



Novel Concepts in Direct Electrochemical C–H Functionalization

Dissertation
for attaining the academic degree of
“Doctor rerum naturalium” (*Dr. rer. nat.*)
in Chemistry

submitted in the Department 09
”Chemistry, Pharmaceutical Sciences, and Geosciences”
at the Johannes Gutenberg University Mainz
by

JOHANNES LUDWIG RÖCKL
born in Regensburg

Mainz, May 2020

Dean: Univ.-Prof. Dr. Tobias Reich

First Reviewer: Univ.-Prof. Dr. Siegfried R. Waldvogel

Second Reviewer: Univ.-Prof. Dr. Holger Frey

Date of Defense:

Declaration

The experimental and written elaboration of this thesis was carried out from March 2018 to May 2020 at the Department of Chemistry (FB 09, Johannes Gutenberg University Mainz) under supervision of Prof. Dr. S. R. Waldvogel.

Hereby, I, Johannes Ludwig Röckl declare that I wrote the dissertation submitted without any unauthorized external assistance and used only sources acknowledged in the work. All textual passages, which are appropriated verbatim or paraphrased from published and unpublished texts, as well as all information obtained from oral sources are duly indicated and listed in accordance with bibliographical rules. In carrying out this research, I complied with the rules of standard scientific practice as formulated in the statutes of Johannes Gutenberg University Mainz to ensure standard of good scientific practice.



“When you know nothing matters, the universe is yours...”
- **Rick Sanchez**

Acknowledgements

Zunächst möchte ich mich für die Unterstützung bei meinem Doktorvater, Prof. Dr. Siegfried Waldvogel und der Managerin des Studiengangs angewandte organische Chemie, Dr. Birgit Janza, an dem ich teilnehmen durfte, bedanken. Ohne euch wäre ich vermutlich nicht auf die Idee gekommen, eine Promotion zu beginnen. Als ich Ende 2016 fragte, ob mich Sigi bei einer Fast-Track Promotion unterstützt und ein einfaches „Ja!“ erklang, ohne große Bedingungen und ausschweifende Erklärungen, war ich gleichermaßen erstaunt und aufgeregt was die Zukunft so bringen würde. Auch an meine Kollegen in der Forschung der BASF (Dörthe und Marco Naujok, Nadine Vogelgesang, Gerd Molle, Peter Schmitt und Yüksel Battal) möchte ich ein großes Dankeschön aussprechen, der Zuspruch über die vielen Jahre und das Aushalten meiner Launen im Labor waren sicher nicht einfach zu ertragen. Im speziellen habe ich Dr. Martin McLaughlin sehr viel zu verdanken, seine stetige Motivation und sein chemischer Input verhalfen mir zu einer guten Grundlage im Bereich der organischen Chemie, die mir während der Promotion sehr zu Gute kam. Auch meinem Gruppenleiter Dr. Jochen Dietz und meinem Mentor Dr. Peter Eckes gilt mein Dank für eine stetige organisatorische Unterstützung und viele lehrreiche Gespräche. Meine zwei engsten Wegbegleiter und Freunde während meiner Zeit bei BASF, Maximilian Blochberger-Claus und Paul Schneide gilt des Weiteren mein Dank und Anerkennung für reichlich Motivation und auch tolle gemeinsame Erlebnisse. Ohne die tatkräftige Hilfe meiner Laborkollegen innerhalb und neben des Labors, wäre diese Arbeit nicht möglich gewesen. Daher danke ich im speziellen Lars Wesenberg, Silja Hofmann, Dennis Pollok, Dimitrij Ryvlin, meinen Vorgängern Anton Wiebe sowie Yasushi Imada für die Hilfe über die letzten Jahre. Bei meinen beiden Bacheloranden Adrian Hauck und Jonas Rein bedanke ich mich für eure tolle Mitarbeit und wünsche alles Gute für eure Zukunft. Eine sehr große Inspiration während meiner Laufbahn stellte für mich Prof. Dr. Bill Morandi dar, da er mich durch seine Art ein Labor zu führen und Forschung zu betreiben auf die Idee brachte, etwas Ähnliches anzustreben. An dieser Stelle auch ein großer Dank an die ganze Morandi-Gruppe für die herzliche Aufnahme in ihrer Mitte. Zu guter Letzt möchte ich mich bei meinen Eltern und Geschwistern für die Erziehung und Unterstützung bedanken und im ganz Besonderen meiner Partnerin Emma Louise Robertson und ihrer Familie für Support in allen Lebenslagen und viel Verständnis danken. Ohne euch wäre das so nicht möglich gewesen.

Abstract

The focus of this Ph.D. thesis was to develop novel electro-organic methods in C–H functionalization; in particular to eliminate the need for additional supporting electrolyte by applying a combination of base with acidic HFIP ($pK_a = 9.3$) to form a supporting electrolyte in situ. This avoids the use of salts and simplifies the work-up procedure, facilitating easy removal of the electrolyte by distillation, simplifying downstream processing and recycling of the electrolyte. The thesis covers studies towards various C–H functionalization reactions of different types of C–H bonds. The benzylic C–H functionalization of methyl groups with HFIP and subsequent cross-coupling has been successfully demonstrated, giving access to valuable diarylmethanes. The unique properties of 1,3-benzodioxoles were used to synthesize orthoesters electrochemically. A closer look at the properties of these structures revealed their extraordinary stability towards acids and bases and their high lipophilicity. Successful introduction of the HFIP moiety with further functionalization of purines and arenes was achieved by applying a Design of Experiment (DoE) approach. Moreover, the first successful electrochemical dehydrogenative homo- and cross-coupling reaction of electron-deficient phenols has been developed. Finally, an electrochemically-enabled isodesmic shuttle reaction of halogens is described. This concept was expanded to SPhBr and SPhCl shuttle reactions, which were thus far unprecedented. The reversibility was utilized in various synthetic applications, such as intramolecular bromine shuttle reactions or the protection and deprotection of double bonds.

Kurzzusammenfassung

Der Schwerpunkt dieser Dissertation lag auf der Entwicklung neuartiger elektro-organischer Methoden zur C–H Funktionalisierung; insbesondere sollte der Bedarf an zusätzlichem Leitsalz durch die Kombination von Base mit HFIP ($pK_s = 9,3$) eliminiert werden. Dies vermeidet die Verwendung von Salzen und vereinfacht die Aufarbeitung, da der Elektrolyt leicht destillativ abgetrennt werden kann und das Recycling des Elektrolyten dadurch vereinfacht wird. Die Arbeit umfasst Studien zu verschiedenen C–H Funktionalisierungsreaktionen an verschiedenen Arten von C-H-Bindungen. Die benzyliche C–H Funktionalisierung von Methylgruppen mit HFIP und anschließender Kreuzkupplung wurde erfolgreich demonstriert, wodurch der Zugang zu wertvollen Diarylmethanen ermöglicht wird. Die einzigartigen Eigenschaften von 1,3-Benzodioxolen wurden genutzt, um Orthoester elektrochemisch zu synthetisieren. Ein

genauerer Blick auf die Eigenschaften dieser Strukturen zeigte ihre außerordentliche Stabilität gegenüber Säuren und Basen und ihre hohe Lipophilie. Die erfolgreiche Einführung der HFIP-Einheit mit weiterer Funktionalisierung von Purinen und Arenen wurde durch Anwendung eines Design of Experiment (DoE)-Ansatzes erreicht. Darüber hinaus wurde die erste erfolgreiche elektrochemische dehydrierende Homo- und Kreuzkupplungsreaktion von elektronenarmen Phenolen entwickelt. Zuletzt wurde eine elektrochemische isodesmische Shuttle-Reaktion von Halogenen beschrieben. Dieses Konzept wurde auf SPhBr- und SPhCl-Shuttle-Reaktionen ausgeweitet, die bisher noch nicht beschrieben waren. Die Reversibilität wurde in verschiedenen synthetischen Anwendungen genutzt, wie z.B. bei intramolekularen Brom-Shuttle-Reaktionen oder zur Schützung und der Entschützung von Doppelbindungen.

Table of Contents

1	INTRODUCTION	17
1.1	ORGANIC ELECTROCHEMISTRY	17
1.2	C–H FUNCTIONALIZATION.....	20
1.2.1	<i>Electrochemical C–H Functionalization</i>	22
1.2.1.1	Benzylic C–H Functionalization.....	23
1.2.1.2	Aromatic C–H Functionalization.....	25
1.2.2	<i>Aryl-Aryl C-C Bond Formation</i>	26
1.3	1,1,1,3,3,3-HEXAFLUOROPROPAN-2-OL (HFIP)/ BASE SYSTEM AS A UNIQUE ELECTROLYTE	28
2	OBJECTIVE	29
3	RESULTS AND DISCUSSION	31
3.1	BENZYL-ARYL CROSS-COUPLING VIA ANODIC C–H FUNCTIONALIZATION WITH HFIP	31
3.2	BENZYLIC ANODIC C–H FUNCTIONALIZATION WITH HFIP AND SUBSEQUENT CYANATION TO GENERATE 2-PHENYLACETONITRILES.....	35
3.3	ANODIC C–H FUNCTIONALIZATION TOWARDS FLUORINATED ORTHOESTERS FROM 1,3-BENZODIOXOLES	38
3.4	ANODIC C–H FUNCTIONALIZATION OF PURINE DERIVATES AND SUBSEQUENT CROSS-COUPLING.....	42
3.5	DEHYDROGENATIVE ANODIC C–C COUPLING OF PHENOLS BEARING ELECTRON-WITHDRAWING GROUPS.....	46
3.6	ELECTROCHEMISTRY-ENABLED ISODESMIC SHUTTLE REACTION	49
4	CONCLUSION	55
5	OUTLOOK	59
6	REFERENCES	62
7	APPENDIX	67
7.1	PUBLICATIONS	67
7.2	SUPERVISED WORK	68
7.3	CURRICULUM VITAE	69
7.4	ATTACHED PUBLICATIONS	71

1 Introduction

1.1 Organic Electrochemistry

Global energy consumption has increased enormously over the last few decades. In the context of global warming, this has become a major topic of social and political discussion. Fossil resources are in limited supply and this will no doubt have a significant impact on the organic synthesis of chemicals in years to come. With the advent of green chemistry,^[1] current research efforts are focused on not only improving efficiency of industrial reactions and processes, but also on the development of sustainable synthetic approaches. Cutbacks on ecological footprint, carbon dioxide emissions and waste generation will become increasingly important for industry. With this shift in focus, electro-organic synthesis is experiencing a renaissance after being overlooked for several decades.^[2,3] The use of electric current to induce oxidation and reduction in lieu of conventional chemical agents poses several advantages from an environmental and economical perspective (Figure 1).^[4] Inexpensive and readily accessible electric current from renewable resources can be harnessed as an inherently safe reagent. This in turn leads to transformations with high atom economy and minimal reagent waste. Electrochemical reactions have already demonstrated robustness across a broad range of current densities, allowing for short reaction times at high current densities without any significant loss in yield versus conventional synthetic routes.^[5,6] Furthermore, an electrochemical approach may open up novel synthetic avenues or enable facile alternatives to otherwise challenging reactions.^[7] Significant progress has been made in electro-organic synthesis over the past two decades, as outlined in reviews by Waldvogel *et al.*, Baran *et al.*, and Kärkäs^[3,8–11]

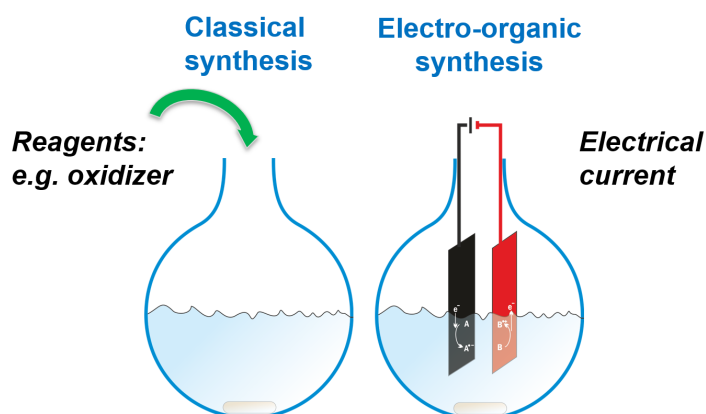


Figure 1. Comparison classical organic synthesis and electro-organic synthesis.

The general principles of organic electrochemistry are based on either cathodic reduction (single electron transfer from electrode to substrate or mediator) or anodic oxidation (single electron transfer from substrate to electrode or mediator). The substrate is dissolved in an ion conductive reaction mixture (electrolyte) and the electrode is usually composed of an electroconductive solid material such as graphite.

There are several reaction parameters which require optimization prior to establishing a novel electro-synthetic method. These include current density, which has direct influence onto the concentration of reactive intermediates; applied charge, which equals the amount of reagent added; temperature, and supporting electrolyte to ensure conductivity (Figure 2).^[8] Single electron transfer occurs at the electrode. For subsequent reactions, these highly reactive intermediates need to diffuse into the bulk, therefore ionic strength and solvation are important factors for the electrolyte system.

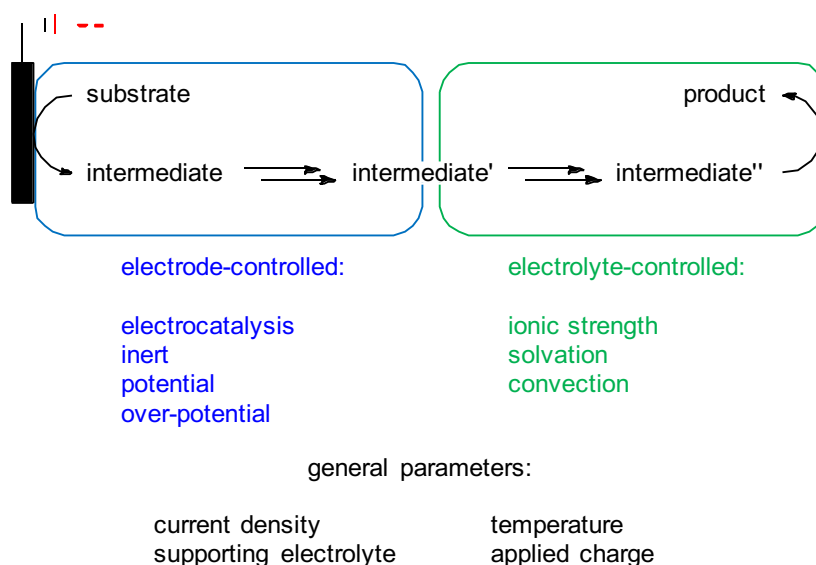


Figure 2. Common parameters in electro-organic synthesis.

The material characteristics of the electrodes must also be considered, as these influence their mode of operation (Figure 3). Inert electrodes are involved exclusively in the electron transfer process, and the selectivity of this process is proportional to the electrode potential. Common inert electrode materials are platinum or carbon-based systems, such as graphite, glassy carbon, or boron-doped diamond (BDD), which share several advantages including simple application and relatively low maintenance.^[9-12] If higher selectivity is needed, active electrodes and mediated electrolysis can be used. Active electrodes generate a non-soluble electrocatalytic

species which forms a layer on the electrode surface and acts as an immobilized redox mediator.^[13] This redox mediator is formed and regenerated in situ, serving as a redox filter. Examples for these electrodes are active Mo,^[14] Ni/NiOOH^[15] or Pb/PbO₂.^[16] Dependence of conversions on the applied electrode potential is reduced compared to that of inert electrode systems. Mediated electrolysis represents a further approach, using a soluble active mediator which converts the substrate and is electrochemically regenerated. A stepwise approach can be taken for even more sensitive substrates, in which a reagent is converted into an active species electrochemically, and the substrate is added in a separate step ex-cell, after complete electrolysis.^[17] In general, oxidized or reduced intermediates generated in situ at the electrode are highly reactive and prone to further reactions.^[18]

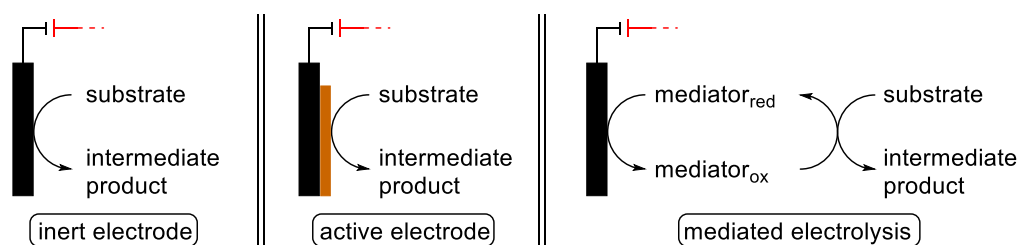


Figure 3. Modes of operation for electrodes in electro-organic synthesis.

There are several different modes of operations in electro-organic synthesis. The galvanostatic protocol operates at constant current, facilitating rapid transformations at low cost (Figure 4). The setup is simple, requiring two electrodes in electrolyte and in a preferentially undivided cell supplied with a source of constant current. Simple direct current power sources which are readily commercially available can be used. The reaction mixture is composed of solvent, and if necessary, an additional supporting electrolyte to facilitate the conductivity. The supporting electrolyte is typically a salt, a strong acid or base. Alternatively, a divided cell setup with an additional semipermeable or porous membrane between the catholyte and anolyte can be used. This is useful for reversible redox reactions or to prevent instability towards the counter electrode.^[3] An alternative setup is required for potentiostatic electrolysis. An additional reference electrode is needed to control the potential, enhancing the selectivity but prolonging reaction time and increasing the associated setup costs.^[19]

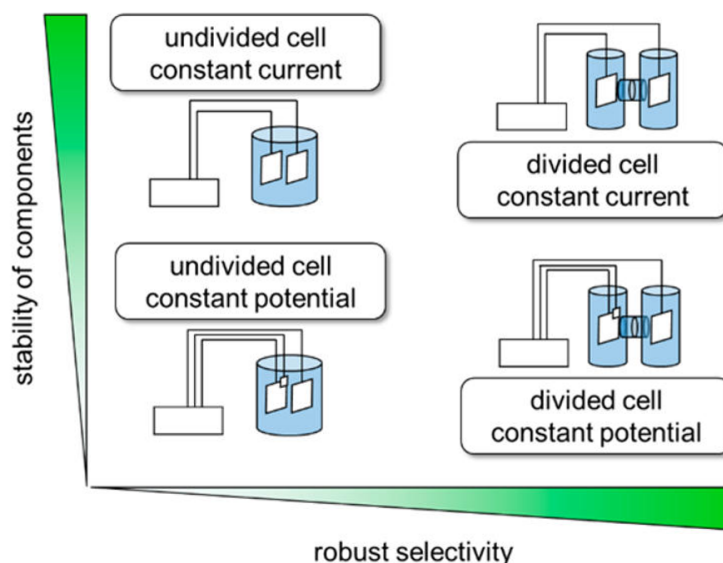
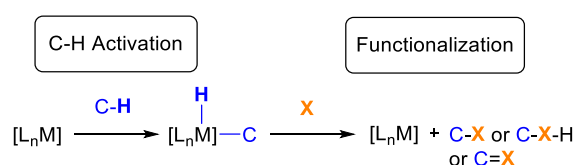


Figure 4. Modes of operation in electro-organic synthesis.

User-friendly setups, such as the ElectraSyn designed by Baran *et al.*,^[20] screening cells,^[21] and electro-organic continuous flow setups developed in the Waldvogel lab are also commercially available.^[22,23] Regardless of the setup used, electrodes should be arranged in parallel to give a homogeneous electric field without local potential peaks which could lower reaction selectivity due to uncontrolled side reactions.^[19] Additionally, the cells should also ensure effective mixing, which was found to be a crucial parameter during this work.

1.2 C–H Functionalization

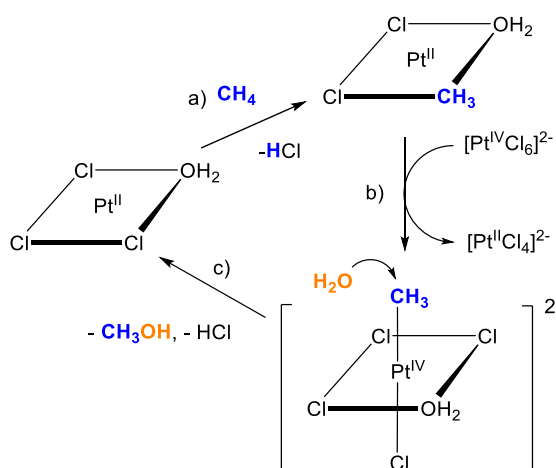
The terms C–H activation and C–H functionalization are often used interchangeably. C–H activation refers to the cleavage of the C–H bond by a transition metal, forming an organometallic complex.^[24–26] This complex can then undergo subsequent reactions leading to C–H functionalization (Scheme 1). For the purposes of the work described in this thesis, C–H functionalization is better defined as any organic transformation of the relatively inert C–H bond into a C–X bond (where X is usually carbon, oxygen or nitrogen), irrespective of the mechanism.



Scheme 1. General equation for metal-catalyzed C–H functionalization.

A notably successful example of C–H functionalization is the Shilov system (Scheme 2).^[27] This system enables direct conversion of methane into methanol in a high-yielding reaction catalyzed by metal salts in solution. This transformation has huge significance for industry, as methanol is the feedstock for many processes including manufacturing of plastics and paints,^[28] and is used as a solvent, antifreeze in pipelines,^[29] and as an efficient energy carrier due to its high energy density.^[30] Direct conversion from methane opens up access to renewable sources such as biogas for industrial processes.

The Shilov reaction was first discovered on observation of a hydrogen-deuterium exchange in deuterated solution using a platinum tetrachloride anion.^[31] Shilov was able to catalytically convert methane into methanol or methyl chloride using a Pt(IV) salt as a stoichiometric oxidant. The process involves three main steps: (a) C–H activation; (b) a redox reaction to form an octahedral complex; followed by (c) attack of water for the formation of the carbon-oxygen bond towards methanol.



Scheme 2. Catalytic cycle of the platinum catalyzed C–H functionalization of methane to methanol.

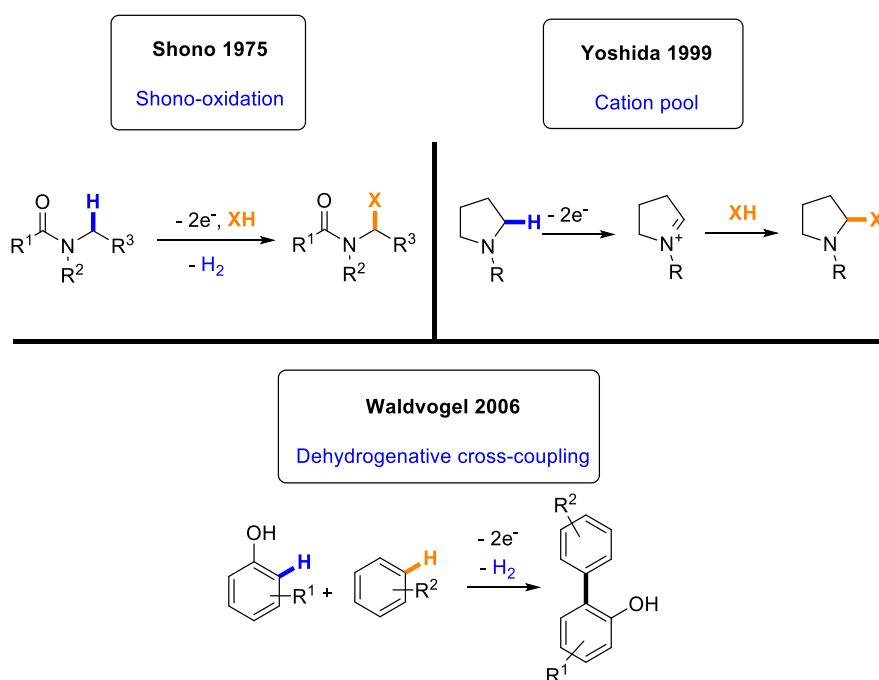
Although C–H bonds are ubiquitous in organic molecules, selective C–H functionalization has yet to be fully exploited.^[32] While transition metal-catalyzed C–H functionalization represents a major breakthrough in organic synthesis, it has its limitations which have led to increasing efforts to develop metal-free alternatives.^[33] C–H functionalization is associated with high cost, due to the need for expensive catalysts and non-commercial ligands. A stoichiometric amount of oxidant is often required, leading to a decrease in atom economy and generation of waste. Toxicity is a further issue, particularly in the production of pharmaceutical products, where certain

threshold values of metals cannot be exceeded.^[34] Sensitivity to air and moisture is a further factor affecting the robustness and ease of setup of metal-catalyzed C–H functionalization reactions.^[35] Limited catalyst turnover in C–H functionalization reactions with a C–H activation step can be another significant problem.

While understanding of the mechanistic aspects of C–H functionalization has deepened in recent years,^[36,37] activation of the kinetically inert C–H bond remains inherently difficult. Electrochemistry can enable reaction pathways which break the C–H bond selectively under mild conditions by generating radicals, cations, anions and other reactive species which can be exploited in subsequent reactions.^[18]

1.2.1 Electrochemical C–H Functionalization

Numerous examples over the past two decades demonstrate the versatility of electrochemical strategies towards C–H functionalization, as detailed in a review by Kärkäs.^[33] Notable contributions to the field include Shono-type oxidations,^[38] Yoshida’s “cation pool” methodology,^[17] and Waldvogel’s selective biaryl cross-coupling (Scheme 3).^[39]



Scheme 3. Important milestones in electrochemical C–H functionalization.

Shono and coworkers developed an electrochemical oxidation of carbamates to *N*-carbamoyl iminium ions as early as 1975.^[40] First, a nitrogen-centered radical is formed which is further oxidized to an iminium ion, which in turn can be reacted with a nucleophile (e.g. alcohol solvent molecule or cyanide). This gives rise to C–H functionalization of nitrogen-containing heterocycles in the alpha position. Of note is that only nucleophiles with oxidation potentials higher than those of the starting material (mostly amides and carbamates) can be applied.

An elegant strategy enabling use of a wider variety of nucleophiles (also with lower oxidation potentials than the starting material) is the “cation pool” method, where electrolysis and addition of the nucleophile are performed in two separate steps.^[17] First, cations are generated and accumulated through electrolysis at low temperatures (such as *N*-acyl iminium ions). The nucleophile is then added to the reaction mixture. Nucleophiles which have been successfully employed include allyl silanes, enol silyl ethers, enol acetates, allyl stannanes, benzyl silanes, Grignard reagents and organo-aluminum compounds, as well as electron-rich arenes and C–H acidic compounds.

In the Waldvogel group, anodic C–H functionalization and coupling reactions of aromatic compounds have been under investigation since 2006.^[39] Initially, the group was focused on the synthesis of 2,2'-biphenols as precursors for catalysts in the hydroformylation process.^[41] After successfully developing procedures for the electrochemical synthesis of biphenols,^[42] selective phenol-arene cross-coupling,^[43] the coupling of anilides,^[44] *meta*- and *para*-terphenyls,^[45] and cross-coupling of different heterocycles with phenols was investigated.^[46–48] Selectivity was achieved by using boron-doped diamond (BDD) electrodes and fluorinated alcohols as a solvent. So far, this methodology has been limited to electron-rich arenes. Therefore, establishing a procedure to successfully couple phenols carrying electron-withdrawing groups is highly desired.

1.2.1.1 Benzylic C–H Functionalization

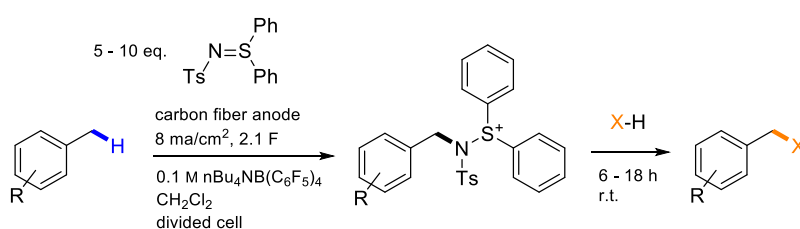
There are several established electrochemical methods towards benzylic C–H functionalization in which a benzylic methyl group is oxidized to the corresponding alcohol^[49] or ketone.^[50] An industrial example is the first step in the synthesis of 3-(4-*tert*-butylphenyl)-2-methylpropanal (Lilial[®], Lysmeral[®]); a twofold anodic oxidation of 4-

4-*tert*-butyl toluene on >10,000 ton per year scale towards an acetal.^[18] Another electrochemical activation of toluene derivatives via initial oxidation of the aromatic core was demonstrated in work by the Wang group.^[51] The aryl radical cation generated can subsequently undergo deprotonation, followed by further oxidation to give a benzylic cation. This cation can then be trapped by a range of oxygen-based nucleophiles, in this case water, which directly undergoes further oxidation from the benzylic alcohol to furnish the corresponding ketone (Scheme 4).



Scheme 4. Selective electrochemical benzylic oxidation towards ketones by Wang *et al.*

Consequently, over-oxidation plays a major role in these kinds of reactions. An elegant strategy to avoid this problem is the “stabilized cation pool” method developed by Yoshida and coworkers.^[52] As in the regular “cation pool” method, the oxidation and coupling events are divided, which leads to bond formation in a selective manner (Scheme 5). However, in this method, accumulation of the electrochemically oxidized species is achieved by trapping the intermediate benzylic cations with an additional reagent. After elimination of the stabilizing reagent, coupling with aromatic nucleophiles was then carried out.



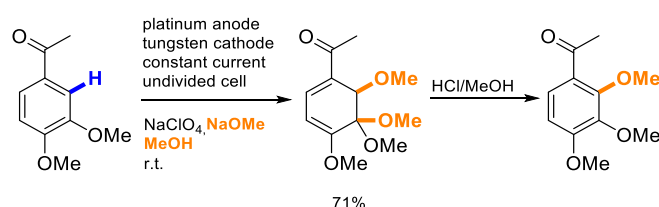
Scheme 5. „Stabilized cation pool“ method by Yoshida *et al.*

Despite the large scope of this method, it exhibits some drawbacks. The stabilizing reagent *S,S*-diphenyl-*N*-(4-methylphenylsulfonyl)sulfimine is not commercially available and needs to be applied in 5- to 10-fold excess. The procedure suffers from long reaction times (up to 35 hours to reach completion) and has only been demonstrated on a small scale (0.1 mmol). Free phenols could not be used in the anodic step. In addition, a complex electrolysis setup has been used (a divided cell

equipped with a very specific carbon fiber anode), limiting the procedure's scalability. In addition, this method suffers from the use of expensive supporting electrolytes and a poor atom efficiency. Consequently, a simple, sustainable, and scalable approach for the synthesis of diarylmethanes remains highly desired.

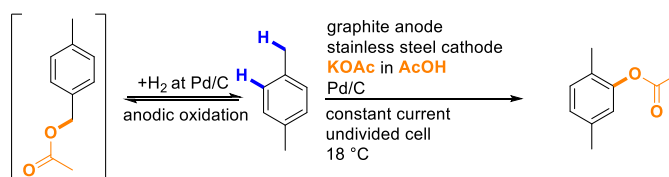
1.2.1.2 Aromatic C–H Functionalization

The direct introduction of alcohols into aromatic systems is challenging, due to the electron-donating nature of alkoxy groups, making the corresponding aryl ethers prone to over-oxidation.^[19] Although monoalkoxylated arenes can be obtained after elimination, the anodic C–H bond alkoxylation is limited to only few examples in low yields (Scheme 6).^[53,54]



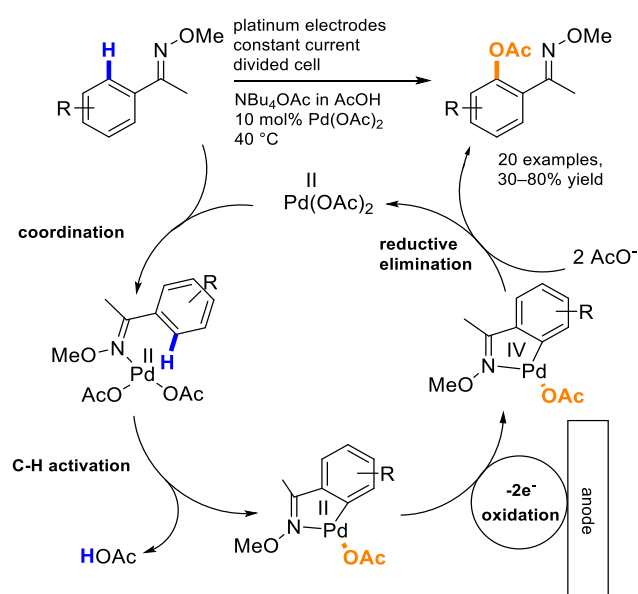
Scheme 6. Anodic methoxylation towards 2,3,4-trimethoxyacetophenone.

Furthermore, the yield of electrochemical C–H acetoxylation of arenes is limited by either over-oxidation or the formation of various regioisomers. Therefore, almost exclusively symmetrical substrates have been explored.^[19] A formal anodic hydroxylation has been achieved in a one-pot sequence, with electrochemical synthesis of aryl acetates followed by hydrolysis (Scheme 7).^[55–57] Benzylic positions are preferentially attacked over aryllic positions by acetic acid as a nucleophile to give benzyl acetate, due to the high stability of benzylic cations. Palladium on carbon reacts with hydrogen generated at the cathode to selectively cleave the benzyl acetates, which leads to accumulation of aryl acetates.^[58]



Scheme 7. Selective anodic core acetoxylation of alkylated benzene derivatives.

Another approach to C(sp²)-H alkoxylation and acetoxylation is transition metal-catalyzed transformation. Anodic oxidation is used as a clean, cheap and safe substitute for oxidizing agents in transition metal-catalyzed C-H functionalization. Ackermann *et al.* developed an electrochemical cobalt-catalyzed *ortho*-C-H alkoxylation of *N*-(pyridine-*N*-oxide)-benzamides utilizing pyridinium-*N*-oxide as a directing group in yields up to 78%.^[59] In contrast to purely non-mediated electrochemical transformations, transition metal-catalysis requires a directing group which allows the pre-coordination of the substrate to the metal (Scheme 8). A variety of directing groups such as oxime ethers, pyridines, pyrazoles, and quinolones are suitable for palladium acetate catalyzed electrochemical C-H acetylation and afford aryl acetates in moderate to good yields.^[60,61] An intrinsic drawback of transition metal-catalyzed C-H activation is the requirement of a directing group and the use of additional metals, which limits the general applicability and the scope.



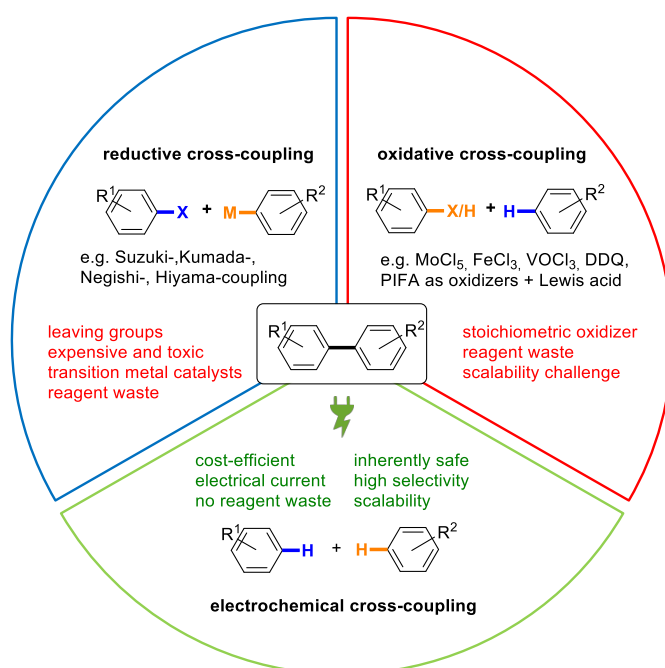
Scheme 8. Catalytic cycle of the Pd-catalyzed C-H activation and acetoxylation of oxime ethers.

1.2.2 Aryl-Aryl C-C Bond Formation

The Suzuki-Miyaura reaction is a well-known general strategy towards the biaryl structural motif. This transition-metal-catalyzed coupling reaction of aryl(pseudo)halides and nucleophilic organometallic species makes use of organoboron reagents (Scheme 9).^[62-64] Although this transformation is highly selective and high-yielding, it is associated with some environmental and economic

disadvantages. Pre-functionalized substrates and expensive transition metal catalysts producing toxic reagent waste are required.

Oxidative, reagent-mediated coupling reactions represent an alternative strategy to access the biaryl motif.^[65–67] Oxidative R¹–H/R²–H cross-coupling is a leaving-group-free, step-economic approach which requires no pre-functionalization. However, the C–C bond formation step with loss of H₂ is typically thermodynamically unfavorable and usually requires a suitable sacrificial oxidant as an external driving force. Conveniently obtained oxidizers such as iron(III) chloride, vanadyl chloride and molybdenum(V) reagents can be used to give selective coupling.^[68] Organo-based reagents like (bis(trifluoroacetoxy)iodo)benzene (PIFA) or 2,3-dichloro-5,6-dicyano-1,4-benzoquinone (DDQ) can also be used but require additional reagents such as Lewis acids.^[69,70] This approach is hindered by limited regioselectivity and over-oxidation to form oligomers and polymers. Additionally, competing reactions to form the homo-coupled products are a significant problem.



Scheme 9. Comparison between different aryl-aryl cross-coupling methodologies.

Electrochemistry poses an environmentally friendly, inherently safe, robust and selective alternative for the formation of carbon-carbon bonds.^[19] Oxidative R¹–H/R²–H cross-coupling with hydrogen gas evolution has recently been achieved via anodic oxidation and concomitant cathodic proton reduction. Further developments and

opportunities for electrochemical C–C bond formation are outlined in a recently published account by Waldvogel *et al.*^[39]

1.3 1,1,1,3,3,3-Hexafluoropropan-2-ol (HFIP)/ Base System as a Unique Electrolyte

Highly fluorinated alcohols such as 1,1,1,3,3,3-hexafluoroisopropanol (HFIP) demonstrate high electrochemical stability and the ability to stabilize intermediary radical cations.^[71–75] Therefore, fluorinated alcohols have emerged as excellent choices for a broad range of applications in organic chemistry, due to their high hydrogen-bonding donor ability,^[76,77] high polarity,^[77,78] outstanding (electro-)chemical stability,^[71,79] and micro-heterogeneity^[80,81]. This is illustrated by their use as solvents, co-solvents or promoters in organic syntheses.^[71,77,82,83] Several examples have showcased the utility of HFIP in transition metal-catalyzed,^[83,84] and metal-free reactions^[85,86]. In combination with bases, HFIP promotes unusual transformations like the generation of aza-oxyallyl cationic intermediates from α -haloamides^[87–89] or HFIP-promoted nucleophilic substitutions.^[82,90] These unique features of HFIP make it particularly well-suited as a solvent for electrochemical reactions, especially its ability to stabilize radical intermediates. HFIP has demonstrated superiority to other solvents when it comes to improving selectivity and yield of various electrochemical transformations.^[8,18,39,91]

2 Objective

A common drawback in electrochemistry is the need for supporting electrolytes, which are often salts which can be harmful to the environment.^[92] For example, perchlorates can lead to explosive events and symmetric tetraalkylammonium salts strongly affect the wastewater treatment.^[93,94] These salts have to be removed upon workup in multiple steps, making recovery and purification difficult. The aim of this work was to find novel electrolytic systems that circumvent these problems and enable new transformations in electrochemical C–H functionalization. When applying a combination of base with acidic HFIP ($pK_a = 9.3$) to electro-organic synthesis, a supporting electrolyte is formed in situ, eliminating the need for additional supporting electrolyte. Avoiding the use of salts simplifies the work-up procedure, facilitating easy removal of the electrolyte by distillation, simplifying downstream processing and recycling of the electrolyte. Additionally, the lack of salts allows for coupling with mass spectrometry for real-time reaction monitoring in, for example, automated synthesis. Furthermore, the enhanced nucleophilicity of deprotonated HFIP allows trapping of reactive intermediates, which can be applied to different coupling reactions to open new pathways in organic synthesis.

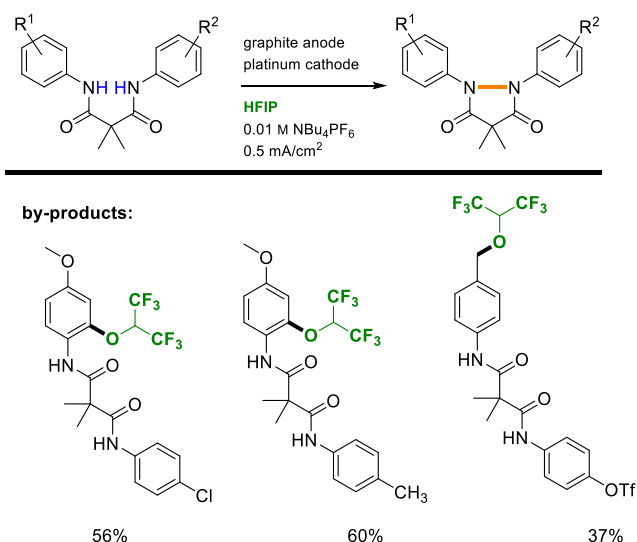
3 Results and Discussion

3.1 Benzyl-Aryl Cross-Coupling via Anodic C–H Functionalization with HFIP

Y. Imada, J. L. Röckl, A. Wiebe, T. Gieshoff, D. Schollmeyer, K. Chiba, R. Franke, S. R. Waldvogel, *Metal- and Reagent-Free Dehydrogenative Benzyl-Aryl Formal Cross-Coupling by Anodic Activation in 1,1,1,3,3,3-Hexafluoropropan-2-ol*, *Angew. Chem. Int. Ed.* **2018**, 57, 12136–12140; (VIP manuscript) (Inside back cover)

Y. Imada, J. L. Röckl, A. Wiebe, T. Gieshoff, D. Schollmeyer, K. Chiba, R. Franke, S. R. Waldvogel, *Metall- und reagensfreie dehydrierende formale Benzyl-Aryl-Kreuzkupplung durch anodische Aktivierung in 1,1,1,3,3,3-Hexafluoropropan-2-ol*, *Angew. Chem.* **2018**, 130, 12312–12317.

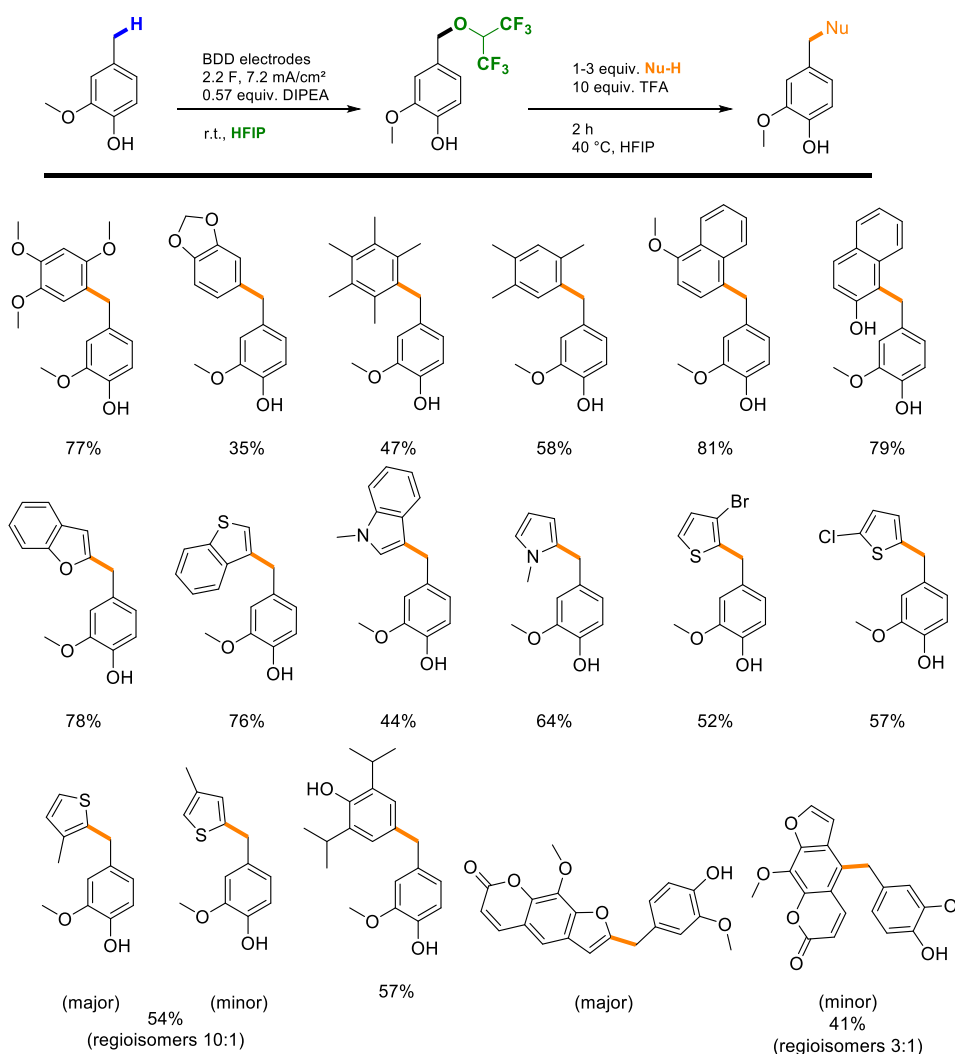
During the work on dehydrogenative *N,N*-coupling, HFIP aryl ethers were discovered as a by-product (Scheme 11).^[95] Of particular interest for subsequent functionalization were the benzylic HFIP ethers, due to their unique reactivity.^[96]



Scheme 11. Discovery of HFIP ethers during the work on anodic *N,N*-bond formation.

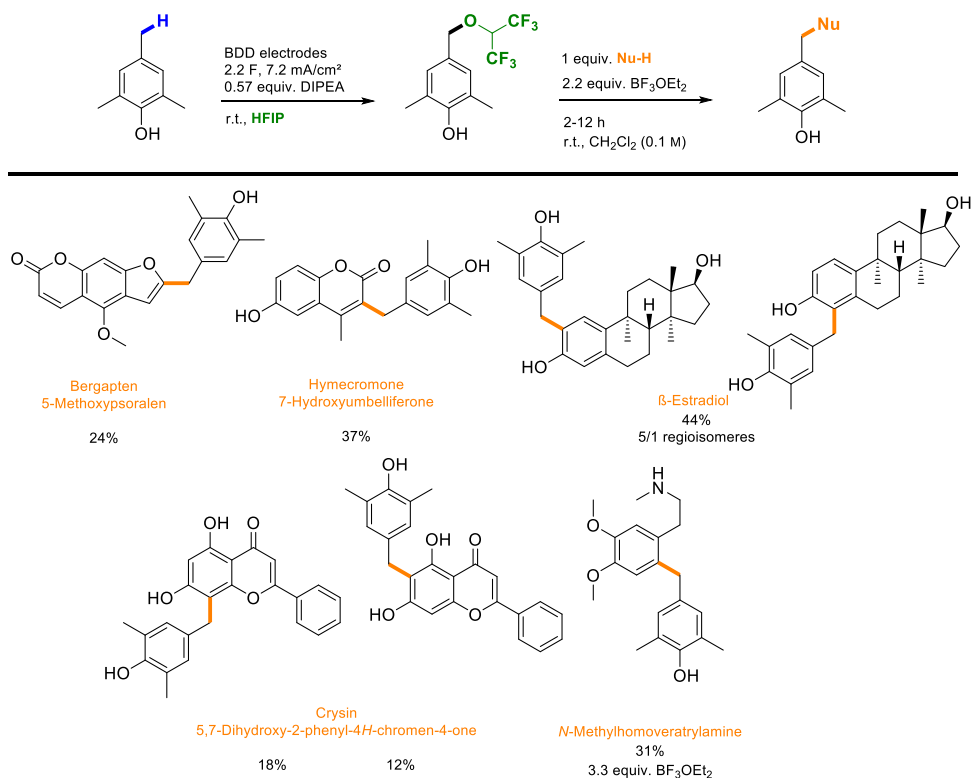
After initial screenings, we found that by adding a base to HFIP as solvent, the anodic oxidation of phenols, anisols and anilids delivers HFIP ethers in very high yields, making additional supporting electrolyte superfluous. Moreover, it was discovered that after treatment of HFIP ethers with acid (acetic acid, trifluoroacetic acid), benzyl cations are formed and HFIP is released again. These benzyl cations are very stable in HFIP^[71] and can easily be trapped with arenes as nucleophiles (Scheme 12). This gives rise to

the cross-coupled products in exceptionally high yields (up to 93% over 2 steps) with a very broad substrate spectrum (Scheme 12).^[96]



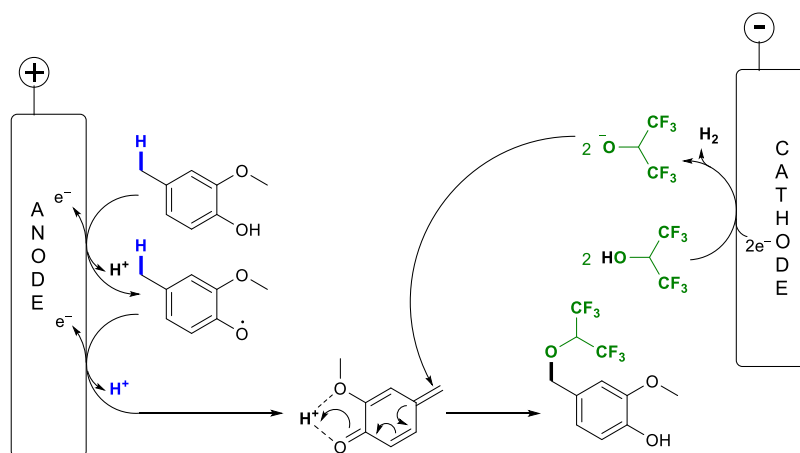
Scheme 12. Benzyl-aryl cross-coupling of phenols with various nucleophiles after anodic activation with HFIP.

Even late-stage functionalization of a variety of natural products and pharmaceuticals was possible in yields up to 44% by slightly changing the protocol and using Lewis acids instead of 2,2,2-trifluoroacetic acid for HFIP ether cleavage (Scheme 13).



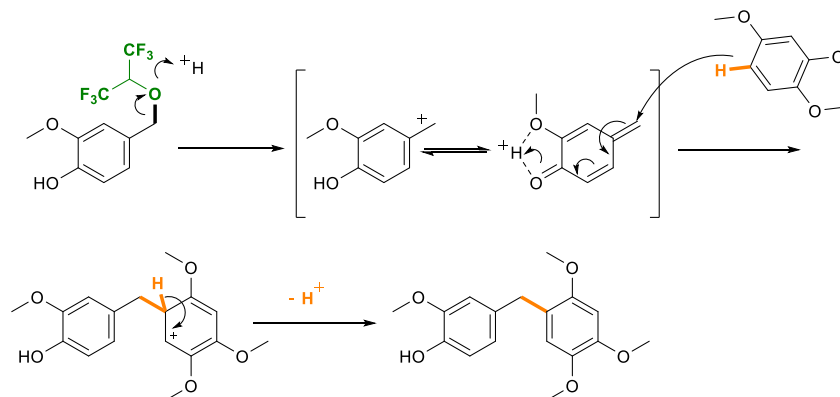
Scheme 13. Lewis acid directed late-stage functionalization of natural products and pharmaceuticals.

Mechanistic investigations revealed that the respective phenol, anisole or even anilide is oxidized twofold at the anode, which after twofold deprotonation results in the formation of a quinone methide derivative (Scheme 14). This intermediate is activated in acidic solution and nucleophilic attack of a HFIP anion in the benzylic position can take place. HFIP anions are present from the beginning of the reaction, due to addition of base. The concentration is maintained by the cathodic formation of hydrogen.



Scheme 14. Proposed mechanism towards benzylic HFIP ethers.

Treatment with acid leads to benzylic cations; these are in equilibrium with quinone methide derivatives which can react with nucleophiles, such as electron-rich arenes, to give valuable diarylmethanes (Scheme 15).



Scheme 15. Mechanistic proposal of HFIP-ether cleavage and benzyl-aryl cross-coupling.

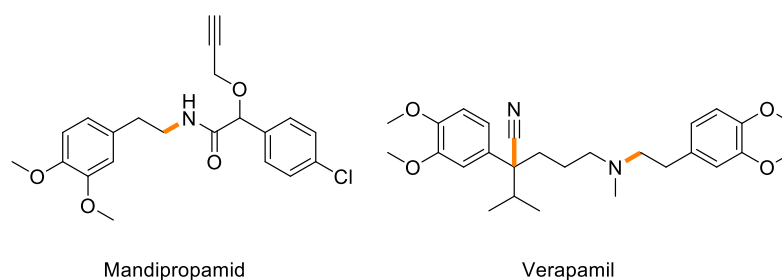
Contribution statement:

Tile Gieshoff (Waldvogel lab) discovered the reaction during other work towards pyrazolidinones via electrochemical *N,N*-bond formation. Anton Wiebe (Waldvogel lab) and Yasushi Imada (Chiba lab) discovered the application of this reaction towards benzyl-aryl cross-coupling. I developed the procedure for the late-stage functionalization, finished the manuscript describing the benzyl-aryl cross-coupling and contributed to further mechanistic investigations. This work was carried out under supervision of Prof. Dr. S. R. Waldvogel at the Johannes Gutenberg University in Mainz.

3.2 Benzylic Anodic C–H Functionalization with HFIP and Subsequent Cyanation to Generate 2-Phenylacetonitriles

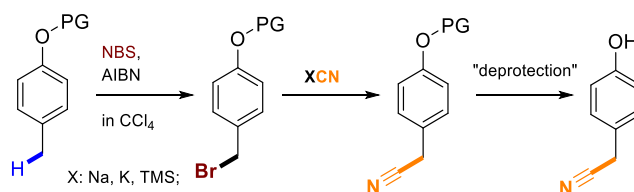
J. L. Röckl, Y. Imada, K. Chiba, R. Franke, S. R. Waldvogel, *Dehydrogenative Anodic Cyanation Reaction of Phenols in Benzylic Positions, ChemElectroChem* **2019**, 6, 4184–4187.

It was found that liberation of the benzylic cation is not necessary to achieve selective bond formation when stronger nucleophiles are used.^[97] With cyanides, a direct substitution reaction is observed to yield 2-phenylacetonitriles, which represent important building blocks in organic synthesis. The structural feature is a precursor to many biologically active molecules such as 2-phenylethylamines^[98] or pharmaceuticals such as the calcium ion channel blocker verapamil or the fungicide mandipropamid (Scheme 16).^[99,100]



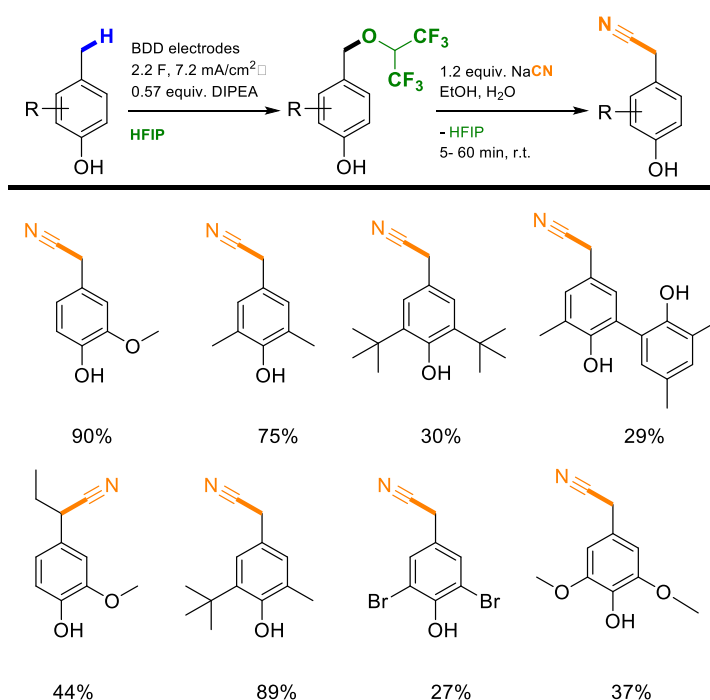
Scheme 16. Representative examples for biologically active molecules incorporating the 2-phenylacetonitrile and/or phenylethyl amine motif.

The reaction only works with *p*-methylphenols, which is noteworthy as phenols typically need to be protected for conversion into 2-phenylacetonitriles using conventional routes. The commonly used route involves a radical bromination and subsequent substitution with cyanide, with additional protection and deprotection steps (Scheme 17).



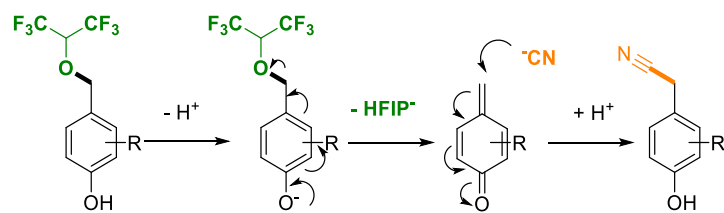
Scheme 17. Common synthetic route to 2-phenylacetonitriles.

The new procedure allows for a simple, sustainable, easily scalable, reagent- and metal-free electrochemical cyanation reaction. It consists of a two-step sequence and the HFIP ether generated in-situ can be used without further purification. The reaction is selective, with yields up to 90% over 2 steps and multiple alkyl groups, halogens, and methoxy groups being tolerated (Scheme 18). Phenols can be converted in a protective-group-free manner, shortening the usual synthetic route by one to two steps. Additionally, only a small excess of cyanide source is used and therefore less toxic reagent waste is generated. The solvent can be redistilled, allowing for a greener procedure.



Scheme 18. Scope of the benzylic anodic activation with HFIP and subsequent cyanation.

The mechanism of the anodic HFIP ether formation is the same as in the benzyl-aryl cross-coupling explained in the previous section. As this method only proceeds well with phenols, the following mechanism is proposed: deprotonation of the phenolic hydroxy group, followed by the loss of the HFIP anion to form a quinone methide intermediate, which can be attacked in a 1,6-addition by cyanide to form the desired 2-phenylacetonitrile (Scheme 19).



Scheme 19. Mechanism of the cyanation of benzylic HFIP ethers.

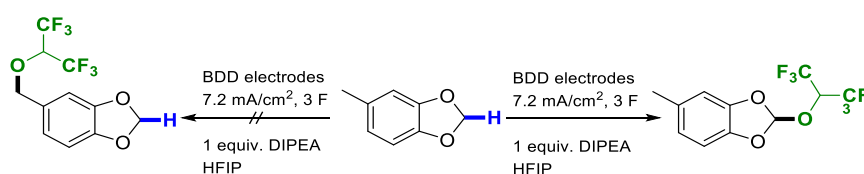
Contribution statement:

The formation of HFIP ethers was developed during previous work. The concept and the optimization of the second reaction were my work. I was responsible for the development of the scope and preparation of the manuscript. Yasushi Imada is listed as a co-author, due to his contribution to the optimization and development of the HFIP ether formation. This work was carried out under supervision of Prof. Dr. S. R. Waldvogel at the Johannes Gutenberg University in Mainz.

3.3 Anodic C–H Functionalization Towards Fluorinated Orthoesters from 1,3-Benzodioxoles

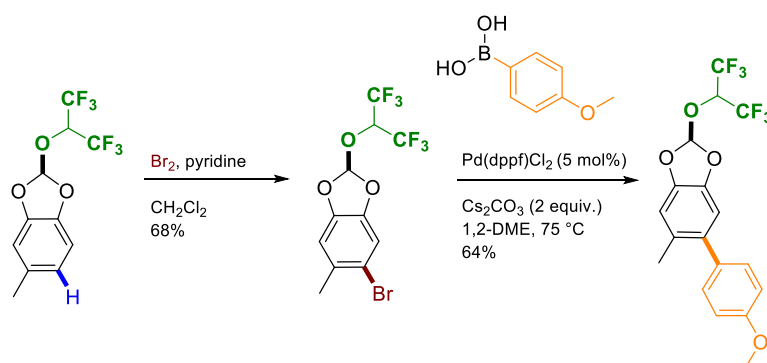
J. L. Röckl, A. V. Hauck, D. Schollmeyer, S. R. Waldvogel, *Electrochemical Synthesis of Fluorinated Orthoesters from 1,3-Benzodioxoles*, *ChemistryOpen*. **2019**, *8*, 1167–1171. (Front cover)

During the substrate screening in previous work, 1,3-benzodioxoles were found to exhibit unexpected reactivity at complete conversion.^[101] Functionalization occurred at position 2, even in the presence of benzylic methyl groups, contrary to previous work where the benzylic position was functionalized (Scheme 20).



Scheme 20. Selectivity of the anodic C–H functionalization of 1,3-benzodioxoles with HFIP.

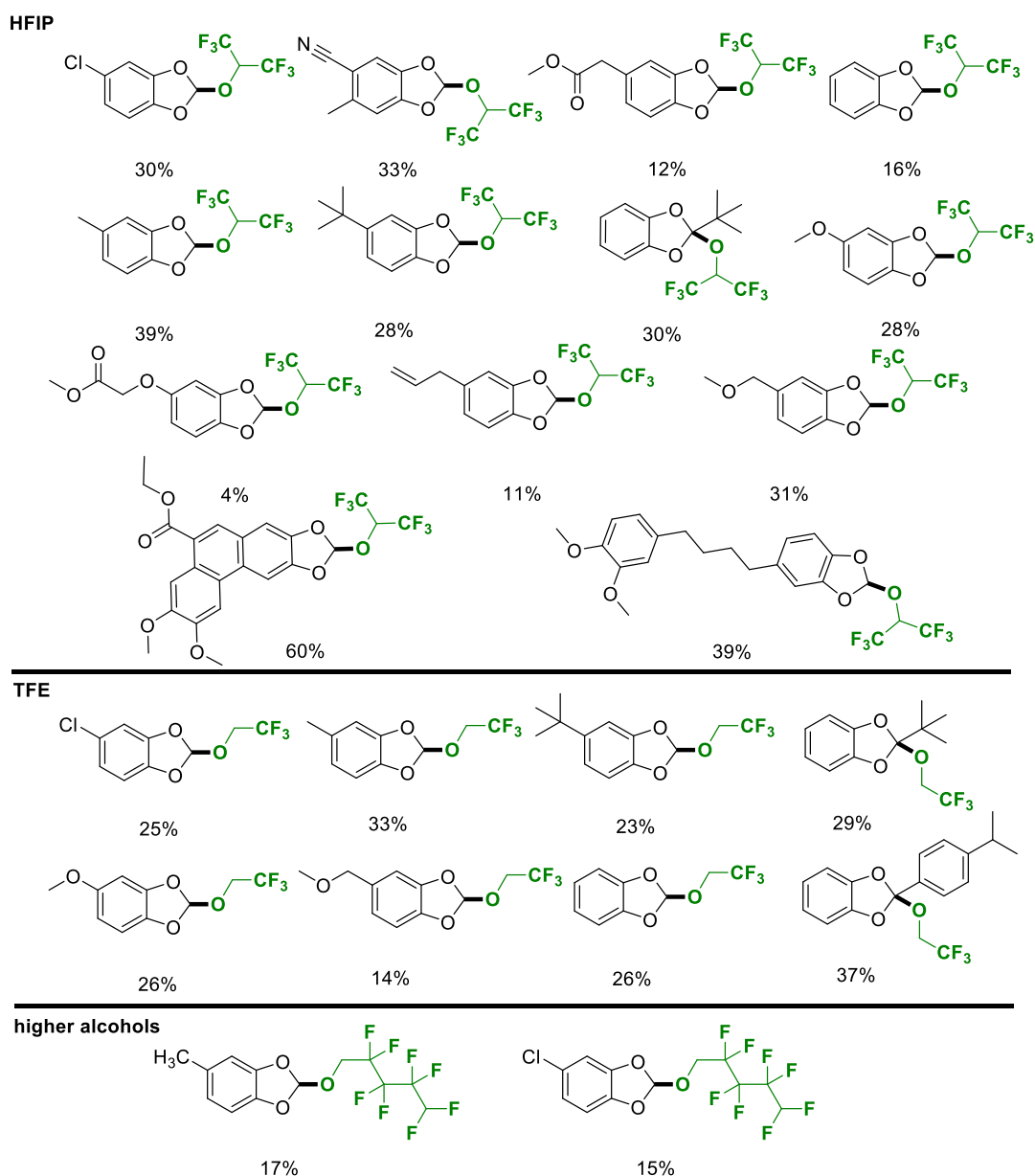
These orthoesters exhibit interesting properties. They are surprisingly stable to acids and bases and do not undergo substitution reactions, even when transition metals are present in the reaction mixture. Therefore, it was possible to perform a bromination, followed by a palladium-catalyzed Suzuki coupling, in the presence of the HFIP orthoester (Scheme 21).



Scheme 21. Synthetic transformations at acidic and transition-metal containing conditions at elevated temperatures in the presence of fluorinated orthoesters, demonstrating their outstanding chemical stability.

It was also possible to install various fluororous groups, allowing for modulation of the properties of the pharmaceutically relevant 1,3-benzodioxole moiety (Scheme 22).^[102] Higher yields and improved selectivity were observed with increasingly larger π -

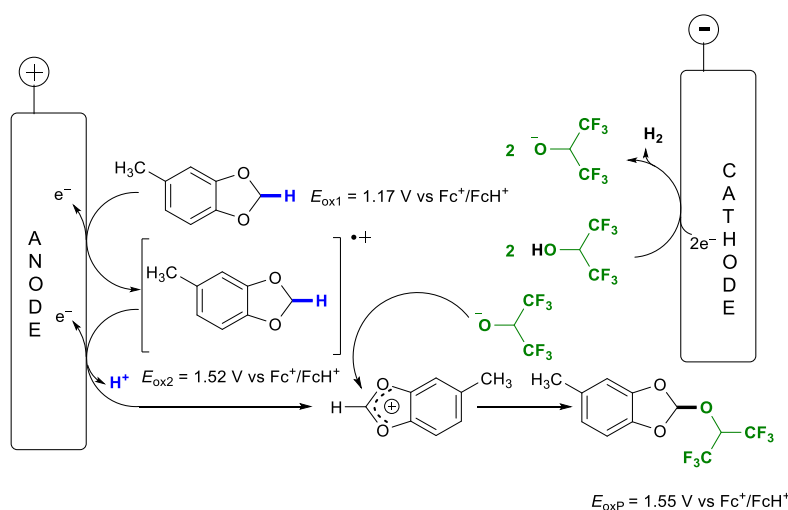
systems. This can be explained by stabilization of the respective cations after twofold oxidation and deprotonation.



Scheme 22. Scope of electrochemically accessible fluorinated orthoesters.

The logP-values of 1,3-benzodioxoles and the corresponding orthoesters were calculated and compared to determine the lipophilicity of the orthoesters in comparison to the respective 1,3-benzodioxoles (see SI of ref.^[101]). It is remarkable that these values increased by a factor of 1.5 to 2 when fluorinated side chains were installed. This transformation could boost the potency of bioactive compounds and impact target selectivity tremendously by influencing pK_a, modulating conformation, and hydrophobic interactions of the 1,3-benzodioxole moiety.^[103]

The mechanism was studied by cyclic voltammetry (Figure 4). Upon initial oxidation, a radical cation is generated which is highly acidic and therefore undergoes deprotonation. After a further oxidation step, a 6 π aromatic 1,3-benzodioxolium species is formed, which can react with a HFIP anion. These intermediates are stabilized by larger π -systems to circumvent side reactions (Scheme 22).



Scheme 22. Proposed mechanism for the formation of fluorinated orthoesters.

The anticipated 6 π aromatic intermediates were isolated as tetrafluoroborate salts and spectroscopically investigated by NMR by Dimroth *et al.*^[104] Studying the CVs, we found that addition of base plays an important role. First, 5-methyl-1,3-benzodioxole in HFIP without base and MTBS as supporting electrolyte was measured. The electron transfer process to the radical cation is reversible, even at a low scan rate of 5 mV/s, indicative of a highly stable radical cation (Figure 4). Upon adding base to this solution, it was found that the process became irreversible. This is due to the subsequent deprotonation reaction. Again, two irreversible oxidation steps ($E_{ox1} = 1.17$ V vs. FcH/FcH⁺, $E_{ox2} = 1.52$ V vs. FcH/FcH⁺) were observed (Figure 4). This confirms an initial oxidation step to the radical cation, followed by the loss of a proton.

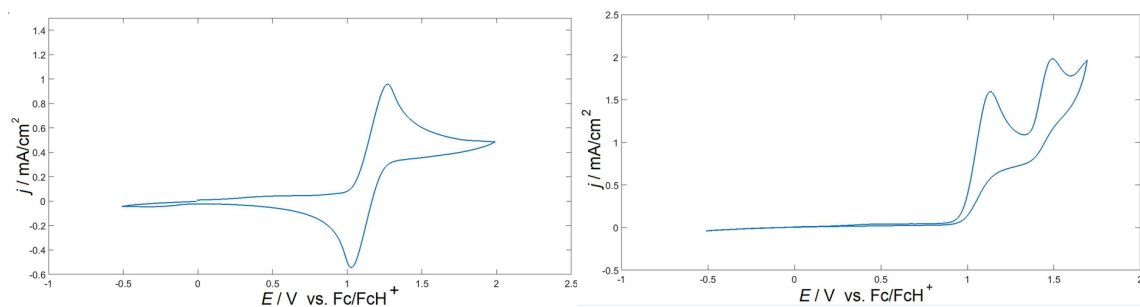


Figure 4. Cyclic voltammograms of a 5 mM solution of 5-methyl-1,3-benzodioxole in HFIP at 50 mV/s; left: HFIP/MTBS; right: HFIP/MTBS + DIPEA.

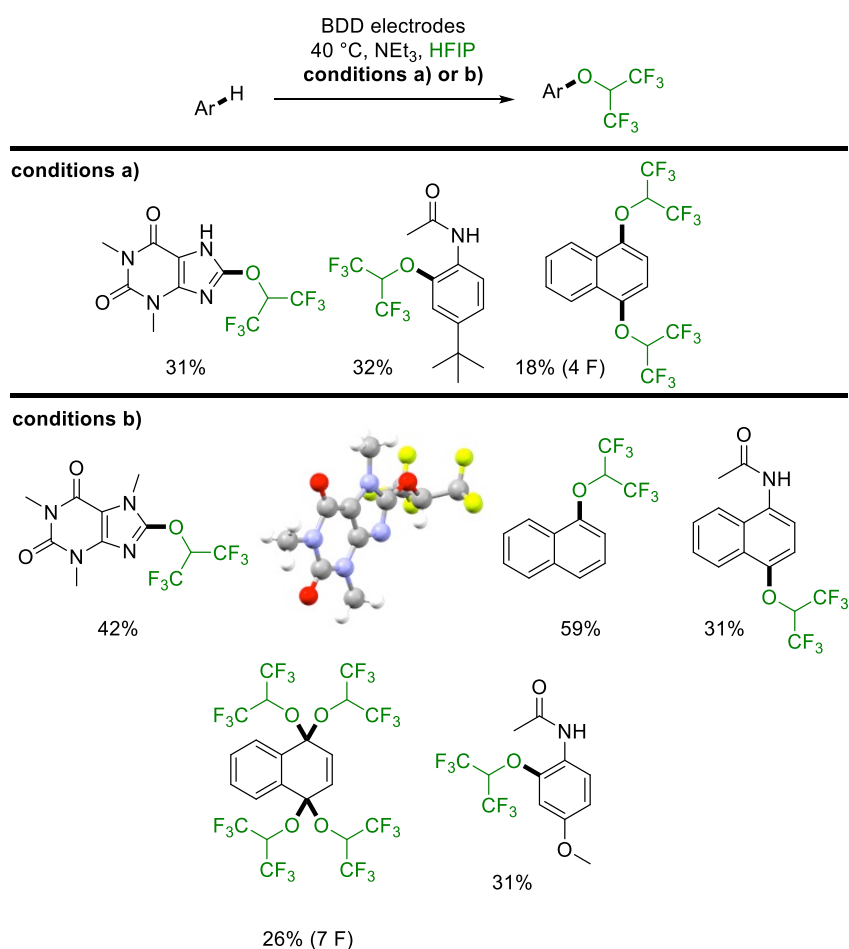
Contribution statement:

I discovered the reaction during screening for a previous project. During his B.Sc. thesis, Adrian Hauck optimized the reaction conditions and finished the scope under my supervision. I studied the mechanism by cyclic voltammetry and prepared the manuscript. This work was carried out under supervision of Prof. Dr. Waldvogel at the Johannes Gutenberg University in Mainz.

3.4 Anodic C–H Functionalization of Purine Derivates and Subsequent Cross-Coupling

M. Dörr, J. L. Röckl, J. Rein, S. R. Waldvogel, *Electrochemical C-H Functionalization of (Hetero)Arenes* – Optimized by DoE, *Chem. Eur. J.*, 2020, accepted.

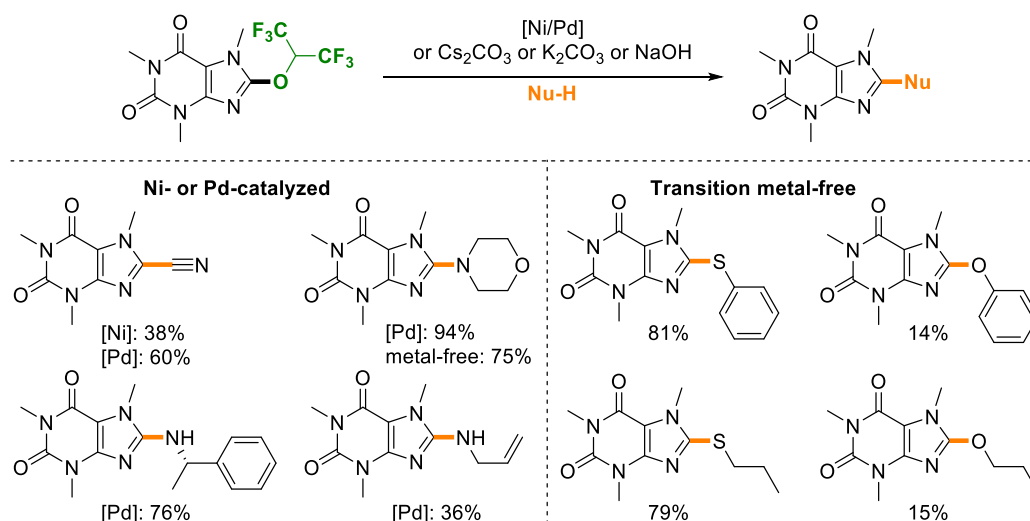
After developing the benzylic activation reactions and isolating aryl HFIP ethers as side components, it was considered to use the HFIP moiety attached to aryls as a leaving group in metal-catalyzed cross-couplings. A selective, scalable, and sustainable electrochemical synthesis of HFIP aryl ethers was thus developed. Of particular interest is the electrochemical modification of bioactive purine derivatives, such as caffeine and theophylline derivatives (Scheme 23).



Scheme 23. Linear and DoE optimized reaction conditions of the anodic oxidation of purines and other arenes to 8-(1,1,1,3,3,3-hexafluoro-2-propoxy)-arenes in the presence of a base. OVAT optimized a) 7.2 mA/cm², 2.0 F, 300 rpm (stirrer velocity), 0.25 M (concentration caffeine), 0.1 M concentration NEt₃, yield 8-(1,1,1,3,3,3-hexafluoro-2-propoxy)caffeine: 33%; DoE optimized a) 22.1 mA/cm², 2.61 F, 700 rpm (stirrer velocity), 0.2 M (concentration caffeine), 0.2 M concentration NEt₃, yield 8-(1,1,1,3,3,3-hexafluoro-2-propoxy)caffeine: 42%.

The optimization to increase the yield for the electrosynthesis of the HFIP caffeyl ether was conducted via a Design of Experiment approach. Optimal reaction conditions were

successfully applied to a variety of aryl substrates to extend the scope to non-purine derivatives. Further, the HFIP caffeine ether was successfully used as the electrophile in transition metal-catalyzed and transition metal-free reactions with excellent yields up to 94% (Scheme 24).



Scheme 24. Derivatization of HFIP caffeine ether with various nucleophiles.

[a] NiCl₂(PPh₃)₂ (10 mol%), PPh₃ (20 mol%), KCN (4 eq.), Zn (1 eq.) in DMF 115 °C, 4 h; [b] Pd(OAc)₂ (5 mol%), XantPhos (10 mol%), KCN (1.5 eq.), DMF, 85 °C, 14 h; [c] Pd(OAc)₂ (5 mol%), XantPhos (10 mol%), amine (2.0–3.0 eq.), DMA, 100 °C, 3–14 h; [d] amine (3.0 eq.), DMA, 100 °C, 14 h; [e] Cs₂CO₃ (3.0 eq.), phenol/thiophenol (2.0 eq.), DMF, r.t. [f] NaOH (15 eq.) in propan-1-ol/water 1/3, 60 °C, 2 h; [g] K₂CO₃ (3.0 eq.), propan-1-thiol (2.0 eq.), in DMF, 65 °C, 2 h;

The cyclic voltammogram (CV) of caffeine in HFIP/NEt₃ with a scan rate of 100 mV/s shows only one peak at 1.80 V (vs. Ag/AgCl in saturated LiCl in EtOH, orange). This indicates that the reaction follows an ECEC pathway, where the oxidation potential of the second oxidation is lower than that of the first oxidation. The oxidations are coupled with an irreversible fast chemical reaction, as indicated by the lack of a cathodic peak at scan rates up to 500 mV/s. The cyclic voltammogram of caffeine in HFIP/MTBS at 100 mV/s shows two distinct anodic peaks at anodic peak potentials of 1.88 V (vs. Ag/AgCl in saturated LiCl in EtOH) for the first oxidation and 2.41 V (vs. Ag/AgCl in saturated LiCl in EtOH) for a second oxidation step. The oxidations are also coupled with an irreversible fast chemical reaction. The second peak in the cyclic voltammogram of caffeine in HFIP/MTBS is evidence for an oxidation pathway that differs from the ECEC mechanism of caffeine in HFIP/NEt₃. The high anodic peak potential (2.41 V vs. Ag/AgCl in saturated LiCl in EtOH) suggests that the second oxidation results in a high energy intermediate. The potential shift of the first anodic peak potential in the anodic direction (+0.08 V) suggests that the follow-up reaction is slower or hindered in HFIP/MTBS.^[105]

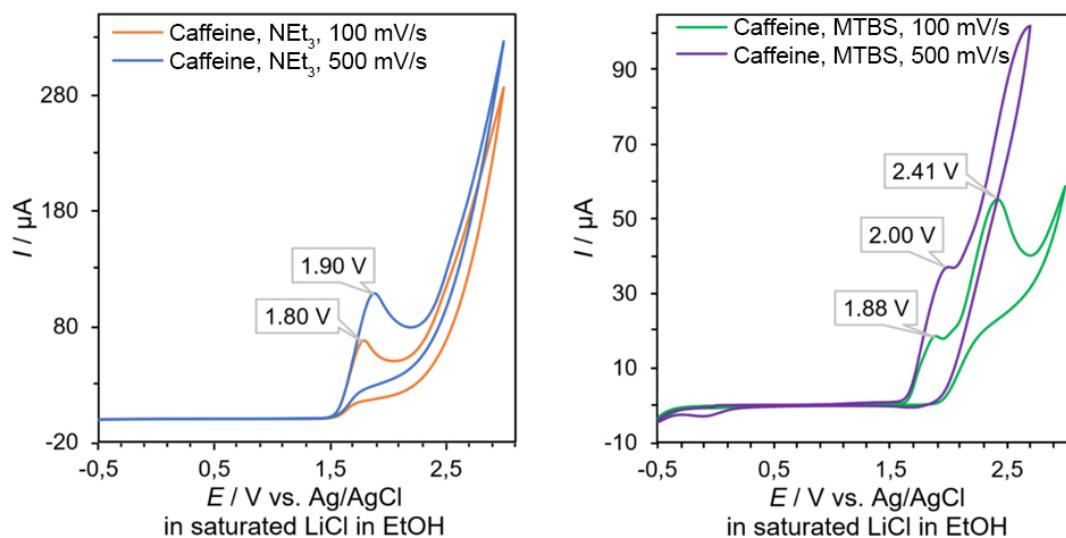
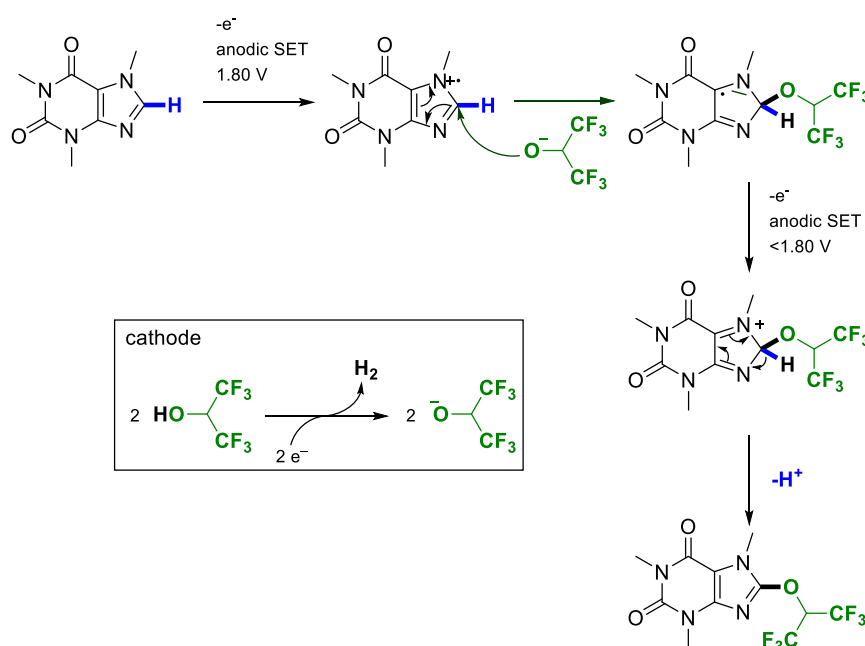


Figure 5. Left: Cyclic voltammogram of a 5 mM solution of caffeine in a 0.1 M solution of NEt_3 in HFIP. With a BDD anode and a glassy carbon cathode at scan rates of 100 mV/s (orange) and 500 mV/s (blue). Right: Cyclic voltammogram of a 5 mM solution of caffeine in a 0.1 M solution of tributylmethylammonium sulfate (MTBS) in HFIP. With a BDD anode and a glassy carbon cathode at scan rates of 100 mV/s (green) and 500 mV/s (purple).

NEt_3 deprotonates HFIP and generates HFIP anions, which either deprotonate or undergo nucleophilic attack of cationic intermediates with second-order rate laws. Therefore, a study of the potential shift which is dependent on the concentration of HFIP anions is not applicable to discern the mechanism of the follow-up reaction, as HFIP anions are involved in both possible ECEC mechanisms.



Scheme 25. Proposed ECEC mechanism of the electrolysis of caffeine in HFIP/TEA.

Contribution statement:

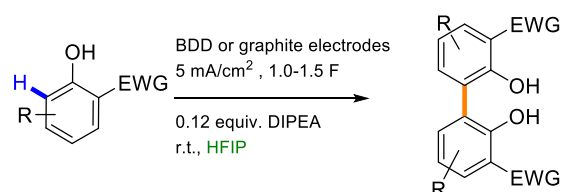
I determined that the application with purines and further derivatizations was viable. Jonas Rein performed a linear optimization approach and looked into Ni-catalyzed cross-couplings using allylic HFIP ethers as leaving groups and investigated the mechanism as part of his B.Sc. thesis under my supervision. Maurice Dörr undertook the DoE approach and found a more robust and reliable method. This work was carried out under supervision of Prof. Dr. S. R. Waldvogel at the Johannes Gutenberg University in Mainz.

3.5 Dehydrogenative Anodic C–C Coupling of Phenols Bearing Electron-withdrawing Groups

J. L. Röckl, D. Schollmeyer, R. Franke, S. R. Waldvogel, *Dehydrogenative C,C – coupling of Phenols bearing Electronwithdrawing Groups*, *Angew. Chem. Int. Ed.* **2020**, 59, 315–319 (Hot Paper);

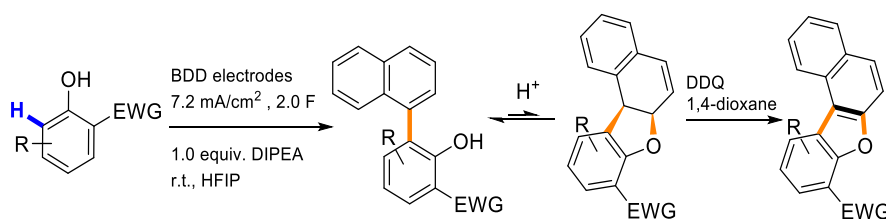
J. L. Röckl, D. Schollmeyer, R. Franke, S. R. Waldvogel, *Dehydrierende anodische C,C – Kupplung von Phenolen mit elektronenziehenden Substituenten*, *Angew. Chem.* **2020**, 132, 323–327.

During the work on the C–H functionalization with alcohols, it was found that specific substrates undergo a different reaction pathway. Interestingly, phenols carrying electron-withdrawing groups (EWGs) in position 2 undergo dehydrodimerization. This posed the first selective electrochemical coupling of phenols bearing EWGs.^[106] After optimization, the reaction was selective and yielded 2,2'-biphenols in up to 64% yield (Scheme 26).



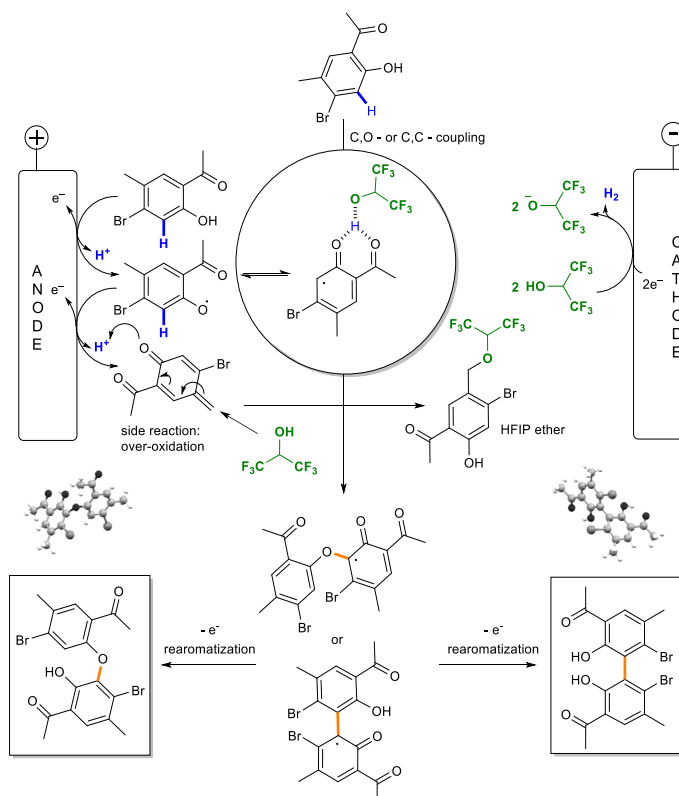
Scheme 26. First selective homo-coupling of phenols bearing electron-withdrawing groups.

These types of structures are used for the synthesis of several binuclear boron^[107] and aluminum complexes,^[108] for application in optoelectronic devices and as catalysts in polymerization reactions^[109,110] and are often produced via sophisticated multi-step syntheses.^[111] Cross-coupling reactions were also investigated. Co-electrolysis with naphthalene unexpectedly yielded polycyclic structures, which were analyzed by X-ray analysis, NMR spectroscopy and ESI/MS. The aromatic system was broken by the nucleophilic attack of the phenolic oxygen, which is quite unusual. It was also found that the equilibrium is influenced by the pH value, which poses a new type of tautomerism. Further oxidation with DDQ yielded dibenzofurans. Therefore, it was possible to choose between the simple cross-coupled or polycyclic product (Scheme 27).



Scheme 27. Cross-coupling of phenols bearing electron-withdrawing groups with naphthalene – discovery of a new form of tautomerism.

To further investigate the mechanism of the reaction, cyclic voltammetry studies were conducted. It was found that the oxidation potential was significantly lower when DIPEA was added. All major side products were isolated, including the *O,C*- and the *C,C*-coupled product. These were crystallized and their structures were determined by X-ray analysis (Scheme 28). The corresponding HFIP ether was also observed by GC-MS and NMR spectroscopy as in previous work.^[96] It is therefore proposed that initial anodic oxidation and subsequent loss of a proton gives the oxygen-centered radical, which can also be written as a carbon-centered radical. This radical can either be attacked by the nucleophilic oxygen or carbon of another molecule of phenol, leading to, after another oxidation step and subsequent re-aromatization, the undesired *O,C*-coupled side product or to the desired *C,C*-coupled product. At high current densities, further oxidation of the radical gives more likely a quinone methide intermediate, which is then trapped by HFIP in a 1,6-addition, giving a HFIP ether. This also explains why at lower current density, as well as a higher concentration of phenol, no HFIP ether can be detected and higher yields of desired 2,2'-biphenol are achieved. At high concentration, the radical is more likely to be trapped immediately by another molecule of starting material or another radical instead of being further oxidized at the anode or undergoing other side reactions.



Scheme 28. Proposed mechanism for the formation of 2,2'-biphenols carrying EWGs.

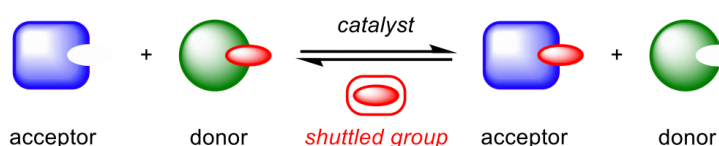
Contribution statement:

I discovered the reactivity and carried out all the work related to this publication. The crystal structure analysis was conducted by Dr. Dieter Schollmeyer. This work was carried out under supervision of Prof. Dr. S. R. Waldvogel at the Johannes Gutenberg University in Mainz.

3.6 Electrochemistry-Enabled Isodesmic Shuttle Reaction

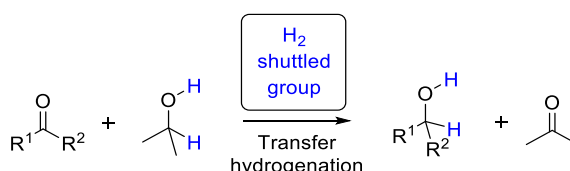
J. L. Röckl, X. Dong, S. R. Waldvogel, B. Morandi, *Electrochemistry enabled isodesmic shuttle reaction*, *Nature*, 2020, in preparation.

During my PhD studies, I had the opportunity to undertake a research stay in Bill Morandi's group at ETH Zurich. The group focuses mainly on isodesmic shuttle reactions, in which the aim is to transfer functional groups from one molecule to another (Scheme 29). Unusually, these reactions are inherently reversible processes, which is the key to their synthetic utility. The shuttled group (also known as the payload) is transferred from a donor molecule to an acceptor molecule.^[112,113]



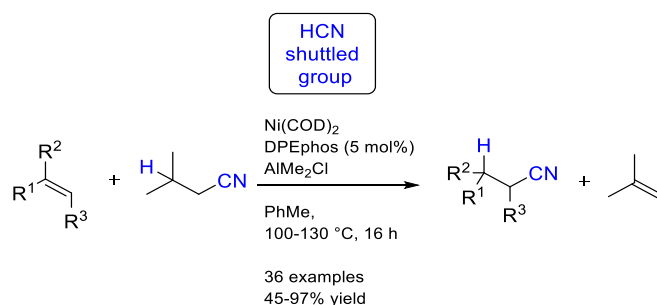
Scheme 29. Shuttle concept.^[113]

While the total number and type of bonds remain unchanged throughout the reaction, the number of bonds in each reaction partner does change. This can be understood by looking at a prime example of shuttle catalysis, transfer hydrogenation (Scheme 30).^[114] Here, hydrogen is transferred between an alcohol donor and a ketone acceptor.

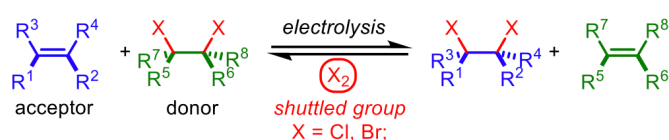


Scheme 30. Transfer hydrogenation as a simple example for a shuttle reaction.

A more sophisticated application of shuttle catalysis is the use of aliphatic nitriles as HCN donors, which are significantly less toxic alternatives to other cyanide sources (Scheme 31). In the work of the Morandi group, isovaleronitrile was employed as an efficient donor, using a Ni catalyst with an Al Lewis acid. It was possible to perform hydrocyanation on a broad range of alkenes using this approach.^[115] The formation of volatile isobutene as a by-product acts as a driving force for the transformation. These examples can be considered as mono-functionalization, because there is always hydrogen involved. We were curious to know if di-functionalization is also possible in e.g. chlorine, bromine or halogen-X transfer reactions, to avoid the use of molecular halogens and use inexpensive, less corrosive liquid donor molecules.

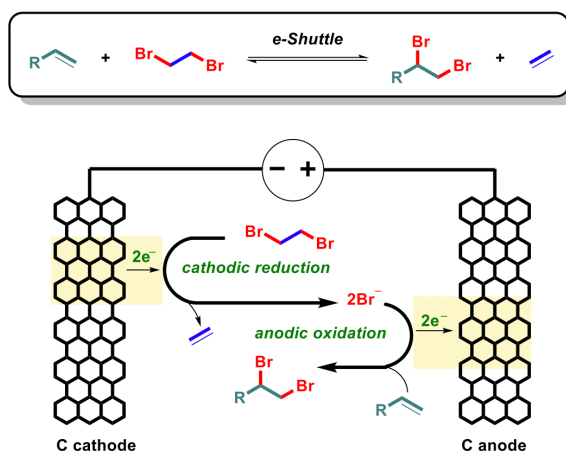
Scheme 31. Catalytic HCN-shuttle by Morandi *et al.*

After more than 3000 experiments towards a metal-catalyzed approach were carried out by Xichang Dong (postdoctoral researcher in the Morandi group), it was considered that electrochemistry could be a promising alternative (Scheme 32).



Scheme 32. Electrochemistry enabled halogen shuttle reaction.

Electrochemistry represents a perfect match for these types of reactions, because the reaction is redox neutral and can therefore be performed as a paired electrolysis. At the cathode, a reduction of the dihalo-donor is performed, two halides and the respective alkene are extruded.

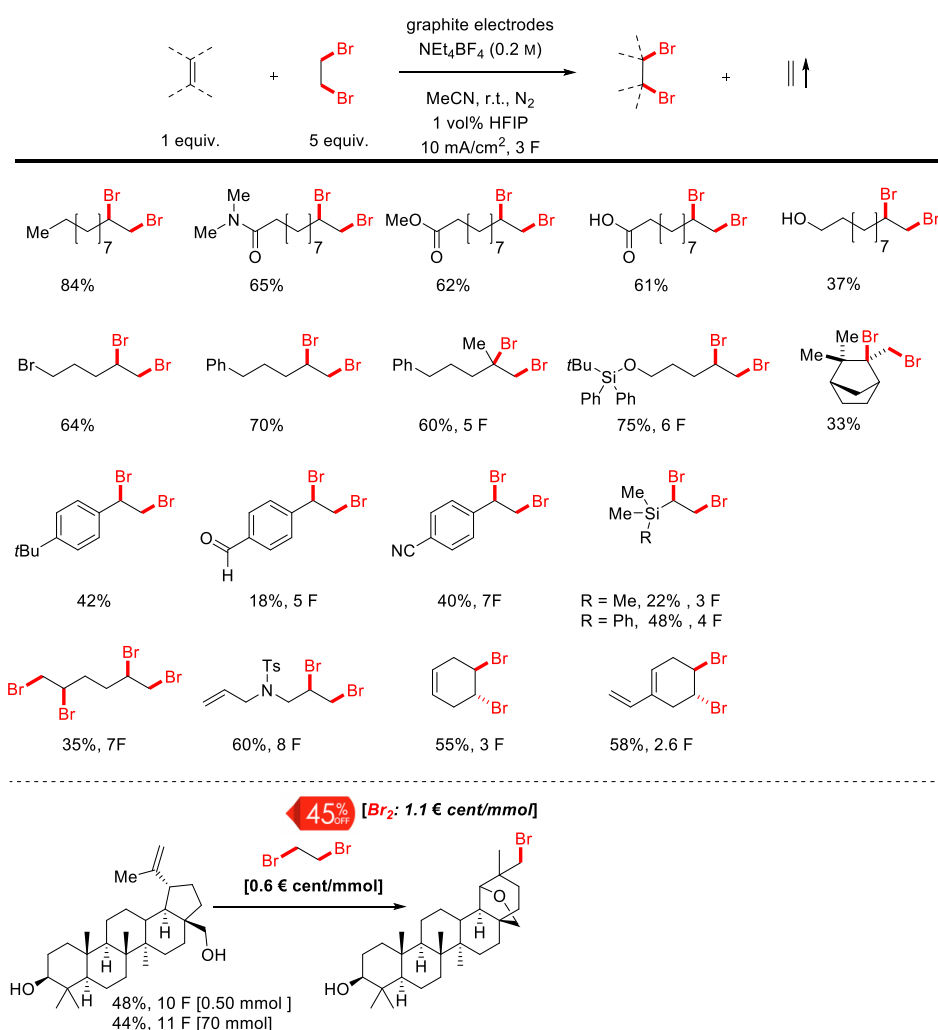


Electrochemistry enabled Shuttle Reaction: Redox-neutral

Scheme 33. Proposed mechanism for the Br₂-shuttle reaction.

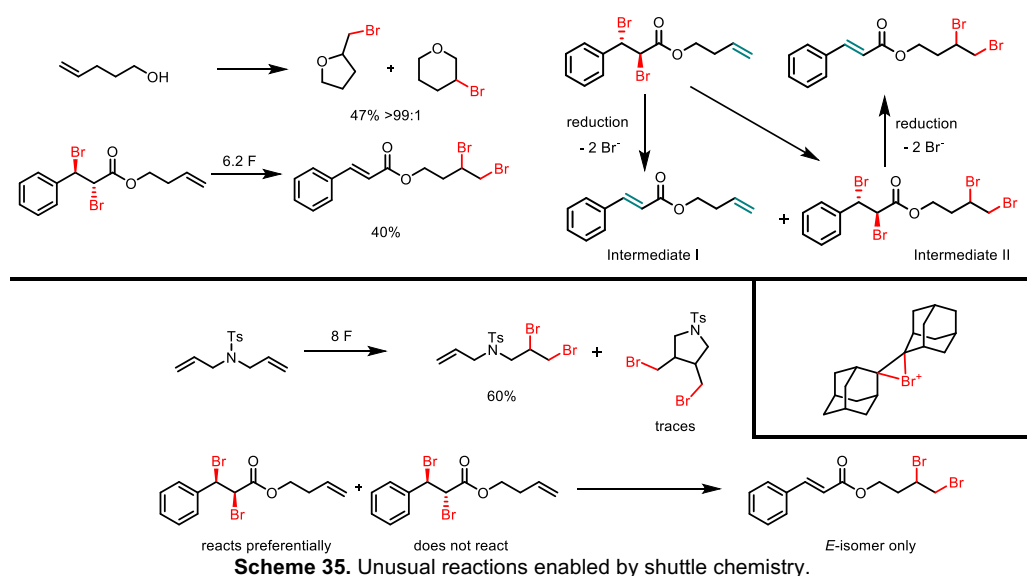
The halides can then be oxidized at the anode to give Br⁺-ions or Cl-radicals, which can then react with another alkene to refurbish the two C–X bonds (Scheme 33). In the case of Br₂-shuttle reactions, simple 1,2-dibromoethane could be used as a donor to extrude ethylene as a driving force, which was shown by headspace GC/MS.

It was possible to apply these conditions to a broad variety of substrates and in late-stage functionalization (Scheme 34).

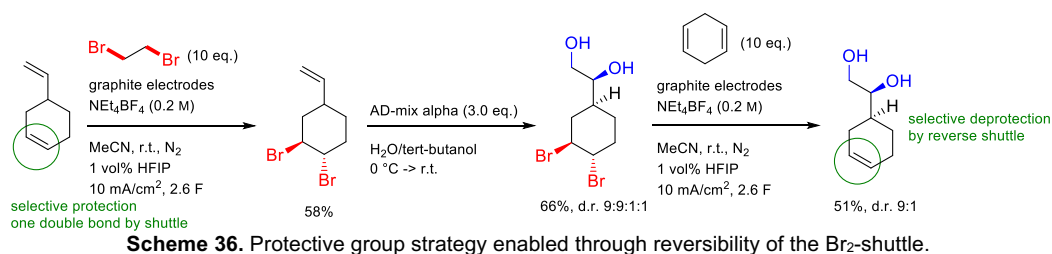


Scheme 34. Scope of the Br₂-shuttle reaction using 1,2-dibromoethane as a donor.

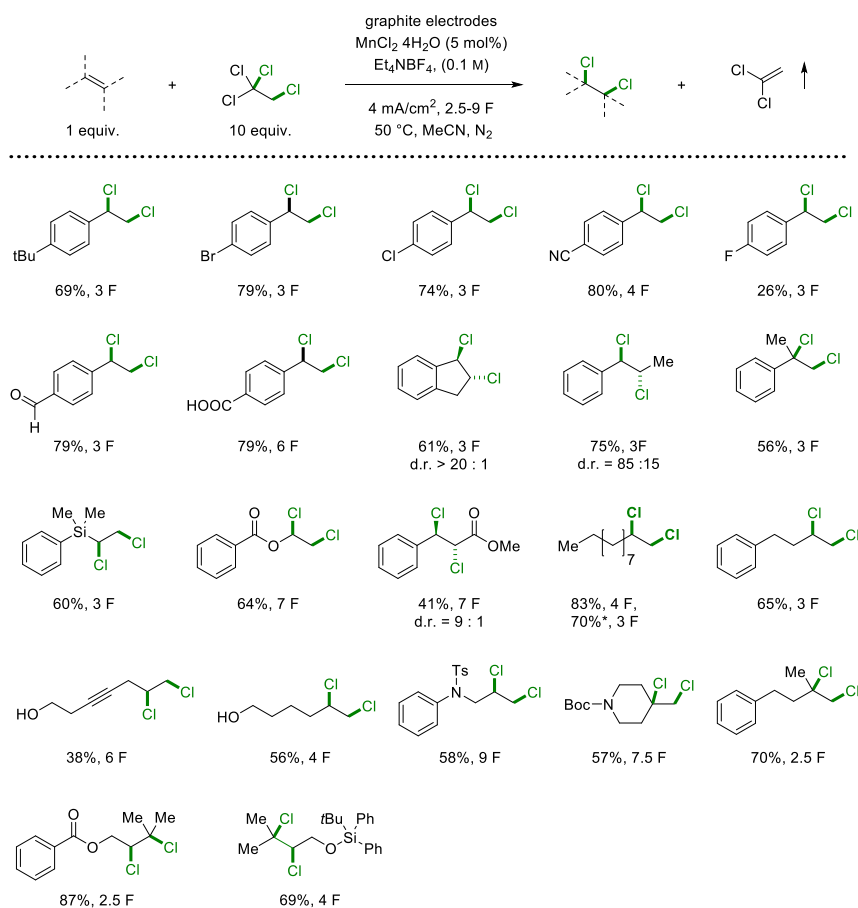
Additionally, unusual reactions were enabled, including a formal intramolecular shuttle and intramolecular ring-closing domino reactions (Scheme 35). The mechanistic proposal was also supported by radical clock experiments, which reveal an ionic mechanism or only short-lived radical intermediates. It is proposed that extrusion of the bromide takes place in a stepwise manner, rather than concerted, because the *threo*-isomer reacts preferentially to give the *E*-alkene. We were also able to trap the bromonium ion using a sterically hindered alkene.



Another interesting application of the shuttle reaction is its use in a protect/deprotect strategy (Scheme 36). Due to the low concentration of reactive agent in the electrochemical reaction, it was possible to achieve regioselective bromination of 4-vinylcyclohex-1-ene. Subsequent epoxidation or dihydroxylation and reverse reaction with an excess of 1,4-cyclohexadiene as acceptor delivered the desired epoxide or dihydroxy compound in the desired position only.

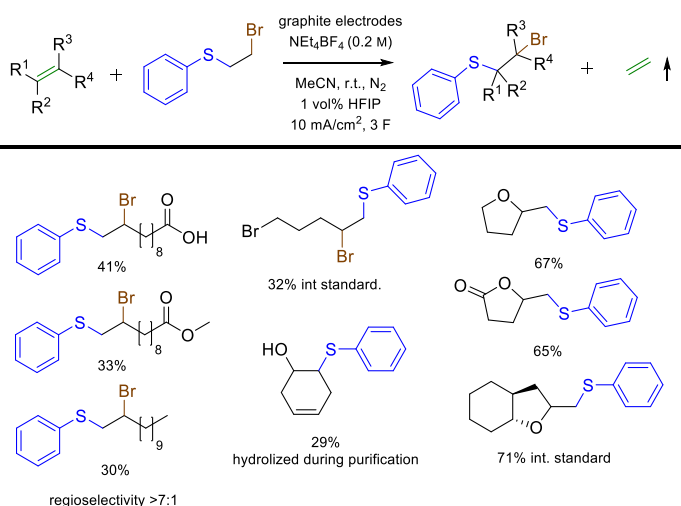


This approach was also applied to the shuttle of Cl₂, which is Mn-catalyzed and works well with a large variety of substrates when 1,1,1,2-tetrachloroethane is used as a donor. Activated systems, as well as acid sensitive substrates, are converted into the respective vicinal dihalides (Scheme 37). The mechanism of this reaction is thought to proceed via a Mn^{II}/Mn^{III} redox couple of the chloride-bound complex, as described in work of Lin *et al.*^[116]



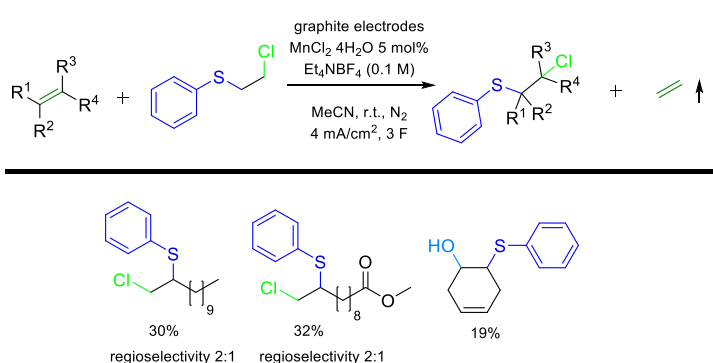
Scheme 37. Scope of the Cl₂-shuttle reactions using 1,1,1,2-tetrachloroethane as a donor.

We also looked into a variety of other di-functionalization reactions, such as SPhBr- and SPhCl-shuttle reactions (Schemes 38 and 39). On applying similar conditions to those of the halogen shuttle, similar reactivity was observed. The reactions proceed particularly well if intramolecular follow-up reactions, such as cyclization, are possible (up to 71% yield).



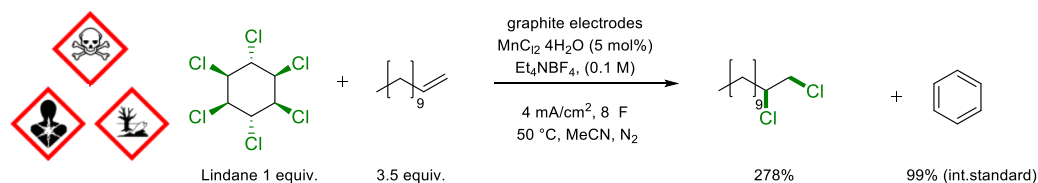
Scheme 38. Scope of the SPhBr-shuttle reaction.

A crucial aspect of these reactions is the regioselectivity: for SPhBr-shuttle reactions the secondary halide is formed primarily, whereas in the SPhCl-case the primary halide is observed. This is probably due to the reversibility and the reaction rate of the sulfonium ion formation. For SPhBr this is a highly reversible process, which leads to the formation of the thermodynamically more stable product, the secondary bromide. In the second case, when chloride is involved, the sulfonium ion formation is disfavored and this leads to the formation of the kinetic product as the major product, which is the primary chloride.



Scheme 39. Scope of the SPhCl-shuttle reaction.

A further fascinating feature of this methodology is the use of polychlorinated waste as a Cl₂ – donor. We were able to selectively degrade lindane, a persistent organic pollutant, to benzene and use the 3 equivalents of Cl₂ to selectively chlorinate alkenes (Scheme 40). The generation of the by-product benzene was quantified by GC using an internal standard.



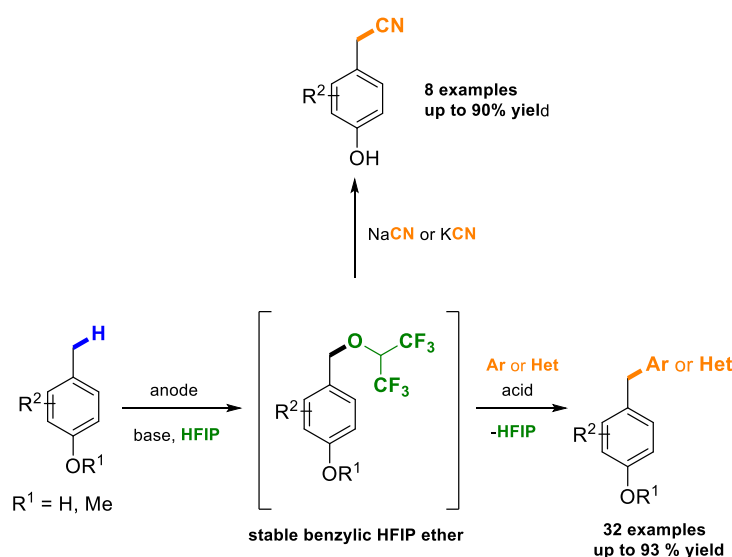
Scheme 40. Degradation of lindane to benzene

Contribution statement:

Xichang Dong (postdoctoral researcher, Morandi group), worked on a transition-metal based solution for the existing concept behind this transformation. Both Xichang and I contributed equally to the ideation and optimization of the methodology.

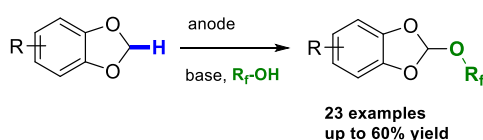
4 Conclusion

This thesis covers studies towards various C–H functionalization reactions of different types of C–H bonds. Benzylic C–H functionalization of methyl groups with HFIP and subsequent cross-coupling was successfully demonstrated (Scheme 41). Valuable insights relating to the leaving group abilities and the stability of HFIP ethers were gained by treating these with a range of nucleophiles, such as cyanides.



Scheme 41. Selective anodic benzylic C-H functionalization and utility of HFIP ethers.

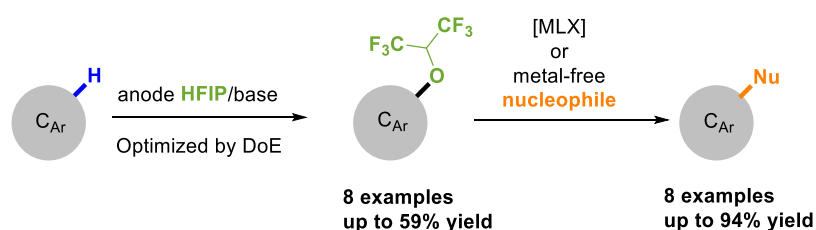
The unique properties of 1,3-benzodioxoles have been used to synthesize orthoesters electrochemically (Scheme 42). A closer look at the properties of these structures revealed their extraordinary stability towards acids and bases and their high lipophilicity.



Scheme 42. Selective anodic C-H functionalization of 1,3-benzodioxoles in position 2.

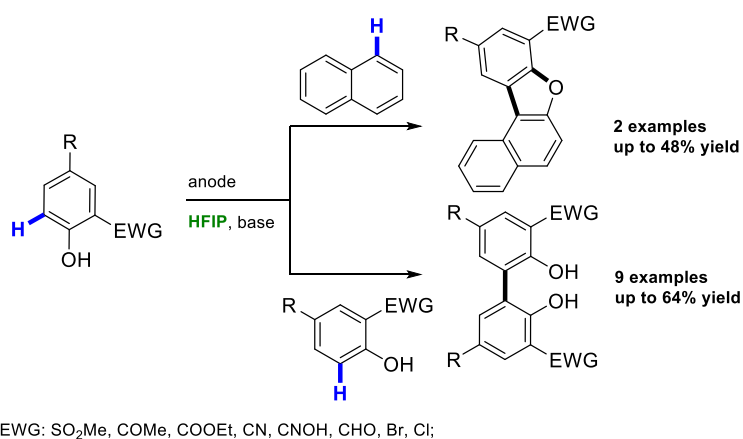
It was attempted to apply the approach to sp^2 -hybridized atoms, such as purines and other aryls. Successful introduction of the HFIP moiety with further functionalization of purines was achieved (Scheme 43). In this context, we encountered a major challenge in the electrochemical synthesis of oxygen substituted arenes, namely over-oxidation. This is due to the mesomeric electron-releasing effect of oxygen substituents that leads

to a lowered oxidation potential compared to the starting material. However, applying a DoE approach we were able to achieve higher yields up to 59%.



Scheme 43. Selective anodic C-H functionalization of arenes and subsequent use in coupling reactions.

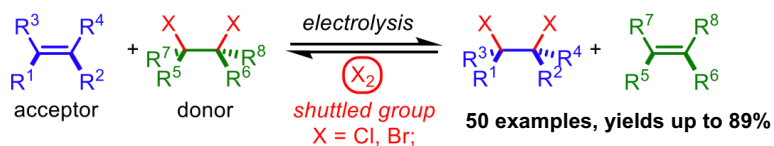
During this work, it was discovered that certain substrates undergo different, interesting reaction pathways, such as phenols bearing EWGs (Scheme 44). These react in dehydrogenative homo-coupling reactions, in the first successful electrochemical synthesis of such electron-deficient phenols to the best of our knowledge. Studies towards cross-coupling of such phenols with naphthalene revealed a novel type of tautomerism, where the aromaticity of the naphthalene moiety is broken to form a polycyclic dihydrodibenzofuran system. This was exploited to synthesize heterocycles by further oxidation towards dibenzofurans.



Scheme 44. Selective anodic homo- and cross-coupling of phenols bearing EWG.

During my work on electrochemically enabled shuttle reactions, the isodesmic difunctionalization of alkenes was investigated (Scheme 45). This was achieved by using a dihalo donor, such as 1,2-dichloroethane or 1,2-dibromoethane, which was reduced at the cathode and the resulting halogenides oxidized to react with the alkene. This formed a new vicinal dihalide with release of ethylene, indicating that novel intramolecular bromine or chlorine shuttle reactions can be achieved. This concept was

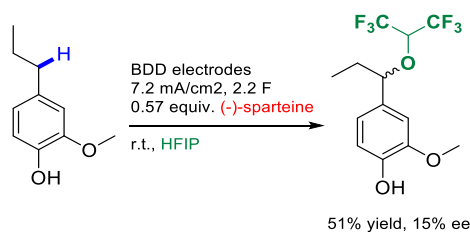
expanded to Br(Cl)SPh shuttle reactions, which were thus far unprecedented. The reversibility was utilized in various synthetic applications, such as intramolecular bromine shuttle reactions or the protection and deprotection of double bonds and the degradation of persistent organic pollutants like lindane.



Scheme 45. Electrochemically enabled halogen shuttle.

5 Outlook

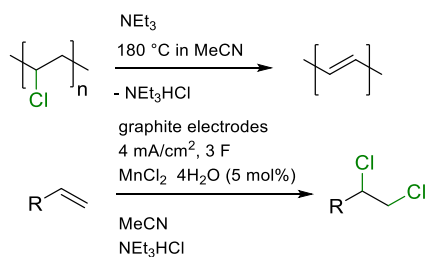
A promising extension of the chemistry shown would be the stereoselective formation of HFIP ethers. In this case, three different approaches would be possible: synthesis in chiral solvents, at chiral electrodes or using a chiral supporting electrolyte. The synthesis using a chiral supporting electrolyte seems very promising, especially because induced formation of helices in HFIP could be possible e.g. by a chiral base. However, electro-organic transformations using chiral supporting electrolytes are under-explored and to date only one report on asymmetric electrochemical reactions in a chiral solvent has been published, by Seebach and Oei in the 1970s.^[117] The first example using a chiral supporting electrolyte by Horner in 1968 was an electroreduction of acetophenone using ephedrine hydrochloride in 4.6% ee.^[118] A similar approach has also been attempted for the formation of HFIP ethers. (-)-Sparteine, which acts as a supporting electrolyte in combination with HFIP, showed an enantiomeric excess of 15% in the reaction with 2-methoxy-4-propylphenol (Scheme 45). However, several other chiral bases and additives have failed to induce chirality. Also, racemization after aqueous work up and purification was observed. Mechanistic studies into the inducement are very challenging and still ongoing. Insights from these studies could help to further improve the enantiomeric excess. Additionally, subsequent stereospecific reactions could help to trap chirality into a more stable molecule.



Scheme 45. Asymmetric synthesis of HFIP ethers using sparteine as a chiral additive.

A major problem of our time is the pollution of the oceans, especially by poorly or non-degradable plastics. One approach to this issue could be to develop strategies to facilitate upcycling or recycling of commodity polymers. One such strategy is to recycle chemically-bound chlorine from polyvinyl chloride (PVC) and transfer it to other molecules to create valuable fine chemicals via our developed shuttle catalysis approach. The most significant potential barrier to success of this approach is the poor solubility of PVC. In initial trials, only DMF and THF, which might have been viable solvents in the e-shuttle reaction, showed dwelling of the polymer. However, these

solvents shut down the reaction even with small molecules as donors, which are similar to the subunit of PVC (e.g. 2-chlorobutane). Only acetonitrile shows sufficient reactivity using these donors. There are many reports of thermal dehydrochlorination of PVC;^[119] if this would be used as a pretreatment to set chloride free, subsequent electrochemical chlorination could be achieved. Indeed, a thermal pretreatment of PVC (2.5 equiv. of Cl₂) in a closed vessel containing acetonitrile and small amounts of triethylamine (2.5 equiv.) as a base enabled selective subsequent electrochemical chlorination of dodecene in a selective manner in 25% yield at 26% conversion thus far and increased upon first screenings up to 50% (Scheme 46). This serves as proof-of-principle for further studies in the future.



Scheme 46. Dehydrochlorination of PVC and subsequent Mn-catalyzed chlorination of alkenes.

6 References

- [1] P. Anastas, N. Eghbali, *Chem. Soc. Rev.* **2010**, 39, 301–312.
- [2] S. R. Waldvogel, B. Janza, *Angew. Chem. Int. Ed.* **2014**, 53, 7122–7123.
- [3] M. Yan, Y. Kawamata, P. S. Baran, *Chem. Rev.* **2017**, 117, 13230–13319.
- [4] B. A. Frontana-Uribe, R. D. Little, J. G. Ibanez, A. Palma, R. Vasquez-Medrano, *Green Chem.* **2010**, 12, 2099.
- [5] A. Wiebe, B. Riehl, S. Lips, R. Franke, S. R. Waldvogel, *Sci. Adv.* **2017**, 3, eaao3920.
- [6] L. Schulz, J.-Å. Husmann, S. R. Waldvogel, *Electrochim. Acta* **2020**, 337, 135786.
- [7] A. Shatskiy, H. Lundberg, M. D. Kärkäs, *ChemElectroChem* **2019**, 6, 4067–4092.
- [8] A. Wiebe, T. Gieshoff, S. Möhle, E. Rodrigo, M. Zirbes, S. R. Waldvogel, *Angew. Chem. Int. Ed.* **2018**, 57, 5594–5619.
- [9] E. Brillas, C. A. Martínez-Huitle, *Synthetic diamond films. Preparation, electrochemistry, characterization, and applications*, Wiley, Hoboken, N.J., **2011**.
- [10] T. A. Ivandini, Y. Einaga, *Chem. Commun.* **2017**, 53, 1338–1347.
- [11] T. A. Ivandini, R. Sato, Y. Makide, A. Fujishima, Y. Einaga, *Diamond Relat. Mater.* **2004**, 13, 2003–2008.
- [12] S. R. Waldvogel, S. Mentizi, A. Kirste, *Top. Curr. Chem.* **2012**, 320, 1–31.
- [13] S. J. Yoo, L.-J. Li, C.-C. Zeng, R. D. Little, *Angew. Chem. Int. Ed.* **2015**, 54, 3744–3747.
- [14] S. B. Beil, T. Müller, S. B. Sillart, P. Franzmann, A. Bomm, M. Holtkamp, U. Karst, W. Schade, S. R. Waldvogel, *Angew. Chem. Int. Ed.* **2018**, 57, 2450–2454.
- [15] M. Chiku in *Encyclopedia of Applied Electrochemistry* (Eds.: G. Kreysa, K.-i. Ota, R. F. Savinell), Springer New York, New York, NY, **2014**, 1366–1368.
- [16] F. I. Danilov, A. B. Velichenko, L. N. Nishcheryakova, *Electrochim. Acta* **1994**, 39, 1603–1605.
- [17] J.-I. Yoshida, S. Suga, *Chem. Eur. J.* **2002**, 8, 2650.
- [18] S. Möhle, M. Zirbes, E. Rodrigo, T. Gieshoff, A. Wiebe, S. R. Waldvogel, *Angew. Chem. Int. Ed.* **2018**, 57, 6018–6041.
- [19] S. R. Waldvogel, S. Lips, M. Selt, B. Riehl, C. J. Kampf, *Chem. Rev.* **2018**, 118, 6706–6765.
- [20] ChemViews, *ChemViews* **2017**.
- [21] C. Gütz, B. Klöckner, S. R. Waldvogel, *Org. Process Res. Dev.* **2016**, 20, 26–32.
- [22] C. Gütz, A. Stenglein, S. R. Waldvogel, *Org. Process Res. Dev.* **2017**, 21, 771–778.
- [23] B. Gleede, M. Selt, C. Gütz, A. Stenglein, S. R. Waldvogel, *Org. Process Res. Dev.* **2019**.
- [24] B. A. Arndtsen, R. G. Bergman, T. A. Mobley, T. H. Peterson, *Acc. Chem. Res.* **1995**, 28, 154–162.
- [25] K. I. Goldberg, A. S. Goldman (Eds.) *ACS Symposium Series*, American Chemical Society, Washington, DC, **2004**.
- [26] R. A. Periana, G. Bhalla, W. J. Tenn, K. J.H. Young, X. Y. Liu, O. Mironov, C. J. Jones, V. R. Ziatdinov, *J. Mol. Catal. A: Chem.* **2004**, 220, 7–25.
- [27] A. E. Shilov, G. B. Shul'pin, *Chem. Rev.* **1997**, 97, 2879–2932.

-
- [28] *Ullmann's Encyclopedia of Industrial Chemistry*, Wiley-VCH Verlag GmbH & Co. KGaA, Weinheim, Germany, **2000**.
- [29] W. P. Yant, H. H. Schrenk, R. R. Sayers, *Ind. Eng. Chem.* **1931**, *23*, 551–555.
- [30] B. Höhle, T. Grube, P. Biedermann, H. Bielawa, G. Erdmann, L. Schlecht, G. Isenberg, R. Edinger, *Methanol als Energieträger*, Forschungszentrum Jülich GmbH, Jülich, **2003**.
- [31] N. F. Gol'dshleger, *Zh. Fiz. Khim.* **1969**, 2174–2175.
- [32] R. G. Bergman, *Nature* **2007**, *446*, 391–393.
- [33] M. D. Kärkäs, *Chem. Soc. Rev.* **2018**, *47*, 5786–5865.
- [34] D. R. Abernethy, A. J. Destefano, T. L. Cecil, K. Zaidi, R. L. Williams, *Pharm. Res.* **2010**, *27*, 750–755.
- [35] C. Ma, P. Fang, T.-S. Mei, *ACS Catal.* **2018**, *8*, 7179–7189.
- [36] D. Gallego, E. A. Baquero, *Open Chem.* **2018**, *16*, 1001–1058.
- [37] X. Qi, Y. Li, R. Bai, Y. Lan, *Acc. Chem. Res.* **2017**, *50*, 2799–2808.
- [38] T. Shono, Y. Matsumura, K. Tsubata, *J. Am. Chem. Soc.* **1981**, *103*, 1172–1176.
- [39] J. L. Röckl, D. Pollok, R. Franke, S. R. Waldvogel, *Acc. Chem. Res.* **2020**, *53*, 45–61.
- [40] T. Shono, H. Hamaguchi, Y. Matsumura, *J. Am. Chem. Soc.* **1975**, *97*, 4264–4268.
- [41] A. Börner, R. Franke, *Hydroformylation. Fundamentals, processes, and applications in organic synthesis*, Wiley-VCH Verlag GmbH & Co, Weinheim, **2016**.
- [42] I. M. Malkowsky, U. Griesbach, H. Pütter, S. R. Waldvogel, *Eur. J. Org. Chem.* **2006**, *2006*, 4569–4572.
- [43] A. Kirste, G. Schnakenburg, F. Stecker, A. Fischer, S. R. Waldvogel, *Angew. Chem. Int. Ed.* **2010**, *49*, 971–975.
- [44] L. Schulz, M. Enders, B. Elsler, D. Schollmeyer, K. M. Dyballa, R. Franke, S. R. Waldvogel, *Angew. Chem. Int. Ed.* **2017**, *56*, 4877–4881.
- [45] S. Lips, A. Wiebe, B. Elsler, D. Schollmeyer, K. M. Dyballa, R. Franke, S. R. Waldvogel, *Angew. Chem. Int. Ed.* **2016**, *55*, 10872–10876.
- [46] S. Lips, B. A. Frontana-Urbe, M. Dörr, D. Schollmeyer, R. Franke, S. R. Waldvogel, *Chem. Eur. J.* **2018**, *24*, 6057–6061.
- [47] S. Lips, D. Schollmeyer, R. Franke, S. R. Waldvogel, *Angew. Chem. Int. Ed.* **2018**, *57*, 13325–13329.
- [48] A. Wiebe, S. Lips, D. Schollmeyer, R. Franke, S. R. Waldvogel, *Angew. Chem. Int. Ed.* **2017**, *56*, 14727–14731.
- [49] Y. Kawamata, M. Yan, Z. Liu, D.-H. Bao, J. Chen, J. T. Starr, P. S. Baran, *J. Am. Chem. Soc.* **2017**, *139*, 7448–7451.
- [50] J. A. Marko, A. Durgham, S. L. Bretz, W. Liu, *Chem. Commun.* **2019**, *55*, 937–940.
- [51] L. Meng, J. Su, Z. Zha, L. Zhang, Z. Zhang, Z. Wang, *Chem. Eur. J.* **2013**, *19*, 5542–5545.
- [52] R. Hayashi, A. Shimizu, J.-I. Yoshida, *J. Am. Chem. Soc.* **2016**, *138*, 8400–8403.
- [53] G. E. Hawkes, J. E. Hawkes, F. C.M. Comninos, V. L. Pardini, H. Viertler, *Tetrahedron Lett.* **1992**, *33*, 8133–8136.
- [54] M. G. Dolson, J. S. Swenton, *J. Am. Chem. Soc.* **1981**, *103*, 2361–2371.
- [55] L. Ebersson, K. Nyberg, J. Simonet, R. B. Jensen, O. Dahl, O. Buchardt, G. Schroll, *Acta Chem. Scand.* **1975**, *29b*, 168–170.

References

- [56] K. Fujimoto, Y. Tokuda, H. Maekawa, Y. Matsubara, T. Mizuno, I. Nishiguchi, *Tetrahedron* **1996**, *52*, 3889–3896.
- [57] K. Nyberg, B. Samuelsson, T. Motzfeldt, U. Ragnarsson, S. E. Rasmussen, E. Sunde, N. A. Sørensen, *Acta Chem. Scand.* **1970**, *24*, 473–481.
- [58] L. Ebersson, E. Oberrauch, K. Schaumburg, C. R. Enzell, *Acta Chem. Scand.* **1981**, *35b*, 193–196.
- [59] N. Sauermann, T. H. Meyer, C. Tian, L. Ackermann, *J. Am. Chem. Soc.* **2017**, *139*, 18452–18455.
- [60] A. Shrestha, M. Lee, A. L. Dunn, M. S. Sanford, *Org. Lett.* **2018**, *20*, 204–207.
- [61] Y.-Q. Li, Q.-L. Yang, P. Fang, T.-S. Mei, D. Zhang, *Org. Lett.* **2017**, *19*, 2905–2908.
- [62] N. Miyaura, A. Suzuki, *J. Chem. Soc., Chem. Commun.* **1979**, 866.
- [63] N. Miyaura, K. Yamada, A. Suzuki, *Tetrahedron Lett.* **1979**, *20*, 3437–3440.
- [64] N. Miyaura, A. Suzuki, *Chem. Rev.* **1995**, *95*, 2457–2483.
- [65] M. Grzybowski, K. Skonieczny, H. Butenschön, D. T. Gryko, *Angew. Chem. Int. Ed.* **2013**, *52*, 9900–9930.
- [66] S. Tang, Y. Liu, A. Lei, *Chem* **2018**, *4*, 27–45.
- [67] H. Yi, G. Zhang, H. Wang, Z. Huang, J. Wang, A. K. Singh, A. Lei, *Chem. Rev.* **2017**, *117*, 9016–9085.
- [68] M. Schubert, S. R. Waldvogel, *Eur. J. Org. Chem.* **2016**, *2016*, 1921–1936.
- [69] B. T. King, J. Kroulík, C. R. Robertson, P. Rempala, C. L. Hilton, J. D. Korinek, L. M. Gortari, *J. Org. Chem.* **2007**, *72*, 2279–2288.
- [70] L. Zhai, R. Shukla, S. H. Wadumethrige, R. Rathore, *J. Org. Chem.* **2010**, *75*, 4748–4760.
- [71] I. Colomer, A. E. R. Chamberlain, M. B. Haughey, T. J. Donohoe, *Nat. Rev. Chem.* **2017**, *1*, 18.
- [72] S. K. Sinha, T. Bhattacharya, D. Maiti, *React. Chem. Eng.* **2019**, *4*, 244–253.
- [73] L. Ebersson, M. P. Hartshorn, O. Persson, *J. Chem. Soc., Perkin Trans. 2* **1995**, 1735.
- [74] A. Kirste, M. Nieger, I. M. Malkowsky, F. Stecker, A. Fischer, S. R. Waldvogel, *Chem. Eur. J.* **2009**, *15*, 2273–2277.
- [75] Y. Tamura, T. Yakura, J. Haruta, Y. Kita, *J. Org. Chem.* **1987**, *52*, 3927–3930.
- [76] M. J. Kamlet, J. L. M. Abboud, M. H. Abraham, R. W. Taft, *J. Org. Chem.* **1983**, *48*, 2877–2887.
- [77] J.-P. Bégué, D. Bonnet-Delpon, B. Crousse, *Synlett* **2004**, 18–29.
- [78] C. Reichardt, *Chem. Rev.* **1994**, *94*, 2319–2358.
- [79] R. Francke, D. Cericola, R. Kötz, D. Weingarh, S. R. Waldvogel, *Electrochimica Acta* **2012**, *62*, 372–380.
- [80] O. Hollóczki, A. Berkessel, J. Mars, M. Mezger, A. Wiebe, S. R. Waldvogel, B. Kirchner, *ACS Catal.* **2017**, *7*, 1846–1852.
- [81] J. T. Gerig, *J. Phys. Chem. B* **2014**, *118*, 1471–1480.
- [82] X.-D. An, J. Xiao, *Chem. Rec.* **2020**, *20*, 142–161.
- [83] I. Shuklov, N. Dubrovina, A. Börner, *Synthesis* **2007**, 2925–2943.
- [84] Y. Cheng, J. Zheng, C. Tian, Y. He, C. Zhang, Q. Tan, G. An, G. Li, *Asian J. Org. Chem.* **2019**, *8*, 526–531.
- [85] A. Heydari, S. Khaksar, M. Tajbakhsh, *Synthesis* **2008**, 3126–3130.
- [86] L.-R. Wen, G.-Y. Ren, R.-S. Geng, L.-B. Zhang, M. Li, *Org. Biomol. Chem.* **2020**, *18*, 225–229.
- [87] C. S. Jeffrey, K. L. Barnes, J. A. Eickhoff, C. R. Carson, *J. Am. Chem. Soc.* **2011**, *133*, 7688–7691.
- [88] A. Acharya, J. Eickhoff, C. Jeffrey, *Synthesis* **2013**, *45*, 1825–1836.

-
- [89] W. Ji, L. Yao, X. Liao, *Org. Lett.* **2016**, *18*, 628–630.
- [90] L. Yu, S.-S. Li, W. Li, S. Yu, Q. Liu, J. Xiao, *J. Org. Chem.* **2018**, *83*, 15277–15283.
- [91] B. Elsler, A. Wiebe, D. Schollmeyer, K. M. Dyballa, R. Franke, S. R. Waldvogel, *Chem. Eur. J.* **2015**, *21*, 12321–12325.
- [92] Y. Yuan, A. Lei, *Nat. Commun.* **2020**, *11*, 802.
- [93] K. Sellers, *Perchlorate. Environmental problems and solutions*, CRC/Taylor & Francis, Boca Raton, **2007**.
- [94] D. T. Chang, D. Park, J.-J. Zhu, H.-J. Fan, *Applied Sciences* **2019**, *9*, 4578.
- [95] T. Gieshoff, A. Kehl, D. Schollmeyer, K. D. Moeller, S. R. Waldvogel, *J. Am. Chem. Soc.* **2017**, *139*, 12317–12324.
- [96] Y. Imada, J. L. Röckl, A. Wiebe, T. Gieshoff, D. Schollmeyer, K. Chiba, R. Franke, S. R. Waldvogel, *Angew. Chem. Int. Ed.* **2018**, *57*, 12136–12140.
- [97] J. L. Röckl, Y. Imada, K. Chiba, R. Franke, S. R. Waldvogel, *ChemElectroChem* **2019**, *6*, 4184–4187.
- [98] M. Irsfeld, M. Spadafore, B. M. Prüß, *WebmedCentral* **2013**, *4*.
- [99] C. Lamberth, A. Jeanguenat, F. Cederbaum, A. de Mesmaeker, M. Zeller, H.-J. Kempf, R. Zeun, *Bioorg. Med. Chem.* **2008**, *16*, 1531–1545.
- [100] R. N. Brogden, P. Benfield, *Drugs* **1996**, *51*, 792–819.
- [101] J. L. Röckl, A. V. Hauck, D. Schollmeyer, S. R. Waldvogel, *ChemistryOpen* **2019**, *8*, 1167–1171.
- [102] M. Murray, *Curr. Drug Metab.* **2000**, *1*, 67–84.
- [103] E. P. Gillis, K. J. Eastman, M. D. Hill, D. J. Donnelly, N. A. Meanwell, *J. med. Chem.* **2015**, *58*, 8315–8359.
- [104] K. Dimroth, P. Heinrich, K. Schromm, *Angew. Chem. Int. Ed.* **1965**, *4*, 873.
- [105] J. Heinze, *Angew. Chem. Int. Ed.* **1984**, *23*, 831–847.
- [106] J. L. Röckl, D. Schollmeyer, R. Franke, S. R. Waldvogel, *Angew. Chem. Int. Ed.* **2020**, *59*, 315–319.
- [107] K. Dhanunjayarao, V. Mukundam, M. Ramesh, K. Venkatasubbaiah, *Eur. J. Inorg. Chem.* **2014**, *2014*, 539–545.
- [108] H.-L. Han, Y. Liu, J.-Y. Liu, K. Nomura, Y.-S. Li, *Dalton trans.* **2013**, *42*, 12346–12353.
- [109] Y. Liu, W.-M. Ren, J. Liu, X.-B. Lu, *Angew. Chem. Int. Ed.* **2013**, *52*, 11594–11598.
- [110] T. Hu, Y.-G. Li, Y.-S. Li, N.-H. Hu, *J. Mol. Catal. A: Chem.* **2006**, *253*, 155–164.
- [111] N. Tsuji, K. Nagashima, *Tetrahedron* **1969**, *25*, 3017–3031.
- [112] B. N. Bhawal, B. Morandi, *Angew. Chem. Int. Ed.* **2019**, *58*, 10074–10103.
- [113] B. N. Bhawal, B. Morandi, *Chem. Eur. J.* **2017**, *23*, 12004–12013.
- [114] D. Wang, D. Astruc, *Chem. Rev.* **2015**, *115*, 6621–6686.
- [115] X. Fang, P. Yu, B. Morandi, *Science* **2016**, *351*, 832–836.
- [116] N. Fu, G. S. Sauer, S. Lin, *J. Am. Chem. Soc.* **2017**, *139*, 15548–15553.
- [117] D. Seebach, H. A. Oei, *Angew. Chem. Int. Ed.* **1975**, *14*, 634–636.
- [118] L. Horner, D. Degner, *Tetrahedron Lett.* **1968**, *9*, 5889–5892.
- [119] J. Yu, L. Sun, C. Ma, Y. Qiao, H. Yao, *J. Waste Manage.* **2016**, *48*, 300–314.

7 Appendix

7.1 Publications

J. L. Röckl, M. Dörr, S. R. Waldvogel, *Electrosynthesis 2.0 in 1,1,1,3,3,3-Hexafluoroisopropanol / Amine mixtures*, **2020**, in preparation.

X. Dong*, **J. L. Röckl***, S. R. Waldvogel, B. Morandi, *Merging shuttle reactions and paired electrolysis: e-shuttle enables the reversible interconversion of alkenes and vicinal dihalides*, **2020**, in preparation.

M. Dörr*, **J. L. Röckl***, J. Rein, S. R. Waldvogel, *Electrochemical C-H Functionalization of (Hetero)Arenes – Optimized by DoE*, *Chem. Eur. J.*, **2020**, accepted, (DOI: 10.1002/chem.202001171).

J. Dickhaut, A. Molt, **J. L. Röckl**, *CYCLOCLAVINE: A NATURAL PRODUCT WITH INSECTICIDAL POTENTIAL*, book chapter, Elsevier **2020**, ASAP.

J. L. Röckl, D. Pollok, R. Franke, S. R. Waldvogel, *A Decade of Electrochemical Dehydrogenative C,C – Coupling of Aryls*, *Acc. Chem. Res.* **2020**, 53, 45–61. (Front Cover)

J. L. Röckl, D. Schollmeyer, R. Franke, S. R. Waldvogel, *Dehydrogenative C,C – coupling of Phenols bearing Electronwithdrawing Groups*, *Angew. Chem. Int. Ed.* **2020**, 59, 315–319; (Hot Paper)

J. L. Röckl, D. Schollmeyer, R. Franke, S. R. Waldvogel, *Dehydrierende anodische C,C – Kupplung von Phenolen mit elektronenziehenden Substituenten*, *Angew. Chem.* **2020**, 132, 323–327.

J. L. Röckl, A. V. Hauck, D. Schollmeyer, S. R. Waldvogel, *Electrochemical Synthesis of Fluorinated Orthoesters from 1,3-Benzodioxoles*, *ChemistryOpen* **2019**, 8, 1167–1171. (Front cover)

J. L. Röckl, Y. Imada, K. Chiba, R. Franke, S. R. Waldvogel, *Dehydrogenative Anodic Cyanation Reaction of Phenols in Benzylic Positions*, *ChemElectroChem* **2019**, 6, 4184–4187.

Y. Imada, **J. L. Röckl**, A. Wiebe, T. Gieshoff, D. Schollmeyer, K. Chiba, R. Franke, S. R. Waldvogel, *Metal- and Reagent-Free Dehydrogenative Benzyl-Aryl Formal Cross-Coupling by Anodic Activation in 1,1,1,3,3,3-Hexafluoropropan-2-ol*, *Angew. Chem. Int. Ed.* **2018**, 57, 12136–12140; (VIP manuscript) (Inside back cover)

Y. Imada, **J. L. Röckl**, A. Wiebe, T. Gieshoff, D. Schollmeyer, K. Chiba, R. Franke, S. R. Waldvogel, *Metall- und reagensfreie dehydrierende formale Benzyl-Aryl-Kreuzkupplung durch anodische Aktivierung in 1,1,1,3,3,3-Hexafluoropropan-2-ol*, *Angew. Chem.* **2018**, 130, 12312–12317.

M. J. McLaughlin, K. Koerber, B. Gockel, P. Bindschaedler, S. Soergel, D. Vyas, **J. Roeckl**, *Oxy-cope rearrangement for the manufacture of insecticidal cyclopentene compounds*, *PCT Int. Appl.* **2018**, WO 2018007175A1.

* Authors contributed equally

7.2 Supervised work

2018 **Adrian Hauck**, B.Sc.–Thesis

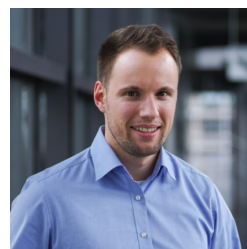
Title: *Elektrochemische Darstellung von Orthoestern*

2019 **Jonas Rein**, B.Sc.–Thesis

Title: *Electrochemical Functionalization of Purine Derivatives*

7.3 Curriculum vitae

Johannes Röckl



Johannes Ludwig Röckl

Department of Organic Chemistry
Johannes Gutenberg University
Room 1.125, Duesbergweg 10-14, 55128 Mainz

Nationality: German
Date of Birth: 20.01.1991
E-mail: joroeckl@uni-mainz.de
Phone: +49 15129109412

Education

2017 – now: **PhD. Candidate Electro-organic Chemistry with Prof. S. R. Waldvogel at Johannes Gutenberg University Mainz**

Fast-Track Ph.D. program: awarded to above-average students.

2013 – 2016: **B.Sc. Applied Organic Chemistry at Johannes Gutenberg University Mainz**

Bachelor-Thesis: "Cycloclavine as a Potential Insecticide"

Total synthesis of Natural Product derivatives under supervision of Prof. Dr. S. R. Waldvogel and Dr. J. Dickhaut.

2010 – 2013: **BBS Naturwissenschaften, Ludwigshafen am Rhein**

Laboratory Technology – Training during apprenticeship.

2001 – 2010: **Benedikt-Stattler-Gymnasium, Bad Kötzing**

Graduation courses: chemistry, sports;

Graduation project: Chemistry in Dental Medicine.

Relevant Experience

2018 – now: **PhD student at Johannes Gutenberg University, Mainz**

Supervision of Master and Bachelor students;

Work on direct electrochemical C,H – functionalization reactions.

2019: **Visiting Researcher at ETH Zurich with Prof. Dr. Bill Morandi, Zurich**

Work on novel amination reactions and electrochemistry enabled halogen transfer reactions.

2016 – 2018: **Scientific Lab Expert at BASF SE, Crop Protection Division, Ludwigshafen**

Scientist in agricultural research

Responsible for early stage projects in insecticide science:

- Evaluation of biological data
- Planning of the synthesis of new target molecules
- Coordinating parallel synthesis of new derivatives
- Scale up of reactions into technical scale
- Route scouting
- Purchase of new compounds for testing.

- 2017: **Lab Associate at BASF India Ltd., Crop Protection Division, Navi Mumbai**
Work on early stage projects in Insecticide science.
- 2013 – 2016: **Lab Technician at BASF SE, Crop Protection Division, Ludwigshafen**
Synthesis of lead structures for novel insecticides.
- 2010 – 2013: **Apprenticeship as a Laboratory Technician at BASF SE, Ludwigshafen**
2012–2013: Combinatorial chemistry for crop protection and LC/MS routine analytics.
2011–2012: Polymers for fiber-bonding - Application technology.
2011–2012: Synthesis of zeolites in catalysis, surface-analytics for zeolites and metal-organic frameworks.
2010–2011: Synthesis of lead structures for fungicides.
- 2012: **Internship at Jotun Group, Sandefjord, Norway (Leonardo da Vinci program)**
Lab assistant at Jotun research and development center.
Studied the application of fungicides in paint.

Awards & Achievements

- 2019: **MPGC – Max-Planck-Graduate Center**
Accepted as a member of the virtual department across two Max Planck Institutes and four facilities of the Johannes Gutenberg University
- 2018: **Prize for best graduate in the degree program Applied Organic Chemistry**
Awarded for high grades during studies at Johannes Gutenberg University, Mainz
- 2018: **MAINZ - Materials Science in Mainz Graduate School**
Scholarship and Graduate School (Uni Mainz/MPI/P /TU Kaiserslautern)
- 2017: **Gutenberg Lehrkolleg Thesis Prize – GLK Johannes Gutenberg University, Mainz**
Awarded for outstanding Bachelor thesis in the department of Chemistry
- 2014 – 2016: **Scholarship: Weiterbildungsstipendium Bundesministerium für Bildung und Forschung**
Scholarship for gifted students, IHK Pfalz
- 2013: **Prize for Best Apprenticeship Graduate Industrie- und Handelskammer Pfalz**
Awarded for high grades during apprenticeship

Languages & Other Relevant Skills

Native: **German**
Other: **English (advanced), French (basic), Swedish (basic)**

Experience with Microsoft Office, electronic laboratory notebook systems, and scientific databases such as SciFinder and Reaxys. Experience using specialist software such as Origin for data presentation & analysis.

7.4 Attached Publications

VIP **Electrochemistry** Very Important PaperInternational Edition: DOI: 10.1002/anie.201804997
German Edition: DOI: 10.1002/ange.201804997**Metal- and Reagent-Free Dehydrogenative Formal Benzyl–Aryl Cross-Coupling by Anodic Activation in 1,1,1,3,3,3-Hexafluoropropan-2-ol**

Yasushi Imada, Johannes L. Röckl, Anton Wiebe, Tile Gieshoff, Dieter Schollmeyer, Kazuhiro Chiba, Robert Franke, and Siegfried R. Waldvogel*

Abstract: A selective dehydrogenative electrochemical functionalization of benzylic positions that employs 1,1,1,3,3,3-hexafluoropropan-2-ol (HFIP) has been developed. The electrogenerated products are versatile intermediates for subsequent functionalizations as they act as masked benzylic cations that can be easily activated. Herein, we report a sustainable, scalable, and reagent- and metal-free dehydrogenative formal benzyl–aryl cross-coupling. Liberation of the benzylic cation was accomplished through the use of acid. Valuable diarylmethanes are accessible in the presence of aromatic nucleophiles. The direct application of electricity enables a safe and environmentally benign chemical transformation as oxidizers are replaced by electrons. A broad variety of different substrates and nucleophiles can be employed.

Diarylmethanes are important motifs in biologically active compounds,^[1] medicinal chemistry,^[2] and materials science.^[3] In general, there are two different synthetic approaches to symmetric and non-symmetric diarylmethanes. Common procedures exploit transition-metal-catalyzed coupling reactions of benzyl halides with prefunctionalized aromatic nucleophiles, or aryl halides with benzylic nucleophiles.^[4] However, conventional cross-coupling reactions (e.g., Suzuki–Miyaura or Kumada–Corriu coupling reactions)

share several major disadvantages: The synthesis of the desired diarylmethanes involves a multistep sequence, is cost-intensive and time-consuming, and lacks atom efficiency. Prefunctionalized starting materials have to be prepared under difficult reaction conditions. Catalysts, mostly palladium-based, are also required for the final coupling reaction. Furthermore, reagent waste is generated in each individual step. The activation of C–H bonds in such reactions has only been achieved in a few examples, with a limited substrate scope.^[5] Friedel–Crafts-type conversions are the second available option. Hydroxy, halogen, or acetoxy substituents in benzylic positions are cleaved by metal catalysts to generate cationic intermediates, which can then undergo coupling reactions with nucleophilic arenes. The activation by metal catalysts is indispensable in most cases, and a variety of catalysts have been employed (RhCl₃,^[6] IrCl₃,^[6] H₂PdCl₄,^[6] H₂PtCl₆,^[6] HAuCl₄,^[7] FeCl₃,^[8] and Bi(OTf)₃).^[9]

In addition to the complex reaction conditions required (elevated temperature, dry solvents, and/or inert atmosphere), low regioselectivities and the generation of large amounts of salts as reagent waste are further disadvantages.^[6]

Avoiding the use of stoichiometric reagents and the generation of reagent waste is an important factor in developing an environmentally benign, “greener” route to diarylmethanes.^[10] For this purpose, methods for dehydrogenative coupling reactions are of great interest. Electrochemistry, in particular anodic conversion, is a valuable tool for the development of such metal- and reagent-free sustainable transformations.^[11] This has been recently demonstrated by the development of an electrochemical benzyl–aryl coupling for the synthesis of diarylmethanes by Yoshida and co-workers.^[12] For accumulation of the electrochemically oxidized species in this procedure, the intermediary generated benzylic cations had to be trapped with an additional reagent owing to their high reactivity. Subsequent elimination of the stabilizing reagent and coupling with aromatic nucleophiles was then carried out. Owing to the separation of the oxidation and coupling events, bond formation occurred in a selective manner. However, this method exhibits some drawbacks. The stabilizing reagent is not commercially available and has to be used in large excess. The coupling reaction can take up to 35 hours to reach completion, and all reactions were only demonstrated on small scale (0.1 mmol). The application of free phenols for the anodic step was not reported. In addition, owing to the complex electrolysis setup (a divided cell equipped with a very specific carbon fiber anode), the procedure is not easily scalable. Consequently, a simple, sustainable, and scalable approach for the synthesis of diarylmethanes is still highly desired. In a recent contribution,

[*] Y. Imada, J. L. Röckl, Dr. A. Wiebe, Dr. T. Gieshoff, Dr. D. Schollmeyer, Prof. Dr. S. R. Waldvogel
Institute of Organic Chemistry
Johannes Gutenberg University Mainz
Duesbergweg 10–14, 55128 Mainz (Germany)
E-mail: waldvogel@uni-mainz.de
Homepage: <http://www.chemie.uni-mainz.de/OC/AK-Waldvogel/>

Y. Imada, Prof. Dr. K. Chiba
Department of Applied Biological Science
Tokyo University of Agriculture and Technology (Japan)

Y. Imada, Dr. T. Gieshoff, Prof. Dr. S. R. Waldvogel
Graduate School Materials Science in Mainz
Johannes Gutenberg University Mainz (Germany)

Dr. A. Wiebe, Prof. Dr. S. R. Waldvogel
Max Planck Graduate Center
Johannes Gutenberg University Mainz (Germany)

Prof. Dr. R. Franke
Evonik Performance Materials GmbH
Marl (Germany)

Prof. Dr. R. Franke
Lehrstuhl für Theoretische Chemie
Ruhr-Universität Bochum (Germany)

Supporting information and the ORCID identification number(s) for the author(s) of this article can be found under:
<https://doi.org/10.1002/anie.201804997>

Stahl and co-workers reported an electrochemical iodination that delivers substrates for benzyl–aryl couplings.^[13]

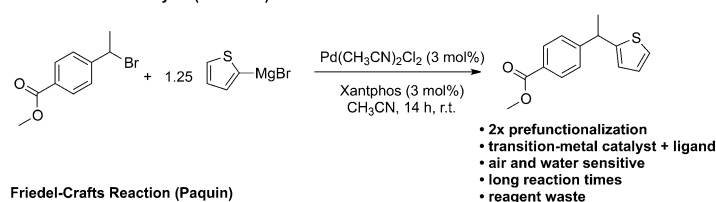
Following our interest in electrochemical reactions, our group has developed efficient electrochemical C–C and N–N coupling reactions involving phenols,^[14] anilides,^[15] and dianilides as substrates.^[16] Key to these conversions was the application of 1,1,1,3,3,3-hexafluoropropan-2-ol (HFIP) as the solvent. HFIP has unique properties. It stabilizes reactive intermediates,^[17] has a unique solvent microstructure,^[18] as well as interesting solvation properties, and as such, it can enable selective transformations.^[14e,19] HFIP was also used as a solvent by Paquin and co-workers in a non-electrochemical approach for the activation of benzyl fluorides in benzyl–aryl coupling reactions.^[20] Owing to its low nucleophilicity, reactions involving nucleophilic attack of HFIP are rarely reported.^[21] Recently, our group described an anodic functionalization of anilides with HFIP at the benzylic and aromatic position.^[16b]

Herein, we report the selective electrochemical functionalization of benzylic positions with HFIP. Such direct electrochemical C–H functionalizations often require catalyst systems.^[22] The generated ether acts as a molecular mask for the benzylic cation, and stabilizes this reactive intermediate by solvent trapping in a less reactive state. The activation of such masked cations to facilitate an efficient and selective benzyl–aryl coupling reaction is reported for the first time. We present a simple, sustainable, easily scalable, and reagent- and metal-free electrochemical benzyl–aryl cross-coupling reaction that proceeds in a two-step, one-pot sequence (Scheme 1).

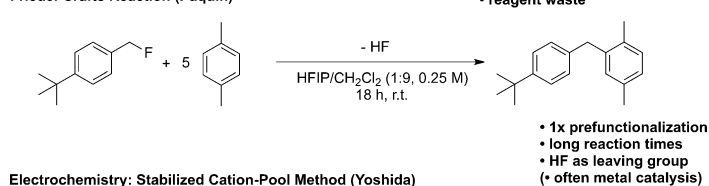
Initially, the electrochemical HFIP ether formation was optimized (Table 1). Phenol **1** was selected as the test substrate. The electrochemical parameters developed for the anodic phenol–thiophene cross-coupling were used as the initial conditions.^[14c] Additive screening resulted in efficient HFIP ether formation with 0.57 equiv of diisopropylethylamine (DIPEA; Table 1, entry 1). We attributed this to the base character of the additive. A similar effect, but with lower yield and selectivity, was observed using triethylamine (TEA), K₂CO₃, or Cs₂CO₃ as the base (Table 1, entry 2; see also the Supporting information). The optimal electrolysis parameters were 2.2 F and 7.2 mA cm⁻² (Table 1, entries 3–7).

Notably, oxidation at graphite anodes, which are less expensive than boron-doped diamond (BDD) anodes, provided the desired HFIP ether in similar yields (Table 1, entry 8). This is particularly interesting for technical large-scale applications. However, it should be noted that we proceeded here with BDD anodes in the subsequent electrolysis because of the slightly better yield according to our optimization studies. A significant step towards a greener procedure was made by noting that DIPEA forms in situ a supporting electrolyte so that additional salt is not required for this transformation (entries 9 and 10). This can be rationalized by salt formation between the solvent HFIP (pK_a = 9.3)^[21] and DIPEAH⁺ (pK_a = 11.4),^[23] which leads to sufficient electrical conductivity. Doubling the amount of

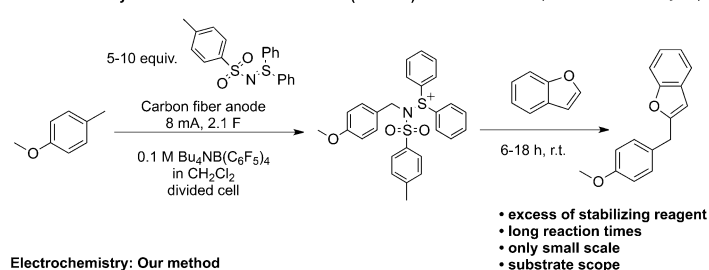
Transition-Metal Catalysis (Carretero)



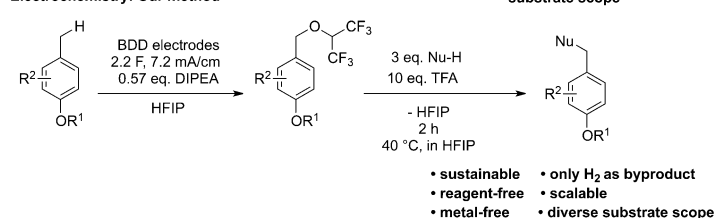
Friedel-Crafts Reaction (Paquin)



Electrochemistry: Stabilized Cation-Pool Method (Yoshida)



Electrochemistry: Our method



Scheme 1. Strategies for benzyl–aryl couplings in comparison to our new method.

Table 1: Optimization of the anodic functionalization of 4-methylguaiaicol with HFIP.^[a]

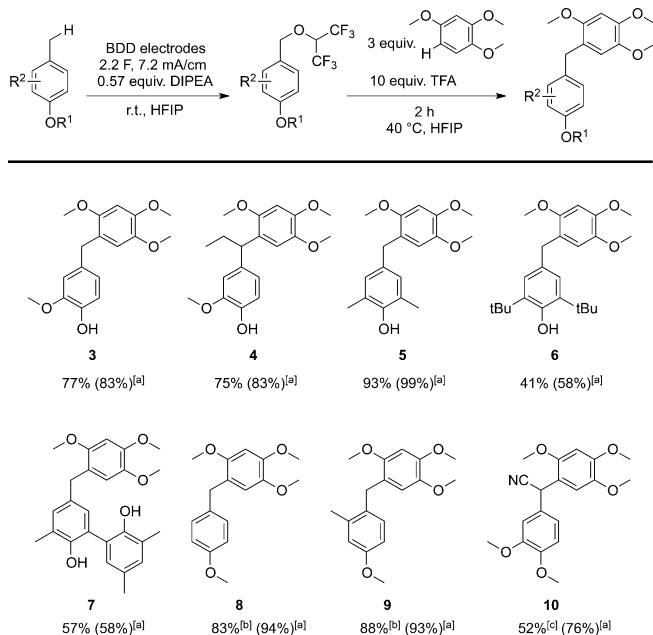
Entry	Deviation from the standard conditions	Yield ^[b] [%]
1	–	72
2	TEA instead of DIPEA	42
3	1.9 F	64
4	2.2 F	78
5	2.4 F	56
6	2.2 F, 5 mA cm ⁻²	67
7	2.2 F, 10 mA cm ⁻²	63
8	graphite electrodes, 2.2 F	76
9	graphite electrodes, without supporting electrolyte, 2.2 F	72
10	without supporting electrolyte, 2.2 F	78
11	without supporting electrolyte, 2.2 F, 1.14 equiv DIPEA	69
12	without DIPEA	0

[a] All reactions were carried out with 1.0 mmol of phenol **1** in 5 mL of HFIP in an undivided cell. [b] Yields determined by ¹H NMR spectroscopy with benzaldehyde as the internal standard. MTBS = methyltributylammonium methyl sulfate.

DIPEA did not improve the yield (entry 11). In a control experiment (entry 12), the significance of DIPEA as an additive was confirmed. Without additive, phenol homocoupling and oligomerization dominated.

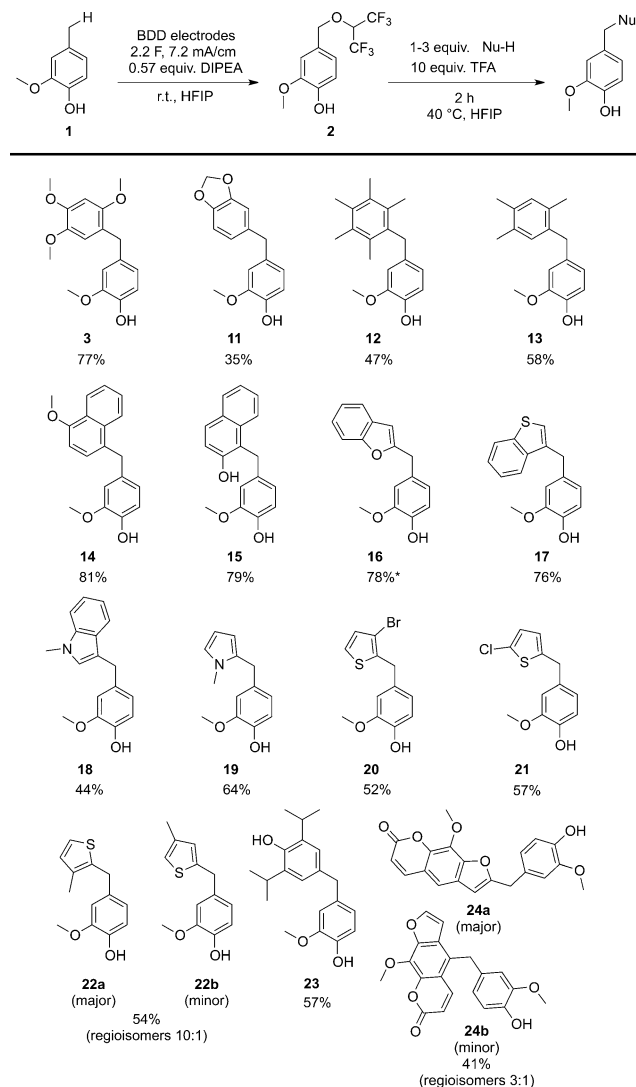
While the selective formation of benzylic HFIP ethers using HFIP as a nucleophile is an unprecedented transformation, we were particularly interested in exploring applications of this motif in further synthesis. The ether can be seen as a molecular mask for the benzylic cation in this case. However, compared to an approach presented in 2013 demonstrating the trapping of cations in the α -position of amides in Shono oxidation products of lactams,^[24] the stabilization and subsequent activation of benzylic cations is a significantly more challenging task. We found that treatment with 2,2,2-trifluoroacetic acid (TFA) led to subsequent formation of an active benzylic cation. When this activation is carried out in the presence of one to three equivalents of an aromatic nucleophile, selective benzyl–aryl cross-coupling can be achieved. We optimized this coupling reaction with 1,2,4-trimethoxybenzene as a test substrate. With optimized conditions for the first and second step in hand, we explored the scope of potential substrates for HFIP ether formation. For the subsequent benzylic cross-coupling reaction, 1,2,4-trimethoxybenzene served as the test nucleophile (Scheme 2).

Electrochemical functionalization with HFIP at the benzylic position and subsequent benzyl–aryl cross-coupling was achieved with a variety of substrates in yields up to 93% (**5**). Unprotected phenols can be coupled at primary (**3**, **5**, **6**) and secondary benzylic positions (**4**). Additionally, a biphenol was functionalized (**7**). Our method proved to be complementary to the “stabilized cation pool” approach as anisole



Scheme 2. Scope of the anodic functionalization with HFIP and the subsequent coupling to 1,2,4-trimethoxybenzene. Electrolysis was carried out in 5 mL HFIP with 1 mmol of substrate in an undivided cell. [a] Yield of the benzylic HFIP ether after electrolysis, determined by ¹⁹F NMR analysis. [b] With 0.5 mmol of substrate and 3.0 F for optimum electrochemical conversion. [c] Electrolysis with 1.8 F; activation with *p*-TsOH instead of TFA, 3 h.

and anisole derivatives could be coupled in high yields (**8–10**). Product **10** is particularly interesting as the nitrile moiety allows for further facile functionalization. When dehydrodimerization or oligomerization became noticeable during electrolysis (**8** and **9**), the concentration of the starting material was reduced, leading to high yields (83% and 88%) of the desired coupling products. As a logical step, we investigated couplings with different nucleophiles. For this approach, the electrolysis was carried out under the optimized reaction conditions with 4-methylguaiacol as the test system, and the subsequent coupling step was investigated (Scheme 3). The reaction was found to be successful with a broad variety of different nucleophiles. Arenes with strongly electron-releasing groups (**3** and **11**), as well as methylated arenes (**12** and **13**), were successfully cross-coupled with 4-methylguaiacol. The reaction with a free phenol proceeded in good yield (**23**). Naphthalene derivatives, including 1-methoxynaphthalene and unprotected 2-naphthol, were coupled in high yields of up to 81% (**14** and **15**). Coupling of 4-methylguaiacol with heterocycles such as benzofuran,



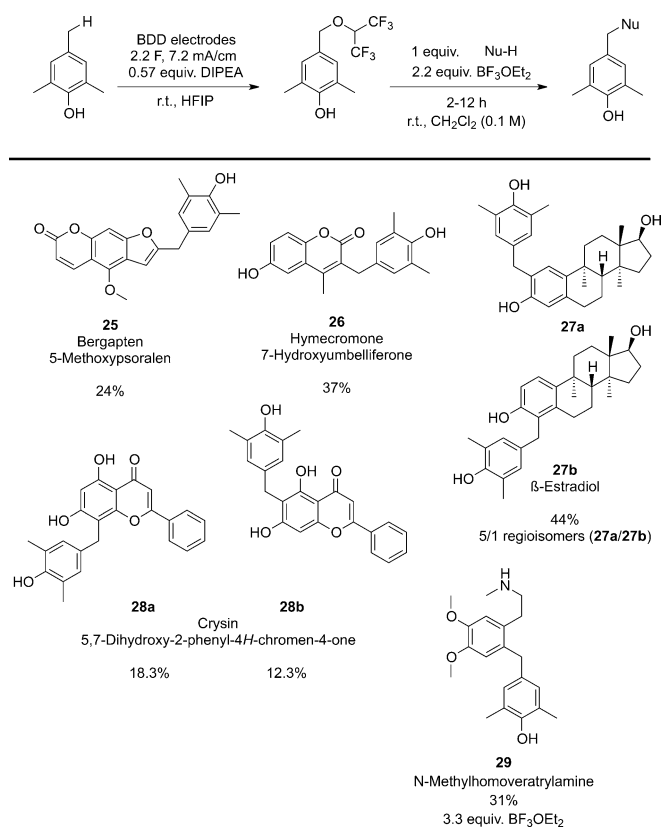
Scheme 3. Variation of the nucleophile in the coupling reaction with 4-methylguaiacol. Electrolysis carried out in 5 mL HFIP with 1 mmol of phenol **1** in an undivided cell.

benzothiophene, *N*-methylindole, *N*-methylpyrrole, and thiophene derivatives is possible in moderate to high yields (**16–22b**). The transformation tolerates a variety of substituents (methoxy, methyl, hydroxy, chlorine, and bromine). In most cases, the coupling reaction proceeded smoothly and selectively. Only in the case of 3-methylthiophene, the formation of regioisomers (**22a** and **22b**) was observed. Importantly, the benzyl–aryl cross-coupling reaction can be conducted in a much shorter period of time compared to Yoshida's process.^[12] It should be noted that HFIP was used as both the solvent and nucleophile in this procedure, and that it can be fully recovered and reused.^[21] This leads to an overall reaction balance with hydrogen as the only byproduct for the C–C cross-coupling reaction.

To explore the full potential of this method, its application to natural product derivatization was of high interest. Our initial approaches to this end using 2,2,2-trifluoroacetic acid led to the generation of complex mixtures. Further attempts using Lewis acids in dichloromethane proved promising. The use of β -estradiol as a nucleophile and aluminum chloride led to a 32% yield of the coupled product. Further optimization of this system using BF_3OEt_2 (2.2 equiv) increased the yield of the coupled product to 44%. Based on these initial results, we were able to carry out late-stage functionalizations of a range of natural products and biologically active compounds in moderate yields (Scheme 4). Five different classes of natural products (steroid **27**, umbelliferone **26**, psolarene **25**, phenylethylamine **29**, and flavone **28**) were successfully derivatized. Couplings were achieved at a range of positions, illustrating the generality of this method for exclusive carbon functionalization even in the presence of nucleophilic oxygen (**26**, **27**, and **28**) or nitrogen moieties (**29**). Additionally, crystal structures of the psolarene and umbelliferone derivatives were obtained (see the Supporting Information). These novel derivatives may be of interest as potentially biologically active compounds. Their biological activities are currently being tested.

To demonstrate the scalability of our method, we chose the synthesis of compound **17** as a model reaction. The structural moiety of **17** is of significant interest for pharmaceutically active compounds.^[25] Therefore, a simple and scalable method for the synthesis of these diarylmethanes would provide a new versatile strategy. The electrolysis was scaled up by a factor of 40, and was conducted with 40 mmol of phenol **1** in a 200 mL beaker-type cell (Figure 1). No erosion of selectivity was observed for the anodic functionalization with HFIP. This mixture was directly subjected to the coupling reaction with benzothiophene to give 6.91 g of the desired product **17** in a single batch (64% yield). The yield is slightly lower compared to that obtained on 5 mL scale (76%). This can be rationalized by the not yet optimized addition of TFA on larger scale. Nevertheless, the reaction time could even be decreased from 2 h to 1 h within this upscaling approach.

In conclusion, we have established a very efficient procedure for the electrochemical functionalization of benzylic groups that is based on the use of HFIP. Small amounts of DIPEA can be used as an additive to selectively enable this reaction pathway and to fully replace any additional support-



Scheme 4. Benzylation of natural products and bioactive compounds using BF_3OEt_2 (2.2 equiv), 0.1 M in CH_2Cl_2 , room temperature, 2–12 h.



Figure 1. For the scale-up studies, 5 mL and 200 mL beaker-type cells were employed. For size comparison, a 2€ coin (diameter: 25.75 mm, ca. 1.01 inches) was placed between the two cells. See the Supporting Information for details.

ing electrolyte. The scope was exemplified with phenols and anisoles as well as through the late-stage functionalization of natural products. The benzylic HFIP ethers can be activated with acid to undergo dehydrogenative benzyl–aryl cross-coupling reactions with a variety of different nucleophiles in high yields. This method provides a scalable, metal-free, and reagent-saving route to diarylmethanes, which has the poten-

tial to shorten a variety of synthetic routes. Activation of electrogenerated HFIP ethers for applications in various reactions with nucleophiles can be imagined. In addition, this method could be extended and optimized for anilides, as already shown by our group for the first step. Therefore, this approach provides a general route for numerous chemical transformations.

Acknowledgements

We thank the DFG (GSC 266, Wa 1276/17-1, Wa 1276/14-1) for financial support. Support of the Advanced Lab of Electrochemistry and Electrosynthesis—ELYSION (Carl Zeiss Stiftung) is gratefully acknowledged. Y.I. gratefully acknowledges support from the Program for Leading Graduate School of TUAT, granted by the Ministry of Education, Culture, Science and Technology (MEXT), Japan. Y.I. and T.G. thank the Material Science in Mainz (MAINZ) graduate school for financial support. A.W. thanks the Max Planck Graduate Center for financial support.

Conflict of interest

The authors declare no conflict of interest.

Keywords: benzylic coupling · electrochemistry · green chemistry · HFIP · natural products

How to cite: *Angew. Chem. Int. Ed.* **2018**, *57*, 12136–12140
Angew. Chem. **2018**, *130*, 12312–12317

- [1] K. L. McPhail, D. E. A. Rivett, D. E. Lack, M. T. Davies-Coleman, *Tetrahedron* **2000**, *56*, 9391–9396.
- [2] Y.-Q. Long, X.-H. Jiang, R. Dayam, T. Sanchez, R. Shoemaker, S. Sei, N. Neamati, *J. Med. Chem.* **2004**, *47*, 2561–2573.
- [3] a) M. Ahmad, J. K. Luo, H. Purnawali, W. M. Huang, P. J. King, P. R. Chalker, M. Mireftab, J. Geng, *J. Mater. Chem.* **2012**, *22*, 8192–8194; b) S. Wang, C. Zhang, Y. Shu, S. Jiang, Q. Xia, L. Chen, S. Jin, I. Hussain, A. I. Cooper, B. Tan, *Sci. Adv.* **2017**, *3*, e1602610.
- [4] a) A. López-Pérez, J. Adrio, J. C. Carretero, *Org. Lett.* **2009**, *11*, 5514–5517; b) M. J. Burns, I. J. S. Fairlamb, A. R. Kapdi, P. Sehnal, R. J. K. Taylor, *Org. Lett.* **2007**, *9*, 5397–5400; c) B. P. Bandgar, S. V. Bettigeri, J. Phopase, *Tetrahedron Lett.* **2004**, *45*, 6959–6962; d) S. M. Nobre, A. L. Monteiro, *Tetrahedron Lett.* **2004**, *45*, 8225–8228; e) J.-Y. Yu, R. Kuwano, *Org. Lett.* **2008**, *10*, 973–976.
- [5] a) T. Mukai, K. Hirano, T. Satoh, M. Miura, *Org. Lett.* **2010**, *12*, 1360–1363; b) D. Lapointe, K. Fagnou, *Org. Lett.* **2009**, *11*, 4160–4163; c) J. Zhang, A. Bellomo, A. D. Creamer, S. D. Dreher, P. J. Walsh, *J. Am. Chem. Soc.* **2012**, *134*, 13765–13772.
- [6] K. Mertins, I. Iovel, J. Kischel, A. Zapf, M. Beller, *Angew. Chem. Int. Ed.* **2005**, *44*, 238–242; *Angew. Chem.* **2005**, *117*, 242–246.
- [7] K. Mertins, I. Iovel, J. Kischel, A. Zapf, M. Beller, *Adv. Synth. Catal.* **2006**, *348*, 691–695.
- [8] I. Iovel, K. Mertins, J. Kischel, A. Zapf, M. Beller, *Angew. Chem. Int. Ed.* **2005**, *44*, 3913–3917; *Angew. Chem.* **2005**, *117*, 3981–3985.
- [9] M. Rueping, B. J. Nachtsheim, W. Ieawsuwan, *Adv. Synth. Catal.* **2006**, *348*, 1033–1037.
- [10] P. Anastas, N. Eghbali, *Chem. Soc. Rev.* **2010**, *39*, 301–312.
- [11] a) A. Wiebe, T. Gieshoff, S. Möhle, E. Rodrigo, M. Zirbes, S. R. Waldvogel, *Angew. Chem. Int. Ed.* **2018**, *57*, 5594–5616; *Angew. Chem.* **2018**, *130*, 5694–5721; b) S. Möhle, M. Zirbes, E. Rodrigo, T. Gieshoff, A. Wiebe, S. R. Waldvogel, *Angew. Chem. Int. Ed.* **2018**, *57*, 6018–6041; *Angew. Chem.* **2018**, *130*, 6124–6149.
- [12] R. Hayashi, A. Shimizu, J.-I. Yoshida, *J. Am. Chem. Soc.* **2016**, *138*, 8400–8403.
- [13] M. Rafiee, F. Wang, D. P. Hruszkewycz, S. S. Stahl, *J. Am. Chem. Soc.* **2018**, *140*, 22–25.
- [14] a) A. Wiebe, D. Schollmeyer, K. M. Dyballa, R. Franke, S. R. Waldvogel, *Angew. Chem. Int. Ed.* **2016**, *55*, 11801–11805; *Angew. Chem.* **2016**, *128*, 11979–11983; b) A. Wiebe, B. Riehl, S. Lips, R. Franke, S. R. Waldvogel, *Sci. Adv.* **2017**, *3*, eaao3920; c) A. Wiebe, S. Lips, D. Schollmeyer, R. Franke, S. R. Waldvogel, *Angew. Chem. Int. Ed.* **2017**, *56*, 14727–14731; *Angew. Chem.* **2017**, *129*, 14920–14925; d) S. Lips, A. Wiebe, B. Elsler, D. Schollmeyer, K. M. Dyballa, R. Franke, S. R. Waldvogel, *Angew. Chem. Int. Ed.* **2016**, *55*, 10872–10876; *Angew. Chem.* **2016**, *128*, 11031–11035; e) B. Elsler, A. Wiebe, D. Schollmeyer, K. M. Dyballa, R. Franke, S. R. Waldvogel, *Chem. Eur. J.* **2015**, *21*, 12321–12325.
- [15] L. Schulz, M. Enders, B. Elsler, D. Schollmeyer, K. M. Dyballa, R. Franke, S. R. Waldvogel, *Angew. Chem. Int. Ed.* **2017**, *56*, 4877–4881; *Angew. Chem.* **2017**, *129*, 4955–4959.
- [16] a) T. Gieshoff, D. Schollmeyer, S. R. Waldvogel, *Angew. Chem. Int. Ed.* **2016**, *55*, 9437–9440; *Angew. Chem.* **2016**, *128*, 9587–9590; b) T. Gieshoff, A. Kehl, D. Schollmeyer, K. D. Moeller, S. R. Waldvogel, *J. Am. Chem. Soc.* **2017**, *139*, 12317–12324.
- [17] L. Ebersson, O. Persson, M. P. Hartshorn, *Angew. Chem. Int. Ed. Engl.* **1995**, *34*, 2268–2269; *Angew. Chem.* **1995**, *107*, 2417–2418.
- [18] O. Hollóczki, A. Berkessel, J. Mars, M. Mezger, A. Wiebe, S. R. Waldvogel, B. Kirchner, *ACS Catal.* **2017**, *7*, 1846–1852.
- [19] a) B. Elsler, D. Schollmeyer, K. M. Dyballa, R. Franke, S. R. Waldvogel, *Angew. Chem. Int. Ed.* **2014**, *53*, 5210–5213; *Angew. Chem.* **2014**, *126*, 5311–5314; b) A. Kirste, B. Elsler, G. Schnakenburg, S. R. Waldvogel, *J. Am. Chem. Soc.* **2012**, *134*, 3571–3576; c) A. Kirste, G. Schnakenburg, F. Stecker, A. Fischer, S. R. Waldvogel, *Angew. Chem. Int. Ed.* **2010**, *49*, 971–975; *Angew. Chem.* **2010**, *122*, 983–987; d) A. Kirste, M. Nieger, I. M. Malkowsky, F. Stecker, A. Fischer, S. R. Waldvogel, *Chem. Eur. J.* **2009**, *15*, 2273–2277.
- [20] P. A. Champagne, Y. Benhassine, J. Desroches, J.-F. Paquin, *Angew. Chem. Int. Ed.* **2014**, *53*, 13835–13839; *Angew. Chem.* **2014**, *126*, 14055–14059.
- [21] I. Colomer, A. E. R. Chamberlain, M. B. Haughey, T. J. Donohoe, *Nat. Rev. Chem.* **2017**, *1*, 0088.
- [22] a) Q.-L. Yang, Y.-Q. Li, C. Ma, P. Fang, X.-J. Zhang, T.-S. Mei, *J. Am. Chem. Soc.* **2017**, *139*, 3293–3298; b) A. Shrestha, M. Lee, A. L. Dunn, M. S. Sanford, *Org. Lett.* **2018**, *20*, 204–207.
- [23] T. Fujii, H. Nishidam, Y. Abiru, M. Yamamoto, M. Kise, *Chem. Pharm. Bull.* **1995**, *43*, 1872–1877.
- [24] T. Tajima, H. Kurihara, S. Shimizu, H. Tateno, *Electrochemistry* **2013**, *81*, 353–355.
- [25] a) T. A. Grese, S. Cho, H. U. Bryant, H. W. Cole, A. L. Glasebrook, D. E. Magee, D. L. Phillips, E. R. Rowley, L. L. Short, *Bioorg. Med. Chem. Lett.* **1996**, *6*, 201–206; b) A. D. Palkowitz, A. L. Glasebrook, K. J. Thrasher, K. L. Hauser, L. L. Short, D. L. Phillips, B. S. Muehl, M. Sato, P. K. Shetler, G. J. Cullinan, T. R. Pell, H. U. Bryant, *J. Med. Chem.* **1997**, *40*, 1407–1416; c) D. J. Sall, S. L. Briggs, N. Y. Chirgadze, D. K. Clawson, D. S. Gifford-Moore, V. J. Klimkowski, J. R. McCowan, G. F. Smith, J. H. Wikel, *Bioorg. Med. Chem. Lett.* **1998**, *8*, 2527–2532.

Manuscript received: April 29, 2018

Accepted manuscript online: May 24, 2018

Version of record online: June 28, 2018



Metall- und reagensfreie dehydrierende formale Benzyl-Aryl-Kreuzkupplung durch anodische Aktivierung in 1,1,1,3,3,3-Hexafluorpropan-2-ol

Yasushi Imada, Johannes L. Röckl, Anton Wiebe, Tile Gieshoff, Dieter Schollmeyer, Kazuhiro Chiba, Robert Franke und Siegfried R. Waldvogel*

Abstract: Eine selektive dehydrierende elektrochemische Funktionalisierung benzyliischer Positionen durch 1,1,1,3,3,3-Hexafluorpropan-2-ol (HFIP) wurde entwickelt. Die elektrolitisch generierten Produkte sind vielseitige Zwischenprodukte für nachfolgende Funktionalisierungen, da sie als maskierte, leicht aktivierbare Benzylkationen reagieren. Hier wird eine nachhaltige, skalierbare, reagens- und metallfreie, dehydrierende, formale Benzyl-Aryl-Kreuzkupplung vorgestellt. Die Freisetzung des benzyliischen Kations erfolgt durch Säure. Wertvolle Diarylmethane sind in Gegenwart von aromatischen Nucleophilen zugänglich. Die direkte Nutzung von Strom ermöglicht eine sichere und umweltverträgliche chemische Umwandlung, da Oxidationsmittel durch Elektronen ersetzt werden. Es kann eine große Vielfalt an Substraten und Nucleophilen eingesetzt werden.

Diarylmethane sind eine wichtige Strukturform für biologisch aktive Verbindungen,^[1] in der medizinischen Chemie^[2] und in den Materialwissenschaften.^[3] Generell stehen zwei Ansätze für die Synthese symmetrischer und nicht-symmetrischer Diarylmethane zur Verfügung. Gängige Vorgehensweisen nutzen Übergangsmetall-katalysierte Kupplungsreaktionen von Benzylhalogeniden mit vorfunktionalisierten

aromatischen Nucleophilen oder Arylhalogeniden mit benzyliischen Nucleophilen.^[4] Herkömmliche Kreuzkupplungen (z. B. Suzuki-Miyaura- oder Kumada-Corriu-Kupplungen) haben jedoch mehrere große Nachteile gemein: Die Synthese der gewünschten Diarylmethane ist mehrstufig, kosten- sowie zeitaufwändig und läuft mit niedriger Atomökonomie ab. Vorfunktionalisierte Ausgangsverbindungen müssen unter schwierigen Reaktionsbedingungen hergestellt werden. Es werden Katalysatoren, meist auf Palladiumbasis, für die finale Kupplungsreaktion benötigt. Darüber hinaus fallen in jedem einzelnen Schritt Reagensabfälle an. Die Aktivierung von C-H-Bindungen in derartigen Reaktionen wurde nur in wenigen Beispielen mit begrenztem Substratumfang erreicht.^[5] Als zweite Möglichkeit kann die Friedel-Crafts-Reaktion angesehen werden. Hydroxy-, Halogen- oder Acetoxysubstituenten in benzyliischen Positionen werden durch Metallkatalysatoren zu kationischen Zwischenstufen gespalten. Diese können Kupplungen mit nucleophilen Arenen eingehen. Die Aktivierung durch Metallkatalysatoren ist in den meisten Fällen unerlässlich, und es wurden verschiedene Katalysatoren eingesetzt (RhCl₃,^[6] IrCl₃,^[6] H₂PdCl₄,^[6] H₂PtCl₆,^[6] HAuCl₄,^[7] FeCl₃^[8] und Bi(OTf)₃).^[9]

Weitere Nachteile sind außer den anspruchsvollen Reaktionsbedingungen (erhöhte Temperatur, wasserfreie Lösungsmittel und/oder inerte Atmosphäre) auch die geringe Regioselektivität und große Mengen an Salzabfällen.^[6]

Die Vermeidung von stöchiometrischen Reagentien und Reagensabfällen ist ein wichtiger Faktor bei der Entwicklung eines umweltverträglicheren, „grüneren“ Weges zu Diarylmethanen.^[10] Zu diesem Zweck sind Methoden für dehydrierende Kupplungsreaktionen von großem Interesse. Die Elektrochemie, besonders die anodische Umwandlung, ist ein wertvolles Hilfsmittel für die Entwicklung von solchen metall- und reagensfreien, nachhaltigen Transformationen.^[11] Dies wurde 2016 mit einer von Yoshida et al. entwickelten, elektrochemischen Benzyl-Aryl-Kupplung für die Synthese von Diarylmethanen gezeigt.^[12] Für die Anreicherung der elektrochemisch oxidierten Spezies in diesem Verfahren müssen die gebildeten Benzylkationen wegen ihrer hohen Reaktivität mit einem zusätzlichen Reagens abgefangen werden. Anschließend erfolgen die Eliminierung des Stabilisierungsreagens und die Kupplung mit aromatischen Nucleophilen. Durch die Trennung von Oxidations- und Kupplungsreaktion erfolgt die Bindungsbildung selektiv. Diese Methode weist jedoch einige Nachteile auf: Das Stabilisierungsreagens ist nicht im Handel erhältlich und muss in großem Überschuss verwendet werden. Die Kupplungsreak-

*] Y. Imada, J. L. Röckl, Dr. A. Wiebe, Dr. T. Gieshoff, Dr. D. Schollmeyer, Prof. Dr. S. R. Waldvogel
 Institut für Organische Chemie
 Johannes Gutenberg-Universität Mainz
 Duesbergweg 10–14, 55128 Mainz (Deutschland)
 E-Mail: waldvogel@uni-mainz.de
 Homepage: <http://www.chemie.uni-mainz.de/OC/AK-Waldvogel/>


Y. Imada, Prof. Dr. K. Chiba
 Department of Applied Biological Science
 Tokyo University of Agriculture and Technology (Japan)

Y. Imada, Dr. T. Gieshoff, Prof. Dr. S. R. Waldvogel
 Graduate School Materials Science in Mainz
 Johannes Gutenberg-Universität Mainz (Deutschland)

Dr. A. Wiebe, Prof. Dr. S. R. Waldvogel
 Max Planck Graduate Center
 Johannes Gutenberg-Universität Mainz (Deutschland)

Prof. Dr. R. Franke
 Evonik Performance Materials GmbH
 Marl (Deutschland)

Prof. Dr. R. Franke
 Lehrstuhl für Theoretische Chemie
 Ruhr-Universität Bochum (Deutschland)

 Hintergrundinformationen und die Identifikationsnummer (ORCID) eines Autors sind unter:
<https://doi.org/10.1002/ange.201804997> zu finden.

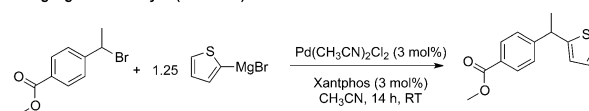
tion kann bis zu 35 h dauern, und alle Umsetzungen wurden nur im kleinen Maßstab (0.1 mmol) demonstriert. Über die Anwendung von freien Phenolen für die anodische Umsetzung wurde nicht berichtet. Zudem ist das Verfahren infolge des komplexen Elektrolyseaufbaus (eine geteilte Zelle mit sehr spezifischer Kohlefaser-Anode) nicht einfach skalierbar. Daher ist ein einfacher, nachhaltiger und skalierbarer Ansatz für die Synthese von Diarylmethanen immer noch von großem Interesse. In einem aktuellen Beitrag von Stahl und Mitarbeitern liefert eine elektrochemisch vermittelte Iodierung Substrate für die Benzyl-Aryl-Kupplung.^[13]

Als Folge unseres Interesses an elektrochemischen Umsetzungen hat unsere Gruppe effiziente elektrochemische C-C- und N-N-Kupplungen mit Phenolen,^[14] Aniliden^[15] und Dianiliden als Substrate entwickelt.^[16] Der Schlüssel zu diesen Umwandlungen war die Verwendung von 1,1,1,3,3,3-Hexafluorpropan-2-ol (HFIP) als Lösungsmittel. HFIP hat einzigartige Eigenschaften. Es stabilisiert reaktive Zwischenprodukte,^[17] hat eine einzigartige Lösungsmittelmikrostruktur^[18] sowie interessante Solvatisierungseigenschaften und kann somit selektive Transformationen ermöglichen.^[14c,19] HFIP wurde auch von Paquin et al. als Lösungsmittel in einem nicht-elektrochemischen Ansatz zur Aktivierung von Benzylfluoriden in Benzyl-Aryl-Kupplungen verwendet.^[20] Wegen der geringen Nukleophilie gibt es kaum Berichte über Reaktionen mit nukleophilem HFIP-Angriff.^[21] Kürzlich hat unsere Gruppe die anodische Funktionalisierung von Aniliden mit HFIP an benzyllischen und aromatischen Positionen gezeigt.^[16b]

Hier berichten wir über die selektive elektrochemische Funktionalisierung von benzyllischen Positionen durch HFIP. Diese direkten elektrochemischen C-H-Funktionalisierungen erfordern oft Katalysatorsysteme.^[22] Der Ether fungiert als molekulare Maske für das Benzylkation und stabilisiert dieses reaktive Zwischenprodukt durch Abfangen mit Lösungsmittel in einem weniger reaktiven Zustand. Eine derartige Aktivierung dieser maskierten Kationen zur Erleichterung einer effizienten und selektiven Benzyl-Aryl-Kupplung wird hier erstmals beschrieben. Wir präsentieren eine einfache, nachhaltige, leicht skalierbare, reagens- und metallfreie elektrochemische Benzyl-Aryl-Kreuzkupplung in einer zweistufigen Eintopfreaktion (Schema 1).

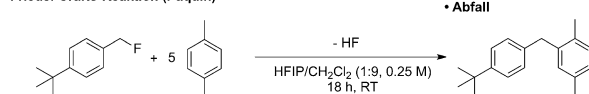
Zunächst wurde die elektrochemische HFIP-Etherbildung optimiert (Tabelle 1). Als Testsubstrat wurde Phenol **1** ausgewählt. Die elektrochemischen Parameter für die anodische Phenol-Thiophen-Kreuzkupplung wurden als Ausgangsbedingungen verwendet.^[14c] Ein Screening von Additiven führte zu einer effizienten HFIP-Etherbildung mit 0.57 Äquivalenten *N*-Ethyl-*N,N*-di(methylethyl)amin (DIPEA; Tabelle 1, Nr. 1). Wir haben dies dem Grundcharakter des Additivs zugeschrieben. Ein ähnlicher Effekt, jedoch bei geringerer Ausbeute und Selektivität, wurde mit Triethylamin (TEA), K₂CO₃ oder Cs₂CO₃ als Basen erreicht (Tabelle 1, Nr. 2 und Hintergrundinformationen (SI)). 2.2 F und 7.2 mA cm⁻² waren die optimalen elektrolytischen Bedingungen (Tabelle 1, Nr. 3–7).

Übergangsmetallkatalyse (Carretero)



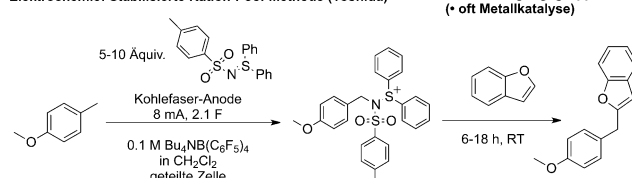
- zweifache Vorfunktionalisierung
- Übergangsmetallkatalysator + Ligand
- luft- und wasserempfindlich
- lange Reaktionszeiten
- Abfall

Friedel-Crafts-Reaktion (Paquin)



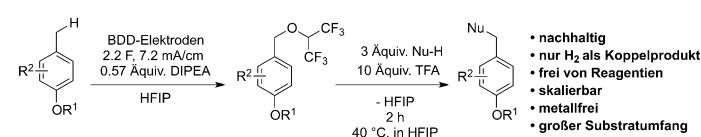
- Vorfunktionalisierung
- lange Reaktionszeiten
- HF als Abgangsgruppe (• oft Metallkatalyse)

Elektrochemie: Stabilisierte Kation-Pool-Methode (Yoshida)



- Überschuss an stabilisierendem Reagens
- lange Reaktionszeiten
- nur kleiner Maßstab
- limitierter Substratumfang

Elektrochemie: Diese Arbeit



- nachhaltig
- nur H₂ als Koppelprodukt
- frei von Reagentien
- skalierbar
- metallfrei
- großer Substratumfang

Schema 1. Strategien zur Benzyl-Aryl-Kupplung im Vergleich zu unserer neuen Methode.

Tabelle 1: Optimierung der anodischen Funktionalisierung von 4-Methylguajacol mit HFIP.^[a]

Nr.	Abweichung von den Standardbedingungen	Ausb. ^[b] [%]
1	–	72
2	TEA statt DIPEA	42
3	1.9 F	64
4	2.2 F	78
5	2.4 F	56
6	2.2 F, 5 mA cm ⁻²	67
7	2.2 F, 10 mA cm ⁻²	63
8	Graphitelektroden, 2.2 F	76
9	Graphitelektroden, ohne Leitsalz, 2.2 F	72
10	ohne Leitsalz, 2.2 F	78
11	ohne Leitsalz, 2.2 F, 1.14 Äquiv. DIPEA	69
12	ohne DIPEA	0

[a] Alle Reaktionen wurden mit 1.0 mmol Phenol **1** in 5 mL HFIP in einer ungeteilten Zelle durchgeführt. MTBS = Methyltributylmethylsulfat.

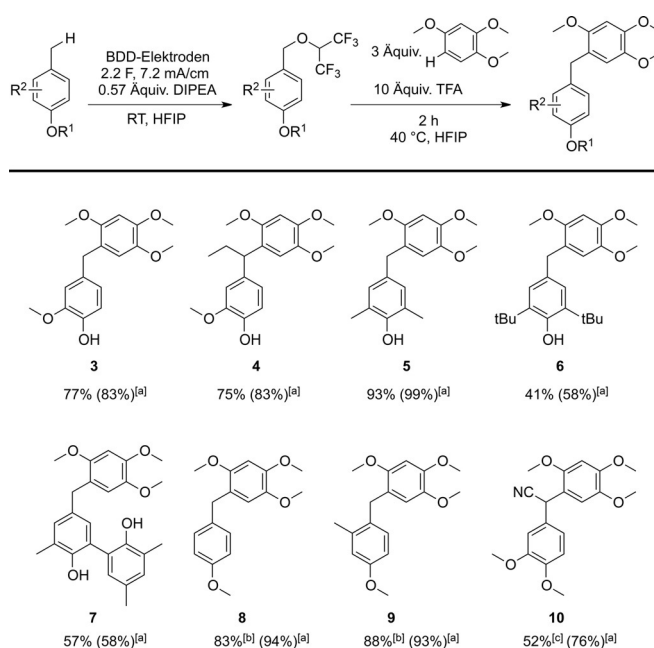
[b] Die Ausbeuten wurden mittels ¹H-NMR-Spektroskopie mit Benzaldehyd als Standard bestimmt.

Die Oxidation an Graphitanoden, die günstiger sind als bordotierte Diamantanoden (BDD-Anoden), liefert den gewünschten HFIP-Ether in ähnlichen Ausbeuten (Tabelle 1, Nr. 8). Dies ist besonders interessant für technische Anwendungen. Wir merken allerdings an, dass wir hier wegen der etwas besseren Ausbeuten auf BDD-Anoden zurückgegriffen

haben. Ein wichtiger Schritt zu einem grüneren Verfahren wurde mit der Feststellung gemacht, dass DIPEA mit HFIP eine ausreichende Leitfähigkeit erzeugt und deshalb kein zusätzliches Leitsalz bei dieser Umwandlung erforderlich ist (Tabelle 1, Nr. 9 und 10). Dies kann durch Salzbildung zwischen dem Lösungsmittel HFIP ($pK_a = 9.3$)^[21] und DIPEAH⁺ ($pK_a = 11.4$)^[23] erklärt werden. Eine Verdoppelung der DIPEA-Menge hat die Ausbeute nicht verbessert (Tabelle 1, Nr. 11). In einem Kontrollversuch (Tabelle 1, Nr. 12) wurde die Bedeutung von DIPEA als Additiv ermittelt. Ohne Additiv dominierten Phenol-Homokupplung sowie -Oligomerisierung.

Während die selektive Bildung von benzylichen HFIP-Ethern unter Verwendung von HFIP als Nukleophil eine beispiellose Transformation darstellt, waren wir besonders daran interessiert, Anwendungen dieses Motivs in der weiteren Synthese zu untersuchen. Gegenüber einem 2013 vorgestellten Ansatz, der das Einfangen von Kationen in der α -Position von Amiden in Shono-Oxidationsprodukten von Lactamen demonstriert,^[24] ist die Stabilisierung und anschließende Aktivierung von Benzylkationen eine deutlich anspruchsvollere Aufgabe. Wir fanden heraus, dass die Umsetzung mit 2,2,2-Trifluoressigsäure (TFA) zur Bildung eines aktiven Benzylkations führte. Erfolgt diese Aktivierung in Gegenwart einer äquimolaren bis hin zu einer dreifachen Menge eines aromatischen Nucleophils, kann eine selektive Benzyl-Aryl-Kreuzkupplung erreicht werden. Wir haben diese Kupplungsreaktion mit 1,2,4-Trimethoxybenzol als Testsubstrat optimiert. Unter den optimierten Bedingungen für den ersten und zweiten Schritt wurde die Bandbreite der möglichen Substrate für die HFIP-Etherbildung untersucht. Für die anschließende benzyliche Kreuzkupplung fungierte 1,2,4-Trimethoxybenzol als Testnucleophil (Schema 2).

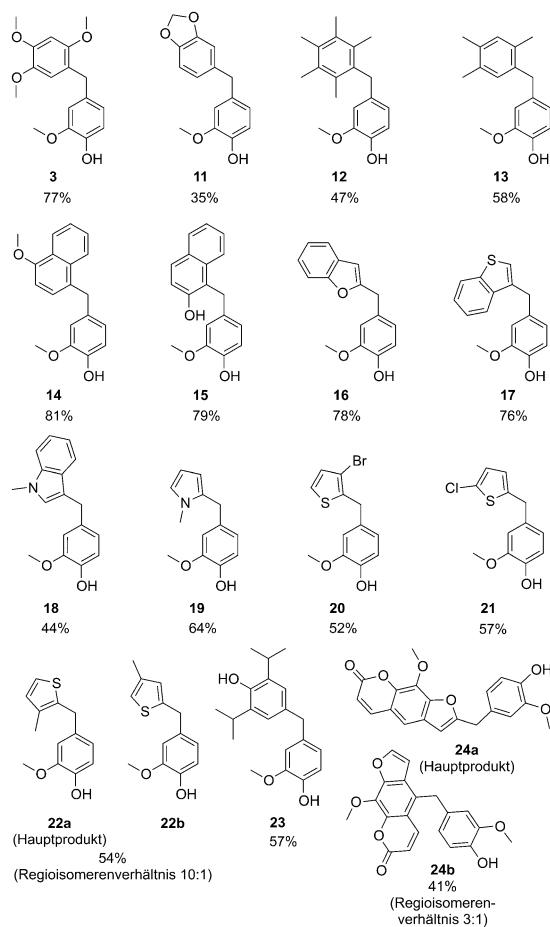
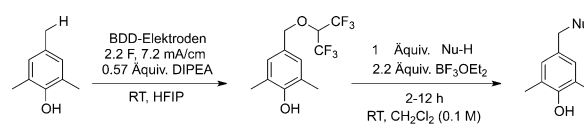
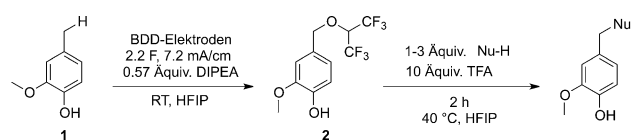
Die elektrochemische Funktionalisierung mit HFIP an der benzylichen Position und anschließende Benzyl-Aryl-Kreuzkupplung wurden mit einer Vielzahl von Substraten in Ausbeuten von bis zu 93% (**5**) erreicht. Ungeschützte Phenole können an primäre (**3**, **5**, **6**) und sekundäre benzyliche Positionen (**4**) gekuppelt werden. Zusätzlich wurde die Funktionalisierung von Biphenolen nachgewiesen (**7**). Unsere Methode erwies sich als komplementär zum „stabilisierten Kation-Pool“, da Anisol und Anisolderivate in hoher Ausbeute gekuppelt werden konnten (**8–10**). Produkt **10** ist besonders interessant, da die Nitrilgruppe eine weitere einfache Funktionalisierung ermöglicht. Falls bei der Elektrolyse (**8** und **9**) eine Dehydromerisierung oder Oligomerisierung zu beobachten waren, wurde die Konzentration des Ausgangsmaterials verringert, was zu hohen Ausbeuten (83 und 88%) der gewünschten Kupplungsprodukte führte. Als logischen Schritt führten wir Untersuchungen zur Kupplung mit verschiedenen Nucleophilen durch. Für diesen Ansatz wurde die Elektrolyse unter optimierten Reaktionsbedingungen mit 4-Methylguajacol als Testsystem durchgeführt und der nachfolgende Kupplungsschritt untersucht (Schema 3). Die Reaktion gelang mit vielfältigen Nucleophilen. Arene mit stark elektronenschiebenden Gruppen (**3** und **11**) sowie methylierte Arene (**12** und **13**) wurden mit 4-Methylguajacol kreuzgekuppelt. Die Reaktion mit einem freien Phenol verlief in guter Ausbeute (**23**). Naphthalinderivate, einschließlich



Scheme 2. Möglichkeit der anodischen Funktionalisierung mit HFIP und anschließende Kupplung an 1,2,4-Trimethoxybenzol. Die Elektrolyse wurde in 5 mL HFIP mit 1 mmol Substrat in einer ungeteilten Zelle durchgeführt. [a] Ausbeute des benzylichen HFIP-Ethers nach der Elektrolyse, bestimmt durch ¹⁹F-NMR-Spektroskopie. [b] 0.5 mmol Substrat und 3.0 F wurden zur optimalen elektrochemischen Umsetzung verwendet. [c] Elektrolyse mit 1.8 F, Aktivierung für die zweite Reaktion mit *p*-Toluolsulfonsäure statt TFA, Reaktionszeit 3 h.

1-Methoxynaphthalin und ungeschütztes 2-Naphthol, wurden in hohen Ausbeuten von bis zu 81% (**14** und **15**) gekuppelt. Die Kupplung von 4-Methylguajacol mit Heterocyclen wie Benzofuran, Benzothiophen, *N*-Methylindol, *N*-Methylpyrrol und Thiophenderivaten ist möglich (**16–22b**). Die Umwandlung ist verträglich mit einer Vielzahl von Substituenten (Methoxy, Methyl, Hydroxy, Chlor und Brom). In den meisten Fällen erfolgt die Kupplung mild und selektiv. Nur bei 3-Methylthiophen wurde die Bildung von Regioisomeren (**22a** und **22b**) beobachtet. Wichtig ist, dass diese Benzyl-Aryl-Kreuzkupplung in wesentlich kürzerer Zeit als die von Yoshida et al. durchgeführt werden kann.^[12] Außerdem ist zu beachten, dass HFIP als Lösungsmittel wie auch als Nucleophil in diesem Verfahren verwendet wurde und vollständig zurückgewonnen sowie wiederverwendet werden kann.^[21] Dies führt zu einer Gesamtreaktionsbilanz mit lediglich Wasserstoff als Nebenprodukt für die C-C-Kreuzkupplung.

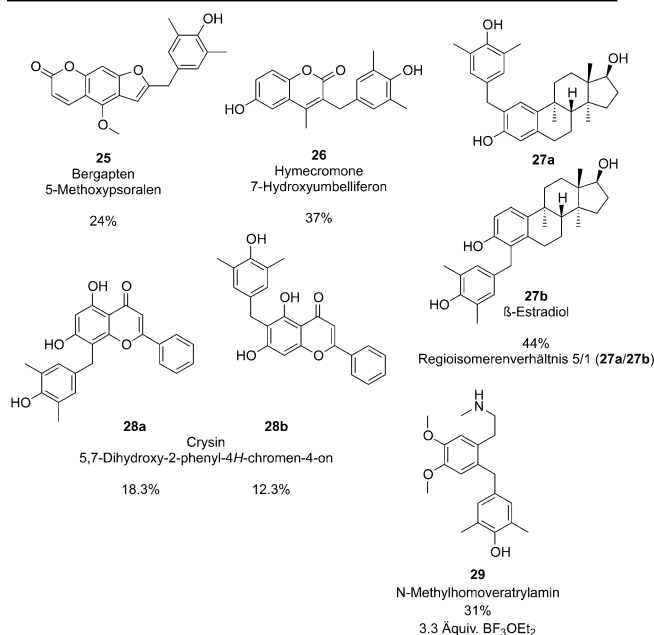
Um das volle Potenzial dieser Methode auszuschöpfen, war die Derivatisierung von Naturstoffen von großem Interesse. Erste Ansätze mit 2,2,2-Trifluoressigsäure führten zu komplexen Mischungen. Weitere Versuche mit Lewis-Säuren in Dichlormethan waren vielversprechend. Die Verwendung von β -Estradiol als Nucleophil und Aluminiumchlorid führte zu einer Ausbeute von 32% des gekuppelten Produktes. Die weitere Optimierung dieses Systems mit BF₃·OEt₂ (2.2 Äquivalente) steigerte die Ausbeute des gekuppelten Produktes auf 44%. Auf Grundlage dieser ersten Ergebnisse konnten wir eine Reihe von Naturstoffen und biologisch aktiven Substanzen in moderaten Ausbeuten funktionalisieren



Scheme 3. Variation des Nucleophils in der Kupplungsreaktion mit 4-Methylguajacol. Die Elektrolyse wurde in 5 mL HFIP mit 1 mmol Phenol **1** in einer ungeteilten Zelle durchgeführt.

(Scheme 4). Fünf Klassen von Naturstoffen (Steroid **27**, Umbelliferon **26**, Psolaren **25**, Phenylethylamin **29** und Flavon **28**) wurden derivatisiert. Die Kupplung wurde an verschiedenen Stellen erreicht, was die Allgemeingültigkeit dieser Methode zur exklusiven C-Funktionalisierung auch in Gegenwart von nukleophilen Sauerstoff- (**26**, **27** und **28**) oder Stickstoffatomen (**29**) verdeutlicht. Zusätzlich wurden Molekülstrukturen durch Röntgenstrukturanalyse der Psolaren- und Umbelliferonderivate gewonnen (siehe Hintergrundinformationen). Diese neuen Derivate könnten als potenziell biologisch aktive Verbindungen von Interesse sein. Die Prüfung der biologischen Aktivität ist im Gange.

Um die Skalierbarkeit unserer Methode zu demonstrieren, haben wir die Synthese von **17** als Modellreaktion gewählt. Die Struktureinheit von **17** ist von großem Interesse für pharmazeutische Wirkstoffe.^[25] Eine einfache und skalierbare Methode zur Synthese dieser Diarylmethane bietet daher eine neue, vielseitige Strategie. Wir haben die Elektrolyse um den Faktor 40 vergrößert. Es wurde also eine Elektrolyse mit



Scheme 4. Benzylierte Naturstoffe und bioaktive Verbindungen unter Verwendung von $\text{BF}_3 \cdot \text{OEt}_2$ (2.2 Äquiv.), 0.1 M in CH_2Cl_2 , RT, 2–12 h.

40 mmol Phenol **1** in einer 200-mL-Becherglaszelle durchgeführt (Abbildung 1). Für die anodische Funktionalisierung mit HFIP wurde kein Abfallen der Selektivität beobachtet. Diese Mischung wurde direkt der Kupplungsreaktion mit Benzothiophen unterzogen, um schließlich 6.91 g des gewünschten Produkts **17** in einem einzigen Ansatz (64% Ausbeute) zu erhalten. Die Ausbeute ist etwas geringer als im 5-mL-Maßstab (76%). Dies kann durch eine noch nicht op-



Abbildung 1. 5-mL- und 200-mL-Becherglaszellen für die Hochskalierung. Zum Größenvergleich wurde eine 2€-Münze (Durchmesser 25.75 mm, ca. 1.01 Zoll) zwischen die beiden Zellen gelegt. Weitere Details finden Sie in den Hintergrundinformationen.

timierte Zugabe von TFA in größerem Maßstab erklärt werden. Dennoch konnte die Reaktionszeit innerhalb dieser Hochskalierung sogar von 2 auf 1 h verringert werden.

Wir haben ein sehr effizientes Verfahren für die elektrochemische Funktionalisierung von benzylicchen Positionen durch HFIP entwickelt. Kleine Mengen DIPEA können als Additiv verwendet werden, um selektiv zu diesem Reaktionsweg zu führen und einen zusätzlichen Hilfselektrolyten vollständig zu ersetzen. Der Anwendungsbereich wurde mit Phenolen, Anisolen und der Funktionalisierung von Naturstoffen demonstriert. Die benzylicche HFIP-Funktionalisierung kann mit Säure aktiviert werden, um eine dehydrierende Benzyl-Aryl-Kreuzkupplung mit einer Vielzahl von verschiedenen Nukleophilen in hoher Ausbeute durchzuführen. Dieses Verfahren bietet einen skalierbaren, metallfreien und reagentiensparenden Weg zu Diarylmethanen, der das Potenzial hat, verschiedene Synthesewege zu verkürzen. Es ist gut vorstellbar, dass die Aktivierung von elektrogenierten HFIP-Ethern in verschiedenen Reaktionen Anwendung finden wird. Zusätzlich könnte diese Methode erweitert und für Anilide optimiert werden, wie bereits in ersten Schritten von unserer Gruppe gezeigt. Diese Route ist damit allgemeingültig für zahlreiche chemische Umwandlungen.

Danksagung

Wir danken der DFG (GSC 266, Wa 1276/17-1, Wa 1276/14-1) für die finanzielle Unterstützung. Die Unterstützung durch das Advanced Lab of Electrochemistry and Electrosynthesis – ELYSION (Carl Zeiss Stiftung) wird dankbar gewürdigt. Y.I. dankt dem Ministerium für Bildung, Kultur, Wissenschaft und Technologie (MEXT), Japan, für die Unterstützung durch das Programm for Leading Graduate School of TUAT. Y.I. und T.G. bedanken sich bei der Graduiertenschule Material Science in Mainz (MAINZ) für die finanzielle Unterstützung. A.W. dankt dem Max-Planck-Graduiertenzentrum für die finanzielle Unterstützung.

Interessenkonflikt

Die Autoren erklären, dass keine Interessenkonflikte vorliegen.

Stichwörter: Benzylicche Kupplungen · Elektrochemie · Grüne Chemie · HFIP · Naturstoffe

Zitierweise: *Angew. Chem. Int. Ed.* **2018**, *57*, 12136–12140
Angew. Chem. **2018**, *130*, 12312–12317

- [1] K. L. McPhail, D. E. A. Rivett, D. E. Lack, M. T. Davies-Coleman, *Tetrahedron* **2000**, *56*, 9391–9396.
- [2] Y.-Q. Long, X.-H. Jiang, R. Dayam, T. Sanchez, R. Shoemaker, S. Sei, N. Neamati, *J. Med. Chem.* **2004**, *47*, 2561–2573.
- [3] a) M. Ahmad, J. K. Luo, H. Purnawali, W. M. Huang, P. J. King, P. R. Chalker, M. Mireftab, J. Geng, *J. Mater. Chem.* **2012**, *22*, 8192–8194; b) S. Wang, C. Zhang, Y. Shu, S. Jiang, Q. Xia, L. Chen, S. Jin, I. Hussain, A. I. Cooper, B. Tan, *Sci. Adv.* **2017**, *3*, e1602610.
- [4] a) A. López-Pérez, J. Adrio, J. C. Carretero, *Org. Lett.* **2009**, *11*, 5514–5517; b) M. J. Burns, I. J. S. Fairlamb, A. R. Kapdi, P. Sehnal, R. J. K. Taylor, *Org. Lett.* **2007**, *9*, 5397–5400; c) B. P. Bandgar, S. V. Bettigeri, J. Phopase, *Tetrahedron Lett.* **2004**, *45*, 6959–6962; d) S. M. Nobre, A. L. Monteiro, *Tetrahedron Lett.* **2004**, *45*, 8225–8228; e) J.-Y. Yu, R. Kuwano, *Org. Lett.* **2008**, *10*, 973–976.
- [5] a) T. Mukai, K. Hirano, T. Satoh, M. Miura, *Org. Lett.* **2010**, *12*, 1360–1363; b) D. Lapointe, K. Fagnou, *Org. Lett.* **2009**, *11*, 4160–4163; c) J. Zhang, A. Bellomo, A. D. Creamer, S. D. Dreher, P. J. Walsh, *J. Am. Chem. Soc.* **2012**, *134*, 13765–13772.
- [6] K. Mertins, I. Iovel, J. Kischel, A. Zapf, M. Beller, *Angew. Chem. Int. Ed.* **2005**, *44*, 238–242; *Angew. Chem.* **2005**, *117*, 242–246.
- [7] K. Mertins, I. Iovel, J. Kischel, A. Zapf, M. Beller, *Adv. Synth. Catal.* **2006**, *348*, 691–695.
- [8] I. Iovel, K. Mertins, J. Kischel, A. Zapf, M. Beller, *Angew. Chem. Int. Ed.* **2005**, *44*, 3913–3917; *Angew. Chem.* **2005**, *117*, 3981–3985.
- [9] M. Rueping, B. J. Nachtsheim, W. Ieawsuwan, *Adv. Synth. Catal.* **2006**, *348*, 1033–1037.
- [10] P. Anastas, N. Eghbali, *Chem. Soc. Rev.* **2010**, *39*, 301–312.
- [11] a) A. Wiebe, T. Gieshoff, S. Möhle, E. Rodrigo, M. Zirbes, S. R. Waldvogel, *Angew. Chem. Int. Ed.* **2018**, *57*, 5594–5619; *Angew. Chem.* **2018**, *130*, 5694–5721; b) S. Möhle, M. Zirbes, E. Rodrigo, T. Gieshoff, A. Wiebe, S. R. Waldvogel, *Angew. Chem. Int. Ed.* **2018**, *57*, 6018–6041; *Angew. Chem.* **2018**, *130*, 6124–6149.
- [12] R. Hayashi, A. Shimizu, J.-I. Yoshida, *J. Am. Chem. Soc.* **2016**, *138*, 8400–8403.
- [13] M. Rafiee, F. Wang, D. P. Hruszkewycz, S. S. Stahl, *J. Am. Chem. Soc.* **2018**, *140*, 22–25.
- [14] a) A. Wiebe, D. Schollmeyer, K. M. Dyballa, R. Franke, S. R. Waldvogel, *Angew. Chem. Int. Ed.* **2016**, *55*, 11801–11805; *Angew. Chem.* **2016**, *128*, 11979–11983; b) A. Wiebe, B. Riehl, S. Lips, R. Franke, S. R. Waldvogel, *Sci. Adv.* **2017**, *3*, eaao3920; c) A. Wiebe, S. Lips, D. Schollmeyer, R. Franke, S. R. Waldvogel, *Angew. Chem. Int. Ed.* **2017**, *56*, 14727–14731; *Angew. Chem.* **2017**, *129*, 14920–14925; d) S. Lips, A. Wiebe, B. Elsler, D. Schollmeyer, K. M. Dyballa, R. Franke, S. R. Waldvogel, *Angew. Chem. Int. Ed.* **2016**, *55*, 10872–10876; *Angew. Chem.* **2016**, *128*, 11031–11035; e) B. Elsler, A. Wiebe, D. Schollmeyer, K. M. Dyballa, R. Franke, S. R. Waldvogel, *Chem. Eur. J.* **2015**, *21*, 12321–12325.
- [15] L. Schulz, M. Enders, B. Elsler, D. Schollmeyer, K. M. Dyballa, R. Franke, S. R. Waldvogel, *Angew. Chem. Int. Ed.* **2017**, *56*, 4877–4881; *Angew. Chem.* **2017**, *129*, 4955–4959.
- [16] a) T. Gieshoff, D. Schollmeyer, S. R. Waldvogel, *Angew. Chem. Int. Ed.* **2016**, *55*, 9437–9440; *Angew. Chem.* **2016**, *128*, 9587–9590; b) T. Gieshoff, A. Kehl, D. Schollmeyer, K. D. Moeller, S. R. Waldvogel, *J. Am. Chem. Soc.* **2017**, *139*, 12317–12324.
- [17] L. Ebersson, O. Persson, M. P. Hartshorn, *Angew. Chem. Int. Ed. Engl.* **1995**, *34*, 2268–2269; *Angew. Chem.* **1995**, *107*, 2417–2418.
- [18] O. Hollóczki, A. Berkessel, J. Mars, M. Mezger, A. Wiebe, S. R. Waldvogel, B. Kirchner, *ACS Catal.* **2017**, *7*, 1846–1852.
- [19] a) B. Elsler, D. Schollmeyer, K. M. Dyballa, R. Franke, S. R. Waldvogel, *Angew. Chem. Int. Ed.* **2014**, *53*, 5210–5213; *Angew. Chem.* **2014**, *126*, 5311–5314; b) A. Kirste, B. Elsler, G. Schnakenburg, S. R. Waldvogel, *J. Am. Chem. Soc.* **2012**, *134*, 3571–3576; c) A. Kirste, G. Schnakenburg, F. Stecker, A. Fischer, S. R. Waldvogel, *Angew. Chem. Int. Ed.* **2010**, *49*, 971–975; *Angew. Chem.* **2010**, *122*, 983–987; d) A. Kirste, M. Nieger, I. M. Malkowsky, F. Stecker, A. Fischer, S. R. Waldvogel, *Chem. Eur. J.* **2009**, *15*, 2273–2277.
- [20] P. A. Champagne, Y. Benhassine, J. Desroches, J.-F. Paquin, *Angew. Chem. Int. Ed.* **2014**, *53*, 13835–13839; *Angew. Chem.* **2014**, *126*, 14055–14059.
- [21] I. Colomer, A. E. R. Chamberlain, M. B. Haughey, T. J. Donohoe, *Nat. Rev. Chem.* **2017**, *1*, 0088.

- [22] a) Q.-L. Yang, Y.-Q. Li, C. Ma, P. Fang, X.-J. Zhang, T.-S. Mei, *J. Am. Chem. Soc.* **2017**, *139*, 3293–3298; b) A. Shrestha, M. Lee, A. L. Dunn, M. S. Sanford, *Org. Lett.* **2018**, *20*, 204–207.
- [23] T. Fujii, H. Nishidam, Y. Abiru, M. Yamamoto, M. Kise, *Chem. Pharm. Bull.* **1995**, *43*, 1872–1877.
- [24] T. Tajima, H. Kurihara, S. Shimizu, H. Tateno, *Electrochemistry* **2013**, *81*, 353–355.
- [25] a) T. A. Grese, S. Cho, H. U. Bryant, H. W. Cole, A. L. Glasebrook, D. E. Magee, D. L. Phillips, E. R. Rowley, L. L. Short, *Bioorg. Med. Chem. Lett.* **1996**, *6*, 201–206; b) A. D. Palkowitz, A. L. Glasebrook, K. J. Thrasher, K. L. Hauser, L. L. Short, D. L. Phillips, B. S. Muehl, M. Sato, P. K. Shetler, G. J. Cullinan, T. R. Pell, H. U. Bryant, *J. Med. Chem.* **1997**, *40*, 1407–1416; c) D. J. Sall, S. L. Briggs, N. Y. Chirgadze, D. K. Clawson, D. S. Gifford-Moore, V. J. Klimkowski, J. R. McCowan, G. F. Smith, J. H. Wikel, *Bioorg. Med. Chem. Lett.* **1998**, *8*, 2527–2532.

Manuskript erhalten: 29. April 2018
Akzeptierte Fassung online: 24. Mai 2018
Endgültige Fassung online: 28. Juni 2018

Supporting Information

Metal- and Reagent-Free Dehydrogenative Formal Benzyl–Aryl Cross-Coupling by Anodic Activation in 1,1,1,3,3,3-Hexafluoropropan-2-ol

*Yasushi Imada, Johannes L. Röckl, Anton Wiebe, Tile Gieshoff, Dieter Schollmeyer, Kazuhiro Chiba, Robert Franke, and Siegfried R. Waldvogel**

anie_201804997_sm_miscellaneous_information.pdf

Table of Contents

General information.....	3
General protocol for benzyl-aryl cross-coupling reaction (GP).....	4
Proposed mechanisms for anodic HFIP ether formation and benzyl-aryl cross-coupling reaction	6
Cyclic voltammetry studies	7
Synthesis of benzylic HFIP ether.....	10
Synthesis of benzyl-aryl cross-coupling product	11
Synthesis of benzylated natural products and bioactive compounds (late-stage functionalization)	34
40 mmol scale synthesis in a 200 mL beaker-type cell	41
NMR spectra	42
References.....	73

General information

All reagents were used in analytical or sufficiently pure grades. Solvents were purified by standard methods.^[1] *N*-Methyl-*N,N,N*-tributylammonium methylsulfate (kindly provided by BASF SE, Ludwigshafen, Germany) was used as supporting electrolyte. Electrochemical reactions were carried out at boron-doped diamond (BDD) electrodes. BDD electrodes were obtained as DIACHEM™ quality from CONDIAS GmbH, Itzehoe, Germany. BDD (15 μm diamond layer) on silicon support.

Column chromatography was performed on silica gel 60 M (0.040–0.063 mm, Macherey-Nagel GmbH & Co, Düren, Germany) with a maximum pressure of 1.6 bar. In addition, a preparative chromatography system (Büchi Labortechnik GmbH, Essen, Germany) was used with a Büchi Control Unit C-620, an UV detector Büchi UV photometer C-635, Büchi fraction collector C-660 and two Pump Modules C-605 for adjusting the solvent mixtures. As eluents mixtures of cyclohexane and ethyl acetate were used. Silica gel 60 sheets on aluminum (F254, Merck, Darmstadt, Germany) were used for thin layer chromatography.

Gas chromatography was performed on a Shimadzu GC-2010 (Shimadzu, Japan) using a ZB-5 column (Phenomenex, USA; length: 30 m, inner diameter: 0.25 mm, film: 0.25 μm, carrier gas: hydrogen/air). GC-MS measurements were carried out on a Shimadzu GC-2010 (Shimadzu, Japan) using a ZB-5 column (Phenomenex, USA; length: 30 m, inner diameter: 0.25 mm, film: 0.25 μm, carrier gas: helium). The chromatograph was coupled to a mass spectrometer: Shimadzu GCMS-QP2010.

High Performance Liquid Chromatography (HPLC) was performed on a Azura preparative HPLC (KNAUER Wissenschaftliche Geräte GmbH, Germany) using a Eurospher II column (pore size: 100 Å, particle size: 5 μm, length: 250 mm, inner diameter: 30 mm), deuterium lamp as a detector and 2.1 L pump.

Melting points were determined with a Melting Point Apparatus B-545 (Büchi, Flawil, Switzerland) and are uncorrected. Heating rate: 2 °C/min.

Spectroscopy and spectrometry ¹H NMR, ¹³C and ¹⁹F NMR spectra were recorded at 25 °C, using a Bruker Avance III HD 400 (400 MHz) (5 mm BBFO-SmartProbe with z gradient and ATM, SampleXPress 60 sample changer, Analytische Messtechnik, Karlsruhe, Germany). Chemical shifts (δ) are reported in parts per million (ppm) relative to traces in the corresponding deuterated solvent. Mass spectra and high-resolution mass spectra were obtained by using a QToF Ultima 3 (Waters, Milford, Massachusetts) apparatus employing ESI⁺.

Cyclic voltammetry was performed with a Metrohm 663 VA Stand equipped with a μAutolab type III potentiostat (Metrohm AG, Herisau, Switzerland). *WE*: BDD electrode tip, 2 mm diameter; *CE*: glassy carbon rod; *RE*: Ag/AgCl in saturated LiCl/EtOH. Solvent: HFIP. $v = 100$ mV/s, $T = 20$ °C, $c = 0.005$ M, supporting electrolyte (if used): ^tBu₃NMe O₃SOMe (MTBS), c (MTBS) = 0.09 M.

General protocol for benzyl-aryl cross-coupling reaction (GP)

GP I: Undivided PTFE cell (5 mL)

The undivided 5 mL PTFE electrolysis cells were homemade by the mechanical shop of the university. Detailed information about used cells are already reported.^[2,3] It is operated with boron-doped diamond electrodes (BDD, 0.3 x 1 x 7 cm, 15 μm diamond layer, support of silicon was used).

A solution of phenol or anisol derivative (0.5–1.0 mmol) and *N*-Ethyl-*N*-(propan-2-yl)propan-2-amine (**DIPEA**) (0.1 mL, 0.57 mmol) in 5 mL 1,1,1,3,3,3-hexafluoropropan-2-ol (**HFIP**) was electrolyzed with a boron-doped Diamond (**BDD**) anode and a BDD cathode. A constant current electrolysis with a current density of 7.2 mA/cm² was performed at room temperature. After 1.8–3.0 F were applied, the reaction solution was diluted with HFIP to 10 mL total volume (to unify the concentration for each reaction). Then, 1.0 eq. - 3.0 eq. of the coupling partner and 10 eq. 2,2,2-trifluoroacetic acid were added to the solution. The mixture was stirred at 40 °C for 2 h. After completion of the reaction, HFIP was recovered by distillation. Residue was dissolved in 30 mL dichloromethane and washed with 70 mL water. The aqueous phase was afterwards washed with 30 mL of dichloromethane. Combined organic phases were dried with MgSO₄ and filtered. After evaporation of the solvent, column chromatography yielded the product.

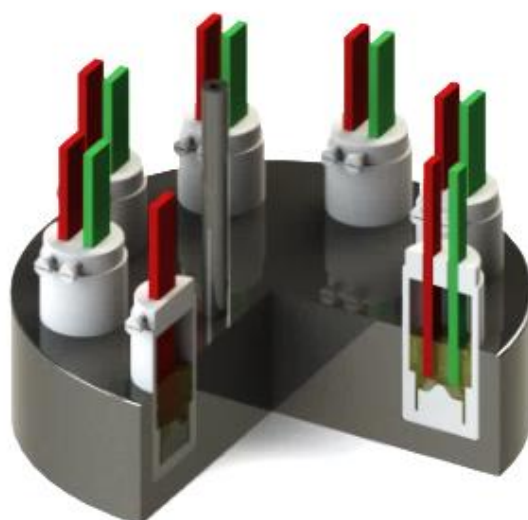


Fig. S1: 5 mL PTFE cells in a stainless steel screening block (for temperature equilibration).

GP II: Beaker-type cell (200 mL)

40 mmol phenol, 200 mL HFIP, and 4.0 mL (0.57 eq.) DIPEA were transferred into an undivided beaker-type electrolysis cell equipped with a BDD anode and a BDD cathode. A constant current electrolysis with a current density of 7.2 mA/cm^2 was performed at room temperature. After 2.2 F were applied, the reaction solution was diluted with HFIP to a total volume of 400 mL. Then, 3.0 eq. of the coupling partner and 10 eq. 2,2,2-trifluoroacetic acid were added to the solution. The mixture was stirred at $40 \text{ }^\circ\text{C}$ for 1 h. The conversion was monitored by GC. After completion of the reaction, HFIP was recovered by distillation. Residue was dissolved in 70 mL dichloromethane and washed with 150 mL water. The aqueous phase was afterwards washed with 70 mL of dichloromethane. Combined organic phases were dried with MgSO_4 and filtered. After evaporation of the solvent, excess amount of the nucleophile was recovered by bulb-to-bulb distillation ($60 \text{ }^\circ\text{C}$, $1 \cdot 10^{-3} \text{ mbar}$). The pure product was obtained by column chromatography of the residue.

The beaker-type cell (200 mL) consists of a simple glass beaker and a glass adapter, closed by a PTFE plug. This cap allows precise arrangement of the BDD electrodes. Total dimension of the BDD electrodes are $14 \text{ cm} \times 3.5 \text{ cm} \times 0.3 \text{ cm}$.

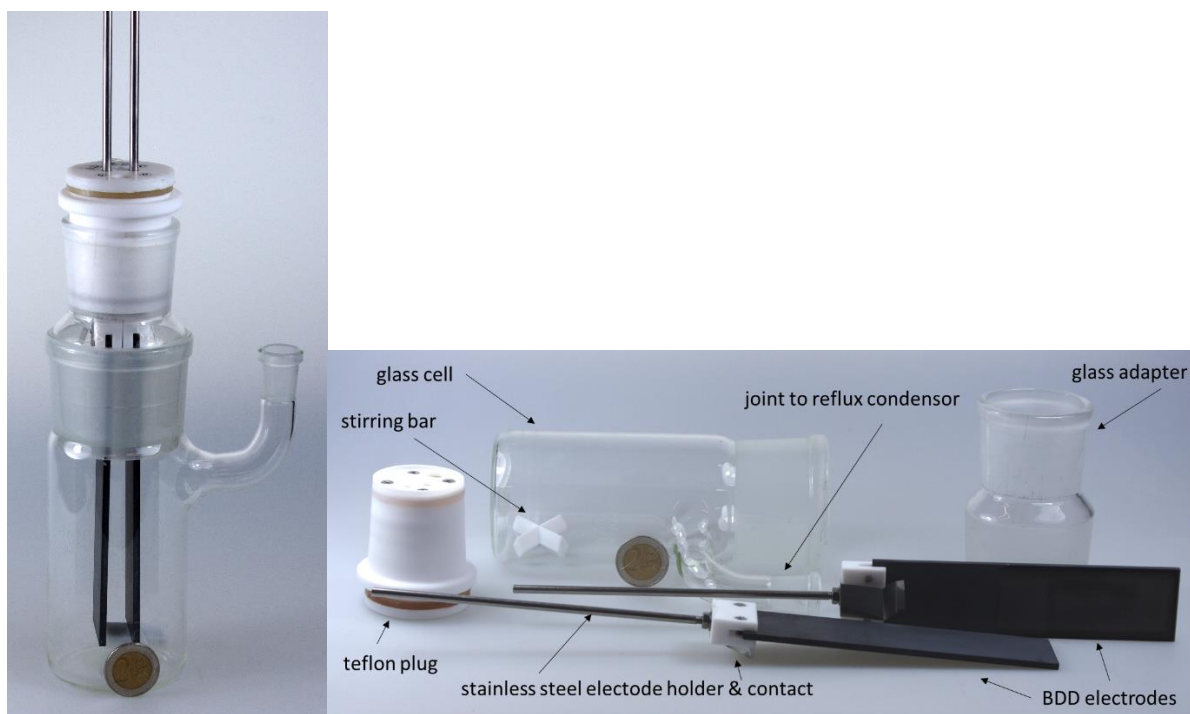


Fig. S2: 200 mL beaker-type cell; left: assembled; right: individual parts. For size comparison one 2 € coin (diameter 25.75 mm \approx 1.01 inches) is placed in front of the glass cell.

GP III: Cyclic voltammetry protocol

A 5 mM solution of the substrate in 5 mL HFIP (with 0.09 M MTBS and/or 0.1 mL DIPEA) was placed in a 10 mL beaker-type glass cell. After degassing of the solution with argon, cyclic voltammetry was performed with a 100 mV/s (or 10 mV/s) scan rate using a BDD working electrode, glassy carbon counter electrode and Ag/AgCl (in saturated LiCl in EtOH) reference electrode. The peak potentials were referenced versus the FcH/FcH⁺ couple.

Proposed mechanisms for anodic HFIP ether formation and benzyl-aryl cross-coupling reaction

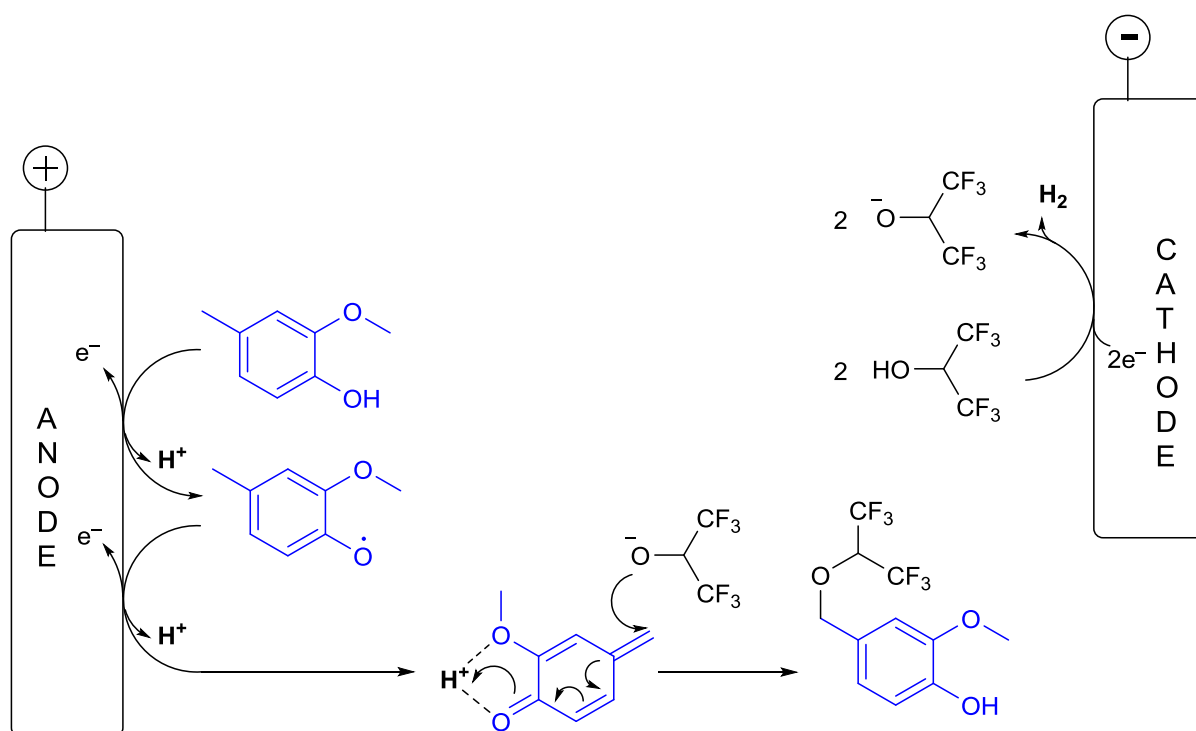


Fig. S3: Proposed mechanism for the electrochemical HFIP ether formation at benzylic position. Mechanism is shown for 4-methylguaiacol and can vary for other substrates.

Twofold oxidation of the phenol at the anode will result in the formation of a quinone methide derivative. This can be activated in the acidic solution to allow nucleophilic attack of the HFIP anion at the benzylic position. The resulting product is a benzylic HFIP ether. Due to addition of DIPEA, HFIP anions are present from the beginning of the reaction. This concentration will be maintained by the cathodic reaction.

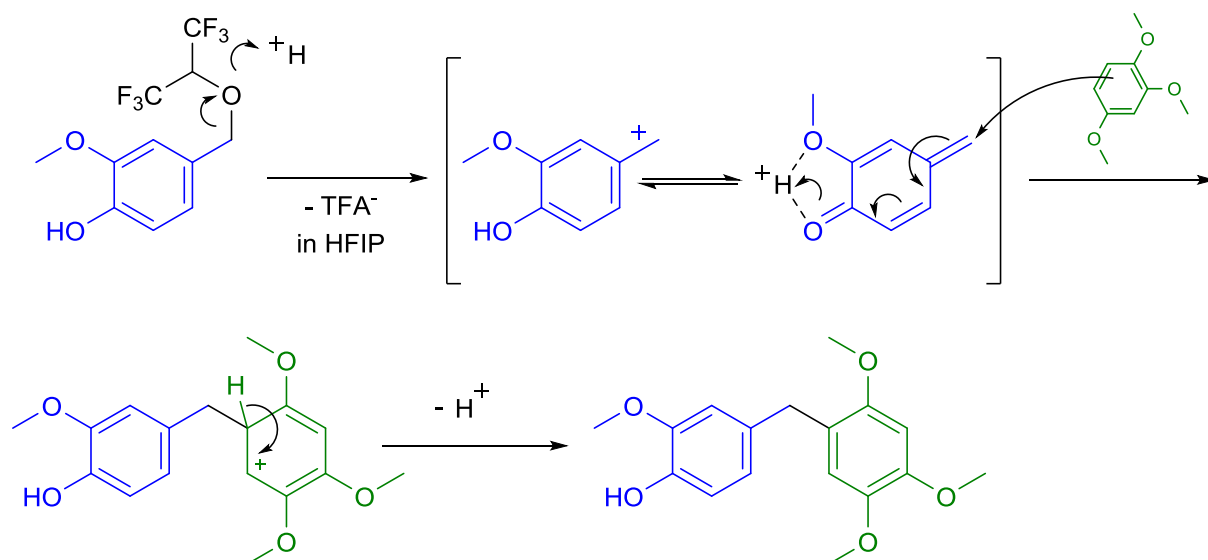


Fig. S4: Proposed mechanism for the benzyl-aryl coupling by cleavage of the HFIP ether with TFA, followed by a nucleophilic attack at benzylic position. Mechanism is shown for 4-methylguaiaicol and can vary for other substrates.

The addition of acids like TFA or *p*-TsOH will lead to the cleavage of the benzylic HFIP ether. The resulting benzylic cation is in equilibrium with the quinone methide species. Both substances are capable and stable enough to be attacked by the coupling partner in a nucleophilic attack. After proton abstraction the desired product is formed.

Cyclic voltammetry studies

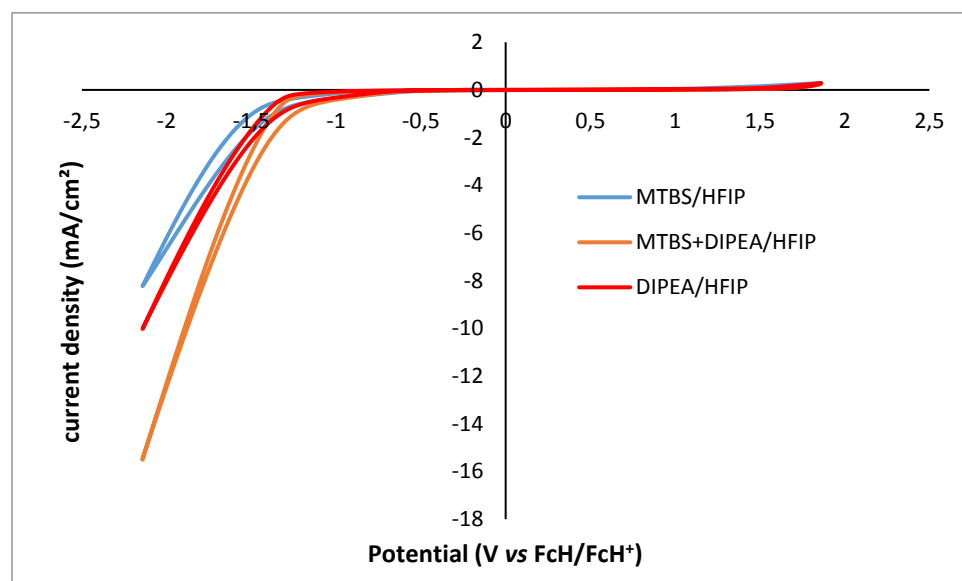


Fig. S5: Cyclic voltammogram of different blank electrolytic solutions (100 mV/s scan rate).

According to **GP III**, cyclic voltammetry was performed using different electrolytes. As expected, the oxidation peak of DIPEA was not observed in HFIP (**Fig. S5**). This suggests that DIPEA is protonated by HFIP and does not act as a mediator in this electrolyte system in the applied potential range.

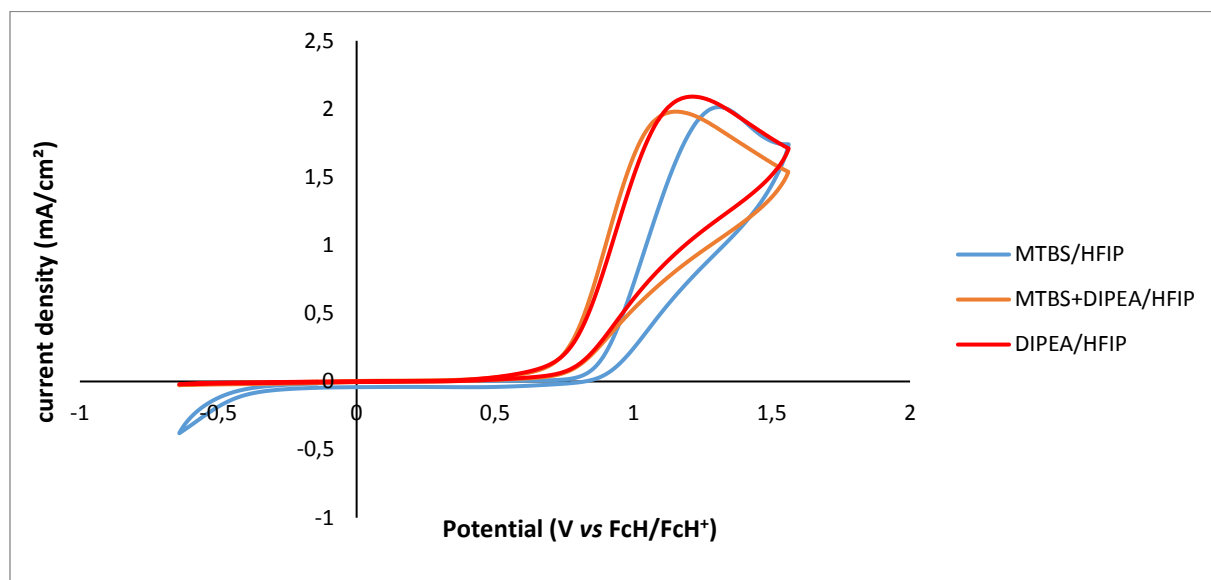


Fig. S6: Cyclic voltammogram of a 5 mM solution of 2-methoxy-4-methylphenol in different electrolytes (100 mV/s scan rate).

According to **GP III**, different electrolytes with 5 mM 2-methoxy-4-methylphenol were conducted and the oxidation potential was measured (100 mV/s scan rate). A decrease of the oxidation peak-potential of the phenol can be measured in electrolytic media containing DIPEA (MTBS+DIPEA/HFIP: $E_{ox} = 1.12 \text{ V vs Fc/FcH}^+$, DIPEA/HFIP: $E_{ox} = 1.21 \text{ V vs Fc/FcH}^+$) compared to HFIP/MTBS solutions (MTBS/HFIP: $E_{ox} = 1.34 \text{ V vs Fc/FcH}^+$) (**Fig. S6**).

We tested faster scan rates for a separation of both oxidation steps to the quinone methide intermediate. Nevertheless, no difference of the cyclic voltammogram in any media was observed for scan rates up to 0.5 V/s. This indicates, that both oxidation steps are too fast to be clearly visible by CV measurements. In contrast, a shift to slow scan rates (10 mV/s) showed interesting differences for the cyclovoltammograms in different electrolytes (**Fig. S7**). According to **GP III**, different electrolytes with 5 mM 2-methoxy-4-methylphenol were prepared and the oxidation potential was measured (10 mV/s scan rate). In electrolytes containing DIPEA two shoulders close to the oxidation potential of the substrate have been observed (**Fig. S7**, orange and red curve). A shift for higher potentials decreases the oxidation current. This is comparable to the oxidation behavior when applying fast scan rates (**Fig. S6**). In contrast, in the electrolyte without any DIPEA (**Fig. S7**, blue curve), the

oxidation current first decreases after reaching the peak potential and then rises fast with increasing potential values. This can be rationalized with subsequent fast oligomerization reactions close and/or on the electrode surface, whereas in solutions with DIPEA formed intermediates seem to be relatively stable in the applied potential range. This clearly indicates a changed reaction pathway by addition of DIPEA to the electrolyte.

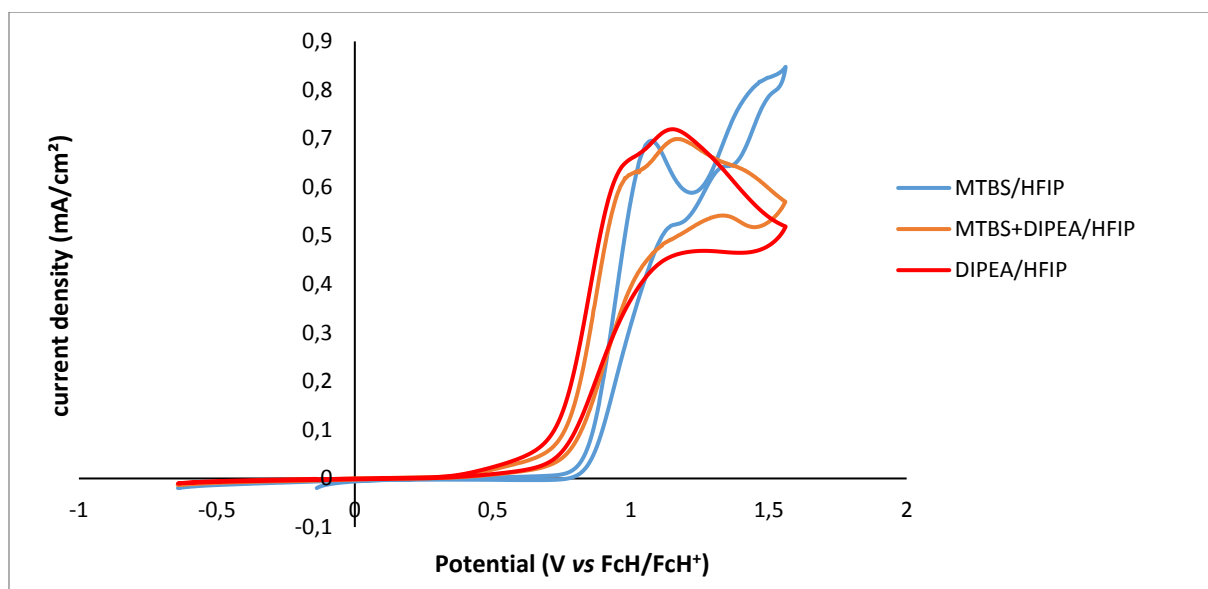
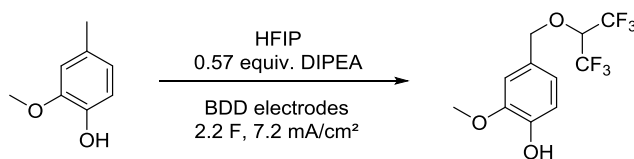
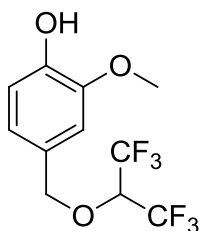


Fig. S7: Cyclic voltammogram of 5 mM 2-methoxy-4-methylphenol in different electrolytic solution (10 mV/s scan rate).

Synthesis of benzylic HFIP ether



4-((1-Trifluoromethyl-2,2,2-trifluoroethyl)oxymethyl)-2-methoxyphenol (2)



According to the **GPI** for the electrochemical HFIP ether formation, 138.16 mg (1.0 mmol) 2-methoxy-4-methylphenol, 5 mL HFIP, and 0.1 mL DIPEA were transferred into an undivided PTFE cell. Electrolysis was carried out at room temperature with a current density of 7.2 mA/cm². After 2.2 F were applied, HFIP was recovered by distillation on the rotary evaporator. The residue was dissolved in 30 mL dichloromethane and washed with 70 mL water. The aqueous phase was afterwards washed with 30 mL of dichloromethane. Combined organic phases were dried with MgSO₄ and filtered. After evaporation of the solvent, column chromatography on a preparative column chromatography apparatus (gradient: cyclohexane:ethyl acetate = from 100:0 for 3 min to 93:7 for 60 min; column 12 mm x 150 mm; flow rate 10 mL/min) yielded the product as colorless oil (yield: 54%, 164 mg, 0.54 mmol). To be mentioned, the HFIP ether is sensitive to silica gel and can decompose during column chromatography.

R_f (cyclohexane:ethyl acetate = 10:3) = 0.52

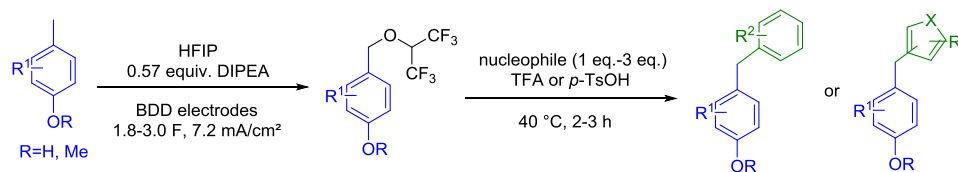
¹H NMR (400 MHz, Chloroform-d) δ = 6.94 (d, *J* = 8.0 Hz, 1H), 6.91 (d, *J* = 1.9 Hz, 1H), 6.87 (dd, *J* = 8.0, 1.9 Hz, 1H), 5.77 (s, 1H), 4.81 (s, 2H), 4.13 (p, *J* = 6.0 Hz, 1H), 3.93 (s, 3H).

¹³C NMR (101 MHz, CDCl₃) δ = 146.86, 146.48, 126.21, 122.61, 114.26, 111.27, 75.72, 73.94, 73.62, 73.29, 72.97, 72.65, 55.91.

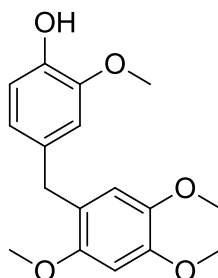
¹⁹F NMR (376 MHz, CDCl₃) δ = -74.61, -74.62.

HRMS for C₁₁H₁₀F₆O₃⁺ (APCI+) [M]⁺: calc.: 304.0529, found: 304.0532.

Synthesis of benzyl-aryl cross-coupling product



2-Methoxy-4-(2,4,5-trimethoxybenzyl)phenol (3)



According to the **GPI** for the electrochemical HFIP ether formation, 138.16 mg (1.0 mmol) 2-methoxy-4-methylphenol, 5 mL HFIP, and 0.1 mL DIPEA were transferred into an undivided 5 mL PTFE cell. Electrolysis was carried out at room temperature with a current density of 7.2 mA/cm². After 2.2 F were applied, the reaction solution was diluted with HFIP to a total volume of 10 mL to unify the concentration for each reaction. Then, 448 μ L (3.0 mmol) 1,2,4-trimethoxybenzene and 766 μ L (10 mmol) trifluoroacetic acid were added to the solution and stirred at 40 °C for 2 h. After completion of the reaction, HFIP was recovered by distillation on the rotary evaporator. The residue was dissolved in 30 mL dichloromethane and washed with 70 mL water. The aqueous phase was afterwards washed with 30 mL of dichloromethane. Combined organic phases were dried with MgSO₄ and filtered. After evaporation of the solvent, column chromatography on a preparative column chromatography apparatus (gradient: cyclohexane:ethyl acetate = from 100:0 for 3 min to 90:10 for 60 min; column 12 mm x 150 mm; flow rate 10 mL/min) yielded the product as colorless oil (yield: 77%, 235 mg, 0.77 mmol).

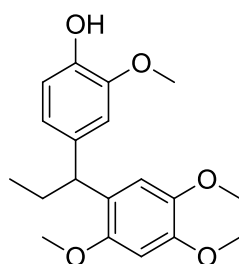
R_f (cyclohexane:ethyl acetate = 10:3) = 0.21

¹H NMR (400 MHz, CDCl₃) δ = 6.83 (d, J = 8.0 Hz, 1H), 6.73 (d, J = 1.9 Hz, 1H), 6.69 (dd, J = 8.0, 1.9 Hz, 1H), 6.65 (s, 1H), 6.56 (s, 1H), 3.88 (s, 3H), 3.86 (s, 2H), 3.82 (s, 3H), 3.80 (s, 3H), 3.77 (s, 3H).

¹³C NMR (101 MHz, CDCl₃) δ = 151.44, 148.02, 146.41, 143.71, 142.99, 133.21, 121.49, 121.34, 114.57, 114.17, 111.42, 98.01, 56.69, 56.54, 56.24, 55.82, 34.92.

HRMS for C₁₇H₂₀NaO₅ (ESI⁺) [M+Na]⁺: calc.: 327.1203, found: 327.1203.

2-Methoxy-4-(1-(2,4,5-trimethoxyphenyl)propyl)phenol (4)



According to the **GPI** for the electrochemical HFIP ether formation, 166.1 mg (1.0 mmol) 2-methoxy-4-propylphenol, 5 mL HFIP, and 0.1 mL DIPEA were transferred into an undivided 5 mL PTFE cell. Electrolysis was carried out at room temperature with a current density of 7.2 mA/cm². After 2.2 F were applied, the reaction solution was diluted with HFIP to a total volume of 10 mL to unify the concentration for each reaction. Then, 448 μ L (3.0 mmol) 1,2,4-trimethoxybenzene and 766 μ L (10 mmol) trifluoroacetic acid were added to the solution and stirred at 40 °C for 2 h. After completion of the reaction, HFIP was recovered by distillation on the rotary evaporator. The residue was dissolved in 30 mL dichloromethane and washed with 70 mL water. The aqueous phase was afterwards washed with 30 mL of dichloromethane. Combined organic phases were dried with MgSO₄ and filtered. After evaporation of the solvent, column chromatography on a preparative column chromatography apparatus (gradient: cyclohexane:ethyl acetate = from 100:0 for 3 min to 90:10 for 60 min; column 12 mm x 150 mm; flow rate 10 mL/min) yielded the product as colorless oil (yield: 75%, 249 mg, 0.75 mmol).

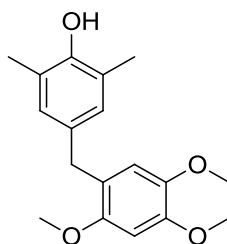
R_f (cyclohexane:ethyl acetate = 10:3) = 0.13

¹H NMR (400 MHz, CDCl₃) δ = 6.83 (d, *J* = 8.0 Hz, 1H), 6.80 – 6.74 (m, 3H), 6.52 (s, 1H), 5.60 (s, 1H), 4.17 (t, *J* = 7.8 Hz, 1H), 3.86 (s, 3H), 3.82 (s, 3H), 3.81 (s, 3H), 3.77 (s, 3H), 2.12 – 1.79 (m, 2H), 0.90 (t, *J* = 7.8 Hz, 3H).

¹³C NMR (101 MHz, CDCl₃) δ = 151.41, 147.72, 146.23, 143.57, 143.08, 125.72, 120.28, 114.01, 112.18, 110.94, 98.19, 56.88, 56.75, 56.11, 55.80, 55.80, 44.35, 28.26, 12.81.

HRMS for C₁₉H₂₄O₅⁺ (APPI+) [M]⁺: calc.: 332.1618, found: 332.1616.

2,6-Dimethyl-4-(2,4,5-trimethoxybenzyl)phenol (5)



According to the **GPI** for the electrochemical HFIP ether formation, 136.2 mg (1.0 mmol) 2,4,6-trimethylphenol, 5 mL HFIP, and 0.1 mL DIPEA were transferred into an undivided 5 mL PTFE cell. Electrolysis was carried out at room temperature with a current density of 7.2 mA/cm². After 2.2 F were applied, the reaction solution was diluted with HFIP to a total volume of 10 mL to unify the concentration for each reaction. Then, 448 μ L (3.0 mmol) 1,2,4-trimethoxybenzene and 766 μ L (10 mmol) trifluoroacetic acid were added to the solution and stirred at 40 °C for 2 h. After completion of the reaction, HFIP was recovered by distillation on the rotary evaporator. The residue was dissolved in 30 mL dichloromethane and washed with 70 mL water. The aqueous phase was afterwards washed with 30 mL of dichloromethane. Combined organic phases were dried with MgSO₄ and filtered. After evaporation of the solvent, column chromatography on a preparative column chromatography apparatus (gradient: cyclohexane:ethyl acetate = from 100:0 for 3 min to 90:10 for 60 min; column 12 mm x 150 mm; flow rate 10 mL/min) yielded the product as white solid (yield: 93%, 281 mg, 0.93 mmol).

Rf (cyclohexane:ethyl acetate = 10:3) = 0.12

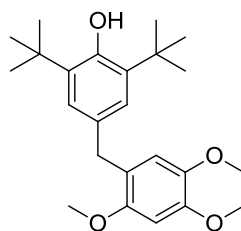
Melting point: 142.0 °C – 142.8 °C

¹H NMR (400 MHz, CDCl₃) δ = 6.81 (s, 2H), 6.66 (s, 1H), 6.56 (s, 1H), 3.89 (s, 3H), 3.81 (s, 3H), 3.80 (s, 2H), 3.79 (s, 3H), 2.21 (s, 6H).

¹³C NMR (101 MHz, CDCl₃) δ = 151.46, 150.29, 147.91, 142.97, 132.85, 128.78, 122.84, 121.75, 114.65, 98.08, 56.69, 56.65, 56.23, 34.32, 15.98.

HRMS for C₁₈H₂₁O₄⁺ (APCI+) [M]⁺: calc.: 301.1434, found: 301.1428.

2,6-Di-*tert*-butyl-4-(2,4,5-trimethoxybenzyl)phenol (6)



According to the **GPI** for the electrochemical HFIP ether formation, 220.6 mg (1.0 mmol) 2,6-Di-*tert*-butyl-4-methylphenol, 5 mL HFIP, and 0.1 mL DIPEA were transferred into an undivided 5 mL PTFE cell. Electrolysis was carried out at room temperature with a current density of 7.2 mA/cm². After 2.2 F were applied, the reaction solution was diluted with HFIP to a total volume of 10 mL to unify the concentration for each reaction. Then, 448 μ L (3.0 mmol) 1,2,4-trimethoxybenzene and 766 μ L (10 mmol) trifluoroacetic acid were added to the solution and stirred at 40 °C for 2 h. After completion of the reaction, HFIP was recovered by distillation on the rotary evaporator. The residue was dissolved in 30 mL dichloromethane and washed with 70 mL water. The aqueous phase was afterwards washed with 30 mL of dichloromethane. Combined organic phases were dried with MgSO₄ and filtered. After evaporation of the solvent, column chromatography on a preparative column chromatography apparatus (gradient: cyclohexane:ethyl acetate = from 100:0 for 3 min to 99:1 for 60 min; column 12 mm x 150 mm; flow rate 10 mL/min) yielded the product as yellow oil (yield: 41%, 158 mg, 0.41 mmol).

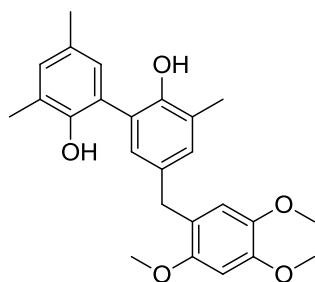
R_f (cyclohexane:ethyl acetate = 10:3) = 0.47

¹H NMR (400 MHz, CDCl₃) δ = 7.06 (s, 2H), 6.69 (s, 1H), 6.57 (s, 1H), 5.06 (s, 1H), 3.91 (s, 3H), 3.86 (s, 2H), 3.84 (s, 3H), 3.80 (s, 3H), 1.44 (s, 18H).

¹³C NMR (101 MHz, CDCl₃) δ = 151.84, 151.41, 147.76, 142.83, 135.58, 131.58, 125.34, 121.85, 114.52, 97.76, 56.58, 56.43, 56.24, 35.11, 34.30, 30.35.

HRMS for C₂₄H₃₄O₄⁺ (APCI+) [M]⁺: calc.: 385.2373, found: 385.2366.

3,3',5-Trimethyl-5'-(2,4,5-trimethoxybenzyl)-[1,1'-biphenyl]-2,2'-diol (7)



According to the **GPI** for the electrochemical HFIP ether formation, 242.3 mg (1.0 mmol) 3,3',5,5'-tetramethyl-[1,1'-biphenyl]-2,2'-diol, 5 mL HFIP, and 0.1 mL DIPEA were transferred into an undivided 5 mL PTFE cell. Electrolysis was carried out at room temperature with a current density of 7.2 mA/cm². After 2.2 F were applied, the reaction solution was diluted with HFIP to a total volume of 10 mL to unify the concentration for each reaction. Then, 448 μ L (3.0 mmol) 1,2,4-trimethoxybenzene and 766 μ L (10 mmol) trifluoroacetic acid were added to the solution and stirred at 40 °C for 2 h. After completion of the reaction, HFIP was recovered by distillation on the rotary evaporator. The residue was dissolved in 30 mL dichloromethane and washed with 70 mL water. The aqueous phase was afterwards washed with 30 mL of dichloromethane. Combined organic phases were dried with MgSO₄ and filtered. After evaporation of the solvent, column chromatography on a preparative column chromatography apparatus (gradient: cyclohexane:ethyl acetate = from 100:0 for 3 min to 90:10 for 60 min; column 12 mm x 150 mm; flow rate 10 mL/min) yielded the product as brown oil (yield: 57%, 233 mg, 0.57 mmol).

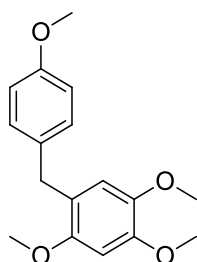
R_f (cyclohexane:ethyl acetate = 10:3) = 0.12

¹H NMR (400 MHz, CDCl₃) δ = 7.01 (d, *J* = 4.0 Hz, 2H), 6.91 (d, *J* = 2.2 Hz, 1H), 6.86 (d, *J* = 2.2 Hz, 1H), 6.69 (s, 1H), 6.54 (s, 1H), 5.17 (s, 2H), 3.88 (s, 3H), 3.85 (s, 2H), 3.80 (s, 6H), 2.27 (s, 9H).

¹³C NMR (101 MHz, CDCl₃) δ = 151.48, 149.50, 149.22, 148.06, 142.95, 133.72, 132.00, 131.56, 129.97, 128.47, 128.19, 125.27, 122.27, 122.10, 121.17, 114.60, 97.96, 56.71, 56.50, 56.21, 34.57, 20.47, 16.34, 16.22.

HRMS for C₂₅H₂₈NaO₅⁺ (ESI+) [M+Na]⁺: calc.: 431.1829, found: 431.1829.

1,2,4-Trimethoxy-5-(4-methoxybenzyl)benzene (8)



According to the **GPI** for the electrochemical HFIP ether formation, 61.1 mg (0.5 mmol) 4-methylanisol, 5 mL HFIP, and 0.05 mL DIPEA were transferred into an undivided 5 mL PTFE cell. Electrolysis was carried out at room temperature with a current density of 7.2 mA/cm². After 3.0 F were applied, the reaction solution was diluted with HFIP to a total volume of 10 mL to unify the concentration for each reaction. Then, 224 μ L (1.5 mmol) 1,2,4-trimethoxybenzene and 383 μ L (5.0 mmol) trifluoroacetic acid were added to the solution and stirred at 40 °C for 2 h. After completion of the reaction, HFIP was recovered by distillation on the rotary evaporator. The residue was dissolved in 30 mL dichloromethane and washed with 70 mL water. The aqueous phase was afterwards washed with 30 mL of dichloromethane. Combined organic phases were dried with MgSO₄ and filtered. After evaporation of the solvent, column chromatography on a preparative column chromatography apparatus (gradient: cyclohexane:ethyl acetate = from 100:0 for 3 min to 90:10 for 60 min; column 12 mm x 150 mm; flow rate 10 mL/min) yielded the product as brown oil (yield: 83%, 120 mg, 0.42 mmol).

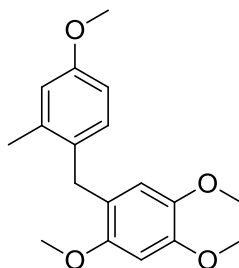
R_f (cyclohexane:ethyl acetate = 10:3) = 0.25

¹H NMR (400 MHz, CDCl₃) δ = 7.12 (d, *J* = 4.0 Hz, 2H), 6.82 (d, *J* = 4.0 Hz, 2H), 6.65 (s, 1H), 6.55 (s, 1H), 3.89 (s, 3H), 3.87 (s, 2H), 3.79 (s, 3H), 3.78 (d, *J* = 1.0 Hz, 6H).

¹³C NMR (101 MHz, CDCl₃) δ = 157.74, 151.44, 147.96, 142.97, 133.45, 129.63, 121.56, 114.52, 113.71, 97.97, 56.63, 56.53, 56.23, 55.23, 34.44.

HRMS for C₁₇H₂₀O₄⁺ (APCI+) [M]⁺: calc.: 288.1356, found: 288.135.

1,2,4-Trimethoxy-5-(4-methoxy-2-methylbenzyl)benzene (9)



According to the **GPI** for the electrochemical HFIP ether formation, 69.9 mg (0.5 mmol) 3,4-Dimethylanisol, 5 mL HFIP, and 0.05 mL DIPEA were transferred into an undivided 5 mL PTFE cell. Electrolysis was carried out at room temperature with a current density of 7.2 mA/cm². After 3.0 F were applied, the reaction solution was diluted with HFIP to a total volume of 10 mL to unify the concentration for each reaction. Then, 224 μ L (1.5 mmol) 1,2,4-trimethoxybenzene and 383 μ L (5.0 mmol) trifluoroacetic acid were added to the solution and stirred at 40 °C for 2 h. After completion of the reaction, HFIP was recovered by distillation on the rotary evaporator. The residue was dissolved in 30 mL dichloromethane and washed with 70 mL water. The aqueous phase was afterwards washed with 30 mL of dichloromethane. Combined organic phases were dried with MgSO₄ and filtered. After evaporation of the solvent, column chromatography on a preparative column chromatography apparatus (gradient: cyclohexane:ethyl acetate = from 100:0 for 3 min to 90:10 for 60 min; column 12 mm x 150 mm; flow rate 10 mL/min) yielded the product as brown oil (yield: 88%, 133 mg, 0.44 mmol).

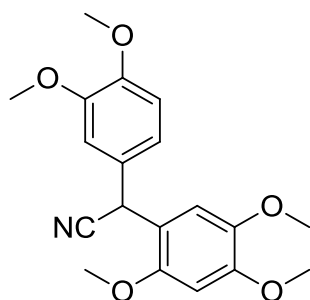
R_f (cyclohexane:ethyl acetate = 10:3) = 0.25

¹H NMR (400 MHz, CDCl₃) δ = 6.93 (d, *J* = 8.4 Hz, 1H), 6.74 (d, *J* = 2.8 Hz, 1H), 6.67 (dd, *J* = 8.4, 2.8 Hz, 1H), 6.56 (s, 1H), 6.46 (s, 1H), 3.89 (s, 3H), 3.82 (s, 2H), 3.81 (s, 3H), 3.78 (s, 3H), 3.70 (s, 3H), 2.25 (s, 3H).

¹³C NMR (101 MHz, CDCl₃) δ = 157.84, 151.49, 147.81, 142.93, 137.87, 131.14, 130.31, 120.65, 115.80, 114.18, 110.81, 97.65, 56.61, 56.46, 56.23, 55.18, 31.76, 19.83.

HRMS for C₁₈H₂₂NaO₄⁺ (ESI+) [M+Na]⁺: calc.: 325.141, found: 325.1401.

2-(3,4-Dimethoxyphenyl)-2-(2,4,5-trimethoxyphenyl)acetonitrile (10)



According to the **GPI** for the electrochemical HFIP ether formation, 177.2 mg (1.0 mmol) (3,4-Dimethoxyphenyl)acetonitrile, 5 mL HFIP, and 0.1 mL DIPEA were transferred into an undivided 5 mL PTFE cell. Electrolysis was carried out at room temperature with a current density of 7.2 mA/cm². After 1.8 F were applied, the reaction solution was diluted with HFIP to a total volume of 10 mL to unify the concentration for each reaction. Then, 448 μ L (3.0 mmol) 1,2,4-trimethoxybenzene and 1.90 g (10 mmol) *p*-Toluenesulfonic acid monohydrate were added to the solution and stirred at 40 °C for 3 h. After completion of the reaction, HFIP was recovered by distillation on the rotary evaporator. The residue was dissolved in 30 mL dichloromethane and washed with 70 mL water. The aqueous phase was afterwards washed with 30 mL of dichloromethane. Combined organic phases were dried with MgSO₄ and filtered. After evaporation of the solvent, column chromatography on a preparative column chromatography apparatus (gradient: cyclohexane:ethyl acetate = from 100:0 for 3 min to 90:10 for 60 min; column 12 mm x 150 mm; flow rate 10 mL/min) yielded the product as yellow oil (yield: 52%, 178 mg, 0.52 mmol).

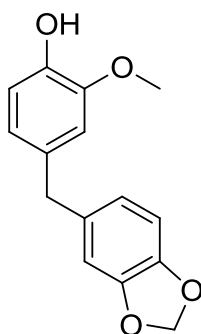
R_f (cyclohexane:ethyl acetate = 1:1) = 0.38

¹H NMR (400 MHz, CDCl₃) δ = 6.89 (dd, *J* = 8.3, 2.9 Hz, 1H), 6.84 (d, *J* = 2.9 Hz, 1H), 6.81 (d, *J* = 8.3 Hz, 1H), 6.79 (s, 1H), 6.53 (s, 1H), 5.47 (s, 1H), 3.88 (s, 3H), 3.85 (s, 3H), 3.84 (s, 3H), 3.83 (s, 3H), 3.78 (s, 3H).

¹³C NMR (101 MHz, CDCl₃) δ = 150.55, 149.84, 149.13, 148.61, 143.36, 128.16, 120.31, 119.76, 115.64, 112.36, 111.18, 110.66, 97.42, 56.70, 56.47, 56.16, 55.94, 55.92, 35.30.

HRMS for C₁₉H₂₂NO₅⁺ (APCI+) [M+H]⁺: calc.: 344.1492, found: 344.1488.

4-(Benzo[d][1,3]dioxol-5-ylmethyl)-2-methoxyphenol (11)



According to the **GPI** for the electrochemical HFIP ether formation, 138.16 mg (1.0 mmol) 2-methoxy-4-methylphenol, 5 mL HFIP, and 0.1 mL DIPEA were transferred into an undivided 5 mL PTFE cell. Electrolysis was carried out at room temperature with a current density of 7.2 mA/cm². After 2.2 F were applied, the reaction solution was diluted with HFIP to a total volume of 10 mL to unify the concentration for each reaction. Then, 344 μ L (3.0 mmol) 1,2-methylenedioxybenzene and 766 μ L (10 mmol) trifluoroacetic acid were added to the solution and stirred at 40 °C for 2 h. After completion of the reaction, HFIP was recovered by distillation on the rotary evaporator. The residue was dissolved in 30 mL dichloromethane and washed with 70 mL water. The aqueous phase was afterwards washed with 30 mL of dichloromethane. Combined organic phases were dried with MgSO₄ and filtered. After evaporation of the solvent, column chromatography on a preparative column chromatography apparatus (gradient: cyclohexane:ethyl acetate = from 100:0 for 3 min to 90:10 for 60 min; column 12 mm x 150 mm; flow rate 10 mL/min) yielded the product as colorless oil (yield: 35%, 90 mg, 0.35 mmol).

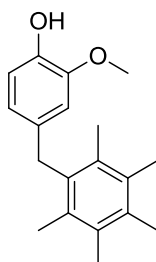
R_f (cyclohexane:ethyl acetate = 10:3) = 0.25

¹H NMR (400 MHz, CDCl₃) δ = 6.85 (d, *J* = 7.9 Hz, 1H), 6.74 (d, *J* = 7.9 Hz, 1H), 6.71 – 6.64 (m, 4H), 5.92 (s, 2H), 5.53 (s, 1H), 3.84 (s, 3H), 3.83 (s, 2H).

¹³C NMR (101 MHz, CDCl₃) δ = 147.69, 146.51, 145.81, 143.97, 135.41, 133.14, 121.52, 114.26, 111.31, 109.27, 108.14, 100.83, 55.87, 41.27.

HRMS for C₁₅H₁₃O₄⁺ (APCI+) [M]⁺: calc.: 257.0808, found: 257.0815.

2-Methoxy-4-(2,3,4,5,6-pentamethylbenzyl)phenol (12)



According to the **GPI** for the electrochemical HFIP ether formation, 138.16 mg (1.0 mmol) 2-methoxy-4-methylphenol, 5 mL HFIP, and 0.1 mL DIPEA were transferred into an undivided 5 mL PTFE cell. Electrolysis was carried out at room temperature with a current density of 7.2 mA/cm². After 2.2 F were applied, the reaction solution was diluted with HFIP to a total volume of 10 mL to unify the concentration for each reaction. Then, 484.9 mg (3.0 mmol) pentamethylbenzene and 766 μ L (10 mmol) trifluoroacetic acid were added to the solution and stirred at 40 °C for 2 h. After completion of the reaction, HFIP was recovered by distillation on the rotary evaporator. The residue was dissolved in 30 mL dichloromethane and washed with 70 mL water. The aqueous phase was afterwards washed with 30 mL of dichloromethane. Combined organic phases were dried with MgSO₄ and filtered. After evaporation of the solvent, column chromatography on a preparative column chromatography apparatus (gradient: cyclohexane:ethyl acetate = from 100:0 for 3 min to 90:10 for 60 min; column 12 mm x 150 mm; flow rate 10 mL/min) yielded the product as white solid (yield: 47%, 133 mg, 0.47 mmol).

R_f (cyclohexane:ethyl acetate = 10:3) = 0.60

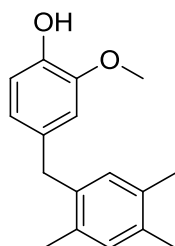
Melting point: 140.0 °C – 140.8 °C

¹H NMR (400 MHz, CDCl₃) δ = 6.80 (d, *J* = 8.1 Hz, 1H), 6.67 (s, 1H), 6.47 (d, *J* = 8.1, 1H), 5.31 (s, 1H), 4.07 (s, 2H), 3.85 (s, 3H), 2.30 (s, 3H), 2.28 (s, 6H), 2.22 (s, 6H).

¹³C NMR (101 MHz, CDCl₃) δ = 146.49, 143.57, 133.94, 133.08, 132.78, 132.49, 120.35, 114.18, 110.72, 55.94, 35.78, 16.99, 16.90, 16.87.

HRMS for C₁₉H₂₃O₂⁺ (APCI+) [M]⁺: calc.: 283.1693, found: 283.1687.

2-Methoxy-4-(2,4,5-trimethylbenzyl)phenol (13)



According to the **GPI** for the electrochemical HFIP ether formation, 138.16 mg (1.0 mmol) 2-methoxy-4-methylphenol, 5 mL HFIP, and 0.1 mL DIPEA were transferred into an undivided 5 mL PTFE cell. Electrolysis was carried out at room temperature with a current density of 7.2 mA/cm². After 2.2 F were applied, the reaction solution was diluted with HFIP to a total volume of 10 mL to unify the concentration for each reaction. Then, 412 μ L (3.0 mmol) 1,2,4-trimethylbenzene and 766 μ L (10 mmol) trifluoroacetic acid were added to the solution and stirred at 40 °C for 2 h. After completion of the reaction, HFIP was recovered by distillation on the rotary evaporator. The residue was dissolved in 30 mL dichloromethane and washed with 70 mL water. The aqueous phase was afterwards washed with 30 mL of dichloromethane. Combined organic phases were dried with MgSO₄ and filtered. After evaporation of the solvent, column chromatography on a preparative column chromatography apparatus (gradient: cyclohexane:ethyl acetate = from 100:0 for 3 min to 90:10 for 60 min; column 12 mm x 150 mm; flow rate 10 mL/min) yielded the product as white solid (yield: 58%, 149 mg, 0.58 mmol).

R_f (cyclohexane:ethyl acetate = 10:3) = 0.60

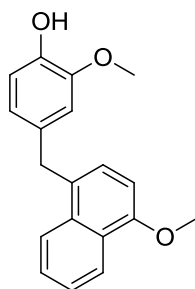
Melting point: 72.7 °C – 73.5 °C

¹H NMR (400 MHz, CDCl₃) δ = 7.00 (s, 1H), 6.91 (s, 1H), 6.88 (d, *J* = 8.1 Hz, 1H), 6.71 (s, 1H), 6.66 (dd, *J* = 8.1, 1.8 Hz, 1H), 3.91 (s, 2H), 3.87 (s, 3H), 2.27 (s, 3H), 2.25 (s, 6H).

¹³C NMR (101 MHz, CDCl₃) δ = 146.50, 143.73, 136.51, 134.35, 133.87, 133.68, 132.73, 131.72, 131.12, 121.44, 114.25, 111.39, 55.91, 38.66, 19.30, 19.24, 19.10.

HRMS for C₁₇H₂₀NaO₂⁺ (ESI+) [M+Na]⁺: calc.: 279.1356, found: 279.1366.

2-Methoxy-4-((4-methoxynaphthalen-1-yl)methyl)phenol (14)



According to the **GPI** for the electrochemical HFIP ether formation, 138.16 mg (1.0 mmol) 2-methoxy-4-methylphenol, 5 mL HFIP, and 0.1 mL DIPEA were transferred into an undivided 5 mL PTFE cell. Electrolysis was carried out at room temperature with a current density of 7.2 mA/cm². After 2.2 F were applied, the reaction solution was diluted with HFIP to a total volume of 10 mL to unify the concentration for each reaction. Then, 432 μ L (3.0 mmol) 1-methoxynaphthalene and 766 μ L (10 mmol) trifluoroacetic acid were added to the solution and stirred at 40 °C for 2 h. After completion of the reaction, HFIP was recovered by distillation on the rotary evaporator. The residue was dissolved in 30 mL dichloromethane and washed with 70 mL water. The aqueous phase was afterwards washed with 30 mL of dichloromethane. Combined organic phases were dried with MgSO₄ and filtered. After evaporation of the solvent, column chromatography on a preparative column chromatography apparatus (gradient: cyclohexane:ethyl acetate = from 100:0 for 3 min to 90:10 for 60 min; column 12 mm x 150 mm; flow rate 10 mL/min) yielded the product as yellow oil (yield: 81%, 238 mg, 0.81 mmol).

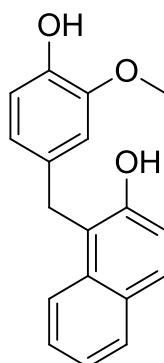
R_f (cyclohexane:ethyl acetate = 10:3) = 0.25

¹H NMR (400 MHz, CDCl₃) δ = 8.39 – 8.29 (m, 1H), 8.00 – 7.85 (m, 1H), 7.56 – 7.44 (m, 2H), 7.19 (d, *J* = 7.8 Hz, 1H), 6.86 (dd, *J* = 7.8, 1.8 Hz, 1H), 6.77 (d, *J* = 7.8 Hz, 1H), 6.74 – 6.68 (m, 2H), 5.30 (s, 1H), 4.32 (s, 2H), 4.01 (s, 3H), 3.78 (s, 3H).

¹³C NMR (101 MHz, CDCl₃) δ = 154.50, 146.52, 143.81, 132.97, 132.91, 128.86, 126.94, 126.46, 126.02, 124.94, 124.10, 122.52, 121.43, 114.24, 111.26, 103.33, 55.84, 55.49, 38.29.

HRMS for C₁₉H₁₈NaO₃⁺ (ESI⁺) [M+Na]⁺: calc.: 317.1148, found: 317.1157.

1-(4-Hydroxy-3-methoxybenzyl)naphthalen-2-ol (15)



According to the **GPI** for the electrochemical HFIP ether formation, 138.16 mg (1.0 mmol) 2-methoxy-4-methylphenol, 5 mL HFIP, and 0.1 mL DIPEA were transferred into an undivided 5 mL PTFE cell. Electrolysis was carried out at room temperature with a current density of 7.2 mA/cm². After 2.2 F were applied, the reaction solution was diluted with HFIP to a total volume of 10 mL to unify the concentration for each reaction. Then, 432.5 mg (3.0 mmol) 2-naphthol and 766 μ L (10 mmol) trifluoroacetic acid were added to the solution and stirred at 40 °C for 2 h. After completion of the reaction, HFIP was recovered by distillation on the rotary evaporator. The residue was dissolved in 30 mL dichloromethane and washed with 70 mL water. The aqueous phase was afterwards washed with 30 mL of dichloromethane. Combined organic phases were dried with MgSO₄ and filtered. After evaporation of the solvent, column chromatography on a preparative column chromatography apparatus (gradient: cyclohexane:ethyl acetate = from 100:0 for 3 min to 90:10 for 60 min; column 12 mm x 150 mm; flow rate 10 mL/min) yielded the product as white solid (yield: 79%, 222 mg, 0.79 mmol).

R_f (cyclohexane:ethyl acetate = 10:3) = 0.05

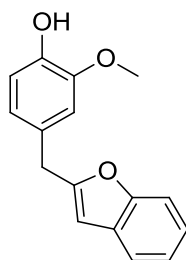
Melting point: 168.7 °C – 169.5 °C

¹H NMR (400 MHz, DMSO-*d*₆) δ = 9.67 (s, 1H), 8.62 (s, 1H), 7.87 (d, *J* = 8.6 Hz, 1H), 7.77 (d, *J* = 8.6 Hz, 1H), 7.68 (d, *J* = 8.6 Hz, 1H), 7.38 (td, *J* = 8.6, 2.0 Hz, 1H), 7.28 – 7.20 (m, 2H), 6.90 (d, *J* = 2.0 Hz, 1H), 6.57 (d, *J* = 8.1 Hz, 1H), 6.50 (dd, *J* = 8.1, 2.0 Hz, 1H), 4.24 (s, 2H), 3.68 (s, 3H).

¹³C NMR (101 MHz, DMSO-*d*₆) δ = 152.86, 147.71, 144.81, 133.79, 132.57, 128.69, 128.04, 126.46, 123.63, 122.64, 120.65, 118.88, 118.61, 115.62, 113.22, 109.98, 56.00, 29.89.

HRMS for C₁₈H₁₆NaO₃⁺ (ESI⁺) [M+Na]⁺: calc.: 303.0997, found: 303.0996.

2-((4-Hydroxy-3-methoxyphenyl)methyl)-benzofuran (16)



According to the **GPI** for the electrochemical HFIP ether formation, 138.16 mg (1.0 mmol) 2-methoxy-4-methylphenol, 5 mL HFIP, and 0.1 mL DIPEA were transferred into an undivided 5 mL PTFE cell. Electrolysis was carried out at room temperature with a current density of 7.2 mA/cm². After 2.2 F were applied, the reaction solution was diluted with HFIP to a total volume of 10 mL to unify the concentration for each reaction. Then, 107 μ L (1.0 mmol) 2,3-benzofuran and 766 μ L (10 mmol) trifluoroacetic acid were added to the solution and stirred at 40 °C for 2 h. After completion of the reaction, HFIP was recovered by distillation on the rotary evaporator. The residue was dissolved in 30 mL dichloromethane and washed with 70 mL water. The aqueous phase was afterwards washed with 30 mL of dichloromethane. Combined organic phases were dried with MgSO₄ and filtered. After evaporation of the solvent, column chromatography on a preparative column chromatography apparatus (gradient: cyclohexane:ethyl acetate = from 100:0 for 3 min to 93:7 for 60 min; column 12 mm x 150 mm; flow rate 10 mL/min) yielded the product as yellow oil (yield: 78%, 199 mg, 0.78 mmol).

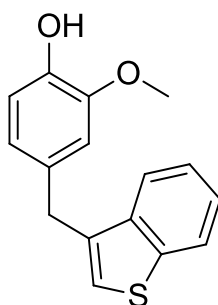
R_f (cyclohexane:ethyl acetate = 20:3) = 0.25

¹H NMR (400 MHz, CDCl₃) δ = 7.52 (d, *J* = 7.0, 1H), 7.47 (d, *J* = 7.0, 1H), 7.30 – 7.20 (m, 2H), 6.94 (d, *J* = 8.6, 1H), 6.86 (d, *J* = 4.0, 2H), 6.41 (s, 1H), 5.64 (s, 1H), 4.08 (s, 2H), 3.89 (s, 3H).

¹³C NMR (101 MHz, CDCl₃) δ = 158.24, 154.97, 146.58, 144.48, 129.02, 128.83, 123.42, 122.55, 121.74, 120.44, 114.45, 111.44, 110.94, 103.20, 55.93, 34.71.

HRMS for C₁₆H₁₄O₃⁺ (APPI+) [M]⁺: calc.: 254.0937, found: 254.0926.

3-((4-Hydroxy-3-methoxyphenyl)methyl)-benzo[*b*]thiophene (17)



According to the **GPI** for the electrochemical HFIP ether formation, 138.16 mg (1.0 mmol) 2-methoxy-4-methylphenol, 5 mL HFIP, and 0.1 mL DIPEA were transferred into an undivided 5 mL PTFE cell. Electrolysis was carried out at room temperature with a current density of 7.2 mA/cm². After 2.2 F were applied, the reaction solution was diluted with HFIP to a total volume of 10 mL to unify the concentration for each reaction. Then, 402.6 mg (3.0 mmol) benzo[*b*]thiophene and 766 μ L (10 mmol) trifluoroacetic acid were added to the solution and stirred at 40 °C for 2 h. After completion of the reaction, HFIP was recovered by distillation on the rotary evaporator. The residue was dissolved in 30 mL dichloromethane and washed with 70 mL water. The aqueous phase was afterwards washed with 30 mL of dichloromethane. Combined organic phases were dried with MgSO₄ and filtered. After evaporation of the solvent, column chromatography on a preparative column chromatography apparatus (gradient: cyclohexane:ethyl acetate = from 100:0 for 3 min to 90:10 for 60 min; column 12 mm x 150 mm; flow rate 10 mL/min) yielded the product as yellow oil (yield: 76%, 205 mg, 0.76 mmol).

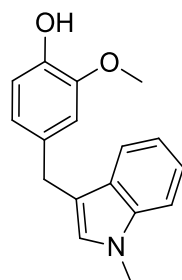
R_f (cyclohexane:ethyl acetate = 10:3) = 0.54

¹H NMR (400 MHz, CDCl₃) δ = 7.91 – 7.84 (m, 1H), 7.76 – 7.71 (m, 1H), 7.40 – 7.35 (m, 2H), 7.01 (s, 1H), 6.89 (d, *J* = 7.9 Hz, 1H), 6.83 – 6.75 (m, 2H), 5.57 (s, 1H), 4.14 (s, 2H), 3.83 (s, 3H).

¹³C NMR (101 MHz, CDCl₃) δ = 146.57, 144.12, 140.63, 138.82, 136.10, 131.17, 124.31, 123.97, 122.90, 121.97, 121.64, 114.35, 111.37, 55.90, 34.75.

HRMS for C₁₆H₁₃O₂S⁻ (ESI-) [M-H]⁻: calc.: 269.0642, found: 269.064.

1-Methyl-3-((4-hydroxy-3-methoxyphenyl)methyl)-indole (18)



According to the **GPI** for the electrochemical HFIP ether formation, 138.16 mg (1.0 mmol) 2-methoxy-4-methylphenol, 5 mL HFIP, and 0.1 mL DIPEA were transferred into an undivided 5 mL PTFE cell. Electrolysis was carried out at room temperature with a current density of 7.2 mA/cm². After 2.2 F were applied, the reaction solution was diluted with HFIP to a total volume of 10 mL to unify the concentration for each reaction. Then, 375 μ L (3.0 mmol) 1-methylindole and 766 μ L (10 mmol) trifluoroacetic acid were added to the solution. The flask was covered with aluminium foil to protect it from light and the solution was stirred at 40 °C for 2 h. After completion of the reaction, HFIP was recovered by distillation on the rotary evaporator. The residue was dissolved in 30 mL dichloromethane and washed with 70 mL water. The aqueous phase was afterwards washed with 30 mL of dichloromethane. Combined organic phases were dried with MgSO₄ and filtered. After evaporation of the solvent, column chromatography on a preparative column chromatography apparatus (gradient: cyclohexane:ethyl acetate = from 100:0 for 3 min to 93:7 for 60 min; column 12 mm x 150 mm; flow rate 10 mL/min) yielded the product as colorless oil (yield: 44%, 117 mg, 0.44 mmol).

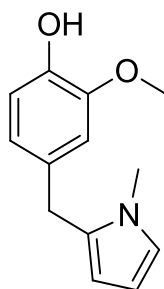
R_f (cyclohexane:ethyl acetate = 10:3) = 0.36

¹H NMR (400 MHz, CDCl₃) δ = 7.54 (d, *J* = 7.9 Hz, 1H), 7.30 (d, *J* = 7.9 Hz, 1H), 7.23 (td, *J* = 7.9, 1.1 Hz, 1H), 7.09 (td, *J* = 7.9, 1.1 Hz, 1H), 6.87 – 6.83 (m, 1H), 6.82 – 6.78 (m, 2H), 6.74 (t, *J* = 1.1 Hz, 1H), 5.48 (s, 1H), 4.04 (s, 2H), 3.83 (s, 3H), 3.74 (s, 3H).

¹³C NMR (101 MHz, CDCl₃) δ = 146.39, 143.71, 137.17, 133.30, 127.77, 127.04, 121.57, 121.31, 119.18, 118.75, 114.72, 114.11, 111.31, 109.15, 55.88, 32.63, 31.24.

HRMS for C₁₇H₁₈NO₂⁺ (ESI+) [M+H]⁺: calc.: 268.1332, found: 268.1323.

1-Methyl-2-((4-Hydroxy-3-methoxyphenyl)methyl)-pyrrole (19)



According to the **GPI** for the electrochemical HFIP ether formation, 138.16 mg (1.0 mmol) 2-methoxy-4-methylphenol, 5 mL HFIP, and 0.1 mL DIPEA were transferred into an undivided 5 mL PTFE cell. Electrolysis was carried out at room temperature with a current density of 7.2 mA/cm². After 2.2 F were applied, the reaction solution was diluted with HFIP to a total volume of 10 mL to unify the concentration for each reaction. Then, 243 μ L (3.0 mmol) 1-methylpyrrole and 766 μ L (10 mmol) trifluoroacetic acid were added to the solution and stirred at 40 °C for 2 h. After completion of the reaction, HFIP was recovered by distillation on the rotary evaporator. The residue was dissolved in 30 mL dichloromethane and washed with 70 mL water. The aqueous phase was afterwards washed with 30 mL of dichloromethane. Combined organic phases were dried with MgSO₄ and filtered. After evaporation of the solvent, column chromatography on a preparative column chromatography apparatus (gradient: cyclohexane:ethyl acetate = from 100:0 for 3 min to 93:7 for 60 min; column 12 mm x 150 mm; flow rate 10 mL/min) yielded the product as colorless oil (yield: 64%, 139 mg, 0.64 mmol).

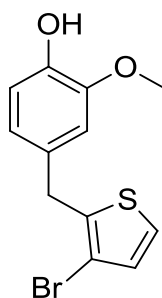
R_f (cyclohexane:ethyl acetate = 10:3) = 0.33

¹H NMR (400 MHz, CDCl₃) δ = 6.85 (d, *J* = 7.9 Hz, 1H), 6.72 - 6.67 (m, 2H), 6.59 (t, *J* = 2.7 Hz, 1H), 6.08 (t, *J* = 2.7 Hz, 1H), 5.92 – 5.86 (m, 1H), 5.53 (s, 1H), 3.88 (s, 2H), 3.84 (s, 3H), 3.45 (s, 3H).

¹³C NMR (101 MHz, CDCl₃) δ = 146.56, 143.95, 131.79, 131.27, 121.77, 121.13, 114.20, 111.02, 107.71, 106.53, 55.89, 33.81, 32.55.

HRMS for C₁₃H₁₆NO₂⁺ (ESI+) [M+H]⁺: calc.: 218.1176, found: 218.1172.

2-((4-Hydroxy-3-methoxyphenyl)methyl)-3-bromothiophene (20)



According to the **GPI** for the electrochemical HFIP ether formation, 138.16 mg (1.0 mmol) 2-methoxy-4-methylphenol, 5 mL HFIP, and 0.1 mL DIPEA were transferred into an undivided 5 mL PTFE cell. Electrolysis was carried out at room temperature with a current density of 7.2 mA/cm². After 2.2 F were applied, the reaction solution was diluted with HFIP to a total volume of 10 mL to unify the concentration for each reaction. Then, 284 μ L (3.0 mmol) 3-bromothiophene and 766 μ L (10 mmol) trifluoroacetic acid were added to the solution and stirred at 40 °C for 2 h. After completion of the reaction, HFIP was recovered by distillation on the rotary evaporator. The residue was dissolved in 30 mL dichloromethane and washed with 70 mL water. The aqueous phase was afterwards washed with 30 mL of dichloromethane. Combined organic phases were dried with MgSO₄ and filtered. After evaporation of the solvent, column chromatography on a preparative column chromatography apparatus (gradient: cyclohexane:ethyl acetate = from 100:0 for 3 min to 93:7 for 60 min; column 12 mm x 150 mm; flow rate 10 mL/min) yielded the product as yellow oil (yield: 52%, 154 mg, 0.52 mmol).

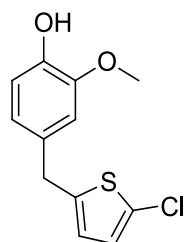
R_f (cyclohexane:ethyl acetate = 10:3) = 0.53

¹H NMR (400 MHz, CDCl₃) δ = 7.14 (d, *J* = 5.3 Hz, 1H), 6.94 (d, *J* = 5.3 Hz, 1H), 6.88 (d, *J* = 8.6 Hz, 1H), 6.80 – 6.75 (m, 2H), 5.61 (s, 1H), 4.05 (s, 2H), 3.86 (s, 3H).

¹³C NMR (101 MHz, CDCl₃) δ = 146.56, 144.41, 139.27, 131.09, 129.92, 123.96, 121.40, 114.42, 111.21, 108.87, 55.91, 34.87.

HRMS for C₁₂H₉BrNaO₂S⁺ (ESI+) [M+Na]⁺: calc.: 318.9399, found: 318.9392.

2-((4-Hydroxy-3-methoxyphenyl)methyl)-5-chlorothiophene (21)



According to the **GPI** for the electrochemical HFIP ether formation, 138.16 mg (1.0 mmol) 2-methoxy-4-methylphenol, 5 mL HFIP, and 0.1 mL DIPEA were transferred into an undivided 5 mL PTFE cell. Electrolysis was carried out at room temperature with a current density of 7.2 mA/cm². After 2.2 F were applied, the reaction solution was diluted with HFIP to a total volume of 10 mL to unify the concentration for each reaction. Then, 277 μ L (3.0 mmol) 2-chlorothiophene and 766 μ L (10 mmol) trifluoroacetic acid were added to the solution and stirred at 40 °C for 2 h. After completion of the reaction, HFIP was recovered by distillation on the rotary evaporator. The residue was dissolved in 30 mL dichloromethane and washed with 70 mL water. The aqueous phase was afterwards washed with 30 mL of dichloromethane. Combined organic phases were dried with MgSO₄ and filtered. After evaporation of the solvent, column chromatography on a preparative column chromatography apparatus (gradient: cyclohexane:ethyl acetate = from 100:0 for 3 min to 93:7 for 60 min; column 12 mm x 150 mm; flow rate 10 mL/min) yielded the product as yellow oil (yield: 57%, 145 mg, 0.57 mmol).

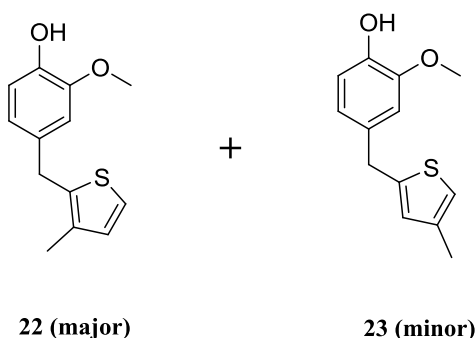
R_f (cyclohexane:ethyl acetate = 10:3) = 0.52

¹H NMR (400 MHz, CDCl₃) δ = 6.87 (d, *J* = 7.9 Hz, 1H), 6.76 – 6.68 (m, 3H), 6.56 (d, *J* = 3.7 Hz, 1H), 5.55 (s, 1H), 3.98 (s, 2H), 3.86 (s, 3H).

¹³C NMR (101 MHz, CDCl₃) δ = 146.59, 144.45, 143.67, 131.39, 127.82, 125.71, 124.07, 121.35, 114.40, 111.07, 55.92, 36.17.

HRMS for C₁₂H₁₀ClO₂S⁺ (APCI+) [M⁺]⁺: calc.: 253.0085, found: 253.0079.

2-((4-Hydroxy-3-methoxyphenyl)methyl)-3-methylthiophene (22a) and 2-((4-Hydroxy-3-methoxyphenyl)methyl)-4-methylthiophene (22b)



According to the **GPI** for the electrochemical HFIP ether formation, 138.16 mg (1.0 mmol) 2-methoxy-4-methylphenol, 5 mL HFIP, and 0.1 mL DIPEA were transferred into an undivided 5 mL PTFE cell. Electrolysis was carried out at room temperature with a current density of 7.2 mA/cm². After 2.2 F were applied, the reaction solution was diluted with HFIP to a total volume of 10 mL to unify the concentration for each reaction. Then, 292 μ L (3.0 mmol) 3-methylthiophene and 766 μ L (10 mmol) trifluoroacetic acid were added to the solution and stirred at 40 °C for 2 h. After completion of the reaction, HFIP was recovered by distillation on the rotary evaporator. The residue was dissolved in 30 mL dichloromethane and washed with 70 mL water. The aqueous phase was afterwards washed with 30 mL of dichloromethane. Combined organic phases were dried with MgSO₄ and filtered. After evaporation of the solvent, column chromatography on a preparative column chromatography apparatus (gradient: cyclohexane:ethyl acetate = from 100:0 for 3 min to 90:10 for 60 min; column 12 mm x 150 mm; flow rate 10 mL/min) yielded the product as yellow oil (yield: 54%, 126 mg, 0.54 mmol). The ration of regioisomers is 10 : 1 determined by ¹H NMR.

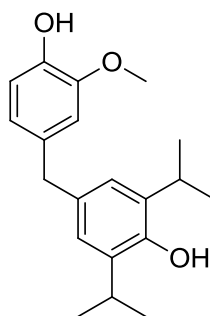
R_f (cyclohexane:ethyl acetate = 10:3) = 0.50

¹H NMR (400 MHz, CDCl₃) δ = 7.06 (d, *J* = 5.1 Hz, 1H), 6.88 – 6.82 (m, 2H), 6.74 – 6.69 (m, 2H), 5.55 (s, 1H), 4.01 (s, 2H), 3.86 (s, 3H), 2.20 (s, 3H).

¹³C NMR (101 MHz, CDCl₃) δ = 146.59, 144.17, 137.33, 133.28, 132.35, 130.17, 121.94, 121.21, 114.36, 111.10, 55.97, 33.58, 13.90.

HRMS for C₁₃H₁₅O₂S⁺ (ESI+) [M+H]⁺: calc.: 235.0787, found: 235.0788.

4-(4-Hydroxy-3-methoxybenzyl)-2,6-diisopropylphenol (23)



According to the **GPI** for the electrochemical HFIP ether formation, 138.16 mg (1.0 mmol) 2-methoxy-4-methylphenol, 5 mL HFIP, and 0.1 mL DIPEA were transferred into an undivided 5 mL PTFE cell. Electrolysis was carried out at room temperature with a current density of 7.2 mA/cm². After 2.2 F were applied, the reaction solution was diluted with HFIP to a total volume of 10 mL to unify the concentration for each reaction. Then, 556 μ L (3.0 mmol) 2,6-diisopropylphenol and 766 μ L (10 mmol) trifluoroacetic acid were added to the solution and stirred at 40 °C for 2 h. After completion of the reaction, HFIP was recovered by distillation on the rotary evaporator. The residue was dissolved in 30 mL dichloromethane and washed with 70 mL water. The aqueous phase was afterwards washed with 30 mL of dichloromethane. Combined organic phases were dried with MgSO₄ and filtered. After evaporation of the solvent, column chromatography on a preparative column chromatography apparatus (gradient: cyclohexane:ethyl acetate = from 100:0 for 3 min to 93:7 for 60 min; column 12 mm x 150 mm; flow rate 10 mL/min) yielded the product as yellow oil (yield: 57%, 179 mg, 0.57 mmol).

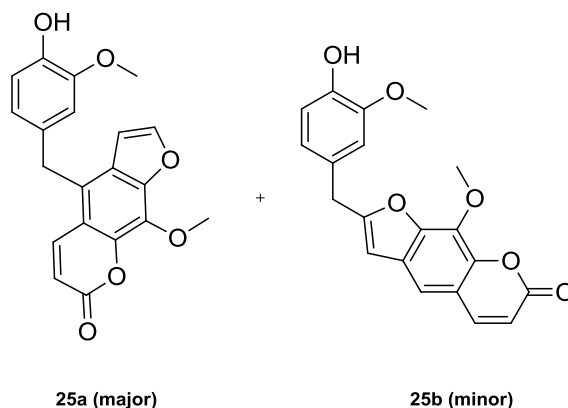
R_f (cyclohexane:ethyl acetate = 10:3) = 0.42

¹H NMR (400 MHz, CDCl₃) δ = 6.94 (s, 2H), 6.92 (d, *J* = 8.5 Hz, 1H), 6.77 – 6.74 (m, 2H), 5.67 (s, 1H), 4.84 (s, 1H), 3.92 (s, 2H), 3.87 (s, 3H), 3.20 (hept, *J* = 6.9 Hz, 2H), 1.30 (d, *J* = 6.9 Hz, 12H).

¹³C NMR (101 MHz, CDCl₃) δ = 148.26, 146.47, 143.74, 133.81, 133.74, 133.14, 123.92, 121.55, 114.30, 111.47, 55.90, 41.27, 27.28, 22.87.

HRMS for C₂₀H₂₆O₃⁺ (APPI+) [M]⁺: calc.: 314.1876, found: 314.1874.

4-(4-Hydroxy-3-methoxybenzyl)-9-methoxy-7H-furo[3,2-g]chromen-7-one (24a) and **2-(4-Hydroxy-3-methoxybenzyl)-9-methoxy-7H-furo[3,2-g]chromen-7-one (24b)**



According to the **GPI** for the electrochemical HFIP ether formation, 138.16 mg (1.0 mmol) 2-methoxy-4-methylphenol, 5 mL HFIP, and 0.1 mL DIPEA were transferred into an undivided 5 mL PTFE cell. Electrolysis was carried out at room temperature with a current density of 7.2 mA/cm². After 2.2 F were applied, the reaction solution was diluted with HFIP to a total volume of 10 mL to unify the concentration for each reaction. Then, 648.6 mg (3.0 mmol) xanthotoxin and 766 μ L (10 mmol) trifluoroacetic acid were added to the solution and stirred at 40 °C for 2 h. After completion of the reaction, HFIP was recovered by distillation on the rotary evaporator. The residue was dissolved in 30 mL dichloromethane and washed with 70 mL water. The aqueous phase was afterwards washed with 30 mL of dichloromethane. Combined organic phases were dried with MgSO₄ and filtered. After evaporation of the solvent, excess amount of the nucleophile was recovered by bulb-to-bulb distillation (120 °C, 1·10⁻³ mbar). Preparative High performance liquid chromatography (prep. HPLC) (solvent: solution A: solution B* = from 30:70 for 10 min to 60:40 for 90 min; Initial flow-rate was 10 mL/min. After 10 seconds, the flow rate was raised to 20 mL/min; column 250 mm x 30 mm) yielded the product **24a** as white solid (yield: 31%, 109 mg, 0.31 mmol) and product **24b** as white solid (yield: 10%, 35 mg, 0.10 mmol) in total 41%.

*A = Acetonitril, B = water with 5% Acetonitril and 0.1% Phosporic acid

R_f (cyclohexane:ethyl acetate = 1:1) = 0.43 (both compounds)

4-(4-Hydroxy-3-methoxybenzyl)-9-methoxy-7H-furo[3,2-g]chromen-7-one (24a)

Melting point: 173.1 °C – 173.8 °C

^1H NMR (400 MHz, CDCl_3) δ = 7.94 (d, J = 9.9 Hz, 1H), 7.67 (d, J = 2.3 Hz, 1H), 6.81 (d, J = 2.3 Hz, 1H), 6.78 (d, J = 8.1 Hz, 1H), 6.56 (d, J = 2.3 Hz, 1H), 6.51 (d, J = 8.1 Hz, 1H), 6.31 (d, J = 9.9 Hz, 1H), 5.57 (s, 1H), 4.31 (s, 2H), 4.27 (s, 3H), 3.76 (s, 3H).

^{13}C NMR (101 MHz, CDCl_3) δ = 160.31, 147.34, 146.78, 146.40, 144.30, 143.94, 141.06, 131.57, 131.30, 126.65, 123.80, 120.61, 114.76, 114.55, 114.33, 110.37, 105.75, 61.43, 55.89, 34.17.

HRMS for $\text{C}_{20}\text{H}_{17}\text{O}_6^+$ (APCI+) $[\text{M}+\text{H}]^+$: calc.: 353.102, found: 353.1016.

2-(4-Hydroxy-3-methoxybenzyl)-9-methoxy-7H-furo[3,2-g]chromen-7-one (24b)

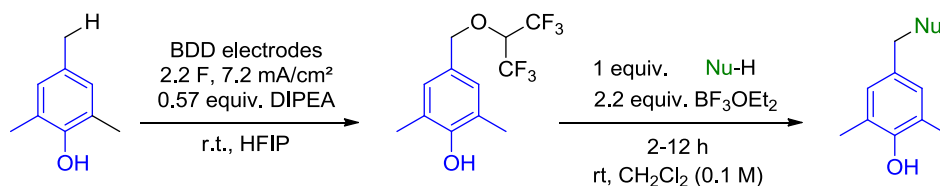
Melting point: 144.1 °C – 144.9 °C

^1H NMR (400 MHz, CDCl_3) δ = 7.73 (d, J = 9.6 Hz, 1H), 7.19 (s, 1H), 6.89 (d, J = 9.6 Hz, 1H), 6.83 – 6.79 (m, 2H), 6.40 – 6.32 (m, 2H), 5.57 (s, 1H), 4.26 (s, 3H), 4.06 (s, 2H), 3.88 (s, 3H).

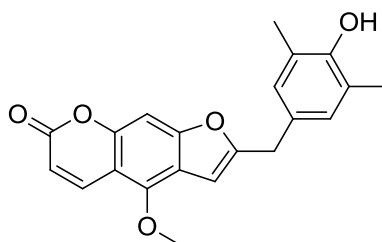
^{13}C NMR (101 MHz, CDCl_3) δ = 160.80, 160.75, 147.85, 146.75, 144.80, 144.57, 142.88, 132.45, 128.27, 127.63, 121.93, 116.32, 114.66, 114.61, 112.23, 111.56, 103.12, 77.16, 61.49, 56.07, 34.83.

HRMS for $\text{C}_{20}\text{H}_{17}\text{O}_6^+$ (ESI+) $[\text{M}+\text{H}]^+$: calc.: 353.102, found: 353.1019.

Synthesis of benzylated natural products and bioactive compounds (late-stage functionalization)



2-(4-Hydroxy-3,5-dimethylbenzyl)-4-methoxy-7H-furo[3,2-g]chromen-7-one (25)



According to the **GPI** for the electrochemical HFIP ether formation, 138.16 mg (1.0 mmol) 2-methoxy-4-methylphenol, 5 mL HFIP, and 0.1 mL DIPEA were transferred into an undivided 5 mL PTFE cell. Electrolysis was carried out at room temperature with a current density of 7.2 mA/cm². After 2.2 F were applied, HFIP was recovered and the residue was taken up in CH₂Cl₂ (10 mL). Then, 216.2 mg (1.0 mmol) of Bergapten and 272 μ L (2.2 mmol) BF₃OEt₂ were added to the solution and stirred at room temperature for 12 h. The reaction was diluted with CH₂Cl₂ (30 mL) and washed with water (70 mL). The aqueous phase was afterwards washed with 30 mL of dichloromethane. Combined organic phases were dried over Na₂SO₄ and filtered. After evaporation of the solvent, preparative high performance liquid chromatography (HPLC) (solvent: solution A:solution B* = from 30:70 for 10 min to 60:40 for 120 min; flow rate 20 mL/min; column 250 mm x 30 mm) yielded the product **25** as white solid (yield: 24%, 84 mg, 0.24 mmol)

*A = Acetonitril, B = water with 5% Acetonitril and 0.1% Phosporic acid

¹H NMR (400 MHz, CDCl₃) δ 8.15 (dd, J = 9.8, 0.7 Hz, 1H), 7.28 (s, 1H), 7.07 (t, J = 0.7 Hz, 1H), 6.93 (s, 2H), 6.59 (q, J = 1.1 Hz, 1H), 6.27 (d, J = 9.8 Hz, 1H), 4.67 (s, 1H), 4.22 (s, 2H), 3.97 (s, 3H), 2.26 (s, 6H).

¹³C NMR (101 MHz, CDCl₃) δ 161.60, 158.79, 158.60, 152.28, 151.37, 148.83, 139.56, 129.12, 127.97, 123.50, 114.23, 112.40, 106.48, 101.13, 93.84, 60.21, 34.12, 16.09.

HRMS for C₂₁H₁₉O₅⁺ (ESI+) [M+H]⁺: calc.: 351.1227, found: 351.1223.

Crystal structure determination of **25** (CCDC 1840040): C₂₁H₁₈O₅, Mr = 350.35 g/mol, yellow needle (0.034 x 0.041 x 0.642 mm³), P 21/c (monoklin), a = 4.8224 Å, b = 14.5298 Å, c = 23.4618 Å, V = 1640.5 Å³, Z = 4, F(000) = 736, ρ = 1.419 g/cm³, μ = 0.101 mm⁻¹, Mo-Kα graphite monochromator, -80 °C, 9491 reflections, 4146 independent reflections, wR2 = 0.1436, R1 = 0.066, 0.26 e/Å³, -0.25 e/Å³, GoF = 1.145

Single crystals for structure determination were obtained by recrystallization from ethyl acetate/cyclohexane at room temperature.

Intermolecular interaction via hydrogen bonds of the phenolic hydroxyl groups with the methoxy group and the lactone is observed (figure 2). Also hydrogen bonds via the furan can be observed (figure 2).

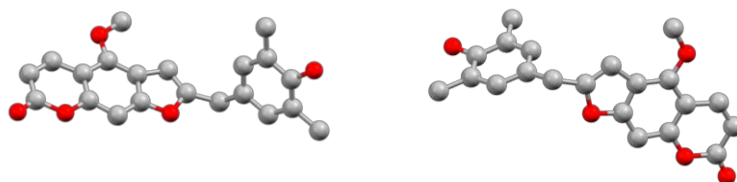


Figure 1 crystal structure of 25

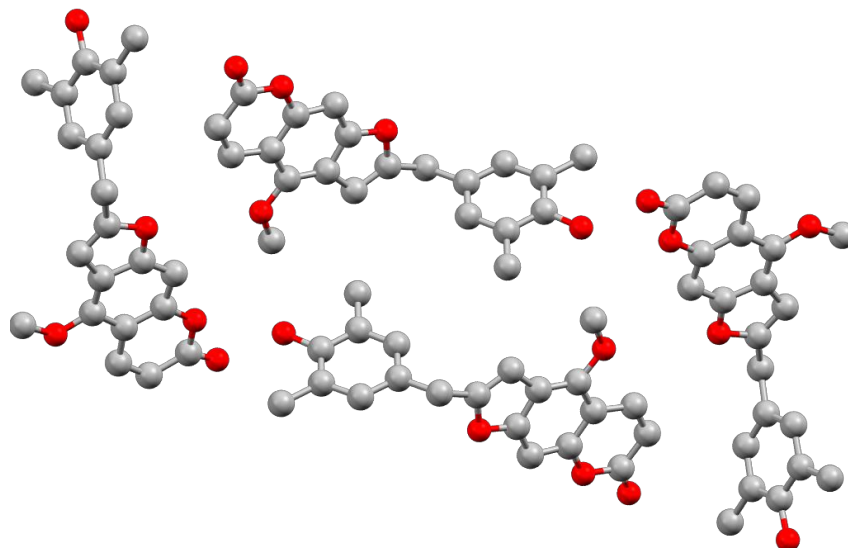
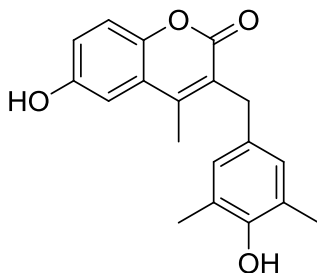


Figure 2 Packing of 25 in the solid state

6-Hydroxy-3-(4-hydroxy-3,5-dimethylbenzyl)-4-methyl-2H-chromen-2-one
(26)



According to the **GPI** for the electrochemical HFIP ether formation, 138.16 mg (1.0 mmol) 2-methoxy-4-methylphenol, 5 mL HFIP, and 0.1 mL DIPEA were transferred into an undivided 5 mL PTFE cell. Electrolysis was carried out at room temperature with a current density of 7.2 mA/cm². After 2.2 F were applied, HFIP was recovered and the residue was taken up in CH₂Cl₂ (10 mL). Then, 216.2 mg (1.0 mmol) of 4-Methylumbelliferone and 272 μ L (2.2 mmol) BF₃OEt₂ were added to the solution and stirred at room temperature for 12 h. The reaction was diluted with CH₂Cl₂ (30 mL) and washed with water (70 mL). The aqueous phase was afterwards washed with 30 mL of dichloromethane. Combined organic phases were dried over Na₂SO₄ and filtered. After evaporation of the solvent, preparative high performance liquid chromatography (prep. HPLC) (solvent: solution A: solution B* = from 30:70 for 10 min to 50:50 for 120 min; flow rate 20 mL/min; column 250 mm x 30 mm) yielded the product **26** as white solid (yield: 37%, 115 mg, 0.37 mmol)

*A = Acetonitril, B = water with 5% Acetonitril and 0.1% Phosporic acid

¹H NMR (400 MHz, DMSO-*d*₆) δ 10.41 (s, 1H), 7.98 (s, 1H), 7.60 (d, *J* = 8.8 Hz, 1H), 6.79 (dd, *J* = 8.8, 2.4 Hz, 1H), 6.72 (s, 2H), 6.69 (d, *J* = 2.4 Hz, 1H), 3.73 (s, 2H), 2.36 (s, 3H), 2.09 (s, 6H).

¹³C NMR (101 MHz, DMSO-*d*₆) δ 161.39, 160.32, 153.38, 151.36, 147.94, 129.66, 127.71, 126.64, 124.10, 120.78, 112.86, 112.53, 101.91, 31.25, 16.67, 15.08.

HRMS for C₁₉H₁₈NaO₄⁺ (ESI+) [M+Na]⁺: calc.: 333.1097, found: 333.1093.

Crystal structure determination of **26** (CCDC 1840041): C₁₉H₁₈O₄, M_r = 310.3 g/mol, colorless needle (0.09 x 0.18 x 0.41 mm³), P -1 (triklin), a = 8.4245 Å, b = 13.3710 Å, c = 14.8922 Å, V = 1522.6 Å³, Z = 4, F(000) = 656, ρ = 1.354 g/cm³, μ = 0.09 mm⁻¹, Mo-Kα graphite monochromator, -20 °C, 14360 reflections, 7522 independent reflections, wR₂ = 0.1475, R₁ = 0.0523, 0.22 e/Å³, -0.20 e/Å³, GoF = 1.015

Single crystals for structure determination were obtained by recrystallization from ethyl acetate/cyclohexane at room temperature.

Intermolecular interaction via hydrogen bonds of the phenolic hydroxyl groups with the lactone is observed (figure 1). Also π /π stacking of the benzyl groups can be seen (figure 2).

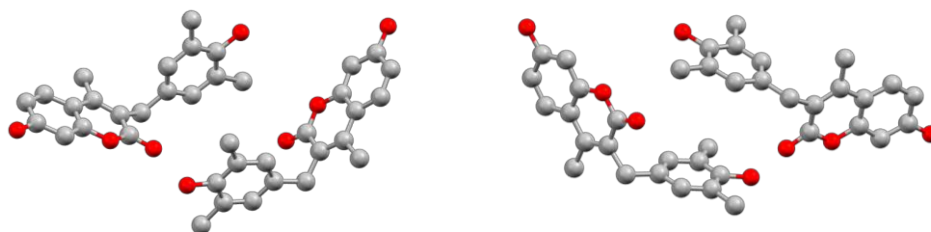


Figure 3 crystal structure of **26** showing two slightly different conformers

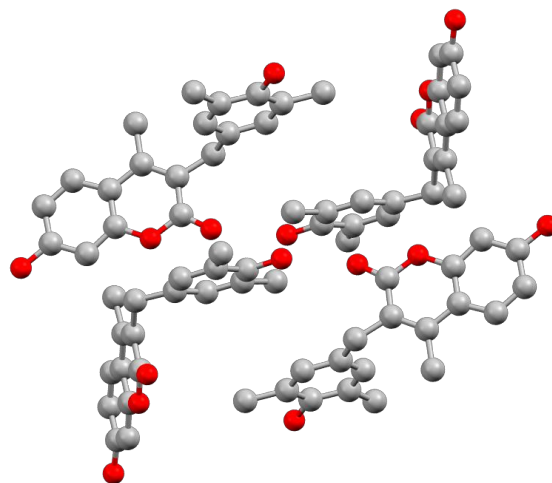
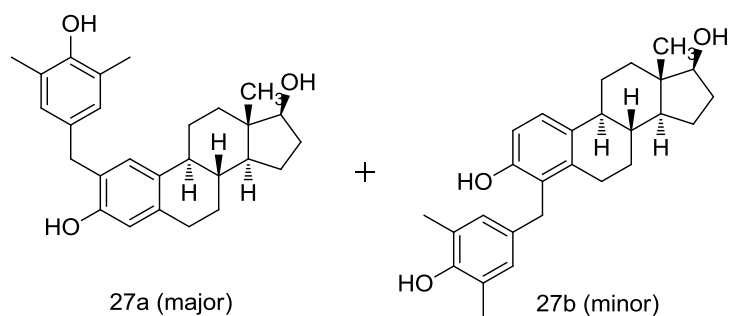


Figure 4 Packing of **26** in the solid state - π /π stacking of the phenols

(8*R*,9*S*,13*S*,14*S*,17*S*)-2-(4-Hydroxy-3,5-dimethylbenzyl)-13-methyl-7,8,9,11,12,13,14,15,16,17-decahydro-6*H*-cyclopenta[*a*]phenanthrene-3,17-diol (27a) and (8*R*,9*S*,13*S*,14*S*,17*S*)-4-(4-Hydroxy-3,5-dimethylbenzyl)-13-methyl-7,8,9,11,12,13,14,15,16,17-decahydro-6*H*-cyclopenta[*a*]phenanthrene-3,17-diol (27b)



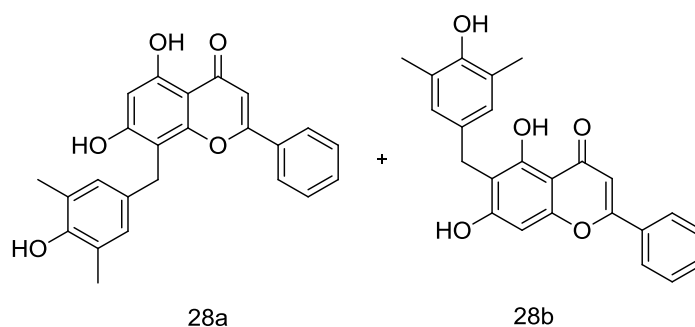
According to the **GPI** for the electrochemical HFIP ether formation, 138.16 mg (1.0 mmol) 2-methoxy-4-methylphenol, 5 mL HFIP, and 0.1 mL DIPEA were transferred into an undivided 5 mL PTFE cell. Electrolysis was carried out at room temperature with a current density of 7.2 mA/cm². After 2.2 F were applied, HFIP was recovered and the residue was taken up in CH₂Cl₂ (10 mL). Then, 272 mg (1.0 mmol) of β-estradiol and 272 μL (2.2 mmol) BF₃OEt₂ were added to the solution and stirred at room temperature for 2 h. The reaction was diluted with CH₂Cl₂ (30 mL) and washed with water (70 mL). The aqueous phase was afterwards washed with 30 mL of dichloromethane. Combined organic phases were dried over Na₂SO₄ and filtered. After evaporation of the solvent, column chromatography on a preparative column chromatography apparatus (gradient: cyclohexane:ethyl acetate = from 100:0 for 3 min to 80:20 for 60 min; column 12 mm x 150 mm; flow rate 15 mL/min) yielded the product **27a and 27b** as a white foam and a mixture of regioisomers 5/1 **27a/27b**, determined by H¹NMR (yield: 44%, 179 mg, 0.44 mmol).

¹H NMR (400 MHz, DMSO-*d*₆) δ 10.41 (s, 1H), 7.98 (s, 1H), 7.60 (d, *J* = 8.7 Hz, 1H), 6.79 (dd, *J* = 8.7, 2.4 Hz, 1H), 6.72 (s, 2H), 6.69 (d, *J* = 2.4 Hz, 1H), 3.73 (s, 2H), 2.36 (s, 3H), 2.09 (s, 6H).

¹³C NMR (101 MHz, CDCl₃) δ 151.93, 150.90, 136.43, 132.68, 131.47, 128.74, 128.28, 127.95, 124.61, 123.47, 116.05, 82.10, 50.17, 44.09, 43.39, 39.00, 36.86, 36.19, 30.72, 29.40, 27.39, 26.51, 23.27, 16.09, 11.24.

HRMS for $C_{27}H_{34}NaO_3^+$ (ESI+) [M+Na]⁺: calc.: 429.2400 found: 429.2390

5,7-Dihydroxy-8-(4-hydroxy-3,5-dimethylbenzyl)-2-phenyl-4H-chromen-4-one (28a) and 5,7-Dihydroxy-6-(4-hydroxy-3,5-dimethylbenzyl)-2-phenyl-4H-chromen-4-one (28b)



According to the **GPI** for the electrochemical HFIP ether formation, 138.16 mg (1.0 mmol) 2-methoxy-4-methylphenol, 5 mL HFIP, and 0.1 mL DIPEA were transferred into an undivided 5 mL PTFE cell. Electrolysis was carried out at room temperature with a current density of 7.2 mA/cm². After 2.2 F were applied, HFIP was recovered and the residue was taken up in CH₂Cl₂ (10 mL). Then, 254 mg (1.0 mmol) of Crysine and 272 μL (2.2 mmol) BF₃OEt₂ were added to the solution and stirred at room temperature for 12 h. The reaction was diluted with CH₂Cl₂ (30 mL) and washed with water (70 mL). The aqueous phase was afterwards washed with 30 mL of dichloromethane. Combined organic phases were dried over Na₂SO₄ and filtered. After evaporation of the solvent, preparative high performance liquid chromatography (prep. HPLC) (solvent: solution A : solution B* = from 50:50 for 10 min to 80:20 for 120 min; flow rate 20 mL/min; column 250 mm x 30 mm) yielded the product **28a** (yield: 18.3%, 71 mg, 0.18 mmol) as yellow solid and **28b** also as a yellow solid (yield: 12.3%, 46 mg, 0.12 mmol)

*A = Acetonitril, B = water with 5% Acetonitril and 0.1% Phosphoric acid

Regioisomer 28a:

¹H NMR (400 MHz, DMSO-*d*₆) δ 12.77 (s, 1H), 11.19 (s, 1H), 8.01 – 7.83 (m, 2H), 7.71 – 7.45 (m, 3H), 6.91 (s, 1H), 6.79 (s, 2H), 6.51 (s, 1H), 3.92 (s, 2H), 2.03 (s, 6H).

¹³C NMR (101 MHz, DMSO) δ 182.14, 163.08, 162.33, 159.18, 154.82, 151.17, 131.96, 130.98, 130.94, 129.10, 127.80, 126.39, 123.98, 106.74, 105.03, 103.90, 98.75, 27.02, 16.71.

HRMS for $C_{24}H_{21}O_5^+$ (ESI+) $[M+H]^+$: calc.: 389.1384, found: 389.1377

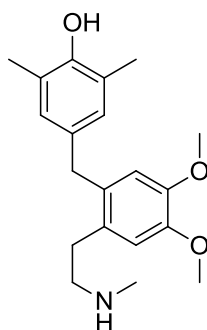
Regioisomer 28b:

1H NMR (400 MHz, DMSO- d_6) δ 13.13 (s, 1H), 11.09 (s, 1H), 8.09 – 8.02 (m, 2H), 7.90 (s, 1H), 7.64 – 7.53 (m, 3H), 6.96 (s, 1H), 6.78 (s, 2H), 6.66 (s, 1H), 3.71 (s, 2H), 2.08 (s, 6H).

^{13}C NMR (101 MHz, DMSO) δ 213.85, 181.94, 162.98, 162.36, 158.55, 155.34, 151.02, 131.95, 130.97, 130.81, 129.16, 128.05, 126.39, 123.66, 111.71, 105.11, 103.74, 93.49, 26.59, 16.72.

HRMS for $C_{24}H_{21}O_5^+$ (ESI+) $[M+H]^+$: calc.: 389.1384, found: 389.1377

4-(4,5-Dimethoxy-2-(2-(methylamino)ethyl)benzyl)-2,6-dimethylphenol(29)



According to the **GPI** for the electrochemical HFIP ether formation, 138.16 mg (1.0 mmol) 2-methoxy-4-methylphenol, 5 mL HFIP, and 0.1 mL DIPEA were transferred into an undivided 5 mL PTFE cell. Electrolysis was carried out at room temperature with a current density of 7.2 mA/cm². After 2.2 F were applied, HFIP was recovered and the residue was taken up in CH₂Cl₂ (10 mL). Then, 206 mg (1.0 mmol) of N-Methylhomoveratrylamine and 408 μ L (3.3 mmol) BF₃OEt₂ were added to the solution and stirred at room temperature for 2 h. The reaction was diluted with CH₂Cl₂ (30 mL) and washed with water (70 mL). The aqueous phase was afterwards washed with 30 mL of dichloromethane. Combined organic phases were dried over Na₂SO₄ and filtered. After evaporation of the solvent, column chromatography on a preparative column chromatography apparatus (gradient: ethyl acetate/MeOH = from 100:0 to 80:20 for 60 min; column 12 mm x 150 mm; flow rate 15 mL/min) yielded the product yielded the product **29** (yield: 31%, 101 mg, 0.31 mmol) as a colourless oil)

1H NMR (400 MHz, CDCl₃) δ 6.69 (s, 1H), 6.66 (s, 2H), 6.64 (s, 1H), 3.84 (s, 3H), 3.80 (s, 2H), 3.79 (s, 3H), 2.75 (ddd, J = 8.3, 6.6, 1.9 Hz, 2H), 2.67 (ddd, J = 8.3, 6.6, 1.9 Hz, 1H), 2.37 (s, 2H), 2.17 (s, 6H).

^{13}C NMR (101 MHz, CDCl_3) δ 150.76, 147.51, 132.57, 131.51, 129.28, 128.60, 123.54, 114.19, 113.22, 56.08, 52.03, 37.75, 35.29, 31.97, 16.22.

HRMS for $\text{C}_{20}\text{H}_{28}\text{NO}_3^+$ (ESI+) $[\text{M}+\text{H}]^+$: calc.: 329.2000, found: 330.2063

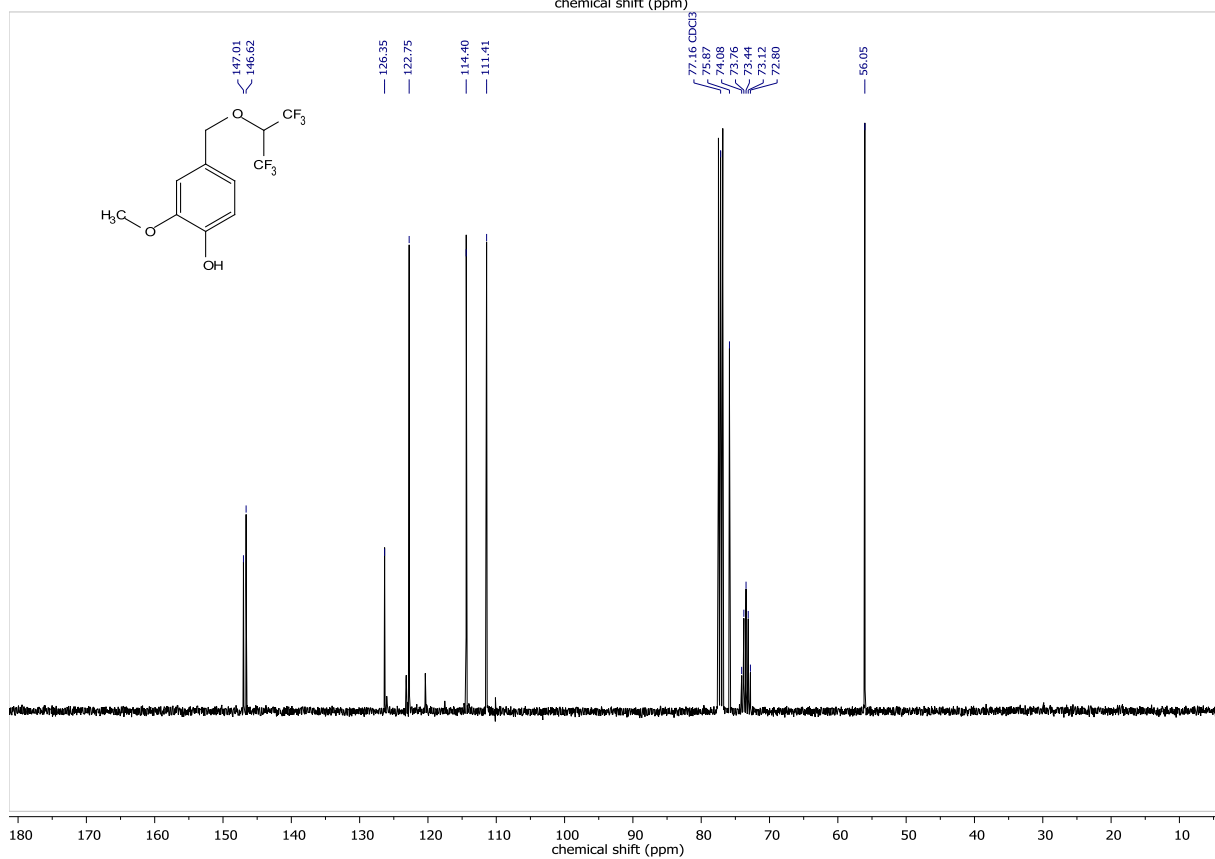
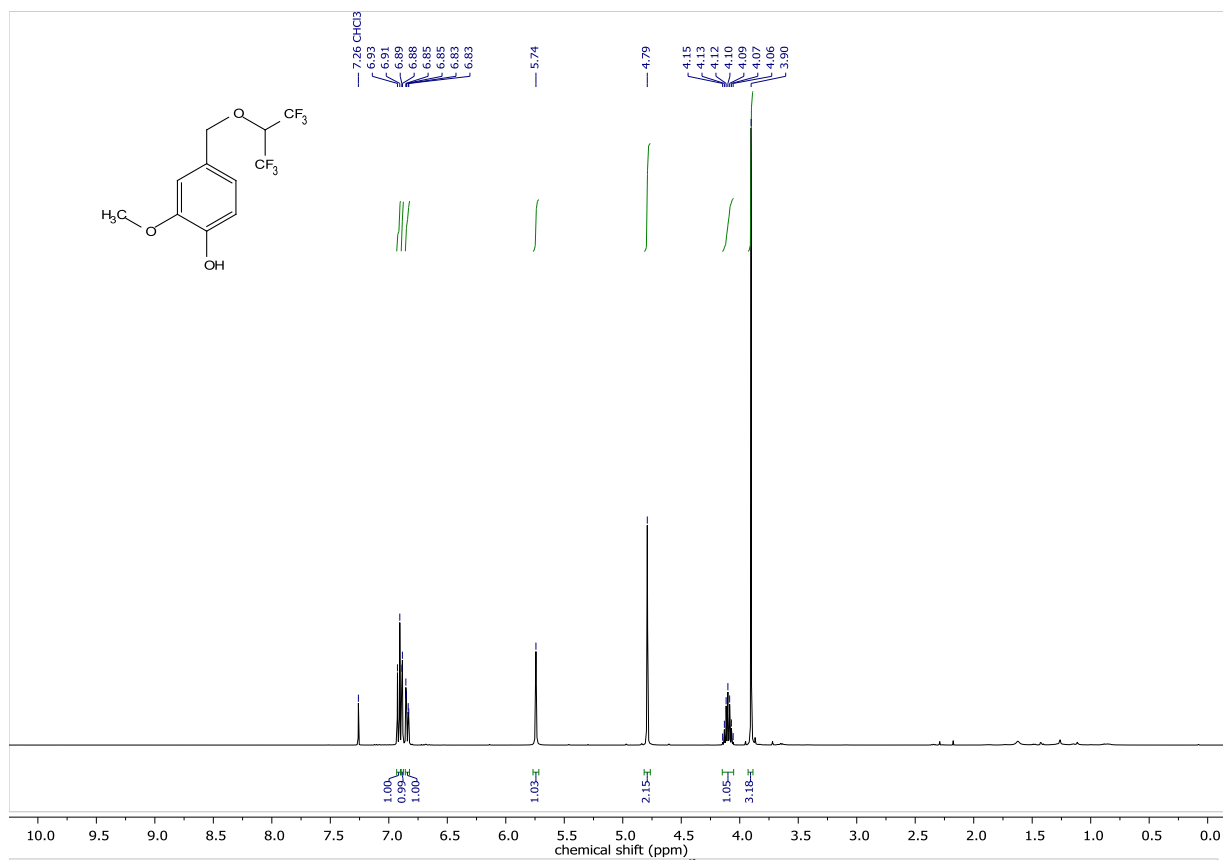
40 mmol scale synthesis in a 200 mL beaker-type cell

According to **GP II** for the electrochemical HFIP ether formation, 5.53 g (40 mmol) 2-methoxy-4-methylphenol, 200 mL HFIP, and 4.0 mL (0.57 equiv) DIPEA were transferred into an undivided beaker-type electrolysis cell. Electrolysis was carried out at room temperature with a current density of 7.2 mA/cm². After 2.2 F were applied, the reaction solution was diluted with HFIP to a total volume of 400 mL (to unify the concentration with the 5 mL scale reaction). Then, 16.1 g (3.0 equiv, 120 mmol) benzo[*b*]thiophene and 30.6 mL (10 equiv, 400 mmol) trifluoroacetic acid were added to the solution and stirred at 40 °C for 1 h. After completion of the reaction, HFIP was recovered by distillation on the rotary evaporator. The residue was dissolved in 30 mL dichloromethane and washed with 70 mL water. The aqueous phase was afterwards washed with 30 mL of dichloromethane. Combined organic phases were dried with MgSO_4 and filtered. After evaporation of the solvent, excess amount of the nucleophile was recovered by bulb-to-bulb distillation (60 °C, $1 \cdot 10^{-3}$ mbar). Then, column chromatography on a preparative column chromatography apparatus (gradient: cyclohexane:ethyl acetate = from 100:0 for 10 min to 98:2 for 60 min; column 40 mm x 150 mm; flow rate 50 mL/min) yielded the product as yellow oil (yield: 64 %, 6.91 g, 25.6 mmol).

NMR spectra

4-((1-Trifluoromethyl-2,2,2-trifluoroethyl)oxymethyl)-2-methoxyphenol

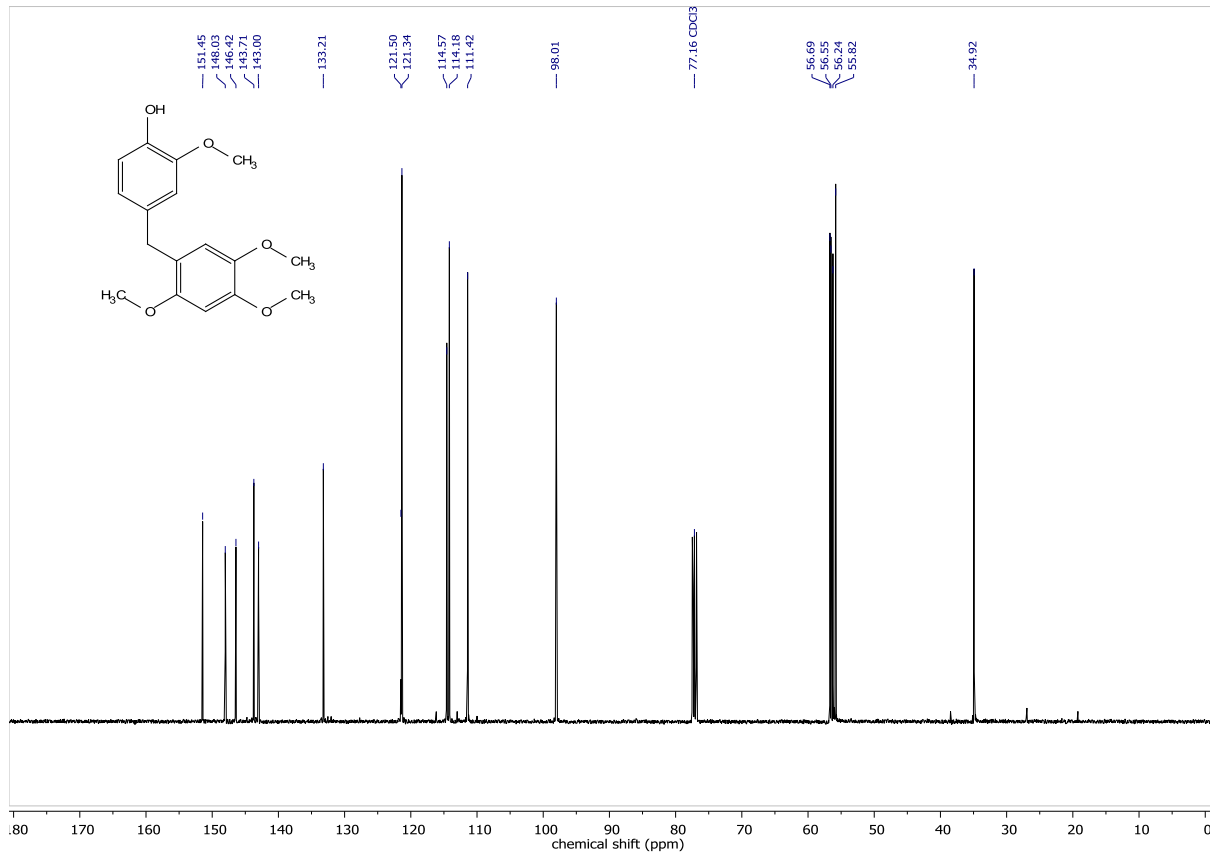
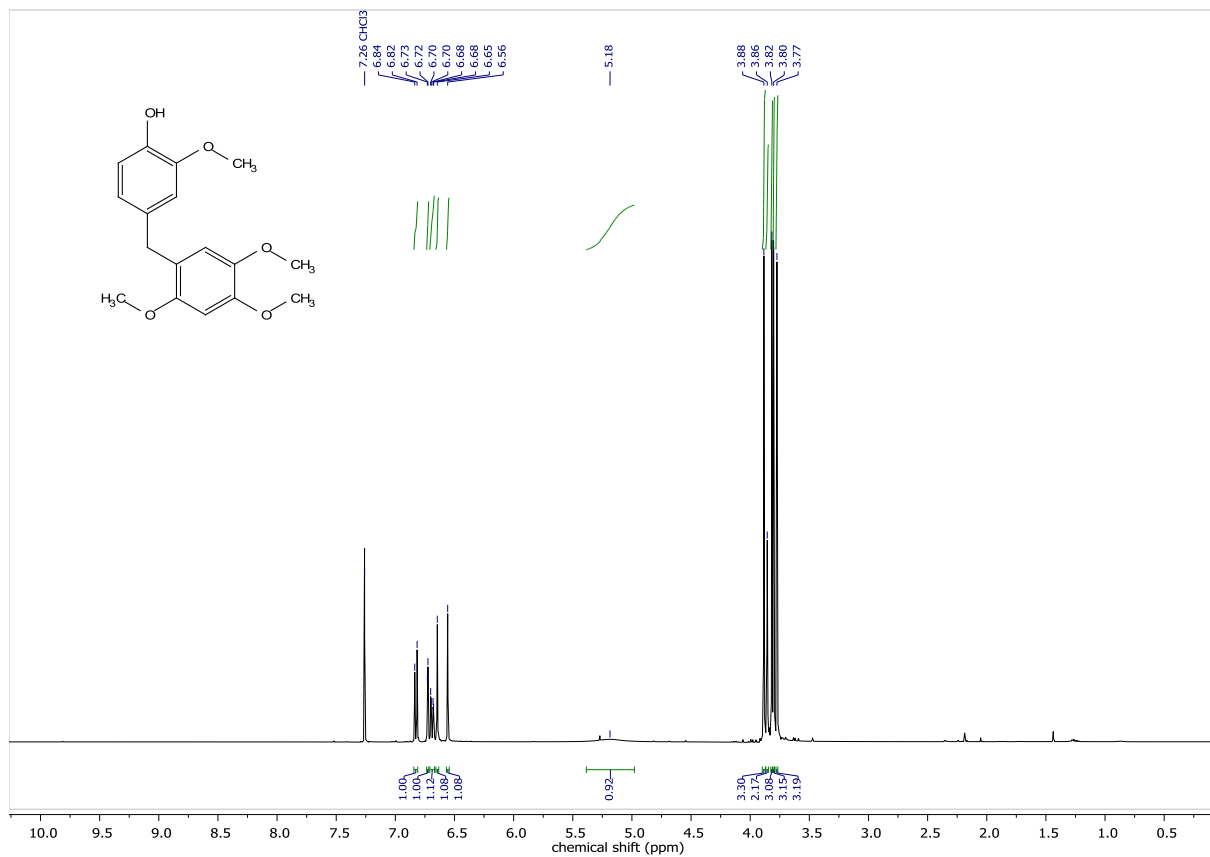
(2)



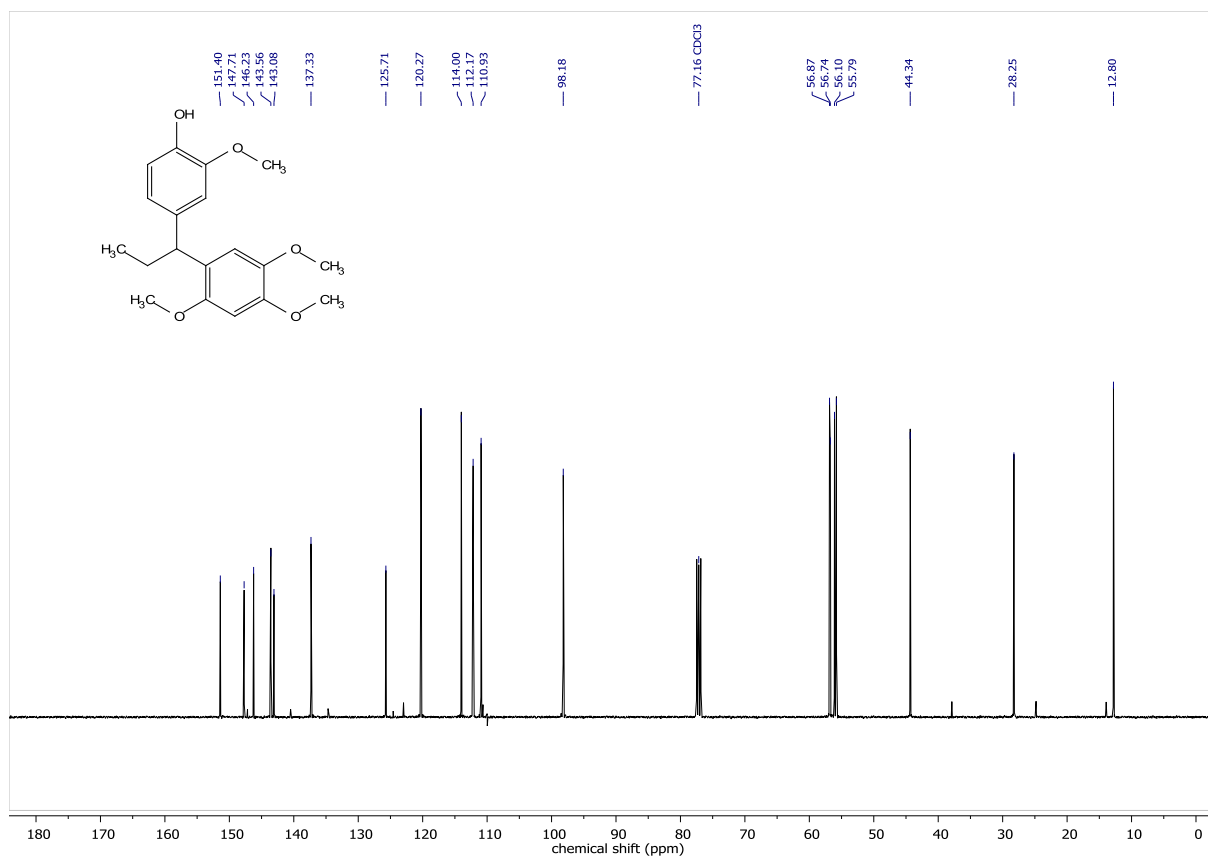
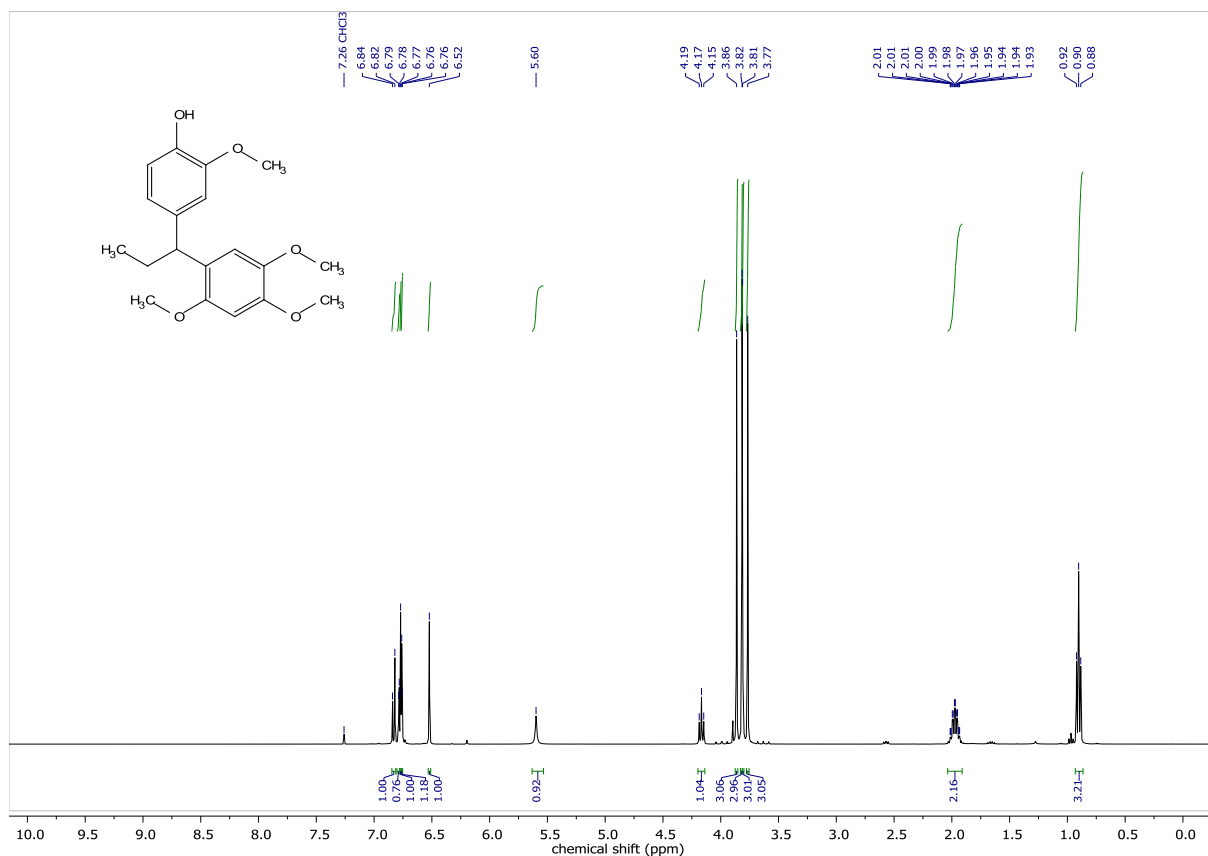


2-Methoxy-4-(2,4,5-trimethoxybenzyl)phenol

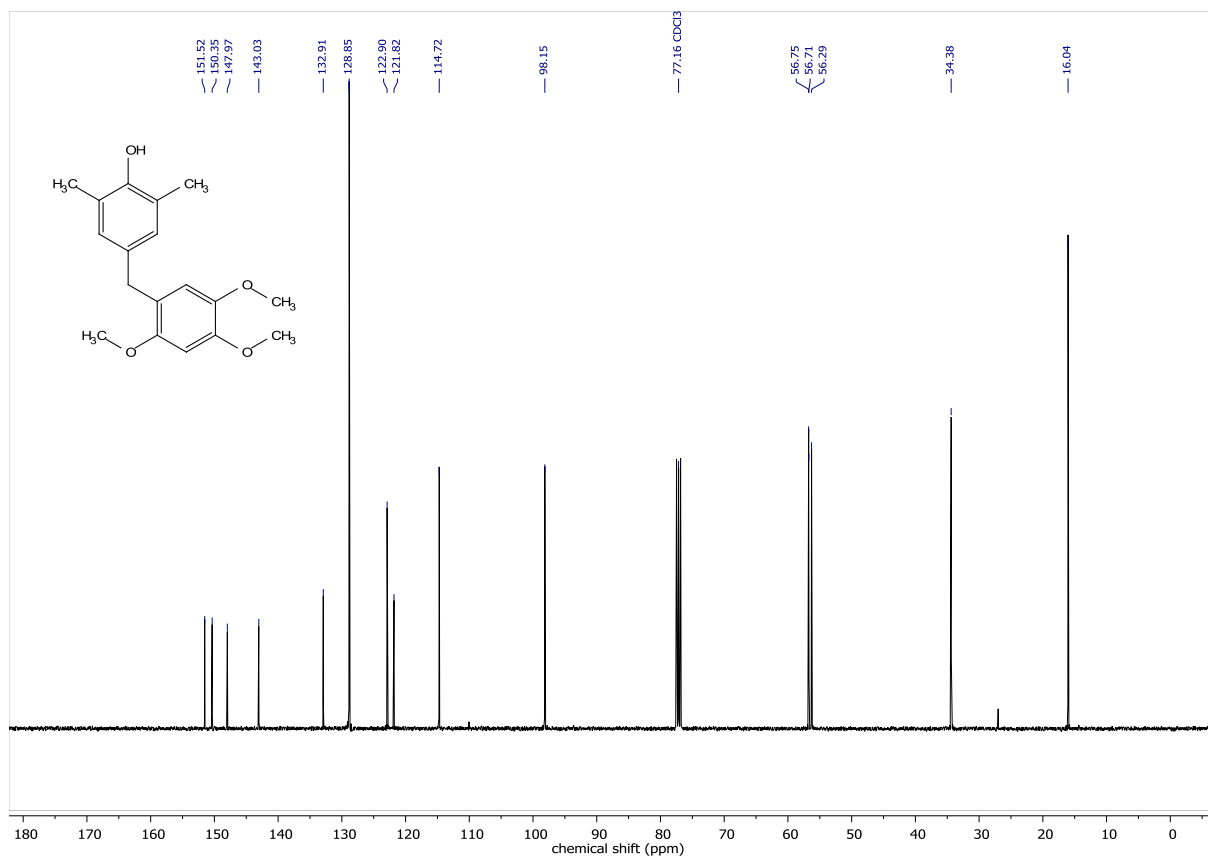
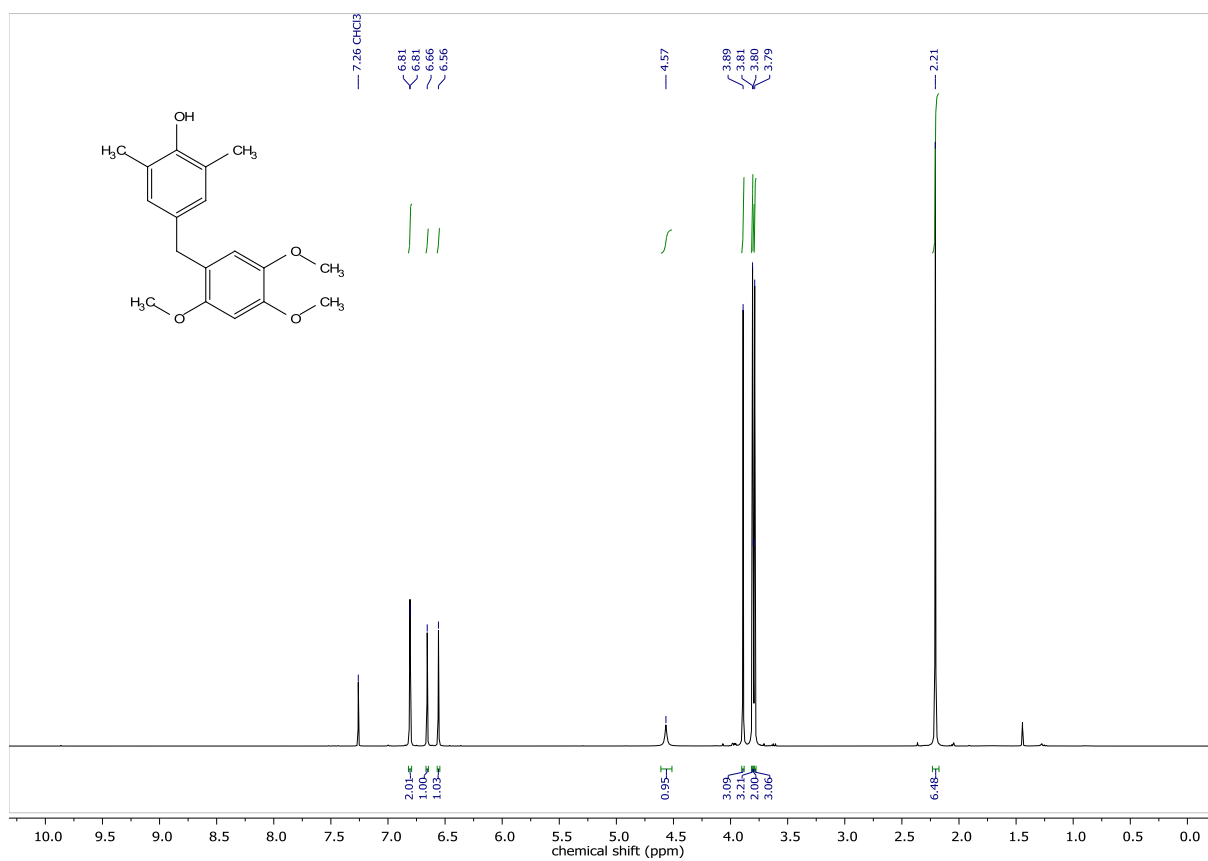
(3)



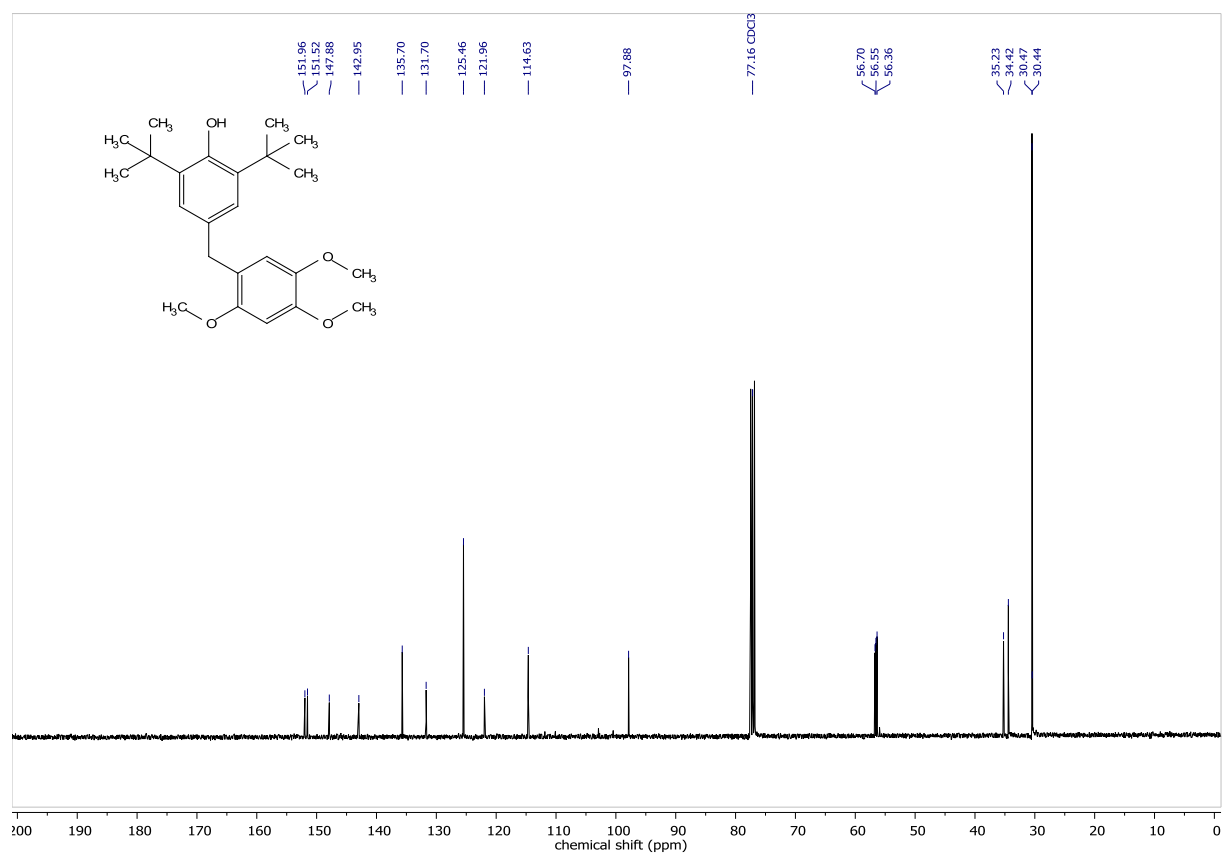
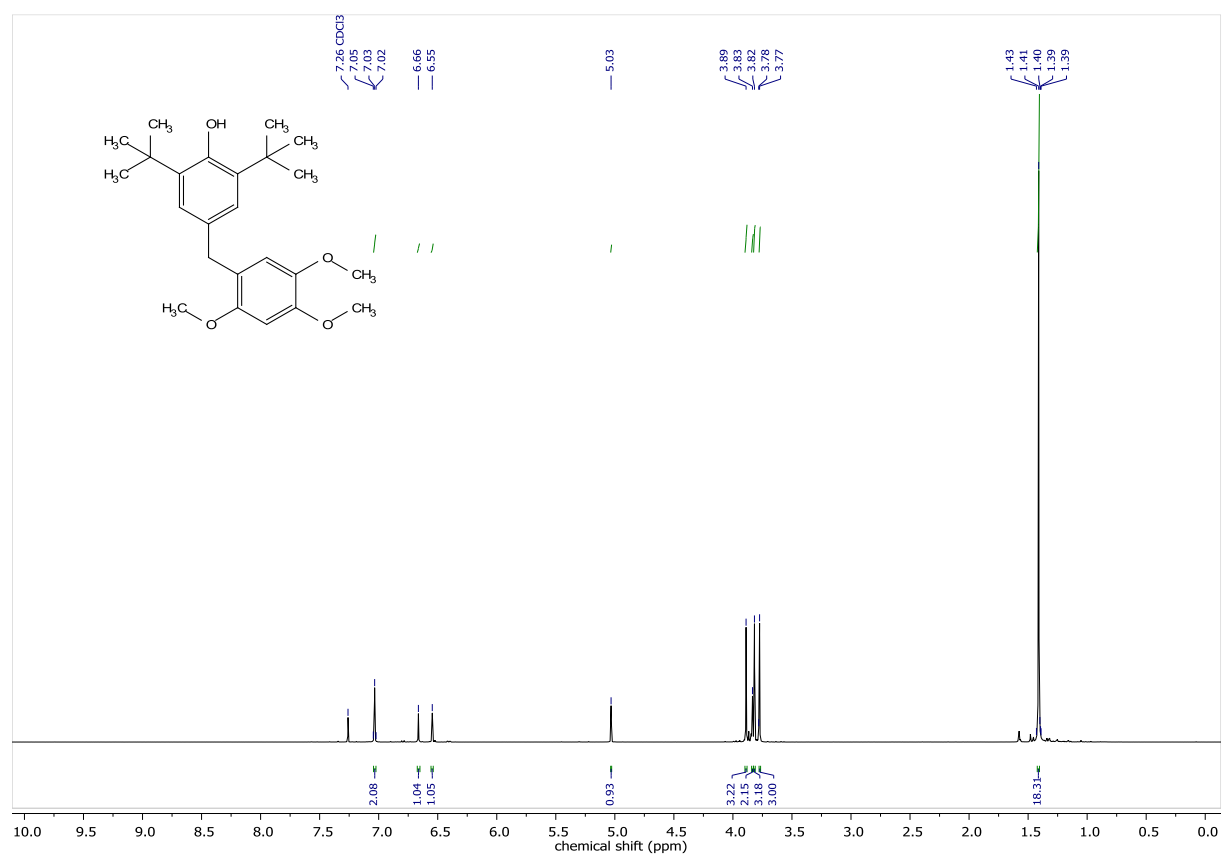
2-Methoxy-4-(1-(2,4,5-trimethoxyphenyl)propyl)phenol (4)



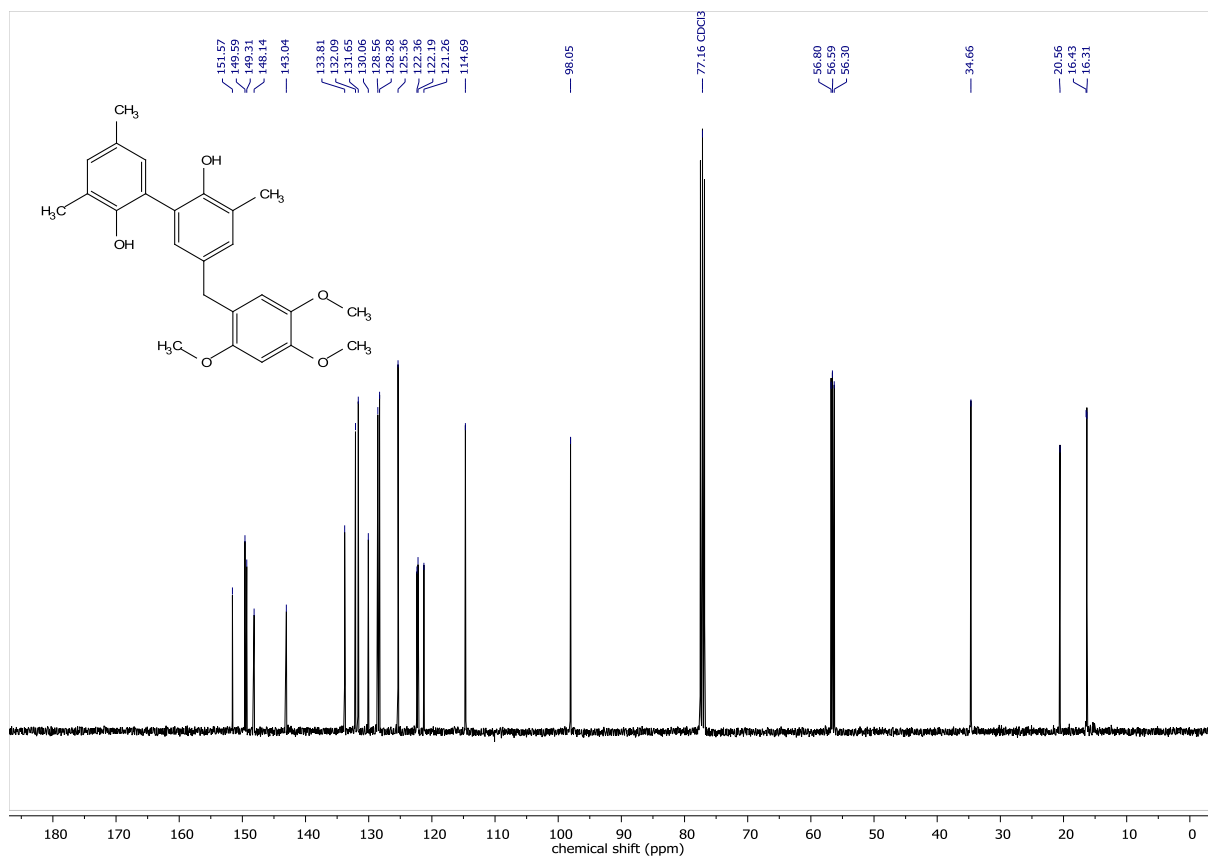
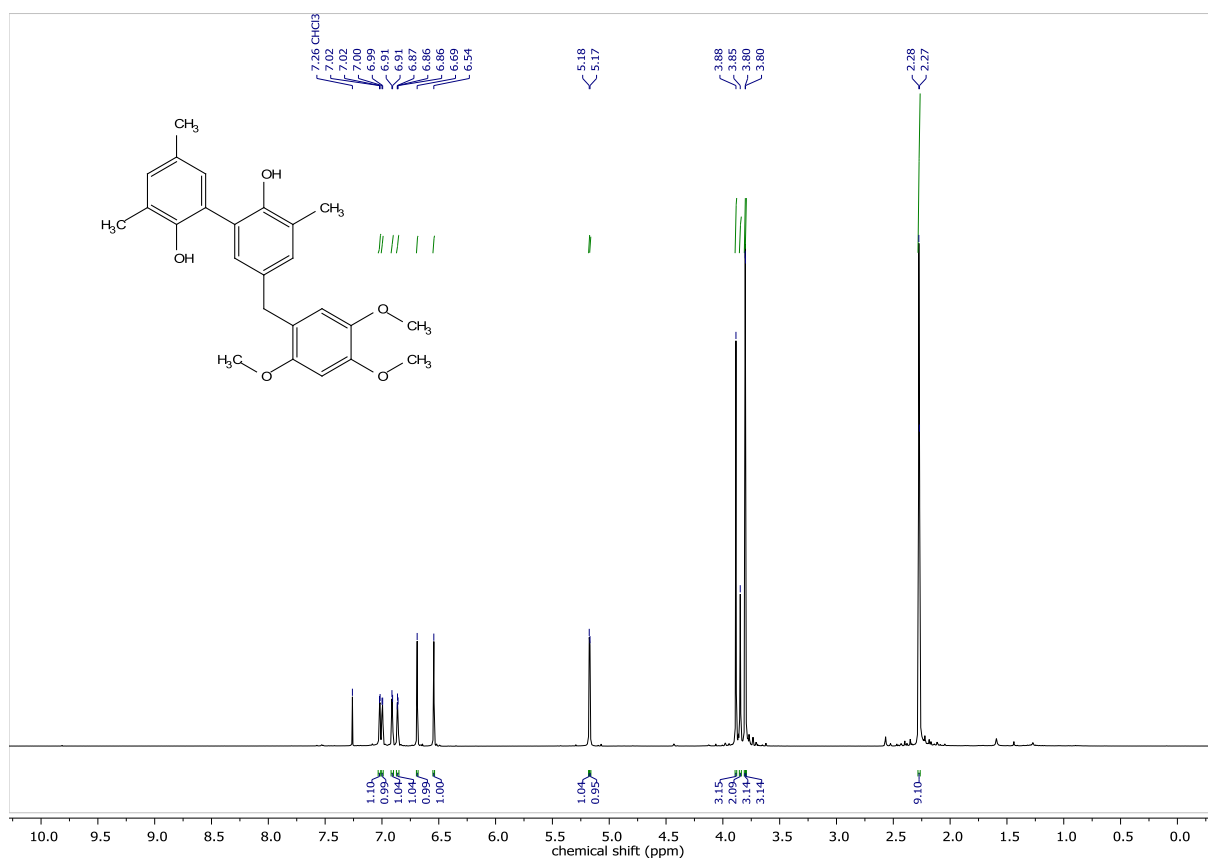
2,6-Dimethyl-4-(2,4,5-trimethoxybenzyl)phenol (5)



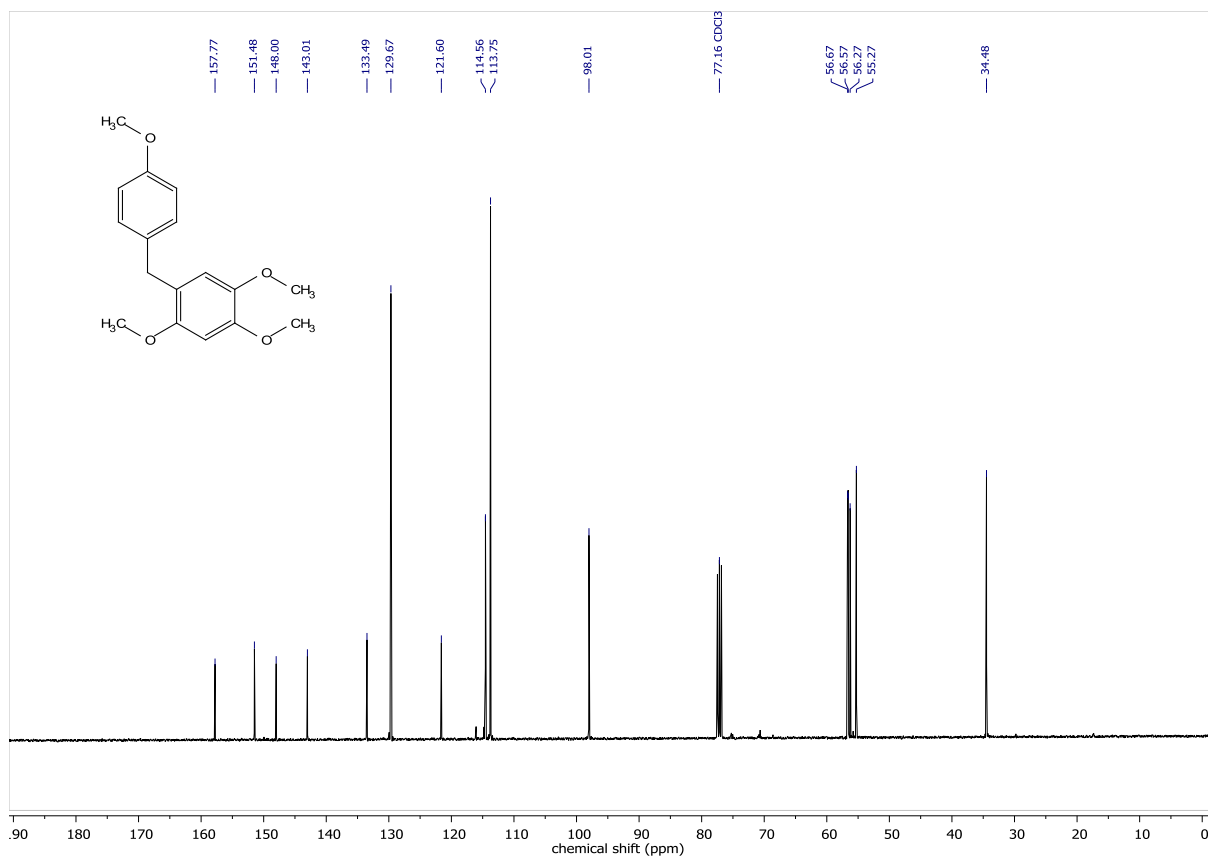
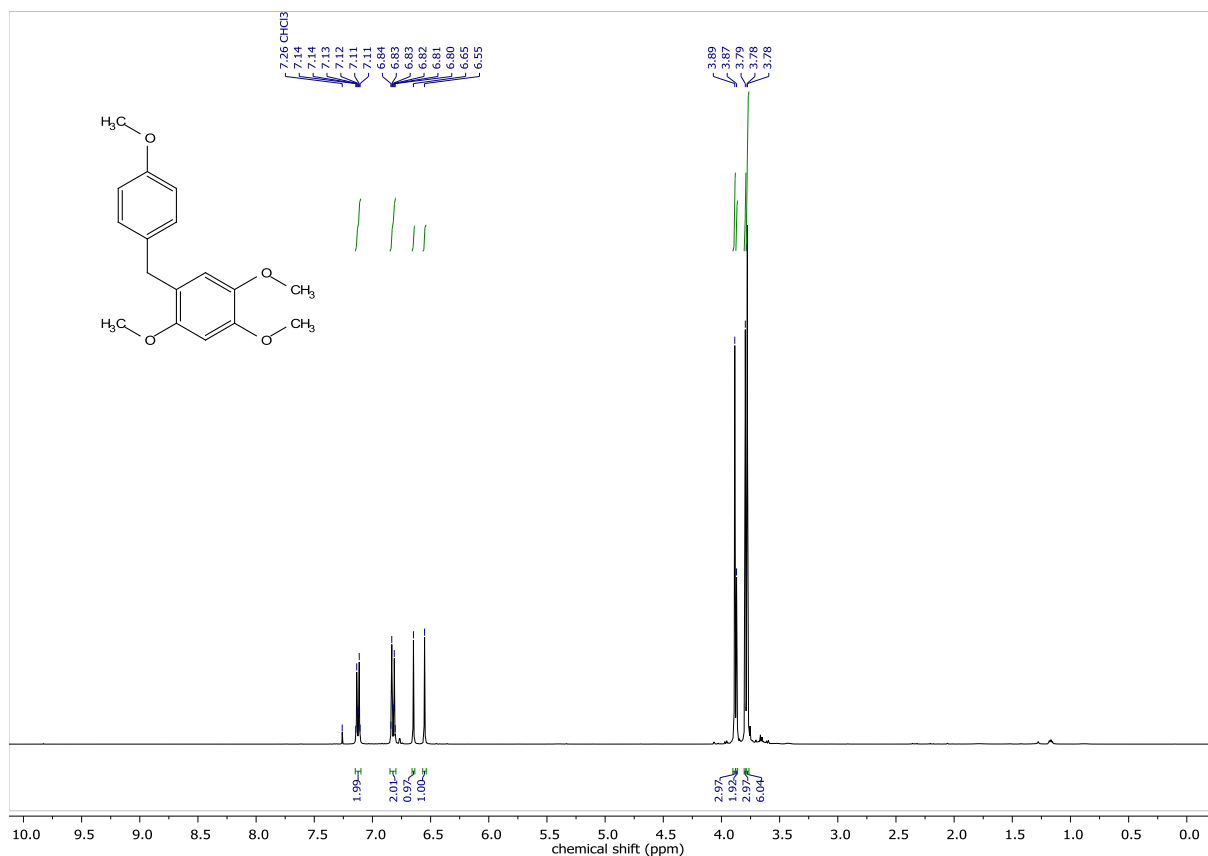
2,6-Di-*tert*-butyl-4-(2,4,5-trimethoxybenzyl)phenol (6)



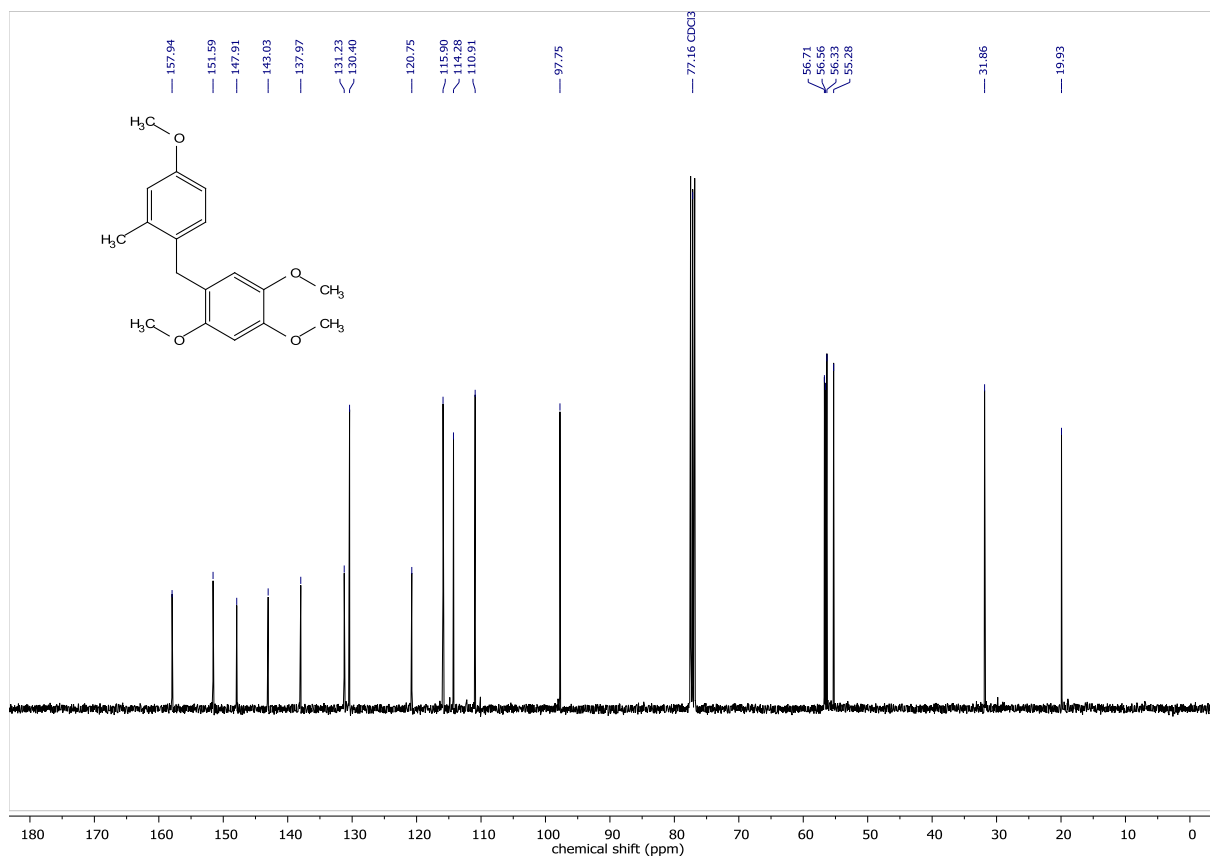
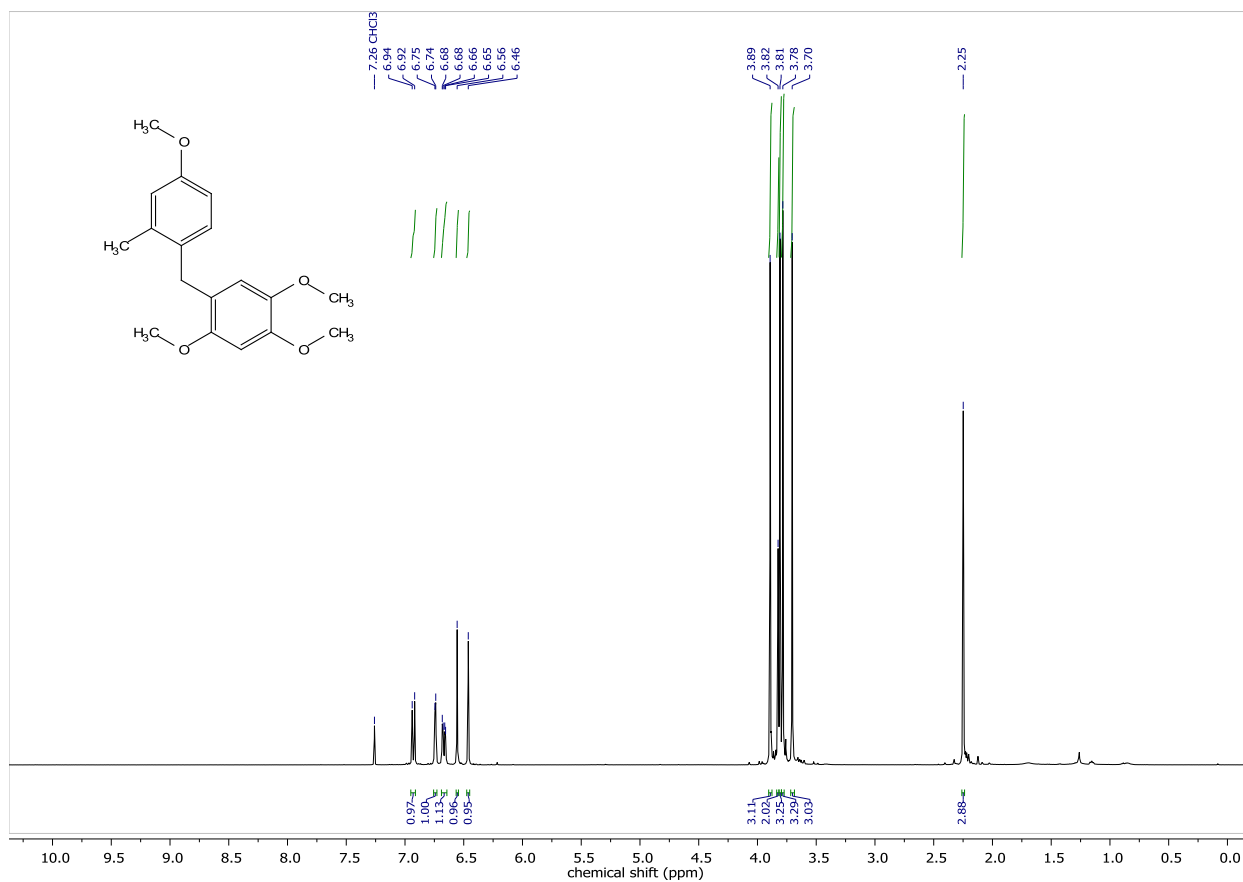
3,3',5-Trimethyl-5'-(2,4,5-trimethoxybenzyl)-[1,1'-biphenyl]-2,2'-diol (7)



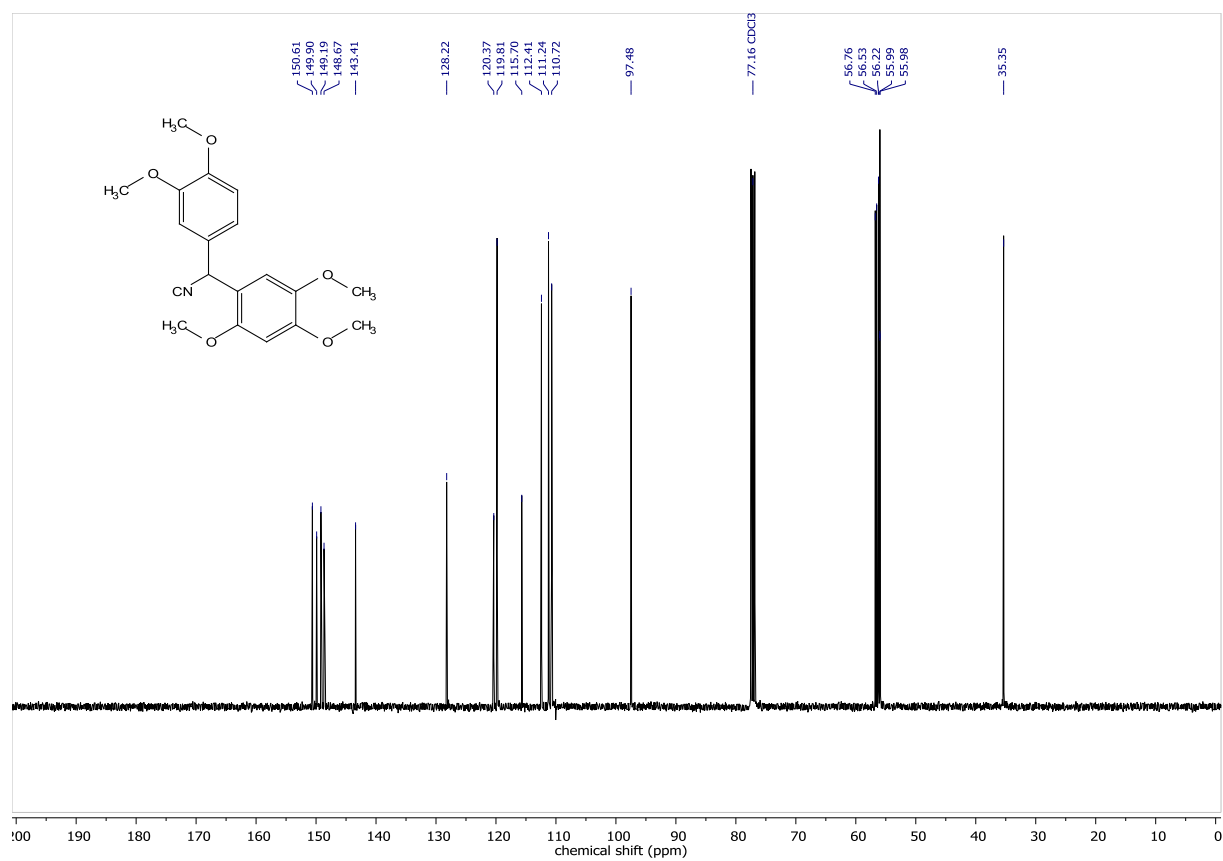
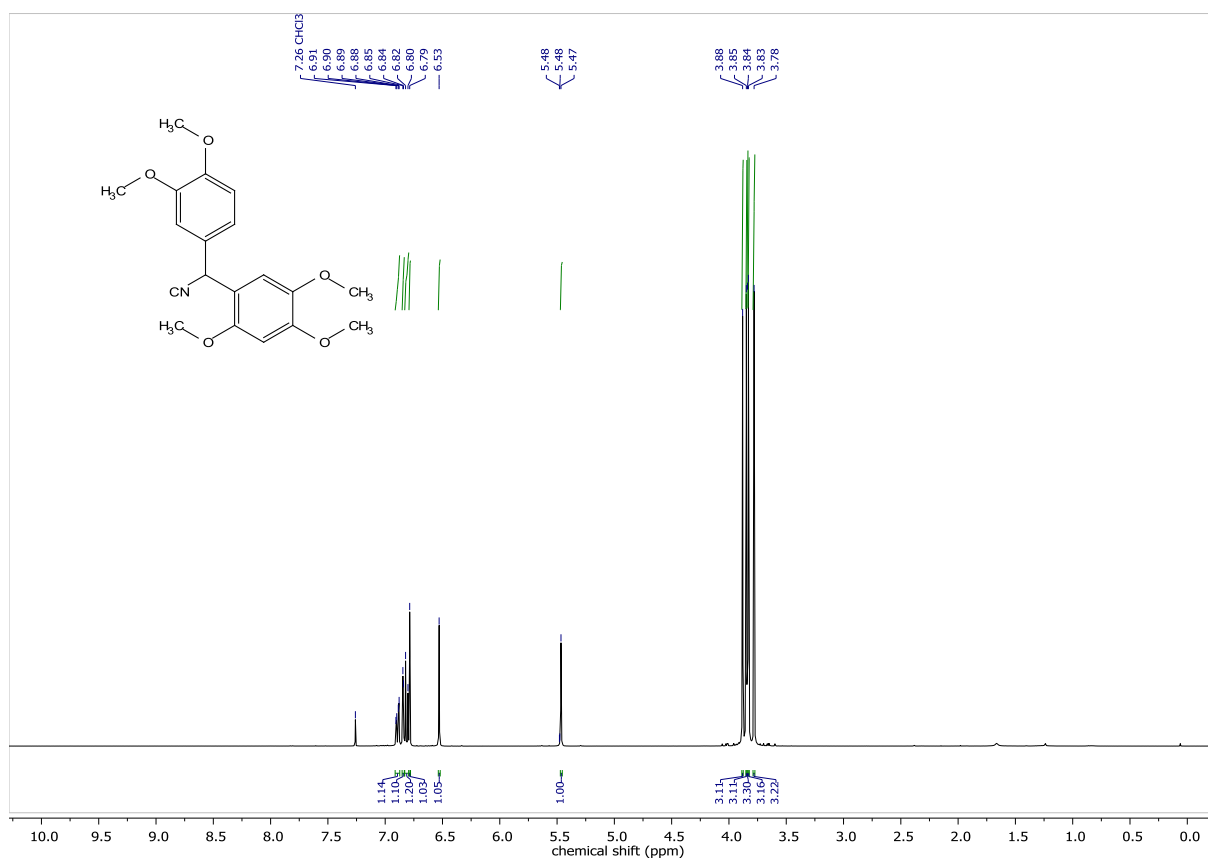
1,2,4-Trimethoxy-5-(4-methoxybenzyl)benzene (8)



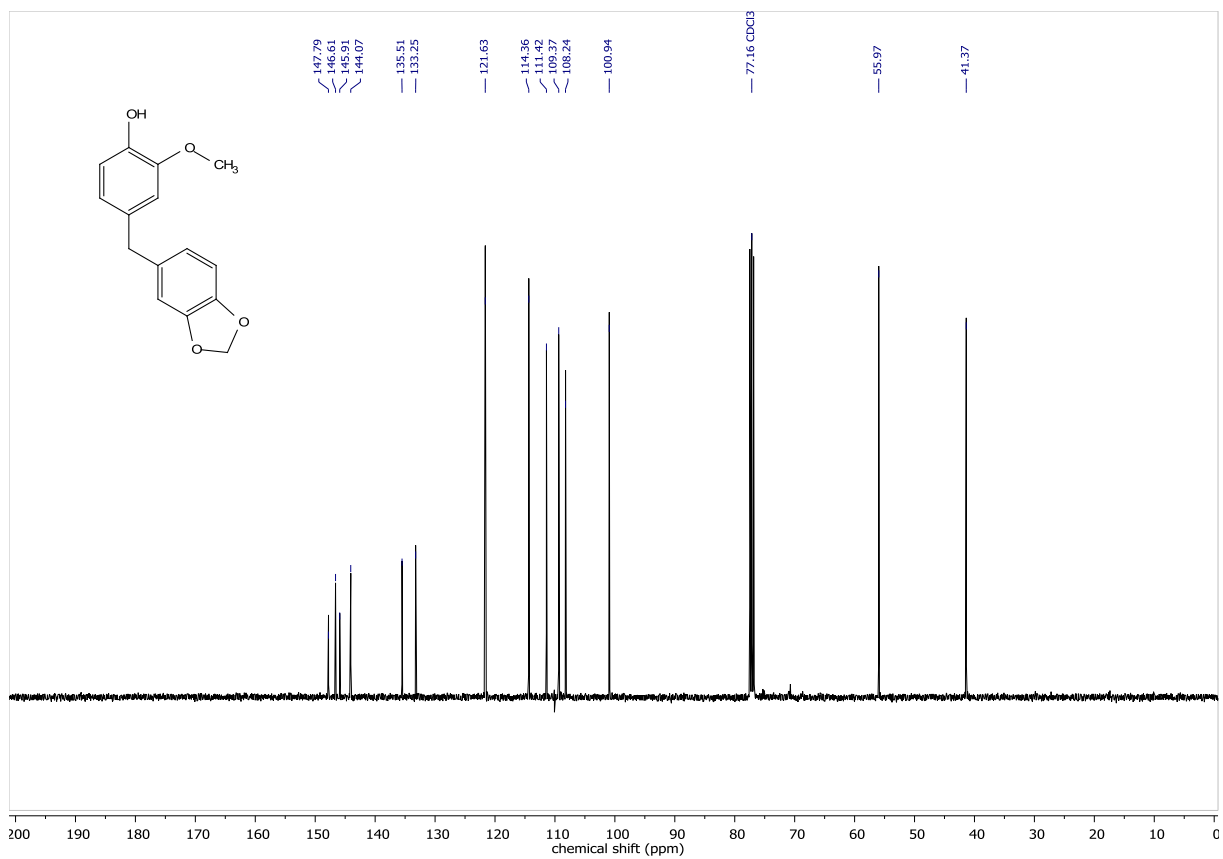
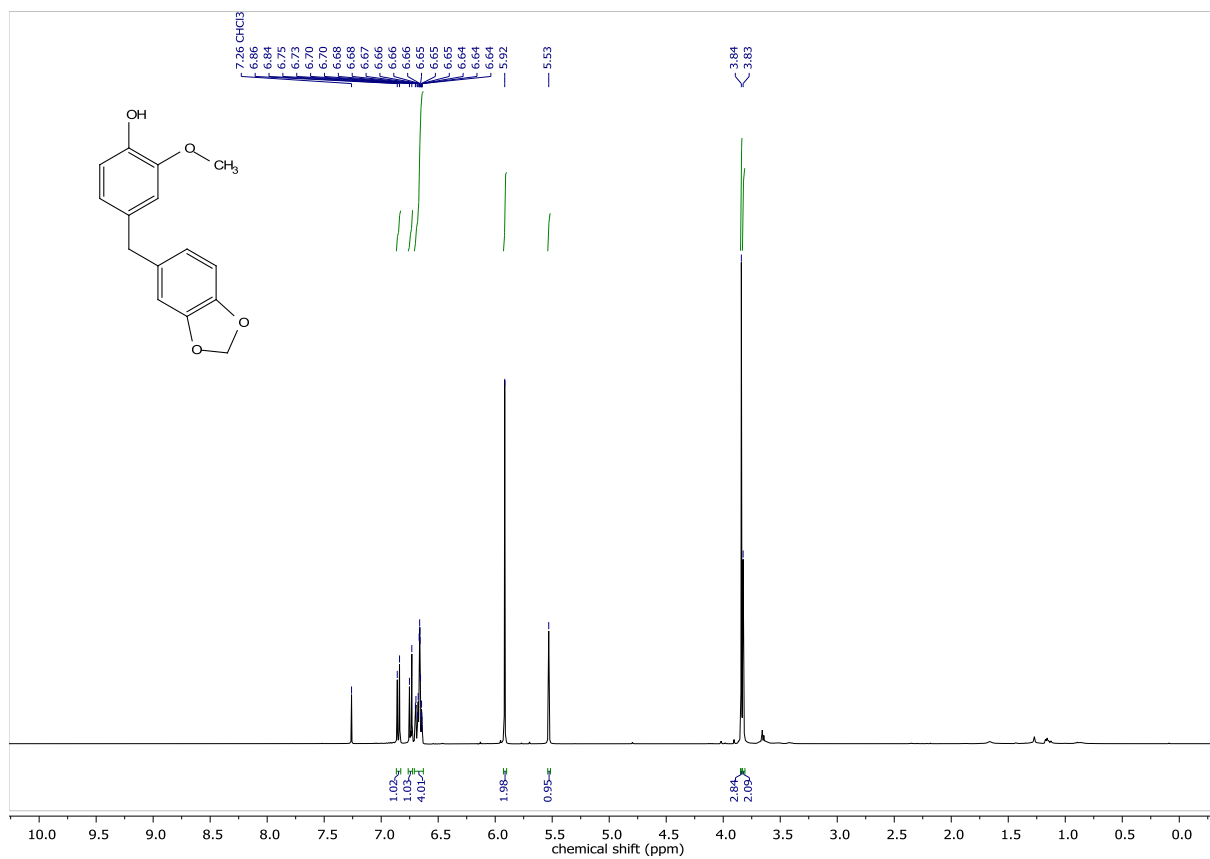
1,2,4-Trimethoxy-5-(4-methoxy-2-methylbenzyl)benzene (9)



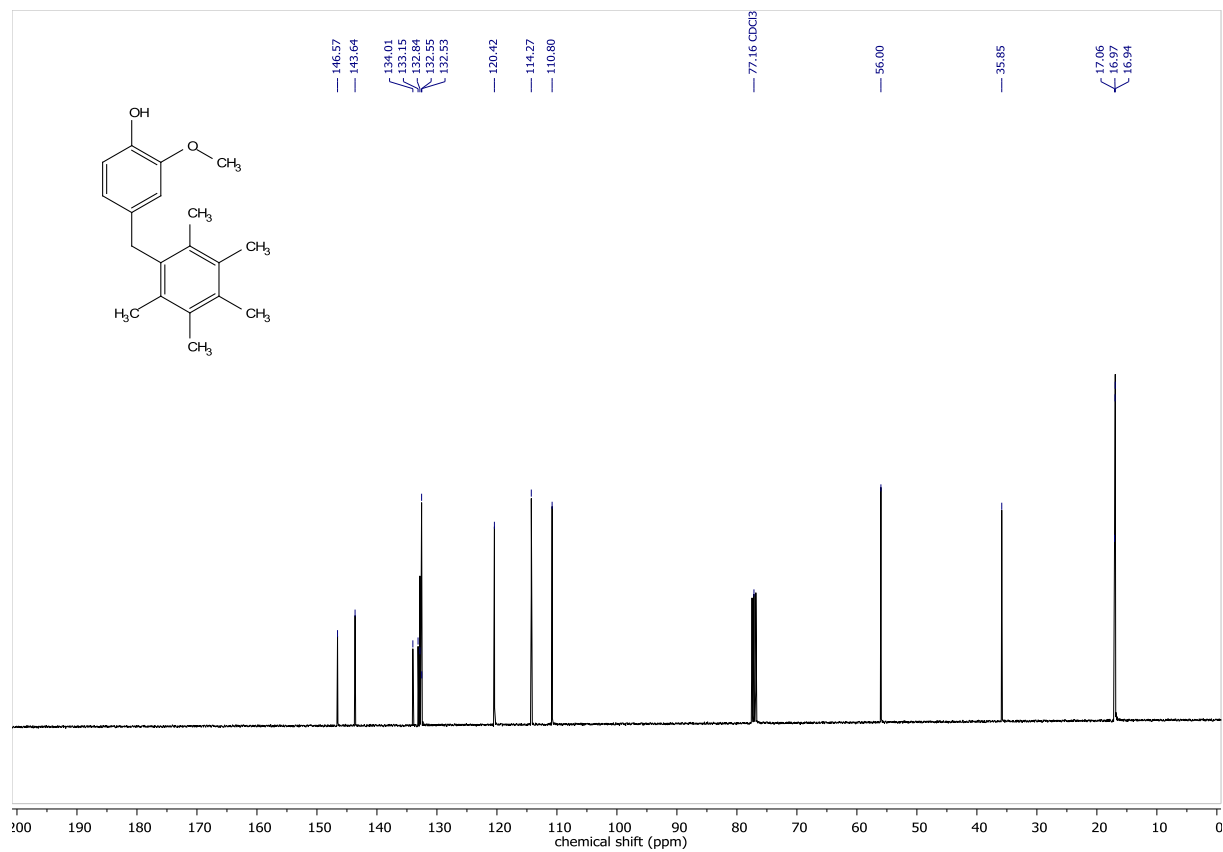
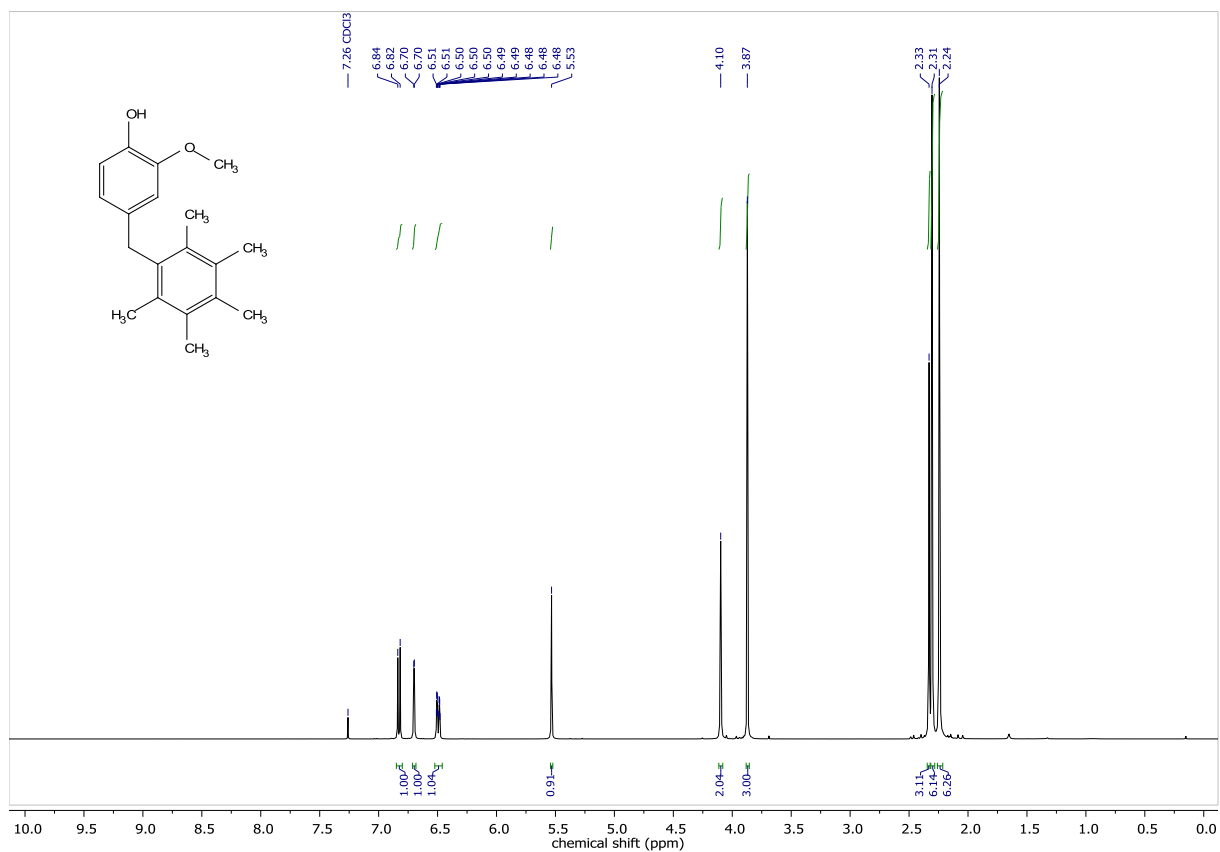
2-(3,4-Dimethoxyphenyl)-2-(2,4,5-trimethoxyphenyl)acetonitrile (10)



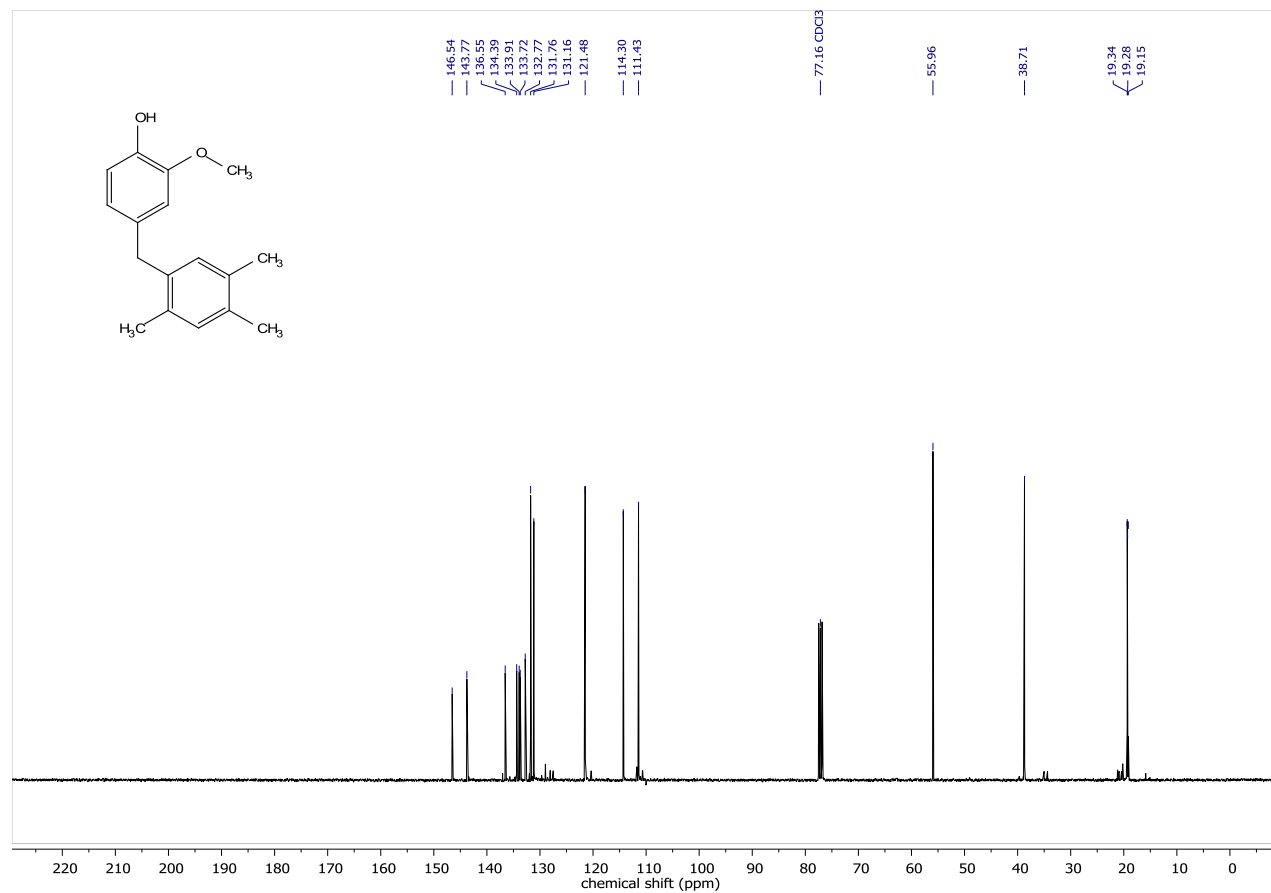
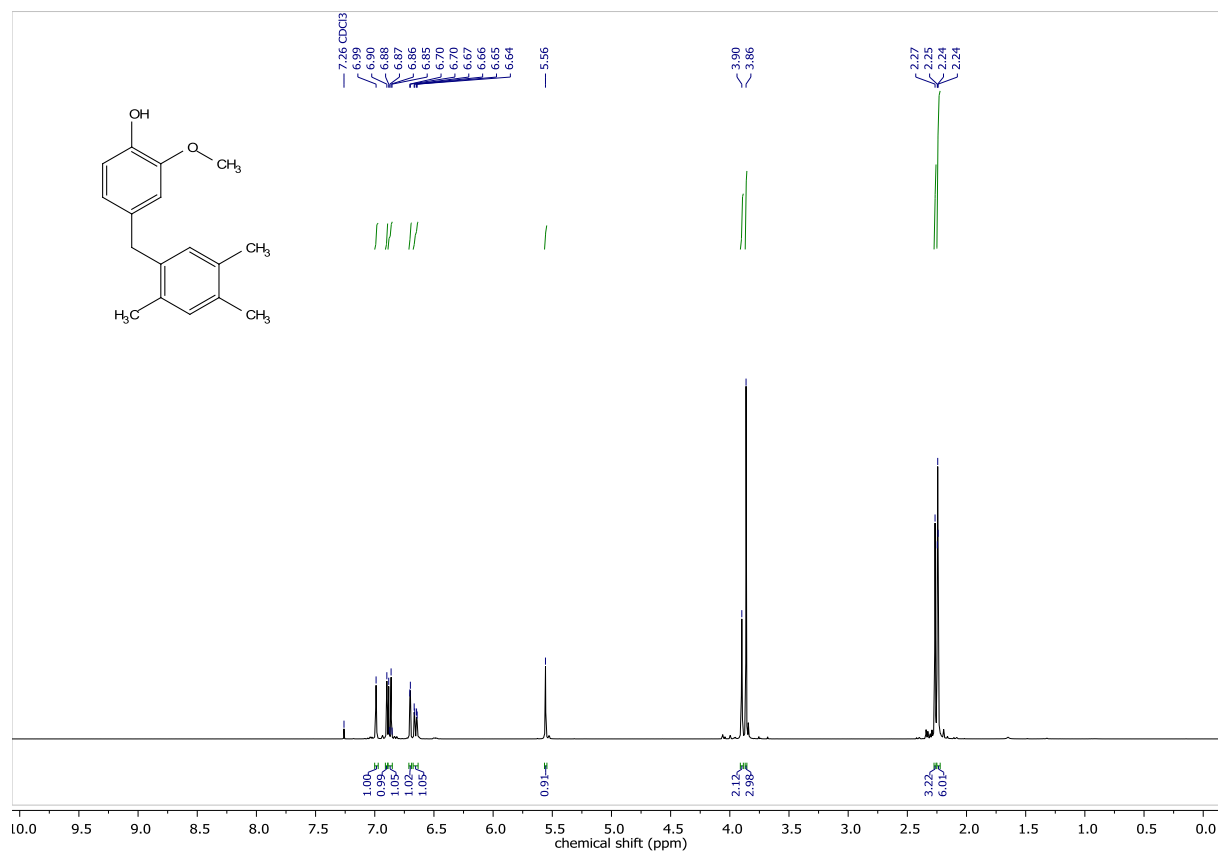
4-(Benzo[d][1,3]dioxol-5-ylmethyl)-2-methoxyphenol (11)



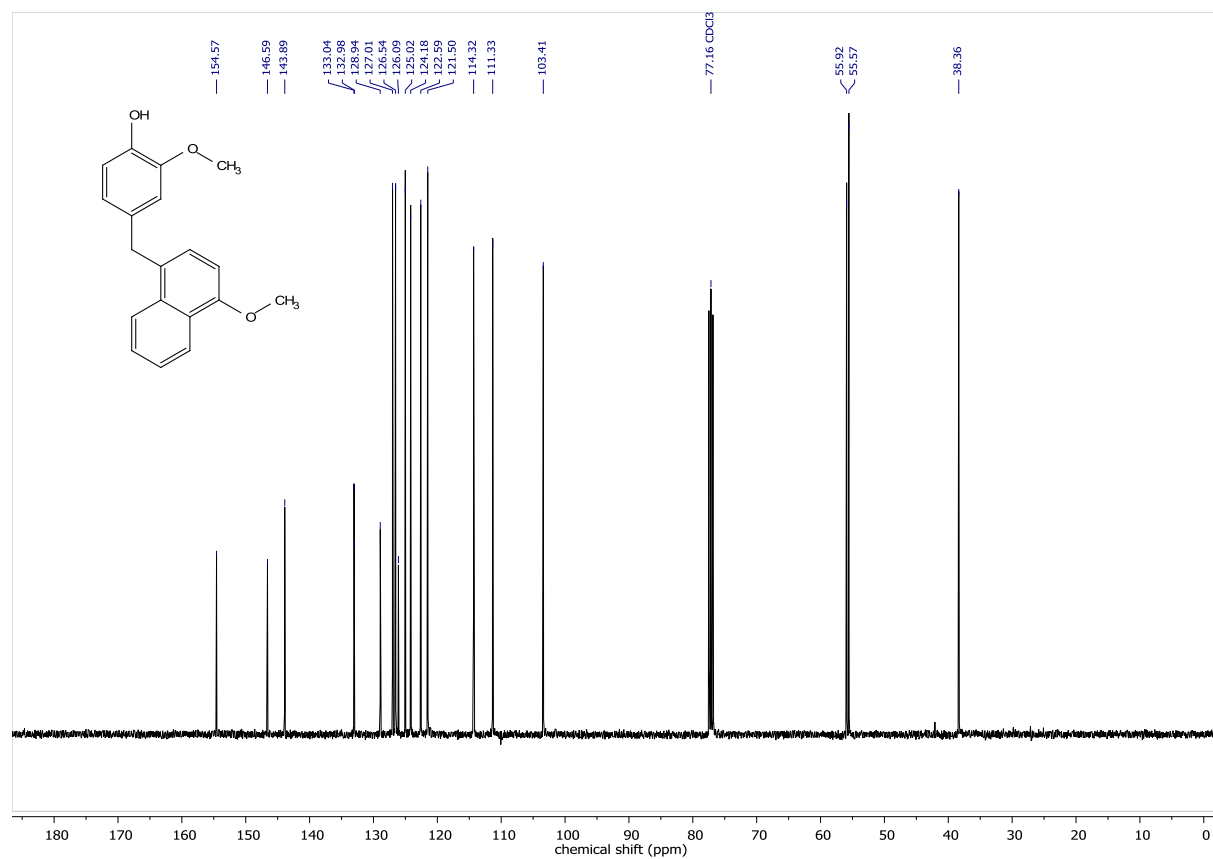
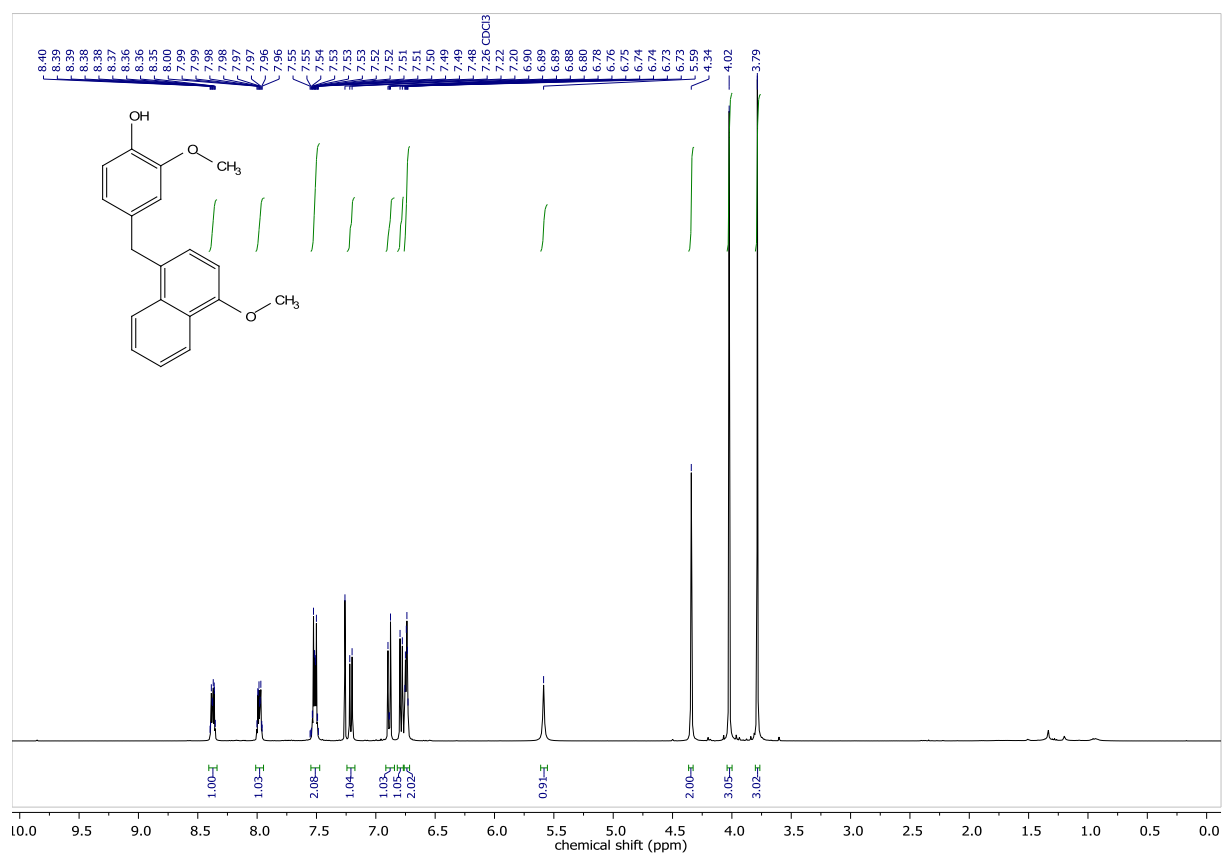
2-Methoxy-4-(2,3,4,5,6-pentamethylbenzyl)phenol (12)



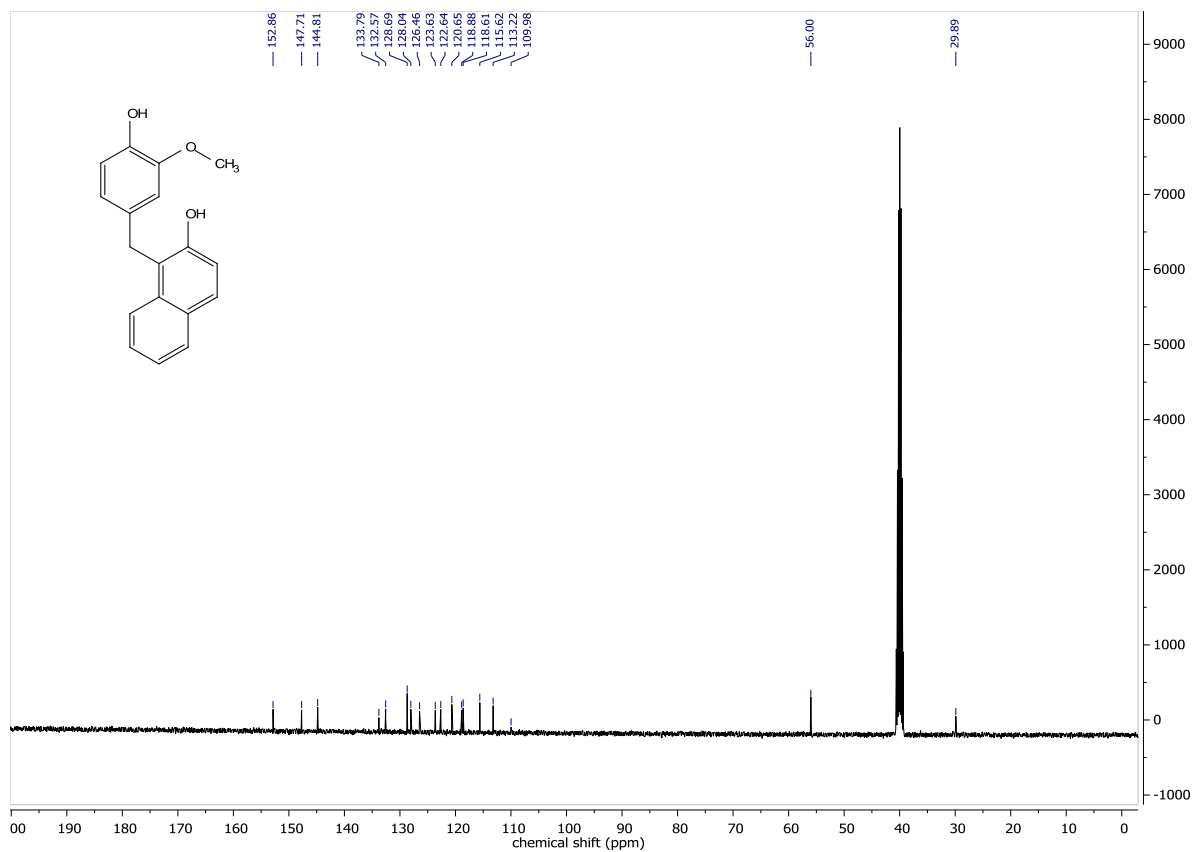
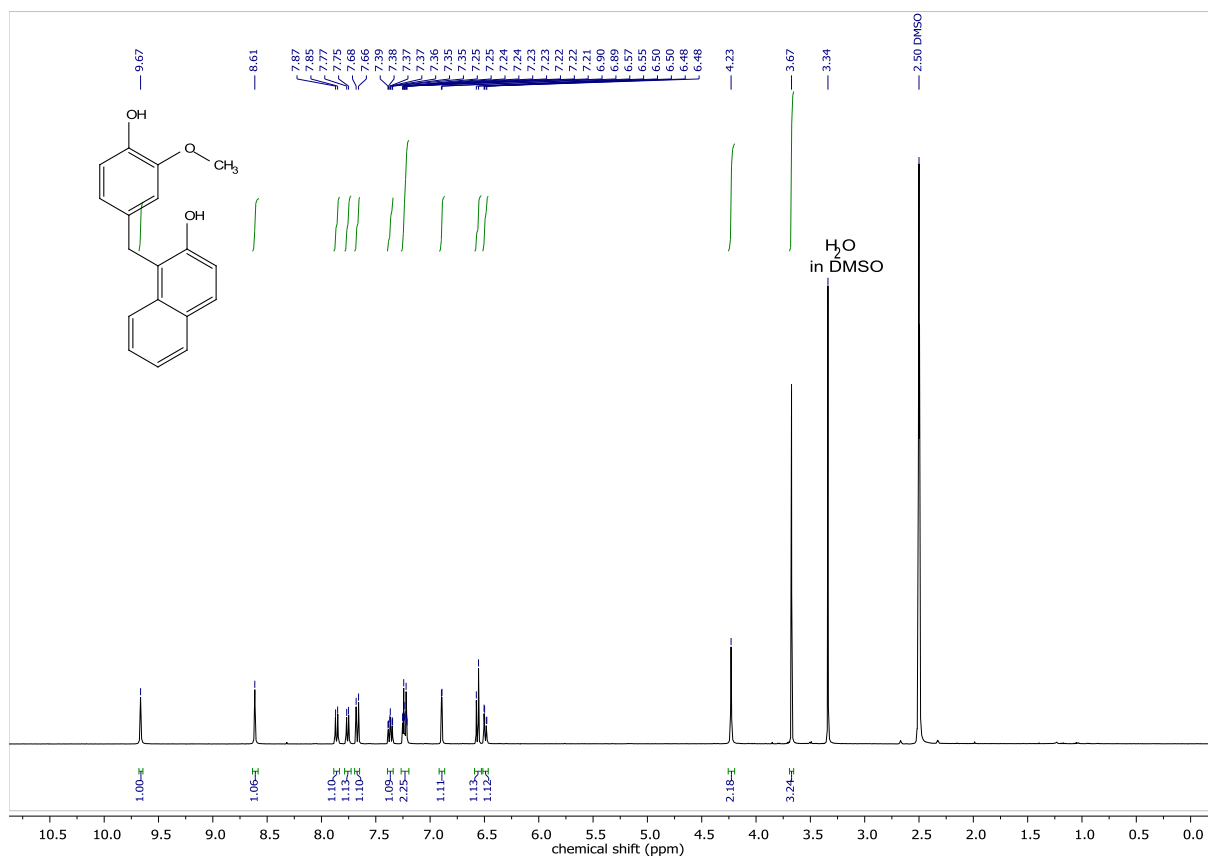
2-Methoxy-4-(2,4,5-trimethylbenzyl)phenol (13)



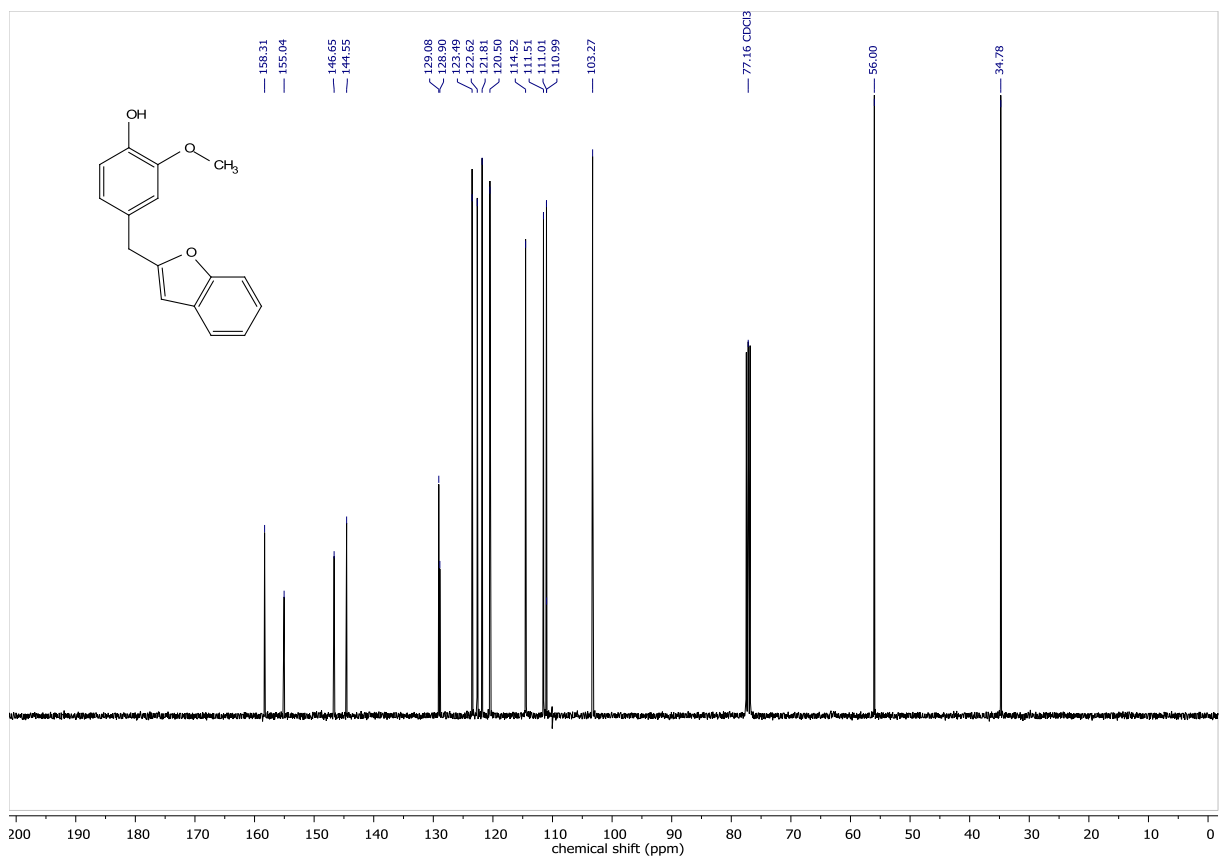
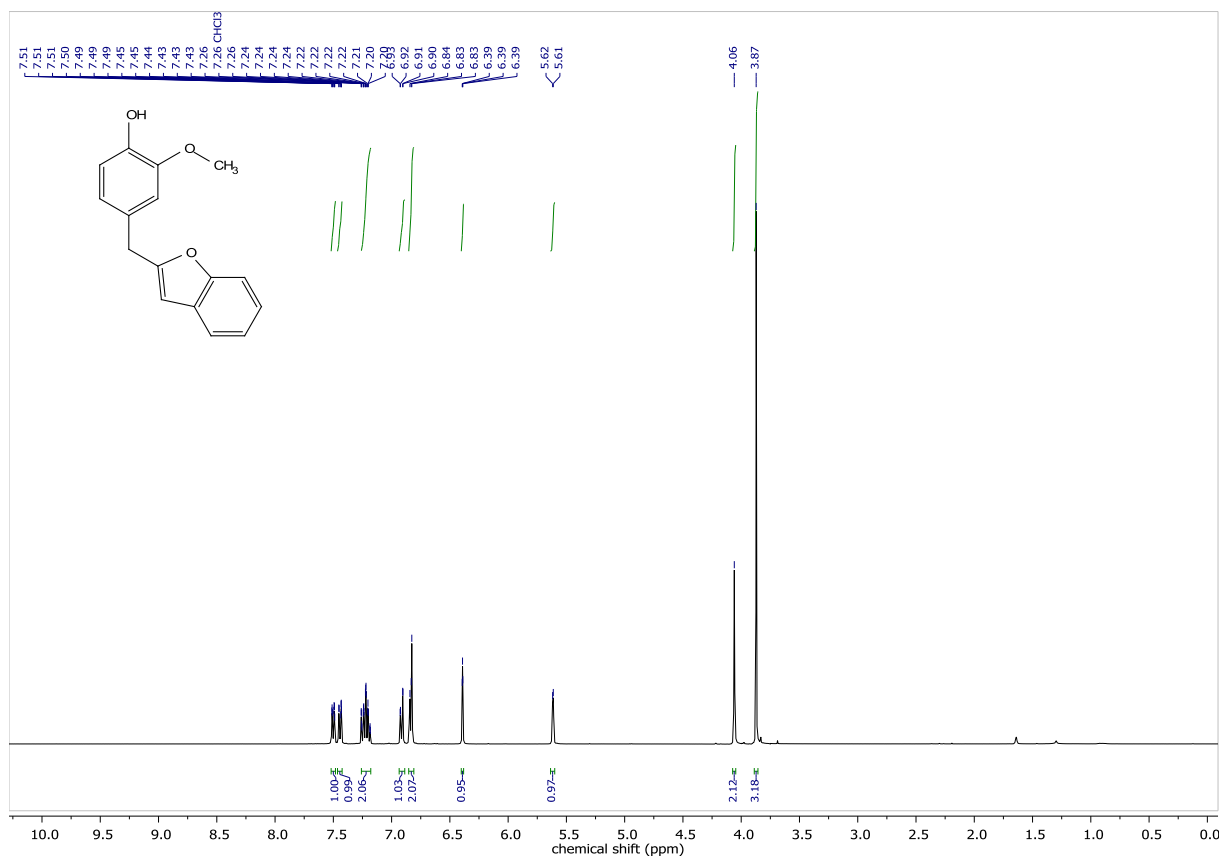
2-Methoxy-4-((4-methoxynaphthalen-1-yl)methyl)phenol (14)



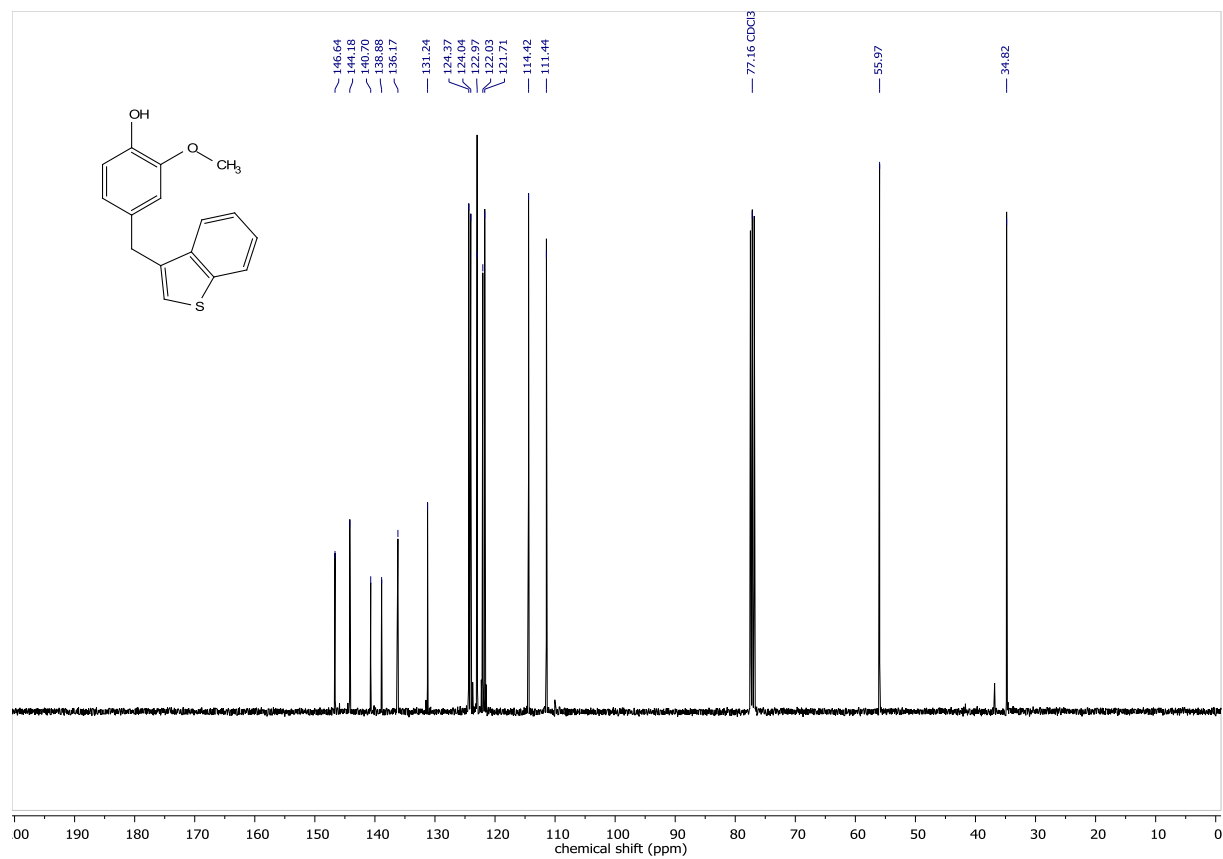
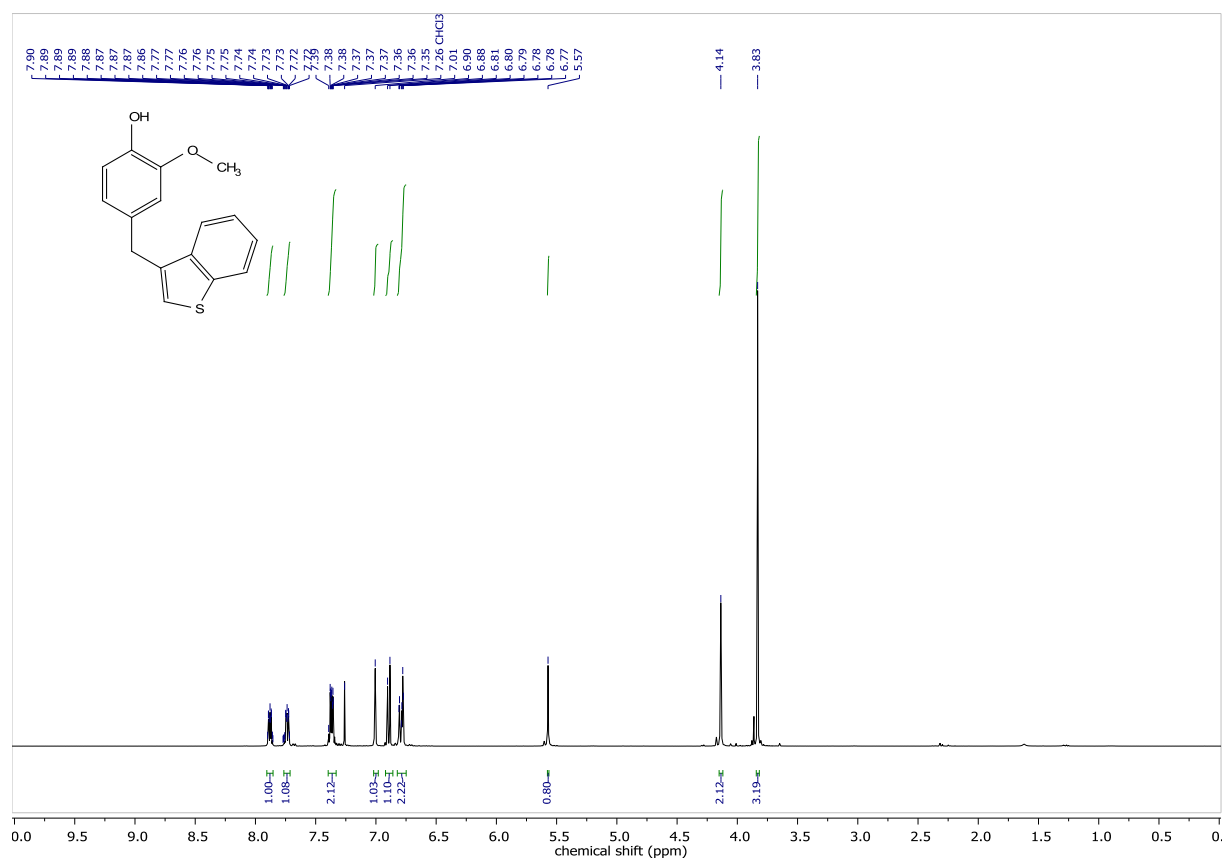
1-(4-Hydroxy-3-methoxybenzyl)naphthalen-2-ol (15)



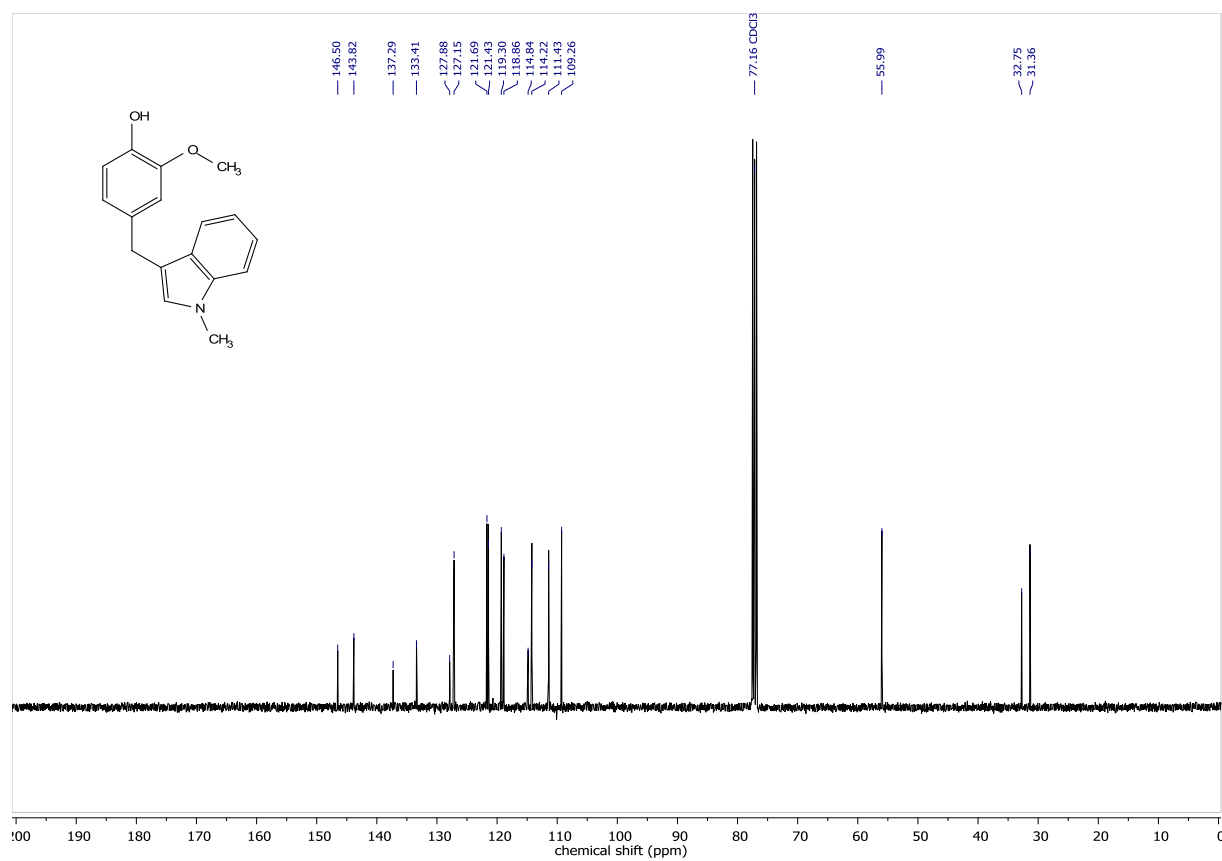
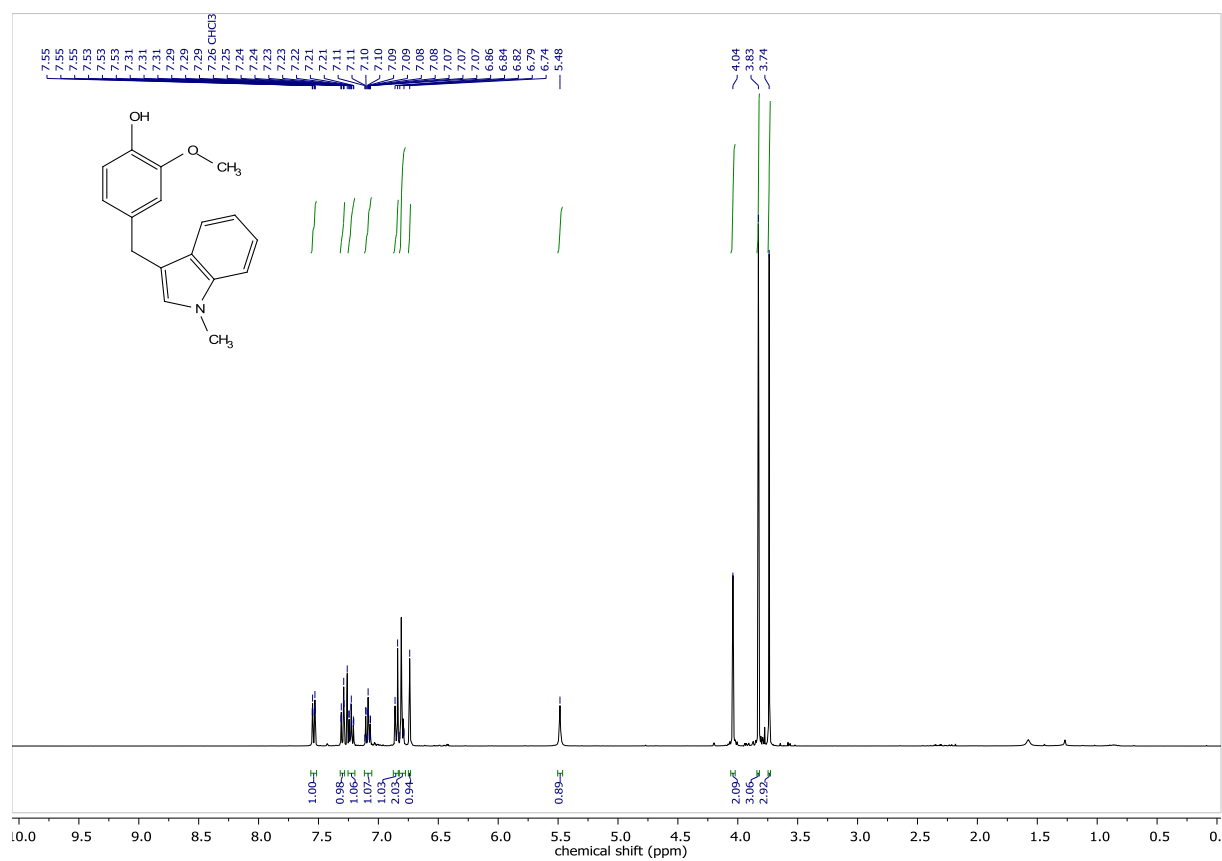
2-((4-Hydroxy-3-methoxyphenyl)methyl)-benzofuran (16)



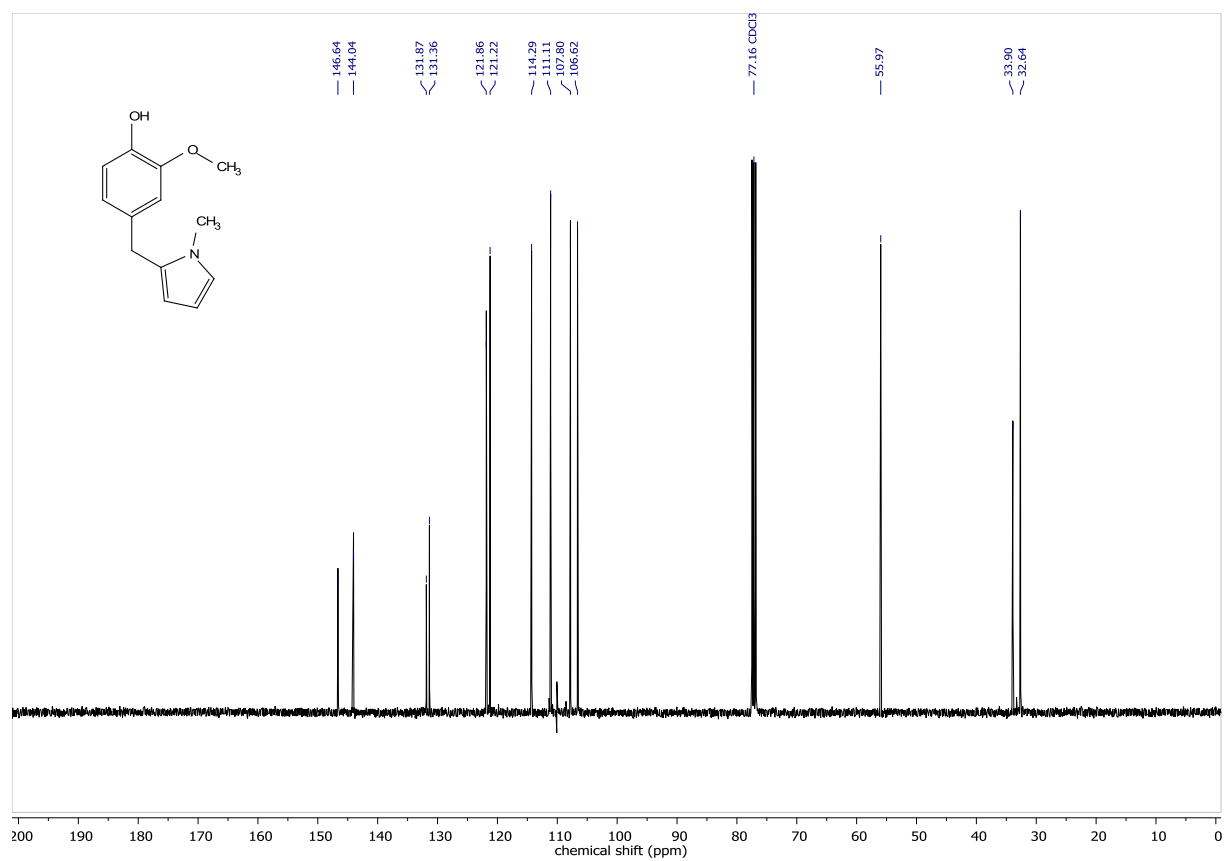
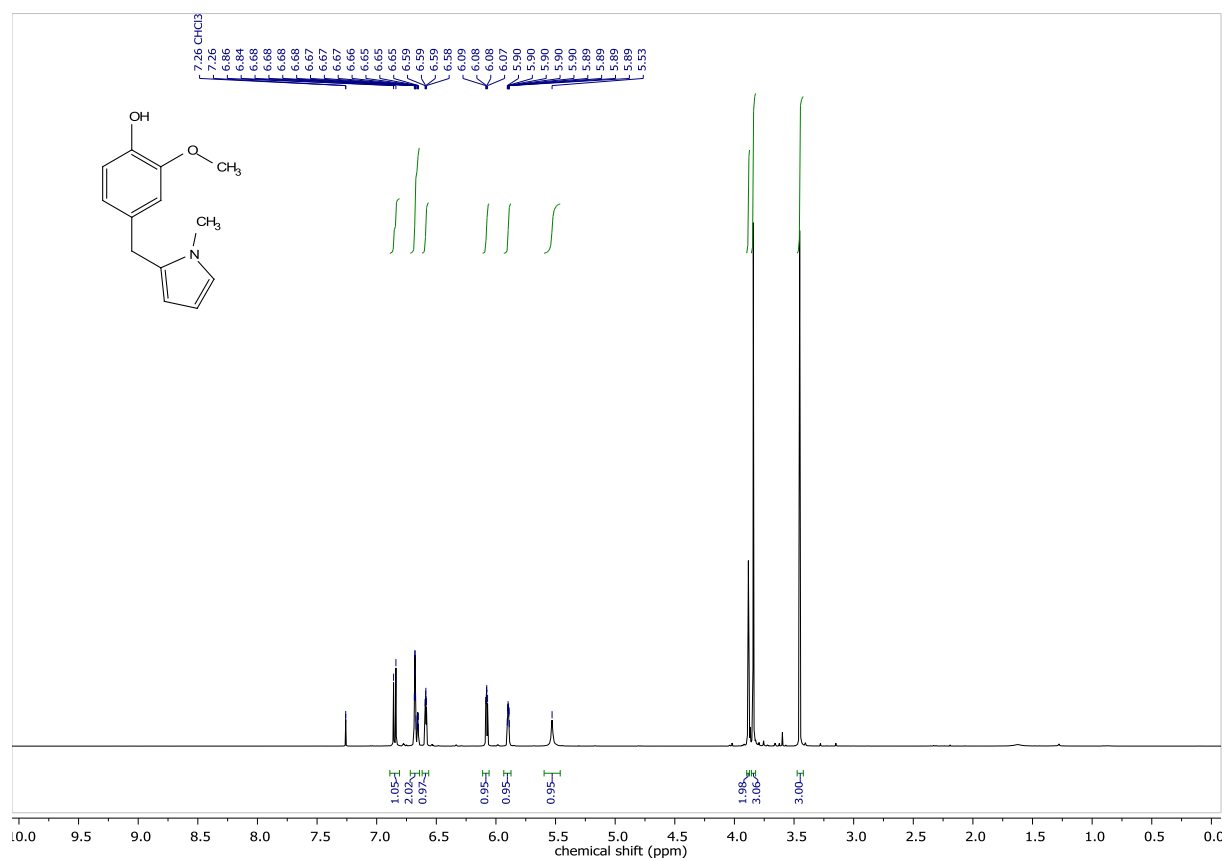
3-((4-Hydroxy-3-methoxyphenyl)methyl)-benzo[b]thiophene (17)



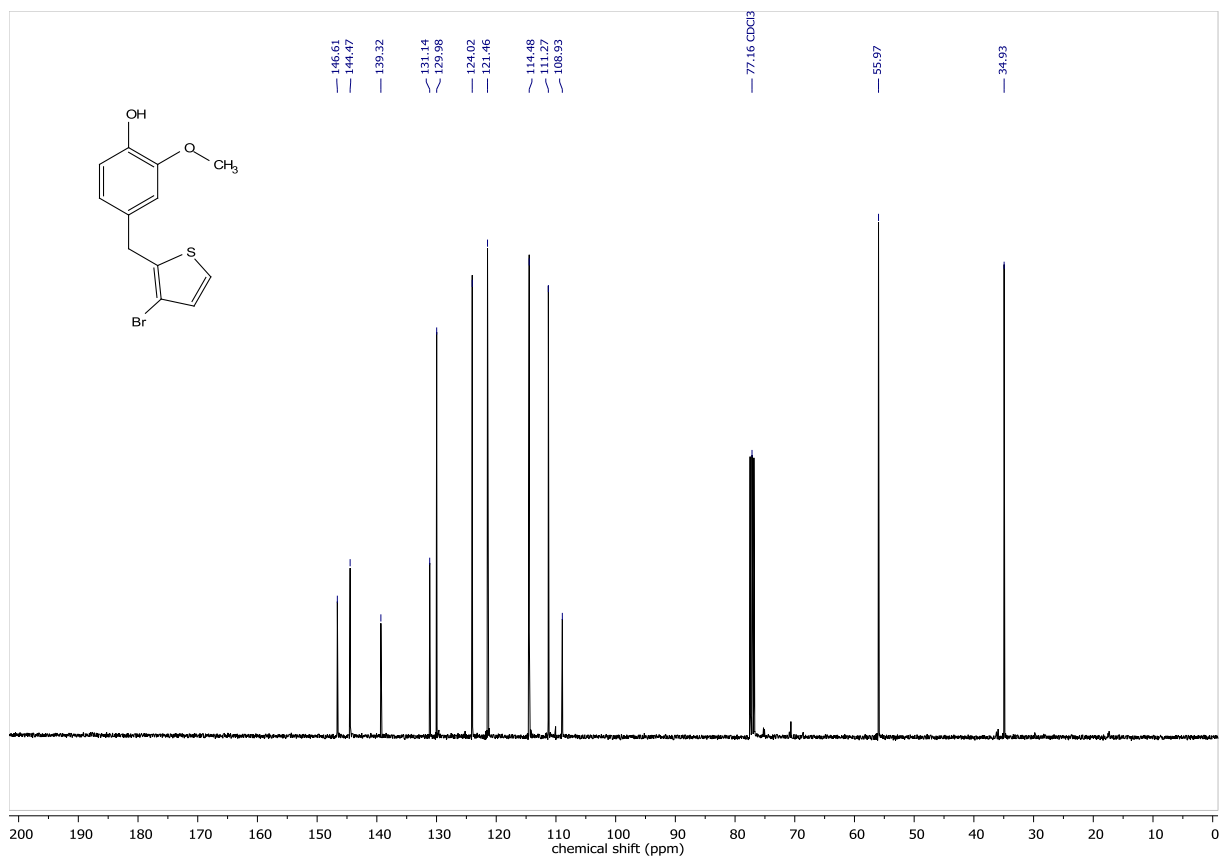
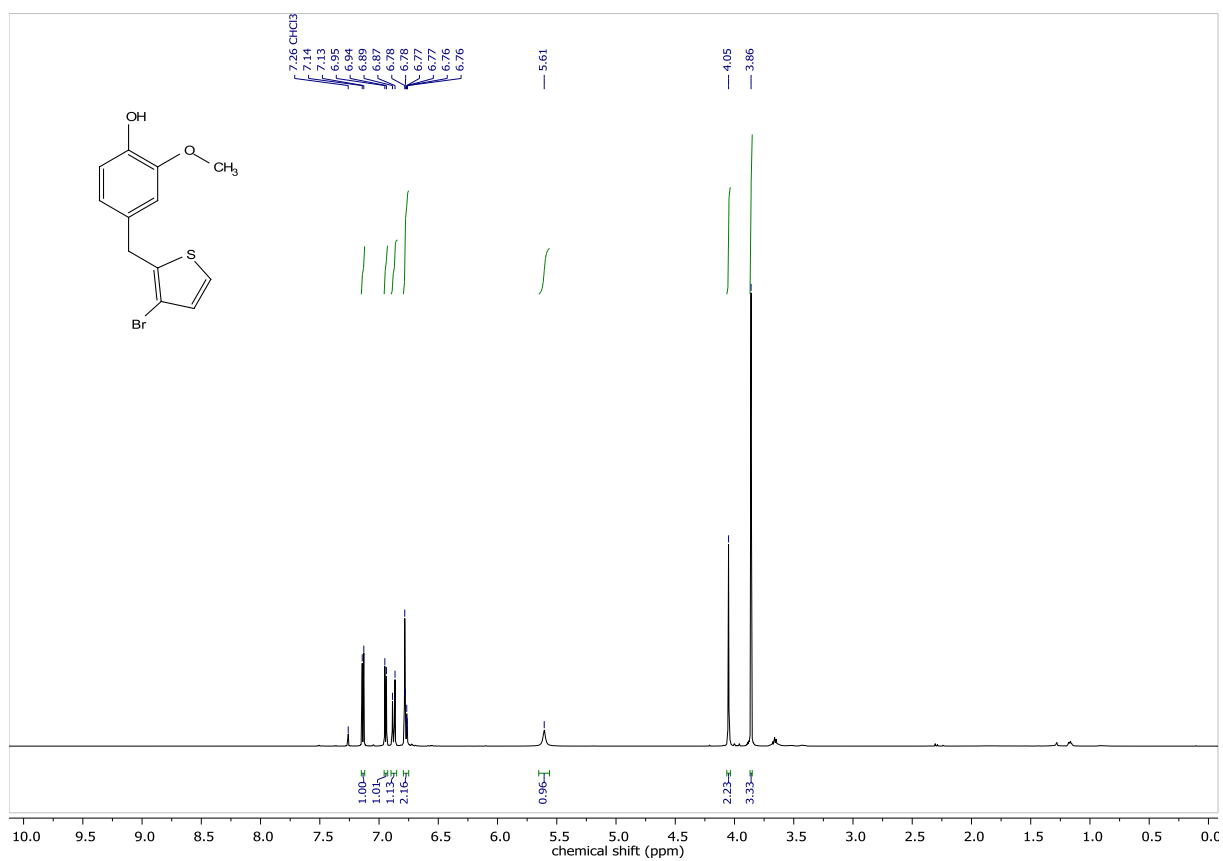
1-Methyl-3-((4-hydroxy-3-methoxyphenyl)methyl)-indole (18)



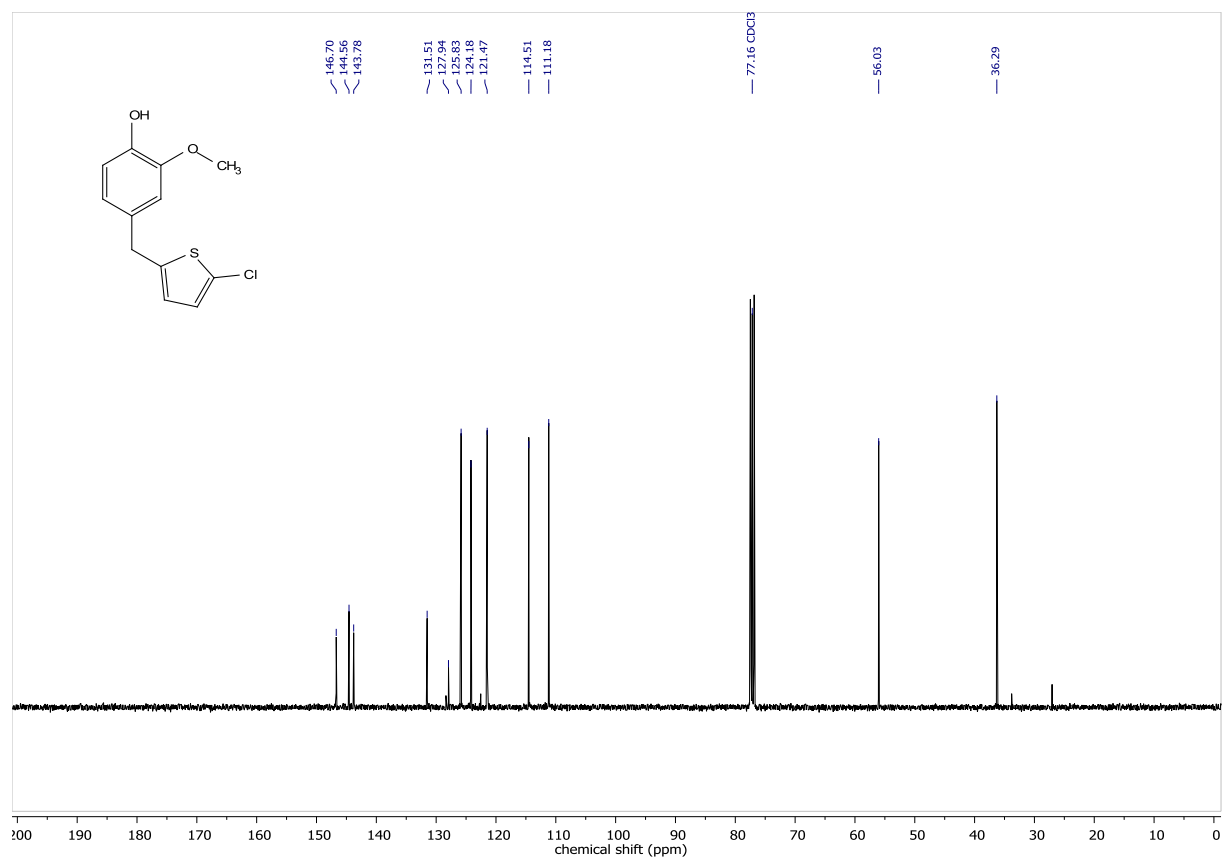
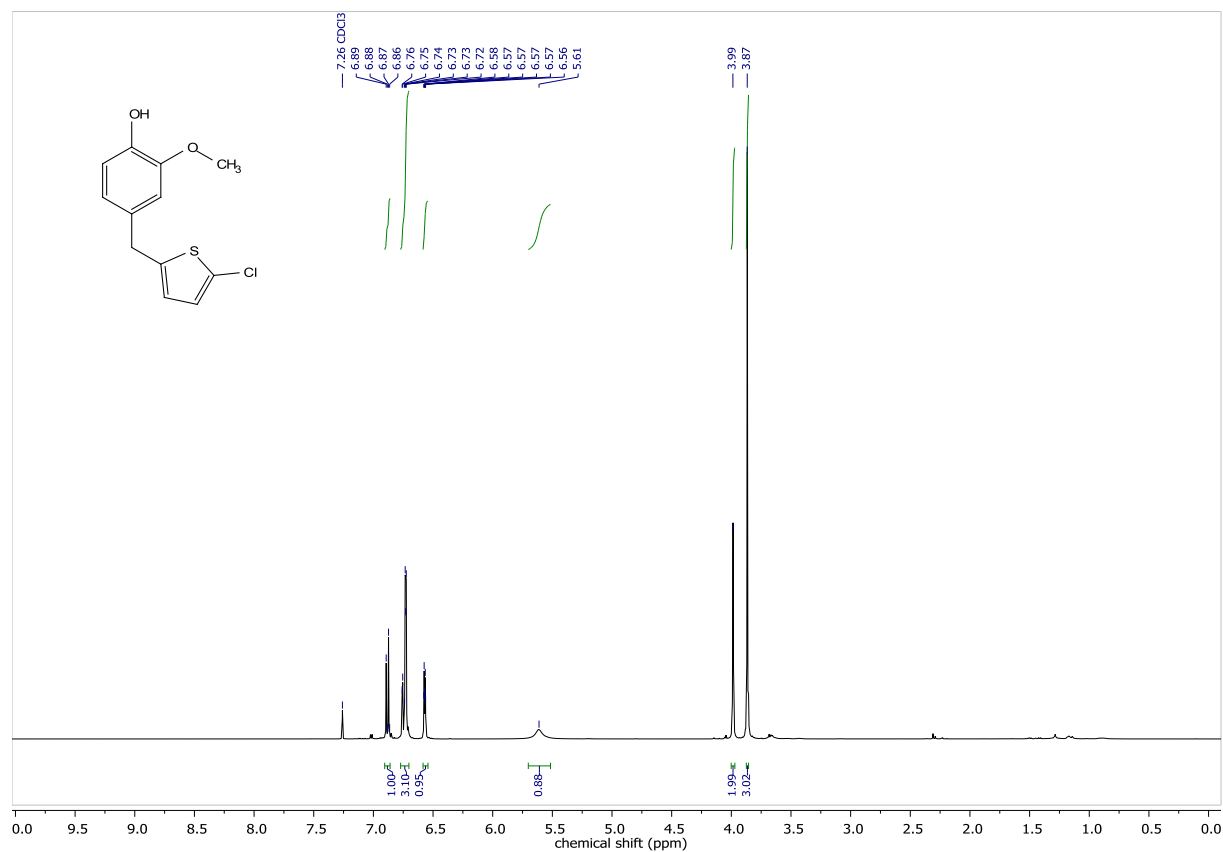
1-Methyl-2-((4-hydroxy-3-methoxyphenyl)methyl)-pyrrole (19)



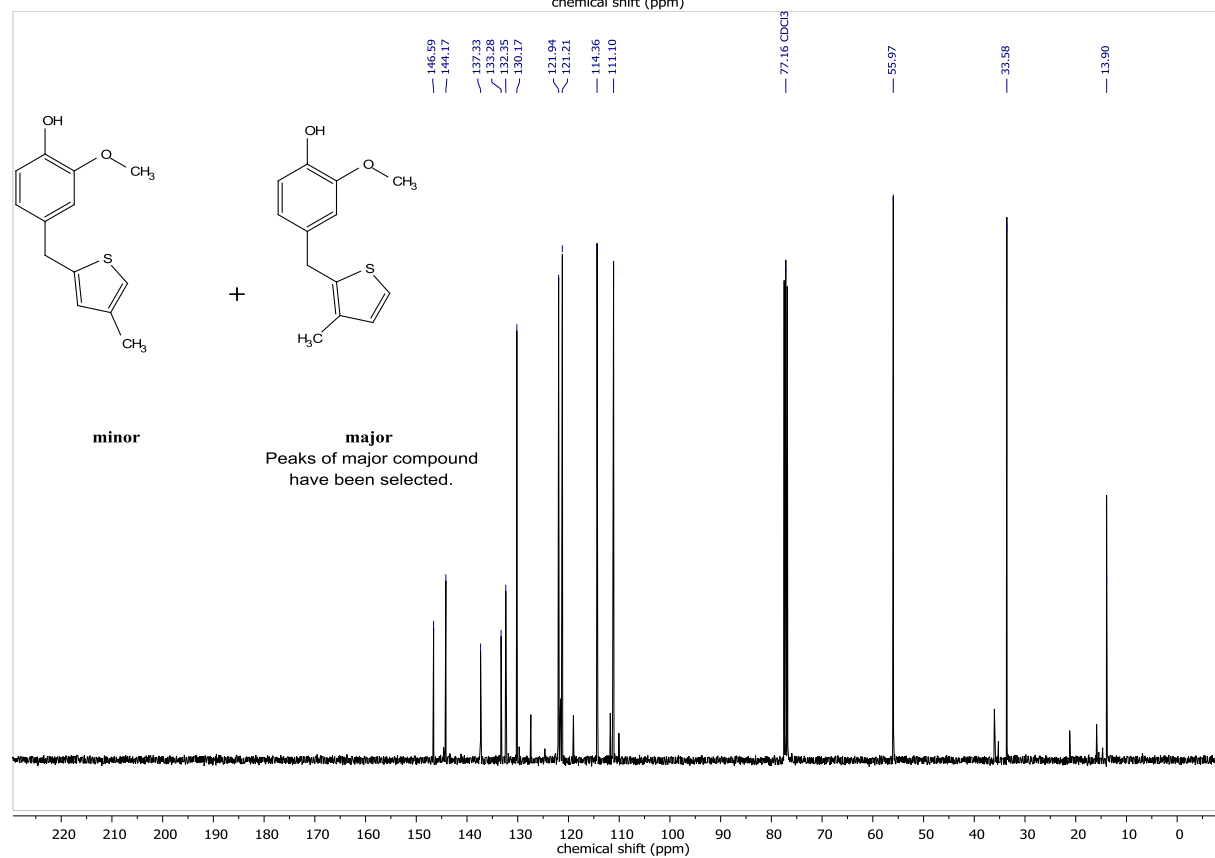
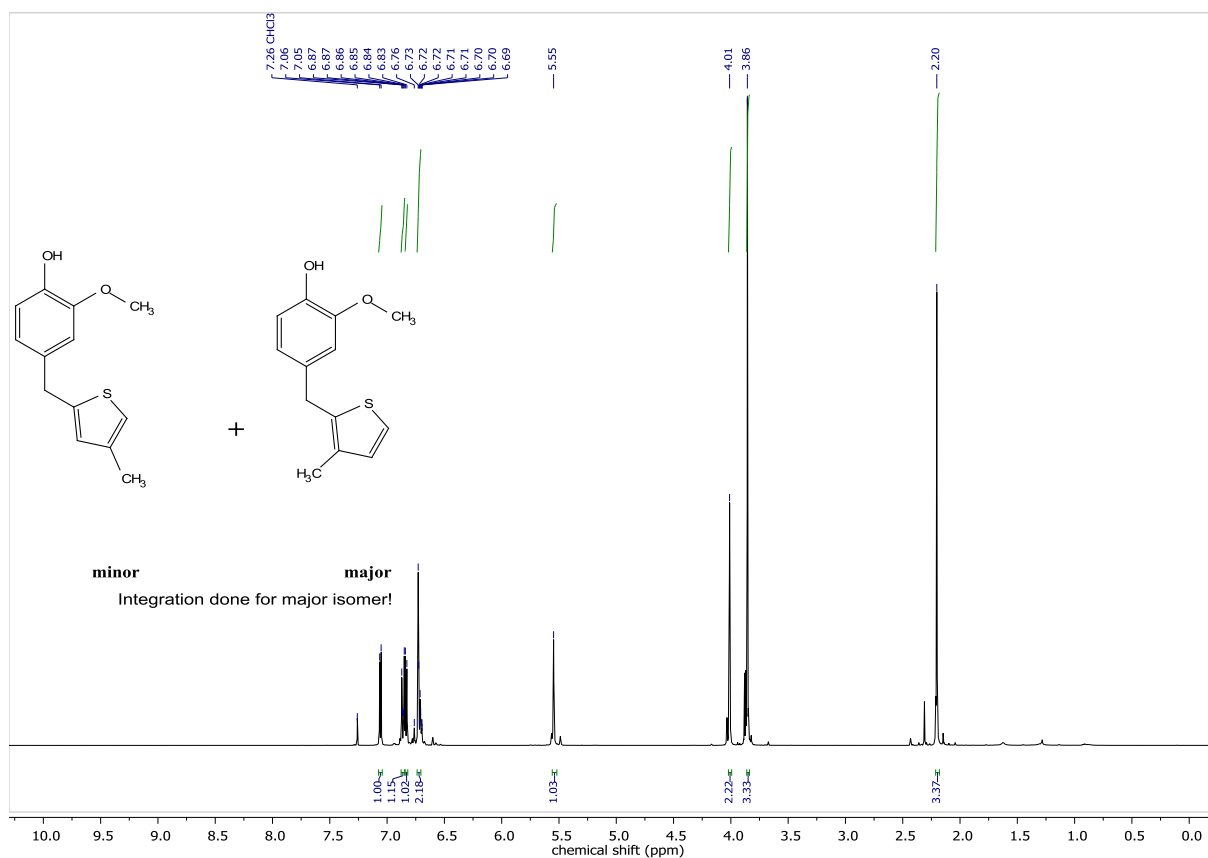
2-((4-Hydroxy-3-methoxyphenyl)methyl)-3-bromothiophene (20)



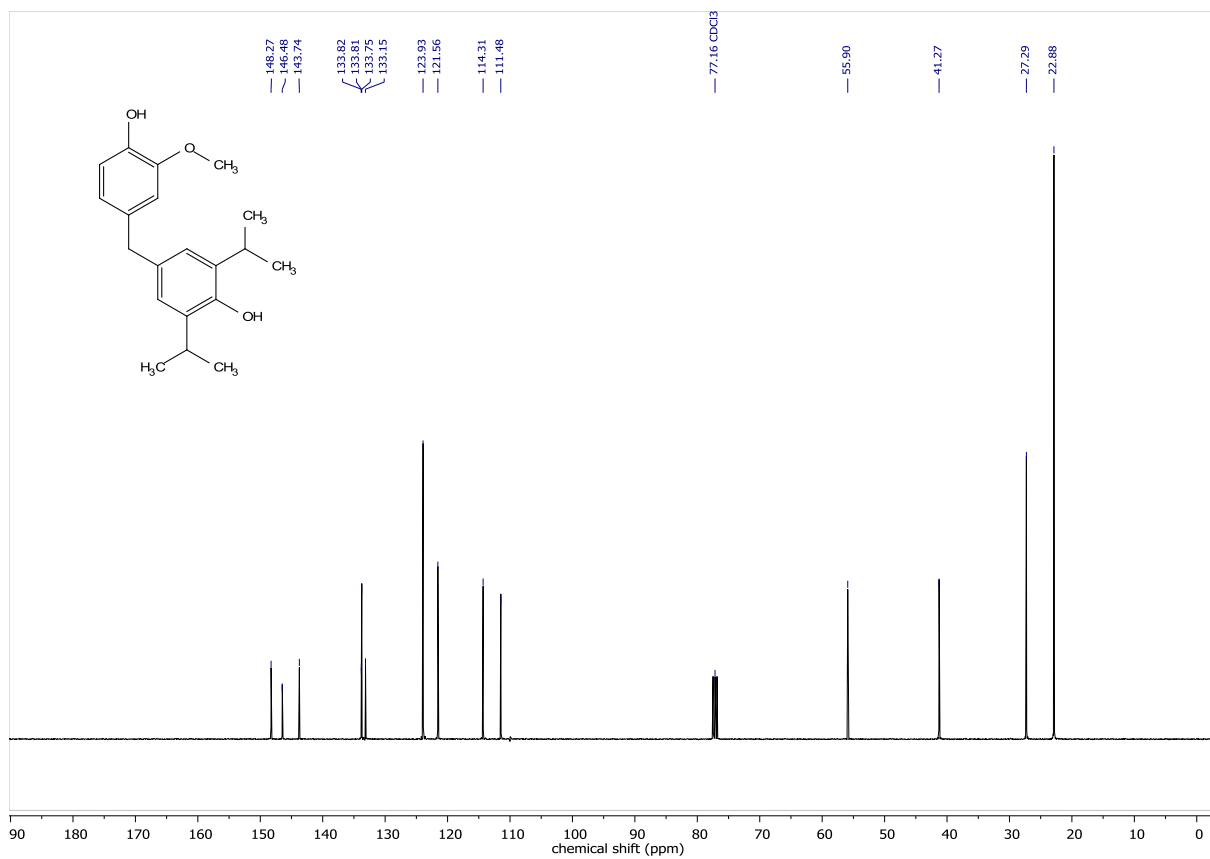
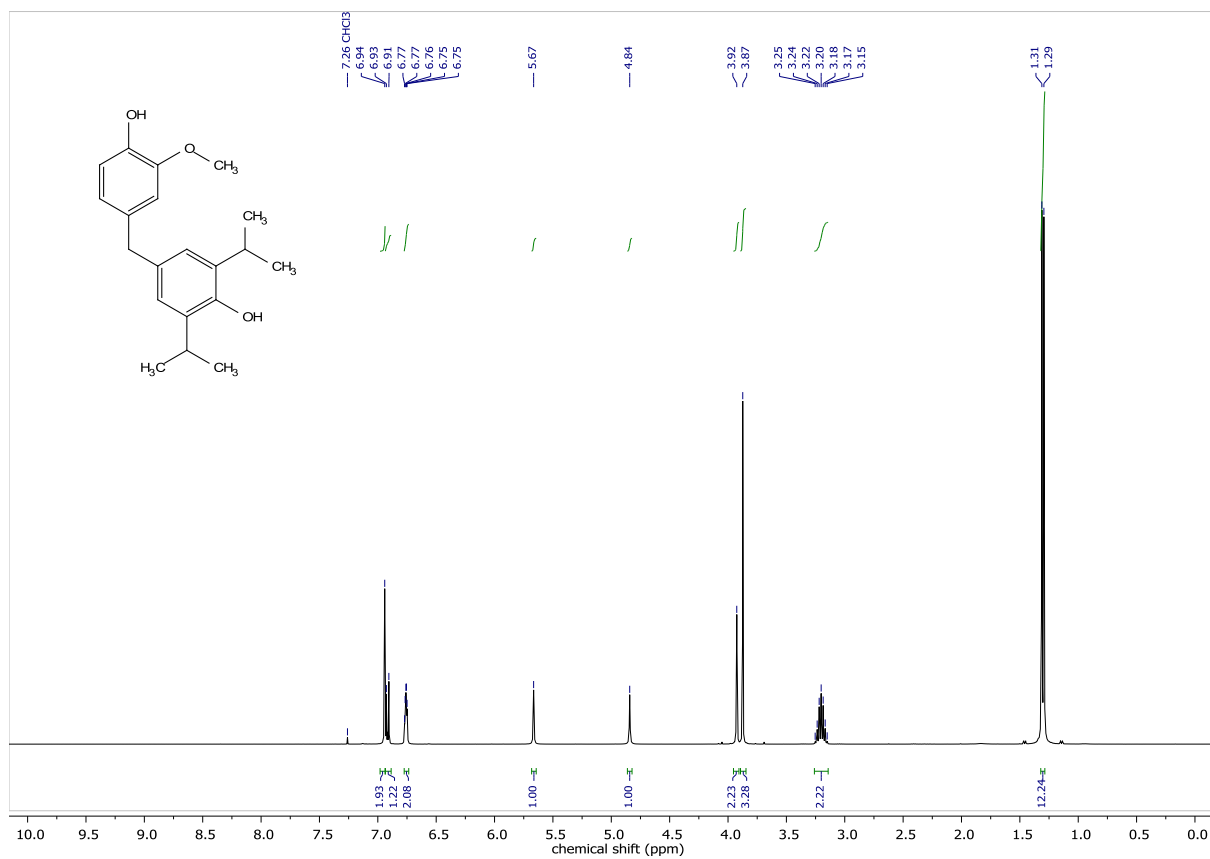
2-((4-Hydroxy-3-methoxyphenyl)methyl)-5-chlorothiophene (21)



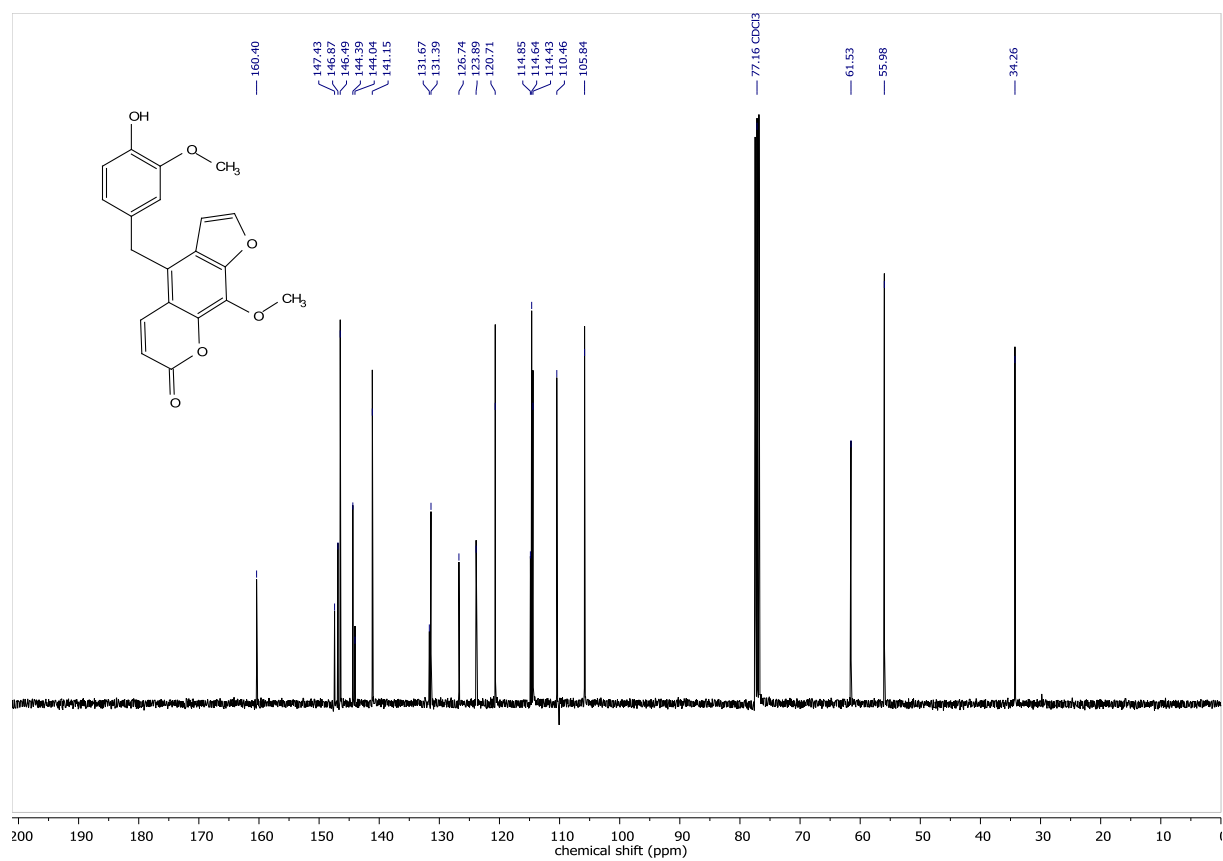
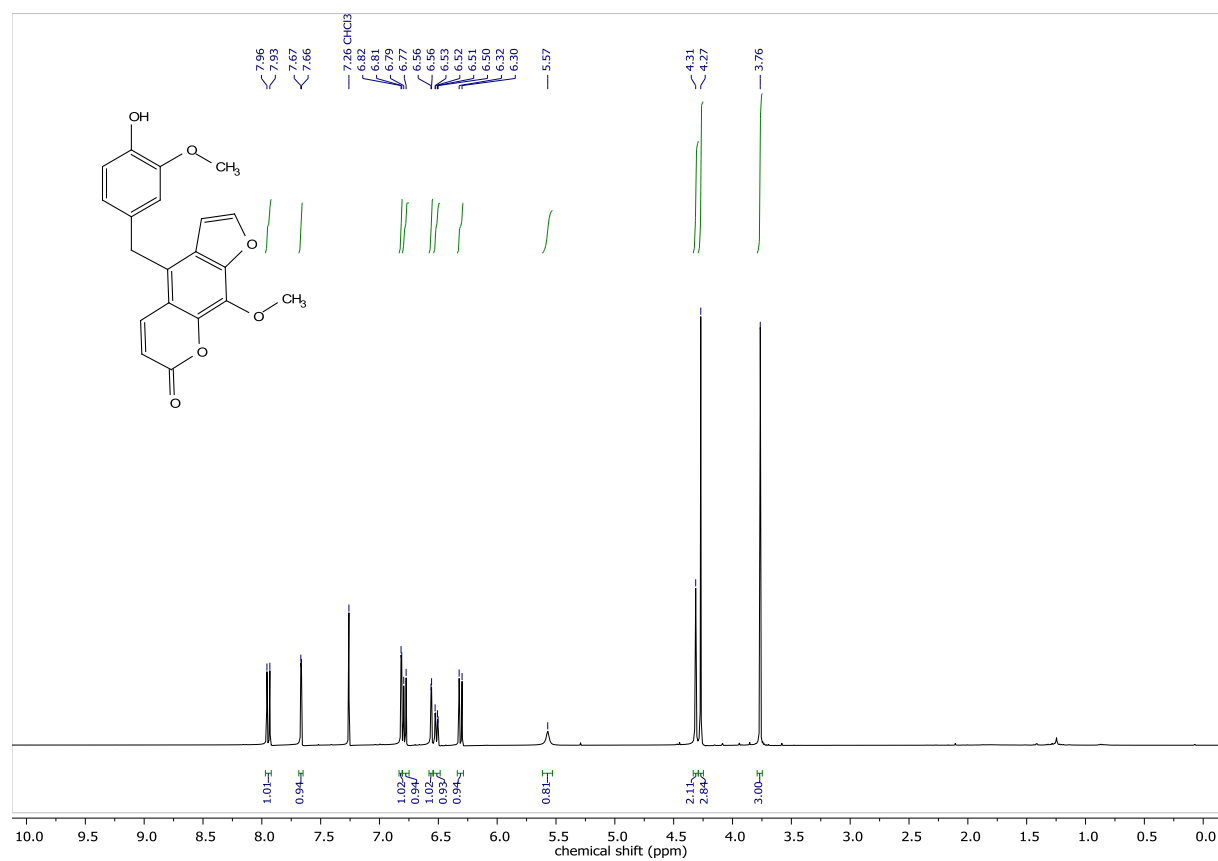
2-((4-Hydroxy-3-methoxyphenyl)methyl)-4-methylthiophene (23) and 2-((4-Hydroxy-3-methoxyphenyl)methyl)-3-methylthiophene (22)



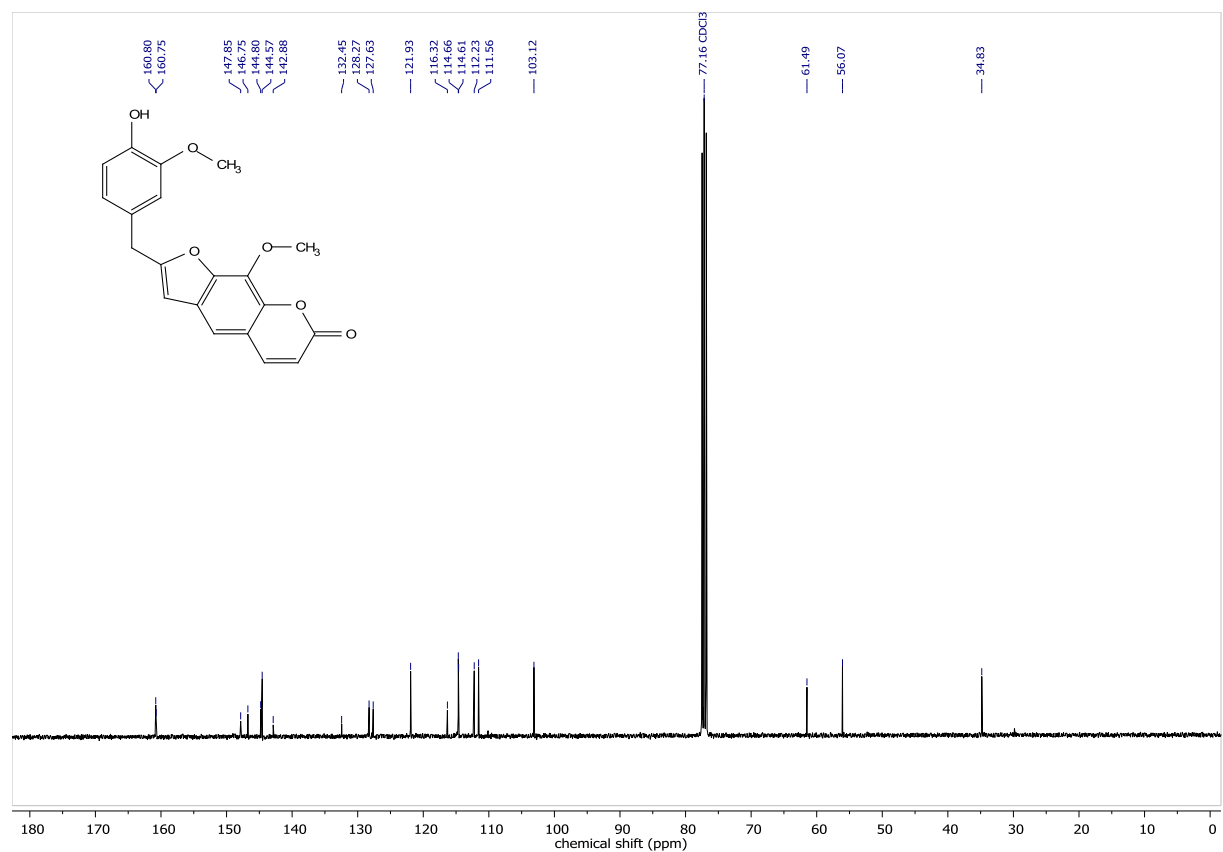
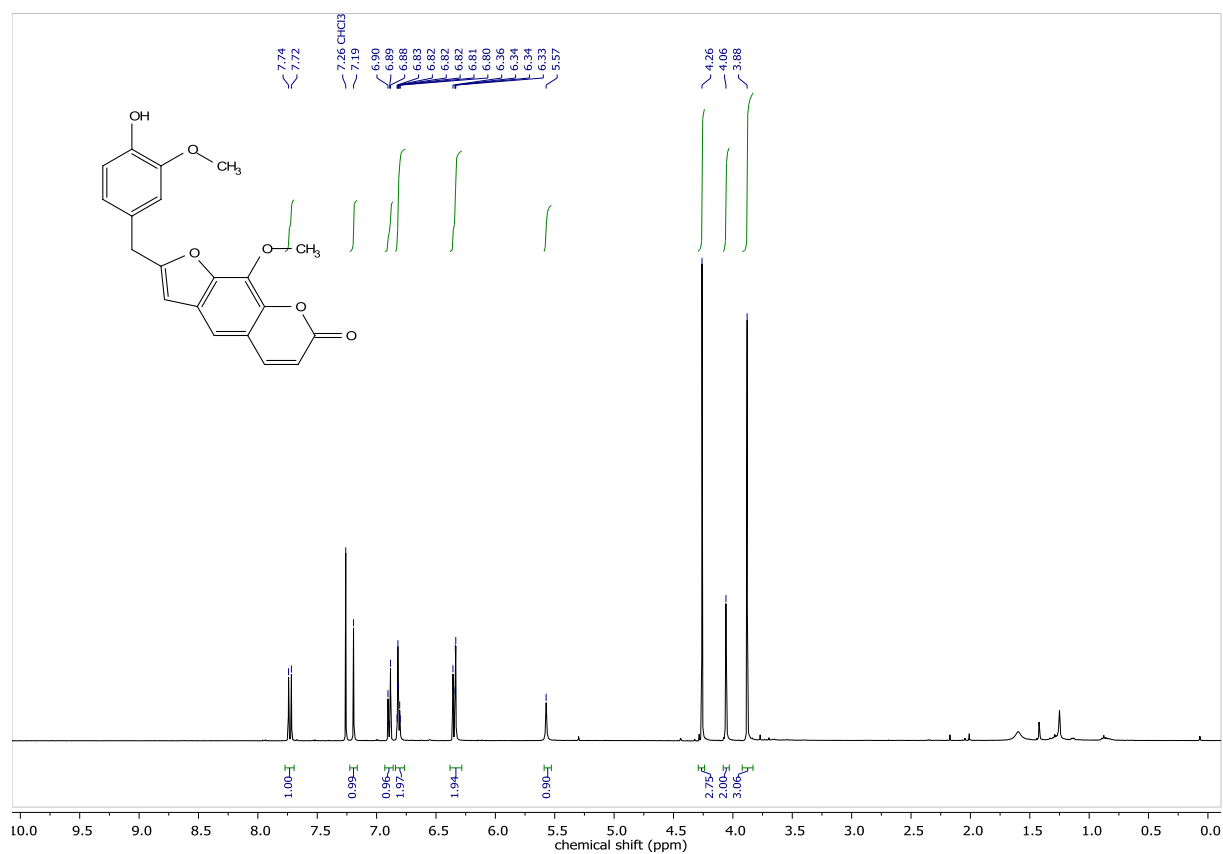
4-(4-Hydroxy-3-methoxybenzyl)-2,6-diisopropylphenol (24)



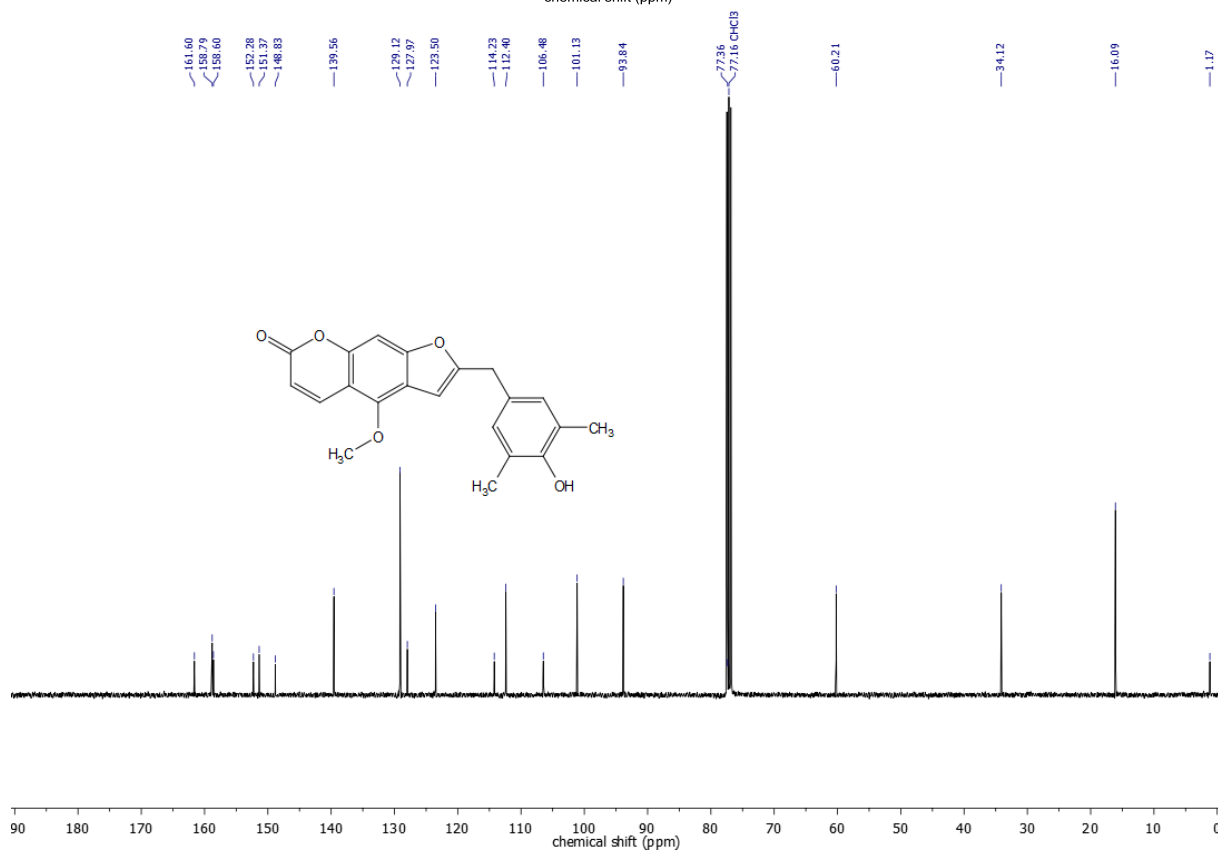
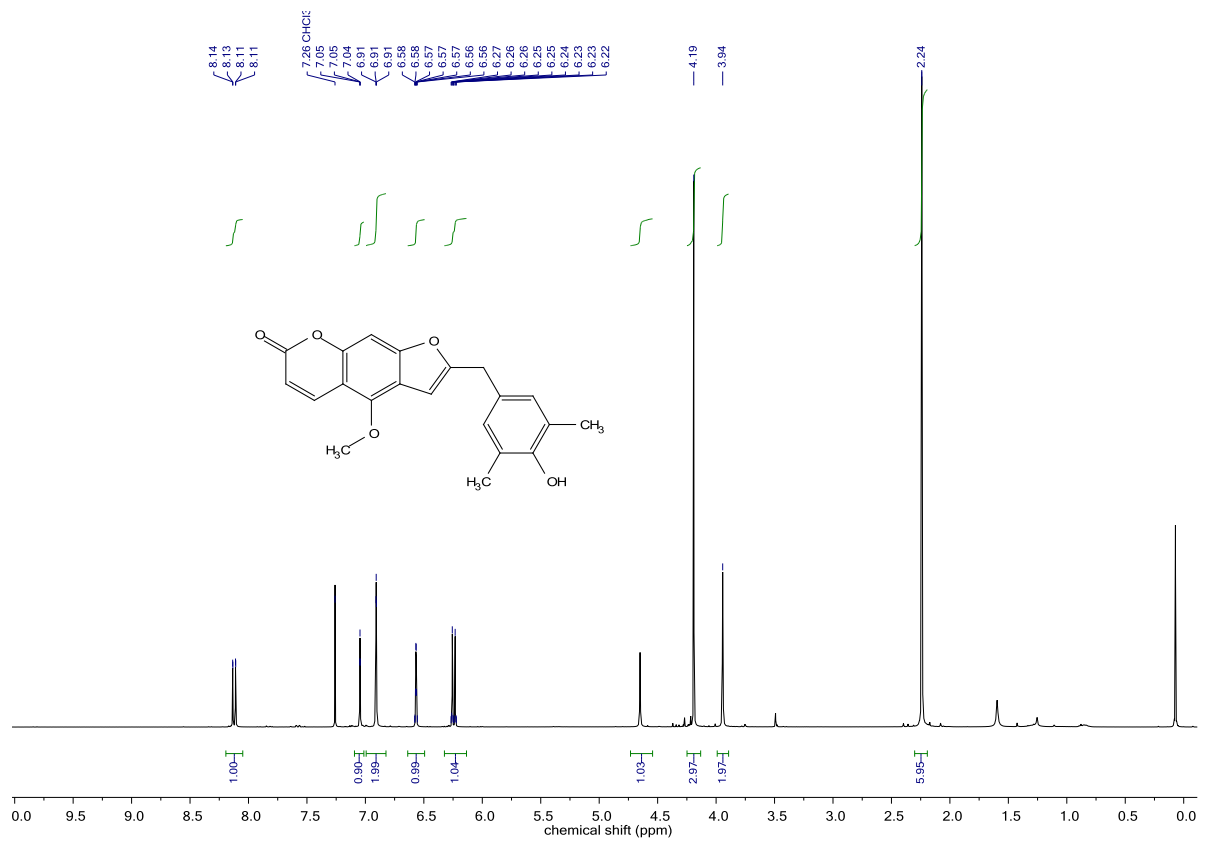
4-(4-Hydroxy-3-methoxybenzyl)-9-methoxy-7H-furo[3,2-g]chromen-7-one (24a)



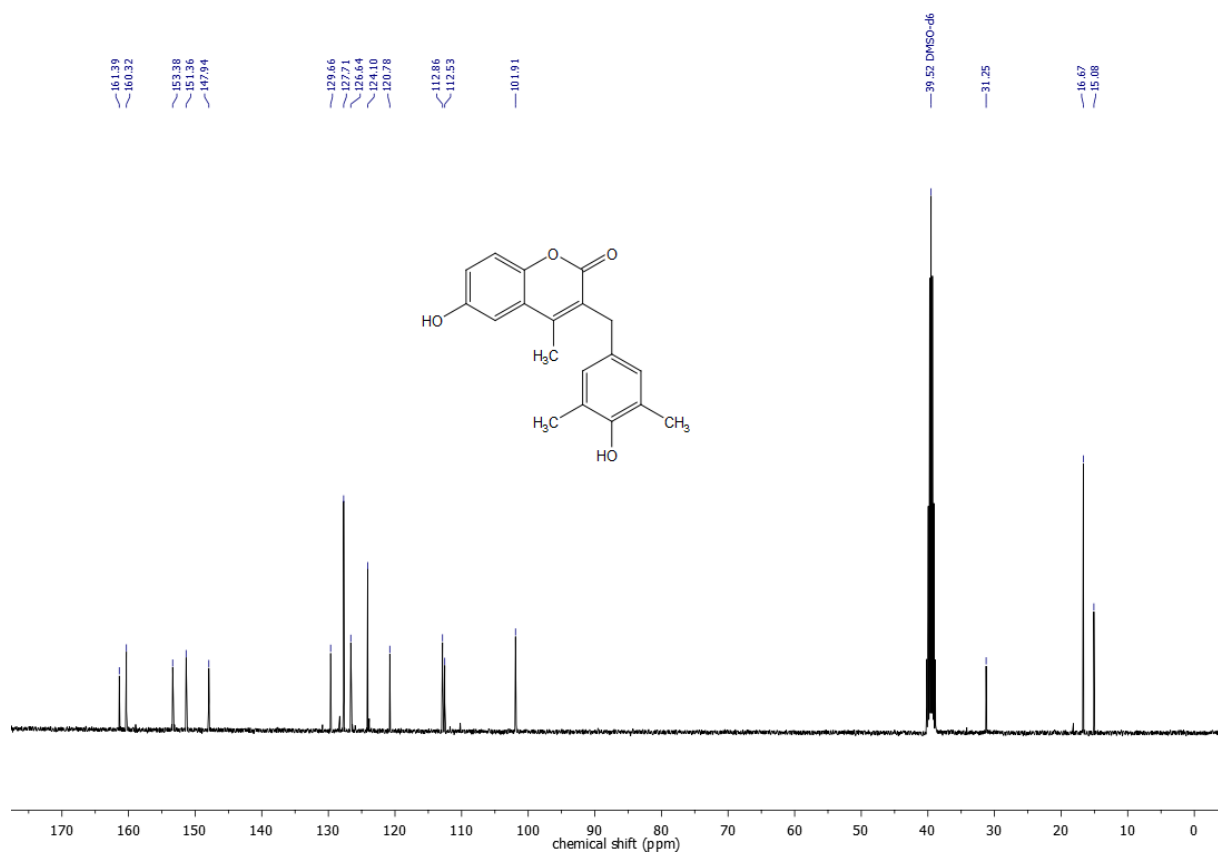
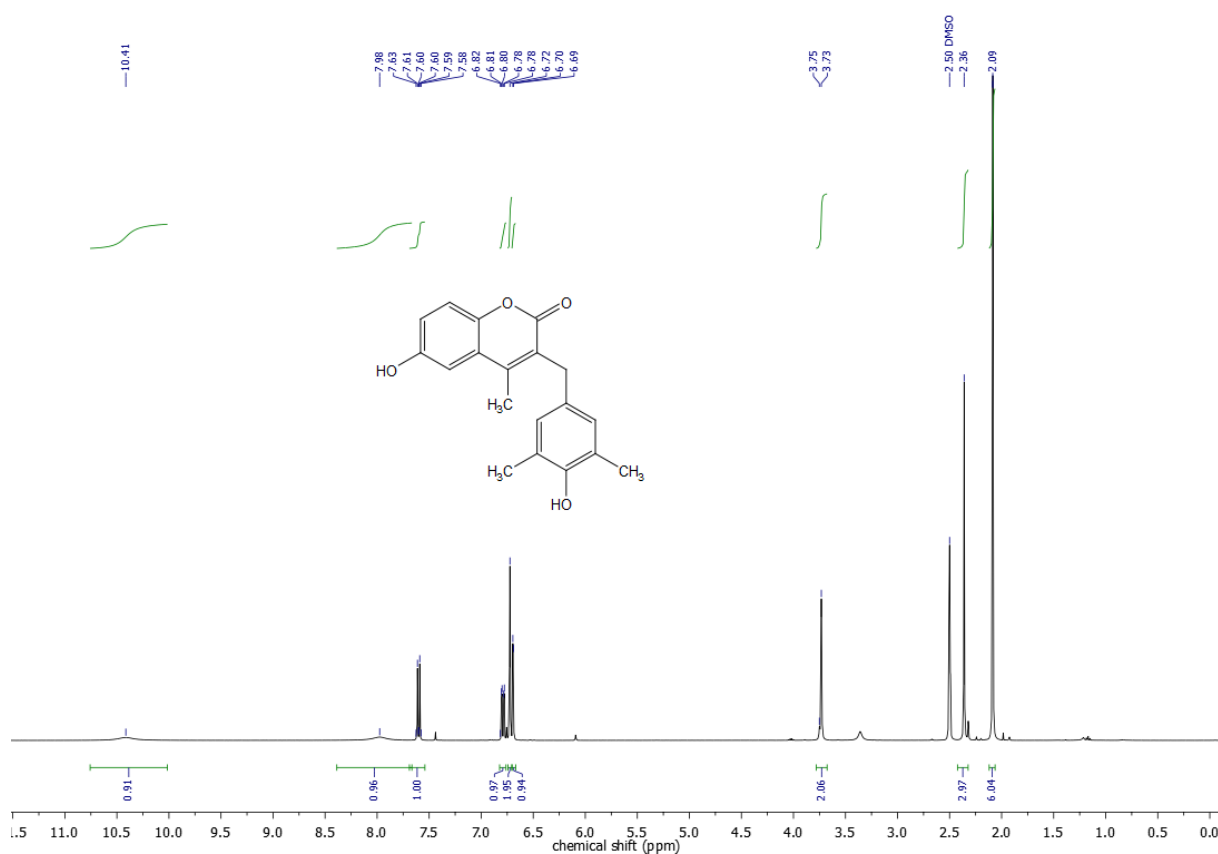
2-(4-Hydroxy-3-methoxybenzyl)-9-methoxy-7H-furo[3,2-g]chromen-7-one (24b)



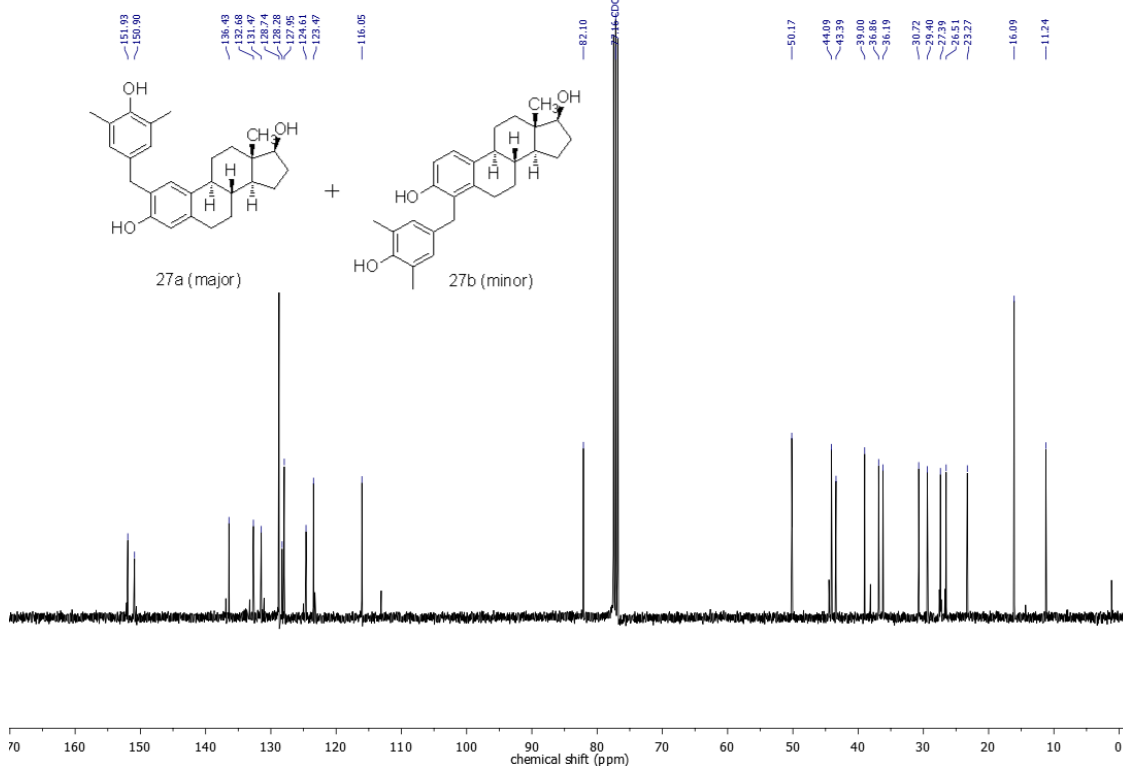
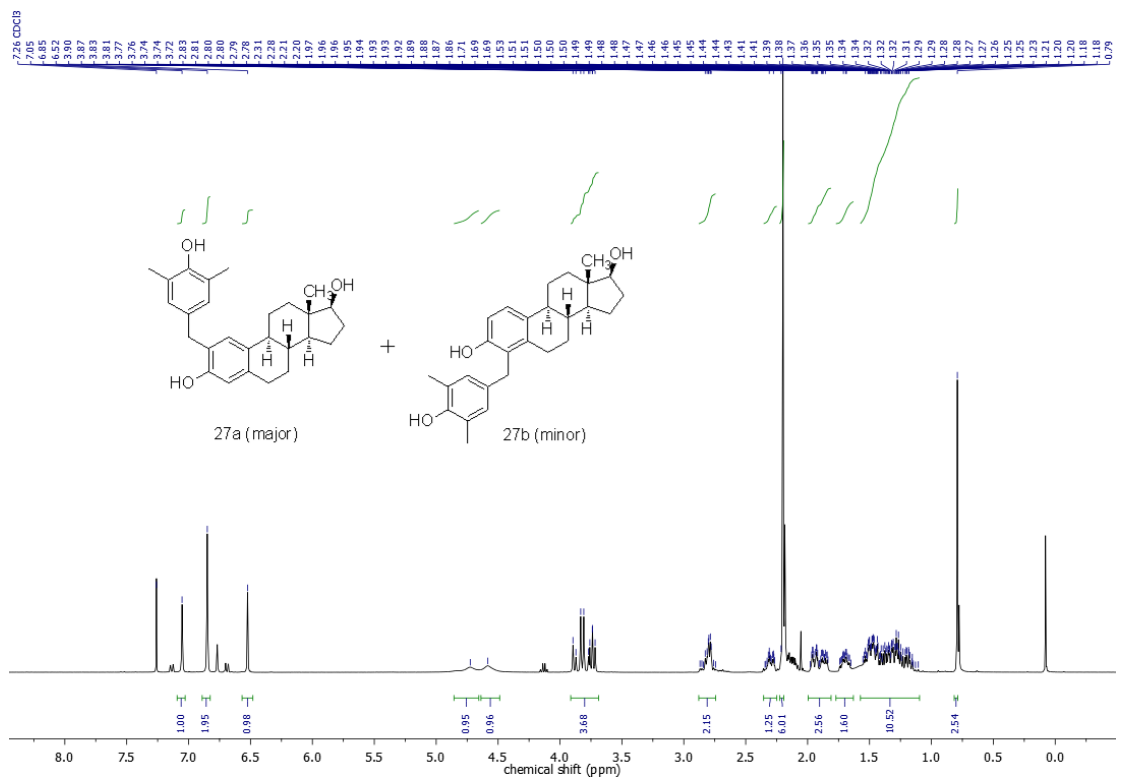
2-(4-Hydroxy-3,5-dimethylbenzyl)-4-methoxy-7H-furo[3,2-g]chromen-7-one (25)



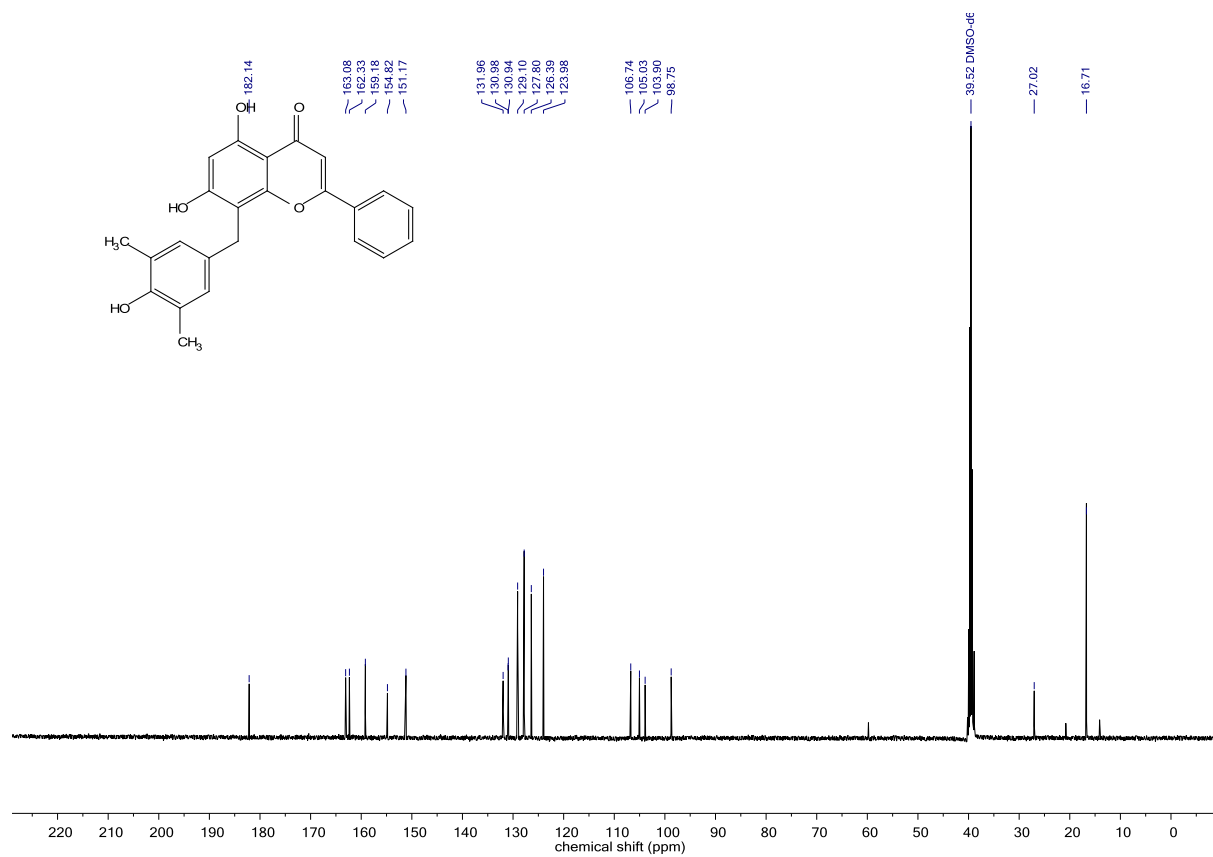
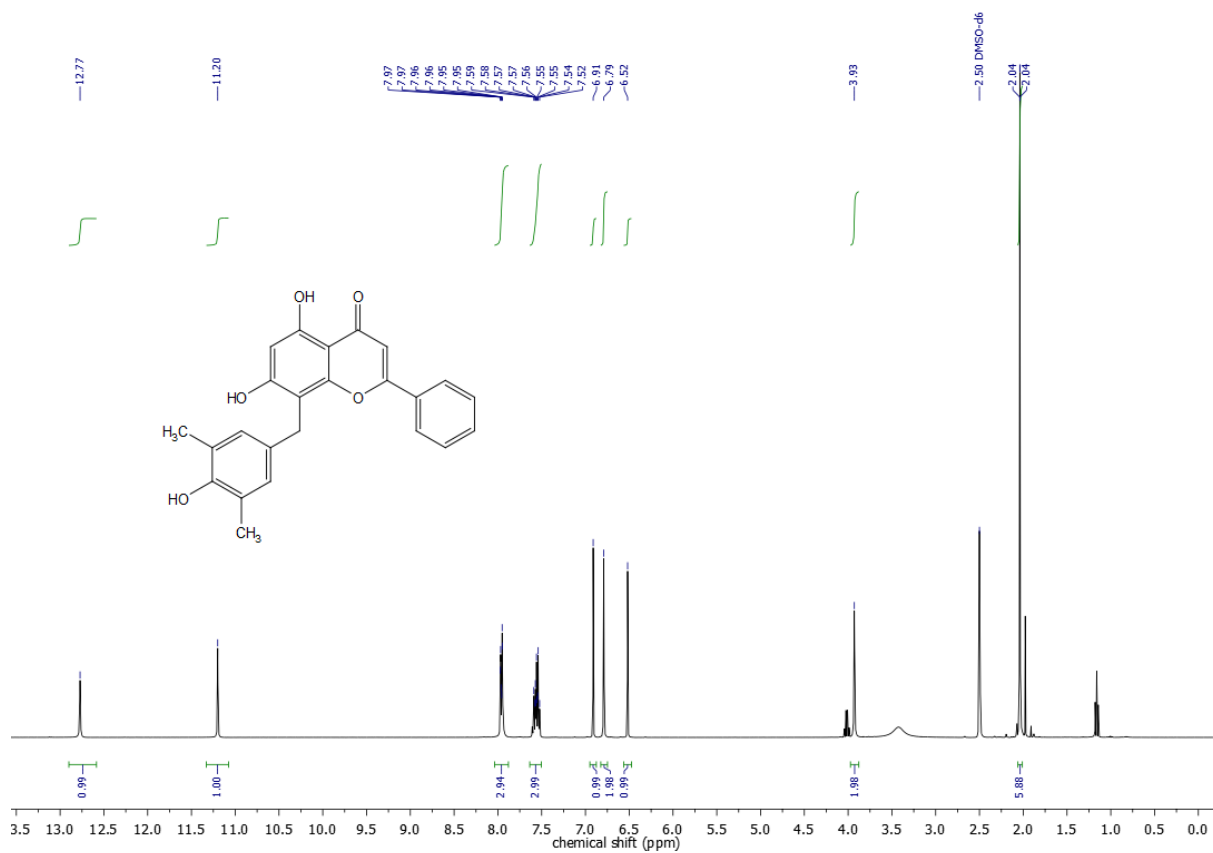
6-Hydroxy-3-(4-hydroxy-3,5-dimethylbenzyl)-4-methyl-2H-chromen-2-one (26)

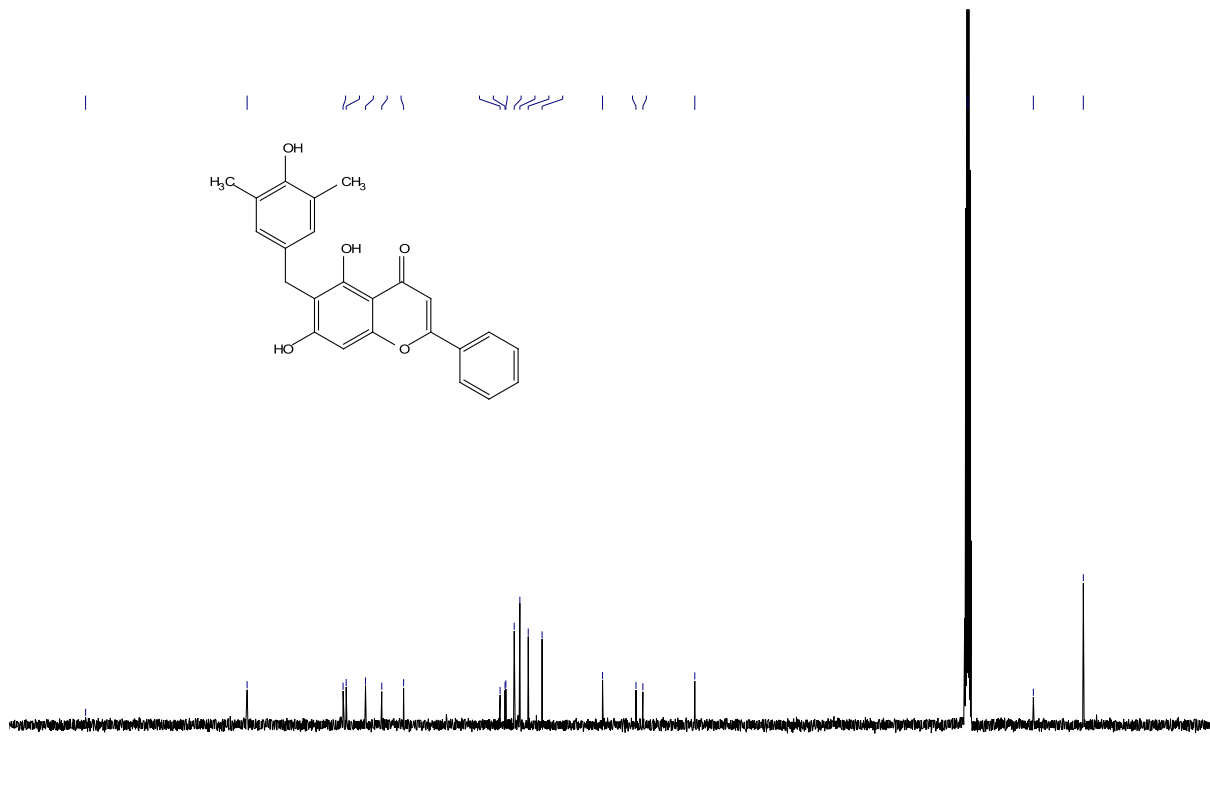
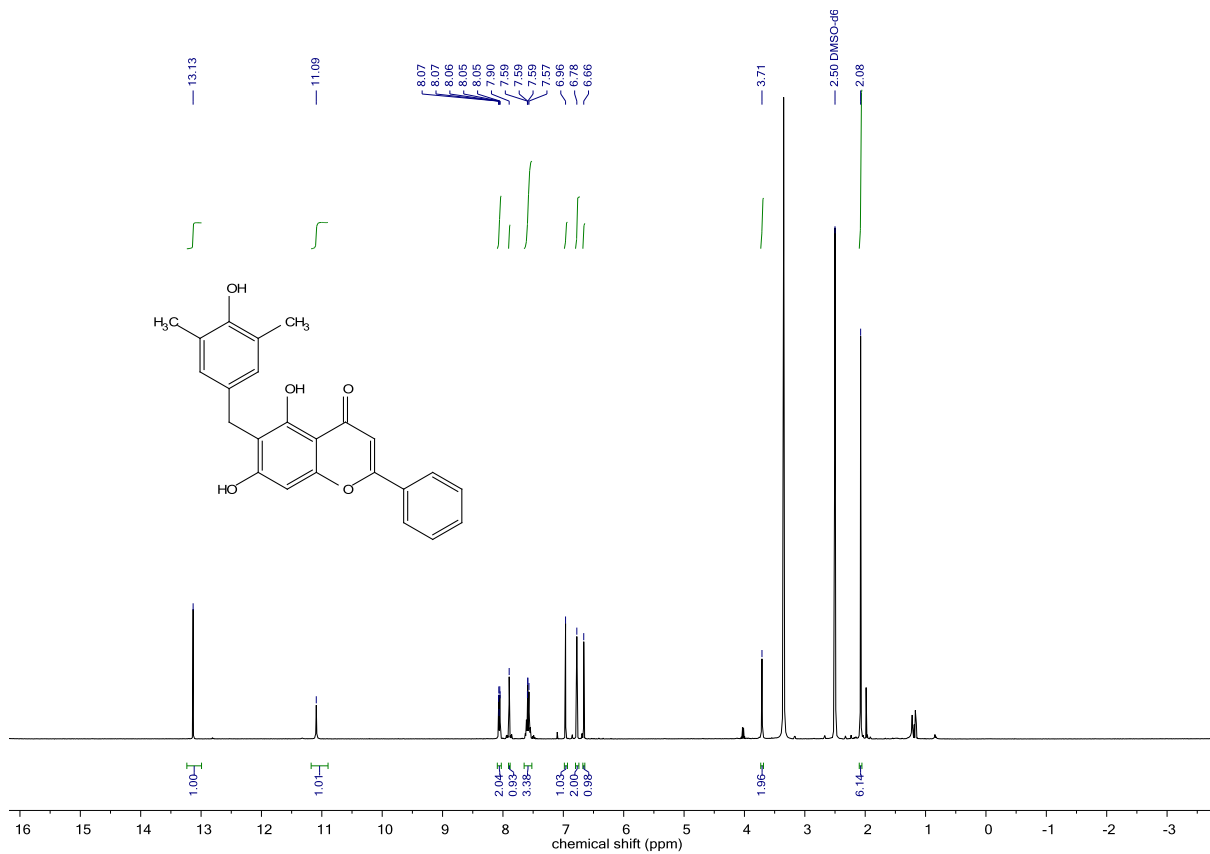


(8R,9S,13S,14S,17S)-2-(4-Hydroxy-3,5-dimethylbenzyl)-13-methyl-7,8,9,11,12,13,14,15,16,17-decahydro-6H-cyclopenta[a]phenanthrene-3,17-diol (27a)
and
(8R,9S,13S,14S,17S)-4-(4-Hydroxy-3,5-dimethylbenzyl)-13-methyl-7,8,9,11,12,13,14,15,16,17-decahydro-6H-cyclopenta[a]phenanthrene-3,17-diol (27b)

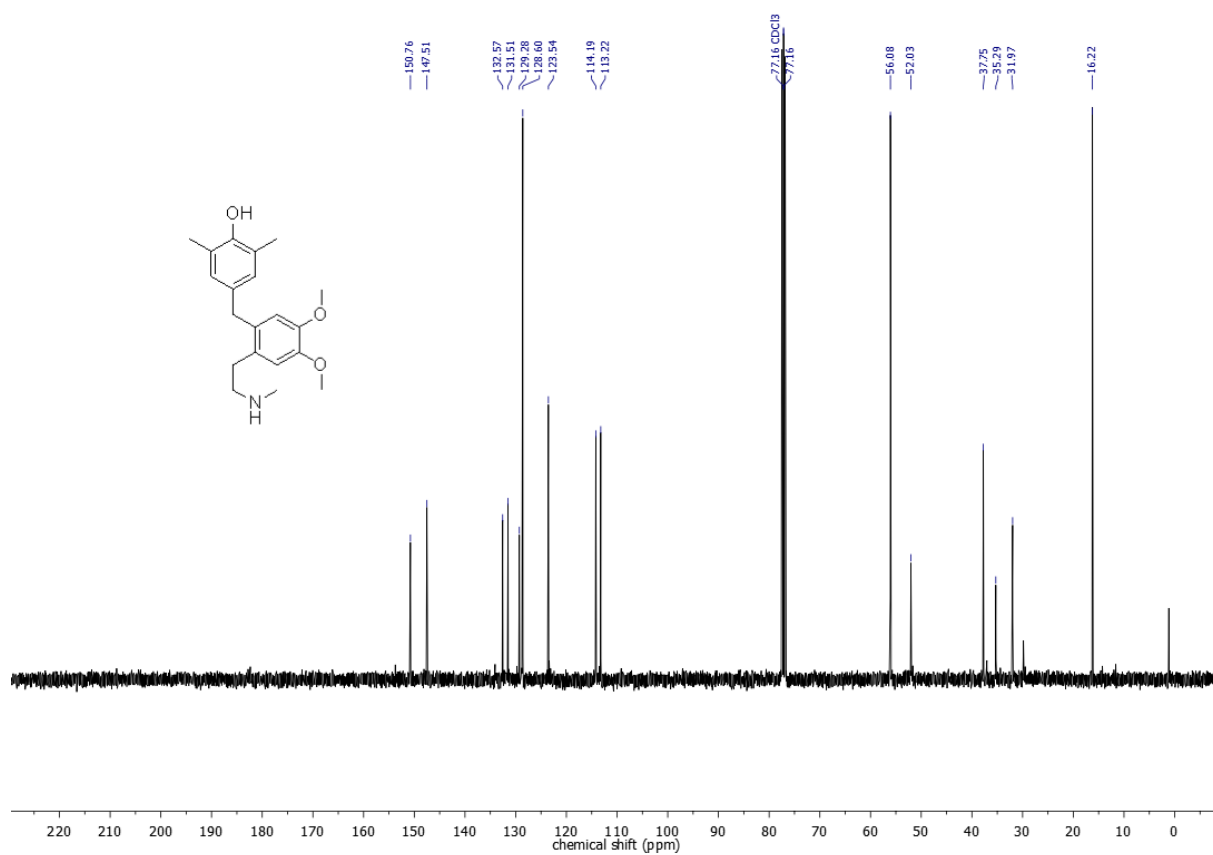
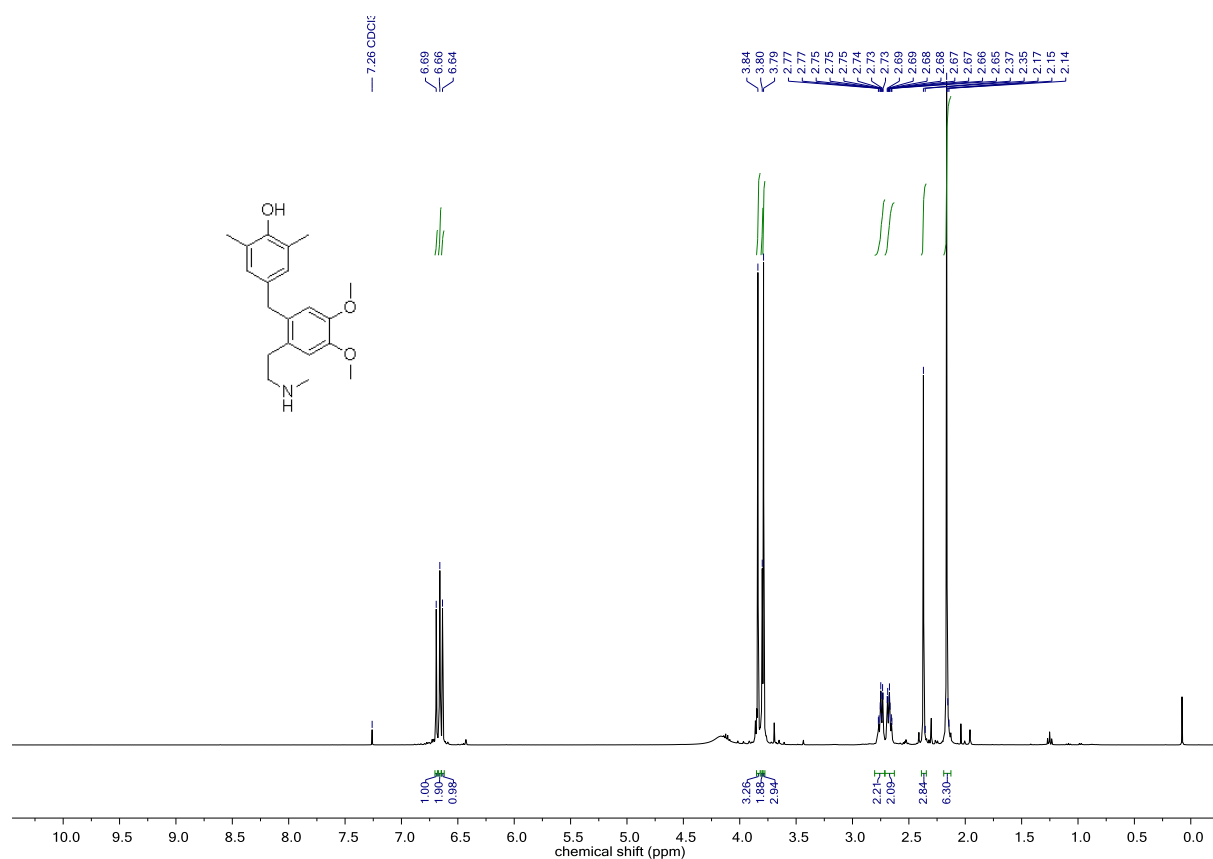


5,7-Dihydroxy-8-(4-hydroxy-3,5-dimethylbenzyl)-2-phenyl-4H-chromen-4-one (28a) and
5,7-Dihydroxy-6-(4-hydroxy-3,5-dimethylbenzyl)-2-phenyl-4H-chromen-4-one (28b)





4-(4,5-Dimethoxy-2-(2-(methylamino)ethyl)benzyl)-2,6-dimethylphenol (29)



References

- [1] W. L. F. Armarego, C. L. L. Chai, *Purification of laboratory chemicals*, Elsevier, Amsterdam, **2013**.
- [2] C. Gütz, B. Klöckner, S. R. Waldvogel, *Org. Process Res. Dev.* **2016**, *20*, 26–32.
- [3] A. Kirste, G. Schnakenburg, F. Stecker, A. Fischer, S. R. Waldvogel, *Angew. Chem. Int. Ed.* **2010**, *49*, 971-975; *Angew. Chem.* **2010**, *122*, 983–987. (see SI thereof).

Special
Issue

Dehydrogenative Anodic Cyanation Reaction of Phenols in Benzylic Positions

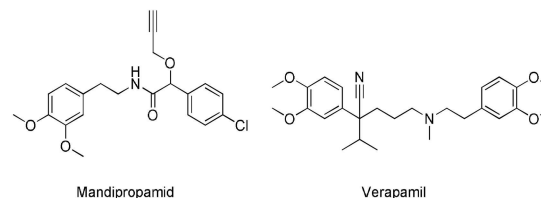
Johannes L. Röckl,^[a, c] Yasushi Imada,^[b, c] Kazuhiro Chiba,^[b] Robert Franke,^[d, e] and Siegfried R. Waldvogel^{*[a, c]}

The selective dehydrogenative electrochemical activation of benzylic positions by 1,1,1,3,3,3-hexafluoropropan-2-ol (HFIP) and subsequent cyanation is presented for the first time. Herein, we report a sustainable, scalable, and metal-free dehydrogenative benzylic cyanation protocol. Valuable 2-phenylacetonitrile derivatives are accessible in the presence of a cyanide source and an electrolytically-derived HFIP ether. The direct application of electricity enables a safe and environmentally benign chemical transformation, since oxidizers are replaced by electricity.

2-Phenylacetonitriles represent important building blocks in organic synthesis and are precursors for biologically active molecules, such as tetrazoles^[1] or 2-phenylethylamines,^[2] including the fungicide mandipropamid,^[3] and the calcium channel blocker verapamil (Scheme 1).^[4]

2-Phenylacetonitriles are amenable to a wide range of synthetic transformations, such as monoalkylation,^[5] reduction to 2-phenylethylamines,^[6] oxidation to acids or amides,^[7] conversion with azides to tetrazoles,^[8] or in Knoevenagel reactions with aldehydes to form alkenes (Scheme 1, Supporting Information).^[9]

Electrochemical installation of cyano groups has been reported for electron-rich arenes several decades ago.^[10] In addition a direct cyanation was feasible on side chains of highly electron-rich pyrroles.^[11] Recently, the dehydrogenative cyana-



Scheme 1. Important biologically active molecules derived from or containing 2-phenylethyl acetonitrile moieties.

tion of activated arenes and heteroarenes was published by Gooßen et al.^[12] Alternatively, cyano groups can also be established by electro-conversion of a renewable feedstock, such as glutamic acid, towards the bulk chemical adiponitrile,^[13] or by a domino electrolysis of aldoximes.^[14] This makes chemical synthesis sustainable and environmentally friendly.^[15] Additionally an electrochemical method for the direct α -cyanation of *N*-protected cyclic amines on graphite electrodes has been reported by Onomura and co-workers.^[16] However, a benzylic electrochemical cyanation is presented here for the first time.

A common synthetic route to 2-phenylacetonitriles consists of initial protection of the phenolic hydroxyl moiety, followed by radical halogenation of the benzyl group (usually by NBS, AIBN in a halogenated solvent). This is followed by substitution of the halo substituent by cyanide, employing sodium,^[17] potassium,^[18] TMS-cyanide,^[19] or tetraethylammonium cyanide^[20] with final liberation of the phenol. This strategy has several major disadvantages: additional alkyl groups are not tolerated, due to poor regioselectivity of the radical halogenation reaction.^[21] Furthermore, this route leads to the generation of significant reagent waste and requires two additional protection and deblocking steps. Additionally, radical halogenation often leads to low yields, due to multiple halogenation processes and elimination reactions.^[21]

An alternative route starts from benzylic alcohols or aldehydes.^[22] The alcohol is converted in a Mitsunobu-type reaction using triphenylphosphine, 2,3-dichloro-5,6-dicyano-1,4-benzoquinone and tetrabutylammonium cyanide in acetonitrile to give the desired 2-phenylacetonitriles. While this route can lead to high yields, with a broad substrate scope tolerating aliphatic branched, linear, and substituted benzylic alcohols, it has significant drawbacks. These include generation of large amounts of waste and low atom efficiency, due to the use of two equivalents of PPh₃, DDQ, and NBu₄CN per equivalent of alcohol. Another route to 2-phenylacetonitriles starts from carbonyl compounds, which are reduced to the corresponding

[a] J. L. Röckl, Prof. Dr. S. R. Waldvogel
Institute of Organic Chemistry
Duesbergweg 10–14, 55128 Mainz, Germany
E-mail: waldvogel@uni-mainz.de
Homepage: <https://www.blogs.uni-mainz.de/fb09akwaldvogel/>

[b] Y. Imada, Prof. Dr. K. Chiba
Department of Applied Biological Science
Tokyo University of Agriculture and Technology
3-5-8 Saiwai-cho, Fuchu, Tokyo 183-8509, Japan

[c] J. L. Röckl, Y. Imada, Prof. Dr. S. R. Waldvogel
Graduate School Materials Science in Mainz
Johannes Gutenberg Universität Mainz
Staudinger Weg 9, 55128 Mainz, Germany

[d] Prof. Dr. R. Franke
Evonik Performance Materials GmbH
Paul-Baumann-Str. 1, 45772 Marl, Germany

[e] Prof. Dr. R. Franke
Lehrstuhl für Theoretische Chemie
Ruhr-Universität Bochum
Universitätsstraße 150, 44801 Bochum, Germany

Supporting information for this article is available on the WWW under <https://doi.org/10.1002/celec.201801727>

An invited contribution to a Special Issue on Organic Electrochemistry

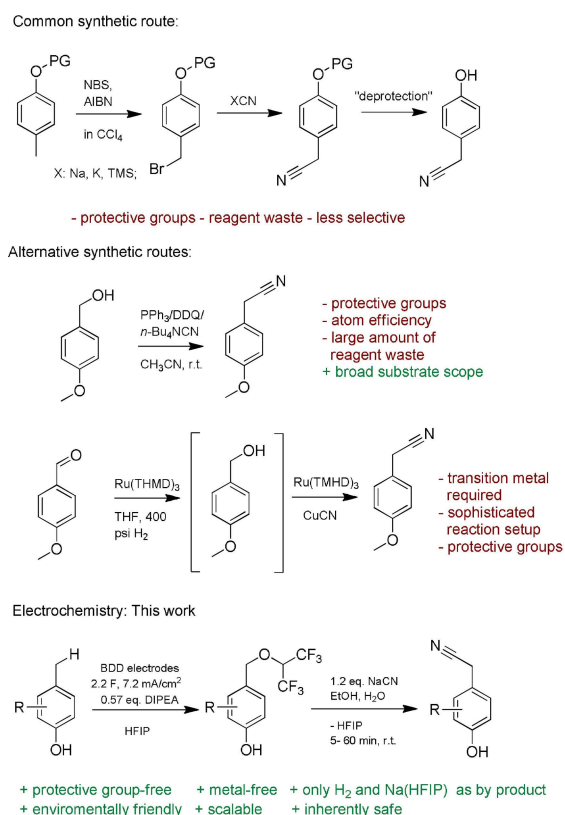
alcohols in the presence of a Ru(TMHD)₂ complex, and are then transformed in-situ into their corresponding nitriles.^[23] One shortcoming of this route is, in the case of phenols, that an additional protective group is needed. Furthermore, the reaction must be carried out under 500 psi H₂, and activation of methyl groups needs to be carried out first, by oxidation to the aldehyde. These disadvantages, coupled with the use of an expensive transition metal catalyst, make this route less attractive. The limits of the current synthetic routes to 2-phenylacetonitriles discussed here highlight the need for a facile and environmentally benign route to these valuable building blocks (Scheme 2).

Recently, we reported the selective electrochemical functionalization of benzylic positions using HFIP,^[24] which has extraordinary properties. It stabilizes reactive intermediates,^[25] and has a unique solvent microstructure.^[26] Its interesting solvation properties can enable various transformations.^[27] The generated ether acts as a molecular mask for the benzylic cation, and stabilizes this reactive intermediate by solvent trapping in a less reactive state. Notably, the oxidation also works on graphite anodes, DIPEA acts together with HFIP as a supporting electrolyte, and HFIP can be reused completely,^[28] which makes this protocol attractive for technical applications. BDD electrodes are used here as they allowed for slightly higher yields.^[29] The HFIP ether can act as a leaving group in a nucleophilic substitution reaction with cyanides. A simple, sustainable, easily scalable, reagent- and metal-free electrochemical cyanation reaction that proceeds in a two-step

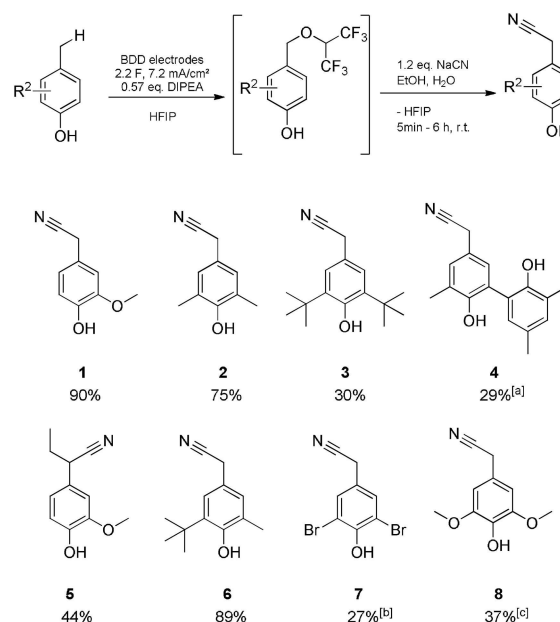
sequence with only one purification step is presented. The electrochemical activation is selective, with multiple alkyl groups being tolerated. It is also protective group-free, shortening the usual synthetic route by one to two steps. Additionally, less toxic reagent waste is generated, allowing for a greener procedure.

The electrolytic conditions of the initial electrochemical step were optimized in our previous work.^[24] Non-protected phenols can be converted into HFIP ethers and subsequently reacted with sodium cyanide or potassium cyanide in yields up to 90% over both steps, with only a single purification within the second step (Scheme 3). Secondary nitriles can be obtained in 37% yield (5). Phenols containing more than one alkyl group can be transformed to the corresponding nitriles in high yields up to 89% (6). Substrates with halo substituents are tolerated, resulting in moderate yields up to 27% (7), and even the dimer (4) underwent the cyanation with 29% yield of the cyanation product. The cyanation reactions proceed rapidly and selectively within 5 to 60 min at room temperature, when NaCN in an ethanol/water mixture (9/1) is used, demonstrating the suitability of HFIP as a leaving group. A suggested mechanism can be found in the SI (Figure S3). In acetonitrile with KCN, the conversions can take up to 6 h. Concentration was found to be crucial in the cyanation step: in some cases a subsequent reaction is faster than the initial cyanation itself, resulting in low yields. Also 4-methylanisoles form the respective HFIP ethers, but do not undergo the cyanation reaction.

To demonstrate the scalability of our method, we chose the synthesis of compound 1 as test reaction. The structural motif of 1 is of significant interest as a precursor for pharmaceutically relevant compounds.^[2] We scaled-up the electrolysis by a factor of 50. The electrolysis was conducted with 50 mmol of 1 in a



Scheme 2. Synthetic strategies to 2-phenylacetonitrile.



Scheme 3. Scope of the reaction. a) 1 mmol, 3 F were applied. KCN (1.5 eq.) in acetonitrile (10 mL); b) 0.5 mmol, polarity reversal of each 10 s, 3 F, KCN (1.5 eq.) in acetonitrile (10 mL); c) 0.5 mmol, KCN (1.5 eq.) in acetonitrile (10 mL);



Figure 1. 500 mL round bottomed flask with Teflon plug and two BDD electrodes (14 cm × 3.5 cm × 0.3 cm) used in the scale up reaction. A 50 Eurocent coin for comparison. (diameter: 24,25 mm)

500 mL round-bottomed flask (Figure 1). No erosion of selectivity was observed for the anodic functionalization with HFIP. The resulting mixture was concentrated and reacted with sodium cyanide in the ethanol/water mixture yielding in 3.5 g of the desired compound **1** in a single batch (41 % yield). The yield is significantly lower compared to that observed on the 5 mL scale (90%). This can be explained by the previously mentioned side-reactions, which take place at high concentrations of HFIP ether. However, the reaction was repeated, adding the HFIP ether to the sodium cyanide solution in ethanol/water dropwise and slowly. The yield of **1** was then increased to 78%. The slightly lower yield can be rationalized as a result of insufficient mixing and therefore localized high concentration of HFIP ether. A mechanical stirrer can raise the yield to the original screening cell result.

In conclusion, we have established a selective, protective-group-free and environmentally benign cyanation protocol, using electrochemically derived HFIP ethers. 2-Phenylacetoneitriles are valuable building blocks in organic synthesis, which can be synthesized in two steps from 4-methylphenol derivatives in high yields. This route provides a scalable, metal-free, and reagent-saving route to 2-phenylacetoneitriles. This has the potential to shorten many synthetic routes towards biologically active structures and relevant intermediates for pharmaceuticals and pesticides.

Acknowledgements

The authors thank the DFG (GSC 266, Wa 1276/17-1, Wa 1276/14-1) for financial support. Support of the Advanced Lab of Electrochemistry and Electrosynthesis – ELYSION (Carl Zeiss Stiftung) is gratefully acknowledged. Y.I. gratefully acknowledges the support from the Program for Leading Graduate School of TUAT granted by the Ministry of Education, Culture, Science and Technology (MEXT), Japan.

Conflict of Interest

The authors declare no conflict of interest.

Keywords: cyanides · electrochemistry · green chemistry · HFIP · oxidation

- [1] V. A. Ostrovskii, R. E. Trifonov, E. A. Popova, *Russ. Chem. Bull.* **2012**, *61*, 768–780.
- [2] M. Irsfeld, M. Spadafore, B. M. Prüß, *WebmedCentral* **2013**, *4*, 4409–4426.
- [3] C. Lamberth, A. Jeanguenat, F. Cederbaum, A. de Mesmaeker, M. Zeller, H.-J. Kempf, R. Zeun, *Bioorg. Med. Chem.* **2008**, *16*, 1531–1545.
- [4] R. N. Brogden, P. Benfield, *Drugs* **1996**, *51*, 792–819.
- [5] I. Choi, H. Chung, J. W. Park, Y. K. Chung, *Org. Lett.* **2016**, *18*, 5508–5511.
- [6] K. Rice, A. Brossi, *J. Org. Chem.* **1980**, *45*, 592–601.
- [7] N. Dittrich, L. I. Pilkington, E. Leung, D. Barker, *Tetrahedron* **2017**, *73*, 1881–1894.
- [8] J. W. Tilley, W. Danho, K. Lovey, R. Wagner, J. Swistok, R. Makofske, J. Michalewsky, J. Triscari, D. Nelson, S. Weatherford, *J. Med. Chem.* **1991**, *34*, 1125–1136.
- [9] Y. Yue, H. Fang, M. Wang, Z. Wang, M. Yu, *J. Chem. Res.* **2009**, 377–381.
- [10] a) L. Ebersson, B. Helgée *Chem. Abstr.* **1974**, *80*, 82473; b) L. Ebersson, B. Helgée, *Acta Chem. Scand.* **1977**, *31*, 813–817; c) S. Andreas, E. W. Zahnow, *J. Am. Chem. Soc.* **1969**, *91*, 4181–4190; d) L. Ebersson, B. Helgée, *Acta Chem. Scand.* **1975**, *29*, 451–456; e) F. Fichter, W. Dietrich, *Helv. Chim. Acta* **1924**, *7*, 131–143.
- [11] Y. Kunihiro, *J. Am. Chem. Soc.* **1979**, *101*, 2116
- [12] D. Hayrapetyan, R. K. Rit, M. Kratz, K. Tschulik, L. J. Gooßen, *Chem. Eur. J.* **2018**, *24*, 11288–11291.
- [13] J.-J. Dai, Y.-B. Huang, C. Fang, Q.-X. Guo, Y. Fu, *ChemSusChem* **2012**, *5*, 617–620.
- [14] a) M. F. Hartmer, S. R. Waldvogel, *Chem. Commun.* **2015**, *51*, 16346–16348; b) C. Gütz, V. Grimaudo, M. Holtkamp, M. Hartmer, J. Werra, L. Frensemeier, A. Kehl, U. Karst, P. Broekmann, S. R. Waldvogel, *ChemElectroChem* **2018**, *5*, 247–252.
- [15] a) S. Möhle, M. Zirbes, E. Rodrigo, T. Gieshoff, A. Wiebe, S. R. Waldvogel, *Angew. Chem. Int. Ed.* **2018**, *57*, 6018–6041; *Angew. Chem.* **2018**, *130*, 6124–6149. b) A. Wiebe, T. Gieshoff, S. Möhle, E. Rodrigo, M. Zirbes, S. R. Waldvogel, *Angew. Chem. Int. Ed.* **2018**, *57*, 5594–5619; *Angew. Chem.* **2018**, *130*, 5694–5721. c) M. Yan, Y. Kawamata, P. S. Baran, *Chem. Rev.* **2017**, *117*, 13230–13319.
- [16] S. S. Libendi, Y. Demizu, O. Onomura, *Org. Biomol. Chem.* **2009**, *7*, 351–356.
- [17] a) Reynold C. Fuson, William C. Hammann, Paul R. Jones, *J. Am. Chem. Soc.* **1957**, *79*, 928–931; b) V. Boelkeheide, T. Miyasaka, *J. Am. Chem. Soc.* **1967**, *89*, 1709–1714.
- [18] A. Saeed, P. A. Mahesar, *Tetrahedron* **2014**, *70* 1401–1407.
- [19] U. Schmidt, A. Lieberknecht, H. Griesser, J. Talbiersky, *J. Org. Chem.* **1982**, *47*, 3261–3264.
- [20] K. Hilpert, F. Hubler, M. Murphy, D. Renneberg; Benzamide derivatives as p2x7 receptor agonists, *Eur. Pat. Appl.* 2678317 A1, **2014**.
- [21] F. A. Carey, *Organic Chemistry*, McGraw-Hill Higher Education, Boston, **2006**.
- [22] N. Iranpoor, H. Firouzabadi, B. Akhlaghinia, N. Nowrouzi, *J. Org. Chem.* **2004**, *69*, 2562–2564.
- [23] M. D. Bhor, A. G. Panda, N. S. Nandurkar, B. M. Bhanage, *Tetrahedron Lett.* **2008**, *49*, 6475–6479.
- [24] Y. Imada, J. L. Röckl, A. Wiebe, T. Gieshoff, D. Schollmeyer, K. Chiba, R. Franke, S. R. Waldvogel, *Angew. Chem. Int. Ed.* **2018**, *57*, 12136–12140; *Angew. Chem.* **2018**, *130*, 12312–12317.
- [25] L. Ebersson, O. Persson, M. P. Hartshorn, *Angew. Chem. Int. Ed.* **1995**, *34*, 2268–2269; *Angew. Chem.* **1995**, *107*, 2417–2418.
- [26] O. Hollóczki, A. Berkessel, J. Mars, M. Mezger, A. Wiebe, S. R. Waldvogel, B. Kirchner, *ACS Catal.* **2017**, *7*, 1846–1852.
- [27] a) B. Elsler, D. Schollmeyer, K. M. Dyballa, R. Franke, S. R. Waldvogel, *Angew. Chem. Int. Ed.* **2014**, *53*, 5210–5213; *Angew. Chem.* **2014**, *126*, 5311–5314; b) A. Kirste, G. Schnakenburg, F. Stecker, A. Fischer, S. R. Waldvogel, *Angew. Chem. Int. Ed.* **2010**, *49*, 971–975; *Angew. Chem.* **2010**, *122*, 983–987; c) A. Kirste, M. Nieger, I. M. Malkowsky, F. Stecker, A. Fischer, S. R. Waldvogel, *Chem. Eur. J.* **2009**, *15*, 2273–2277; d) A. Wiebe, S. Lips, D. Schollmeyer, R. Franke, S. R. Waldvogel, *Angew. Chem.*

- Int. Ed.* **2017**, *56*, 14727–14731; *Angew. Chem.* **2017**, *129*, 14920–14925; e) S. Lips, D. Schollmeyer, R. Franke, S. R. Waldvogel, *Angew. Chem. Int. Ed.* **2018**, *57*, 13325–1332; *Angew. Chem.* **2018**, *130*, 13509–13513; f) L. Schulz, M. Enders, B. Elsler, D. Schollmeyer, K. M. Dyballa, R. Franke, S. R. Waldvogel, *Angew. Chem. Int. Ed.* **2017**, *56*, 4877–4881; *Angew. Chem.* **2017**, *129*, 4955–4959; g) S. Lips, A. Wiebe, B. Elsler, D. Schollmeyer, K. M. Dyballa, R. Franke, S. R. Waldvogel, *Angew. Chem. Int. Ed.* **2016**, *55*, 10872–10876; *Angew. Chem.* **2016**, *128*, 11031–11035; h) A. Wiebe, D. Schollmeyer, K. M. Dyballa, R. Franke, S. R. Waldvogel, *Angew. Chem. Int. Ed.* **2016**, *55*, 11801–11805; *Angew. Chem.* **2016**, *128*, 11979–11983.
- [28] I. Colomer, A. E. R. Chamberlain, M. B. Haughey, T. J. Donohoe, *Nat. Rev. Chem.* **2017**, *1*, 88, 1–12.
- [29] A. Kirste, B. Elsler, G. Schnakenburg, S. R. Waldvogel, *J. Am. Chem. Soc.* **2012**, *134*, 3571–3576.

Manuscript received: November 30, 2018
Revised manuscript received: December 20, 2018
Accepted manuscript online: December 20, 2018
Version of record online: January 22, 2019

Supporting Information

© Copyright Wiley-VCH Verlag GmbH & Co. KGaA, 69451 Weinheim, 2019

Dehydrogenative Anodic Cyanation Reaction of Phenols in Benzylic Positions

Johannes L. Röckl, Yasushi Imada, Kazuhiro Chiba, Robert Franke, and Siegfried R. Waldvogel*An invited contribution to a Special Issue on Organic Electrosynthesis

Table of Contents

General information.....	3
General protocol for electrolytic cyanation reaction (GP)	4
Proposed mechanisms for anodic HFIP ether formation	6
Synthesis of benzylic HFIP ether	8
Synthesis of 2-phenylacetonitriles.....	9
NMR spectra	17
References.....	27

General information

All reagents were used in analytical or sufficiently pure grades. Solvents were purified by standard methods.^[1] Electrochemical reactions were carried out at boron-doped diamond (BDD) electrodes. BDD electrodes were obtained as DIACHEM™ quality from CONDIAS GmbH, Itzehoe, Germany. BDD (15 μm diamond layer) on silicon support.

Column chromatography was performed on silica gel 60 M (0.040–0.063 mm, Macherey-Nagel GmbH & Co, Düren, Germany) with a maximum pressure of 1.6 bar. In addition, a preparative chromatography system (Büchi Labortechnik GmbH, Essen, Germany) was used with a Büchi Control Unit C-620, an UV detector Büchi UV photometer C-635, Büchi fraction collector C-660 and two Pump Modules C-605 for adjusting the solvent mixtures. As eluents mixtures of cyclohexane and ethyl acetate were used. Silica gel 60 sheets on aluminum (F254, Merck, Darmstadt, Germany) were used for thin layer chromatography.

Gas chromatography was performed on a Shimadzu GC-2010 (Shimadzu, Japan) using a ZB-5 column (Phenomenex, USA; length: 30 m, inner diameter: 0.25 mm, film: 0.25 μm, carrier gas: hydrogen/air). GC-MS measurements were carried out on a Shimadzu GC-2010 (Shimadzu, Japan) using a ZB-5 column (Phenomenex, USA; length: 30 m, inner diameter: 0.25 mm, film: 0.25 μm, carrier gas: helium). The chromatograph was coupled to a mass spectrometer: Shimadzu GCMS-QP2010.

High Performance Liquid Chromatography (HPLC) was performed on a Azura preparative HPLC (KNAUER Wissenschaftliche Geräte GmbH, Germany) using a Eurospher II column (pore size: 100 Å, particle size: 5 μm, length: 250 mm, inner diameter: 30 mm), deuterium lamp as a detector and 2.1 L pomp.

Melting points were determined with a Melting Point Apparatus B-545 (Büchi, Flawil, Switzerland) and are uncorrected. Heating rate: 2 °C/min.

Spectroscopy and spectrometry ¹H NMR, ¹³C and ¹⁹F NMR spectra were recorded at 25 °C, using a Bruker Avance III HD 400 (400 MHz) (5 mm BBFO-SmartProbe with z gradient and ATM, SampleXPress 60 sample changer, Analytische Messtechnik, Karlsruhe, Germany). Chemical shifts (δ) are reported in parts per million (ppm) relative to traces in the corresponding deuterated solvent. Mass spectra and high-resolution mass spectra were obtained by using a QToF Ultima 3 (Waters, Milford, Massachusetts) apparatus employing ESI⁺.

Cyclic voltammetry was performed with a Metrohm 663 VA Stand equipped with a μAutolab type III potentiostat (Metrohm AG, Herisau, Switzerland). *WE*: BDD electrode tip, 2 mm diameter; *CE*: glassy carbon rod; *RE*: Ag/AgCl in saturated LiCl/EtOH. Solvent: HFIP. $v = 100$ mV/s, $T = 20$ °C, $c = 0.005$ M, supporting electrolyte (if used): ⁿBu₃NMe O₃SOMe (MTBS), c (MTBS) = 0.09 M.

General protocol for electrolytic cyanation reaction (GP)

GP I: Undivided PTFE cell (5 mL)

The undivided 5 mL PTFE electrolysis cells can be homemade. Detailed information about used cells are already reported.^[2,3] However, the complete setup with these cells are also commercially available as IKA Screening System, IKA-Werke GmbH & Co. KG, Staufen, Germany. It is operated with boron-doped diamond electrodes (BDD, 0.3 x 1 x 7 cm, 15 μm diamond layer, support of silicon was used).

A solution of a phenol derivative (0.5–1.0 mmol) and *N*-ethyl-*N*-(prop-2-yl)propan-2-amine (**DIPEA**) (0.1 mL, 0.57 mmol) in 5 mL 1,1,1,3,3,3-hexafluoropropan-2-ol (**HFIP**) was electrolyzed at a boron-doped diamond (**BDD**) anode and a BDD cathode. A constant current electrolysis with a current density of 7.2 mA/cm² was performed at room temperature. After 1.8–3.0 F were applied, HFIP was recovered by distillation. Then, the reaction was taken up in EtOH/water or MeCN (10 mL) and 1.2 eq. - 2.0 eq. sodium or potassium cyanide were added. The mixture was stirred at r.t. for 5 min to 12 h. After completion of the reaction, the solvent was removed under reduced pressure and the residue was dissolved in 50 mL ethyl acetate and washed with 70 mL water. The aqueous phase was afterwards extracted to 30 mL of ethyl acetate. Combined organic phases were washed with 50 mL brine and dried with Na₂SO₄. After evaporation of the solvent, column chromatography yielded the pure product.

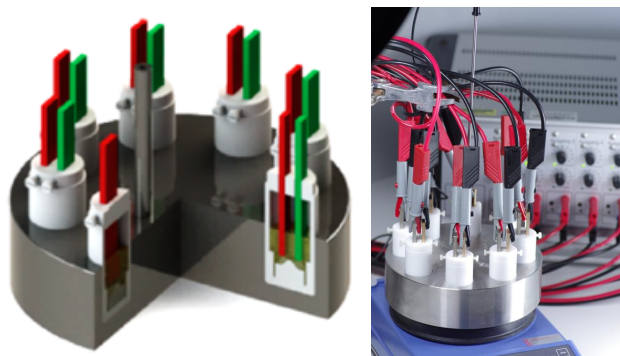


Fig. S1: Left: schematic 5 mL Teflon cells; Right: The commercially available IKA Screenings System, IKA-Werke GmbH & Co. KG, Staufen, Germany.

GP II: Round bottomed flask cell (500 mL) – Scale-up

50 mmol phenol, 250 mL HFIP, and 5.0 mL (0.57 eq.) DIPEA were transferred into a 500 mL round-bottomed flask equipped with a BDD anode and a BDD cathode. A constant current electrolysis with a current density of 7.2 mA/cm^2 was performed at room temperature. After 2.2 F were applied, HFIP was recovered by distillation. Then, sodium cyanide (2 eq.) was dissolved in 1000 mL EtOH/water (9/1) and the reaction mixture was added slowly dropwise under vigorous stirring. The mixture was stirred at r.t. for 5 min. After completion of the reaction, the solvent was removed under reduced pressure and the residue was dissolved in 200 mL ethyl acetate and washed with 200 mL water (3x). The aqueous layer was afterwards extracted to 100 mL of ethyl acetate. Combined organic fractions were first washed with 100 mL brine and dried with Na_2SO_4 . After evaporation of the solvent, column chromatography yielded the product.

The flask (500 mL) is closed by a PTFE plug. This cap allows precise arrangement of the BDD electrodes. Total dimension of the BDD electrodes are 14 cm x 3.5 cm x 0.3 cm.



Fig. S2: 500 mL flask cell; left: BDD electrode removed; right: assembled. For size comparison one 50 Eurocent coin is placed in front of the glass cell.

Proposed mechanisms for anodic HFIP ether formation

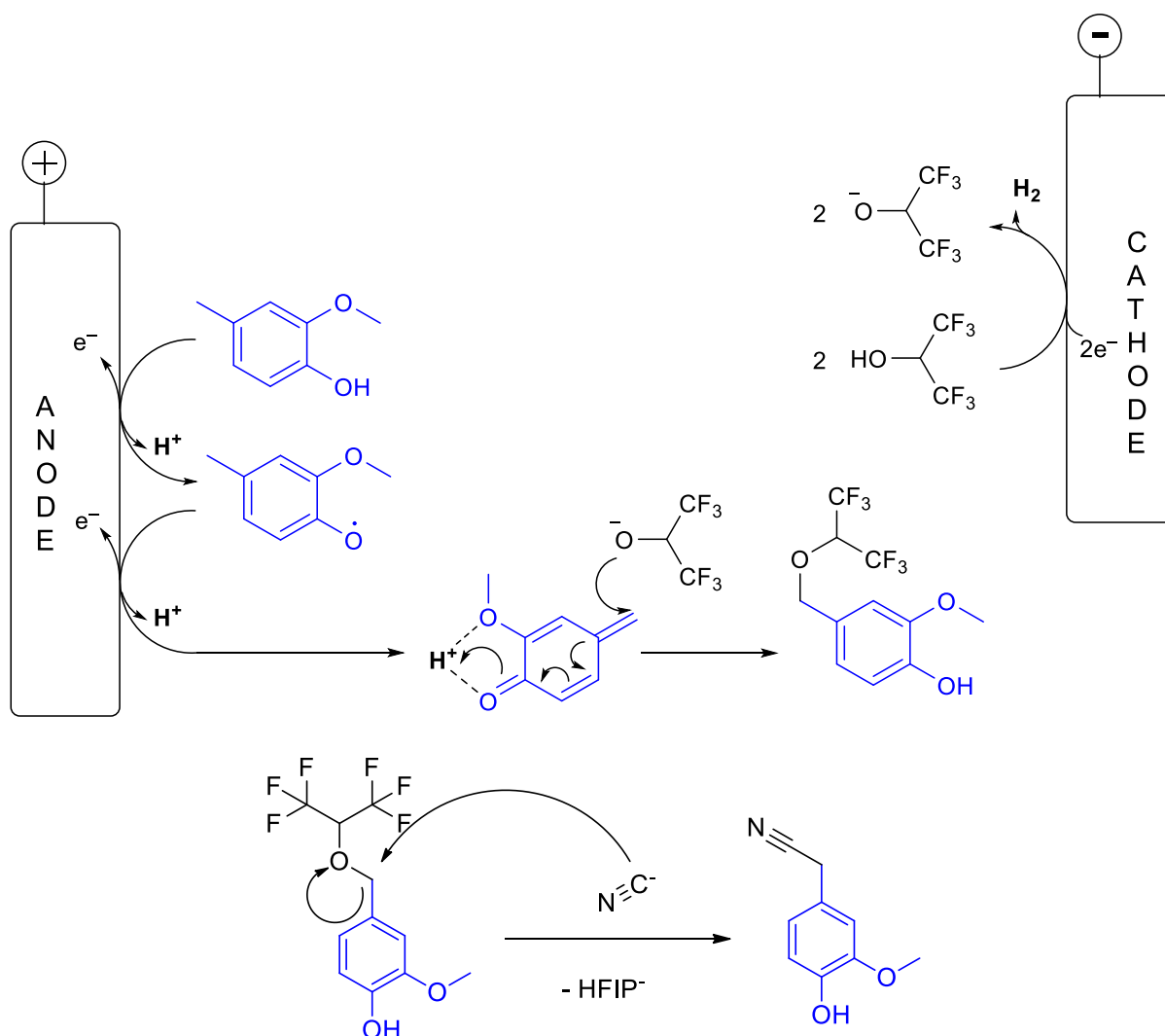
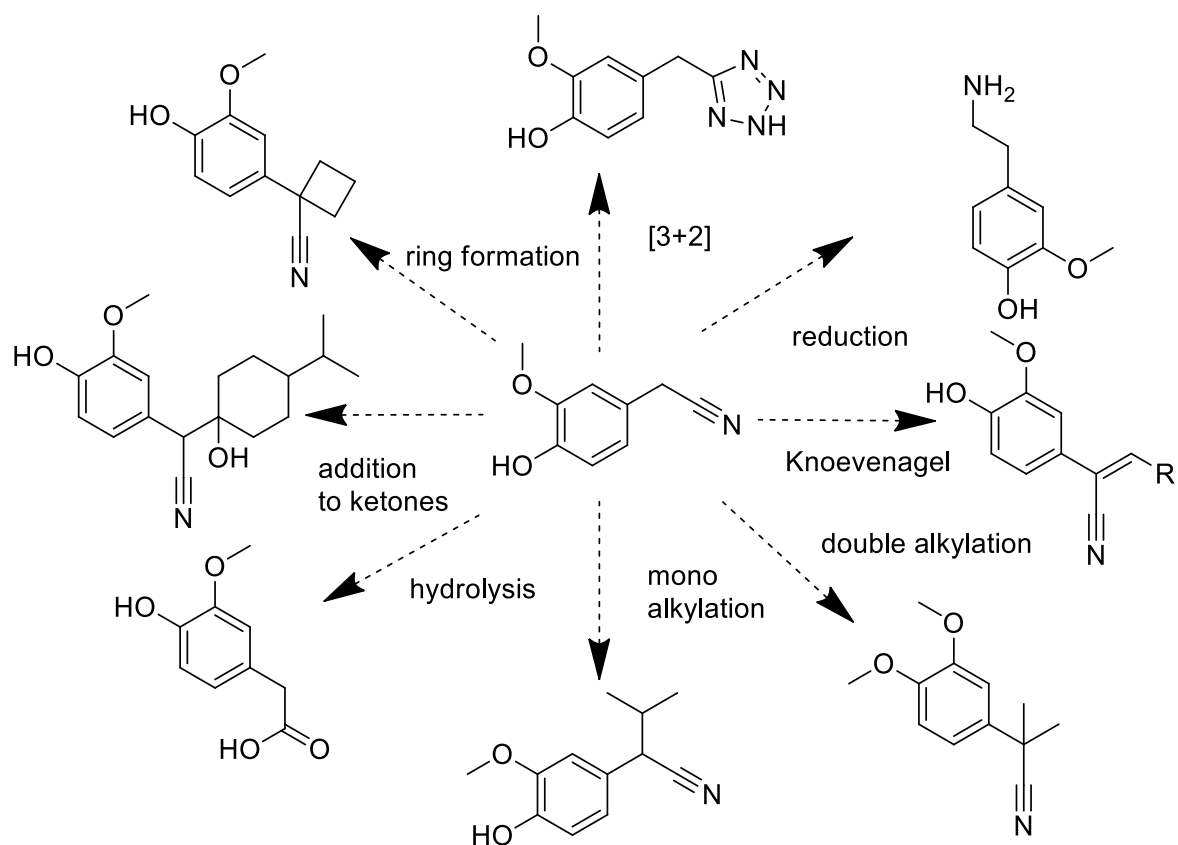


Fig. S3: Proposed mechanism for the electrochemical HFIP ether formation at benzylic position. Mechanism is shown for 4-methylguaiacol and can vary for other substrates.

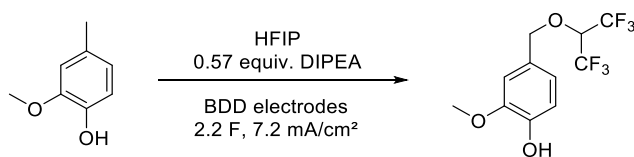
Twofold oxidation of the phenol at the anode will result in the formation of a quinone methide derivative. This can be activated in the acidic solution to allow nucleophilic attack of the HFIP anion at the benzylic position. The resulting product is a benzylic HFIP ether. Due to addition of DIPEA, HFIP anions are present from the beginning of the reaction. This concentration will be maintained by the cathodic reaction. The HFIP ether moiety is then substituted in a S_{N}^- reaction to yield the desired 2-phenylacetonitriles.

Previous CV measurements are inline to this mechanism assumption.^[4]

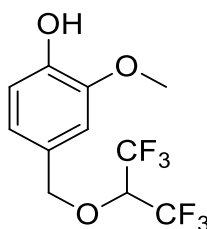


Scheme 1: Significance of 2-phenylacetonitriles as important building blocks in organic synthesis.

Synthesis of benzylic HFIP ether



4-((1-Trifluoromethyl-2,2,2-trifluoroethyl)oxymethyl)-2-methoxyphenol



According to the **GPI** for the electrochemical HFIP ether formation, 138 mg (1.0 mmol) 2-methoxy-4-methylphenol, 5 mL HFIP, and 0.1 mL DIPEA were transferred into an undivided PTFE cell. Electrolysis was carried out at room temperature with a current density of 7.2 mA/cm². After 2.2 F were applied, HFIP was recovered *in vacuo*. The residue was dissolved dichloromethane (30 mL) and washed with water (70 mL). The aqueous layer was afterwards extracted to dichloromethane (30 mL). Combined organic phases were dried over MgSO₄. After evaporation of the solvent, column chromatography (gradient: cyclohexane:ethyl acetate = from 100:0 for 3 min to 93:7 for 60 min; column 12 mm x 150 mm; flow rate 10 mL/min) yielded the product as colorless oil (yield: 54%, 164 mg, 0.54 mmol). Noteworthy, the HFIP ether is sensitive to silica gel and can decompose during column chromatography.

R_f (cyclohexane:ethyl acetate = 10:3) = 0.52

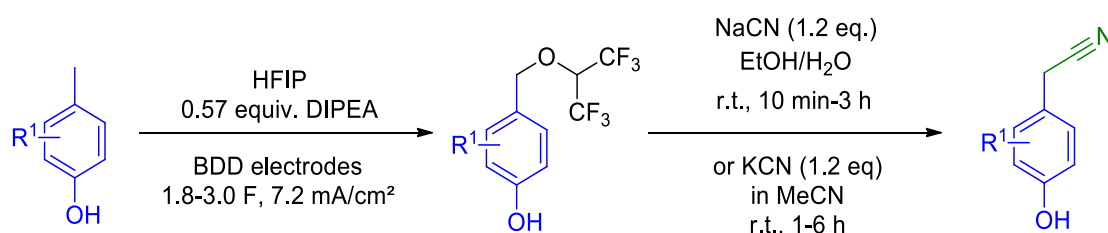
¹H NMR (400 MHz, CDCl₃) δ = 6.94 (d, *J* = 8.0 Hz, 1H), 6.91 (d, *J* = 1.9 Hz, 1H), 6.87 (dd, *J* = 8.0, 1.9 Hz, 1H), 5.77 (s, 1H), 4.81 (s, 2H), 4.13 (s, *J* = 6.0 Hz, 1H), 3.93 (s, 3H).

¹³C NMR (101 MHz, CDCl₃) δ = 146.86, 146.48, 126.21, 122.61, 114.26, 111.27, 75.72, 73.44 (p, *J* = 32.3 Hz), 55.91.

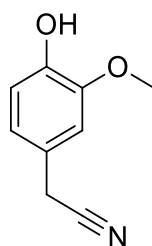
¹⁹F NMR (376 MHz, CDCl₃) δ = -74.61, -74.62.

HRMS for C₁₁H₁₀F₆O₃⁺ (APCI+) [M]⁺: calc.: 304.0529, found: 304.0532.

Synthesis of 2-phenylacetonitriles



2-(4-Hydroxy-3-methoxyphenyl)acetonitrile (1)



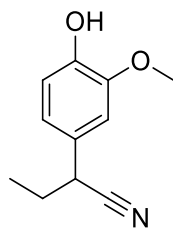
According to the **GPI** for the electrochemical HFIP ether formation, 138.16 mg (1.0 mmol) 2-methoxy-4-methylphenol (1 eq.), HFIP (5 mL), and DIPEA (0.1 mL) were transferred into an undivided 5 mL PTFE cell. Electrolysis was carried out at room temperature with a current density of 7.2 mA/cm². After 2.2 F were applied, HFIP was recovered *in vacuo*. The crude HFIP ether was dissolved in a mixture of ethanol (9 mL) and water (1 mL). Sodium cyanide (1.2 eq.) was then added and the reaction mixture was stirred at room temperature for 10 min. After completion, the reaction mixture was evaporated *in vacuo*. The residue was dissolved in ethyl acetate (30 mL) and washed with water (70 mL). The aqueous layer was afterwards extracted to ethyl acetate (30 mL). The combined organic fractions were dried over Na₂SO₄. After evaporation of the solvent, column chromatography (gradient: cyclohexane:ethyl acetate = from 100:0 for 3 min to 80:20 for 60 min; column 12 mm x 150 mm; flow rate 12.5 mL/min) yielded the product as colorless oil (yield: 90%, 147 mg, 0.90 mmol).

¹H NMR (400 MHz, CDCl₃) δ 6.89 (d, *J* = 8.0 Hz, 1H), 6.83 – 6.75 (m, 2H), 5.71 (s, 1H), 3.89 (s, 3H), 3.67 (s, 2H).

¹³C NMR (101 MHz, CDCl₃) δ 147.02, 145.52, 121.55, 121.04, 118.34, 114.92, 110.44, 56.11, 23.34.

HRMS for C₁₀H₁₁NaNO⁺ (ESI⁺) [M+Na]⁺: calc.: 186.0522, found: 186.0520.

2-(4-Hydroxy-3-methoxyphenyl)butanenitrile (2)



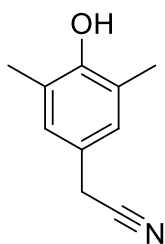
According to the **GPI** for the electrochemical HFIP ether formation, 191 mg (1.0 mmol) 2-methoxy-4-propylphenol (1 eq.), HFIP (5 mL), and DIPEA (0.1 mL) were transferred into an undivided 5 mL PTFE cell. Electrolysis was carried out at room temperature with a current density of 7.2 mA/cm². After 2.2 F were applied, HFIP was recovered *in vacuo*. The crude HFIP ether was dissolved in a mixture of ethanol (9 mL) and water (1 mL). Sodium cyanide (1.2 eq.) was then added and the reaction mixture was stirred at room temperature for 10 min. After completion, the reaction mixture was evaporated *in vacuo*. The residue was dissolved in ethyl acetate (30 mL) and washed with water (70 mL). The aqueous layer was afterwards extracted to ethyl acetate (30 mL). The combined organic fractions were dried over Na₂SO₄. After evaporation of the solvent, column chromatography (gradient: cyclohexane:ethyl acetate = from 100:0 for 3 min to 80:20 for 60 min; column 12 mm x 150 mm; flow rate 12.5 mL/min) yielded the product as colorless oil (yield: 44%, 84 mg, 0.44 mmol).

¹H NMR (400 MHz, CDCl₃) δ 6.88 (d, *J* = 8.1 Hz, 1H), 6.84 – 6.73 (m, 2H), 5.77 (s, 1H), 3.88 (s, 3H), 3.65 (dd, *J* = 7.5, 6.6 Hz, 1H), 1.91 (m, 2H), 1.05 (t, *J* = 7.5 Hz, 3H).

¹³C NMR (101 MHz, CDCl₃) δ 146.93, 145.48, 127.61, 120.41, 114.79, 109.70, 56.11, 38.67, 29.42, 11.59.

HRMS for C₁₁H₁₃NO₂⁺ (APCI+) [M]⁺: calc.: 191.0941, found: 191.0939.

2-(4-Hydroxy-3,5-dimethylphenyl)acetonitrile (3)



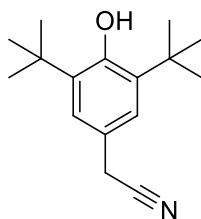
According to the **GPI** for the electrochemical HFIP ether formation, 136 mg (1.0 mmol) 2,4,6-trimethylphenol (1 eq.), HFIP (5 mL), and DIPEA (0.1 mL) were transferred into an undivided 5 mL PTFE cell. Electrolysis was carried out at room temperature with a current density of 7.2 mA/cm². After 2.2 F were applied, HFIP was recovered *in vacuo*. The crude HFIP ether was dissolved in a mixture of ethanol (9 mL) and water (1 mL). Sodium cyanide (1.2 eq.) was then added and the reaction mixture was stirred at room temperature for 10 min. After completion, the reaction mixture was evaporated *in vacuo*. The residue was dissolved in ethyl acetate (30 mL) and washed with water (70 mL). The aqueous layer was afterwards extracted to ethyl acetate (30 mL). The combined organic fractions were dried over Na₂SO₄. After evaporation of the solvent, column chromatography (gradient: cyclohexane:ethyl acetate = from 100:0 for 3 min to 80:20 for 60 min; column 12 mm x 150 mm; flow rate 12.5 mL/min) yielded the product as colorless oil (yield: 75%, 119 mg, 0.75 mmol).

¹H NMR (400 MHz, CDCl₃) δ 6.94 (s, 2H), 4.99 (s, 1H), 3.63 (s, 2H), 2.26 (s, 6H).

¹³C NMR (101 MHz, CDCl₃) δ 152.09, 128.12, 124.09, 121.07, 118.63, 22.80, 16.01.

HRMS for C₁₀H₁₁NO⁺ (APCI+) [M]⁺: calc.: 161.0841, found: 161.0831.

2-(3,5-Di-tert-butyl-4-hydroxyphenyl)acetonitrile (4)



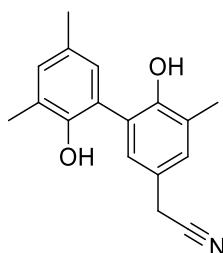
According to the **GPI** for the electrochemical HFIP ether formation, 220 mg (1.0 mmol) 2,6-di-tert-butyl-4-methylphenol (1 eq.), HFIP (5 mL), and DIPEA (0.1 mL) were transferred into an undivided 5 mL PTFE cell. Electrolysis was carried out at room temperature with a current density of 7.2 mA/cm². After 2.2 F were applied, HFIP was recovered *in vacuo*. The crude HFIP ether was dissolved in a mixture of ethanol (9 mL) and water (1 mL). Sodium cyanide (1.2 eq.) was then added and the reaction mixture was stirred at room temperature for 30 min. After completion, the reaction mixture was evaporated *in vacuo*. The residue was dissolved in ethyl acetate (30 mL) and washed with water (70 mL). The aqueous layer was afterwards extracted to ethyl acetate (30 mL). The combined organic fractions were dried over Na₂SO₄. After evaporation of the solvent, column chromatography (gradient: cyclohexane:ethyl acetate = from 100:0 for 3 min to 90:10 for 60 min; column 12 mm x 150 mm; flow rate 10 mL/min) yielded the product as crystalline solid (yield: 30%, 72 mg, 0.30 mmol).

¹H NMR (400 MHz, CDCl₃) δ 7.11 (s, 2H), 5.26 (s, 1H), 3.66 (s, 2H), 1.45 (s, 18H).

¹³C NMR (101 MHz, CDCl₃) δ 153.61, 136.85, 124.82, 120.58, 118.73, 34.51, 30.26, 23.56.

HRMS for C₁₆H₂₄NO⁺ (ESI+) [M+H]⁺: calc.: 246.1852, found: 246.1813.

5-Cyanomethyl-3,3',5'-trimethyl-2,2'-biphenol (5)



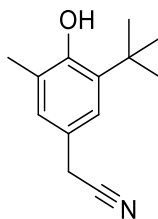
According to the **GPI** for the electrochemical HFIP ether formation, 242 mg (1 mmol) 3,3',5,5'-tetramethyl-2,2'-biphenol (1 eq.), HFIP (5 mL), and DIPEA (0.1 mL) were transferred into an undivided 5 mL PTFE cell. Electrolysis was carried out at room temperature with a current density of 7.2 mA/cm². After 2.2 F were applied, HFIP was recovered *in vacuo*. The crude HFIP ether was dissolved in acetonitrile (10 mL). Potassium cyanide (1.2 eq.) was then added and the reaction mixture was stirred at room temperature for 5 h. After completion, the reaction mixture was evaporated *in vacuo*. The residue was dissolved in ethyl acetate (30 mL) and washed with water (70 mL). The aqueous layer was afterwards extracted to ethyl acetate (30 mL). The combined organic fractions were dried over Na₂SO₄. After evaporation of the solvent, column chromatography (gradient: cyclohexane:ethyl acetate = from 100:0 for 3 min to 80:20 for 60 min; column 12 mm x 150 mm; flow rate 12.5 mL/min) yielded the product as crystalline solid (yield: 29%, 75 mg, 0.29 mmol).

¹H NMR (400 MHz, CDCl₃) δ 7.14 (d, *J* = 2.3 Hz, 1H), 7.05 – 7.00 (m, 2H), 6.87 – 6.83 (m, 1H), 5.45 (d, *J* = 2.3 Hz, 1H), 4.98 (d, *J* = 2.3 Hz, 1H), 3.67 (s, 2H), 2.31 (s, 3H), 2.29 (s, 6H).

¹³C NMR (101 MHz, CDCl₃) δ 151.33, 148.90, 132.40, 130.65, 130.49, 128.77, 127.91, 126.60, 125.23, 123.65, 121.89, 121.59, 118.16, 22.82, 20.44, 16.28, 16.14.

HRMS for C₁₇H₁₇NNaO₂⁺ (ESI+) [M+Na]⁺: calc.: 290.1151, found: 290.1149.

2-(3-(tert-Butyl)-4-hydroxy-5-methylphenyl)acetonitrile (6)



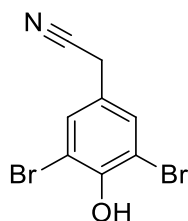
According to the **GPI** for the electrochemical HFIP ether formation, 178 mg (1.0 mmol) 2-(tert-butyl)-4,6-dimethylphenol (1 eq.), HFIP (5 mL), and DIPEA (0.1 mL) were transferred into an undivided 5 mL PTFE cell. Electrolysis was carried out at room temperature with a current density of 7.2 mA/cm². After 2.2 F were applied, HFIP was recovered *in vacuo*. The crude HFIP ether was dissolved in a mixture of ethanol (9 mL) and water (1 mL). Sodium cyanide (1.2 eq.) was then added and the reaction mixture was stirred at room temperature for 10 min. After completion, the reaction mixture was evaporated *in vacuo*. The residue was dissolved in ethyl acetate (30 mL) and washed with water (70 mL). The aqueous layer was afterwards extracted to ethyl acetate (30 mL). The combined organic fractions were dried over Na₂SO₄. After evaporation of the solvent, column chromatography (gradient: cyclohexane:ethyl acetate = from 100:0 for 3 min to 90:10 for 60 min; column 12 mm x 150 mm; flow rate 10 mL/min) yielded the product as crystalline solid (yield: 89%, 180 mg, 0.89 mmol).

¹H NMR (400 MHz, CDCl₃) δ 7.05 (d, *J* = 2.4 Hz, 1H), 6.98 (dd, *J* = 2.4, 0.8 Hz, 1H), 5.01 (s, 1H), 3.64 (s, 2H), 2.25 (s, 3H), 1.42 (s, 9H).

¹³C NMR (101 MHz, CDCl₃) δ 152.54, 136.67, 128.04, 124.83, 124.12, 120.83, 118.68, 34.69, 29.66, 23.12, 16.10.

HRMS for C₁₃H₁₇O⁺ (APCI+) [M]⁺: calc.: 203.1310, found: 203.1261.

2-(3,5-Dibromo-4-hydroxyphenyl)acetonitrile (7)



According to the **GPI** for the electrochemical HFIP ether formation, 133 mg (0.5 mmol) 2,6-dibromo-4-methylphenol (1 eq.), diol (1 eq.), HFIP (5 mL), and DIPEA (0.1 mL) were transferred into an undivided 5 mL PTFE cell. Electrolysis was carried out at room temperature with a current density of 7.2 mA/cm². After 2.2 F were applied, HFIP was recovered *in vacuo*. The crude HFIP ether was dissolved in acetonitrile (10 mL). Potassium cyanide (1.2 eq.) was then added and the reaction mixture was stirred at room temperature for 12 h. After completion, the reaction mixture was evaporated *in vacuo*. The residue was dissolved in ethyl acetate (30 mL) and washed with water (70 mL). The aqueous layer was afterwards extracted to ethyl acetate (30 mL). The combined organic fractions were dried over Na₂SO₄. After evaporation of the solvent, column chromatography (gradient: cyclohexane:ethyl acetate = from 100:0 for 3 min to 80:20 for 60 min; column 12 mm x 150 mm; flow rate 12.5 mL/min) yielded the product as crystalline solid (yield: 27%, 39 mg, 0.135 mmol).

¹H NMR (400 MHz, DMSO-*d*₆) δ 10.11 (s, 1H), 7.55 (s, 1H), 3.95 (s, 1H).

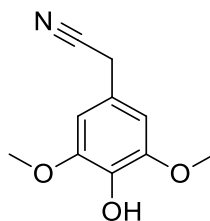
¹³C NMR (101 MHz, DMSO-*d*₆) δ 150.79, 132.47, 125.98, 119.39, 112.55, 21.17.

HRMS for C₈H₄⁷⁹Br₂NO⁻ (ESI-) [M-H]⁻: calc.: 287.8665, found: 287.8661

for C₈H₄⁷⁹Br⁸¹BrNO⁻ (ESI-) [M-H]⁻: calc.: 289.8639, found: 289.8640

for C₈H₄⁸¹Br₂NO⁻ (ESI-) [M-H]⁻: calc.: 291.8619, found: 291.8623

2-(4-Hydroxy-3,5-dimethoxyphenyl)acetonitrile (8)



According to the **GPI** for the electrochemical HFIP ether formation, 84 mg (0.5 mmol) 2,6-dimethoxy-4-methylphenoldiol (1 eq.), HFIP (5 mL), and DIPEA (0.1 mL) were transferred into an undivided 5 mL PTFE cell. Electrolysis was carried out at room temperature with a current density of 7.2 mA/cm². After 2.2 F were applied, HFIP was recovered *in vacuo*. The crude HFIP ether was dissolved in acetonitrile (10 mL). Potassium cyanide (1.2 eq.) was then added and the reaction mixture was stirred at room temperature for 5 h. After completion, the reaction mixture was evaporated *in vacuo*. The residue was dissolved in ethyl acetate (30 mL) and washed with water (70 mL). The aqueous layer was afterwards extracted to ethyl acetate (30 mL). The combined organic fractions were dried over Na₂SO₄. After evaporation of the solvent, column chromatography (gradient: cyclohexane:ethyl acetate = from 100:0 for 3 min to 75:25 for 60 min; column 12 mm x 150 mm; flow rate 12.5 mL/min) yielded the product as crystalline solid (yield: 37%, 36 mg, 0.18 mmol).

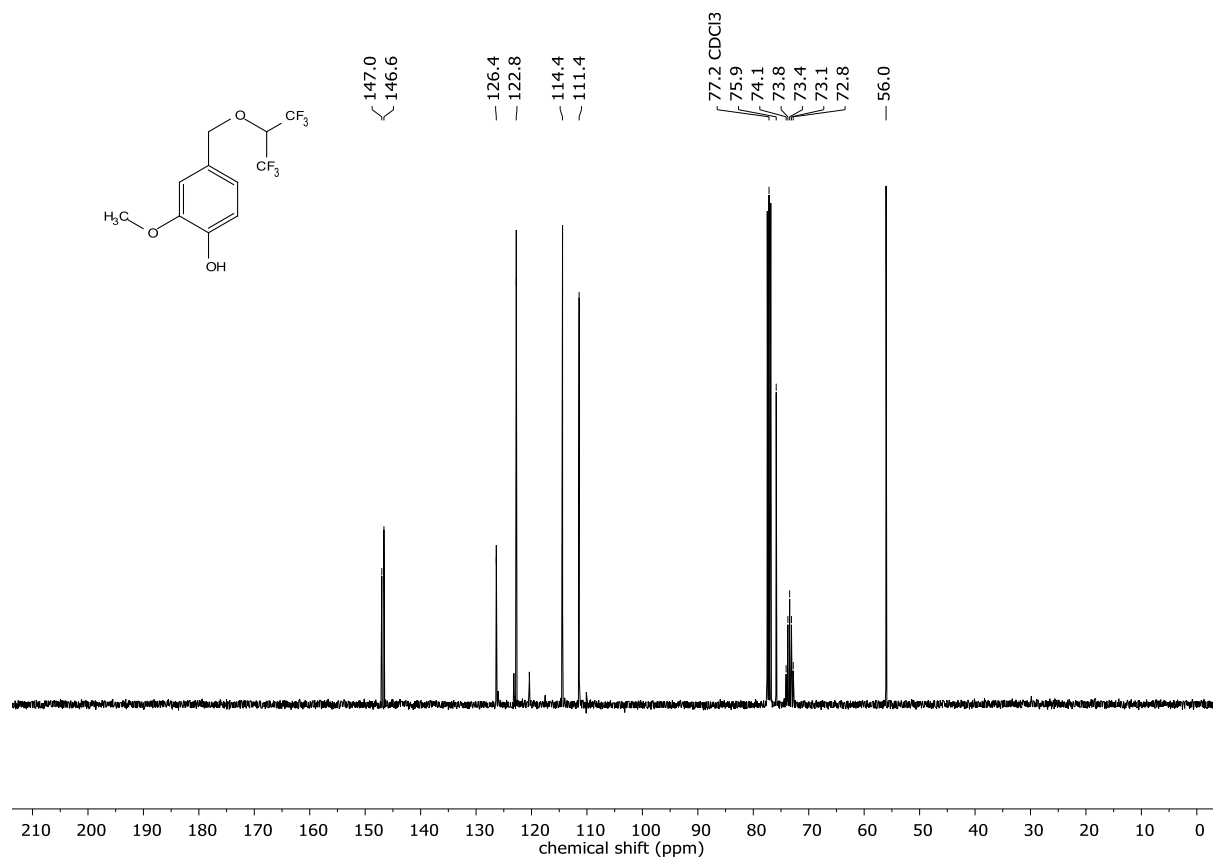
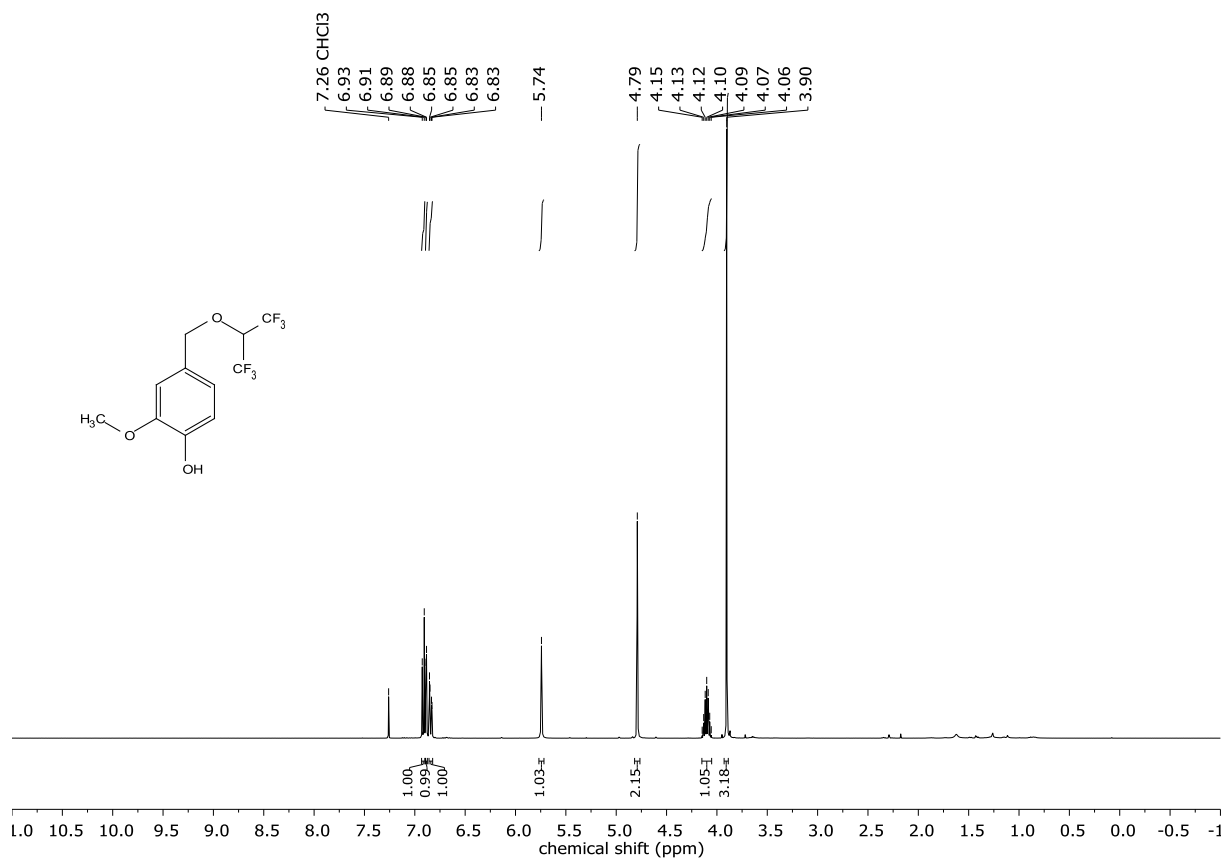
¹H NMR (400 MHz, CDCl₃) δ 6.51 (s, 2H), 5.56 (s, 1H), 3.88 (s, 6H), 3.67 (s, 2H).

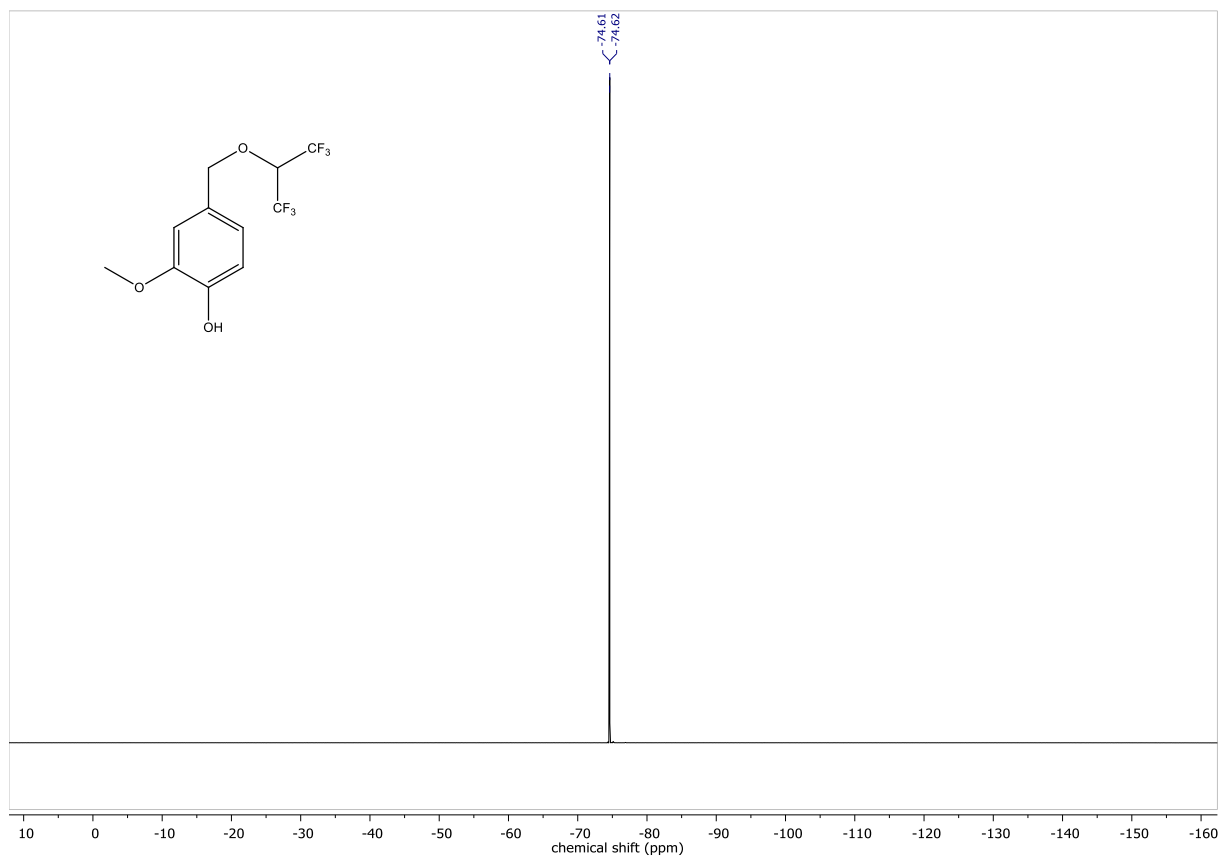
¹³C NMR (101 MHz, CDCl₃) δ 147.39, 134.45, 120.75, 118.13, 104.74, 56.41, 23.63.

HRMS for C₁₀H₁₀NO₃⁺ (APCI+) [M]⁺: calc.: 192.0655, found: 192.0656

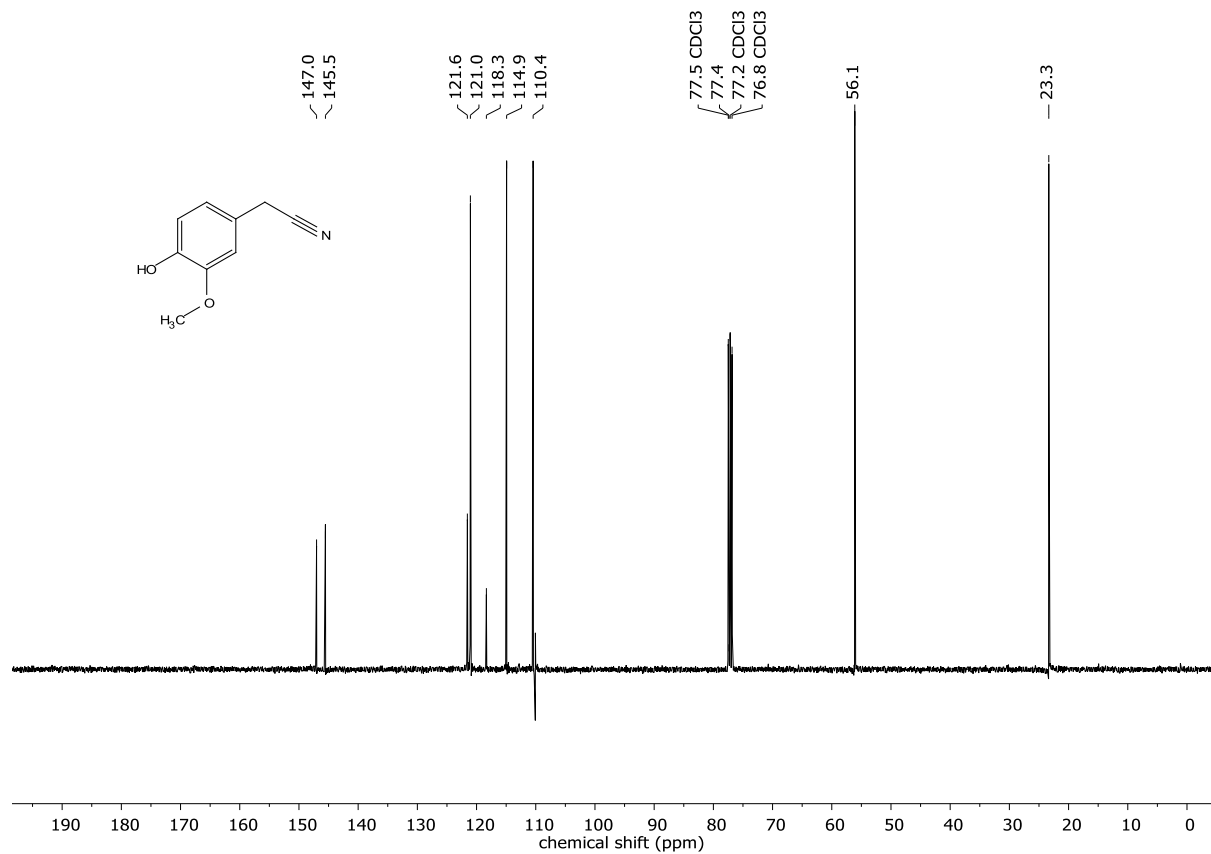
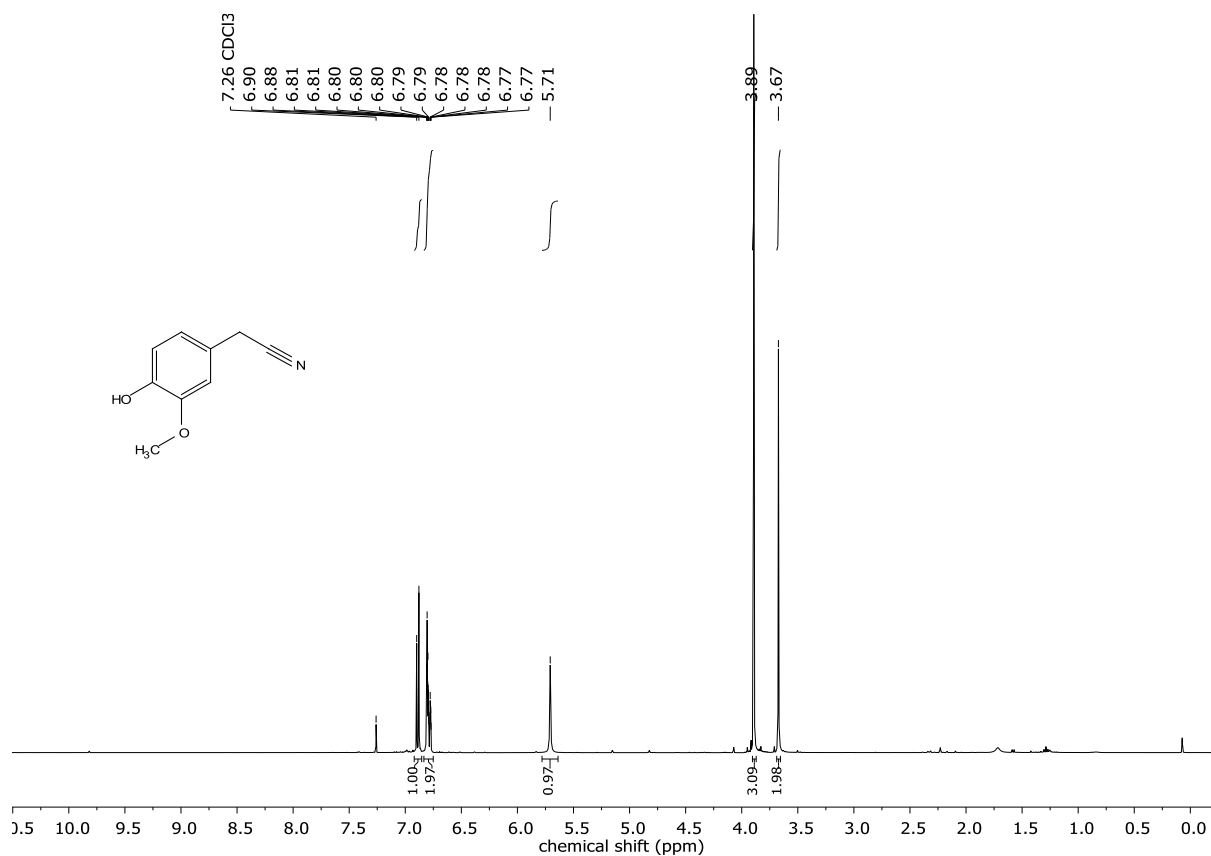
NMR spectra

4-((1-Trifluoromethyl-2,2,2-trifluoroethyl)oxymethyl)-2-methoxyphenol

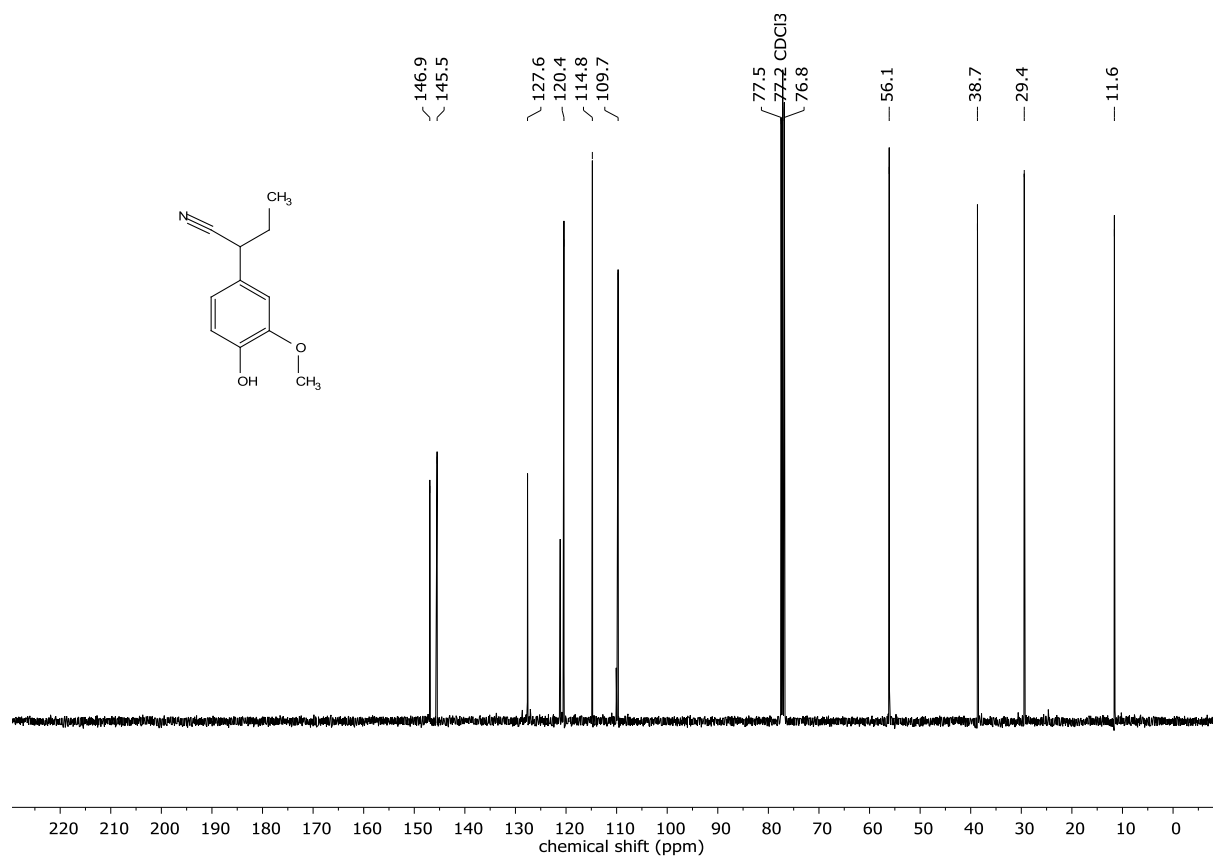
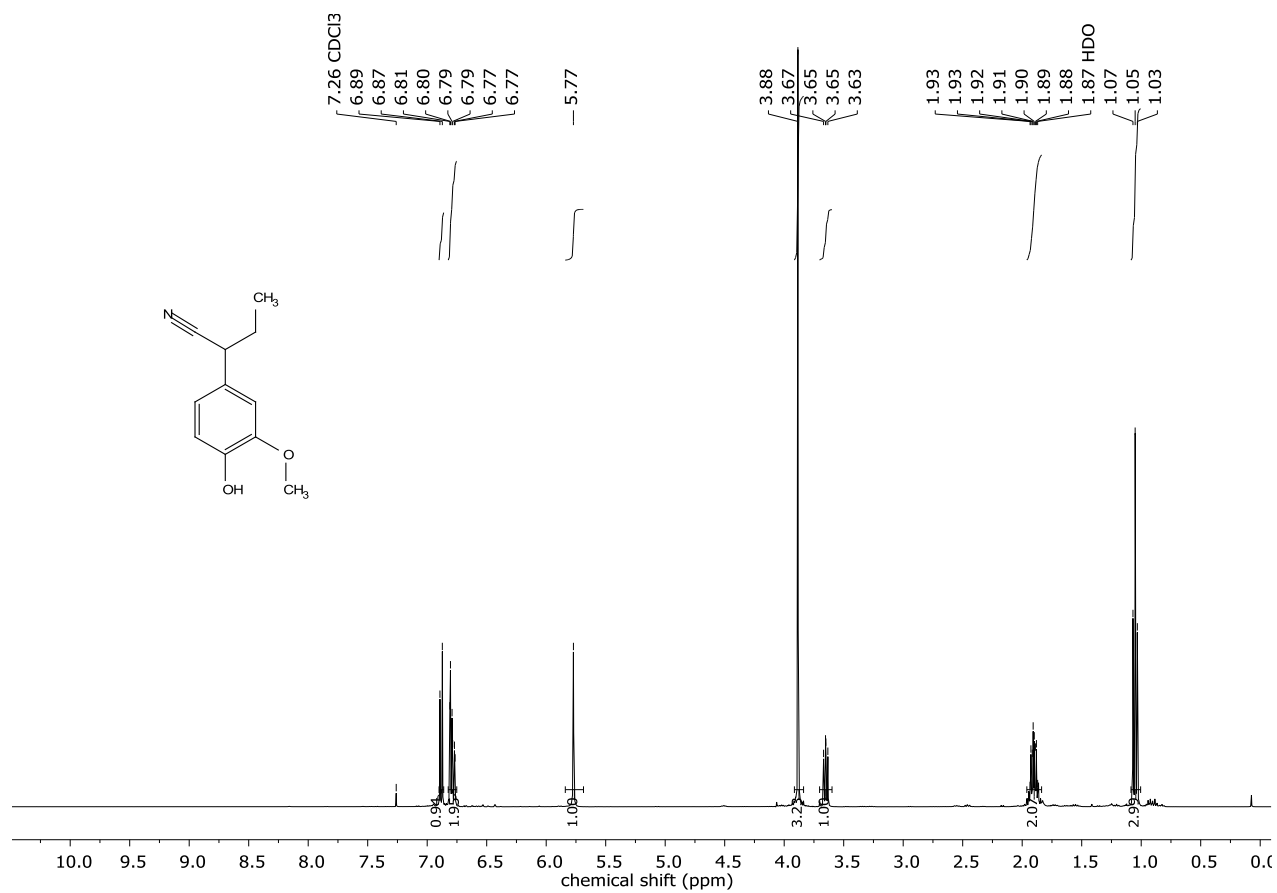




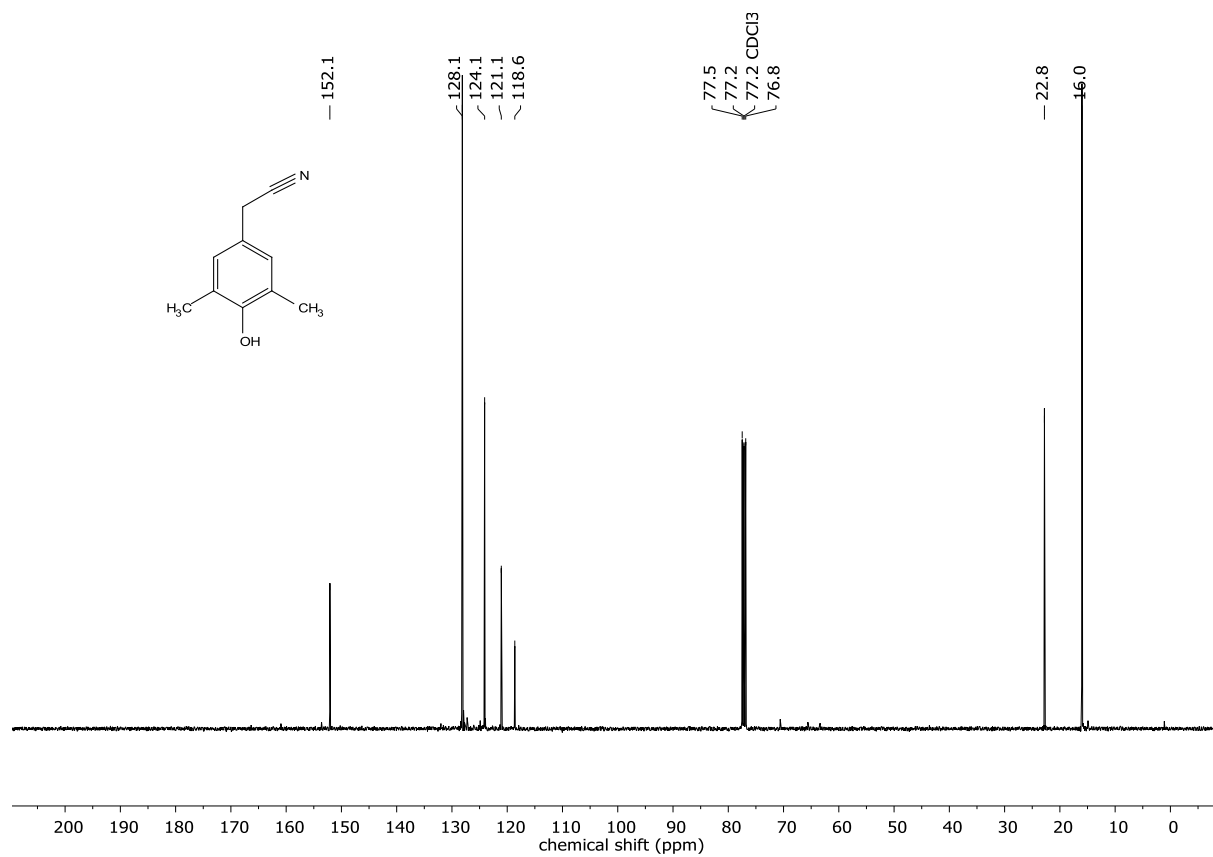
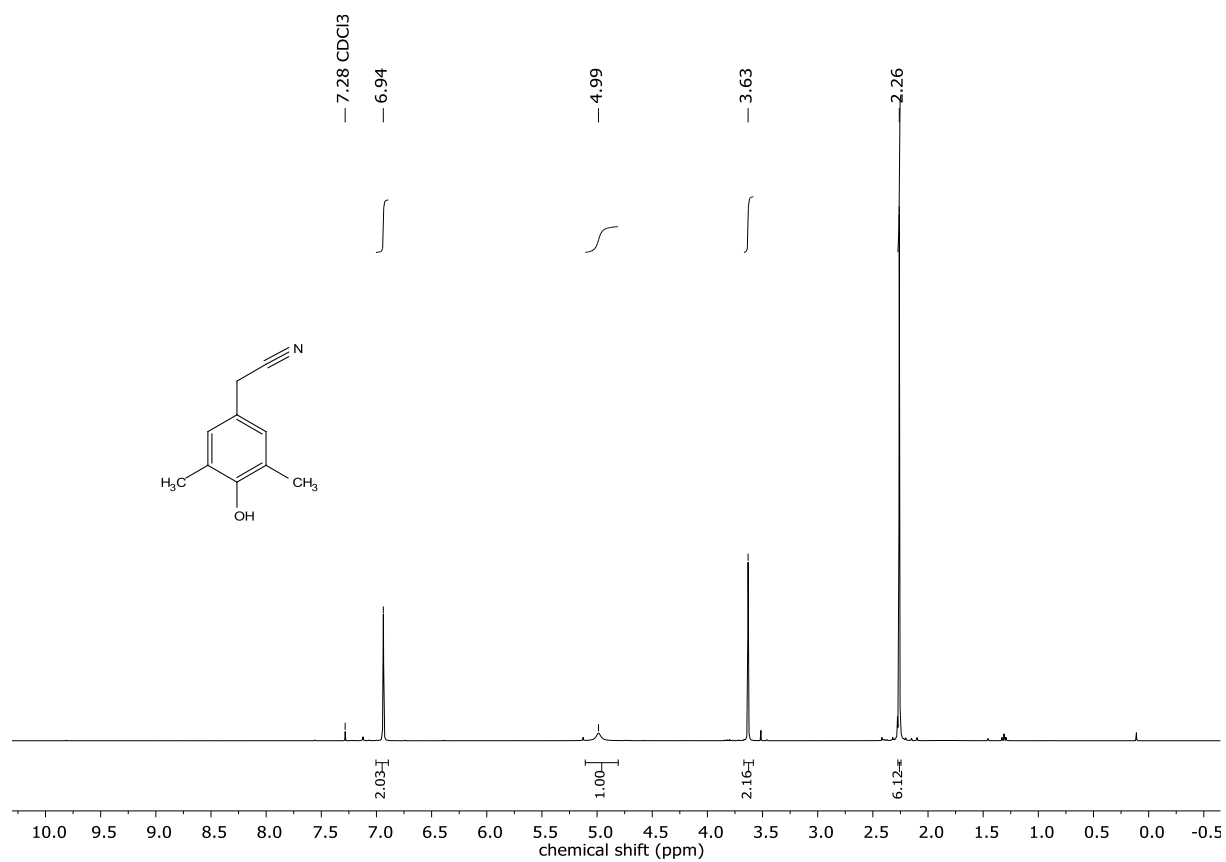
2-(4-Hydroxy-3-methoxyphenyl)acetonitrile (1)



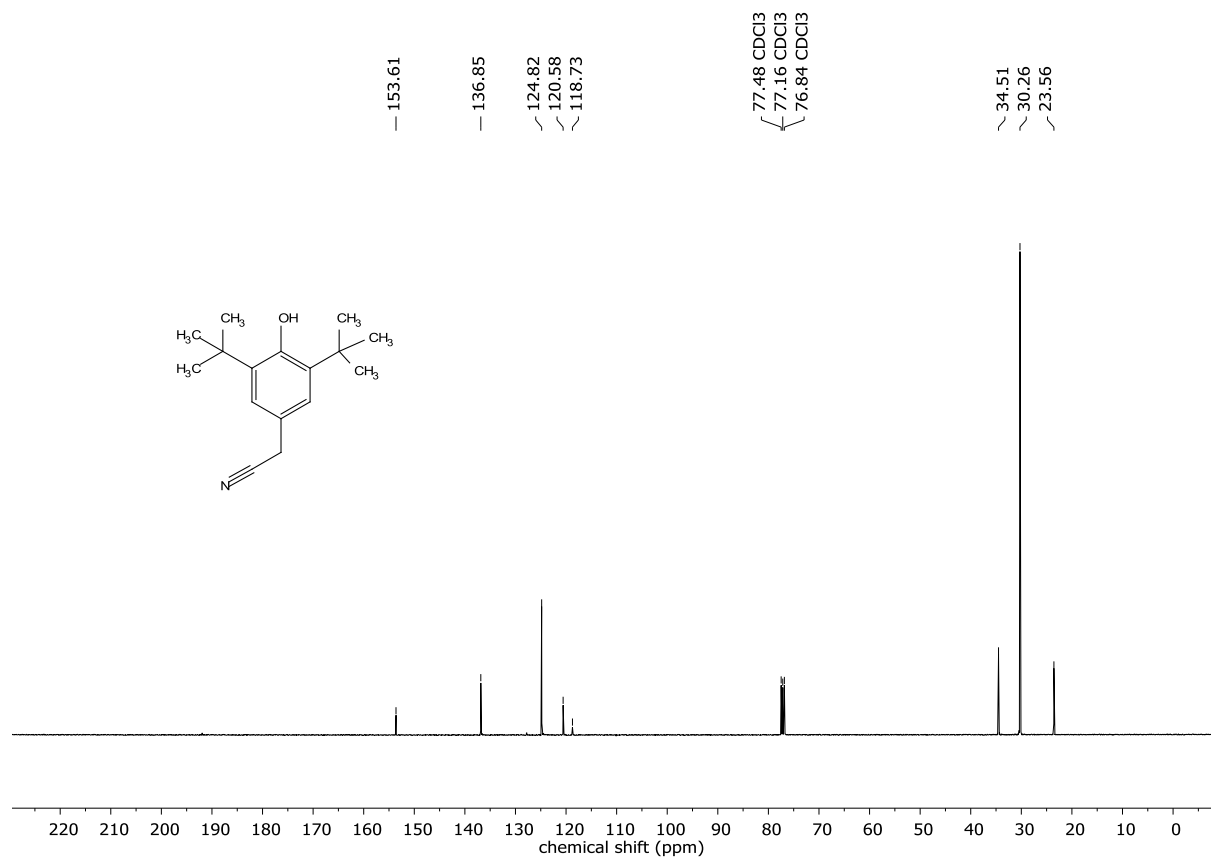
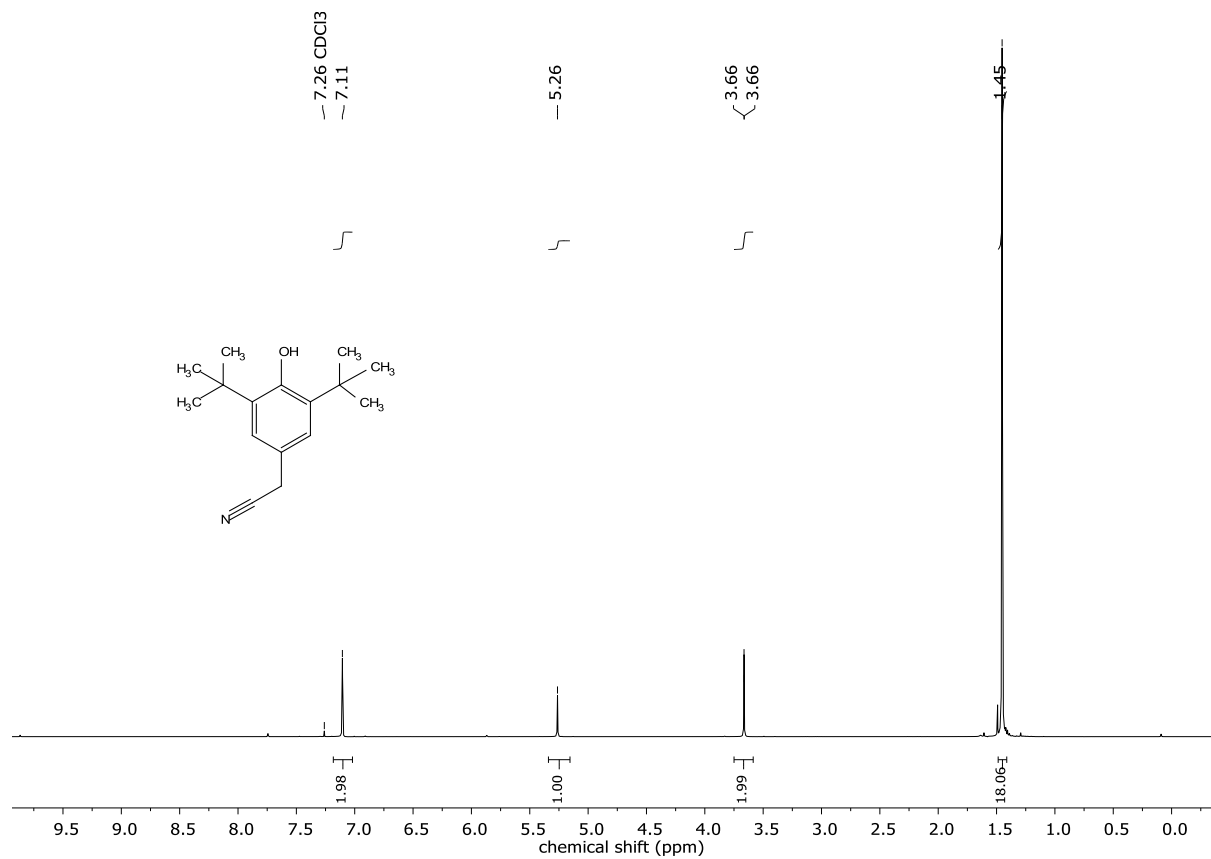
2-(4-Hydroxy-3-methoxyphenyl)butanenitrile (2)



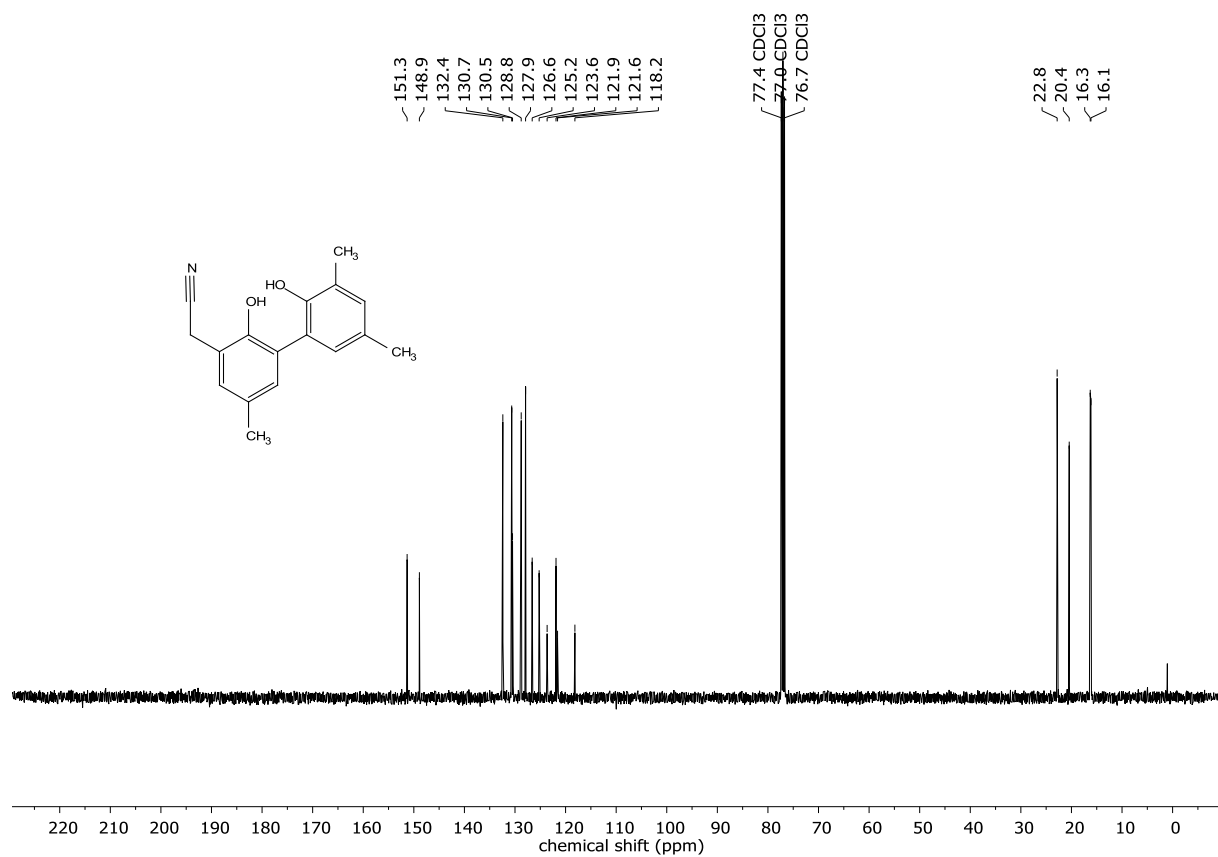
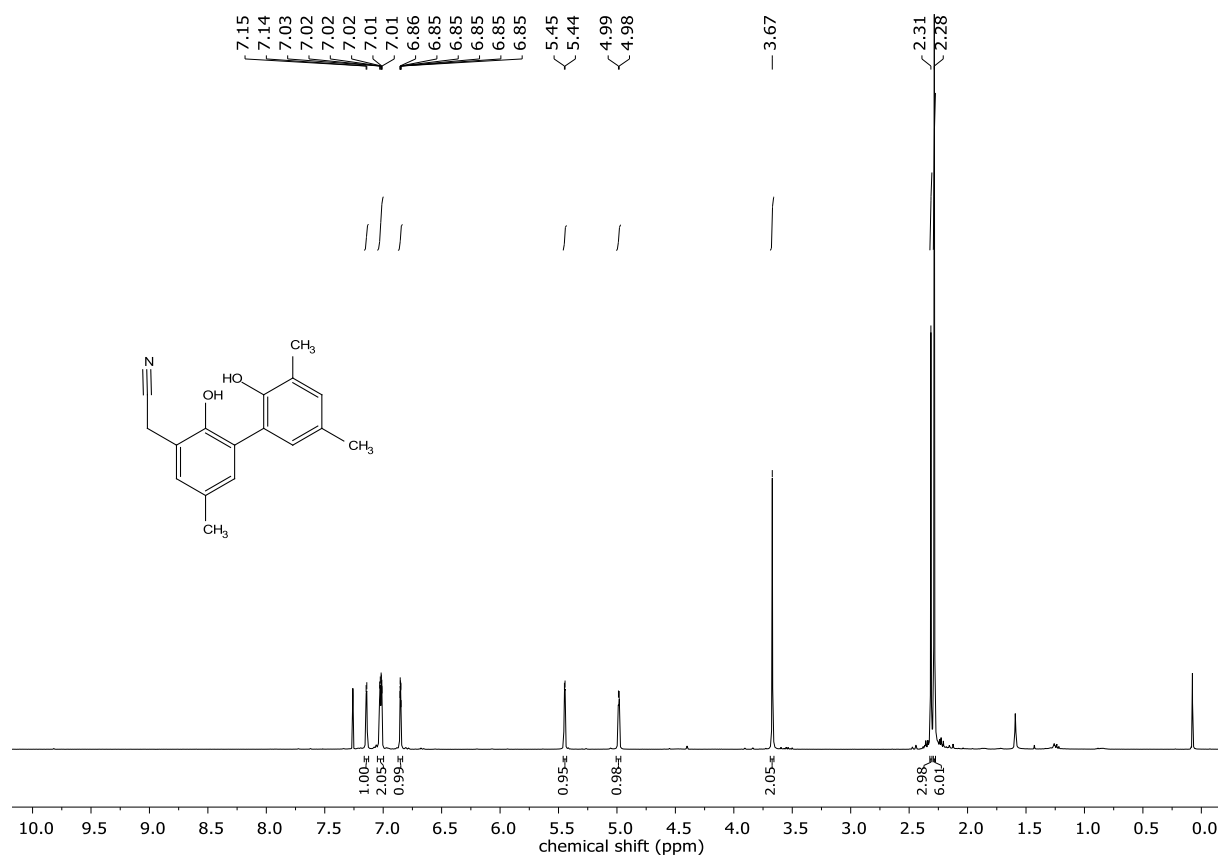
2,6-Dimethyl-4-(2,4,5-trimethoxybenzyl)phenol (3)



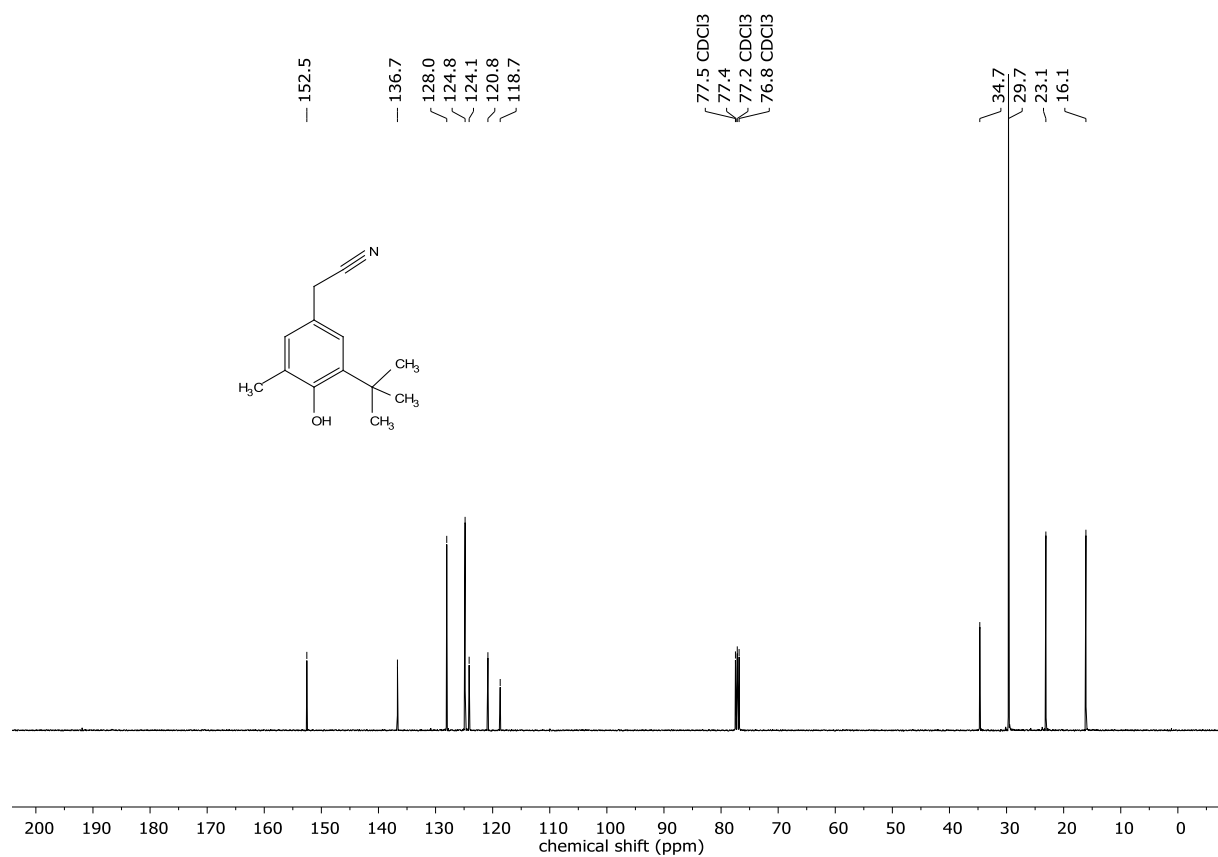
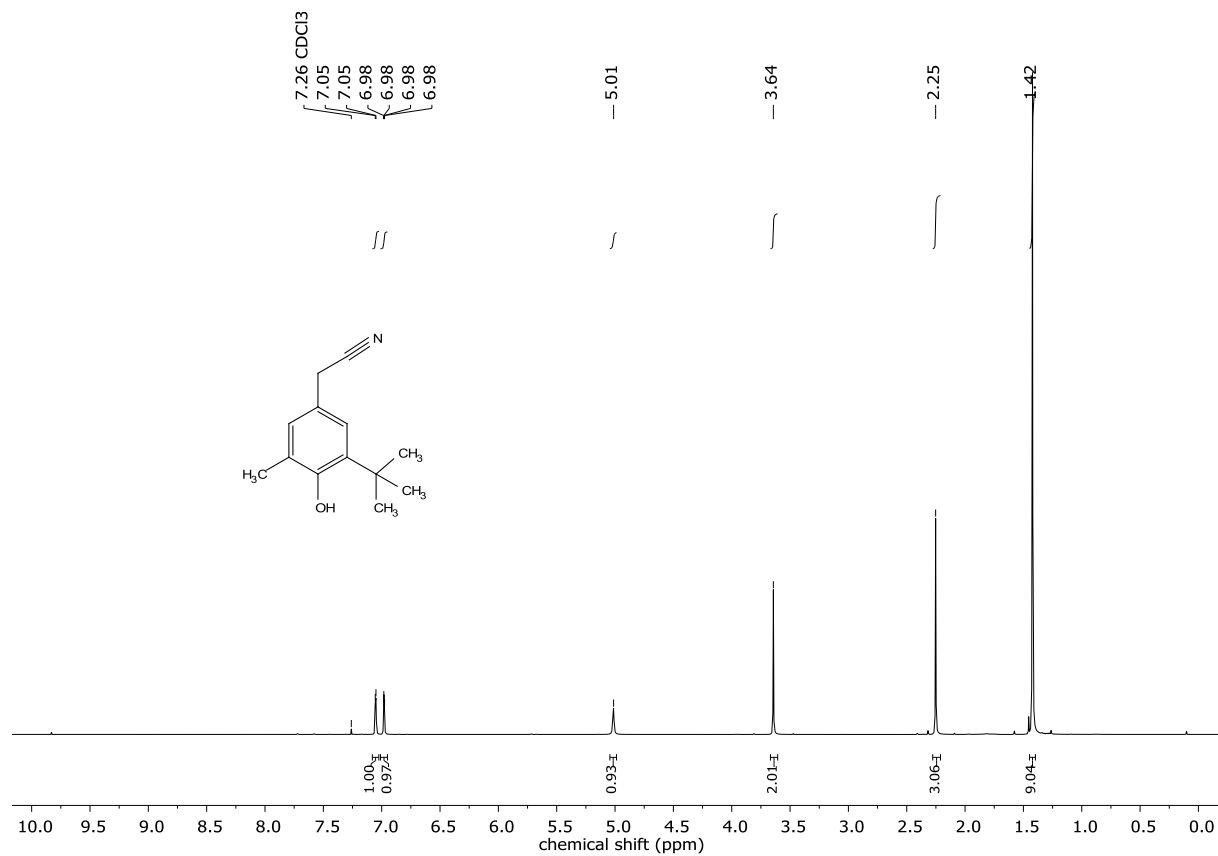
2-(3,5-Di-*tert*-butyl-4-hydroxyphenyl)acetonitrile (4)



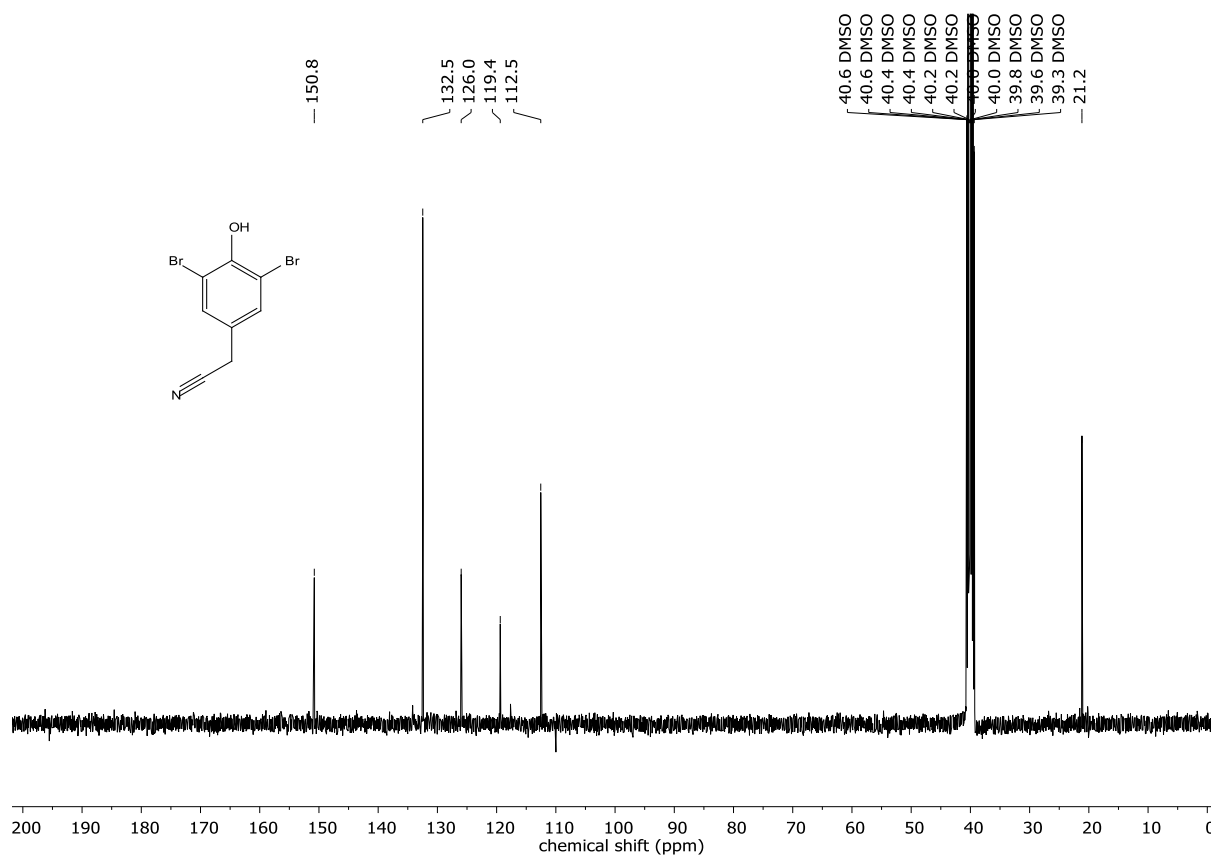
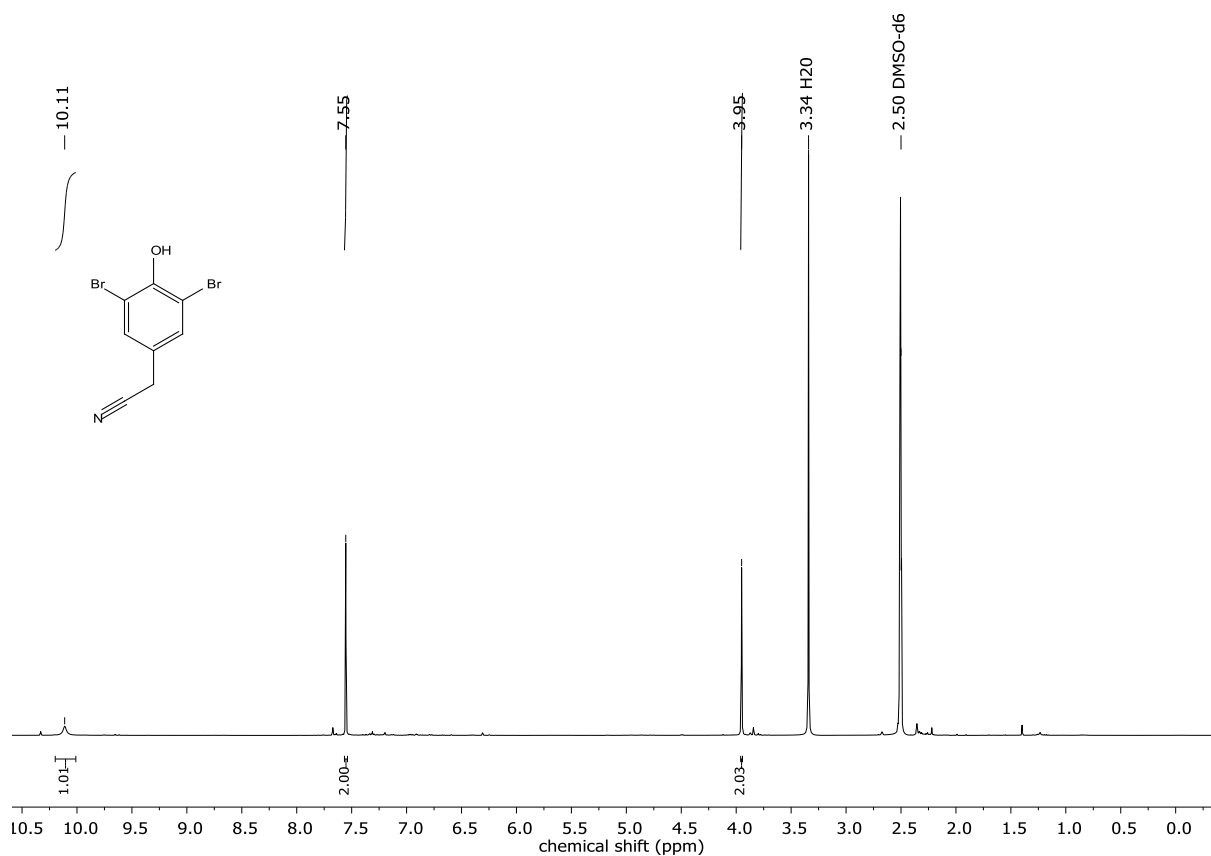
5-Cyanomethyl-3,3',5'-trimethyl-2,2'-biphenol (5)



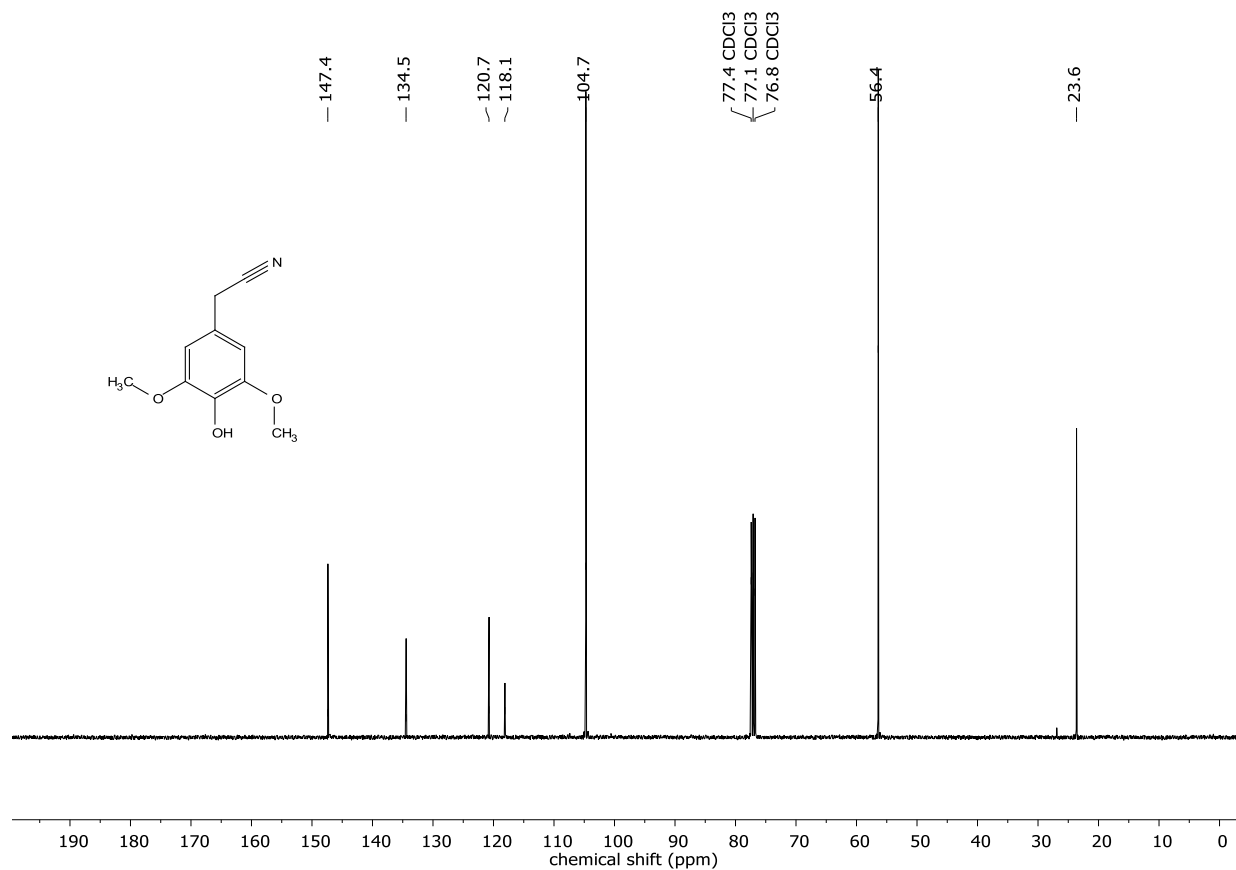
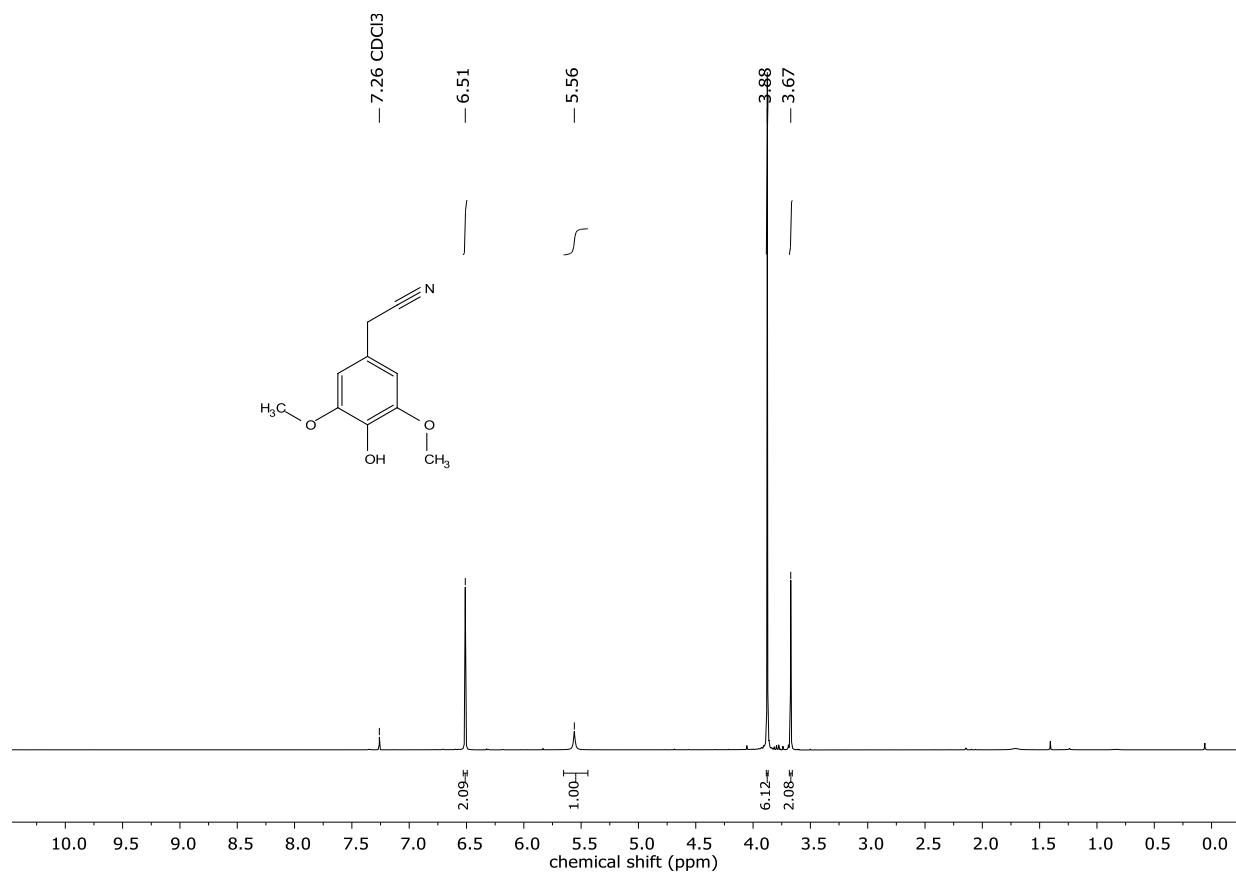
2-(3-(*tert*-Butyl)-4-hydroxy-5-methylphenyl)acetonitrile (6)



2-(3,5-Dibromo-4-hydroxyphenyl)acetonitrile (7)



2-(4-Hydroxy-3,5-dimethoxyphenyl)acetonitrile (8)



References

- [1] W. L. F. Armarego, C. L. L. Chai, *Purification of laboratory chemicals*, Elsevier, Amsterdam, **2013**.
- [2] C. Gütz, B. Klöckner, S. R. Waldvogel, *Org. Process Res. Dev.* **2016**, *20*, 26–32.
- [3] A. Kirste, G. Schnakenburg, F. Stecker, A. Fischer, S. R. Waldvogel, *Angew. Chem. Int. Ed.* **2010**, *49*, 971-975; *Angew. Chem.* **2010**, *122*, 983–987. (see SI thereof).
- [4] Y. Imada, J. L. Röckl, A. Wiebe, T. Gieshoff, D. Schollmeyer, K. Chiba, R. Franke, S. R. Waldvogel, *Angew.Chem. Int. Ed.* **2018**, *57*,12136–1214

Electrochemical Synthesis of Fluorinated Orthoesters from 1,3-Benzodioxoles

Johannes L. Röckl,^[a, b] Adrian V. Hauck,^[a] Dieter Schollmeyer,^[a] and Siegfried R. Waldvogel^{*[a, b]}

A scalable, dehydrogenative, and electrochemical synthesis of novel highly fluorinated orthoesters is reported. This protocol provides easy and direct access to a wide variety of derivatives, using a very simple electrolysis setup. These compounds are surprisingly robust towards base and acid with an unusual high lipophilicity, making them interesting motifs for potentially active compounds in medicinal chemistry or agro applications. The use of electricity enables a safe and environmentally benign chemical transformation as only electrons serve as oxidants.

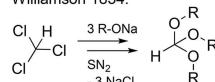
The orthoester is an extremely versatile structural feature, used as a protective group for esters^[1] in peptide synthesis^[2] and for alcohols in nucleoside synthesis.^[3] This functional group is vital for transformations such as the Claisen-Johnson rearrangement,^[4] the synthesis of a variety of nitrogen-based heterocycles^[5] and various condensation reactions.^[6] Orthoesters were first prepared via conversion of chloroform with alcoholates by Williamson and Kay in 1854.^[7] This route generates a large amount of salt waste and results in low yields.^[8] A common alternative is the Pinner route to orthoesters involving conversion of nitriles with alcohols in the presence of strong acids.^[9] Hydrogen cyanide is often used in these reactions, which should be avoided. Additionally, a large amount of waste is generated. This can be avoided using an electrochemical approach, which was developed in 2000 by Fischer et al. at BASF.^[10] This process is particularly suitable for the preparation of methyl orthoformate, from 1,1,2,2-tetraethoxy-ethane via anodic oxidation. Additionally, orthoesters can be synthesized using the Hofer-Moest reaction, a Kolbe-type electrolysis. This reaction leads to high yields ($\geq 95\%$) and can

also be applied to a broader variety of substrates compared to the Pinner approach. However, this reaction only proceeds with aliphatic moieties in the position β to the carboxylic acid (R^2 , Scheme 1).^[11] First reports on the direct anodic conversion of 1,3-benzodioxoles was given by Thomas et al.^[12] The installation of the methoxy moiety at the heterocyclic skeleton could be achieved. However, the reaction is limited to a narrow scope. Only a few substrates with substituents on the aromatic system are tolerated. Furthermore, the setup for the electrolytic conversion is not straightforward, since carbon dioxide has to be applied and the reaction is carried out with cooling to 10 °C. The use of expensive platinum electrodes incorporates an additional disadvantage (Scheme 1).

Here, a scalable electrosynthetic method towards novel highly fluorinated orthoesters is presented. These molecules are a new class for potentially biologically active compounds with a high lipophilicity (Scheme 1).^[13] LogP values were found to increase dramatically compared to those of the corresponding substrates, while the volatility remains almost the same like the

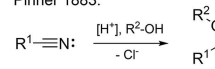
Conventional approaches:

Williamson 1854:



- large amount of reagent waste
- low yields

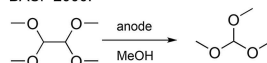
Pinner 1883:



- use of hazardous acids
- significant amount of reagent waste

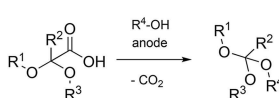
Electrosynthetic approaches:

BASF 2000:



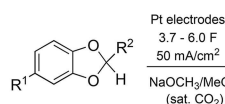
+ avoidance of hydrogen cyanide

Hofer-Moest 2005:



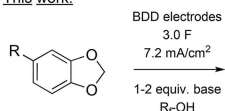
- prefunctionalized starting materials
- only aliphatic moieties R²
+ high yields

Thomas 1985:



- narrow substrate scope
- sophisticated electrolysis setup

This work:



+ broad substrate scope
+ simple reaction setup
+ access towards fluorinated orthoesters with a high stability and lipophilicity

Scheme 1. Synthetic strategies to orthoesters.

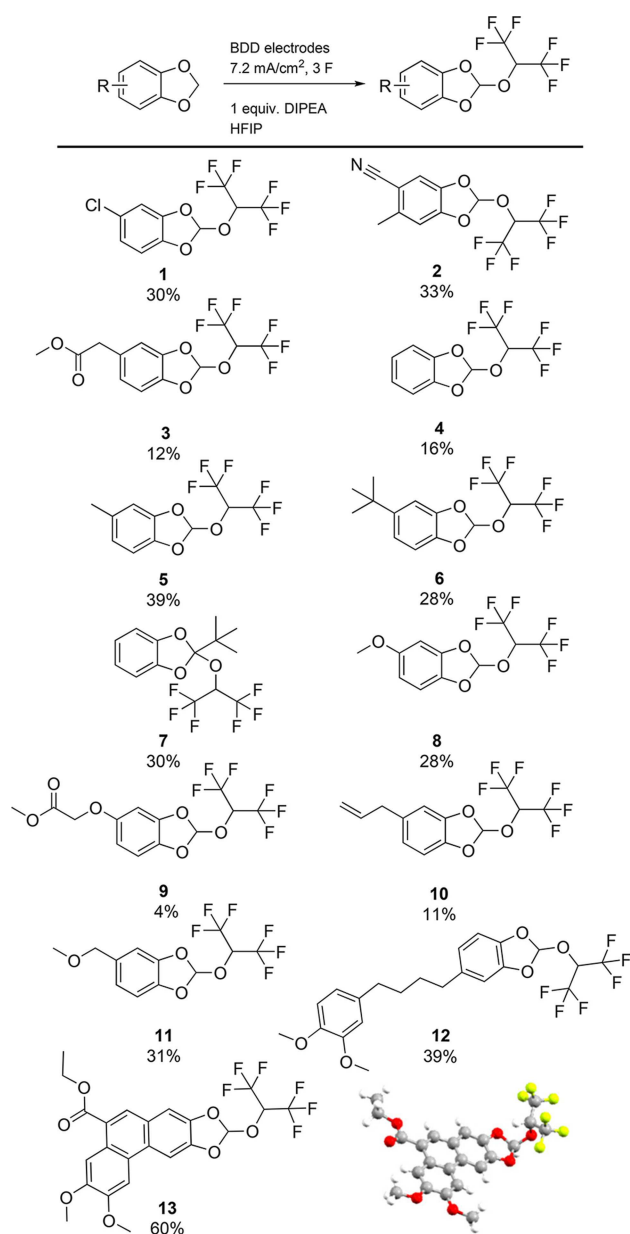
[a] J. L. Röckl, A. V. Hauck, D. Schollmeyer, Prof. Dr. S. R. Waldvogel
Johannes Gutenberg University Mainz
Institute of Organic Chemistry
Duesbergweg 10–14, 55128 Mainz, Germany
E-mail: waldvogel@uni-mainz.de
Homepage: <https://www.blogs.uni-mainz.de/fb09akwaldvogel/>

[b] J. L. Röckl, Prof. Dr. S. R. Waldvogel
Johannes Gutenberg Universität Mainz
Graduate School Materials Science in Mainz
Staudingerweg 9, 55128 Mainz, Germany

Supporting information for this article is available on the WWW under <https://doi.org/10.1002/open.201900127>

©2019 The Authors. Published by Wiley-VCH Verlag GmbH & Co. KGaA.
This is an open access article under the terms of the Creative Commons Attribution Non-Commercial NoDerivs License, which permits use and distribution in any medium, provided the original work is properly cited, the use is non-commercial and no modifications or adaptations are made.

starting materials (see SI). Furthermore, this reaction allows the lipophilicity to be modulated via the installation of various highly fluorinated side-chains in the difficult-to-address position 2 of 1,3-benzodioxoles. These products proved to be surprisingly inert towards acids and bases, suggesting they are amenable to further functionalization or applicable in active ingredients. A broad substrate scope is tolerated (Scheme 2–4), providing access to a wide variety of derivatives in moderate yields. Graphite, glassy carbon, or boron-doped diamond (BDD) can be used as electrode material and no additional supporting electrolyte is needed. The constant current electrolysis is carried out in a simple undivided electrolytic cell at room temperature with the corresponding alcohols as solvent. This simple reaction



Scheme 2. Scope of the reaction with HFIP. Electrolysis was carried out in HFIP (5 mL) with 0.5 mmol substrate, 0.02 vol% of DIPEA, using BDD electrodes and 3.0 F at 7.2 mA/cm² in an undivided cell. Molecular structure (based on X-ray crystallography) of **13** is displayed. Isolated yields are given.

Table 1. Constant current electrolysis of 5-chloro-1,3-benzodioxole **1** (0.5 mmol) was performed in HFIP/TFE (5 mL) and 1.0 equiv. of a base (DIPEA/DBU) in an undivided Teflon cell. Isolated yields. BDD: Boron-doped diamond.

Entry	Current density [mA/cm ²]	Anode	Charge [F]	Yield 1 [%]
1	1.0	BDD	3.0	0
2	15	BDD	3.0	24
3	90	BDD	3.0	23
4	7.2	BDD	2.2	19
5	7.2	BDD	2.8	26
6	7.2	BDD	4.0	13
7	7.2	BDD	3.0	30
8	7.2	Graphite	3.0	23
9	7.2	Glassy carbon	3.0	27
10	7.2	Mo	3.0	0

setup makes this reaction easily scalable and therefore particularly attractive for technical applications.

Electrochemistry is an attractive concept in performing organic synthesis, because it can potentially diminish the amount of reagent waste, plus renewable energy can be used to contribute to more sustainable conversions.^[14] The use of fluoroalcohols (in particular 1,1,1,3,3,3-hexafluoroisopropanol, HFIP) in electrochemistry has major advantages, as it modulates the reactivity of intermediates,^[15] and has an exceptional solvent microheterogeneity.^[16] This has been recently demonstrated by conversion of electrogenerated HFIP ethers with nucleophiles towards diarylmethanes^[17] and 2-phenylacetone nitriles.^[18] We have also developed efficient electrochemical C–N, S–S, C–C, and N–N coupling reactions involving phenols,^[19] anilides,^[20] and dianilides as substrates.^[21]

By electrochemical screening, the ideal reaction conditions such as concentration, electrode material, applied charge and current density were identified (Table 1).^[22] The screening experiments were performed with 5-chloro-1,3-benzodioxole (**1**) as test system. Optimal reaction conditions were achieved when working with BDD electrodes at a concentration of 0.1 mol/L and an applied charge of 3.0 F. When more charge was applied, the respective orthocarbonates were observed as by-products, resulting in lower yields (Table 1, Entry 6). The optimal current density identified^[15] was 7.2 mA/cm². (Table 1, Entry 7). It should be noted that the protocol is very robust, since the yield remains almost unchanged up to a current density of 90 mA/cm² (Table 1, Entry 3). Inexpensive electrode materials can also be used, such as glassy carbon or graphite (Table 1, Entries 8 and 9). However, BDD is slightly superior. Sufficient conductivity was achieved, when using 0.02 vol% of *N,N*-diisopropylethylamine (DIPEA) consequently no additional supporting electrolyte is needed.^[17] In addition, the concentration played an important role, as increased oligomerization was observed on the electrodes at higher concentrations (see SI).

Electrochemical functionalization with HFIP was achieved in yields up to 60%. Various functional groups are tolerated. Substrates carrying an electron-withdrawing substituent such as halogen or nitrile (**1**, **2**) can be converted in yields up to 33%. The yields were significantly lower for substrates involving

phenyl-acetates (3), allylic groups (10), or methoxyacetates (9). The unsubstituted 1,3-benzodioxole undergoes the reaction in 16% yield (4). Electron-releasing groups such as alkyl- (5–7) and methoxy groups (8) were also tolerated. Interestingly, benzylic positions (5) were not oxidized to the corresponding HFIP ethers.^[17] Sterically demanding groups such as *tert*-butyl groups in 2- and 4-positions had no significant influence onto the yields (6, 7). Substrates carrying a second aromatic system also formed the desired products (12). Substrates involving larger π systems form the corresponding 2-alkoxy-1,3-benzodioxoles in enhanced yields (13, 21) (Scheme 2).

This can be rationalized upon analysis of the mechanism: First, a radical cation is generated, which undergoes the loss of a proton and a further oxidation step to a 1,3-benzodioxolium species. This cation will be trapped by a HFIP anion. Larger π systems can stabilize these cations and avoid unwanted side reactions (Scheme 3).

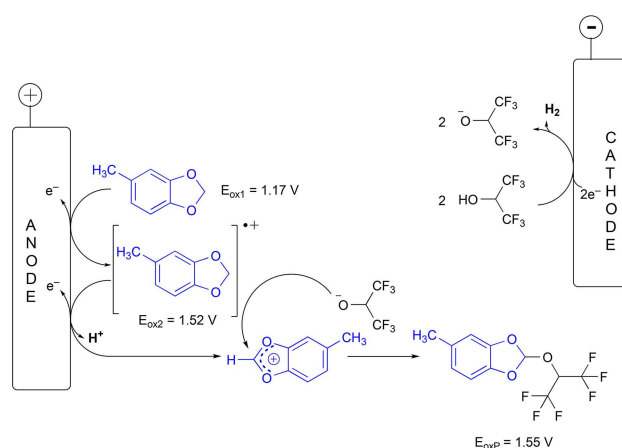
The proposed mechanism is supported by cyclic voltammetry (Figure S4 and Figure S5 in SI) and the anticipated 6 π aromatic intermediates were isolated as BF₄⁻-salts and spectroscopically investigated by NMR.^[23] We also found that the addition of base plays a crucial role.

Subsequently, we investigated the starting material in HFIP without any base and MTBS as supporting electrolyte. We found that this electron transfer process to the radical cation is reversible (Figure 1).

Afterwards, we added base to this solution and found that the process is now irreversible, due to the subsequent deprotonation reaction and we can again observe the two

irreversible oxidation steps ($E_{\text{ox1}} = 1.17 \text{ V vs Fc/FcH}^+$, $E_{\text{ox2}} = 1.52 \text{ V vs Fc/FcH}^+$) (Figure 2). This confirms our assumption that initially an oxidation step to a radical cation and then a deprotonation step occurs.

The reaction could be applied to other fluorinated alcohols, such as 2,2,2-trifluoroethanol (TFE) or, 2,2,3,3,4,4,5,5-octafluoropentanol-1-ol. Therefore, stronger bases like 1,8-diazabicyclo[5.4.0]undec-7-ene (DBU) and 1,8-bis(dimethylamino)naphthalene, are required in order to achieve sufficient conductivity. It was possible to convert the 1,3-benzodioxoles to TFE orthoesters in slightly lower yields, compared to the HFIP orthoesters. However, the trends are similar. Larger π systems also resulted in enhanced yields (21, 37%) (Scheme 4). Recently, an electro-



Scheme 3. Proposed mechanism for the formation of orthoesters.

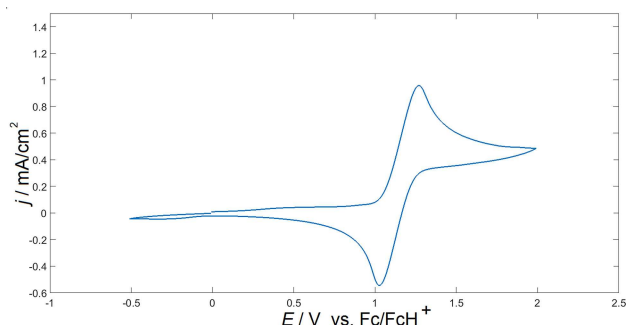


Figure 1. Cyclic voltammogram of a 5 mM solution of 5-methyl-1,3-benzodioxol in HFIP/MTBS at 50 mV/s.

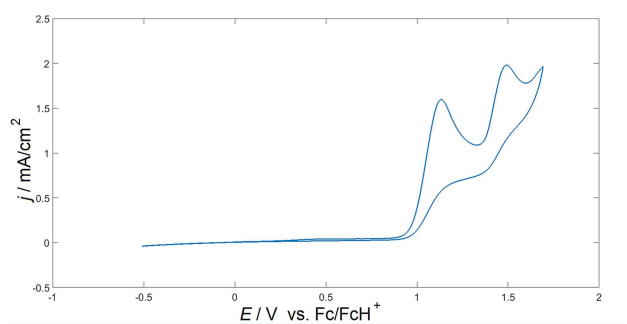
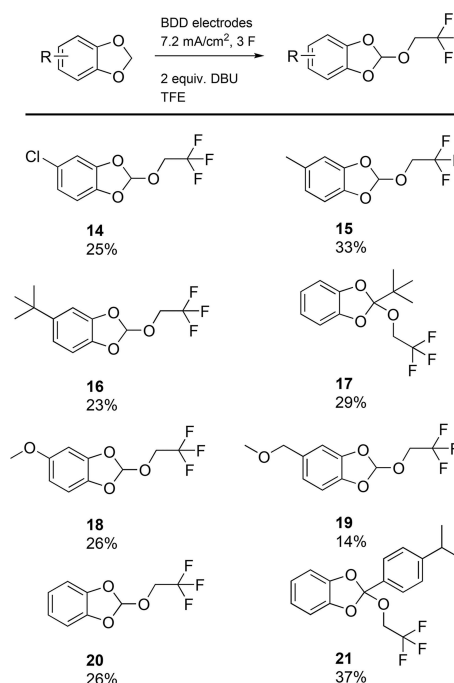


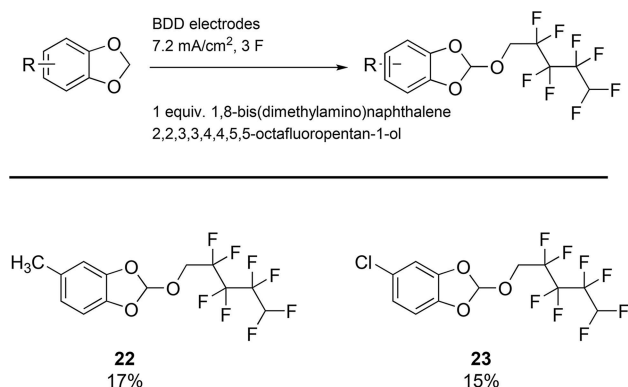
Figure 2. Cyclic voltammogram of a 5 mM solution of 5-methyl-1,3-benzodioxol in HFIP/MTBS + DIPEA at 50 mV/s.



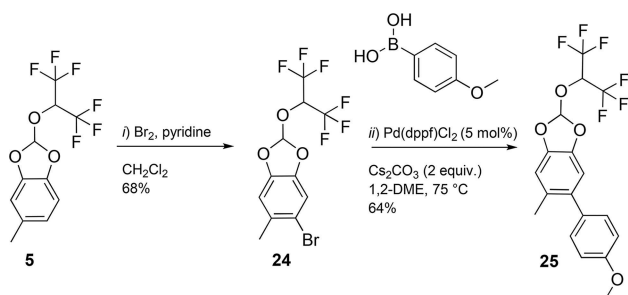
Scheme 4. Scope of the reaction with TFE. Electrolysis was carried out in TFE (5 mL) with 0.5 mmol substrate, 0.03 vol% of DBU and BDD electrodes using BDD electrodes and 3.0 F at 7.2 mA/cm² in an undivided cell. Isolated yields are displayed.

chemical installation of TFE has been reported by an iodine(III)-mediated cyclisation reaction for the synthesis of 4-(2,2,2-trifluoroethoxy)isochroman-1-ones.^[24]

For longer fluorinated alkyl chains the yields decreased to 15–17% (**22**, **23**). This can be explained by the higher viscosity of the solvent and therefore high local concentrations, and less conductivity (Scheme 5).



Scheme 5. Scope of the reaction with 2,2,3,3,4,4,5,5-octafluoropentan-1-ol. Electrolysis was carried out in the corresponding alcohol (5 mL) with 0.5 mmol substrate, 1 equiv. of 1,8-bis(dimethylamino)naphthalene using BDD electrodes and 3.0 F at 7.2 mA/cm² in an undivided cell. Isolated yields are given.



Scheme 6. Further conversions of fluorinated orthoesters. *i*) Bromine (1.5 equiv.) was added to pyridine (2 equiv.) and **5** (1 equiv.) in dichloromethane (2 mL) at 0 °C. *ii*) Pd(dppf)Cl₂ (0.05 equiv.), 4-methoxyphenylboronic acid (1.2 equiv.), caesium carbonate (2 equiv.) and **24** (1 equiv.) was added to 1,2-dimethoxyethane and heated to 75 °C for 8 h.

In addition, to demonstrate the scalability of our method, the electrolysis was scaled-up by a factor of 50. For this, we used 25 mmol of 5-methyl-1,3-benzodioxole in a 500 mL round-bottomed flask cell (Figure S2 in SI). No erosion of selectivity was observed. HFIP was then recovered and the residue was directly purified to give 2.75 g of the desired product **5** in a single batch (37% yield). The yield is not significantly lower compared to that obtained on 5 mL scale (39%), which supports the robustness and scalability of the developed reaction.

Further conversion of products **1** and **5** were investigated. When treated with 4-methylbenzene-1-sulfonic acid in THF (tetrahydrofuran), BF₃-etherate in ether, ethylmagnesium bromide in THF, or even *n*-butyllithium in THF absolutely no

conversion could be observed, leading to complete recovery of the orthoesters. Methoxy orthoesters usually undergo rapid reactions with Grignard reagents,^[25] Lewis acids^[26] and even water.^[12,27] It was therefore possible to convert these molecules in presence of the orthoester moiety: **5** was selectively brominated in 68% yield, using bromine in CH₂Cl₂ with pyridine as additive. The resulting product **24** was then subjected to a Suzuki-Miyaura coupling in 64% yield (**25**) without affecting the orthoester functionality (Scheme 6). This proves the usefulness and robustness of these functionalities. The logP values of 1,3-benzodioxoles and the corresponding orthoesters have been calculated and compared (see SI). It was remarkable that these values increase by a factor of 1.5 to 2 when fluorinated side chains were installed. This transformation could boost the potency and impact target selectivity tremendously by influencing pK_a, modulating conformation, and hydrophobic interactions.^[28] The unprecedented robustness and the high lipophilicity further enhance the potential of bioactive compounds involving 1,3-benzodioxoles.

In conclusion, we have established a scalable and simple protocol towards novel highly fluorinated orthoesters. This transformation allows the functionalization of 1,3-benzodioxoles in position 2 with different fluorinated alcohols. This makes it possible to adjust the physicochemical properties of a broad variety of potentially bioactive substrates. The high robustness towards acids and bases gives rise to subsequent conversions without affecting the moiety. This makes these structural motives particularly interesting for applications in medicinal and agrochemistry.

Acknowledgements

J. L. Röckl is a recipient of a DFG fellowship through the Excellence Initiative by the Graduate School Materials Science in Mainz (GSC 266). Support of the Advanced Lab of Electrochemistry and Electrosynthesis – ELYSION (Carl-Zeiss-Stiftung) is gratefully acknowledged.

Conflict of Interest

The authors declare no conflict of interest.

Keywords: oxygen heterocycles · electrochemistry · oxidation · orthoesters · fluorine

- [1] J. L. Giner, *Org. Lett.* **2005**, *7*, 499–501.
 [2] F. Vellaccio, J. M. Phelan, R. L. Trottier, T. W. Napier, *J. Org. Chem.* **1981**, *46*, 3087–3091.
 [3] M. Sekine, T. Hata, *J. Am. Chem. Soc.* **1983**, *105*, 2044–2049.
 [4] a) Montero, E. Mann, B. Herradon, *Eur. J. Org. Chem.* **2004**, *14*, 3063–3073; b) W. S. Johnson, L. Werthemann, W. R. Bartlett, T. J. Brocksom, T.-T. Li, D. J. Faulkner, M. R. Petersen, *J. Am. Chem. Soc.* **1970**, *92*, 741–743.
 [5] a) A. Kudelko, W. Zielinski, *Heterocycles* **2006**, *68*, 2269–2284; b) W. Zielinski, A. Kudelko, W. Czardybon, *J. Heterocycl. Chem.* **2005**, *42*, 1393–1397; c) D. Villemin, M. Hammadi, B. Martin, *Synth. Commun.* **1996**, *26*, 2895–2899.

- [6] N. Maulide, I. E. Markó, *Chem. Commun.* **2006**, 1200–1202.
- [7] A. W. Williamson, G. Kay, *Ann. Chem.* **1854**, 92, 346–363.
- [8] J. Houben, *Methods of Organic Chemistry Vol. III, 2nd Edition: Oxygen-, Sulfur-, Halogen-Compounds*, Georg Thieme Verlag, **2014**, p. 163.
- [9] A. Pinner, *Chem. Ber.* **1883**, 16, 1643–1655.
- [10] A. Fischer, H. Puetter (BASF SE) DE10043789 A1 **2000**.
- [11] a) H. Kolbe, *Liebigs Ann. Chem.* **1849**, 69, 257–294. b) F. Lebreux, F. Buzzo, I. E. Markó, *J. Electrochem. Soc.* **2008**, 13, 1–10.
- [12] H. G. Thomas, A. Schmitz, *Synthesis* **1985**, 31–33.
- [13] M. Murray, *Curr. Drug Metab.* **2000**, 1, 67–84.
- [14] a) A. Wiebe, T. Gieshoff, S. Möhle, E. Rodrigo, M. Zirbes, S. R. Waldvogel, *Angew. Chem. Int. Ed.* **2018**, 57, 5594–5616; *Angew. Chem.* **2018**, 130, 5694–5721; b) S. Möhle, M. Zirbes, E. Rodrigo, T. Gieshoff, A. Wiebe, S. R. Waldvogel, *Angew. Chem. Int. Ed.* **2018**, 57, 6018–6041; *Angew. Chem.* **2018**, 130, 6124–6149; c) M. D. Karkas, *Chem. Soc. Rev.* **2018**, 47, 5786–5865; d) M. Yam, Y. Kawamata, P. S. Baran, *Chem. Rev.* **2017**, 117, 13230–1331; e) S. R. Waldvogel, S. Lips, M. Selt, B. Riehl, C. J. Kampf, *Chem. Rev.* **2018**, 118, 6706–6765; f) K. D. Moeller, *Chem. Rev.* **2018**, 118, 4817–4833.
- [15] a) I. Colomer, A. E. R. Chamberlain, M. B. Haughey, T. J. Donohoe, *Nat. Rev. Chem.* **2017**, 1, 88, 1–12; b) B. Elsler, A. Wiebe, D. Schollmeyer, K. M. Dyballa, R. Franke, S. R. Waldvogel, *Chem. Eur. J.* **2015**, 21, 12321–12325.
- [16] a) O. Hollóczki, A. Berkessel, J. Mars, M. Mezger, A. Wiebe, S. R. Waldvogel, B. Kirchner, *ACS Catal.* **2017**, 7, 1846–1852; b) O. Hollóczki, R. Macchieraldo, B. Gleede, S. R. Waldvogel, B. Kirchner, *J. Phys. Chem. Lett.* **2019**, in press. For early view: [10.1021/acs.jpcllett.9b00112]
- [17] Y. Imada, J. L. Röckl, A. Wiebe, T. Gieshoff, D. Schollmeyer, K. Chiba, R. Franke, S. R. Waldvogel, *Angew. Chem. Int. Ed.* **2018**, 57, 12136–12140; *Angew. Chem.* **2018**, 130, 12312–12317.
- [18] J. Röckl, Y. Imada, K. Chiba, R. Franke, S. R. Waldvogel, *ChemElectroChem* **2018**, in press. For early view: [10.1002/celc.201801727]
- [19] a) A. Lipp, D. Ferenc, C. Gütz, M. Geffe, N. Vierengel, D. Schollmeyer, H. J. Schäfer, S. R. Waldvogel, T. Opatz, *Angew. Chem. Int. Ed.* **2018**, 57, 11055–11059; *Angew. Chem.* **2018**, 34, 11221–11225; b) S. Lips, D. Schollmeyer, R. Franke, S. R. Waldvogel, *Angew. Chem. Int. Ed.* **2018**, 57, 13325–13329; *Angew. Chem.* **2018**, 130, 13509–13513; c) B. Elsler, D. Schollmeyer, K. M. Dyballa, R. Franke, S. R. Waldvogel, *Angew. Chem. Int. Ed.* **2014** 126, 5311–5314; *Angew. Chem.* **2014**, 34, 11221–11225; d) A. Wiebe, D. Schollmeyer, K. M. Dyballa, R. Franke, S. R. Waldvogel, *Angew. Chem. Int. Ed.* **2016**, 55, 11801–11805; *Angew. Chem.* **2016**, 128, 11979–11983; e) S. Lips, A. Wiebe, B. Elsler, D. Schollmeyer, K. M. Dyballa, R. Franke, S. R. Waldvogel, *Angew. Chem. Int. Ed.* **2016**, 55, 10872–10876; *Angew. Chem.* **2016**, 128, 11031–11035. f) B. Dahms, R. Franke, S. R. Waldvogel, *ChemElectroChem* **2018**, 5, 1249–1252; g) A. Wiebe, S. Lips, D. Schollmeyer, R. Franke, S. R. Waldvogel, *Angew. Chem. Int. Ed.* **2017**, 56, 14727–14731; *Angew. Chem.* **2017**, 129, 14920–14925; h) S. Lips, B. A. Frontana-Urbe, M. Dörr, D. Schollmeyer, R. Franke, S. R. Waldvogel, *Chem. Eur. J.* **2018**, 24, 6057–6061.
- [20] a) L. Schulz, M. Enders, B. Elsler, D. Schollmeyer, K. M. Dyballa, R. Franke, S. R. Waldvogel, *Angew. Chem. Int. Ed.* **2017**, 56, 4877–4881; *Angew. Chem.* **2017**, 129, 4955–4959; b) A. Kehl, V. Breising, D. Schollmeyer, *Chem. Eur. J.* **2018**, 24, 17230–17233.
- [21] a) T. Gieshoff, D. Schollmeyer, S. R. Waldvogel, *Angew. Chem. Int. Ed.* **2016**, 55, 9437–9440; *Angew. Chem.* **2016**, 128, 9587–9590; b) T. Gieshoff, A. Kehl, D. Schollmeyer, K. D. Moeller, S. R. Waldvogel, *J. Am. Chem. Soc.* **2017**, 139, 12317–12324; c) V. Breising, T. Gieshoff, A. Kehl, V. Kilian, D. Schollmeyer, S. R. Waldvogel, *Org. Lett.* **2018**, 20, 6785–6788.
- [22] C. Gütz, B. Klöckner, S. R. Waldvogel, *Org. Process Res. Dev.* **2016**, 20, 26–32.
- [23] a) H. Volz, G. Zimmermann, *Tetrahedron Lett.* **1970**, 41, 1597–3800; b) K. Dimroth, P. Heinrich, K. Schromm, *Angew. Chem. Int. Ed.* **1965**, 4, 873; *Angew. Chem.* **1965**, 77, 863.
- [24] R. Möckel, E. Babaoglu, G. Hilt, *Chem. Eur. J.* **2018**, 24, 15781–15785.
- [25] a) A. E. Tschitschibabin, *Chem. Ber.* **1904**, 37, 186–188. b) W. F. Bailey, A. A. Croteau, *Tetrahedron Lett.* **1981**, 22, 545–540.
- [26] U. von der Brueggen, R. Lammers, H. Mayr, *J. Org. Chem.* **1988**, 53, 2920–2925.
- [27] J. Clayden, N. Greeves, S. Warren, P. Wothers, *Organic Chemistry* (1st ed.). **2001** Oxford University Press. p. 345.
- [28] E. P. Gillis, K. J. Eastman, M. D. Hill, D. J. Donnelly, N. A. Meanwell, *J. Med. Chem.* **2015**, 58, 8315–8359.

Manuscript received: April 8, 2019



Supporting Information

© Copyright Wiley-VCH Verlag GmbH & Co. KGaA, 69451 Weinheim, 2019



Electrochemical Synthesis of Fluorinated Orthoesters from 1,3-Benzodioxoles

Johannes L. Röckl, Adrian V. Hauck, Dieter Schollmeyer, and Siegfried R. Waldvogel*©2019 The Authors. Published by Wiley-VCH Verlag GmbH & Co. KGaA.

This is an open access article under the terms of the Creative Commons Attribution Non-Commercial NoDerivs License, which permits use and distribution in any medium, provided the original work is properly cited, the use is non-commercial and no modifications or adaptations are made.

Table of Contents

1.	GENERAL INFORMATION	2
2.	GENERAL PROTOCOL FOR ELECTROLYTIC SYNTHESIS OF ORTHOESTERS (GP)	3
2.1.	GPI: SYNTHESIS OF HFIP-ORTHOESTERS.....	3
2.2.	GPII: SYNTHESIS OF TFE-ORTHOESTERS	3
2.3.	GPIII: SYNTHESIS OF FP-ORTHOESTERS	4
2.4.	GPIV: SCALEUP OF HFIP-ORTHOESTERS.....	4
3.	CYCLIC VOLTAMMETRY STUDIES	5
4.	POSTULATED MECHANISM FOR THE ANODIC ORTHOESTER FORMATION.....	7
5.	EXPERIMENTAL SECTION.....	8
5.1.	SYNTHESIS OF 1,3-BENZODIOXOLES	8
5.2.	SYNTHESIS OF HFIP-ORTHOESTERS	15
5.3.	SYNTHESIS OF TFE-ORTHOESTERS.....	29
5.4.	SYNTHESIS OF OFP-ORTHOESTERS	37
5.5.	ORTHOCARBONATES	39
5.6.	FURTHER FUNCTIONALIZATIONS OF HFIP-ORTHOESTERS	40
5.7.	OPTIMIZATION OF REACTION PARAMETERS	42
6.	LIPOPHILICITY: LOGP – VALUES OF 1,3-BENZODIOXOLES AND THE CORRESPONDING ORTHOESTERS	43
7.	NMR SPECTRA	44
8.	REFERENCES	89

1. General information

All reagents were used in analytical or sufficiently pure grades. Solvents were purified by standard methods.^[1] Electrochemical reactions were carried out at boron-doped diamond (BDD) electrodes. BDD electrodes were obtained as DIACHEMTM quality from CONDIAS GmbH, Itzehoe, Germany. BDD (15 μm diamond layer) on silicon support.

Column chromatography was performed on basic aluminiumoxide (0.05-0.15 mm; pH 9.5 \pm 0.5). In addition, a preparative chromatography system (Büchi Labortechnik GmbH, Essen, Germany) was used with a Büchi Control Unit C-620, an UV detector Büchi UV photometer C-635, Büchi fraction collector C-660 and two Pump Modules C-605 for adjusting the solvent mixtures. As eluents mixtures of cyclohexane and ethyl acetate were used. Silica gel 60 sheets on aluminum (F254, Merck, Darmstadt, Germany) were used for thin layer chromatography.

Spectroscopy and spectrometry ¹H NMR, ¹³C and ¹⁹F NMR spectra were recorded at 25 °C, using a Bruker Avance III HD 400 (400 MHz) (5 mm BBFO-SmartProbe with z gradient and ATM, SampleXPress 60 sample changer, Analytische Messtechnik, Karlsruhe, Germany). Chemical shifts (δ) are reported in parts per million (ppm) relative to TMS as internal standard or traces of CHCl₃ or DMSO-d₆ in the corresponding deuterated solvent. For the ¹⁹F spectra, ethyl fluoroacetate served as external standard ($\delta = -231.1\text{ppm}$). Mass spectra and high-resolution mass spectra were obtained by using a QToF Ultima 3 (Waters, Milford, Massachusetts) apparatus employing ESI⁺ or APCI.

Melting points were determined with a Melting Point Apparatus B-545 (Büchi, Flawil, Switzerland) and are uncorrected. Heating rate: 1 °C/min.

Cyclic voltammetry was performed with a Metrohm 663 VA Stand equipped with a μ Autolab type III potentiostat (Metrohm AG, Herisau, Switzerland). *WE*: BDD electrode tip, 2 mm diameter; *CE*: glassy carbon rod; *RE*: Ag/AgCl in saturated LiCl/EtOH. Solvent: HFIP. $\nu = 100\text{ mV/s}$, $T = 20.0\text{ }^\circ\text{C}$, $c = 0.00500\text{ M}$, supporting electrolyte DIPEA: $c = 0.100\text{ M}$.

2. General protocol for electrolytic synthesis of orthoesters (GP)

The undivided 5 mL PTFE electrolysis cells are homemade. Detailed information about used cells are already reported.^[2,3] However, the complete setup with these cells are also commercially available as IKA Screening System, IKA-Werke GmbH & Co. KG, Staufen, Germany. It is operated with boron-doped diamond electrodes (BDD, 0.3 x 1 x 7 cm, 15 μm diamond layer, the support material is silicon).

2.1. GPI: Synthesis of HFIP-orthoesters

The 1,3-benzodioxole substrate (0.5 mmol) was dissolved in HFIP (5.0 mL, 47 mmol, 95 equiv.) in an undivided 5 mL PTFE electrolysis cell and mixed with DIPEA (0.1 mL, 0.6 mmol, 1 equiv.). The electrolysis was carried out with BDD electrodes at room temperature and a current density of 7.2 mA/cm². After applying a charge of 3.0 F, HFIP was recovered by evaporation. The crude product was purified by column chromatography on basic aluminiumoxide (0.05-0.15 mm; pH 9.5 \pm 0.5) to yield the desired product.

2.2. GPII: Synthesis of TFE-orthoesters

The 1,3-benzodioxole substrate (0.50 mmol, 1.0 equiv.) was dissolved in HFIP (5.0 mL, 69 mmol, 138 equiv.) in an undivided 5 mL PTFE electrolysis cell and mixed with DBU (0.15 mL, 1.0 mmol, 2.0 equiv.). The electrolysis was carried out with BDD electrodes at room temperature and a current density of 7.2 mA/cm². After applying a charge of 3.0 F, TFE was recovered by evaporation. The crude product was purified by column chromatography on basic aluminiumoxide (0.05-0.15 mm; pH 9.5 \pm 0.5) to yield the desired product.



Fig. S1: Left: schematic 5 mL Teflon cells; Middle: The commercially available IKA Screenings System, IKA-Werke GmbH & Co. KG, Staufen, Germany; right: 5 mL Teflon cell with two parallel electrodes (size: 3 x 10 x 70 mm, 1 Euro coin for comparison, diameter: 23,25 mm).

2.3. GPIII: Synthesis OFP-orthoesters

The 1,3-benzodioxole substrate (0.50 mmol, 1.0 equiv.) was dissolved in 2,2,3,3,4,4,5,5 -octafluoropentan-1-ol (OFP) (5.0 mL, 36 mmol, 72 equiv.) in an undivided 5 mL PTFE electrolysis cell and mixed with 1,8-bis(dimethylamino)naphthalene (0.107 g, 0.50 mmol, 1.0 equiv.). The electrolysis was carried out with BDD electrodes at room temperature and a current density of 7.2 mA/cm². After applying a charge of 3.0 F, the solvent was recovered by evaporation. The crude product was purified by column chromatography on basic aluminiumoxide (0.05-0.15 mm; pH 9.5±0.5) to yield the desired product.

2.4. GPIV: Scaleup of HFIP-orthoesters

The 1,3-benzodioxole substrate (25 mmol, 1.0 equiv.) was dissolved in HFIP (250 mL) in an undivided 500 mL glass electrolysis cell and mixed with DIPEA (5.0 mL, 10 mmol, 1.0 equiv.). The electrolysis was carried out with BDD electrodes at room temperature and a current density of 7.2 mA/cm². After applying a charge of 3.0 F, HFIP was recovered by evaporation. The crude product was purified by column chromatography on basic aluminiumoxide (0.05-0.15 mm; pH 9.5±0.5) to yield of the desired product.

For **2-(1-Trifluoromethyl-(2,2,2-trifluoroethyl))-5-methyl-1,3-benzodioxole (5)** 2.75 g were isolated as a colourless liquid (yield: 37%).

The flask (500 mL) is closed by a PTFE plug. This cap allows precise arrangement of the BDD electrodes. Total dimension of the BDD electrodes are 6.0 cm x 2.0 cm x 0.3 cm.



Fig. S2: 500 mL flask cell; left: BDD electrode removed; right: assembled. For size comparison one 50 Eurocent (diameter: 24,25 mm) coin is placed in front of the glass cell.

3. Cyclic voltammetry studies

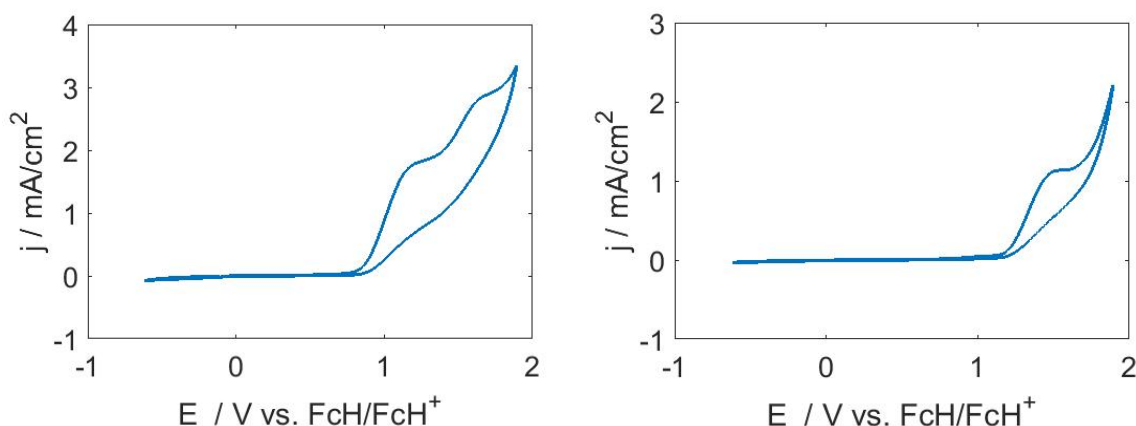


Fig. S4: left: cyclic voltammogram of a 5 mM solution of 5-methyl-1,3-benzodioxol in HFIP/DIPEA at 100 mV/s right: cyclic voltammogram of a 5 mM solution of 2-(1-trifluoromethyl-(2,2,2-trifluoroethyl))-5-methyl-1,3-benzodioxole in HFIP/DIPEA at 100 mV/s.

In the cyclic voltammogram of the starting material (Fig. S4 left), two oxidation steps were observed ($E_{ox1} = 1.17$ V vs Fc/FcH⁺, $E_{ox2} = 1.52$ V vs Fc/FcH⁺). This suggests that first a radical cation is produced, which is then further converted by deprotonation and a further oxidation step to a benzodioxolium ion. This cation represents a 6 π - aromatic system, which is rather stable. This benzodioxolium ion can then be trapped with the corresponding alcoholate to form the orthoester. The oxidation potential of the product is found to be higher ($E_{ox} = 1.55$ V vs Fc/FcH⁺) (Fig. S4 right).

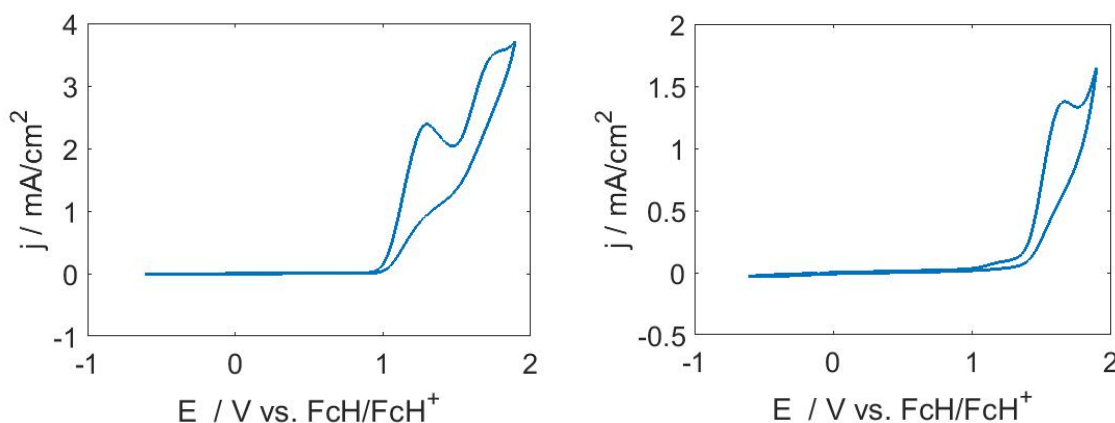


Fig. S5: left: cyclic voltammogram of a 5 mM solution of 5-Chloro-1,3-benzodioxol in HFIP/DIPEA at 100 mV/s right: cyclic voltammogram of a 5 mM solution of 2-(1-Trifluoromethyl-(2,2,2-trifluoroethyl))-5-chloro-1,3-benzodioxole in HFIP/DIPEA at 100 mV/s.

The same trends were found for 5-chloro-1,3-benzodioxole, even though the oxidation potentials were higher ($E_{ox1} = 1.30$ V vs Fc/FcH⁺, $E_{ox2} = 1.89$ V vs Fc/FcH⁺) (Fig. S5

left). For the product $E_{\text{ox}} = 1.66 \text{ V vs Fc/FcH}^+$ was found (Fig. S6 right). The lower oxidation potential of the product in comparison to $E_{\text{ox}2}$ of the starting material explains the lower yield for this substrate.

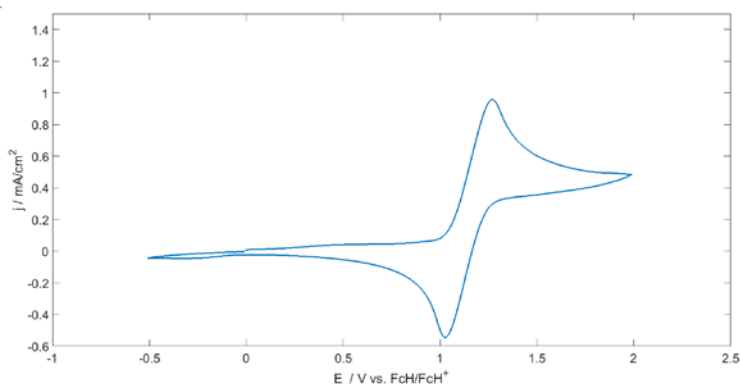


Fig. S6: cyclic voltammogram of a 5 mM solution of 5-methyl-1,3-benzodioxol in HFIP/MTBS at 50 mV/s

Subsequently, we investigated the starting material in HFIP without any base and with MTBS as supporting electrolyte. We found that this electron transfer process to the radical cation is reversible (Fig. S6).

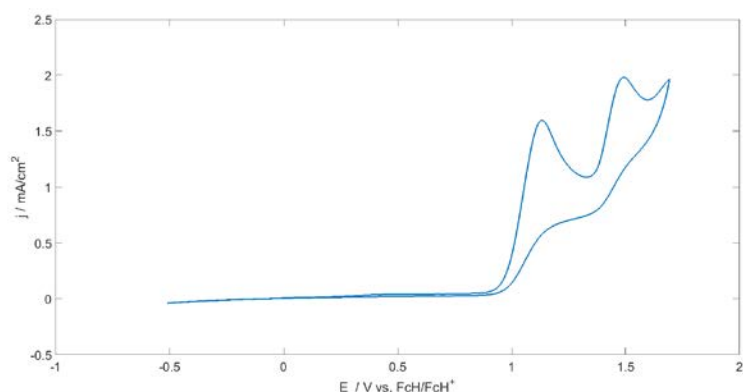


Fig. S7: cyclic voltammogram of a 5 mM solution of 5-methyl-1,3-benzodioxol in HFIP/MTBS + DIPEA at 50 mV/s

Afterwards, we added base to this solution and found that the process is now irreversible, due to the subsequent deprotonation reaction and we can again observe the two irreversible oxidation steps ($E_{\text{ox}1} = 1.17 \text{ V vs Fc/FcH}^+$, $E_{\text{ox}2} = 1.52 \text{ V vs Fc/FcH}^+$) (Fig. S7). This confirms our assumption that initially an oxidation step to a radical cation and then a deprotonation step occurs.

It could be shown by cyclic voltammetry that the reaction proceeds via an ECEC-mechanism. This was also suggested by Thomas et al.^[4] This ionic mechanism is also in

accordance with works, in which benzodioxolium ions were isolated as tetrafluoroborates and characterized by NMR spectroscopy.^[5] This hypothesis is supported by our observation that reactions of substrates with larger π systems result in higher yields.

4. Postulated mechanism for the anodic orthoester formation

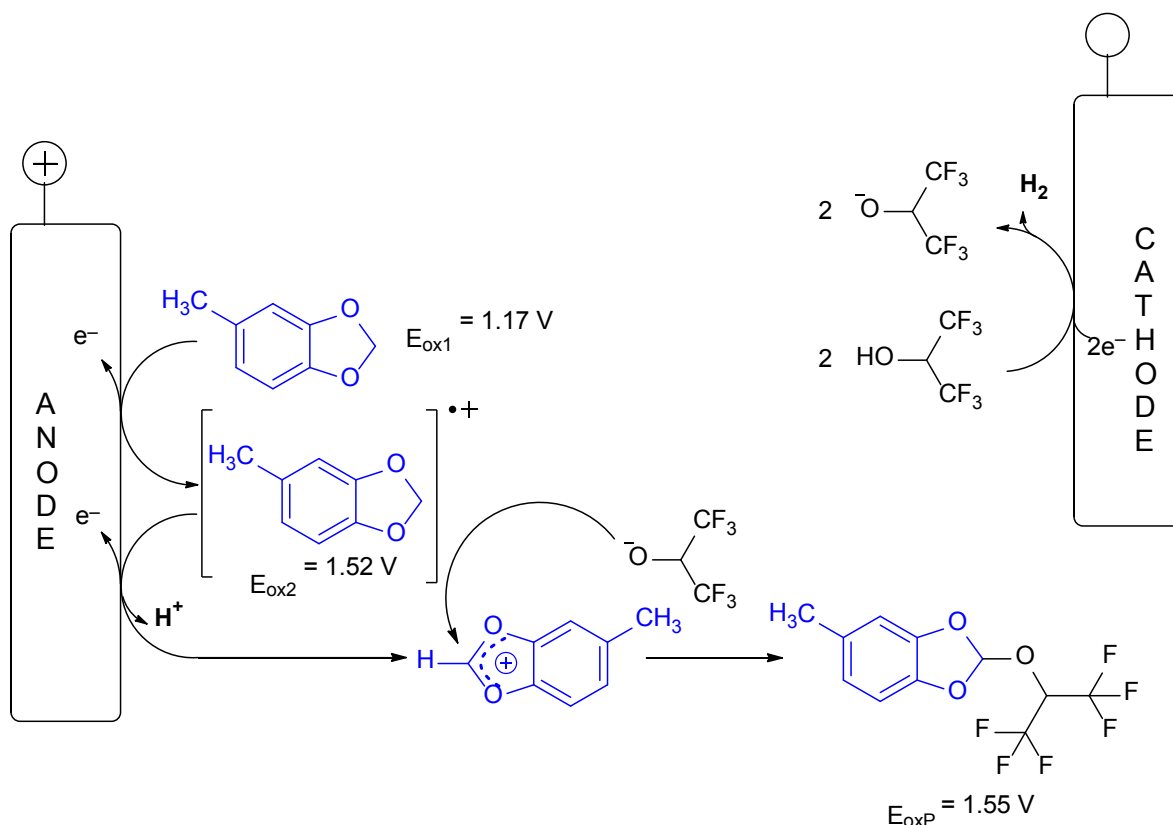


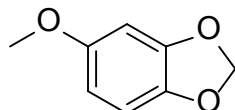
Fig. S8: Postulated mechanism for the electrochemical orthoester formation of 1,3-benzodioxoles.

First a radical cation is produced, which is then further converted by deprotonation and a further oxidation step to a benzodioxolium ion. This cation represents a 6π -aromatic system, which is rather stable. This benzodioxolium ion can then be trapped with the corresponding alcoholate to form the orthoester. Due to addition of base, alcoholates are present from the beginning of the reaction. This concentration will be maintained by the cathodic reaction.

5. Experimental section

5.1. Synthesis of 1,3-Benzodioxoles

5-Methoxy-1,3-benzodioxole



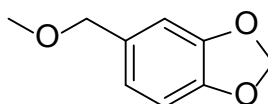
In a 50 mL round-bottomed flask, 5-hydroxy-1,3-benzodioxole (3.0 g, 22 mmol, 1 equiv.) was dissolved in *N,N*-dimethylformamide (25 mL). Potassium carbonate (6.0 g, 43 mmol, 2 equiv.) was added to the solution. Iodomethane (13.5 mL, 168 mmol, 8 equiv.) was added slowly while stirring. After three hours, the solvent was distilled off in vacuum. The residue was mixed with water (350 mL) and extracted three times with ethyl acetate (50 mL). The combined extracts were dried over sodium sulfate and concentrated. The residue was purified by column chromatography using silica gel 60 (0.040-0.063 mm). The product was obtained as a colourless oil (yield: 70%, 2.31 g, 15.18 mmol).

^1H NMR (400 MHz, CDCl_3) δ 6.71 (d, $J = 8.5$ Hz, 1H), 6.50 (d, $J = 2.5$ Hz, 1H), 6.32 (dd, $J = 8.5, 2.5$ Hz, 1H), 5.91 (s, 2H), 3.75 (s, 3H).

^{13}C NMR (101 MHz, CDCl_3) δ 155.3, 148.4, 141.7, 108.0, 104.8, 101.2, 97.6, 56.1.

HRMS of $\text{C}_8\text{H}_8\text{O}_3^+$ (APCI+) $[\text{M}]^+$: calc.: 152.0468, found: 152.0464.

The analytical data are consistent with the literature.^[6]

5-(Methoxymethyl)-1,3-benzodioxole

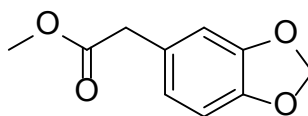
5-(Hydroxymethyl)-1,3-benzodioxole (3.0 g, 20 mmol, 1 equiv.) was dissolved in *N,N*-dimethylformamide (25 mL) in a 50 mL round-bottomed flask. Sodium hydride (2.4 g, 99 mmol, 5 equiv.) was added to the solution as a 60% mineral oil dispersion (3.95 g). Iodomethane (12.3 mL, 153 mmol, 8 equiv.) was added slowly while stirring. After three hours the solvent was distilled off in vacuum. The residue was mixed with water (350 mL) and extracted three times with ethyl acetate (50 mL). The combined extracts were dried over sodium sulfate and concentrated. The residue was purified by column chromatography using silica gel 60 (0.040-0.063 mm). The product was obtained as colorless oil (yield: 82%, 2.72 g, 16.37 mmol).

¹H NMR (400 MHz, CDCl₃) δ 6.85-6.76 (m, 3H), 5.95 (s, 2H), 4.35 (s, 2H), 3.35 (s, 3H).

¹³C NMR (101 MHz, CDCl₃) δ 147.9, 147.2, 132.2, 121.5, 108.6, 108.2, 101.1, 74.7, 57.9.

HRMS of C₉H₁₀O₃⁺ (APCI+) [M]⁺: calc.: 166.0624, found: 166.0622.

The analytical data are consistent with the literature.^[7]

5-(Methoxycarbonylmethyl)-1,3-benzodioxole

5-(Carboxymethyl)-1,3-benzodioxole (1.00 g, 5.6 mmol, 1 equiv.) was dissolved in methanol in a 50 mL round-bottomed flask. Thionyl chloride (0.5 mL, 7 mmol, 1 equiv.) was added while stirring. After two hours the solvent was distilled off. The residue was purified by column chromatography using silica gel 60 (0.040-0.063 mm). The product was obtained as colourless oil (yield: 78%, 0.84 g, 4.34 mmol).

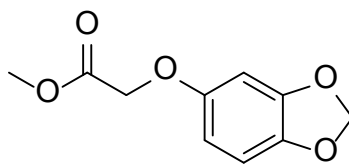
GCMS (Methode „hart“) t_R : 10.0 min; m/z : 194 $[M]^+$

^1H NMR (400 MHz, CDCl_3) δ 6.78 (d, $J = 1.7$ Hz, 1H), 6.76 (d, $J = 7.9$ Hz, 1H), 6.71 (dd, $J = 7.9, 1.7$ Hz, 1H), 5.94 (s, 2H), 3.69 (s, 3H), 3.53 (s, 2H).

^{13}C NMR (101 MHz, CDCl_3) δ 172.2, 147.9, 146.8, 127.6, 122.5, 109.8, 108.4, 101.2, 52.2, 40.9.

HRMS of $\text{C}_{10}\text{H}_{10}\text{O}_4^+$ (APCI+) $[M]^+$: calc.: 194.0574, found: 194.0573.

The analytical data are consistent with the literature.^[8]

5-(Methoxycarbonylmethoxy)-1,3-benzodioxole

5-(Carboxymethoxy)-1,3-benzodioxole (0.53 g, 2.7 mmol, 1 equivalent) was dissolved in methanol in a 50 mL round-bottomed flask. *p*-Toluenesulfonic acid monohydrate (0.11 g, 0.64 mmol, 0.2 equiv.) was added with stirring. After one hour the solvent was distilled off. The residue was purified by acid chromatography using silica gel 60 (0.040-0.063 mm). The product precipitated as a colorless crystalline solid (yield: 83%, 0.47 g, 2.23 mmol).

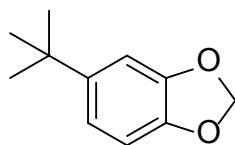
GCMS (Methode „hart“) t_R : 11.0 min; m/z : 210 $[M]^+$

^1H NMR (400 MHz, CDCl_3) δ 6.96 (d, $J = 8.5$ Hz, 1H), 6.53 (d, $J = 2.6$ Hz, 1H), 6.31 (dd, $J = 8.5, 2.6$ Hz, 1H), 5.92 (s, 2H), 4.56 (s, 2H), 3.80 (s, 3H).

^{13}C NMR (101 MHz, CDCl_3) δ 169.6, 153.4, 148.5, 142.6, 108.0, 106.0, 101.5, 98.7, 66.5, 52.4.

HRMS of $\text{C}_{10}\text{H}_{10}\text{O}_5^+$ (APCI+) $[M]^+$: calc.: 210.0523, found: 210.0519 .

The analytical data are consistent with the literature.^[9]

5-(2,2-Dimethylethyl)-1,3-benzodioxole

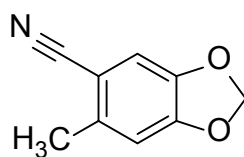
To a solution of 4-(2-methyl-2-propanyl)-1,2-benzenediol (2.06 g, 12,39 mmol, 1 equiv.) in DMSO (25 mL), an aqueous sodium hydroxide solution (2.04 g, 51 mmol, 4 equiv.) was slowly added at 90 °C. After heating for two hours at 90 °C, diiodomethane (2.5 mL, 31 mmol, 2.5 equiv.) was added. After a further two hours, the reaction mixture was extracted with ethyl acetate and then purified by column chromatography using silica gel 60 (0.040-0.063 mm). The product was obtained as colourless oil (yield: 39%, 0.87 mg, 4.86 mmol).

^1H NMR (400 MHz, CDCl_3) δ 6.97-6.96 (m, 1H), 6.82-6.77 (m, 2H), 5.95 (s, 2H), 1.23 (s, 9H).

^{13}C NMR (101 MHz, CDCl_3) δ 147.1, 144.8, 144.8, 117.6, 107.5, 106.2, 100.6, 34.3, 31.3.

HRMS of $\text{C}_{11}\text{H}_{14}\text{O}_2^+$ (APCI+) $[\text{M}]^+$: calc.:178.0988, found: 178.0985.

The analytical data are consistent with the literature.^[10]

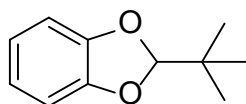
5-Cyano-6-methyl-1,3-benzodioxole

6-Bromo-5-cyano-1,3-benzodioxole (0.5 g, 2.2 mmol, 1.0 eq), trimethylboroxine (304 mg, 2.4 mmol, 1.1 equiv.), Pd(dppf)Cl₂ (82 mg, 5 mol%) was dissolved in 1,4-dioxane (9 mL) and water (1 mL). Cs₂CO₃ (1.1g, 3.4 mmol, 1.5 equiv) was added to the solution and the reaction was stirred for 16 h at 110 °C. The reaction mixture was filtered and concentrated *in vacuo*. Purification by column chromatography using silica gel 60 (0.040-0.063 mm) and a gradient (cyclohexan/ethyl acetate 97/3) at a flow of 12.5 mL/min yielded 280 mg of the desired product as a white solid (yield: 78%, 270 mg, 1.7 mmol).

¹H NMR (400 MHz, CDCl₃) δ 6.96 (s, 1H), 6.73 (s, 1H), 6.02 (s, 2H), 2.46 (s, 3H).

¹³C NMR (101 MHz, CDCl₃) δ 151.6, 146.0, 138.6, 118.5, 111.2, 110.5, 104.6, 102.2, 20.6.

HRMS of C₉H₈NO₂⁺ (ESI+) [M]⁺: calc.:162.0550, found: 162.0550.

2-(1,1-Dimethylethyl)-1,3-benzodioxole

To Catechol (5 g, 46 mmol, 1 eq.) in toluene (50 mL) was added pivaldehyde (4 g, 46 mmol, 1 eq.) and *p*-toluenesulfonic acid monohydrate (0.1 g, 0.5 mmol, 0.01 eq.) refluxed for 3 h using a Dean-Stark trap. After completion of the reaction, toluene was evaporated and the residue was purified by column chromatography using silica gel 60 (0.040-0.063 mm) and a gradient (cyclohexan/ethyl acetate 90/10) at a flow of 45.0 mL/min. This yielded 0.5 g of the desired product as a white solid (yield: 11%, 500 mg, 2.8 mmol).

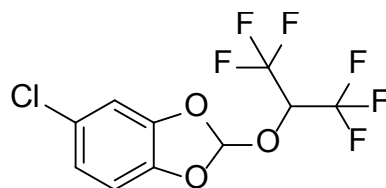
^1H NMR (400 MHz, CDCl_3) δ 6.78 (s, 1H), 5.75 (s, 0H), 1.05 (s, 3H).

^{13}C NMR (101 MHz, CDCl_3) δ 148.4, 121.2, 117.1, 108.1, 35.8, 23.6.

HRMS of $\text{C}_{11}\text{H}_8\text{NO}_2^+$ (ESI+) $[\text{M}]^+$: calc.:179.1065, found: 179.1067.

5.2. Synthesis of HFIP-Orthoesters

5-Chloro-2-(1-trifluoromethyl-(2,2,2-trifluoroethyl)oxy)-1,3-benzodioxole (1)



The compound was synthesized according to GPI. The product was obtained as a colourless oil (51 mg, 0.16 mmol, yield: 30%).

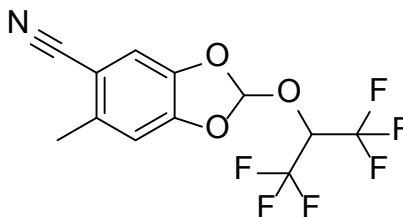
^1H NMR (400 MHz, $\text{DMSO-}d_6$) δ 7.44 (s, 1H), 7.36 (d, $J = 2.1$, 1H), 7.18 (d, $J = 8.4$ Hz, 1H), 7.07 (dd, $J = 8.4$, 2.1 Hz, 1H), 6.22 (hept, $J = 6.3$ Hz, 1H)

^{13}C NMR (101 MHz, $\text{DMSO-}d_6$) δ 145.0, 143.3, 126.4, 122.6, 119.1, 110.3, 110.2, 69.7 (hept, $J = 33.2$ Hz).

^{19}F NMR (376 MHz, $\text{DMSO-}d_6$) $\delta = -74.28, -74.30$.

HRMS of $\text{C}_{10}\text{H}_5^{35}\text{ClF}_6\text{O}_3^+$ (APCI+) $[\text{M}]^+$: calc.: 321.9826, found: 321.9826.

2-(1-Trifluoromethyl-(2,2,2-trifluoroethyl)oxy)-5-cyano-6-methyl-1,3-benzodioxole (2)



The compound was synthesized according to GPI. The product was obtained as colourless wax (54 mg, 0.17 mmol, 33%).

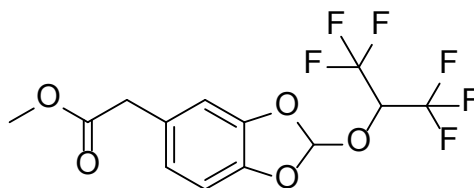
^1H NMR (400 MHz, $\text{DMSO-}d_6$) δ 7.64 (s, 1H), 7.51 (s, 1H), 7.31 (s, 1H), 6.26 (hept, J = 6.3 Hz, 1H), 2.44 (s, 3H).

^{13}C NMR (101 MHz, $\text{DMSO-}d_6$) δ 147.9, 142.6, 139.2, 119.3, 117.7, 112.3, 111.3, 105.0, 69.7 (hept, J = 33.2 Hz), 19.9.

^{19}F NMR (376 MHz, $\text{DMSO-}d_6$) δ -74.31, -74.32.

HRMS of $\text{C}_{12}\text{H}_7\text{F}_6\text{NO}_3^+$ (APCI+) $[\text{M}+\text{H}]^+$: calc.: 327.0325, found: 327.0313.

2-(1-Trifluoromethyl-(2,2,2-trifluoroethyl)oxy)-5-(methoxycarbonylmethyl)-1,3-benzodioxole (3)



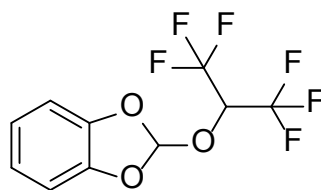
The compound was synthesized according to GPI. The product was obtained as a colourless oil (36 mg, 0.10 mmol, yield: 19%).

^1H NMR (400 MHz, $\text{DMSO-}d_6$) δ 7.35 (s, 1H), 7.08 (d, $J = 8.1$ Hz, 2H), 6.90 (dd, $J = 8.1$ Hz, 1H), 6.19 (hept, $J = 6.3$ Hz, 1H), 3.66 (s, 2H), 3.61 (s, 3H).

^{13}C NMR (101 MHz, $\text{DMSO-}d_6$) δ 171.6, 144.0, 143.0, 129.3, 123.8, 122.5, 119.6, 118.6, 110.5, 108.9, 69.7 (hept, $J = 33.2$ Hz), 51.7, 40.2.

^{19}F NMR (376 MHz, $\text{DMSO-}d_6$) $\delta = -74.30, -74.32$.

HRMS of $\text{C}_{13}\text{H}_{10}\text{F}_6\text{O}_5^+$ (APCI+) $[\text{M}]^+$: calc.: 360.0432, found: 360.0425.

2-(1-Trifluoromethyl-(2,2,2-trifluoroethyl)oxy)-methoxy-1,3-benzodioxole (4)

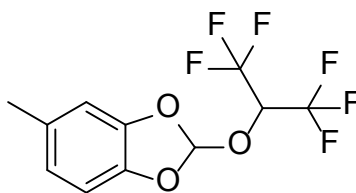
The compound was synthesized according to GPI. The product was obtained as colourless oil (24 mg, 0.083 mmol, yield: 16%).

^1H NMR (400 MHz, $\text{DMSO-}d_6$) δ 7.35 (s, 1H), 7.18-7.13, (m, 2H), 7.03-6.99 (m, 2H), 6.19 (hept, $J = 6.4$ Hz, 1H).

^{13}C NMR (101 MHz, $\text{DMSO-}d_6$) δ 144.0, 122.9, 118.2, 109.5, 109.4, 69.7 (hept, $J = 33.2$ Hz).

^{19}F NMR (376 MHz, $\text{DMSO-}d_6$) $\delta = -74.28, -74.30$.

HRMS of $\text{C}_{10}\text{H}_6\text{O}_6\text{F}_3^+$ (APCI+) $[\text{M}]^+$: calc.: 288.0221, found: 288.0212.

2-(1-Trifluoromethyl-(2,2,2-trifluoroethyl)oxy)-5-methyl-1,3-benzodioxole (5)

The compound was synthesized according to GPI. The product was obtained as colourless oil (64 mg, 0.21 mmol, yield: 39%).

^1H NMR (400 MHz, $\text{DMSO-}d_6$) δ 7.30 (s, 1H), 7.04-6.97 (m, 2H), 6.80 (m, 1H), 6.15 (hept, $J = 6.3$ Hz, 1H), 2.27 (s, 3H).

^{13}C NMR (101 MHz, $\text{DMSO-}d_6$) δ 144.0, 141.9, 132.4, 122.8, 118.3, 110.0, 108.8, 69.7 (hept, $J = 33.2$ Hz), 20.7.

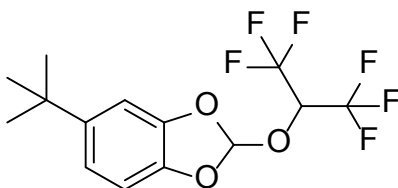
^{19}F NMR (376 MHz, $\text{DMSO-}d_6$) $\delta = -74.28, -74.30$.

HRMS of $\text{C}_{11}\text{H}_8\text{F}_6\text{O}_3^+$ (APCI+) $[\text{M}]^+$: calc.: 302.0372, found: 302.0379.

Boiling point: 49 °C (1.2 mbar).

Boiling point starting material: 49 °C (2.0 mbar).

2-(1-Trifluoromethyl-(2,2,2-trifluoroethyl)oxy)-5-(1,1-dimethylethyl)-1,3-benzodioxole (6)



The compound was synthesized according to GPI. The product was obtained as a slightly greenish oil (48 mg, 0.14 mmol, yield: 28%).

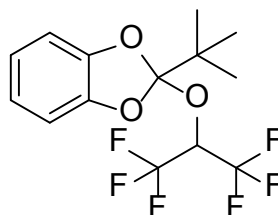
$^1\text{H-NMR}$ (400 MHz, $\text{DMSO-}d_6$) δ 7.31 (s, 1H), 7.19 (d, $J = 1.5$ Hz, 1H), 7.03 (d, $J = 8.0$ Hz, 1H), 6.98 (dd, $J = 8.0, 1.5$ Hz, 1H), 6.17 (hept, $J = 6.3$ Hz, 1H), 1.26, (s, 9H).

$^{13}\text{C-NMR}$ (101 MHz, $\text{DMSO-}d_6$) δ 146.1, 144.1, 141.7, 119.0, 118.6, 108.3, 106.8, 69.8 (hept, $J = 33.2$ Hz), 34.6, 31.3.

$^{19}\text{F-NMR}$ (376 MHz, $\text{DMSO-}d_6$) $\delta = -74.27, -74.29$.

HRMS von $\text{C}_{14}\text{H}_{14}\text{F}_6\text{O}_3^+$ (APCI+) $[\text{M}]^+$: calc.: 344.0842, found: 344.0842.

2-(1-Trifluoromethyl-(2,2,2-trifluoroethyl)oxy)-2-(1,1-dimethylethyl)-1,3-benzodioxole (7)



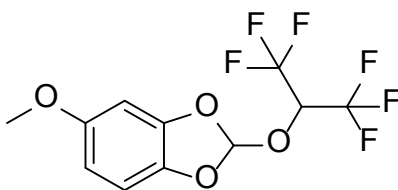
The compound was synthesized according to GPI. The product was obtained as colourless oil (53 mg, 0.15 mmol, yield: 30%).

^1H NMR (400 MHz, $\text{DMSO-}d_6$) δ 7.06 (dd, $J = 5.8, 3.3$ Hz, 1H), 6.93 (dd, $J = 5.8, 3.3$ Hz, 1H), 5.47 (hept, $J = 6.0$ Hz, 1H), 1.04 (s, 5H).

^{13}C NMR (101 MHz, $\text{DMSO-}d_6$) δ 147.7, 146.1, 130.2, 122.3, 121.2, 116.1, 108.4, 107.9, 68.0 (hept, $J = 33.2$ Hz), 40.6, 23.3.

^{19}F NMR (376 MHz, $\text{DMSO-}d_6$) δ -73.54, -73.56.

HRMS von $\text{C}_{14}\text{H}_{14}\text{F}_6\text{O}_3^+$ (APCI+) $[\text{M}]^+$: berechnet: 344.0847, gefunden: 344.0845.

2-(1-Trifluoromethyl-(2,2,2-trifluoroethyl)oxy)-5-methoxy-1,3-benzodioxole (8)

The compound was synthesized according to GPI. The product was obtained as a colourless oil (45 mg, 0.14 mmol, yield: 28%).

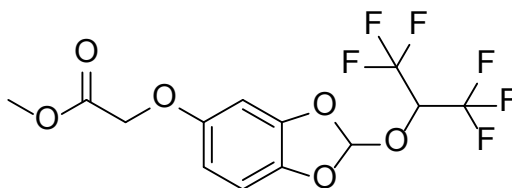
^1H NMR (400 MHz, $\text{DMSO-}d_6$) δ 7.31 (s, 1H), 7.04 (d, $J = 8.6$ Hz, 1H), 6.84 (d, $J = 2.5$ Hz, 1H), 6.53 (dd, $J = 8.6, 2.5$ Hz, 1H), 6.14 (hept, $J = 6.3$, 1H), 3.71 (s, 3H).

^{13}C NMR (101 MHz, $\text{DMSO-}d_6$) δ 155.5, 144.8, 138.0, 122.5, 119.7, 118.8, 109.0, 106.6, 97.5, 69.7 (hept, $J = 33.2$ Hz), 55.9.

^{19}F NMR (376 MHz, $\text{DMSO-}d_6$) $\delta = -74.34, -74.36$.

HRMS of $\text{C}_{11}\text{H}_8\text{F}_6\text{O}_4^+$ (APCI+) $[\text{M}]^+$: calc.: 318.0321, found: 318.0319.

2-(1-Trifluoromethyl-(2,2,2-trifluoroethyl)oxy)-5-(methoxycarbonylmethoxy)-1,3-benzodioxole (9)



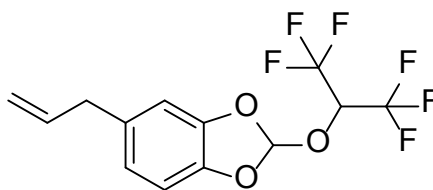
The compound was synthesized according to GPI. The product was obtained as a colourless oil (7 mg, 0.02 mmol, yield: 4%).

^1H NMR (400 MHz, $\text{DMSO-}d_6$) δ 7.32 (s, 1H), 7.04 (d, $J = 8.6$ Hz, 1H), 6.89 (m, 1H), 6.53 (m, 1H), 6.16 (hept, $J = 6.3$ Hz, 1H), 4.76 (s, 2H), 3.69 (s, 3H).

^{13}C NMR (101 MHz, $\text{DMSO-}d_6$) δ 169.2, 153.7, 144.8, 138.5, 118.9, 109.6, 109.0, 107.6, 98.3, 69.7 (hept, $J = 33.2$ Hz), 65.4, 51.8.

^{19}F NMR (376 MHz, $\text{DMSO-}d_6$) $\delta = -74.27, -74.29$.

HRMS of $\text{C}_{13}\text{H}_{10}\text{F}_6\text{O}_6^+$ (APCI+) $[\text{M}]^+$: calc.: 376.0382, found: 376.0384.

5-Allyl-2-(1-trifluoromethyl-(2,2,2-trifluoroethyl)oxy)-1,3-benzodioxole (10)

The compound was synthesized according to GPI. The product was obtained as a colourless oil (24 mg, 0.073 mmol, yield: 11%).

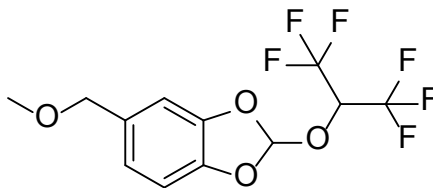
^1H NMR (400 MHz, $\text{DMSO-}d_6$) δ 7.32 (s, 1H), 7.06 (d, $J = 8.0$ Hz, 1H), 6.98 (d, $J = 1.6$ Hz, 1H), 6.82 (dd, $J = 8.0, 1.6$ Hz, 1H), 6.17 (hept, $J = 6.3$ Hz, 1H), 5.98-5.88 (m, 1H), 5.10-5.01 (m, 2H), 3.32 (d, 2H).

^{13}C NMR (101 MHz, $\text{DMSO-}d_6$) δ 144.2, 142.4, 137.7, 135.0, 122.5, 118.4, 115.9, 109.5, 109.0, 69.6 (hept, $J = 33.2$ Hz), 48.6.

^{19}F NMR (376 MHz, $\text{DMSO-}d_6$) $\delta = -74.29, -74.31$.

HRMS of $\text{C}_{13}\text{H}_{10}\text{F}_6\text{O}_3^+$ (APCI+) $[\text{M}]^+$: calc.: 328.0534, found: 328.0525.

2-(1-Trifluoromethyl-(2,2,2-trifluoroethyl)oxy)-5-(methoxymethyl)-1,3-benzodioxole (11)



The compound was synthesized according to GPI. The product was obtained as a colourless oil (50 mg, 0.15 mmol, yield: 31%).

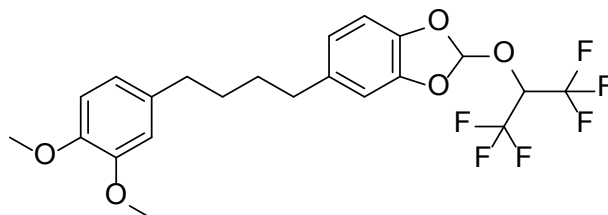
^1H NMR (400 MHz, $\text{DMSO-}d_6$) δ 7.36 (s, 1H, 7.12-7.09 (m, 2H), 6.98-6.95 (m, 1H), 6.19 (hept, $J = 6.3$ Hz, 1H), 4.35 (s, 2H), 3.26 (s, 3H).

^{13}C NMR (101 MHz, $\text{DMSO-}d_6$) δ 144.1, 143.4, 133.5, 118.5, 108.8, 73.2, 69.6 (hept, $J = 33.2$ Hz), 57.3.

^{19}F NMR (376 MHz, $\text{DMSO-}d_6$) $\delta = -74.29, -74.31$.

HRMS of $\text{C}_{12}\text{H}_{10}\text{F}_6\text{O}_4^+$ (APCI+) $[\text{M}]^+$: calc.: 331.0400, found: 331.0399.

2-(1-Trifluoromethyl-(2,2,2-trifluoroethyl)oxy)-5-(4-(3,4-dimethoxyphenyl)butyl)-1,3-benzodioxole (12)



The compound was synthesized according to GPI. The product was obtained as colourless wax (53 mg, 0.19 mmol, 38%).

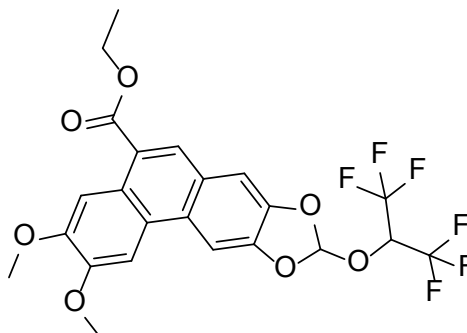
^1H NMR (400 MHz, $\text{DMSO-}d_6$) δ 7.30 (s, 1H), 7.02 (d, $J = 8.0$ Hz, 1H), 6.99 (d, $J = 1.4$ Hz, 1H), 6.83 – 6.78 (m, 2H), 6.75 (d, $J = 1.9$ Hz, 1H), 6.66 (dd, $J = 8.0, 1.9$ Hz, 1H), 6.16 (hept, $J = 6.3$ Hz, 1H), 3.71 (s, 3H), 3.69 (s, 3H), 2.56 (t, $J = 6.8$ Hz, 2H), 2.53 (s, 2H), 1.54 (t, $J = 6.8$ Hz, 4H).

^{19}F NMR (376 MHz, $\text{DMSO-}d_6$) δ -74.28, -74.30.

^{13}C NMR (101 MHz, $\text{DMSO-}d_6$) δ 148.6, 146.8, 144.1, 142.1, 137.5, 134.7, 122.3, 120.0, 118.4, 112.2, 111.8, 109.3, 108.8, 69.7 (hept, $J = 33.2$ Hz), 55.5, 55.3, 39.5, 34.6, 34.5, 30.8, 30.7.

HRMS of $\text{C}_{22}\text{H}_{22}\text{F}_6\text{O}_5^+$ (APCI+) $[\text{M}]^+$: calc.: 480.1366, found: 480.1354.

Ethyl 9-(1-Trifluoromethyl-(2,2,2-trifluoroethyl)oxy)-2,3-dimethoxyphenanthro[2,3-d][1,3]dioxole-5-carboxylate (13**)**



The compound was synthesized according to GPI. The product was obtained as colourless crystals (155 mg, 0.076 mmol, 60%).

^1H NMR (600 MHz, $\text{DMSO-}d_6$) δ 8.66 (s, 1H), 8.43 (s, 1H), 8.36 (s, 1H), 8.15 (s, 1H), 7.86 (s, 1H), 7.60 (s, 1H), 6.35 (hept, $J = 6.3, 5.9$ Hz, 1H), 4.44 (q, $J = 7.1$ Hz, 2H), 4.04 (s, 3H), 3.91 (s, 3H), 1.43 (t, $J = 7.1$ Hz, 3H).

^{13}C NMR (151 MHz, $\text{DMSO-}d_6$) δ 167.2, 149.3, 146.7, 143.9, 129.6, 128.7, 125.7, 125.6, 123.4, 123.2, 120.1, 119.1, 107.6, 106.1, 104.3, 102.4, 69.8, 60.9, 56.0, 55.3, 14.3.

^{19}F NMR (377 MHz, $\text{DMSO-}d_6$) δ -74.11, -74.14, -74.15, -74.17, -74.18, -74.20, -74.22, -74.24.

HRMS of $\text{C}_{12}\text{H}_{19}\text{F}_6\text{O}_7^+$ (APCI+) $[\text{M}+\text{H}]^+$: calc.: 521.1029, found: 521.1029.

Melting point: 204 °C.

Crystal structure determination of **13**: $\text{C}_{23}\text{H}_{18}\text{F}_6\text{O}_7$, $M_r = 520.37$ g/mol, colourless plates (0.03 x 0.05 x 0.11 mm^3), $P -1$ (triklin), $a = 9.4787$ Å, $b = 10.5740$ Å, $c = 12.0956$ Å, $V = 1078.2$ Å 3 , $z = 2$, $F(000) = 532$, $\rho = 1.603$ g/cm 3 , $\mu = 0.151$ mm $^{-1}$, Mo-K α graphite monochromator, -80 °C, 9976 reflections, 3786 reflections, $wR_2 = 0.2474$, $R_1 = 0.0859$, 0.3 eÅ $^{-3}$, -0.27 eÅ $^{-3}$, GoF = 1.012;

Single crystals for structure determination were obtained by recrystallization from acetone at room temperature.

Surprisingly no π / π - stacking was observed. The HFIP – moieties interlock into each other.

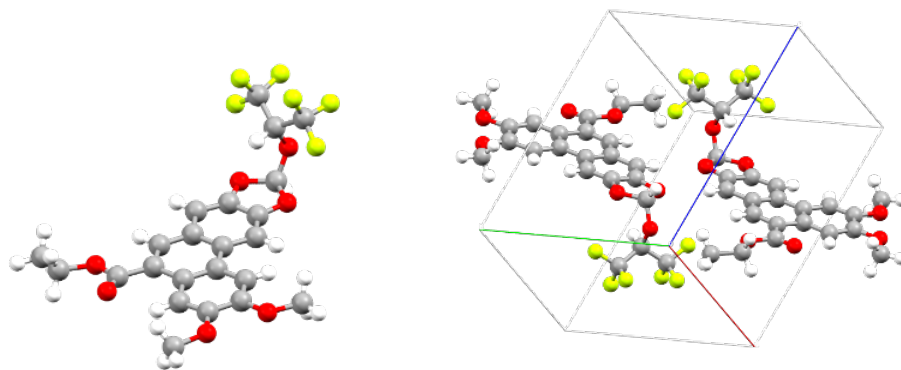
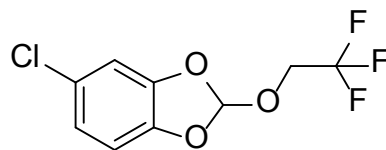


Fig. S9: left: crystal structure of **13**; right: Packing of **13** in the solid state.

5.3. Synthesis of TFE-Orthoesters

5-Chlor-2-(2,2,2-trifluoroethoxy)-1,3-benzodioxole (14)



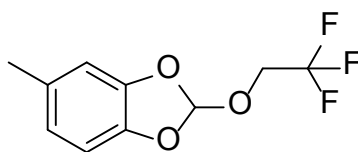
The compound was synthesized according to GP11. The product was obtained as colourless oil (33 mg, 0.13 mmol, yield: 25%).

^1H NMR (400 MHz, DMSO- d_6) δ 7.32 (s, 1H), 7.25 (d, J = 2.1 Hz, 1H), 7.10 (d, J = 8.4 Hz, 1H), 7.01 (dd, J = 8.4, 2.1 Hz 1H), 4.40 (q, J = 9.0 Hz, 2H).

^{13}C NMR (101 MHz, DMSO- d_6) δ 145.7, 144.0, 125.8, 124.6, 122.7, 122.0, 119.0, 109.8, 109.7, 61.5 (q, J = 34.6 Hz).

^{19}F NMR (376 MHz, DMSO- d_6) δ = -74.05, -74.05, -74.10.

HRMS of $\text{C}_9\text{H}_6\text{Cl}^{35}\text{F}_3\text{O}_3^+$ (APCI+) $[\text{M}]^+$: calc.: 253.9958, found: 253,9938.

2-(2,2,2-Trifluoroethoxy)-5-methyl-1,3-benzodioxole (15)

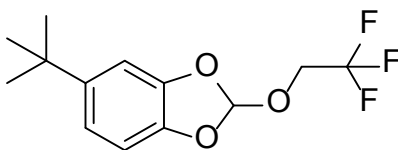
The compound was synthesized according to GPII. The product was obtained as colourless oil (39 mg, 0.17 mmol, yield: 33%).

^1H NMR (400 MHz, DMSO- d_6) δ 7.20 (s, 1H), 6.93 (d, J = 8.0 Hz, 1H), 6.90 (m, 1H), 6.76-6.72 (m, 1H), 4.34 (q, J = 9.0 Hz, 2H), 2.25 (s, 3H).

^{13}C NMR (101 MHz, DMSO- d_6) δ 144.7, 142.6, 122.2, 121.4, 118.0, 109.6, 108.3, 61.2 (q, J = 34.6 Hz), 20.7.

^{19}F NMR (376 MHz, DMSO- d_6) δ = -74.04, -74.06, -74.08.

HRMS of $\text{C}_{10}\text{H}_9\text{F}_3\text{O}_3^+$ (APCI+) $[\text{M}]^+$: calc.: 234.0498, found: 234.0496.

2-(2,2,2-Trifluoroethoxy)-5-(1,1-dimethylethyl)-1,3-benzodioxole (16)

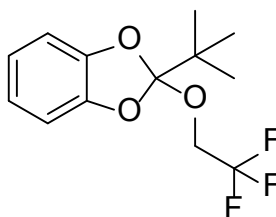
The compound was synthesized according to GPII. The product was obtained as colourless oil (33 mg, 0.12 mmol, yield: 23%).

^1H NMR (400 MHz, DMSO- d_6) δ 7.20 (s, 1H), 7.12 (m, 1H), 6.95-6.93 (m, 2H), 4.36 (q, J = 9.0 Hz, 2H), 1.25 (s, 9H).

^{13}C NMR (101 MHz, DMSO- d_6) δ 145.6, 144.7, 142.2, 118.4, 118.2, 107.9, 106.4, 49.0, 61.3 (q, J = 34.6 Hz), 34.5, 31.4.

^{19}F NMR (376 MHz, DMSO- d_6) δ = -74.02, -74.05, -74.07.

HRMS of $\text{C}_{13}\text{H}_{15}\text{F}_3\text{O}_3^+$ (APCI+) $[\text{M}]^+$: calc.: 276.0968, found: 276.0971.

2-(2,2,2-Trifluoroethoxy)-2-(1,1-dimethylethyl)-1,3-benzodioxole (17)

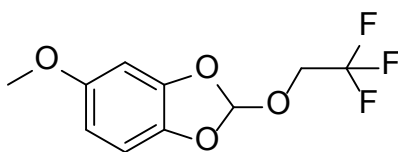
The compound was synthesized according to GPII. The product was obtained as colourless oil (53 mg, 0.15 mmol, 29%).

^1H NMR (400 MHz, $\text{DMSO-}d_6$) δ 7.04 (dd, $J = 5.7, 3.3$ Hz, 2H), 6.91 (dd, $J = 5.8, 3.3$ Hz, 2H), 4.01 (q, $J = 8.9$ Hz, 2H), 1.04 (s, 9H).

^{13}C NMR (101 MHz, $\text{DMSO-}d_6$) δ 146.2, 130.0, 122.0, 108.0, 60.0 (q, $J = 34.6$ Hz), 59.7, 59.3, 59.0, 40.0, 23.5.

^{19}F NMR (376 MHz, $\text{DMSO-}d_6$) δ -73.82, -73.84, -73.87.

HRMS of $\text{C}_{13}\text{H}_{15}\text{F}_3\text{O}_3^+$ (APCI+) $[\text{M}]^+$: calc.: 276.0968, found: 276.0967.

2-(2,2,2-Trifluoroethoxy)-5-methoxy-1,3-benzodioxole (18)

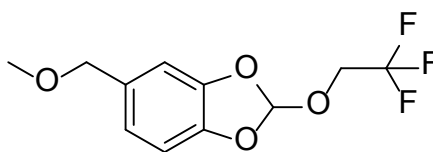
The compound was synthesized according to GPII. The product was obtained as colourless oil (33 mg, 0.13 mmol, 26%).

^1H NMR (400 MHz, DMSO- d_6) δ 7.20 (s, 1H), 6.96 (d, J = 8.6 Hz, 1H), 6.76 (d, J = 2.5 Hz, 1H), 6.47 (dd, J = 8.6, 2.5 Hz, 1H), 4.35 (q, J = 9.0 Hz, 2H), 3.70 (s, 3H).

^{13}C NMR (101 MHz, DMSO- d_6) δ 155.6, 145.9, 139.1, 125.5, 122.8, 118.9, 106.4, 97.6, 61.7 (q, J = 34.6 Hz), 56.3.

^{19}F NMR (376 MHz, DMSO- d_6) δ = -74.03, -74.06, -74.08.

HRMS of $\text{C}_{10}\text{H}_9\text{F}_3\text{O}_4^+$ (APCI+) $[\text{M}]^+$: calc.: 250.0447, found: 250.0441.

2-(2,2,2-Trifluoroethoxy)-5-(methoxymethyl)-1,3-benzodioxole (19)

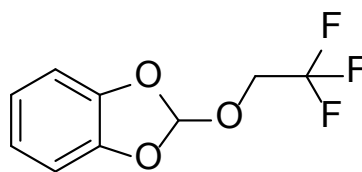
The compound was synthesized according to GPII. The product was obtained as colourless oil (20 mg, 0.076 mmol, 15%).

^1H NMR (400 MHz, DMSO- d_6) δ 7.25 (s, 1H), 7.04-7.01 (m, 2H), 6.92-6.89 (m, 1H), 4.41-4.34 (q, J = 9.0 Hz, 2H), 4.33 (s, 2H), 3.25 (s, 3H).

^{13}C NMR (101 MHz, DMSO- d_6) δ 145.2, 144.5, 133.3, 125.5, 122.7, 122.2, 118.7, 108.9, 73.7, 61.8 (q, J = 34.6 Hz), 57.7.

^{19}F NMR (376 MHz, DMSO- d_6) δ = -74.06, -74.08, -74.11.

HRMS of $\text{C}_{11}\text{H}_{11}\text{F}_3\text{O}_4^+$ (APCI+) $[\text{M}]^+$: calc.: 264.0609, found: 264.0611.

2-(2,2,2-Trifluoroethoxy)-1,3-benzodioxole (20)

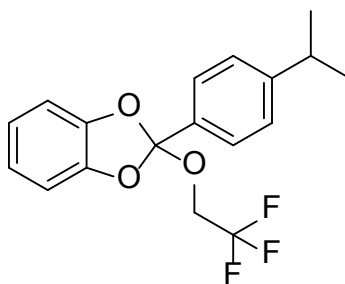
The compound was synthesized according to GP11. The product was obtained as colourless oil (29 mg, 0.13 mmol, yield: 26%).

^1H NMR (400 MHz, DMSO- d_6) δ 7.24 (s, 1H), 7.07 (m, 2H), 6.95 (m, 2H), 4.37 (q, J = 9.0 Hz, 2H).

^{13}C NMR (101 MHz, DMSO- d_6) δ 144.6, 125.1, 122.4, 117.9, 108.9, 61.3 (q, J = 34.6 Hz).

^{19}F NMR (376 MHz, DMSO- d_6) δ = -74.05, -74.08, -74.10.

HRMS of $\text{C}_9\text{H}_7\text{F}_3\text{O}_3^+$ (APCI+) $[\text{M}]^+$: calc.: 220.0366, found: 220.0344.

2-(2,2,2-Trifluoroethoxy)-2-(4-isopropylphenyl)-1,3-benzodioxole (21)

The compound was synthesized according to GPII. The product was obtained as colourless oil (64 mg, 0.19 mmol, yield: 38%).

^1H NMR (400 MHz, $\text{DMSO-}d_6$) δ 7.53 – 7.46 (m, 2H), 7.38 – 7.31 (m, 2H), 7.11 (dd, J = 5.8, 3.3 Hz, 2H), 6.98 (dd, J = 5.8, 3.3 Hz, 2H), 4.26 (q, J = 8.9 Hz, 2H), 2.90 (h, J = 6.9 Hz, 1H), 1.19 (d, J = 6.9 Hz, 6H).

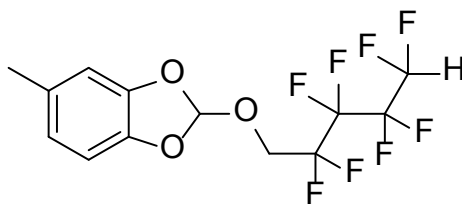
^{13}C NMR (101 MHz, $\text{DMSO-}d_6$) δ 151.4, 145.7, 133.2, 127.1, 125.7, 125.6, 122.9, 109.2, 61.2 (q, J = 34.6 Hz), 60.9, 60.5, 60.2, 33.7, 24.1.

^{19}F NMR (376 MHz, $\text{DMSO-}d_6$) δ -73.63, -73.66, -73.68.

HRMS of $\text{C}_{18}\text{H}_{18}\text{F}_3\text{O}_3^+$ (ESI+) $[\text{M}+\text{H}]^+$: calc.: 339.1203, found: 339.1199.

5.4. Synthesis of OFP-orthoesters

5-Methyl-2-((2,2,3,3,4,4,5,5-octafluoropentyl)oxy)-1,3-benzodioxole (22)



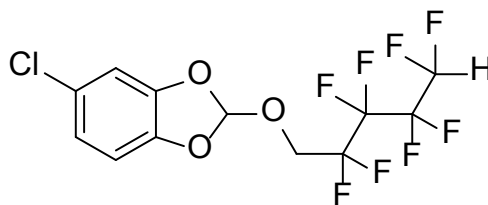
The compound was synthesized according to GPIII. The product was obtained as yellowish oil (31 mg, 0.09 mmol, yield: 17%).

^1H NMR (400 MHz, $\text{DMSO-}d_6$) δ 7.22 (s, 1H), 7.05 (tt, $J = 50.1$ Hz, 5.6 Hz, 1H), 6.74 (ddd, $J = 8.0$, 1.6, 0.9 Hz, 1H), 4.40 (tt, $J = 14.7$, 1.6 Hz, 2H), 2.25 (s, 3H).

^{13}C NMR (101 MHz, DMSO) δ 145.1, 143.0, 132.2, 122.7, 118.5, 110.9, 110.6, 110.0, 108.8, 108.4, 61.1 (t, $J = 26.9$ Hz), 21.2.

^{19}F NMR (376 MHz, $\text{DMSO-}d_6$) δ -120.41 – -120.69 (m), -125.80 (t, $J = 8.6$ Hz), -130.91 (tq, $J = 11.8$, 5.55 Hz), -139.67 (dp, $J = 50.3$, 7.3 Hz).

HRMS of $\text{C}_{13}\text{H}_{10}\text{F}_8\text{O}_3^+$ (APCI+) [M^+]: calc.: 366.0497, found: 366.501.

5-Chloro-2-((2,2,3,3,4,4,5,5-octafluoropentyl)oxy)-1,3-benzodioxole (23)

The compound was synthesized according to GPIII. The product was obtained as yellowish oil (29 mg, 0.08 mmol, yield: 15%).

^1H NMR (400 MHz, $\text{DMSO-}d_6$) δ 7.33 (s, 1H), 7.26 (d, $J = 2.1$ Hz, 1H), 7.11 (d, $J = 8.4$ Hz, 1H), 7.06 (tt, $J = 50.3, 5.6$ Hz, 1H), 7.01 (dd, $J = 8.4, 2.1$ Hz, 1H), 4.47 (t, $J = 14.5$ Hz, 2H).

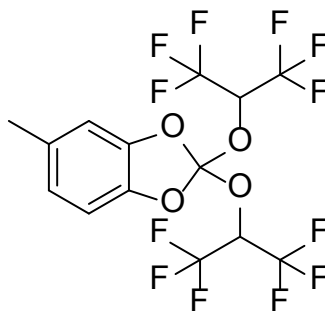
^{13}C NMR (101 MHz, DMSO) δ 146.1, 144.4, 126.3, 122.5, 119.5, 110.2, 110.2, 86.5, 61.5 (t, $J = 26.9$ Hz).

^{19}F NMR (376 MHz, $\text{DMSO-}d_6$) δ -120.56 (p, $J = 13.4, 12.5$ Hz), -125.74 (t, $J = 8.8$ Hz), -130.88 (dq, $J = 11.2, 5.7$ Hz), -139.64 (dq, $J = 51.9, 8.4, 6.9$ Hz).

HRMS of $\text{C}_{12}\text{H}_7\text{ClF}_8\text{O}_3^+$ (APCI+) [M^+]: calc.: 385,9956, found: 385,9955.

5.5. Orthocarbonates

2,2-Bis(1-trifluoromethyl-(2,2,2-trifluoroethyl)oxy)-5-methyl-1,3-benzodioxole



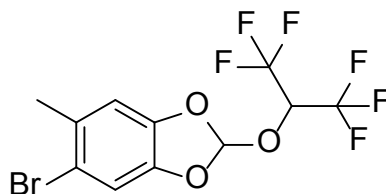
This compound was isolated as a side component in the reaction to **5** using 4 F applied charge. (2 mg were isolated and characterized).

^1H NMR (400 MHz, $\text{DMSO-}d_6$) δ 7.14 – 7.08 (m, 1H), 6.91 (ddd, $J = 8.1, 1.7, 0.8$ Hz, 1H), 6.29 (hept, $J = 5.9$ Hz, 1H).

HRMS of $\text{C}_{14}\text{H}_8\text{F}_{14}\text{O}_4^+$ (APCI+) [M^+]: calc.: 468,0231, found: 468,0230.

5.6. Further functionalizations of HFIP-orthoesters

5-Bromo-2-(1-trifluoromethyl-(2,2,2-trifluoroethyl)oxy)-6-methyl-1,3-benzodioxole (24)



Bromine (60 mg, 0.38 mmol, 1.5 equiv.) was added dropwise to a solution of 2-(1-Trifluoromethyl-(2,2,2-trifluoroethyl)oxy)-5-methyl-1,3-benzodioxole (76 mg, 0.25 mmol, 1.0 equiv.) and pyridine (79 mg, 0.5 mmol, 2.0 equiv.) in CH_2Cl_2 (2 mL) at 0 °C. It was then allowed to warm up to r.t. and stirred for 48 h at r.t.. The reaction was quenched with saturated NaHCO_3 -solution. The phases were separated and the organic phase dried over anhydrous sodium sulfate. The crude mixture was concentrated under reduced pressure and purified by column chromatography on basic aluminiumoxide (0.05-0.15 mm; pH 9.5 ± 0.5) to yield the product as a colourless oil (65 mg, 0.17 mmol, 68% yield).

^1H NMR (400 MHz, $\text{DMSO}-d_6$) δ 7.45 (s, 1H), 7.39 (s, 1H), 7.22 (s, 1H), 6.19 (hept, $J = 6.3$ Hz, 1H), 2.29 (s, 3H).

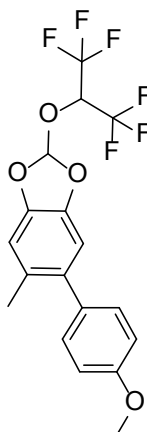
^{13}C NMR (101 MHz, $\text{DMSO}-d_6$) δ 144.3, 143.6, 132.1, 122.9, 119.3, 115.9, 113.3, 111.9, 70.3, 70.0, 69.7, 22.8.

^{19}F NMR (376 MHz, $\text{DMSO}-d_6$) δ -74.25, -74.27.

HRMS of $\text{C}_{11}\text{H}_7^{79}\text{BrF}_6\text{O}_3^+$ (APCI+) [M^+]: calc.: 379.9483, found: 379.9487.

$\text{C}_{11}\text{H}_7^{81}\text{BrF}_6\text{O}_3^+$ (APCI+) [M^+]: calc.: 381.9462, found: 379.9461.

2-(1-Trifluoromethyl-(2,2,2-trifluoroethyl)oxy)-5-(4-methoxyphenyl)-6-methyl-1,3-benzodioxole (25)



A mixture of 5-bromo-2-(1-trifluoromethyl-(2,2,2-trifluoroethyl)oxy)-6-methyl-1,3-benzodioxole (90 mg, 0.24 mmol, 1.0 equiv.), 4-methoxyphenylboronic acid (53.8 mg, 0.35 mmol, 1.50 equiv.), Pd(dppf)Cl₂ (8.6 mg, 0.012 mmol, 0.050 equiv.) and Cs₂CO₃ (153.8 mg, 0.47 mmol, 2.0 equiv.) in 1,2-dimethoxyethane was heated to 75 °C for 6 h under an argon atmosphere. After cooling to r.t., the mixture was diluted with EtOAc and filtered through a pad of celite. The filtrate was washed with NaOH solution (1 M) three times (10 mL) and was then dried over sodium sulfate. After removal of the solvent *in vacuo*, the residue was purified by column chromatography using silica gel (eluent: cyclohexane/EtOAc: 99/1) to afford the desired product as a colourless wax (65 mg, 0.15 mmol, 64% yield).

¹H NMR (400 MHz, CDCl₃) δ 7.22 – 7.17 (m, 2H), 6.97 (s, 1H), 6.96 – 6.92 (m, 2H), 6.88 (s, 1H), 6.85 (s, 1H), 4.58 (hept, *J* = 5.8 Hz, 1H), 3.85 (s, 3H), 2.21 (s, 3H).

¹³C NMR (101 MHz, CDCl₃) δ 158.6, 143.5, 142.7, 136.2, 133.6, 130.3, 117.4, 113.6, 110.64, 110.6, 110.0, 69.3 (p, *J* = 34.3 Hz), 55.3, 20.5.

¹⁹F NMR (376 MHz, CDCl₃) δ -74.57, -74.58.

HRMS of C₁₈H₁₄F₆O₄⁺ (APCI+) [*M*⁺]: calc.: 408.0801, found: 408.0796.

5.7. Optimization of reaction parameters

Table S1: (left) and **Fig. S10** (right): Yield (%) as a function of current density (mA/cm²).

current density [mA/cm ²]	yield
1	0%
2.5	3%
5	11%
7.2	30%
10	21%
15	24%
20	22%
30	22%
50	22%
70	21%
90	23%

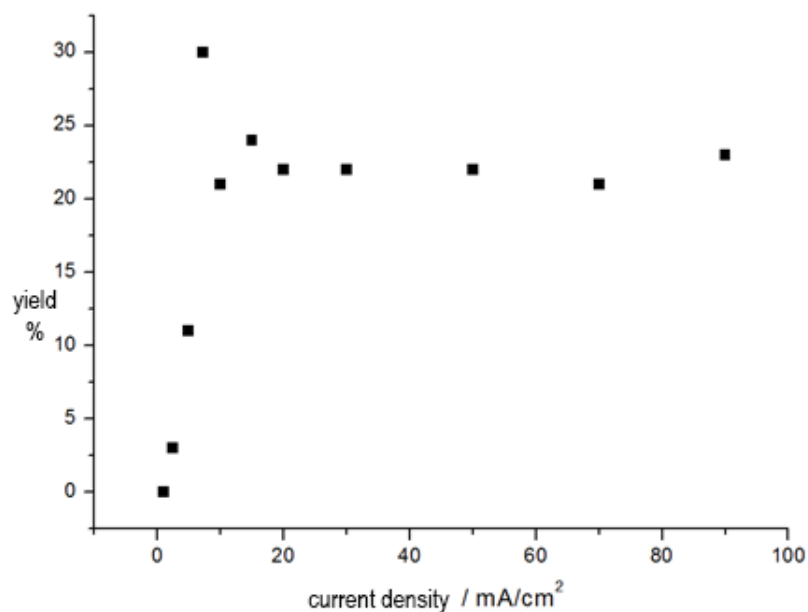
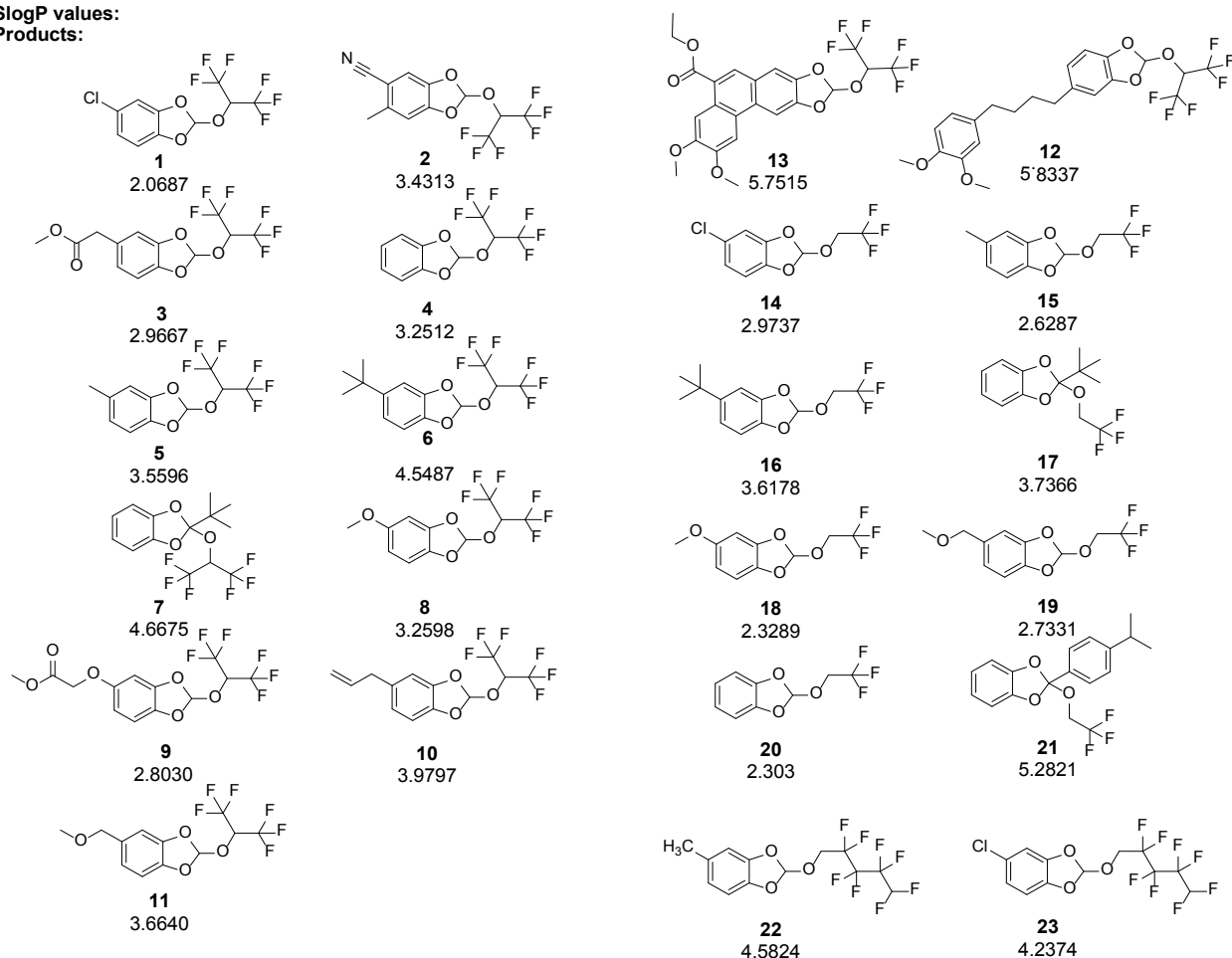


Table S2: Optimized parameters: substrate concentration, applied charge and electrode material

concentration [mol/L]	yield	applied charge [F]	yield	electrode	yield
0.40	10%	2.2	19%	BDD	30%
0.20	13%	2.4	25%	Nickel	2%
0.11	19%	2.6	25%	Graphite	23%
0.07	18%	2.8	26%	Glassy carbon	27%
		3.0	30%	Molybdenum	0%
		4.0	13%		

6. Lipophilicity: LogP – Values of 1,3-benzodioxoles and the corresponding orthoesters

SlogP values:
Products:



Starting materials:

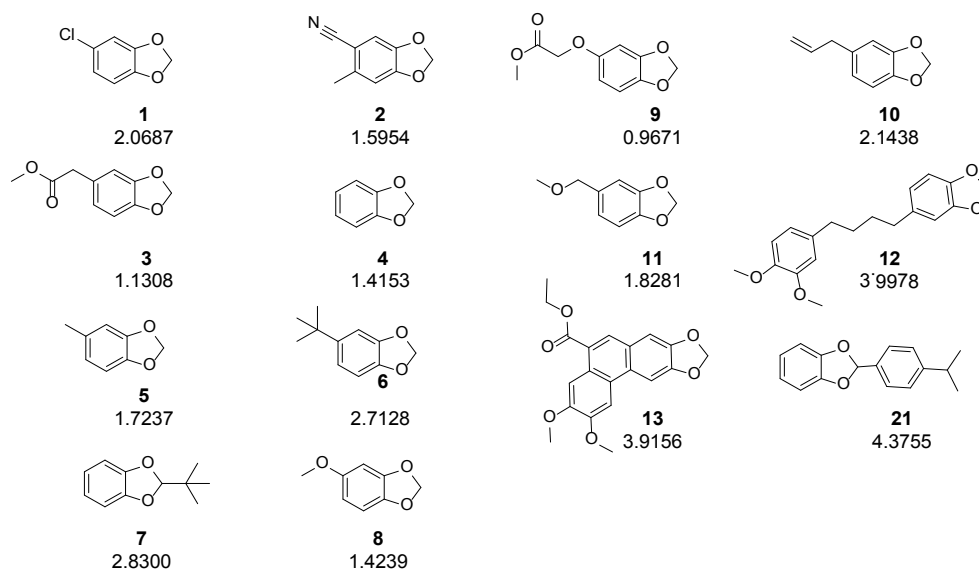
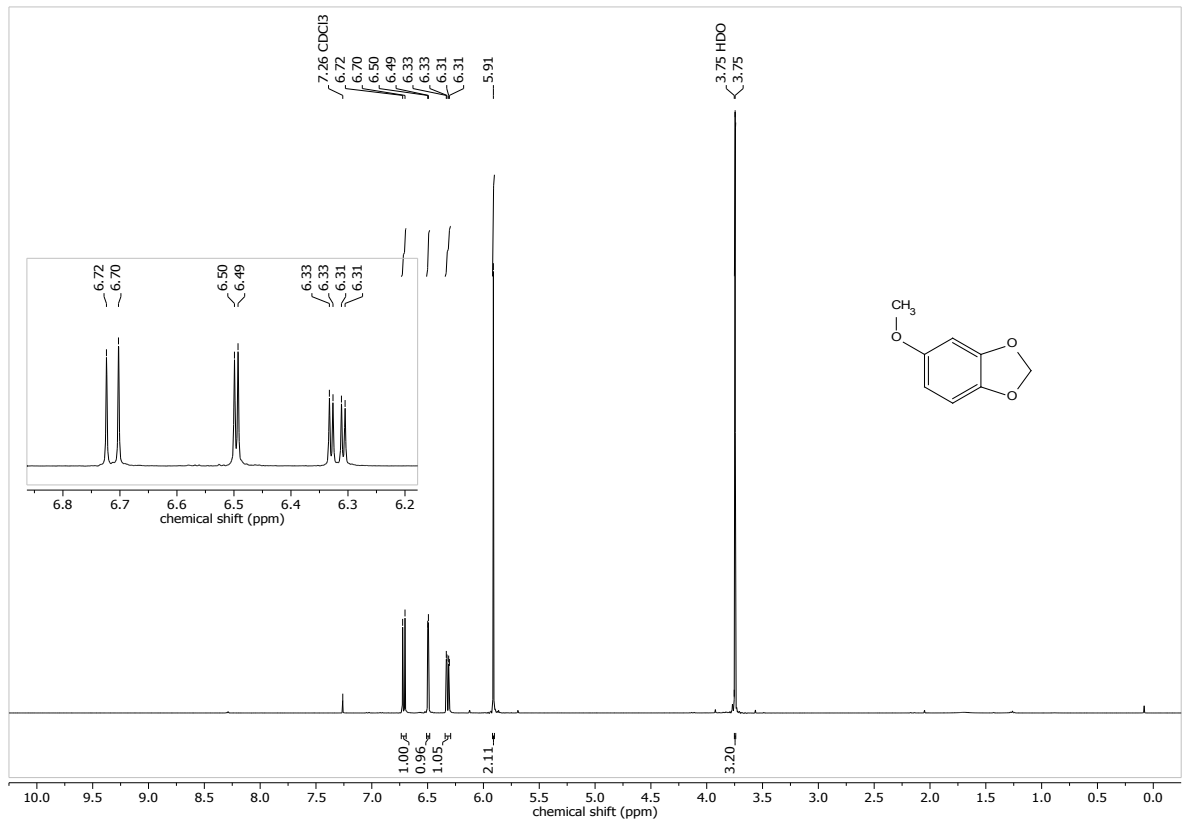
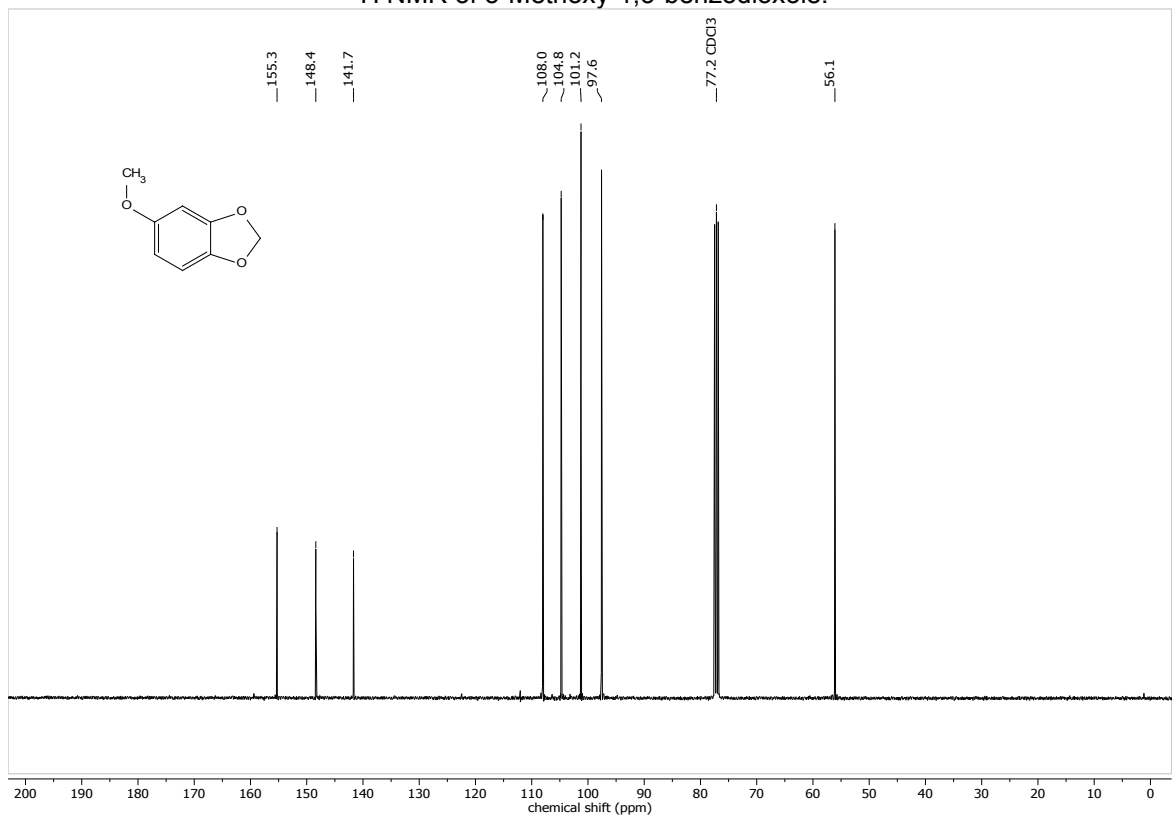


Fig. S11: slogP-values, calculation according to S.A. Wildman, G.M. Crippen, Prediction of Physicochemical Parameters by Atomic Contributions, *J. Chem. Inf. Comput. Sci.* **1999**, 39, 868–873.

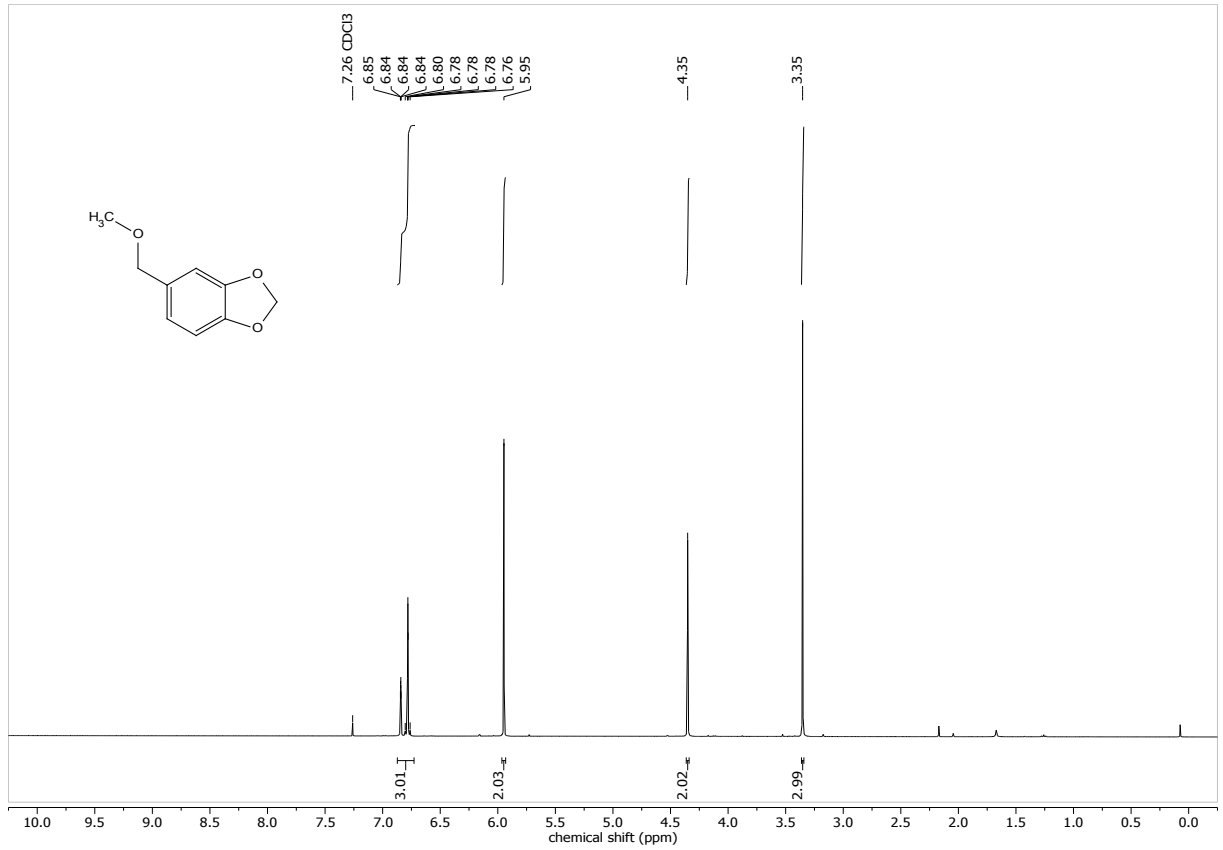
7. NMR spectra



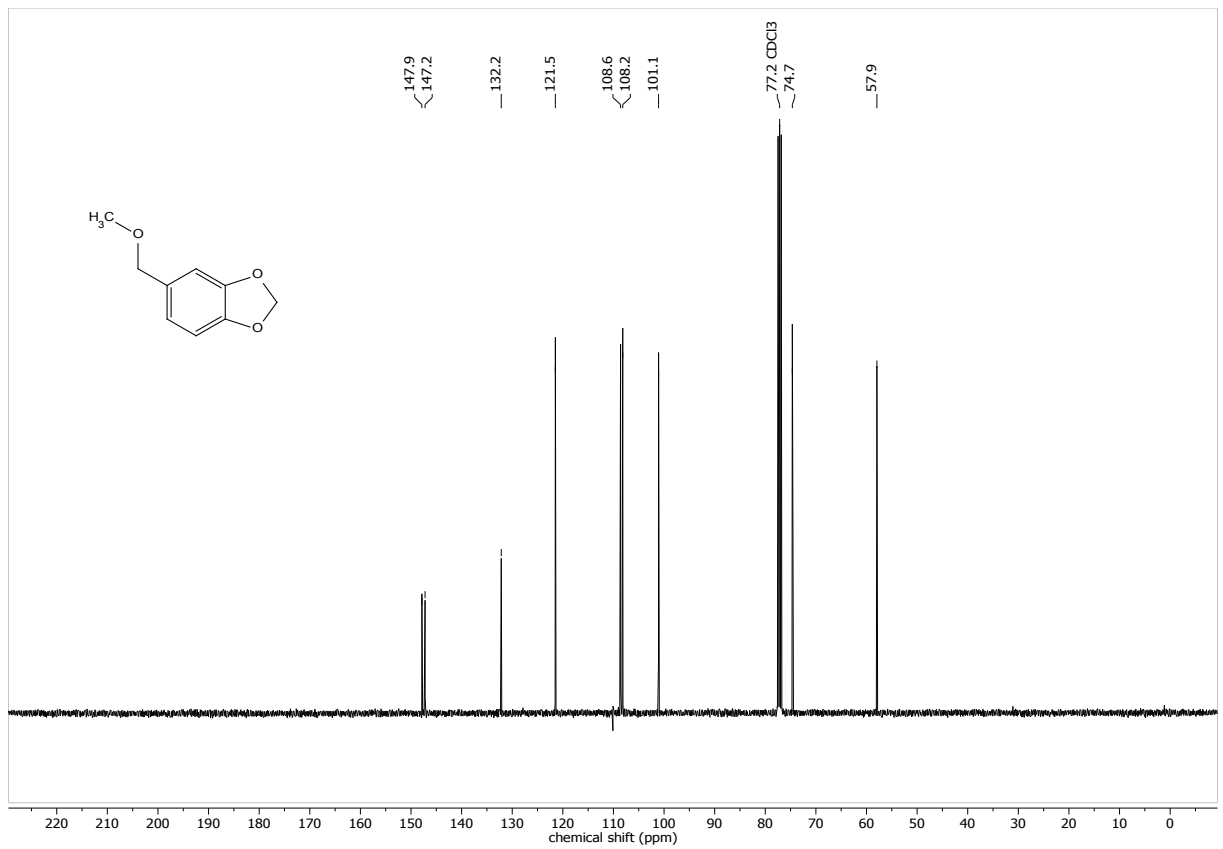
¹H NMR of 5-Methoxy-1,3-benzodioxole.



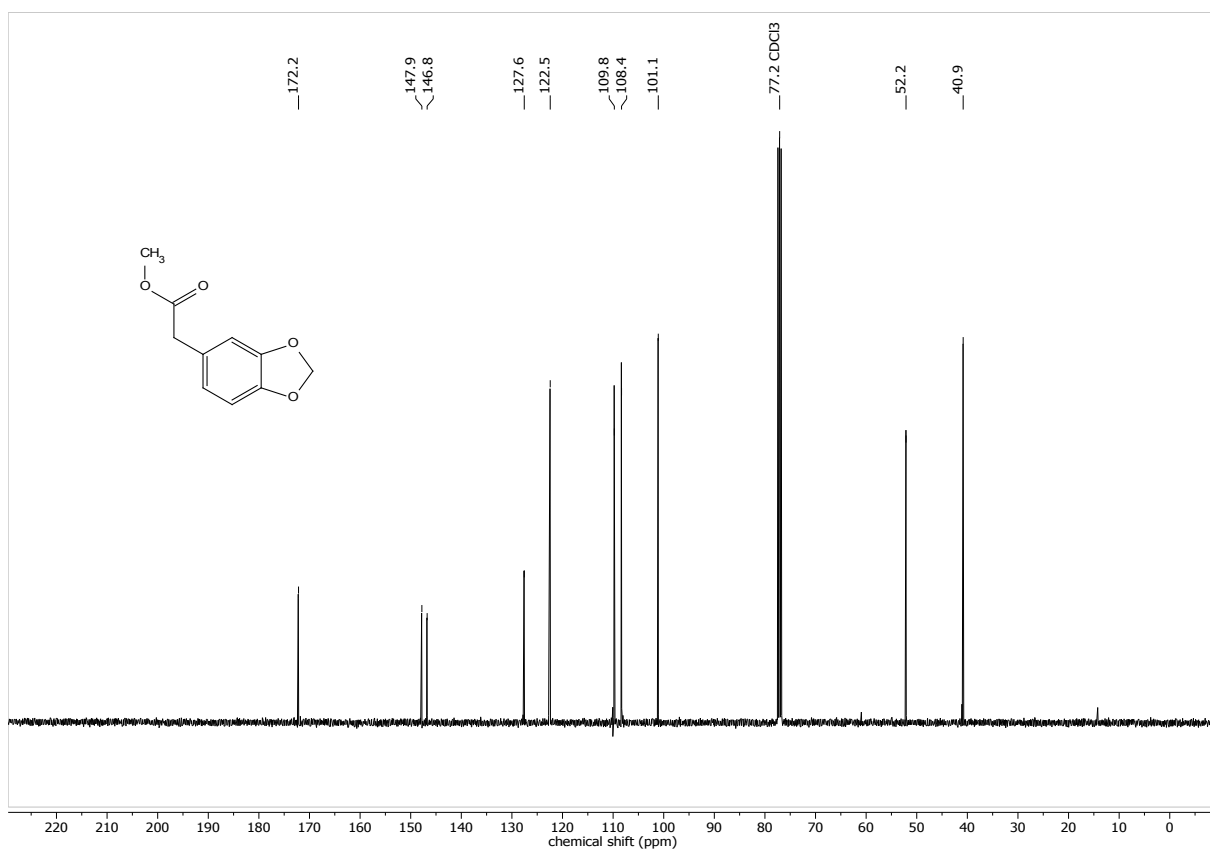
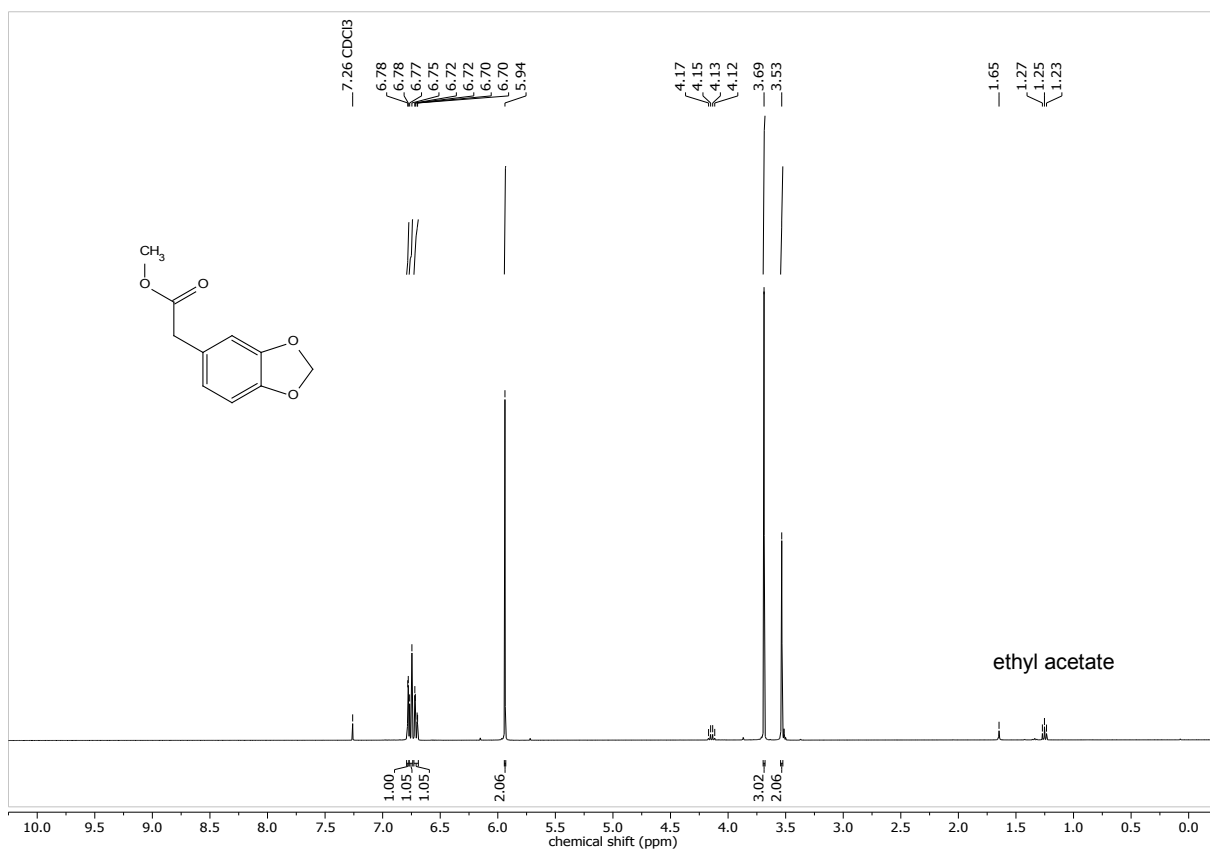
¹³C NMR of 5-Methoxy-1,3-benzodioxol.

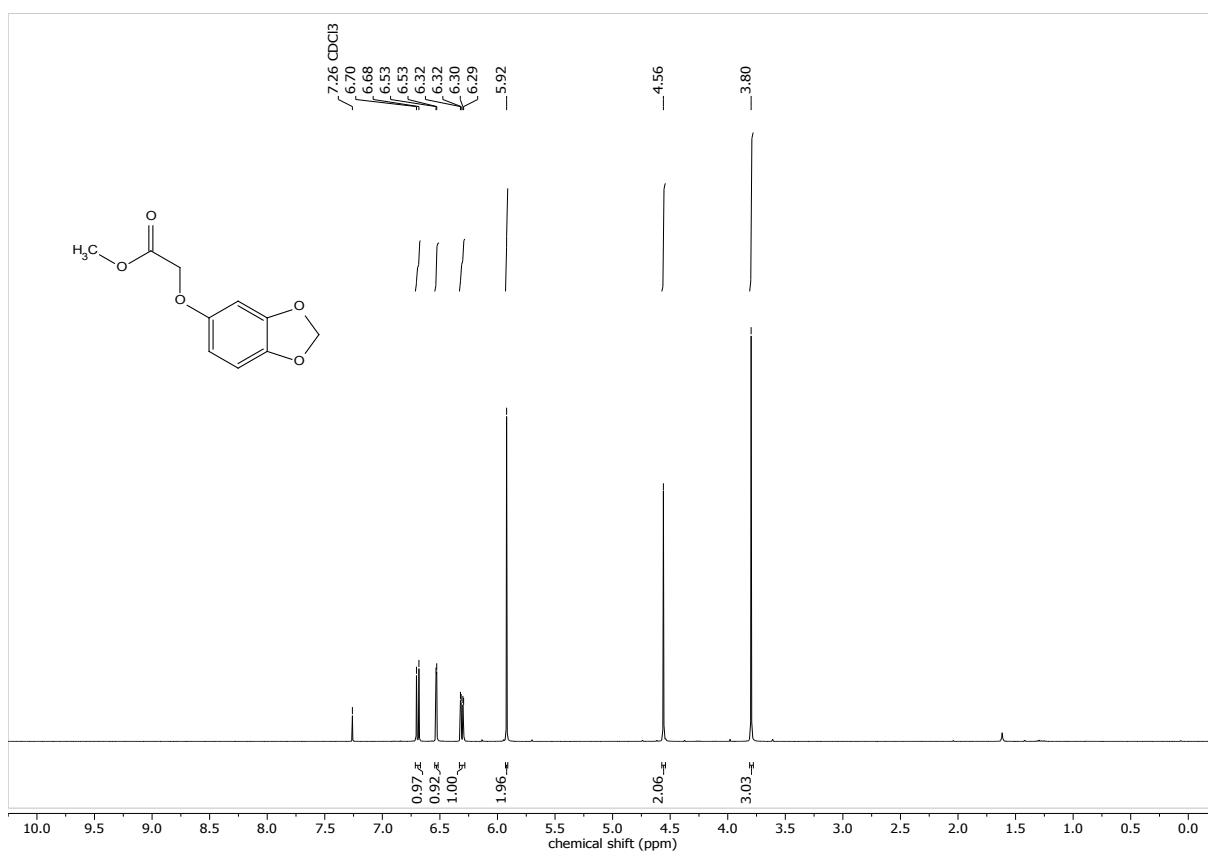


¹H NMR of 5-(Methoxymethyl)-1,3-benzodioxole.

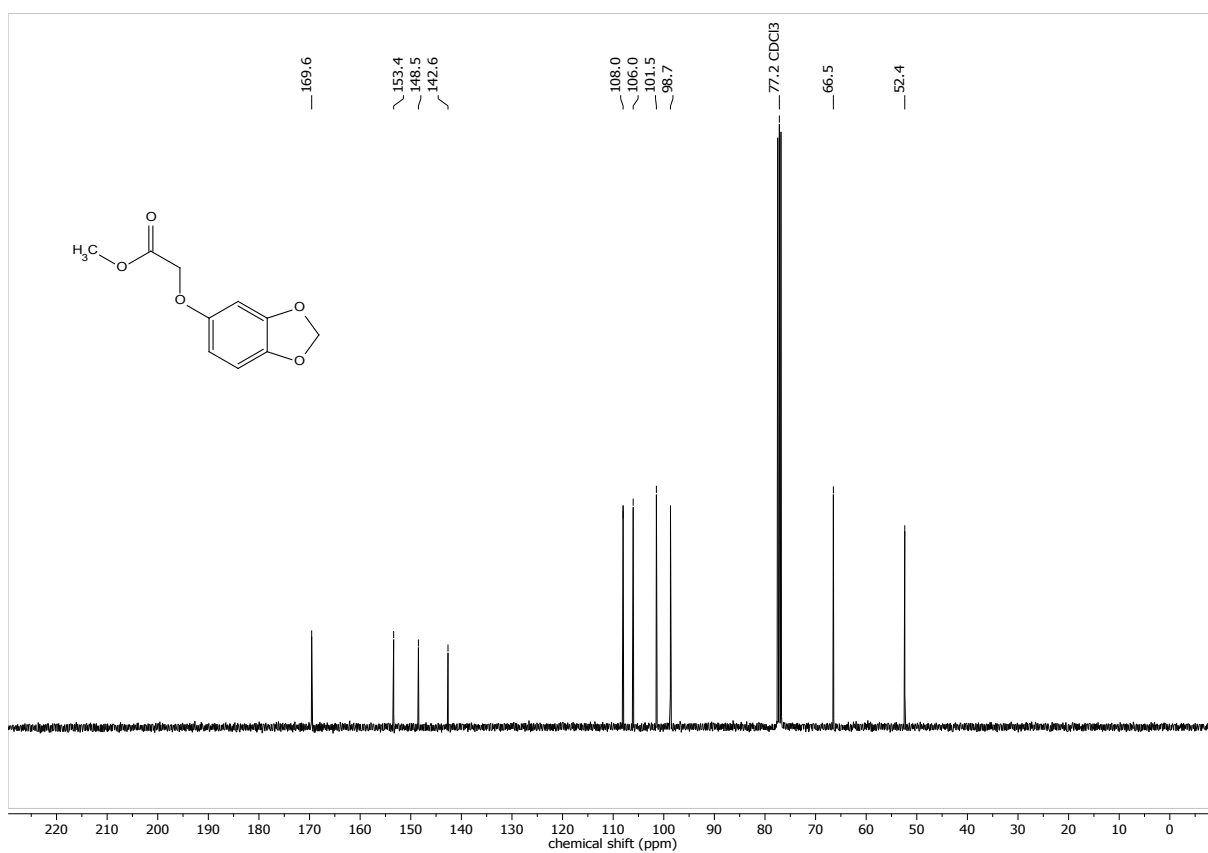


¹³C NMR of 5-(Methoxymethyl)-1,3-benzodioxole.

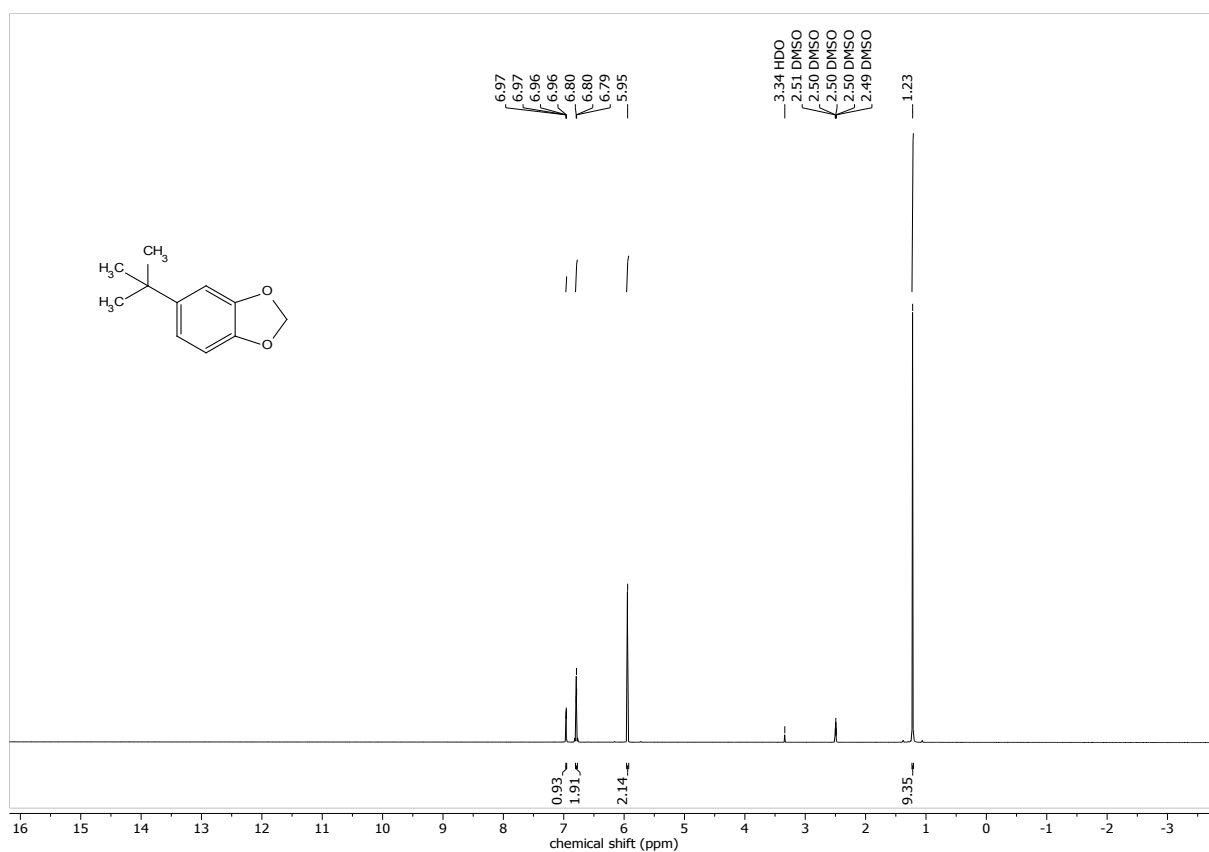




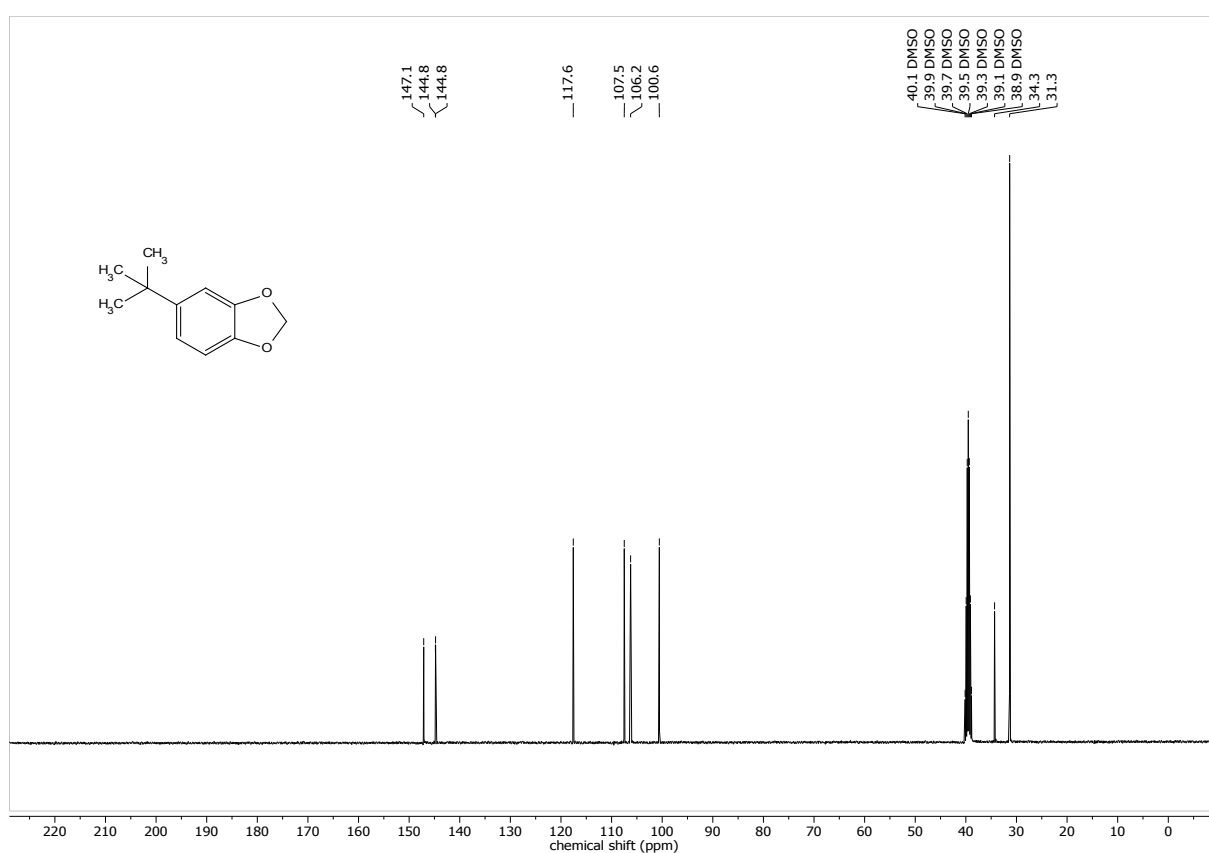
¹H NMR of 5-(Methoxycarbonylmethoxy)-1,3-benzodioxole.



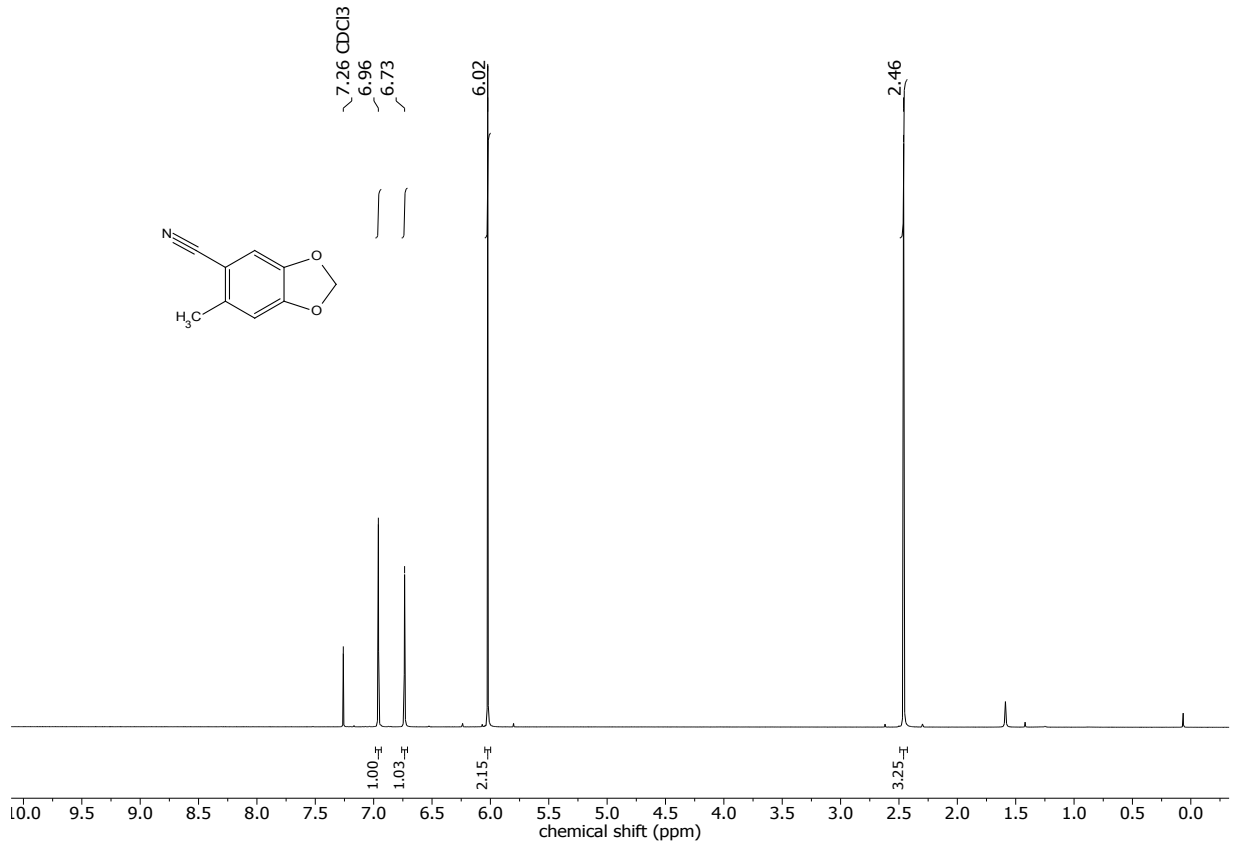
¹³C NMR of 5-(Methoxycarbonylmethoxy)-1,3-benzodioxole.



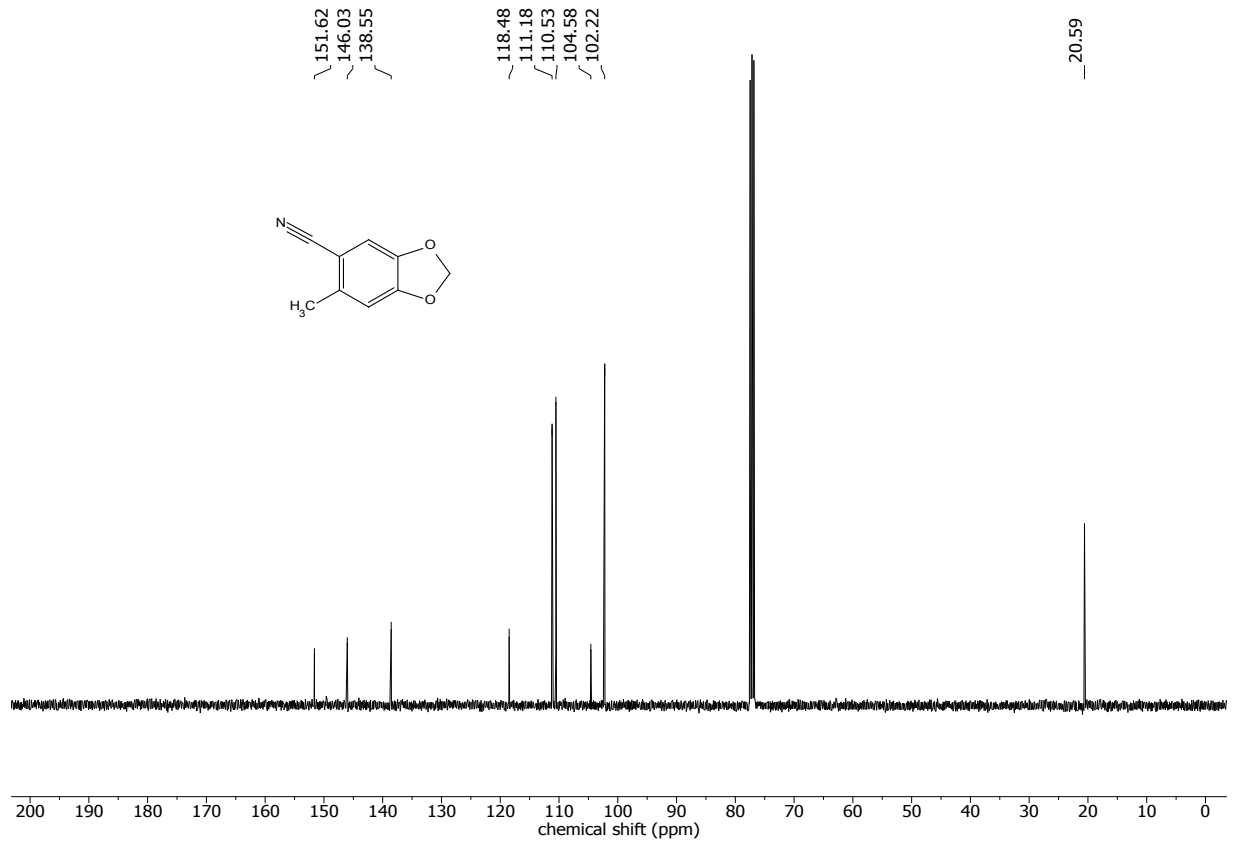
¹H NMR of 5-(2,2-Dimethylethyl)-1,3-benzodioxole.



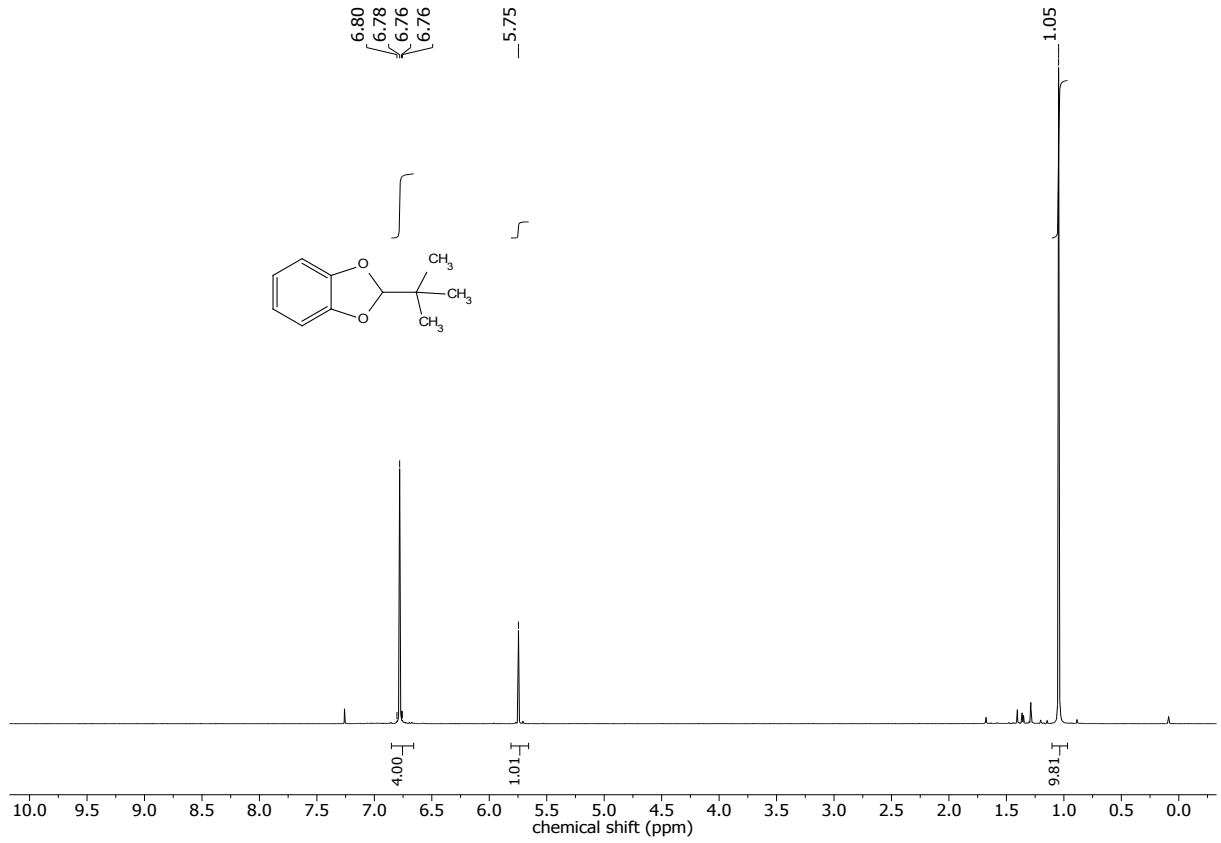
¹³C NMR of 5-(1,1-Dimethylethyl)-1,3-benzodioxole.



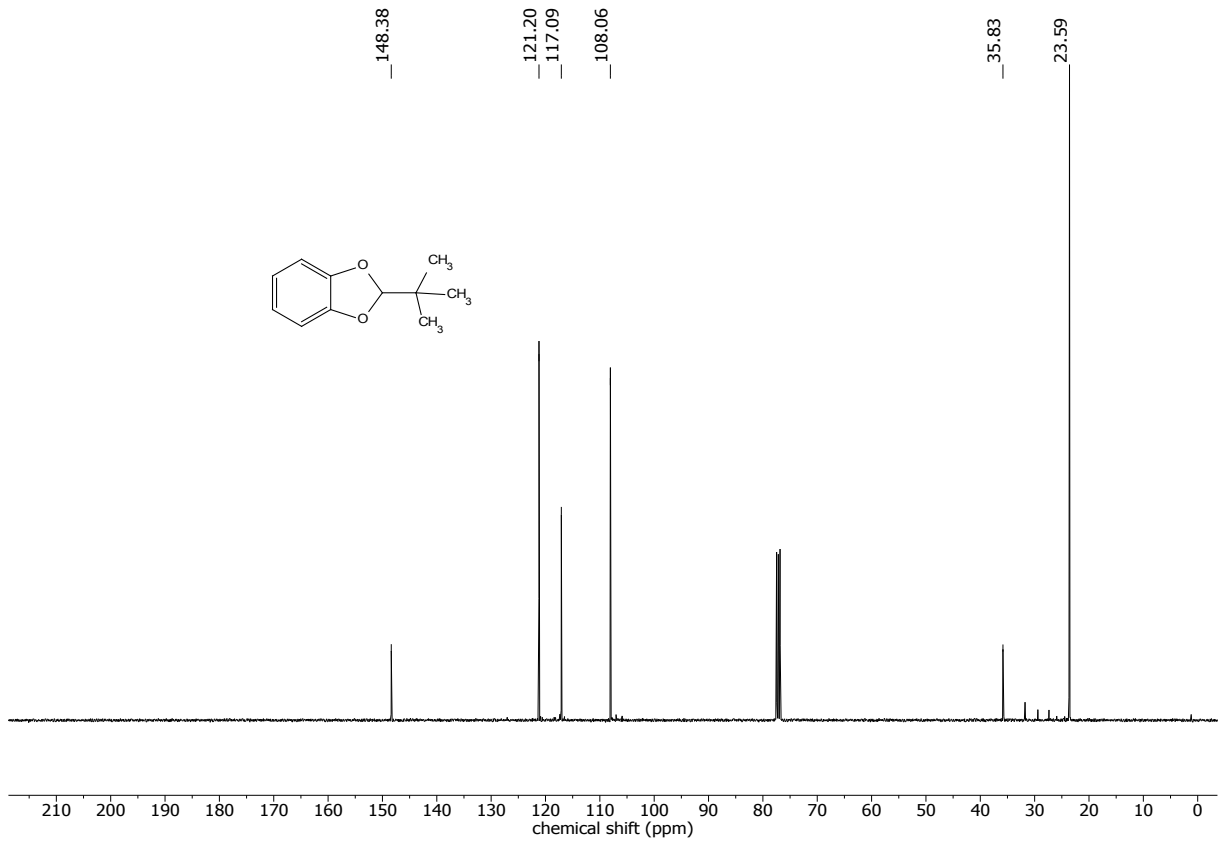
¹H NMR of 5-Cyano-6-methyl-1,3-benzodioxole.



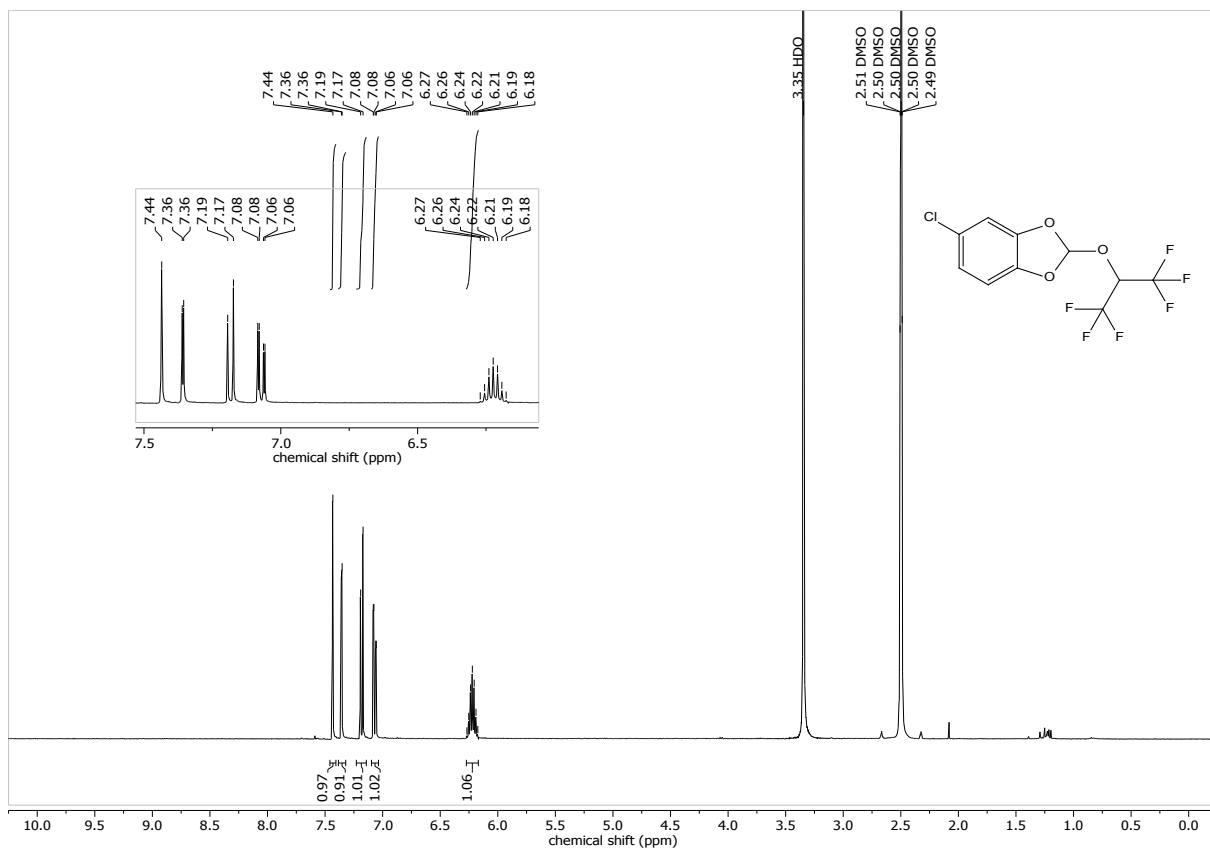
¹³C NMR of 5-Cyano-6-methyl-1,3-benzodioxole.



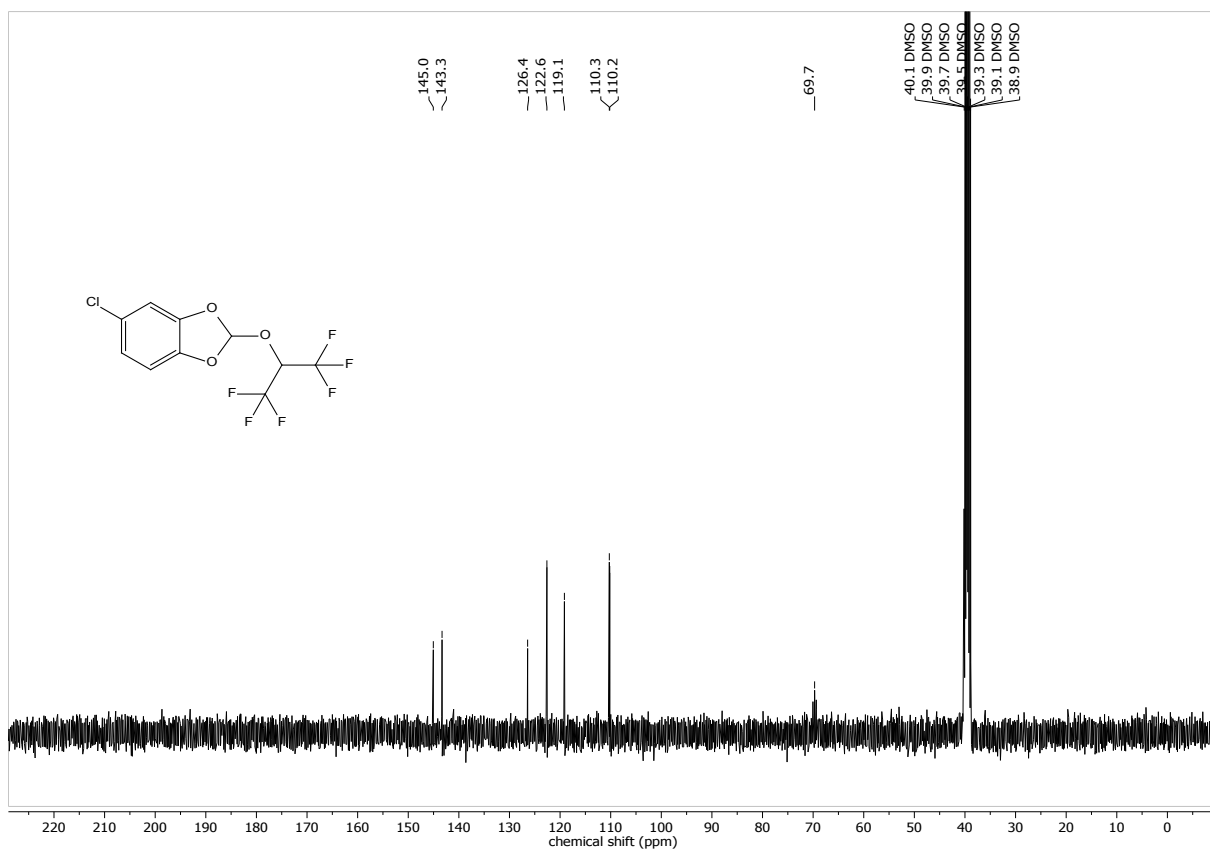
¹H NMR of 2-(1,1-Dimethylethyl)-1,3-benzodioxole.



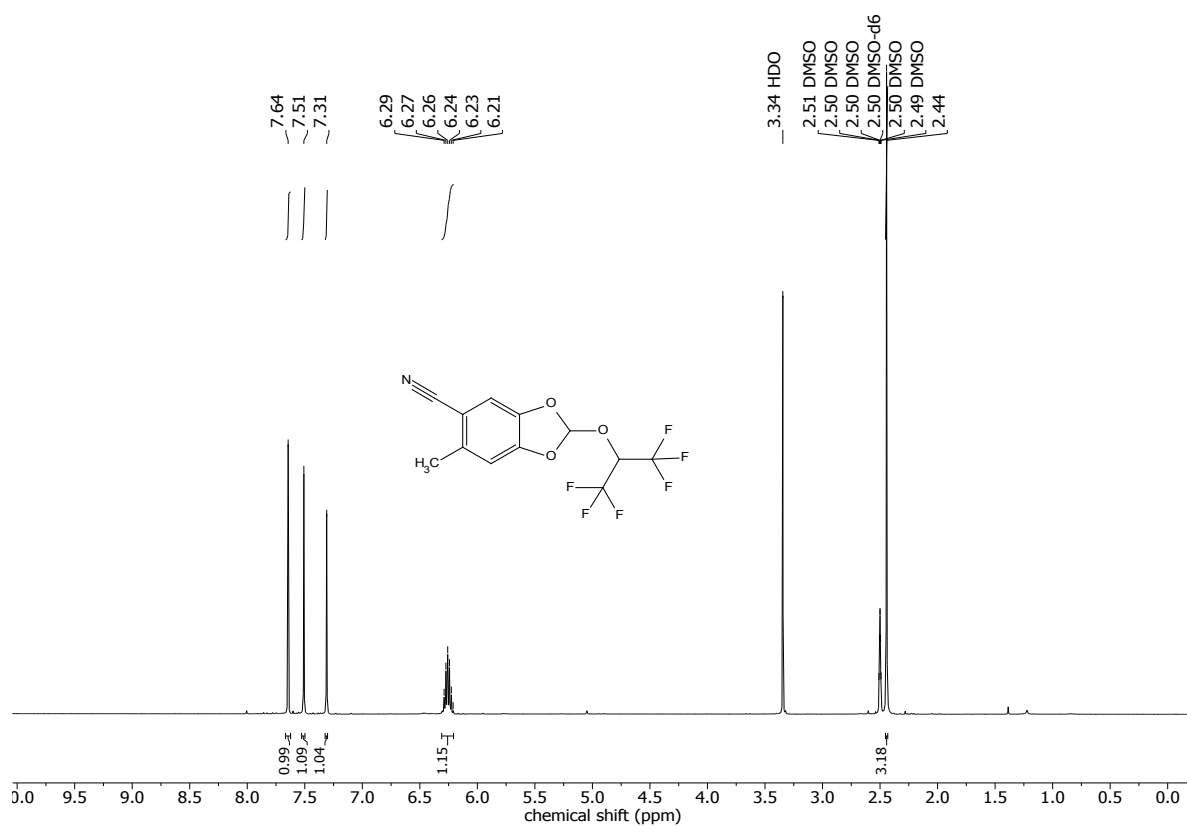
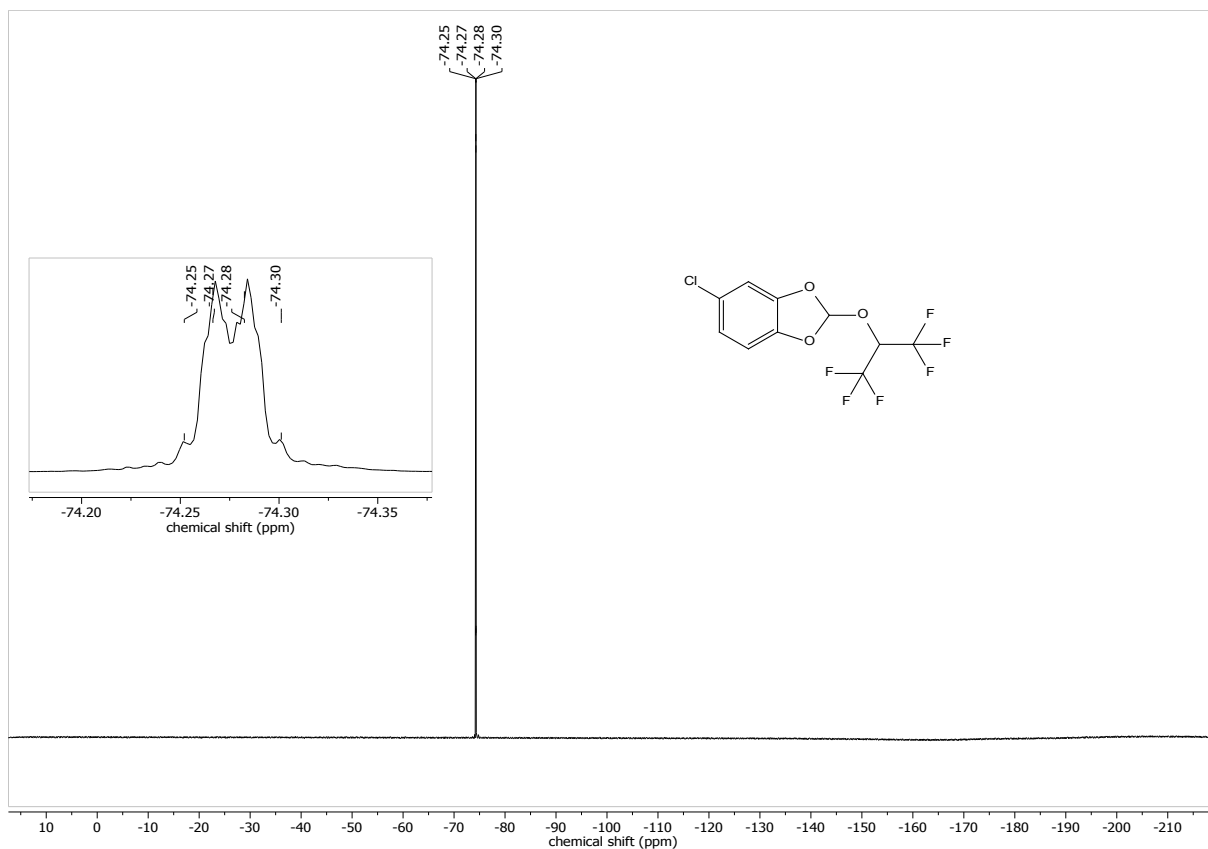
¹³C NMR of 2-(1,1-Dimethylethyl)-1,3-benzodioxole.

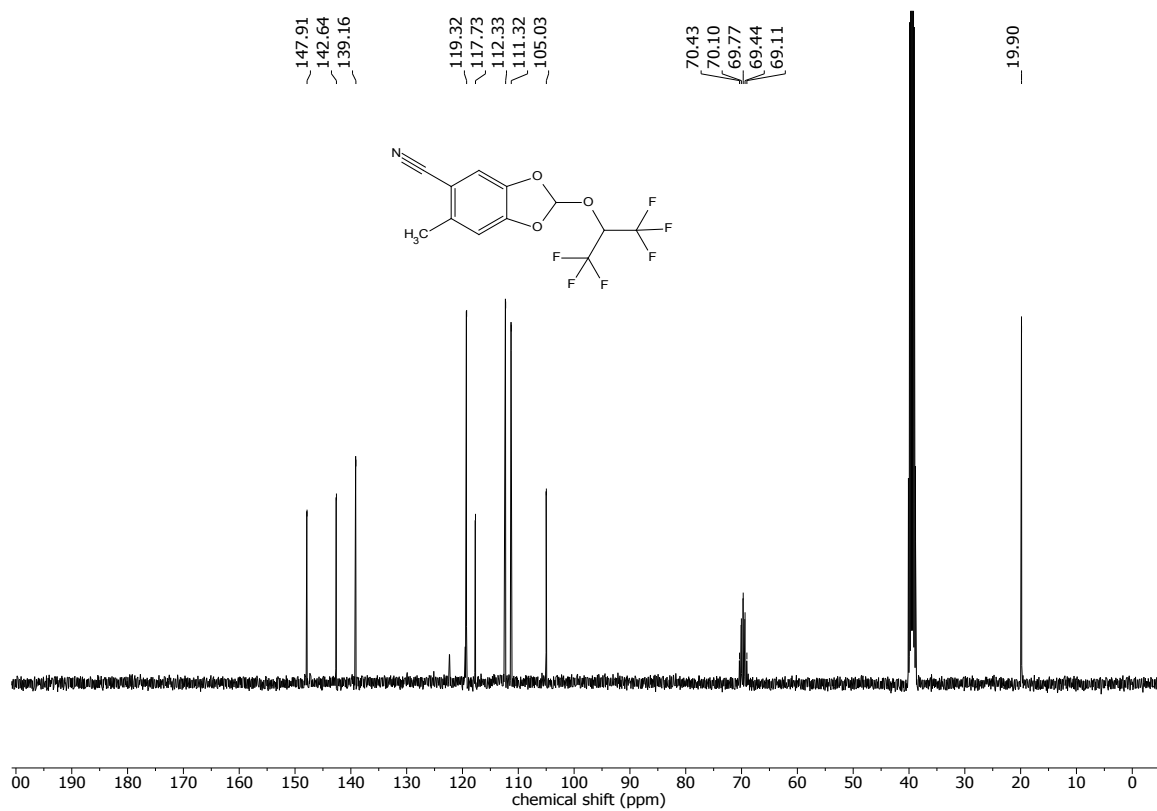


¹H NMR of 5-Chlor-2-(1-trifluoromethyl-(2,2,2-trifluoroethyl)oxy)-1,3-benzodioxole (1).

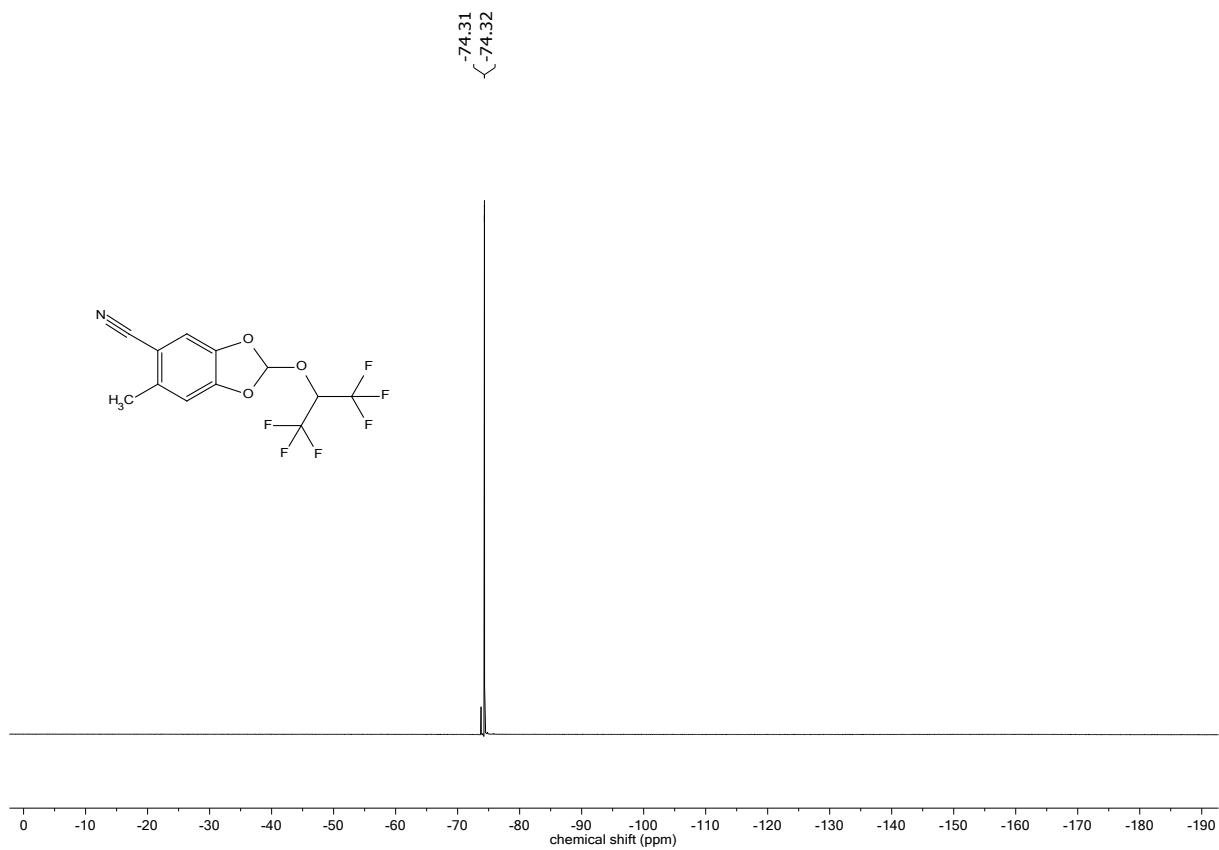


¹³C NMR of 5-Chlor-2-(1-trifluoromethyl-(2,2,2-trifluoroethyl)oxy)-1,3-benzodioxole (1).

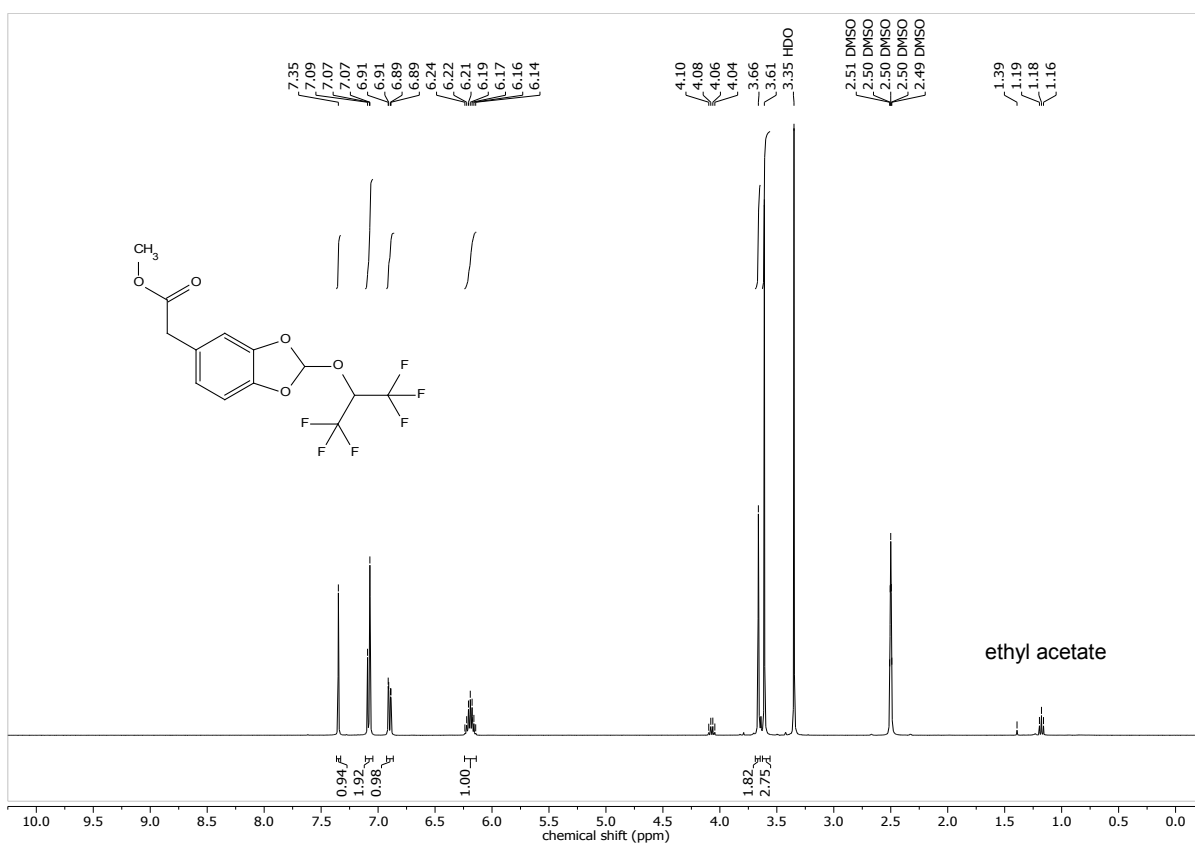




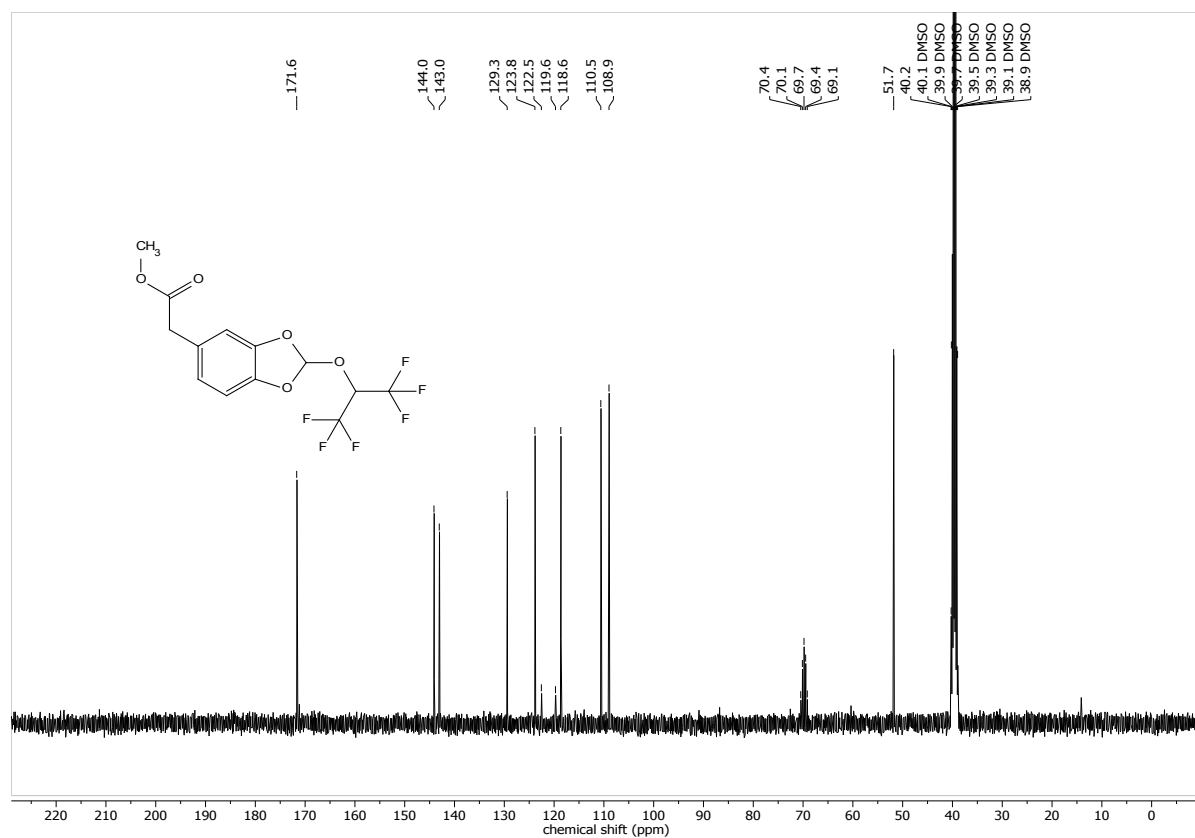
¹³C NMR of 2-(1-Trifluoromethyl-(2,2,2-trifluoroethyl)oxy)-5-cyano-6-methyl-1,3-benzodioxole (2).



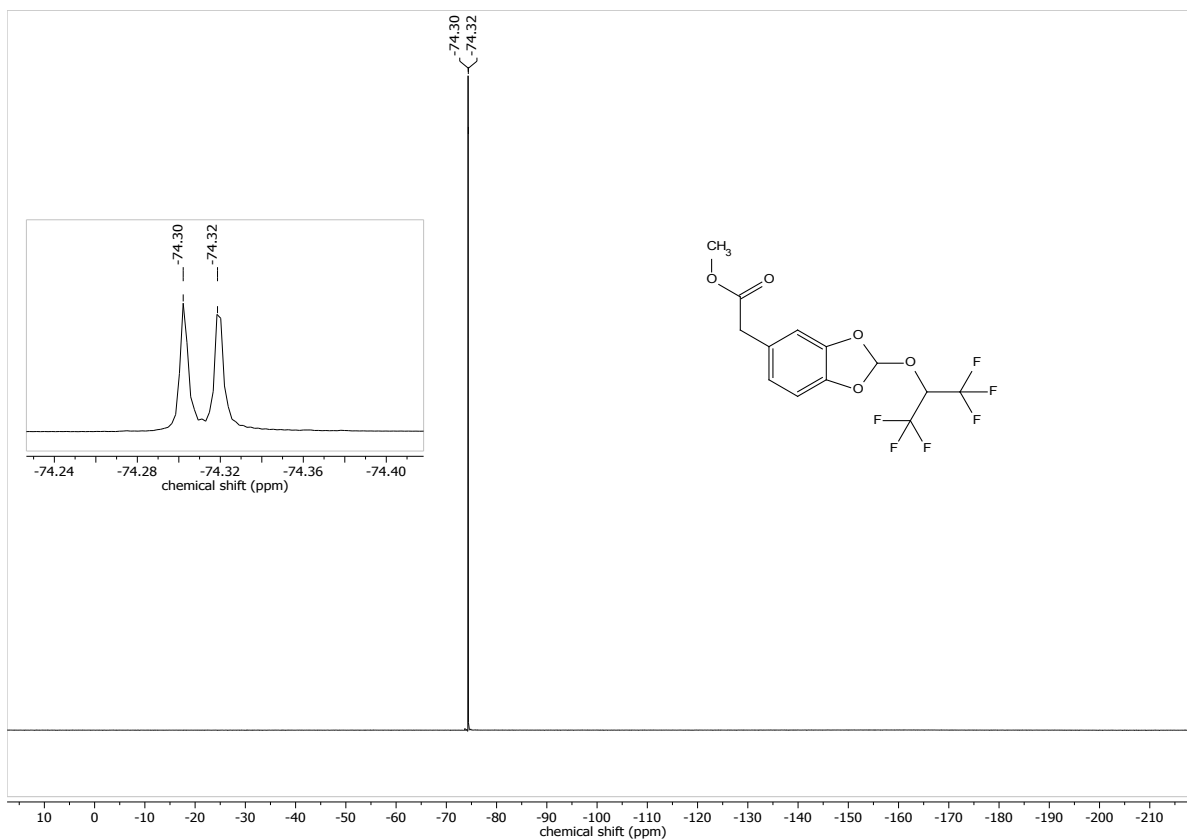
¹⁹F NMR of 2-(1-Trifluoromethyl-(2,2,2-trifluoroethyl)oxy)-5-cyano-6-methyl-1,3-benzodioxole (2).



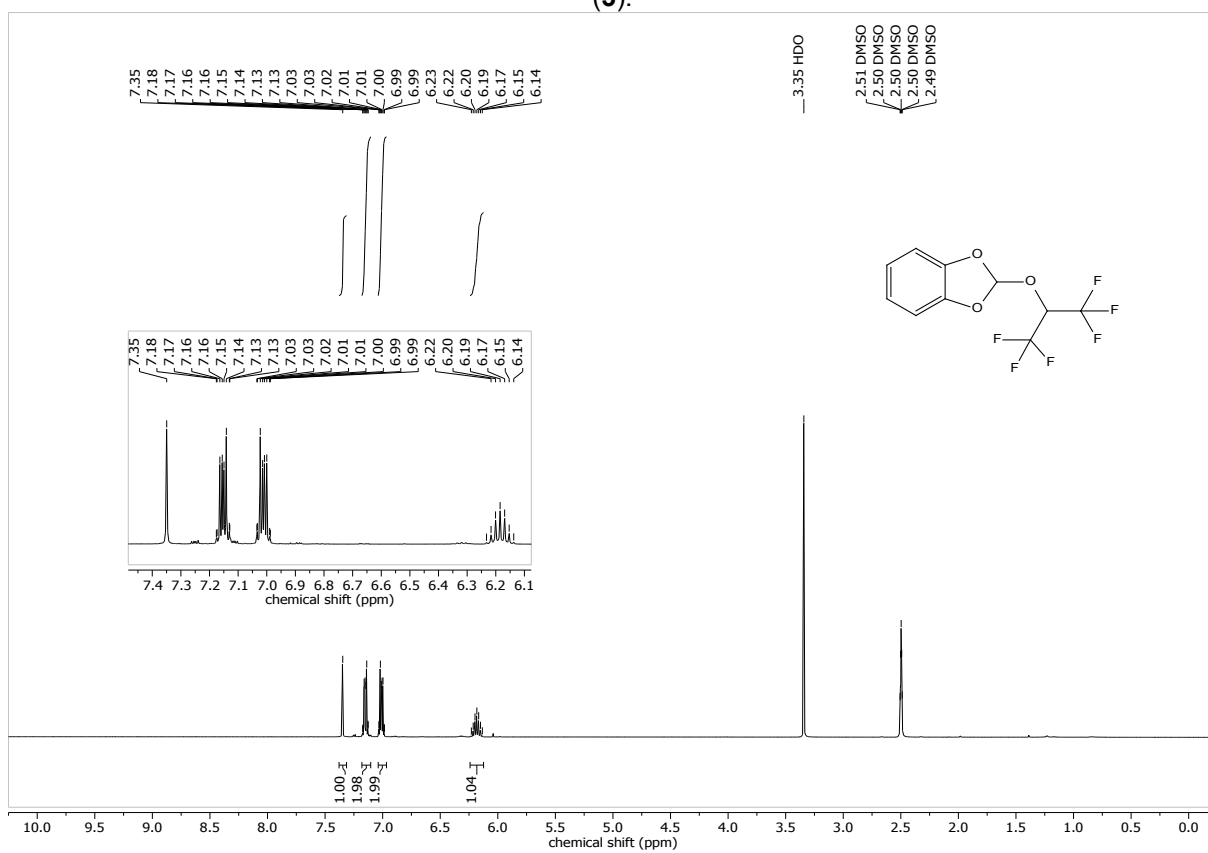
¹H NMR of 2-(1-Trifluoromethyl-(2,2,2-trifluoroethyl)oxy)-5-(methoxycarbonylmethyl)-1,3-benzodioxole (3).



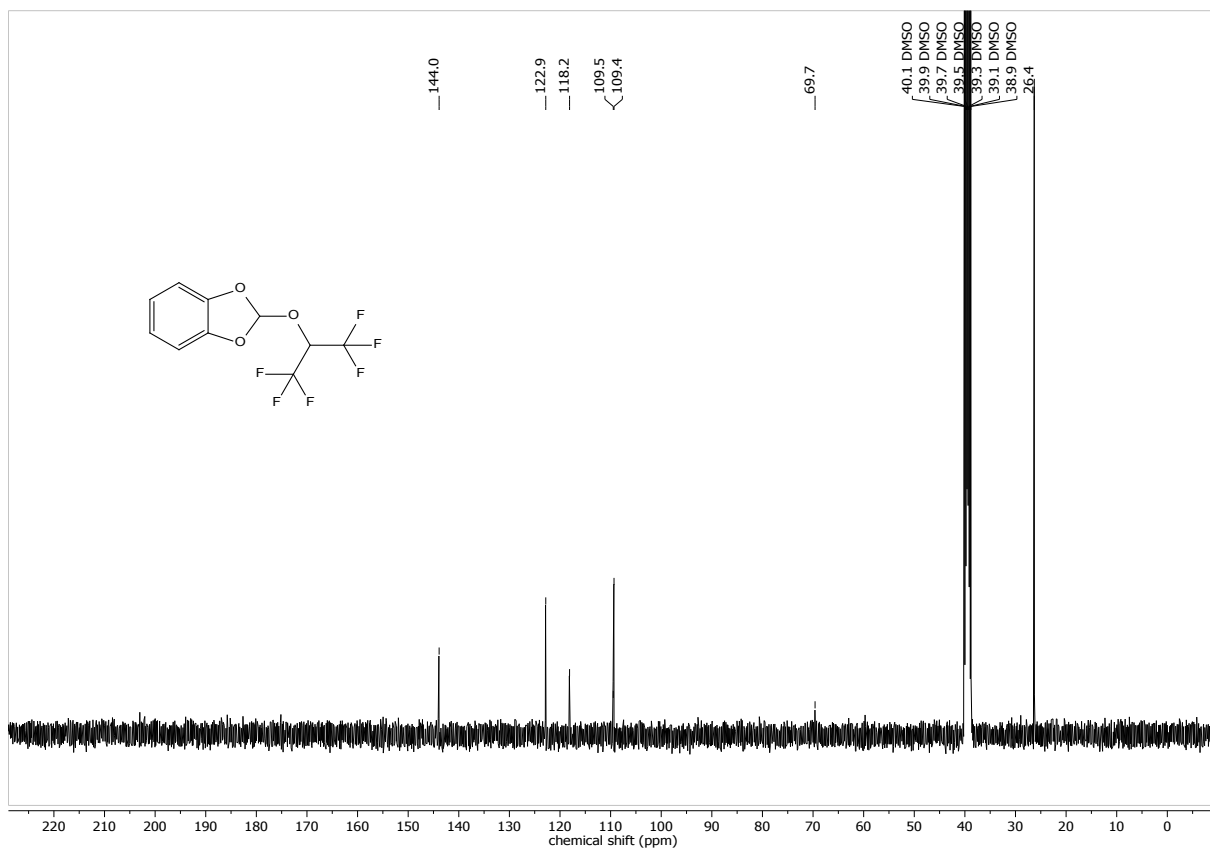
¹³C NMR of 2-(1-Trifluoromethyl-(2,2,2-trifluoroethyl)oxy)-5-(methoxycarbonylmethyl)-1,3-benzodioxole (3).



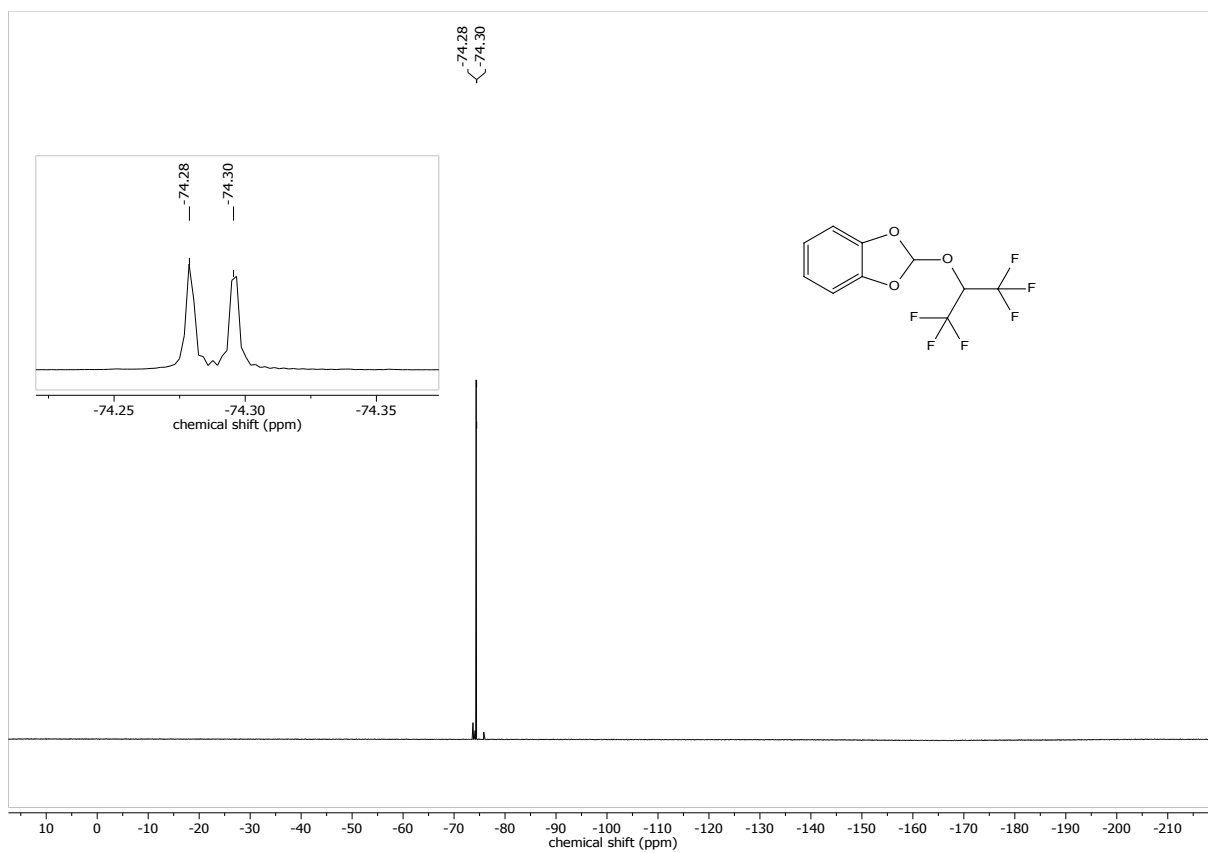
¹⁹F NMR of 2-(1-Trifluoromethyl-(2,2,2-trifluoroethyl)oxy)-5-(methoxycarbonylmethyl)-1,3-benzodioxole (3).



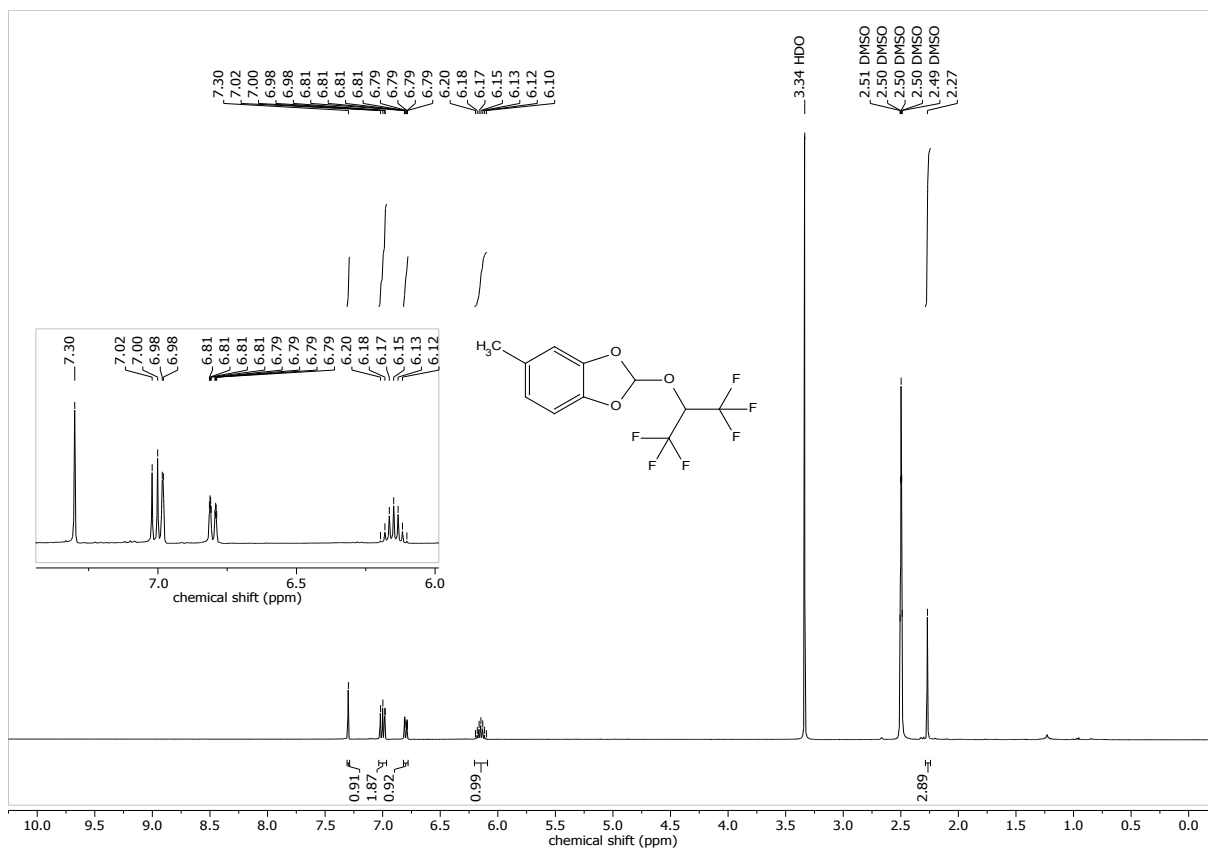
¹H NMR of 2-(1-Trifluoromethyl-(2,2,2-trifluoroethyl)oxy)-1,3-benzodioxole (4).



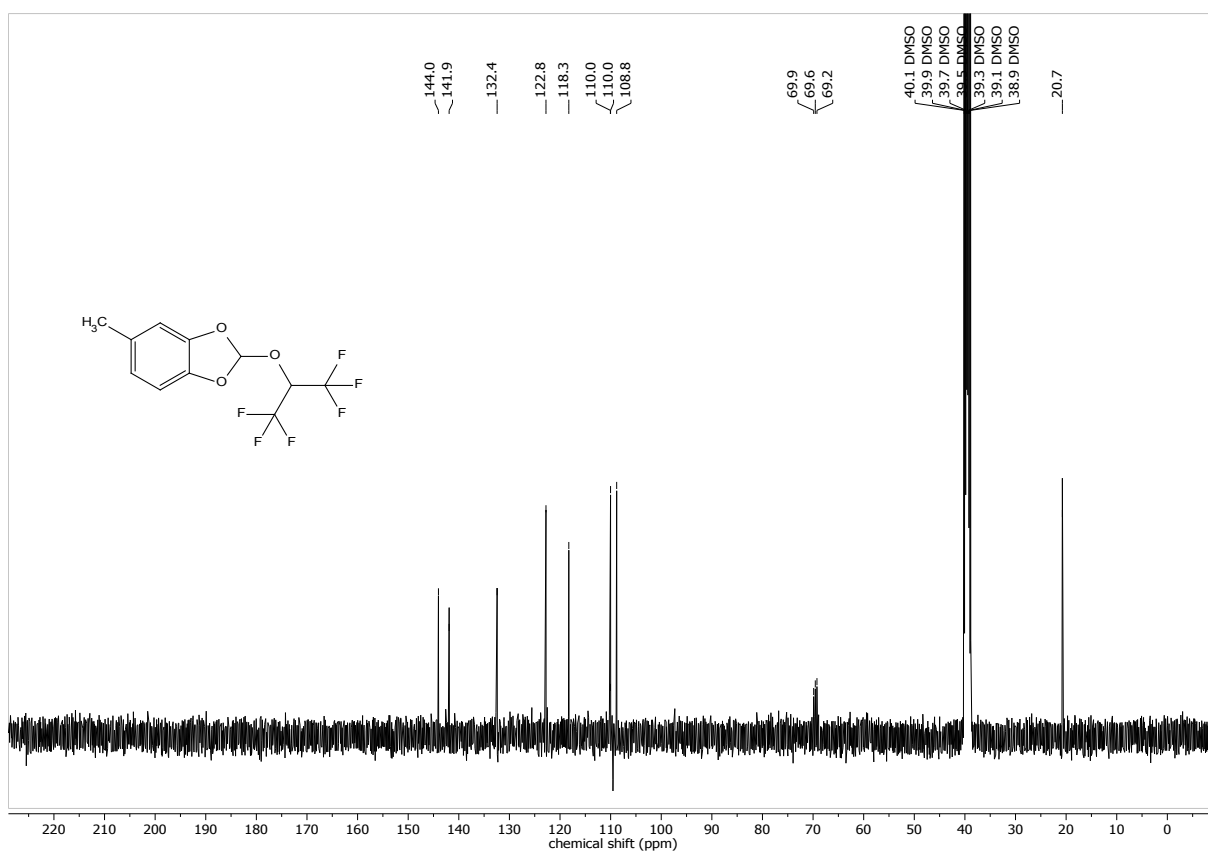
¹³C NMR of 2-(1-Trifluoromethyl-(2,2,2-trifluoroethyl)oxy)-1,3-benzodioxole (4).



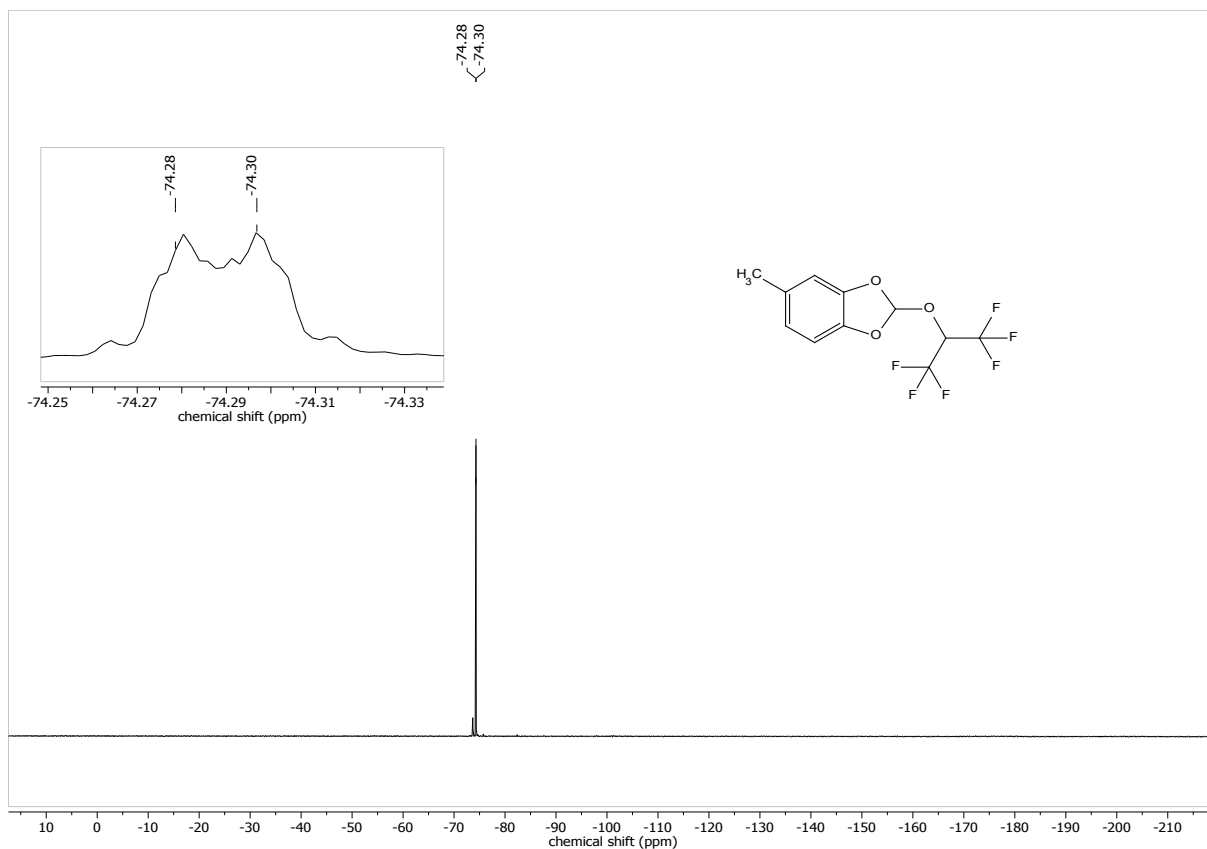
¹⁹F NMR of 2-(1-Trifluoromethyl-(2,2,2-trifluoroethyl)oxy)-1,3-benzodioxole (4).



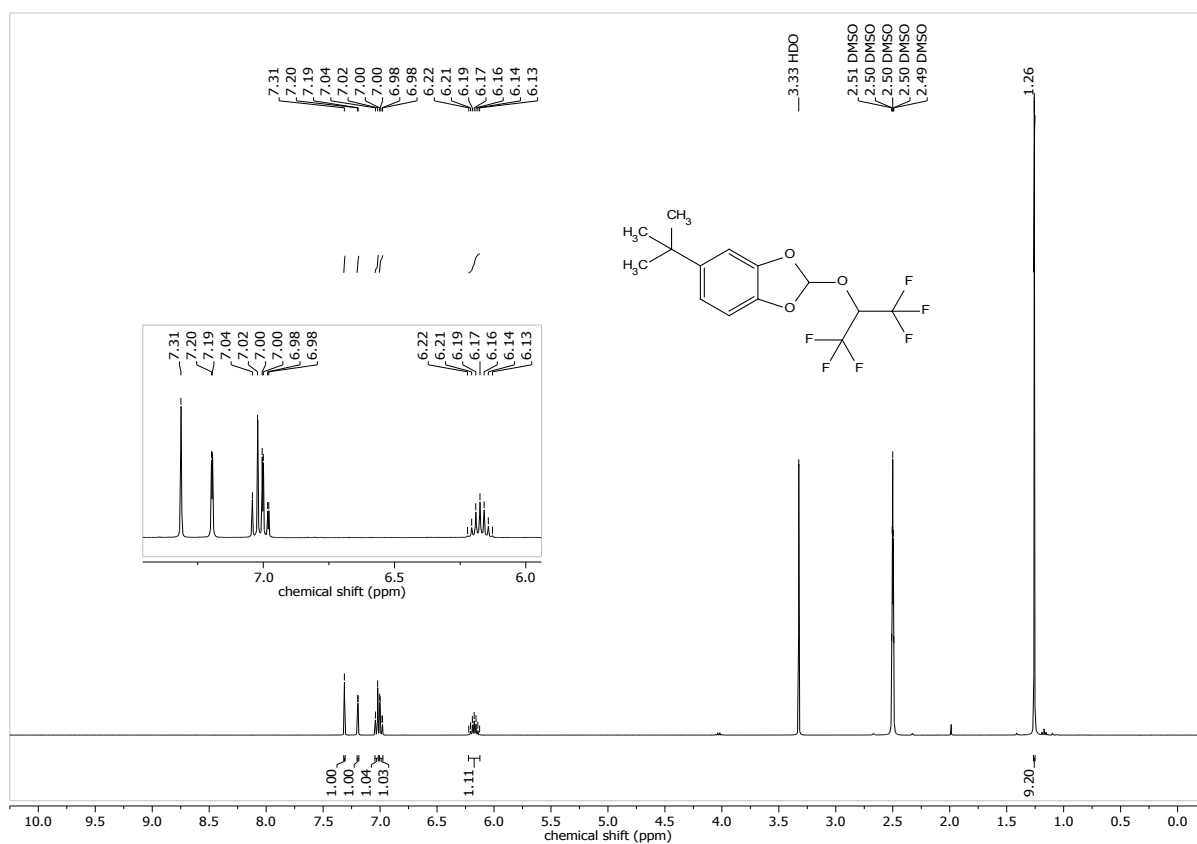
¹H NMR of 2-(1-Trifluoromethyl-(2,2,2-trifluoroethoxy)-5-methyl-1,3-benzodioxole (5).



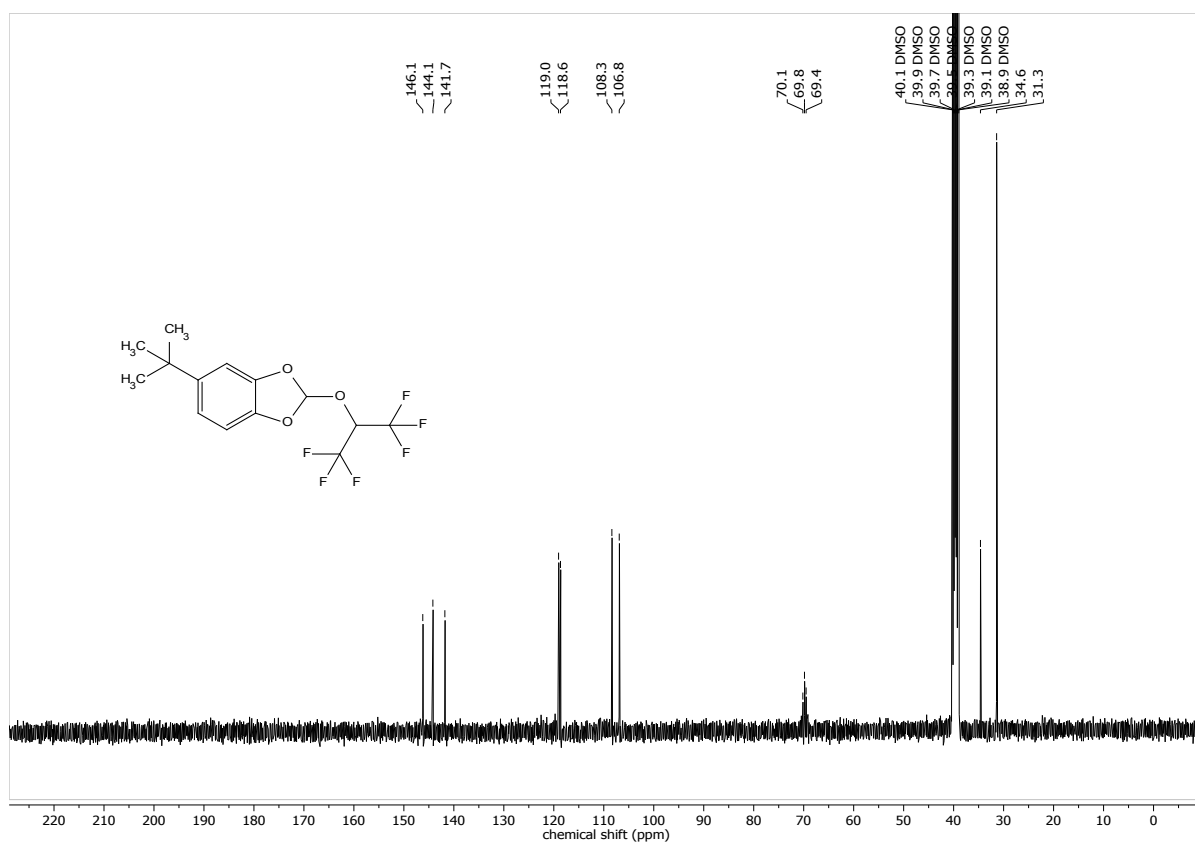
¹³C NMR of 2-(1-Trifluoromethyl-(2,2,2-trifluoroethoxy)-5-methyl-1,3-benzodioxole (5).



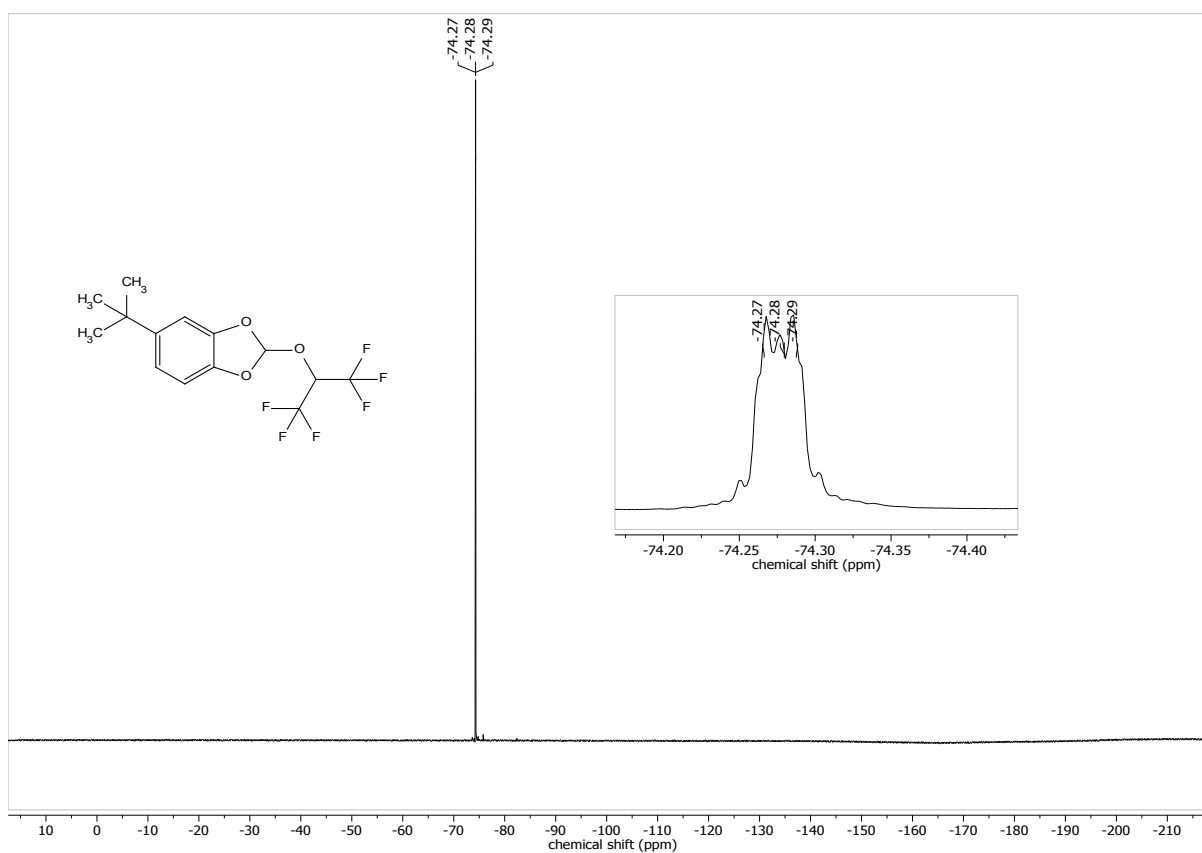
^{19}F NMR of 2-(1-Trifluoromethyl-(2,2,2-trifluoroethyl)oxy)-5-methyl-1,3-benzodioxole (**5**).



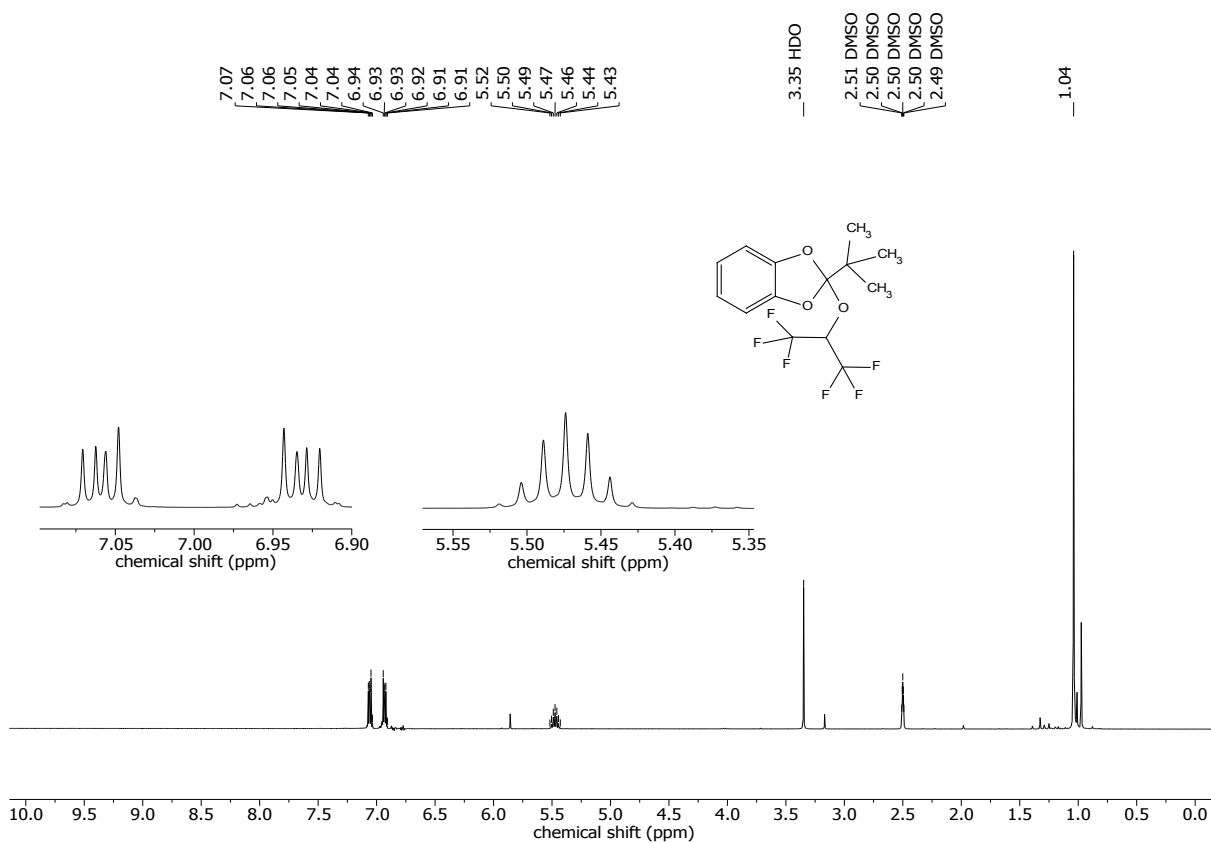
^1H NMR of 2-(1-Trifluoromethyl-(2,2,2-trifluoroethyl)oxy)-5-(1,1-dimethylethyl)-1,3-benzodioxole (**6**).



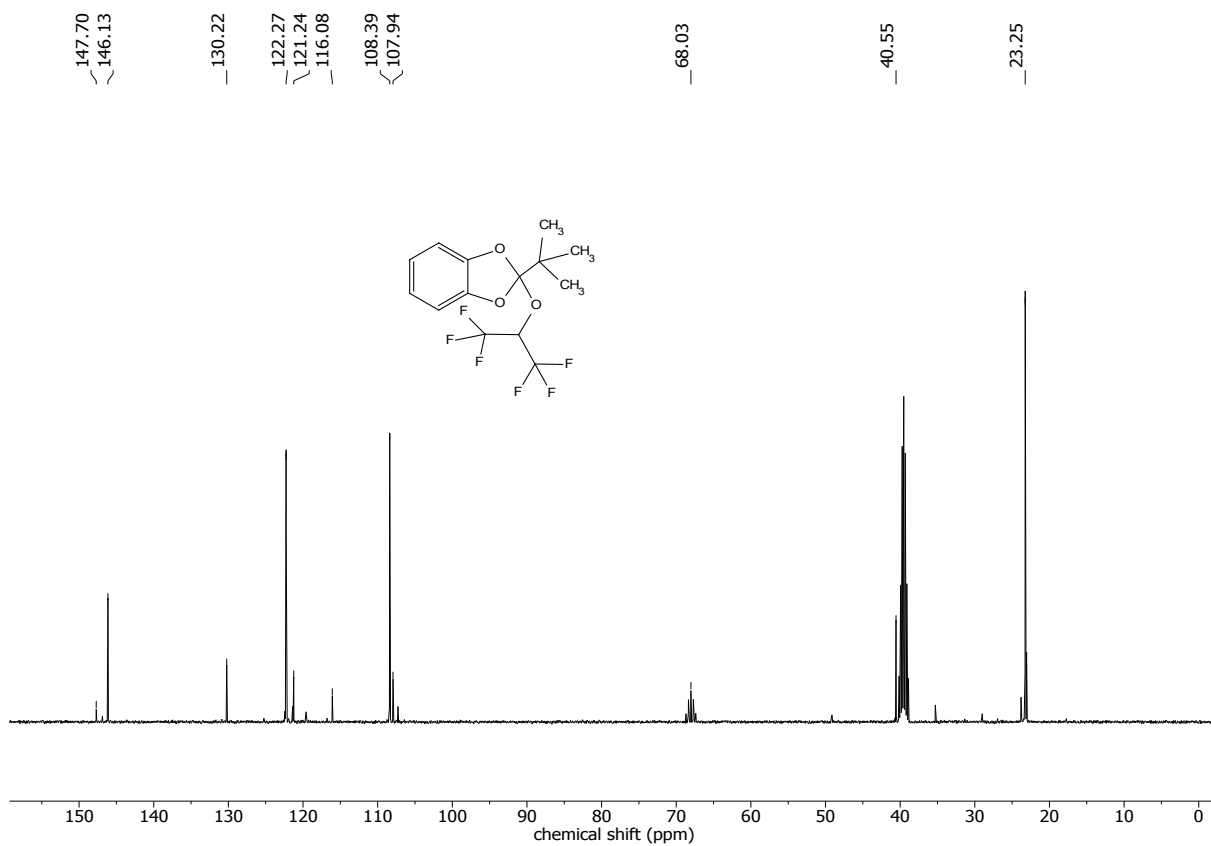
¹³C NMR of 2-(1-Trifluoromethyl-(2,2,2-trifluoroethyl)oxy)-5-(1,1-dimethylethyl)-1,3-benzodioxole (**6**).



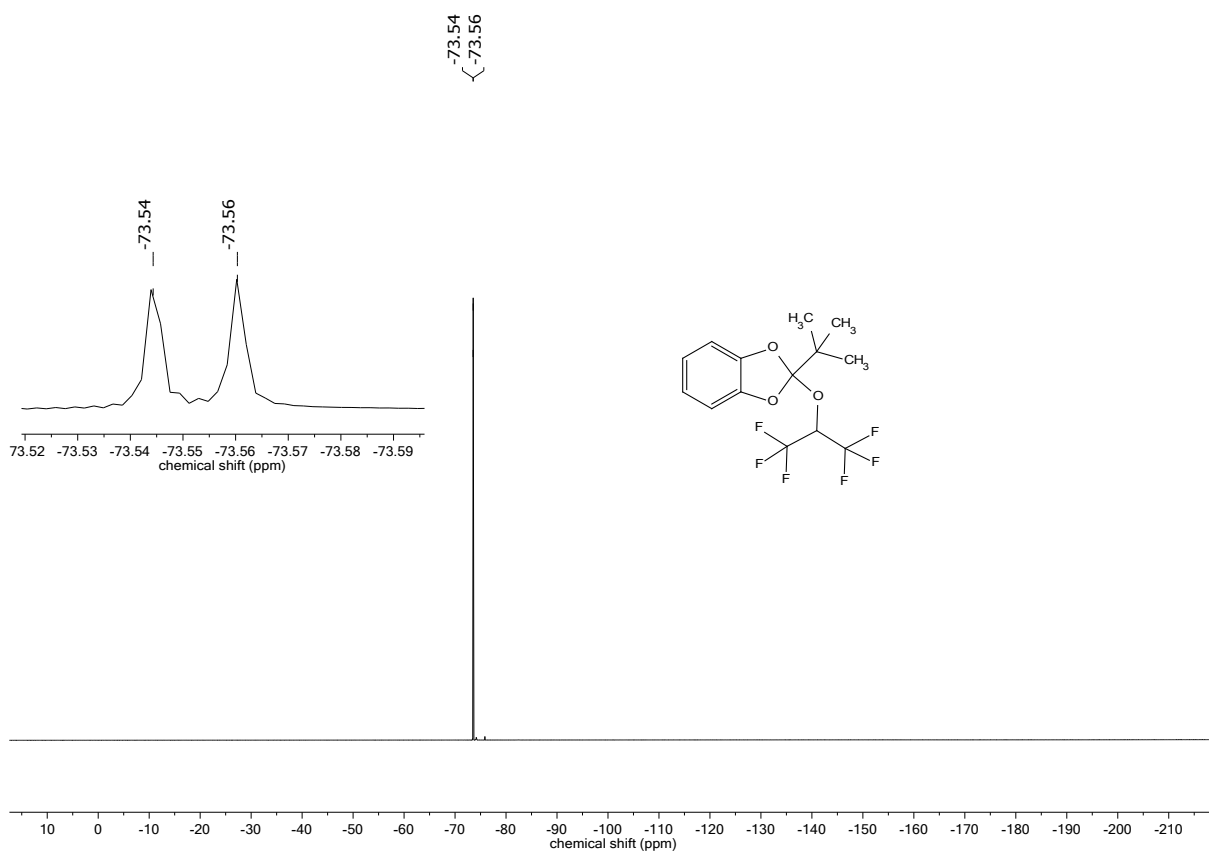
¹⁹F NMR of 2-(1-Trifluoromethyl-(2,2,2-trifluoroethyl)oxy)-5-(1,1-dimethylethyl)-1,3-benzodioxole (**6**).



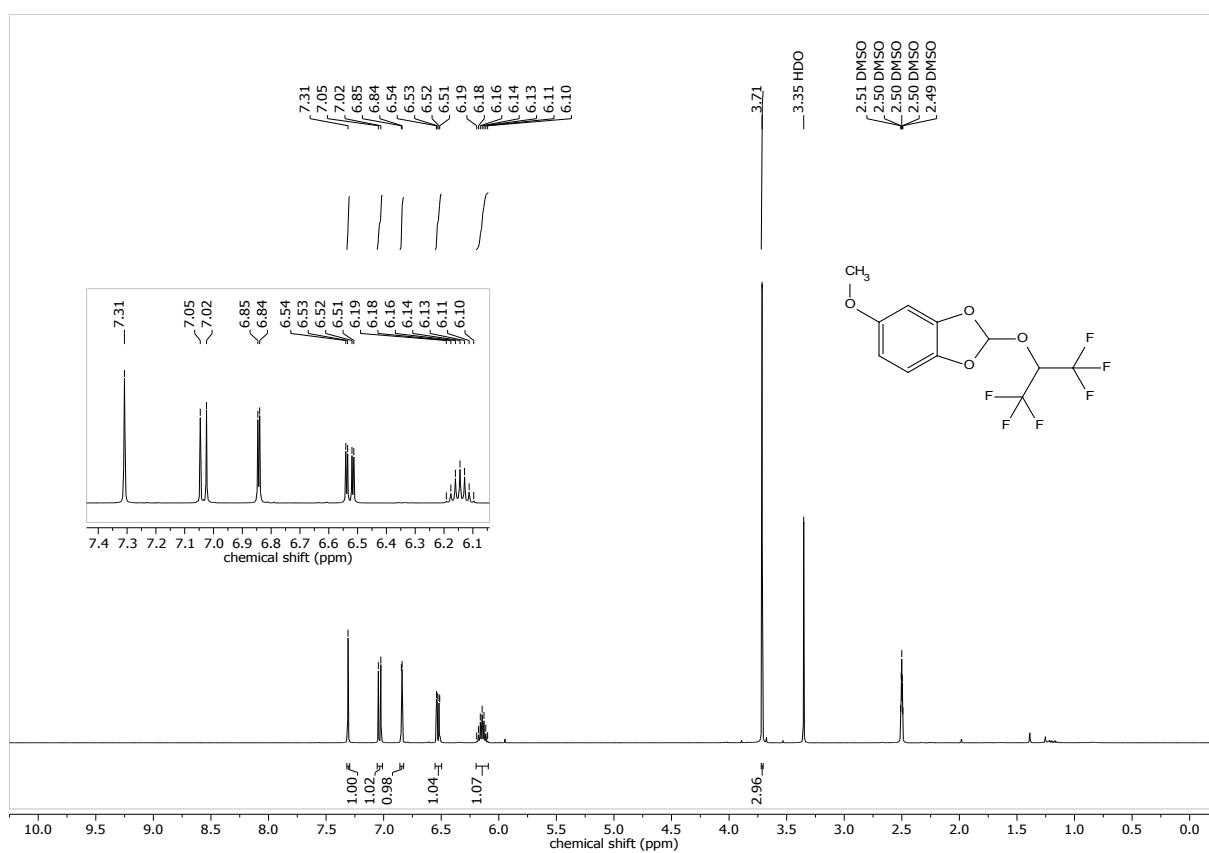
^1H NMR of 2-(1-Trifluoromethyl-(2,2,2-trifluoroethyl)oxy)-2-(1,1-dimethylethyl)-1,3-benzodioxole (7).



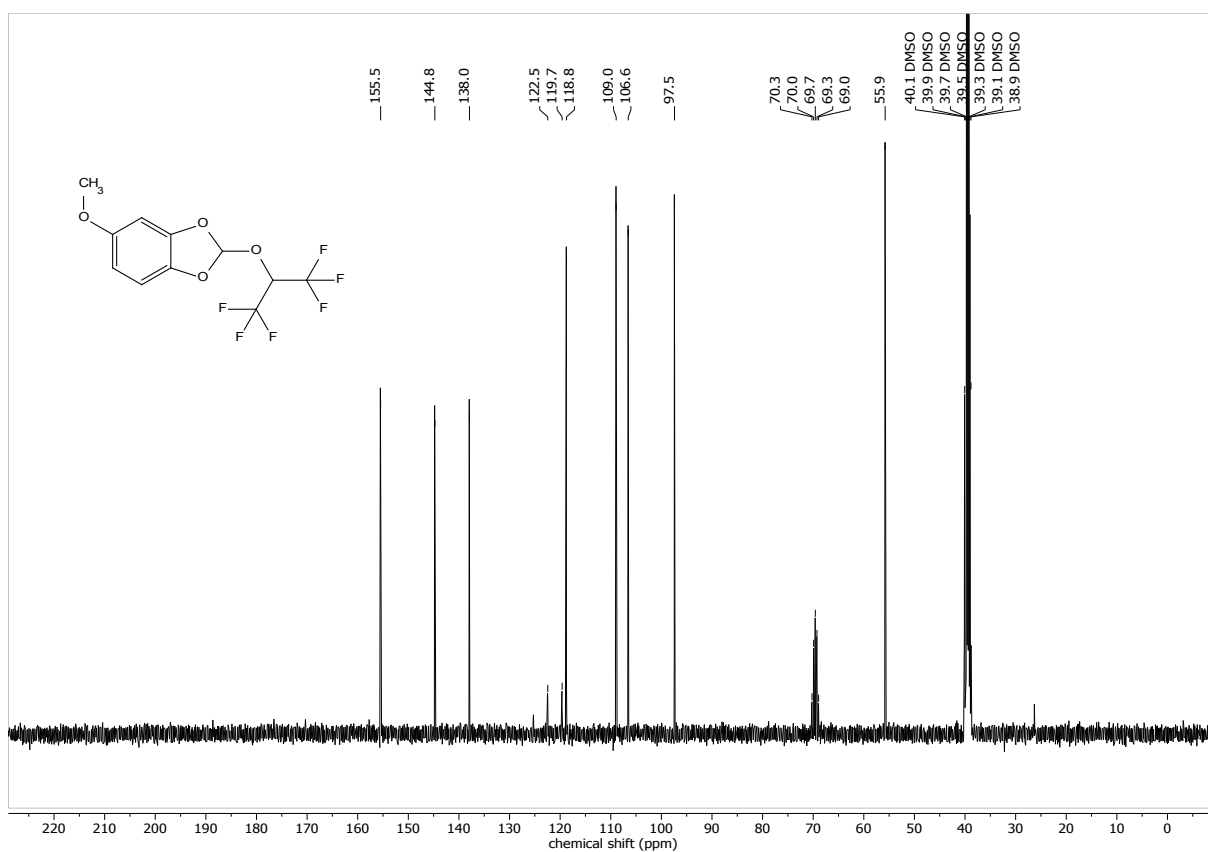
^{13}C NMR of 2-(1-Trifluoromethyl-(2,2,2-trifluoroethyl)oxy)-2-(1,1-dimethylethyl)-1,3-benzodioxole (7).



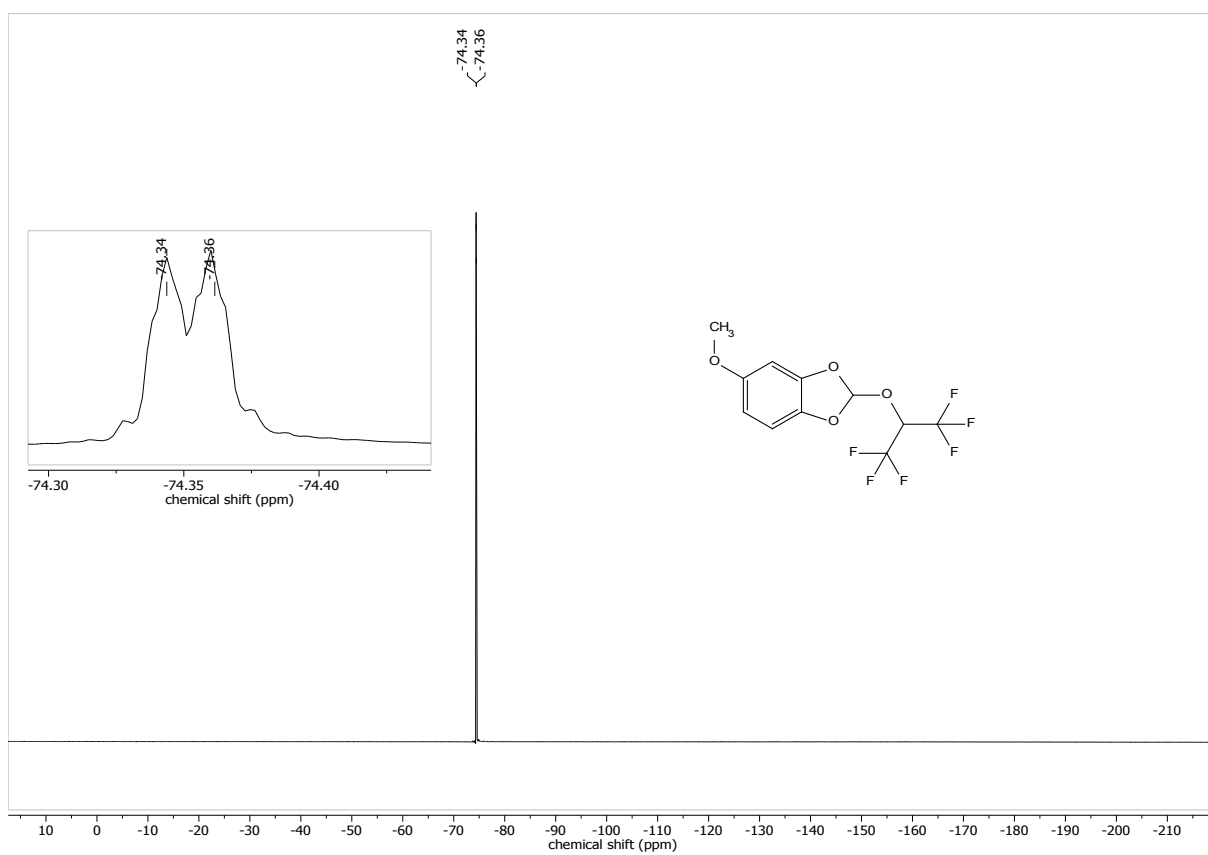
¹⁹F NMR of 2-(1-Trifluoromethyl-(2,2,2-trifluoroethyl)oxy)-2-(1,1-dimethylethyl)-1,3-benzodioxole (7).



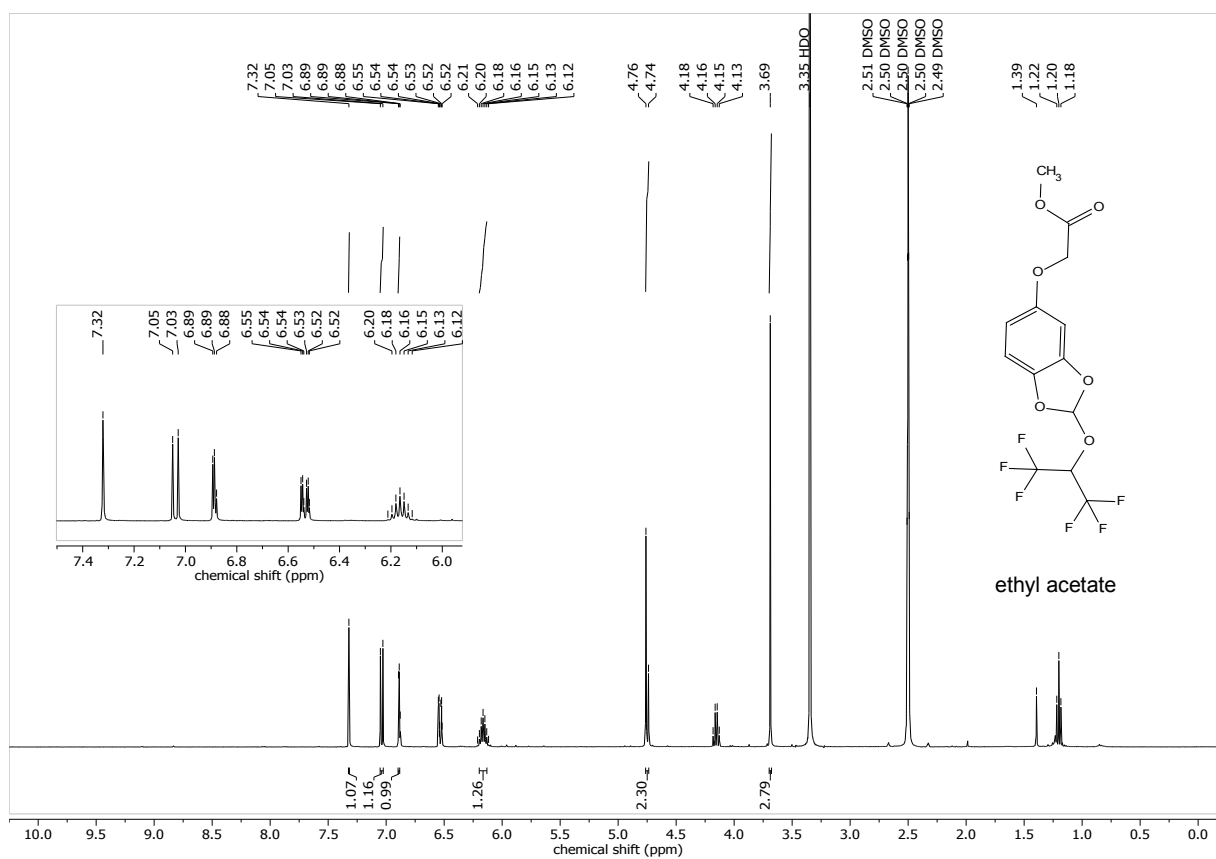
¹H NMR of 2-(1-Trifluoromethyl-(2,2,2-trifluoroethyl)oxy)-5-methoxy-1,3-benzodioxole (8).



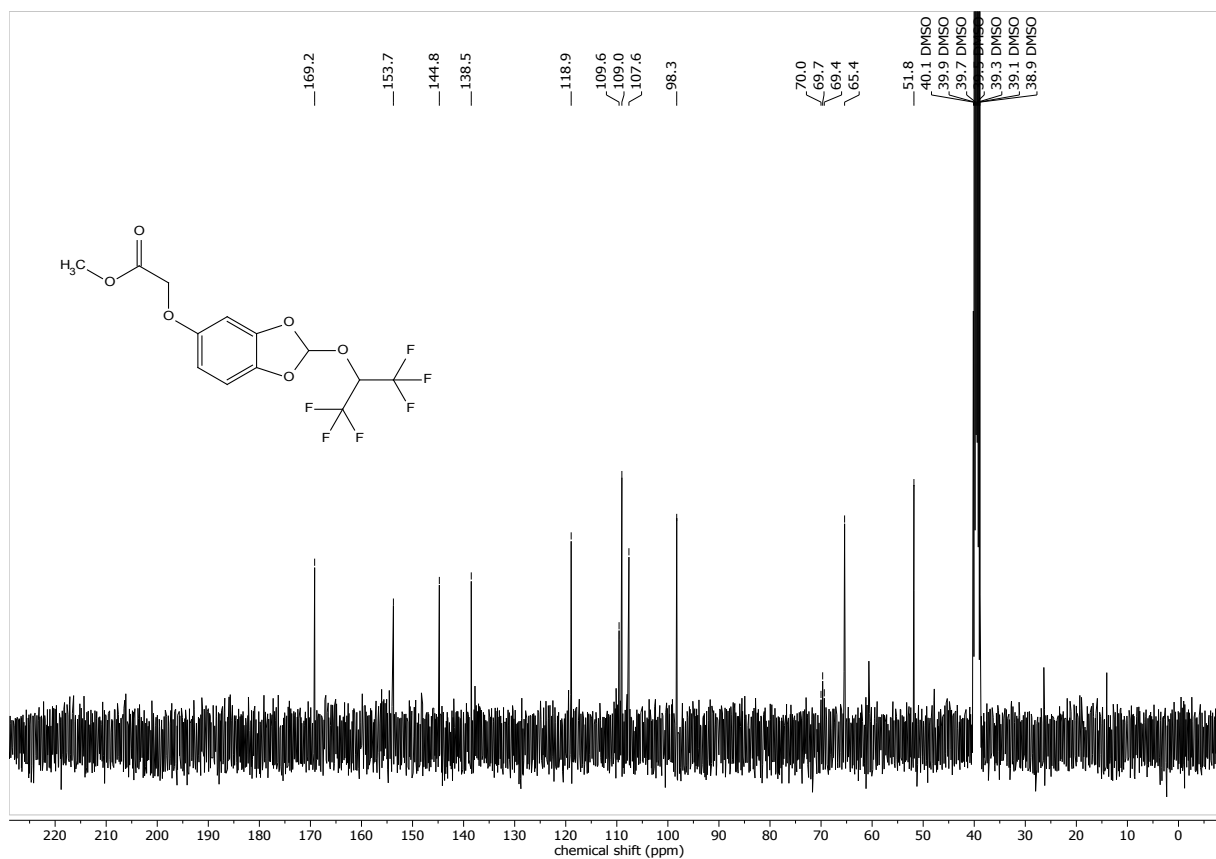
¹³C NMR of 2-(1-Trifluoromethyl-(2,2,2-trifluoroethyl)oxy)-5-methoxy-1,3-benzodioxole (**8**).



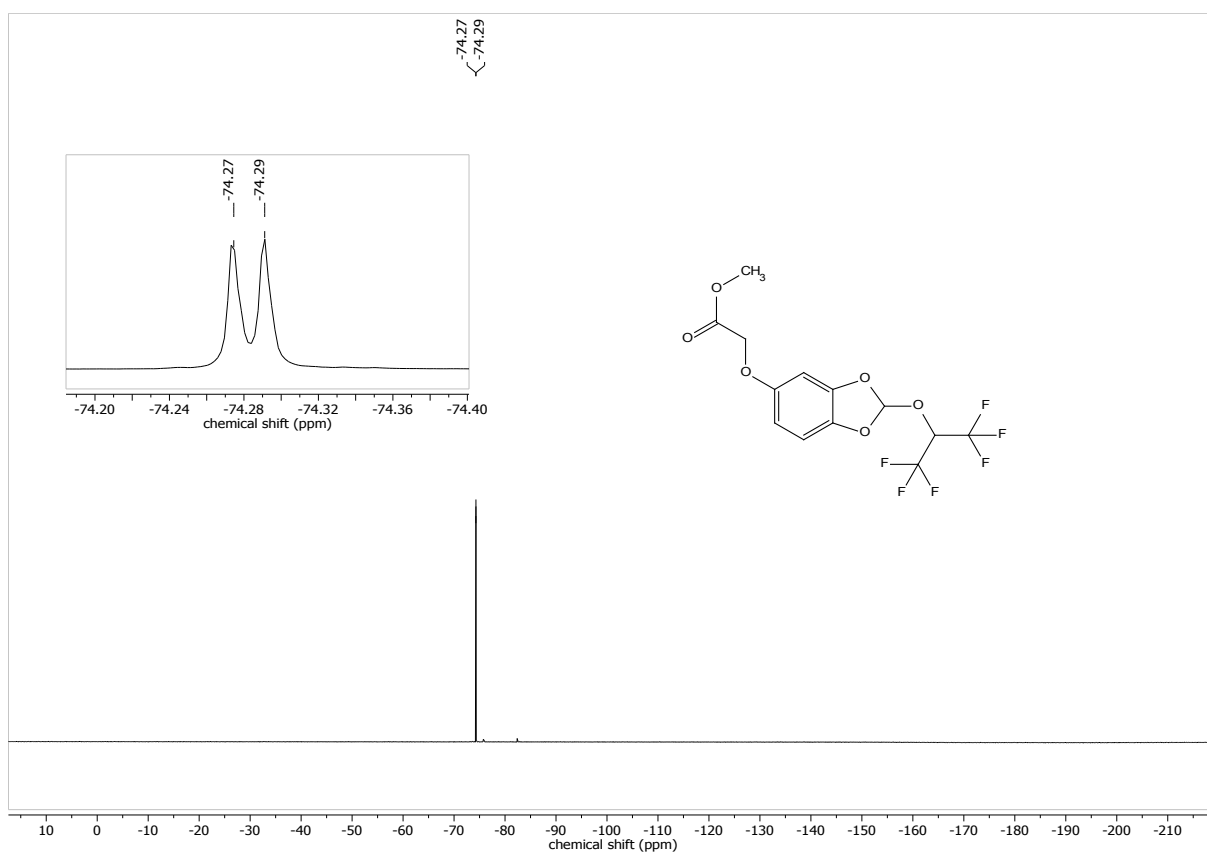
¹⁹F NMR of 2-(1-Trifluoromethyl-(2,2,2-trifluoroethyl)oxy)-5-methoxy-1,3-benzodioxole (**8**).



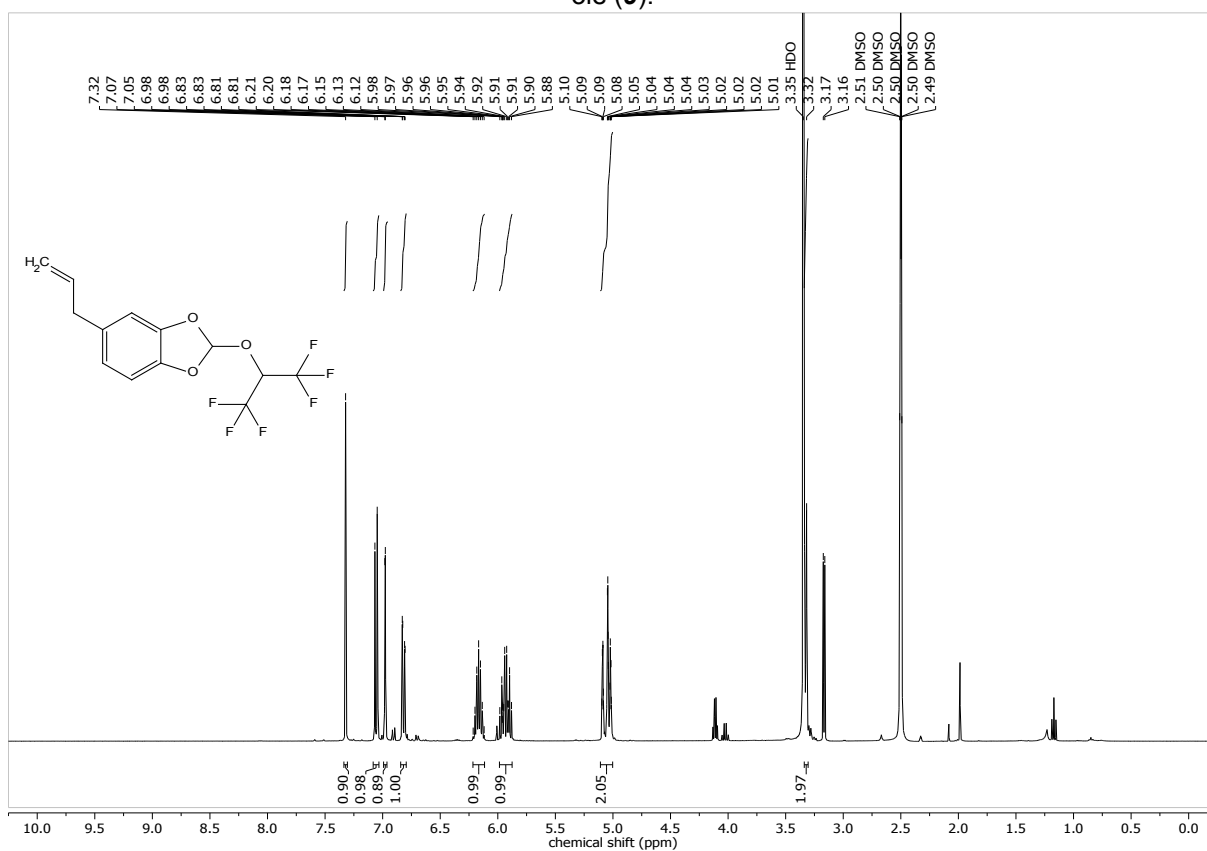
¹H NMR of 2-(1-Trifluoromethyl-(2,2,2-trifluoroethyl)oxy)-5-(methoxycarbonylmethoxy)-1,3-benzodioxole (9).



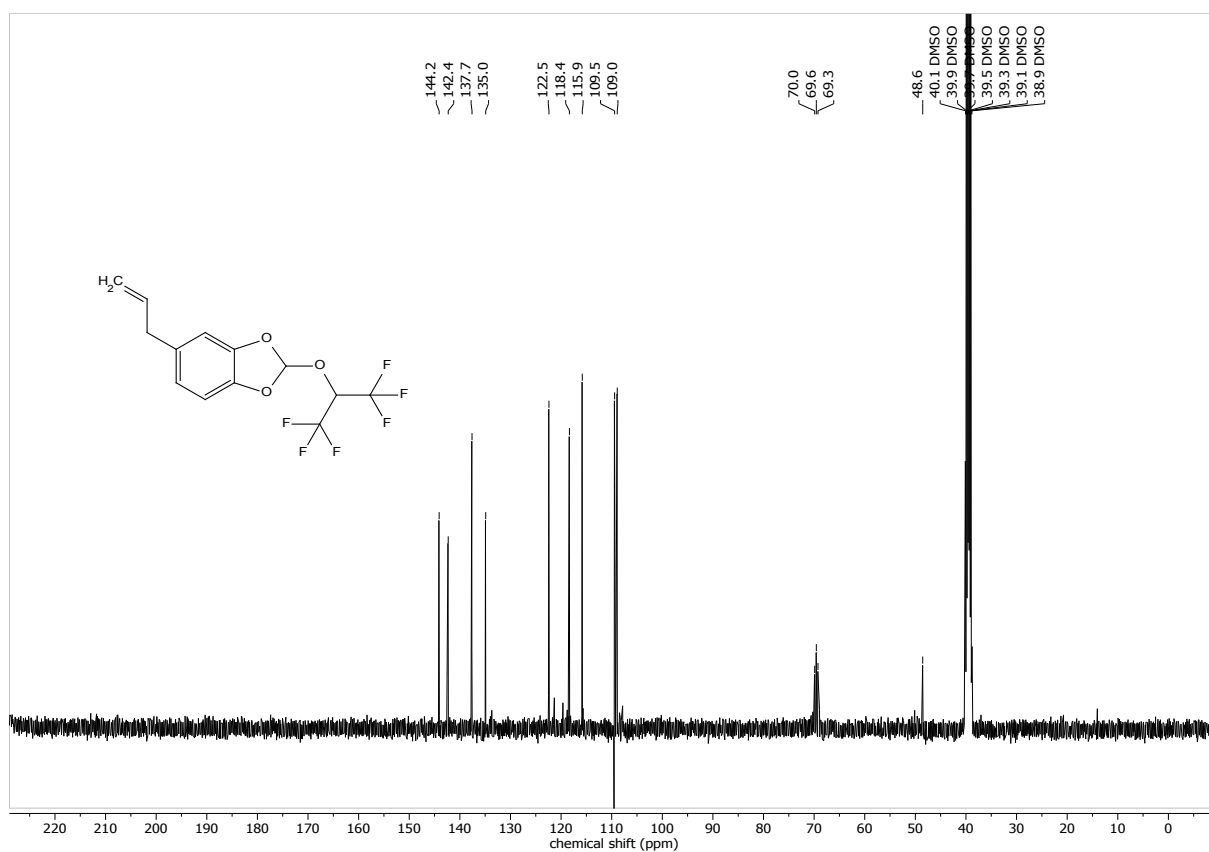
¹³C NMR 2-(1-Trifluoromethyl-(2,2,2-trifluoroethyl)-5-(methoxycarbonylmethoxy)-1,3-benzodioxole (9).



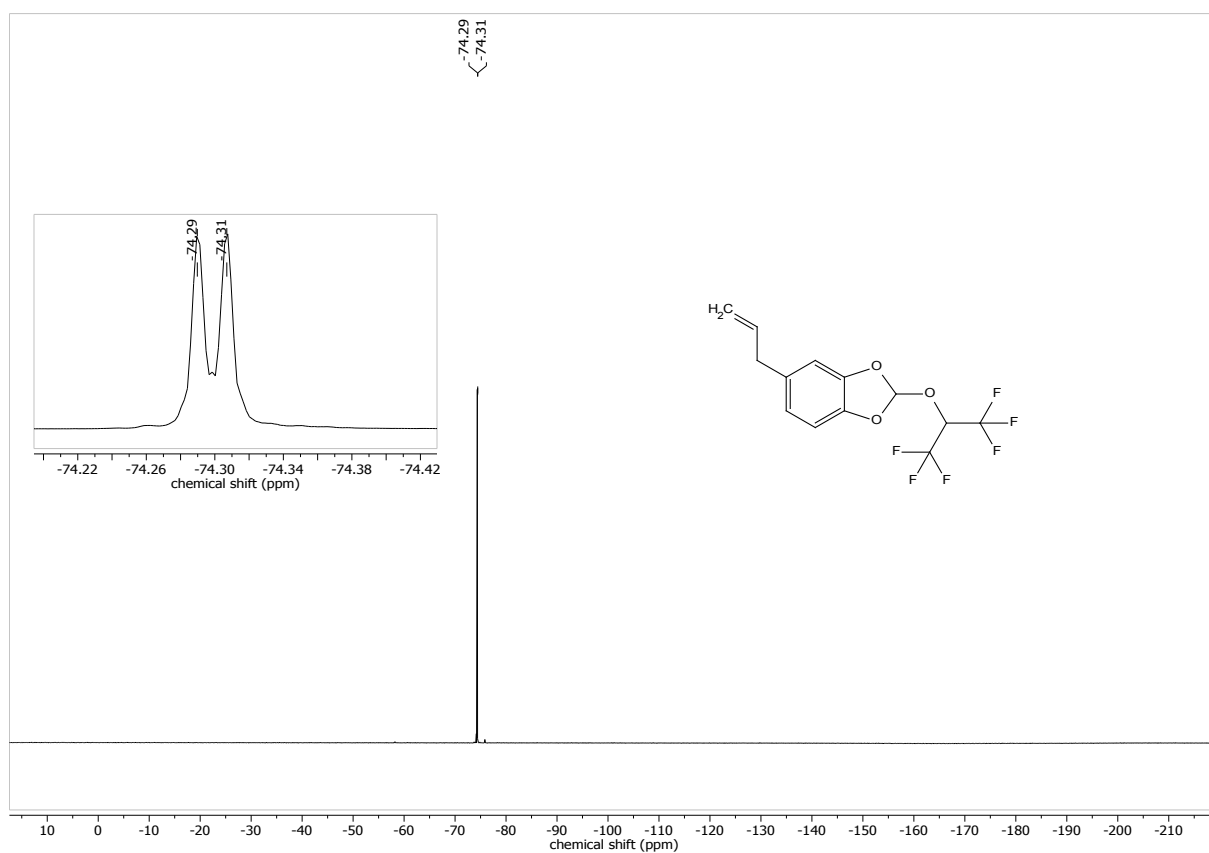
^{19}F NMR of 2-(1-Trifluoromethyl-(2,2,2-trifluoroethyl)oxy)-5-(methoxycarbonylmethoxy)-1,3-benzodioxole (**9**).



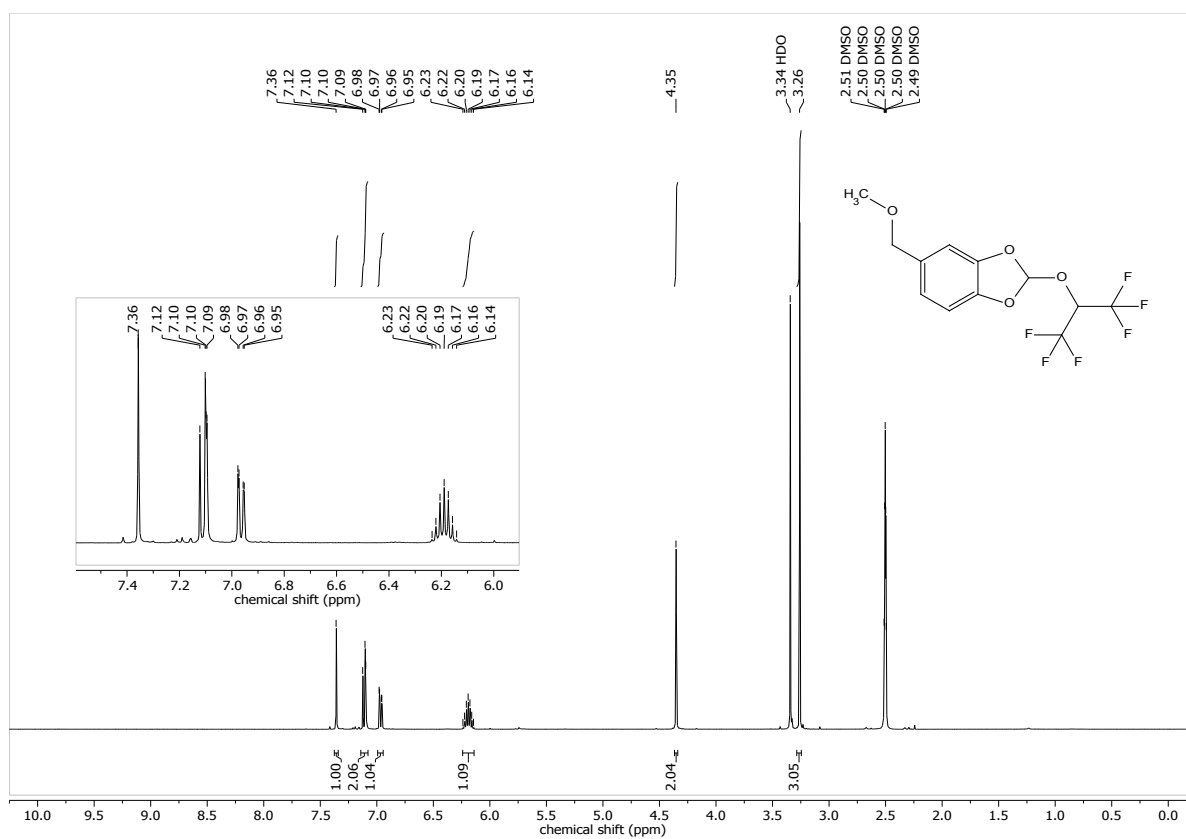
^1H NMR of 5-Allyl-2-(1-trifluoromethyl-(2,2,2-trifluoroethyl)oxy)-1,3-benzodioxole (**10**).



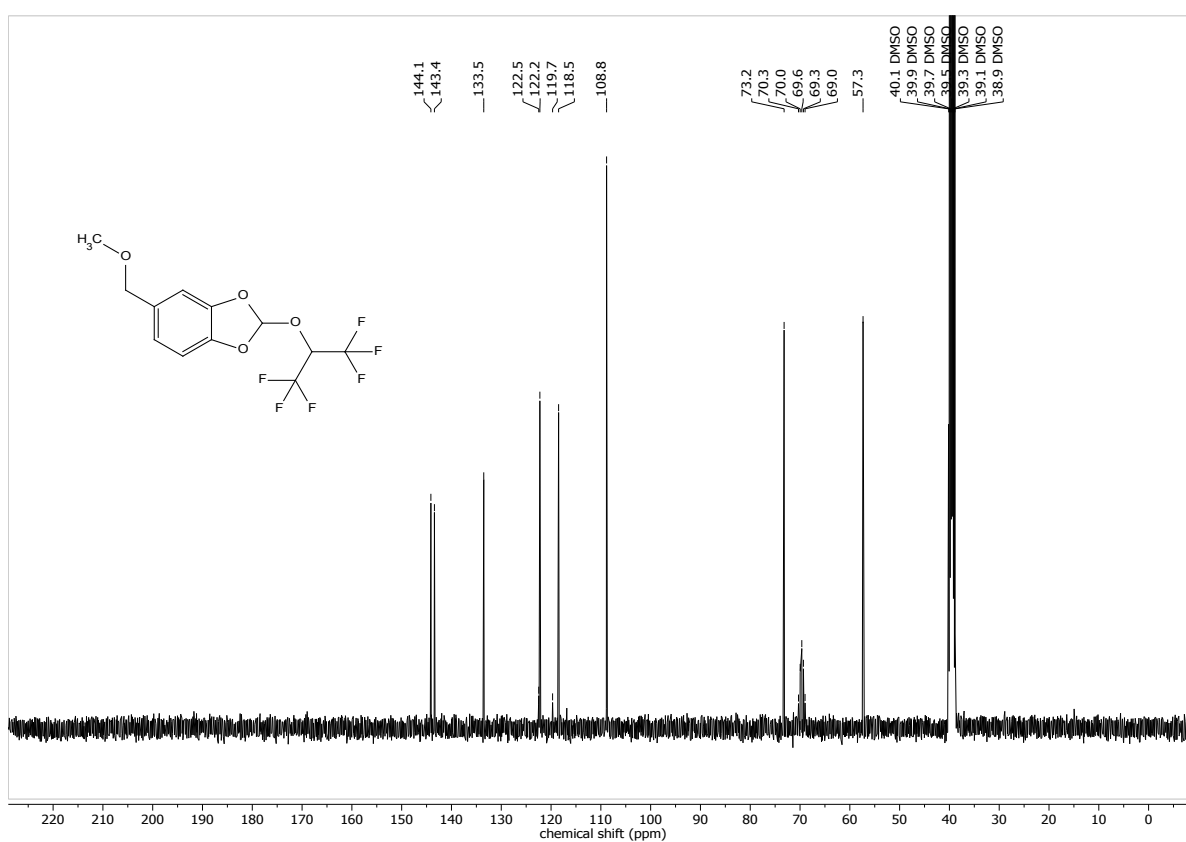
¹³C NMR of 5-Allyl-2-(1-trifluoromethyl-(2,2,2-trifluoroethyl)oxy)-1,3-benzodioxole (**10**).



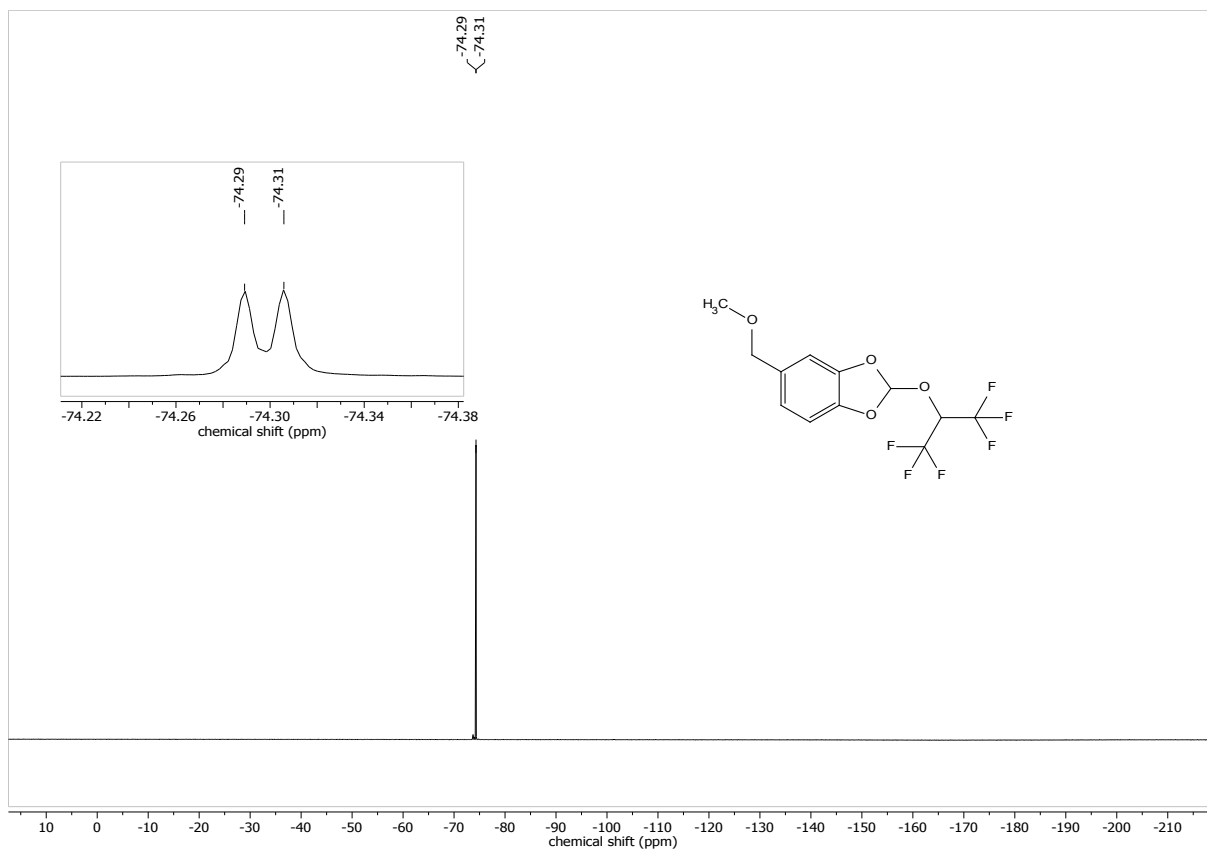
¹⁹F NMR of 5-Allyl-2-(1-trifluoromethyl-(2,2,2-trifluoroethyl)oxy)-1,3-benzodioxole (**10**).



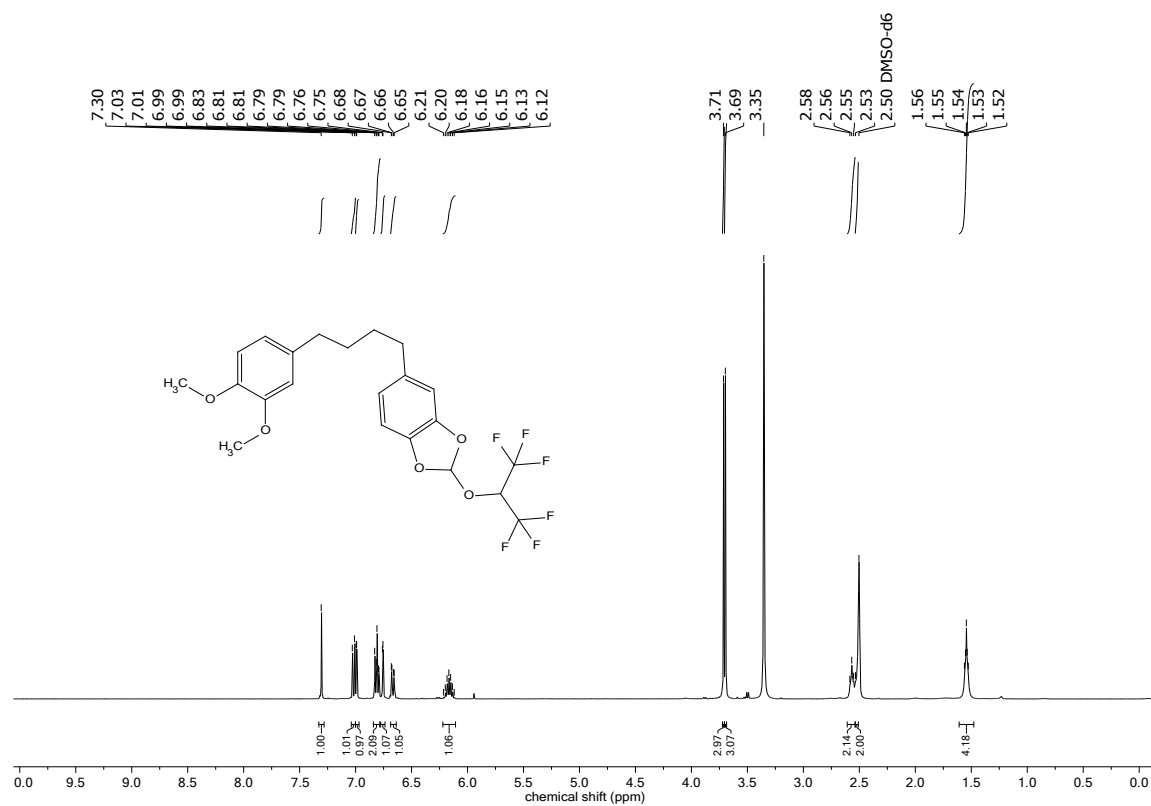
¹H NMR of 2-(1-Trifluoromethyl-(2,2,2-trifluoroethyl)oxy)-5-(methoxymethyl)-1,3-benzodioxole (11).



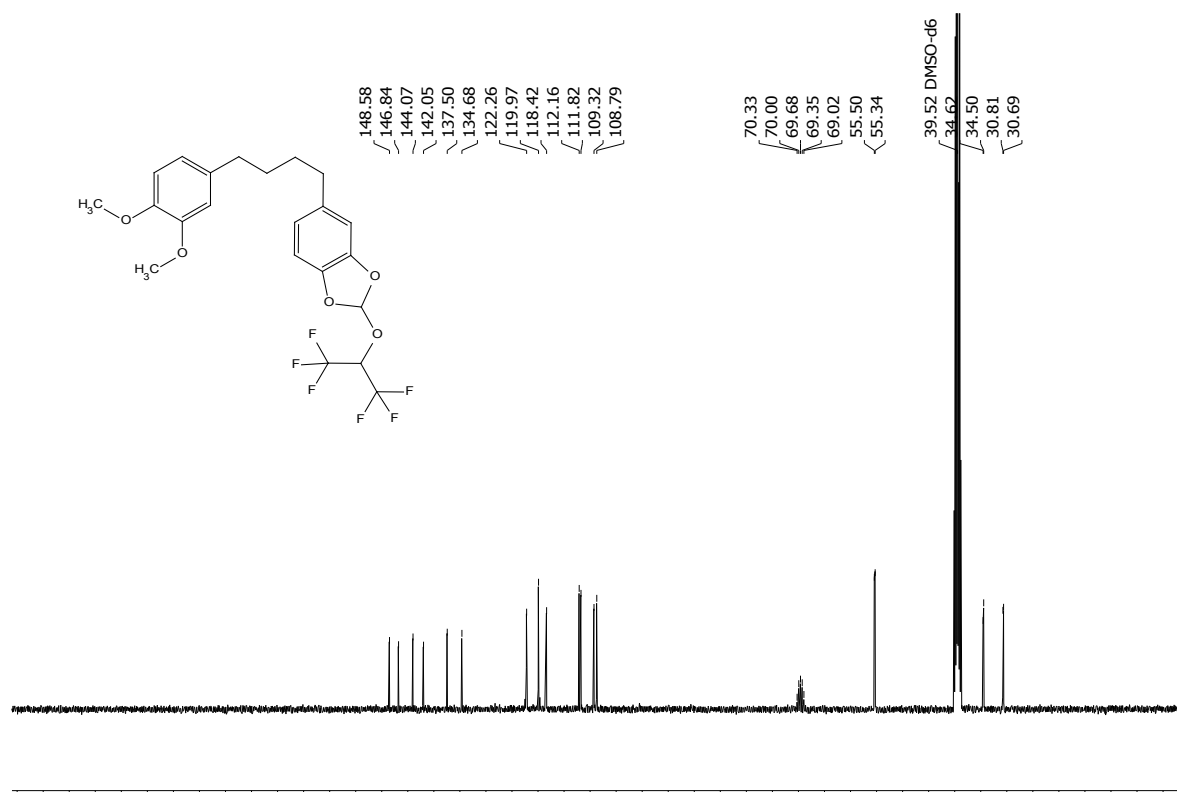
¹³C NMR of 2-(1-Trifluoromethyl-(2,2,2-trifluoroethyl)oxy)-5-(methoxymethyl)-1,3-benzodioxole (11).



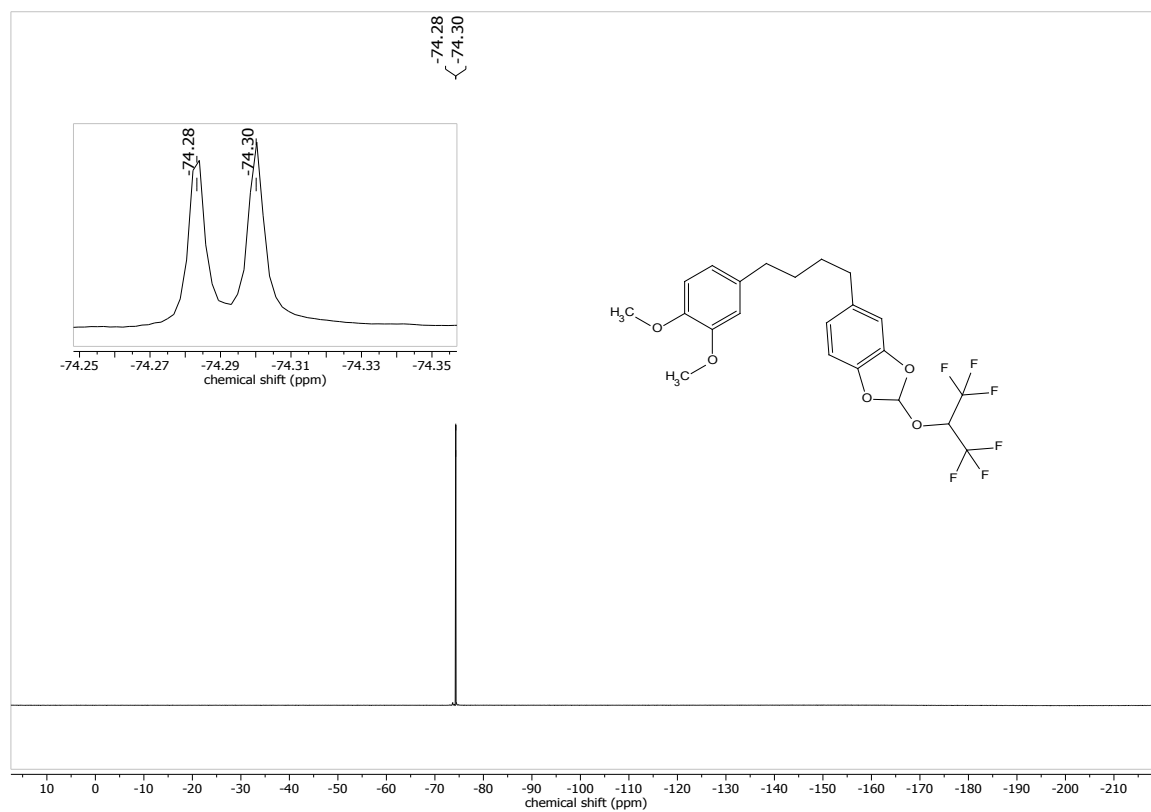
^{19}F NMR of 2-(1-Trifluoromethyl-(2,2,2-trifluoroethyl)oxy)-5-(methoxymethyl)-1,3-benzodioxole (**11**).



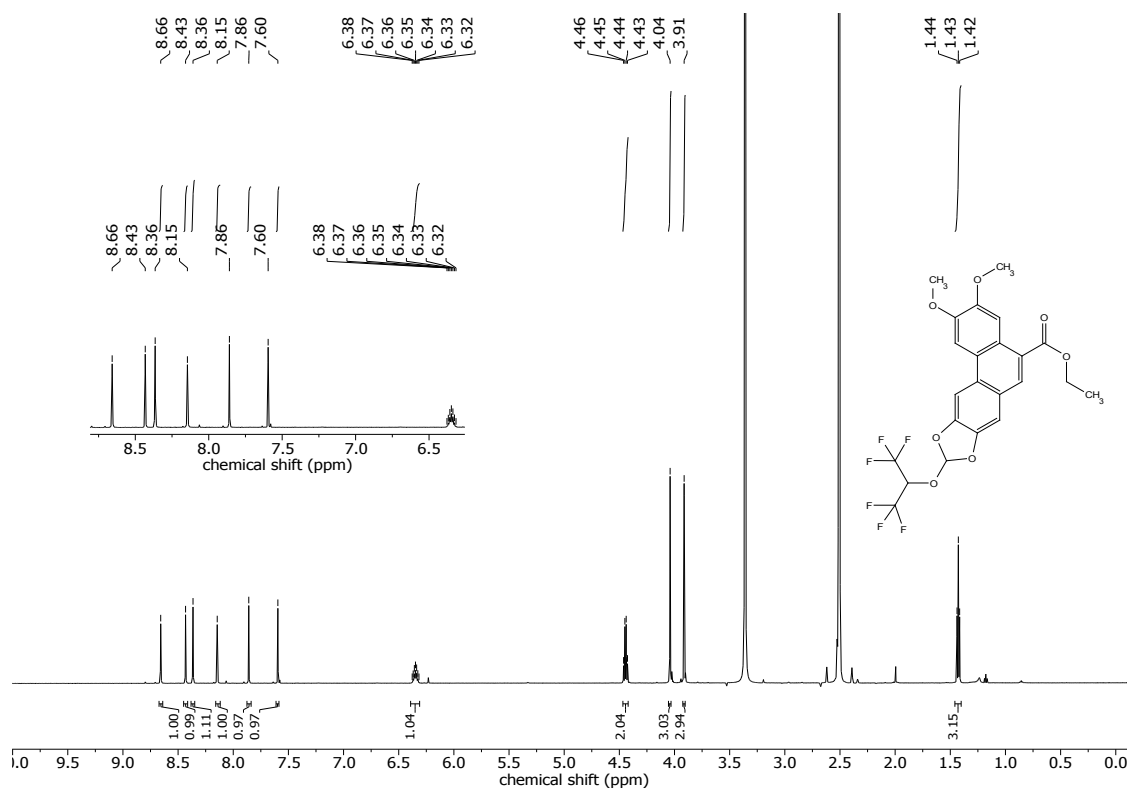
^1H -NMR of 2-(1-Trifluoromethyl-(2,2,2-trifluoroethyl)oxy)-5-(4-(3,4-dimethoxyphenyl)butyl)-1,3-benzodioxole (**12**).



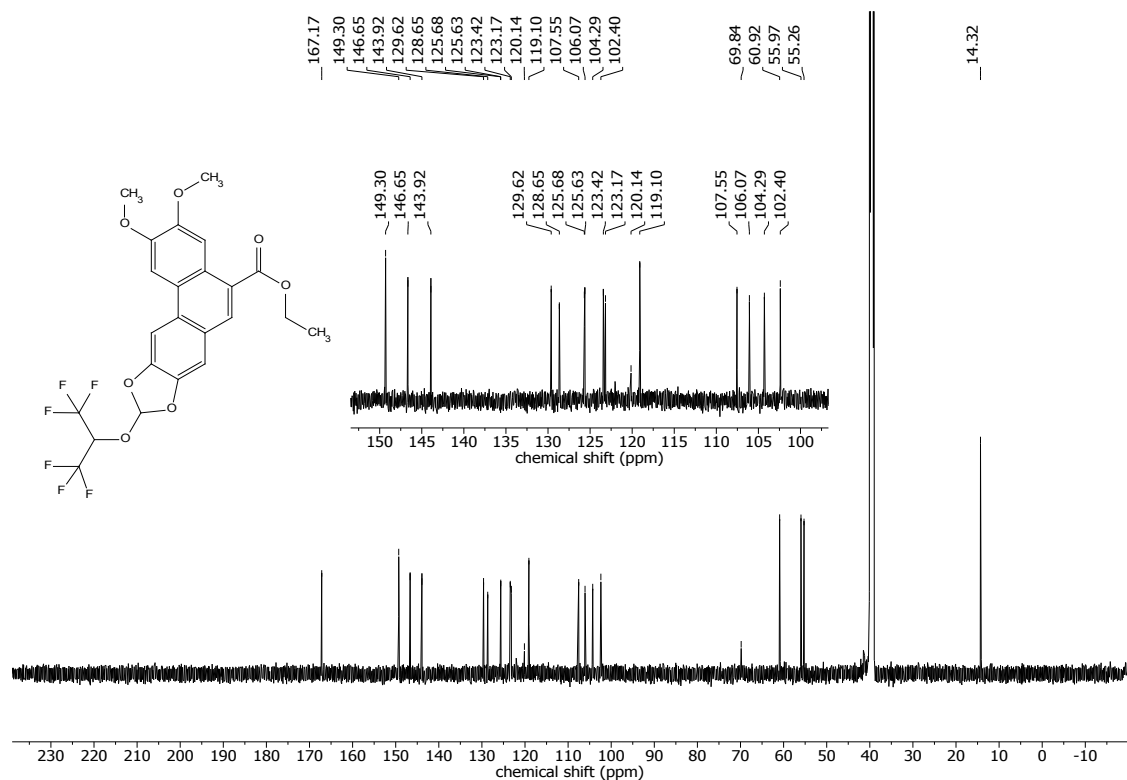
^{13}C NMR of 2-(1-Trifluoromethyl-(2,2,2-trifluoroethyl)oxy)-5-(4-(3,4-dimethoxyphenyl)butyl)-1,3-benzodioxole (**12**).



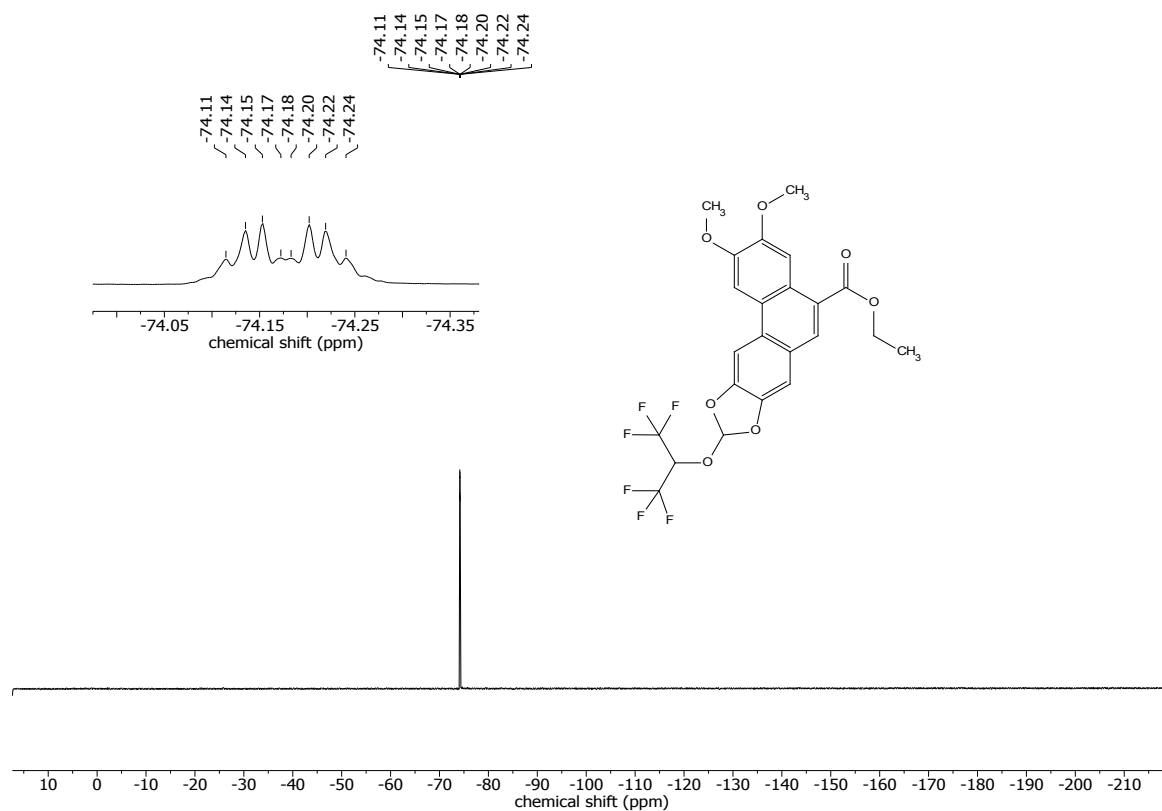
^{19}F -NMR of 2-(1-Trifluoromethyl-(2,2,2-trifluoroethyl)oxy)-5-(4-(3,4-dimethoxyphenyl)butyl)-1,3-benzodioxole (**12**).



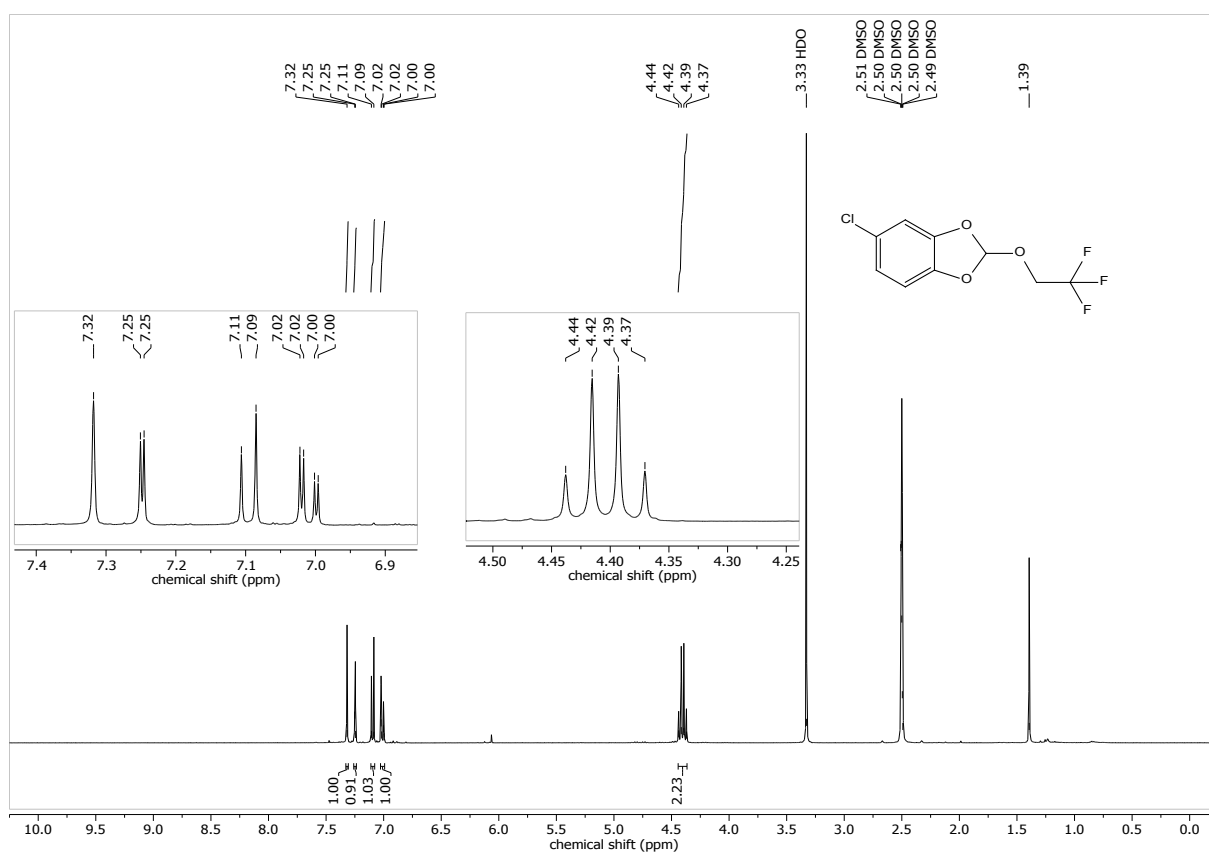
¹H NMR of Ethyl 9-(1-Trifluoromethyl-(2,2,2-trifluoroethyl))-2,3-dimethoxyphenanthro[2,3-d][1,3]dioxole-5-carboxylate (13).



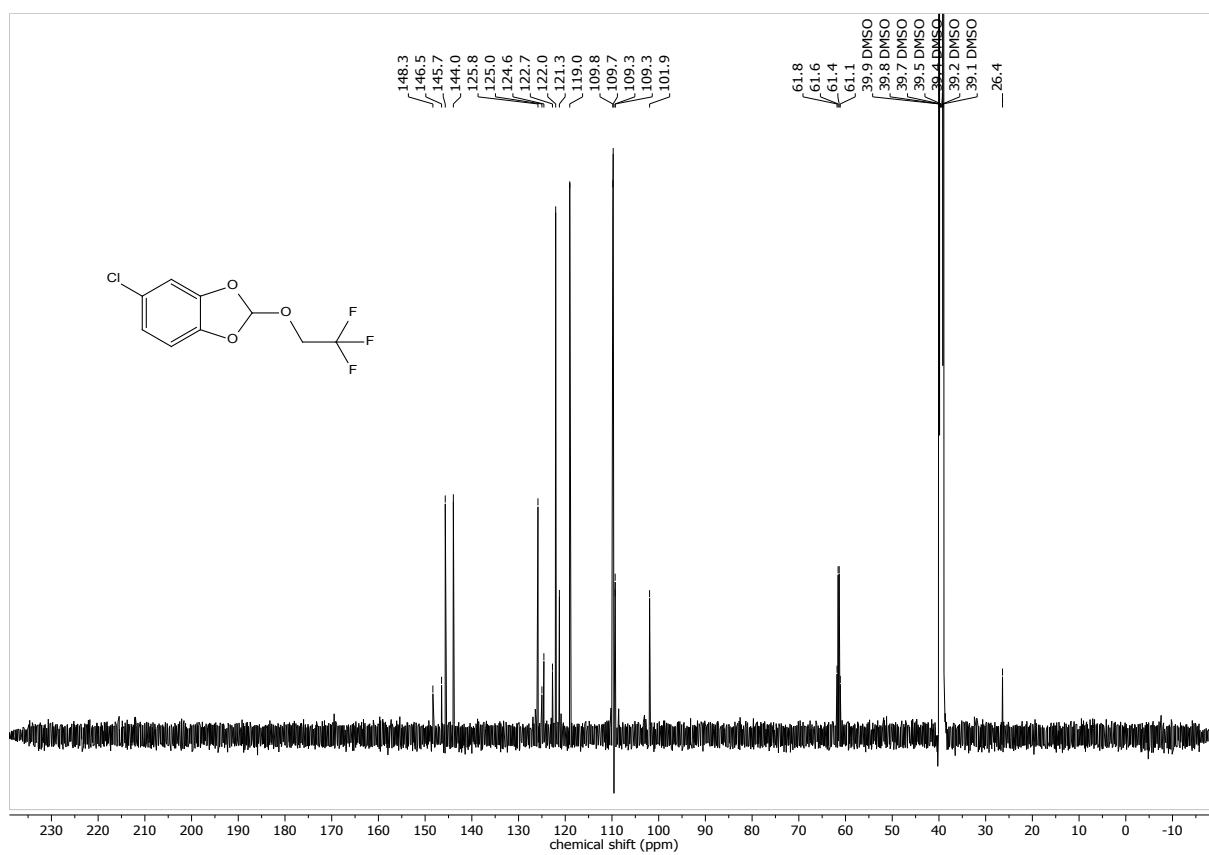
¹³C NMR of Ethyl 9-(1-Trifluoromethyl-(2,2,2-trifluoroethyl)oxy)-2,3-dimethoxyphenanthro[2,3-d][1,3]dioxole-5-carboxylate (13).



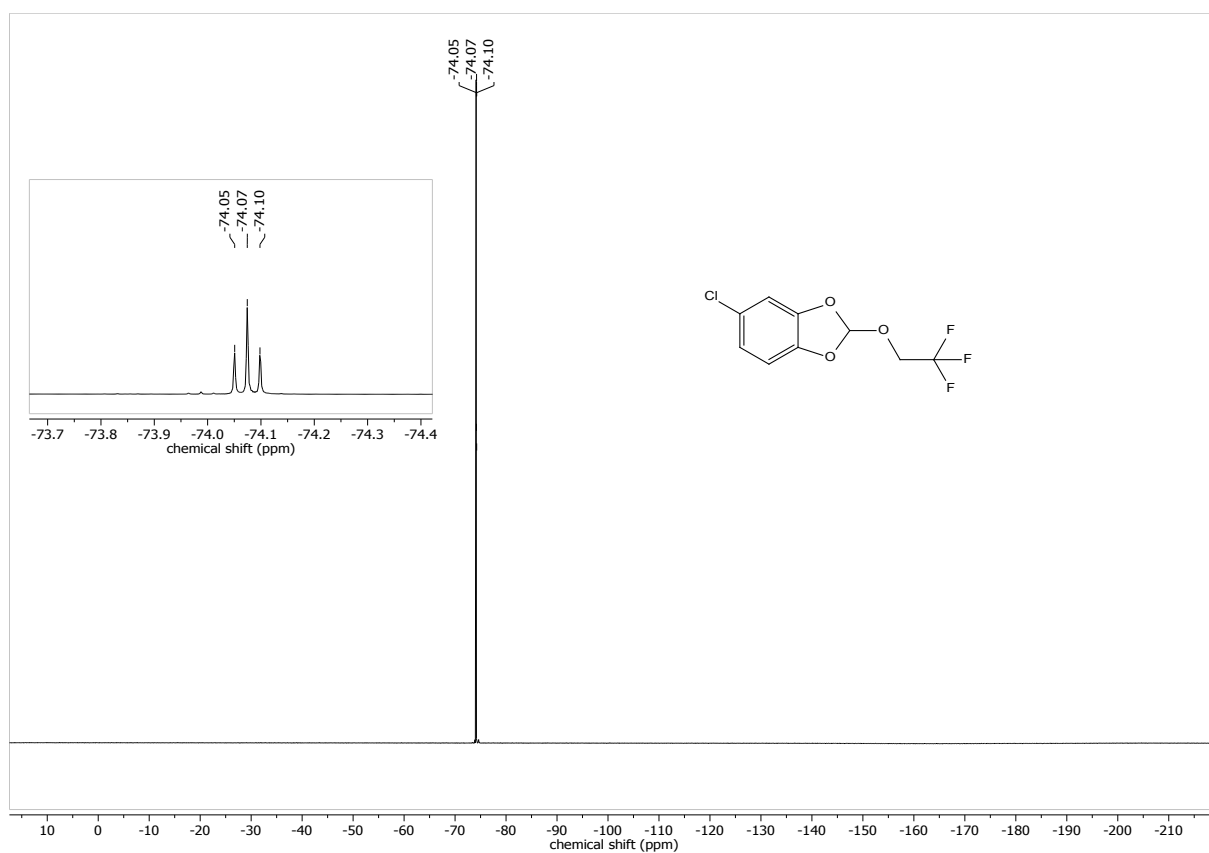
^{19}F NMR of Ethyl 9-(1-(2,2,2-trifluoroethyl)oxy)-2,3-dimethoxyphenanthro[2,3-d][1,3]dioxole-5-carboxylate (**13**).



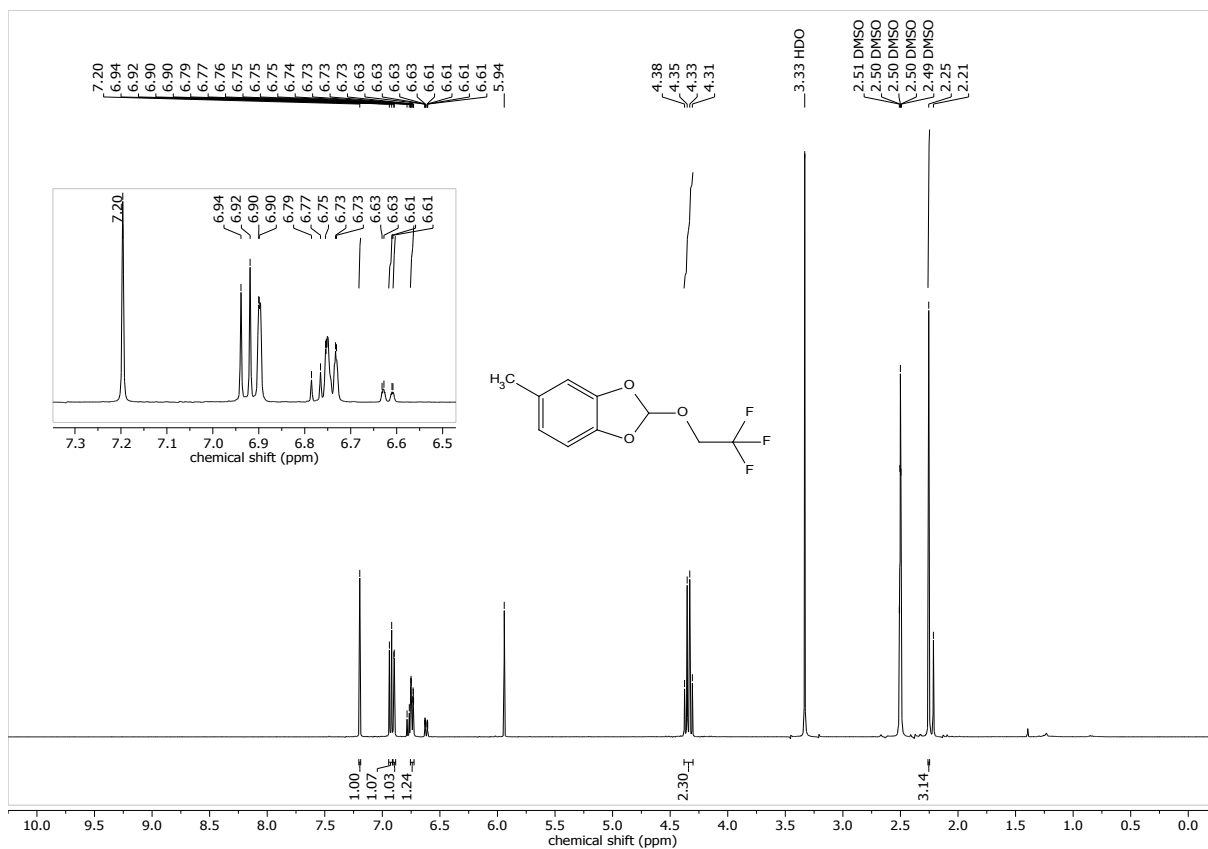
^1H NMR of 5-Chloro-2-(2,2,2-trifluoroethoxy)-1,3-benzodioxole (**14**).



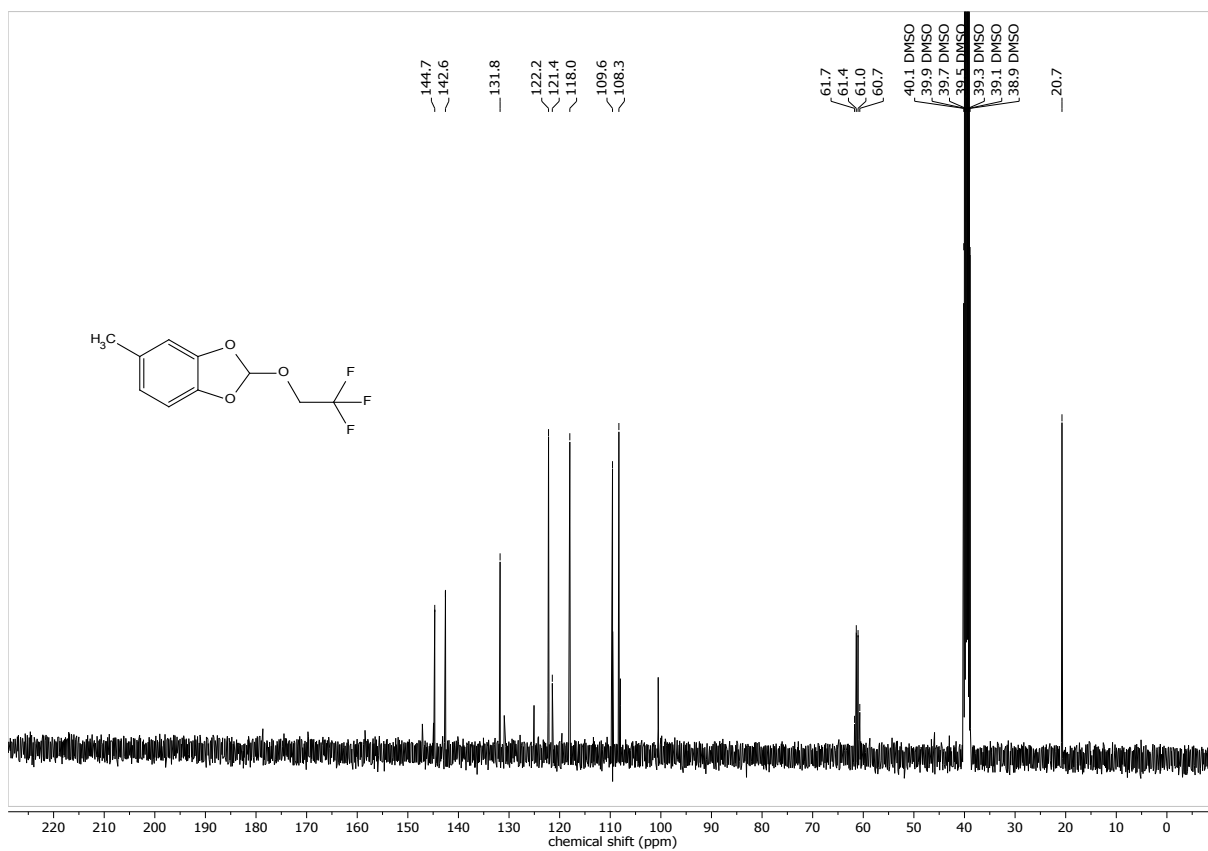
¹³C NMR of 5-Chlor-2-(2,2,2-trifluoroethoxy)-1,3-benzodioxole (**14**).



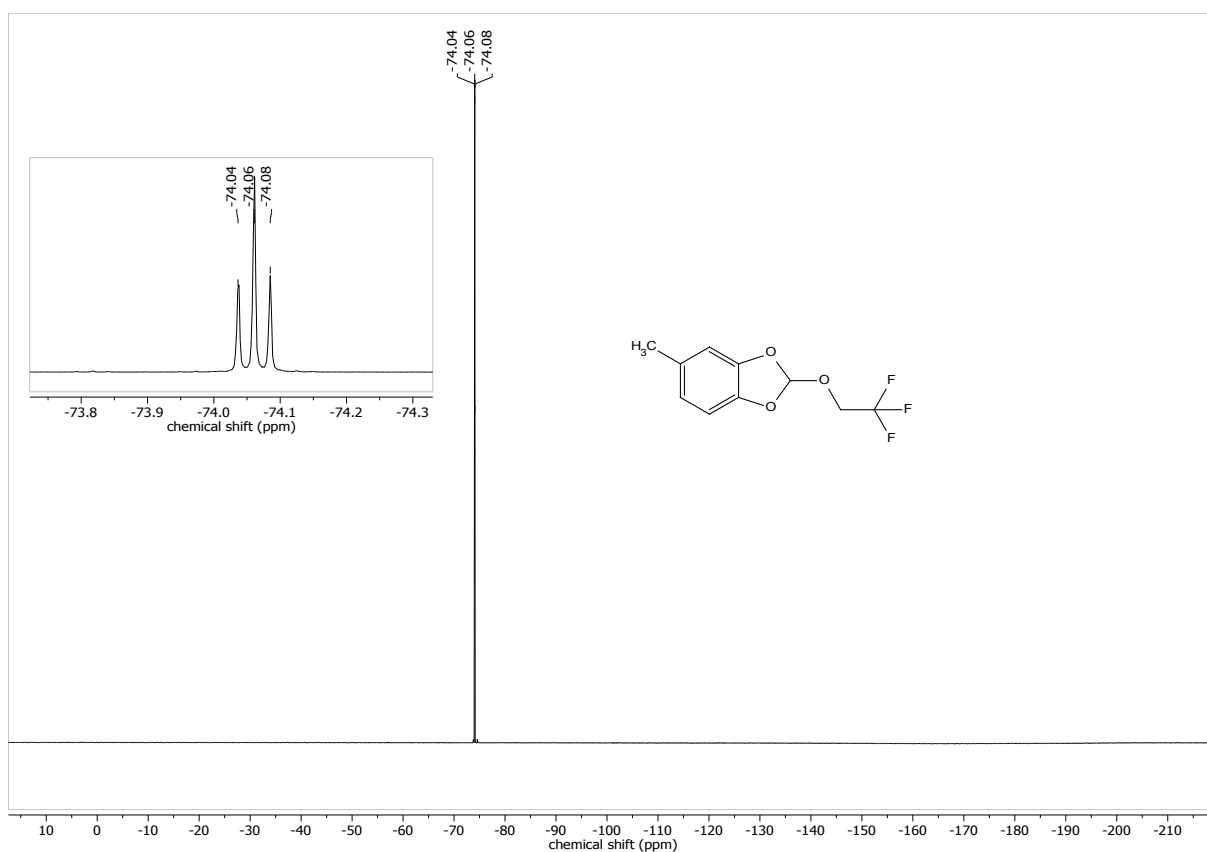
¹⁹F NMR of 5-Chlor-2-(2,2,2-trifluoroethoxy)-1,3-benzodioxole (**14**).



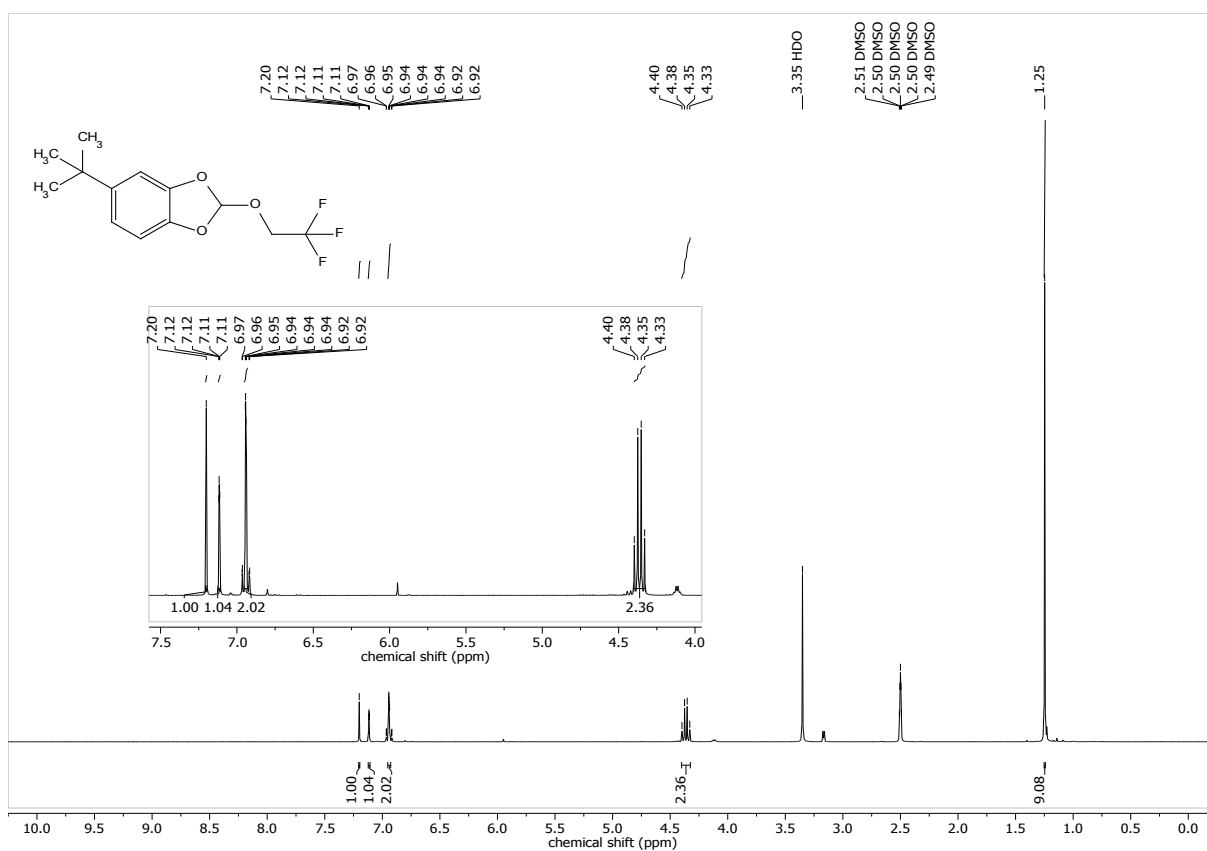
¹H NMR of 2-(2,2,2-Trifluoroethoxy)-5-methyl-1,3-benzodioxole (**15**).



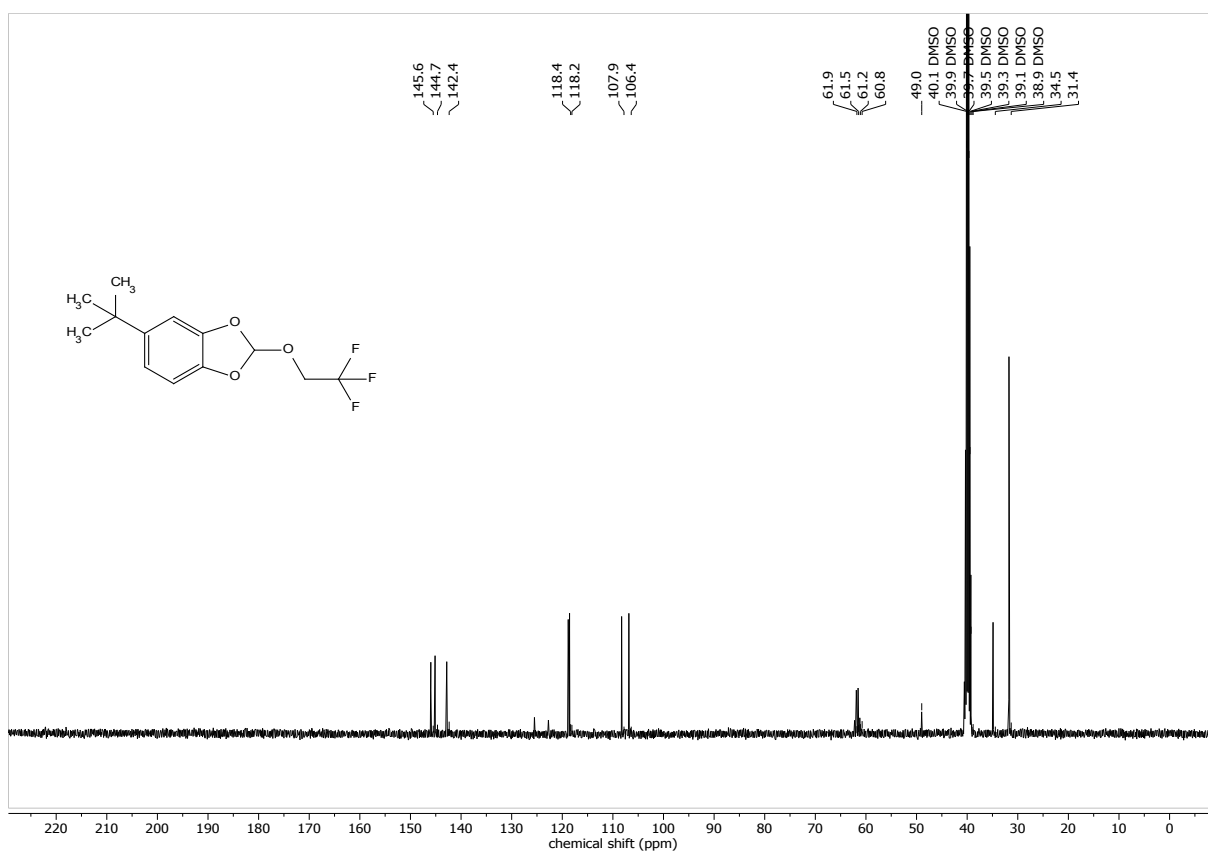
¹³C NMR of 2-(2,2,2-Trifluoroethoxy)-5-methyl-1,3-benzodioxole (**15**).



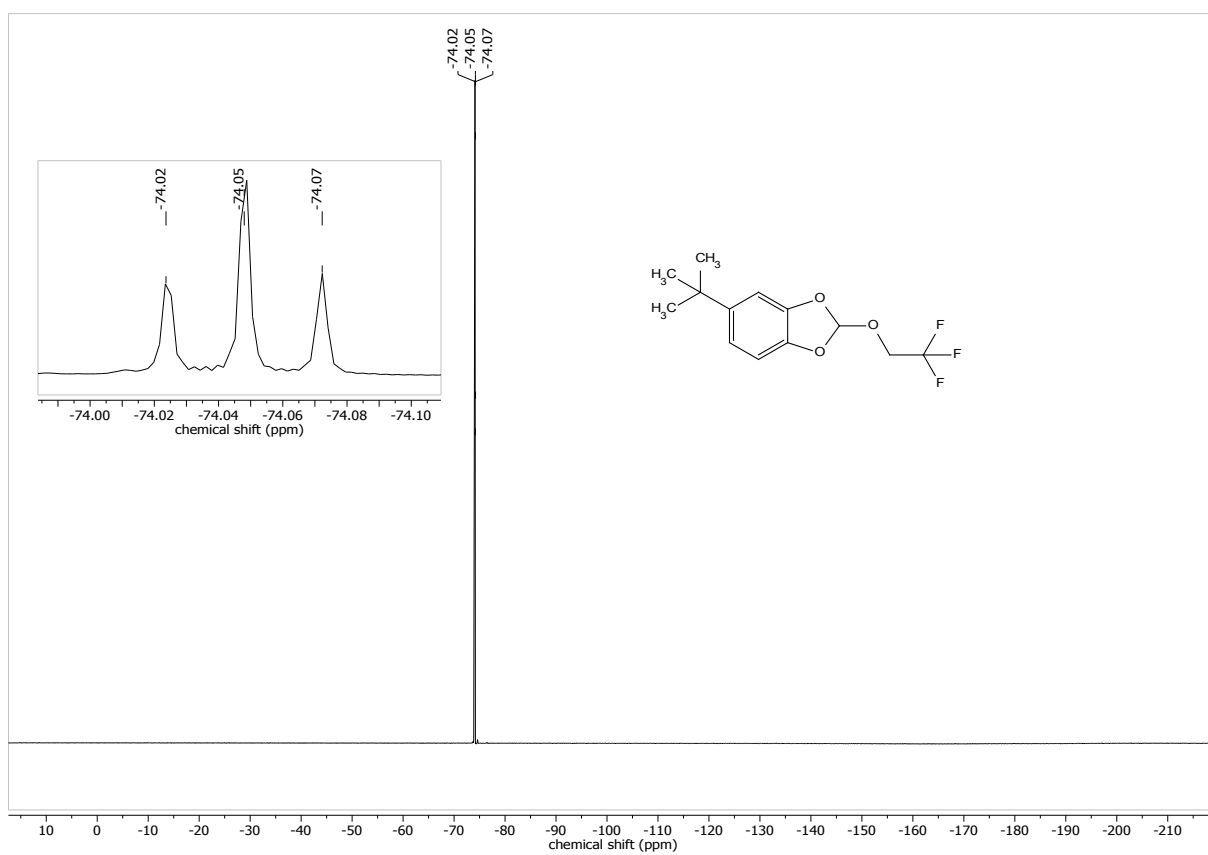
^{19}F NMR of 2-(2,2,2-Trifluoroethoxy)-5-methyl-1,3-benzodioxole (**15**).



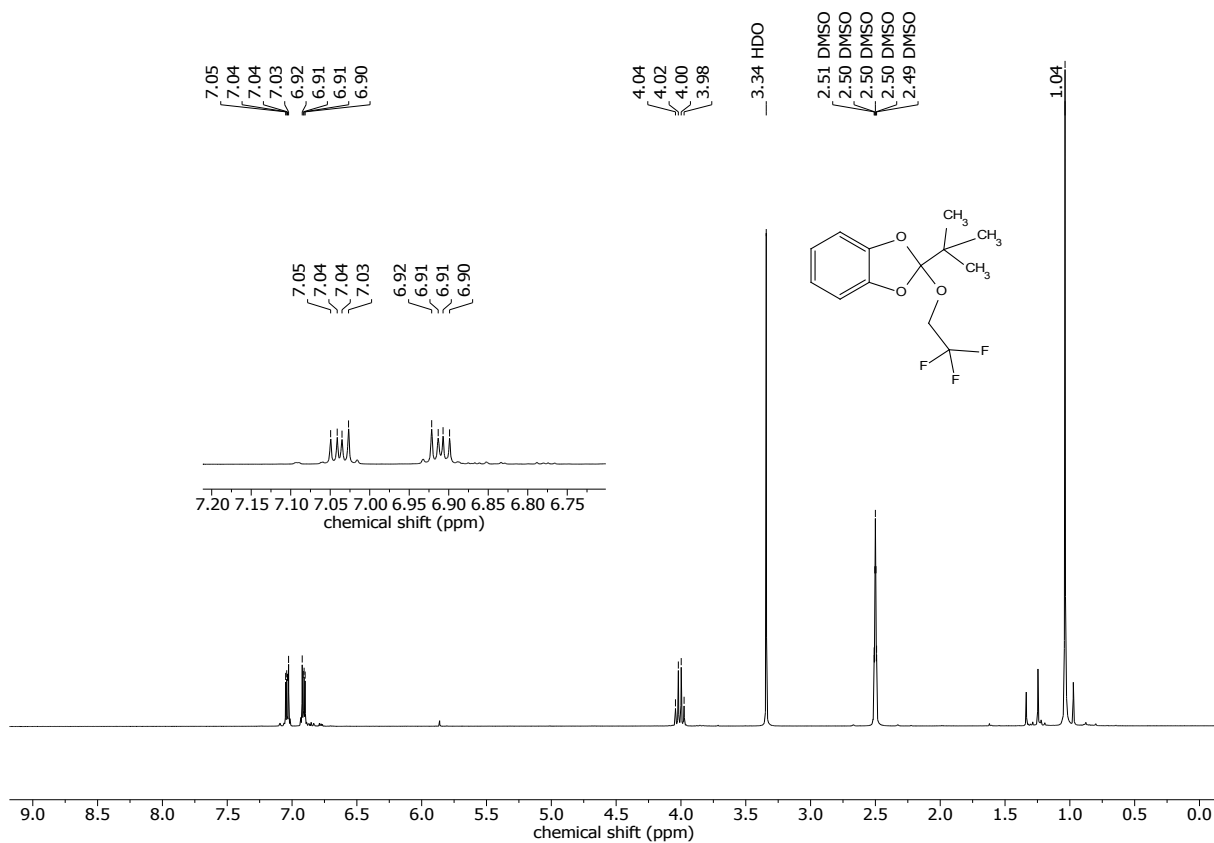
^1H NMR of 2-(2,2,2-Trifluoroethoxy)-5-(2,2-dimethylethyl)-1,3-benzodioxole (**16**).



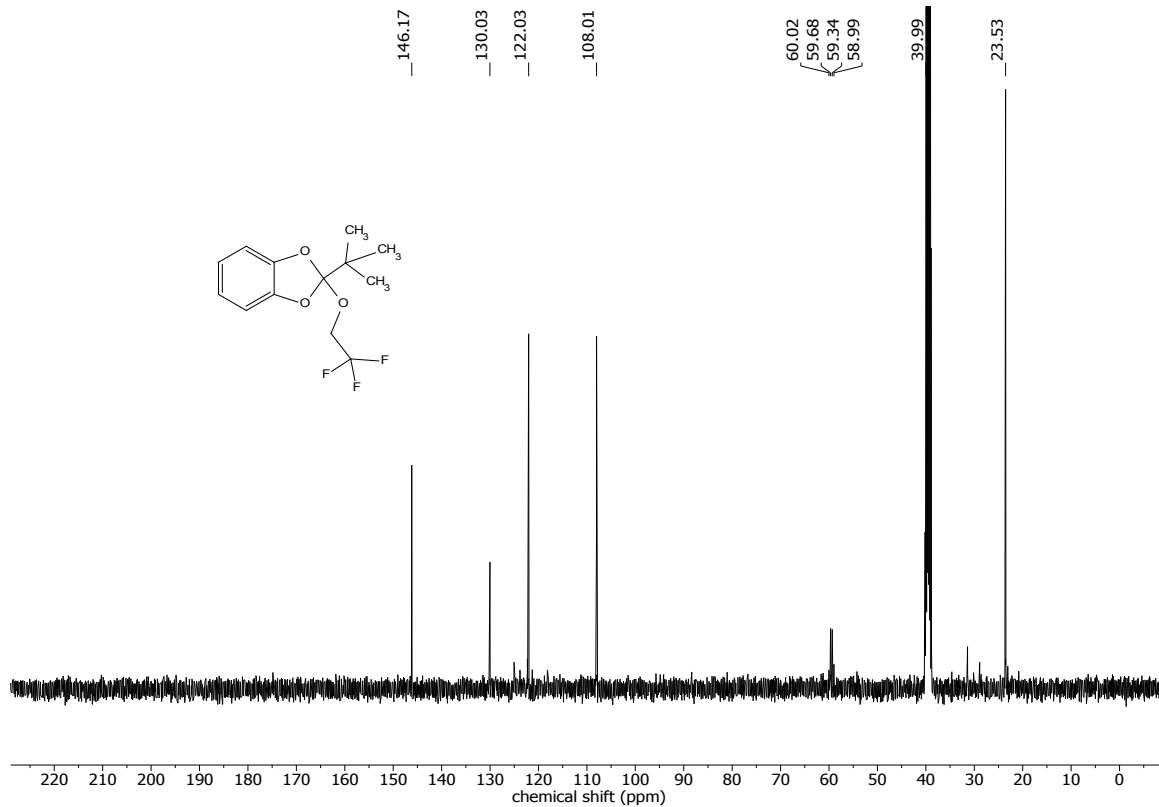
¹³C NMR of 2-(2,2,2-Trifluoroethoxy)-5-(2,2-dimethylethyl)-1,3-benzodioxole (**16**).



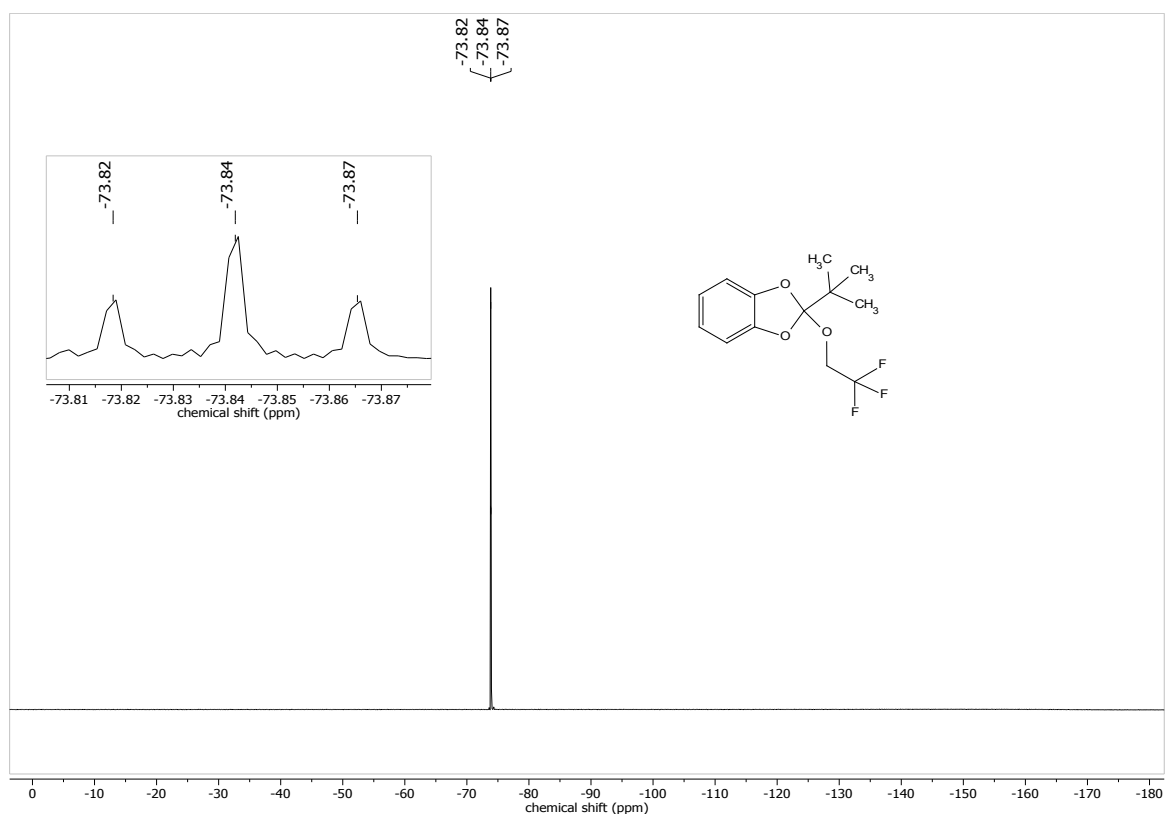
¹⁹F NMR of 2-(2,2,2-Trifluoroethoxy)-5-(2,2-dimethylethyl)-1,3-benzodioxole (**16**).



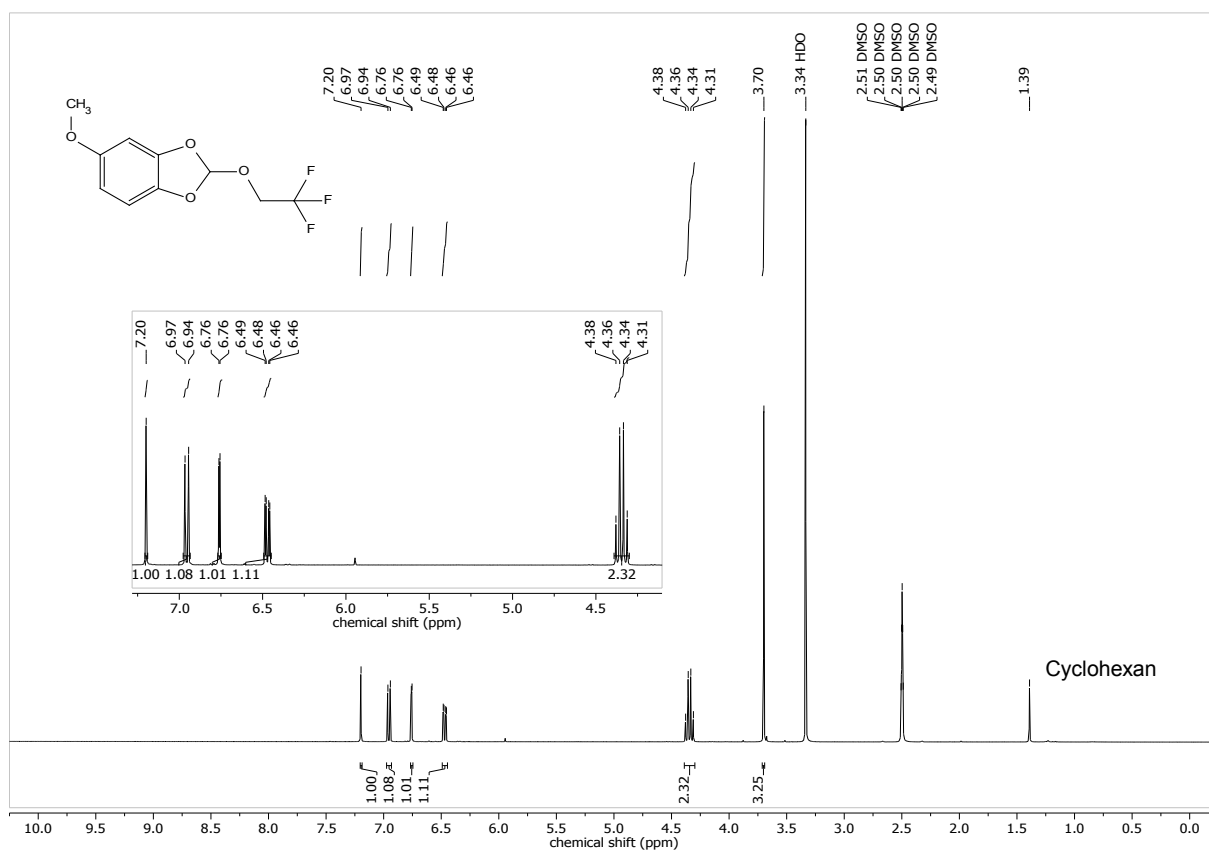
¹H NMR of 2-(2,2,2-trifluoroethoxy)-2-(1,1-dimethylethyl)-1,3-benzodioxole (**17**).



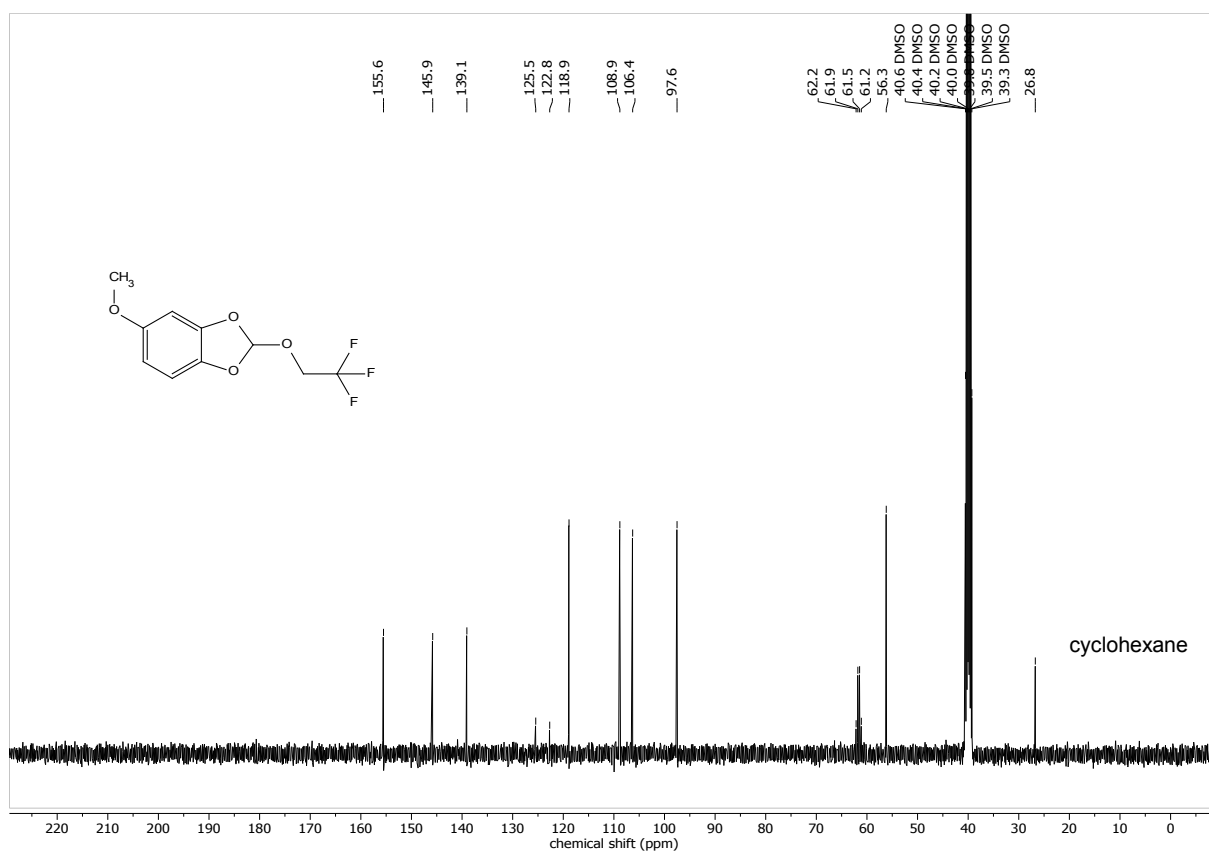
¹³C NMR of 2-(2,2,2-trifluoroethoxy)-2-(1,1-dimethylethyl)-1,3-benzodioxole (**17**).



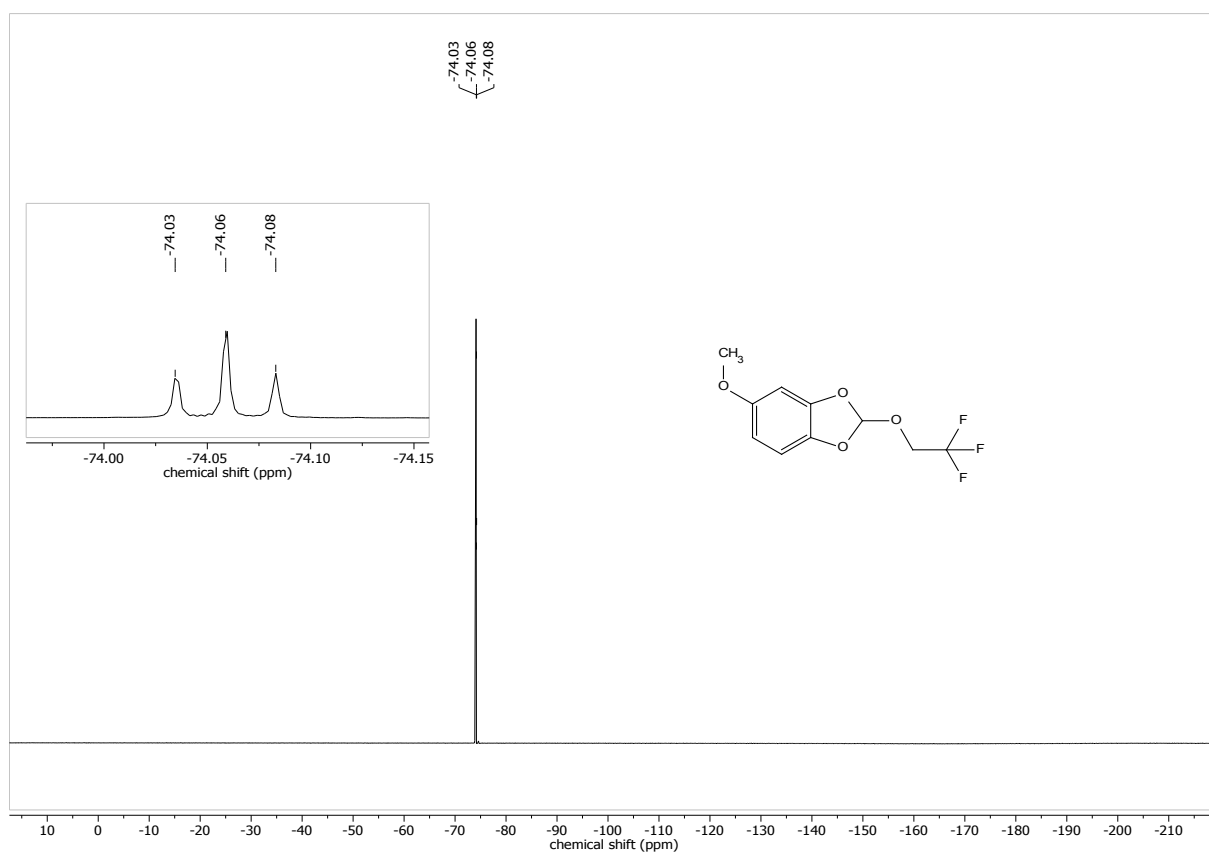
^{19}F NMR of 2-(2,2,2-trifluoroethoxy)-2-(1,1-dimethylethyl)-1,3-benzodioxole (**17**).



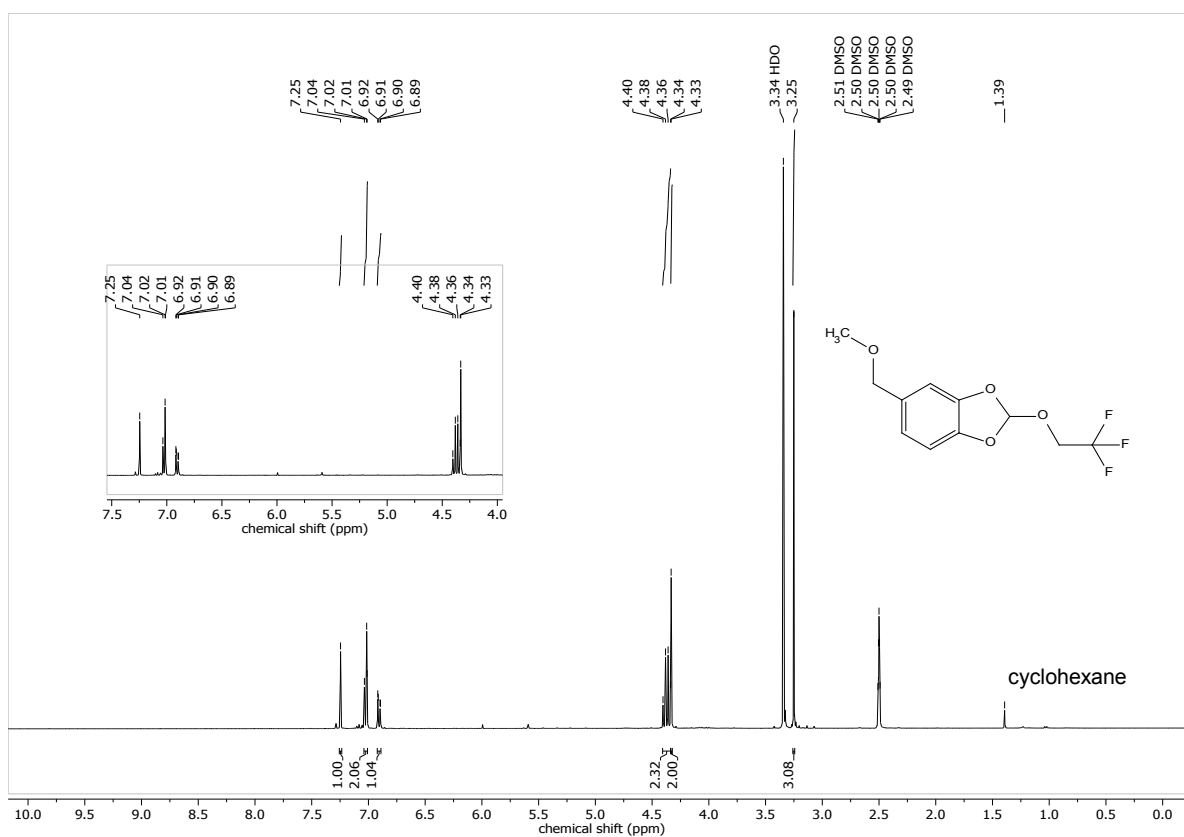
^1H NMR of 2-(2,2,2-Trifluoroethoxy)-5-methoxy-1,3-benzodioxole (**18**).



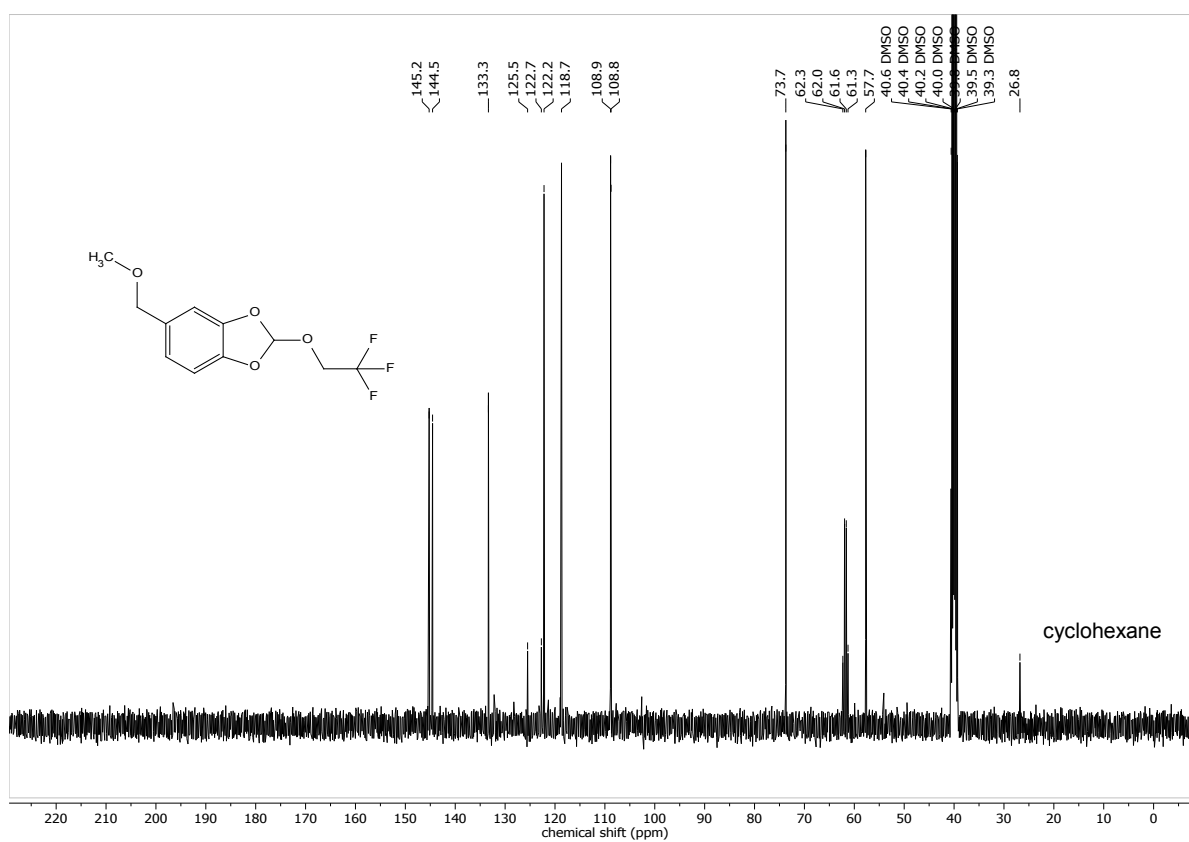
¹³C NMR of 2-(2,2,2-Trifluoroethoxy)-5-methoxy-1,3-benzodioxole (**18**).



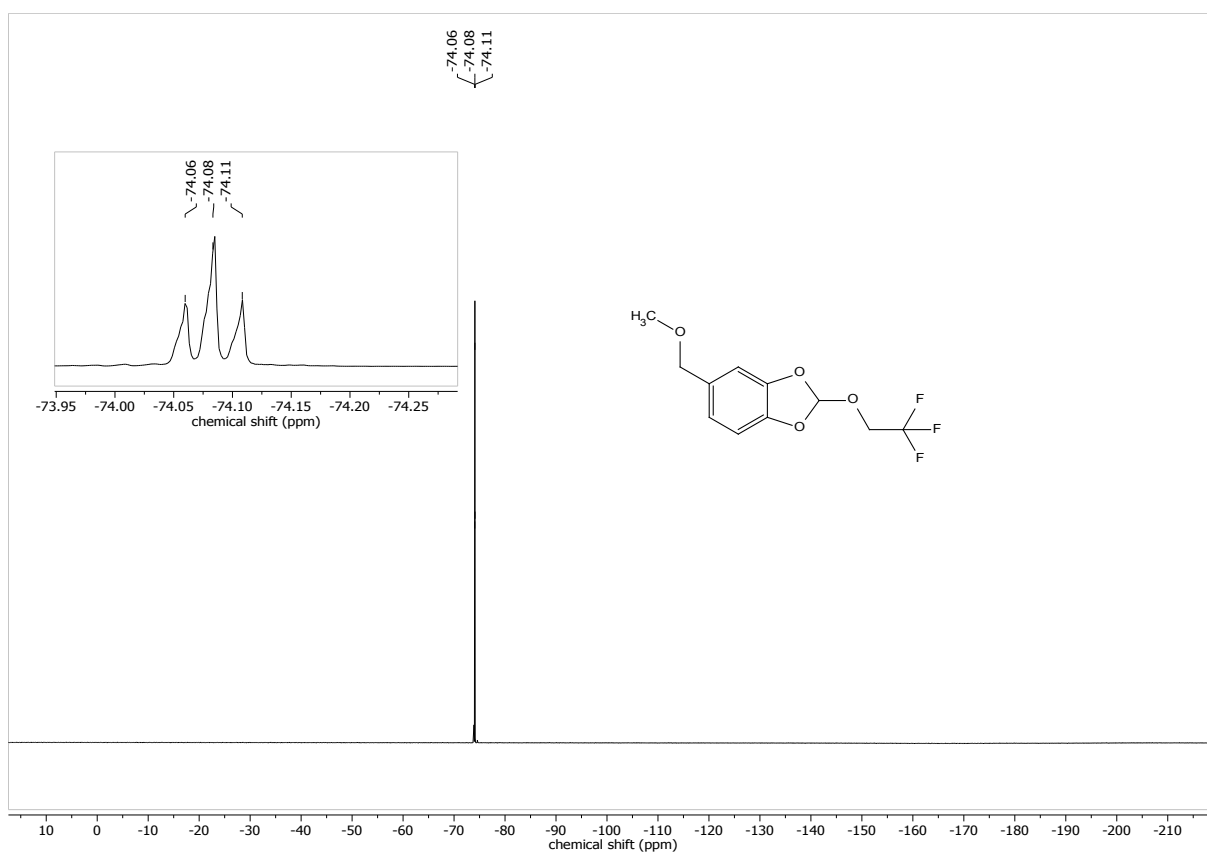
¹⁹F NMR of 2-(2,2,2-Trifluoroethoxy)-5-methoxy-1,3-benzodioxole (**18**).



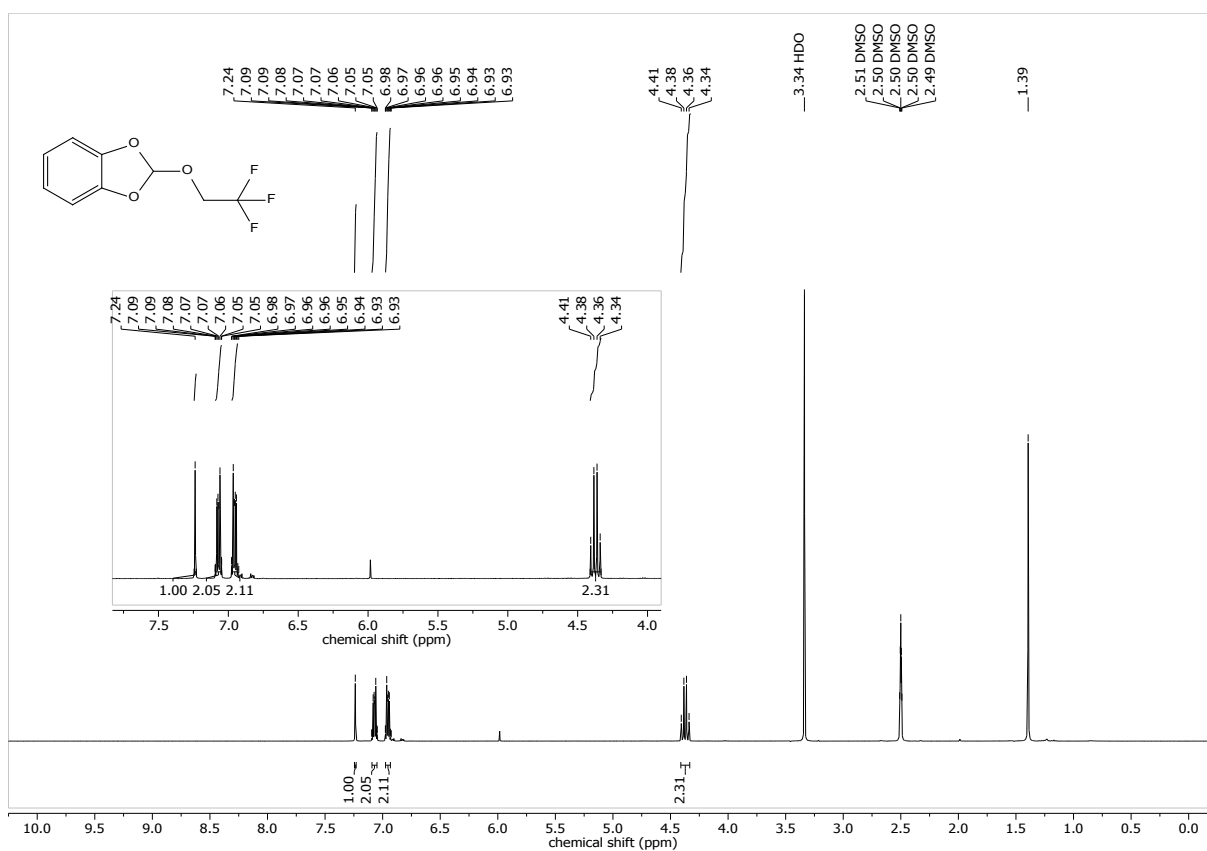
¹H NMR of 2-(2,2,2-Trifluoroethoxy)-5-(methoxymethyl)-1,3-benzodioxole (19).



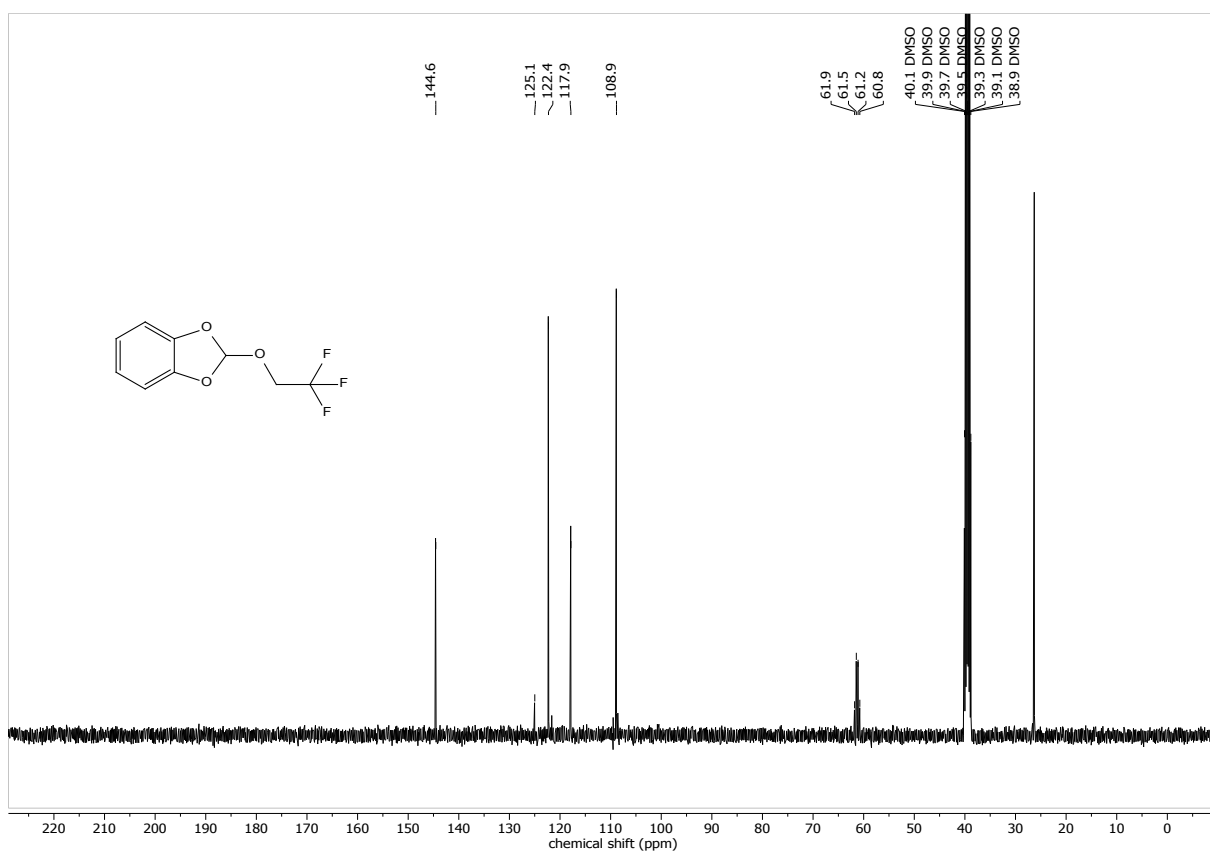
¹³C NMR of 2-(2,2,2-Trifluoroethoxy)-5-(methoxymethyl)-1,3-benzodioxole (19).



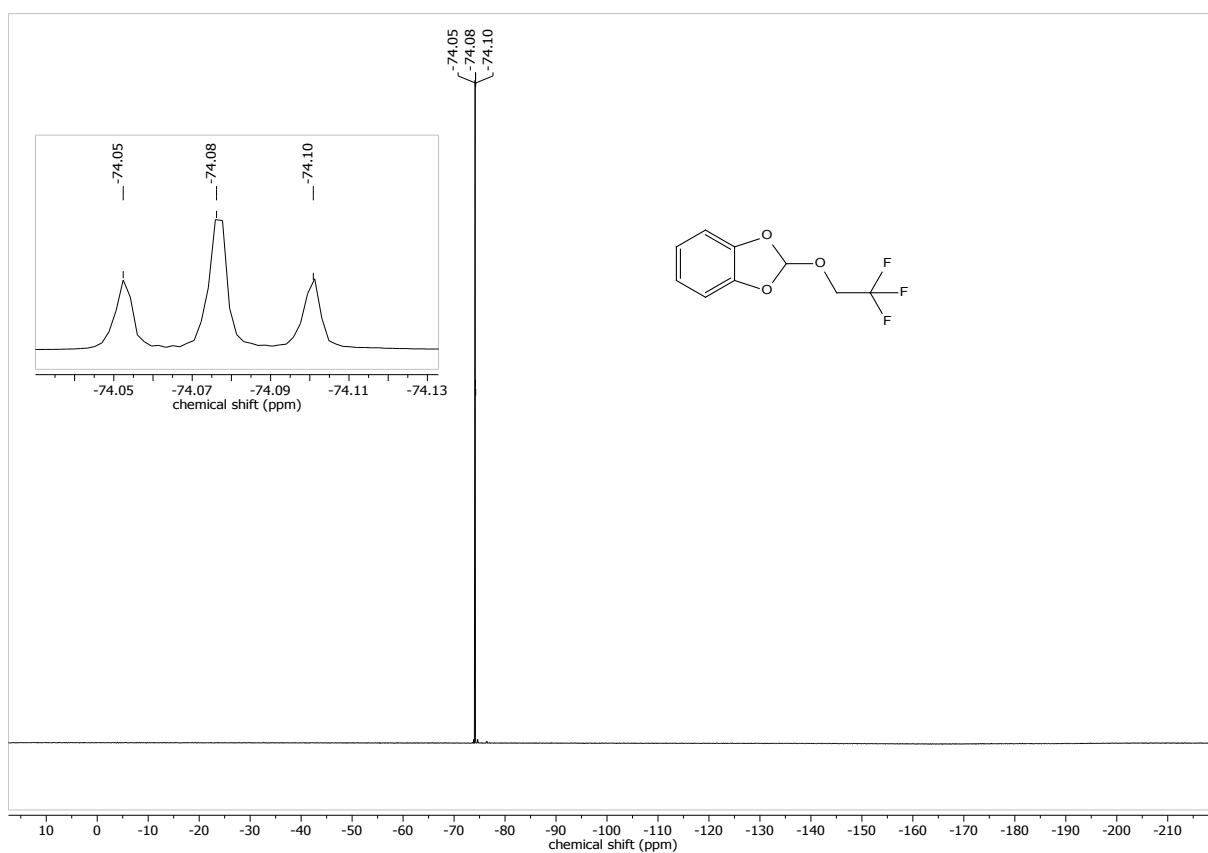
^{19}F NMR of 2-(2,2,2-Trifluoroethoxy)-5-(methoxymethyl)-1,3-benzodioxole (**19**).



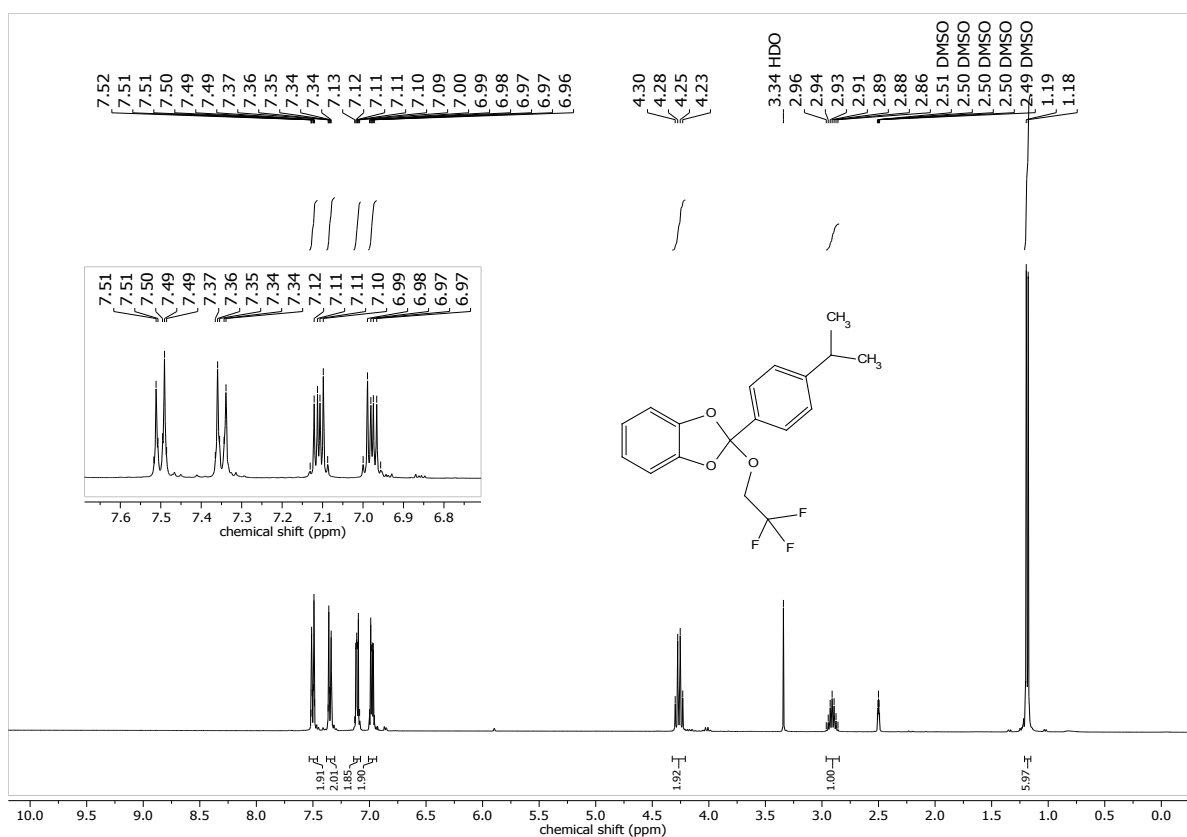
^1H NMR of 2-(2,2,2-Trifluoroethoxy)-1,3-benzodioxole (**20**).



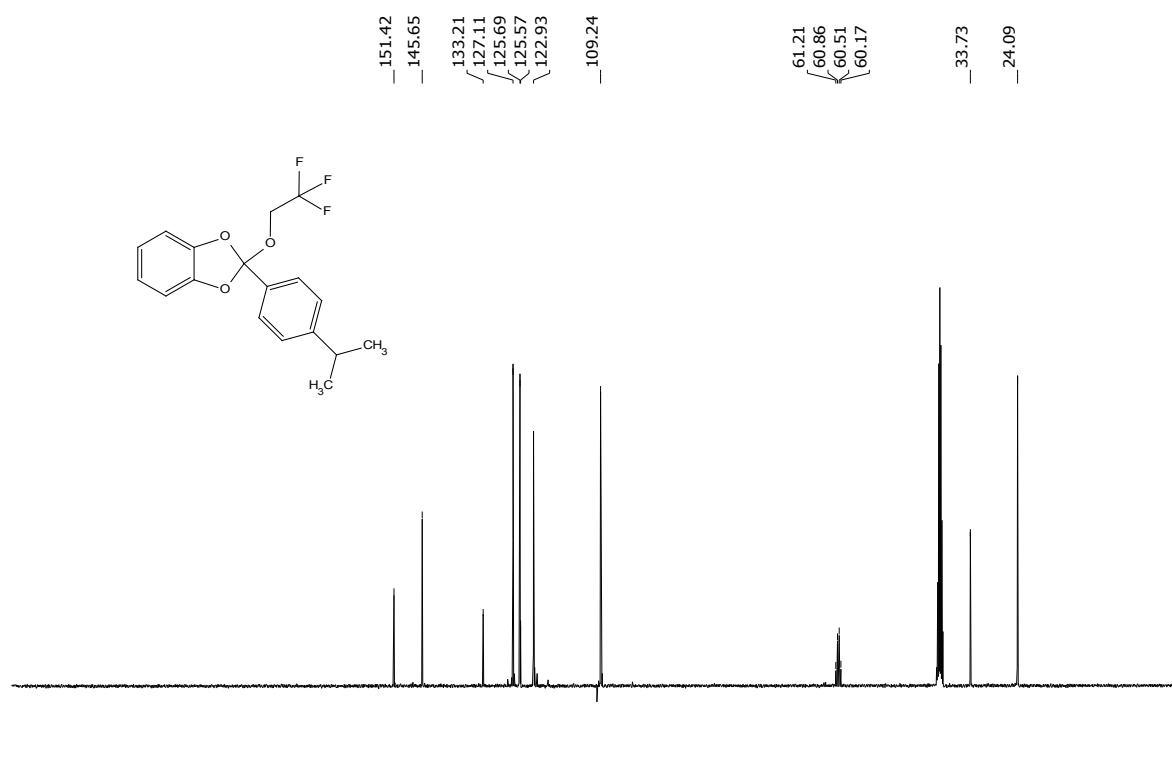
¹³C NMR of 2-(2,2,2-Trifluoroethoxy)-1,3-benzodioxole (**20**).



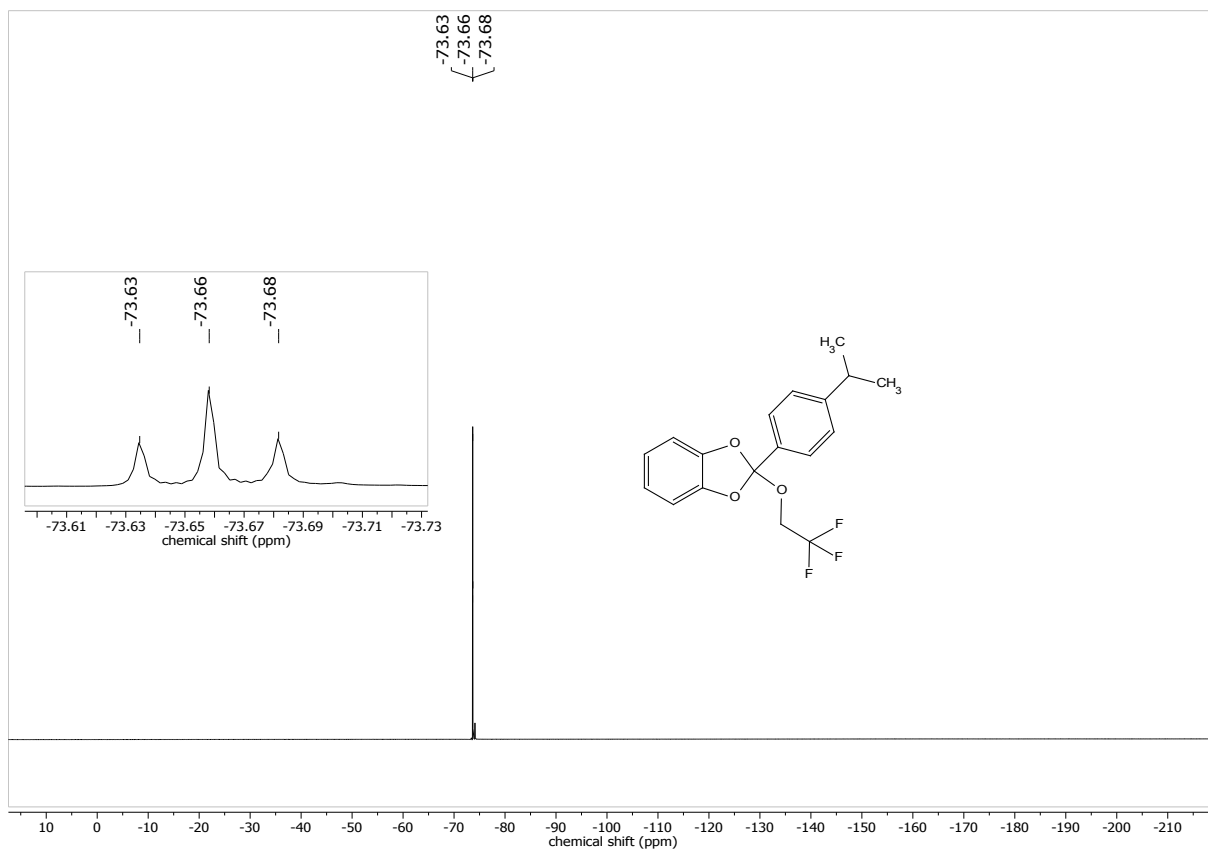
¹⁹F NMR of 2-(2,2,2-Trifluoroethoxy)-1,3-benzodioxole (**20**).



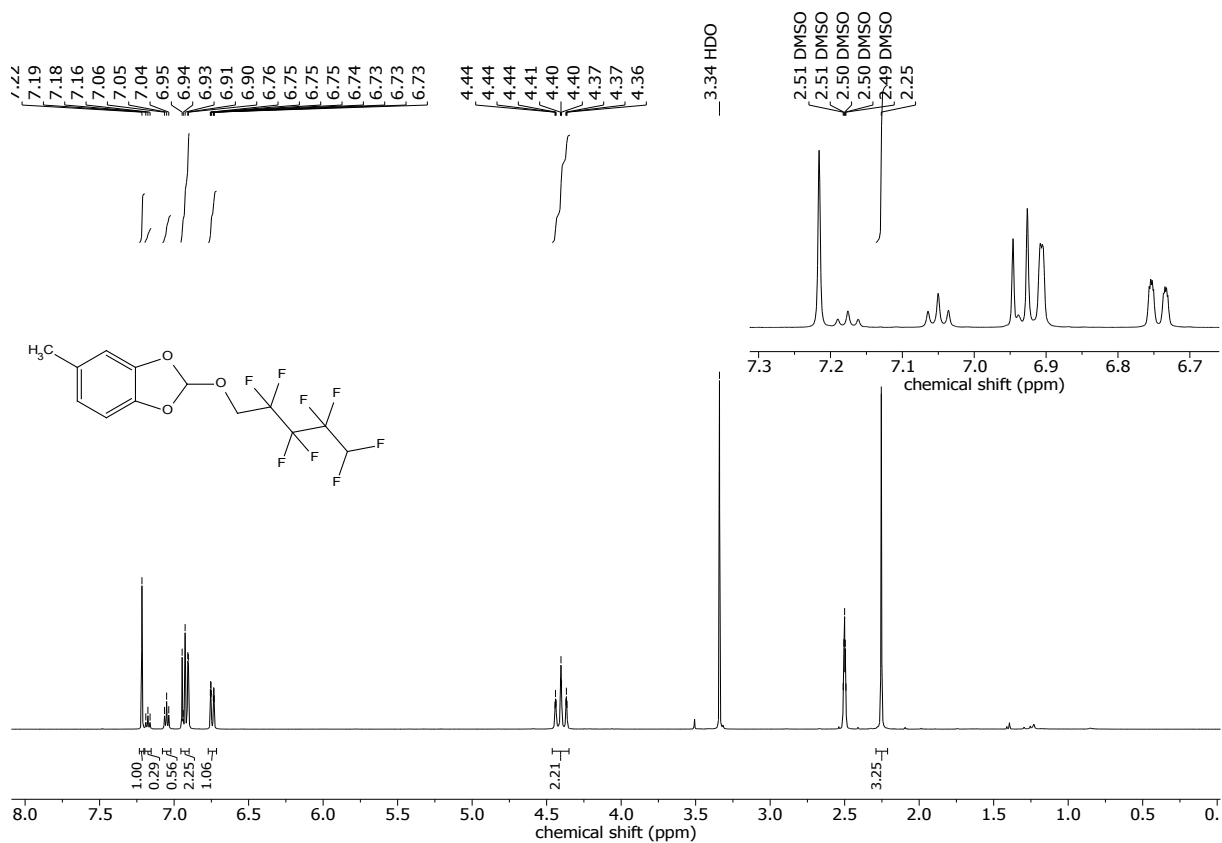
¹H NMR of 2-(2,2,2-Trifluoroethoxy)-2-(4-isopropylphenyl)-1,3-benzodioxole (21).



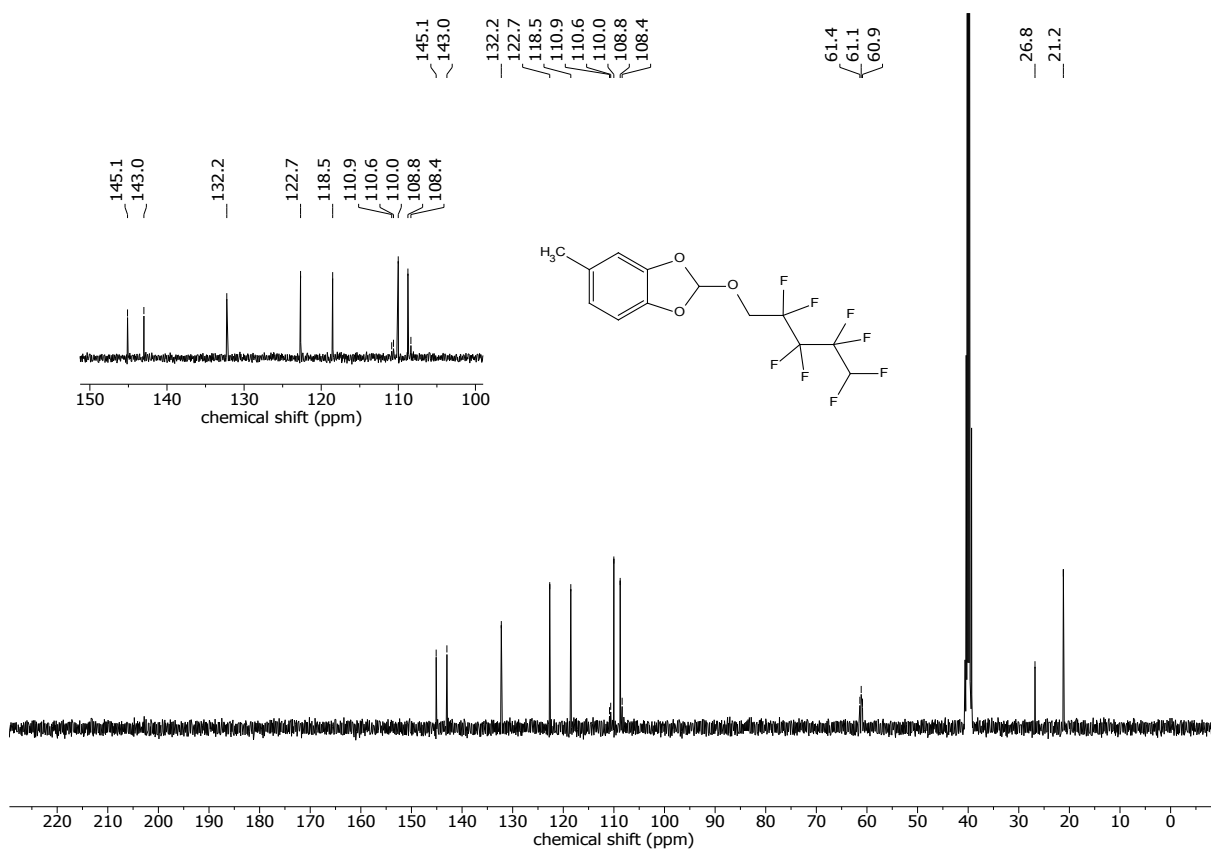
¹³C NMR of 2-(2,2,2-Trifluoroethoxy)-2-(4-isopropylphenyl)-1,3-benzodioxole (21).



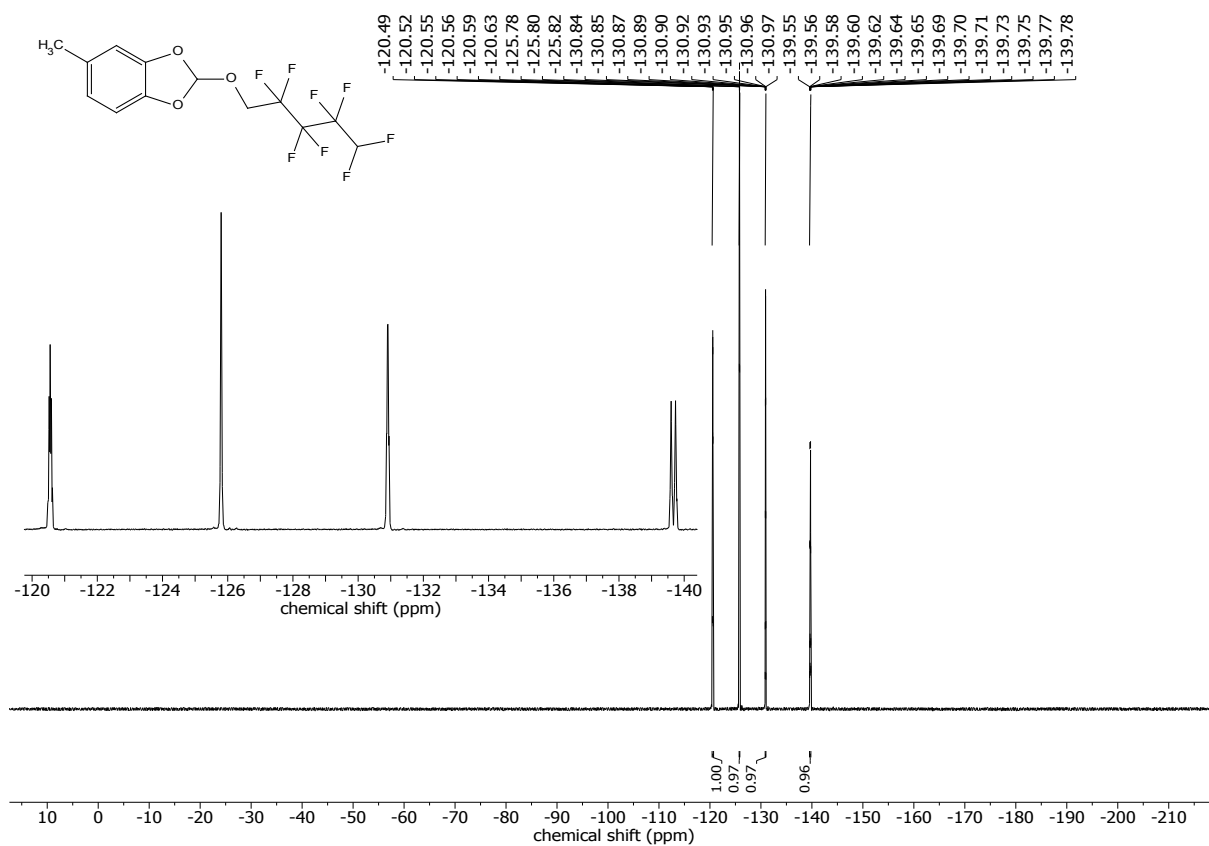
¹⁹F NMR of 2-(2,2,2-Trifluoroethoxy)-2-(4-isopropylphenyl)-1,3-benzodioxole (**21**).



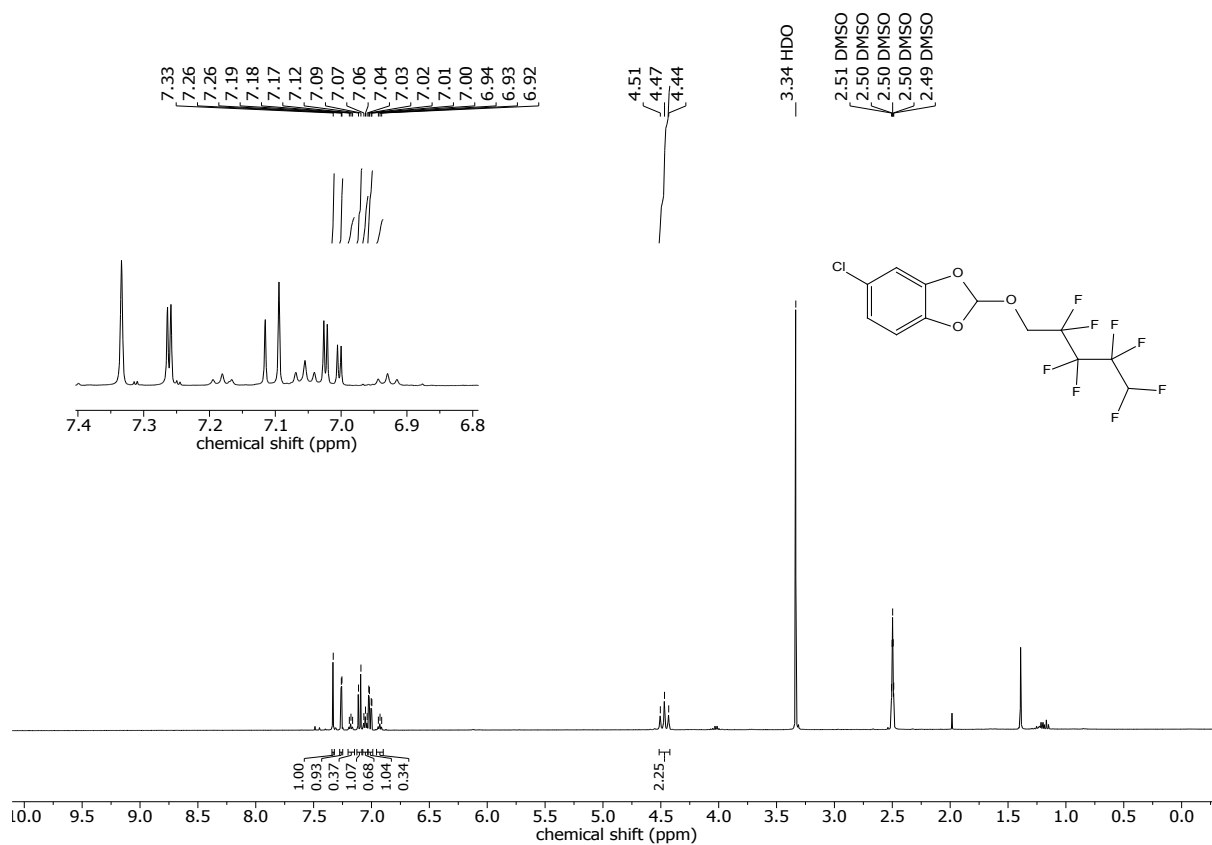
¹H NMR of 5-Methyl-2-((2,2,3,3,4,4,5,5-octafluoropentyl)oxy)-1,3-benzodioxole. (**22**)



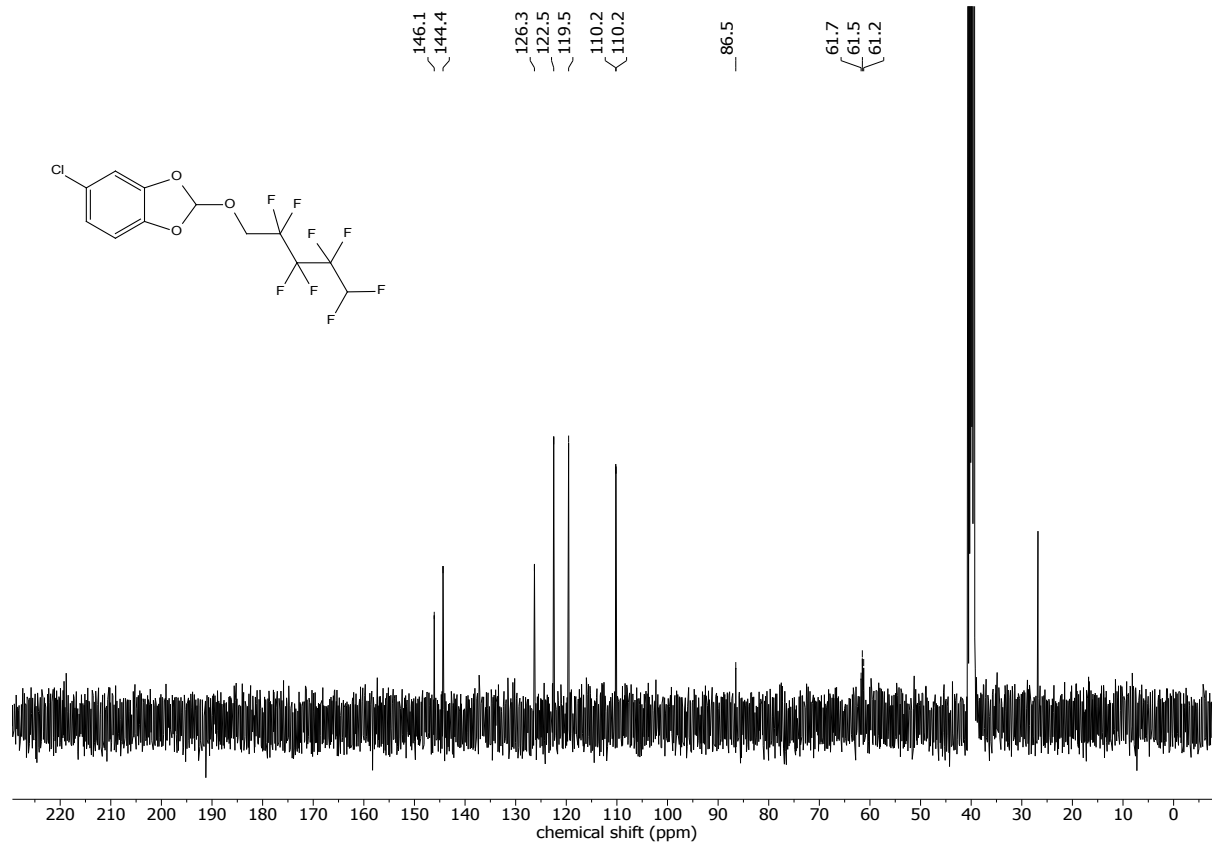
¹³C NMR of 5-Methyl-2-((2,2,3,3,4,4,5,5-octafluoropentyl)oxy)-1,3-benzodioxole. (22)



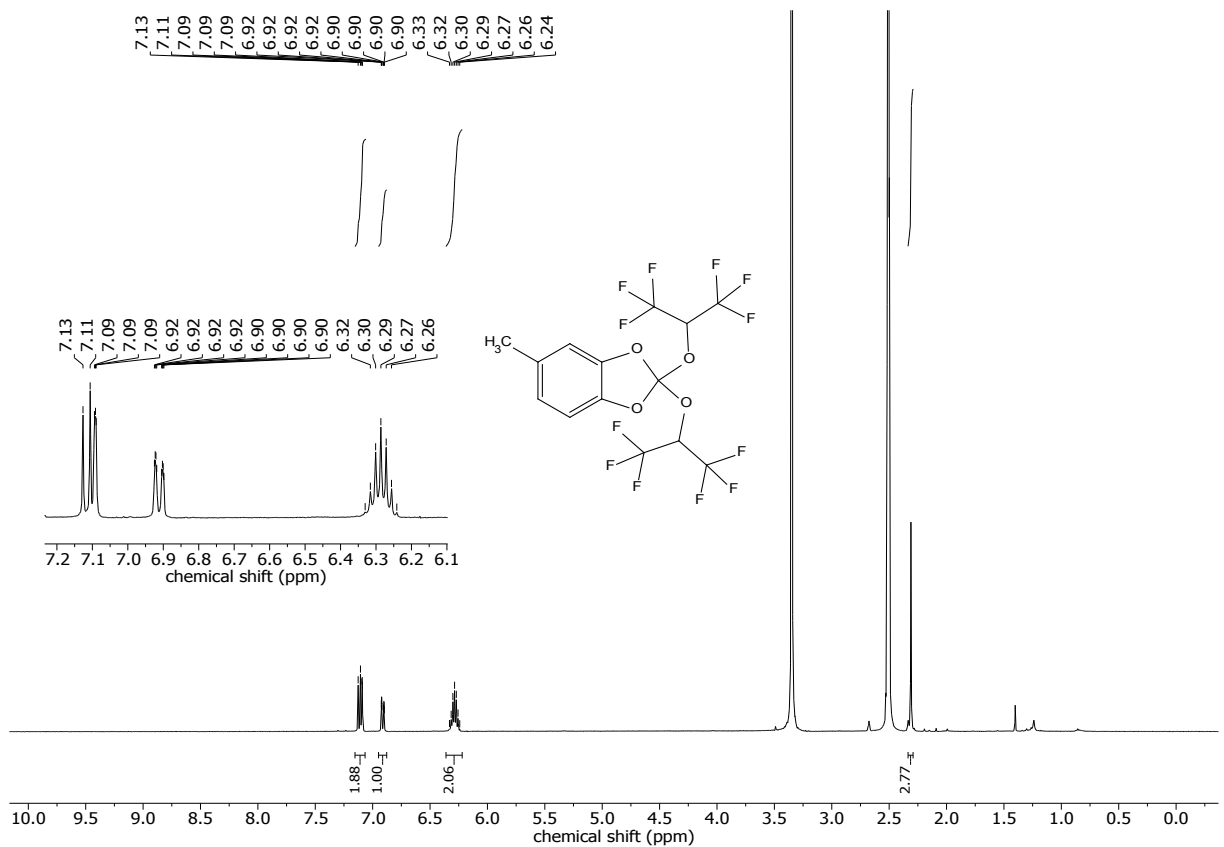
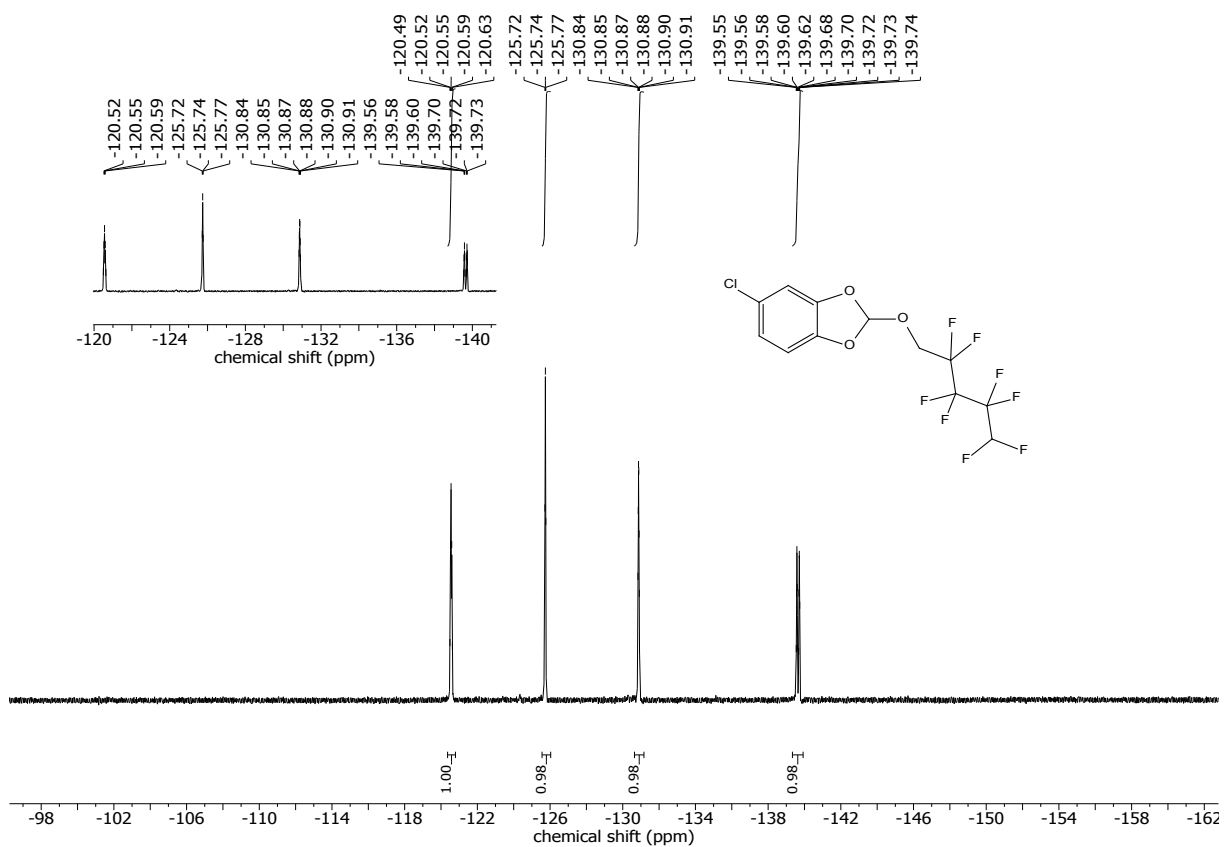
¹⁹F NMR of 5-Methyl-2-((2,2,3,3,4,4,5,5-octafluoropentyl)oxy)-1,3-benzodioxole. (22)

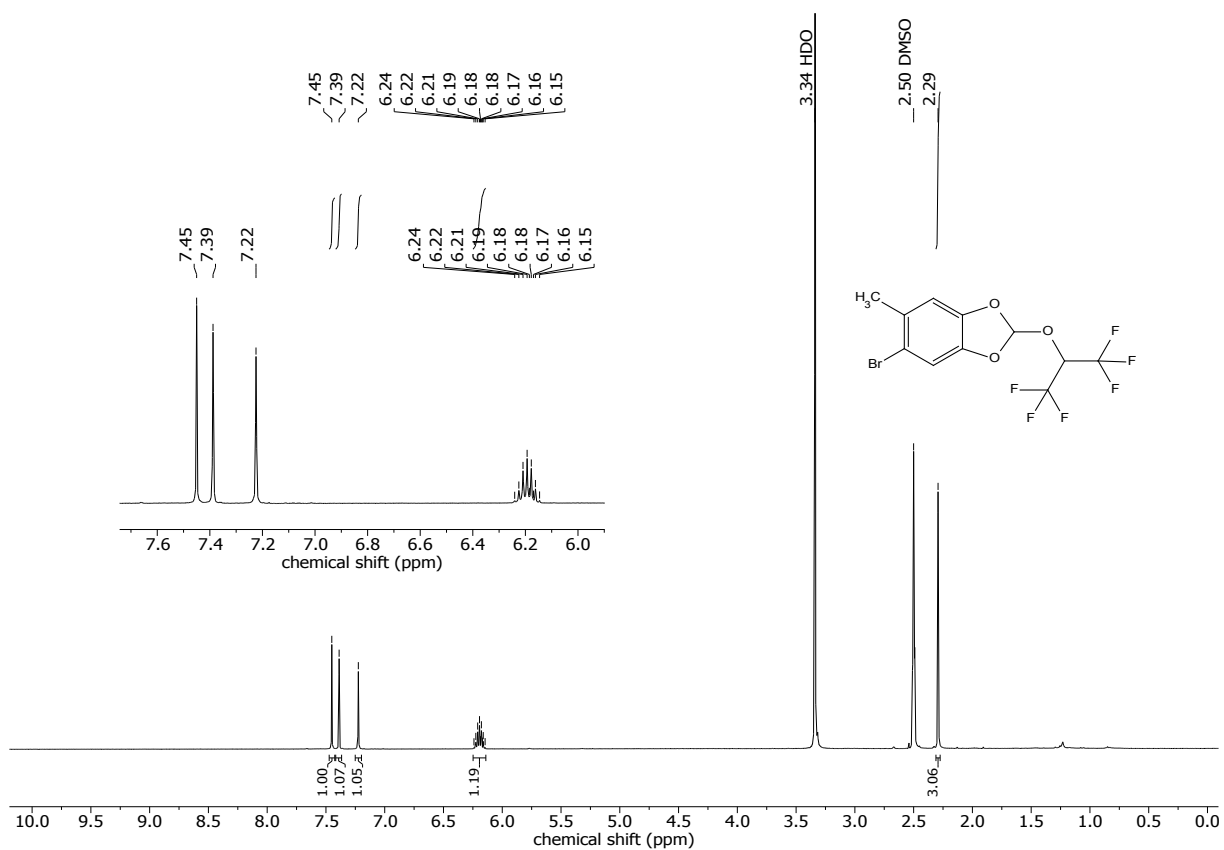


¹H NMR of 5-Chloro-2-((2,2,3,3,4,4,5,5-octafluoropentyl)oxy)-1,3-benzodioxole. (23)

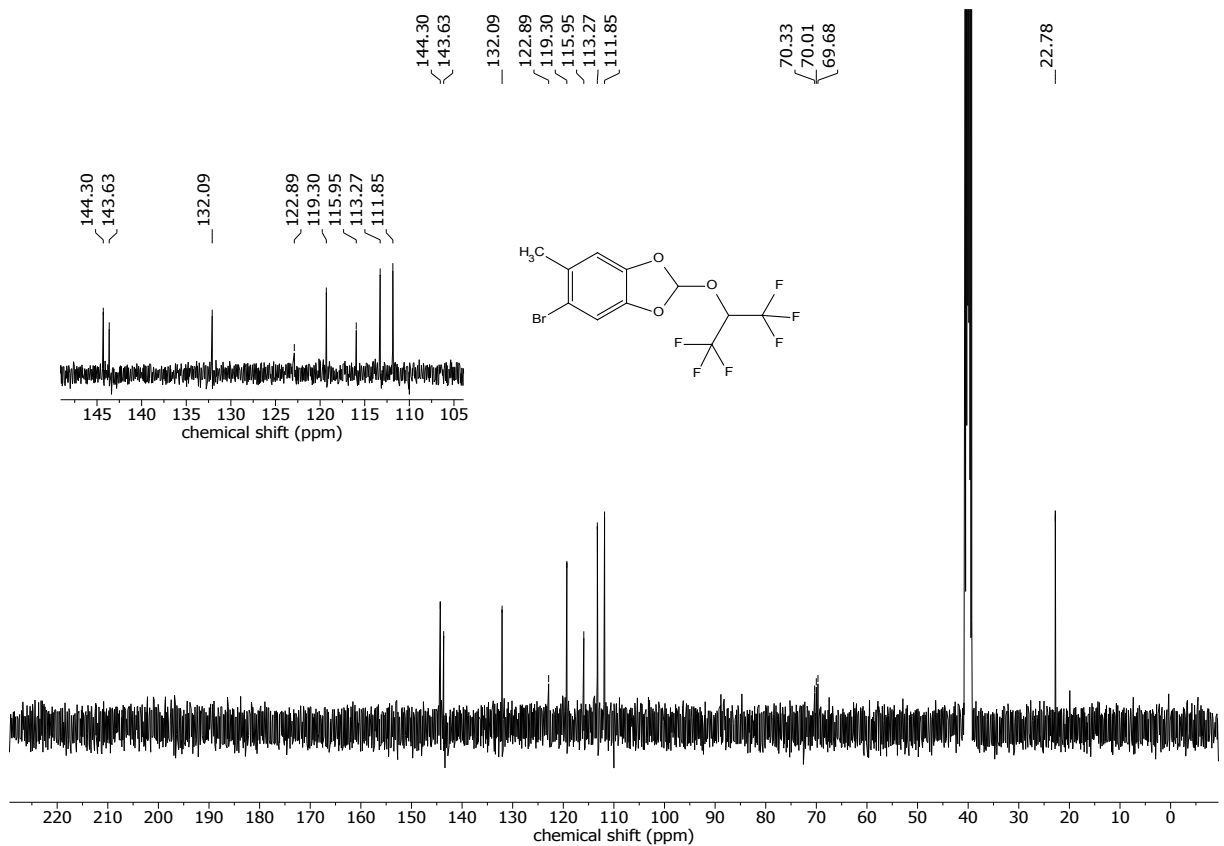


¹³C NMR of 5-Chloro-2-((2,2,3,3,4,4,5,5-octafluoropentyl)oxy)-1,3-benzodioxole. (23)

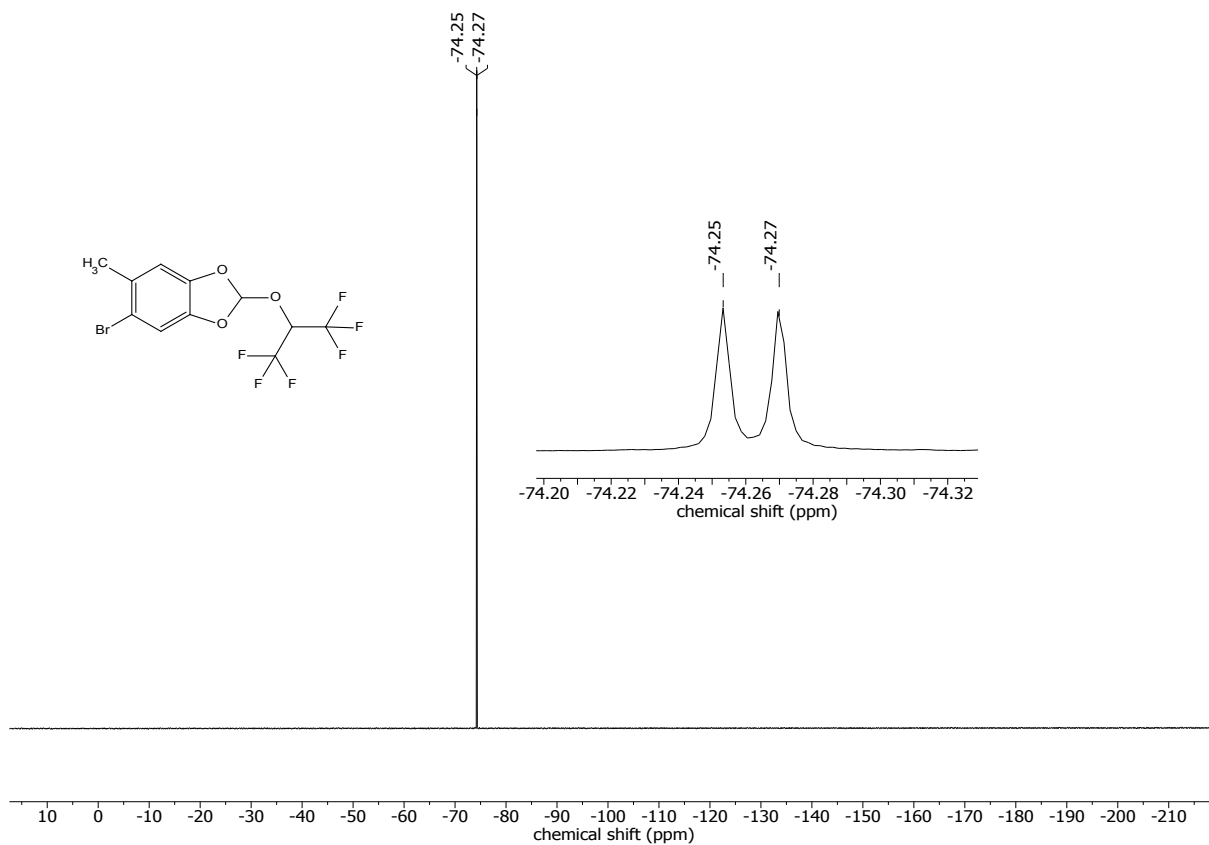




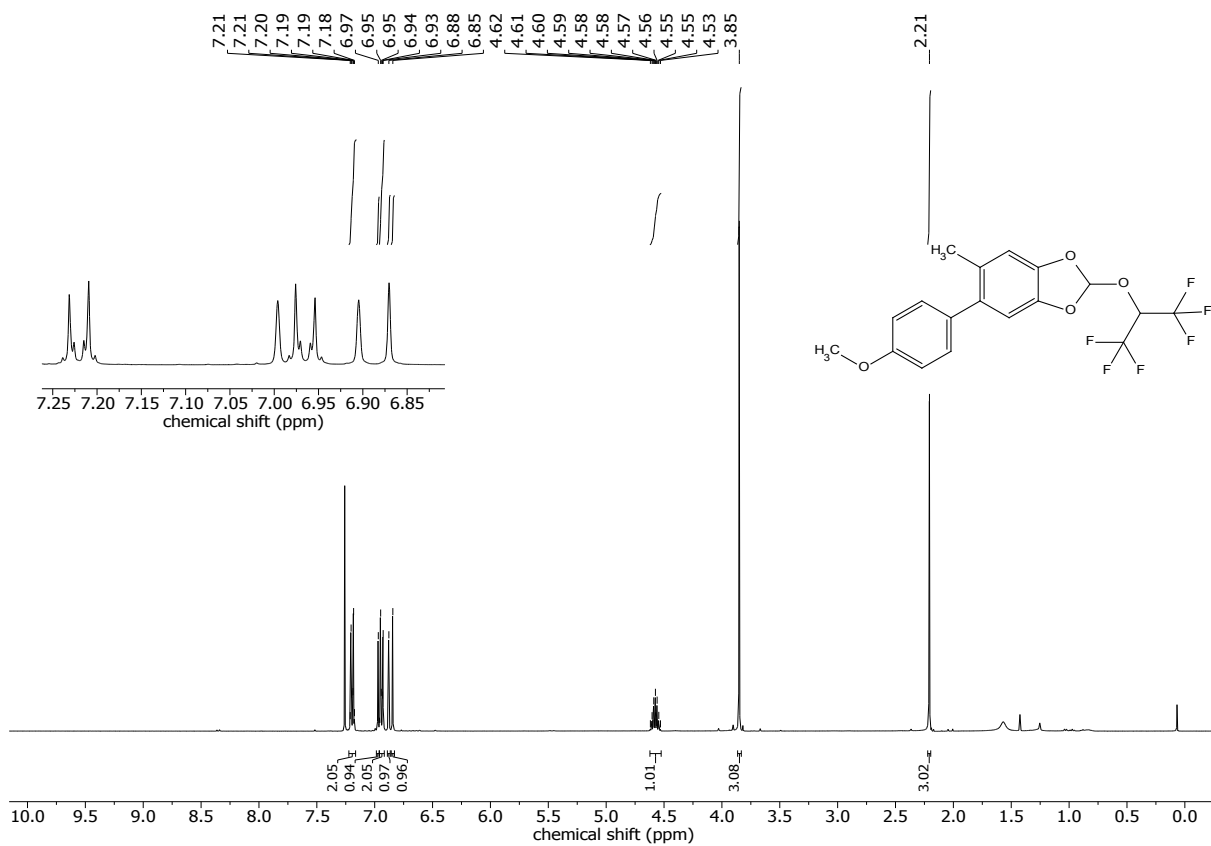
¹H NMR of 5-Bromo-2-(1-trifluoromethyl-(2,2,2-trifluoroethyl)oxy)-6-methyl-1,3-benzodioxole (24)



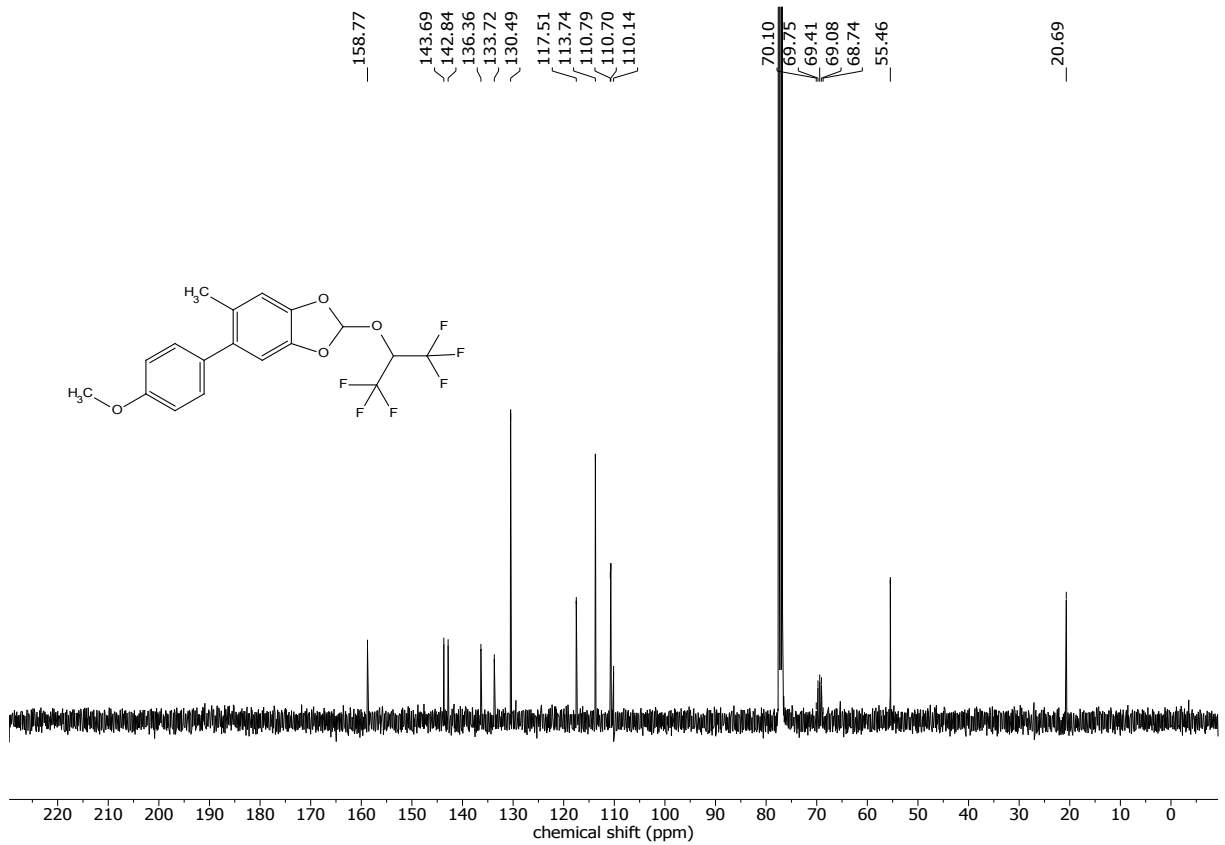
¹³C NMR of 5-Bromo-2-(1-trifluoromethyl-(2,2,2-trifluoroethyl)oxy)-6-methyl-1,3-benzodioxole (24)



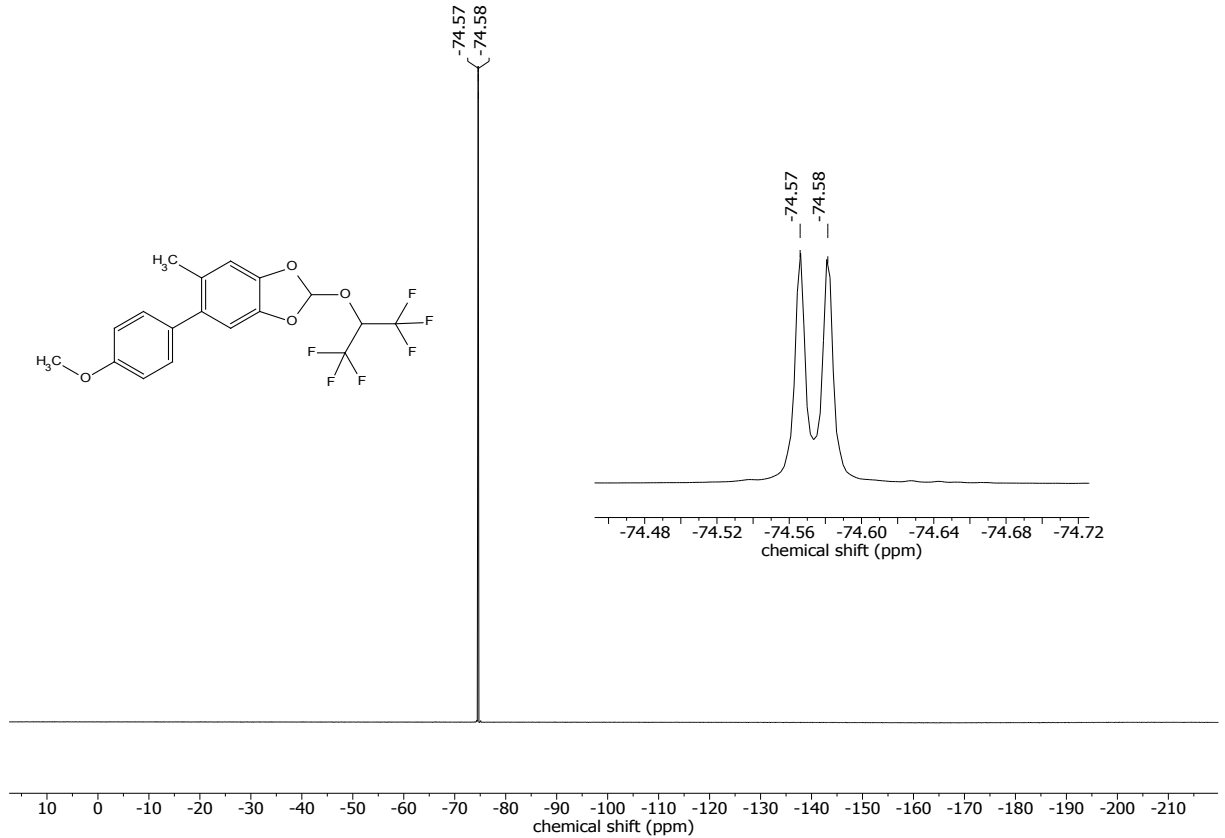
¹⁹F NMR of 5-Bromo-2-(1-trifluoromethyl-(2,2,2-trifluoroethyl)oxy)-6-methyl-1,3-benzodioxole (24**)**



¹H NMR of 2-(1-Trifluoromethyl-(2,2,2-trifluoroethyl)oxy)-5-(4-methoxyphenyl)-6-methyl-1,3-benzodioxole (25**)**



¹³C NMR of 2-(1-Trifluoromethyl-(2,2,2-trifluoroethyl)oxy)-5-(4-methoxyphenyl)-6-methyl-1,3-benzodioxole (**25**)



¹⁹F NMR of 2-(1-Trifluoromethyl-(2,2,2-trifluoroethyl)oxy)-5-(4-methoxyphenyl)-6-methyl-1,3-benzodioxole (**25**)

8. References

- [1] W. L. F. Armarego, C. L. L. Chai, *Purification of laboratory chemicals*, Elsevier, Amsterdam, **2013**.
- [2] C. Gütz, B. Klöckner, S. R. Waldvogel, *Org. Process Res. Dev.* **2016**, *20*, 26–32. (see SI thereof).
- [3] A. Kirste, G. Schnakenburg, F. Stecker, A. Fischer, S. R. Waldvogel, *Angew. Chem. Int. Ed.* **2010**, *49*, 971-975; *Angew. Chem.* **2010**, *122*, 983–987. (see SI thereof).
- [4] H.G. Thomas, A. Schmitz, *Synthesis* **1985**, 31–33.
- [5] a) H. Volz, G. Zimmermann, *Tet. Lett.* **1970**, *41*, 1597-3800; b) K. Dimroth, P. Heinrich, K. Schromm, *Angew. Chem.* **1965**, *77*, 873.
- [6] De Hardo, T.; Nevado, C. *J. Am. Chem. Soc.*, **2010**, *132*, 1512–1513.
- [7] Victor, S. R.; Crisóstomo, F. R.; Bueno, F. C.; Pagnocca, F. C.; Fernandes, J. B.; Correa, A. G.; Bueno, O. C.; Hebling, M. J.; Bacci, M.; Vieira, P. C.; da Silva, M. F. *Pest Management Science*, **2001**, *57* (7), 603–608.
- [8] Li, Y.; Wang, Z.; Wu, X.-F. *Green Chemistry*, **2018**, *20* (5), 969–972.
- [9] Del Carmen Cruz, M.; Tamariz, J. *Tetrahedron* **2005**, *61*, 10061–10072.
- [10] Cai, X.; Qian, C.; Zhai, H. US2008/234314, **2008**.



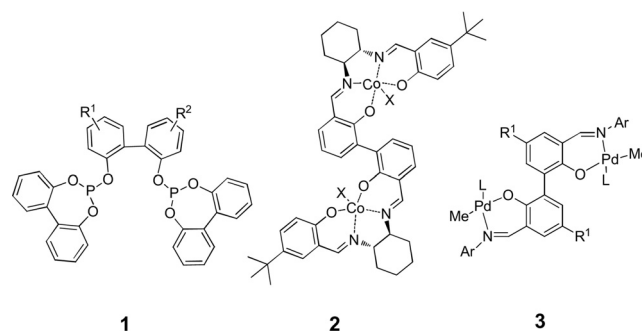
Dehydrogenative Anodic C–C Coupling of Phenols Bearing Electron-Withdrawing Groups

Johannes L. Röckl, Dieter Schollmeyer, Robert Franke, and Siegfried R. Waldvogel*

Abstract: We herein present a metal-free, electrochemical method that enables the direct dehydrogenative coupling reactions of phenols carrying electron-withdrawing groups for the first time. The reactions are easy to conduct and scalable, as they are carried out in undivided cells and obviate the necessity for additional supporting electrolyte. As such, this conversion is efficient, practical, and thereby environmentally friendly, as production of waste is minimized. The method features a broad substrate scope, and a variety of functional groups are tolerated, providing easy access to precursors for novel polydentate ligands and even heterocycles such as dibenzofurans.

2,2'-Biphenols are an important structural feature of a variety of ligands in transition metal catalysis.^[1] Phosphite ligands **1** are used on the industrial scale in the hydroformylation process.^[2] The biphenols carrying electron-withdrawing groups are excellent precursors for salen-type ligands **2**, which can be employed in various polymerization reactions, such as in the asymmetric copolymerization of CO₂ with *meso*-epoxides to give optically active polycarbonates, and in neutral nickel and palladium complexes **3** used as precatalysts for norbornene polymerization (Scheme 1).^[3]

The dehydrogenative coupling plays an important role in modern organic chemistry, since it is a very efficient way to selectively form C–C bonds.^[4] Therefore, numerous studies on the syntheses of biaryls have been reported, but the direct



Scheme 1. Important ligands for transition metal catalysis involving the 2,2'-biphenol motif.

synthesis of 2,2'-biphenols exhibiting electron-withdrawing moieties in 3,3'-positions have been rarely reported. A very efficient copper-catalyzed reaction providing symmetrical and unsymmetrical 2,2'-BINOL derivatives in >90% *ee* in the presence of O₂ was developed by Kozłowski et al.^[5] The protocol tolerates a variety of electron-withdrawing groups in position 3 and proceeds in good yields and high selectivity. However, the synthesis of cross-coupled naphthols proceeded with low selectivity. Furthermore, this method seems to be limited to naphthols as substrates. To the best of our knowledge, only substrates carrying electron-releasing groups or halogens have been successfully converted by electrochemistry so far.^[6] Halo-2,2'-biphenols have been successfully synthesized via anodic oxidation of *o,o'*-dihalogenated phenols by the Nishiyama group.^[7] The reaction was conducted at a very low current density and using undesirable LiClO₄ as an additional supporting electrolyte provided the coupled product in only 25% yield (Scheme 2).

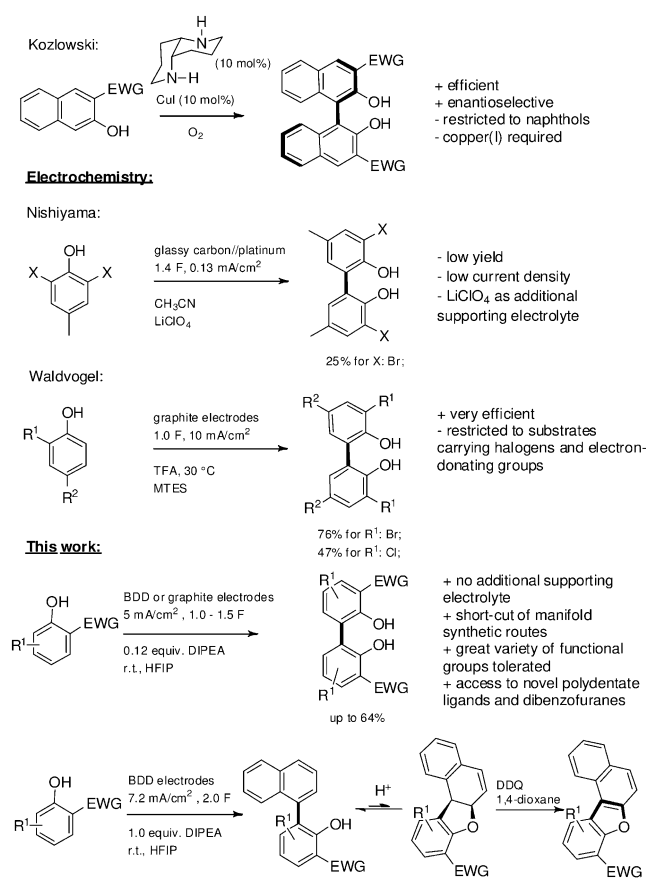
In previous work, our group was also able to access 3,3'-dihalo-2,2'-biphenols.^[8] When trifluoroacetic acid in combination with methyltriethylammonium methylsulfate as the supporting electrolyte is used, 2-halophenols can be converted in high current efficiency when a high current density is applied. Noteworthy are the high yields of 76% for the 3,3'-dibromo-2,2'-biphenol and 47% for the 3,3'-dichloro-2,2'-biphenol. However, this methodology is still limited to substrates equipped with electron-releasing substituents. As a complementary method, the anodic C–C coupling of phenols with electron-withdrawing groups is presented here for the first time. This electrolytic conversion represents an efficient, metal-free route to symmetric 2,2'-biphenols having electron-withdrawing groups in good yields and high selectivity. Coupling these phenols with naphthalenes leads to polycyclic intermediates, which can be further oxidized to dibenzofurans or cleaved to access the desired cross-coupled

[*] J. L. Röckl, Dr. D. Schollmeyer, Prof. Dr. S. R. Waldvogel
Institute of Organic Chemistry
Johannes Gutenberg University Mainz
Duesbergweg 10–14, 55128 Mainz (Germany)
E-mail: waldvogel@uni-mainz.de
Homepage: <https://www.aksw.uni-mainz.de>

J. L. Röckl, Prof. Dr. S. R. Waldvogel
Graduate School Materials Science in Mainz (Germany)
Prof. Dr. R. Franke
Evonik Performance Materials GmbH
Paul-Baumann-Str. 1, 45772 Marl (Germany)
Prof. Dr. R. Franke
Lehrstuhl für Theoretische Chemie, Ruhr-Universität Bochum
Universitätsstraße 150, 44801 Bochum (Germany)

Supporting information and the ORCID identification number(s) for the author(s) of this article can be found under <https://doi.org/10.1002/anie.201910077>.

© 2019 The Authors. Published by Wiley-VCH Verlag GmbH & Co. KGaA. This is an open access article under the terms of the Creative Commons Attribution Non-Commercial NoDerivs License, which permits use and distribution in any medium, provided the original work is properly cited, the use is non-commercial, and no modifications or adaptations are made.



Scheme 2. Synthetic strategies to 2,2'-biphenols incorporating electron-withdrawing groups. EWG = electron-withdrawing group; TFA = trifluoroacetic acid; MTES = methyltriethylammonium methylsulfate; BDD = boron-doped diamond; DIPEA = diisopropylamine; HFIP = 1,1,1,3,3,3-hexafluoroisopropanol.

products. The use of base as an additive in 1,1,1,3,3,3-hexafluoroisopropanol (HFIP) obviates additional supporting electrolyte. The reactions are easy to conduct and scalable.

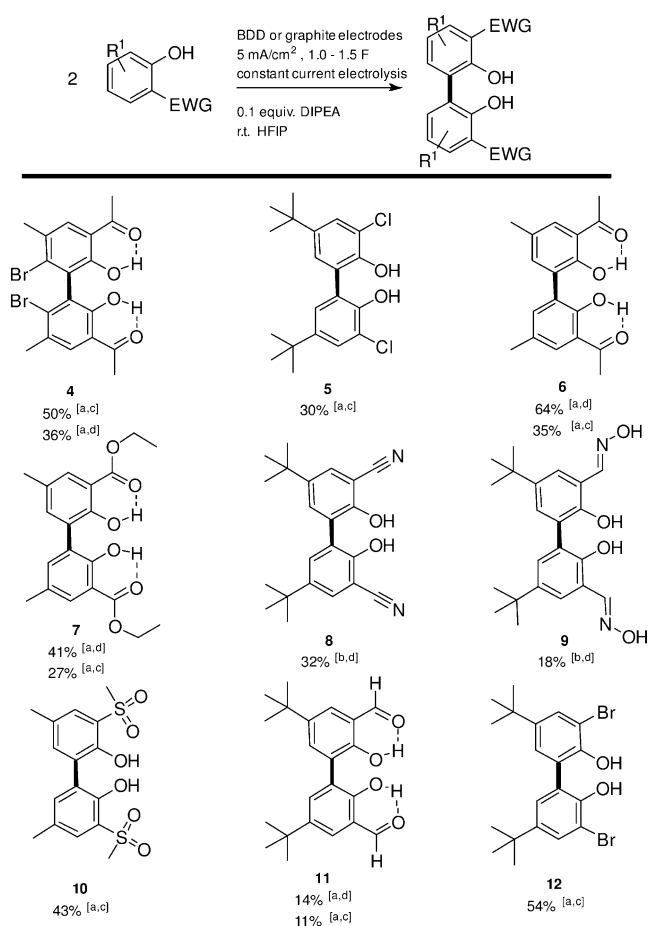
Electro-organic synthesis has become an important part of the synthetic organic toolkit which offers a number of advantages over conventional chemical processes. As well as facilitating novel routes to obtain desired structures, electro-organic synthesis is inherently safe and step-economical.^[9] Reaction conditions are typically mild and importantly, electrons can be used as a sustainable reagent. Consequently, no reagent waste is produced. As a result, conventional chemical oxidizers and reducing agents can be replaced by electric current as an inexpensive, renewable, and safe alternative. Usually, electrochemistry is associated with oxidative or reductive transformations, but this mild method to generate radicals from the substrates allows a much broader and versatile scope of reactivity.^[11] Moreover, such electrosyntheses may be performed discontinuously or on different power levels,^[12] making it compatible with fluctuating renewable energy sources. In our work, the control of selectivity is achieved by HFIP. This solvent is capable of stabilizing reactive intermediates generated at the anode while being very electrochemically stable with a very broad potential window of 4.5 V.^[13] Notably, this solvent can be

easily recovered and reused. Aside from stabilization, HFIP can decouple nucleophilicity from oxidation potential.^[14] For the anodic coupling, it was found that HFIP performed best in combination with boron-doped diamond (BDD) as the electrode material, but here inexpensive graphite serves just as well.

In order to achieve high selectivity in the homo-coupling reaction, the formation of HFIP benzylic ether had to be suppressed.^[15] This was accomplished by using a low current density of 5 mA cm⁻². The greatest impact on the yield of this reaction was the concentration of starting material. The highest yield of **4** was obtained at a starting material concentration of 0.5 M. However, the solubility limit of the starting material was also reached at this concentration, preventing higher concentrations from being obtained. The minimum amount of diisopropylethylamine (DIPEA) required in this reaction to ensure sufficient conductivity is as low as 0.12 equivalents relative to the phenolic substrate. When other bases such as pyridine are used, O–C coupling becomes dominant and the yield drops dramatically. The applied charge can be as low as 1.0–1.5 F (per mole of phenol), resulting in high current efficiency; when higher charge was applied, over-oxidation and oligomerization took place. The preferred electrode material is BDD, but in some cases, graphite is superior. The low cost of graphite is beneficial for latter technical applications.^[16] Additionally, when halogens are present (**4**, **5**, **12**), BDD is preferred as electrode material, because graphite can promote formation of the O–C coupled product (Scheme 3). Other solvents, such as acetonitrile, proved unsuccessful, as they lead to dehalogenation reactions and were not observed to facilitate any C–C or C–O coupling. For ketone (**6**) and ester (**7**) as functional groups, graphite lead to significantly higher yields up to 64%. Halogenated 2,2'-biphenols (**4**, **5**, **12**) can be synthesized yields up to 54%. Nitriles (**8**), oximes (**9**), and sulfones (**10**) are also tolerated, providing polydentate ligand precursors in a straightforward manner in yields up to 43%. Even an aldehyde (**11**) was tolerated to give the product in low yields; the electrode material was not found to play a significant role here. Notably, the very sterically hindered ketone (**4**) was accessible in a yield of 50%. The application of nitro groups yielded only a small amount of biphenol and phosphonates were not tolerated at all.

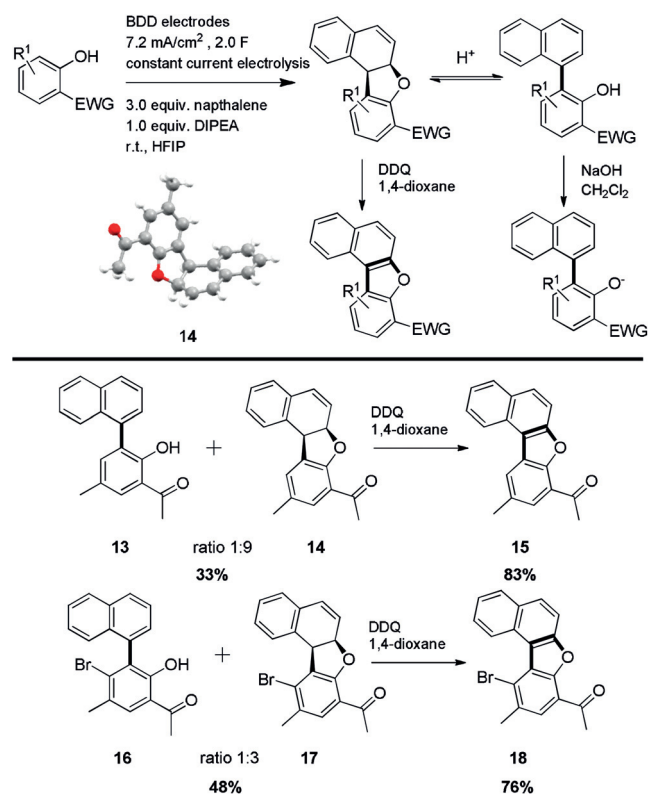
The bromo moiety of **4** is amenable to further derivatizations and X-ray analysis revealed an angle about the aryl–aryl axis of almost 90° (Scheme 5). Conjugation of the π -systems is no longer possible, which makes the product less prone to over-oxidation, as previously investigated by our group.^[6c] Also, the product shows strong hydrogen bonds between the keto moiety and the phenolic proton.

In addition, access to cross-coupling employing phenols carrying electron-withdrawing groups was explored using our methodology. When 2-hydroxy-5-methylacetophenone and naphthalene were co-electrolyzed, a polycyclic structure **14** was obtained as the main product, instead of the expected cross-coupled derivative **13** (Scheme 4). The highest yields were obtained at a concentration of 0.1 M and with an excess of naphthalene (3.0 equivalents). An applied charge of 2.0 F was sufficient and with BDD electrodes the best yields were



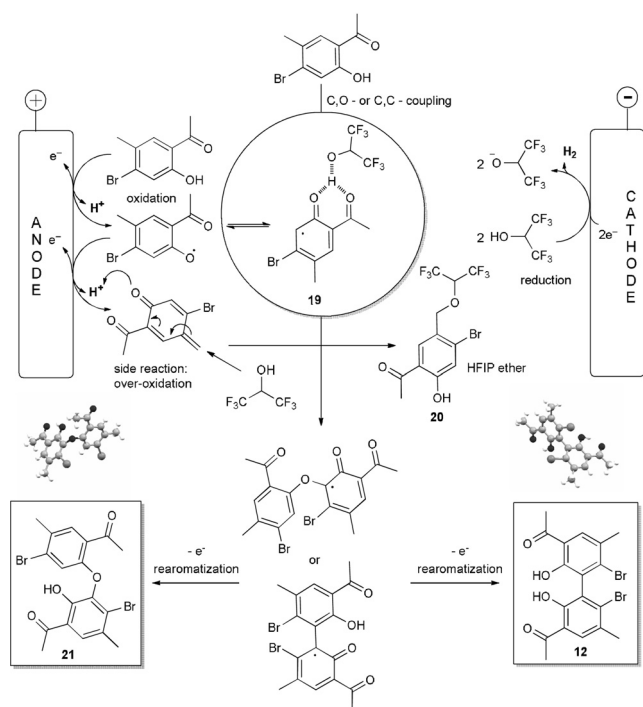
obtained. Product **14** could only be selectively oxidized to the corresponding dibenzofuran **15** using 2,3-dichloro-5,6-dicyano-1,4-benzoquinone (DDQ) in 1,4-dioxane in 83% yield. Further application of current did not yield the desired **15**, contrary to our expectations. The same reaction pathway could be shown for 4-bromo-2-hydroxy-5-methylacetophenone, and gave an even higher overall yield, but a lower selectivity towards the polycyclic intermediate **17**. This mixture was then subjected to further oxidation with DDQ to furnish **18** in 76% yield. When the cyclic product **14** is treated with 1M HCl, a ring opening leading to formation of phenol **16** occurred. After work-up of the mixture, the polycyclic product **17** could again be observed in NMR, which indicates that these two isomers are in equilibrium. This represents an interesting, to our knowledge, previously unknown form of tautomerism. When treated with an excess of 1M NaOH, this equilibrium is completely shifted to the phenolate (Scheme 4). When aldehydes instead of ketones were employed, the yield dropped dramatically, due to over-oxidation (see the Supporting Information).

To demonstrate the scalability of our method, we synthesized compound **6** on a 66.6 mmol scale. The substrates



carrying the carbonyl moiety showed not only the highest yield in the 5 mL beaker cells, but they also represent precursors for a variety of polydentate ligands, for example, salen-type ligands (**2**). In addition, these types of structures are used for the synthesis of several binuclear boron^[17] and aluminum^[18] complexes, for application in optoelectronic devices and as catalysts in polymerization reactions.^[3,18] Therefore, a simple and scalable method for the synthesis of these structural motifs is of high interest. The synthesis routes to this structural motif are mostly complicated, multistep, and low-yielding: Compound **6** can be prepared starting from *p*-cresol in a five-step procedure in an overall yield of 1.1%, involving an iodination, *p*-tosyl protection, a reductive coupling using copper, and a Fries-type rearrangement.^[19] The electrolysis was scaled up by a factor of 13.3 and was conducted in a 500 mL flask-type cell (Figure S2 in the Supporting Information). The achieved yield of 59% corresponds approximately to the yield in the 5 mL beaker-type cell (64%) and therefore clearly shows the scalability of this method.

Both the O,C-**21** and the C,C-coupled product **12** could be crystallized and their structures were determined by X-ray analysis (Scheme 5). HFIP ether **20** could be observed during the optimization (confirmed by GC-MS and NMR), which is in accordance with observations in our previous work.^[15] We therefore propose that an oxidation step and a subsequent deprotonation leads to **19**. This intermediate can either be attacked by the nucleophilic oxygen or carbon, leading, after a further oxidation and subsequent rearomatization, to **21** or



Scheme 5. Proposed mechanisms for the C–C and O–C coupling of phenols carrying electron-withdrawing groups and the formation of HFIP ethers. Molecular structures of **21** and **12** determined by X-ray analysis are displayed.

to the desired product **12**. Further oxidation of **19** provides a quinone methide intermediate which is likely to be attacked by HFIP in a 1,6-addition, leading to **20**. This explains why a lower current density, as well as a higher concentration of phenol, leads to higher yields of desired 2,2'-biphenol. The radical can then be trapped immediately by phenol instead of being further oxidized or undergoing other side reactions. Also, the recombination of such two radicals seems to be a possible pathway to the desired product.

In conclusion, we have established a highly efficient and scalable method for the electrochemical dehydrogenative homo- and cross-coupling of a broad variety of phenols carrying electron-withdrawing groups in good yields. The resulting products represent precursors for polydentate ligands, which have great importance in transition metal catalysis. By electrochemistry the route towards an important example could be shortened by three steps (when started from *p*-cresol) and the overall yield enhanced by a factor of 50. Cross-coupling reactions with naphthalenes deliver biaryls and precursors for dibenzofurans. The reactions are easy to conduct and no additional supporting electrolyte is needed, since a very low amount of base ensures sufficient conductivity, resulting in a high atom efficiency. In addition, the reaction proceeds with a high current efficiency.

Acknowledgements

J.L. Röckl is a recipient of a DFG fellowship through the Excellence Initiative by the Graduate School Materials

Science in Mainz (GSC 266). Support of the Advanced Lab of Electrochemistry and Electrosynthesis – ELYSION (Carl-Zeiss-Stiftung) is gratefully acknowledged.

Conflict of interest

The authors declare no conflict of interest.

Keywords: C–C coupling · cross-coupling · electrochemistry · oxidation · oxygen heterocycles

How to cite: *Angew. Chem. Int. Ed.* **2020**, *59*, 315–319
Angew. Chem. **2020**, *132*, 323–327

- [1] a) P. J. Walsh, A. E. Lurain, J. Balsells, *Chem. Rev.* **2003**, *103*, 3297–3344; b) A. Alexakis, D. Polet, S. Rosset, S. March, *J. Org. Chem.* **2004**, *69*, 5660–5667.
- [2] R. Franke, D. Selent, A. Börner, *Chem. Rev.* **2012**, *112*, 5675–5732.
- [3] a) T. Hu, Y.-G. Li, Y.-S. Li, N.-H. Hu, *J. Mol. Catal. Chem.* **2006**, *253*, 155–164; b) Y. Liu, W.-M. Ren, J. Liu, X.-B. Lu, *Angew. Chem. Int. Ed.* **2013**, *52*, 11594–11598; *Angew. Chem.* **2013**, *125*, 11808–11812; c) H.-C. Zhang, W.-S. Huang, L. Pu, *J. Org. Chem.* **2001**, *66*, 481–487.
- [4] a) C.-J. Li, *Acc. Chem. Res.* **2009**, *42*, 335–344; b) S. Tang, Y. Liu, A. Lei, *Chem* **2018**, *4*, 27–45; c) H. Yi, G. Zhang, H. Wang, Z. Huang, J. Wang, A. Lei, *Chem. Rev.* **2017**, *117*, 9016–9085; d) Z.-J. Wu, S.-R. Li, H. Long, H.-C. Xu, *Chem. Commun.* **2018**, *54*, 4601–4604; e) Z.-J. Wu, S. R. Li, H.-C. Xu, *Angew. Chem. Int. Ed.* **2018**, *57*, 14070–14074; *Angew. Chem.* **2018**, *130*, 14266–14270; f) S. R. Waldvogel, S. Lips, M. Selt, B. Riehl, C. J. Kampf, *Chem. Rev.* **2018**, *118*, 6706–6765; g) H. Shalit, A. Dyadyuk, D. Pappo, *J. Org. Chem.* **2019**, *84*, 1677–1686.
- [5] X. Li, B. Hewgley, C. A. Mulrooney, J. Yang, M. C. Kozlowski, *J. Org. Chem.* **2003**, *68*, 5500–5511.
- [6] a) B. Riehl, K. Dyballa, R. Franke, S. R. Waldvogel, *Synthesis* **2016**, *49*, 252–259; b) B. Elsler, D. Schollmeyer, K. M. Dyballa, R. Franke, S. R. Waldvogel, *Angew. Chem. Int. Ed.* **2014**, *53*, 5210–5213; *Angew. Chem.* **2014**, *126*, 5311–5314; c) A. Wiebe, D. Schollmeyer, K. M. Dyballa, R. Franke, S. R. Waldvogel, *Angew. Chem. Int. Ed.* **2016**, *55*, 11801–11805; *Angew. Chem.* **2016**, *128*, 11979–11983; d) B. Dahms, P. J. Kohlpaintner, A. Wiebe, R. Breinbauer, D. Schollmeyer, S. R. Waldvogel, *Chem. Eur. J.* **2019**, *25*, 2713–2716; e) S. Lips, A. Wiebe, B. Elsler, D. Schollmeyer, K. M. Dyballa, R. Franke, S. R. Waldvogel, *Angew. Chem. Int. Ed.* **2016**, *55*, 10872–10876; *Angew. Chem.* **2016**, *128*, 11031–11035; f) B. Dahms, R. Franke, S. R. Waldvogel, *Chem-ElectroChem* **2018**, *5*, 1249–1252; g) A. Wiebe, S. Lips, D. Schollmeyer, R. Franke, S. R. Waldvogel, *Angew. Chem. Int. Ed.* **2017**, *56*, 14727–14731; *Angew. Chem.* **2017**, *129*, 14920–14925; h) S. Lips, D. Schollmeyer, R. Franke, S. R. Waldvogel, *Angew. Chem. Int. Ed.* **2018**, *57*, 13325–13329; *Angew. Chem.* **2018**, *130*, 13509–13513; i) S. Lips, B. A. Frontana-Urbe, M. Dörr, D. Schollmeyer, R. Franke, S. R. Waldvogel, *Chem. Eur. J.* **2018**, *24*, 6057–6061.
- [7] M. Takahashi, H. Konishi, S. Iida, K. Nakamura, S. Yamamura, S. Nishiyama, *Tetrahedron* **1999**, *55*, 5295–5302.
- [8] A. Kirste, S. Hayashi, G. Schnakenburg, I. Malkowsky, F. Stecker, A. Fischer, T. Fuchigami, S. R. Waldvogel, *Chem. Eur. J.* **2011**, *17*, 14164–14169.
- [9] a) E. J. Horn, B. R. Rosen, P. S. Baran, *ACS Cent. Sci.* **2016**, *2*, 302–308; b) E. J. Horn, B. R. Rosen, Y. Chen, J. Tang, K. Chen, M. D. Eastgate, P. S. Baran, *Nature* **2016**, *533*, 77–81.

- [10] a) S. R. Waldvogel, B. Janza, *Angew. Chem. Int. Ed.* **2014**, *53*, 7122–7123; *Angew. Chem.* **2014**, *126*, 7248–7249; b) S. R. Waldvogel, S. Möhle, *Angew. Chem. Int. Ed.* **2015**, *54*, 6398–6399; *Angew. Chem.* **2015**, *127*, 6496–6497; c) S. R. Waldvogel, M. Selt, *Angew. Chem. Int. Ed.* **2016**, *55*, 12578–12580; *Angew. Chem.* **2016**, *128*, 12766–12768.
- [11] a) A. Wiebe, T. Gieshoff, S. Möhle, E. Rodrigo, M. Zirbes, S. R. Waldvogel, *Angew. Chem. Int. Ed.* **2018**, *57*, 5594–5619; *Angew. Chem.* **2018**, *130*, 5694–5721; b) S. Möhle, M. Zirbes, E. Rodrigo, T. Gieshoff, A. Wiebe, S. R. Waldvogel, *Angew. Chem. Int. Ed.* **2018**, *57*, 6018–6041; *Angew. Chem.* **2018**, *130*, 6124–6149.
- [12] A. Wiebe, B. Riehl, S. Lips, R. Franke, S. R. Waldvogel, *Sci. Adv.* **2017**, *3*, eaao3920.
- [13] a) R. Francke, D. Cericola, R. Kötz, D. Weingarth, S. R. Waldvogel, *Electrochim. Acta* **2012**, *62*, 372; b) L. Ebersson, M. P. Hartshorn, O. Persson, *J. Chem. Soc. Perkin Trans. 2* **1995**, 1735–1744; c) M. Lucarini, V. Mugnaini, G. F. Pedulli, M. Guerra, *J. Am. Chem. Soc.* **2003**, *125*, 8318–8329; d) L. Ebersson, O. Persson, M. P. Hartshorn, *Angew. Chem. Int. Ed. Engl.* **1995**, *34*, 2268–2269; *Angew. Chem.* **1995**, *107*, 2417–2418.
- [14] B. Elsler, A. Wiebe, D. Schollmeyer, K. M. Dyballa, R. Franke, S. R. Waldvogel, *Chem. Eur. J.* **2015**, *21*, 12321–12325.
- [15] a) Y. Imada, J. L. Röckl, A. Wiebe, T. Gieshoff, D. Schollmeyer, K. Chiba, R. Franke, S. R. Waldvogel, *Angew. Chem. Int. Ed.* **2018**, *57*, 12136–12140; *Angew. Chem.* **2018**, *130*, 12312–12317; b) J. L. Röckl, Y. Imada, K. Chiba, S. R. Waldvogel, *ChemElectroChem* **2019**, *6*, 4184–4187; c) J. L. Röckl, A. V. Hauck, D. Schollmeyer, S. R. Waldvogel, *ChemistryOpen* **2019**, *8*, 1167–1171.
- [16] J. Kotz, P. Treichel, G. Weaver, *Chemistry and Chemical Reactivity*, 6th ed., Enhanced Review Edition, Brooks/Cole Thomson Learning, Belmont, CA, **2006**.
- [17] K. Dhanunjayarao, V. Mukundam, M. Ramesh, K. Venkatasubbaiah, *Eur. J. Inorg. Chem.* **2014**, 539–545.
- [18] H.-L. Han, Y. Liu, J.-Y. Liu, K. Nomura, Y. S. Li, *Dalton Trans.* **2013**, *42*, 12346–12353.
- [19] N. Tsu, K. Nagashima, *Tetrahedron* **1969**, *25*, 3017–3031.

Manuscript received: August 8, 2019

Accepted manuscript online: September 9, 2019

Version of record online: November 19, 2019

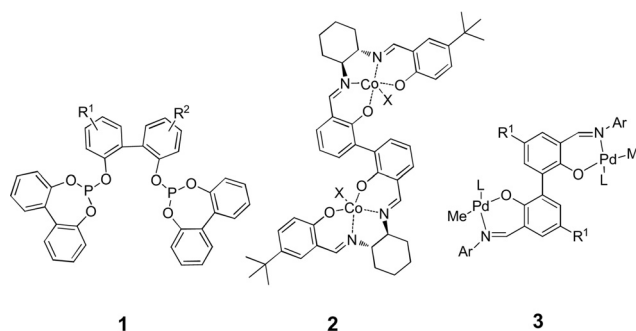


Dehydrierende anodische C-C-Kupplung von Phenolen mit elektronenziehenden Substituenten

Johannes L. Röckl, Dieter Schollmeyer, Robert Franke und Siegfried R. Waldvogel*

Abstract: Wir stellen hier eine metallfreie, elektrosynthetische Methode vor, die erstmals eine direkte dehydrierende Kupplungsreaktionen von Phenolen mit elektronenziehenden Gruppen ermöglicht. Die Reaktionen sind einfach durchzuführen und skalierbar, da sie in ungeteilten Zellen durchgeführt werden und kein zusätzliches Leitsalz benötigt wird. Hierdurch ist diese Umsetzung effizient, praktisch und dadurch besonders umweltfreundlich, da Reagenzabfall minimiert wird. Das Verfahren zeichnet sich durch ein breites Spektrum an möglichen Substraten aus und es werden eine Vielzahl von funktionellen Gruppen toleriert. Das ermöglicht einen einfachen Zugang zu Vorläufern für neuartige mehrzählige Liganden und sogar zu Heterocyclen wie Dibenzofuranen.

Die 2,2'-Biphenole stellen eine wichtige Struktureinheit einer Vielzahl von Liganden in der Übergangsmetallkatalyse dar.^[1] Phosphitliganden **1** werden im industriellen Maßstab im Hydroformylierungsprozess eingesetzt. Biphenole mit elektronenziehenden Gruppen sind ausgezeichnete Vorläufer für mehrkernige Salenliganden **2**, die in verschiedenen Polymerisationsreaktionen eingesetzt werden können, z. B. in einer asymmetrischen Co-Polymerisation von CO₂ mit *meso*-Epoxyden zu optisch aktiven Polycarbonaten (**2**) oder für neutrale Nickel- und Palladiumkomplexe, die als Vorläufer für Katalysatoren für die Norbornenpolymerisation verwendet werden (**3**, Schema 1).^[3]



Schema 1. Wichtige Liganden in der Übergangsmetallkatalyse, welche die 2,2'-Biphenol Struktureinheit beinhalten.

Die dehydrierende Kupplung spielt in der modernen organischen Chemie eine wichtige Rolle, da sie eine sehr effiziente Möglichkeit darstellt, selektiv C-C-Bindungen zu bilden.^[4] Es gibt daher zahlreiche Studien zur Synthese von Biarylverbindungen, aber der direkte Zugang zu 2,2'-Biphenolen mit elektronenziehenden Einheiten in 3,3'-Positionen wurde selten berichtet. Eine sehr effiziente kupferkatalysierte Reaktion zu symmetrischen und unsymmetrischen 2,2'-BINOL-Derivaten in Gegenwart von Sauerstoff wurde von Kozlowski et al. entwickelt.^[5] Das Verfahren toleriert eine Vielzahl von elektronenziehenden Gruppen in 3-Position in guter Ausbeute und hoher Selektivität. Die Synthese von kreuzgekuppelten Naphtholen verlief jedoch mit geringer Selektivität. Darüber hinaus scheint sich diese Methode auf Naphthole als Substrate beschränkt zu sein. Bisher konnten, nach unserem Wissen, nur Substrate mit elektronenschiebenden Gruppen oder Halogenen elektrochemisch erfolgreich umgesetzt werden.^[6] Halo-2,2'-biphenole wurden durch anodische Oxidation von *o,o'*-dihalogenierten Phenolen von Nishiyama und Mitarbeiter erfolgreich synthetisiert.^[7] Die Reaktion lieferte das gekuppelte Produkt bei einer sehr geringen Stromdichte und mit unerwünschtem LiClO₄ als zusätzlichem Leitsalz in lediglich 25 % Ausbeute (Schema 2).

In früheren Arbeiten konnte unsere Gruppe die Synthese von 3,3'-Dihalogen-2,2'-biphenole zeigen.^[8] Bei Verwendung von Trifluoressigsäure in Kombination mit Methyltriethylammoniummethylsulfat als Leitsalz können 2-Halogenphenole bei hohen Stromdichten erfolgreich in hoher Stromausbeute erhalten werden. Bemerkenswert sind die hohen Ausbeuten von 76 % für 3,3'-Dibrom-2,2'-biphenol und 47 % für 3,3'-Dichlor-2,2'-biphenol. Diese Methode ist jedoch immer noch auf Substrate beschränkt, die mit elektronenschiebenden Substituenten oder Halogengruppen ausgestattet sind. Als ergänzendes Verfahren wird hier erstmals die anodische C-C-Kupplung von Phenolen mit elektronenziehenden Gruppen vorgestellt. Diese elektrolytische Umwandlung


[*] J. L. Röckl, Dr. D. Schollmeyer, Prof. Dr. S. R. Waldvogel


Institut für Organische Chemie
 Johannes Gutenberg Universität Mainz
 Duesbergweg 10–14, 55128 Mainz (Deutschland)
 E-Mail: waldvogel@uni-mainz.de
 Homepage: <https://www.aksw.uni-mainz.de>

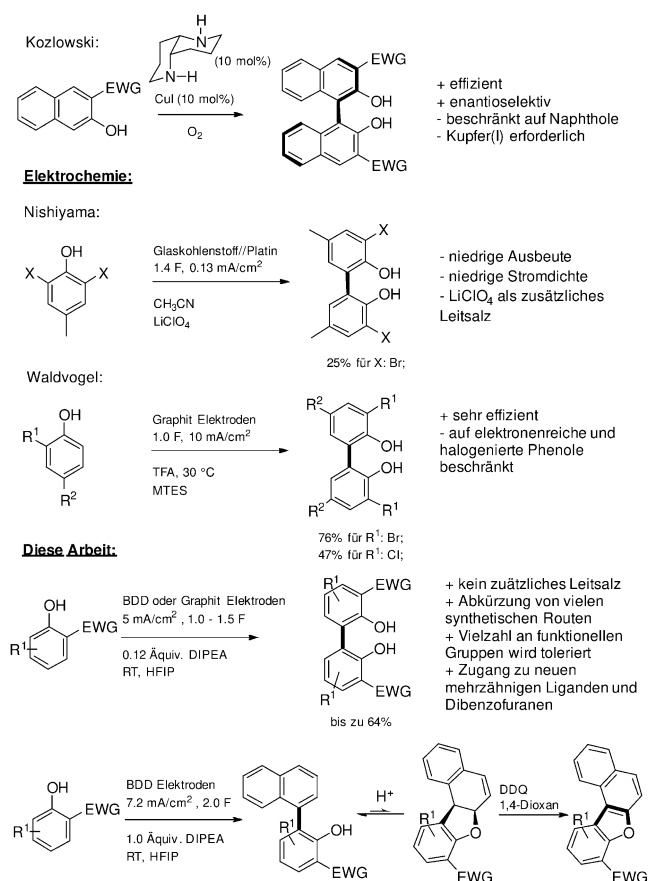
J. L. Röckl, Prof. Dr. S. R. Waldvogel
 Graduate School Materials Science in Mainz (Deutschland)

Prof. Dr. R. Franke
 Evonik Performance Materials GmbH
 Paul-Baumann-Straße 1, 45772 Marl (Deutschland)

Prof. Dr. R. Franke
 Lehrstuhl für Theoretische Chemie, Ruhr-Universität Bochum
 Universitätsstraße 150, 44801 Bochum (Deutschland)

 Hintergrundinformationen und die Identifikationsnummer (ORCID) eines Autors sind unter <https://doi.org/10.1002/ange.201910077> zu finden.

 © 2019 Die Autoren. Veröffentlicht von Wiley-VCH Verlag GmbH & Co. KGaA. Dieser Open Access Beitrag steht unter den Bedingungen der Creative Commons Attribution Non-Commercial NoDerivs License, die eine Nutzung und Verbreitung in allen Medien gestattet, sofern der ursprüngliche Beitrag ordnungsgemäß zitiert und nicht für kommerzielle Zwecke genutzt wird und keine Änderungen und Anpassungen vorgenommen werden.



Schema 2. Synthetische Strategien zu 2,2'-Biphenolen mit elektronenziehenden Gruppen. EWG = elektronenziehende Gruppe; TFA = Trifluoressigsäure; MTES = Methyltriethylammonium-methylsulfat; BDD = bordotierter Diamant; DIPEA = Diisopropylamin; HFIP = 1,1,1,3,3,3-Hexafluorisopropanol.

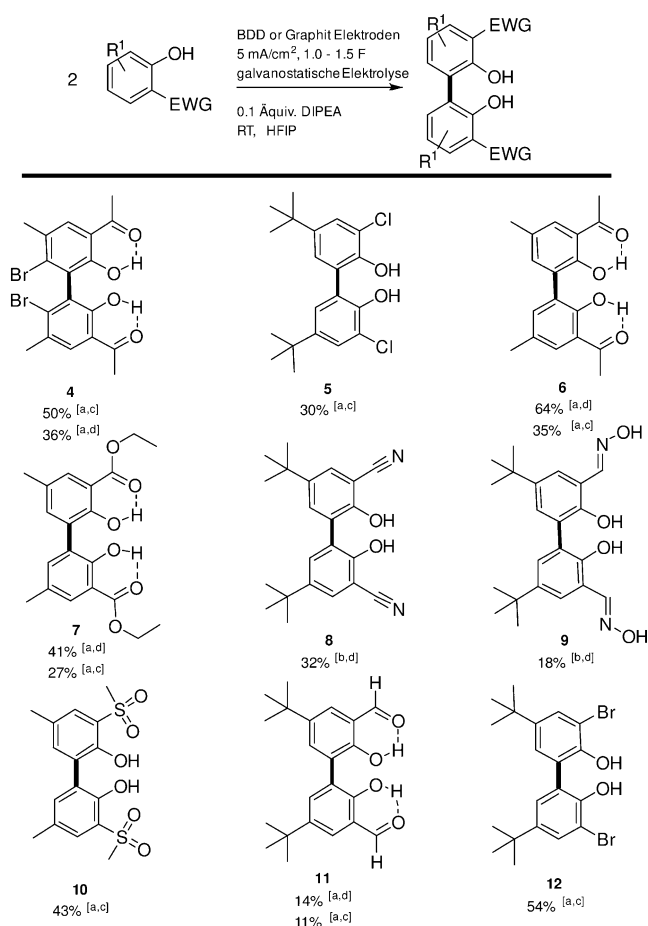
stellt einen effizienten, metallfreien Weg zu symmetrischen 2,2'-Biphenolen dar, die in guter Ausbeute und mit hoher Selektivität abläuft. Die Kupplung dieser Phenole mit Naphthalinen führt zu polycyclischen Zwischenprodukten, die zu Dibenzofuranen oxidiert oder gespalten werden können, um das gewünschte kreuzgekuppelte Produkt zu erhalten. Die Verwendung von Base als Additiv in 1,1,1,3,3,3-Hexafluorisopropanol (HFIP) vermeidet die Verwendung von zusätzlichem Leitsalz. Außerdem sind die Reaktionen einfach durchzuführen und skalierbar.

Die elektroorganische Synthese ist zu einem wichtigen Bestandteil des synthetischen organischen Handwerkszeugs geworden, da sie eine Reihe von Vorteilen gegenüber herkömmlichen chemischen Verfahren bietet. Neben Zugang zu neuartigen Strukturen ist elektroorganische Synthese von Grund auf sicher und stufenökonomisch.^[9] Die Reaktionsbedingungen sind typischerweise mild und Elektronen können als nachhaltiges Reagenz betrachtet werden. Dadurch entsteht kein Reagenzabfall. Als Folge davon werden herkömmliche chemische Oxidationsmittel oder Reduktionsmittel durch elektrischen Strom als kostengünstige, erneuerbare und sichere Alternative ersetzt. Normalerweise ist die Elektrochemie mit oxidativen oder reduktiven Transformationen verbunden, aber die milde Methode zur Erzeugung

von Radikalen aus den Substraten eröffnet einen viel breiteren und vielseitigeren chemischen Raum.^[11] Darüber hinaus können Elektrosynthesen diskontinuierlich oder auf unterschiedlichen Leistungsstufen betrieben werden,^[12] was die Kompatibilität mit schwankenden erneuerbaren Energien ermöglicht. In unserer Arbeit wird die Kontrolle der Selektivität durch HFIP erreicht. Dieses Lösungsmittel ist in der Lage, reaktive Zwischenprodukte, die an der Anode erzeugt werden, zu stabilisieren und gleichzeitig elektrochemisch stabil, mit einem sehr breiten Potentialfenster von 4,5 V, zu sein.^[13] Des Weiteren kann das Lösungsmittel leicht durch einfache Destillation zurückgewonnen und wiederverwendet werden. Neben der Stabilisierung kann HFIP die Nukleophilie vom Oxidationspotential entkoppeln.^[14] Für die anodische Kupplung wurde gefunden, dass HFIP am besten in Kombination mit bordotiertem Diamanten (BDD) als Elektrodenmaterial funktioniert, aber hier kann auch kostengünstiger Graphit erfolgreich eingesetzt werden.

Um eine hohe Selektivität in der Homokupplung der Phenole zu erreichen, musste die benzyliche HFIP-Etherbildung unterdrückt werden.^[15] Dies wurde durch die Verwendung einer geringen Stromdichte von 5 mA cm⁻² erreicht. Den größten Einfluss auf die Ausbeute dieser Reaktion hat die Konzentration des Ausgangsmaterials. Die höchste Ausbeute von **4** wurde bei einer Ausgangsstoffkonzentration von 0,5 M erzielt. Das Löslichkeitslimit des Ausgangsmaterials in HFIP wurde jedoch bereits bei dieser Konzentration erreicht. Die Mindestmenge an Diisopropylethylamin (DIPEA), die in dieser Reaktion benötigt wird, um eine ausreichende Leitfähigkeit zu gewährleisten, beträgt nur 0,12 Äquivalente (bezogen auf das Phenolsubstrat). Wenn andere Basen wie Pyridin verwendet werden, tritt die unerwünschte O-C-Kupplung vermehrt auf und die Ausbeute sinkt drastisch. Die benötigte applizierte Strommenge beträgt 1,0–1,5 F (pro Mol Phenol), was zu einer hohen Stromausbeute führt. Das bevorzugte Elektrodenmaterial ist BDD, aber in einigen Fällen ist Graphit überlegen. Darüber hinaus wird bei Anwesenheit von Halogenen (**4**, **5**, **12**) BDD als Elektrodenmaterial bevorzugt, da Graphit die Bildung des O-C-gekuppelten Produkts fördern kann (Schema 3). Andere Lösungsmittel, wie beispielsweise Acetonitril, erwiesen sich als ungeeignet, da sie zu Dehalogenierungsreaktionen begünstigen. Für Ketone (**6**) und Ester (**7**) als funktionelle Gruppen führt Graphit zu deutlich höheren Ausbeuten von bis zu 64%. Halogenierte 2,2'-Biphenole (**4,5,12**) können in einer Ausbeute von bis zu 54% synthetisiert werden. Nitrile (**8**), Oxime (**9**) und Sulfone (**10**) werden ebenfalls toleriert und ergeben auf einfache Weise Vorläufer von mehrzähligen Liganden mit Ausbeuten von bis zu 43%. Sogar Aldehyde (**11**) wurde toleriert, um das Produkt in niedrigen Ausbeuten zu erhalten; das Elektrodenmaterial spielte dabei keine wesentliche Rolle. Insbesondere das sehr sterisch gehinderte Keton (**4**) war in einer Ausbeute von 50% zugänglich. Die Verwendung von Nitrogruppen ergab nur einen geringen Anteil an Biphenol und Phosphonate wurden überhaupt nicht toleriert.

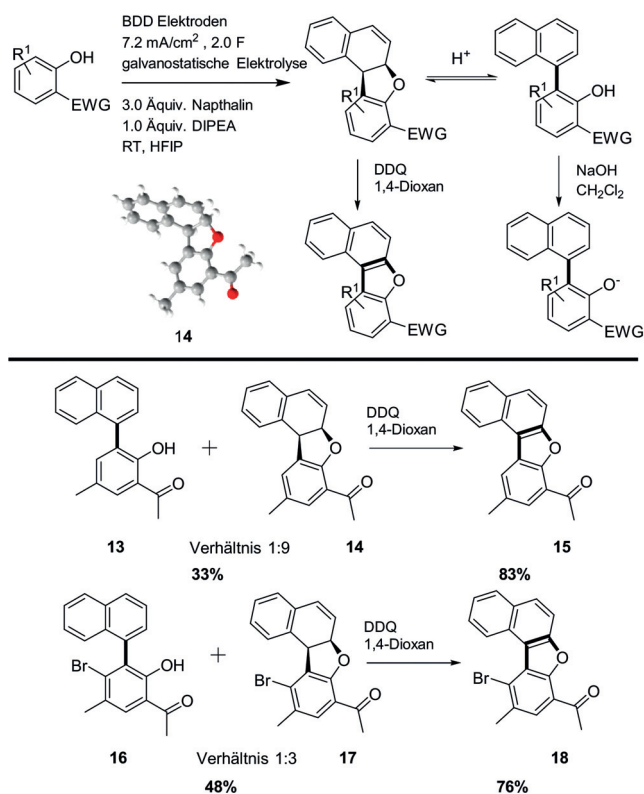
Der Brom-Substituent bei **4** macht weitere Derivatisierungen in dieser Position möglich und die Röntgenstrukturanalyse von geeigneten Einkristallen ergab einen Aryl-Aryl-Achsenwinkel von fast 90° (Schema 5). Die Konjugation der



Schema 3. Substratumfang der Reaktion. [a] Die Elektrolyse wurde in 5 mL HFIP mit 2.5 mmol Substrat in einer ungeteilten Zelle und 0.12 Äquivalenten durchgeführt. DIPEA. [b] Die Elektrolyse wurde in 5 mL HFIP mit 1.0 mmol Substrat in einer ungeteilten Zelle und 0,3 Äquivalenten durchgeführt. DIPEA. [c] Isolierte Ausbeute mit BDD-Elektroden. [d] Isolierte Ausbeute mit Graphitelektroden.

π -Systeme ist daher nicht mehr möglich, was dieses Produkt weniger anfällig für Überoxidation macht, wie bereits von unserer Gruppe untersucht wurde.^[6c] Außerdem zeigt das Produkt starke Wasserstoffbrückenbindungen zwischen der Ketogruppe und dem phenolischen Proton.

Darüber hinaus wurde der Zugang zur Kreuzkupplung mit Phenolen, die elektronenziehende Gruppen tragen, mit unserer Methodik untersucht. Wenn 2-Hydroxy-5-methylacetophenon und Naphthalin gemeinsam elektrolysiert wurden, wurde anstelle des erwarteten kreuzgekuppelten Derivats **13** (Schema 4) eine polycyclische Struktur **14** als Hauptprodukt erhalten. Die höchsten Ausbeuten wurden bei Konzentrationen von 0.1M und einem Überschuss an Naphthalin (3.0 Äquivalente) erzielt. Eine Ladungsmenge von 2.0 F war ausreichend und mit BDD-Elektroden wurden die besten Ausbeuten erzielt. **14** konnte selektiv zu dem entsprechenden Dibenzofuran **15** mit 2,3-Dichlor-5,6-dicyano-1,4-benzochinon (DDQ) in 1,4-Dioxan in 83% Ausbeute oxidiert werden. Eine höhere Ladungsmenge hat entgegen unseren Erwartungen nicht das gewünschte Produkt **15** ergeben. Der gleiche Reaktionsweg konnte für 4-Brom-2-hy-



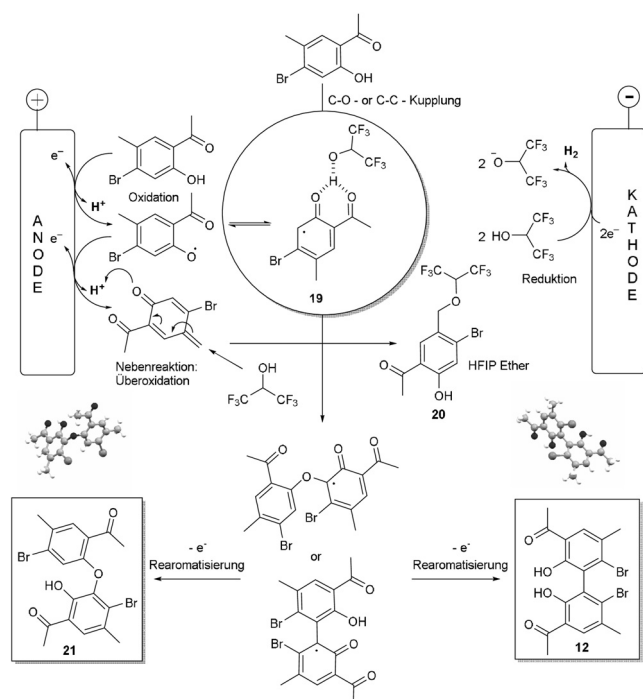
Schema 4. Reaktionsweg der Kreuzkupplung mit Naphthalin. Es werden isolierte Ausbeuten angegeben. Die durch die Röntgenstrukturanalyse bestimmte Molekülstruktur von **14** in *cis*-Konfiguration (*rac*) ist abgebildet.

droxy-5-methylacetophenon gezeigt werden, was zu noch höheren Gesamtausbeuten, aber einer geringeren Selektivität gegenüber dem polycyclischen Zwischenprodukt **17** führt. Diese Mischung wurde dann einer weiteren Oxidation mit DDQ unterzogen, um **18** in 76% Ausbeute zu erhalten. Wenn das cyclische Produkt **14** mit 1M HCl behandelt wird, trat eine Ringöffnung auf, die zur Bildung des Phenols **16** führt. Nach der Aufarbeitung des Reaktionsgemisches konnte das polycyclische Produkt **17** erneut via NMR beobachtet werden, was darauf hindeutet, dass sich diese beiden Isomere im Gleichgewicht befinden. Dies stellt eine nach unserem Kenntnisstand interessante, unbekannt Form der Tautomerie dar. Bei Behandlung mit einem Überschuss von 1M NaOH wird dieses Gleichgewicht vollständig auf die Seite des Phenolats verschoben (Schema 4). Wenn Aldehyde anstelle von Ketonen verwendet wurden, sank die Ausbeute dramatisch (siehe Hintergrundinformationen).

Um die Skalierbarkeit unserer Methode zu demonstrieren, haben wir die Verbindung **6** im 66.6 mmol-Maßstab synthetisiert. Die Substrate die eine Carbonyl-Einheit tragen, zeigten nicht nur die höchste Ausbeute in den 5 mL Bechergläsern, sondern sind auch Vorläufer für eine Vielzahl von mehrzähligen Liganden, z.B. Salenliganden (**2**). Darüber hinaus werden diese Arten von Strukturen für die Synthese mehrerer binuklearer Bor-^[17] und Aluminiumkomplexe,^[18] für den Einsatz in optoelektronischen Vorrichtungen oder als Katalysatoren in Polymerisationsreaktionen verwendet.^[3,18] Daher ist eine einfache und skalierbare Methode zur Syn-

these dieser strukturellen Motive von großem Interesse. Die Synthesewege zu diesem strukturellen Motiv sind meist kompliziert, mehrstufig und verlaufen mit geringen Ausbeuten: **6** wird in einem 5-stufigen Verfahren aus *p*-Kresol in einer Gesamtausbeute von 1,1% synthetisiert, wobei eine Jodierung, ein *p*-Tosyl-Schützung, eine reduktive Kupplung mit Kupfer und eine Fries-Umlagerung durchgeführt werden müssen.^[19] Die Elektrolyse wurde um den Faktor 13.3 hochskaliert und in einem 500-mL-Kolben durchgeführt (Hintergrundinformationen, Abbildung S2). Die erzielte Ausbeute von 59% entspricht in etwa der Ausbeute in der 5 mL Bechercelle (64%) und zeigt damit deutlich die Skalierbarkeit dieses Verfahrens.

Sowohl das O-C- **21** als auch das C-C-gekuppelte Produkt **12** konnten kristallisiert werden und ihre Strukturen wurden durch Röntgenstrukturanalyse bestimmt (Schema 5). Der



Schema 5. Vorgeschlagener Mechanismus für die C-C- und O-C-Kupplung von Phenolen mit elektronenziehenden Gruppen, sowie die Bildung von HFIP-Ethern. Es werden die durch die Röntgenstrukturanalyse bestimmten Molekülstrukturen von **21** und **12** dargestellt.

HFIP-Ether **20** konnte während der Optimierung beobachtet werden (bestätigt durch GC/MS und NMR), was mit den Beobachtungen in unseren früheren Arbeiten übereinstimmt.^[15] Wir schlagen daher vor, dass ein Oxidationsschritt und eine anschließende Deprotonierung zu **19** führt. Dieses Zwischenprodukt kann entweder durch den nucleophilen Sauerstoff oder Kohlenstoff angegriffen werden, was nach einer weiteren Oxidation und anschließender Rearomatisierung zu **21** oder zum gewünschten Produkt **12** führt. Die weitere Oxidation von **19** ergibt ein Chinonmethid-Zwischenprodukt, das wahrscheinlich von HFIP in einer 1,6-Addition angegriffen wird, was zu **20** führt. Dies erklärt,

warum eine geringere Stromdichte sowie eine höhere Konzentration an Phenol zu einer höheren Ausbeute an gewünschtem 2,2'-Biphenol führt. Das Radikal kann dann sofort durch Phenol abgefangen werden, anstatt weiter oxidiert zu werden oder andere Nebenreaktionen einzugehen. Auch die Rekombination dieser beiden Radikale scheint ein möglicher Weg zum gewünschten Produkt zu sein.

Zusammenfassend lässt sich sagen, dass wir eine hocheffiziente und skalierbare Methode für die elektrochemische dehydrierende Homo- und Kreuzkupplung einer breiten Palette von Phenolen mit elektronenziehenden Gruppen in guten Ausbeuten etabliert haben. Die daraus resultierenden Produkte sind Vorläufer für mehrzählige Liganden, die für die Übergangsmetallkatalyse von großer Bedeutung sind. Durch Elektrosynthese konnte die Syntheseroute zu einem wichtigen Beispiel um drei Schritte verkürzt werden (wenn man von *p*-Kresol ausgeht) und die Gesamtausbeute um den Faktor 50 erhöht werden. Kreuzkupplungsreaktionen mit Naphthalinen liefern Biaryle und Vorläufer für Dibenzofurane. Die Reaktionen sind einfach durchzuführen und es wird kein zusätzliches Leitsalz benötigt, da eine sehr geringe Basenmenge eine ausreichende Leitfähigkeit gewährleistet, was zu einem hohen Atomwirkungsgrad führt. Darüber hinaus verläuft die Reaktion mit hoher Stromausbeute.

Danksagung

J.L. Röckl erhält ein DFG-Stipendium im Rahmen der Exzellenzinitiative der Graduate School Materials Science in Mainz (GSC 266). Die Unterstützung des Advanced Lab of Electrochemistry and Electrosynthesis – ELYSION (Carl-Zeiss-Stiftung) wird dankbar angenommen.

Interessenkonflikt

Die Autoren erklären, dass keine Interessenkonflikte vorliegen.

Stichwörter: C-C-Kupplungen · Elektrochemie · Kreuzkupplungen · Oxidation · Sauerstoffheterocyclen

Zitierweise: *Angew. Chem. Int. Ed.* **2020**, *59*, 315–319
Angew. Chem. **2020**, *132*, 323–327

- [1] a) P. J. Walsh, A. E. Lurain, J. Balsells, *Chem. Rev.* **2003**, *103*, 3297–3344; b) A. Alexakis, D. Polet, S. Rosset, S. March, *J. Org. Chem.* **2004**, *69*, 5660–5667.
- [2] R. Franke, D. Selent, A. Börner, *Chem. Rev.* **2012**, *112*, 5675–5732.
- [3] a) T. Hu, Y.-G. Li, Y.-S. Li, N.-H. Hu, *J. Mol. Catal. Chem.* **2006**, *253*, 155–164; b) Y. Liu, W.-M. Ren, J. Liu, X.-B. Lu, *Angew. Chem. Int. Ed.* **2013**, *52*, 11594–11598; *Angew. Chem.* **2013**, *125*, 11808–11812; c) H.-C. Zhang, W.-S. Huang, L. Pu, *J. Org. Chem.* **2001**, *66*, 481–487.
- [4] a) C.-J. Li, *Acc. Chem. Res.* **2009**, *42*, 335–344; b) S. Tang, Y. Liu, A. Lei, *Chem* **2018**, *4*, 27–45; c) H. Yi, G. Zhang, H. Wang, Z. Huang, J. Wang, A. Lei, *Chem. Rev.* **2017**, *117*, 9016–9085; d) Z.-J. Wu, S.-R. Li, H. Long, H.-C. Xu, *Chem. Commun.* **2018**, *54*, 4601–4604; e) Z.-J. Wu, S. R. Li, H.-C. Xu, *Angew. Chem. Int.*

- Ed.* **2018**, *57*, 14070–14074; *Angew. Chem.* **2018**, *130*, 14266–14270; f) S. R. Waldvogel, S. Lips, M. Selt, B. Riehl, C. J. Kampf, *Chem. Rev.* **2018**, *118*, 6706–6765; g) H. Shalit, A. Dyadyuk, D. Pappo, *J. Org. Chem.* **2019**, *84*, 1677–1686.
- [5] X. Li, B. Hewgley, C. A. Mulrooney, J. Yang, M. C. Kozlowski, *J. Org. Chem.* **2003**, *68*, 5500–5511.
- [6] a) B. Riehl, K. Dyballa, R. Franke, S. R. Waldvogel, *Synthesis* **2016**, *49*, 252–259; b) B. Elsler, D. Schollmeyer, K. M. Dyballa, R. Franke, S. R. Waldvogel, *Angew. Chem. Int. Ed.* **2014**, *53*, 5210–5213; *Angew. Chem.* **2014**, *126*, 5311–5314; c) A. Wiebe, D. Schollmeyer, K. M. Dyballa, R. Franke, S. R. Waldvogel, *Angew. Chem. Int. Ed.* **2016**, *55*, 11801–11805; *Angew. Chem.* **2016**, *128*, 11979–11983; d) B. Dahms, P. J. Kohlpaintner, A. Wiebe, R. Breinbauer, D. Schollmeyer, S. R. Waldvogel, *Chem. Eur. J.* **2019**, *25*, 2713–2716; e) S. Lips, A. Wiebe, B. Elsler, D. Schollmeyer, K. M. Dyballa, R. Franke, S. R. Waldvogel, *Angew. Chem. Int. Ed.* **2016**, *55*, 10872–10876; *Angew. Chem.* **2016**, *128*, 11031–11035; f) B. Dahms, R. Franke, S. R. Waldvogel, *ChemElectroChem* **2018**, *5*, 1249–1252; g) A. Wiebe, S. Lips, D. Schollmeyer, R. Franke, S. R. Waldvogel, *Angew. Chem. Int. Ed.* **2017**, *56*, 14727–14731; *Angew. Chem.* **2017**, *129*, 14920–14925; h) S. Lips, D. Schollmeyer, R. Franke, S. R. Waldvogel, *Angew. Chem. Int. Ed.* **2018**, *57*, 13325–13329; *Angew. Chem.* **2018**, *130*, 13509–13513; i) S. Lips, B. A. Frontana-Urbe, M. Dörr, D. Schollmeyer, R. Franke, S. R. Waldvogel, *Chem. Eur. J.* **2018**, *24*, 6057–6061.
- [7] M. Takahashi, H. Konishi, S. Iida, K. Nakamura, S. Yamamura, S. Nishiyama, *Tetrahedron* **1999**, *55*, 5295–5302.
- [8] A. Kirste, S. Hayashi, G. Schnakenburg, I. Malkowsky, F. Stecker, A. Fischer, T. Fuchigami, S. R. Waldvogel, *Chem. Eur. J.* **2011**, *17*, 14164–14169.
- [9] a) E. J. Horn, B. R. Rosen, P. S. Baran, *ACS Cent. Sci.* **2016**, *2*, 302–308; b) E. J. Horn, B. R. Rosen, Y. Chen, J. Tang, K. Chen, M. D. Eastgate, P. S. Baran, *Nature* **2016**, *533*, 77–81.
- [10] a) S. R. Waldvogel, B. Janza, *Angew. Chem. Int. Ed.* **2014**, *53*, 7122–7123; *Angew. Chem.* **2014**, *126*, 7248–7249; b) S. R. Waldvogel, S. Möhle, *Angew. Chem. Int. Ed.* **2015**, *54*, 6398–6399; *Angew. Chem.* **2015**, *127*, 6496–6497; c) S. R. Waldvogel, M. Selt, *Angew. Chem. Int. Ed.* **2016**, *55*, 12578–12580; *Angew. Chem.* **2016**, *128*, 12766–12768.
- [11] a) A. Wiebe, T. Gieshoff, S. Möhle, E. Rodrigo, M. Zirbes, S. R. Waldvogel, *Angew. Chem. Int. Ed.* **2018**, *57*, 5594–5619; *Angew. Chem.* **2018**, *130*, 5694–5721; b) S. Möhle, M. Zirbes, E. Rodrigo, T. Gieshoff, A. Wiebe, S. R. Waldvogel, *Angew. Chem. Int. Ed.* **2018**, *57*, 6018–6041; *Angew. Chem.* **2018**, *130*, 6124–6149.
- [12] A. Wiebe, B. Riehl, S. Lips, R. Franke, S. R. Waldvogel, *Sci. Adv.* **2017**, *3*, eaao3920.
- [13] a) R. Francke, D. Cericola, R. Kötz, D. Weingarh, S. R. Waldvogel, *Electrochim. Acta* **2012**, *62*, 372; b) L. Ebersson, M. P. Hartshorn, O. Persson, *J. Chem. Soc. Perkin Trans. 2* **1995**, 1735–1744; c) M. Lucarini, V. Mugnaini, G. F. Pedulli, M. Guerra, *J. Am. Chem. Soc.* **2003**, *125*, 8318–8329; d) L. Ebersson, O. Persson, M. P. Hartshorn, *Angew. Chem. Int. Ed. Engl.* **1995**, *34*, 2268–2269; *Angew. Chem.* **1995**, *107*, 2417–2418.
- [14] B. Elsler, A. Wiebe, D. Schollmeyer, K. M. Dyballa, R. Franke, S. R. Waldvogel, *Chem. Eur. J.* **2015**, *21*, 12321–12325.
- [15] a) Y. Imada, J. L. Röckl, A. Wiebe, T. Gieshoff, D. Schollmeyer, K. Chiba, R. Franke, S. R. Waldvogel, *Angew. Chem. Int. Ed.* **2018**, *57*, 12136–12140; *Angew. Chem.* **2018**, *130*, 12312–12317; b) J. L. Röckl, Y. Imada, K. Chiba, S. R. Waldvogel, *ChemElectroChem* **2019**, *6*, 4184–4187; c) J. L. Röckl, A. V. Hauck, D. Schollmeyer, S. R. Waldvogel, *ChemistryOpen* **2019**, *8*, 1167–1171.
- [16] J. Kotz, P. Treichel, G. Weaver, *Chemistry and Chemical Reactivity*, 6th ed., Enhanced Review Edition, Brooks/Cole Thomson Learning, Belmont, CA, **2006**.
- [17] K. Dhanunjayarao, V. Mukundam, M. Ramesh, K. Venkatasubbaiah, *Eur. J. Inorg. Chem.* **2014**, 539–545.
- [18] H.-L. Han, Y. Liu, J.-Y. Liu, K. Nomura, Y. S. Li, *Dalton Trans.* **2013**, *42*, 12346–12353.
- [19] N. Tsu, K. Nagashima, *Tetrahedron* **1969**, *25*, 3017–3031.

Manuskript erhalten: 8. August 2019

Akzeptierte Fassung online: 9. September 2019

Endgültige Fassung online: 19. November 2019

Supporting Information

Dehydrogenative Anodic C–C Coupling of Phenols Bearing Electron-Withdrawing Groups

*Johannes L. Röckl, Dieter Schollmeyer, Robert Franke, and Siegfried R. Waldvogel**

anie_201910077_sm_miscellaneous_information.pdf

Table of Contents

General information.....	3
General protocol for electrolytic coupling of phenols carrying EWG (GP)	4
CV studies.....	7
Synthesis of starting materials.....	12
Homo-coupling of phenols carrying EWG	15
Cross-coupling of phenols carrying EWG	25
NMR spectra	33
References.....	52

General information

All reagents were used in analytical or sufficiently pure grades. Solvents were purified by standard methods.^[1] Electrochemical reactions were carried out at boron-doped diamond (BDD) electrodes. BDD electrodes were obtained as DIACHEM™ quality from CONDIAS GmbH, Itzehoe, Germany. BDD (15 μm diamond layer) on silicon support and with isostatic graphite electrodes (SIGRAFINE®V2100, SGL Carbon, Bonn-Bad Godesberg, Germany).

Column chromatography was performed on silica gel 60 M (0.040–0.063 mm, Macherey-Nagel GmbH & Co, Düren, Germany) with a maximum pressure of 1.6 bar. In addition, a preparative chromatography system (Büchi Labortechnik GmbH, Essen, Germany) was used with a Büchi Control Unit C-620, an UV detector Büchi UV photometer C-635, Büchi fraction collector C-660 and two Pump Modules C-605 for adjusting the solvent mixtures. As eluents mixtures of cyclohexane and ethyl acetate were used. Silica gel 60 sheets on aluminum (F254, Merck, Darmstadt, Germany) were used for thin layer chromatography.

Spectroscopy and spectrometry ¹H NMR, ¹³C and ¹⁹F NMR spectra were recorded at 25 °C, using a Bruker Avance III HD 400 (400 MHz) (5 mm BBFO-SmartProbe with z gradient and ATM, SampleXPress 60 sample changer, Analytische Messtechnik, Karlsruhe, Germany). Chemical shifts (δ) are reported in parts per million (ppm) relative to TMS as internal standard or traces of CHCl₃ or DMSO-d₆ in the corresponding deuterated solvent. For the ¹⁹F spectra, ethyl fluoroacetate served as external standard (δ = -231.1 ppm). Mass spectra and high-resolution mass spectra were obtained by using a QToF Ultima 3 (Waters, Milford, Massachusetts) apparatus employing ESI⁺ or APCI.

Melting points were determined with a Melting Point Apparatus B-545 (Büchi, Flawil, Switzerland) and are uncorrected. Heating rate: 1 °C/min.

Cyclic voltammetry was performed with a Metrohm 663 VA Stand equipped with a μAutolab type III potentiostat (Metrohm AG, Herisau, Switzerland). *WE*: BDD electrode tip, 2 mm diameter; *CE*: glassy carbon rod; *RE*: Ag/AgCl in saturated LiCl/EtOH. Sol-vent: HFIP. *v* = 100 mV/s, *T* = 20.0 °C, *c* = 0.00500 M, supporting electrolyte DIPEA: *c* = 0.100 M, MTBS: *c* = 0.200 M.

X-ray analysis: All data were collected on a STOE IPDS2T diffractometer (Oxford Cryostream 700er series, Oxford Cryosystems) using graphite monochromated Mo *K*_α radiation (λ = 0.71073 Å). Intensities were measured using fine-slicing ω and φ-scans and corrected for background, polarization and Lorentz effects. The structures were solved by direct methods and refined anisotropically by the least-squares procedure implemented in the SHELX program system.

The supplementary crystallographic data for this paper can be obtained free of charge from The Cambridge Crystallographic Data Center via www.ccdc.cam.ac.uk/data_request/cif. Deposition numbers and further details are given with the individual characterization data.

General protocol for electrolytic coupling of phenols carrying EWG (GP)

The undivided 5 mL PTFE electrolysis cells are homemade. Detailed information about used cells are already reported.^[2,3] However, the complete setup with these cells are also commercially available as IKA Screening System, IKA-Werke GmbH & Co. KG, Staufen, Germany. It is operated with boron-doped diamond electrodes (BDD, 0.3 x 1 x 7 cm, 15 μ m diamond layer, the support material is silicon) or graphite electrodes (0.3 x 1 x 7 cm SIGRAFINE®V2100, SGL Carbon, Bonn-Bad Godesberg, Germany).

GP I: Homocoupling of phenols undivided PTFE cell (1 mmol / 5 mL)

A solution of a phenol derivative (1.0 – 2.5 mmol, 1.0 equiv.) and *N*-ethyl-*N*-(prop-2-yl)propan-2-amine (**DIPEA**) (0.05 mL, 0.29 mmol, 0.12 equiv. – 0.3 equiv.) in 1,1,1,3,3,3-hexafluoropropan-2-ol (**HFIP**) (5 mL) was electrolyzed at a boron-doped diamond (**BDD**) or graphite anode and a BDD or graphite cathode. A constant current electrolysis with a current density of 5.0 mA/cm² was performed at room temperature. After 1.0 - 1.5 F (per mole) were applied, HFIP was recovered by distillation. The residue was purified by column chromatography.

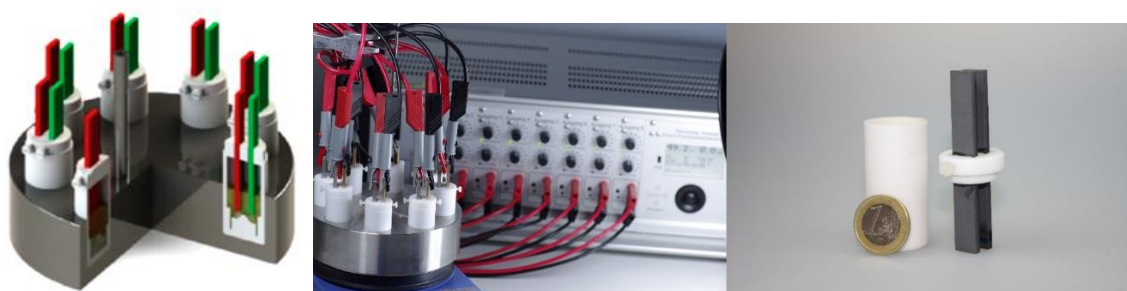


Fig. S1: Left: schematic 5 mL Teflon cells; Middle: The commercially available IKA Screenings System, IKA-Werke GmbH & Co. KG, Staufen, Germany; right: 5 mL Teflon cell with two parallel electrodes (size: 3 x 10 x 70 mm, 1 Euro coin for comparison, diameter: 23,25 mm).

GP II: Flask-type cell (66 mmol / 500 mL) – Scale-up

Phenol derivative (66.6 mmol, 1.0 equiv.) HFIP (134 mL), and 5.0 mL (1.5 mmol, 0.12 equiv.) DIPEA were transferred into an undivided 500 mL electrolysis cell equipped with a graphite anode and a graphite cathode. A constant current electrolysis with a current density of 5.0 mA/cm² was performed at room temperature. After 1.0 F - 1.5 F (per mole) were applied, HFIP was recovered by distillation. Purification by column chromatography yielded the clean product as a yellow solid.

For 3,3'-Diacetyl-5,5'-dimethyl-2,2'-biphenol (**6**): yellow solid (5.9 g, 19.6 mmol, 59%).

The flask (500 mL) is closed by a PTFE plug. This cap allows precise arrangement of the electrodes. Total dimension of the graphite electrodes are 6.0 cm x 2.0 cm x 0.3 cm.

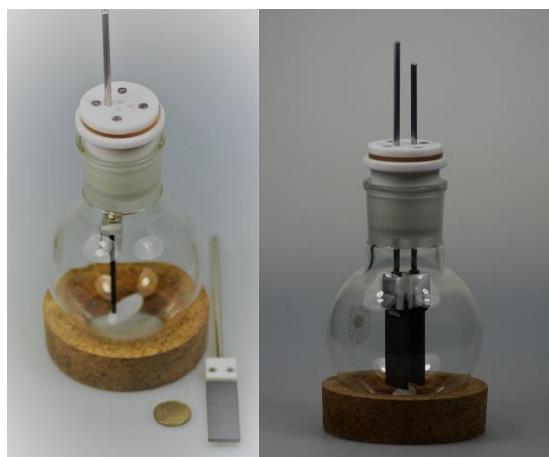


Fig. S2: 500 mL flask cell; left: Electrode removed; right: assembled. For size comparison one 50 Eurocent (diameter: 24,25 mm) coin is placed in front of the glass cell.

GP III: Cross-coupling of phenols with naphthalenes undivided PTFE cell (5 mL)

A solution of a phenol derivative (0.5 mmol, 1.0 equiv.) naphthalene (1.5 mmol, 3.0 equiv.) and *N*-ethyl-*N*-(prop-2-yl)propan-2-amine (**DIPEA**) (0.1 mL, 0.57 mmol 1.15 equiv.) in 1,1,1,3,3,3-hexafluoropropan-2-ol (**HFIP**) (5 mL) was electrolyzed at a boron-doped diamond (**BDD**) anode and a BDD cathode. A constant current electrolysis with a current density of 5.0 mA/cm² was performed at room temperature. After 2.0 F were applied, HFIP was recovered by distillation. The residue was purified by column chromatography.

Procedure with ElectraSyn

ElectraSyn 2.0 (IKA, cat. no. 0020008980)

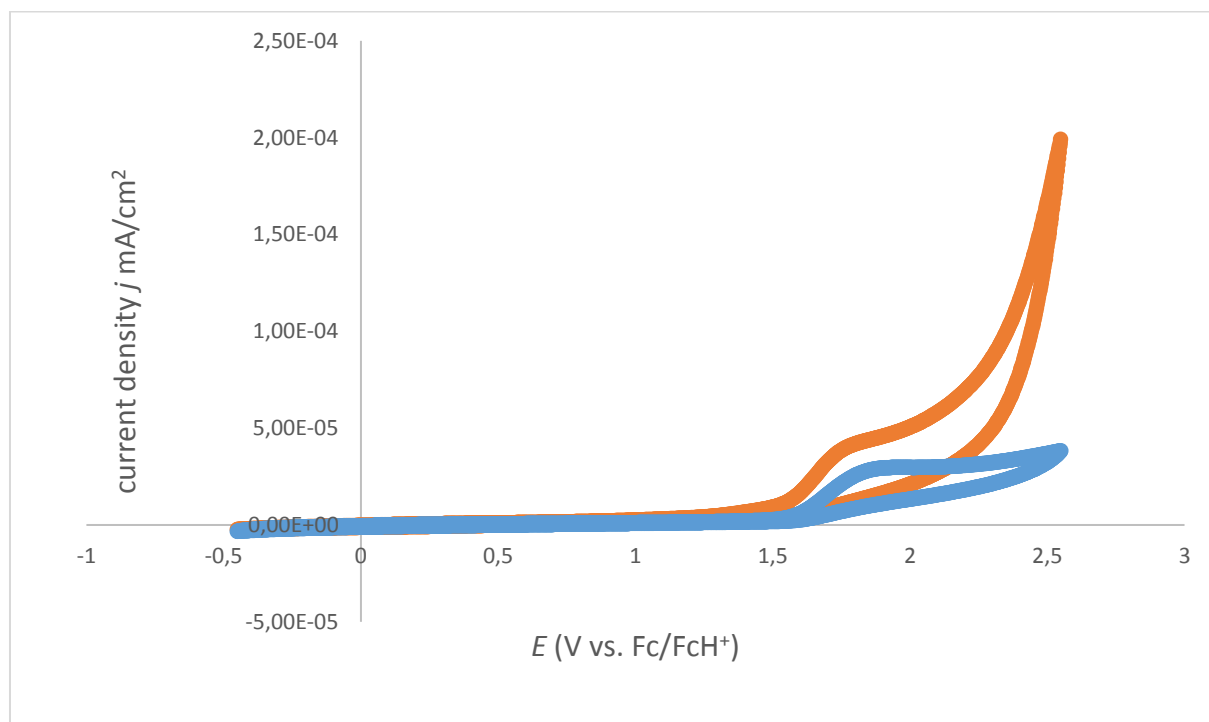
Graphite electrode assembly (IKA, cat. no. 0040002858)

Charge the ElectraSyn vial (10 mL volume) with a Teflon-coated magnetic stir bar, 2-hydroxy-5-methylacetophenone (375 mg, 2.5 mmol, 1.0 equiv.), HFIP (5 mL), and DIPEA (0.05 mL, 0.29 mmol, 0.12 equiv.). Adapt the graphite (W) and platinum or graphite (C) electrodes to the ElectraSyn vial cap. Screw the vial cap onto the vial. Premix the reaction mixture until a clear solution is obtained. Adapt the electrochemical cell to the ElectraSyn 2.0 vial holder. Select 'New experiments' and then 'Constant current'. Set '5 mA' for 'desired current'. Select 'No' for 'Are you using a reference electrode?' Choose 'Total charge'. Adjust 'mmols substrate' to '2.5 mmol' and '1.5' for 'equiv. of electrons'. Select 'No' for 'Would you like to alternate the polarity'. After electrolysis for ca. 18 h, disconnect the reaction vial from the ElectraSyn 2.0, gently remove the cap with electrodes from the vial, and transfer the reaction mixture to a flask (recover HFIP, if wished), then rinse both electrodes with ethyl acetate (10 mL) to transfer any residual product. Remove the solvent using a rotary evaporator. The residue was purified by column chromatography to yield the desired biphenol (155 mg, 0.52 mmol of **6**, 42%).

CV studies

A general trend that has been observed in all CV measurements is the decrease of oxidation potentials with the addition of base (ca. 0.1 – 0.2 V). In orange the CVs with addition of base and in blue the CVs measured with MTBS as supporting electrolyte are shown. One rationale would be, that upon deprotonation of the phenol the aromatic system becomes more electron-rich and therefore can be more easily oxidized.

4-bromo-2-hydroxy-5-methylacetophenone



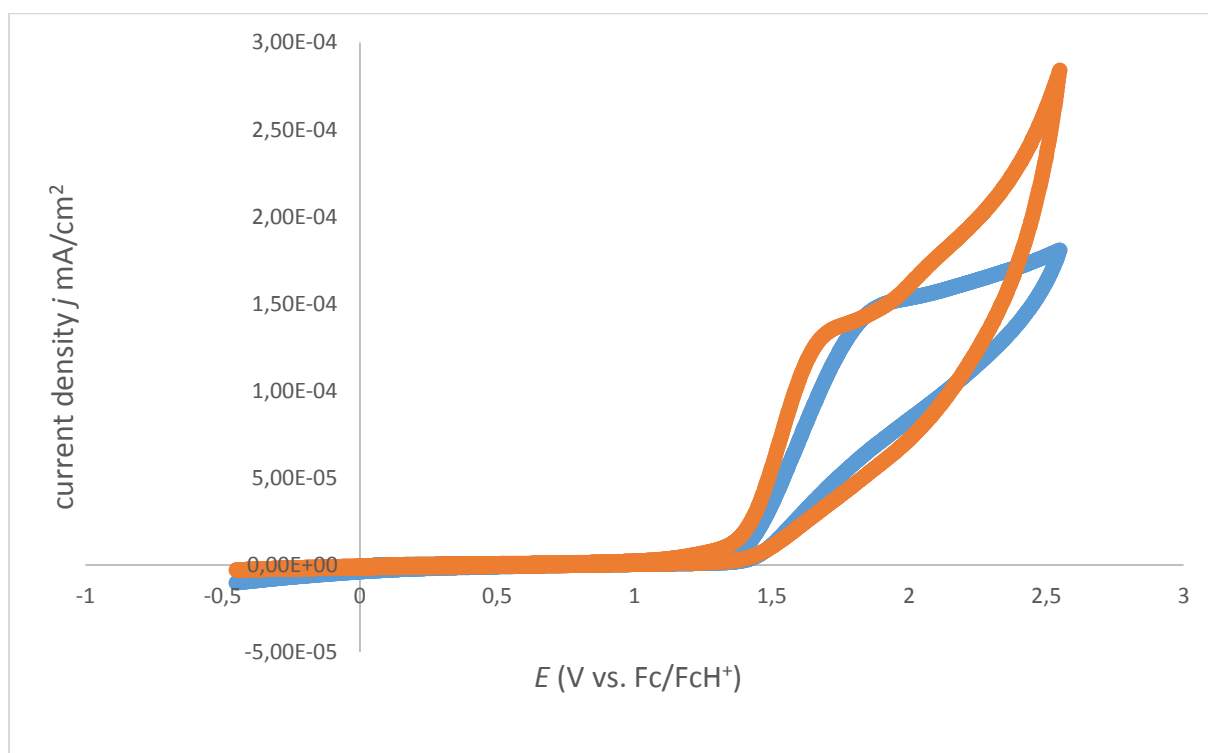
Blue: cyclic voltammogram of a 5 mM solution of 4-bromo-2-hydroxy-5-methylacetophenone in HFIP/MTBS at 100 mV/s

$E_{ox1} = 1.85 \text{ V vs Fc/FcH}^+$

Orange: cyclic voltammogram of a 5 mM solution of 4-bromo-2-hydroxy-5-methylacetophenone in HFIP/DIPEA at 100 mV/s

$E_{ox2} = 1.78 \text{ V vs Fc/FcH}^+$

2-hydroxy-5-methylacetophenone



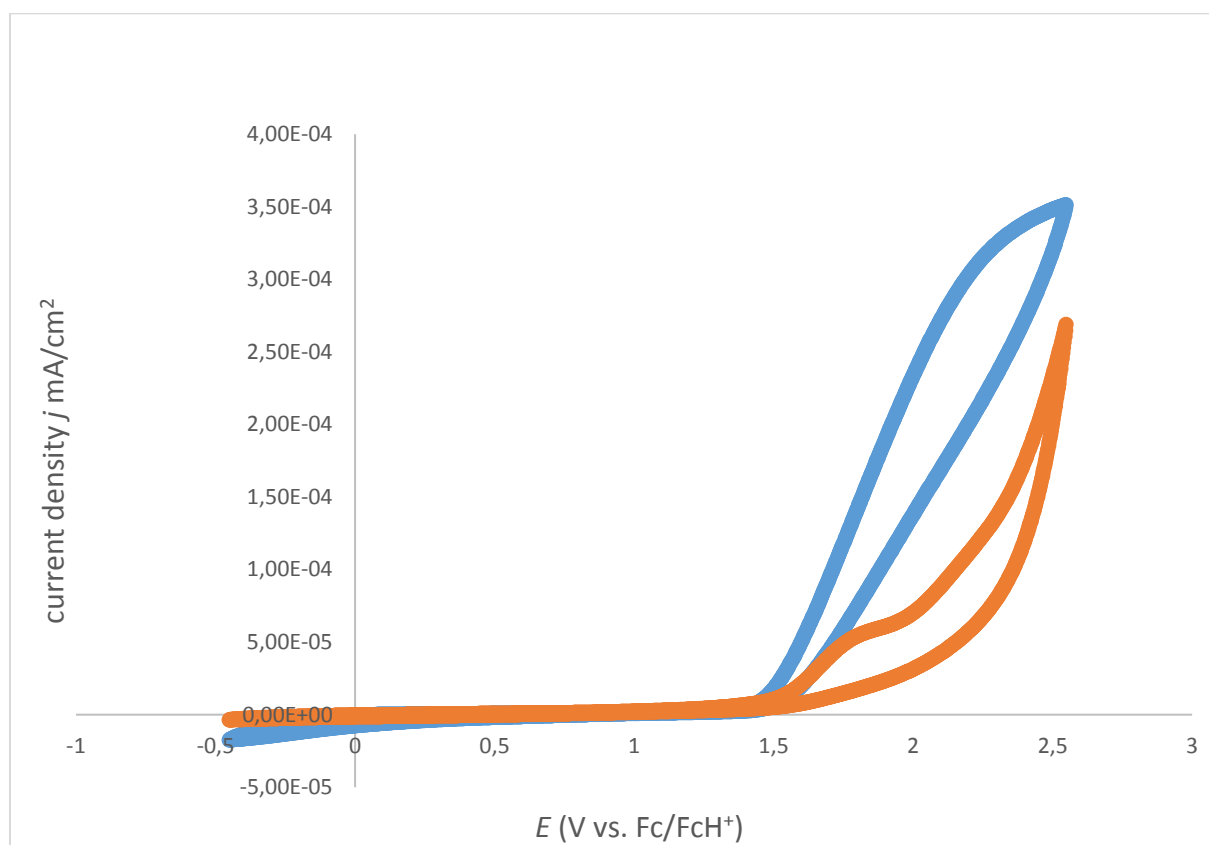
Blue: cyclic voltammogram of a 5 mM solution of 2-hydroxy-5-methylacetophenone in HFIP/MTBS at 100 mV/s

$E_{ox1} = 1.90$ V vs Fc/FcH⁺

Orange: cyclic voltammogram of a 5 mM solution of 2-hydroxy-5-methylacetophenone in HFIP/DIPEA at 100 mV/s

$E_{ox2} = 1.72$ V vs Fc/FcH⁺

5-(*tert*-butyl)-2-hydroxybenzaldehyde



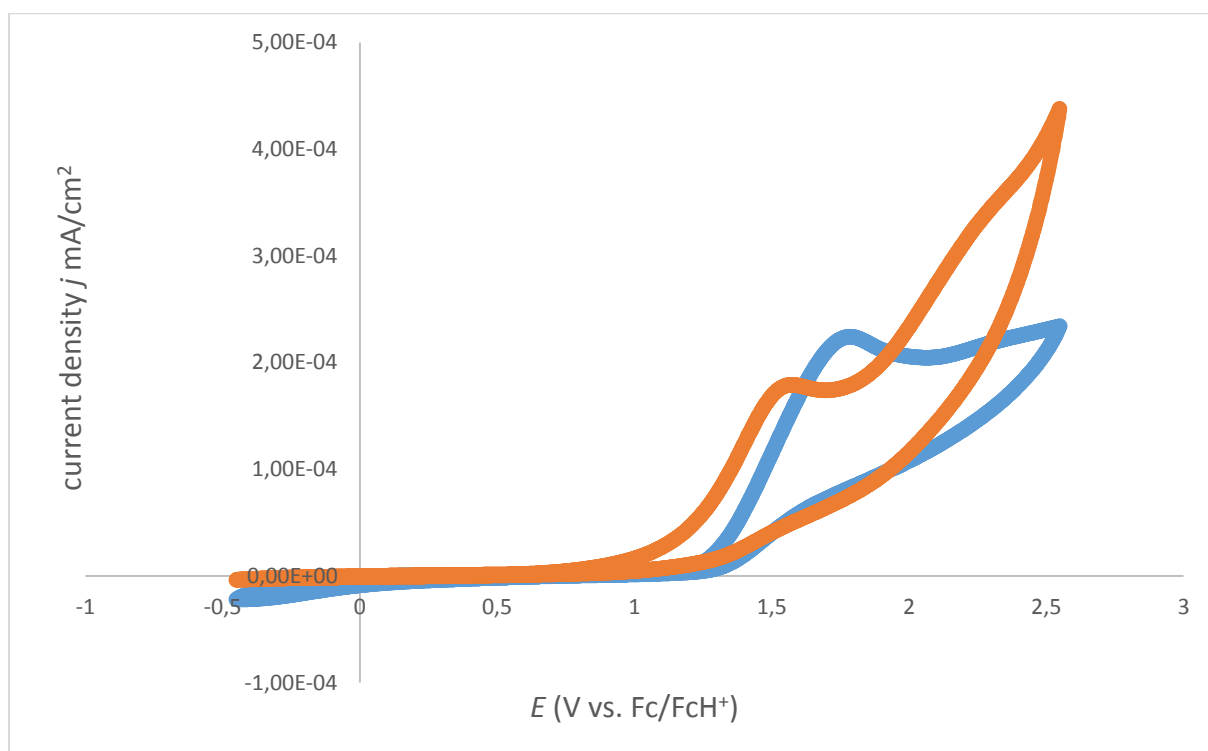
Blue: cyclic voltammogram of a 5 mM solution of 5-(*tert*-butyl)-2-hydroxybenzaldehyde in HFIP/MTBS at 100 mV/s

$E_{ox1} = 2.50$ V vs Fc/FcH⁺

Orange: cyclic voltammogram of a 5 mM solution of 5-(*tert*-butyl)-2-hydroxybenzaldehyde in HFIP/DIPEA at 100 mV/s

$E_{ox2} = 1.79$ V vs Fc/FcH⁺

2-chloro-4-(*tert*-butyl)phenol



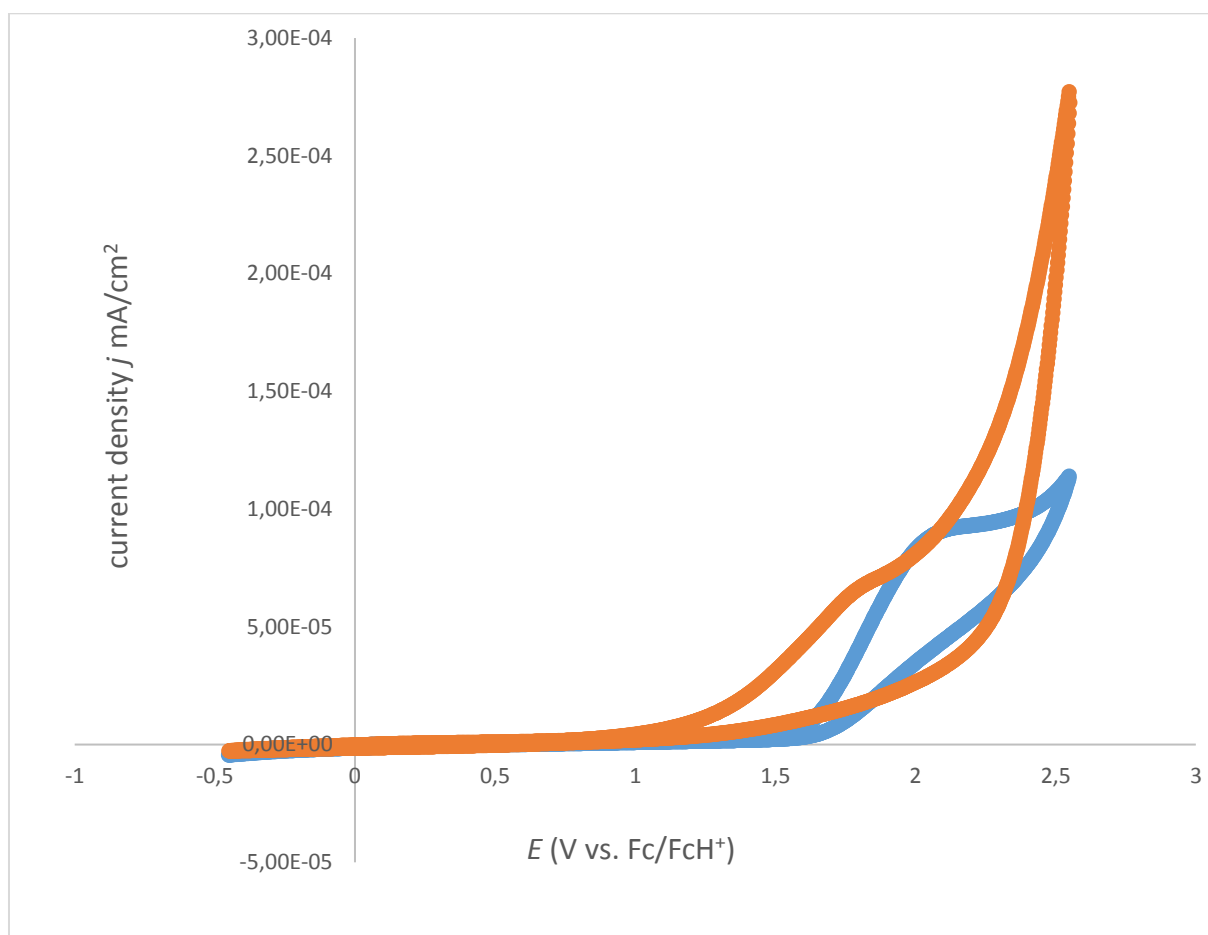
Blue: cyclic voltammogram of a 5 mM solution of 2-chloro-4-(*tert*-butyl)phenol in HFIP/MTBS at 100 mV/s

$E_{ox1} = 1.78$ V vs Fc/FcH⁺

Orange: cyclic voltammogram of a 5 mM solution of 2-chloro-4-(*tert*-butyl)phenol in HFIP/DIPEA at 100 mV/s

$E_{ox2} = 1.56$ V vs Fc/FcH⁺

4-methyl-2-(methylsulfonyl)phenol



Blue: cyclic voltammogram of a 5 mM solution of 4-methyl-2-(methylsulfonyl)phenol in HFIP/MTBS at 100 mV/s

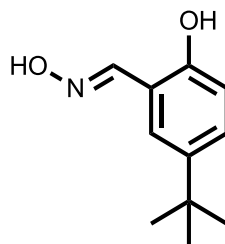
$E_{ox1} = 2.05$ V vs Fc/FcH⁺

Orange: cyclic voltammogram of a 5 mM solution of 4-methyl-2-(methylsulfonyl)phenol in HFIP/DIPEA at 100 mV/s

$E_{ox1} = 1.80$ V vs Fc/FcH⁺

Synthesis of starting materials

5-(*tert*-Butyl)-2-hydroxybenzaldehyde oxime



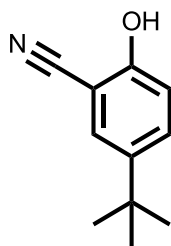
5-(*tert*-Butyl)-2-hydroxybenzaldehyde (0.89 g, 5.0 mmol, 1.0 equiv.) was dissolved in EtOH (35 mL), pyridine (0.79 g, 10 mmol, 2.0 equiv.), hydroxylammonium hydrochloride (1.7 g, 25 mmol, 5.0 equiv.) were added and the resulting mixture was stirred for 3h at 60 °C. It was then partitioned between EtOAc (100 mL) and water (100 mL). The organic fraction was then dried over sodium sulfate and evaporated under vacuum to yield 1.0 g (6.2 mmol, quantitative yield) of a colorless crystalline solid. This crude product was directly used in the next reaction.

^1H NMR (400 MHz, CDCl_3) δ 8.24 (s, 1H), 7.32 (dd, $J = 8.6, 2.4$ Hz, 1H), 7.15 (d, $J = 2.4$ Hz, 1H), 6.92 (d, $J = 8.6$ Hz, 1H), 1.30 (s, 10H).

^{13}C NMR (101 MHz, CDCl_3) δ 154.9, 153.3, 142.4, 128.5, 127.3, 116.2, 115.7, 34.0, 31.4.

HRMS for $\text{C}_{11}\text{H}_{16}\text{NO}_2^+$ (ESI+) $[\text{M}+\text{H}]^+$: calc. 194.1176, found: 194.1176.

5-(*tert*-Butyl)-2-hydroxybenzonitrile



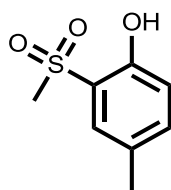
To a solution of the salicylaldehyde (386 mg, 2.0 mmol, 1 equiv.) and triphenylphosphine (PPh₃) (1.3 g, 5.0 mmol, 2.5 equiv.) in anhydrous CH₂Cl₂ (28 mL) was added diisopropyl azodicarboxylate (DIAD) (1.0 g, 5.0 mmol, 2.5 equiv.) dropwise at room temperature. The reaction was stirred at the same temperature under an inert atmosphere until completion (TLC). The reaction mixture was partitioned between further CH₂Cl₂ (100 mL) and 0.1 M NaOH (50 mL). The aqueous layer was washed with CH₂Cl₂ (3×50 mL), and then acidified with 1 M HCl (10 mL). The acidic aqueous layer was then extracted by CH₂Cl₂ (2×50 mL). These organic fractions were combined, dried over Na₂SO₄, filtered, and concentrated. The residue was purified by column chromatography (gradient: cyclohexane:ethyl acetate = from 100:0 for 3 min to 50:50 for 60 min; column 12 mm x 150 mm; flow rate 12.5 mL/min) yielding the product as a colorless solid (yield: 53%, 185 mg, 1.06 mmol).

¹H NMR (400 MHz, CDCl₃) δ 7.54 – 7.44 (m, 2H), 6.93 (dd, *J* = 8.6, 0.6 Hz, 1H), 1.29 (s, 8H).

¹³C NMR (101 MHz, CDCl₃) δ 156.2, 144.4, 132.4, 129.3, 116.9, 116.4, 98.9, 77.2, 34.4, 31.3.

HRMS for C₁₁H₁₄NO⁺ (ESI⁺) [M+H]⁺: calc. 176.1070, found: 176.1068.

4-Methyl-2-(methylsulfonyl)phenol



4-Methyl-2-(methylthio)phenol (2.0 g, 13 mmol, 1.0 equiv.) was dissolved in CH₂Cl₂ (25 mL). Then *meta*-chloroperoxybenzoic acid (5.6 g, 32.5 mmol, 2.5 equiv.) was added portionwise and the reaction was stirred overnight at room temperature. The reaction was then quenched with sat. sodium thiosulfate solution and extracted to CH₂Cl₂ (20 mL). The combined organic fractions were dried over sodium sulfate and evaporated *in vacuo*. The residue was purified by column chromatography to yield the desired product as a colorless solid (33%, 0.8 g, 4.3 mmol).

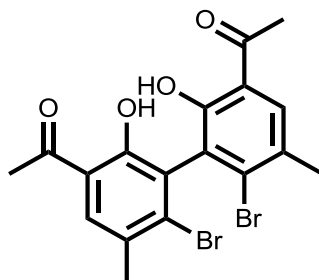
¹H NMR (400 MHz, CDCl₃) δ 8.64 (s, 1H), 7.47 (dd, *J* = 2.3, 0.8 Hz, 1H), 7.33 (ddd, *J* = 8.5, 2.3, 0.8 Hz, 1H), 6.94 (d, *J* = 8.5 Hz, 1H), 3.11 (s, 3H), 2.32 (s, 2H).

¹³C NMR (101 MHz, CDCl₃) δ 153.8, 137.6, 130.6, 128.3, 122.4, 119.1, 77.2, 45.1, 20.4.

HRMS for C₈H₉O₃S⁺ (ESI+) [M+H]⁺: calc. 185.0272, found: 185.0280.

Homo-coupling of phenols carrying EWG

3,3'-Diacetyl-6,6'-dibromo-5,5'-dimethyl-2,2'-biphenol (4)



According to the **GPI** for the electrochemical homocoupling of phenols, 4-bromo-2-hydroxy-5-methylacetophenone (573 mg, 2.5 mmol, 1.0 equiv.), HFIP (5 mL), and DIPEA (0.05 mL, 0.29 mmol, 0.12 equiv.) were transferred into an undivided PTFE cell. Electrolysis was carried out at room temperature with a current density of 5.0 mA/cm² using BDD electrodes. After 1.5 F was applied, HFIP was recovered *in vacuo*. The residue was purified by column chromatography (gradient: cyclohexane:ethyl acetate = from 100:0 for 3 min to 95:5 for 60 min; column 12 mm x 150 mm; flow rate 12.5 mL/min) yielding the product as an off white solid (yield: 50%, 285 mg, 0.63 mmol).

¹H NMR (400 MHz, DMSO-*d*₆) δ 12.35 (s, 2H), 8.03 (s, 2H), 2.70 (s, 6H), 2.41 (s, 6H).

¹³C NMR (101 MHz, DMSO-*d*₆) δ 205.4, 157.3, 134.7, 132.4, 128.1, 127.6, 118.5, 27.2, 22.4.

HRMS for C₁₈H₁₇⁷⁹Br₂O₄⁺ (ESI+) [M+H]⁺: calc.: 454.9488, found: 454.9493

for C₁₈H₁₇⁷⁹Br⁸¹BrO₄⁺ (ESI+) [M+H]⁺: calc.: 456.9473, found: 456.9471

for C₁₈H₁₇⁸¹Br₂O₄⁺ (ESI+) [M+H]⁺: calc.: 458.9540, found: 458.9456

Melting point: >240 °C (decomposition).

Crystal structure determination of **4**: C₁₈H₁₆Br₂O₄, M_r = 456.1 g/mol, colourless needles (0.06 x 0.12 x 0.34 mm³), I 2/C (monoklin), a = 13.1111(11) Å, b = 9.5924(7) Å, c = 14.1624(12) Å, V = 1770.5(2) Å³, z = 4, F(000) = 904, ρ = 1.711 g/cm³, μ = 4.60 mm⁻¹, Mo-Kα graphite monochromator, -80 °C, 5553 reflections, 2189 reflections, wR₂ = 0.1710, R₁ = 0.0859, 1.06 eÅ⁻³, -0.71 eÅ⁻³, GoF = 1.051. Single crystals for structure determination were obtained by recrystallization from acetone at room temperature. **Deposition Number 1920410**

A strong twist of the C-C – axis is observed (circa 90° angle). The molecules interact amongst each other via π-π – stacking of the respective aromatic systems.

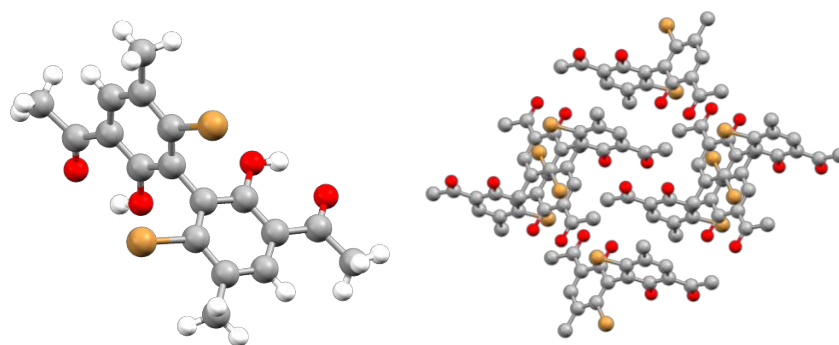


Fig. S3: left: molecular structure of **4**; right: Packing of **4** in the solid state.

1-(3-(2-Acetyl-5-bromo-4-methylphenoxy)-3-acetyl-5-bromo-4-methylphenol (21) was found as a minor side component in the reaction via GC/MS and could be identified by X-ray analysis.

Crystal structure determination of **21** (O-C – coupled product): $C_{18}H_{16}Br_2O_4$, $M_r = 456.13$ g/mol, colourless block (0.06 x 0.7 x 0.13 mm³), C 2/C (monoklin), $a = 18.8729$ (11) Å, $b = 8.7562$ (4) Å, $c = 21.8974$ (10) Å, $V = 3445.7$ (3) Å³, $z = 8$, $F(000) = 1808$, $\rho = 1.759$ g/cm³, $\mu = 4.724$ mm⁻¹, Mo-K α graphite monochromator, -80 °C, 4250 reflections, 2618 reflections, $wR_2 = 0.1234$, $R_1 = 0.0554$, 0.42 eÅ⁻³, -0.45 eÅ⁻³, GoF = 1.102. Single crystals for structure determination were obtained by recrystallization from acetone at room temperature.

Deposition Number 1920411

The molecules are strongly twisted and interact amongst each other via π - π – stacking of the respective aromatic systems.

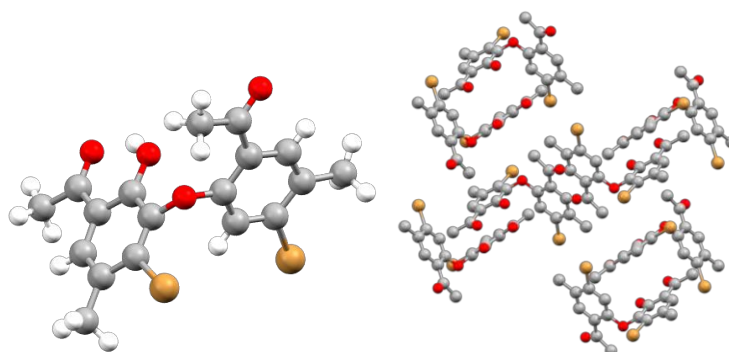
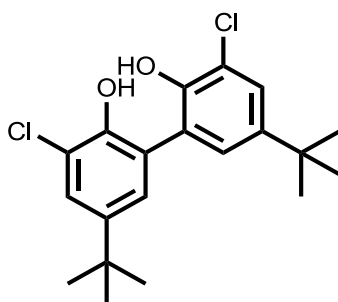


Fig. S4: left: molecular structure of **21**; right: Packing of **21** in the solid state.

3,3'-Dichloro-5,5'-di(2,2-dimethylethyl)-2,2'-biphenol (5)



According to the **GPI** for the electrochemical homocoupling of phenols, 2-chloro-4-(*tert*-butyl)phenol (462 mg, 2.5 mmol, 1.0 equiv.), HFIP (5 mL), and DIPEA (0.05 mL, 0.29 mmol, 0.12 equiv.) were transferred into an undivided PTFE cell. Electrolysis was carried out at room temperature with a current density of 5.0 mA/cm² using BDD electrodes. After 1.0 F was applied, HFIP was recovered *in vacuo*. The residue was purified by column chromatography (gradient: cyclohexane:ethyl acetate = from 100:0 for 3 min to 10:90 for 60 min; column 12 mm x 150 mm; flow rate 12.5 mL/min) yielding the product as a yellow wax, which crystallized upon standing (yield: 30%, 137 mg, 0.37 mmol).

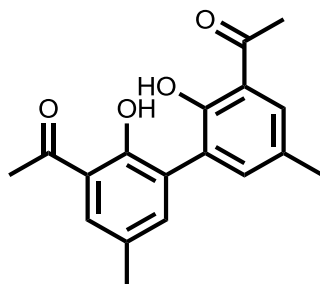
¹H NMR (400 MHz, CDCl₃) δ 7.40 (d, *J* = 2.4 Hz, 1H), 7.20 (d, *J* = 2.4 Hz, 1H), 5.81 (s, 1H), 1.33 (s, 9H).

¹³C NMR (101 MHz, CDCl₃) δ 146.4, 144.8, 127.5, 126.4, 125.4, 120.9, 34.6, 31.5.

HRMS for C₂₀H₂₄Cl₂O₂⁺ (APCI+) [M]⁺: calc.: 366.1148, found: 366.1149.

Melting point: 160 °C.

3,3'-Diacetyl-5,5'-dimethyl-2,2'-biphenol (6)



According to the **GPI** for the electrochemical homocoupling of phenols, 2-hydroxy-5-methylacetophenone (375 mg, 2.5 mmol, 1.0 equiv.), HFIP (5 mL), and DIPEA (0.05 mL, 0.29 mmol, 0.12 equiv.) were transferred into an undivided PTFE cell. Electrolysis was carried out at room temperature with a current density of 5.0 mA/cm² using graphite electrodes. After 1.0 F was applied, HFIP was recovered *in vacuo*. The residue was purified by column chromatography (gradient: cyclohexane:ethyl acetate = from 100:0 for 3 min to 95:5 for 60 min; column 12 mm x 150 mm; flow rate 12.5 mL/min) yielding the product as a yellow solid (yield: 64%, 238 mg, 0.8 mmol).

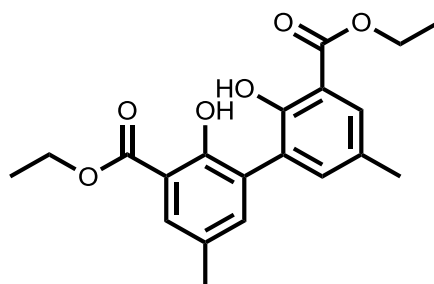
¹H NMR (400 MHz, CDCl₃) δ 12.53 (s, 2H), 7.56 (s, 2H), 7.35 (s, 2H), 2.66 (s, 6H), 2.35 (s, 6H).

¹³C NMR (101 MHz, CDCl₃) δ 204.8, 158.0, 139.3, 130.5, 127.6, 126.5, 119.6, 27.0, 20.7.

HRMS for C₁₈H₁₈NaO₄⁺ (ESI+) [M]⁺: calc.: 321.1098, found: 321.1098.

Melting point: 180.5 °C.

3,3'-Di(ethoxycarbonyl)-5,5'-dimethyl-2,2'-biphenol (7)



According to the **GPI** for the electrochemical homocoupling of phenols, ethyl 2-hydroxy-5-methylbenzoate (450 mg, 2.5 mmol, 1.0 equiv.), HFIP (5 mL), and DIPEA (0.05 mL, 0.29 mmol, 0.12 equiv.) were transferred into an undivided PTFE cell. Electrolysis was carried out at room temperature with a current density of 5.0 mA/cm² using graphite electrodes. After 1.0 F was applied, HFIP was recovered *in vacuo*. The residue was purified by column chromatography (gradient: cyclohexane:ethyl acetate = from 100:0 for 3 min to 50:50 for 60 min; column 12 mm x 150 mm; flow rate 12.5 mL/min) yielding the product as a white solid (yield: 41%, 184 mg, 0.51 mmol).

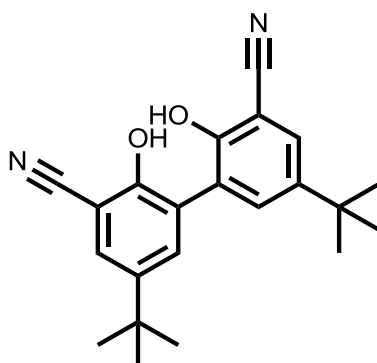
¹H NMR (400 MHz, CDCl₃) δ 11.08 (s, 2H), 7.71 (dd, *J* = 2.3, 0.9 Hz, 2H), 7.32 (d, *J* = 2.3 Hz, 2H), 4.42 (q, *J* = 7.1 Hz, 4H), 2.34 (s, 6H), 1.43 (t, *J* = 7.1 Hz, 6H).

¹³C NMR (101 MHz, CDCl₃) δ 170.6, 157.2, 138.3, 129.6, 127.8, 126.1, 112.4, 61.5, 20.5, 14.6.

HRMS for C₂₀H₂₃O₆⁺ (ESI+) [M+H]⁺: calc.: 359.1489, found: 359.1491.

Melting point: 161.5 °C.

3,3'-Dicyano-5,5'-di(2,2-dimethylethyl)-2,2'-biphenol (8)



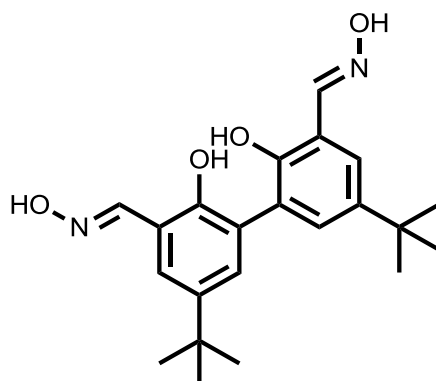
According to the **GPI** for the electrochemical homocoupling of phenols, 5-(*tert*-butyl)-2-hydroxybenzonitrile (175 mg, 1.0 mmol, 1.0 equiv.), HFIP (5 mL), and DIPEA (0.05 mL, 0.29 mmol, 0.12 equiv.) were transferred into an undivided PTFE cell. Electrolysis was carried out at room temperature with a current density of 5.0 mA/cm² using graphite electrodes. After 1.2 F was applied, HFIP was recovered *in vacuo*. The residue was purified by column chromatography (gradient: cyclohexane:ethyl acetate = from 100:0 for 3 min to 50:50 for 60 min; column 12 mm x 150 mm; flow rate 12.5 mL/min) yielding the product as an off white solid (yield: 32%, 55 mg, 0.16 mmol).

¹H NMR (400 MHz, DMSO-*d*₆) δ 7.41 (d, *J* = 2.6 Hz, 2H), 7.32 (d, *J* = 2.6 Hz, 2H), 1.24 (s, 18H).

¹³C NMR (101 MHz, DMSO-*d*₆) δ 132.5, 128.7, 128.0, 119.0, 118.2, 100.6, 59.8, 33.8, 31.1.

HRMS for C₂₂H₂₅N₂O₂⁺ (ESI+) [M+H]⁺: calc.: 349.1911, found: 349.1899.

3,3'-Dicarboxime-5,5'-di(2,2-dimethylethyl)-2,2'-biphenol (9)



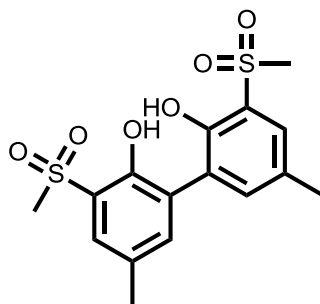
According to the **GPI** for the electrochemical homocoupling of phenols, 5-(*tert*-butyl)-2-hydroxybenzaldehyde oxime (193 mg, 1.0 mmol, 1.0 equiv.), HFIP (5 mL), and DIPEA (0.05 mL, 0.29 mmol, 0.30 equiv.) were transferred into an undivided PTFE cell. Electrolysis was carried out at room temperature with a current density of 5.0 mA/cm² using graphite electrodes. After 1.25 F was applied, HFIP was recovered *in vacuo*. The residue was purified by column chromatography (gradient: cyclohexane:ethyl acetate = from 100:0 for 3 min to 0:100 for 60 min; column 12 mm x 150 mm; flow rate 12.5 mL/min) yielding the product as a yellow wax, which crystallized upon standing (yield: 18%, 35 mg, 0.51 mmol).

¹H NMR (400 MHz, Chloroform-*d*) δ 10.25 (s, 2H), 8.26 (s, 2H), 7.35 (d, *J* = 2.4 Hz, 2H), 7.20 (d, *J* = 2.4 Hz, 2H), 1.33 (s, 18H).

¹³C NMR (101 MHz, CDCl₃) δ 153.1, 152.3, 142.4, 130.7, 127.2, 125.9, 116.3, 77.2, 34.2, 31.6.

HRMS for C₂₂H₁₉N₂O₄⁺ (ESI+) [M+H]⁺: calc.: 385.2122, found: 385.2121.

5,5'-Dimethyl-3,3'-di(methylsulfonyl)-2,2'-biphenol (10)



According to the **GPI** for the electrochemical homocoupling of phenols, 4-methyl-2-(methylsulfonyl)phenol (450 mg, 2.5 mmol, 1.0 equiv.), HFIP (5 mL), and DIPEA (0.05 mL, 0.29 mmol, 0.12 equiv.) were transferred into an undivided PTFE cell. Electrolysis was carried out at room temperature with a current density of 5.0 mA/cm² using BDD electrodes. After 1.5 F was applied, HFIP was recovered *in vacuo*. The residue was purified by column chromatography (gradient: cyclohexane:ethyl acetate = from 100:0 for 3 min to 0:100 for 60 min; column 12 mm x 150 mm; flow rate 12.5 mL/min) yielding the product as a yellow wax which crystallized upon standing (yield: 43%, 198 mg, 0.51 mmol).

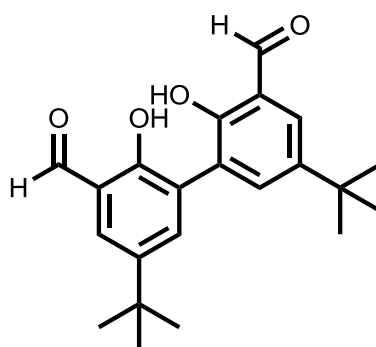
¹H NMR (400 MHz, DMSO-*d*₆) δ 7.40 (dd, *J* = 2.4, 0.8 Hz, 1H), 7.35 (d, *J* = 2.4 Hz, 1H), 3.24 (s, 3H), 2.26 (s, 3H).

¹³C NMR (101 MHz, DMSO-*d*₆) δ 159.5, 136.1, 131.2, 127.8, 126.5, 122.4, 42.0, 39.5, 20.1.

HRMS for C₁₆H₁₈NaO₆S₂⁺ (ESI+) [M+H]⁺: calc.: 393.0437, found: 393.0434.

Melting point: 173.5 °C.

3,3'-Diformyl-5,5'-di(2,2-dimethylethyl)-2,2'-biphenol (11)



According to the **GPI** for the electrochemical homocoupling of phenols, 5-(*tert*-butyl)-2-hydroxybenzaldehyde (445.5 mg, 2.5 mmol, 1.0 equiv.), HFIP (5 mL), and DIPEA (0.05 mL, 0.29 mmol, 0.12 equiv.) were transferred into an undivided PTFE cell. Electrolysis was carried out at room temperature with a current density of 5.0 mA/cm² using graphite electrodes. After 1.0 F was applied, HFIP was recovered *in vacuo*. The residue was purified by column chromatography (gradient: cyclohexane:ethyl acetate = from 100:0 for 3 min to 10:90 for 60 min; column 12 mm x 150 mm; flow rate 12.5 mL/min) yielding the product as a colourless wax, which solidified upon standing (yield: 14%, 63 mg, 0.18 mmol).

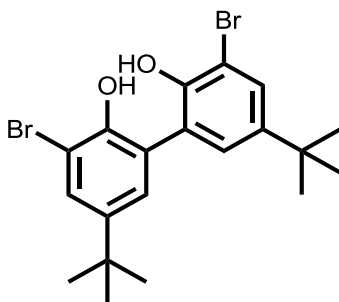
¹H NMR (400 MHz, CDCl₃) δ 11.25 (s, 2H), 9.95 (s, 2H), 7.72 (dd, *J* = 2.5, 0.6 Hz, 2H), 7.58 (d, *J* = 2.5 Hz, 2H), 1.37 (s, 18H).

¹³C NMR (101 MHz, CDCl₃) δ 197.0, 157.1, 142.4, 137.1, 130.1, 125.0, 120.5, 77.2, 34.4, 31.4.

HRMS for C₂₂H₁₇O₄⁺ (ESI+) [M+H]⁺: calc.: 355.1904, found: 355.1914.

Melting point: 213.5 °C.

3,3'-Dibromo-5,5'-di(2,2-dimethylethyl)-2,2'-biphenol (12)



According to the **GPI** for the electrochemical homocoupling of phenols, 2-bromo-4-(*tert*-butyl)phenol (573 mg, 2.5 mmol, 1.0 equiv.), HFIP (5 mL), and DIPEA (0.05 mL, 0.29 mmol, 0.12 equiv.) were transferred into an undivided PTFE cell. Electrolysis was carried out at room temperature with a current density of 5.0 mA/cm² using BDD electrodes. After 1.0 F was applied, HFIP was recovered *in vacuo*. The residue was purified by column chromatography (gradient: cyclohexane:ethyl acetate = from 100:0 for 3 min to 10:90 for 60 min; column 12 mm x 150 mm; flow rate 12.5 mL/min) yielding the product as a yellow wax, which solidified upon standing (yield: 54%, 250 mg, 0.55 mmol).

¹H NMR (400 MHz, CDCl₃) δ 8.27 (s, 2H), 7.35 (d, *J* = 2.5 Hz, 2H), 7.20 (d, *J* = 2.5 Hz, 2H), 1.33 (s, 18H).

¹³C NMR (101 MHz, CDCl₃) δ 153.1, 152.3, 130.7, 127.2, 125.9, 116.3, 77.2, 34.2, 31.6.

HRMS for C₂₀H₂₄⁷⁹Br₂O₂⁺ (ESI+) [M+H]⁺: calc.: 454.0143, found: 454.0148.

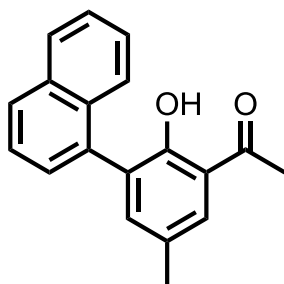
for C₂₀H₂₄⁸¹Br₂O₂⁺ (ESI+) [M+H]⁺: calc.: 458.0102, found: 458.0105.

for C₂₀H₂₄⁷⁹Br⁸¹BrO₂⁺ (ESI+) [M+H]⁺: calc.: 457.0156, found: 457.0157.

Melting point: 180 – 182 °C.

Cross-coupling of phenols carrying EWG

2-Acetyl-4-methyl-6-(naphthyl)phenol (13)

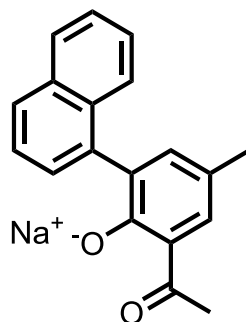


^1H NMR (400 MHz, Chloroform-*d*) δ 12.41 (s, 1H), 7.89 (ddt, J = 8.2, 4.6, 1.0 Hz, 2H), 7.65 (dd, J = 2.2, 1.0 Hz, 1H), 7.63 – 7.58 (m, 1H), 7.54 (dd, J = 8.2, 7.0 Hz, 1H), 7.48 (ddd, J = 8.2, 7.0, 1.4 Hz, 1H), 7.44 – 7.38 (m, 2H), 7.36 (d, J = 2.2 Hz, 1H), 2.72 (s, 3H), 2.39 (s, 3H).

HRMS for $\text{C}_{19}\text{H}_{17}\text{O}_2^+$ (ESI+) $[\text{M}+\text{H}]^+$: calc.: 277.1223, found: 277.1225.

In a mixture with **14**.

Sodium 2-acetyl-4-methyl-6-(naphthyl)phenolate (phenolate of 13)

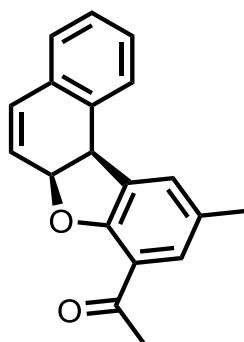


cis-8-Acetyl-6a,11b-dihydro-10-methylnaphtho[2,1-*b*]benzo[*d*]furan was taken up in CH_2Cl_2 (0.5 mL) and treated with 1 M NaOH solution (5 mL). The reaction mixture was stirred vigorously over night at room temperature. CH_2Cl_2 and water were removed under vacuum.

^1H NMR (300 MHz, DMSO- d_6) δ 7.83 (dd, J = 8.1, 1.4 Hz, 1H), 7.76 – 7.69 (m, 2H), 7.41 (td, J = 8.1, 6.9, 2.2 Hz, 2H), 7.35 – 7.27 (m, 2H), 7.23 (dd, J = 7.0, 1.4 Hz, 1H), 6.75 (d, J = 2.8 Hz, 1H), 2.44 (s, 2H), 2.07 (s, 3H).

^{13}C NMR (101 MHz, DMSO) δ 198.0, 159.9, 136.3, 135.3, 133.1, 132.5, 130.2, 127.9, 127.5, 127.5, 126.8, 125.5, 125.4, 124.9, 124.6, 80.6, 48.6, 39.5, 30.9, 20.4.

cis-8-Acetyl-6a,11b-dihydro-10-methylnaphtho[2,1-b]benzo[d]furan (14)



rac.

According to the **GPIII** for the electrochemical cross-coupling of phenols with naphthalenes, 2-hydroxy-5-methylacetophenone (75 mg, 0.5 mmol, 1.0 equiv.), naphthalene (192 mg, 1.5 mmol, 3.0 equiv.), HFIP (5 mL), and DIPEA (0.1 mL, 0.57 mmol 1.15 equiv.) were transferred into an undivided PTFE cell. Electrolysis was carried out at room temperature with a current density of 5.0 mA/cm² using graphite electrodes. After 2.0 F was applied, HFIP was recovered *in vacuo*. The residue was purified by column chromatography (gradient: cyclohexane:ethyl acetate = from 100:0 for 3 min to 97:3 for 60 min; column 12 mm x 150 mm; flow rate 12.5 mL/min) yielding the product as colourless crystals (yield: 35%, 48 mg, 0.17 mmol).

¹H NMR (400 MHz, CDCl₃) δ 7.50 (dt, *J* = 2.0, 0.9 Hz, 1H), 7.40 (ddd, *J* = 7.4, 1.5, 0.9 Hz, 1H), 7.32 (td, *J* = 7.4, 1.5 Hz, 1H), 7.29 – 7.23 (m, 1H), 7.10 (dd, *J* = 7.4, 1.5 Hz, 1H), 7.00 (ddd, *J* = 2.0, 1.5, 0.9 Hz, 1H), 6.52 (dd, *J* = 10.0, 1.5 Hz, 1H), 5.96 (ddd, *J* = 10.0, 3.0, 1.5 Hz, 1H), 5.87 (dd, *J* = 10.0, 3.0 Hz, 1H), 4.68 (d, *J* = 10.0 Hz, 1H), 2.24 (s, 3H).

¹³C NMR (101 MHz, CDCl₃) δ 197.2, 156.7, 132.5, 132.3, 130.6, 130.3, 130.2, 129.9, 128.8, 128.6, 128.4, 128.1, 127.9, 124.6, 120.8, 82.5, 43.3, 31.2, 20.8.

HRMS for C₁₉H₁₇O₂⁺ (ESI+) [M+H]⁺: calc.: 277.1223, found: 277.1225.

Melting point: 133.5 °C.

Crystal structure determination of **14**: C₁₉H₁₆O₄, M_r = 276.32 g/mol, colourless needle (0.09 x 0.1 x 0.77 mm³), P na₂₁ (orthorombisch), a = 18.9656(16) Å, b = 4.7241(3) Å, c = 15.4178(10) Å, V = 1381.36(17) Å³, z = 4, F(000) = 584, ρ = 1.329 g/cm³, μ = 0.085 mm⁻¹, Mo-Kα graphite monochromator, 120 K, 5378 reflections, 2753 reflections, wR₂ = 0.0949, R₁ = 0.0371, 0.15 eÅ⁻³, -0.16 eÅ⁻³, GoF = 1.005;

Single crystals for structure determination were obtained by slowly evaporating acetone at room temperature. **Deposition Number 1920412**

The structure analysis revealed that the aromatic system is suspended and a dihydrobenzofurane system in Z-conformation is formed.

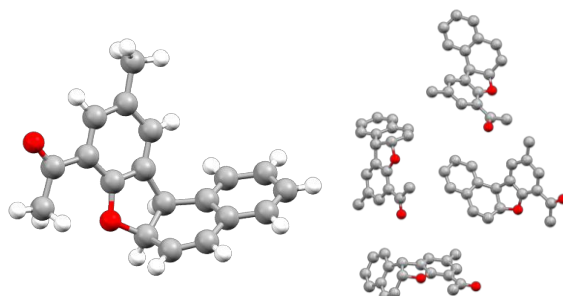


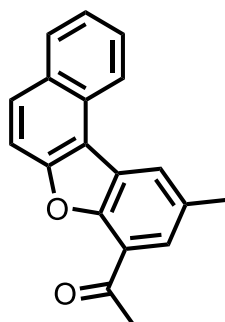
Fig. S5: left: molecular structure of **14**; right: Packing of **14** in the solid state.

Due to the equilibrium of **13** and **14** only mixtures could be obtained.

14 could be crystallized easily, whereas **13** could not be crystallized in a clean fashion.

The phenolate of **13** could be analyzed. (see page 19 in SI).

8-Acetyl-10-methylnaphtho[2,1-*b*]benzo[*d*]furan (15)



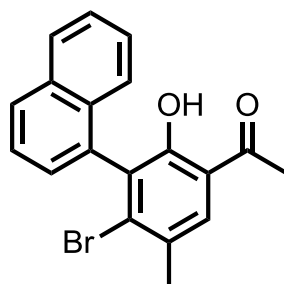
cis-8-Acetyl-6a,11b-dihydro-10-methylnaphtho[2,1-*b*]benzo[*d*]furan (50 mg, 0.18 mmol, 1.0 equiv.) were dissolved in 1,4-dioxane (1 mL) and 2,3-dichloro-5,6-dicyano-1,4-benzoquinone (50 mg, 0.22 mmol, 1.2 equiv.) were added. The mixture was stirred at reflux for 12 h. The resulting red mixture was diluted with ethyl acetate (10 mL) and washed with sat. NaHCO₃ solution (10 mL) twice. The organic layer was dried over sodium sulfate and evaporated under vacuum. The residue was purified by column chromatography (gradient: cyclohexane:ethyl acetate = from 100:0 for 3 min to 97:3 for 60 min; column 12 mm x 150 mm; flow rate 12.5 mL/min) yielding the product as a white solid (yield: 83%, 40 mg, 0.15 mmol).

¹H NMR (300 MHz, CDCl₃) δ 8.62 – 8.51 (m, 1H), 8.34 (dd, *J* = 1.9, 0.9 Hz, 1H), 8.07 – 7.99 (m, 1H), 7.95 (d, *J* = 9.0 Hz, 1H), 7.87 (dd, *J* = 1.9, 0.9 Hz, 1H), 7.79 (d, *J* = 9.0 Hz, 1H), 7.73 (ddd, *J* = 8.2, 6.9, 1.2 Hz, 1H), 7.57 (ddd, *J* = 8.2, 6.9, 1.2 Hz, 1H), 2.97 (s, 3H), 2.62 (d, *J* = 0.9 Hz, 3H).

¹³C NMR (101 MHz, CDCl₃) δ 196.6, 154.8, 153.1, 132.9, 130.8, 129.5, 129.3, 128.9, 127.6, 127.3, 127.2, 126.8, 124.8, 123.4, 122.2, 116.5, 112.8, 77.2, 31.3, 21.6.

HRMS for C₁₉H₁₅O₂⁺ (ESI⁺) [M+H]⁺: calc.: 274.0994, found: 275.1071.

2-Acetyl-5-bromo-4-methyl-6-naphthylphenol (**16**)



According to the **GPIII** for the electrochemical cross-coupling of phenols with naphthalenes, 1-4-bromo-2-hydroxy-5-methyl-acetophenone (115 mg, 0.5 mmol, 1.0 equiv.), naphthalene (192 mg, 1.5 mmol, 3.0 equiv.), HFIP (5 mL), and DIPEA (0.1 mL, 0.57 mmol 1.15 equiv.) were transferred into an undivided PTFE cell. Electrolysis was carried out at room temperature with a current density of 5.0 mA/cm² using graphite electrodes. After 2.0 F was applied, HFIP was recovered *in vacuo*. The residue was purified by column chromatography (gradient: cyclohexane:ethyl acetate = from 100:0 for 3 min to 97:3 for 60 min; column 12 mm x 150 mm; flow rate 12.5 mL/min) yielding the product as a colorless solid (yield: 42%, 75 mg, 0.21 mmol).

¹H NMR (400 MHz, CDCl₃) δ 12.43 (s, 1H), 7.93 (tt, *J* = 7.0, 1.0 Hz, 2H), 7.73 (d, *J* = 1.0 Hz, 1H), 7.59 (dd, *J* = 8.3, 7.0 Hz, 1H), 7.48 (dq, *J* = 8.9, 4.9, 4.5 Hz, 1H), 7.44 – 7.37 (m, 2H), 7.34 (dd, *J* = 7.0, 1.0 Hz, 1H), 2.70 (s, 3H), 2.50 (s, 2H).

¹³C NMR (101 MHz, CDCl₃) δ 204.2, 159.0, 136.4, 135.2, 133.8, 131.6, 131.4, 130.8, 128.9, 128.7, 128.6, 127.6, 126.4, 126.1, 125.6, 125.1, 118.5, 77.2, 27.1, 23.6.

HRMS for C₁₉H₁₅⁷⁹BrO₂ (ESI+) [M+H]⁺: calc.: 355.0289, found: 355.0333.

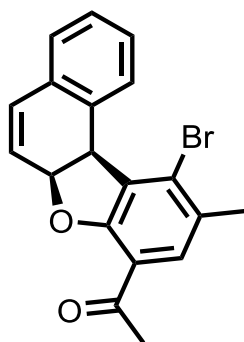
for C₁₉H₁₅⁸¹BrO₂ (ESI+) [M+H]⁺: calc.: 357.0269, found: 357.0315.

Melting point: 148.5 °C.

Due to the equilibrium of **16** and **17** only mixtures could be obtained.

16 could be crystallized easily, whereas **17** could not be crystallized in a clean fashion.

cis-8-Acetyl-11-bromo-6a,11b-dihydro-10-methylnaphtho[2,1-b]benzo[d]furan (17)



rac.

^1H NMR (400 MHz, CDCl_3) δ 7.67 (ddt, $J = 5.6, 1.9, 1.0$ Hz, 1H), 7.26 – 7.22 (m, 2H), 7.20 (dt, $J = 6.1, 3.1$ Hz, 1H), 6.88 (dd, $J = 9.6, 0.7$ Hz, 1H), 6.23 (dd, $J = 9.6, 5.6$ Hz, 1H), 5.26 (dd, $J = 7.7, 5.6$ Hz, 1H), 4.60 – 4.54 (m, 1H), 2.56 (s, 3H), 2.44 (s, 3H).

HRMS for $\text{C}_{19}\text{H}_{15}^{79}\text{BrO}_2$ (ESI+) $[\text{M}+\text{H}]^+$: calc.: 355.0289, found: 355.0333.

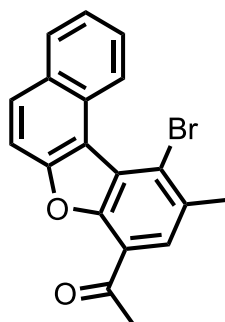
for $\text{C}_{19}\text{H}_{15}^{81}\text{BrO}_2$ (ESI+) $[\text{M}+\text{H}]^+$: calc.: 357.0269, found: 357.0315.

Due to the equilibrium of **16** and **17** only mixtures of **17** with **16** could be obtained.

16 could be crystallized easily, whereas **17** could not be crystallized in a clean fashion.

^{13}C NMR spectra of the mixture is shown on page 42.

8-Acetyl-11-bromo-10-methylnaphtho[2,1-*b*]benzo[*d*]furan (18)



cis-8-Acetyl-11-bromo-6a,11b-dihydro-10-methylnaphtho[2,1-*b*]benzo[*d*]furan (20 mg, 0.056 mmol, 1.0 equiv.) were dissolved in 1,4-dioxane (2 mL) and 2,3-dichloro-5,6-dicyano-1,4-benzoquinone (50 mg, 0.22 mmol, 3.9 equiv.) were added. The mixture was stirred at reflux for 36 h. The resulting red mixture was diluted with ethyl acetate (10 mL) and washed with sat. NaHCO₃ solution (10 mL) twice. The organic layer was dried over sodium sulfate and evaporated under vacuum. The residue was purified by reversed phase column chromatography (gradient: water:acetonitrile = from 50:50 for 3 min to 30:70 for 60 min;) yielding the product as an off white solid (yield: 76%, 15 mg, 0.042 mmol).

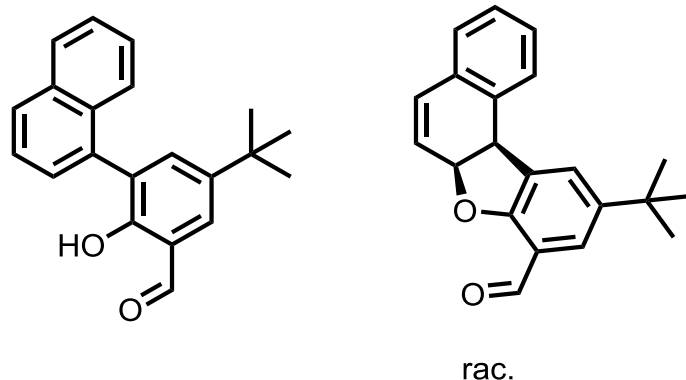
¹H NMR (400 MHz, CDCl₃) δ 9.77 (d, *J* = 8.8 Hz, 1H), 8.06 – 8.00 (m, 2H), 7.96 (s, 1H), 7.79 (d, *J* = 8.8 Hz, 1H), 7.70 (ddd, *J* = 8.0, 6.9, 1.5 Hz, 1H), 7.58 (ddd, *J* = 8.0, 6.9, 1.1 Hz, 1H), 2.98 (s, 2H), 2.68 (s, 3H).

¹³C NMR (101 MHz, CDCl₃) δ 196.1, 155.3, 153.7, 134.4, 131.7, 131.4, 129.5, 128.6, 128.5, 128.4, 128.3, 126.4, 124.8, 121.3, 116.7, 112.5, 110.1, 77.2, 31.6, 24.7.

HRMS for C₁₉H₁₃⁷⁹BrO₂ (APCI+) [M+H]⁺: calc.: 353.0177, found: 353.0165.

for C₁₉H₁₃⁸¹BrO₂ (APCI+) [M+H]⁺: calc.: 355.0157, found: 355.0147.

***cis*-8-Formyl-6a,11b-dihydro-10-(2,2-dimethylethyl)naphtho[2,1-*b*]benzo[*d*]furan and 2-hydroxy-5-(2,2-dimethylethyl)-3-(naphthyl)benzaldehyde (mixture with a ratio of 1:3.3)**



According to the **GPIII** for the electrochemical cross-coupling of phenols with naphthalenes, 5-(*tert*-butyl)-2-hydroxybenzaldehyde (89 mg, 0.5 mmol, 1.0 equiv.), naphthalene (192 mg, 1.5 mmol, 3 equiv.), HFIP (5 mL), and DIPEA (0.1 mL, 0.48 mmol, 0.96 equiv.) were transferred into an undivided PTFE cell. Electrolysis was carried out at room temperature with a current density of 5.0 mA/cm² using graphite electrodes. After 2.0 F was applied, HFIP was recovered *in vacuo*. The residue was purified by column chromatography (gradient: cyclohexane:ethyl acetate = from 100:0 for 3 min to 97:3 for 60 min; column 12 mm x 150 mm; flow rate 12.5 mL/min) yielding the product as a white solid (yield: 3.3%, 5 mg).

Data phenolic structure:

¹H NMR (400 MHz, CDCl₃) δ 10.87 (s, 1H), 9.89 (d, *J* = 0.6 Hz, 1H), 7.62 (dd, *J* = 2.2, 0.9 Hz, 3H), 7.59 (dd, *J* = 8.8, 2.5 Hz, 1H), 7.51 (d, *J* = 2.5 Hz, 1H), 7.37 (dd, *J* = 2.2, 1.4 Hz, 3H), 6.94 (d, *J* = 8.8 Hz, 1H), 1.33 (s, 9H).

Data cyclized structure:

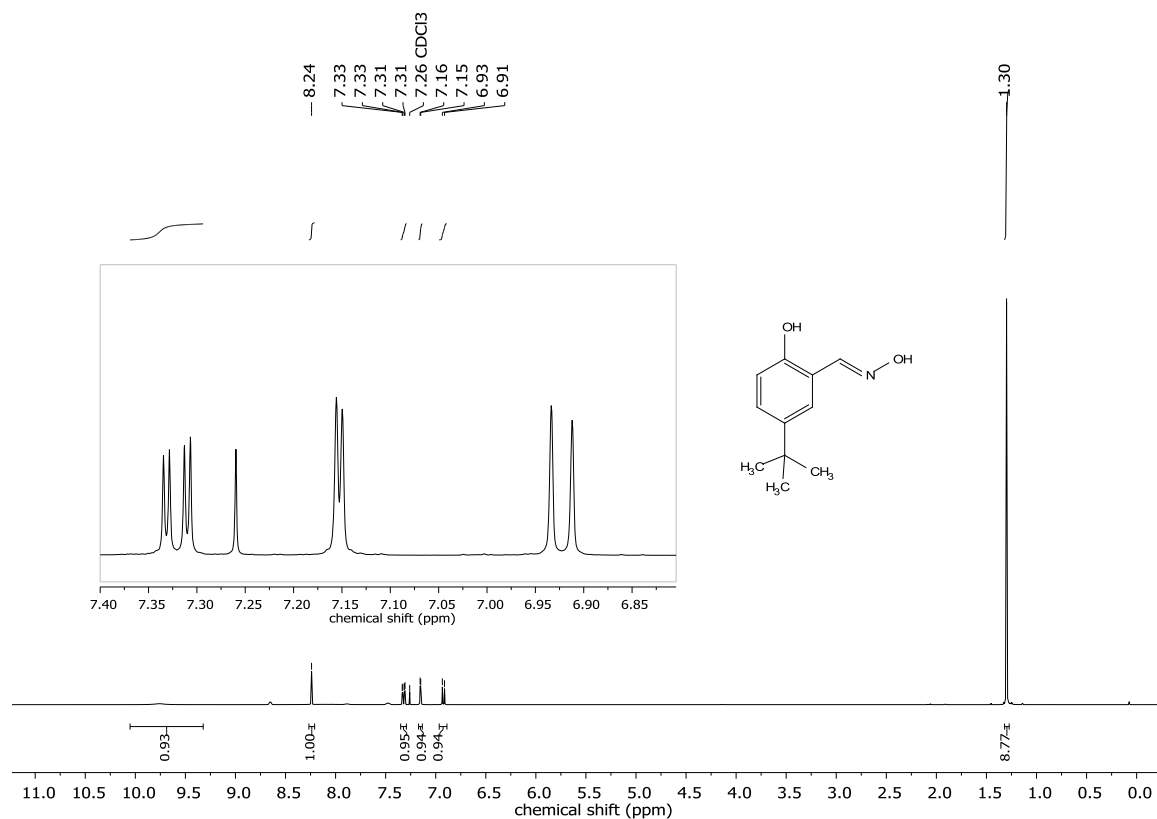
¹H NMR (400 MHz, CDCl₃) δ 10.24 (s, 1H), 7.42 (ddd, *J* = 7.5, 1.5, 0.7 Hz, 1H), 7.37 (dd, *J* = 2.2, 1.4 Hz, 1H), 7.33 (td, *J* = 7.5, 1.5 Hz, 1H), 7.26 (s, 1H), 7.11 (dd, *J* = 7.5, 1.5 Hz, 1H), 6.58 – 6.53 (m, 1H), 6.00 – 5.92 (m, 2H), 4.71 (d, *J* = 9.9 Hz, 1H), 1.33 (s, 3H), 1.26 (s, 9H).

Mixture:

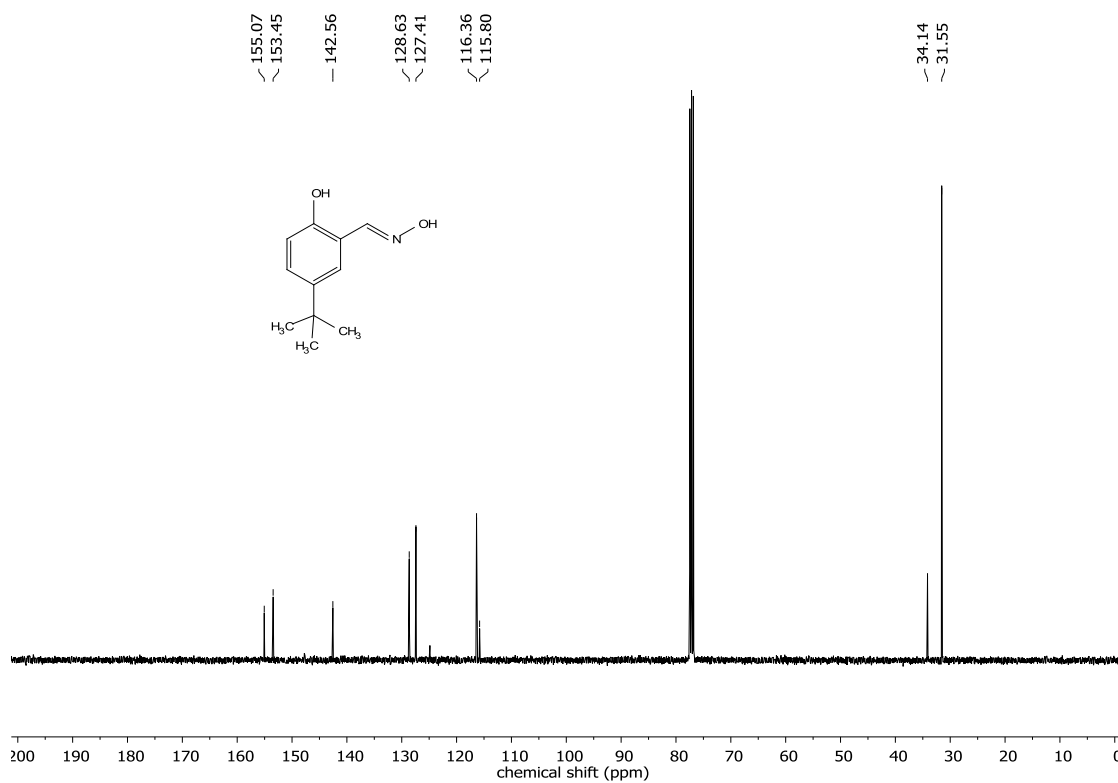
¹³C NMR (101 MHz, CDCl₃) δ 197.0, 189.2, 159.6, 158.7, 144.4, 142.9, 134.9, 132.4, 130.5, 130.1, 129.9, 128.5, 128.4, 128.2, 127.9, 124.1, 123.8, 120.1, 119.2, 117.4, 83.1, 77.2, 42.9, 34.6, 31.6, 27.1.

NMR spectra

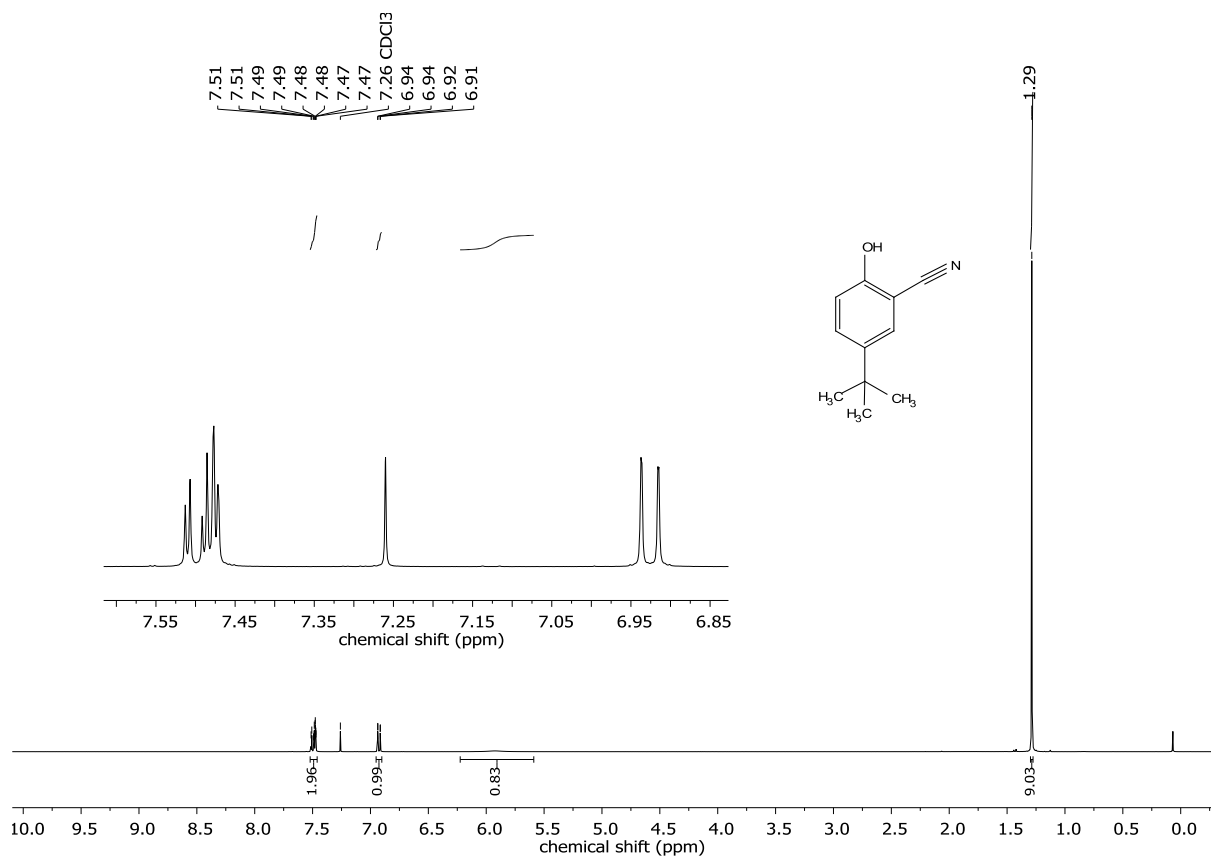
Starting materials:



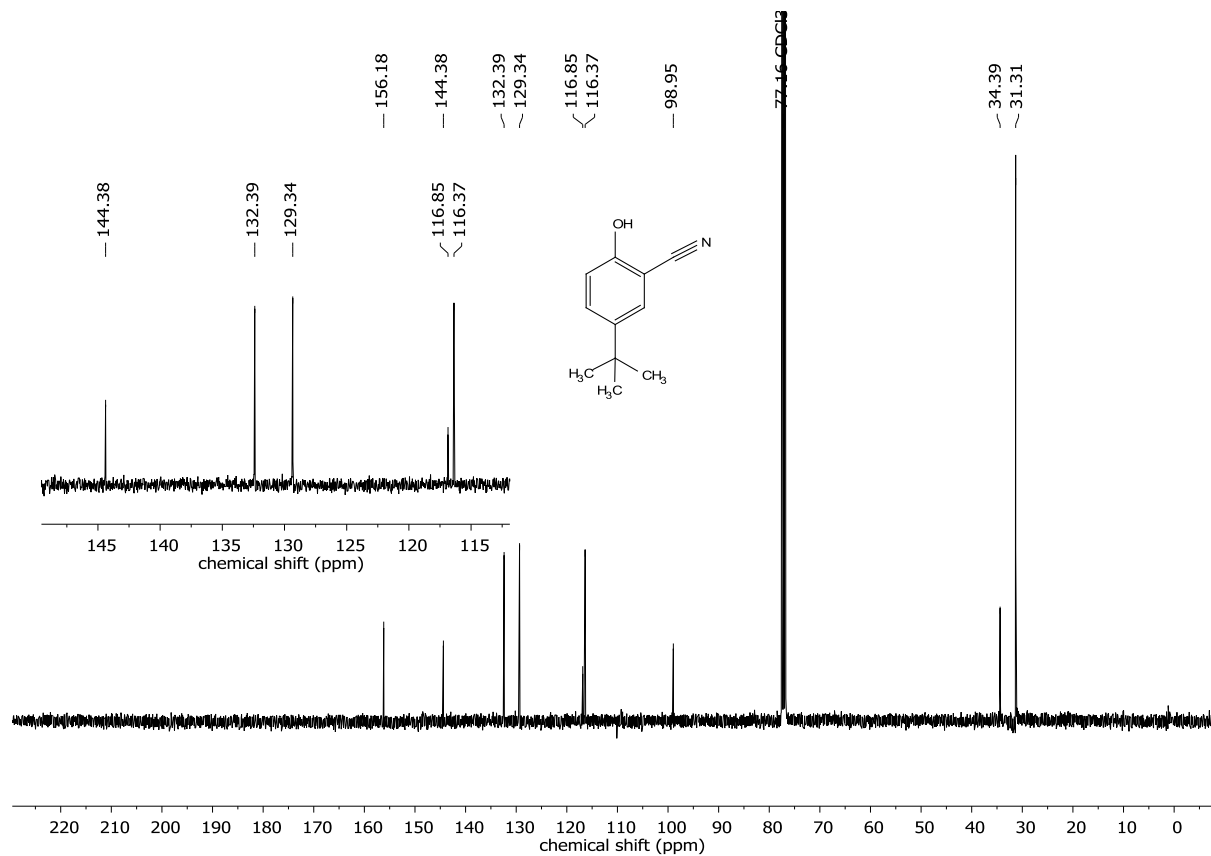
¹H NMR of 5-(*tert*-Butyl)-2-hydroxybenzaldehyde oxime.



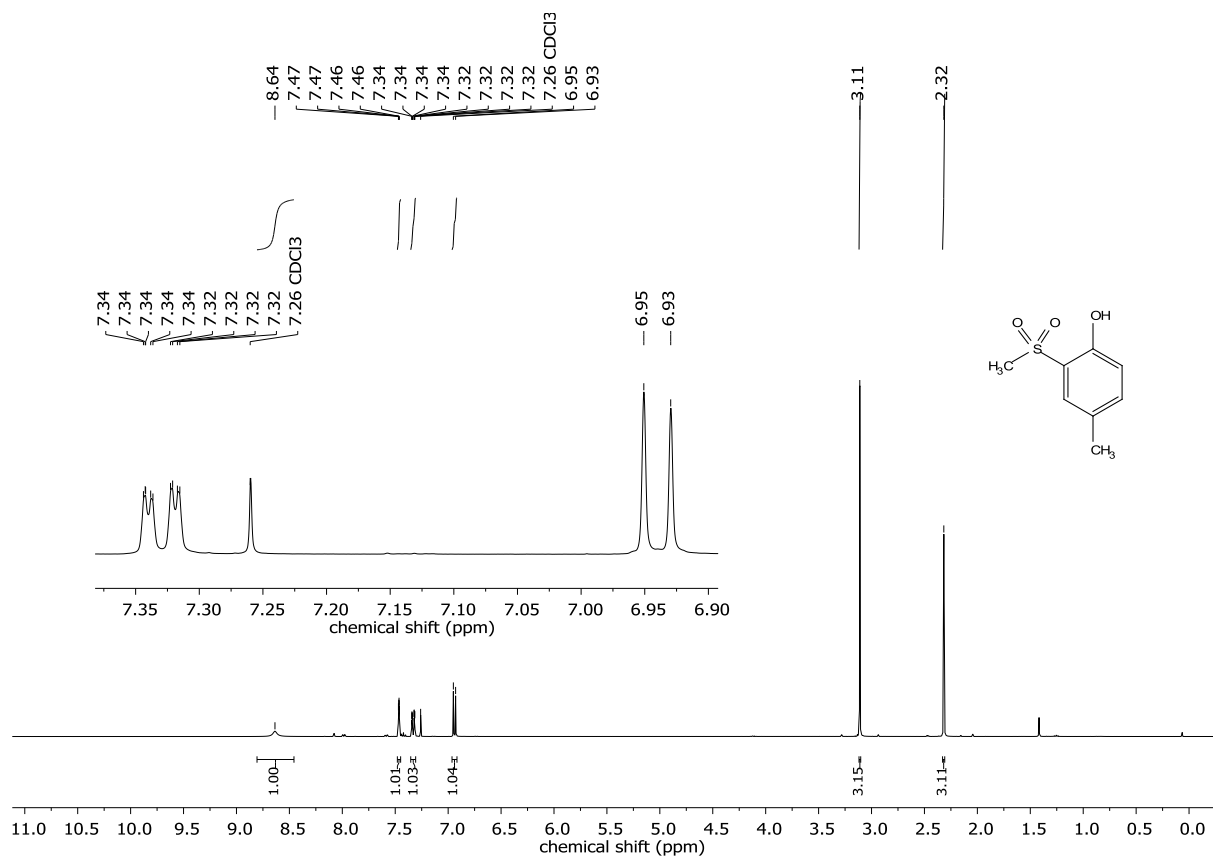
¹³C NMR of 5-(*tert*-Butyl)-2-hydroxybenzaldehyde oxime.



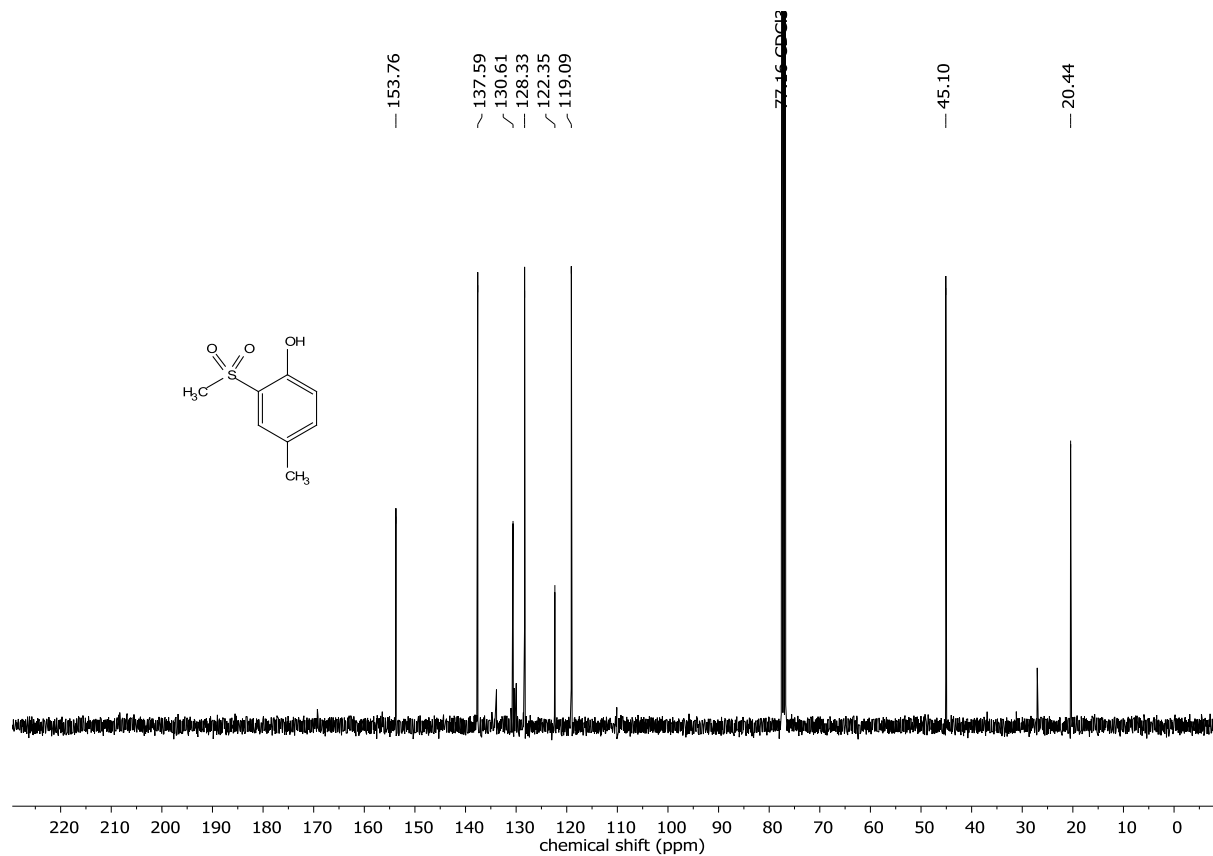
¹H NMR of 5-(*tert*-Butyl)-2-hydroxybenzonitrile.



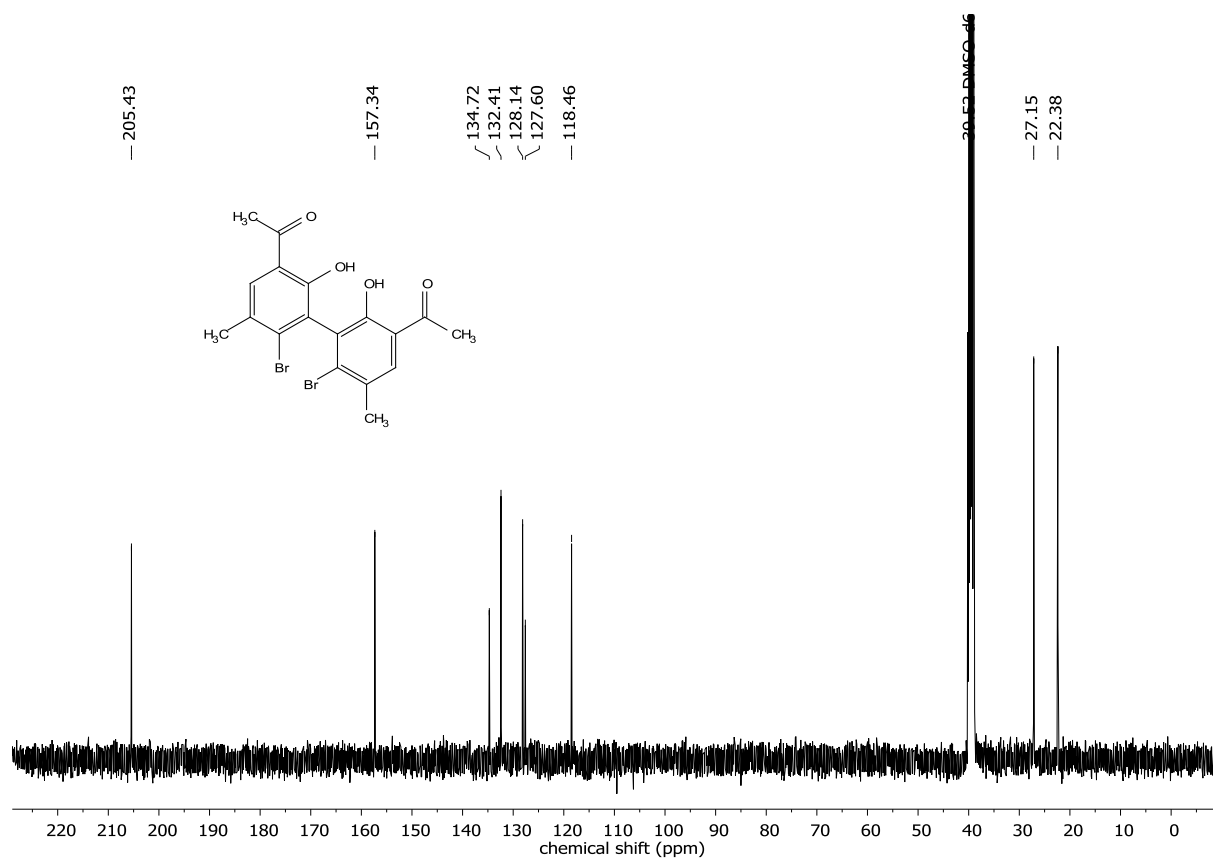
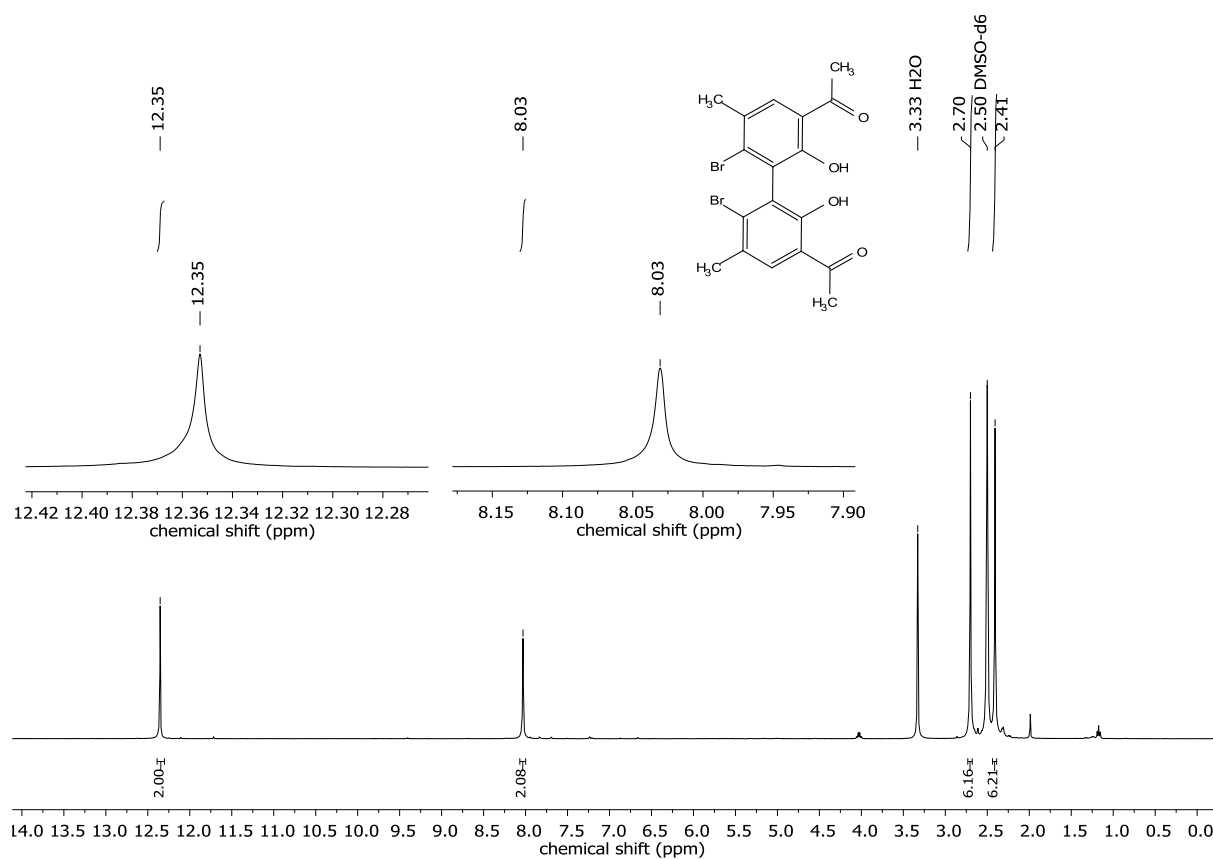
¹³C NMR of 5-(*tert*-Butyl)-2-hydroxybenzonitrile.



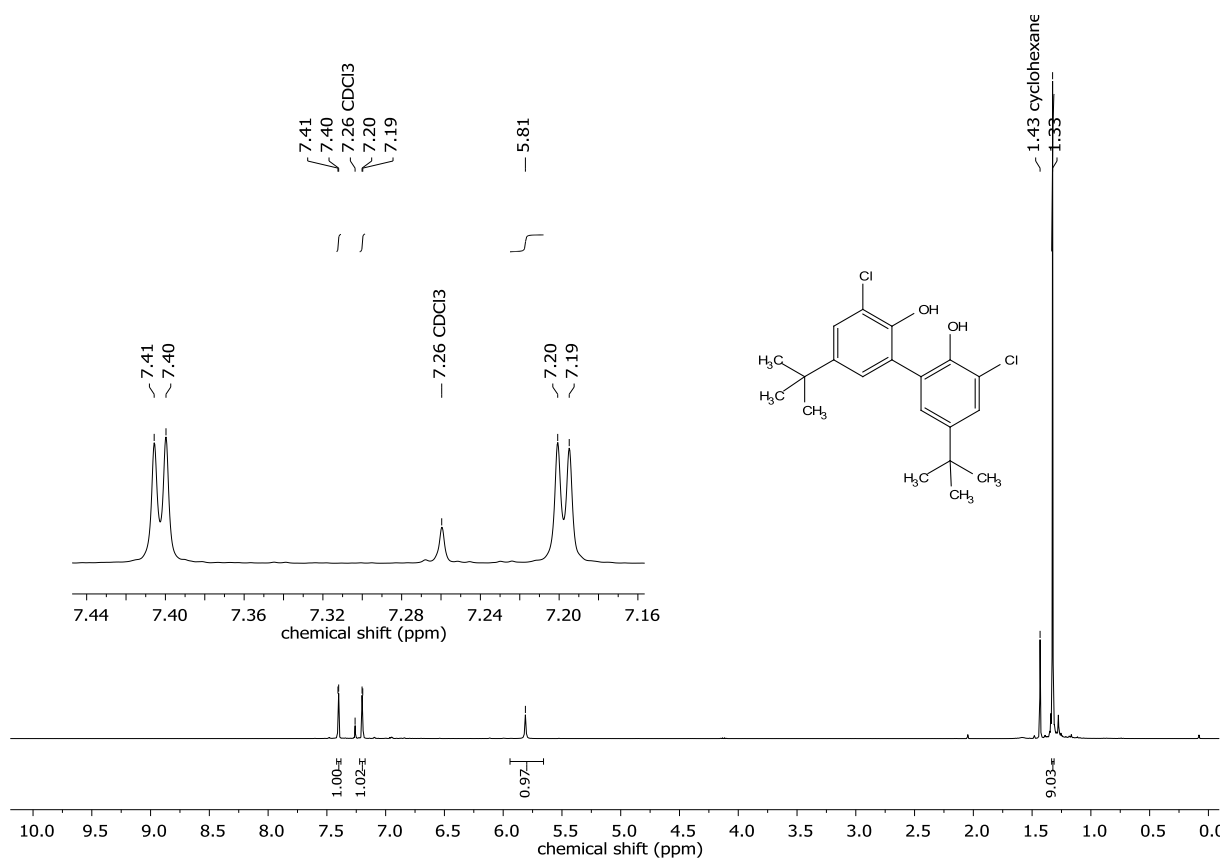
¹H NMR of 4-Methyl-2-(methylsulfonyl)phenol.



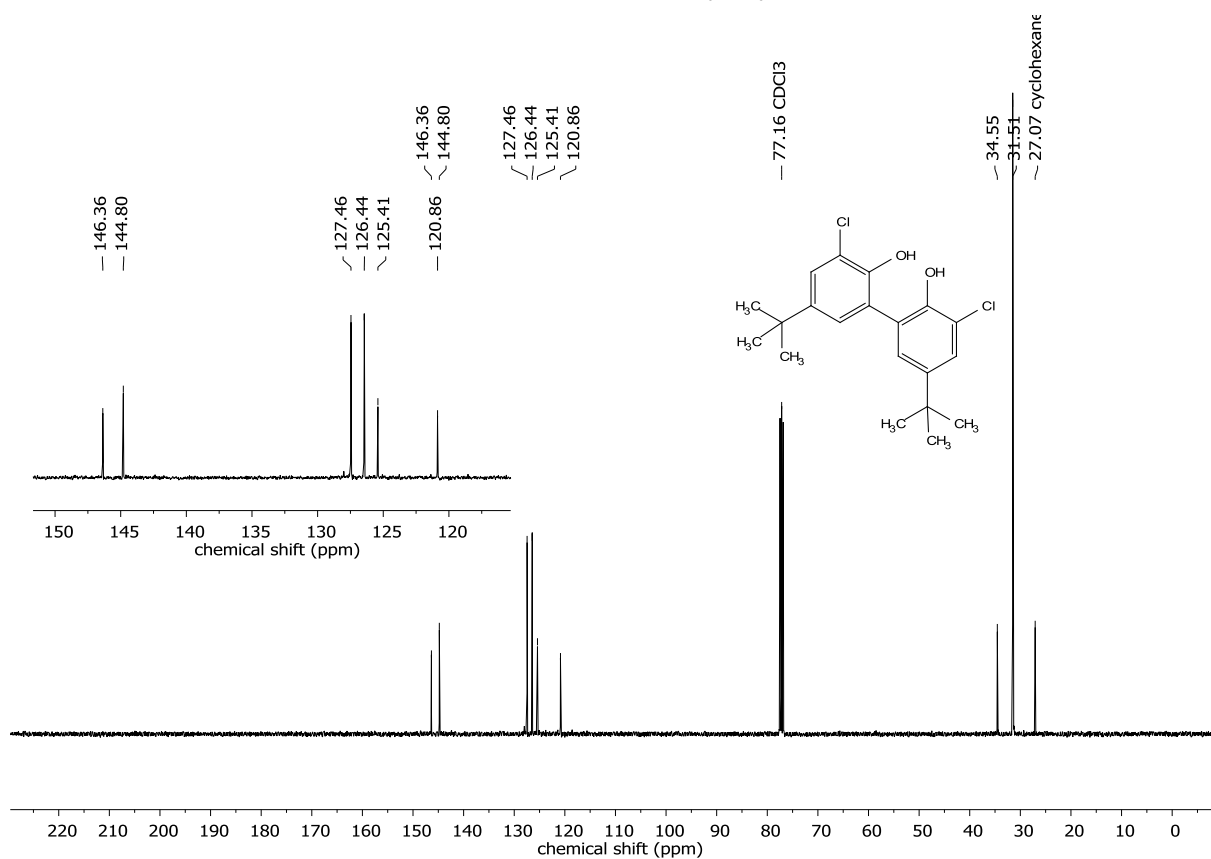
¹³C NMR of 4-Methyl-2-(methylsulfonyl)phenol.



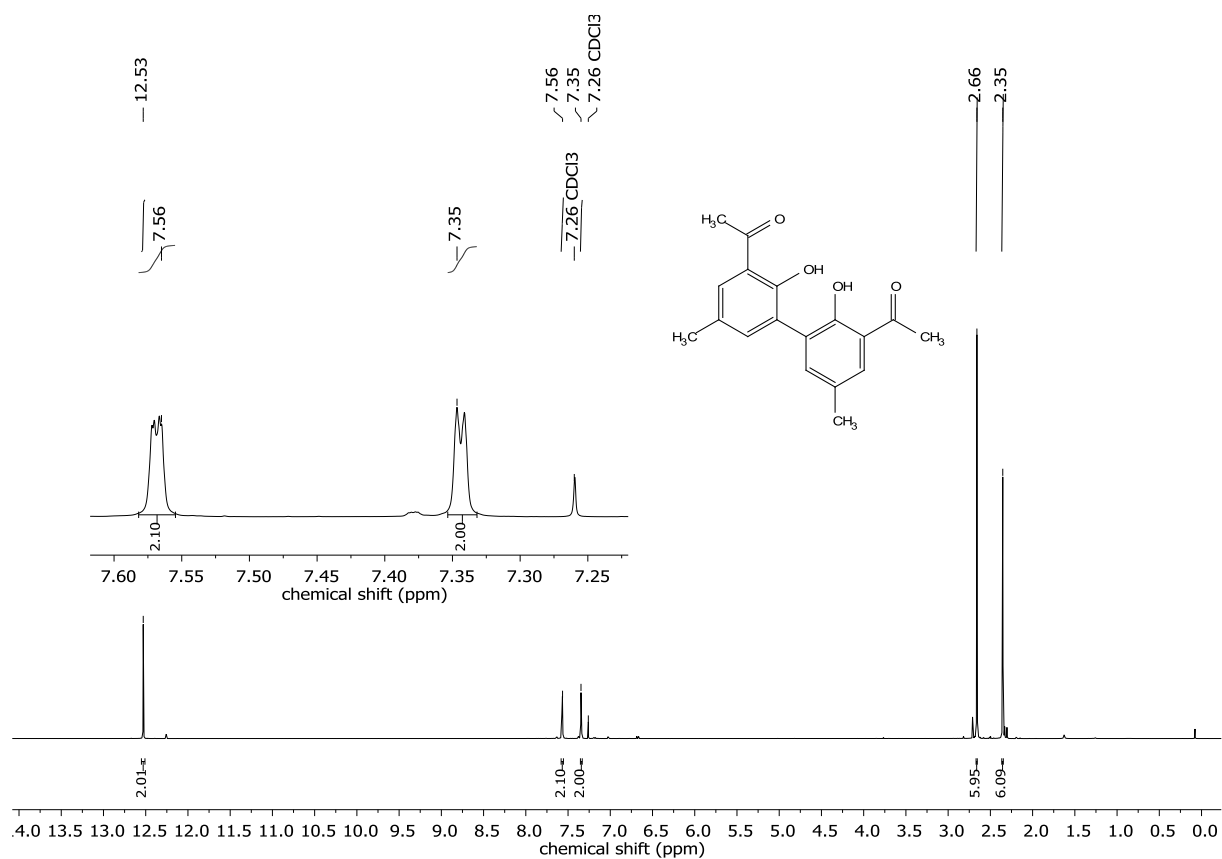
¹³C NMR of 3,3'-Diacetyl-6,6'-dibromo-5,5'-dimethyl-2,2'-biphenol (4).



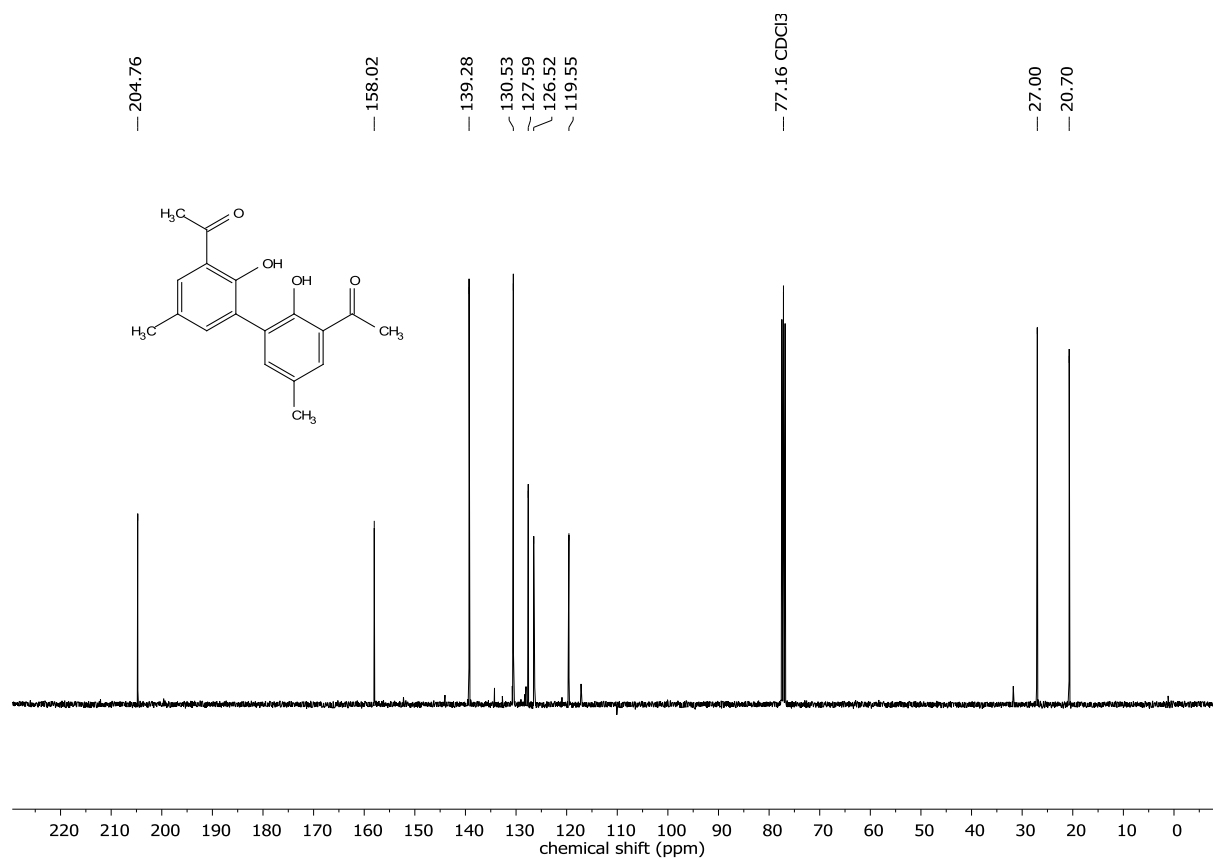
¹H NMR of 3,3'-Dichloro-5,5'-di(2,2-dimethylethyl)-2,2'-biphenol (5).



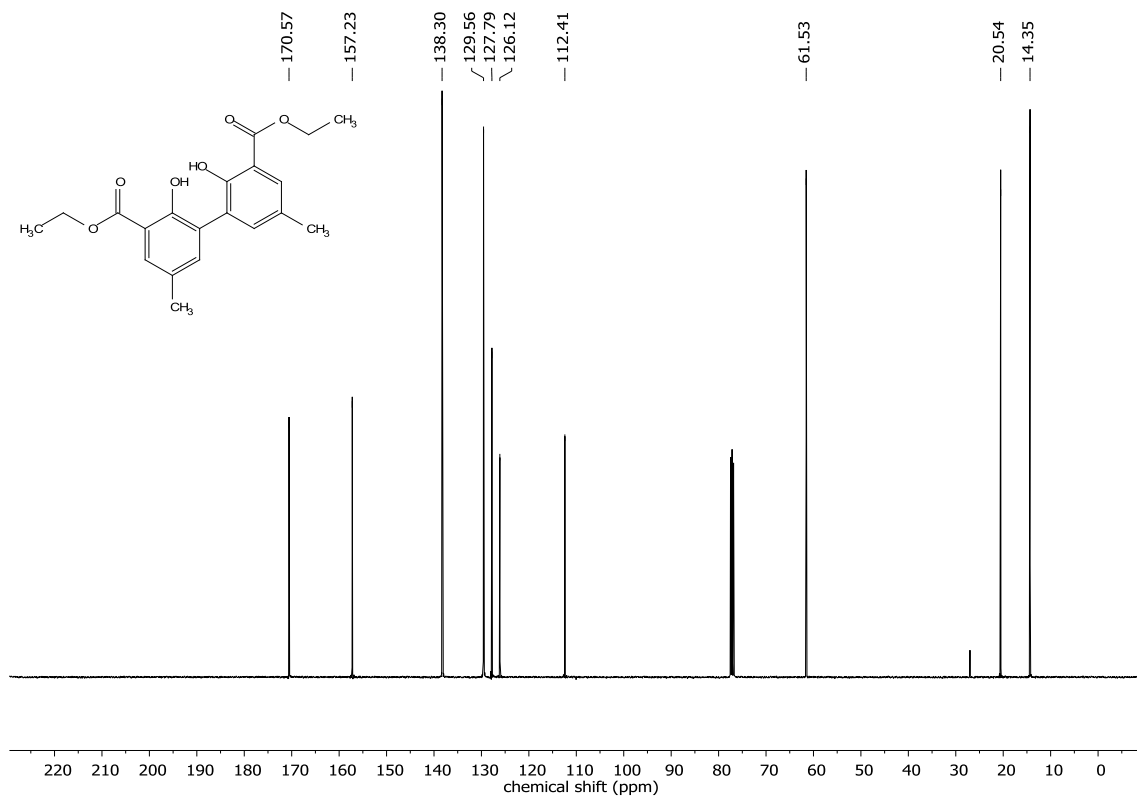
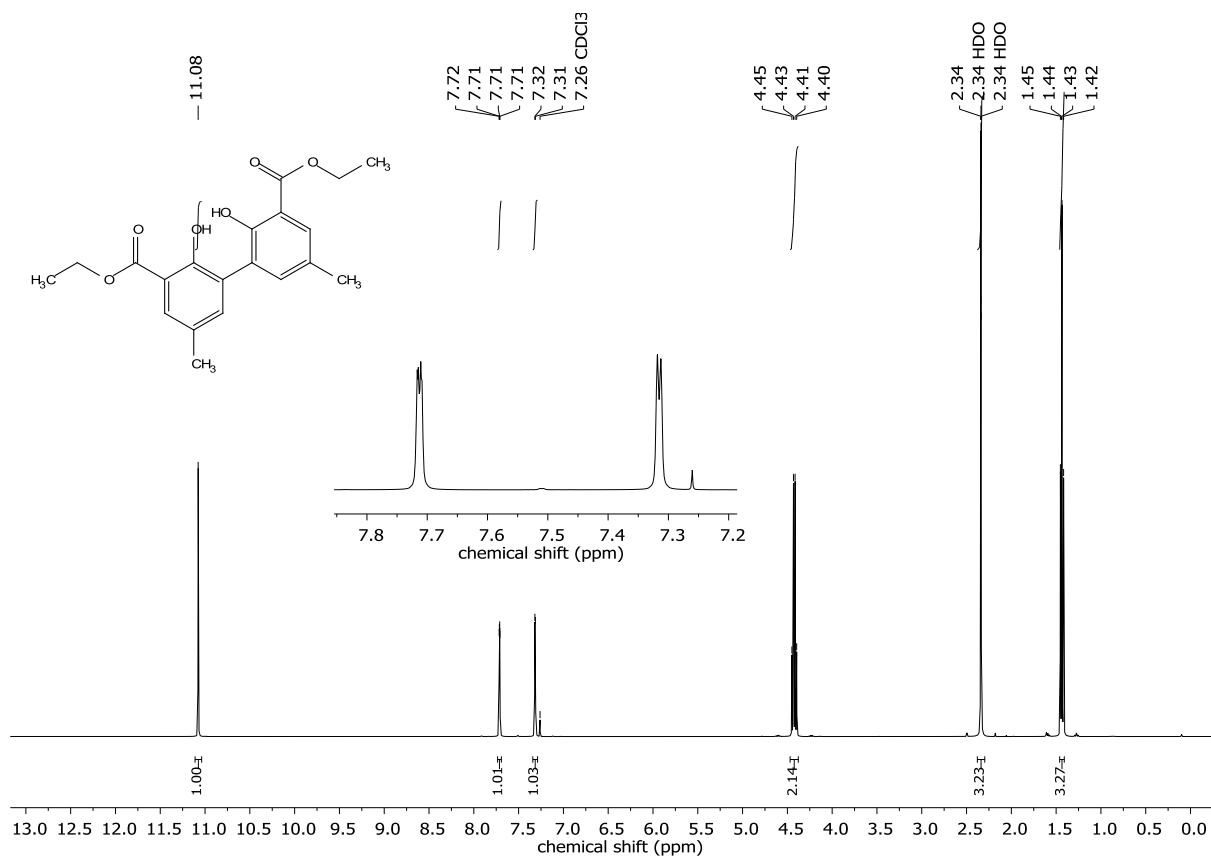
¹³C NMR of 3,3'-Dichloro-5,5'-di(2,2-dimethylethyl)-2,2'-biphenol (5).



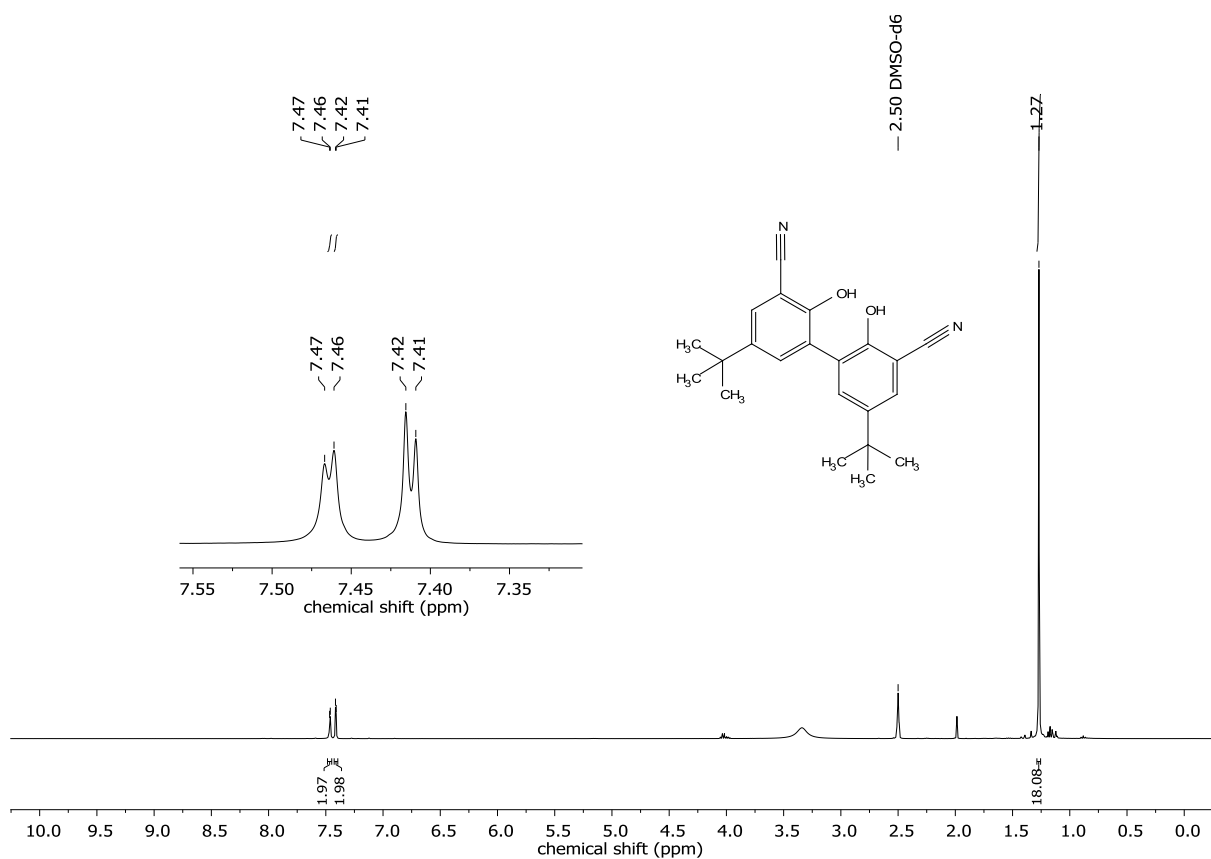
¹H NMR of 3,3'-Diacetyl-5,5'-dimethyl-2,2'-biphenol. (6)



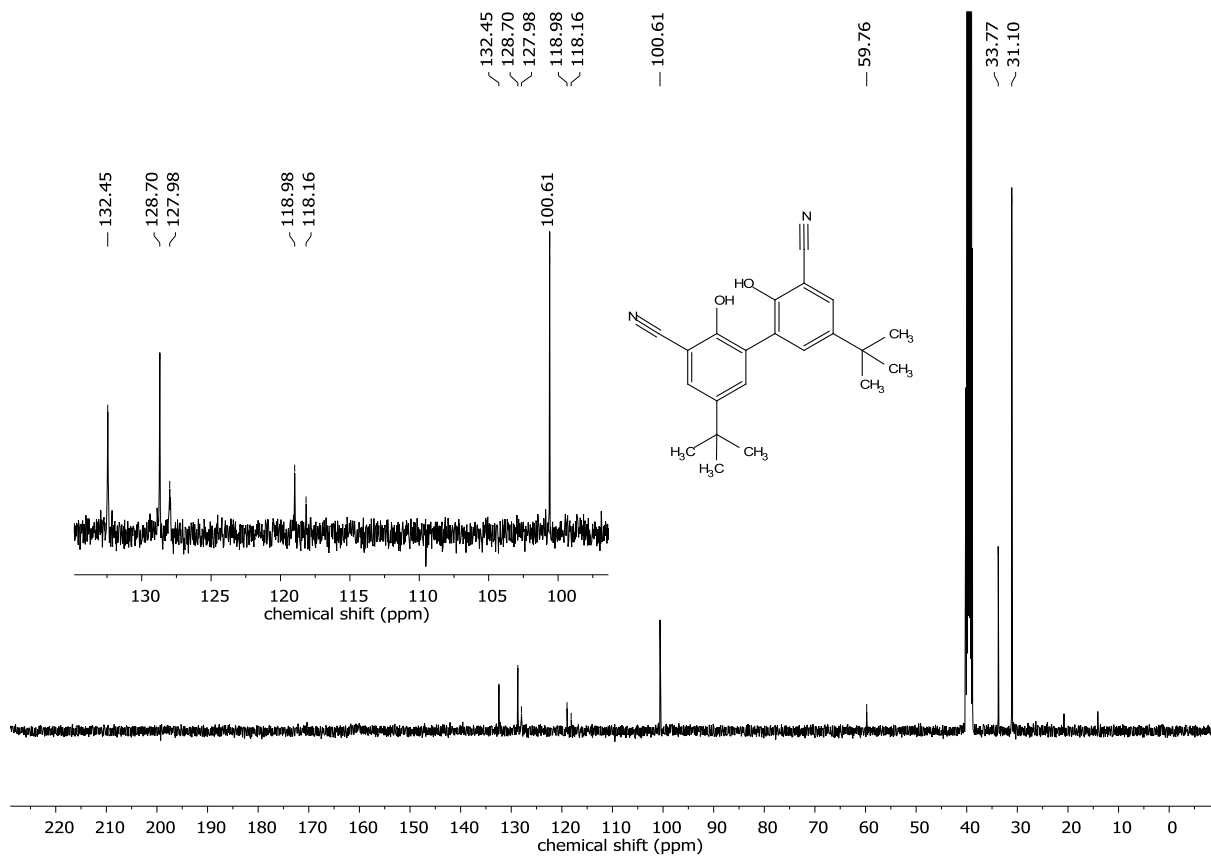
¹³C NMR of 3,3'-Diacetyl-5,5'-dimethyl-2,2'-biphenol. (6).



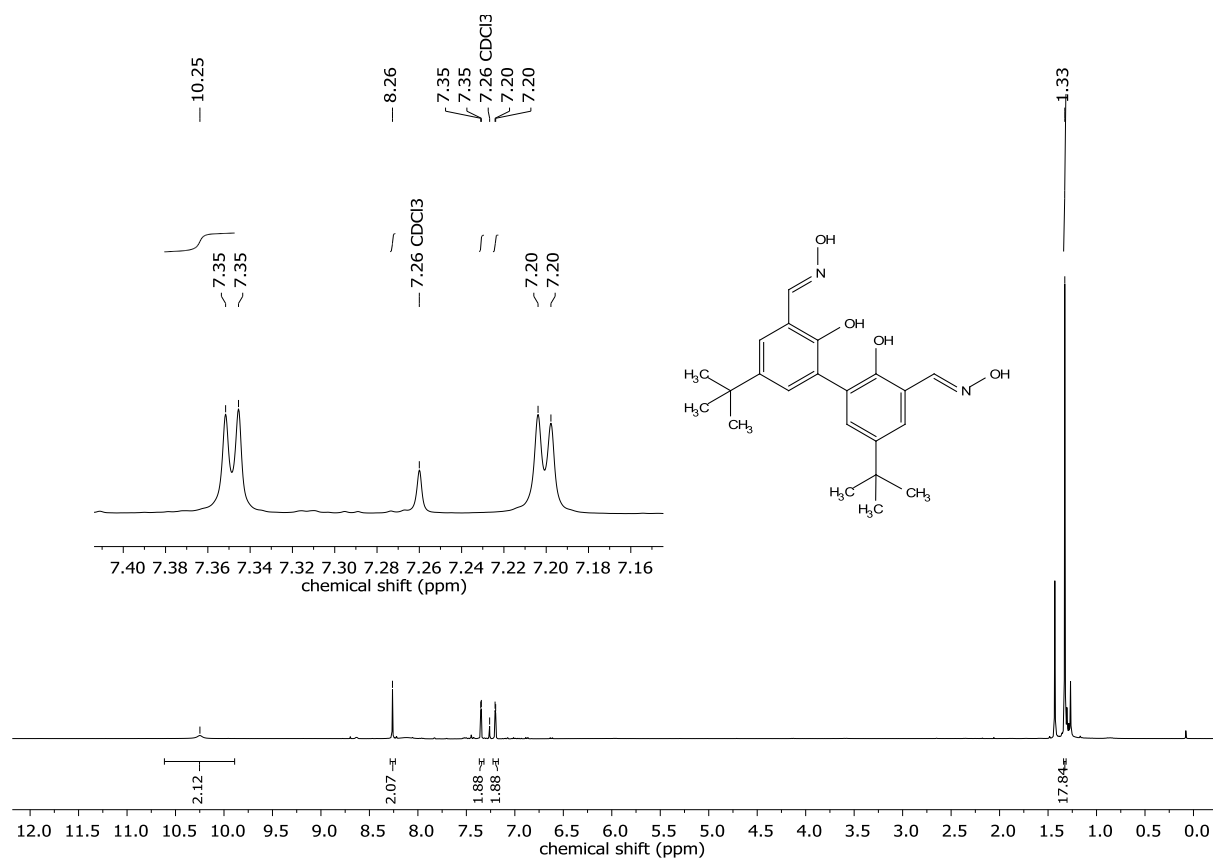
¹³C NMR of 3,3'-Di(ethoxycarbonyl)-5,5'-dimethyl-2,2'-biphenol (7).



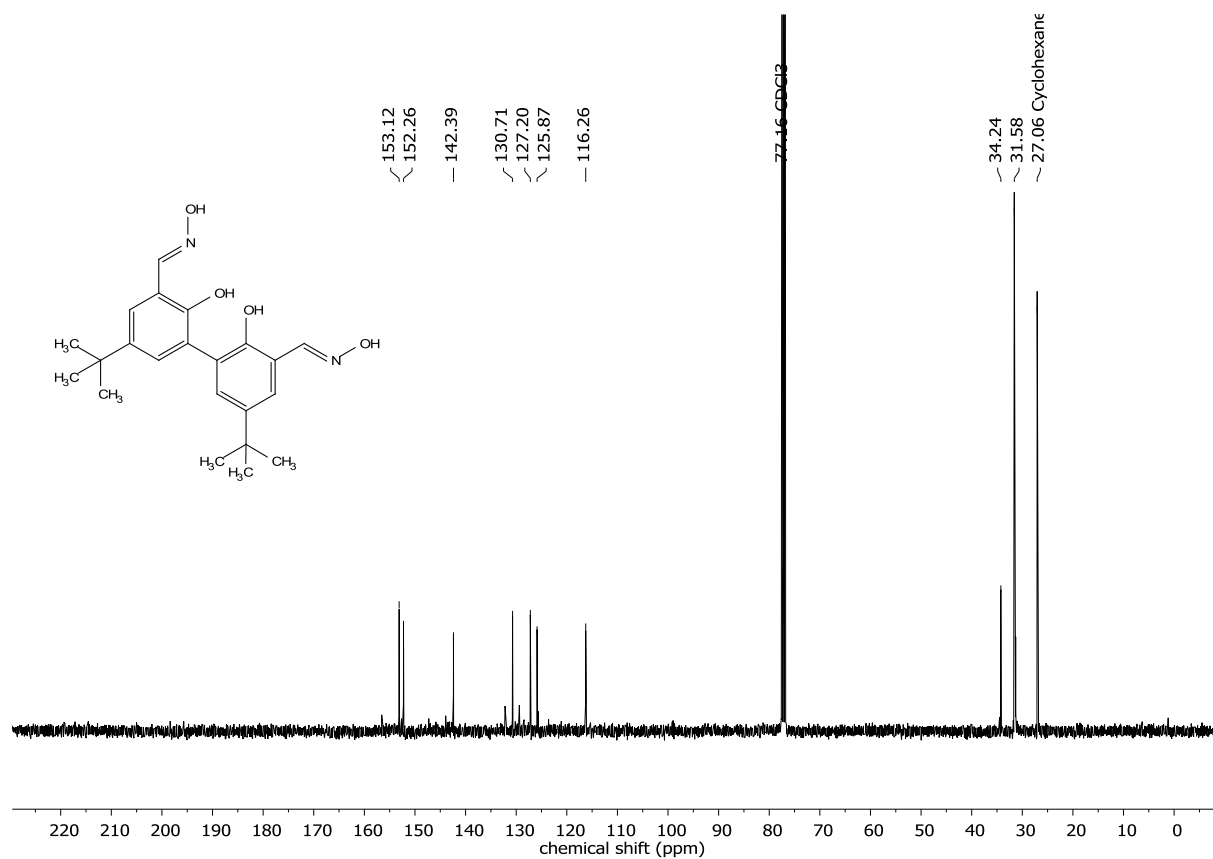
¹H NMR of 3,3'-Dicyano-5,5'-di(2,2-dimethylethyl)-2,2'-biphenol (8).



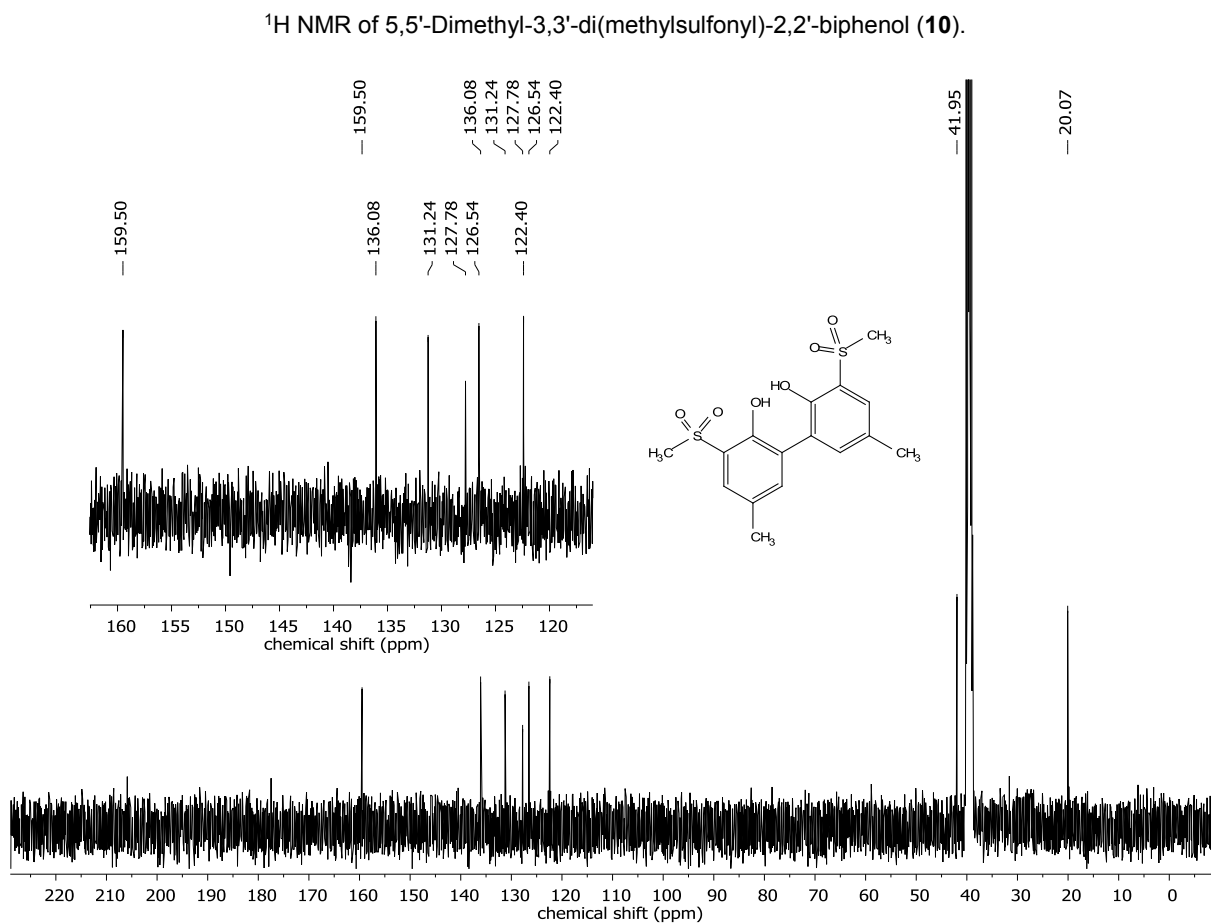
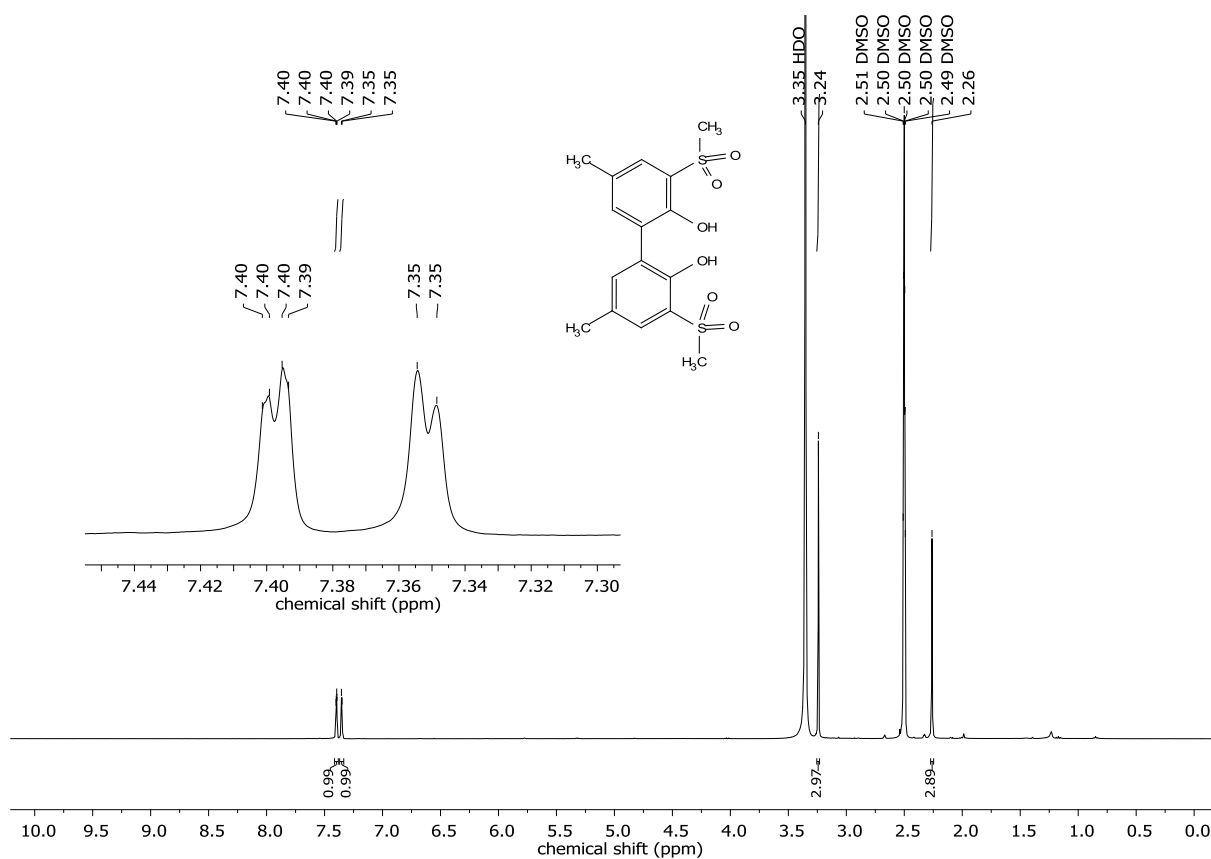
¹³C NMR of 3,3'-Dicyano-5,5'-di(2,2-dimethylethyl)-2,2'-biphenol (8).

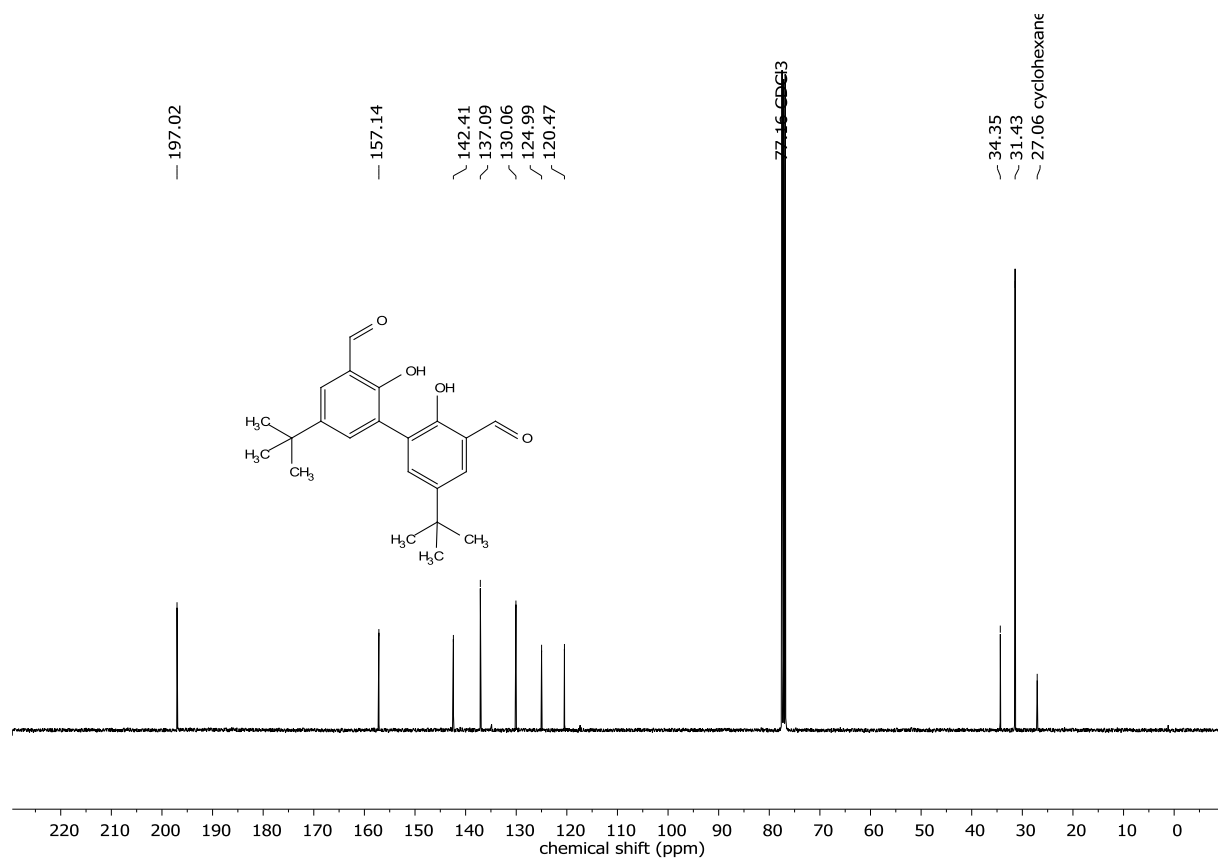
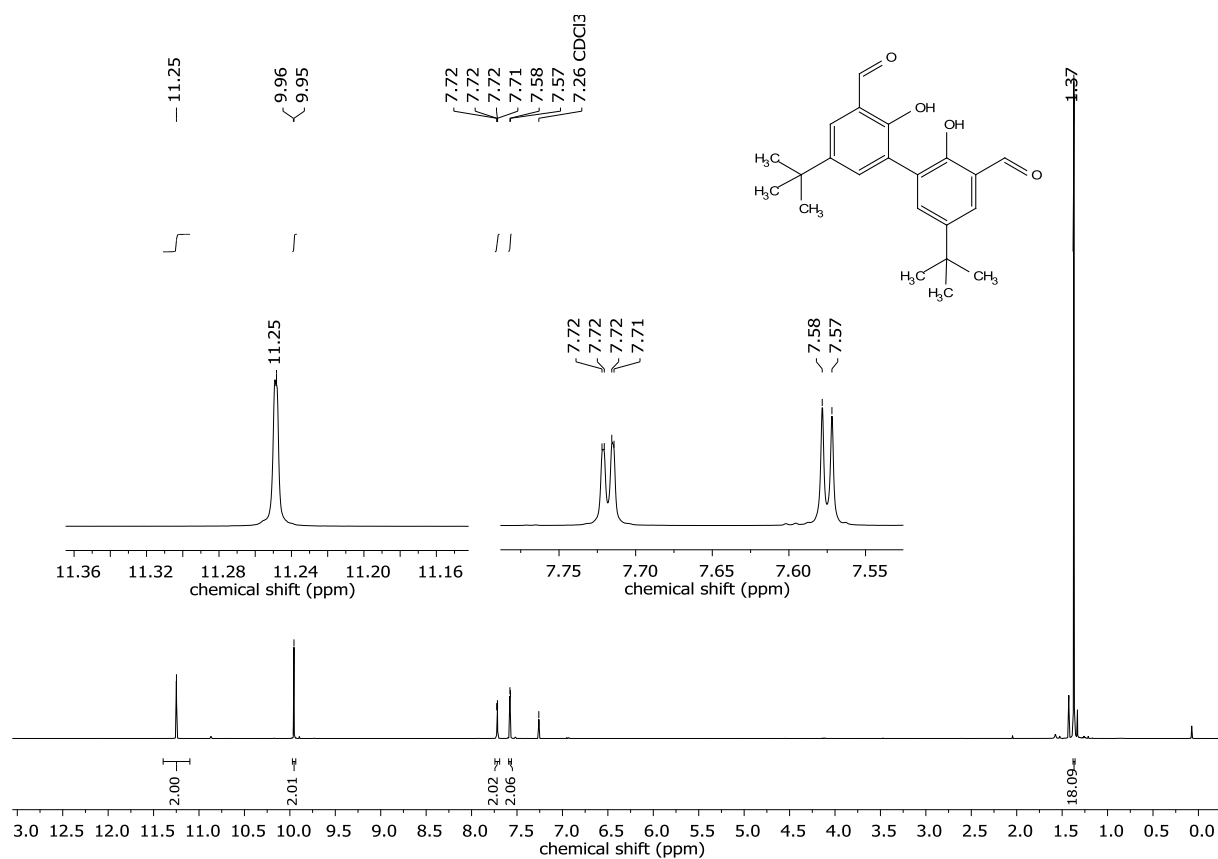


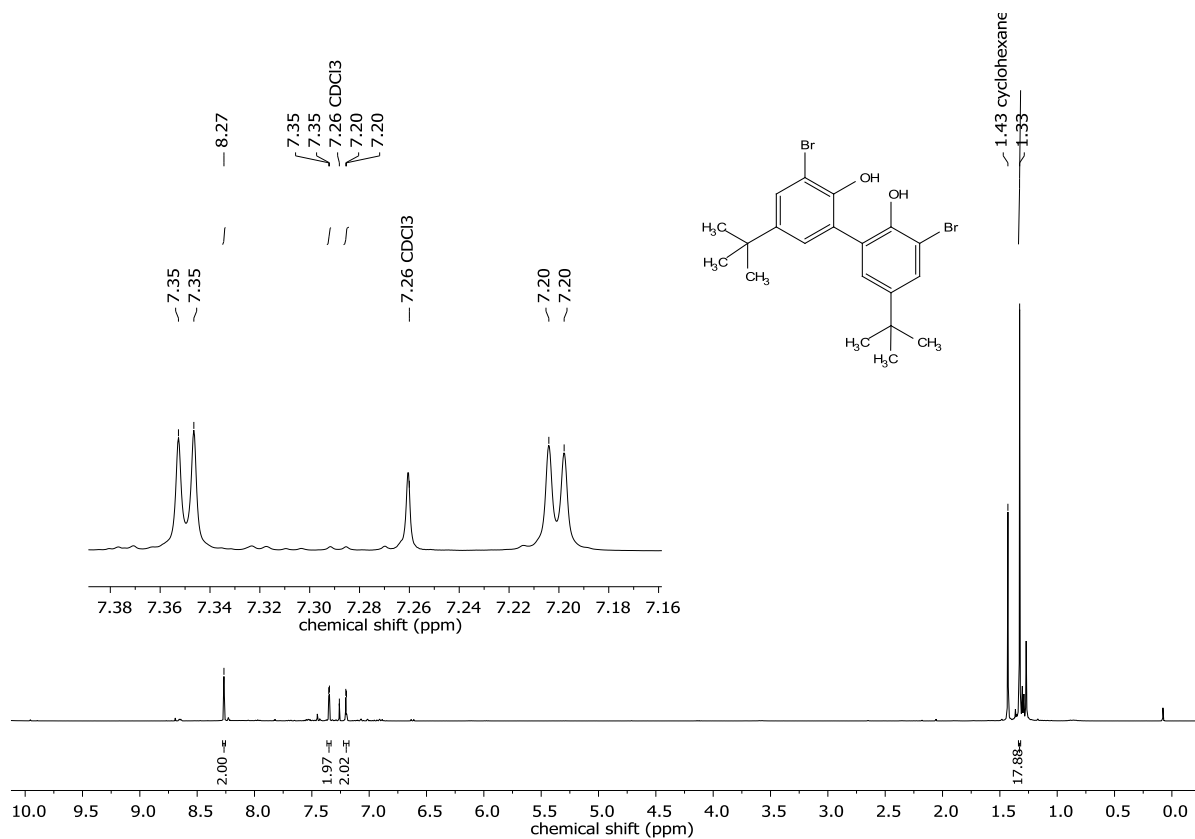
¹H NMR of 3,3'-Dicarboxime-5,5'-di(2,2-dimethylethyl)-2,2'-biphenol (9).



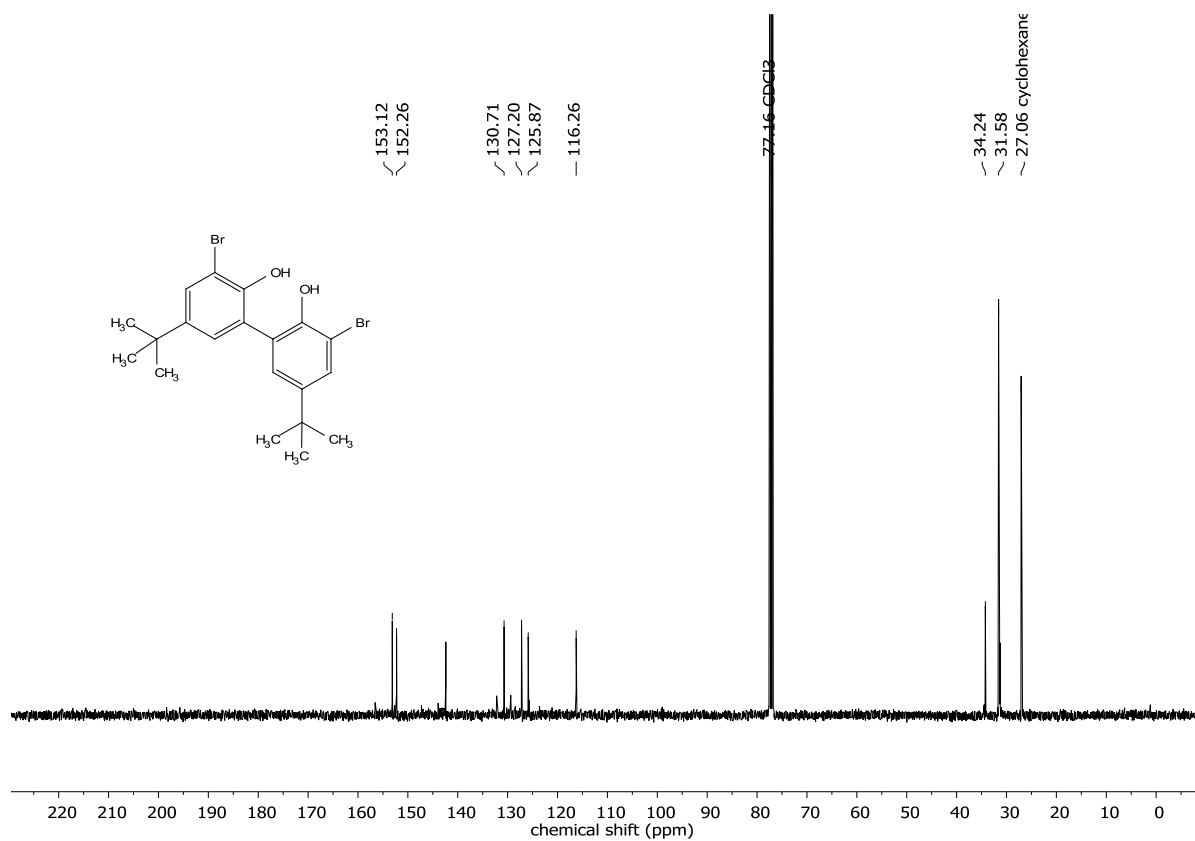
¹³C NMR of 3,3'-Dicarboxime-5,5'-di(2,2-dimethylethyl)-2,2'-biphenol (9).



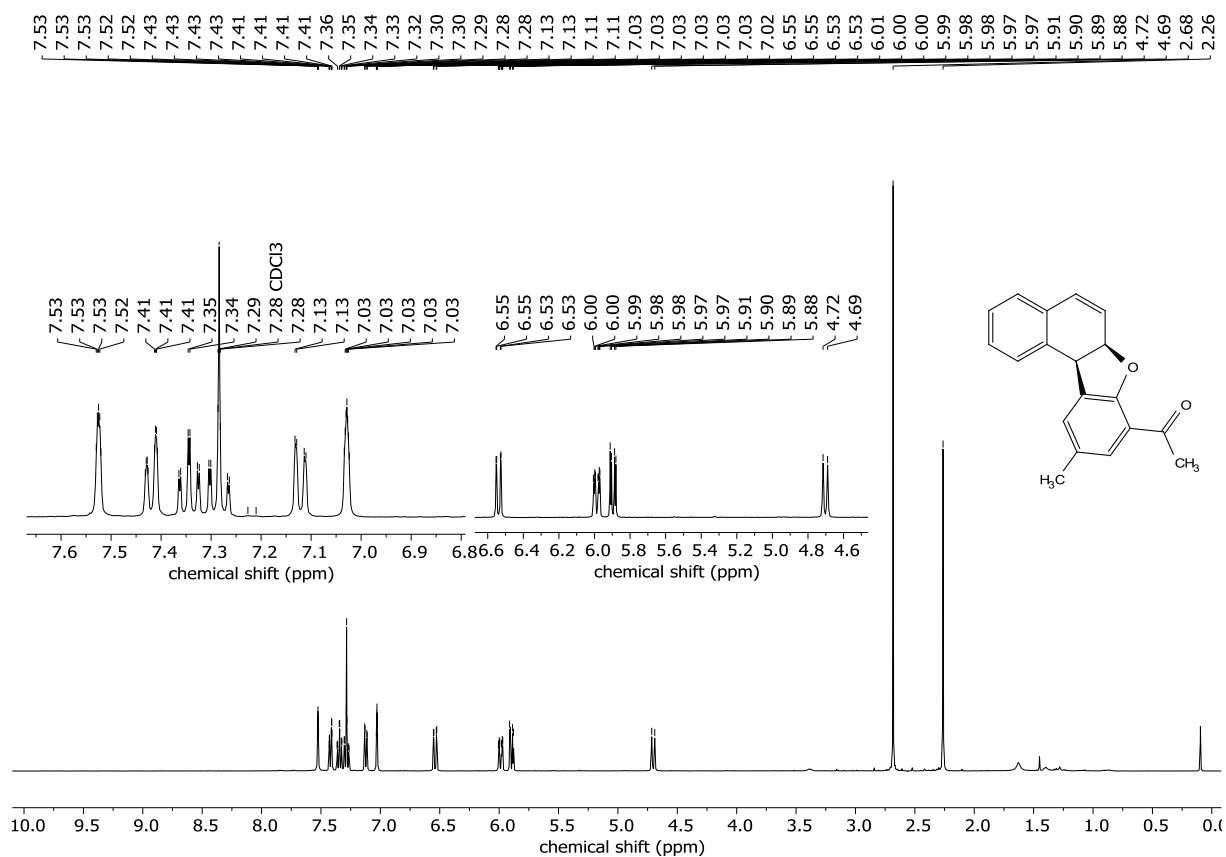




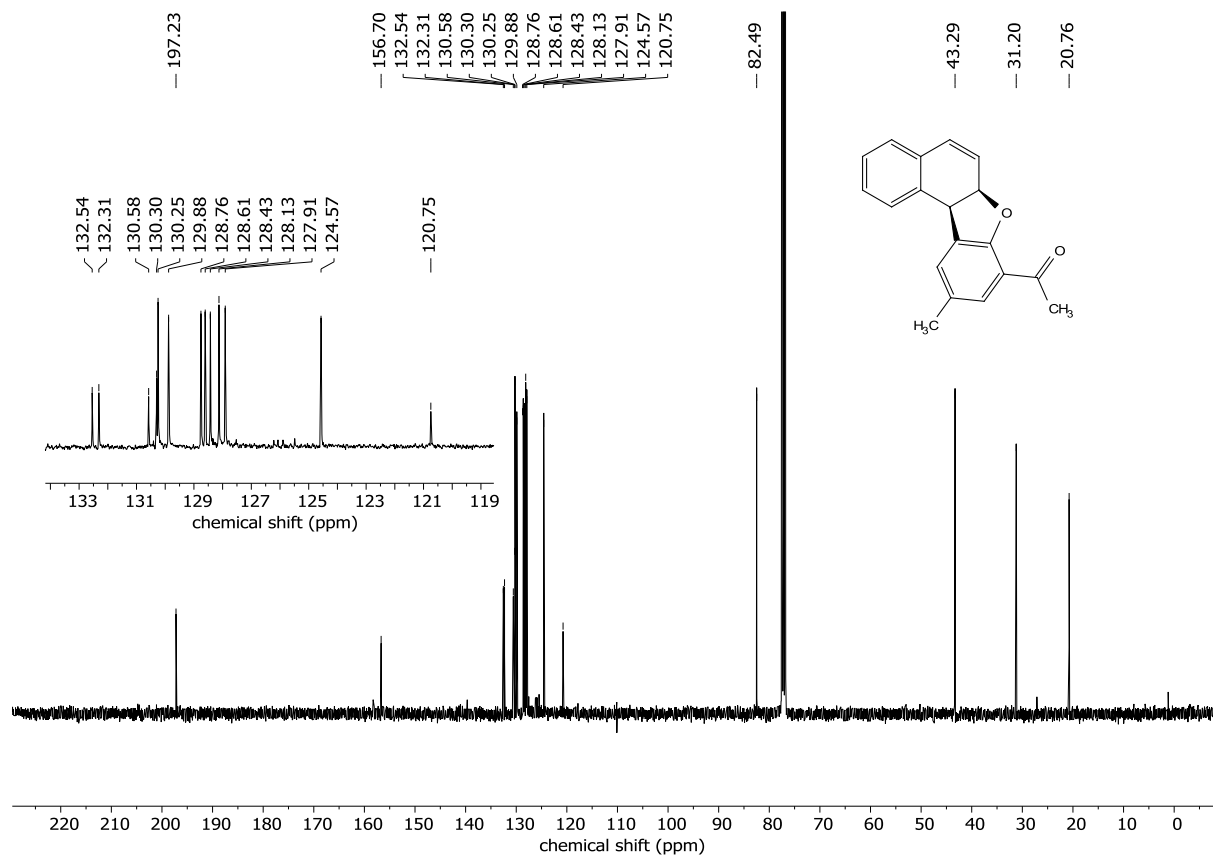
¹H NMR of 3,3'-Dibromo-5,5'-di(2,2-dimethylethyl)-2,2'-biphenol (12).



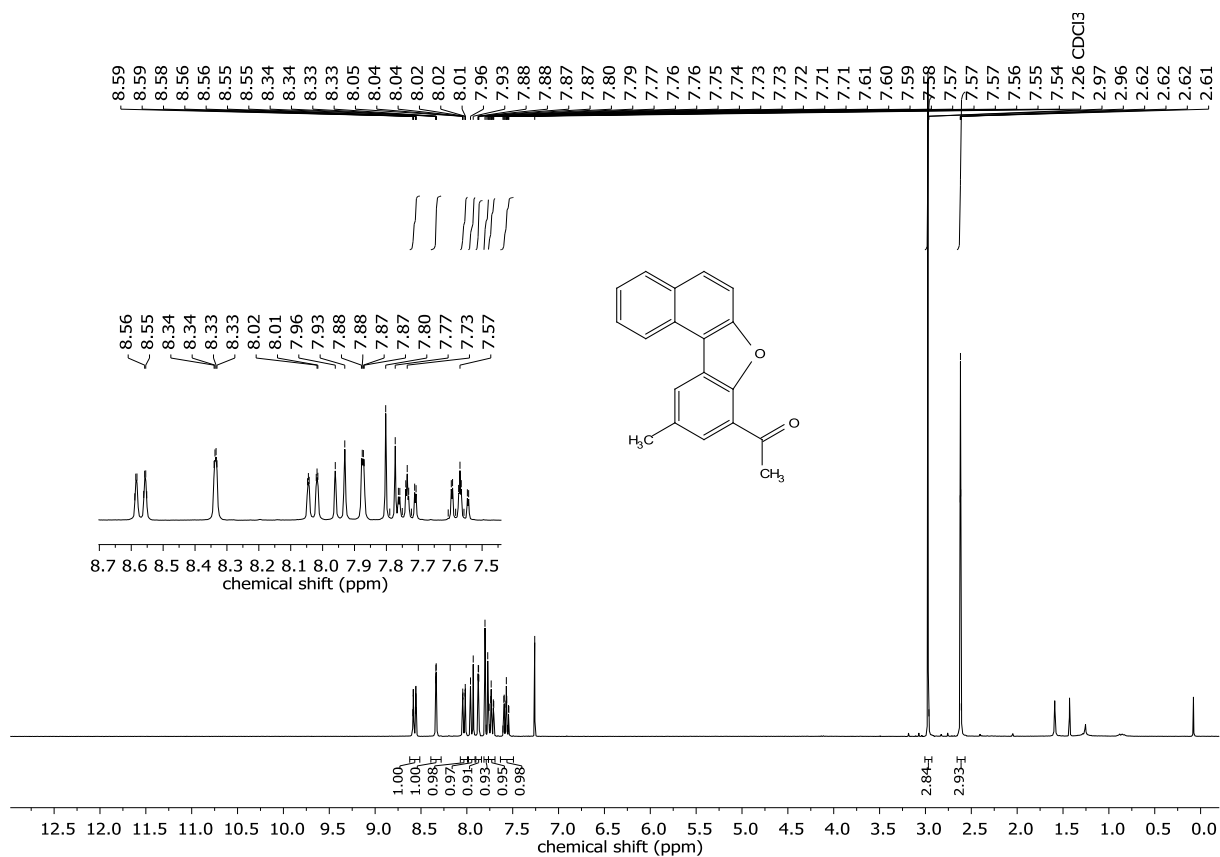
¹³C NMR of 3,3'-Dibromo-5,5'-di(2,2-dimethylethyl)-2,2'-biphenol (12).



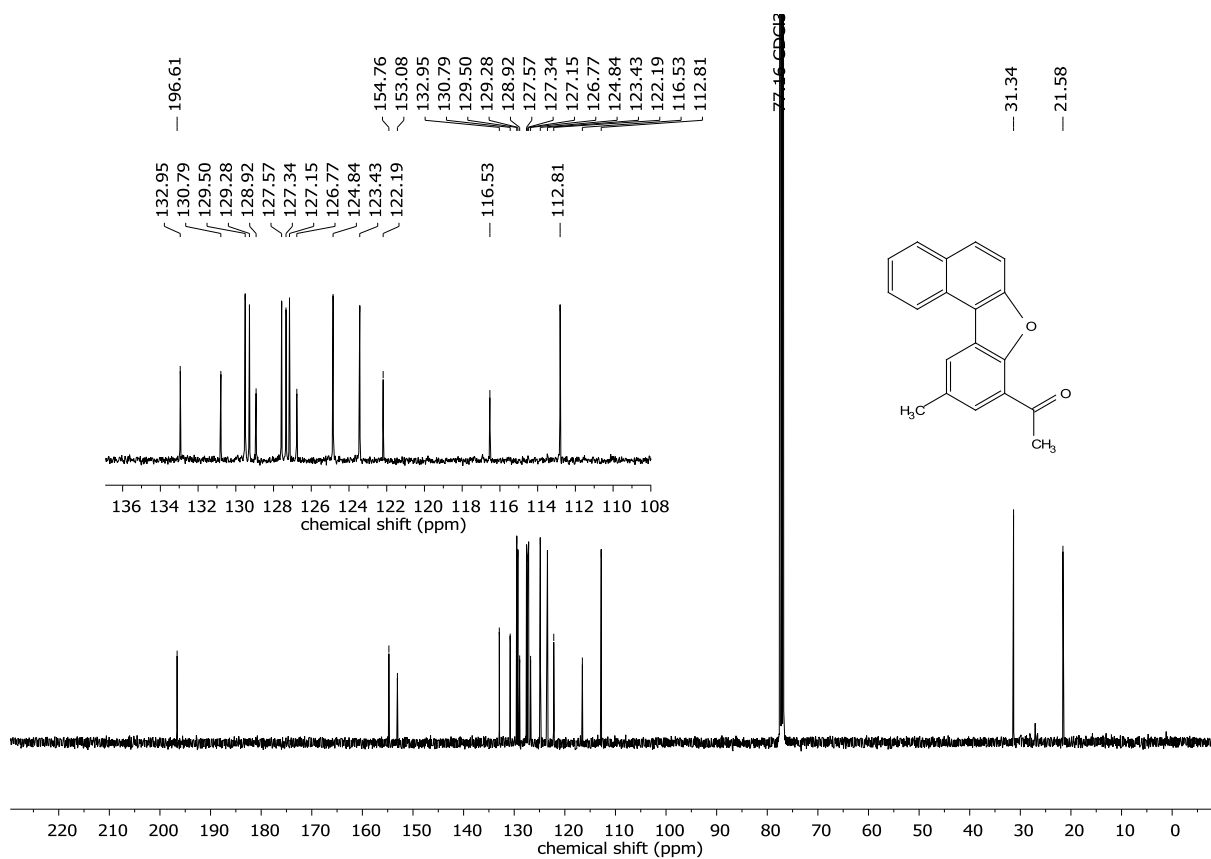
¹H NMR of *cis*-8-Acetyl-6a,11b-dihydro-10-methylnaphtho[2,1-b]benzo[d]furan (**14**).



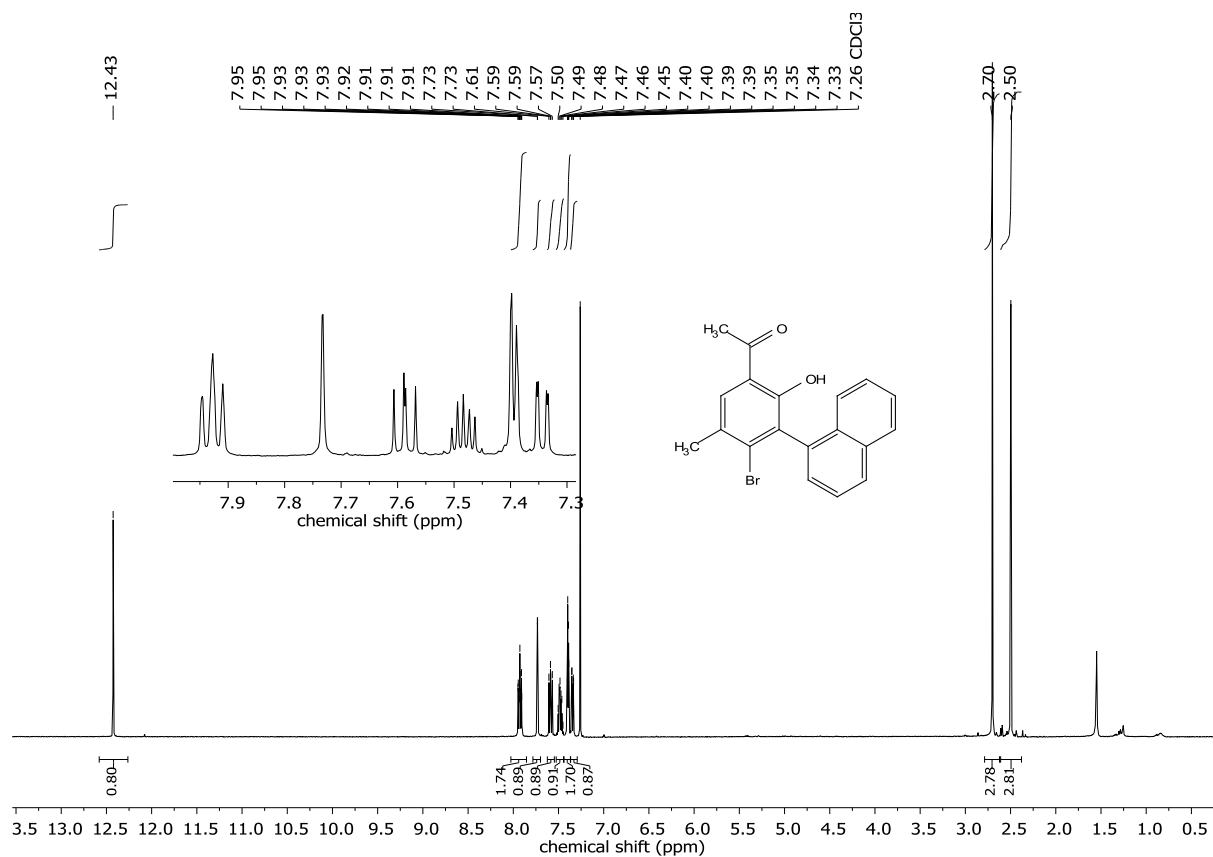
¹³C NMR of *cis*-8-Acetyl-6a,11b-dihydro-10-methylnaphtho[2,1-b]benzo[d]furan (**14**).



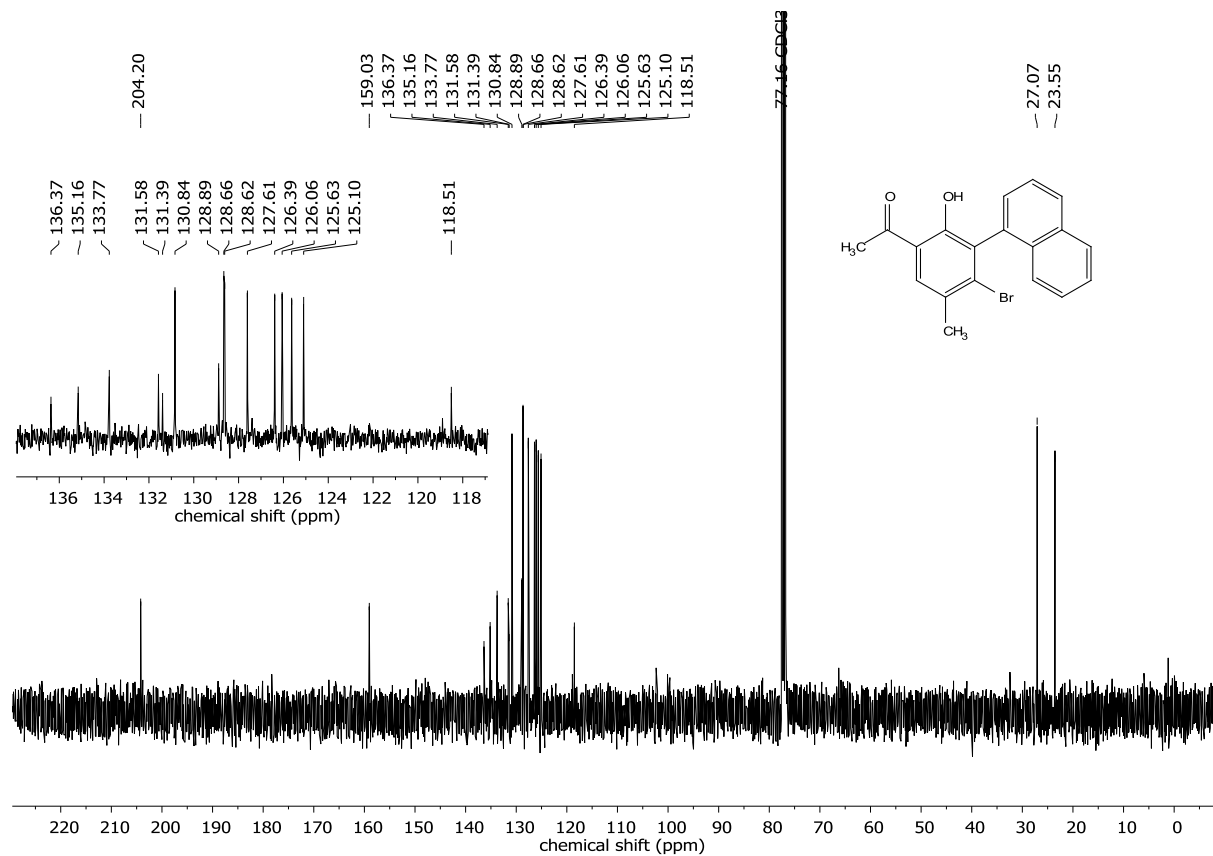
¹H NMR of 8-Acetyl-10-methylbenzo[2,1-*b*]dibenzo[*d*]furan (**15**).



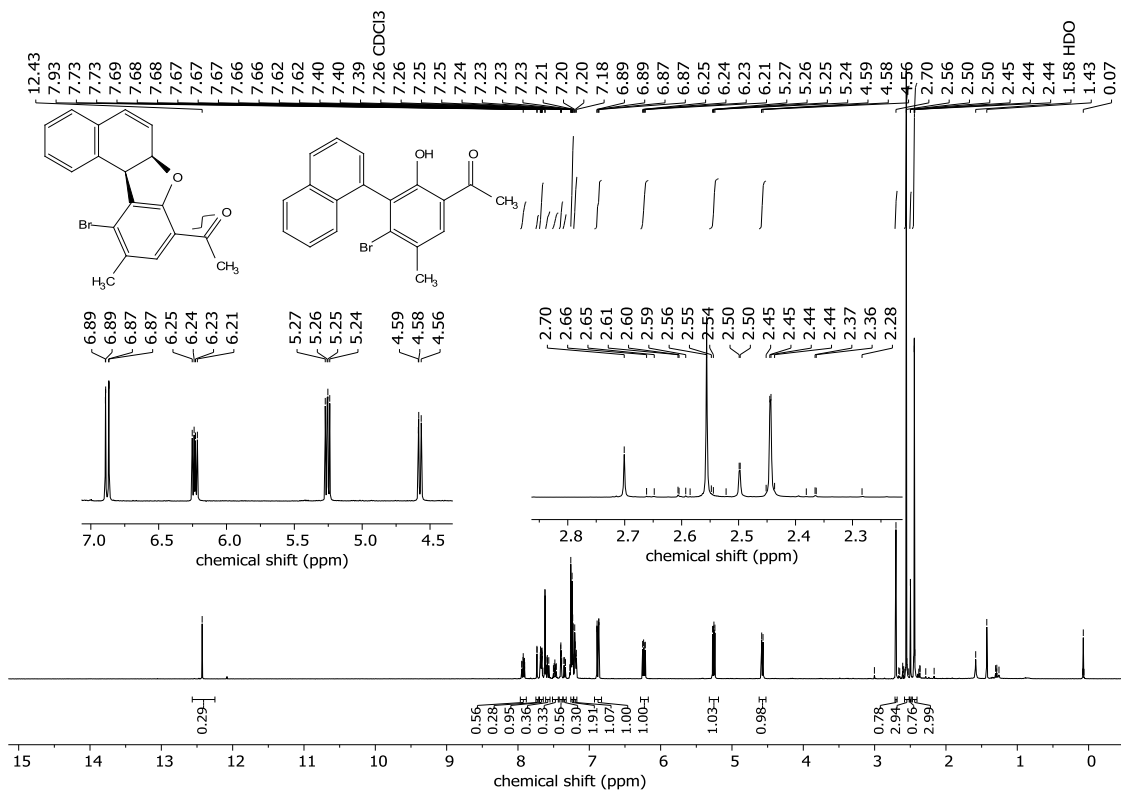
¹³C NMR of 8-Acetyl-10-methylbenzo[2,1-*b*]dibenzo[*d*]furan (**15**).



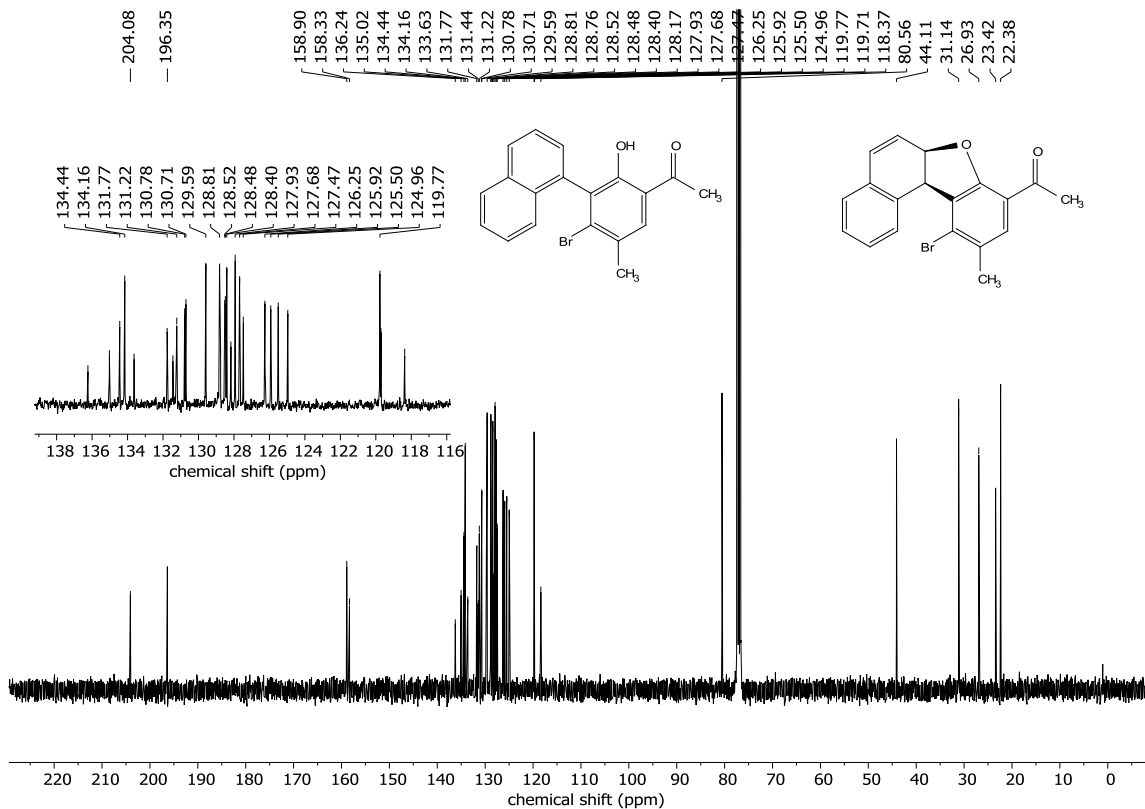
¹H NMR of 2-Acetyl-5-bromo-4-methyl-6-(naphthalen-1-yl)phenol (16).



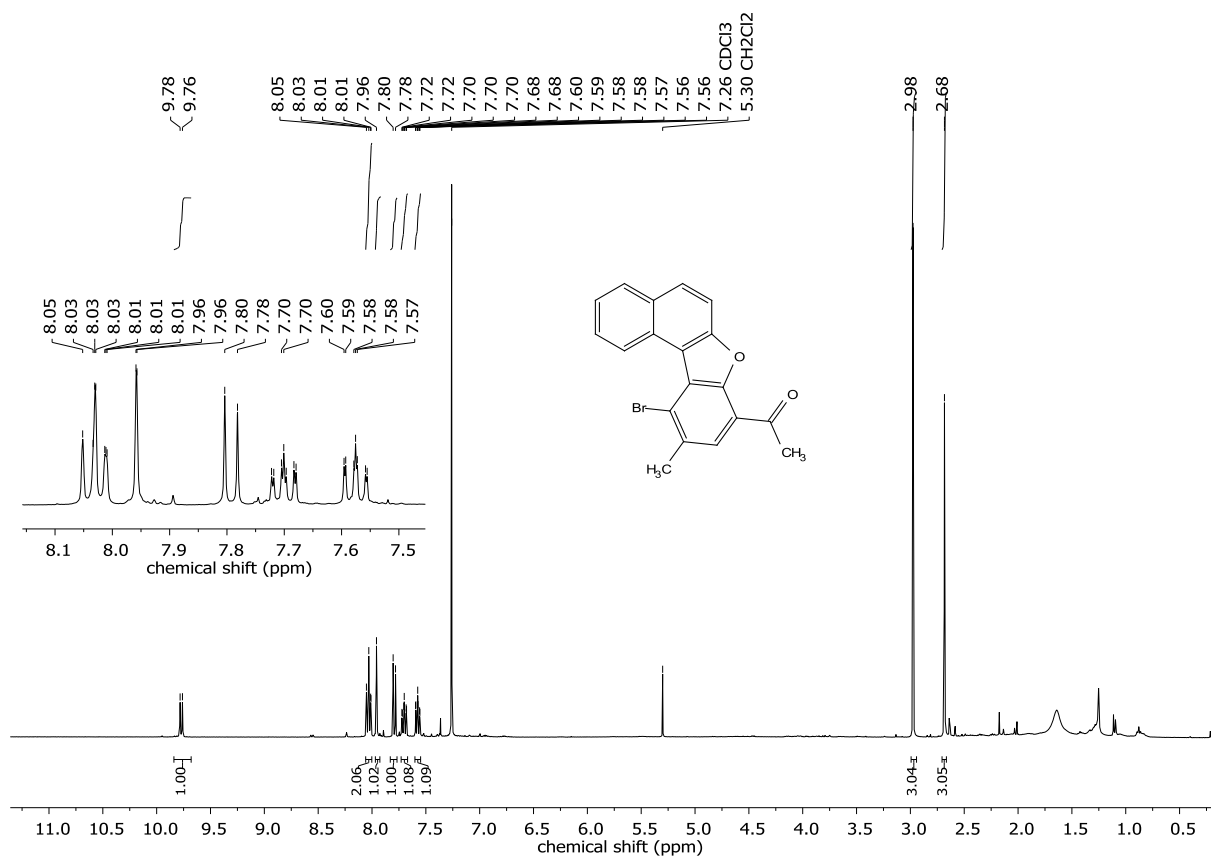
¹³C NMR of 2-Acetyl-5-bromo-4-methyl-6-(naphthalen-1-yl)phenol (16).



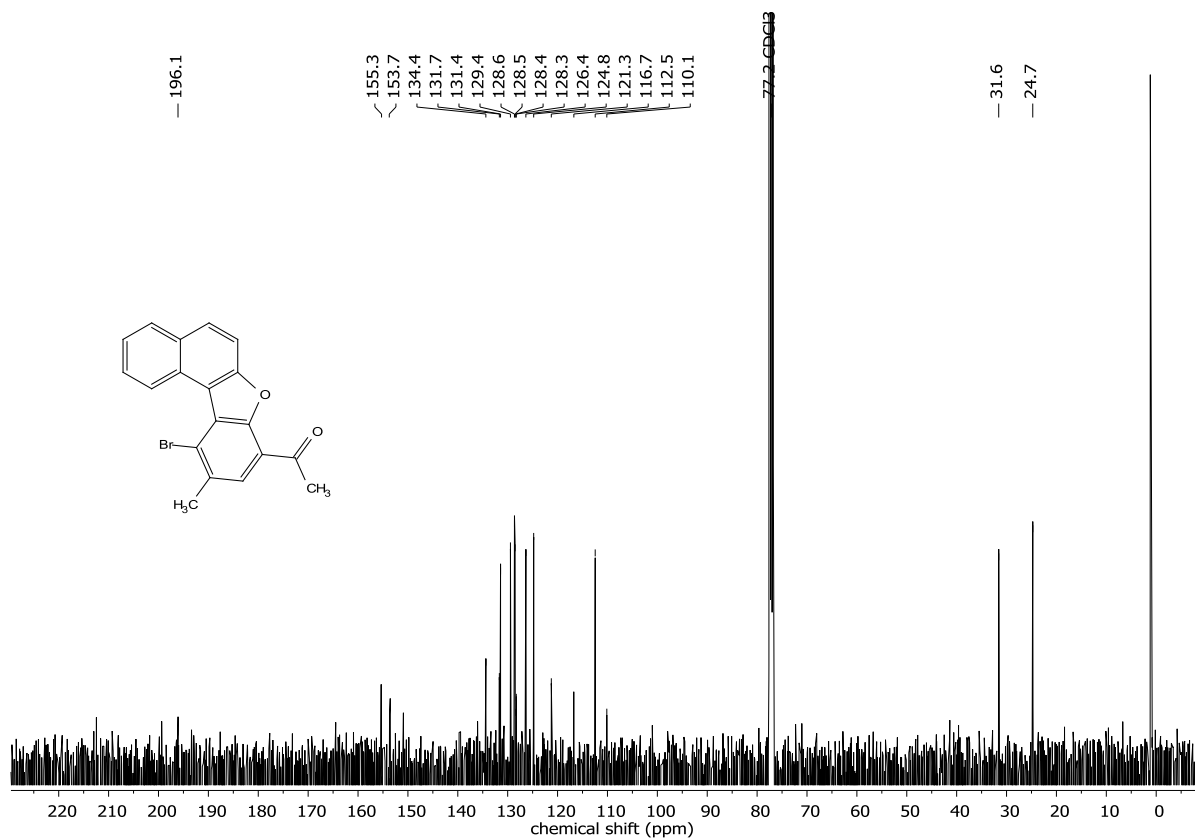
¹H NMR of 2-Acetyl-5-bromo-4-methyl-6-(naphthalen-1-yl)phenol (**16**) and *cis*-8-Acetyl-11-bromo-6a,11b-dihydro-10-methylnaphtho[2,1-*b*]benzo[*d*]furan (**17**) (mixture; ratio 1:3).



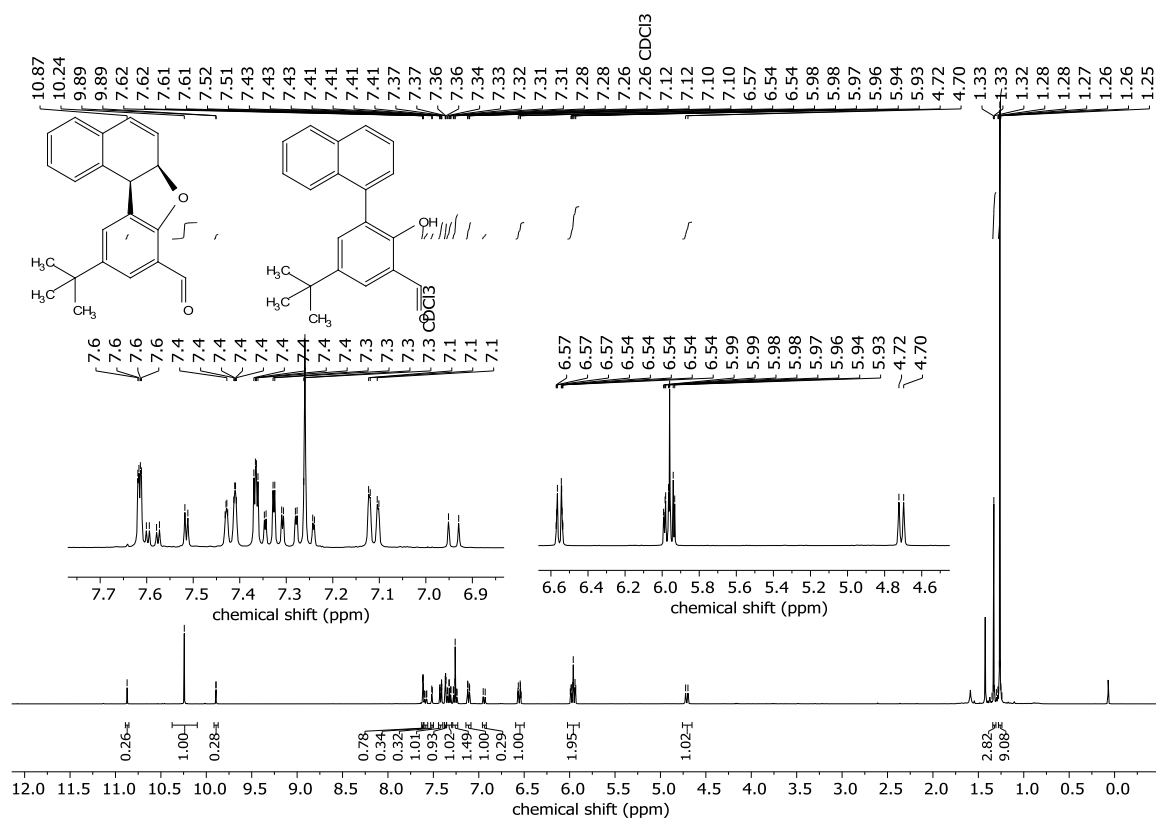
¹³C NMR of 2-Acetyl-5-bromo-4-methyl-6-(naphthalen-1-yl)phenol (**16**) and *cis*-8-Acetyl-11-bromo-6a,11b-dihydro-10-methylnaphtho[2,1-*b*]benzo[*d*]furan (**17**) (mixture; ratio 1:3).



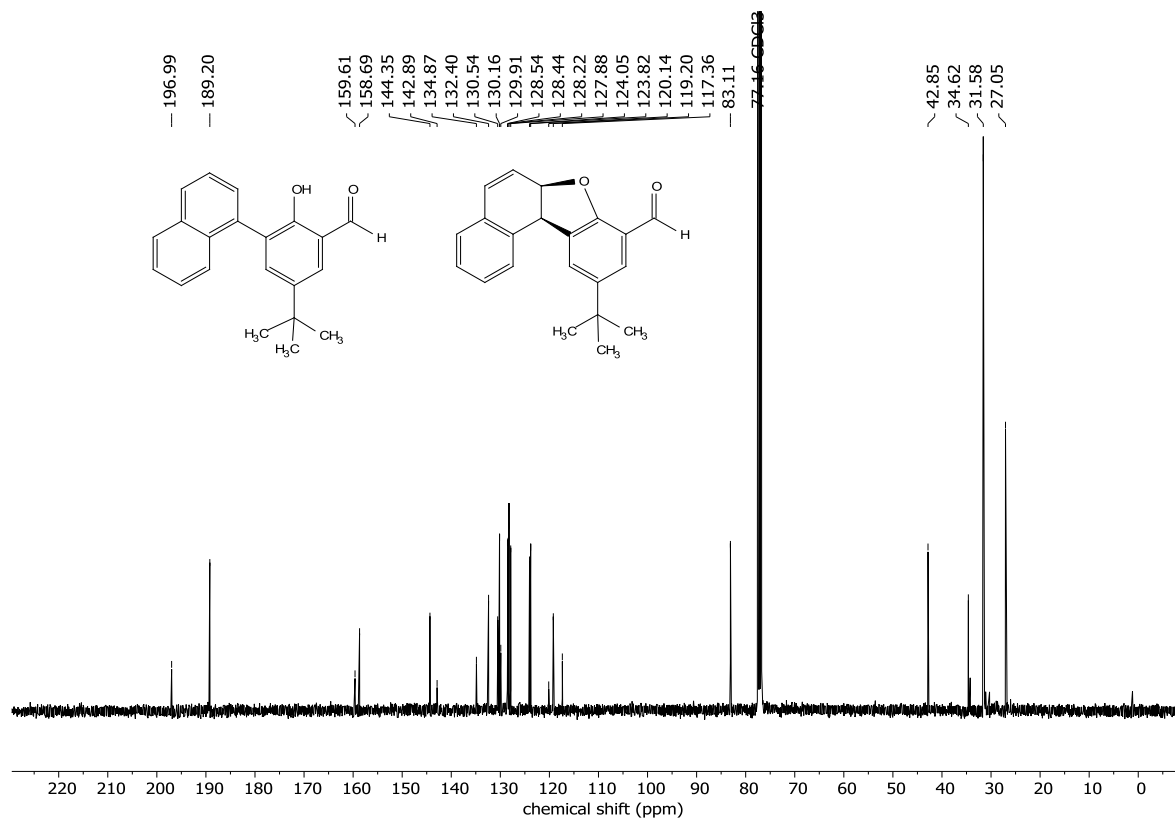
¹H NMR of 8-Acetyl-11-bromo-10-methylnaphtho[2,1-b]dibenzo[d]furan (18).



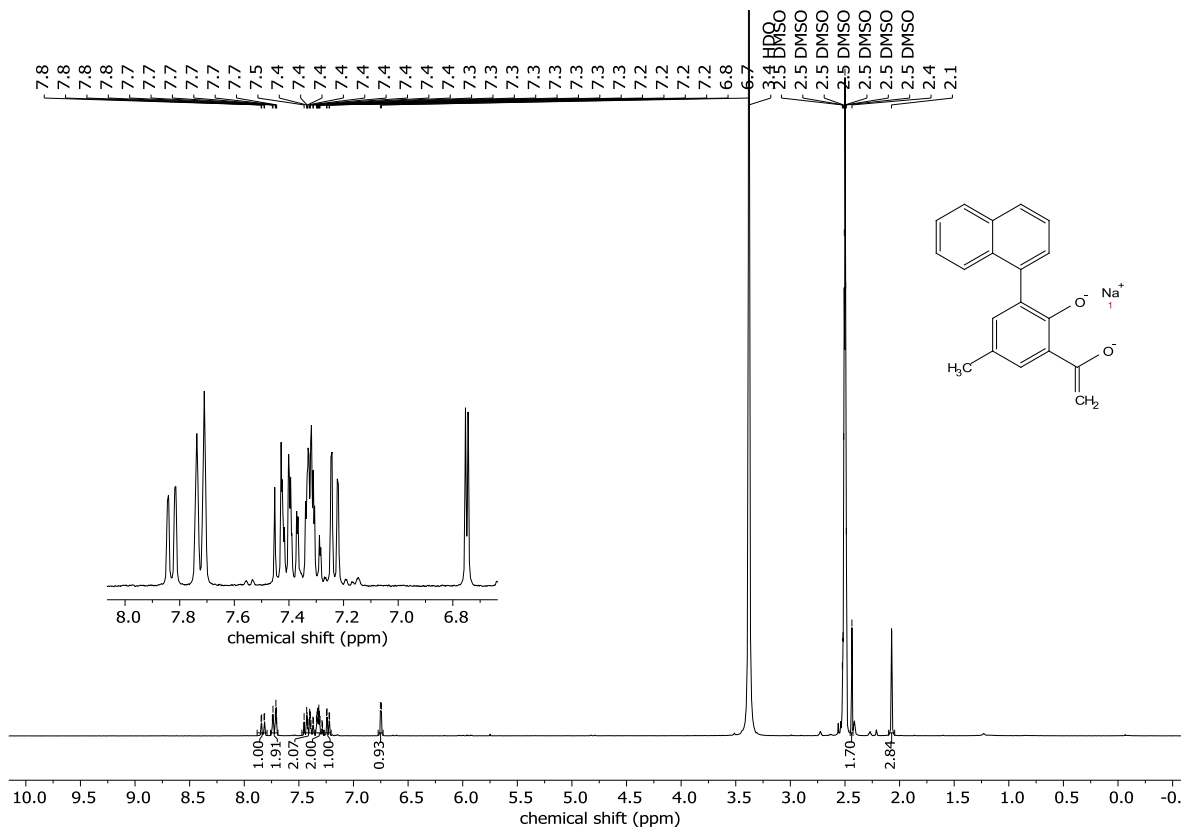
¹³C NMR of 8-Acetyl-11-bromo-10-methylnaphtho[2,1-b]dibenzo[d]furan (18).



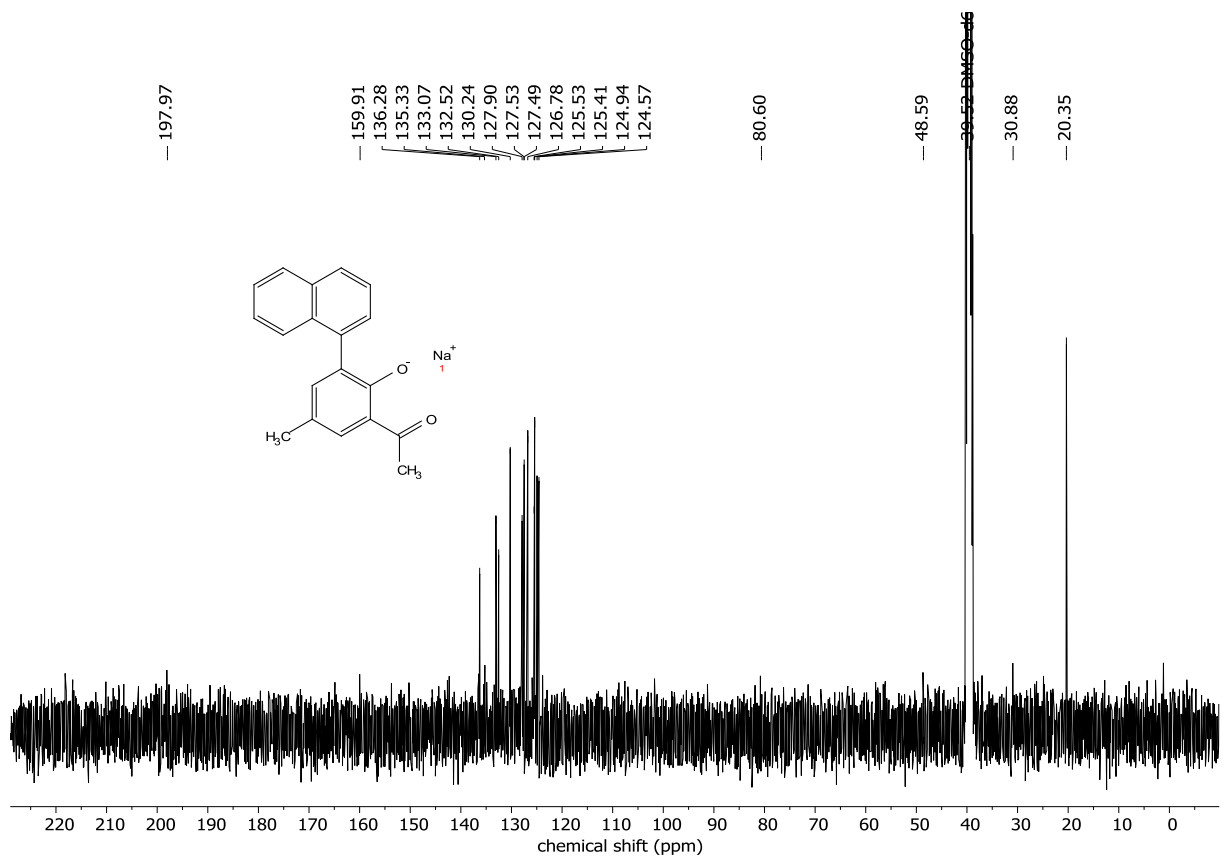
¹H NMR *cis*-8-Formyl-10-methyl-6a,11b-dihydrobenzo[2,1-b]benzofuran and 5-(tert-butyl)-2-hydroxy-3-(naphthalen-1-yl)benzaldehyde mixture (ratio 1:3.3).



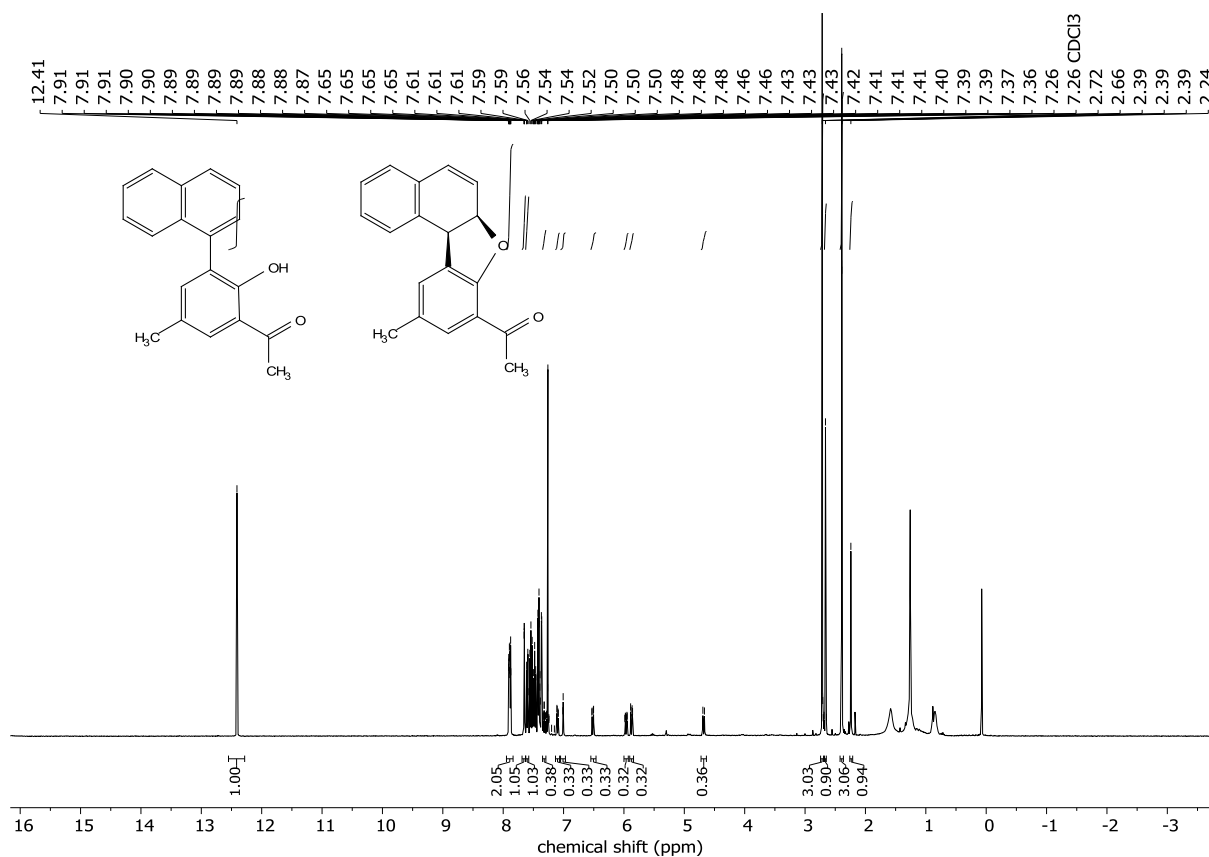
¹³C NMR *cis*-8-Formyl-6a,11b-dihydro-10-(2,2-dimethylethyl)naphtho[2,1-b]benzo[d]furan and 5-(tert-butyl)-2-hydroxy-3-(naphthalen-1-yl)benzaldehyde mixture (ratio 1:3.3).



¹H NMR of Sodium 2-acetyl-4-methyl-6-(naphthalen-1-yl)phenolate



¹³C NMR of Sodium 2-acetyl-4-methyl-6-(naphthalen-1-yl)phenolate.



^1H NMR Equilibrium of **13** and **14** after treatment with 1 M HCl.

References

- [1] W. L. F. Armarego, C. L. L. Chai, *Purification of laboratory chemicals*, Elsevier, Amsterdam, **2013**.
- [2] C. Gütz, B. Klöckner, S. R. Waldvogel, *Org. Process Res. Dev.* **2016**, *20*, 26–32.
- [3] A. Kirste, G. Schnakenburg, F. Stecker, A. Fischer, S. R. Waldvogel, *Angew. Chem. Int. Ed.* **2010**, *49*, 971–975; *Angew. Chem.* **2010**, *122*, 983–987. (see SI thereof).

A Decade of Electrochemical Dehydrogenative C,C-Coupling of Aryls

Published as part of the *Accounts of Chemical Research* special issue “*Electrifying Synthesis*”.

Johannes L. Röckl,^{‡,⊥} Dennis Pollok,^{†,⊥} Robert Franke,^{§,||} and Siegfried R. Waldvogel^{*,†,‡,⊥}

[†]Institute of Organic Chemistry, Johannes Gutenberg University Mainz, Duesbergweg 10-14, 55128 Mainz, Germany

[‡]Graduate School Materials Science in Mainz, Staudingerweg 9, 55128 Mainz, Germany

[§]Evonik Performance Materials GmbH, Paul-Baumann-Str. 1, 45772 Marl, Germany

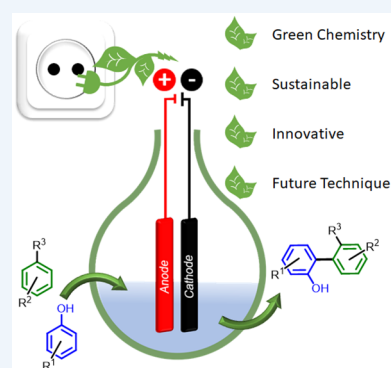
^{||}Lehrstuhl für Theoretische Chemie, Ruhr-Universität Bochum, Universitätsstraße 150, 44801 Bochum, Germany

CONSPECTUS: The importance of sustainable and green synthetic protocols for the synthesis of fine chemicals has rapidly increased during the last decades in an effort to reduce the use of fossil fuels and other finite resources. The replacement of common reagents by electricity provides a cost- and atom-efficient, environmentally friendly, and inherently safe access to novel synthetic routes. The selective formation of carbon–carbon bonds between two distinct substrates is a crucial tool in organic chemistry. This fundamental transformation enables access to a broad variety of complex molecular architectures. In particular, the aryl–aryl bond formation has high significance for the preparation of organic materials, drugs, and natural products. Besides well-known and well-established reductive- and oxidative-reagent-mediated or transition-metal-catalyzed coupling reactions, novel synthetic protocols have arisen, which require fewer steps than conventional synthetic approaches.

Electroorganic conversions can be categorized according to the nature of the electron transfer processes occurring. Direct transformations at inert electrode materials are environmentally benign and cost-effective, whereas catalytic processes at active electrodes and mediated electrosynthesis using an additional soluble reagent can have beneficial properties in terms of selectivity and reactivity. In general, these conversions require challenging optimization of the reaction parameters and the appropriate cell design. Galvanostatic reactions enable fast conversions with a rather simple setup, whereas potentiostatic electrolysis may enhance selectivity.

This Account discusses the development of seminal carbon–carbon bond formations over the past two decades, focusing on phenols leading to precursors for ligands in, e.g., hydroformylation reaction. A key element in the success of these electrochemical transformations is the application of electrochemically inert, non-nucleophilic, highly fluorinated alcohols such as 1,1,1,3,3,3-hexafluoro-2-propanol (HFIP), which exhibit a large potential window for transformations and enable selective cross-coupling reactions. This selectivity is based on the capability of HFIP to stabilize organic radicals. Inert, carbon-based and metal-free electrode materials like graphite or boron-doped diamond (BDD) open up novel electroorganic pathways. Furthermore, novel active electrode materials have been developed to enable intra- and intermolecular dehydrogenative coupling reactions of electron-rich aryls.

The application of 2,2'-biphenol derivatives as ligand components for catalysts requires reactions to be carried out on larger scale. In order to achieve this, continuous flow transformations have been established to overcome the drawbacks of heat transfer, overconversion, and conductivity. Modular cell designs enable the transfer of a broad variety of electroorganic conversions into continuous processes. Recent results demonstrate the application of organic electrochemistry to natural product synthesis of the pharmaceutically relevant opiate alkaloids (–)-thebaine or (–)-oxycodone.



INTRODUCTION

Electroorganic Synthesis

Over the past decades, the tremendous increase of global energy consumption has become a major topic in political and social discussions.¹ The limited supply of fossil resources will also have significant influence on the organic synthesis of chemicals. Current research is focused not only on efficient reactions and processes, but also on sustainable synthetic approaches with a minor ecological footprint. A strict cutback in carbon dioxide emissions and waste generation can be achieved with sustainable synthetic approaches.^{2–4} In this context, electroorganic syn-

thesis has emerged as an innovative approach which is experiencing a renaissance after being overlooked by the organic synthetic community for several decades.^{5–9} Electric current can be used to induce reduction and oxidation reactions, which are superior to conventional chemical oxidizing or reducing agents from an economic and environmental perspective. The opportunity to use inexpensive and readily accessible electrical current from renewable resources as an inherently safe reagent enhances the sustainability aspect of electroorganic synthesis and

Received: September 29, 2019

Published: December 18, 2019

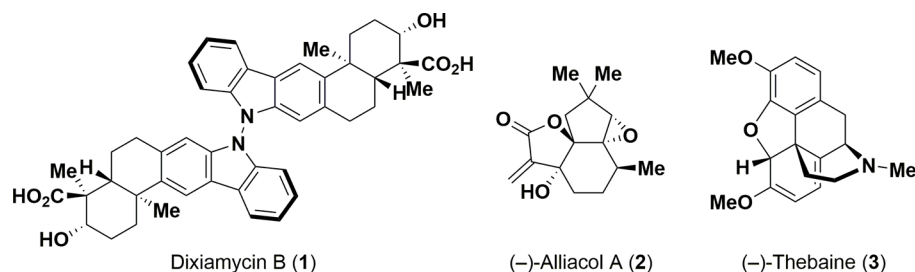


Figure 1. Natural products synthesized using electrochemical key steps.

Scheme 1. Electrolysis Parameters and Mode of Operations for Electrodes in Electroorganic Synthesis

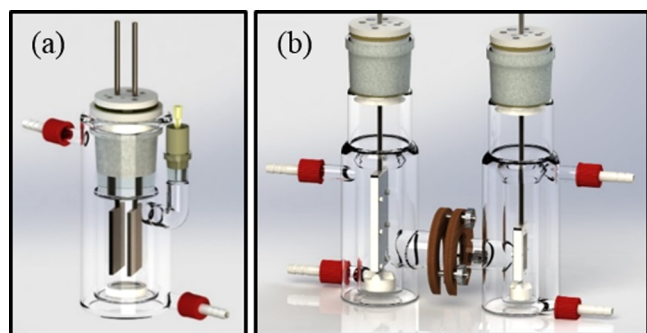
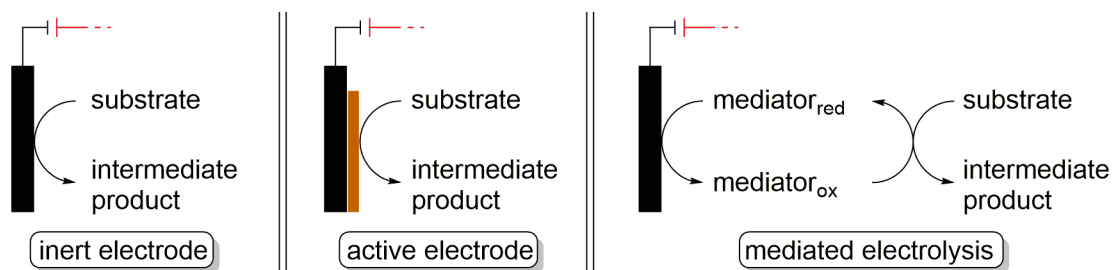
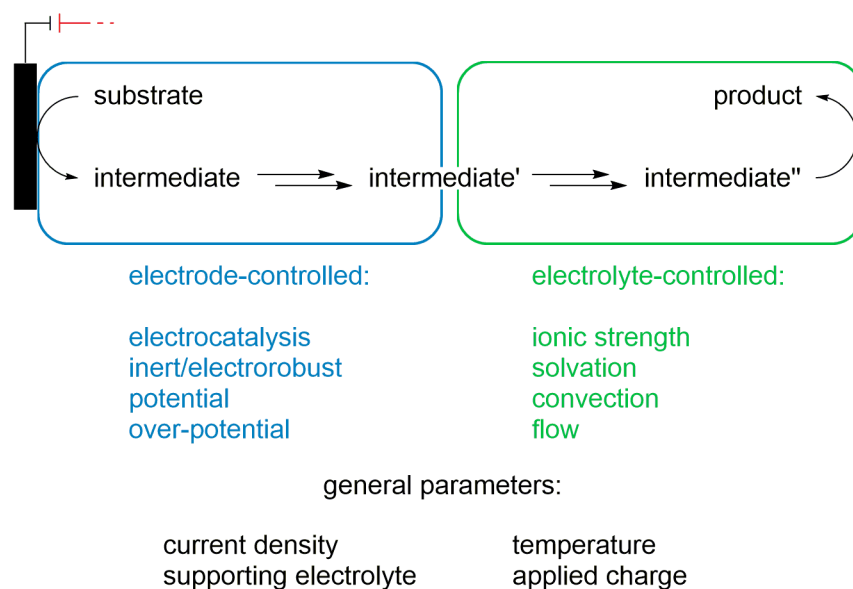


Figure 2. Choice of cell design for electroorganic synthesis: Undivided (a) and divided (b) beaker-type cell. Reproduced with permission from ref 9. Copyright 2018 American Chemical Society.

enables otherwise challenging reactions with few steps compared to traditional approaches. This leads to atom-

economic transformations with a minimum of reagent waste produced if durable and nonsacrificial electrode materials are used.¹⁰ Research has demonstrated the robustness of electrochemical reactions, which demonstrate outstanding performance across a broad range of current densities. These high current densities enable short reaction times without significantly reducing the yield compared to other synthetic routes.¹¹ Relevant progress has been achieved in the field of electroorganic synthesis in the past decades with the synthesis of complex organic molecules including natural products,¹² as well as the development of organocatalysis and flow electrochemistry.^{13,14} Examples include the synthesis of dixiamycin B (1) via N,N' -dehydrodimerization,¹⁵ (-)-alliacol A (2) via anodic cyclization,¹⁶ and (-)-thebaine (3) via anodic coupling (Figure 1).¹⁷ A comprehensive review on developments in electroorganic synthesis since the year 2000 has been recently provided by Baran et al.⁶

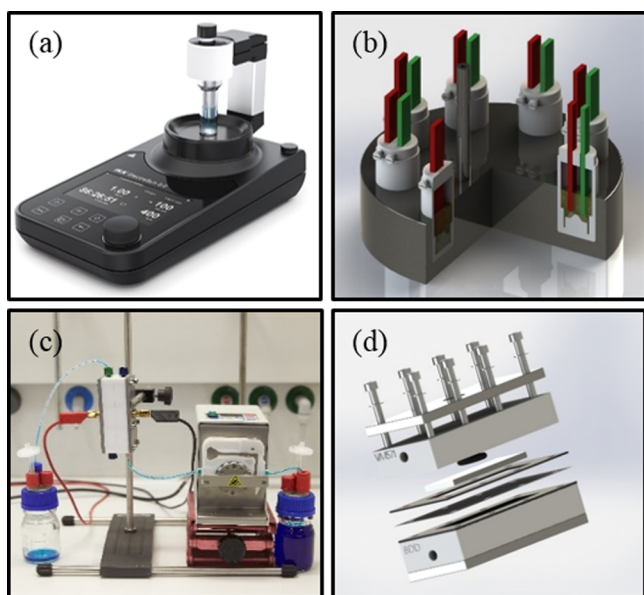


Figure 3. (a) ElectraSyn. Reproduced with permission from ref 29. Copyright 2019 IKA-Werke GmbH & CO. KG. (b) Setup for electrochemical screening experiments. Reproduced with permission from ref 30. Copyright 2016 American Chemical Society. (c) Setup for continuous flow electrolysis with (d) enlarged view drawing developed in the Waldvogel lab and commercialized by IKA. Reproduced with permission from ref 14. Copyright 2017 American Chemical Society.

The general concept of electrosynthesis is based on single electron transfers at the interface between a solid electrode material and a substrate (cathodic reduction) dissolved in the ion conductive reaction mixture (electrolyte), or from a substrate to the electrode (anodic oxidation). In comparison to conventional organic synthesis, the reaction setup offers a large variety of reaction parameters which need optimization

prior to establishing a new synthetic method. These parameters differ in their impact on different intermediates. Besides parameters which are in direct correlation with the electrode surface, further diffusion of the intermediates into the electrolyte system depends on parameters such as the ionic strength or solvation (Scheme 1). General parameters include the current density, applied charge, temperature, and addition of supporting electrolytes.⁸ The electrodes differ in their ability to work as inert or active electrodes according to their material characteristics (Scheme 1).¹⁸ The simplest way is the use of inert electrodes, which are only involved in the electron transfer and the selectivity is proportional to the electrode potential. Common inert electrodes are platinum or carbon-based materials like graphite, glassy carbon, or boron-doped diamond (BDD). Of particular interest is boron-doped diamond which has strong σ -bonds between sp^3 -hybridized atoms, resulting in the highest (electro)chemical robustness. Additionally, BDD is self-cleaning, enables very clean electron transfers, and can even be considered as sustainable, because it can be produced from methane.^{19–23} These properties make BDD particularly applicable to electroorganic synthesis as a metal-free electrode material.^{24–26} This is highly favorable in the synthesis of pharmaceutically active compounds as it allows the prevention of heavy metal contamination. A second approach uses an active electrode material which generates a nonsoluble electrocatalytic active species.²⁷ This layer represents an immobilized redox mediator which is formed and regenerated in situ. This electrocatalyst enables electroorganic conversions, being less dependent on the applied potential since it serves as redox filter. Further approaches use a soluble active mediator which converts the substrate and is electrochemically regenerated. This can be thought of as the electrochemical regeneration of common chemical reagents. An adaption of the conventional one-pot electrolysis for sensitive substrates, whereby all components are present at the time of electrolysis (in-cell) is demonstrated in the

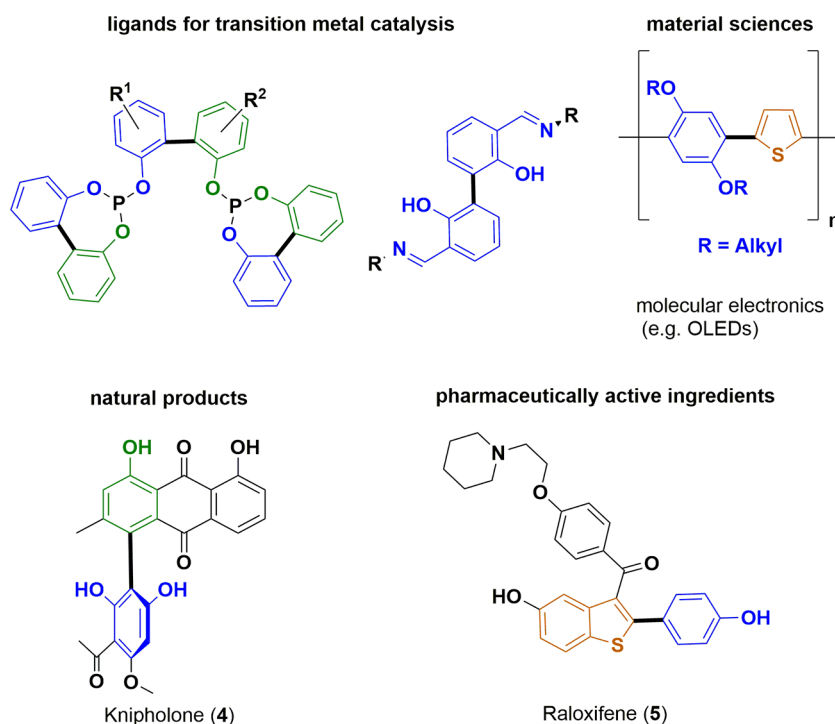
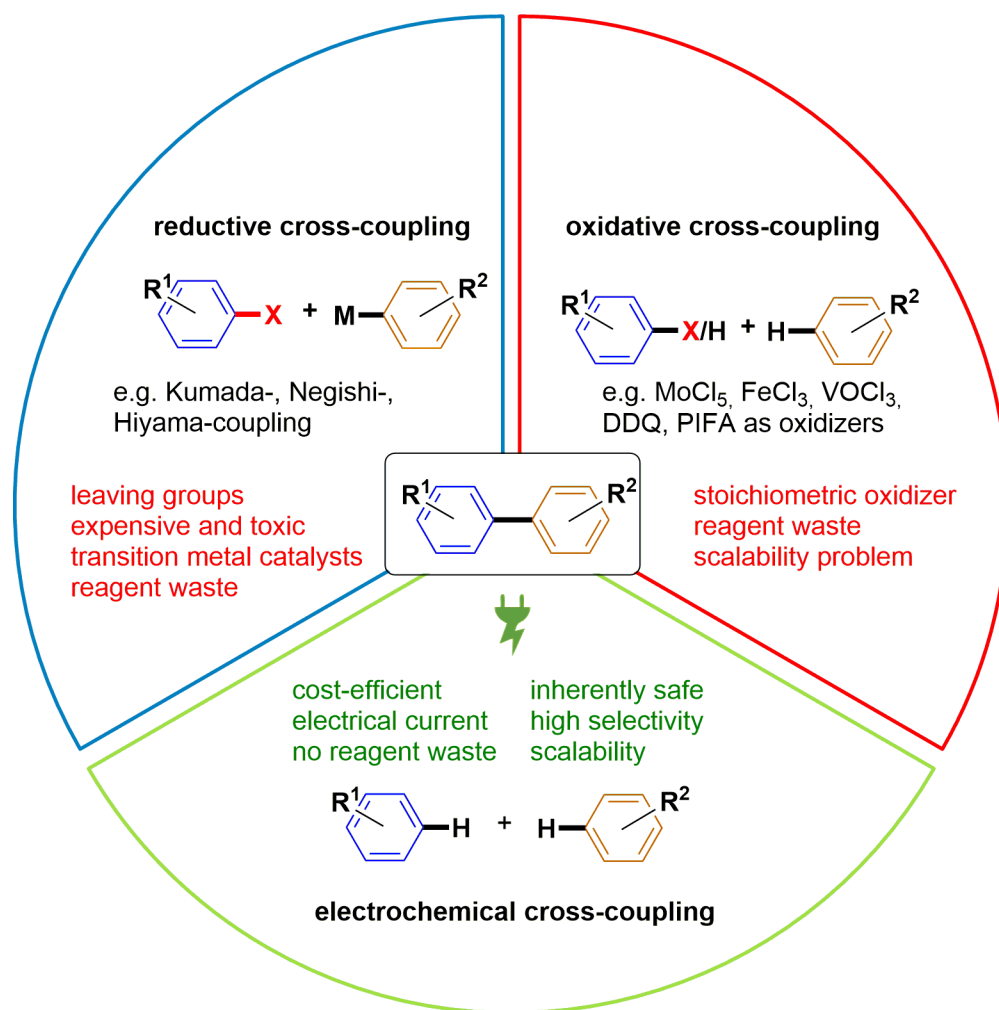
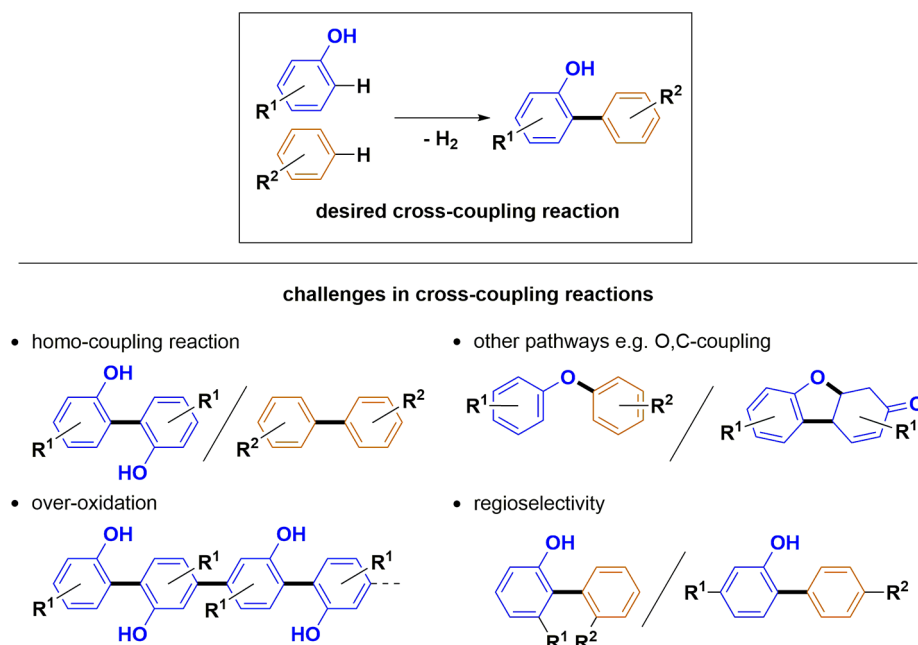


Figure 4. Biaryl structures in catalysts, natural products, pharmaceutically active compounds, and materials science.

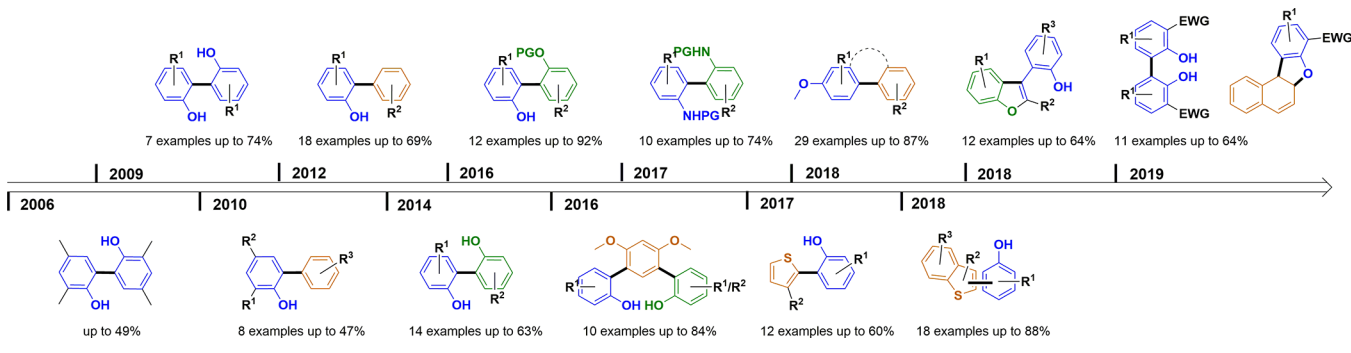
Scheme 2. Different Approaches for Aryl–Aryl Cross-Coupling toward Biaryls



Scheme 3. Challenges in Oxidative Cross-Coupling Reactions of Aryls



Scheme 4. Research on Anodic Dehydrogenative C,C-Coupling in the Waldvogel lab over More than the Past Decade



stepwise reaction. A reagent is converted into an active species electrochemically and after complete electrolysis the substrate is added to the active reagent which has already been synthesized (ex-cell).²⁸ Despite the unique reactivity and avoidance of large overpotentials, the necessity of additional reagents is disadvantageous for scale-up in terms of economic and ecological aspects. In general, oxidized or reduced intermediates generated in situ at the electrode are highly reactive and prone to further reactions.¹⁸

Besides the choice of the electrode material, electrochemical approaches differ in the setup. The advantageous galvanostatic protocol works at constant current which enables rapid transformations at low cost due to a minimum number of very simple electronic devices and is therefore amenable to scale-up. This simple setup requires two electrodes in the electrolyte in an undivided cell connected to a constant current source (Figure 2a). Such simple DC power sources can be obtained easily from hardware stores. The reaction solution consists of an electrolyte based on a solvent and, if necessary, additional supporting electrolyte to facilitate the conductivity. The supporting electrolyte can be a salt, base, or a strong acid. A divided cell setup has an additional semipermeable or porous membrane between the catholyte and anolyte, which is used for reversible redox reactions or to prevent instability toward the counter electrode (Figure 2b).⁶ Potentiostatic electrolysis requires an additional reference electrode to control the potential which enhances the selectivity but prolongs the reaction time and tremendously affords higher investment into the setup (reference electrode and electrical appliances).⁹

In this context, various setups are known besides reactions in commercially available round-bottom flasks, including the ElectraSyn designed by Baran et al., screening setups (Figure 3a) and beaker-type cells, as well as electroorganic continuous flow setups (Figure 3c) developed in the Waldvogel lab. A parallel setup of the electrodes is desired to perform transformations in a homogeneous electric field without local potential peaks which would lead to uncontrolled and undesired side reactions, lowering the selectivity and efficiency of the reactions.⁹

Carbon–Carbon Bond Formation

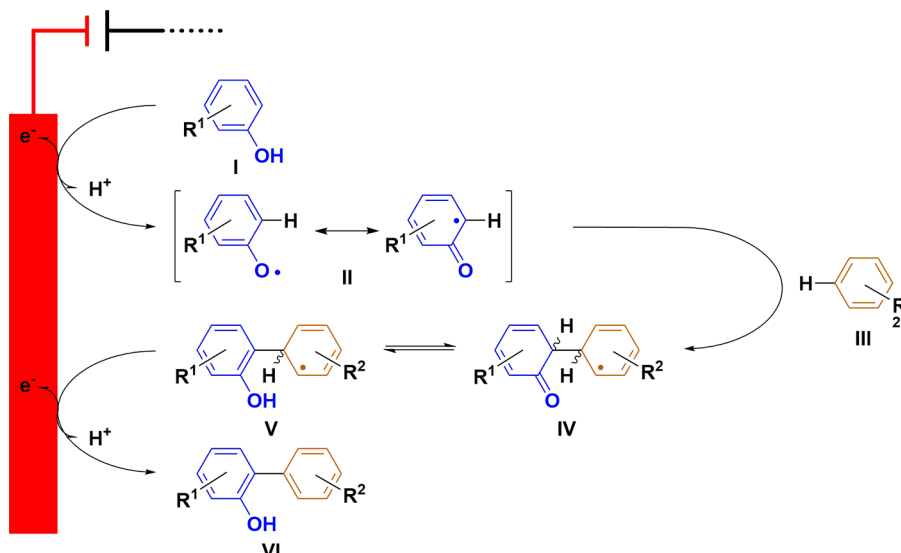
In the context of sustainable chemistry, a deeper insight into the major challenge of organic synthesis, the selective carbon–carbon bond formation, is crucial. Transformations enabling the intra- and intermolecular formation of these bonds enable access to a broad variety of complex organic structural motifs. These motifs have potential for further modification toward natural products, pharmaceutically active compounds, and ligands for catalytic transformations.^{31–35} In this context, a versatile synthetic approach toward the connection of two aromatic

components (sp^2 -hybridized carbon atoms) to give biaryl structures is therefore of utmost importance (Figure 4).³² There are many examples of biologically active compounds which exhibit the biaryl structural motif, such as Kniphofone (4), extracted from *Kniphofia foliosa*, which demonstrates antiparasitic and antitumoral effects.³⁶ In addition, these compounds find application in material sciences, e.g., in molecular electronics like organic light-emitting diodes.³⁷ The broadest and most important field of application is the use of biphenols as ligand precursors for a large variety of transition-metal-catalyzed reactions. Phosphite ligands, for example, are used on industrial scale in the hydroformylation process.³⁸ Biphenols carrying electron-withdrawing groups (EWGs) are excellent precursors for salen-type ligands. These ligands can, for example, be used in an asymmetric copolymerization of CO_2 with *meso*-epoxides to give optically active polycarbonates.³⁹ 1,1'-Binaphthyl-2,2'-diamine (BINAM) is a promising ligand system which can be used in asymmetric Michael-type additions⁴⁰ as well as hydrogenations of ketones and olefins.⁴¹

A general strategy providing access to this biaryl structural motif is the Suzuki–Miyaura reaction, based on the transition metal-catalyzed coupling reaction of aryl(pseudo)halogenides and nucleophilic organometallic species (Scheme 2). The Suzuki–Miyaura coupling reaction uses organoboron reagents,^{42–44} whereas other commonly employed organometallic reagent classes are based on Mg,⁴⁵ Zn,⁴⁶ and Sn.^{47,48} Despite excellent selectivity and high yields, this transformation suffers from environmental and economic drawbacks. These synthetic protocols need prefunctionalized substrates as well as expensive transition-metal based catalysts, which result in (toxic) reagent waste. Additionally, sophisticated reaction conditions are required.

Modern and more sophisticated alternatives to access biaryl structural motifs are oxidative, reagent-mediated coupling reactions with direct C–H activation (Scheme 2).⁴⁹ An overview on oxidative coupling reactions with C–H activation in comparison with electrochemical reactions has been recently provided by Lei and co-workers.^{50,51} The use of convenient oxidizers such as iron(III) chloride, vanadyl chloride, and molybdenum(V) reagents removes the need for prefunctionalization for selective coupling reactions.⁵² Organo-based reagents like (bis(trifluoroacetoxy)iodo)benzene (PIFA) or 2,3-dichloro-5,6-dicyano-1,4-benzoquinone (DDQ) can also simplify synthetic routes, but they always require additional agents, such as Lewis acids.^{49,53,54} However, these reactions suffer from limited regioselectivity as well as overoxidation, forming oligomers and polymers (Scheme 3). The desired cross-coupling reactions compete with the formation of homocoupled products and demonstrate the challenge of oxidative coupling

Scheme 5. Mechanistic Rationale of Anodic Transformation of Phenols with Arenes



reactions. These undesired byproducts, as well as the use of over-stoichiometric amounts of the oxidizer, lead to a large amount of reagent waste.

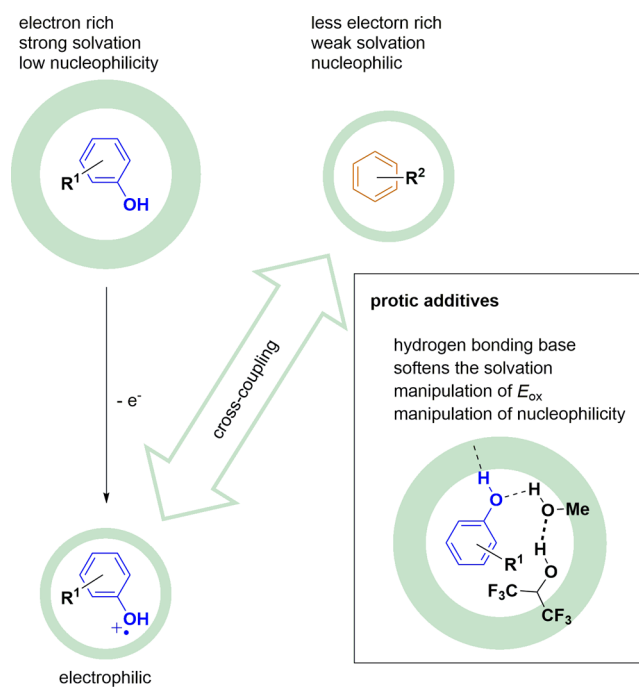
From this point of view, the Waldvogel lab has been interested in the development of a sustainable approach to the synthesis of biaryls to overcome the challenges of oxidative coupling reactions. Novel developments in electrochemical transformations have opened up the possibility of aryl–aryl bond formation using only electric current as the reagent. This leads to an economic and ecologically friendly, inherently safe, robust, and selective synthesis of biaryls.⁵ Electrical current is considered the future primary energy.⁵⁵ Due to the fluctuation in the electric grid, supplies of electricity can be extremely inexpensive and will be attractive as a reagent for synthesis. For producers, low costs in the range of 0.005–0.02 US\$/kWh are anticipated.⁵⁶ The use of renewable sources of electricity, such as wind power, photovoltaics, or hydro power, are increasing.⁵⁷

■ ANODIC DEHYDROGENATIVE C,C-COUPLING REACTIONS OF ARYLS

Waldvogel et al. have been investigating anodic C–H functionalization and coupling reactions of aromatic compounds since 2006 (Scheme 4).⁵⁸ In the early days, the group was devoted to the synthesis of 2,2'-biphenols as precursors for catalysts. After successful development of procedures for the electrochemical synthesis of biphenols, access toward arene-phenols,⁵⁹ bianilides,⁶⁰ *meta*- and *para*-terphenyls,⁶¹ as well as cross-coupled products of various heterocycles with phenols was achieved.^{62–64} Besides the inter- and intramolecular synthesis of electron-rich arenes on active molybdenum anodes,⁶⁵ phenols carrying electron-withdrawing groups were successfully synthesized by adjusting the established procedure and switching to a 1,1,1,3,3,3-hexafluoro-2-propanol (HFIP)/base electrolyte system.⁶⁶

Postulated Mechanism and Source of Selectivity

While working on the phenol-arene cross-coupling reactions, a mechanistic rationale for this conversion (Scheme 5) was postulated by Waldvogel et al. which explains why electrochemical cross-coupling reactions overcome the mentioned challenges (Scheme 3).⁵⁹ It is noteworthy that this mechanism also applies when using this HFIP system with conventional

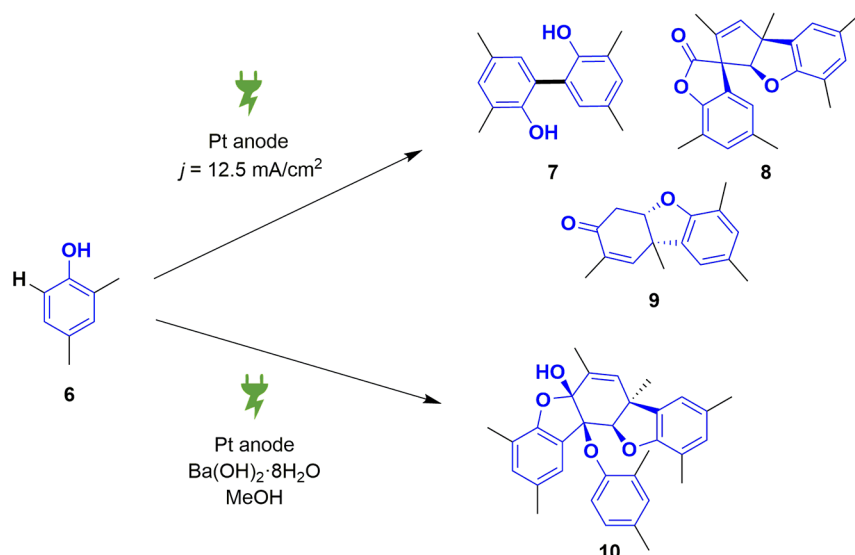
Scheme 6. Source of Selectivity in Anodic Transformations of Phenols with Arenes^a

^aSolvation shell is indicated in green.

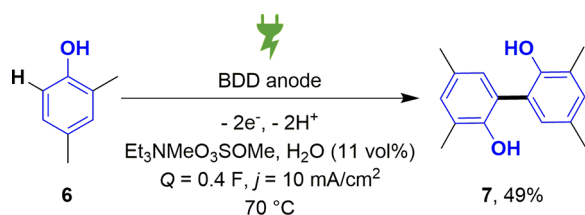
oxidizers.^{67–69} In this mechanism, an initial oxidation of a phenol I occurs, having the lowest oxidation potential at the anode. Subsequently, the deprotonation occurs almost immediately, since the radical cation is extremely acidic. This phenoxyl radical II still represents an electrophile and can be attacked by an arene III or a phenol that exhibits a higher oxidation potential than the initial phenol component. Rearomatization of intermediates IV and V followed by a second anodic oxidation gives rise to the desired biaryl VI.^{26,59,70,71}

Highly fluorinated alcohols like HFIP have been revealed as a unique solvent class, showing a high electrochemical stability and ability to stabilize intermediary radical(-cations).^{72–77} This protic and polar solvent has a larger solvate effect on phenols

Scheme 7. First Attempts on Anodic Transformation of 2,4-Dimethylphenol toward C,C-Homocoupled Product Yield Polycycles

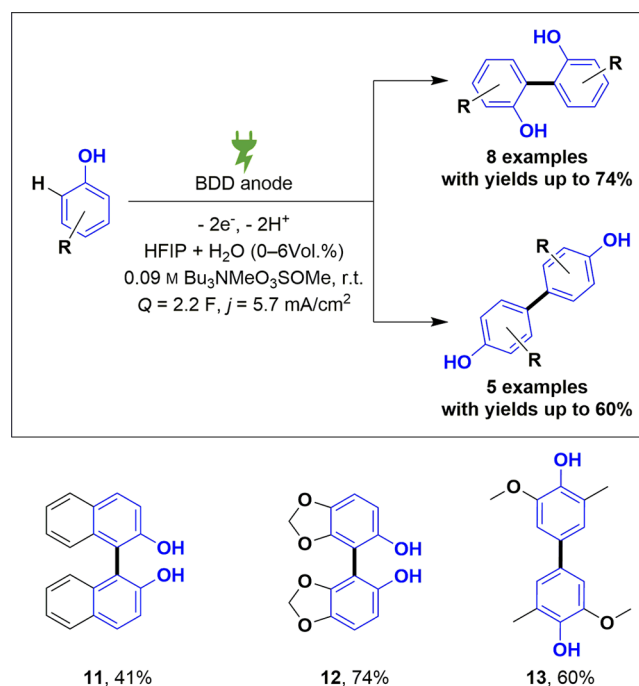
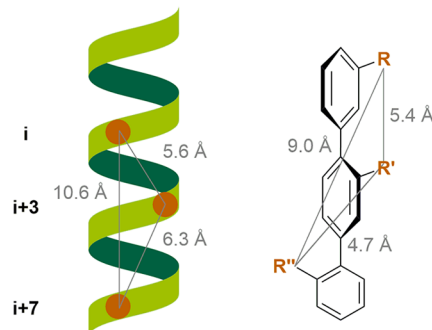


Scheme 8. First Efficient C,C-Homocoupling of 2,4-Dimethylphenol under Solvent-Free Conditions

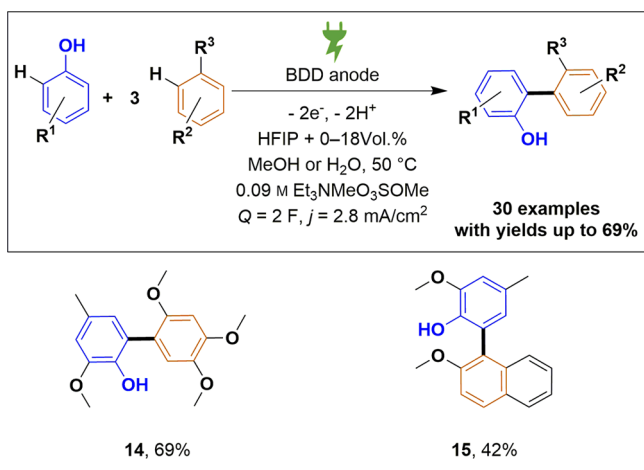


than on arenes, due to its ability of hydrogen bonding. An electron-rich substrate is more prone to oxidation and further follow-up reactions like homocoupling in a nucleophilic attack. These follow-up reactions are likely to occur after diffusion of the intermediates from the electrode surface into the bulk electrolyte.⁷¹ The inherent challenge in engineering selectivity for the cross-coupling reaction derives from the direct linkage of oxidation potential and nucleophilicity. The more electron-rich species, the phenol, is (i) more nucleophilic than the arene and therefore (ii) oxidized more easily to create the electrophilic coupling partner in the reaction. Thus, the natural selectivity favors the formation of the homocoupled product. However, it was found that the nucleophilicity of the phenol can be selectively reduced by the use of HFIP as solvent, which facilitates the creation of a solvent shield via hydrogen bonding interactions. Furthermore, water and methanol are slightly basic in HFIP and are used as additives to lower the oxidation potential of the phenol by weakening the solvate shell and favor the deprotonation. These combined effects favor the formation of the desired cross-coupled product through a shift in the oxidation potential (Scheme 6).^{26,70,71}

By theoretical studies employing ab initio molecular dynamics, it could be confirmed that HFIP in combination with additives interacts with the substrates, influencing the electronic structure of a phenoxyl radical intermediate in a cooperative manner to achieve maximum efficiency and selectivity. This is due to the microheterogeneous structure of HFIP, a segregation of polar, apolar, and fluoruous phases, resulting in chemically active domains.⁷⁸ Another rationale for the efficient coupling reaction is that an enrichment of the substrates at the electrode surface (shown for BDD) takes place.

Scheme 9. HFIP/BDD System Enables Efficient Homocoupling Reactions of Phenols and Comparison of a Linear Terphenyl with a Protein α -Helixconceptual comparison of α -helix with linear terphenyl:

Scheme 10. Additives Such as Methanol or Water Allow Cross-Coupling of Activated Arenes with Phenols in Good Yields



The adsorption of the substrates at the electrode is favored by the attractive lipophilic–lipophilic interactions between the lipophilic electrode and the substrate as well as by the decrease in the repelling lipophilic–fluorous areas.⁷⁹

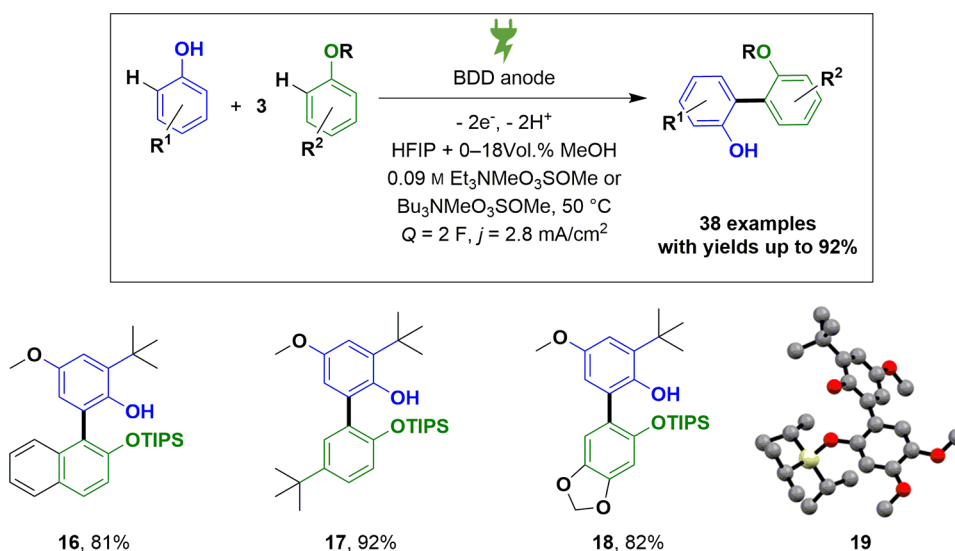
Phenol–Phenol Homocoupling

The selective homocoupling of phenols has faced a significant challenge, before the special features of HFIP were known, because, upon direct electrolysis in most solvents, overoxidation and therefore formation of polycyclic structures occurs (Scheme 7).⁵⁸ The Pummerer's ketone (9) is usually formed as the main product, which occurs as skeleton in many natural products, e.g., (–)-galanthamine or lunarin.⁸⁰ When Ba(OH)₂ is used as supporting electrolyte, the pentacyclic dehydrotetramer 10 is formed in a yield up to 52% in a diastereoselective manner. Depending on the condition of the following up conditions, this unusual scaffold 10 can undergo various transformations to access a great variety of interesting polycyclic natural product like structures.^{81–85}

The first direct selective anodic homocoupling of simple phenols was shown by our group in 2006.⁵⁸ Anodic coupling reaction of 2,4-dimethylphenol using BDD as anode material selectively provides the homocoupled biphenol 7 (Scheme 8). The electrolysis was performed under solvent-free conditions with small amounts of water and supporting electrolyte being required to enhance conductivity. The commonly used supporting electrolytes in the authors' work, triethylmethylammonium methylsulfate and tributylmethylammonium methylsulfate, are both technically common and nonsymmetric which enhances biodegradability. Methylsulfate is an inert and inexpensive anion, and the different chain length enables adjustment of the polarity. When tetraphenoxy borates of the corresponding phenol 6 serve as substrates and supporting electrolyte at the same time, this reaction provides the desired 2,2'-biphenol 7 in 85% yield after hydrolytic workup and enables an electroorganic synthesis of pure product from the simple template precursor⁸⁶ on a multi-kilogram scale using either platinum⁵⁹ or graphite electrodes.^{86,87}

In 2009 an efficient general method for coupling of phenols was established for the first time. It was clearly shown that HFIP as solvent and BDD as anode material is a very suitable combination for carrying out these reactions selectively toward 2,2'-biphenol derivatives (Scheme 9).⁷⁶ The obtained yields were high for the benzodioxole derivative (12), and rather good for 2-naphthol (11), but dropped when applied to different phenols. Ten years later, the very efficient synthesis of 4,4'-biphenols could be demonstrated by applying this method, in up to 60% yield, when the *ortho*-positions are blocked (13).⁸⁸ This electrochemical approach allows not only the synthesis of biaryl structures, but also the access to teraryl structures. Linear teraryls are potential α -helix mimetics, because the substituents of these teraryls are in sufficient accordance in angle and distance to amino acid side chains (i , $i + 3$, $i + 7$) as stated by Hamilton et al.⁸⁹ Furthermore, these linear teraryls are more stable regarding conformational and proteolytic stability than peptide-based drugs for inhibiting protein–protein interactions.⁹⁰

Scheme 11. Installation of a TIPS-Protecting Group Enhances the Yield of the Phenol–Phenol Cross-Coupling Reaction Tremendously^a



^aTIPS = triisopropylsilyl.

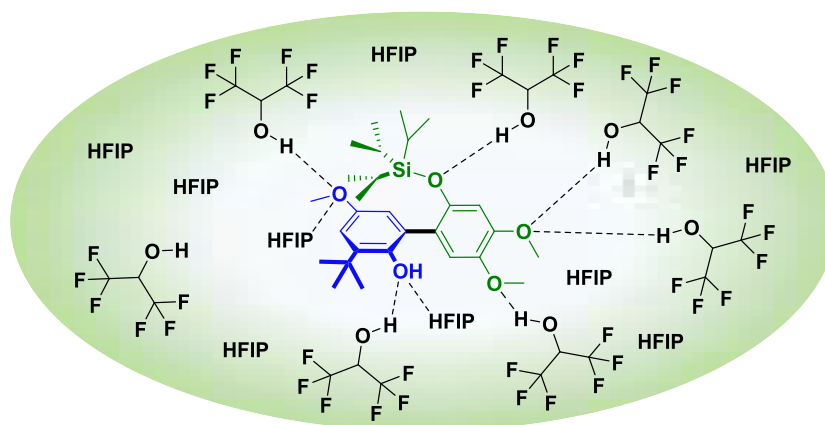
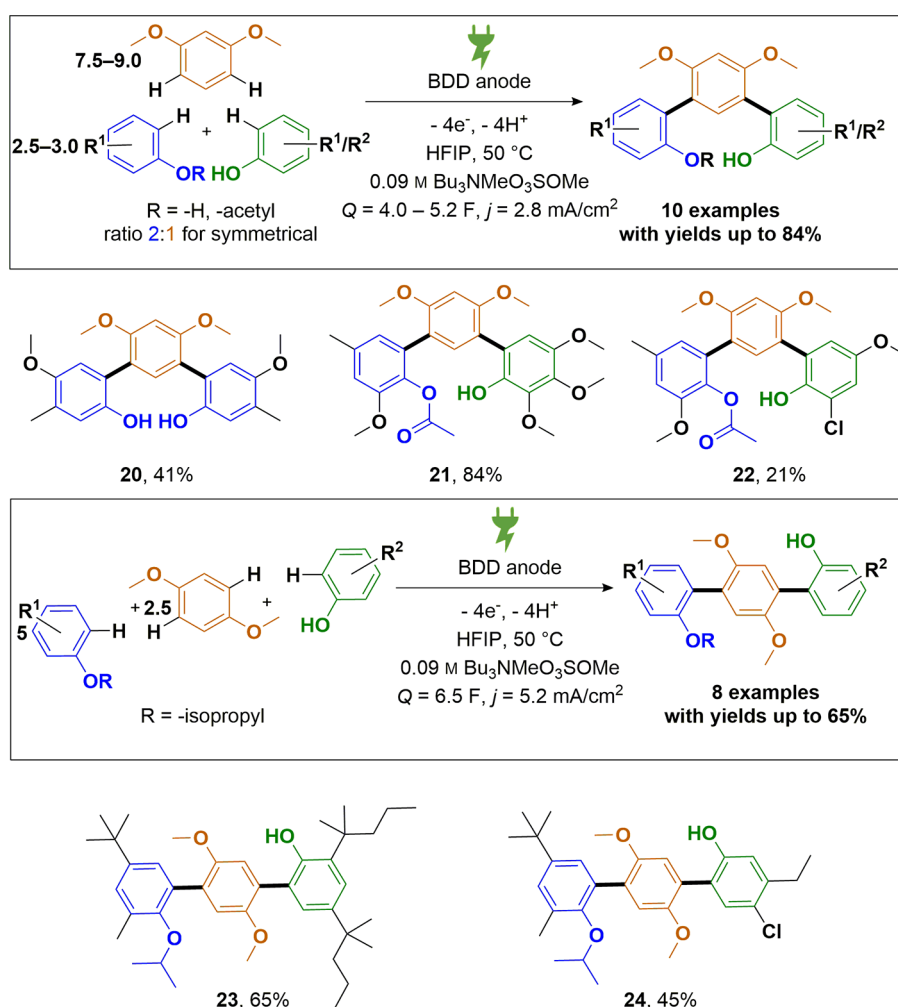


Figure 5. Twist of biaryl axis of a TIPS-protected 2,2'-biphenol with HFIP solvation.

Scheme 12. Synthesis of Terphenyls as OCO-Pincer Ligands or α -Helix Mimetics



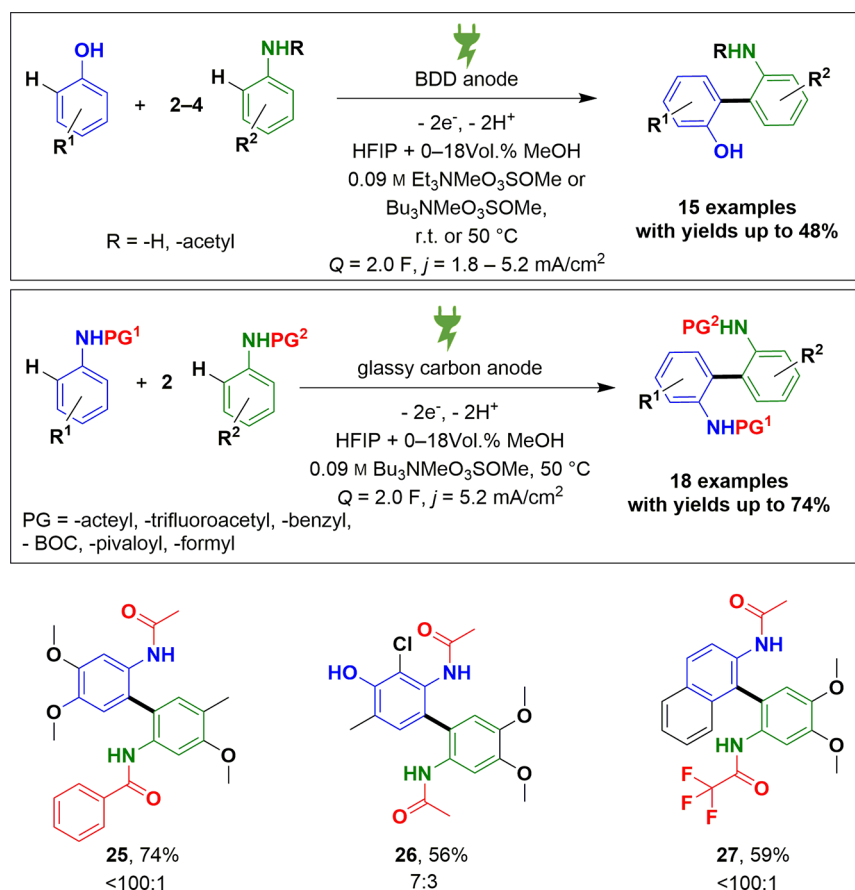
Phenol–Arene Cross-Coupling

In 2010, the first cross-coupling reactions were successfully performed using phenols and activated arenes.⁵⁹ Although initial attempts showed only low yields (up to 39%), an initial proof of concept was achieved. An optimized protocol used water or methanol as additives, increasing the yields up to 69% (**14**, Scheme 10).²⁶ The key parameter to this selectivity is based on the electrolyte (see Scheme 1) used, due to the possibility of using other electrodes like graphite or glassy carbon without

dramatic loss of yield. It was then possible to broaden the scope of these reactions to 30 different phenol-arene combinations. The reaction proceeds selectively in position 2 of the phenol and works with naphthalenes as arene components (**15**).

Phenol–Phenol Cross-Coupling

Afterward, Waldvogel et al. focused upon cross-coupling reactions between different phenols, enabling the synthesis of nonsymmetric 2,2'-biphenols. Direct cross-coupling of non-modified phenols was achieved in yields up to 86%.⁹¹ A

Scheme 13. First Efficient Anilide–Anilide C,C-Cross-Couplings^a^aPG = protective group.

significant increase of the yield up to 92% was achieved by employing a triisopropylsilyl (TIPS) protective group on component B (**17**, 92%, Scheme 11), and the reaction was found to proceed with a broader range of substrates, such as benzodioxoles (**18**).⁹² The protective group can easily be cleaved after the dehydrogenative coupling reaction or could serve already a suitably protected building block to install different phosphorus moieties.

The extraordinary high yields can be rationalized by complementary effects due to the bulky TIPS protective group. First, the TIPS-group causes a strong twist of the biaryl axis of least 53°, which prevents conjugation of the π -systems (Figure 5).⁹² Therefore, the products obtained are less prone to overoxidation. Additionally, increased lipophilicity combined with an unchanged electron-rich nature leads to solvation by HFIP and therefore diminishes the nucleophilicity. This prevents subsequent coupling reactions.

meta-Terphenyl-2,2'-diols and 2-Hydroxy-*para*-terphenyls

So far, the stepwise synthesis of symmetric and nonsymmetric *meta*-terphenyl-2,2''-diols and nonsymmetric 2-hydroxy-*para*-terphenyls has been investigated (Scheme 12).^{61,93} First a phenol-arene system was synthesized, which is later protected. This allows an adjustment of oxidation potentials. Subsequently, a second coupling reaction with a phenol was conducted. This method provides access toward OCO-pincer ligands in moderate to high yields, which have manifold applications in catalysis, synthesis and material science.⁹⁴ When an acetyl group

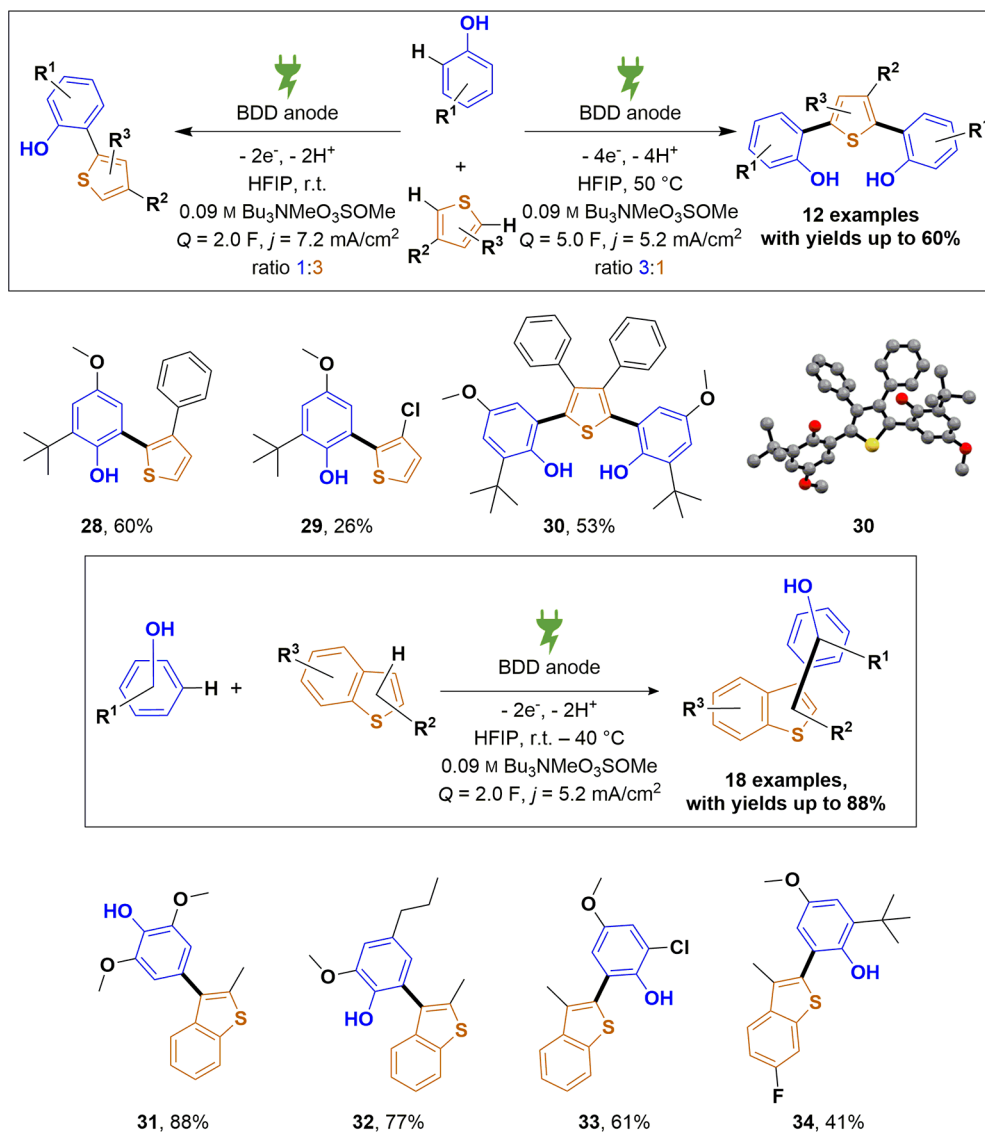
is applied, the yield can be as high as 84% (**21**), whereas halo substituents on phenols lead to yields up to 21% (**22**).

Cross-Coupling Reactions Involving Anilines

The C,C-coupling of anilines poses a particular challenge. The oxidation of aniline with various oxidizers such as potassium chlorate leads to aniline black, which is a complex mixture of condensed aniline molecules and is used as a black pigment.⁹⁵ The anilines must therefore be protected to suppress oligomerization. Since anilines are poor hydrogen bonding acceptors, hydrogen-bonding-based control of selectivity is limited. When a protecting group is installed this situation alters. The developed coupling strategy allows the synthesis of different coupling products between phenols and anilides or protected naphthylamines (Scheme 13).⁹⁶ It was also shown that this methodology rises easy access to nonsymmetrical axially chiral N,O-biaryl structures, derived from enantio-enriched naphthylamines and phenols.⁹⁷ Derivative **25** was synthesized in 74% yield, using acetyl- and benzoyl-protective groups. Also halogenated dianilides (**26**) and naphthylamines (**27**) could be successfully converted as well as formamides.^{60,98}

Phenol-Heterocycle Cross-Coupling

Furthermore, the use of heterocycles within these electrochemical conversions is viable as well. The initial investigations were conducted with thiophenes, allowing highly selective coupling to bi- and teraryl structures in yields up to 60% (**28**) depending on the electrochemical parameters applied (Scheme 14).⁶⁴ When using benzo[*b*]thiophenes, both substitution patterns, in either position 2 or 3 of the benzothiophene, can

Scheme 14. Cross-Coupling of Phenols with Thiophenes and Benzo[*b*]thiophenes

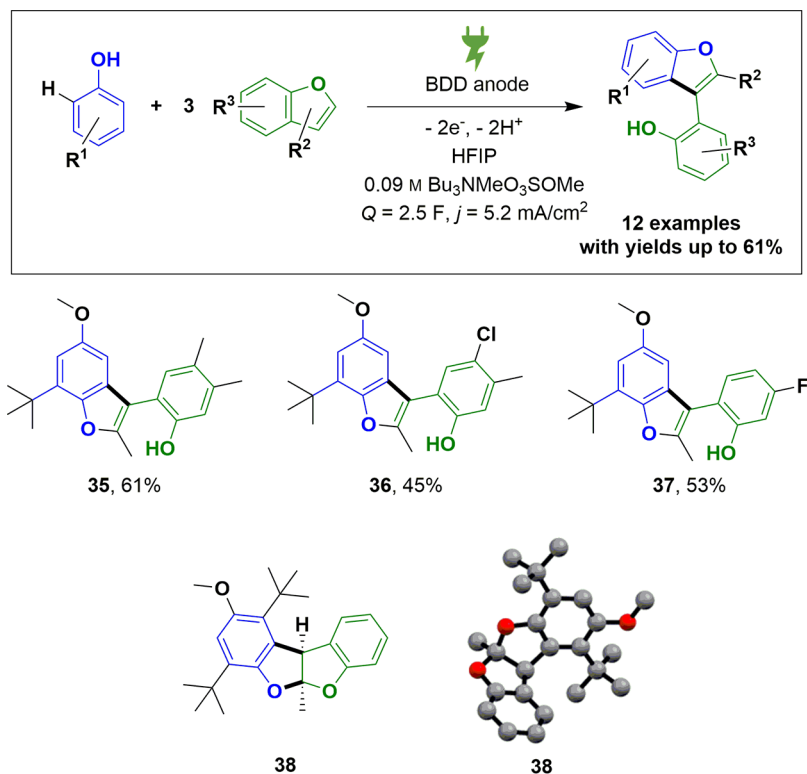
be addressed selectively by the phenol, by simply blocking the other position. Moreover, coupling of phenols in position 2 or 4 is possible, leading to large scope of accessible scaffolds in yields up to 88% (31).⁶³

Using benzofurans within the anodic C,C-coupling reaction, a simple C,C bond formation was not observed, but rather a furan metathesis leading to an exchange of the substituents of phenol and benzofuran occurred (Scheme 15).⁶² The reaction tolerates halogens such as fluoride (37) and chloride (36) and reaches yields up to 61% (35). It takes place via a protonated dihydrobenzofuro[2,3-*b*]benzofuran similar to the isolated intermediate (38). Ring opening of these intermediates (39, 42) to phenols (40, 43), subsequent β -phenonium shift for 3-substituted derivatives, and deprotonation lead to the respective product (41). After workup, unexpectedly, the more nucleophilic oxygen of the electron-rich phenol was found within the benzofuran.

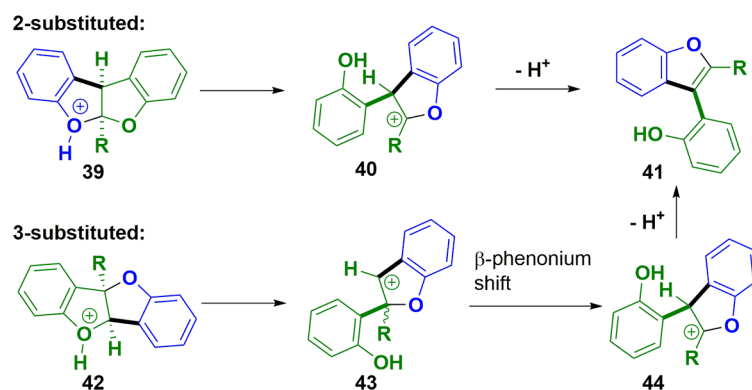
Active Molybdenum Anode for Dehydrogenative Coupling Reactions of Activated Arenes

To date, the anodic coupling reactions have been applied to phenols or anilides in cross-coupling reactions with arenes at

inert electrode materials. Changing the electrode material to an active anode, like molybdenum, in HFIP enabled access to anodic dehydrogenative coupling reactions of electron-rich arenes analogous to molybdenum(V) reagent-mediated reactions.⁶⁵ It was shown that only traces of molybdenum were found in the electrolyte after electrolysis, which does not result from dissolved active species but rather active $Mo(HFIP)_x$ species, likely Mo(IV) and Mo(V), at the surface. The established protocol enabled intermolecular access to biaryl structures, starting from anisole derivatives in yields up to 67% and starting from veratrole derivatives in yields up to 87% (Scheme 16). This reaction is valuable for postfunctionalization reactions due to the tolerance of iodo functionalities (45). Furthermore, the application of this protocol on intramolecular coupling reactions gave access to five- to eight-membered rings as well as heterocycles in yields up to 80%, and substrates which notoriously tend to be chlorinated by the stoichiometric reagent (46) or equipped with carboxylic acids could also be transformed for the first time (47).

Scheme 15. Metathesis of Benzo[*b*]furans with Phenols^a

postulated mechanism for the product formation



^aScope of the reaction and isolated yields are shown. Molecular structure of the isolated tetracyclic intermediate, determined by X-ray analysis including the postulated mechanism for product formation is shown.

Coupling of Phenols Carrying EWGs

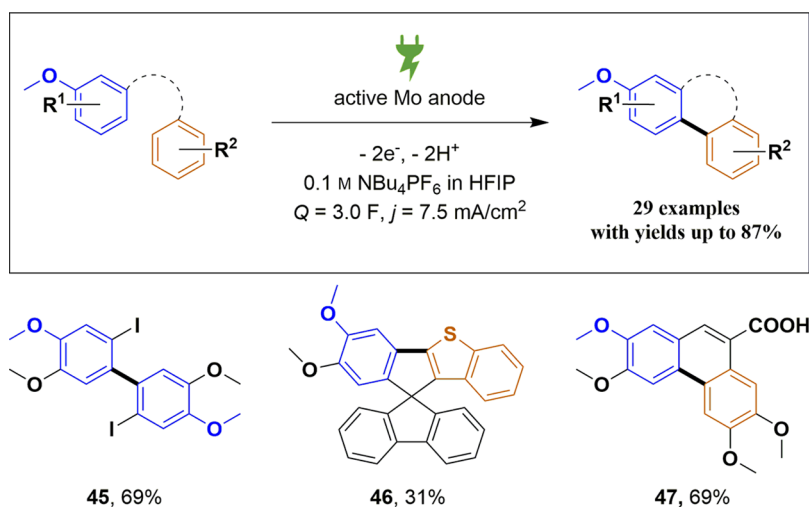
So far, only phenols carrying electron-donating groups could be converted into the desired biphenols. By changing the protocol and switching to base as additive, without any further supporting electrolyte, it is possible to achieve the selective homo- and cross-coupling of phenols carrying EWGs. The base lowers the oxidation potential of the respective starting materials, facilitating the oxidation, as shown by cyclic voltammetry studies. This gives easy access to novel polydentate ligands and precursors for binuclear salen complexes.^{39,99,100} The cross-coupling with naphthalene yields cyclic dihydrodibenzofurans (**52**), which can be easily oxidized to dibenzofurans (**54**). Interestingly cross-coupled phenol (**53**) is in equilibrium with (**54**), which represents an unreported tautomerism. The reaction works with a variety of electron-withdrawing groups,

such as halogens (**48**), acetoxy (**49**), sulfonyls (**51**), and carbonyls (**50**) in yields up to 64% (Scheme 17).

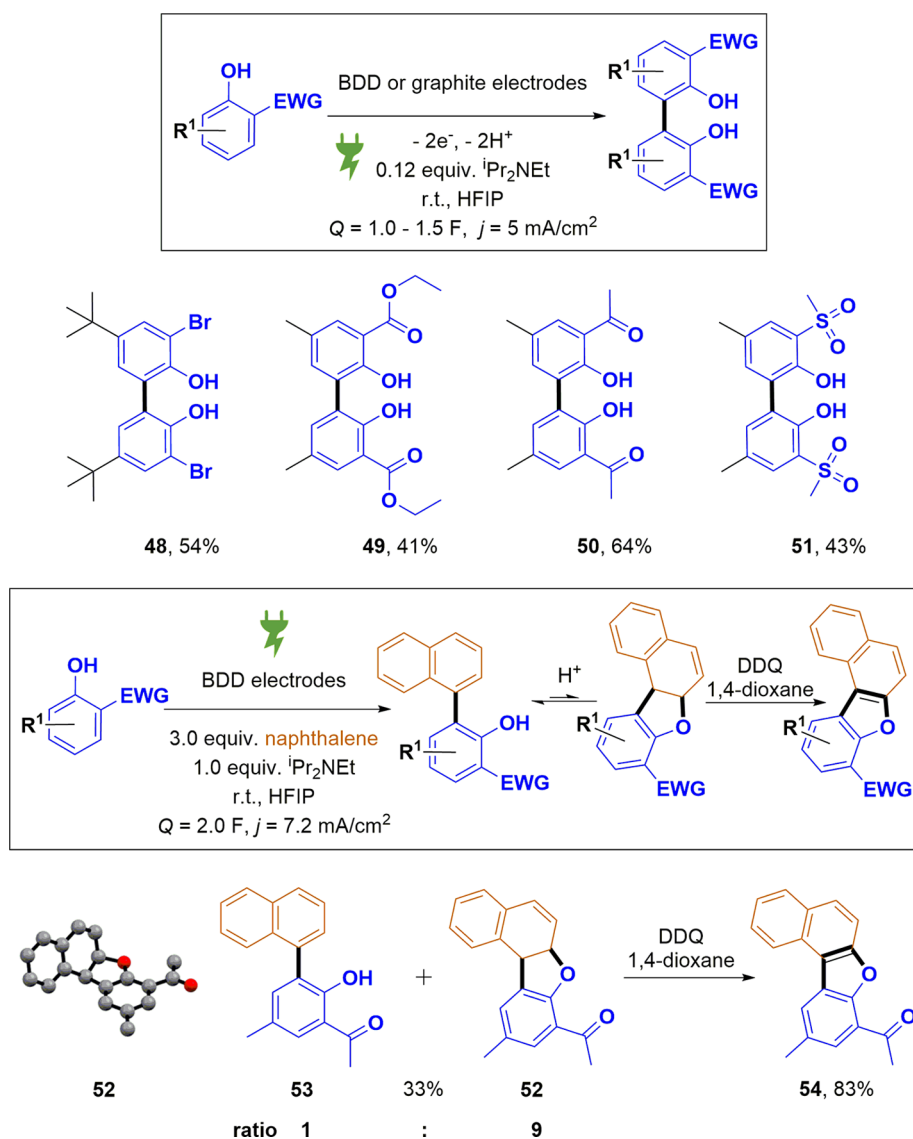
Application in the Synthesis of Natural Products and Pharmaceutically Active Compounds

The isolation of natural products and pharmaceutically active compounds from naturally abundant sources or total synthesis is challenging, cost- and time-demanding. Thus, the idea of applying electroorganic transformations on these compounds is of high interest to enable an environmentally friendly and cost-effective synthesis. Electroorganic key reactions have been applied to the regio- and stereoselective synthesis of the naturally occurring opium alkaloids (–)-thebaine (**3**) and (–)-oxycodone (**56**) (Scheme 18) by our group in a recent collaboration with Opatz et al.^{13,17} The absence of metal-based reagents in the electrochemical key step is of high interest for

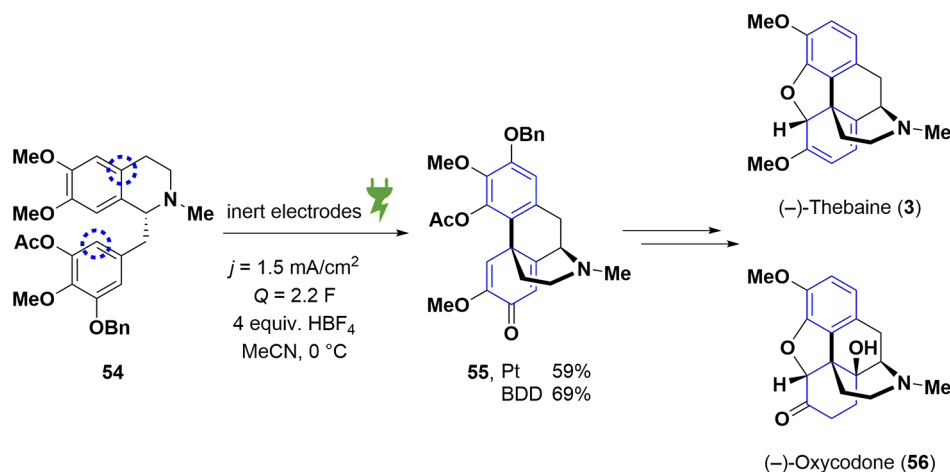
Scheme 16. Intra- and Intermolecular Dehydrogenative Coupling Reaction of Activated Arenes on Active Molybdenum Anodes



Scheme 17. Access to 2,2'-Biphenols Carrying Electron-Withdrawing Groups in HFIP/DIPEA Systems and Access to Tetracyclic Compounds



Scheme 18. Synthesis of (–)-Thebaine and (–)-Oxycodone Using an Anodic Cyclization as a Key Step



further medical applications. The key to this electrochemical transformation is the use of a nonsymmetric set of protective groups at the benzylic moiety. This allows cyclization with excellent selectivity and enables suitable downstream processing to the morphine series. It turned out that BDD electrodes provide even higher yields for the intermediate and enables synthesis in flow electrolysis as well.

SUMMARY AND OUTLOOK

In a decade of research, electroorganic transformations have emerged as a powerful and atom-efficient tool for arene–arene C,C-homo- and cross-coupling reactions. Starting from readily available compounds, a broad variety of different biaryl structures have been obtained. The focus has been drawn toward phenols which find applications in different areas, like catalysis for chemical synthesis as well as potential pharmaceuticals. The total synthesis of natural products can be further simplified and shortened by leveraging electrochemistry, using metal-free key steps.

We anticipate that future research will focus on optimizing electrochemical processes, utilizing effective screening techniques to maximize efficiency. Design of Experiments (DoE) is one such technique which is commonly used in industry and can also be applied effectively to academic research. The synthesis of different substrate classes to offer a broad variety of methods including the selective synthesis of carbon–heteroatom bonds will be a challenge in aryl–aryl coupling reactions. Moreover, the practical elements of the methods presented here have to be improved to enable large-scale reactions, which do not require chromatographic purification but rather distillation or crystallization. Therefore, a continuous flow electroorganic setup would enable a transformation which is not interrupted by purification processes and which could rather be performed in an external setup. This would allow for the transfer of the methods to technical applications for pioneering sustainable chemical synthesis on an industrial scale.

AUTHOR INFORMATION

Corresponding Author

*Email: waldvogel@uni-mainz.de.

ORCID

Siegfried R. Waldvogel: [0000-0002-7949-9638](https://orcid.org/0000-0002-7949-9638)

Author Contributions

[†]J.L.R. and D.P. contributed equally to this work.

Funding

J.L.R. is a recipient of a DFG fellowship through the Excellence Initiative by the Graduate School Materials Science in Mainz (GSC 266). D.P. thanks the Verband der Chemischen Industrie (VCI) for a Kekulé Fellowship.

Notes

The authors declare no competing financial interest.

Biographies

Johannes L. Röckl finished his apprenticeship as a laboratory technician in 2013 at BASF SE, Ludwigshafen and received his B.Sc. from Johannes Gutenberg University in a collaboration with BASF SE working on the total synthesis of natural product derivatives under supervision of Prof. Dr. Siegfried R. Waldvogel and Dr. Joachim Dickhaut in 2016. Afterwards, he was appointed as a scientist in insecticide science working on early stage projects, thereof spending 2 months at the Innovation Campus of BASF India Ltd. as a delegate in Navi Mumbai, India. After acceptance as a fast-track Ph.D. candidate, he started working on electroorganic synthesis in the Waldvogel lab. Currently, he is a visiting researcher at the ETH, Zurich working on transition metal catalysis under the supervision of Prof. Dr. Bill Morandi.

Dennis Pollok received his B.Sc. degree from Johannes Gutenberg University Mainz in collaboration with the Max Planck Institute for Polymer Research in Mainz working on polyphosphate based flame retardants under supervision of Dr. habil. Frederik R. Wurm. During an internship at the University of Toronto he was working in the group of Prof. Dr. Dwight S. Seferos on polyselenophenes. He received his M.Sc. from Johannes Gutenberg University Mainz working under supervision of Prof. Dr. Siegfried R. Waldvogel where he is currently conducting research as a graduate student on electroorganic synthesis.

Robert Franke studied chemistry with focus on industrial chemistry and theoretical chemistry at the University of Bochum in Germany. He earned his doctorate degree in 1994 in the field of relativistic quantum chemistry under Prof. Dr. Werner Kutzelnigg. After working for a period as a research assistant, in 1998 he joined the process engineering department of the former Hüls AG, a predecessor company of Evonik Industries AG. He is now Director Innovation Management Hydroformylation. He was awarded his professorial research degree (Habilitation) in 2002, and since then he has taught at the University

of Bochum. In 2011, he was promoted to an adjunct professor. His research focuses on homogeneous catalysis, process intensification, and computational chemistry.

Siegfried R. Waldvogel studied chemistry in Konstanz and received his Ph.D. in 1996 from the University of Bochum/Max Planck Institute for Coal Research with Prof. Dr. M. T. Reetz as supervisor. After Postdoctoral research at the Scripps Research Institute in La Jolla, CA (Prof. Dr. J. Rebek, jr.), he started his own research career in 1998 with a habilitation at the University of Münster. In 2004, he moved to the University of Bonn as professor for organic chemistry. In 2010, he became full professor at the Johannes Gutenberg University Mainz. His main research interests are electroorganic synthesis ranging from screening to scale-up, novel electroconversions and transformations of renewables as well as supramolecular sensing. In 2018, he cofounded a start-up which provides custom electrosynthesis (ESy-laboratories GmbH).

ACKNOWLEDGMENTS

Support of the Advanced Lab of Electrochemistry and Electrosynthesis – ELYSION (Carl Zeiss Stiftung) is gratefully acknowledged.

REFERENCES

- (1) Olivier, J. G. J.; Peters, J. A. H.W. *Trends in Global CO₂ and Total Greenhouse Gas Emissions: 2018 Report*, 2018. https://www.pbl.nl/sites/default/files/downloads/pbl-2018-trends-in-global-co2-and-total-greenhouse-gas-emissions-2018-report_3125_0.pdf.
- (2) Cernansky, R. Chemistry: Green Refill. *Nature* **2015**, *519*, 379–380.
- (3) Clark, J. H.; Luque, R.; Matharu, A. S. Green Chemistry, Biofuels, and Biorefinery. *Annu. Rev. Chem. Biomol. Eng.* **2012**, *3*, 183–207.
- (4) de Marco, B. A.; Rechelo, B. S.; Totoli, E. G.; Kogawa, A. C.; Salgado, H. R. N. Evolution of Green Chemistry and Its Multidimensional Impacts: A Review. *Saudi Pharm. J.* **2019**, *27*, 1–8.
- (5) Waldvogel, S. R.; Janza, B. Renaissance of Electrosynthetic Methods for the Construction of Complex Molecules. *Angew. Chem., Int. Ed.* **2014**, *53*, 7122–7123.
- (6) Yan, M.; Kawamata, Y.; Baran, P. S. Synthetic Organic Electrochemical Methods Since 2000: On the Verge of a Renaissance. *Chem. Rev.* **2017**, *117*, 13230–13319.
- (7) Horn, E. J.; Rosen, B. R.; Baran, P. S. Synthetic Organic Electrochemistry: An Enabling and Innately Sustainable Method. *ACS Cent. Sci.* **2016**, *2*, 302–308.
- (8) Wiebe, A.; Gieshoff, T.; Möhle, S.; Rodrigo, E.; Zirbes, M.; Waldvogel, S. R. Electrifying Organic Synthesis. *Angew. Chem., Int. Ed.* **2018**, *57*, 5594–5619.
- (9) Waldvogel, S. R.; Lips, S.; Selt, M.; Riehl, B.; Kampf, C. J. Electrochemical Arylation Reaction. *Chem. Rev.* **2018**, *118*, 6706–6765.
- (10) Frontana-Urbe, B. A.; Little, R. D.; Ibanez, J. G.; Palma, A.; Vasquez-Medrano, R. Organic Electrosynthesis: A Promising Green Methodology in Organic Chemistry. *Green Chem.* **2010**, *12*, 2099–2119.
- (11) Wiebe, A.; Riehl, B.; Lips, S.; Franke, R.; Waldvogel, S. R. Unexpected High Robustness of Electrochemical Cross-coupling for a Broad Range of Current Density. *Sci. Adv.* **2017**, *3*, No. ea03920.
- (12) Shatskiy, A.; Lundberg, H.; Kärkäs, M. Organic Electrosynthesis: Applications in Complex Molecule Synthesis. *ChemElectroChem* **2019**, *6*, 4067–4092.
- (13) Lipp, A.; Selt, M.; Ferenc, D.; Schollmeyer, D.; Waldvogel, S. R.; Opatz, T. Total Synthesis of (–)-Oxycodone via Anodic Aryl-Aryl Coupling. *Org. Lett.* **2019**, *21*, 1828–1831.
- (14) Gütz, C.; Stenglein, A.; Waldvogel, S. R. Highly Modular Flow Cell for Electroorganic Synthesis. *Org. Process Res. Dev.* **2017**, *21*, 771–778.
- (15) Rosen, B. R.; Werner, E. W.; O'Brien, A. G.; Baran, P. S. Total Synthesis of Dixiamycin B by Electrochemical Oxidation. *J. Am. Chem. Soc.* **2014**, *136*, 5571–5574.
- (16) Mihelcic, J.; Moeller, K. D. Oxidative Cyclizations: The Asymmetric Synthesis of (–)-Alliacol A. *J. Am. Chem. Soc.* **2004**, *126*, 9106–9111.
- (17) Lipp, A.; Ferenc, D.; Gütz, C.; Geffe, M.; Vierengel, N.; Schollmeyer, D.; Schäfer, H. J.; Waldvogel, S. R.; Opatz, T. A Regio- and Diastereoselective Anodic Aryl-Aryl Coupling in the Biomimetic Total Synthesis of (–)-Thebaine. *Angew. Chem., Int. Ed.* **2018**, *57*, 11055–11059.
- (18) Möhle, S.; Zirbes, M.; Rodrigo, E.; Gieshoff, T.; Wiebe, A.; Waldvogel, S. R. Modern Electrochemical Aspects for the Synthesis of Value-Added Organic Products. *Angew. Chem., Int. Ed.* **2018**, *57*, 6018–6041.
- (19) Martínez-Huitle, C. A.; Brillas, E. *Synthetic Diamond Films: Preparation, Electrochemistry, Characterization, and Applications*; The Wiley Series on Electrocatalysis and Electrochemistry; Wiley: Hoboken, NJ, 2011.
- (20) Macpherson, J. V. A Practical Guide to Using Boron Doped Diamond in Electrochemical Research. *Phys. Chem. Chem. Phys.* **2015**, *17*, 2935–2949.
- (21) Waldvogel, S. R.; Mentizi, S.; Kirste, A. Boron-doped Diamond Electrodes for Electroorganic Chemistry. *Top. Curr. Chem.* **2011**, *320*, 1–31.
- (22) Ivandini, T. A.; Einaga, Y. Polycrystalline Boron-doped Diamond Electrodes for Electrocatalytic and Electrosynthetic Applications. *Chem. Commun.* **2017**, *53*, 1338–1347.
- (23) Ivandini, T. A.; Sato, R.; Makide, Y.; Fujishima, A.; Einaga, Y. Electroanalytical Application of Modified Diamond Electrodes. *Diamond Relat. Mater.* **2004**, *13*, 2003–2008.
- (24) Lips, S.; Waldvogel, S. R. Use of Boron-Doped Diamond Electrodes in Electro-Organic Synthesis. *ChemElectroChem* **2019**, *6*, 1649–1660.
- (25) Kraft, A. Doped Diamond: A Compact Review on a New, Versatile Electrode Material. *Int. J. Electrochem. Sci.* **2007**, *355*–443.
- (26) Kirste, A.; Elsler, B.; Schnakenburg, G.; Waldvogel, S. R. Efficient Anodic and Direct Phenol-Arene C, C Cross-Coupling: The Benign Role of Water or Methanol. *J. Am. Chem. Soc.* **2012**, *134*, 3571–3576.
- (27) Yoo, S. J.; Li, L.-J.; Zeng, C.-C.; Little, R. D. Polymeric Ionic Liquid and Carbon Black Composite as a Reusable Supporting Electrolyte: Modification of the Electrode Surface. *Angew. Chem., Int. Ed.* **2015**, *54*, 3744–3747.
- (28) Yoshida, J.-i.; Suga, S. Basic Concepts of “Cation Pool” and “Cation Flow” Methods and Their Applications in Conventional and Combinatorial Organic Synthesis. *Chem. - Eur. J.* **2002**, *8*, 2650–2658.
- (29) IKA-Werke GmbH & CO. KG. *Electra Syn 2.0 Package*, 2019. www.ika.com/de/Produkte-Lab-Eq/Electrochemistry-Kit-csp-516/ElectraSyn-20-Package-cpdt-20008980 (accessed October 21, 2019).
- (30) Gütz, C.; Klöckner, B.; Waldvogel, S. R. Electrochemical Screening for Electroorganic Synthesis. *Org. Process Res. Dev.* **2016**, *20*, 26–32.
- (31) Alberico, D.; Scott, M. E.; Lautens, M. Aryl-Aryl Bond Formation by Transition-Metal-Catalyzed Direct Arylation. *Chem. Rev.* **2007**, *107*, 174–238.
- (32) Hassan, J.; Sévignon, M.; Gozzi, C.; Schulz, E.; Lemaire, M. Aryl-Aryl Bond Formation One Century after the Discovery of the Ullmann Reaction. *Chem. Rev.* **2002**, *102*, 1359–1470.
- (33) Bringmann, G.; Price Mortimer, A. J.; Keller, P. A.; Gresser, M. J.; Garner, J.; Breuning, M. Atroposelective Synthesis of Axially Chiral Biaryl Compounds. *Angew. Chem., Int. Ed.* **2005**, *44*, 5384–5427.
- (34) McCarthy, M.; Guiry, P. J. Axially Chiral Bidentate Ligands in Asymmetric Catalysis. *Tetrahedron* **2001**, *57*, 3809–3844.
- (35) Zhang, S.-S.; Wang, Z.-Q.; Xu, M.-H.; Lin, G.-Q. Chiral Diene as the Ligand for the Synthesis of Axially Chiral Compounds via Palladium-Catalyzed Suzuki-Miyaura Coupling Reaction. *Org. Lett.* **2010**, *12*, 5546–5549.

- (36) Kuroda, M.; Mimaki, Y.; Sakagami, H.; Sashida, Y. Bulbinelonesides A-E, Phenylanthraquinone Glycosides from the Roots of *Bulbinella Floribunda*. *J. Nat. Prod.* **2003**, *66*, 894–897.
- (37) Perepichka, I. F.; Perepichka, D. F.; Meng, H.; Wudl, F. Light-Emitting Polythiophenes. *Adv. Mater.* **2005**, *17*, 2281–2305.
- (38) Franke, R.; Selent, D.; Börner, A. Applied Hydroformylation. *Chem. Rev.* **2012**, *112*, 5675–5732.
- (39) Liu, Y.; Ren, W.-M.; Liu, J.; Lu, X.-B. Asymmetric Copolymerization of CO₂ with Meso-Epoxides Mediated by Dinuclear Cobalt(III) Complexes: Unprecedented Enantioselectivity and Activity. *Angew. Chem., Int. Ed.* **2013**, *52*, 11594–11598.
- (40) Wang, J.; Li, H.; Duan, W.; Zu, L.; Wang, W. Organocatalytic Asymmetric Michael Addition of 2,4-Pentandione to Nitroolefins. *Org. Lett.* **2005**, *7*, 4713–4716.
- (41) Zhang, F.-Y.; Pai, C.-C.; Chan, A. S. C. Asymmetric Synthesis of Chiral Amine Derivatives through Enantioselective Hydrogenation with a Highly Effective Rhodium Catalyst Containing a Chiral Bisaminophosphine Ligand. *J. Am. Chem. Soc.* **1998**, *120*, 5808–5809.
- (42) Miyaura, N.; Yamada, K.; Suzuki, A. A New Stereospecific Cross-Coupling by the Palladium-Catalyzed Reaction of 1-Alkenylboranes with 1-Alkenyl or 1-Alkynyl Halides. *Tetrahedron Lett.* **1979**, *20*, 3437–3440.
- (43) Miyaura, N.; Suzuki, A. Stereoselective Synthesis of Arylated (E)-Alkenes by the Reaction of Alk-1-enylboranes with Aryl Halides in the Presence of Palladium Catalyst. *J. Chem. Soc., Chem. Commun.* **1979**, 866–867.
- (44) Miyaura, N.; Suzuki, A. Palladium-Catalyzed Cross-Coupling Reactions of Organoboron Compounds. *Chem. Rev.* **1995**, *95*, 2457–2483.
- (45) Tamao, K.; Sumitani, K.; Kumada, M. Selective Carbon-Carbon Bond Formation by Cross-Coupling of Grignard Reagents with Organic Halides. Catalysis by Nickel-Phosphine Complexes. *J. Am. Chem. Soc.* **1972**, *94*, 4374–4376.
- (46) King, A. O.; Okukado, N.; Negishi, E.-i. Highly General Stereo-, Regio-, and Chemo-Selective Synthesis of Terminal and Internal Conjugated Enynes by the Pd-Catalyzed Reaction of Alkynylzinc Reagents with Alkenyl Halides. *J. Chem. Soc., Chem. Commun.* **1977**, 683–684.
- (47) Milstein, D.; Stille, J. K. A General, Selective, and Facile Method for Ketone Synthesis from Acid Chlorides and Organotin Compounds Catalyzed by Palladium. *J. Am. Chem. Soc.* **1978**, *100*, 3636–3638.
- (48) Stille, J. K. The Palladium-Catalyzed Cross-Coupling Reactions of Organotin Reagents with Organic Electrophiles [New Synthetic Methods (58)]. *Angew. Chem., Int. Ed. Engl.* **1986**, *25*, 508–524.
- (49) Grzybowski, M.; Skonieczny, K.; Butenschön, H.; Gryko, D. T. Comparison of Oxidative Aromatic Coupling and the Scholl Reaction. *Angew. Chem., Int. Ed.* **2013**, *52*, 9900–9930.
- (50) Yi, H.; Zhang, G.; Wang, H.; Huang, Z.; Wang, J.; Singh, A. K.; Lei, A. Recent Advances in Radical C-H Activation/Radical Cross-Coupling. *Chem. Rev.* **2017**, *117*, 9016–9085.
- (51) Tang, S.; Liu, Y.; Lei, A. Electrochemical Oxidative Cross-coupling with Hydrogen Evolution: A Green and Sustainable Way for Bond Formation. *Chem.* **2018**, *4*, 27–45.
- (52) Schubert, M.; Waldvogel, S. R. Mo^V Reagents in Organic Synthesis. *Eur. J. Org. Chem.* **2016**, *2016*, 1921–1936.
- (53) King, B. T.; Kroulik, J.; Robertson, C. R.; Rempala, P.; Hilton, C. L.; Korinek, J. D.; Gortari, L. M. Controlling the Scholl Reaction. *J. Org. Chem.* **2007**, *72*, 2279–2288.
- (54) Zhai, L.; Shukla, R.; Wadumethrige, S. H.; Rathore, R. Probing the Arenium-Ion (Proton Transfer) Versus the Cation-Radical (Electron Transfer) Mechanism of Scholl Reaction Using DDQ as Oxidant. *J. Org. Chem.* **2010**, *75*, 4748–4760.
- (55) International Energy Agency. *Energy Access Outlook 2017: From Poverty to Prosperity*, 2017. www.iea.org/publications/freepublications/publication/WEO2017SpecialReport_EnergyAccessOutlook.pdf (accessed August 5, 2019).
- (56) European Energy Exchange AG. *Strom - Spotmarkt: Marktdaten*. <http://www.eex.com/de/marktdaten/strom>.
- (57) REN21. *Renewables 2019 Global Status Report*, 2019. www.ren21.net/wp-content/uploads/2019/05/gsr_2019_full_report_en.pdf (accessed August 5, 2019).
- (58) Malkowsky, I. M.; Griesbach, U.; Pütter, H.; Waldvogel, S. R. Unexpected Highly Chemoselective Anodicortho-Coupling Reaction of 2,4-Dimethylphenol on Boron-Doped Diamond Electrodes. *Eur. J. Org. Chem.* **2006**, *2006*, 4569–4572.
- (59) Kirste, A.; Schnakenburg, G.; Stecker, F.; Fischer, A.; Waldvogel, S. R. Anodic Phenol-Arene Cross-Coupling Reaction on Boron-Doped Diamond Electrodes. *Angew. Chem., Int. Ed.* **2010**, *49*, 971–975.
- (60) Schulz, L.; Enders, M.; Elsler, B.; Schollmeyer, D.; Dyballa, K. M.; Franke, R.; Waldvogel, S. R. Reagent- and Metal-Free Anodic C-C Cross-Coupling of Aniline Derivatives. *Angew. Chem., Int. Ed.* **2017**, *56*, 4877–4881.
- (61) Lips, S.; Wiebe, A.; Elsler, B.; Schollmeyer, D.; Dyballa, K. M.; Franke, R.; Waldvogel, S. R. Synthesis of meta-Terphenyl-2,2''-diols by Anodic C-C Cross-Coupling Reactions. *Angew. Chem., Int. Ed.* **2016**, *55*, 10872–10876.
- (62) Lips, S.; Frontana-Urbe, B. A.; Dörr, M.; Schollmeyer, D.; Franke, R.; Waldvogel, S. R. Metal- and Reagent-Free Anodic C-C Cross-Coupling of Phenols with Benzofurans Leading to a Furan Metathesis. *Chem. - Eur. J.* **2018**, *24*, 6057–6061.
- (63) Lips, S.; Schollmeyer, D.; Franke, R.; Waldvogel, S. R. Regioselective Metal- and Reagent-Free Arylation of Benzothiophenes by Dehydrogenative Electrosynthesis. *Angew. Chem., Int. Ed.* **2018**, *57*, 13325–13329.
- (64) Wiebe, A.; Lips, S.; Schollmeyer, D.; Franke, R.; Waldvogel, S. R. Single and Twofold Metal- and Reagent-Free Anodic C-C Cross-Coupling of Phenols with Thiophenes. *Angew. Chem., Int. Ed.* **2017**, *56*, 14727–14731.
- (65) Beil, S. B.; Müller, T.; Sillart, S. B.; Franzmann, P.; Bomm, A.; Holtkamp, M.; Karst, U.; Schade, W.; Waldvogel, S. R. Active Molybdenum-Based Anode for Dehydrogenative Coupling Reactions. *Angew. Chem., Int. Ed.* **2018**, *57*, 2450–2454.
- (66) Röckl, J. L.; Schollmeyer, D.; Franke, R.; Waldvogel, S. R. Dehydrogenative Anodic C–C Coupling of Phenols Exhibiting Electron-Withdrawing Groups. *Angew. Chem., Int. Ed.* **2019**, DOI: 10.1002/anie.201910077.
- (67) Morimoto, K.; Sakamoto, K.; Ohnishi, Y.; Miyamoto, T.; Ito, M.; Dohi, T.; Kita, Y. Metal-free Oxidative Para Cross-coupling of Phenols. *Chem. - Eur. J.* **2013**, *19*, 8726–8731.
- (68) Libman, A.; Shalit, H.; Vainer, Y.; Narute, S.; Kozuch, S.; Pappo, D. Synthetic and Predictive Approach to Unsymmetrical Biphenols by Iron-Catalyzed Chelated Radical-Anion Oxidative Coupling. *J. Am. Chem. Soc.* **2015**, *137*, 11453–11460.
- (69) Riehl, B.; Dyballa, K.; Franke, R.; Waldvogel, S. Electro-organic Synthesis as a Sustainable Alternative for Dehydrogenative Cross-coupling of Phenols and Naphthols. *Synthesis* **2016**, *49*, 252–259.
- (70) Elsler, B.; Wiebe, A.; Schollmeyer, D.; Dyballa, K. M.; Franke, R.; Waldvogel, S. R. Source of Selectivity in Oxidative Cross-Coupling of Aryls by Solvent Effect of 1,1,1,3,3,3-Hexafluoropropan-2-ol. *Chem. - Eur. J.* **2015**, *21*, 12321–12325.
- (71) Lips, S.; Waldvogel, S. R. Solvent-Controlled Electrochemical Arylation Reaction. *Chem. Chem. Ind.* **2019**, *72*, 476–479.
- (72) Colomer, I.; Chamberlain, A. E. R.; Haughey, M. B.; Donohoe, T. J. Hexafluoroisopropanol as a Highly Versatile Solvent. *Nat. Rev. Chem.* **2017**, *1*, 18.
- (73) Sinha, S. K.; Bhattacharya, T.; Maiti, D. Role of Hexafluoroisopropanol in C-H Activation. *React. Chem. Eng.* **2019**, *4*, 244–253.
- (74) Ebersson, L.; Hartshorn, M. P.; Persson, O. 1,1,1,3,3,3-Hexafluoropropan-2-ol as a Solvent for the Generation of Highly Persistent Radical Cations. *J. Chem. Soc., Perkin Trans. 2* **1995**, *2*, 1735–1744.
- (75) Dohi, T.; Yamaoka, N.; Kita, Y. Fluoroalcohols: Versatile Solvents in Hypervalent Iodine Chemistry and Syntheses of Diaryliodonium(III) Salts. *Tetrahedron* **2010**, *66*, 5775–5785.
- (76) Kirste, A.; Nieger, M.; Malkowsky, I. M.; Stecker, F.; Fischer, A.; Waldvogel, S. R. Ortho-Selective Phenol-Coupling Reaction by Anodic

Treatment on Boron-Doped Diamond Electrode Using Fluorinated Alcohols. *Chem. - Eur. J.* **2009**, *15*, 2273–2277.

(77) Waldvogel, S. R. Novel Anodic Concepts for the Selective Phenol Coupling Reaction. *Pure Appl. Chem.* **2010**, *82*, 1055–1063.

(78) Hollóczki, O.; Berkessel, A.; Mars, J.; Mezger, M.; Wiebe, A.; Waldvogel, S. R.; Kirchner, B. The Catalytic Effect of Fluoroalcohol Mixtures Depends on Domain Formation. *ACS Catal.* **2017**, *7*, 1846–1852.

(79) Hollóczki, O.; Macchieraldo, R.; Gleede, B.; Waldvogel, S. R.; Kirchner, B. Interfacial Domain Formation Enhances Electrochemical Synthesis. *J. Phys. Chem. Lett.* **2019**, *10*, 1192–1197.

(80) Malkowsky, I. M.; Rommel, C. E.; Wedeking, K.; Fröhlich, R.; Bergander, K.; Nieger, M.; Quaiser, C.; Griesbach, U.; Pütter, H.; Waldvogel, S. R. Facile and Highly Diastereoselective Formation of a Novel Pentacyclic Scaffold by Direct Anodic Oxidation of 2,4-Dimethylphenol. *Eur. J. Org. Chem.* **2006**, *2006*, 241–245.

(81) Barjau, J.; Schnakenburg, G.; Waldvogel, S. R. Diversity-oriented Synthesis of Polycyclic Scaffolds by Modification of an Anodic Product Derived from 2,4-Dimethylphenol. *Angew. Chem., Int. Ed.* **2011**, *50*, 1415–1419.

(82) Barjau, J.; Königs, P.; Kataeva, O.; Waldvogel, S. Reinvestigation of Highly Diastereoselective Pentacyclic Spirolactone Formation by Direct Anodic Oxidation of 2,4-Dimethylphenol. *Synlett* **2008**, *2008*, 2309–2312.

(83) Barjau, J.; Schnakenburg, G.; Waldvogel, S. Short Domino Sequence to Dioxo[4.3.3]propellanes. *Synthesis* **2011**, *2011*, 2054–2061.

(84) Barjau, J.; Fleischhauer, J.; Schnakenburg, G.; Waldvogel, S. R. Installation of Amine Moieties into a Polycyclic Anodic Product Derived from 2,4-Dimethylphenol. *Chem. - Eur. J.* **2011**, *17*, 14785–14791.

(85) Mirion, M.; Andernach, L.; Stobe, C.; Barjau, J.; Schollmeyer, D.; Opatz, T.; Lützen, A.; Waldvogel, S. R. Synthesis and Isolation of Enantiomerically Enriched Cyclopenta[*b*]benzofurans Based on Products from Anodic Oxidation of 2,4-Dimethylphenol. *Eur. J. Org. Chem.* **2015**, *2015*, 4876–4882.

(86) Malkowsky, I. M.; Rommel, C. E.; Fröhlich, R.; Griesbach, U.; Pütter, H.; Waldvogel, S. R. Novel Template-Directed Anodic Phenol-Coupling Reaction. *Chem. - Eur. J.* **2006**, *12*, 7482–7488.

(87) Griesbach, U.; Pütter, H.; Waldvogel, S. R.; Malkowsky, I. M. Anodic Dimerisation of Hydroxy-Substituted Aromatics. Patent WO 2006077204 A2, January 16, 2006.

(88) Dahms, B.; Kohlpaintner, P. J.; Wiebe, A.; Breinbauer, R.; Schollmeyer, D.; Waldvogel, S. R. Selective Formation of 4,4'-Biphenols by Anodic Dehydrogenative Cross- and Homo-Coupling Reaction. *Chem. - Eur. J.* **2019**, *25*, 2713–2716.

(89) Orner, B. P.; Ernst, J. T.; Hamilton, A. D. Toward Proteomimetics: Terphenyl Derivatives as Structural and Functional Mimics of Extended Regions of an α -Helix. *J. Am. Chem. Soc.* **2001**, *123*, 5382–5383.

(90) Cummings, C. G.; Hamilton, A. D. Disrupting Protein-Protein Interactions with Non-Peptidic, Small Molecule Alpha-Helix Mimetics. *Curr. Opin. Chem. Biol.* **2010**, *14*, 341–346.

(91) Elsler, B.; Schollmeyer, D.; Dyballa, K. M.; Franke, R.; Waldvogel, S. R. Metal- and Reagent-Free Highly Selective Anodic Cross-Coupling Reaction of Phenols. *Angew. Chem., Int. Ed.* **2014**, *53*, 5210–5213.

(92) Wiebe, A.; Schollmeyer, D.; Dyballa, K. M.; Franke, R.; Waldvogel, S. R. Selective Synthesis of Partially Protected Non-symmetric Biphenols by Reagent- and Metal-Free Anodic Cross-Coupling Reaction. *Angew. Chem., Int. Ed.* **2016**, *55*, 11801–11805.

(93) Lips, S.; Franke, R.; Waldvogel, S. R. Electrochemical Synthesis of 2-Hydroxy-para-Terphenyls by Dehydrogenative Anodic C-C Cross-Coupling Reaction. *Synlett* **2019**, *30*, 1174–1177.

(94) Morales-Morales, D. *Pincer Compounds: Chemistry and Applications*, 1st ed.; Elsevier: Amsterdam, 2018.

(95) Kittel, H. Pigmente, Füllstoffe und Farbmeterik. In *Lehrbuch der Lacke und Beschichtungen*, 2nd ed.; Spille, J., Ed.; Lehrbuch der Lacke und Beschichtungen 5 Bd.; S. Hirzel: Stuttgart, Leipzig, 2003.

(96) Dyballa, K. M.; Franke, R.; Fridag, D.; Waldvogel, S. R. Electrochemical Method for Coupling Phenol to Aniline. Patent WO 2014135371 A1, September 12, 2014.

(97) Dahms, B.; Franke, R.; Waldvogel, S. R. Metal- and Reagent-Free Anodic Dehydrogenative Cross-Coupling of Naphthylamines with Phenols. *ChemElectroChem* **2018**, *5*, 1249–1252.

(98) Schulz, L.; Franke, R.; Waldvogel, S. R. Direct Anodic Dehydrogenative Cross- and Homo-Coupling of Formanilides. *ChemElectroChem* **2018**, *5*, 2069–2072.

(99) Hu, T.; Li, Y.-G.; Li, Y.-S.; Hu, N.-H. Novel Highly Active Binuclear Neutral Nickel and Palladium Complexes as Precatalysts for Norbornene Polymerization. *J. Mol. Catal. A: Chem.* **2006**, *253*, 155–164.

(100) Zhang, H.-C.; Huang, W.-S.; Pu, L. Biaryl-Based Macrocyclic and Polymeric Chiral (Salophen)Ni(II) Complexes: Synthesis and Spectroscopic Study. *J. Org. Chem.* **2001**, *66*, 481–487.



Chemistry A European Journal

 **Chemistry
Europe**
European Chemical
Societies Publishing

Accepted Article

Title: Electrochemical C-H Functionalization of (Hetero)Arenes –
Optimized by DoE

Authors: Siegfried R Waldvogel, Maurice Dörr, Johannes Röckl, Jonas
Rein, and Dieter Schollmeyer

This manuscript has been accepted after peer review and appears as an Accepted Article online prior to editing, proofing, and formal publication of the final Version of Record (VoR). This work is currently citable by using the Digital Object Identifier (DOI) given below. The VoR will be published online in Early View as soon as possible and may be different to this Accepted Article as a result of editing. Readers should obtain the VoR from the journal website shown below when it is published to ensure accuracy of information. The authors are responsible for the content of this Accepted Article.

To be cited as: *Chem. Eur. J.* 10.1002/chem.202001171

Link to VoR: <https://doi.org/10.1002/chem.202001171>

WILEY-VCH

COMMUNICATION

Electrochemical C-H Functionalization of (Hetero)Arenes – Optimized by DoE

Maurice Dörr,^{[a]†} Johannes L. Röckl,^{[a,b]†} Jonas Rein,^[a] Dieter Schollmeyer,^[a] Siegfried R. Waldvogel^{*[a,b]}

[a] M. Dörr, J. L. Röckl, J. Rein, Prof. Dr. S. R. Waldvogel
Department of Chemistry
Johannes Gutenberg University Mainz
Duesbergweg 10–14, 55128 Mainz (Germany)
E-mail: waldvogel@uni-mainz.de
Homepage: <https://www.aksw.uni-mainz.de>

[b] J. L. Röckl, Prof. Dr. S. R. Waldvogel
Graduate School Materials Science in Mainz
Staudingerweg 9, 55128 Mainz (Germany)

[†] These authors contributed equally to this work.

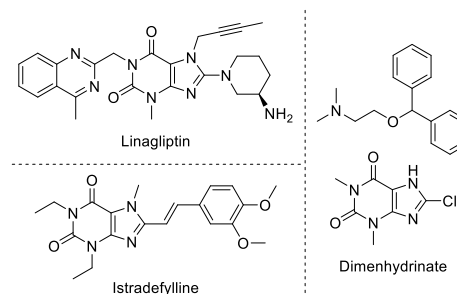
Supporting information for this article is given via a link at the end of the document.

Abstract: A novel approach towards the activation of different arenes and purines including caffeine and theophylline is presented. The simple, safe and scalable electrochemical synthesis of 1,1,1,3,3,3-hexafluoroisopropanol (HFIP) aryl ethers was conducted using an easy electrolysis setup with boron-doped diamond (BDD) electrodes. Good yields up to 59% were achieved. Triethylamine was used as a base as it forms a highly conductive media with HFIP, making additional supporting electrolytes superfluous. The synthesis was optimized using Design of Experiment techniques giving a detailed insight to the significance of the reaction parameters. The mechanism was investigated by cyclic voltammetry (CV). Subsequent transition metal-catalyzed as well as metal-free functionalization led to interesting motifs in excellent yields up to 94%.

Cross-coupling reactions represent a very important synthetic tool used for the formation of aryl-carbon or aryl-heteroatom bonds. Substantial efforts have been taken to develop simple and sustainable reactions of this kind, using methods like electrochemistry^{[1]–[8]} or photoredox catalysis.^[9] However, transition metal catalysis remains dominant in the field of cross-coupling reactions,^[10] despite that often it requires synthesis of precursors to introduce e.g. halides or pseudohalides. Furthermore, the costs rise for Rh, Pd or Pt constantly and strongly, which further increases the desire to avoid transition metals in organic synthesis.^[11] The high selectivity and efficiency of the cross-coupling reaction itself might be diminished by the lack of selectivity and the use of partly hazardous reagents such as bromine, chlorinating agents, trifluoromethanesulfonic anhydride or tosyl chloride during the pre-functionalization.^[12] Besides the risks associated with handling such compounds, they generate stoichiometric amounts of reagent waste. In the case of direct oxidative cross-coupling reactions, pre-functionalization is not necessary but stoichiometric amounts of an oxidizer must be used, again resulting in stoichiometric amounts of reagent waste.^[13] Electro-organic synthesis, on the other hand, fulfills many of the green chemistry postulates and uses only electrons as an inherently clean reactant, hence minimizing reagent waste to a certain degree.^{[1]–[8],[14]} Furthermore, it offers safe-to-conduct protocols and simple cell setups. Combining the benefits of both worlds we designed an electrochemical protocol for the pre-

functionalization of different aromatic compounds for a subsequent metal-free or Ni- or Pd-catalyzed cross-coupling reaction. The electroorganic reactions conducted in simple beaker type cells left many parameters to optimize. Using a simple but not very efficient one-variable-at-a-time approach (OVAT) does not always lead to satisfying results. Design of Experiment techniques provide high quality information from a comparably low number of experiments.^{[15],[16],[17]} In order to make this efficient, an appropriate screening tool is required, providing good quality results with sufficient accuracy.^[18] In our previous work, benzylic C-H functionalization using HFIP as both solvent and reagent was reported.^{[19]–[22]} In addition, our group has a long-standing interest in using HFIP based electrolytes in electro-organic synthesis, since unique reactivity can be attributed to solvent effects and stabilization of intermediates.^{[5],[23]} In the work described here, the scope of the reaction has been successfully expanded to further aromatic compounds using a DoE approach, demonstrating the broad applicability of this method.

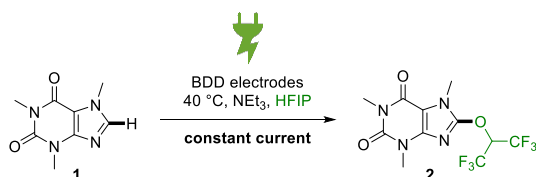
The functionalization of xanthine derivatives like caffeine or theophylline is of great interest for the development of pharmaceuticals.^[24] The examples shown in Scheme 1 are approved drugs used for the treatment of type II diabetes (Linagliptin)^[25] and Parkinson's disease (Istradefylline)^{[26],[27]} or to prevent postoperative vomiting and symptoms of motion sickness (Dimenhydrinate)^{[28],[29]}. Lei et al. recently demonstrated the electrochemical oxidative functionalization of caffeine.^[30]



Scheme 1. Xanthine derived pharmaceuticals functionalized in position 8 of the purine scaffold.^{[25]–[29]}

COMMUNICATION

We present the activation of position 8 of the purine scaffold in caffeine and theophylline, as well as derivatization of naphthalene and aromatic acetamides by installation of the 1,1,1,3,3,3-hexafluoroisopropoxide moiety (HFIP). Furthermore, the resulting HFIP ethers were amenable to subsequent derivatization by metal-catalyzed as well as metal-free nucleophilic substitution reactions. The first electrochemical step is easy to conduct, free from metals, does not require inert conditions and the substrates used are readily available, making this method cost-efficient, simple and quick (Scheme 2). The screening was conducted in undivided cells made of PTFE equipped with two BDD electrodes. This allows for the parallel operation of 8. The limited number of electrolysis cells is rewarded by highly accurate electrochemical data.^[18]



Scheme 2. Constant current electrolysis of caffeine. The oxidative peak potentials are 1.80 V for **1** and 1.60 V for **2** vs. Ag/AgCl, respectively (see Supporting Information).

The electrochemical installation of alcohols to arenes involves a major challenge, due to the electron-releasing properties of the ether moiety. Cyclic voltammetry studies have revealed the mechanism to be of the ECEC type (see Supporting Information) and the products were found to have a lower redox potential than the starting materials. Therefore, over-oxidation is a significant problem, hence careful optimization of the reaction conditions is needed. The caffeine HFIP ether synthesis was first optimized in initial screening reactions using an OVAT approach. The isolated yield of **2** was 33% by these conditions. With the aim of increasing the yield and to obtain detailed information about the importance of the parameters investigated, we turned to a DoE approach and started with a 2^{5-1} -plan with a center point added.^{[15],[17]} The yields during the optimization were determined by qNMR using 1,3,5-trimethoxybenzene as an internal standard. The factors examined and their settings are shown in Table 1.

Table 1. Factors used in the initial 2^{5-1} -plan.

factor	- (lower level)	0 (center point)	+ (upper level)
v_{stirrer} / rpm	200	300	400
c_{caffeine} / $\frac{\text{mol}}{\text{L}}$	0.15	0.25	0.20
c_{NEt_3} / $\frac{\text{mol}}{\text{L}}$	0.10	0.20	0.15
Q / F	2.50	2.0	2.25
j / $\frac{\text{mA}}{\text{cm}^2}$	30	45	60

v_{stirrer} is the stirring rate, c_{caffeine} and c_{NEt_3} are the concentrations of caffeine and NEt₃, Q is the amount of charge and j is the current density.

It was observed that the current density, the stirring rate and the concentration of caffeine were significant for the yield in this area of the experimental space. With the best settings being the

low current density, high stirring rate and high concentration. The yield at the center point did not indicate any curvature, so we did not expect to be close to the maximum yet. With the obtained data a second plan was designed with these three significant factors and, considering that the reaction is electrochemically driven, the amount of charge was taken into consideration. A 2^{4-1} -plan was conducted and analysed. This time the center point did not match the linear model and hence indicated curvature in the yield in this area of the experimental space. Star points were added to convert this plan into a central composite design (CCD).^{[15],[17]} From the results it could be seen that a maximum was reached regarding the amount of charge Q and the current density j . The optimal conditions in this area were found using the *Response Optimizer* in *Minitab*.

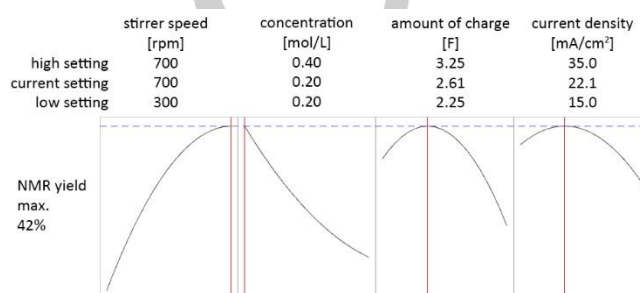


Figure 1. Minitab's *Response Optimizer* was used to maximize the yield from the model obtained through a CCD plan. The predicted yield was 42%. The labelling was rearranged for better readability.

The result shown in Figure 1 indicates that an increase in stirring rate and a decrease in concentration would improve the yield even further. Due to the high stirring rates we experienced a lot of failures, so we used the conditions from this step (**conditions b**) for all further reactions. This is discussed in more detail in the supporting information. To verify the model, we isolated **2** using these conditions and obtained exactly 42% yield.

Table 2. Comparison between the results of the optimization processes.

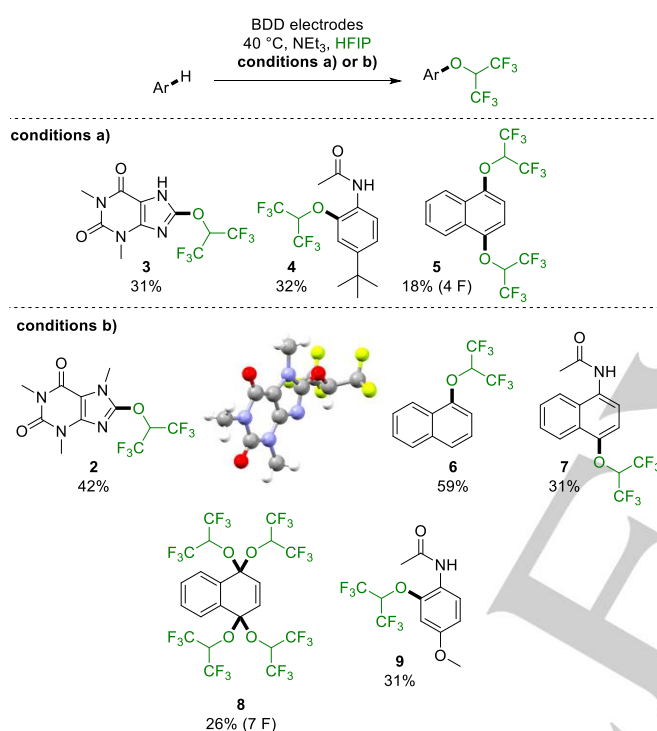
	conditions a) OVAT optimized	conditions b) DoE optimized
j / $\frac{\text{mA}}{\text{cm}^2}$	7.2	22.1
Q / F	2	2.61
v_{stirrer} / rpm	300	700
c_{caffeine} / $\frac{\text{mol}}{\text{L}}$	0.25	0.2
c_{NEt_3} / $\frac{\text{mol}}{\text{L}}$	0.1	0.2
electrolysis time	5 h 10 min	1 h 45 min
product	0.41 mmol	0.42 mmol
Isolated yield	33%	42%

Comparing **conditions a**) and **b**), significant improvements introduced by the optimization via DoE are apparent. The time needed for the electrolysis dropped to about one third and at the same time, the isolated yield increased by 9%. The significant influence of the stirring rate on the reaction suggests that convection was crucial. Therefore, the setup was changed to

COMMUNICATION

investigate temperature, electrode distance and stirring rate more effectively. With these parameters, a 2³-plan and a subsequent 2²-plan excluding electrode distance (see Supporting Information) was explored. This way we were able to isolate **2** in 45% yield in a 10 mmol scale. The larger cell setup for these plans demonstrated the scalability of the electrolysis and considering a few parameters during the scale-up, the yield could even be improved further. Besides using a different batch setup, we tried to bypass the problem of over-oxidation using a flow setup but the yields obtained could not meet those of the batch electrolyses.^[31]

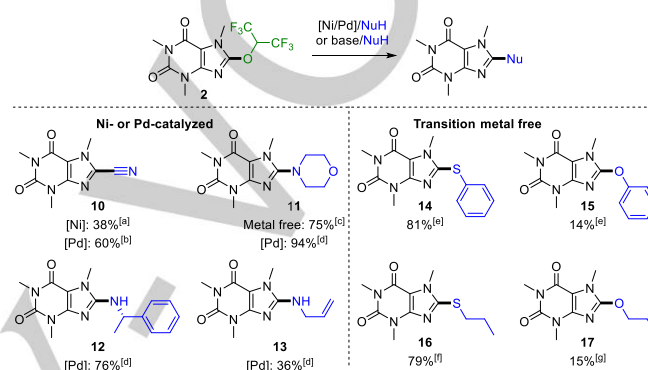
The scope was extended conducting reactions on a 1.00 to 1.25 mmol scale and both **conditions a)** and **b)** (see Table 2) were investigated. Improved results with yields up to 59% could be achieved (Scheme 3).



Scheme 3. Scope of the reaction and yields of the isolated products. The conditions working better are displayed.

As shown in previous work, the HFIP moiety can be used as a leaving group.^{[20],[21]} We wanted to show that this strategy can also be applied to arenes and therefore various functionalization reactions were conducted. Cyanides could be installed by transition metal-catalysis using nickel or palladium in 38% and 60% yield, respectively. Metal-free cyanation was not possible in this case. Also, higher yields were achieved in amination reactions with morpholine (**11**), when Pd was used (94% vs. 75%). Allylic amine (**13**) and benzylic amine (**12**) provided yields up to 76%. The direct metal-free reaction with thiophenol (**14**) and propane-1-thiol (**16**) with **2** gave high yields up to 81%. Application of the respective oxygen derivatives such as phenol and propan-1-ol yielded the desired ethers in up to 15% yield. When submitting **8** to *Kumada*-type couplings only small amounts of desired product could be detected. Other transition metal-catalyzed did not deliver the desired product.

In conclusion, we expanded the scope of the electroorganic synthesis of aryl HFIP ethers from our previous work to heterocycles. Key for these conversions is the amine-HFIP electrolyte.^{[19]–[21]} In addition, the value of these intermediates was demonstrated in the activation within subsequent reactions. A sustainable alternative to common pre-functionalization using hazardous compounds was presented. A DoE approach led to efficient optimization with mild reaction conditions, and shorter electrolysis times across a range of substrates. The subsequent reactions of the caffeyl HFIP ether gave access to various functionalized caffeine derivatives.



Scheme 4. Scope of the reaction of the caffeyl HFIP ether and yields of the isolated products. [a] NiCl₂(PPh₃)₂ (10 mol%), PPh₃ (20 mol%), KCN (4 eq.), Zn (1 eq.) in DMF 115 °C, 4 h; [b] Pd(OAc)₂ (5 mol%), XantPhos (10 mol%), KCN (1.5 eq), DMF, 85 °C, 14 h; [c] Pd(OAc)₂ (5 mol%), XantPhos (10 mol%), amine (2.0 - 3.0 eq), DMA, 100 °C, 3-14 h; [d] amine (3.0 eq), DMA, 100 °C, 14 h; [e] Cs₂CO₃ (3.0 eq), phenol/thiophenol (2.0 eq.), DMF, r.t. [f] NaOH (15 eq.) in propan-1-ol/water 1/3, 60 °C, 2 h; [g] K₂CO₃ (3.0 eq.), propan-1-thiol (2.0 eq.), in DMF, 65 °C, 2h;

Experimental Section

Detailed information on general procedures, electrolytic conversions and product characterization can be found in the Supporting Information.

Acknowledgements

J. L. Röckl is a recipient of a DFG fellowship through the Excellence Initiative by the Graduate School Materials Science in Mainz (GSC 266). J. Rein is a recipient of an undergraduate Scholarship by the Heinrich Böll Foundation. Support of the Advanced Lab of Electrochemistry and Electrosynthesis – ELYSION (Carl-Zeiss-Stiftung) is gratefully acknowledged.

Keywords: electrolysis • CH functionalization • anode • boron-doped diamond • caffeine

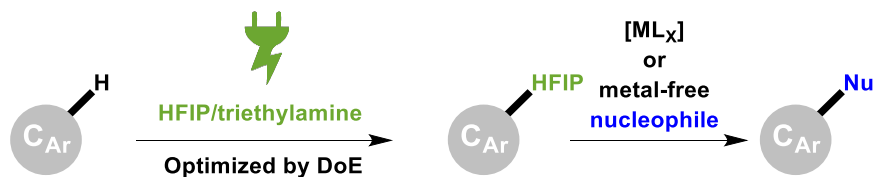
- [1] E. J. Horn, B. R. Rosen, P. S. Baran, *ACS Cent. Sci.* **2016**, *2*, 302–308.
 [2] M. D. Kärkäs, *Chem. Soc. Rev.* **2018**, *47*, 5786–5865.
 [3] S. Möhle, M. Zirbes, E. Rodrigo, T. Gieshoff, A. Wiebe, S. R. Waldvogel, *Angew. Chem. Int. Ed.* **2018**, *57*, 6018–6041; *Angew. Chem.* **2018**, *130*, 6124–6149.

COMMUNICATION

- [4] J. L. Röckl, D. Pollok, R. Franke, S. R. Waldvogel, *Acc. Chem. Res.* **2020**, *53*, 45–61.
- [5] S. R. Waldvogel, S. Lips, M. Selt, B. Riehl, C. J. Kampf, *Chem. Rev.* **2018**, *118*, 6706–6765.
- [6] A. Wiebe, T. Gieshoff, S. Möhle, E. Rodrigo, M. Zirbes, S. R. Waldvogel, *Angew. Chem. Int. Ed.* **2018**, *57*, 5594–5619; *Angew. Chem.* **2018**, *130*, 5694–5721.
- [7] M. Yan, Y. Kawamata, P. S. Baran, *Chem. Rev.* **2017**, *117*, 13230–13319.
- [8] Y. Yang, J. Lan, J. You, *Chem. Rev.* **2017**, *117*, 8787–8863.
- [9] a) N. A. Romero, D. A. Nicewicz, *Chem. Rev.* **2016**, *116*, 10075–10166; b) S. Fukuzumi, K. Ohkubo, *Org. Biomol. Chem.* **2014**, *12*, 6059–6071; c) Y. Xi, H. Yi, A. Lei, *Org. Biomol. Chem.* **2013**, *11*, 2387–2403; d) D. A. Nicewicz, T. M. Nguyen, *ACS Catal.* **2014**, *4*, 355–360; e) B. M. Hockin, C. Li, N. Robertson, E. Zysman-Colman, *Catal. Sci. Technol.* **2019**, *9*, 889–915.
- [10] a) C. C. C. Johansson Seechurn, M. O. Kitching, T. J. Colacot, V. Snieckus, *Angew. Chem. Int. Ed.* **2012**, *51*, 5062–5085; *Angew. Chem.* **2012**, *124*, 5150–5174.; b) Q. Zeng, L. Zhang, Y. Zhou, *Chem. Rec.* **2018**, *18*, 1278–1291; c) Y. Yang, J. Lan, J. You, *Chem. Rev.* **2017**, *117*, 8787–8863.
- [11] "Precious Metal Trading", zu finden unter https://pm-prices.heraeus.com/Heraeus_CurrentPrices.aspx, **2020**. Zuletzt geprüft am 03.03.2020.
- [12] a) J. P. Wolfe, S. Wagaw, J.-F. Marcoux, S. L. Buchwald, *Acc. Chem. Res.* **1998**, *31*, 805–818; b) J. F. Hartwig, *Acc. Chem. Res.* **1998**, *31*, 852–860; c) N. Miyaura, A. Suzuki, *Chem. Rev.* **1995**, *95*, 2457–2483; d) K. Tamao, K. Sumitani, M. Kumada, *J. Am. Chem. Soc.* **1972**, *94*, 4374–4376; e) A. O. King, N. Okukado, E.-i. Negishi, *J. Chem. Soc., Chem. Commun.* **1977**, 683; f) N. Miyaura, A. Suzuki, *J. Chem. Soc., Chem. Commun.* **1979**, 866; g) J. F. Hartwig, *Pure Appl. Chem.* **1999**, *71*, 1417–1423; h) N. Miyaura, K. Yamada, A. Suzuki, *Tetrahedron Lett.* **1979**, *20*, 3437–3440.
- [13] a) Y. Cheng, Y. Wu, G. Tan, J. You, *Angew. Chem. Int. Ed.* **2016**, *55*, 12275–12279; b) J. Dong, Z. Long, F. Song, N. Wu, Q. Guo, J. Lan, J. You, *Angew. Chem. Int. Ed.* **2013**, *52*, 580–584; c) P. Xi, F. Yang, S. Qin, D. Zhao, J. Lan, G. Gao, C. Hu, J. You, *J. Am. Chem. Soc.* **2010**, *132*, 1822–1824.
- [14] B. A. Frontana-Urbe, R. D. Little, J. G. Ibanez, A. Palma, R. Vasquez-Medrano, *Green Chem.* **2010**, *12*, 2099.
- [15] R. Lee, *Chem. Ing. Tech.* **2019**, *91*, 191–200.
- [16] a) R. Möckel, J. Hille, E. Winterling, S. Weidemüller, T. M. Faber, G. Hilt, *Angew. Chem. Int. Ed.* **2018**, *57*, 442–445; *Angew. Chem.* **2018**, *130*, 450–454.; b) P. M. Murray, F. Bellany, L. Benhamou, D.-K. Bučar, A. B. Tabor, T. D. Sheppard, *Org. Biomol. Chem.* **2016**, *14*, 2373–2384; c) X. Zhang, R. Wang, X. Yang, J. Yu, *Chemom. Intell. Lab. Syst.* **2007**, *89*, 45–50; d) S. A. Weissman, N. G. Anderson, *Org. Process Res. Dev.* **2015**, *19*, 1605–1633; e) P. Renzi, M. Bella, *Synlett* **2017**, *28*, 306–315.
- [17] R. Leardi, *Anal. Chim. Acta* **2009**, *652*, 161–172.
- [18] C. Gütz, B. Klöckner, S. R. Waldvogel, *Org. Process Res. Dev.* **2016**, *20*, 26–32.
- [19] J. L. Röckl, A. V. Hauck, D. Schollmeyer, S. R. Waldvogel, *ChemistryOpen* **2019**, *8*, 1167–1171.
- [20] J. L. Röckl, Y. Imada, K. Chiba, R. Franke, S. R. Waldvogel, *ChemElectroChem* **2019**, *6*, 4184–4187.
- [21] Y. Imada, J. L. Röckl, A. Wiebe, T. Gieshoff, D. Schollmeyer, K. Chiba, R. Franke, S. R. Waldvogel, *Angew. Chem. Int. Ed.* **2018**, *57*, 12136–12140; *Angew. Chem.* **2018**, *130*, 12312–12317.
- [22] T. Gieshoff, A. Kehl, D. Schollmeyer, K. D. Moeller, S. R. Waldvogel, *J. Am. Chem. Soc.* **2017**, *139*, 12317–12324.
- [23] a) A. Wiebe, S. Lips, D. Schollmeyer, R. Franke, S. R. Waldvogel, *Angew. Chem. Int. Ed.* **2017**, *56*, 14727–14731; *Angew. Chem.* **2017**, *129*, 14920–14925.; b) T. Gieshoff, D. Schollmeyer, S. R. Waldvogel, *Angew. Chem. Int. Ed.* **2016**, *55*, 9437–9440; *Angew. Chem.* **2016**, *128*, 9587–9590.; c) T. Gieshoff, A. Kehl, D. Schollmeyer, K. D. Moeller, S. R. Waldvogel, *Chem. Commun.* **2017**, *53*, 2974–2977; d) B. Elsler, A. Wiebe, D. Schollmeyer, K. M. Dyballa, R. Franke, S. R. Waldvogel, *Chem. Eur. J.* **2015**, *21*, 12321–12325; e) A. Kehl, T. Gieshoff, D. Schollmeyer, S. R. Waldvogel, *Chem. Eur. J.* **2018**, *24*, 590–593; f) P. Franzmann, S. B. Beil, D. Schollmeyer, S. R. Waldvogel, *Chem. Eur. J.* **2019**, *25*, 1936–1940; g) O. Hollóczki, R. Macchieraldo, B. Gleede, S. R. Waldvogel, B. Kirchner, *J. Phys. Chem. Lett.* **2019**, *10*, 1192–1197; h) V. M. Breising, T. Gieshoff, A. Kehl, V. Kilian, D. Schollmeyer, S. R. Waldvogel, *Org. Lett.* **2018**, *20*, 6785–6788; i) O. Hollóczki, A. Berkessel, J. Mars, M. Mezger, A. Wiebe, S. R. Waldvogel, B. Kirchner, *ACS Catal.* **2017**, *7*, 1846–1852; j) L. Schulz, S. Waldvogel, *Synlett* **2019**, *30*, 275–286; k) M. Selt, S. Mentizi, D. Schollmeyer, R. Franke, S. R. Waldvogel, *Synlett* **2019**, *30*, 2062–2067.
- [24] N. Singh, A. K. Shreshtha, M. S. Thakur, S. Patra, *Heliyon* **2018**, *4*, e00829.
- [25] T. Forst, A. Pfützner, *Expert Opin. Pharmacother.* **2012**, *13*, 101–110.
- [26] R. Dungo, E. D. Deeks, *Drugs* **2013**, *73*, 875–882.
- [27] M. Takahashi, M. Fujita, N. Asai, M. Saki, A. Mori, *Expert Opin. Pharmacother.* **2018**, *19*, 1635–1642.
- [28] C. K. Özkan, U. Taşdemir, Ç. Taş, A. Savaşer, H. Erol, Y. Özkan, *Chromatographia* **2013**, *76*, 1521–1525.
- [29] A. Halpert, *Neurosci. Biobehav. Rev.* **2002**, *26*, 61–67.
- [30] X. - A. Liang, D. Liu, H. Sun, C. Jiang, H. Chen, L. Niu, K. Mahato, T. Abdellilah, H. Zhang, A. Lei, *Adv. Synth. Catal.* **2020**, *51*, 83.
- [31] F. Xu, X.-Y. Qian, Y.-J. Li, H.-C. Xu, *Org. Lett.* **2017**, *19*, 6332–6335.

COMMUNICATION

Entry for the Table of Contents



An alternative route for the activation of different arenes including caffeine and theophylline, optimized by design of experiment techniques is presented. We provide a simple electroorganic protocol using BDD electrodes in undivided cells for the synthesis of aryl 1,1,1,3,3,3-hexafluoroisopropyl ethers. The value of these fluorinated ethers for subsequent functionalization with a variety of nucleophiles has been proved.

Contents

1	GENERAL METHODS.....	1
2	KINETIC AND MECHANISTIC CONSIDERATIONS	6
3	OPTIMIZATION BY DESIGN OF EXPERIMENT	12
4	GENERAL PROTOCOLS.....	27
5	SYNTHESIS.....	28
6	REFERENCES	47
7	¹H, ¹³C AND ¹⁹F NMR SPECTRA	48

1 General Methods

1.1 Gas Chromatography (GC/GC-MS)

Crude reaction mixtures and purified products were analyzed by gas chromatography (GC) with a GC-2010 (*Shimadzu*, Kyōto, Japan). A quartz capillary column ZB-5 (length: 30 cm, inner diameter: 0.25 mm, layer thickness of stationary phase: 0.25 μm, carrier gas: hydrogen, stationary phase: (5%-phenyl)-methylpolysiloxane (*Phenomenex*, Torrance, USA) was used. The carrier gas rate was 45.5 cm·s⁻¹ and the injection temperature 250 °C. A flame ionization detector (FID) with an inlet temperature of 310 °C was used.

Further analysis by gas chromatography mass spectra (GC-MS) using a GC-2010 with a similar column, combined with a GC-MS-QP2010 (*Shimadzu*, Kyōto, Japan) detector with an injection temperature of 250 °C and detection inlet temperature of 310 °C was conducted.

All chromatographic data was recorded using the method “*hart*”, which starts at 50 °C with a heating rate of 15 °C·min⁻¹ to 290 °C which is held for 8 min.

1.2 Liquid Chromatography

Thin layer chromatography (TLC) was performed with “DC Kieselgel 60 F₂₅₄” (*Merck KGaA*, Darmstadt, Germany) on aluminum plates and an UV lamp ($\lambda = 254$ nm, NU-4 KL, Benda, Wiesloch, Germany). No stain was utilized as all starting materials and products absorbed in the UV light at $\lambda = 254$ nm. An automatic silica flash column chromatography system with a control unit C-620, a fraction collector C-666 and a UV photometer C-635 (*Büchi*, Flawil, Switzerland) was used for all isolations. Silica gel 60 M (0.040 – 0.063 mm, *Macherey-Nagel GmbH & Co.*, Düren, Germany) was used as the stationary phase. Cyclohexane and ethyl acetate or dichloromethane and methanol were used as eluents.

The system connected to a computer and controlled with the software *BÜCHI Sepacore Control 1.2 Standard Edition*.

1.3 High Resolution Mass Spectrometry

High resolution electrospray ionization mass spectrometry (HR-ESI) and high resolution atmospheric pressure chemical ionization (HR-APCI) was performed using an Agilent 6545 QTOF-MS (*Agilent*, Santa Clara, USA). The data given displays the mass-charge-ratio (m/z) of the corresponding compounds.

1.4 NMR Spectroscopy

Nuclear magnetic resonance spectroscopy (NMR) was measured using a multi nuclear magnetic resonance spectrometer Bruker Avance III HD 400 (400 MHz) (5 mm BBFO-SmartProbe with z gradient and ATM, *SampleXPress* 60 sample changer, Analytische Messtechnik, Karlsruhe, Germany). The chemical shifts (δ) are reported in parts per million (ppm) relative to the residue signal of the deuterated solvent (CDCl_3 or $\text{DMSO-}d_6$) used for the measurements by the solvent data chart from Cambridge Isotopes Laboratories, USA. For the ^{19}F spectra, ethyl fluoroacetate served as external standard ($\delta = -231.1\text{ppm}$).

The evaluations of ^1H and ^{13}C were executed using the software MestReNova 10.0.1-14719 (*Mestrelab Research S.L.*, Spain) with the assistance of H,H -COSY, C,H -HSQC and C,H -HMBC experiments. The multiplicity of the signals were abbreviated in the following manner: s (singlet), d (doublet), t (triplet), hept (heptet) pseudo-quart (pseudo-quartet), pseudo-quint (pseudo-quintet), m (multiplet), dd (doublet of doublets), ddd (doublet of doublets of doublets). The coupling constants J have been given in Hertz (Hz).

1.5 Melting Point

The melting ranges of purified products were measured using M-565 (*Büchi*, Flawil, Switzerland) with a heating rate of 2 °C·min⁻¹. The given melting ranges are not further corrected.

1.6 Cyclic voltammetry

Cyclic voltammetry (CV) was performed with a Metrohm 663 VA Stand equipped with a μ Autolab type III potentiostat (*Metrohm AG*, Herisau, Switzerland). Working electrode: BDD electrode tip, 2 mm diameter; counter electrode: glassy carbon rod; reference electrode: Ag/AgCl in saturated LiCl/EtOH. Solvent: HFIP, scan rate (unless stated otherwise) $v = 100$ mV/s, $T = 20$ °C, $c = 5$ mM, supporting electrolyte (if used): n-Bu₃NMe O₃SOMe (MTBS), $c(\text{MTBS}) = 90$ mM.

1.7 X-ray Analysis

All data were collected on a STOE IPDS2T diffractometer (*Oxford Cryostream 700er series*, *Oxford Cryosystems*, Oxford, United Kingdom) using graphite monochromated Mo K α radiation ($\lambda = 0.71073$ Å). Intensities were measured using fine-slicing ω and φ -scans and corrected for background, polarization and Lorentz effects. The structures were solved by direct methods and refined anisotropically by the least-squares procedure implemented in the SHELX program system.

The supplementary crystallographic data for this paper can be obtained free of charge from The Cambridge Crystallographic Data Center via www.ccdc.cam.ac.uk/data_request/cif. Deposition numbers and further details are given with the individual characterization data.

1.8 Data Processing

This work was created using the text processing program Word 2016 (*Microsoft*, Redmond, USA) and ChemDraw Ultra 12.0 (*PerkinElmer Inc.*, Waltham, USA) for the design of the chemical structures and schemes. Figures and graphs have been designed using Excel 2016 (*Microsoft*, Redmond, USA) and Origin 7.5 (*OriginLab Corporation*, Northampton, USA). The planning and evaluation of the experiments during the optimization by design of experiments was done in Minitab 19.2 (*Minitab, LLC*, State College, USA).

1.9 Electrochemistry Setup

An undivided electrolysis cell made of polytetrafluoroethylene (PTFE) are used as the screening cells. The electrolysis cell has a maximum volume of 6 mL and can be capped with a cover made of PTFE. Detailed information about used cells are already reported.^[1] Further, the complete setup with these cells is commercially available as the IKA Screening System, *IKA-Werke GmbH & Co. KG*, Staufen, Germany. The electrodes (boron-doped diamond electrodes, 0.3 cm x 1 cm x 7 cm, 15 μm diamond layer, the support material is silicon) are attached to the cover. Since they dip about 1.8 cm into the reaction solution if 5.1 mL are used, they have an effective area of 1.8 cm^2 . Eight PTFE cells can be positioned in an arrangement of steel (Figure 5), which can be heated and cooled by connecting the steel block to a thermostat. The electrodes of the electrolysis cells are connected to an eight-channel galvanostat, made by the technical workshop at the University Bonn. The latter has an integrated charge counter so that it automatically stops the current supply and thus the electrolysis when a specified charge quantity is applied. The galvanostat allows electrolysis up to a voltage of 30 V and a current of 50 mA to be operated. Alternatively, the corresponding IKA System can be used.

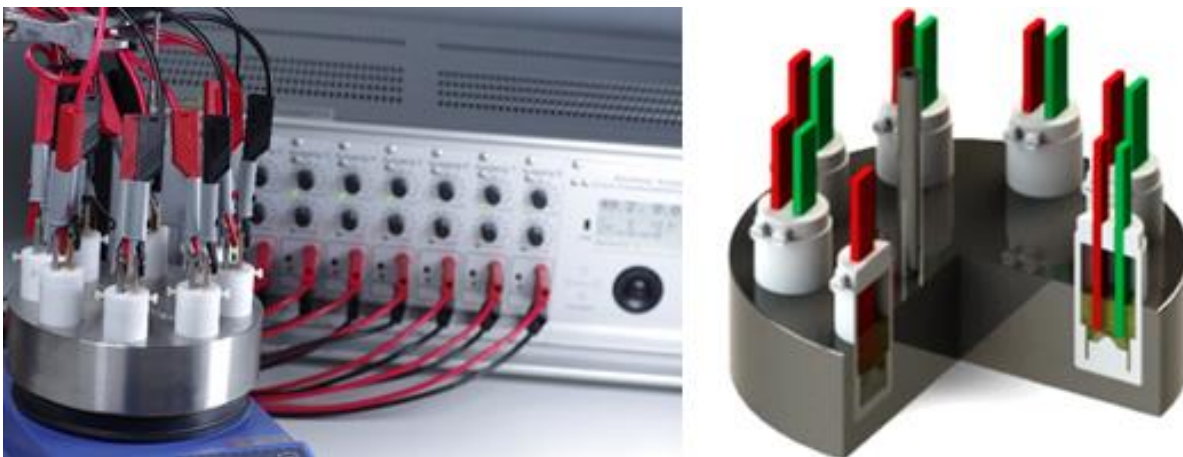


Figure 1: Screening setup with eight undivided screening cells operated with an eight channel galvanostat (left) and a cross section of a metal screening arrangement equipped with undivided screening cells (right).^[1]

2 Kinetic and Mechanistic Considerations

The major challenge in the electrochemical synthesis of oxygen substituted arenes is over-oxidation. This is due to the mesomeric electron-releasing effect of oxygen substituents that leads to a lowered oxidation potential compared to the starting material. In the case of the anodic oxidation of naphthalene in an acetone-water mixture 1-naphthol is only observed in traces as an intermediate.^[2]

In contrast the HFIP naphthyl ether was isolated as the major product of the electrolysis of naphthalene in HFIP, which is also a result of the strong negative inductive effect of the trifluoromethyl substituents increasing the oxidation potential, compared to non-fluorinated naphthyl ethers.

As stated in subsection 3.1.3 and section 3.2, over-oxidation still limits yields of the electrolysis, as the reaction must be stopped prior to full conversion to achieve the maximal yield. Mechanistic insight can provide valuable information on how to limit over-oxidation.

2.1 Mechanism of the Formation of HFIP Caffeyl Ether

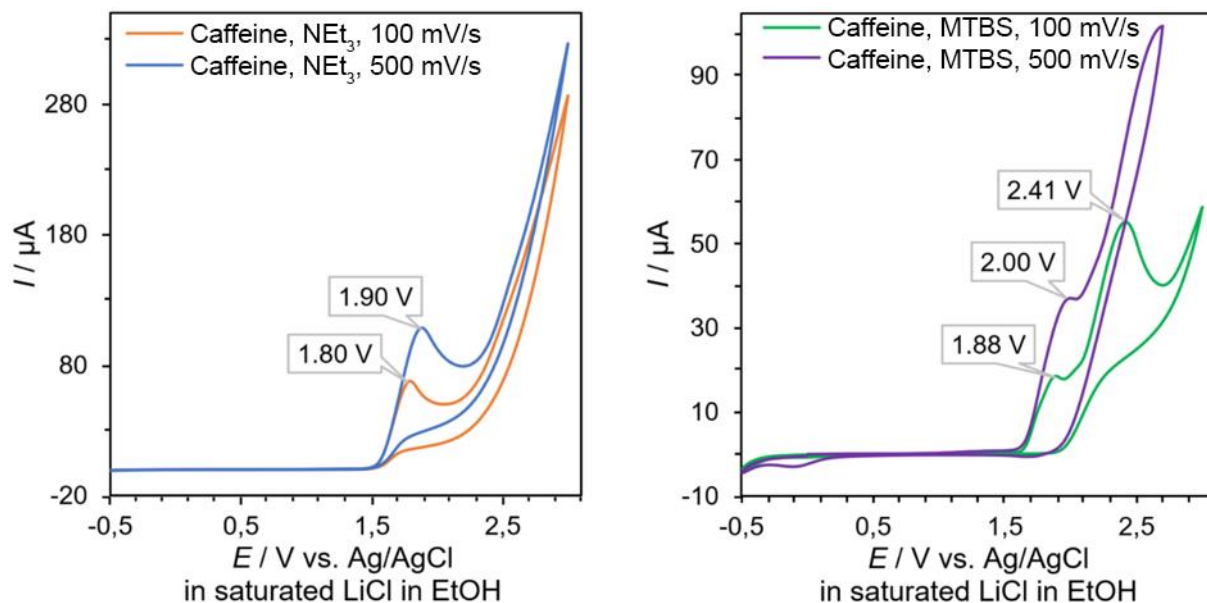


Figure 2: (left) Cyclic voltammogram of a 5 mM solution of caffeine in a 0.1 M solution of NEt_3 in HFIP. With a BDD anode and a glassy carbon cathode at scan rates of 100 mV/s (orange) and 500 mV/s (blue). (right) Cyclic voltammogram of a 5 mM solution of caffeine in a 0.1 M solution of tributylmethylammonium sulfate (MTBS) in HFIP. With a BDD anode and a glassy carbon cathode at scan rates of 100 mV/s (green) and 500 mV/s (purple).

The oxidative formation of HFIP ethers requires at least four elementary steps: twofold oxidation of the aryl (E), deprotonation (C), and nucleophilic attack by HFIP (C), the order of the steps differs between different substrates. For instance, the formation of the HFIP benzyl ether from 4-methylguaiacol follows a ECECC mechanism, where the first and second homogeneous follow-up reactions (C) steps are deprotonations and the last step is the conjugated 1,6-addition of a HFIP.

The cyclic voltammogram (CV) of caffeine in HFIP/ NEt_3 with a scan rate of 100 mV/s has only one peak at 1.80 V (vs. Ag/AgCl in saturated LiCl in EtOH) (orange). This indicates that the reaction follows an ECEC pathway, where the oxidation potential of the second oxidation is lower than that of the first oxidation. The oxidations are coupled with an irreversible fast chemical reaction, as indicated by the lack of a cathodic peaks at scan rates up to 500 mV/s.

The cyclic voltammogram of caffeine in HFIP/MTBS at 100 mV/s shows two distinct anodic peaks at anodic peak potentials of 1.88 V (vs. Ag/AgCl in saturated LiCl in EtOH) for the first oxidation and 2.41 V (vs. Ag/AgCl in saturated LiCl in EtOH) for a second oxidation step. The oxidations are also coupled with an irreversible fast chemical reaction. The second peak in the cyclic voltammogram of caffeine in HFIP/MTBS is evidence for an oxidation pathway that differs from the ECEC mechanism of caffeine in HFIP/NEt₃. The high anodic peak potential (2.41 V) suggests that the second oxidation results in high energy intermediate.

The potential shift of the first anodic peak potential in anodic direction (+0.08 V) suggest that the follow-up reaction is slower or hindered in HFIP/MTBS.^[3] NEt₃ deprotonates HFIP and generates HFIP anions, which either deprotonate or nucleophilicity attack cationic intermediates with second-order rate laws. Therefore, a study of the potential shift depending on the concentration of HFIP anions, cannot be used to determine the follow-up reaction, as HFIP anions are involved in both possible ECEC mechanisms.

Computational calculations performed at the B3LYP/6-31G* level found that the electron density of caffeine's HOMO is mostly located in C-8, N-7 and in the double bond between C-4 and C-5.^[4] The LUMO is mostly located at C-8, N-9 and in the double bond between C-4 and C-5. According to Koopmans' theorem for open shell intermediates the SOMO and LUMO have a similar electronic structure after a SET oxidation.^[5] Thus, a big C-8 LUMO coefficient is in line with a high regioselectivity of a nucleophilic attack of HFIP anions to that position, in caffeine and other xanthines. Figure 3 shows two mechanism for the electrolysis of caffeine in HFIP/NEt₃, for simplicity all oxidation steps are assumed to occur at the anode without involvement of homogeneous electron-transfer, as the data is insufficient to make such predictions.

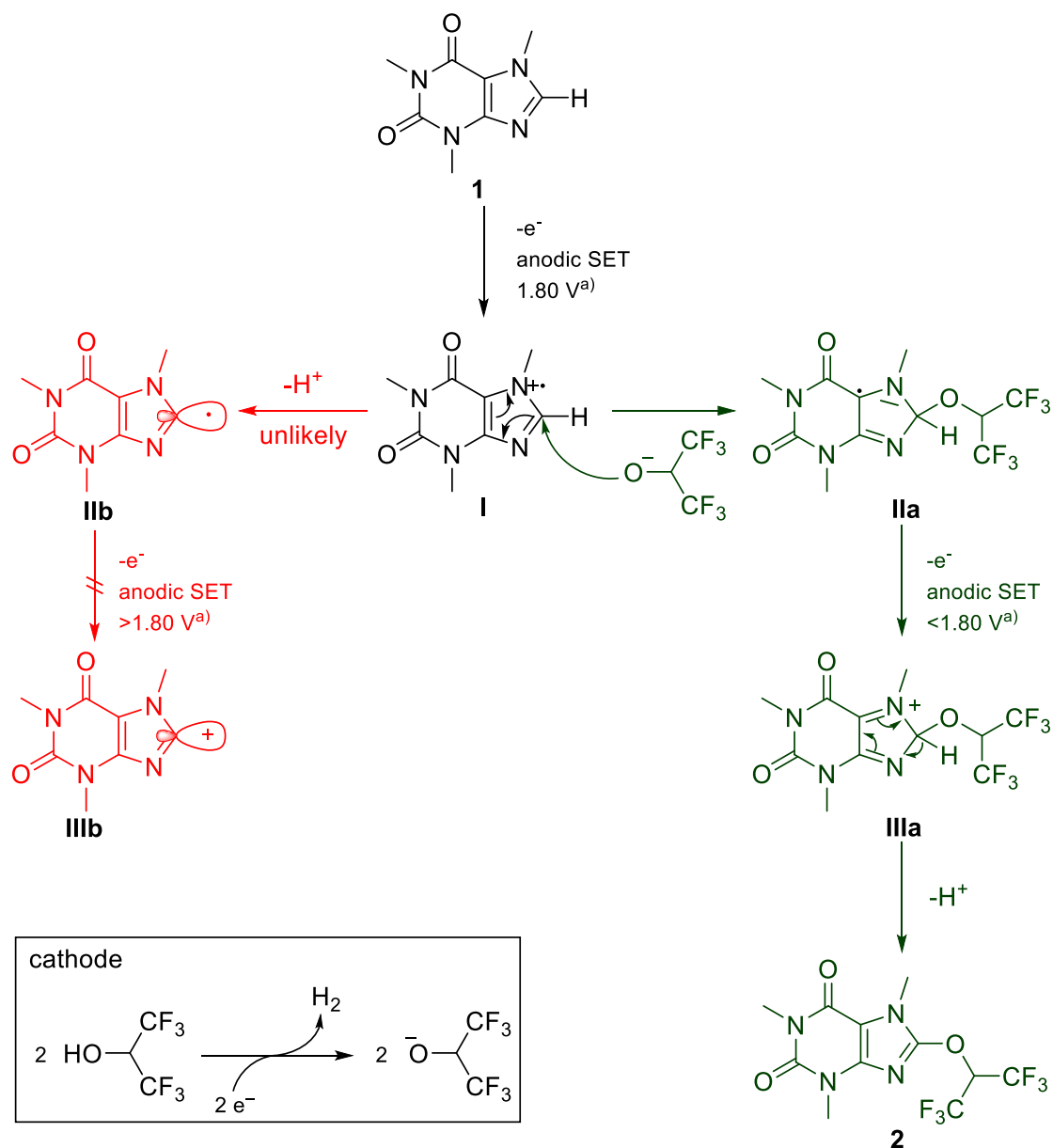


Figure 3: Different ECEC mechanisms of the electrolysis of caffeine in HFIP/ NEt_3 (red and green).

a) E vs. Ag/AgCl in saturated LiCl in EtOH .

The first elementary reaction of the electrosynthesis of HFIP caffeine ether (**2**) is a SET oxidation of caffeine (**1**) to the caffeine radical cation (**I**). The spin density is delocalized across C-8, N-7, C-4 and C-5.

In HFIP/ NEt_3 solution an ECEC mechanism takes place. The open-shell intermediate **IIa** is formed after a second-order nucleophilic attack, of HFIP anions, to the LUMO orbital of the **I** (green). The spin density is delocalized as a π -radical. **IIa** is anodically oxidized

to the delocalized iminium cation **IIIa**. The SOMO orbital of **IIa** is antibonding, as visualized by the valence bond structure displayed above, which has a high unpaired spin density in the antibonding π^* -orbital of the C8–N7 double bond. Hence, the oxidation leads to a delocalized iminium cation with an increased bond order, as no antibonding orbitals are occupied. This is in line with the CV data, that the oxidation potential of the second SET is lower than that of the first oxidation. Deprotonation **IIIa** with HFIP anions or NEt₃ leads to the formation of the desired HFIP caffeyl ether (**2**).

In the alternative ECEC mechanism (red) the caffeine radical cation (**I**) is deprotonated by HFIP/NEt₃. This step has a high activation barrier, compared with the deprotonation of anilide or phenol radical cation, as the C8–H bond is orthogonal to the SOMO orbital. A resonance stabilized radical cation (**I**) reacting to a radical occupying a sp²-orbitals (**IIc**) is hence unlikely. The SET oxidation of this radical would lead to a sp²-cation (**IIIb**), which is highly unstable because sp²-orbitals are low in energy orthogonal to the π -system of the imidazole subunit. Thus, the oxidation would require more energy than the initial oxidation of caffeine, which contrary to the cyclic voltammogram. Therefore, this reaction mechanism (red) can be excluded.

The oxidation of caffeine in HFIP/MTBS follows a different pathway. This can be attributed to the lower nucleophilicity of HFIP, which stabilizes cationic intermediates such as the radical cation **I**, compared to HFIP anions.^[6] Thus, the chemical follow-up reaction, which furnishes **IIa**, is a lot slower and enables other reaction pathways as evident by the second anodic peak at 2.41 V (vs. Ag/AgCl in saturated LiCl in EtOH).

2.2 Oxidation Potential of HFIP Ether

Cyclic voltammograms of HFIP caffeyl ether, Naphthalene, and HFIP naphthyl ether in HFIP/NEt₃ were recorded to examine the oxidation potential of the HFIP ethers compare to the starting materials (Figure 4). At a scan rate of 100 mV/s HFIP caffeyl ether is irreversible oxidized with an anodic peak potential of 1.60 V (vs. Ag/AgCl in saturated LiCl in EtOH), which is lower the anodic peak potential of caffeine 1.80 V (vs. Ag/AgCl in saturated LiCl in EtOH).

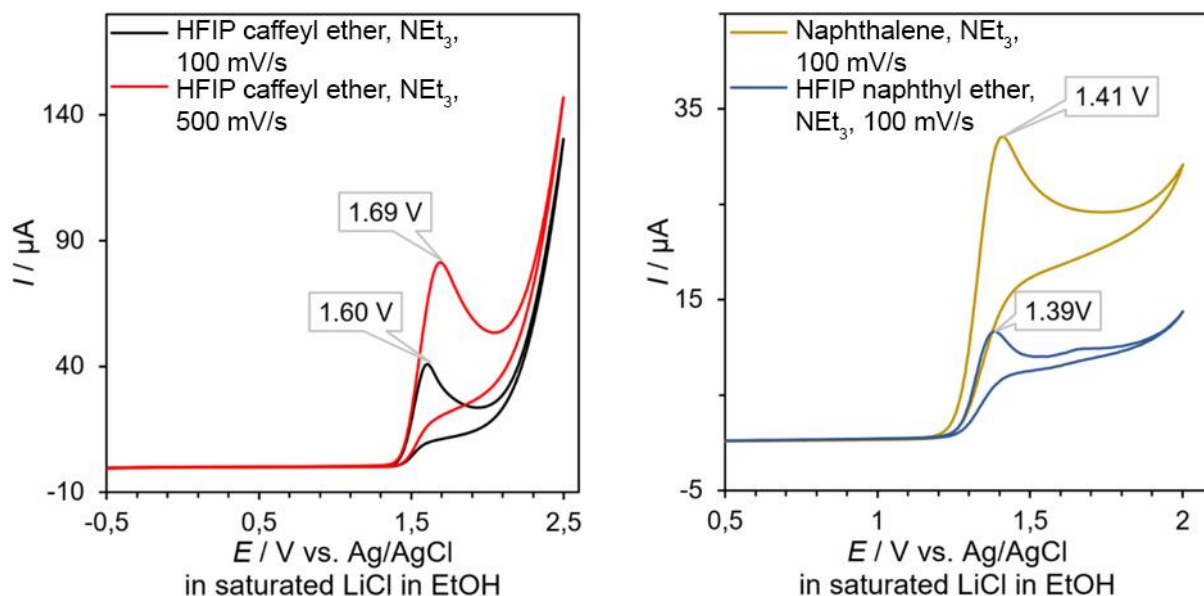


Figure 4: Left: Cyclic voltammogram of a 5 mM solution of HFIP caffeyl ether in a 0.1 M solution of NEt₃ in HFIP. With a BDD anode and a glassy carbon cathode at scan rates of 100 mV/s (black) and 500 mV/s (red). Right: Cyclic voltammograms of 5 mM solutions of naphthalene (yellow) and HFIP naphthyl ether (blue) in a 0.1 M solution of NEt₃ in HFIP. With a BDD anode and a glassy carbon cathode at scan rates of 100 mV/s.

The anodic peak potential of HFIP naphthyl ether (1.39 V vs. Ag/AgCl in saturated LiCl in EtOH) is slightly lower than that naphthalene (1.41 V vs. Ag/AgCl in saturated LiCl in EtOH). This indicates that the mesomeric electron-donating effect is not fully suppressed by the negative inductive effect of the trifluoromethyl-groups, and results in an activation of the product. The similar or lower oxidation potential of the products lead to competing reaction. Thus, the maximal yields are achieved before full conversion of the starting material.

3 Optimization by Design of Experiment

The following experimental designs were planned and evaluated with Minitab 19.2. The given NMR Yields were obtained using 1,3,5-trimethoxybenzene as an internal standard. It was added after removing the solvent in vacuo.

The experiments were conducted according to GP1 with the given changes to the experimental factors (Table 1, Table 2, Table 3 and Table 4). Caffeine was used to optimize the reaction conditions.

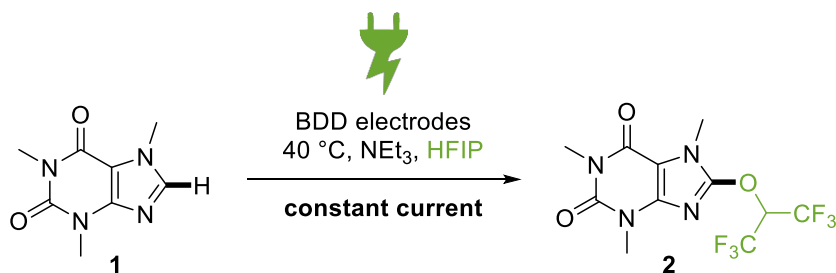


Figure 5: Reaction optimized by DoE.

3.1 Initial experimental design (2⁵⁻¹-Plan) in 0.75–2.0 mmol scale

The first design was a 2⁵⁻¹-plan, consisting of 34 experiments (2 x 16 corners, + 2 x 1 central point) and had a resolution of V. The factors investigated on, were the speed of the magnetic stirrer, the concentrations of caffeine and the base, the amount of charge applied to the system and the current density. The run order was randomized regarding their factor settings except for the stirrer speed. By having the experiments sorted by stirrer speed we could make use of the screening setup and perform 8 reactions simultaneously.

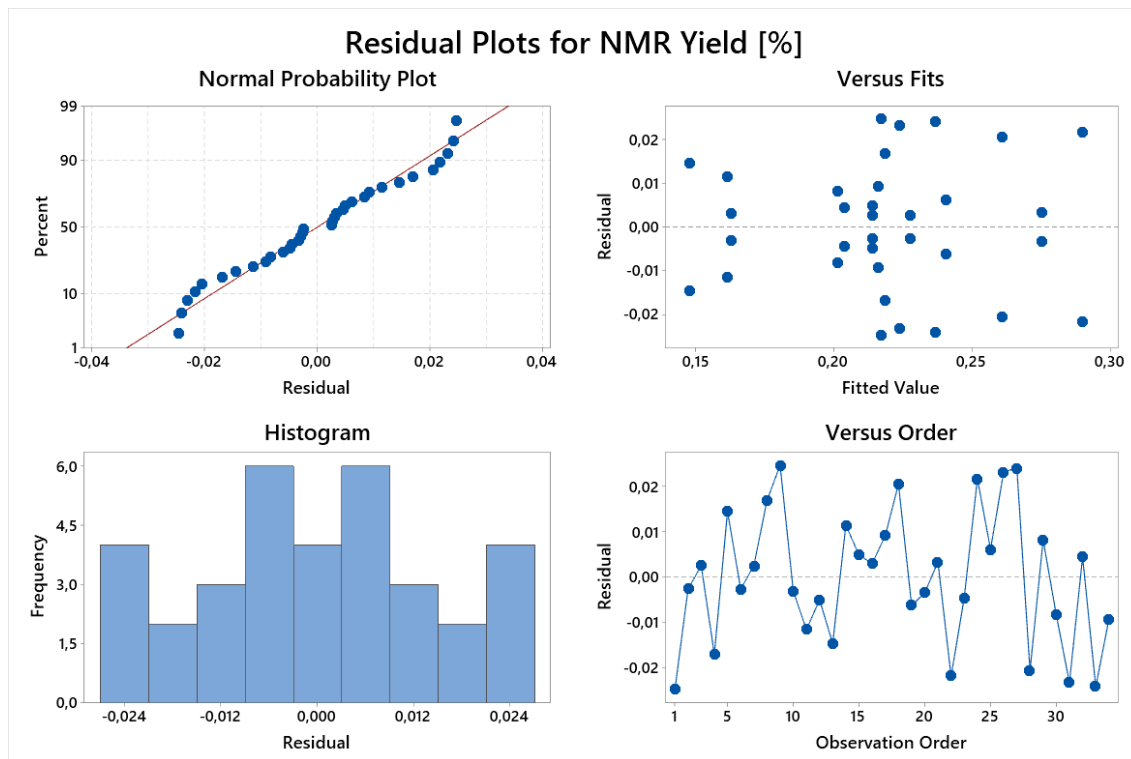
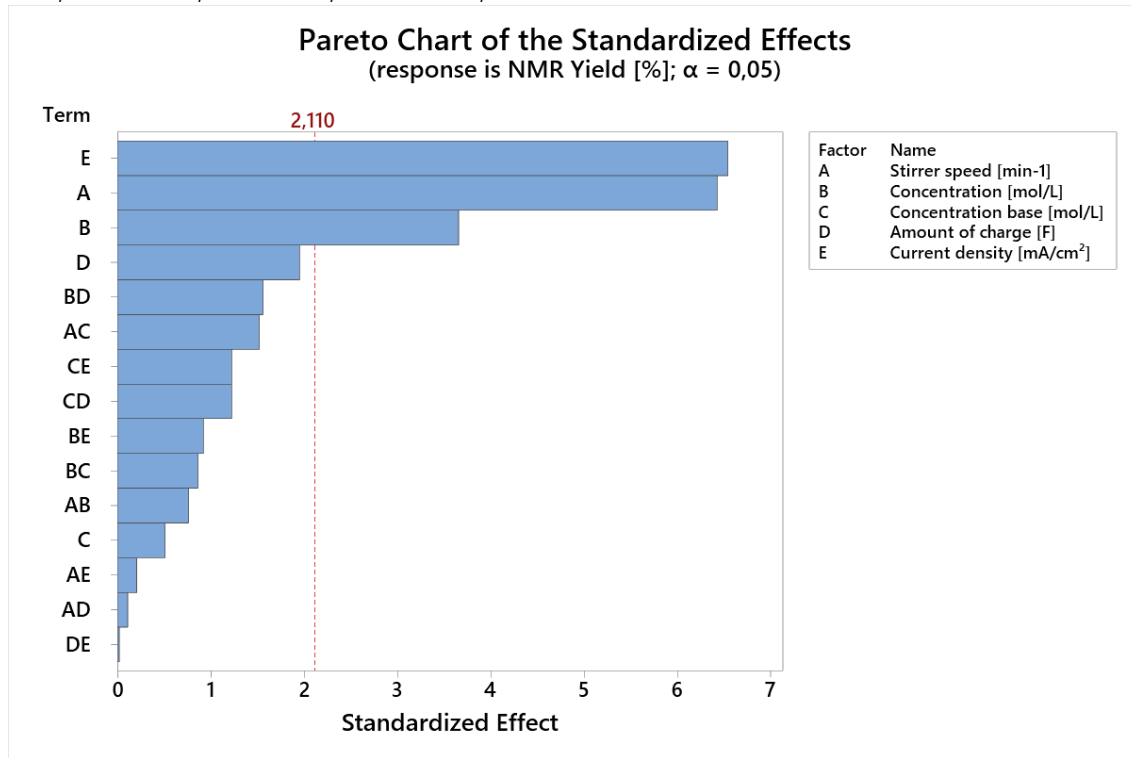
Table 1: Parameters of the first experimental design. Static parameters: 5 mL HFIP + NEt₃, BDD-electrodes, 40 °C.

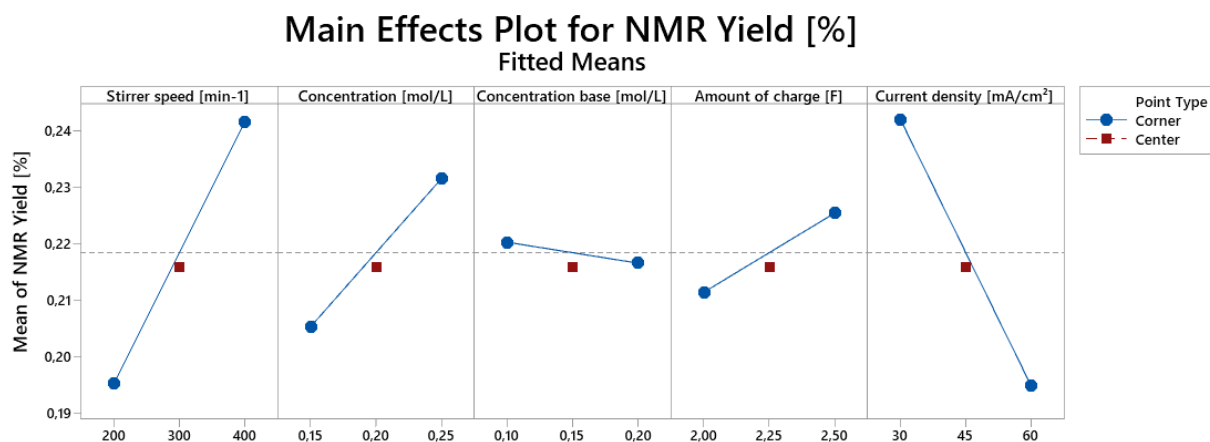
Standard Order	Run Order	Stirrer speed [min ⁻¹]	Concentration [mol/L]	Concentration NEt ₃ [mol/L]	Amount of charge [F]	Current density [mA/cm ²]	NMR Yield [%]
25	1	200	0,15	0,10	2,50	30	19,2%
15	2	200	0,25	0,20	2,50	30	22,5%
5	3	200	0,15	0,20	2,00	30	21,7%
27	4	200	0,25	0,10	2,50	60	20,2%
13	5	200	0,15	0,20	2,50	60	16,2%
21	6	200	0,15	0,20	2,00	30	21,1%
31	7	200	0,25	0,20	2,50	30	23,0%
11	8	200	0,25	0,10	2,50	60	23,6%
9	9	200	0,15	0,10	2,50	30	24,2%
7	10	200	0,25	0,20	2,00	60	16,0%
1	11	200	0,15	0,10	2,00	60	15,0%
19	12	200	0,25	0,10	2,00	30	20,9%
29	13	200	0,15	0,20	2,50	60	13,3%
17	14	200	0,15	0,10	2,00	60	17,3%
3	15	200	0,25	0,10	2,00	30	21,9%
23	16	200	0,25	0,20	2,00	60	16,6%
33	17	300	0,20	0,15	2,25	45	22,5%
14	18	400	0,15	0,20	2,50	30	28,1%
32	19	400	0,25	0,20	2,50	60	23,4%
8	20	400	0,25	0,20	2,00	30	27,2%
24	21	400	0,25	0,20	2,00	30	27,9%
12	22	400	0,25	0,10	2,50	30	26,8%
6	23	400	0,15	0,20	2,00	60	19,9%
28	24	400	0,25	0,10	2,50	30	31,2%
16	25	400	0,25	0,20	2,50	60	24,7%
20	26	400	0,25	0,10	2,00	60	24,7%
18	27	400	0,15	0,10	2,00	30	26,1%
30	28	400	0,15	0,20	2,50	30	24,0%
26	29	400	0,15	0,10	2,50	60	20,9%
10	30	400	0,15	0,10	2,50	60	19,3%
4	31	400	0,25	0,10	2,00	60	20,1%
22	32	400	0,15	0,20	2,00	60	20,8%
2	33	400	0,15	0,10	2,00	30	21,3%
34	34	300	0,20	0,15	2,25	45	20,7%

The models summary as well as a Pareto Chart, Residual Plots and the Main Effects Plot of the fit for the NMR yield are given below:

Model Summary

S	R-sq	R-sq(adj)	R-sq(pred)
0,0203403	86,78%	74,33%	47,11%



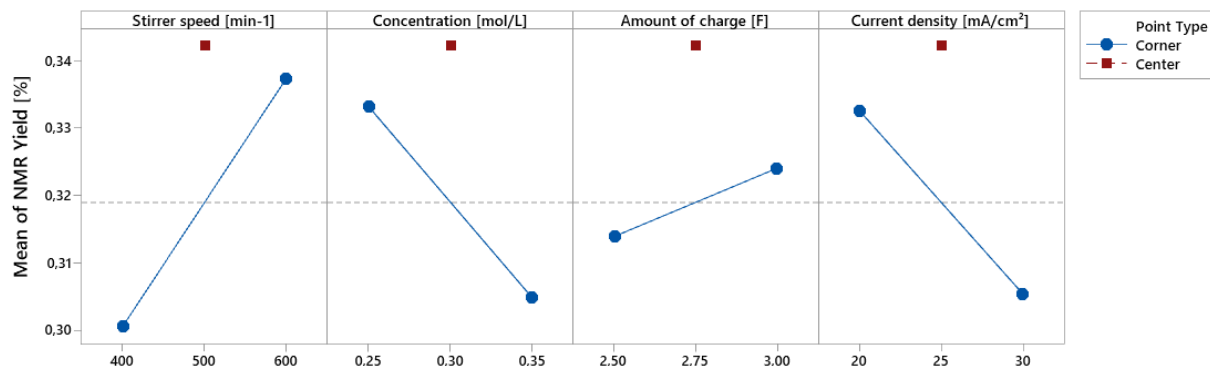


There are three significant factors to the system as can be seen from the Pareto Chart above. Those are the current density, the stirrer speed and the concentration of caffeine. The Main Effects Plot shows, that high stirrer speeds, high concentrations and low current densities seem to be beneficial in this area of the experimental space. Therefore, the next experiments were designed to follow this trend.

3.2 Second experimental design (2^{4-1} -Plan + CCD) in 5 mL-cells

The experimental settings are shown in the upper part of Table 2. The concentration of the base was considered not significant and was not further investigated on in this design. The higher concentration was used to promote a good conductivity. With a confidence level of 95% the amount of charge showed no significant effect in the last design but was considered relevant anyway, since the reaction is driven electrochemically and therefore the amount of charge should be relevant even if the effect might be small between the chosen levels. With the four factors left we used a 2^{4-1} -Plan with a resolution of IV consisting of 18 experiments (2 x 8 corners + 2 x 1 central point). The central point did not fit the linear model as can be seen in the Main Effects Plot shown below.

Main Effects Plot for NMR Yield [%] Fitted Means



Therefore the plan was expanded to a Central Composite Design (CCD) by adding star points and repeating the central point one more time (lower part of Table 2).

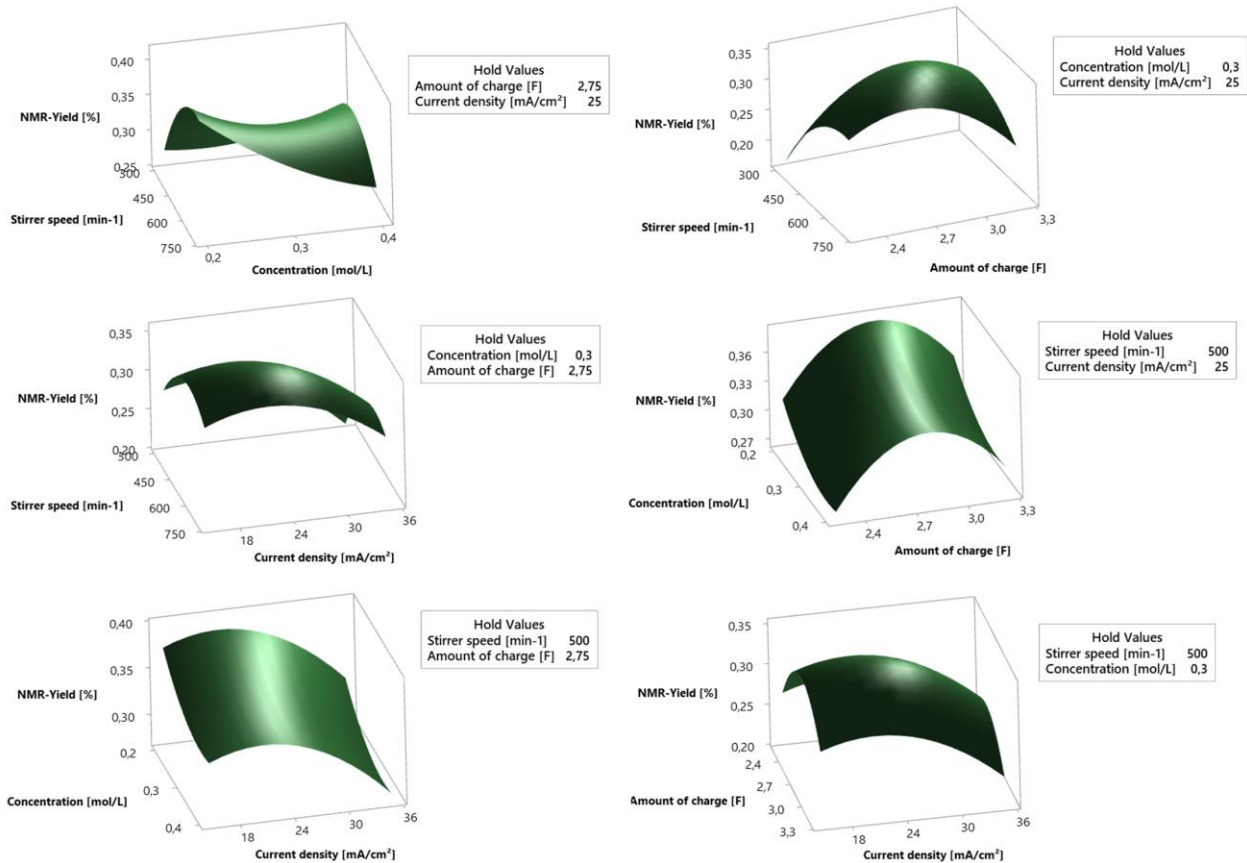
Table 2: Parameters of the second experimental design. Static parameters: 5 mL HFIP + NEt₃ (0.2 M), BDD electrodes, 40 °C.

	Standard Order	Run Order	Stirrer speed [min ⁻¹]	Concentration [mol/L]	Amount of charge [F]	Current density [mA/cm ²]	NMR yield [%]
2 ⁴⁻¹ Plan	5	1	400	0.25	3.00	30	34.6%
	7	2	400	0.35	3.00	20	33.4%
	9	3	400	0.25	2.50	20	29.4%
	15	4	400	0.35	3.00	20	32.1%
	18	5	500	0.30	2.75	25	35.0%
	2	6	600	0.25	2.50	30	36.9%
	4	7	600	0.35	2.50	20	34.4%
	12	8	600	0.35	2.50	20	31.6%
	10	9	600	0.25	2.50	30	34.2%
	17	10	500	0.30	2.75	25	33.4%
	6	11	600	0.25	3.00	20	36.8%
	16	12	600	0.35	3.00	30	29.0%
	14	13	600	0.25	3.00	20	36.8%
	8	14	600	0.35	3.00	30	30.3%
	13	15	400	0.25	3.00	30	26.3%
	1	16	400	0.25	2.50	20	31.5%
	11	17	400	0.35	2.50	30	26.4%
	3	18	400	0.35	2.50	30	26.6%
CCD	19	19	300	0.30	2.75	25	28.7%
	20	20	700	0.30	2.75	25	31.0%
	21	21	500	0.20	2.75	25	36.2%
	22	22	500	0.40	2.75	25	34.6%
	23	23	500	0.30	2.25	25	26.9%
	24	24	500	0.30	3.25	25	28.9%
	25	25	500	0.30	2.75	15	33.1%
	26	26	500	0.30	2.75	35	27.3%
	27	27	500	0.30	2.75	25	34.6%

The resulting Response Surface Plots as well as a model summary are given below. It can be seen that a maximum was found regarding the stirrer speed, the current density and the amount of charge with the other factors held at their central settings. For the stirrer speed there is one exception to the maximum. The upper left plot suggests an increase in yield towards high stirrer speeds and low concentrations.

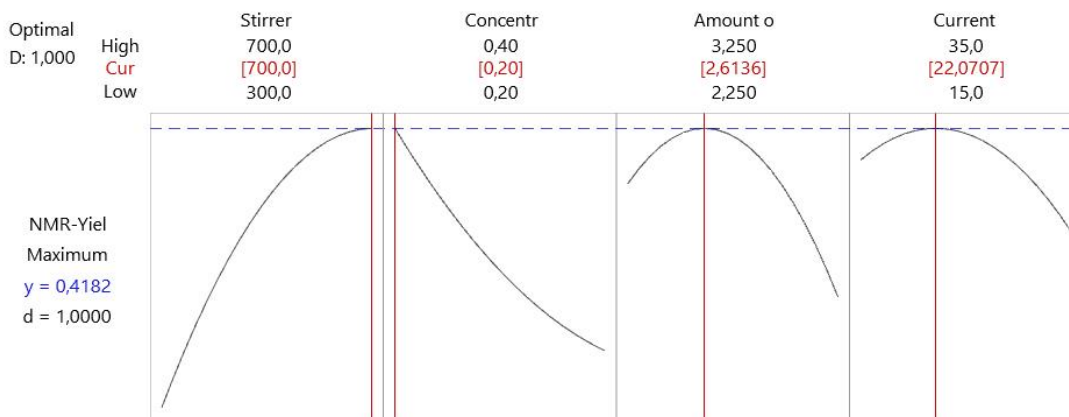
Model Summary

S	R-sq	R-sq(adj)	R-sq(pred)
0,0212351	79,82%	62,52%	24,27%



Using the Response Optimizer of Minitab 19.2 to maximize the NMR yield by the obtained non-linear model, we found that the best conditions would be at the corners of the investigated experimental space regarding the stirrer speed and concentration, while for the amount of charge and current density again a maximum was found. Using those

settings and isolating the product by column chromatography we achieved exactly 42% isolated yield as predicted by the model. The Response Optimizers output is given below.



We tried to use even higher stirrer speeds with lower concentrations in a subsequent design, but this led to a significant number of failures since the stirring bars couldn't keep up with the high speeds and were only shaking after a while. Changing the Magnetic stirrer helped improve that but led to overall lower yields. Therefore, the conditions shown above were used for all following reactions.

3.3 First experimental design (2^3 -Plan) on a 10 mmol scale in a temperable beaker type cell

Since the stirrer speed was crucial, increasing the yield in the 5 mL-cells, we investigated on the distance of the electrodes and the temperature expecting them to influence diffusion and the availability of deprotonated HFIP to the oxidized caffeine species. In order to change the distance of the electrodes we turned the electrode mounting to the same direction, towards or away from each other. Furthermore, we used a bigger, temperable cell and charged it with 50 mL HFIP, 1.39 mL NEt_3 (1.01 g, 10.0 mmol, 1 eq.) and 1.94 g caffeine (10.0 mmol).



Figure 6: Beaker type-cell used for electrolysis of 50 mL electrolyte. The inner diameter is 4.69 cm. The outer shell is used in combination with a thermostat to control the temperature. Left: fully assembled cell, a condenser was added at the open end on the right. Right: parts of the setup with a 1 € coin for size comparison.

To increase reproducibility, we cleaned the BDD electrodes by electrolyzing 70 mL diluted sulfuric (20 mM) acid with 900 mA until 200 C passed before starting the experiment. The used settings of the chosen 2^3 -plan are given in Table 3.

Table 3: Parameters of the third experimental design. Static parameters: 50 mL HFIP + NEt₃ (0.2 M), caffeine 0.2 M, BDD electrodes (decentrally mounted), 2.61 F, 22.07 mA/cm².

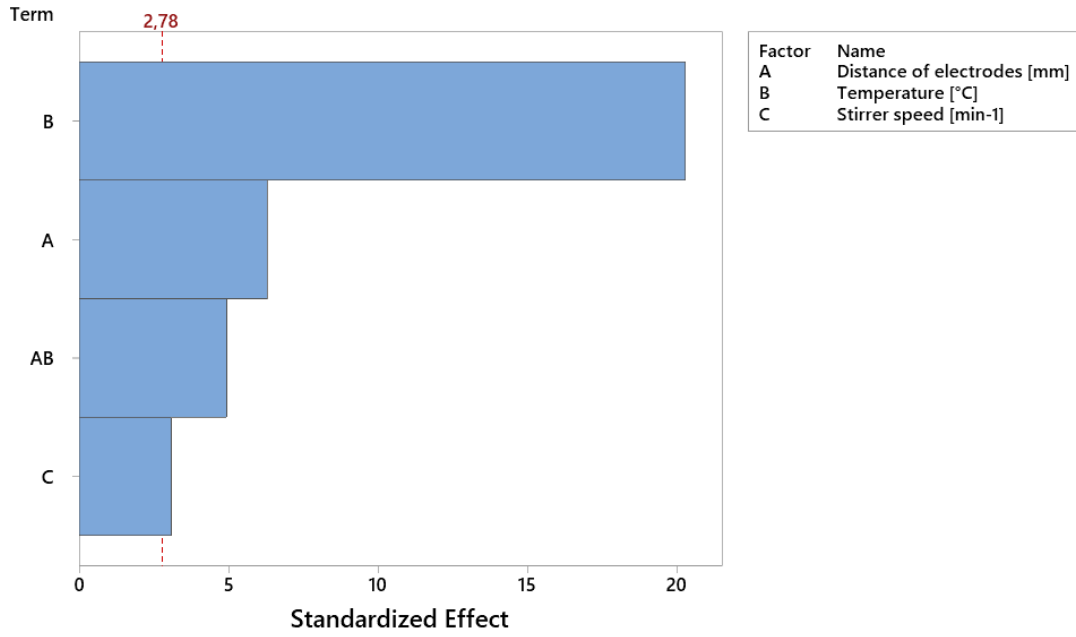
Standard Order	Run Order	Distance of electrodes [mm]	Temperature [°C]	Stirrer speed [min-1]	NMR yield [%]
9	1	10,75	30	600	37.3%
8	2	17,00	40	700	43.0%
5	3	4,50	20	700	29.8%
10	4	10,75	30	600	37.0%
2	5	17,00	20	500	28.4%
3	6	4,50	40	500	36.5%
1	7	4,50	20	500	28.9%
6	8	17,00	20	700	31.6%
4	9	17,00	40	500	41.8%
7	10	4,50	40	700	37.3%

Bearing in mind, that a parallel execution of experiments was not possible because of the changed setup, we tried to keep the number of experiments as little as possible and only repeated the central point. To be able to estimate the residues, despite the small number of degrees of freedom in this plan, we did a backwards elimination of the model's terms while evaluating the results, choosing an "α to remove" of 5%. Doing so, the software will iteratively remove the term with the smallest p-value (least significant term) from the model and evaluate the data again. The resulting model's summary as well as a Pareto Chart, Residual Plots, the Main Effects Plot and the Interaction Plot of the fit for the NMR yield are given below:

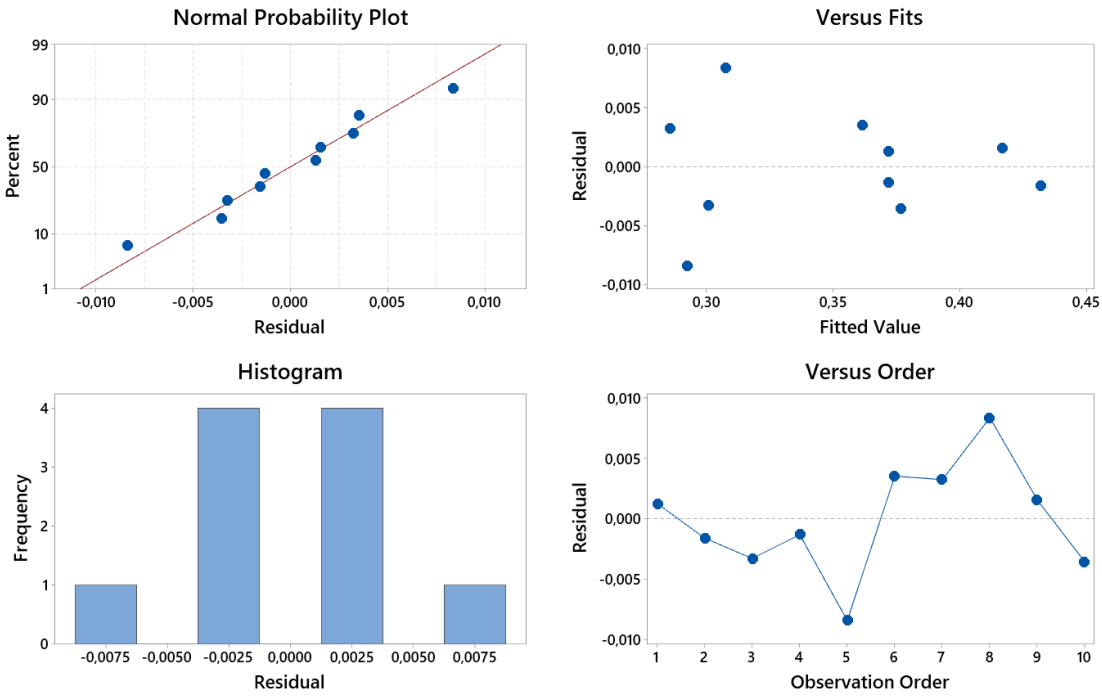
Model Summary

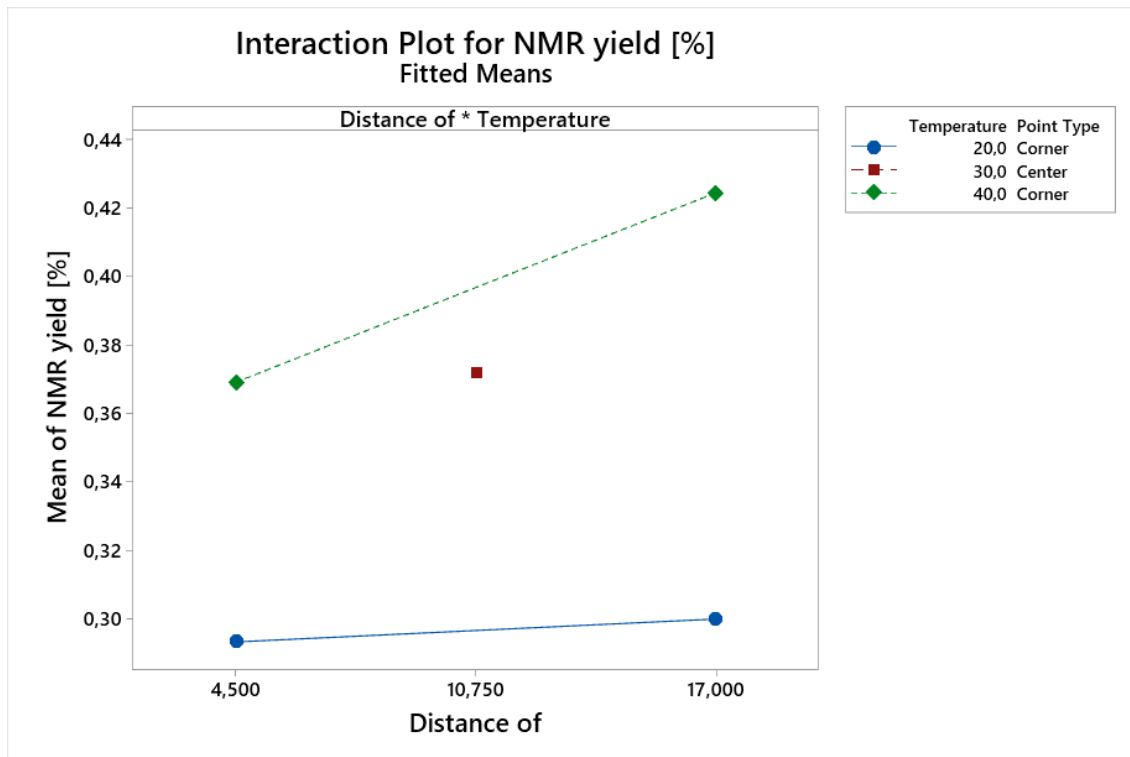
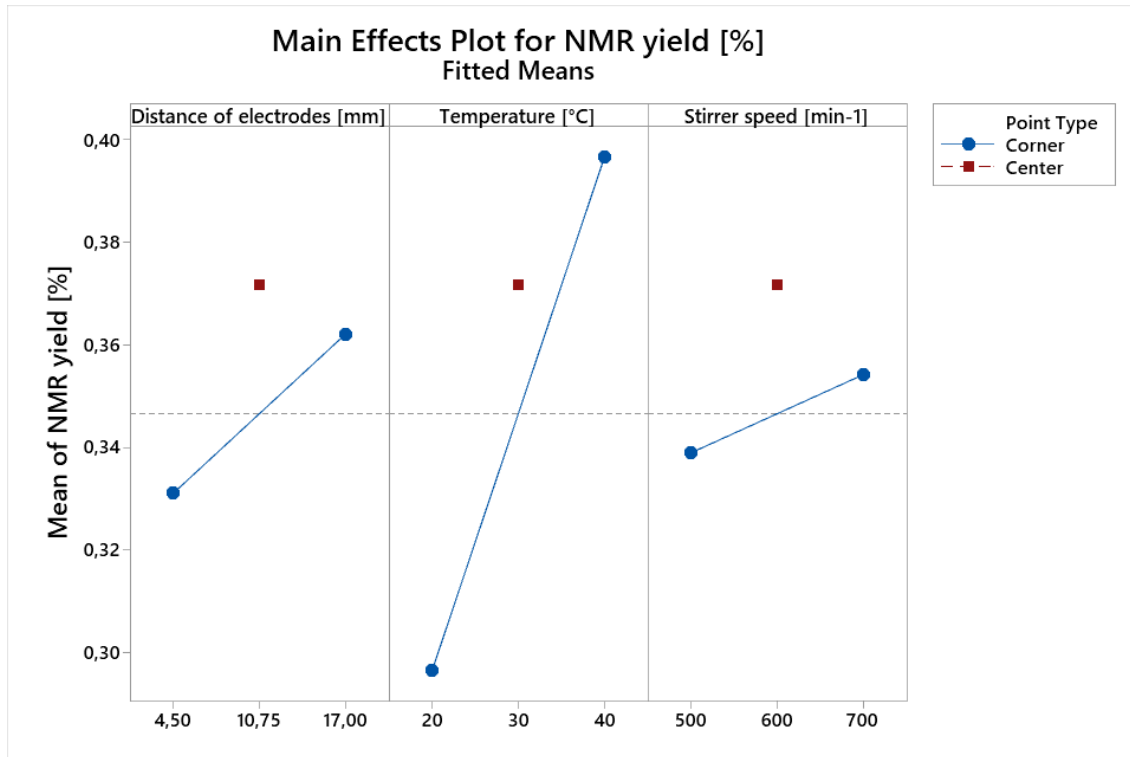
S	R-sq	R-sq(adj)	R-sq(pred)
0,0069778	99,22%	98,24%	94,46%

Pareto Chart of the Standardized Effects
(response is NMR yield [%]; $\alpha = 0,05$)



Residual Plots for NMR yield [%]





The setup used, allowed only the given distances of the electrodes. Therefore, we used the one that gave best results, which was 17 mm, for the following, final experimental design.

3.4 Final experimental design (2²-Plan)

Only the Temperature and the stirrer speed were left to optimize in the given setup. The used settings of the chosen 2²-plan are given in Table 4.

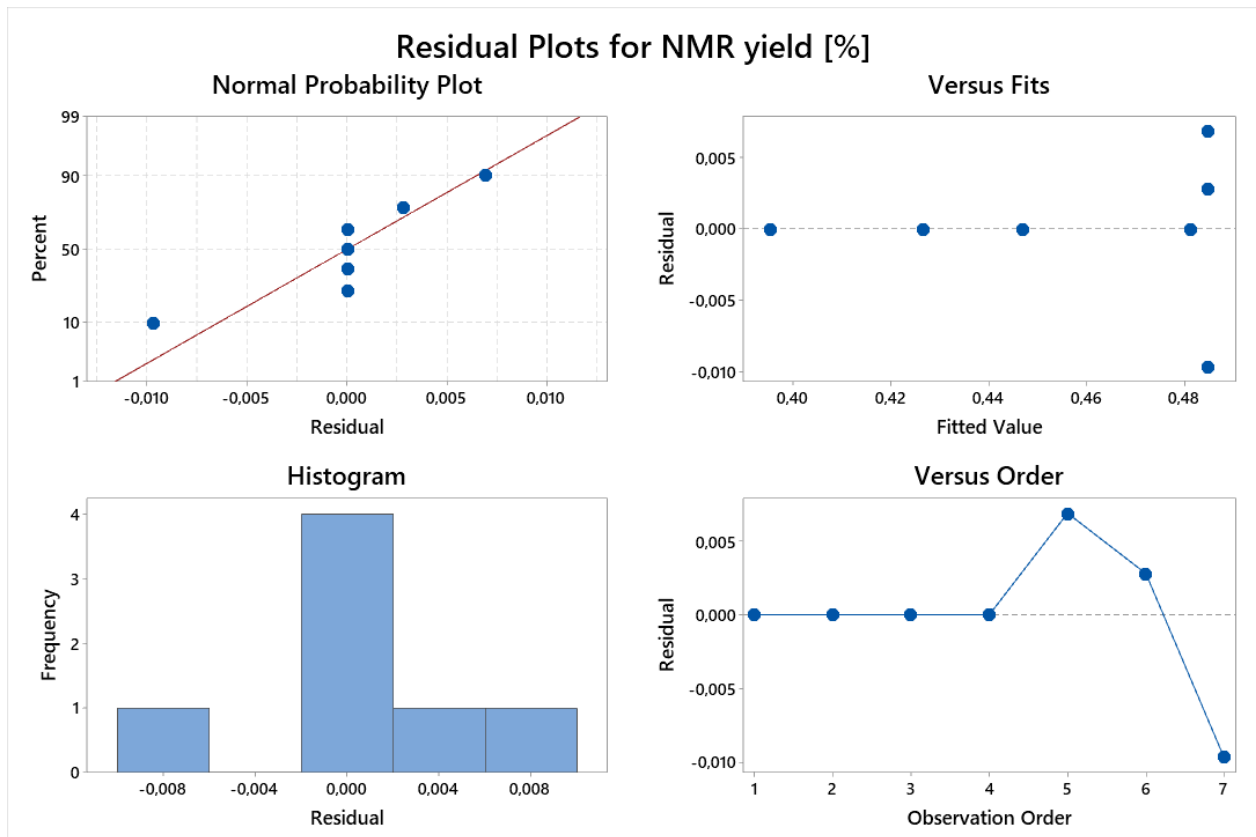
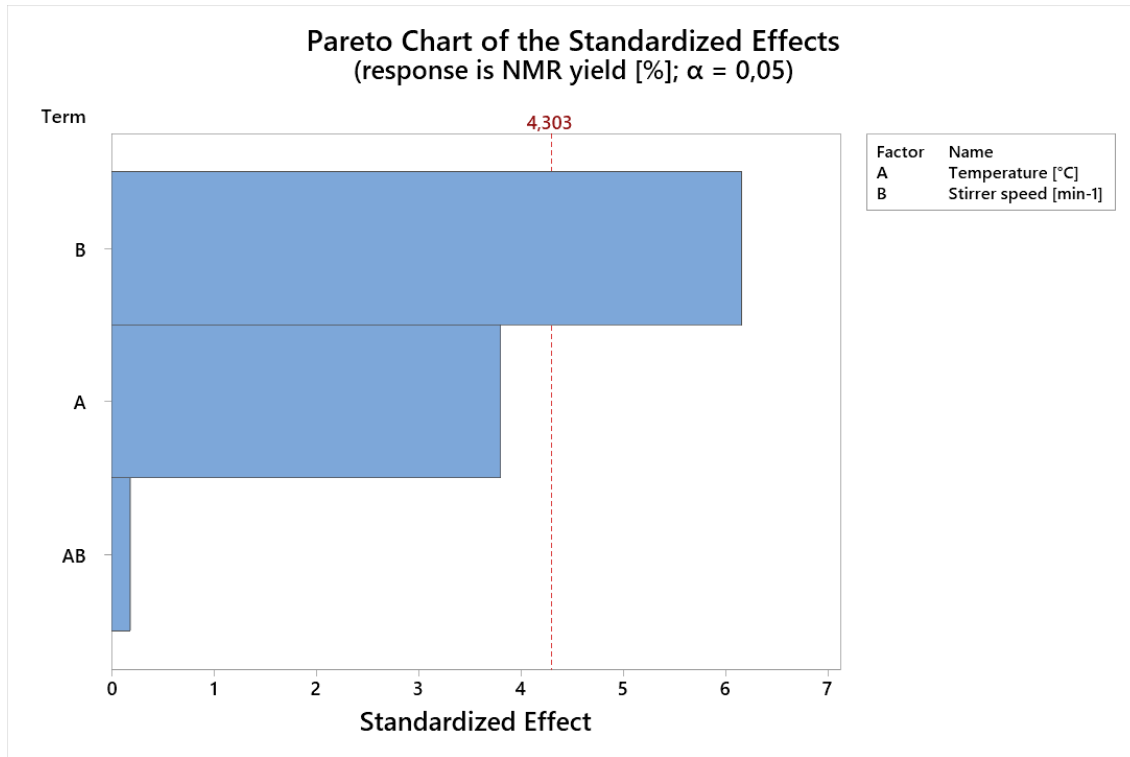
Table 4: Parameters of the fourth experimental design. Static parameters: 50 mL HFIP + NEt₃ (0.2 M), caffeine 0.2 M, BDD-electrodes, 17 mm between the electrodes, 2.61 F, 22.07 mA/cm².

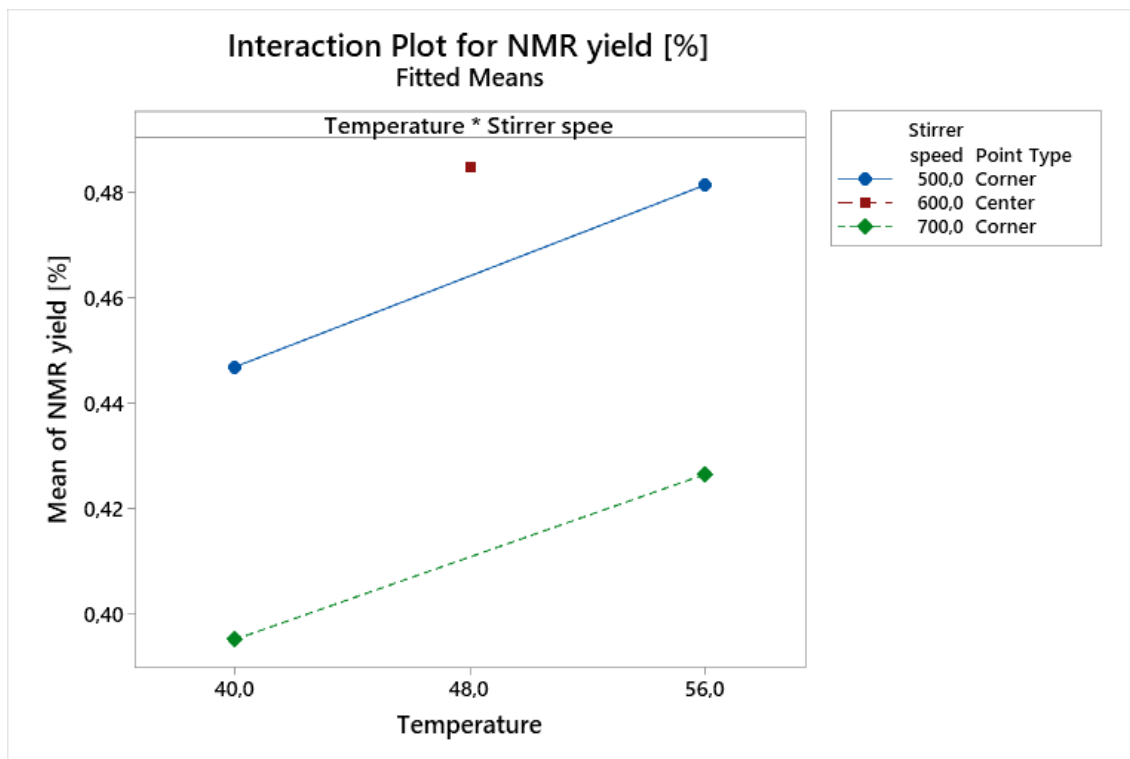
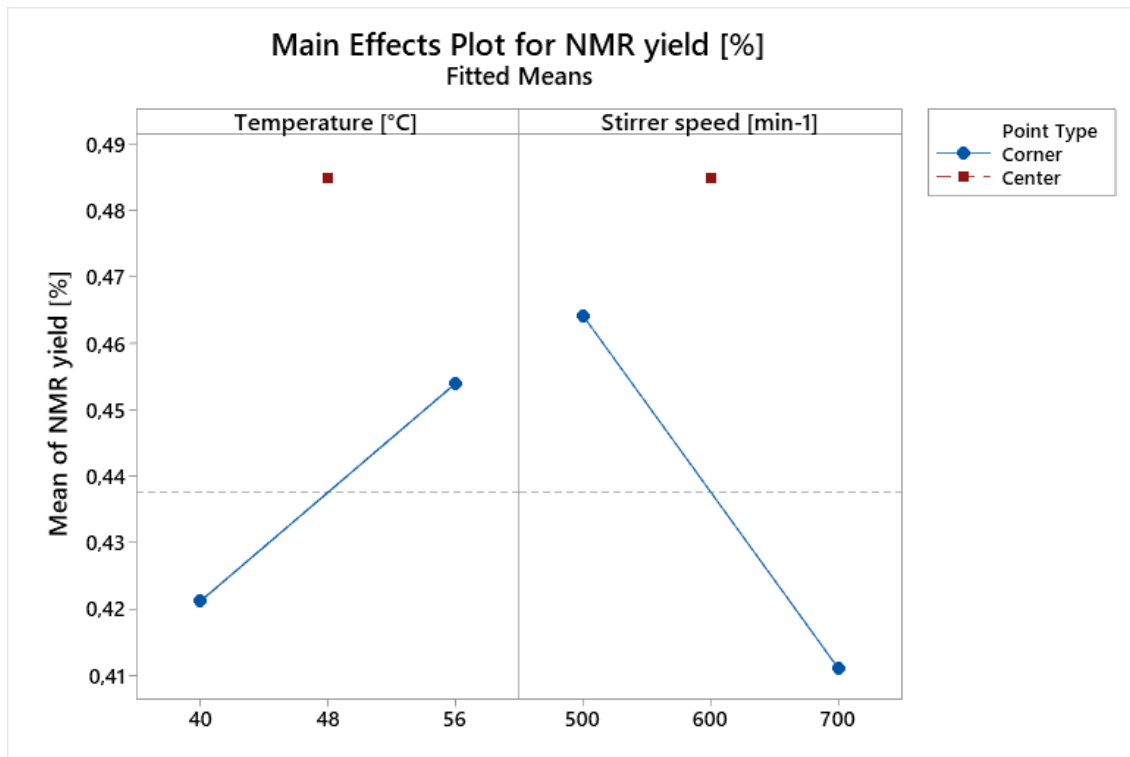
Standard Order	Run Order	Temperature [°C]	Stirrer speed [min-1]	NMR yield [%]
1	1	40	500	44,7%
4	2	56	700	42,7%
3	3	40	700	39,5%
2	4	56	500	48,1%
5	5	48	600	49,2%
6	6	48	600	48,8%
7	7	48	600	47,5%

The resulting model's summary as well as a Pareto Chart, Residual Plots, the Main Effects Plot and the Interaction Plot of the fit for the NMR yield are given below:

Model Summary

S	R-sq	R-sq(adj)	R-sq(pred)
0,0086416	98,12%	94,35%	*





It can be seen from the Main Effects Plot as well as the Interaction Plot that the center point does not fit into the linear model. Indeed, it is way above the expected value from a

linear system. Therefore, we assume, that the center point is somewhere close to the maximum and isolated the product with these settings with 45% yield.

4 General Protocols

4.1 GP1 Electrochemical synthesis of HFIP ethers optimized by OVAT

(conditions a)

An undivided screening cell equipped with a stirring bar and heated to 40°C was charged with the respective purine or arene (1.25 mmol, 1.0 eq.), HFIP (5 mL) and NEt₃ (51 mg, 70 µL, 0.50 mmol, 0.4 eq.). The solution was electrolyzed with BDD electrodes (distance: 4.5 mm, surface in the solution: 1.00 cm x 1.80 cm) applying a current density of 7.2 mA/cm² while stirring at 300 rpm until the required charge was applied. The reactions were monitored by TLC and GC-MS. HFIP was recovered *in vacuo*. Purification was performed using flash column chromatography.

4.2 GP2 Electrochemical synthesis of HFIP ethers optimized by DoE (conditions

b)

An undivided screening cell equipped with a stirring bar and heated to 40°C was charged with the respective purine or arene (1.00 mmol), HFIP (5 mL) and NEt₃ (101 mg, 139 µL, 1.00 mmol, 1.0 eq.). The solution was electrolyzed with BDD electrodes (distance: 4.5 mm, surface in the solution: 1.00 cm x 1.80 cm) applying a current density of 22.1 mA/cm² while stirring at 700 rpm until the required charge was applied. The reactions were monitored by TLC and GC-MS. HFIP was recovered *in vacuo*. Purification was performed using flash column chromatography.

5 Synthesis

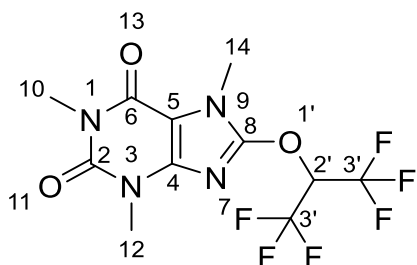
5.1 8-((1,1,1,3,3,3-Hexafluoropropan-2-yl)oxy)caffeine (2)

5.1.1 Synthesis in 1.00 mmol scale

The electrolysis of caffeine (149.2 mg, 1.00 mmol) was conducted according to GP2 until a charge of 2.61 F was applied. The crude product was purified using flash chromatography on silica gel eluting with ethyl acetate in cyclohexane (0–60% in 60 min, then 60-100% in 20 min), yielding a crystalline colorless solid (152.0 mg, 0.422 mmol, 42%).

5.1.2 Synthesis in 10.0 mmol scale

An undivided beaker type-cell (see Figure 6) equipped with a stirring bar and heated to 48°C was charged with caffeine (1.942 g, 10.0 mmol, 1.0 eq.), HFIP (50 mL) and NEt₃ (1.010 g, 1.390 mL, 10.00 mmol, 1.0 eq.). The solution was electrolyzed with BDD electrodes (distance: 17 mm, surface in the solution: 2.00 cm x 2.17 cm) applying a current density of 22.1 mA/cm² while stirring at 600 rpm until the 2.61 F was applied. HFIP was recovered *in vacuo*. Purification was performed using flash column chromatography on silica gel eluting with ethyl acetate in cyclohexane (0–60% in 60 min, then 60-100% in 20 min), yielding a crystalline colorless solid (1.623 g, 4.51 mmol, 45%).



¹H NMR (400 MHz, CDCl₃): δ [ppm] = 6.06 (hept, J = 6.0 Hz, 1H, H -2'), 3.77 (s, 3H, H -14), 3.44 (s, 3H, H -11), 3.31 (s, 3H, H -13).

^{13}C NMR (101 MHz, CDCl_3): δ [ppm] = 154.8 (C-3), 152.1 (C-8), 151.3 (C-5), 144.7 (C-1), 120.1 (qd, J = 283 Hz, 2.4 Hz, C-3'), 104.7 (C-2), 73.0 (hept, 35.7 Hz, C-2'), 30.2 (C-14), 29.7 (C-11), 27.7 (C-13).

^{19}F NMR (376 MHz, $\text{DMSO-}d_6$): δ [ppm] = -73.89 (d, J = 6.1 Hz).

Mp: 159.1 °C (crystallized from ethyl acetate).

HRMS of $([\text{C}_{11}\text{H}_{10}\text{F}_6\text{N}_4\text{O}_3+\text{H}]^+)$ (ESI+) $[\text{M}+\text{H}]^+$: calculated: 361.0735, found: 361.0738.

Crystal structure determination of **2**: $\text{C}_{10}\text{H}_{10}\text{F}_6\text{N}_4\text{O}_3$, M_r = 360.23 g/mol, colorless block ($0.23 \times 0.35 \times 0.57 \text{ mm}^3$), $P 2_1/c$ (monocline), a = 13.3525(8) Å, b = 8.4536(4) Å, c = 13.1687(15) Å, V = 1444.06(15) Å³, z = 4, $F(000)$ = 728, ρ = 1.657 g/cm³, μ = 0.171 mm⁻¹, Mo-K α graphite monochromator, -80 °C, 8332 reflections, 3436 reflections, wR_2 = 0.1096, R_1 = 0.0385, 1.06 eÅ⁻³, -0.24 eÅ⁻³, GoF = 1.03. (CCDC deposition number: 1988067) A suitable single crystal for structure determination was obtained by recrystallization from acetone at room temperature.

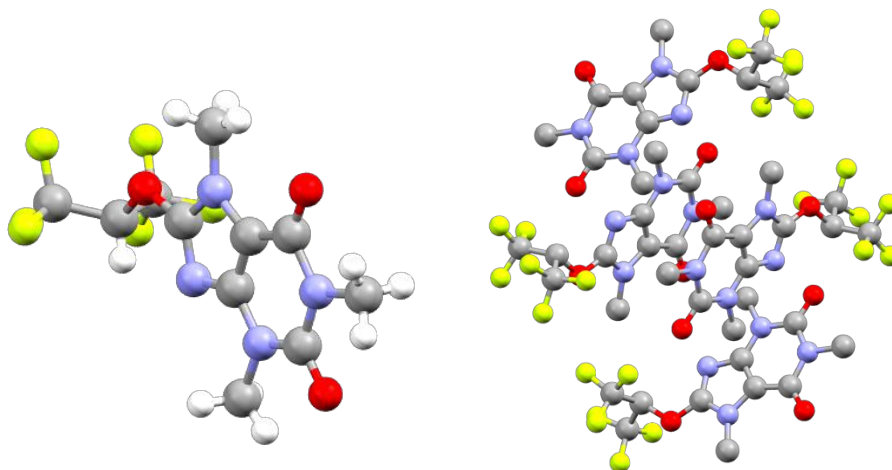
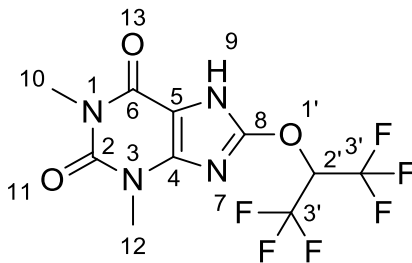


Figure 7: left: molecular structure of **2**; right: Packing of **2** in the solid state.

The molecules interact amongst each other via π - π – stacking of the respective purine scaffolds.

5.2 8-((1,1,1,3,3,3-Hexafluoropropan-2-yl)oxy)theophylline (3)

The electrolysis of theophylline (225.2 mg, 1.25 mmol) was conducted according to GP1 until a charge of 2.00 F was applied. The crude product was purified using flash chromatography on silica gel eluting with methanol in dichloromethane (0–5% in 45 min, then 5–10% in 25 min), yielding a crystalline colorless solid (135.8 mg, 0.393 mmol, 31%).



^1H NMR (400 MHz, $\text{DMSO-}d_6$): δ [ppm] = 13.76 (s, 1H, H -9), 7.05 (hept, J = 6.1 Hz, 1H, H -3'), 3.41 (s, 3H, H -12), 3.22 (s, 3H, H -10).

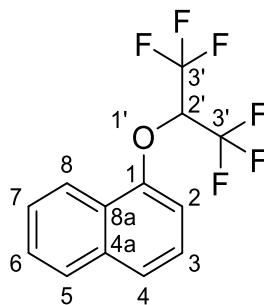
^{13}C NMR (101 MHz, $\text{DMSO-}d_6$): δ [ppm] = 154.3 (C-6), 153.2 (C-8), 151.5 (C-2), 145.5 (C-4), 122.4 (qd, J = 283.0 Hz, 3.9 Hz, C-3'), 104.3 (C-5), 72.6 (hept, J = 33 Hz, C-2'), 30.44 (C-12), 28.2 (C-10).

^{19}F NMR (376 MHz, $\text{DMSO-}d_6$): δ [ppm] = -73.87 (d, J = 6.2 Hz).

HRMS of $([\text{C}_{10}\text{H}_8\text{F}_6\text{N}_4\text{O}_3+\text{H}]^+)$ (APCI+) $[\text{M}+\text{H}]^+$: calculated: 347.0579, found: 347.0573.

5.3 1-((1,1,1,3,3,3-Hexafluoropropan-2-yl)oxy)naphthalene (6)

The electrolysis of naphthalene (128.2 mg, 1.00 mmol) was conducted according to GP2 until a charge of 2.61 F was applied. The crude product was purified using flash chromatography on silica gel eluting with cyclohexane, yielding a crystalline colorless solid (174 mg, 0.591 mmol, 59%).



^1H NMR (400 MHz, CDCl_3): δ [ppm] = 8.32 – 8.22 (m, 1H, $H-8$), 7.93 – 7.83 (m, 1H, $H-5$), 7.66 (d, J = 8.0 Hz, 1H, $H-4$), 7.63 – 7.54 (m, 2H, $H-6$, $H-7$), 7.44 (t, J = 8.0 Hz, 1H, $H-3$), 7.05 (d, J = 8.0 Hz, 1H, $H-2$), 5.15 (hept, J = 5.7 Hz, 1H, $H-2'$).

^{13}C NMR (101 MHz, CDCl_3): δ [ppm] = 153.5 (C-1), 134.7 (C-4a), 127.6 (C-5), 127.2 (C-6), 126.5 (C-7), 125.8 (C-8a), 125.2 (C-3), 124.2 (C-4), 121.0 (q, J = 283 Hz, C-3'), 121.6 (C-8), 108.1 (C-2), 76.1 (hept, J = 4 Hz, C-2').

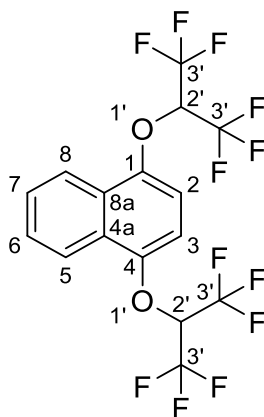
^{19}F NMR (376 MHz, CDCl_3): δ [ppm] = -74.46 (d, J = 5.9 Hz).

Mp: 63.2 °C (crystallized from ethyl acetate).

HRMS of $[\text{C}_{13}\text{H}_8\text{F}_6\text{O}]^+$ (APCI+) $[\text{M}]^+$: calculated: 295.0479, found: 294.0479.

5.4 1,4-Bis((1,1,1,3,3,3-hexafluoropropan-2-yl)oxy)naphthalene (5)

The electrolysis of naphthalene (160.1 mg, 1.25 mmol) was conducted according to GP1 until a charge of 4 F was applied. The crude product was purified using flash chromatography on silica gel eluting with cyclohexane, yielding a crystalline colorless solid (104.1 mg, 0.226 mmol, 18%).



^1H NMR (400 MHz, CDCl_3): δ [ppm] = 8.38 – 8.16 (m, 2H, H -5, H -8), 7.73 – 7.61 (m, 2H, H -6, H -7), 6.98 (s, 2H, H -1, H -4), 5.06 (hept, J = 5.7 Hz, 2H, H -2').

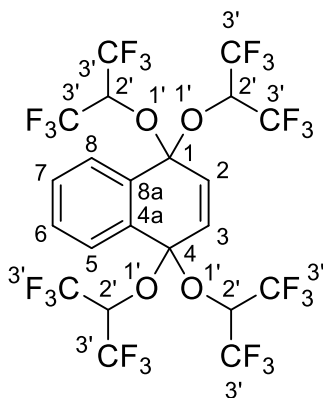
^{13}C NMR (101 MHz, CDCl_3): δ [ppm] = 150.0 (C-1, C-4), 127.8 (C-5, C-8), 126.8 (C-4a, C-8a), 121.6 (C-6, C-7), 121.1 (q, J = 284.0 Hz, C-3'), 107.6 (C-2, C-3), 76.5 (C-2').

^{19}F NMR (376 MHz, CDCl_3): δ [ppm] = -74.45 (d, J = 6.2 Hz).

Mp: 149.8 °C (crystallized from ethyl acetate).

5.5 1,1,4,4-Tetrakis((1,1,1,3,3,3-hexafluoropropan-2-yl)oxy)-1,4-dihydronaphthalene (8)

The electrolysis of naphthalene (128.2 mg, 1.00 mmol) was conducted according to GP2 until a charge of 7 F was applied. The crude product was purified using flash chromatography on silica gel eluting with ethyl acetate in cyclohexane (0-3% in 2 h), yielding a highly viscous orange oil (208 mg, 0.262 mmol, 26%).



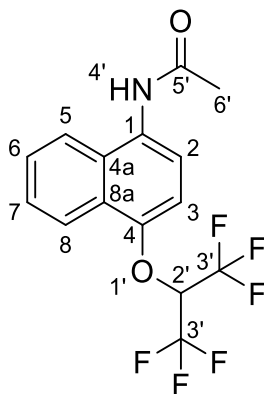
^1H NMR (400 MHz, CDCl_3): δ [ppm] = 7.82 – 7.74 (m, 2H, $H-6$, $H-7$), 7.70 – 7.63 (m, 2H, $H-5$, $H-8$), 6.42 (s, 2H, $H-2$, $H-3$), 4.42 (hept, J = 5.5 Hz, 4H, $H-2'$).

^{13}C NMR (101 MHz, CDCl_3): δ [ppm] = 131.96 ($C-5$, $C-8$), 131.64 ($C-4a$, $C-8a$), 129.35 ($C-2$, $C-3$), 127.97 ($C-6$, $C-7$), 125.51 – 115.76 (m, $C-3'$), 97.99 ($C-1$, $C-4$), 70.61 (hept, J = 33.8 Hz, $C-2'$).

^{19}F NMR (376 MHz, CDCl_3): δ [ppm] = -73.70 (d, J = 5.7 Hz).

5.6 *N*-(4-((1,1,1,3,3,3-Hexafluoropropan-2-yl)oxy)naphthyl)-acetamide (7)

The electrolysis of *N*-(1-naphthyl)acetamide (185.23 mg, 1.00 mmol) was conducted according to GP2 until a charge of 2.61 F was applied. The crude product was purified using flash chromatography on silica gel eluting with ethyl acetate in cyclohexane (0–30% in 3 h), yielding a crystalline colorless solid (110 mg, 0.313 mmol, 31%).



^1H NMR (400 MHz, $\text{DMSO-}d_6$): δ [ppm] = 9.91 (s, 1H, H -4'), 8.17 – 8.02 (m, 2H, H -8, H -5), 7.72 – 7.63 (m, 2H, H -7, H -6), 7.62 (d, J = 8.4 Hz, 1H, H -2), 7.41 (d, J = 8.4 Hz, 1H, H -3), 6.76 (hept, J = 6.0 Hz, 1H, H -2'), 2.18 (s, 3H, H -6').

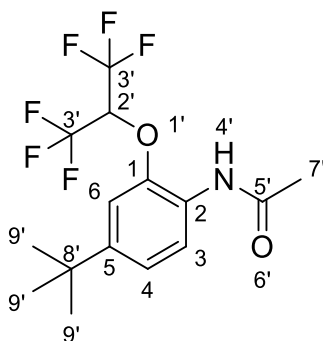
^{13}C NMR (101 MHz, $\text{DMSO-}d_6$): δ [ppm] = 169.5 (C-5'), 149.7 (C-1), 130.2 (C-8a), 129.5 (C-4a), 127.4 (C-6), 127.1 (C-7), 125.5 (C-4), 123.6 (C-5), 122.2 (C-3), 122.0, (C-3') 121.3 (C-8), 108.9, 73.5 (hept, J = 33 Hz, C-2'), 23.8 (C-6').

^{19}F NMR (376 MHz, $\text{DMSO-}d_6$): δ [ppm] = -74.04 (d, J = 6.4 Hz).

HRMS of $([\text{C}_{15}\text{H}_{11}\text{F}_6\text{NO}_2+\text{H}]^+)$ (ESI+) $[\text{M}+\text{H}]^+$: calculated: 352.0771, found: 352.0772.

5.7 *N*-(4-(*tert*-Butyl)-2-((1,1,1,3,3,3-hexafluoropropan-2-yl)oxy)phenyl)acetamide (4)

The electrolysis of 4-(*tert*-butyl)acetanilide (238.9 mg, 1.25 mmol) was conducted according to GP1 until a charge of 2.00 F was applied. The crude product was purified using flash chromatography on silica gel eluting with ethyl acetate in cyclohexane (0–12% in 3 h), yielding a crystalline red solid (144.7 mg, 0.405 mmol, 32%).



^1H NMR (400 MHz, CDCl_3): δ [ppm] = 8.24 (d, J = 8.6 Hz, 1H, H -3), 7.49 (s, 1H, H -4'), 7.21 (dd, J = 8.6, 2.0 Hz, 1H, H -4), 7.03 (d, J = 2.0 Hz, 1H, H -6), 4.84 (hept, J = 5.7 Hz, 1H, H -2'), 2.22 (s, 3H, H -7'), 1.32 (s, 9H, H -9').

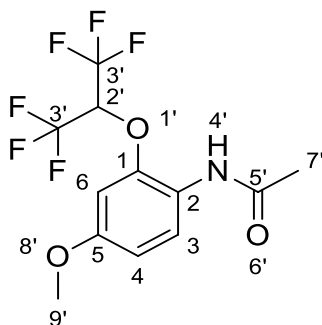
^{13}C NMR (101 MHz, CDCl_3): δ [ppm] = 168.2 (C-5'), 148.3 (C-5), 146.0 (C-1), 126.63 (C-2), 122.4 (C-4), 121.5 (C-3), 121.0 (C-3'), 112.1 (C-6), 77.0 (C-2'), 34.7 (C-8'), 31.2 (C-9'), 24.6 (C-7').

^{19}F NMR (376 MHz, CDCl_3): δ [ppm] = -74.61 (d, J = 5.9 Hz).

HRMS of $([\text{C}_{15}\text{H}_{17}\text{F}_6\text{NO}_2+\text{H}]^+)$ (ESI+) $[\text{M}+\text{H}]^+$: calculated: 358.1242, found: 358.1243.

5.8 *N*-(2-((1,1,1,3,3,3-Hexafluoropropan-2-yl)oxy)-4-methoxyphenyl)acetamide (9)

The electrolysis of 4-(methoxy)acetanilide (165.2 mg, 1.00 mmol) was conducted according to GP2 until a charge of 2.61 F was applied. The crude product was purified using flash chromatography on silica gel eluting with ethyl acetate in cyclohexane (0–20% in 1.5 h), yielding a crystalline red solid (103 mg, 0.311 mmol, 31%).



^1H NMR (400 MHz, CDCl_3): δ [ppm] = 8.19 (d, J = 9.0 Hz, 1H, H -3), 7.37 (s, 1H, H -4'), 6.71 (dd, J = 9.0 Hz, 2.6 Hz 1H, H -4), 6.60 (d, J = 2.6 Hz, 1H, H -6), 4.87 (hept, J = 4.9 Hz, 1H, H -2'), 3.81 (s, 4H, H -9'), 2.20 (s, 3H, H -7').

^{13}C NMR (101 MHz, CDCl_3): δ [ppm] = 167.1 (C-5'), 156.6 (C-5), 147.4 (C-1), 123.3 (C-3), 122.4 (C-2), 120.9 (qd, J = 284.4, 3.0 Hz, C-3'), 109.0 (C-4), 102.6 (C-6), 77.4 (C-3'), 55.7 (C-9'), 24.4 (C-7').

^{19}F NMR (376 MHz, CDCl_3): δ [ppm] = -74.70 (d, J = 5.8 Hz).

Mp: 82.7 °C (crystallized from ethyl acetate).

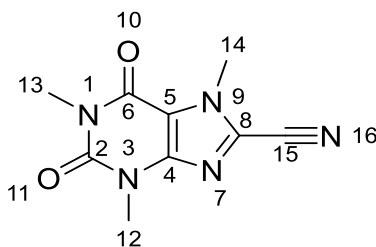
HRMS of $([\text{C}_{15}\text{H}_{17}\text{F}_6\text{NO}_2+\text{H}]^+)$ (ESI+) $[\text{M}+\text{H}]^+$: calculated: 332.0721, found: 332.0721.

5.9 8-Cyanocaffeine (10)

8-Cyanocaffeine was synthesized using nickel-catalysis (Method 1) and palladium-catalysis (Method 2) :

Method 1: The nickel-catalyzed cyanation of HFIP caffeyl ether (**81**) was carried out using standard Schlenk techniques under argon atmosphere. HFIP caffeyl ether (**81**) (90.6 mg, 0.25 mmol, 1 eq.), KCN (65.1 mg, 1 mmol, 4 eq.), PPh₃ (13.1 mg, 0.05 mmol, 20 mol%), NiCl₂(PPh₃)₂ (16.4 mg, 0.025 mmol, 10 mol%), and Zn (16.3 mg, 0.25 mmol, 1 eq.) were added into a Schlenk tube, which was dried by heating under reduced pressure and backfilling with argon three times. The tube was sealed with a rubber septum and the reagents were dried for one hour at reduced pressure. Then dimethylformamide (1 mL) was added. The reaction mixture was stirred at 115 °C for 14 h and conversion monitored by GC-MS. The crude product was purified using flash chromatography on silica gel eluting with ethyl acetate in cyclohexane (0–15% in 1.5 h), yielding a crystalline yellow solid (21.0 mg, 0.096 mmol, 38%).

Method 2: For the palladium-catalyzed cyanation of HFIP caffeyl ether (**81**) a round bottom flask was charged with HFIP caffeyl ether (**81**) (90.6 mg, 0.25 mmol 1 eq.), KCN (24.4 mg, 0.375 mmol, 1.5 eq.), XantPhos (14.5 mg, 0.025 mmol, 10 mol%), Pd(OAc)₂ (2.8 mg, 0.0125 mmol, 5 mol%), and dimethylformamide (1 mL). The reaction mixture was stirred at 85 °C for 14 h and monitored by GC-MS. The crude product was purified using flash chromatography on silica gel eluting with ethyl acetate in cyclohexane (0–15% in 1.5 h), yielding a crystalline yellow solid (33.2 mg, 0.15 mmol, 60%).



^1H NMR (400 MHz, CDCl_3): δ [ppm] = 4.19 (s, 1H, *H*-14), 3.59 (s, 1H, *H*-11), 3.44 (s, 1H, *H*-12).

^{13}C NMR (101 MHz, CDCl_3): δ [ppm] = 154.8 (*C*-1), 151.3 (*C*-5), 147.6 (*C*-3), 124.9 (*C*-8), 109.9 (*C*-2), 109.7 (*C*-15), 34.2 (*C*-14), 30.1 (*C*-11), 28.4 (*C*-12).

Mp: 152.2 °C (crystallized from ethyl acetate).

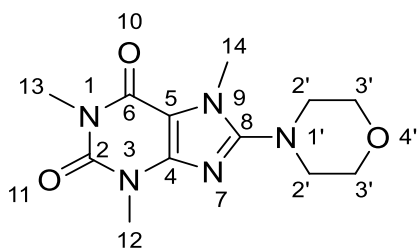
HRMS of $([\text{C}_9\text{H}_9\text{N}_5\text{O}_2+\text{H}]^+)$ (ESI+) $[\text{M}+\text{H}]^+$: calculated: 220.0834, found: 220.0833.

The analytical data match the literature.^[7]

5.10 8-Morpholinocaffeine (11)

Prep. 1: A round bottom flask equipped with a reflux condenser was charged with HFIP caffeyl ether (**100**) (90.6 mg, 0.25 mmol 1eq.), morpholine (0.065 mL, 65.3 mg, 0.75 mmol, 3 eq.), XantPhos (14.5 mg, 0.025 mmol, 10 mol%), Pd(OAc)₂ (2.8 mg, 0.0125 mmol, 5 mol%), and dimethylacetamide (1.5 mL). The reaction mixture was stirred at 100 °C for 14 h and monitored by GC-MS. The crude product was purified using flash chromatography on silica gel eluting with ethyl acetate in cyclohexane (0–15% in 1.5 h), yielding a crystalline beige solid (65.4 mg, 0.234 mmol, 94%).

Prep. 2: A round bottom flask equipped with a reflux condenser was charged with HFIP caffeyl ether (**100**) (90.6 mg, 0.25 mmol 1eq.), morpholine (0.065 mL, 65.3 mg, 0.75 mmol, 3 eq.), and dimethylacetamide (1.5 mL). The reaction mixture was stirred at 100 °C for 14 h and monitored by GC-MS. The crude product was purified using flash chromatography on silica gel eluting with ethyl acetate in cyclohexane (0–15% in 1.5 h), yielding a crystalline beige solid (52.2 mg, 0.234 mmol, 75%).



¹H NMR (400 MHz, DMSO-*d*₆): δ [ppm] = 3.74 (dd, *J* = 6.6, 3.5 Hz, 1H, *H*-2'), 3.69 (s, 1H, *H*-14), 3.37 (s, 1H, *H*-13), 3.22 (dd, *J* = 6.6, 3.5 Hz, 1H, *H*-3'), 3.20 (s, 1H, *H*-12).

¹³C NMR (101 MHz, DMSO-*d*₆): δ [ppm] = 156.0 (C-8), 154.4 (C-4), 151.4 (C-2), 147.2 (C-6), 104.9 (C-5), 66.1 (C-2'), 49.9 (C-3'), 32.8 (C-14), 29.9 (C-13), 27.8 (C-12)

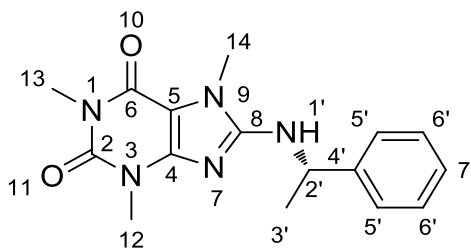
Mp: 143.9 °C (crystallized from ethyl acetate).

HRMS of $[\text{C}_{12}\text{H}_{17}\text{N}_5\text{O}_3+\text{H}]^+$ (ESI+) $[\text{M}+\text{H}]^+$: calculated: 280.1410, found: 280.1409.

The analytical data match the literature.^[8]

5.11 (S)-8-((1-Phenylethyl)amino)caffeine (12)

A round bottom flask equipped with a reflux condenser was charged with HFIP caffeine ether (**102**) (90.6 mg, 0.25 mmol 1eq.), (S)-1-phenylethylamine (0.097 mL, 90.8 mg, 0.75 mmol, 3 eq.), XantPhos (36.2 mg, 0.0625 mmol, 25 mol%), Pd(OAc)₂ (2.8 mg, 0.0125 mmol, 5 mol%), and 1.5 mL dimethylacetamide. The reaction mixture was stirred at 100 °C for 14 h and monitored by GC-MS. The crude product was purified using flash chromatography on silica gel eluting with methanol in dichloromethane (0–4% in 40 min), yielding a crystalline colorless solid (59.5 mg, 0.190 mmol, 76%).



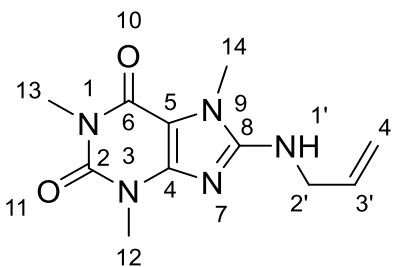
¹H NMR (400 MHz, CDCl₃): δ [ppm] = 7.42 (m, 2H, *H*-5'), 7.37 (m, 2H, *H*-6'), 7.30 (m, 1H, *H*-7'), 5.19 (pseudo-quintett, *J* = 6.8 Hz, 1H, *H*-2'), 4.57 (d, *J* = 6.8 Hz, 1H, *H*-1'), 3.68 (s, 3H, *H*-14), 3.51 (s, 3H, *H*-13), 3.36 (s, 3H, *H*-12), 1.65 (d, *J* = 6.8 Hz, 3H, *H*-3')

¹³C NMR (101 MHz, CDCl₃): δ [ppm] = 154.3 (C-4), 152.6 (C-8), 151.8 (C-2), 148.6 (C-6), 143.3 (C-4'), 128.7 (C-6'), 127.7 (C-7'), 126.2 (C-5'), 103.2 (C-5), 52.7 (C-2'), 29.8 (C-14), 29.6 (C-13), 27.6 (C-12), 22.5 (C-3')

HRMS of ([C₁₆H₁₉N₅O₂]+H)⁺ (ESI+) [M+H]⁺: calculated: 314.1617, found: 314.1617.

5.12 8-Allylaminocaffeine (13)

A round bottom flask equipped with a reflux condenser was charged with HFIP caffeine ether (**102**) (180 mg, 0.5 mmol 1eq.), allylamine (0.073 mL, 57 mg, 1.0 mmol, 2 eq.), XantPhos (28.9 mg, 0.05 mmol, 10 mol%), Pd(OAc)₂ (5.6 mg, 0.025 mmol, 5 mol%), and 3 mL dimethylacetamide. The reaction mixture was stirred at 100 °C for 3 h and monitored was GC-MS. The crude product was purified using flash chromatography on silica gel eluting with methanol in dichloromethane (0–1% in 40 min), yielding a crystalline colorless solid (45 mg, 0.18 mmol, 36%).



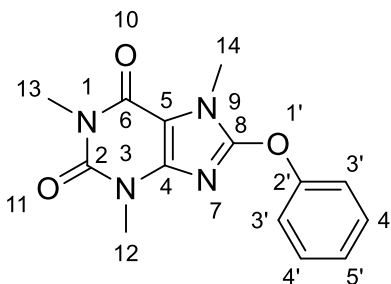
¹H NMR (400 MHz, CDCl₃) δ 5.97 (ddt, *J* = 17.1, 10.2, 5.8 Hz, 1H), 5.28 (dq, *J* = 17.1, 1.4 Hz, 1H), 5.20 (dq, *J* = 10.2, 1.4 Hz, 1H), 4.13 (d, *J* = 5.8 Hz, 2H), 3.69 (s, 3H), 3.52 (s, 3H), 3.36 (s, 3H).

¹³C NMR (101 MHz, CDCl₃) δ 154.4, 153.0, 151.8, 148.2, 134.4, 117.3, 103.3, 77.5, 77.4, 77.2, 76.8, 46.0, 30.0, 29.8, 27.8.

HRMS of ([C₁₁H₁₅N₅O₂]+H)⁺ (ESI+) [M+H]⁺: calculated: 250.1299, found: 250.1304.

5.13 8-Phenoxycaffeine (15)

A round bottom flask equipped with a reflux condenser was charged with HFIP caffeyl ether (**102**) (360 mg, 1.0 mmol 1 eq.), phenol (188 mg, 2.0 mmol, 2 eq.), cesium carbonate (977 mg, 3.0 mmol, 3 eq.) and 5 mL dimethylformamide. The reaction mixture was stirred at room temperature for 3 h and monitored by GC-MS. The crude product was purified using flash chromatography on silica gel eluting with cyclohexane/ethyl acetate (0–25% in 45 min), yielding a colorless solid (40 mg, 0.14 mmol, 14%).



HRMS of $[(C_{14}H_{14}N_4O_3)+H]^+$ (ESI+) $[M+H]^+$: calculated: 287.1139, found: 287.1139.

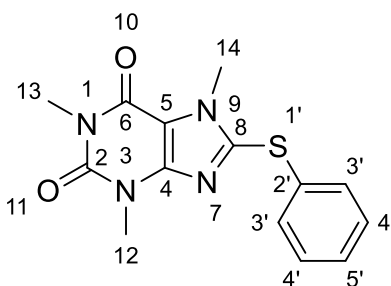
1H NMR (400 MHz, $CDCl_3$) δ 7.47 – 7.39 (m, 2H), 7.31 – 7.23 (m, 3H), 3.88 (s, 3H), 3.46 (s, 3H), 3.41 (s, 3H).

^{13}C NMR (101 MHz, $CDCl_3$) δ 155.1, 153.6, 153.5, 151.8, 146.0, 129.9, 125.8, 119.5, 104.0, 76.8, 30.6, 30.0, 28.0.

The analytical data match the literature.^[9]

5.14 8-(Phenylsulfanyl)caffeine (14)

A round bottom flask equipped with a reflux condenser was charged with HFIP caffeine ether (**102**) (360 mg, 1.0 mmol 1 eq.), thiophenol (0.204 mL, 220 mg, 2.0 mmol, 2 eq.), cesium carbonate (977 mg, 3.0 mmol, 3 eq.) and 5 mL dimethylformamide. The reaction mixture was stirred at room temperature for 3 h and monitored by GC-MS. The crude product was purified using flash chromatography on silica gel eluting with cyclohexane/ethyl acetate (0–45% in 45 min), yielding a colorless solid (246 mg, 0.814 mmol, 81.4%).



¹H NMR (400 MHz, CDCl₃) δ 7.36 – 7.27 (m, 5H), 3.90 (s, 3H), 3.54 (s, 3H), 3.37 (s, 3H).

¹³C NMR (101 MHz, CDCl₃) δ 155.0, 151.5, 148.1, 146.4, 130.9, 130.6, 129.7, 128.3, 109.6, 33.2, 30.0, 28.1.

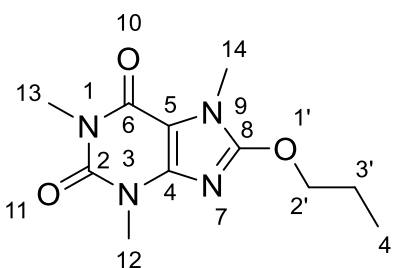
HRMS of ([C₁₄H₁₄N₄O₃]+H)⁺ (ESI⁺) [M+H]⁺: calculated: 303.0910, found: 303.0912.

Mp: 146.5 °C (crystallized from ethyl acetate).

The analytical data match the literature.^[10]

5.15 8-Propyloxycaffeine (17)

A round bottom flask equipped with a reflux condenser was charged with HFIP caffeine ether (**102**) (360 mg, 1.0 mmol 1 eq.), was dissolved in n-propanol (5 mL). A solution of NaOH (0.6 g, 15 mmol, 15 eq.) in 15 ml of water was added. The reaction mixture was stirred at 60 °C for 2 h. and monitored by GC-MS. The crude product was purified using flash chromatography on silica gel eluting with cyclohexane/ethyl acetate (0–40% in 45 min), yielding a crystalline colorless solid (38.0 mg, 0.15 mmol, 15%).



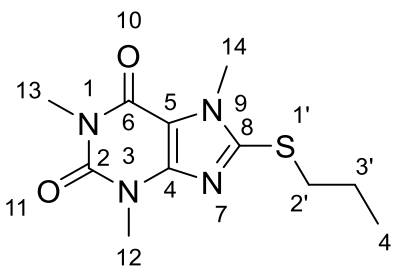
^1H NMR (400 MHz, CDCl_3) δ 4.41 (t, $J = 6.7$ Hz, 2H), 3.69 (s, 3H), 3.51 (s, 3H), 3.38 (s, 3H), 1.84 (dtd, $J = 14.0, 7.4, 6.7$ Hz, 2H), 1.03 (t, $J = 7.4$ Hz, 3H).

^{13}C NMR (101 MHz, CDCl_3) δ 156.0, 155.0, 151.9, 146.5, 103.5, 77.5, 77.2, 76.8, 72.8, 29.9, 29.8, 27.9, 22.4, 10.3.

HRMS of $[(\text{C}_{11}\text{H}_{16}\text{N}_4\text{O}_3)+\text{H}]^+$ (ESI+) $[\text{M}+\text{H}]^+$: calculated: 253.1295, found: 253.1296.

5.16 8-Propylsulfanylcaffeine (16)

A round bottom flask equipped with a reflux condenser was charged with HFIP caffeine ether (**102**) (360 mg, 1.0 mmol 1eq.), propan-1-thiol (0.18 mL, 152 mg, 2.0 mmol, 2 eq.), potassium carbonate (415 mg, 3.0 mmol, 3 eq.) and 5 mL dimethylformamide. The reaction mixture was stirred at 65 °C for 2 h and monitored by GC-MS. The crude product was purified using flash chromatography on silica gel eluting with eluting with cyclohexane/ethyl acetate (0–35% in 45 min), yielding a crystalline colorless solid (213 mg, 0.794 mmol, 79.4%).



^1H NMR (400 MHz, CDCl_3) δ 3.81 (s, 3H), 3.52 (s, 3H), 3.35 (s, 3H), 3.22 (t, $J = 7.3$ Hz, 2H), 1.76 (h, $J = 7.3$ Hz, 2H), 1.03 (t, $J = 7.3$ Hz, 3H).

^{13}C NMR (101 MHz, CDCl_3) δ 154.5, 151.5, 151.3, 148.4, 108.4, 77.4, 77.1, 76.8, 34.7, 32.1, 29.7, 27.8, 23.0, 13.2.

HRMS of $([\text{C}_{11}\text{H}_{16}\text{N}_4\text{O}_2\text{S}+\text{H}]^+)$ (ESI+) $[\text{M}+\text{H}]^+$: calculated: 269.1067, found: 269.1069.

Mp: 130.9 °C (crystallized from ethyl acetate).

The analytical data match the literature.^[11]

6 References

- [1] C. Gütz, B. Klöckner, S. R. Waldvogel, *Org. Process Res. Dev.* **2016**, *20*, 26–32.
- [2] R. E. Sioda, B. Frankowska, E. B. Lesiak, *Monatsh. Chem.* **2008**, *139*, 513–519.
- [3] J. Heinze, *Angew. Chem. Int. Ed.* **1984**, *23*, 831–847; *Angew. Chem.* **1984**, *23*, 823–840.
- [4] M. Salihovic, H. Š, S. Spirtovic-Halilovic, A. Osmanović, A. Dedić, Z. Asimovic, D. Završnik, *Glas. hem. tehnol. Bosne Herceg.* **2014**, *42*.
- [5] B. N. Plakhutin, E. R. Davidson, *J. Phys. Chem. A* **2009**, *113*, 12386–12395.
- [6] B. Elsler, A. Wiebe, D. Schollmeyer, K. M. Dyballa, R. Franke, S. R. Waldvogel, *Chem. Eur. J.* **2015**, *21*, 12321–12325.
- [7] a) H.-Q. Do, O. Daugulis, *Org. Lett.* **2010**, *12*, 2517–2519; b) L.-L. Gundersen, K. Bechgaard, J. Songstad, M. Leskelä, M. Polamo, M. N. Homsı, F. K. H. Kuske, M. Haugg, N. Trabesinger-Rüf, E. G. Weinhold, *Acta Chem. Scand.* **1996**, *50*, 58–63.
- [8] S. Yoshikawa, E. Emori, F. Matsuura, R. Clark, H. Ikuta, N. Yasuda, T. Nagakura, K. Yamazaki, M. Aoki, EP1338595, **2003**.
- [9] B. Strydom, J. J. Bergh, J. P. Petzer, *Eur. J. Med. Chem* **2011**, *46*, 3474–3485.
- [10] P. H. Gehrtz, V. Geiger, T. Schmidt, L. Sršan, I. Fleischer, *Org. Lett.* **2019**, *21*, 50–55.
- [11] M. Jouffroy, C. B. Kelly, G. A. Molander, *Org. Lett.* **2016**, *18*, 876–879.

7 ^1H , ^{13}C and ^{19}F NMR spectra

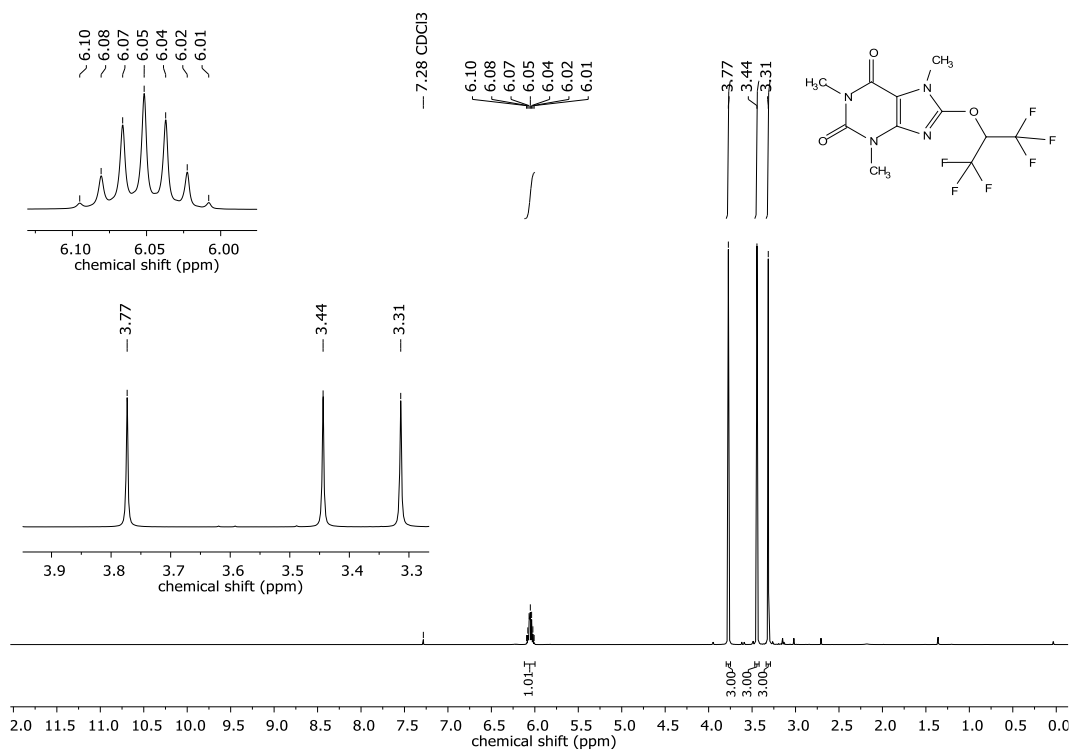


Figure 8: ^1H NMR spectrum of 8-((1,1,1,3,3,3-hexafluoropropan-2-yl)oxy)caffeine (**2**) in CDCl_3

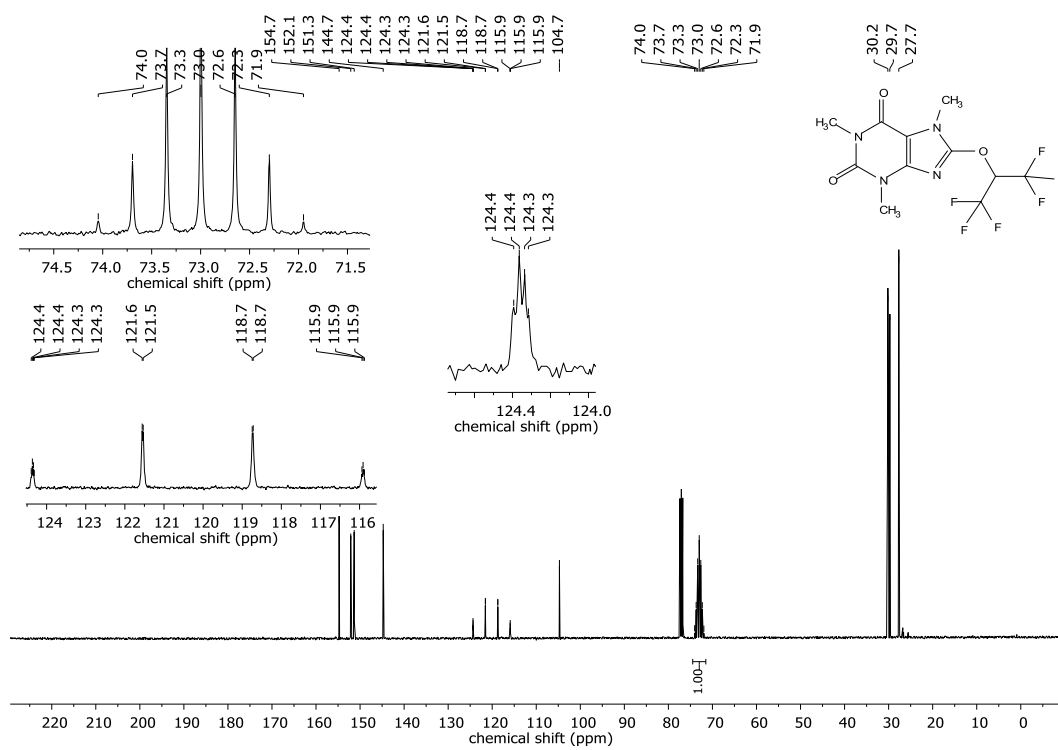


Figure 9: ^{13}C NMR spectrum of 8-((1,1,1,3,3,3-hexafluoropropan-2-yl)oxy)caffeine (**2**) in CDCl_3

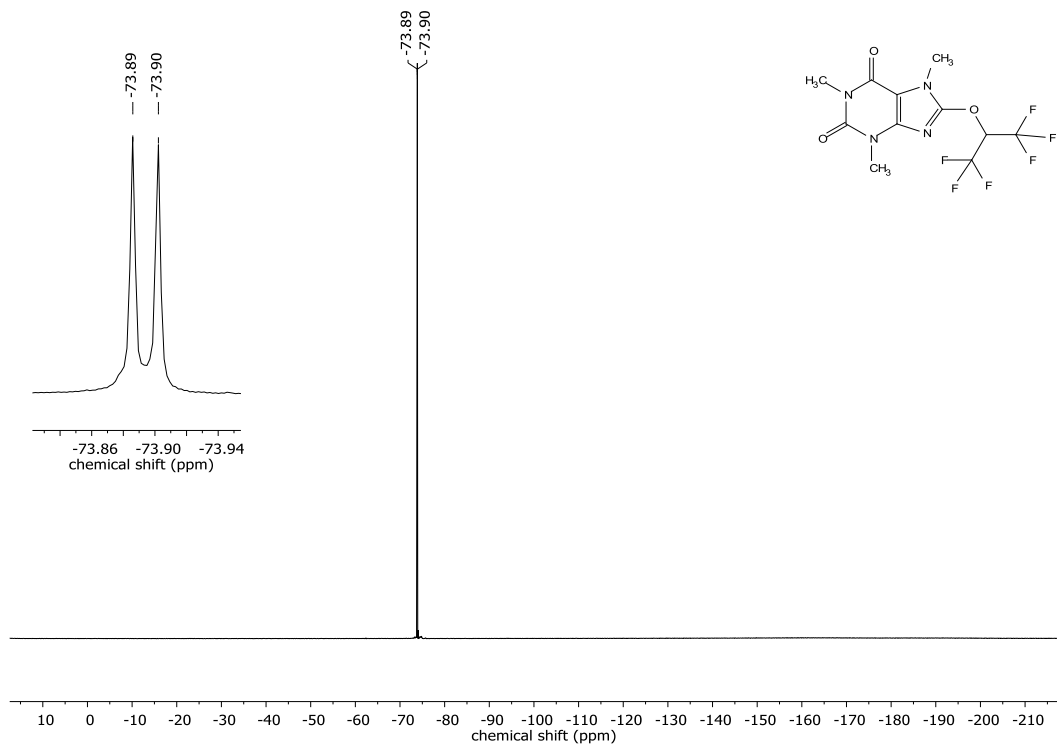


Figure 10: ¹⁹F NMR spectrum of 8-((1,1,1,3,3,3-hexafluoropropan-2-yl)oxy)caffeine (2) in DMSO-*d*₆

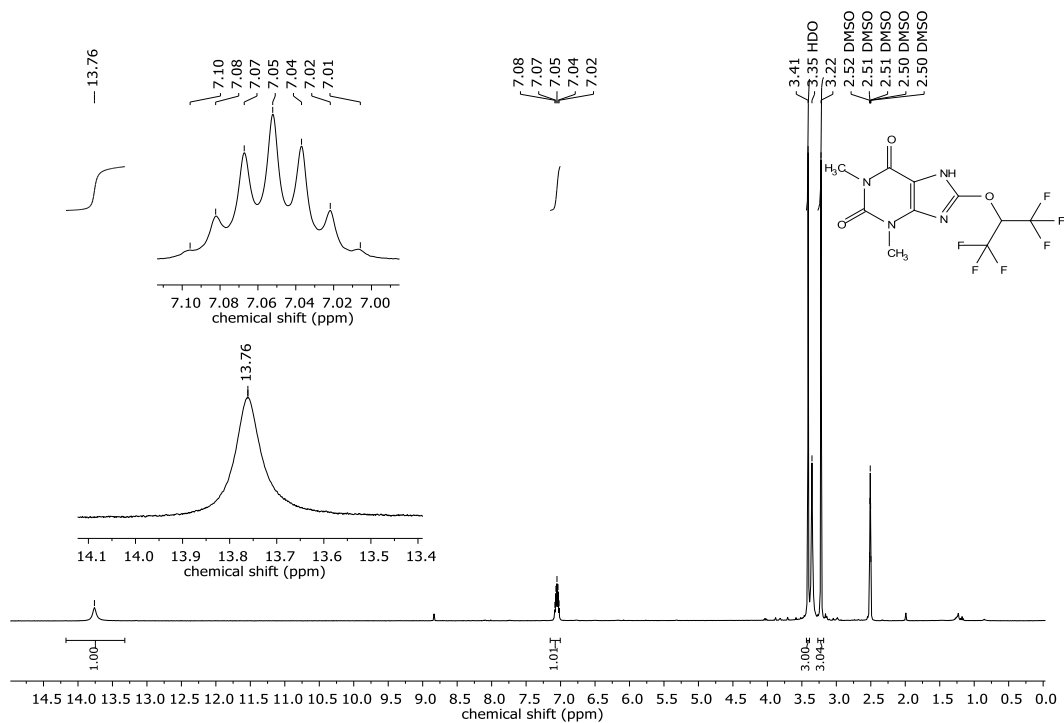


Figure 11: ¹H NMR spectrum of 8-((1,1,1,3,3,3-hexafluoropropan-2-yl)oxy)theophylline (3) in DMSO-*d*₆

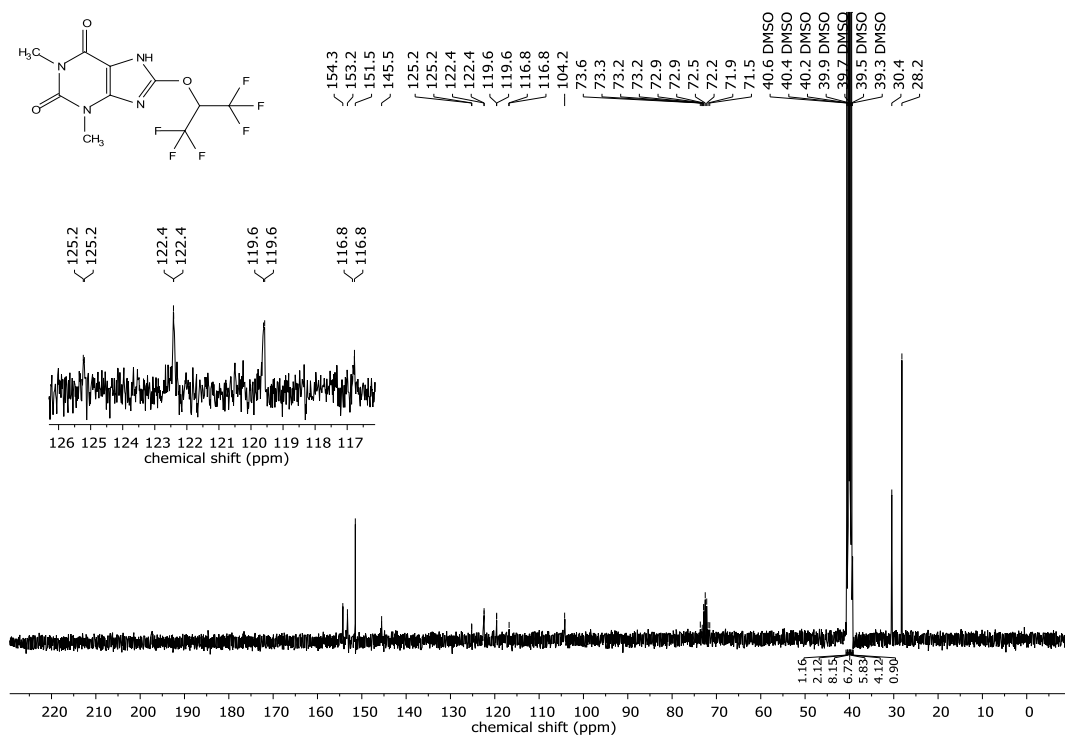


Figure 12: ¹³C NMR spectrum of 8-((1,1,1,3,3,3-hexafluoropropan-2-yl)oxy)theophylline (**3**) in DMSO-*d*₆

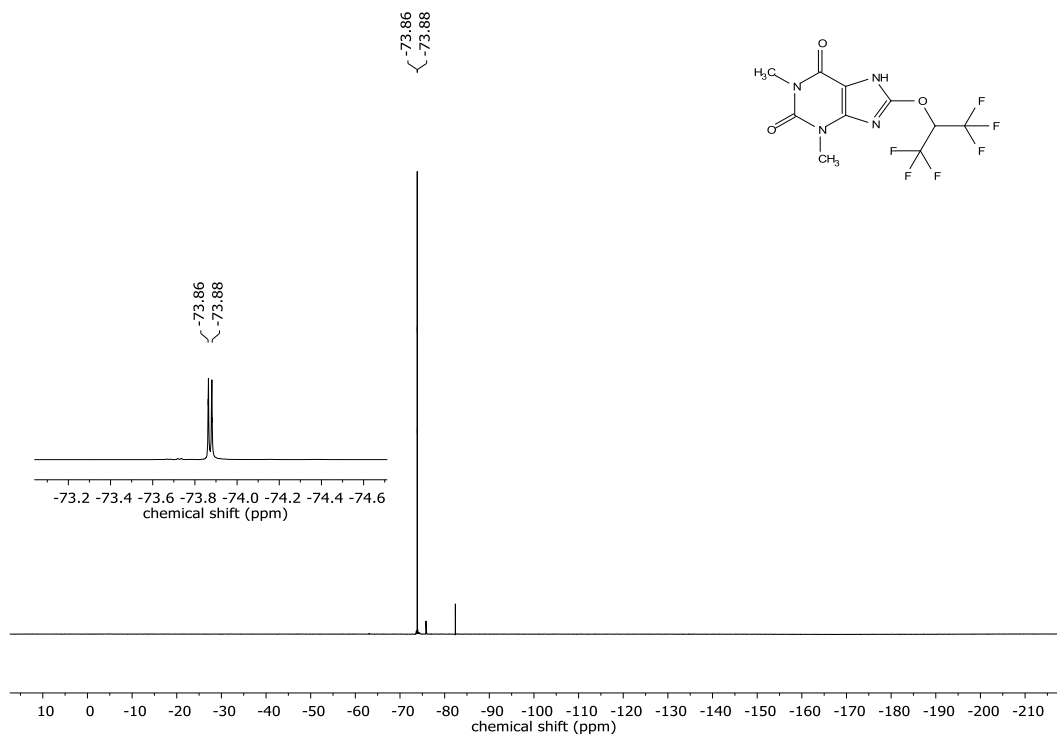


Figure 13: ¹⁹F NMR spectrum of 8-((1,1,1,3,3,3-hexafluoropropan-2-yl)oxy)theophylline (**3**) in DMSO-*d*₆

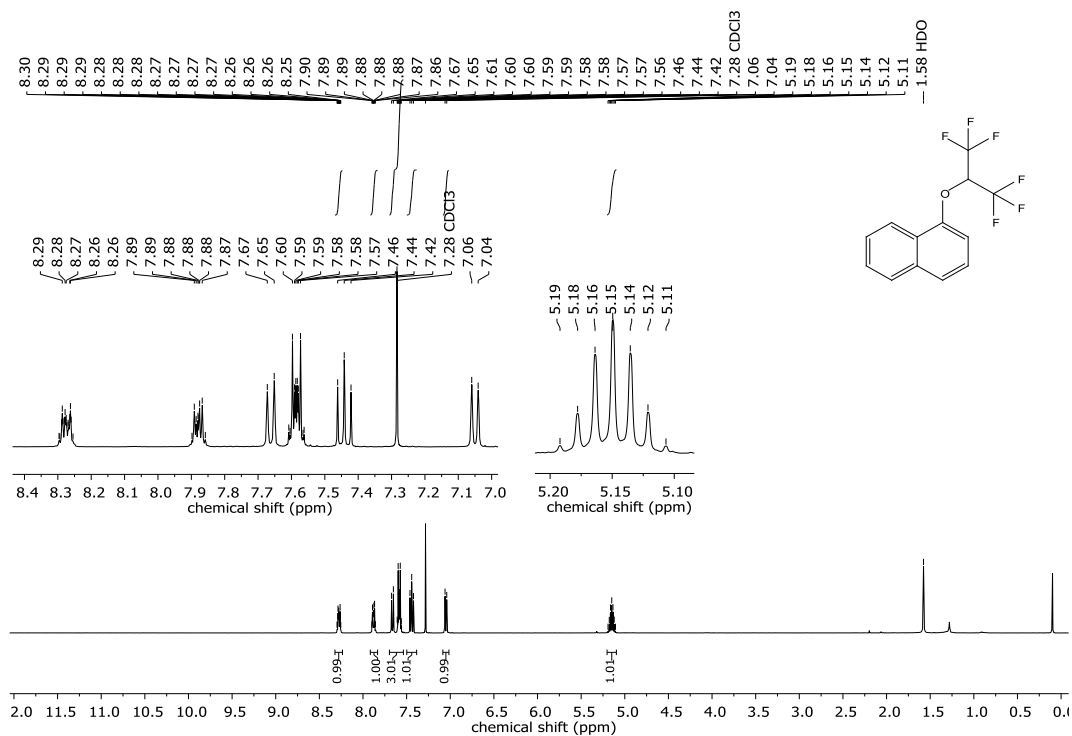


Figure 14: ^1H NMR spectrum of 1-((1,1,1,3,3,3-hexafluoropropan-2-yl)oxy)naphthalene (**6**) in CDCl_3

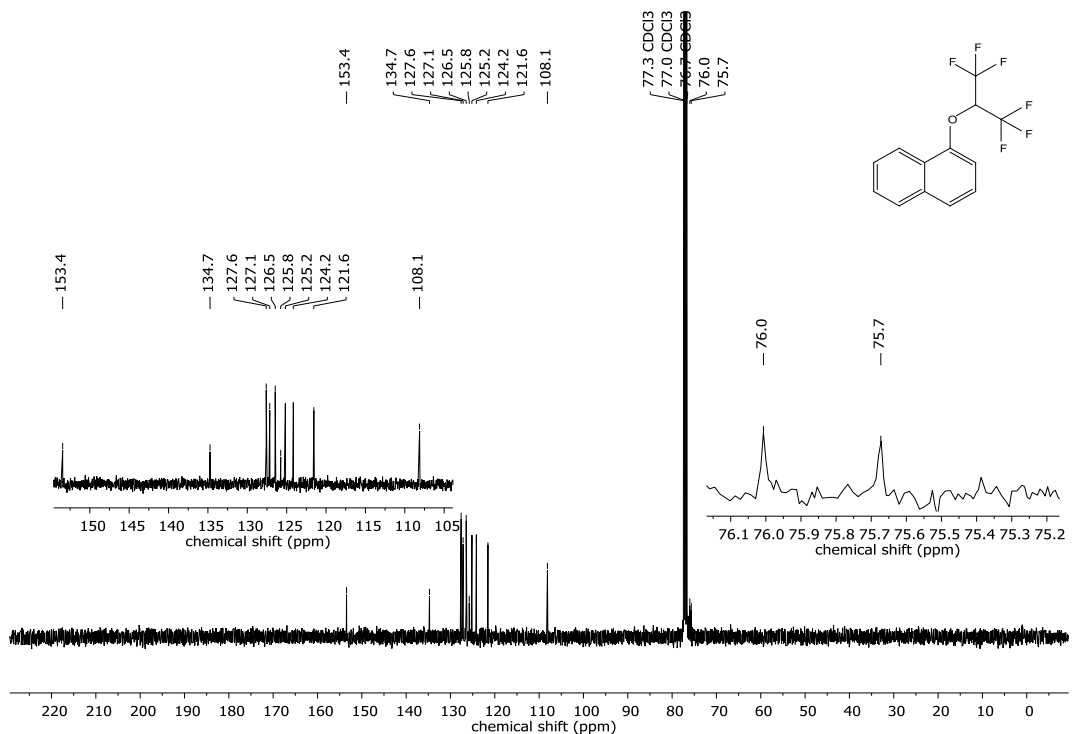


Figure 15: ^{13}C NMR spectrum of 1-((1,1,1,3,3,3-hexafluoropropan-2-yl)oxy)naphthalene (**6**) in CDCl_3

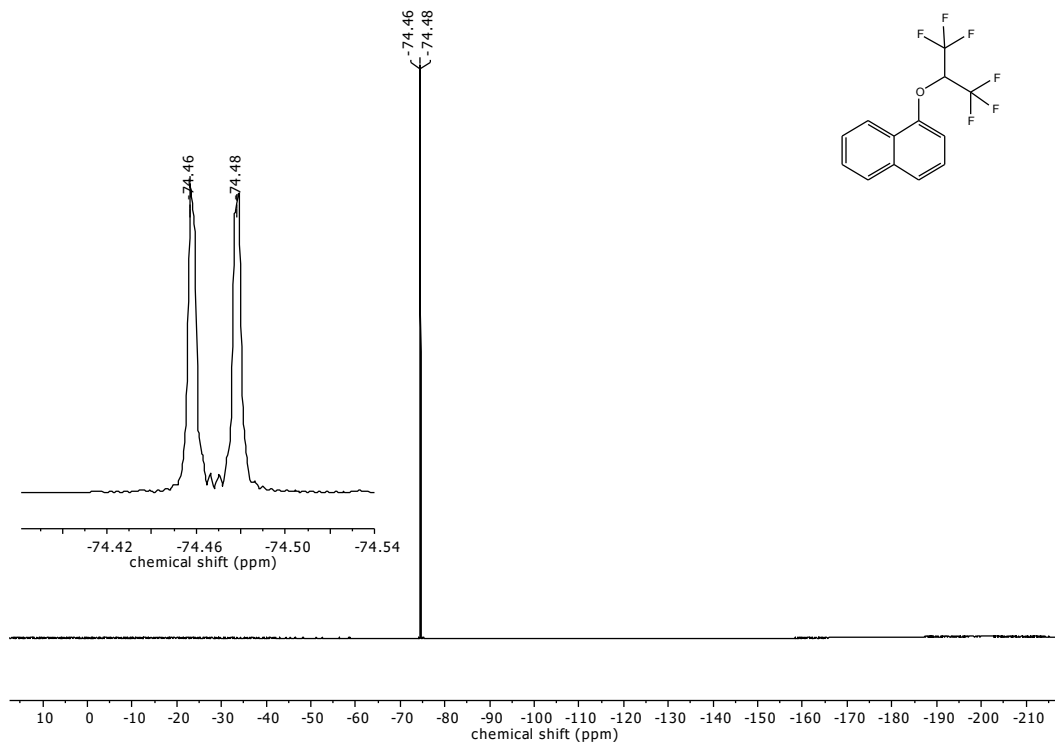


Figure 16: ^{19}F NMR spectrum of 1-((1,1,1,3,3,3-hexafluoropropan-2-yl)oxy)naphthalene (**6**) in CDCl_3

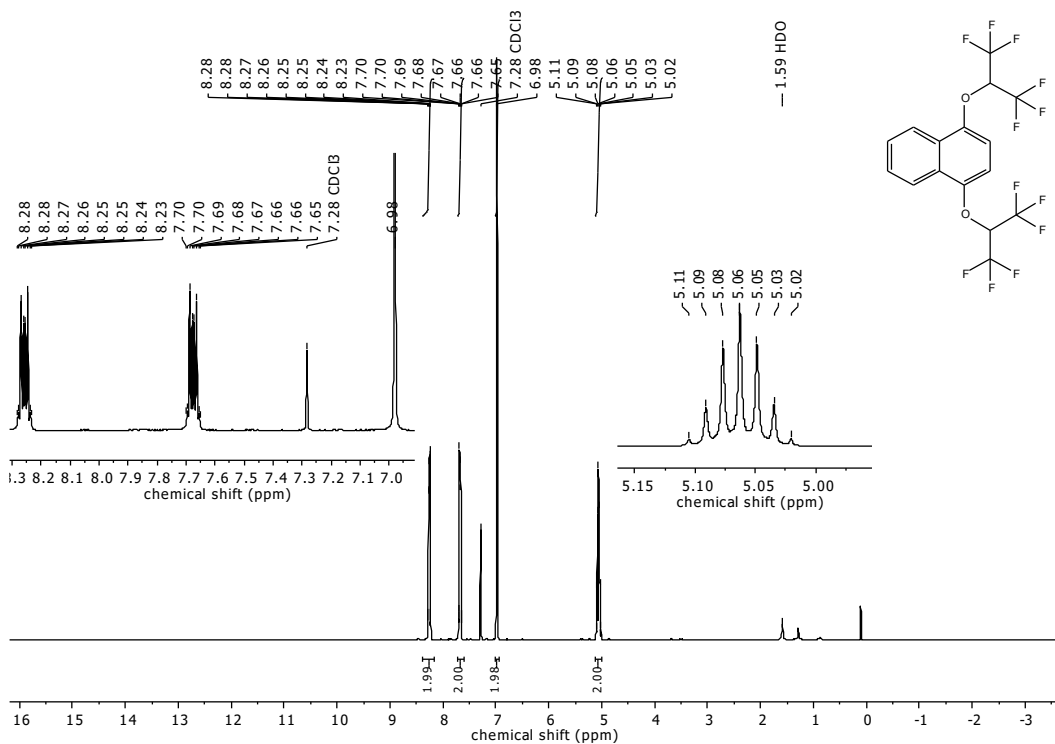


Figure 17: ^1H NMR spectrum of 1,4-bis((1,1,1,3,3,3-hexafluoropropan-2-yl)oxy)naphthalene (**5**) in CDCl_3

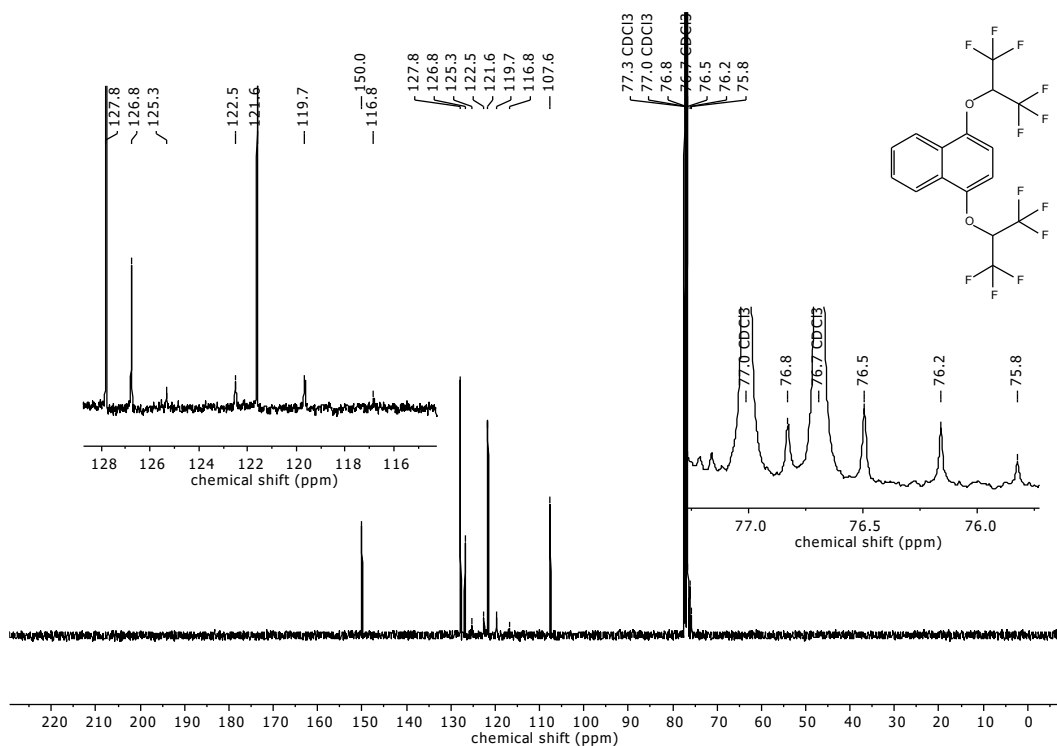


Figure 18: ¹³C NMR spectrum of 1,4-bis((1,1,1,3,3,3-hexafluoropropan-2-yl)oxy)naphthalene (**5**) in CDCl₃

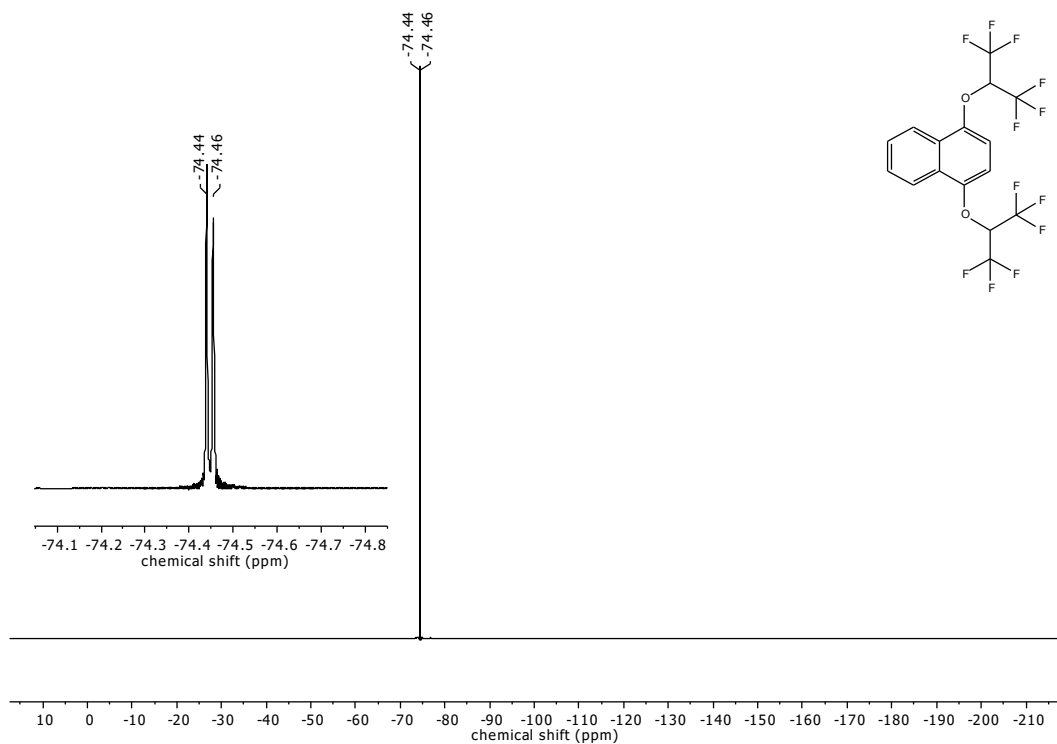


Figure 19: ¹⁹F NMR spectrum of 1,4-bis((1,1,1,3,3,3-hexafluoropropan-2-yl)oxy)naphthalene (**5**) in CDCl₃

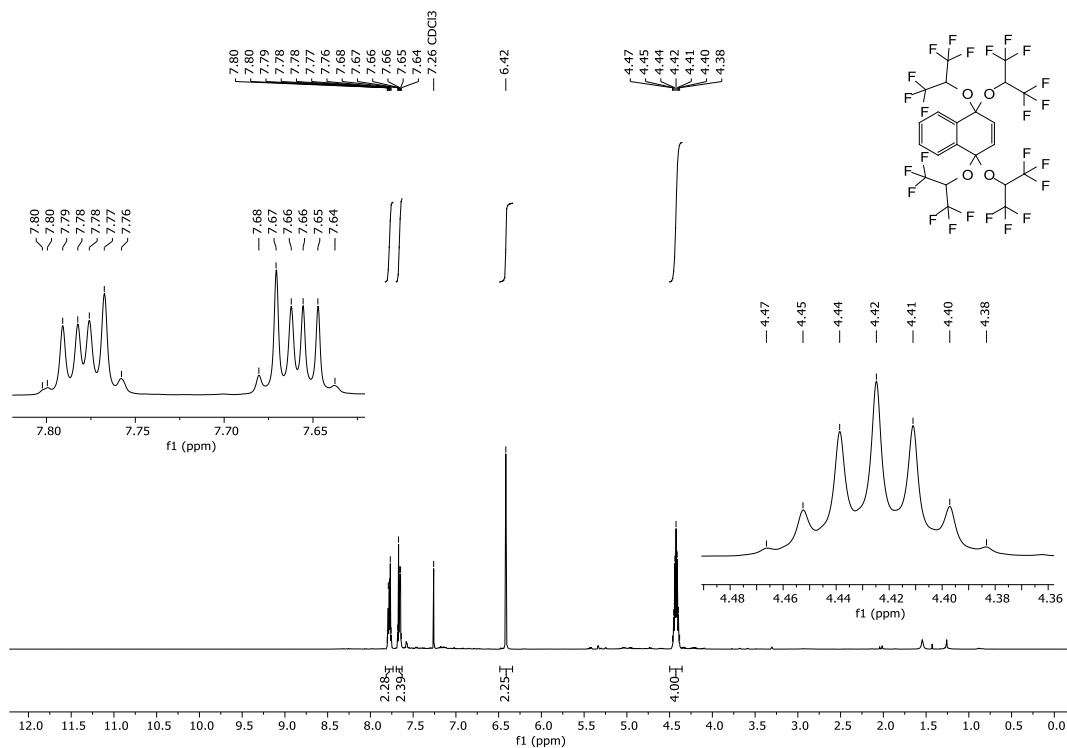


Figure 20: ^1H NMR spectrum of 1,1,4,4-Tetrakis((1,1,1,3,3,3-hexafluoropropan-2-yl)oxy)-1,4-dihydronaphthalene (**8**) in CDCl_3

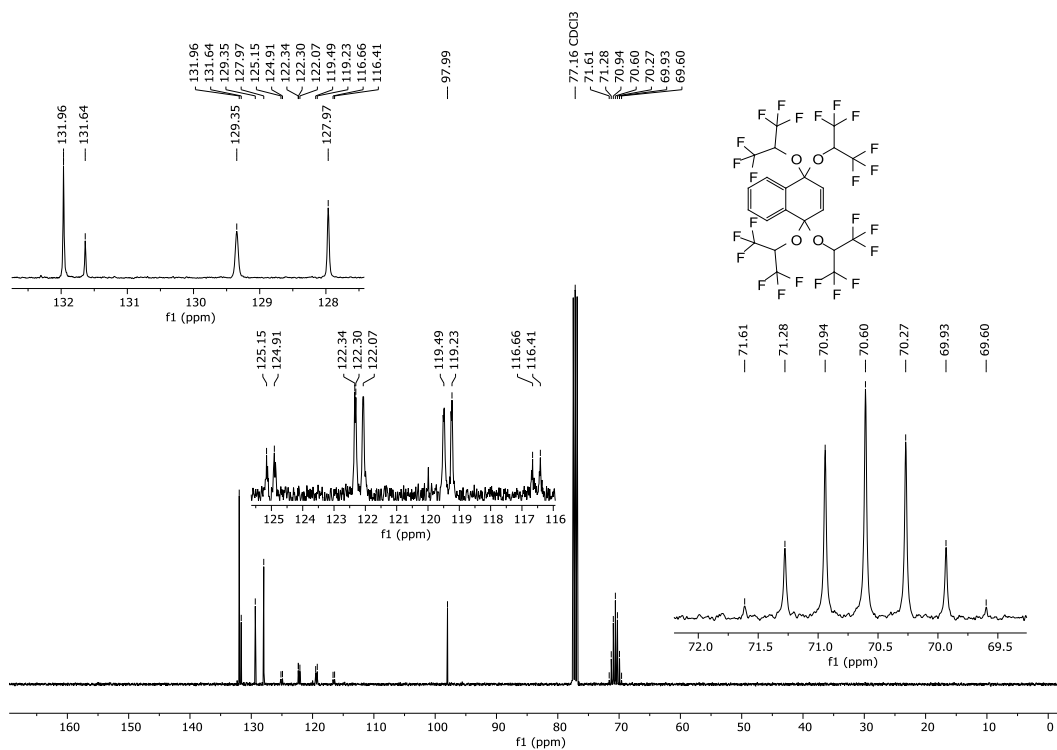


Figure 21: ^{13}C NMR spectrum of 1,1,4,4-Tetrakis((1,1,1,3,3,3-hexafluoropropan-2-yl)oxy)-1,4-dihydronaphthalene (**8**) in CDCl_3

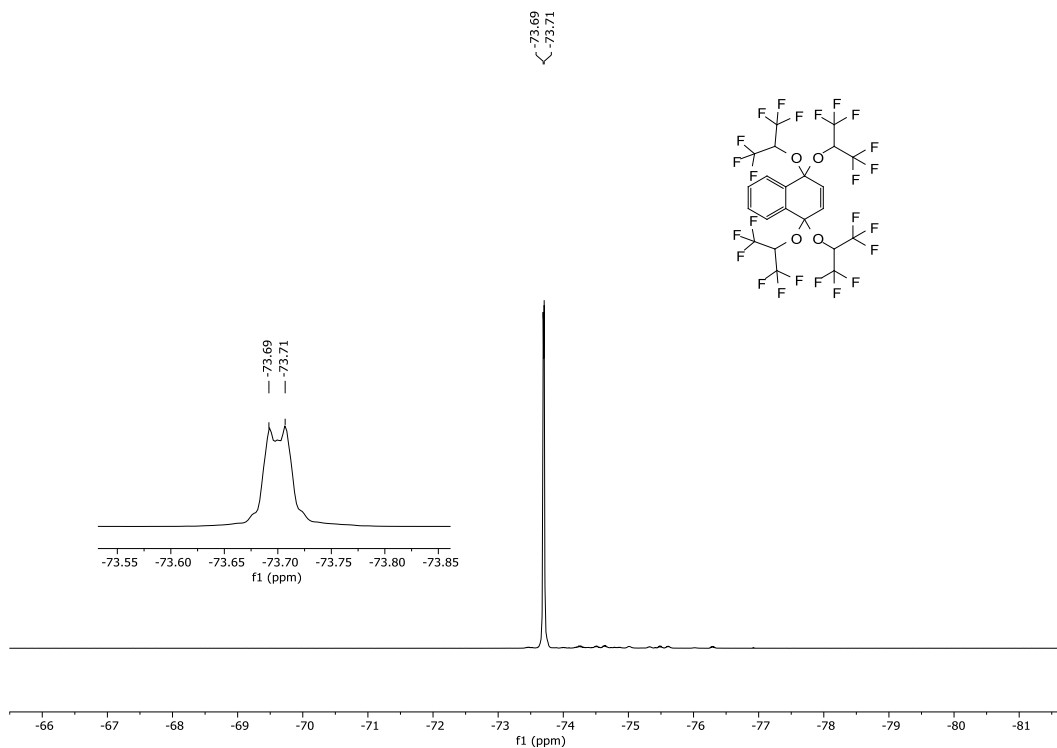


Figure 22: ^{19}F NMR spectrum of 1,1,4-Tetrakis((1,1,1,3,3,3-hexafluoropropan-2-yl)oxy)-1,4-dihydronaphthalene (**8**) in CDCl_3

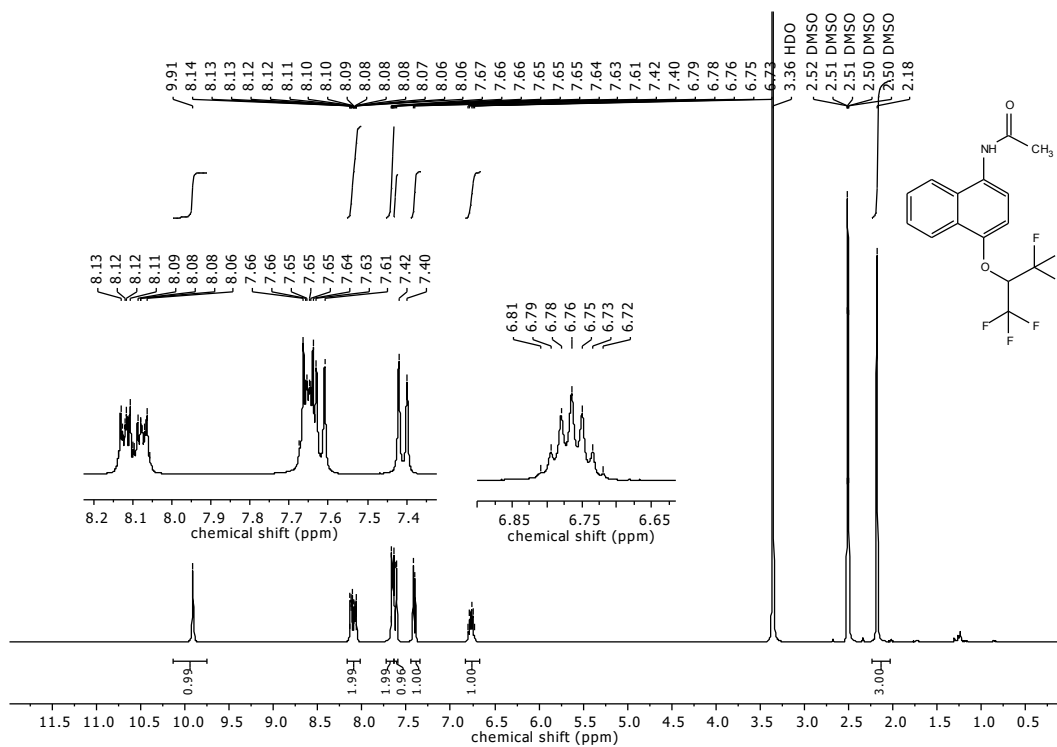


Figure 23: ^1H NMR spectrum of *N*-(4-((1,1,1,3,3,3-hexafluoropropan-2-yl)oxy)naphthyl)acetamide (**7**) in $\text{DMSO}-d_6$

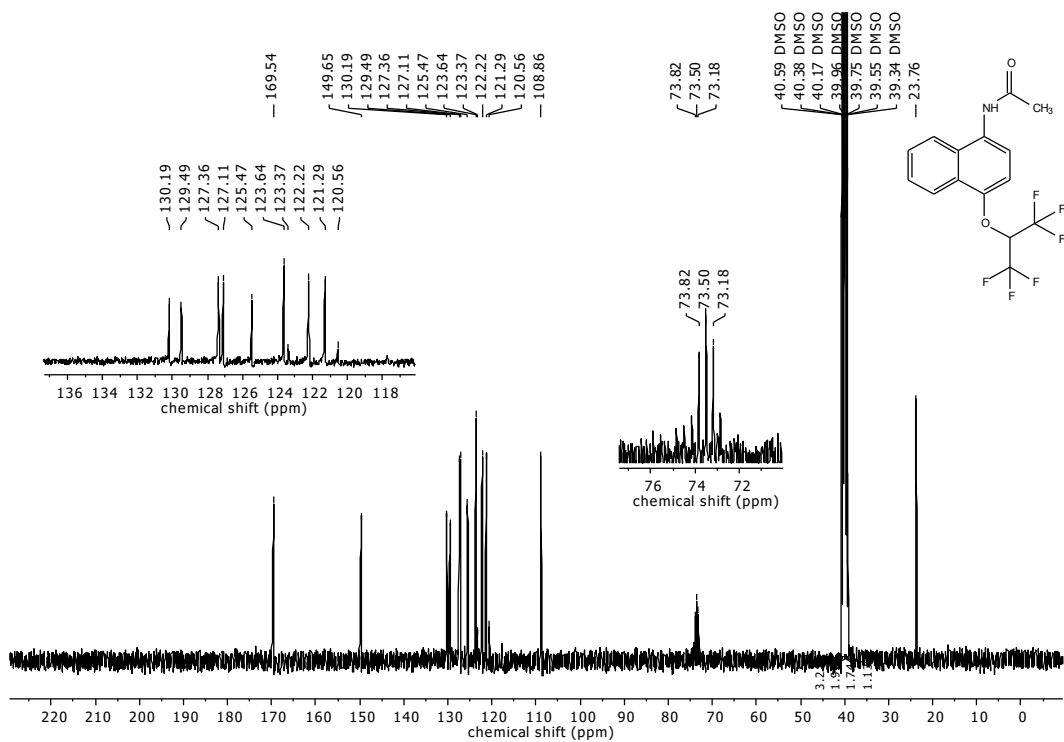


Figure 24: ¹³C NMR spectrum of *N*-(4-((1,1,1,3,3,3-hexafluoropropan-2-yl)oxy)naphthyl)acetamide (**7**) in DMSO-*d*₆

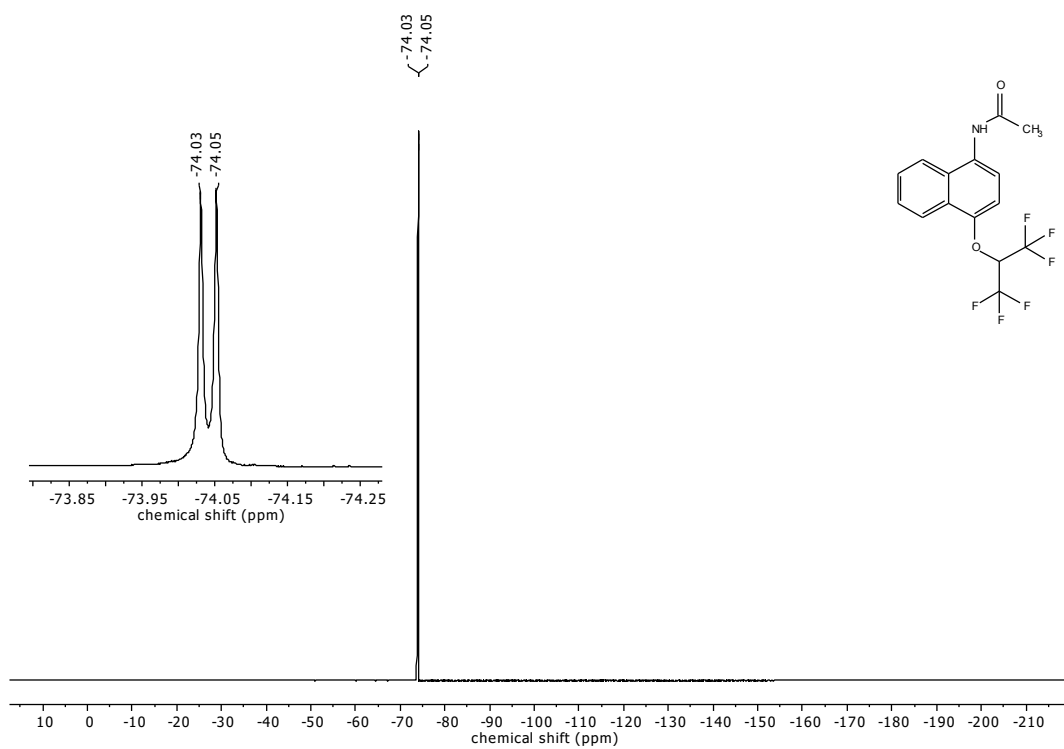


Figure 25: ¹⁹F NMR spectrum of *N*-(4-((1,1,1,3,3,3-hexafluoropropan-2-yl)oxy)naphthyl)acetamide (**7**) in DMSO-*d*₆

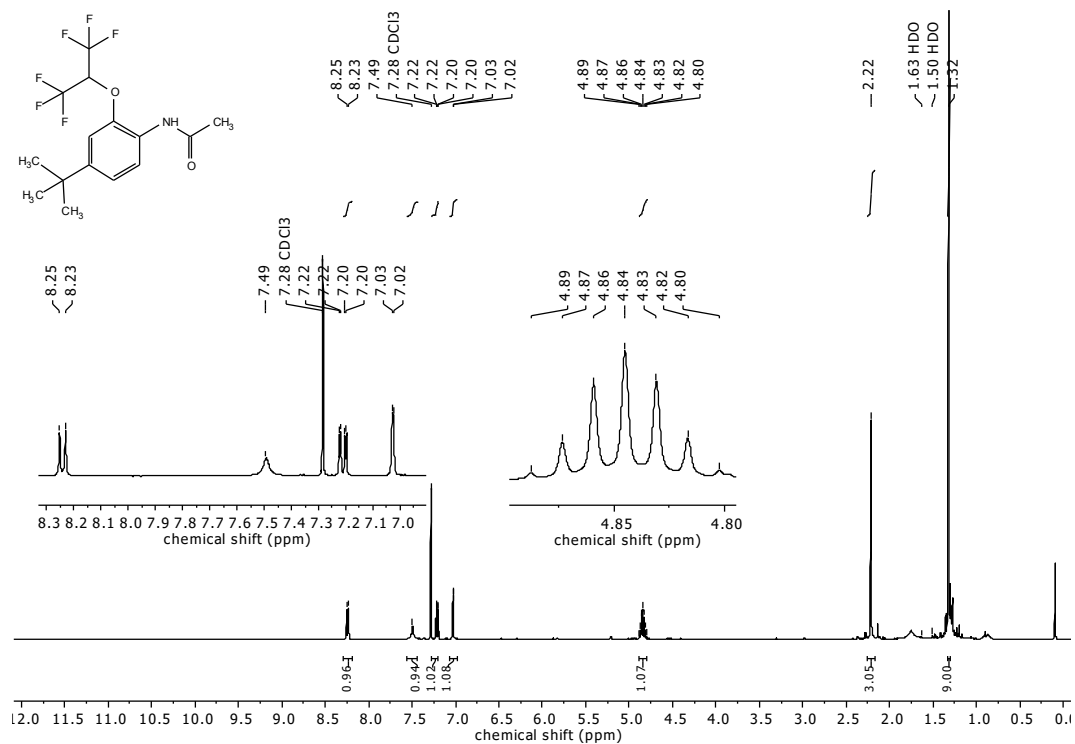


Figure 26: ¹H NMR spectrum of *N*-(4-(tert-butyl)-2-((1,1,1,3,3,3-hexafluoropropan-2-yl)oxy)phenyl)acetamide (**4**) in CDCl₃

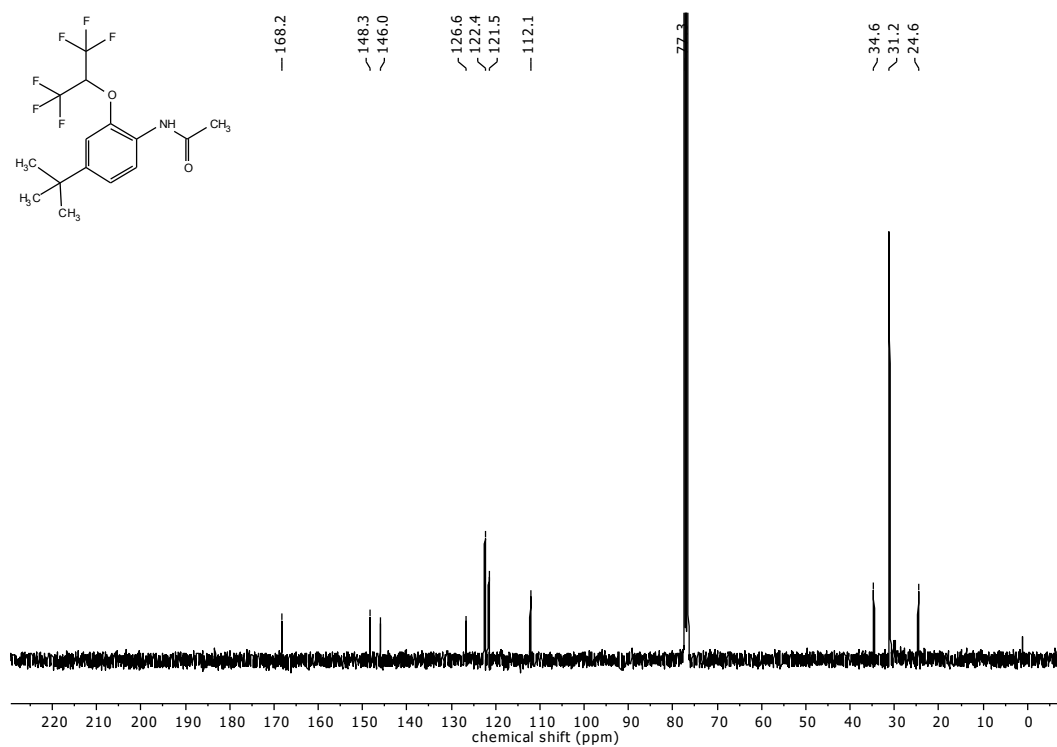


Figure 27: ¹³C NMR spectrum of *N*-(4-(tert-butyl)-2-((1,1,1,3,3,3-hexafluoropropan-2-yl)oxy)phenyl)acetamide (**4**) in CDCl₃

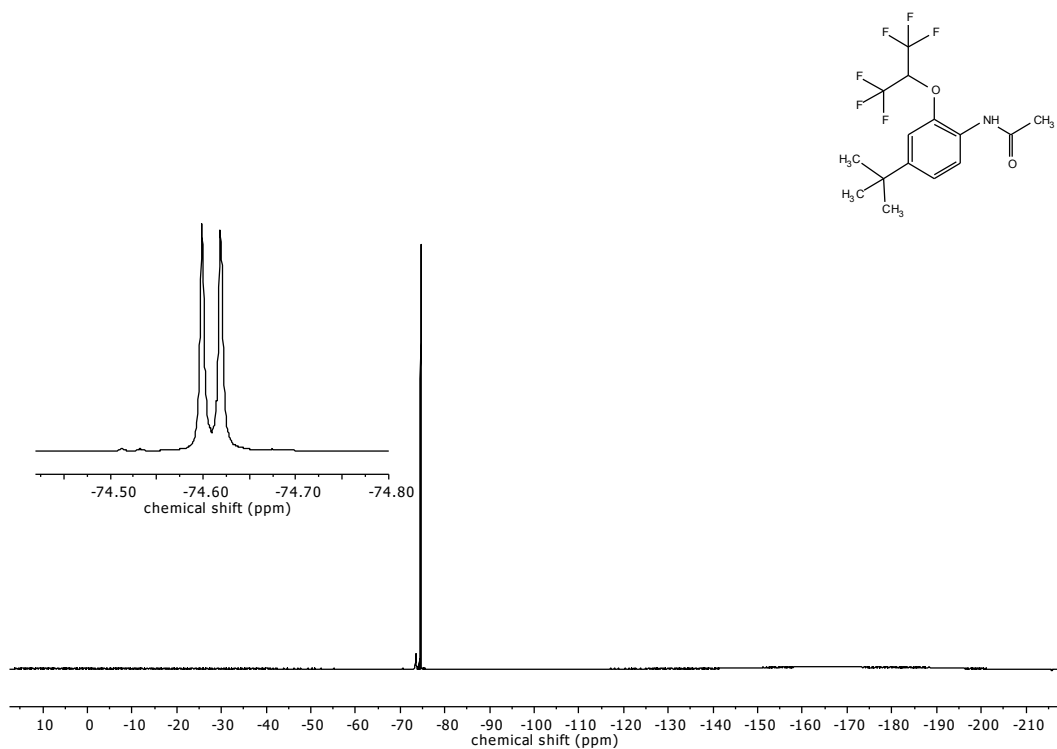


Figure 28: ^{19}F NMR spectrum of *N*-(4-(tert-butyl)-2-((1,1,1,3,3,3-hexafluoropropan-2-yl)oxy)phenyl)acetamide (**4**) in CDCl_3

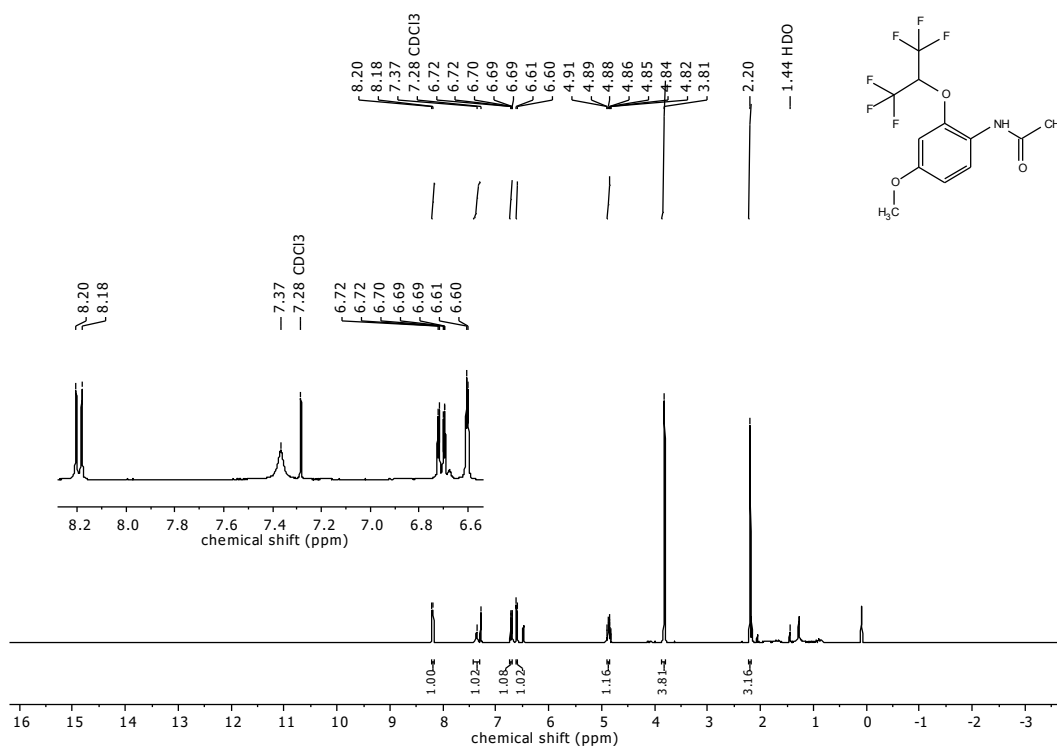


Figure 29: ^1H NMR spectrum of *N*-(2-((1,1,1,3,3,3-hexafluoropropan-2-yl)oxy)-4-methoxyphenyl)acetamide (**9**) in CDCl_3

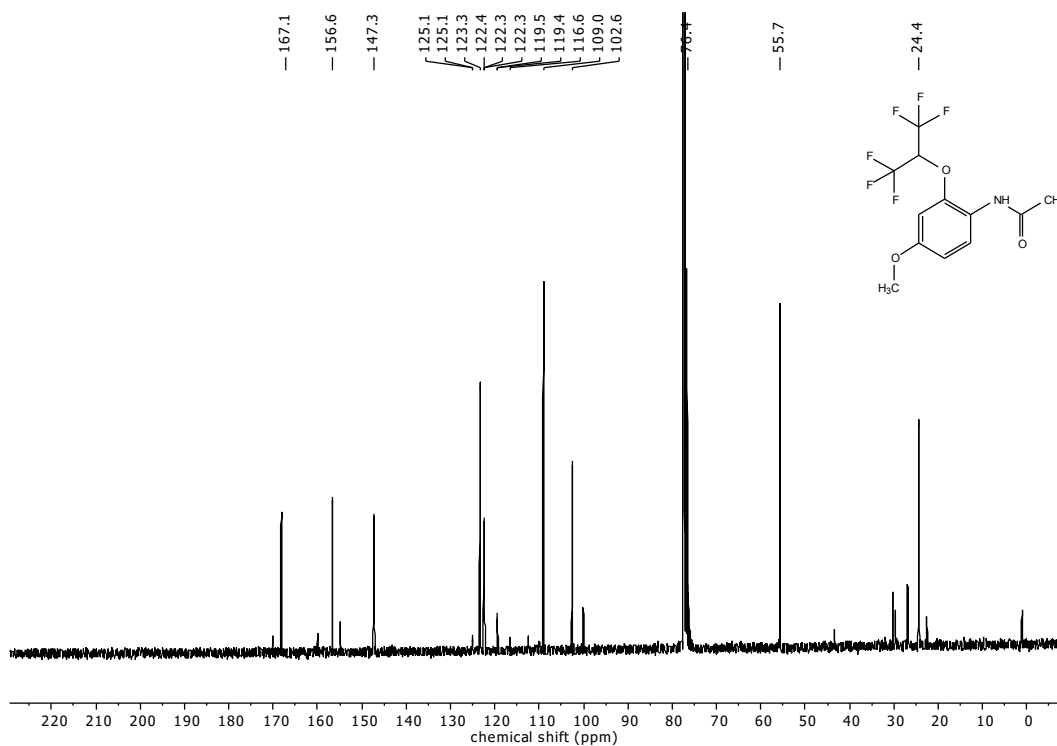


Figure 30: ^{13}C NMR spectrum of *N*-(2-((1,1,1,3,3,3-hexafluoropropan-2-yl)oxy)-4-methoxyphenyl)acetamide (**9**) in CDCl_3

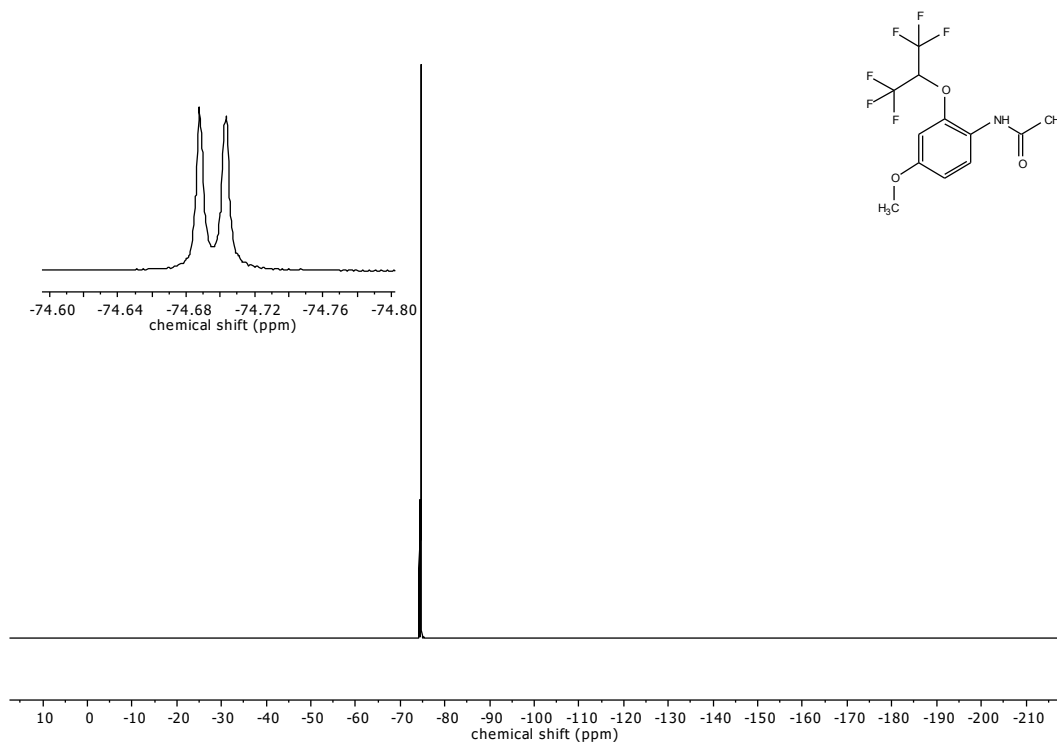


Figure 31: ^{19}F NMR spectrum of *N*-(2-((1,1,1,3,3,3-hexafluoropropan-2-yl)oxy)-4-methoxyphenyl)acetamide (**9**) in CDCl_3

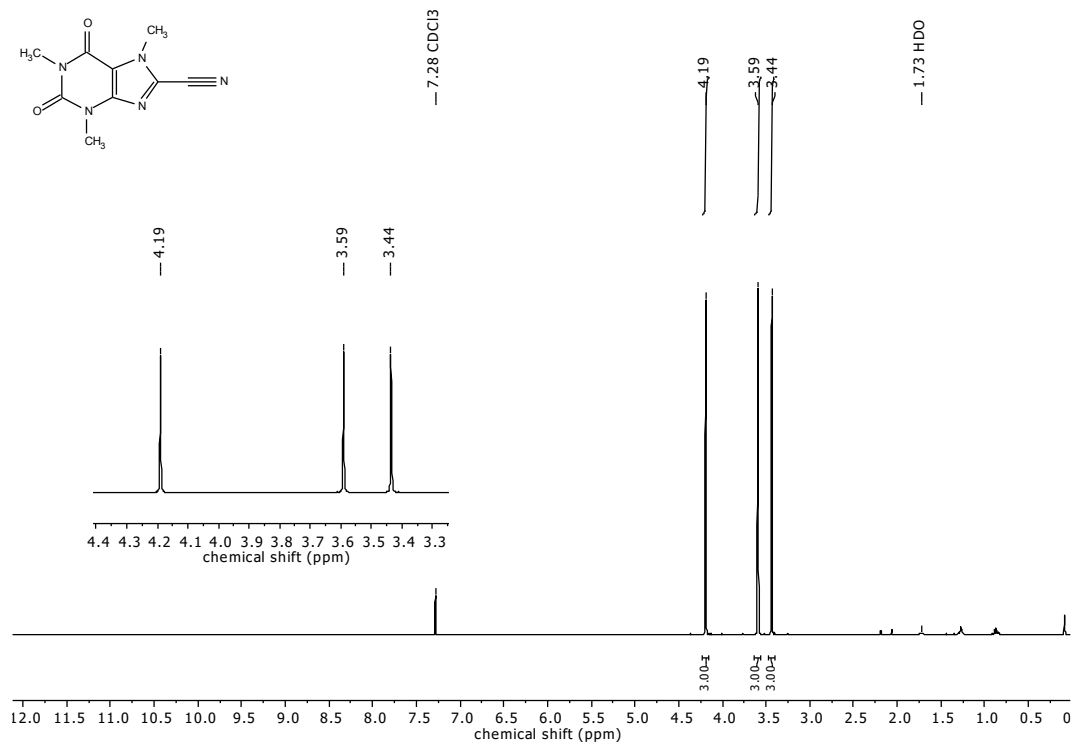


Figure 32: ¹H NMR spectrum of 8-cyanocaffeine (10) in CDCl₃

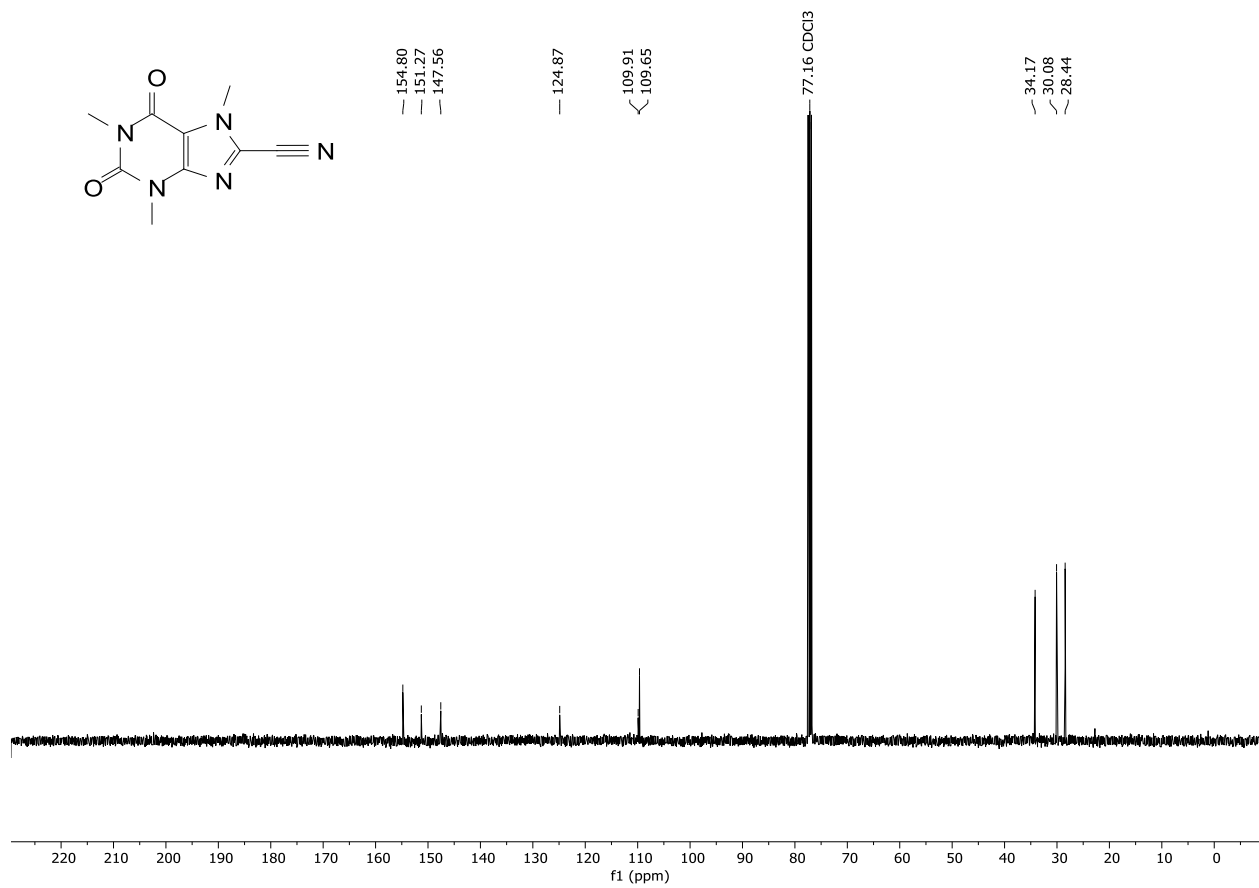


Figure 33: ¹³C NMR spectrum of 8-cyanocaffeine (10) in CDCl₃

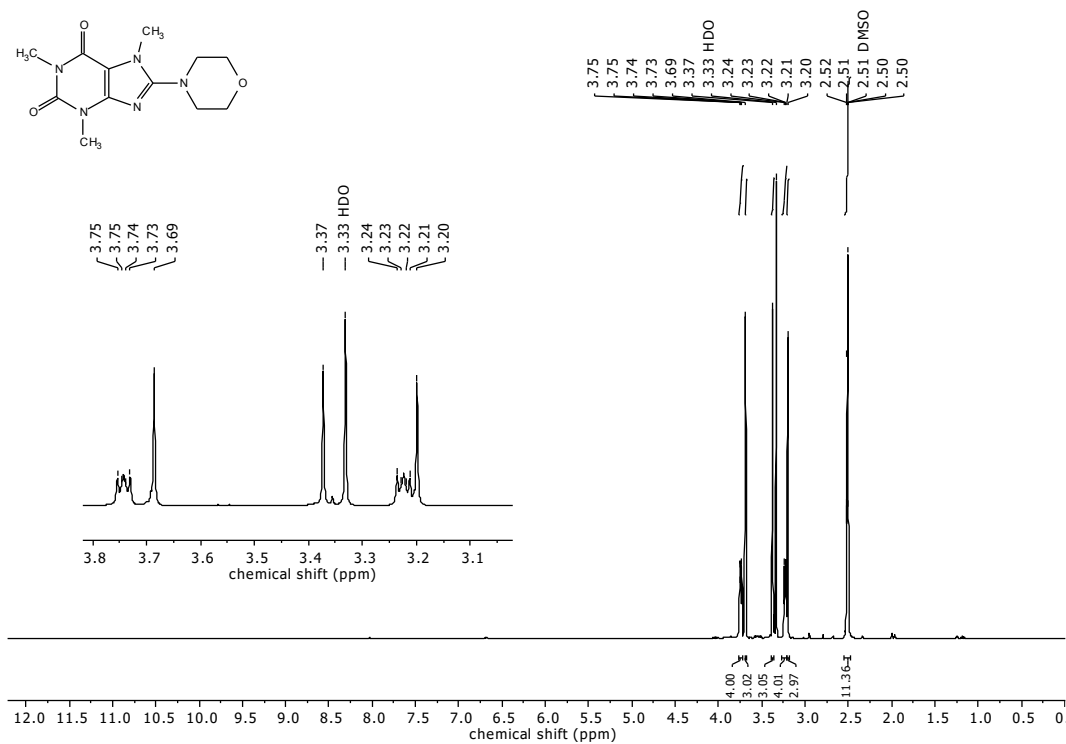


Figure 34: ¹H NMR spectrum of 8-morpholinocaffeine (11) in CDCl₃

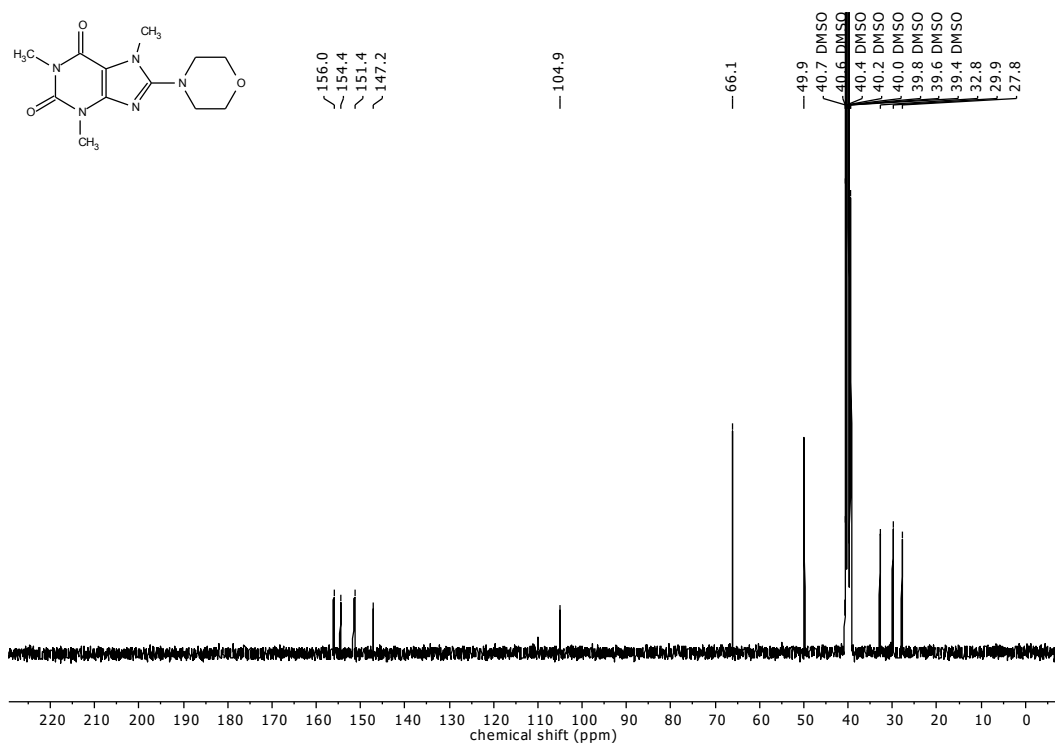


Figure 35: ¹³C NMR spectrum of 8-morpholinocaffeine (11) in CDCl₃

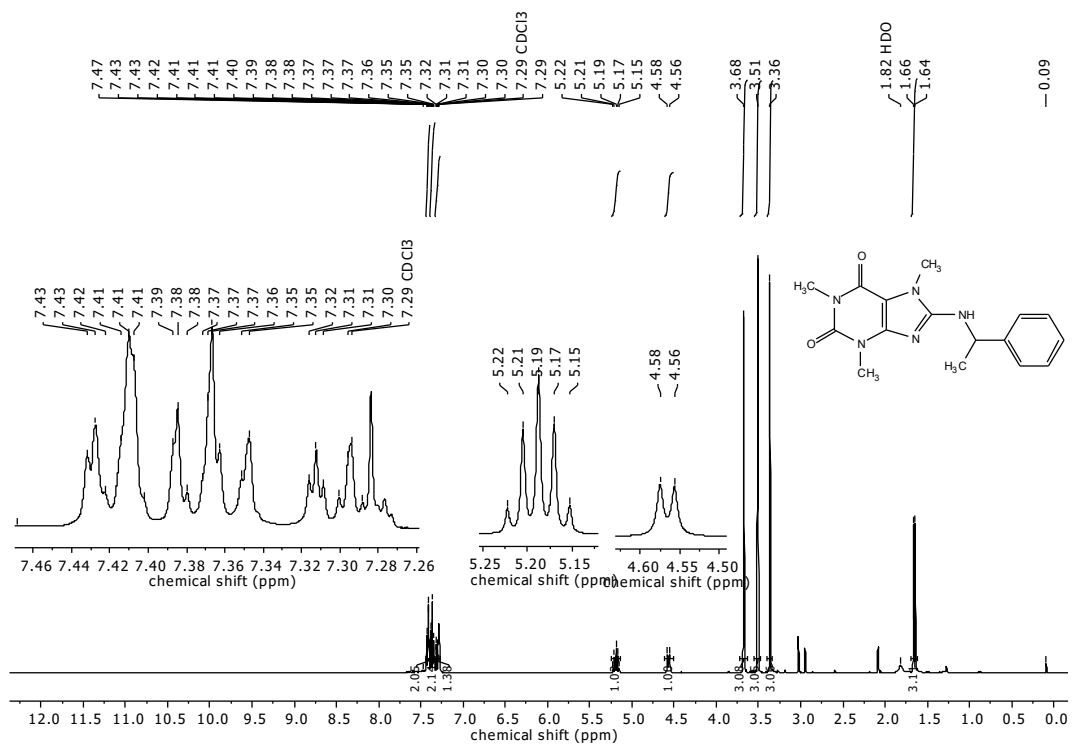


Figure 36: ¹H NMR spectrum of (S)-8-((1-Phenylethyl)amino)caffeine (**12**) in CDCl₃

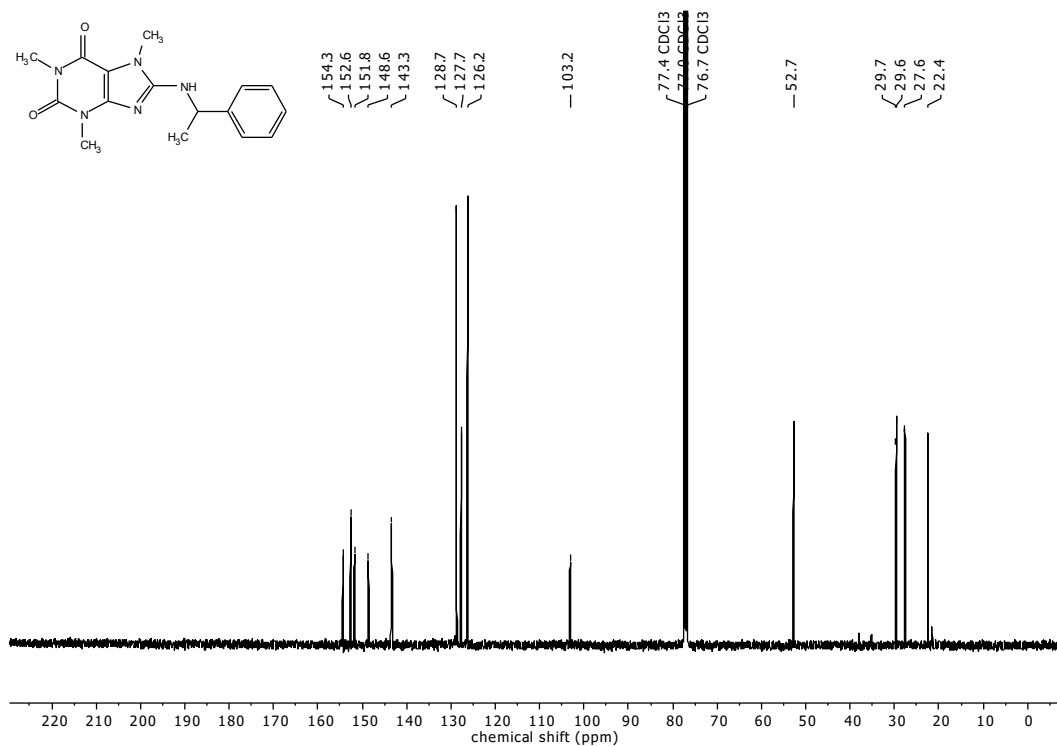


Figure 37 ¹³C NMR spectrum of (S)-8-((1-Phenylethyl)amino)caffeine (**12**) in CDCl₃

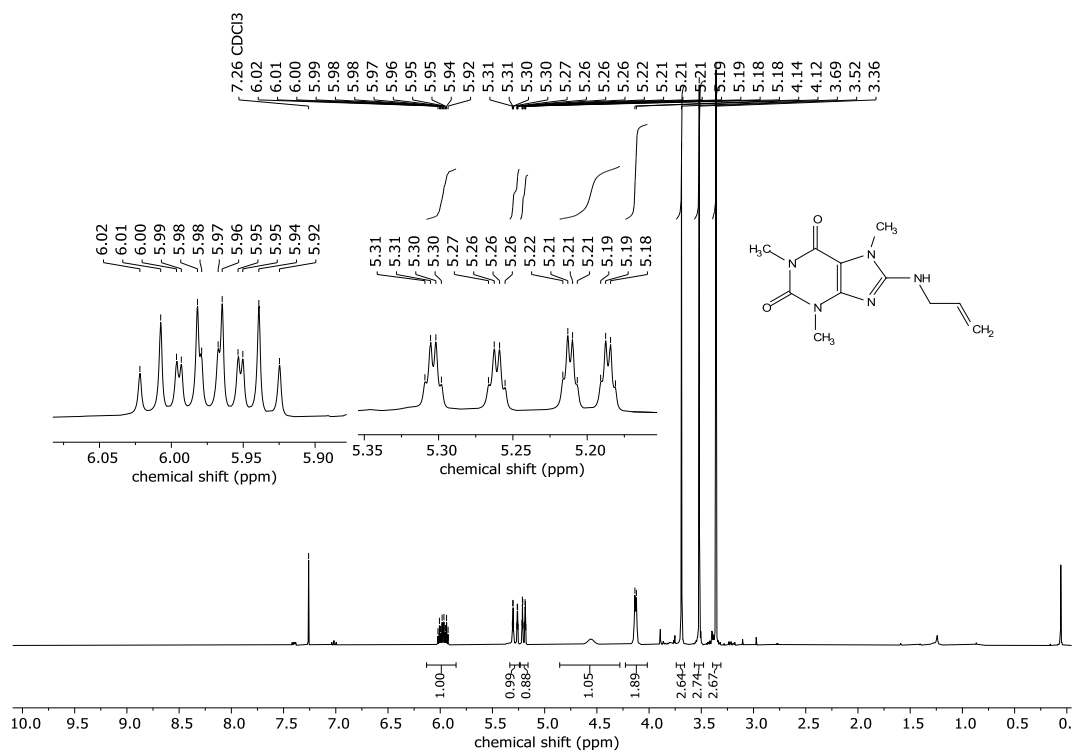


Figure 38 ^1H NMR spectrum of 8-allylaminocaffeine (**13**) in CDCl_3

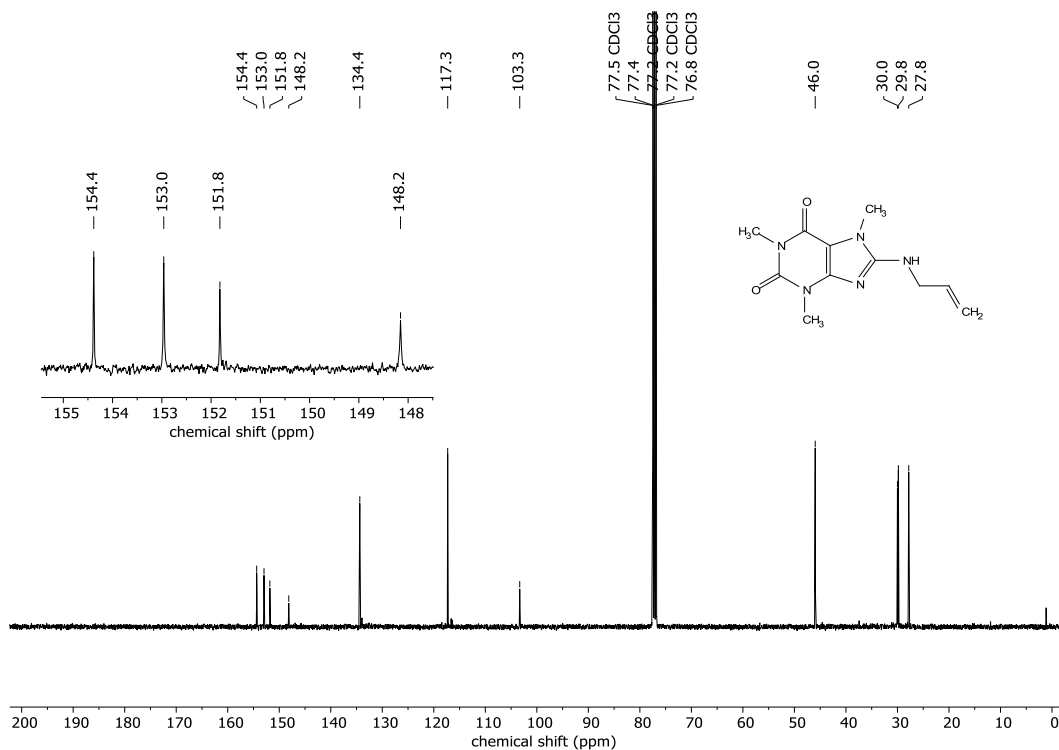


Figure 39 ^{13}C NMR spectrum of 8-allylaminocaffeine (**13**) in CDCl_3

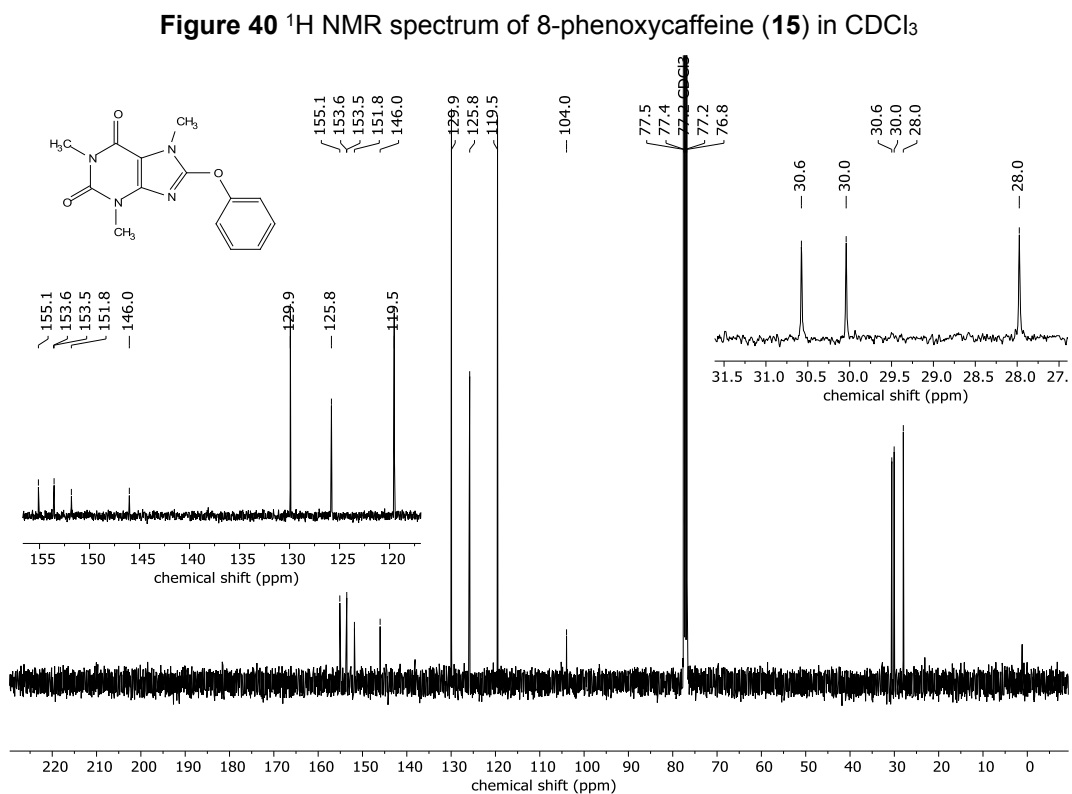
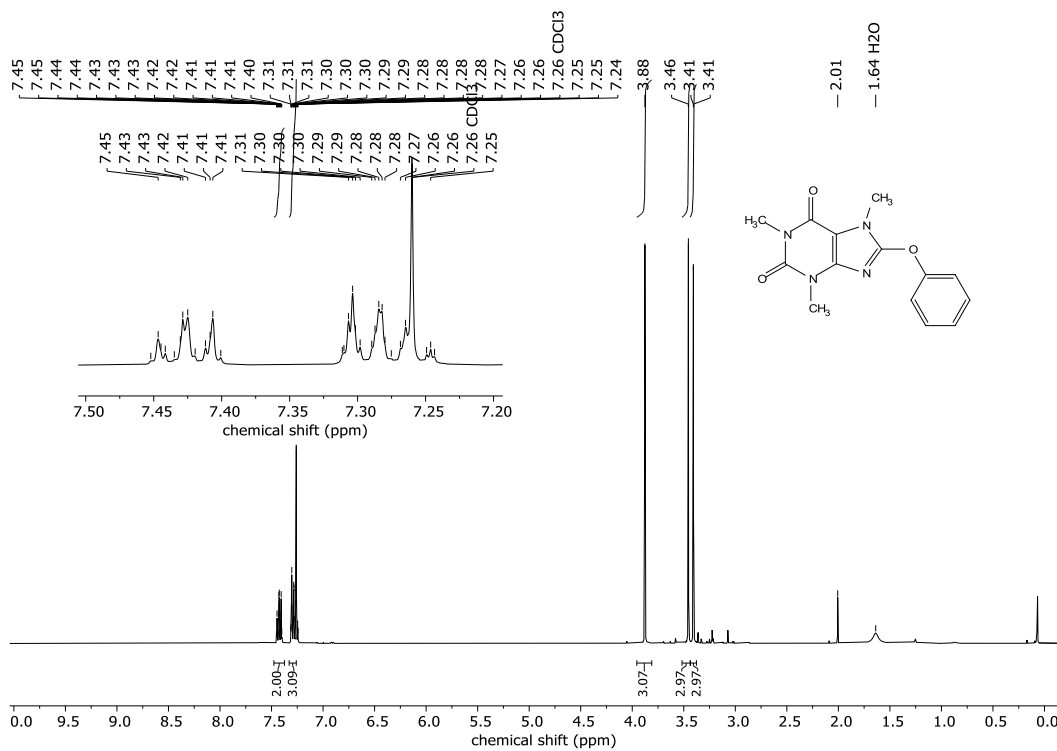


Figure 41 ^{13}C NMR spectrum of 8-phenoxycaffeine (**15**) in CDCl_3

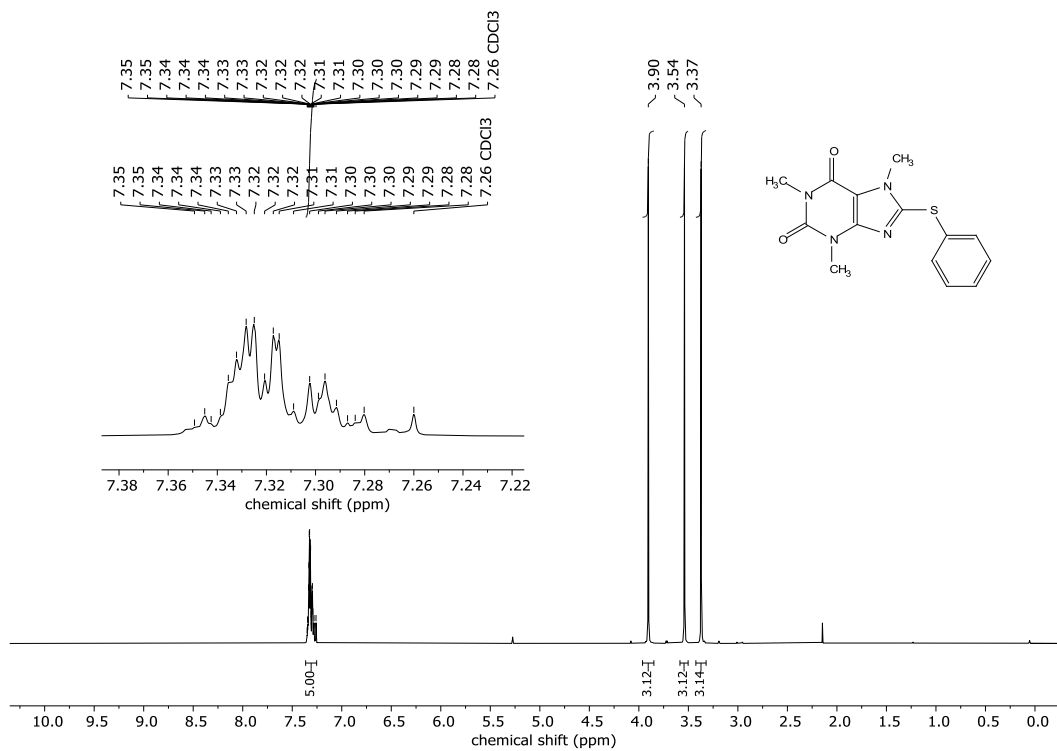


Figure 42 ¹H NMR spectrum of 8-(phenylthio)caffeine (14) in CDCl₃

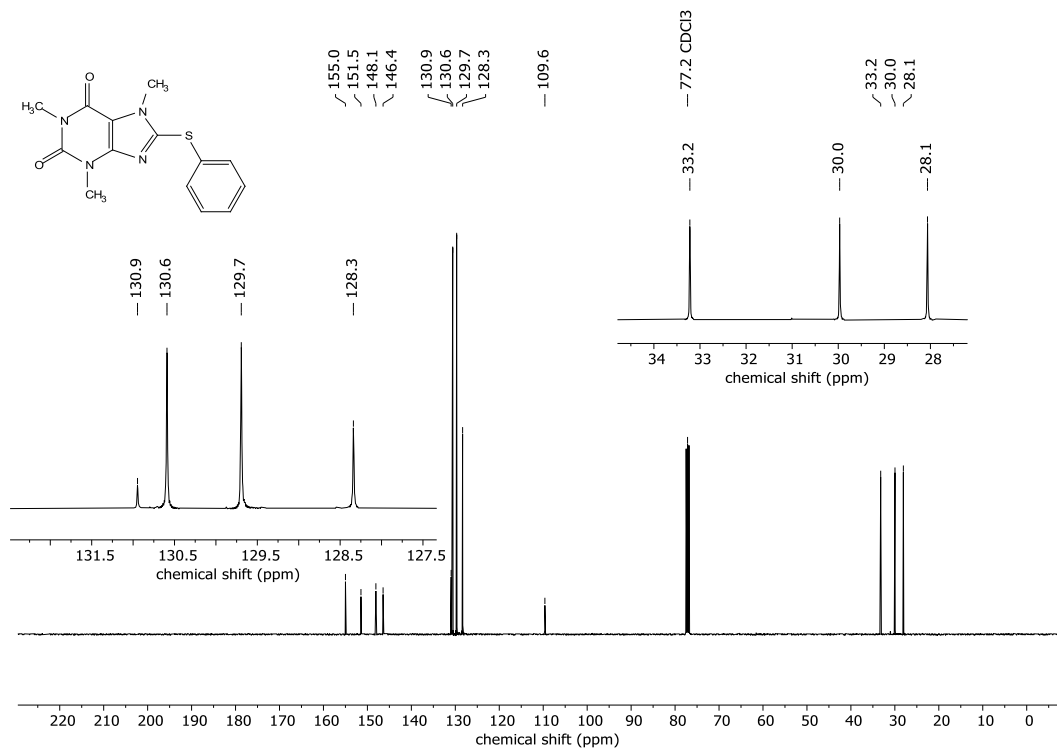


Figure 43 ¹³C NMR spectrum of 8-(phenylthio)caffeine (14) in CDCl₃

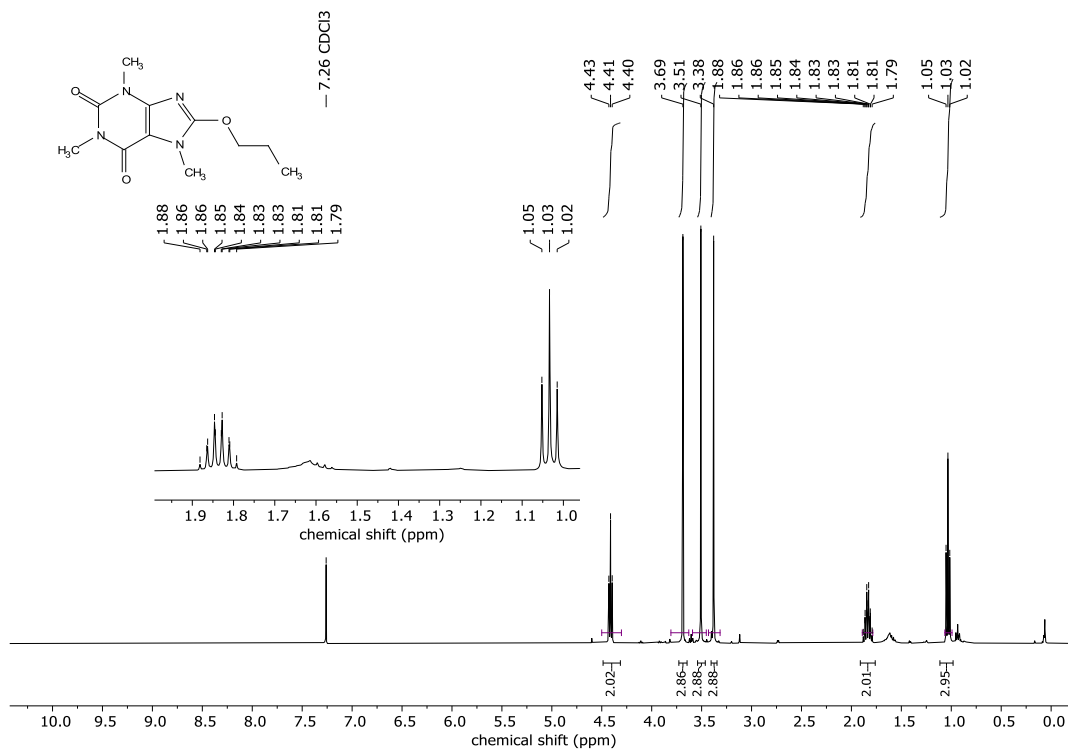


Figure 44 ^1H NMR spectrum of 8-propyloxycaffeine (17) in CDCl_3

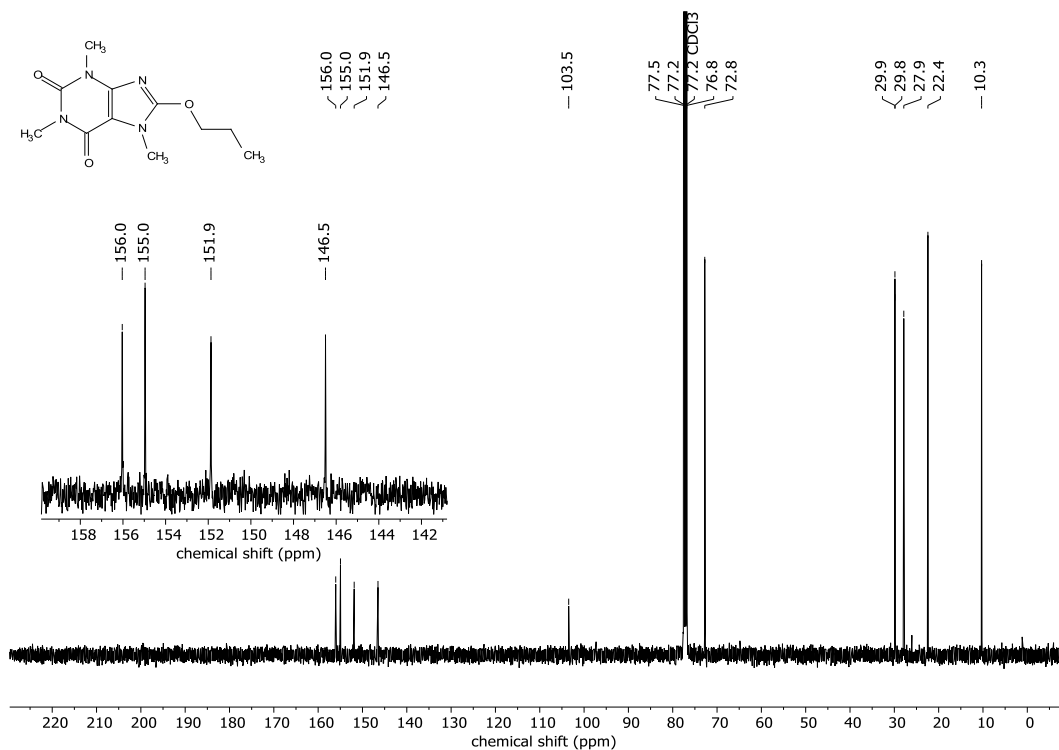


Figure 45 ^{13}C NMR spectrum of 8-propyloxycaffeine (17) in CDCl_3

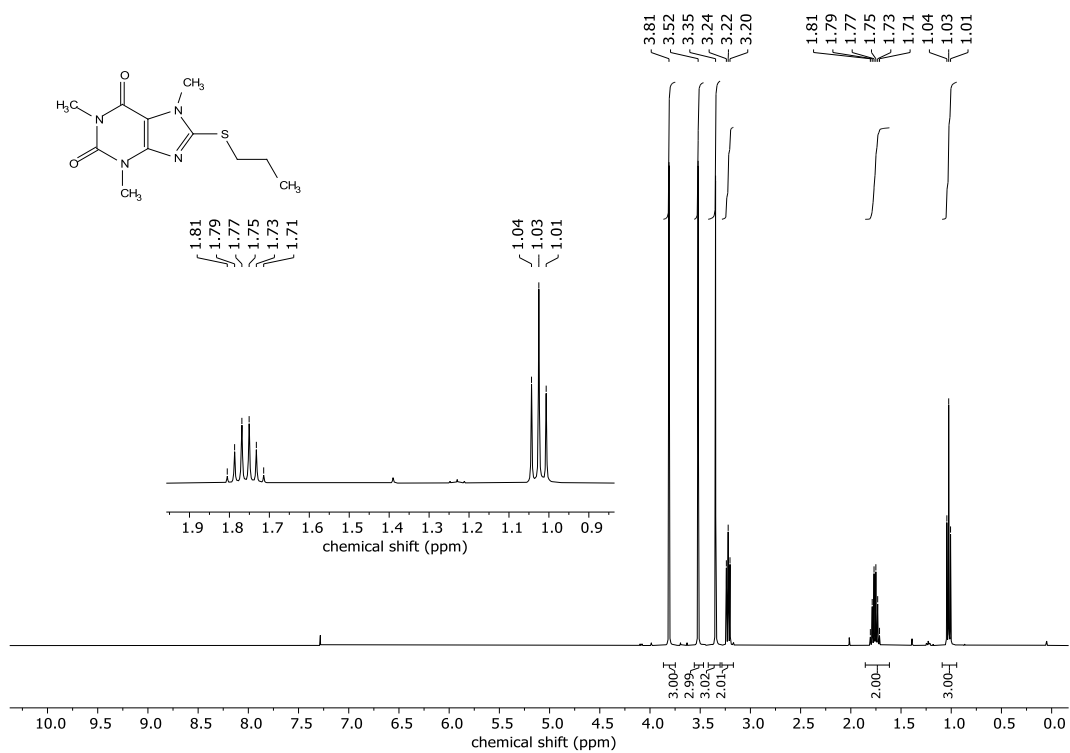


Figure 46 ^1H NMR spectrum of 8-propylthiocaffeine (**16**) in CDCl_3

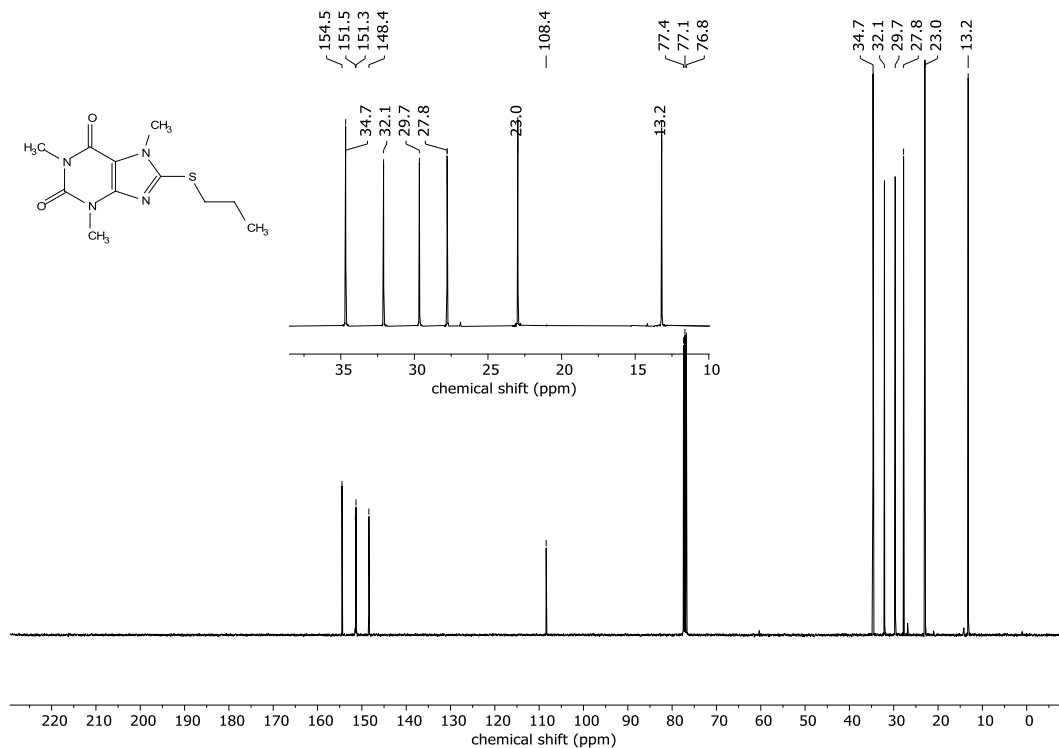


Figure 47 ^{13}C NMR spectrum of 8-propylthiocaffeine (**16**) in CDCl_3

Electrosynthesis 2.0 in 1,1,1,3,3,3-Hexafluoroisopropanol / Amine mixtures

Johannes L. Röckl,^[a,b] Maurice Dörr,^[a] Siegfried R. Waldvogel^{*[a,b]}

In the memory of Prof. Dr. Dennis G. Peters.



MINIREVIEW

- [a] J. L. Röckl, M. Dörr, Prof. Dr. S. R. Waldvogel
Department of Chemistry
Johannes Gutenberg University Mainz
Duesbergweg 10–14, 55128 Mainz (Germany)
E-mail: waldvogel@uni-mainz.de
Homepage: <https://www.aksw.uni-mainz.de>
- [b] J. L. Röckl, Prof. Dr. S. R. Waldvogel
Graduate School Materials Science in Mainz
Staudingerweg 9, 55128 Mainz (Germany)

Abstract: The intention of this survey is to highlight the innovative electrolyte combination of 1,1,1,3,3,3-hexafluoroisopropanol (HFIP) with tertiary nitrogen bases in electro-organic synthesis. This easy applicable and promising mixture is not yet well established in electro-organic synthesis but expands the various possibilities in the latter. Combinations of fluorinated alcohols with nitrogen bases form highly conductive electrolyte systems which can be evaporated completely. Consequently, no additional supporting electrolyte is required and work-up procedures are tremendously simplified. With this electrolyte mixture carbon-carbon homo- and cross-coupling reactions of arenes and phenols have been established with substrates, which have not been previously susceptible to the anodic dehydrogenative coupling reaction. The intermediate installation of highly fluorinated alkoxy moieties can be exploited for subsequent conversions as well as various benzylic functionalization, including asymmetric transformations. These transformations show unique selectivity and functional group tolerance making them highly applicable to the synthesis of sophisticated structural motifs, including natural products.

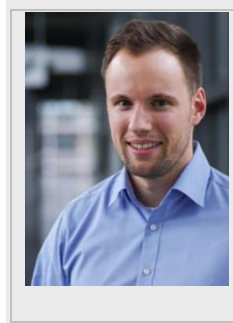
Introduction

Fluorinated alcohols have emerged as excellent choices for a broad range of applications in organic chemistry, due to their high hydrogen-bond donor ability,^[1,2] high polarity,^[2,3] outstanding (electro-)chemical stability,^[4,5] and micro-heterogeneity.^[6–8] This is illustrated by their use as solvents, co-solvents or promoters in organic syntheses.^[2,5,9,10] Several examples have showcased the utility of 1,1,1,3,3,3-hexafluoroisopropanol (HFIP) in transition metal-catalyzed,^[10,11] and metal-free reactions.^[12] In combination with bases, HFIP promotes unusual transformations like the generation of aza-oxyallyl cationic intermediates from α -haloamides^[13] or HFIP-promoted nucleophilic substitutions^[9,14]. These unique features of HFIP make it particularly well-suited as a solvent for electrochemical reactions, especially its ability to stabilize radical intermediates.^[15,16] HFIP has demonstrated superior effects compared to other solvents when it comes to improving selectivity and yield of various electrochemical transformations.^[17–21] In particular, the solvate formation modulates nucleophilicity and oxidation potential.^[7,17] The unusual electrochemical stability of HFIP is ensured as long as inert anodes are employed for direct electrode processes,^[22] whereas hypervalent iodine mediators are capable to convert HFIP to highly toxic hexafluoroacetone.^[23]

Electrochemistry has experienced a renaissance in recent years since it offers benefits over classical synthetic methodologies.^[18–20,24] Electric current, as an inexpensive and inherently safe reagent, facilitates sustainable synthetic pathways, and is compatible with renewable energy sources.^[25] A direct contribution for the stabilizing of the electric grid is provided, when the electro-conversions are robust and fluctuating electricity can

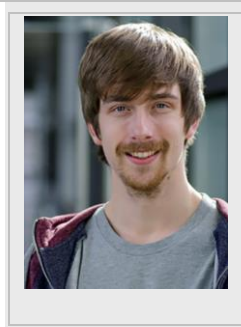
be employed without loss of selectivity and reactivity. Here, HFIP based electrolytes seem to play an outstanding role.^[26] The avoidance of chemical reagents minimizes the amount of reagent waste produced by the process. Thus, many of the “green chemistry” principles may be fulfilled by applying electro-organic methods.^[26,27] A common drawback in electrochemistry is the need for supporting electrolytes, which are often salts with significant environmental impact.^[28] The subsequent workup is complicated due to difficult removal or recovery of the salt. Noteworthy, perchlorates can lead to explosive events and symmetric tetraalkylammonium salts strongly affect the wastewater treatment.^[29] When applying a combination of base with acidic HFIP ($pK_a = 9.3$ ^[15]) to electro-organic synthesis, a supporting electrolyte is formed in-situ, eliminating the need for additional supporting electrolyte. Avoiding the use of salts simplifies the workup procedure, facilitating easy removal of the electrolyte by distillation, simplifying downstream processing and recycling of the electrolyte. Additionally, the lack of salts allows the coupling with mass spectrometry for real-time reaction monitoring in, for example, automated synthesis. In addition, the enhanced nucleophilicity of deprotonated HFIP allows trapping of reactive intermediates, which can be submitted to different coupling reactions to open new pathways in organic synthesis. For example, in 2013 Tajima et al. first described the use of a solid-supported base in HFIP in a one-pot sequence of alkoxylation followed by the reaction with allyltrimethylsilane (Scheme 1).^[30] Subsequently, our group first used a simple tertiary amine base without additional salt or reagents in a formal benzyl-aryl cross-coupling reaction, demonstrating the potential of this approach (Scheme 3).^[31] Many more seminal applications of this powerful combination have been recently published and will be discussed within this review.^[32–36]

Johannes L. Röckl finished his apprenticeship as a laboratory technician in 2013 at BASF SE, Ludwigshafen and received his B.Sc. from Johannes Gutenberg University in a collaboration with BASF SE working on the total synthesis of natural product derivatives under supervision of Prof. Dr. Siegfried R. Waldvogel and Dr. Joachim Dickhaut in 2016. Afterwards, he was appointed as a scientist in insecticide science working on early stage projects for BASF. Upon acceptance as a fast-track Ph.D. candidate, he started working on electro-organic synthesis in the Waldvogel lab. After working as a visiting researcher at ETH, Zurich under the supervision of Prof. Dr. Bill Morandi in 2019, he returned to Mainz to conclude his Ph.D. in electro-organic synthesis.



MINIREVIEW

Maurice Dörr received his B.Sc. degree in chemistry from Johannes Gutenberg University Mainz working on anodic C–C cross-coupling reactions in 2016 and his M.Sc. working on anodic C–N cross-coupling reactions in 2018 supervised by Prof. Dr. Siegfried R. Waldvogel. Currently, he is engaged in the application of Design of Experiments (DoE) towards electro-organic synthesis as a graduate student in the Waldvogel lab.

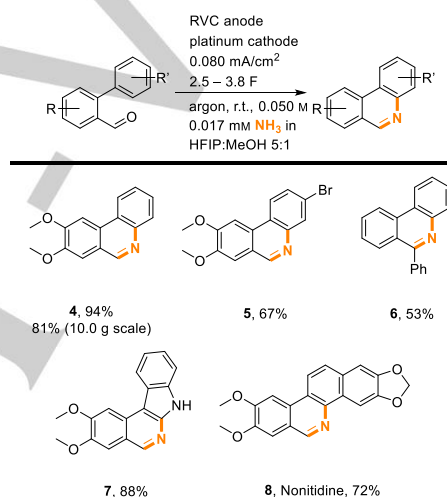


Siegfried R. Waldvogel studied chemistry in Konstanz and received his Ph.D. in 1996 from University of Bochum/Max Planck Institute for Coal Research with Prof. Dr. M. T. Reetz as supervisor. After Postdoctoral research at Scripps Research Institute in La Jolla, CA (Prof. Dr. J. Rebeck, jr.), he started his own research career in 1998 at University of Münster. After his professorship in 2004 at University of Bonn, he became full professor for organic chemistry at Johannes Gutenberg University Mainz in 2010. His research interests are novel electro-organic transformations including bio-based feedstocks, from electrosynthetic screening to scale-up in flow electrolyzers and innovative cell concepts. In 2018, he cofounded ESy-Labs GmbH, which provides custom electrosynthesis and contract R&D.



Electro-organic Formation of Nitrogen Heterocycles using Ammonia in HFIP

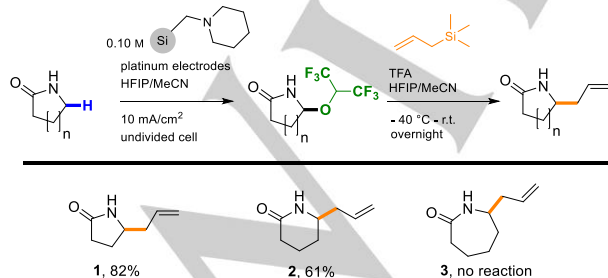
The ubiquity of nitrogen moieties in natural products, pharmaceutically active compounds, and advanced materials highlights the necessity for sustainable formation of nitrogen heterocycles.^[37] Several approaches have been described along with electro-organic C–N bond construction.^[38] A regioselective anodic approach towards phenanthridines and pyridine-fused polycyclic structures exploits ammonia as an inexpensive and stable nitrogen donor and base with high atom economy in HFIP (Scheme 2).^[39] Ammonia ($pK_a(\text{NH}_4^+) = 9.2$)^[40] is used as a reagent and additive for ensuring sufficient conductivity by an acid-base equilibrium with the solvent HFIP. This galvanostatic protocol was also performed in a decagram-scale towards **4** in 81% yield to highlight the utility in organic synthesis. In addition, access to the natural product nonitidine **8** could be accomplished in 72% yield.



Scheme 2. Electro-organic access to phenanthridines and related structures using 1,1,1,3,3,3-hexafluoroisopropanol (HFIP) and ammonia.

Anodic Alkoxylation promoted by Solid-supported Base as Part of a One-Pot Sequence

The Tateno group developed an elegant anodic alkoxylation of lactams followed by allylation in a one-pot sequence using HFIP in combination with a solid-supported amine base.^[30] This gives rise to allylated five- and six-membered lactams (**1**) and (**2**) in yields up to 82% over both steps (Scheme 1). After electrolysis the silica-supported piperidine can be easily removed by filtration. In case of a 7-membered ring (**3**) the intermediate *N*-acyliminium ion was not formed and therefore no reaction took place.

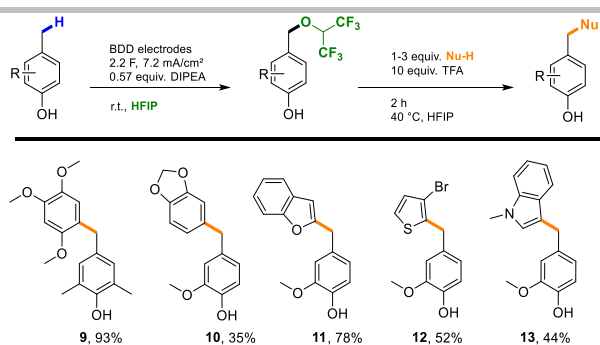


Scheme 1. One-pot sequence enabling allyl-substituted lactams utilizing a solid-supported amine base in 1,1,1,3,3,3-hexafluoroisopropanol (HFIP).

Benzyl-Aryl Cross-coupling reaction via Anodic C–H Functionalization by HFIP

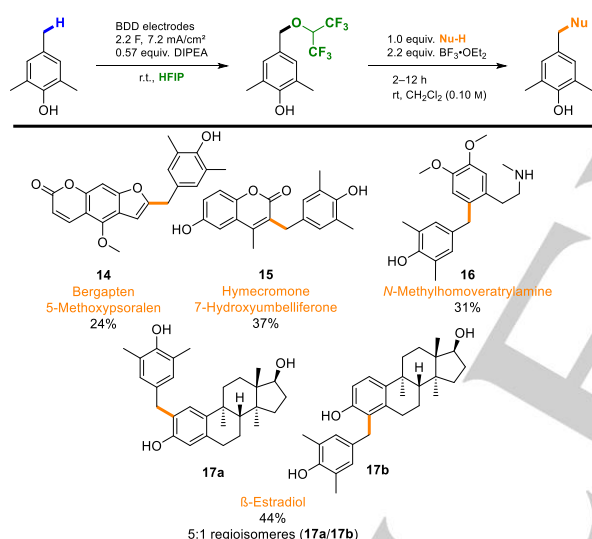
A selective dehydrogenative electrochemical functionalization of benzylic positions with HFIP has been developed by Waldvogel et al.^[31] These electro-generated HFIP ethers are versatile intermediates for subsequent functionalization, as they act as masked benzylic cations, which can be easily activated. Best results were obtained in combination with *N,N*-diisopropylethylamine (DIPEA). Liberation of the benzylic cation was accomplished by acidic treatment. These cations can readily react with aromatic nucleophiles to provide valuable diarylmethanes. Overall, 28 examples in yields up to 93% (**9**) over both steps have been accessed (Scheme 3). Various heterocycles could be alkylated by this way, such as 1,3-benzodioxoles (**10**), benzo[*b*]furanes (**11**), thiophenes (**12**) and indoles (**13**) in high yields up to 78% over 2 steps.

MINIREVIEW



Scheme 3. Benzyl-aryl cross-coupling of phenols with various nucleophiles after anodic activation with 1,1,1,3,3,3-hexafluoroisopropanol (HFIP).

Even late-stage functionalization of a variety of natural products and pharmaceutically active ingredients was possible in yields up to 44% (**17a** and **17b**) with slight alteration of the protocol employing Lewis acids instead of 2,2,2-trifluoroacetic acid for HFIP ether cleavage (Scheme 4). Bergapten (**14**), hymecromone (**15**) and even phenylethylamines (**16**) could be converted in this reaction in yields up to 37%.

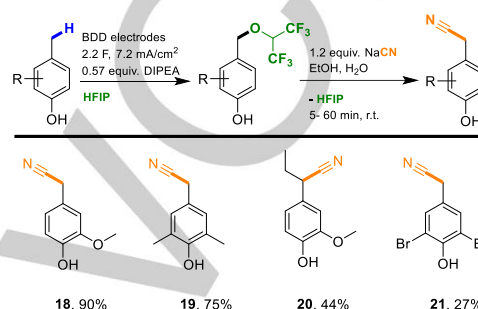


Scheme 4. Lewis acid-directed late-stage functionalization of natural products and pharmaceutically active compounds.

Benzylic anodic C–H Functionalization with HFIP and subsequent Cyanation to generate 2-Phenylacetonitriles

The HFIP ether concept has been expanded to other valuable building blocks by the Waldvogel group. It was found that liberation of the benzylic cation is not necessary to achieve selective bond formation when stronger nucleophiles are used.^[33] With cyanides, a direct substitution reaction is observed to yield 2-phenylacetonitriles, which represent important building blocks in organic synthesis. This structural feature is a precursor to many biologically active molecules such as 2-phenylethylamines^[41] or pharmaceuticals, such as the calcium ion channel blocker verapamil or the fungicide mandipropamid.^[42] This procedure allows a simple, sustainable, easily scalable, reagent- and metal-

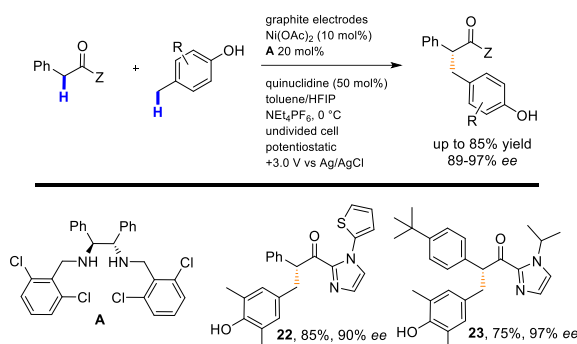
free electrochemical cyanation reaction (Scheme 5). It consists of a two-step sequence and the HFIP ether generated in-situ can be used without further purification. The reaction is selective with yields up to 90% over 2 steps and methoxy groups (**18**), multiple alkyl groups (**19**), propyl moieties (**20**) and halogens (**21**) being tolerated (Scheme 5). Phenols can be converted in a protective group-free manner, shortening the usual synthetic route by one or two steps. Additionally, only a small excess of cyanide source is used and therefore less toxic reagent waste is generated. The HFIP released during the reaction can be recovered and redistilled, improving the sustainability of this reaction.



Scheme 5. Scope of the benzylic anodic activation with 1,1,1,3,3,3-hexafluoroisopropanol (HFIP) and subsequent cyanation reaction.

Asymmetric Lewis Acid-catalyzed Alkylation in a toluene/HFIP/quinuclidine Electrolyte

Inspired by the benzylic-aryl coupling via HFIP ethers by Waldvogel et al., the Guo group developed an outstanding asymmetric nickel-catalyzed electrochemical alkylation.^[35] Asymmetric induction is achieved through the radical–radical coupling of a chiral Ni(II) complex chelated radical with an electrochemically formed benzylic radical. The resulting alkylation products could be isolated in yields up to 85% (**22**) and enantiomeric excess up to 97% (**23**) (Scheme 6). However, the well conductive nature of the HFIP/amine mixture was not exploited, since an additional supporting electrolyte was employed.

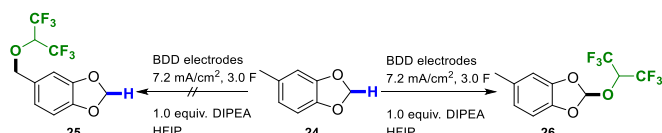


Scheme 6. Quinuclidine in toluene/1,1,1,3,3,3-hexafluoroisopropanol (HFIP) mixture as electrolyte in a Lewis acid-catalyzed asymmetric alkylation.

MINIREVIEW

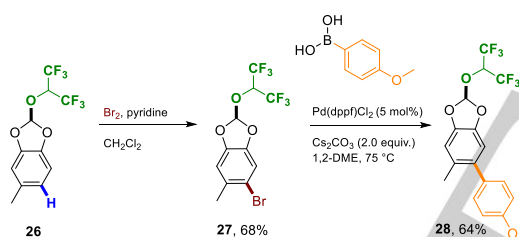
Anodic C–H Functionalization towards fluorinated Orthoesters from 1,3-Benzodioxoles

In contrast to benzylic anodic oxidation of phenols, anisoles and anilides, 1,3-benzodioxoles were found to exhibit unexpected reactivity at complete conversion.^[32] Functionalization of **24** occurred at position 2 (**26**), even in the presence of benzylic methyl groups. This is in contrast to previous work, wherein the benzylic position was functionalized (**25**) (Scheme 7).



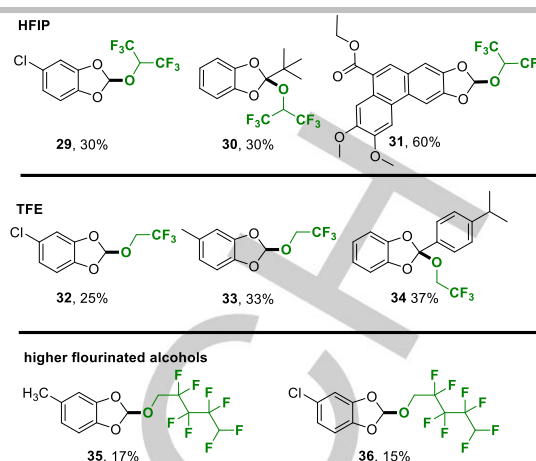
Scheme 7. Selectivity of the anodic C–H functionalization of 1,3-benzodioxoles with HFIP.

These orthoesters exhibit unusual and unique properties. Surprisingly, **26** proved to be extraordinarily stable towards acids and bases and does not undergo substitution reactions, even when transition metals are present within the reaction mixture. Therefore, it was possible to perform a bromination on **26**, followed by a Pd-catalyzed Suzuki coupling to give **28** in 64% yield, in the presence of the HFIP orthoester (Scheme 8).



Scheme 8. Bromination reaction under acidic conditions followed by Suzuki coupling at elevated temperatures in the presence of fluorinated orthoesters.

It was also possible to install various fluorinated alkoxy moieties, allowing the modulation of the bioactive properties of the pharmaceutically relevant 1,3-benzodioxole moiety in **28** examples in yields up to 60% (**31**) (Scheme 9).^[43]



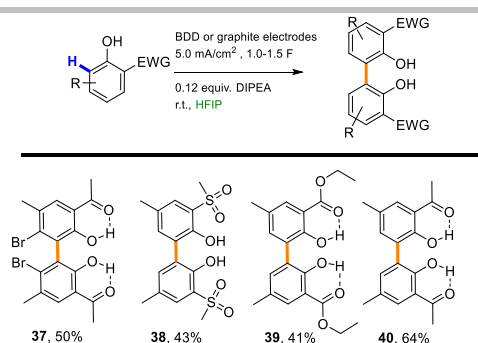
Scheme 9. Scope of electrochemically accessible fluorinated orthoesters.

Higher yields and improved selectivity were observed with increasingly larger π -systems (**31** and **34**). This can be explained by stabilization of the respective cations after twofold oxidation and deprotonation. Halo substituents (**29**, **32**, **36**), as well as a substitution pattern in position 2 and 5 were tolerated (**33**, **34**, **35**). The logP-values of 1,3-benzodioxoles and the corresponding orthoesters were calculated and compared, to determine the lipophilicity of the orthoesters in comparison to the respective 1,3-benzodioxoles (see SI of ref.^[32]). Remarkably, these values increased by a factor of 1.5 to 2 when fluorinated side chains were installed. Such an enhancement of lipophilicity is very unusual. This transformation could boost the potency of bioactive compounds and impact target selectivity tremendously by influencing pK_a, modulating conformation, and hydrophobic interactions of the 1,3-benzodioxole moiety.^[44]

Dehydrogenative anodic C–C Coupling of Phenols bearing electron-withdrawing Groups

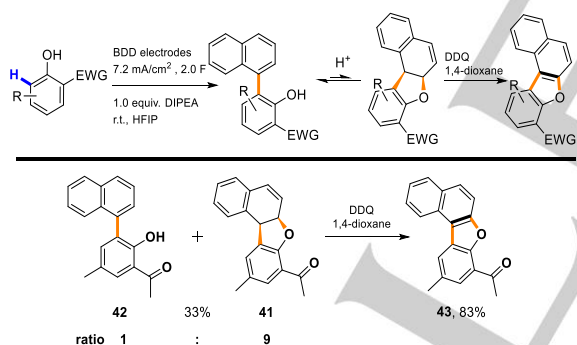
Electron-rich phenols and related substrates such as arenes, anilides or heterocycles could be selectively cross-coupled due to the solvent effect of HFIP.^[6,17,45] However, the method failed when the components were not electron-rich enough. Interestingly, phenols carrying electron-withdrawing groups (EWG) in position 2 undergo dehydrodimerization reaction instead of HFIP ether formation. To the best of our knowledge, this represents the first selective electrochemical coupling of phenols bearing EWGs.^[34] The reaction is highly selective and yields 2,2'-biphenols in up to 64% yield (Scheme 10). This reaction showed a high tolerance to functional groups like ketones (**37** and **40**), halogens (**37**), sulfoxides (**38**), as well as esters (**39**).

MINIREVIEW



Scheme 10. First selective homo-coupling of phenols bearing electron-withdrawing groups.

These types of structures are used as ligands in the synthesis of several binuclear boron^[46] and aluminum complexes,^[47] for application in optoelectronic devices and as catalysts in polymerization reactions^[48] and most of them need sophisticated multi-step syntheses.^[49] Cross-coupling reactions were also investigated in the HFIP/amine electrolyte system. Co-electrolysis with naphthalene unexpectedly yielded polycyclic structures (**41**), which were unequivocally analyzed by X-ray analysis, NMR and ESI/MS techniques (Scheme 11). The aromatic system was intercepted by the nucleophilic attack of the phenolic oxygen, which is quite unusual. It was also found that these are in equilibrium with the common cross-coupled products (**42**). This equilibrium is influenced by the pH, which poses a new type of isomerism. Further oxidation with DDQ provided dibenzofurans (**43**) in yields up to 83%. Therefore, it is possible to obtain both, the simple cross-coupled or polycyclic product selectively.

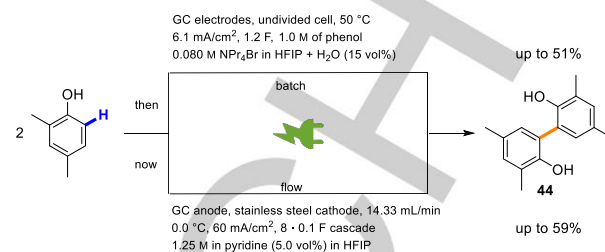


Scheme 11. Cross-coupling of phenols bearing electron-withdrawing groups with naphthalene – discovery of a new form of isomerism.

Scalable Synthesis of 2,2'-Biphenols using HFIP/pyridine as Electrolyte

2,2'-Biphenols are important ligand building blocks for the transition metal-catalyzed hydroformylation as a major branch of transition metal catalysis.^[50] The synthesis of this particular structural motif either requires economically and ecologically unfavorable transition metal catalysis or can be performed in an electro-organic transformation which requires supporting electrolytes.^[51] The use of HFIP is vital to avoid undesired C–O coupling reactions and formation of polycyclic products.^[52] The electrochemical synthesis of **44** was major research topic within

the Waldvogel group^[53] because of the technical relevance. A novel approach surmounting the laborious recovery of supporting electrolyte using a HFIP-pyridine system (Scheme 12) was established.^[54]



Scheme 12. Electro-organic synthesis of 3,3',5,5'-tetramethyl-2,2'-biphenol using 1,1,1,3,3,3-hexafluoroisopropanol (HFIP)/supporting electrolyte and HFIP/pyridine system as electrolyte.

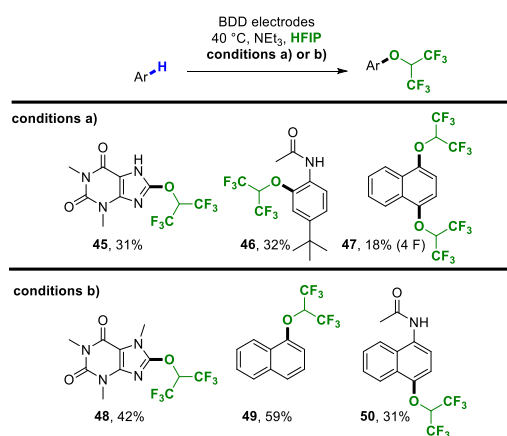
The straightforward removal of HFIP and pyridine after electrolysis by simple distillation is a major advantage of this synthetic protocol. This is of particular interest when scalability of the electro-conversion in a technical range is intended. Scale-up in continuous flow-electrolysis cells^[55] using a glassy carbon (GC) anode gives the desired ligand precursor in yields up to 58% in a 12 cm² and 59% a 48 cm² flow-cell. High current densities of 60 mA/cm² and high flow rates in a cascade electrolysis result in a high time efficiency. Numbering up of flow-cells and a simple work-up strategy make this process viable for a technical scale.

Table 1. Optimized parameters of the different flow cells and yields obtained. 2,4-Dimethylphenol *c* = 1.25 mol/L and pyridine (5 vol %) in HFIP, cathode: stainless steel, anode: glassy carbon, cascade electrolysis with 8 steps of 0.1 F, total applied charge: 0.8 F

	2 cm x 6 cm-flow cell	4 cm x 12 cm-flow cell
Anode surface	12 cm ²	48 cm ²
Current density	60 mA/cm ²	60 mA/cm ²
Flow rate	3.58 mL/min	14.33 mL/min
Temperature	20 °C	0 °C
Isolated yield (44)	58%	59%

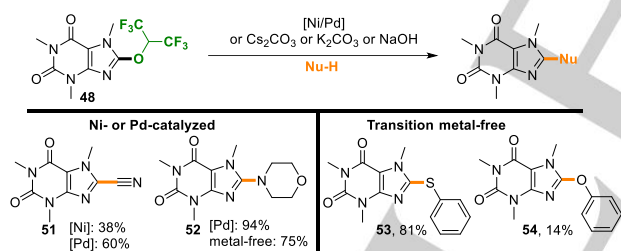
Anodic C–H Functionalization of Purine derivatives and subsequent Cross-coupling reaction (sp²)

After developing benzylic activation reactions and isolating aryl HFIP ethers as side components, it was considered to use the HFIP moiety attached to aryls as a leaving group in metal-catalyzed cross-coupling reactions. A selective, scalable, and sustainable electrochemical synthesis of HFIP aryl ethers was thus developed.^[56] Of particular interest is the electrochemical modification of bioactive purine derivatives, such as theophylline (**45**) and caffeine (**48**) derivatives (Scheme 13). Anilides (**46**, **50**) as well as naphthalene (**47** and **49**) could be converted successfully in yields up to 59%.



Scheme 13. One variable at a time (OVAT) and Design of Experiment (DoE) optimized reaction conditions of the anodic oxidation of purines and other arenes to 8-(1,1,1,3,3,3-hexafluoro-2-propoxy)-arenes in the presence of a base. OVAT optimized a) 7.2 mA/cm², 2.0 F, 300 rpm (stirrer velocity), 0.25 M caffeine, 0.1 M NEt₃, yield of **48** 33%; DoE optimized b) 22.1 mA/cm², 2.61 F, 700 rpm (stirrer velocity), 0.2 M caffeine, 0.2 M NEt₃, yield of **48** 42%;

The optimization to increase the yield for the electrocatalysis of HFIP caffeyl ether (**48**) was conducted via a Design of Experiment (DoE) approach. Optimal reaction conditions were successfully applied to a variety of aryl substrates to extend the scope to non-purine derivatives. Furthermore, the HFIP caffeyl ether was successfully used as the electrophile in transition metal-catalyzed and transition metal-free reactions with cyanides (**51**) and amines with excellent yields up to 94% (**52**) (Scheme 14). Even under metal-free conditions most of the conversions worked, accessing thioethers (**53**) and ethers (**54**) in yields up to 81%.

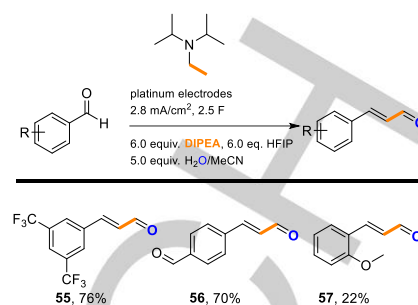


Scheme 14. Derivatization of 1,1,1,3,3,3-hexafluoroisopropanol (HFIP) caffeyl ether with various nucleophiles.

Anodic formation of Cinnamaldehydes with DIPEA as reagent

The Chiba group recently identified a novel mode of reactivity and reported a HFIP/DIPEA-based aldol reaction, whereby the ethyl group of DIPEA additionally serves as a C₂ source.^[36] Mechanistic studies revealed that DIPEA and HFIP play a significant role within this reaction. DIPEA forms not only an electrolyte with HFIP, but also generates acetaldehyde in-situ. A broad scope of benzaldehyde derivatives and heteroarene-aldehydes could be employed in this reaction, forming the cinnamaldehydes in yields up to 76% (**55**) (Scheme 15). Even selective reaction of only one of two aldehyde groups was achieved in yield of 70% (**56**).

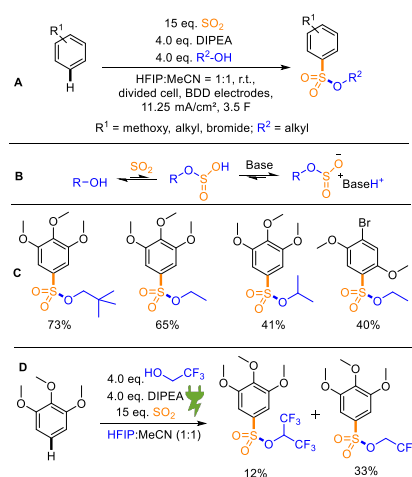
Electron-releasing groups lowered the yield significantly down to 22%, as seen for a methoxy group in ortho position (**57**).



Scheme 15. *N,N*-Diisopropylethylamine (DIPEA) as C₂ feedstock and base promoting conductivity in the anodic formation of cinnamaldehydes.

Electrosynthesis of Alkyl Arylsulfonates in a Multi-Component Reaction

The combination of DIPEA and HFIP has also been applied in the concise electrochemical synthesis of alkyl arylsulfonates by direct anodic oxidation of electron-rich arenes in a multi-component reaction (Scheme 16, A). The combination of SO₂, an alcohol, and DIPEA leads to an in-situ generation of monoalkyl sulfites (**B**) with bifunctional purpose. Firstly, this species functions as nucleophile and secondly, excellent conductivity is provided. Several primary and secondary alcohols and electron-rich arenes are implemented in this reaction to generate the alkyl arylsulfonates in yields up to 73% with exquisite selectivity (**C**). A competition reaction was observed between 1,1,1-trifluoroethanol and HFIP resulting in a product mixture (**D**). BDD electrodes are employed in divided cells at galvanostatic conditions, separated by a simple commercially available glass frit.^[57]



Scheme 16. Electrochemical synthesis of alkyl arylsulfonates in a multi-component reaction.

Summary and Perspectives

Within this review, the outstanding impact and unique reactivity of organic substrates in HFIP/amine electrolytes during electrolysis are surveyed. The important advantage of this approach in

MINIREVIEW

comparison to conventional electro-organic synthesis using additional salts as supporting electrolytes is the simple purification process, which can mostly be performed by distillation of the electrolyte. The direct evaporative recovery of the HFIP/amines mixtures and subsequent reuse diminishes the environmental footprint. Although, besides aryls several aliphatic compounds have been transformed and a large functional group tolerance has been demonstrated. Moreover, the scope of most electrosynthetic transformations is significantly expanded by using HFIP/amines instead of the traditional HFIP electrolytes. The successful conversion of and towards natural products and pharmaceutically active compounds is of exceptional importance and underlines the versatility for the application of this technique. This development will open a new field in electro-organic synthesis and should encourage scientists towards novel processes using these particular HFIP/amine mixtures in sustainable electrosynthesis protocols.

Acknowledgements

J. L. Röckl is a recipient of a DFG fellowship through the Excellence Initiative by the Graduate School Materials Science in Mainz (GSC 266). Funding by the DFG in frame of FOR 2982 – UNDODE (Wa1276/23-1) is highly appreciated. Support by the Advanced Lab of Electrochemistry and Electrosynthesis – ELYSION (Carl-Zeiss-Stiftung) is gratefully acknowledged.

Conflict of Interest

The authors declare no conflict of interest.

Keywords: amines • 1,1,1,3,3,3-hexafluoroisopropanol • oxidation • CH functionalization • ethers

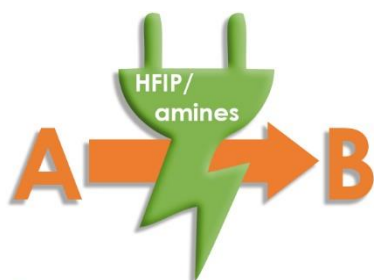
- [1] M. J. Kamlet, J. L. M. Abboud, M. H. Abraham, R. W. Taft, *J. Org. Chem.* **1983**, *48*, 2877–2887.
- [2] J.-P. Bégué, D. Bonnet-Delpon, B. Crousse, *Synlett* **2004**, 18–29.
- [3] C. Reichardt, *Chem. Rev.* **1994**, *94*, 2319–2358.
- [4] R. Francke, D. Cericola, R. Kötz, D. Weingarh, S. R. Waldvogel, *Electrochim. Acta* **2012**, *62*, 372–380.
- [5] I. Colomer, A. E. R. Chamberlain, M. B. Haughey, T. J. Donohoe, *Nat. Rev. Chem.* **2017**, *1*, 88.
- [6] O. Hollóczki, A. Berkessel, J. Mars, M. Mezger, A. Wiebe, S. R. Waldvogel, B. Kirchner, *ACS Catal.* **2017**, *7*, 1846–1852.
- [7] O. Hollóczki, R. Macchieraldo, B. Gleede, S. R. Waldvogel, B. Kirchner, *J. Phys. Chem. Lett.* **2019**, *10*, 1192–1197.
- [8] J. T. Gerig, *J. Phys. Chem. B* **2014**, *118*, 1471–1480.
- [9] X.-D. An, J. Xiao, *Chem. Rec.* **2020**, *20*, 142–161.
- [10] N. V. Dubrovina, I. A. Shuklov, M.-N. Birkholz, D. Michalik, R. Paciello, A. Börner, *Adv. Synth. Catal.* **2007**, *349*, 2183–2187.
- [11] Y. Cheng, J. Zheng, C. Tian, Y. He, C. Zhang, Q. Tan, G. An, G. Li, *Asian J. Org. Chem.* **2019**, *8*, 526–531.
- [12] a) A. Heydari, S. Khaksar, M. Tajbakhsh, *Synthesis* **2008**, 3126–3130; b) L.-R. Wen, G.-Y. Ren, R.-S. Geng, L.-B. Zhang, M. Li, *Org. Biomol. Chem.* **2020**, *18*, 225–229.
- [13] a) C. S. Jeffrey, K. L. Barnes, J. A. Eickhoff, C. R. Carson, *J. Am. Chem. Soc.* **2011**, *133*, 7688–7691; b) A. Acharya, J. Eickhoff, C. Jeffrey, *Synthesis* **2013**, *45*, 1825–1836; c) W. Ji, L. Yao, X. Liao, *Org. Lett.* **2016**, *18*, 628–630.
- [14] L. Yu, S.-S. Li, W. Li, S. Yu, Q. Liu, J. Xiao, *J. Org. Chem.* **2018**, *83*, 15277–15283.
- [15] L. Ebersson, M. P. Hartshorn, O. Persson, *J. Chem. Soc., Perkin Trans. 2* **1995**, 1735.
- [16] a) L. Ebersson, M. P. Hartshorn, O. Persson, *J. Chem. Soc., Chem. Commun.* **1995**, 1131; b) L. Ebersson, O. Persson, M. P. Hartshorn, *Angew. Chem. Int. Ed.* **1995**, *34*, 2268–2269; *Angew. Chem.* **1995**, *107*, 2417–2418.
- [17] B. Elsler, A. Wiebe, D. Schollmeyer, K. M. Dyballa, R. Franke, S. R. Waldvogel, *Chem. Eur. J.* **2015**, *21*, 12321–12325.
- [18] A. Wiebe, T. Gieshoff, S. Möhle, E. Rodrigo, M. Zirbes, S. R. Waldvogel, *Angew. Chem. Int. Ed.* **2018**, *57*, 5594–5619; *Angew. Chem.* **2018**, *130*, 5694–5721.
- [19] S. Möhle, M. Zirbes, E. Rodrigo, T. Gieshoff, A. Wiebe, S. R. Waldvogel, *Angew. Chem. Int. Ed.* **2018**, *57*, 6018–6041; *Angew. Chem.* **2018**, *130*, 6124–6149.
- [20] J. L. Röckl, D. Pollok, R. Franke, S. R. Waldvogel, *Acc. Chem. Res.* **2020**, *53*, 45–61.
- [21] L. Schulz, S. Waldvogel, *Synlett* **2019**, *30*, 275–286.
- [22] a) T. Gieshoff, D. Schollmeyer, S. R. Waldvogel, *Angew. Chem. Int. Ed.* **2016**, *55*, 9437–9440; *Angew. Chem.* **2016**, *128*, 9587–9590; b) T. Gieshoff, A. Kehl, D. Schollmeyer, K. D. Moeller, S. R. Waldvogel, *J. Am. Chem. Soc.* **2017**, *139*, 12317–12324; c) T. Gieshoff, A. Kehl, D. Schollmeyer, K. D. Moeller, S. R. Waldvogel, *Chem. Commun.* **2017**, 53, 2974–2977; d) A. Kehl, T. Gieshoff, D. Schollmeyer, S. R. Waldvogel, *Chem. Eur. J.* **2018**, *24*, 590–593; e) B. Elsler, D. Schollmeyer, K. M. Dyballa, R. Franke, S. R. Waldvogel, *Angew. Chem. Int. Ed.* **2014**, *53*, 5210–5213; *Angew. Chem.* **2014**, *126*, 5311–5314; f) S. Lips, A. Wiebe, B. Elsler, D. Schollmeyer, K. M. Dyballa, R. Franke, S. R. Waldvogel, *Angew. Chem. Int. Ed.* **2016**, *55*, 10872–10876; *Angew. Chem.* **2016**, *128*, 11031–11035; g) L. Schulz, M. Enders, B. Elsler, D. Schollmeyer, K. M. Dyballa, R. Franke, S. R. Waldvogel, *Angew. Chem. Int. Ed.* **2017**, *56*, 4877–4881; *Angew. Chem.* **2017**, *129*, 4955–4959; h) A. Wiebe, D. Schollmeyer, K. M. Dyballa, R. Franke, S. R. Waldvogel, *Angew. Chem. Int. Ed.* **2016**, *55*, 11801–11805; *Angew. Chem.* **2016**, *128*, 11979–11983; i) L. Schulz, R. Franke, S. R. Waldvogel, *ChemElectroChem* **2018**, *5*, 2069–2072; j) A. Wiebe, S. Lips, D. Schollmeyer, R. Franke, S. R. Waldvogel, *Angew. Chem. Int. Ed.* **2017**, *56*, 14727–14731; *Angew. Chem.* **2017**, *129*, 14920–14925.
- [23] a) T. Broese, R. Francke, *Org. Lett.* **2016**, *18*, 5896–5899; b) R. Francke, *Curr. Opin. Electrochem.* **2019**, *15*, 83–88.
- [24] a) S. R. Waldvogel, B. Janza, *Angew. Chem. Int. Ed.* **2014**, *53*, 7122–7123; *Angew. Chem.* **2014**, *126*, 7248–7249; b) S. R. Waldvogel, S. Lips, M. Selt, B. Riehl, C. J. Kampf, *Chem. Rev.* **2018**, *118*, 6706–6765; c) M. Yan, Y. Kawamata, P. S. Baran, *Chem. Rev.* **2017**, *117*, 13230–13319; d) E. J. Horn, B. R. Rosen, P. S. Baran, *ACS Cent. Sci.* **2016**, *2*, 302–308.
- [25] B. A. Frontana-Urbe, R. D. Little, J. G. Ibanez, A. Palma, R. Vasquez-Medrano, *Green Chem.* **2010**, *12*, 2099.
- [26] A. Wiebe, B. Riehl, S. Lips, R. Franke, S. R. Waldvogel, *Sci. Adv.* **2017**, *3*, eaao3920.
- [27] P. Anastas, N. Eghbali, *Chem. Soc. Rev.* **2010**, *39*, 301–312.
- [28] Y. Yuan, A. Lei, *Nat. Commun.* **2020**, *11*, 802.
- [29] a) K. Sellers, *Perchlorate. Environmental problems and solutions*, CRC/Taylor & Francis, Boca Raton, **2007**.; b) D. T. Chang, D. Park, J.-J. Zhu, H.-J. Fan, *Applied Sciences* **2019**, *9*, 4578.
- [30] T. TAJIMA, H. KURIHARA, S. SHIMIZU, H. TATENO, *Electrochemistry* **2013**, *81*, 353–355.
- [31] Y. Imada, J. L. Röckl, A. Wiebe, T. Gieshoff, D. Schollmeyer, K. Chiba, R. Franke, S. R. Waldvogel, *Angew. Chem. Int. Ed.* **2018**, *57*, 12136–12140; *Angew. Chem.* **2018**, *130*, 12312–12317.
- [32] J. L. Röckl, A. V. Hauck, D. Schollmeyer, S. R. Waldvogel, *ChemistryOpen* **2019**, *8*, 1167–1171.
- [33] J. L. Röckl, Y. Imada, K. Chiba, R. Franke, S. R. Waldvogel, *ChemElectroChem* **2019**, *6*, 4184–4187.
- [34] J. L. Röckl, D. Schollmeyer, R. Franke, S. R. Waldvogel, *Angew. Chem. Int. Ed.* **2020**, *59*, 315–319; *Angew. Chem.* **2020**, *132*, 323–327.
- [35] Q. Zhang, X. Chang, L. Peng, C. Guo, *Angew. Chem. Int. Ed.* **2019**, *58*, 6999–7003; *Angew. Chem.* **2019**, *131*, 7073–7077.
- [36] Y. Imada, Y. Okada, K. Chiba, *ChemElectroChem.* **2020**, DOI: 10.1002/celec.202000275.

MINIREVIEW

- [37] a) L. Ackermann, *Acc. Chem. Res.* **2020**, *53*, 84–104; b) E. Vitaku, D. T. Smith, J. T. Njardarson, *J. Med. Chem.* **2014**, *57*, 10257–10274.
- [38] a) A. Kehl, V. M. Breising, D. Schollmeyer, S. R. Waldvogel, *Chem. Eur. J.* **2018**, *24*, 17230–17233; b) A. Kehl, N. Schupp, V. M. Breising, D. Schollmeyer, S. R. Waldvogel, *Electrochemical Synthesis of Carbazoles by Dehydrogenative Coupling Reaction*; manuscript in preparation, **2020**.
- [39] H.-B. Zhao, Z.-J. Liu, J. Song, H.-C. Xu, *Angew. Chem. Int. Ed.* **2017**, *56*, 12732–12735; *Angew. Chem.* **2017**, *129*, 12906–12909.
- [40] E. Nam, P. E. Alokolaro, R. D. Swartz, M. C. Gleaves, J. Pikul, J. A. Kovacs, *Inorganic Chemistry* **2011**, *50*, 1592–1602.
- [41] M. Irsfeld, M. Spadafore, B. M. Prüß, *WebmedCentral* **2013**, *4*, 4409.
- [42] C. Lamberth, A. Jeanguenat, F. Cederbaum, A. de Mesmaeker, M. Zeller, H.-J. Kempf, R. Zeun, *Bioorg. Med. Chem.* **2008**, *16*, 1531–1545.
- [43] M. Murray, *Curr. Drug Metab.* **2000**, *1*, 67–84.
- [44] E. P. Gillis, K. J. Eastman, M. D. Hill, D. J. Donnelly, N. A. Meanwell, *J. Med. Chem.* **2015**, *58*, 8315–8359.
- [45] a) M. Dörr, S. Lips, C. A. Martínez-Huitle, D. Schollmeyer, R. Franke, S. R. Waldvogel, *Chem. Eur. J.* **2019**, *25*, 7835–7838; b) A. Kirste, B. Elsler, G. Schnakenburg, S. R. Waldvogel, *J. Am. Chem. Soc.* **2012**, *134*, 3571–3576; c) S. Lips, B. A. Frontana-Urbe, M. Dörr, D. Schollmeyer, R. Franke, S. R. Waldvogel, *Chem. Eur. J.* **2018**, *24*, 6057–6061; d) J. Nikl, S. Lips, D. Schollmeyer, R. Franke, S. R. Waldvogel, *Chem. Eur. J.* **2019**, *25*, 6891–6895.
- [46] K. Dhanunjayarao, V. Mukundam, M. Ramesh, K. Venkatasubbiah, *Eur. J. Inorg. Chem.* **2014**, *2014*, 539–545.
- [47] H.-L. Han, Y. Liu, J.-Y. Liu, K. Nomura, Y.-S. Li, *Dalton Trans.* **2013**, *42*, 12346–12353.
- [48] Y. Liu, W.-M. Ren, J. Liu, X.-B. Lu, *Angew. Chem. Int. Ed.* **2013**, *52*, 11594–11598; *Angew. Chem.* **2013**, *125*, 11808–11812.
- [49] N. Tsuji, K. Nagashima, *Tetrahedron* **1969**, *25*, 3017–3031.
- [50] a) R. Franke, D. Selent, A. Börner, *Chem. Rev.* **2012**, *112*, 5675–5732; b) S. E. Smith, T. Rosendahl, P. Hofmann, *Organometallics* **2011**, *30*, 3643–3651.
- [51] M. Selt, S. Mentizi, D. Schollmeyer, R. Franke, S. R. Waldvogel, *Synlett* **2019**, *30*, 2062–2067.
- [52] a) J. Barjau, P. Königs, O. Kataeva, S. Waldvogel, *Synlett* **2008**, *2008*, 2309–2312; b) J. Barjau, G. Schnakenburg, S. R. Waldvogel, *Angew. Chem. Int. Ed.* **2011**, *50*, 1415–1419; *Angew. Chem.* **2011**, *123*, 1451–1455; c) I. M. Malkowsky, C. E. Rommel, K. Wedeking, R. Fröhlich, K. Bergander, M. Nieger, C. Quaiser, U. Griesbach, H. Pütter, S. R. Waldvogel, *Eur. J. Org. Chem.* **2006**, *2006*, 241–245; d) M. Mirion, L. Andernach, C. Stobe, J. Barjau, D. Schollmeyer, T. Opatz, A. Lützen, S. R. Waldvogel, *Eur. J. Org. Chem.* **2015**, *2015*, 4876–4882.
- [53] a) A. Kirste, M. Nieger, I. M. Malkowsky, F. Stecker, A. Fischer, S. R. Waldvogel, *Chem. Eur. J.* **2009**, *15*, 2273–2277; b) I. M. Malkowsky, U. Griesbach, H. Pütter, S. R. Waldvogel, *Eur. J. Org. Chem.* **2006**, *2006*, 4569–4572; c) I. M. Malkowsky, C. E. Rommel, R. Fröhlich, U. Griesbach, H. Pütter, S. R. Waldvogel, *Chem. Eur. J.* **2006**, *12*, 7482–7488; d) S. R. Waldvogel, *Pure Appl. Chem.* **2010**, *82*, 1055–1063; e) C. E. Rommel, I. Malkowsky, S. R. Waldvogel, H. Puetter, U. Griesbach (BASF AG), WO2005075709A2, **2005**.; f) U. Griesbach, H. Pütter, S. R. Waldvogel, I. M. Malkowsky (BASF AG), WO2006077204A2, **2006**.; g) K. M. Dyballa, R. Franke, D. Fridag, S. R. Waldvogel, B. Elsler (Evonik Degussa GmbH), US9,879,353, **2013**.; h) K. M. Dyballa, R. Franke, D. Fridag, S. R. Waldvogel, B. Elsler (EVONIK INDUSTRIES AG), DE102013203865A1, **2014**.; i) K. M. Dyballa, R. Franke, D. Fridag, S. R. Waldvogel, B. Elsler (EVONIK INDUSTRIES AG), WO2014135236A1, **2014**.; j) K. M. Dyballa, R. Franke, D. Fridag, S. R. Waldvogel, B. Elsler (EVONIK INDUSTRIES AG), DE102013203866A1, **2014**.; k) K. M. Dyballa, R. Franke, D. Fridag, S. R. Waldvogel, B. Elsler (EVONIK INDUSTRIES AG), WO2014135237A1, **2014**.
- [54] M. Selt, S. R. Waldvogel, *Supporting Electrolyte-free and Scalable Flow Process for the Electrochemical Synthesis of 3,3',5,5'-Tetramethyl-2,2'-biphenol*; manuscript in preparation, **2020**.
- [55] B. Gleede, M. Selt, C. Gütz, A. Stenglein, S. R. Waldvogel, *Org. Process Res. Dev.* **2019**, DOI: 10.1021/acs.oprd.9b00451.
- [56] S. R. Waldvogel, M. Dörr, J. Röckl, J. Rein, D. Schollmeyer, *Chem. Eur. J.* **2020**, DOI: 10.1002/chem.202001171.
- [57] Siegfried R Waldvogel, Stephan Blum, Dieter Schollmeyer, Maris Turks, *Chem. Eur. J.* **2020**, DOI: 10.1002/chem.202001180.

MINIREVIEW

Entry for the Table of Contents



- ✓ Supporting electrolyte-free
- ✓ Completely evaporable
- ✓ Facile work-up
- ✓ Technically viable downstream processing

Electrosynthesis 2.0: The well conductive electrolyte system based on HFIP and amines offers not only intriguing features for practically performing the electrosynthesis, but also novel reactivity and expansion of the scope of the well-established HFIP electrolytes. With an almost complete recovery of the HFIP-amine mixtures a substantial contribution to greener electrosynthesis is established and might lead to a new area in electrosynthesis.

Title:**Merging shuttle reactions and paired electrolysis: e-shuttle enables the reversible interconversion of alkenes and vicinal dihalides****Authors:**

Xichang Dong^{1,3}, Johannes L. Röckl^{1,2,3}, Siegfried R. Waldvogel^{2*} & Bill Morandi^{1*}

¹Laboratory of Organic Chemistry, Department of Chemistry and Applied Biosciences, ETH Zurich, Zurich, Switzerland.

²Department of Organic Chemistry, Johannes Gutenberg-University Mainz, Germany.

³These authors contributed equally: Xichang Dong, Johannes L. Röckl.

✉e-mail: bill.morandi@org.chem.ethz.ch; waldvogel@uni-mainz.de

Abstract (Nature format):

Polyhalogenated molecules have found widespread applications as flame retardants, pesticides, polymers and pharmaceuticals^{1,2}. Moreover, they serve as versatile synthetic intermediates in organic chemistry due to the inherent reactivity of carbon-halogen bonds^{3,4}. Despite these attractive features, the preparation of polyhalogenated molecules still relies on the use of highly toxic and reactive halogenating reagents, such as Cl₂ and Br₂, which are hazardous compounds to transport, store, and handle^{4,5}. Moreover, the use of such highly reactive reagents inherently prevents the possibility to perform the reverse reactions, retro-dihalogenations, despite their potential for the recycling of persistent halogenated pollutants. Here, we introduce an electrochemically-assisted shuttle (*e-shuttle*) paradigm for the facile and scalable interconversion of alkenes and halogenated molecules, a class of reactions which can be used to either synthesize useful polyhalogenated molecules from simple alkenes or recycle waste material. The power of this reaction is best highlighted by an example, in which an inexpensive persistent environmental pollutant (Lindane), can be used as a donor reagent for the functionalization of simple feedstock alkenes, merging a recycling process with a synthetically relevant dichlorination reaction. We further demonstrate that this paired electrolysis-enabled shuttle protocol, which uses a simple setup and inexpensive electrodes, is applicable to four different, synthetically useful transfer halogenation reactions, and can be readily scaled up to decagrams of product. The synthetic potential offered by the reaction's reversibility was further demonstrated in a unique *e-shuttle*-mediated alkene protection/deprotection sequence and an intramolecular transfer dibromination. In a broader context, the symbiotic merging of shuttle reactions and electrochemistry introduced in this work opens new horizons for safe transfer functionalization reactions that will address important challenges across the molecular science.

Main text:

Transfer hydrofunctionalization proceeding through a shuttle catalysis⁶ paradigm has emerged as a powerful strategy to reversibly functionalize and defunctionalize organic molecules without employing or releasing hazardous reagents^{7,8,9,10,11,12}, such as HCN⁷. However, catalytic and reversible transfer reactions have so far been limited to alkene *monofunctionalization* reactions which usually involve the transfer of an HX molecule^{6,12}. In contrast, the synthetically appealing, simultaneous transfer of two functional groups, in a catalytic reversible transfer *difunctionalization* process, has so far remained elusive, despite the vast synthetic potential of these reactions in organic synthesis. In particular, reactions involving the formal transfer of extremely hazardous molecules, such as Cl₂¹³ or Br₂, from inexpensive and non-toxic bulk chemicals, such as dichloro- and dibromoethane, would be highly desirable because of the widespread synthetic applications of polyhalogenated molecules in flame retardants, pesticides, materials and natural products^{1,2,14}. (Scheme 1). The inherent reversibility of a shuttle reaction would further unlock the retro-dihalogenations of waste compounds, such as flame retardants and pesticides, providing a new entry into a circular economy approach to these products.

The challenge in developing transfer difunctionalizations originates from the catalytic approach generally employed in shuttle catalysis. Transfer hydrofunctionalizations, such as hydrocyanation⁷, rely on the intermediacy of an alkyl-M complex which readily undergoes fast and reversible β -hydride elimination, thus triggering the transfer of an H group alongside the desired functional group¹². Unfortunately, the ease of β -hydride elimination makes the selective, competitive elimination of other synthetically useful groups extremely challenging¹⁵. Furthermore, while β -hydride elimination is a fast and reversible process, the subsequent migratory re-insertion of an alkene into the M-X bond is often kinetically and thermodynamically disfavored due to the high stability of metal-halogen bonds¹⁶. Thus, a mechanistically distinct approach to favor X-cleavage over H cleavage is crucial to unlock this important class of transfer difunctionalization reactions.

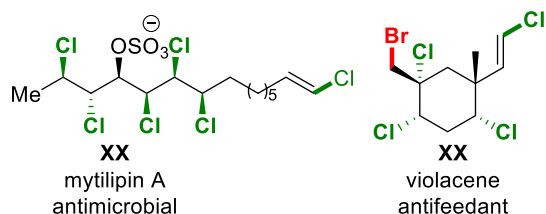
Electrochemistry has recently experienced a renaissance in organic chemistry, as it utilizes inexpensive and readily available electrical current from renewable resources as a sustainable and inherently safe redox reagent^{17,18,19}. Notable advances have been made in halogenation reactions, as illustrated by an elegant example of dichlorination reaction from Lin et al²⁰. However, this reaction, as well as the vast majority of other electrochemical reactions, has to be coupled to another sacrificial half reaction at the counter-electrode. Besides this limitation, current protocols can often be further limited by the use of complex reaction setups including expensive metal electrodes, or the generation of hazardous/flammable by-products (e.g. hydrogen gas)²¹. Moreover, they are inherently irreversible processes and thus cannot be easily used for other synthetically useful applications, such as the degradation of waste molecules, as well rearrangement reactions and new protecting strategies which rely on a process' reversibility.

We envisaged that paired electrolysis^{22,23}, a class of ideal yet extremely rare electrochemical reactions wherein all electrons are employed in the desired transformation, could provide a totally unexplored path to reversible electrochemically-mediated shuttle reactions (e-shuttle). We

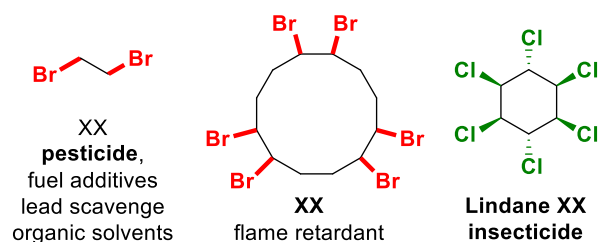
surmised that the reversible cleavage of two strong C—X bonds through a controlled electron transfer process initiated by simple reduction and/or oxidation of key intermediates at the anode and cathode, simultaneously and respectively, would unlock this new class of reactions. More specifically, the single-electron reduction of the dihalide at the cathode releases the X anion and generates the carbon radical Z, which is almost instantly reduced again to an anion²⁴. As a central design, the following selective departure of anion X instead of the hydride breaks the second C—X bond, releasing the alkene simultaneously. Considering that a halide anion is a much better leaving group than a hydride, the competing undesired β -H elimination, which is often the preferred pathway with transition metal intermediates, can be effectively suppressed by this electrochemical approach. The subsequent oxidation of the anion X at the anode followed by reaction with the alkene delivers the desired product, which closes the cycle by rebuilding the C—X and C—Y bonds in a fully isodesmic process. The highly precise control of the potential applied on the electrode and the highly tunable cell potential would make this strategy extremely versatile with regard to the group transferred, opening new horizons for further shuttle reaction development. This is a great advantage over the organometallic strategy, where each shuttle reaction relies on a completely different combination of metal and catalyst requiring tedious optimization campaigns¹².

A: Examples of dihalide compounds of high interest

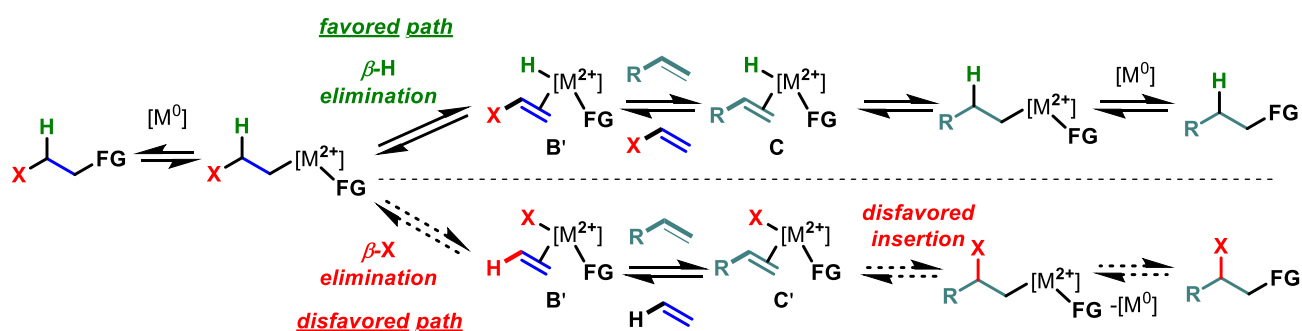
Bioactive dihalides



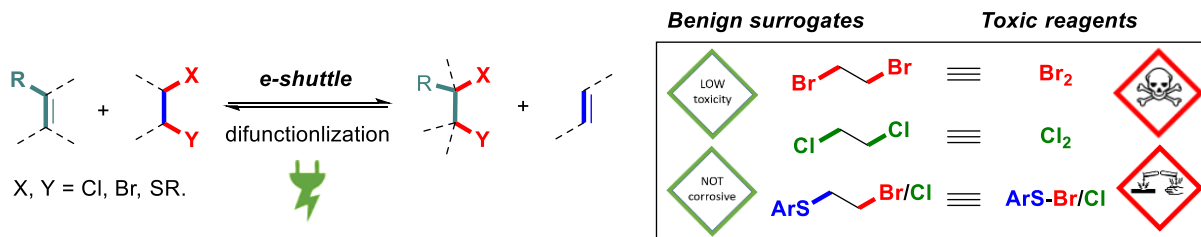
Persistent Organic Pollutants



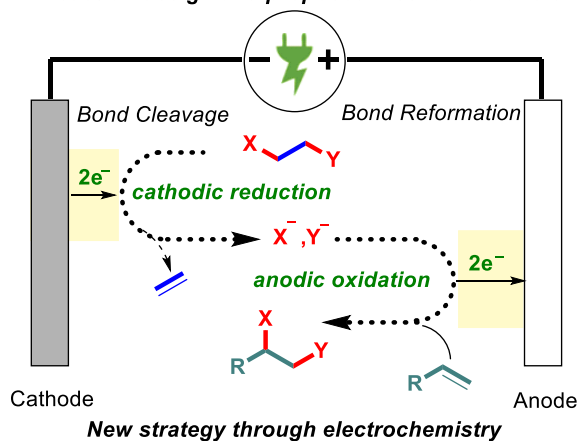
B: Transfer hydrofunctionalization and challenges to develop transfer difunctionalization



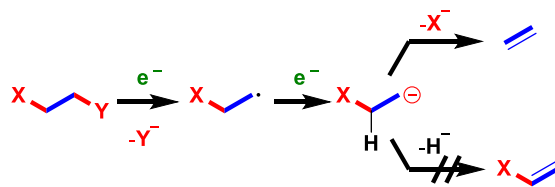
C: Paired Electrolysis Enabled Redox-neutral Shuttle Reaction (e-shuttle)



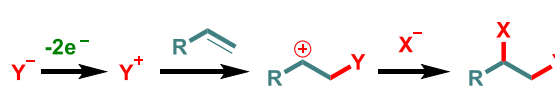
D: Reaction design and proposed mechanism of e-shuttle



a) Cathodic reduction: bond cleavage

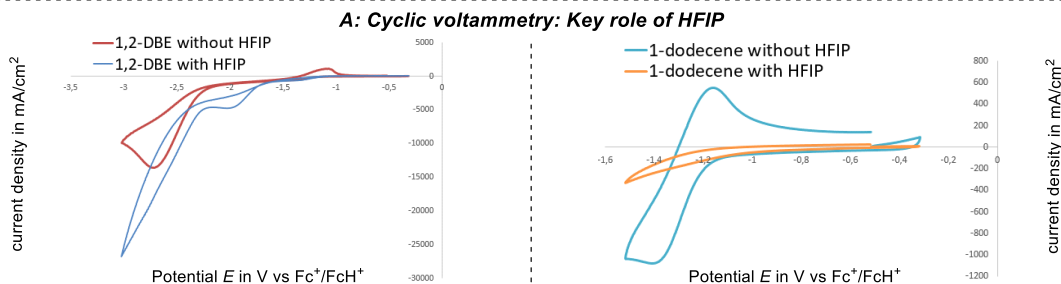
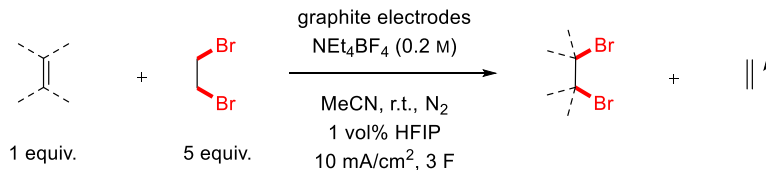


b) Anodic oxidation: bond reformation

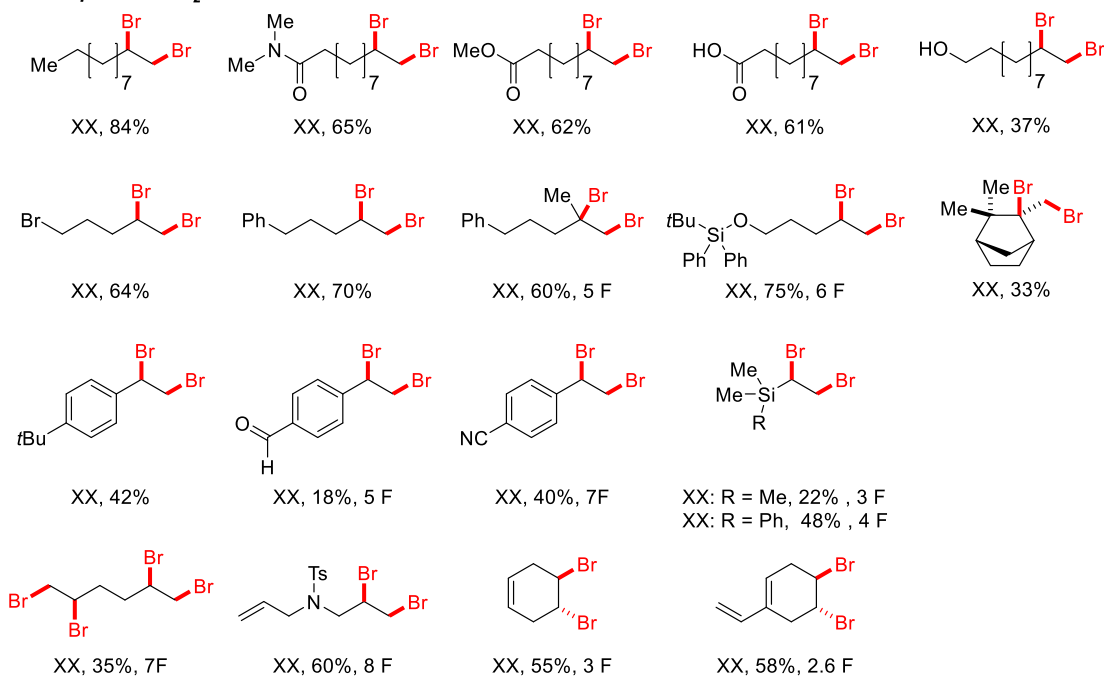


At the outset of our investigations, a transfer dibromination was uniformly optimized in an undivided cell using inexpensive isostatic graphite as the electrode material under a constant current conditions at room temperature, a reaction setup easily accessible to non-specialized laboratories. 1,2-Dibromoethane (DBE) was selected as a formal Br₂ donor because it is an inexpensive reagent, produced on a bulk scale, that would solely release benign ethylene as a by-product. It is also notable that most commercial suppliers offer this reagent at an even lower price (per mol of Br₂) than Br₂ itself, probably reflecting additional costs occurring during transportation and storage of toxic and volatile Br₂²⁵. Optimal results were obtained with 5 equiv. of 1,2-dibromoethane as the Br₂ donor, as little as 1 vol% HFIP as the key additive, and 2 equiv. of Et₄NBF₄ as electrolyte, providing the targeted 1,2-dibromide XX in 84% NMR yield when 3.0 F of electricity with respect to alkene XX was applied. As indicated by cyclic voltammetry (CV) studies, the HFIP additive plays a key role in facilitating the reduction of the DBE donor and suppressing the undesired and unproductive cathode reductive oligo/polymerization of alkene acceptors (see Scheme 2 and SI for more details).

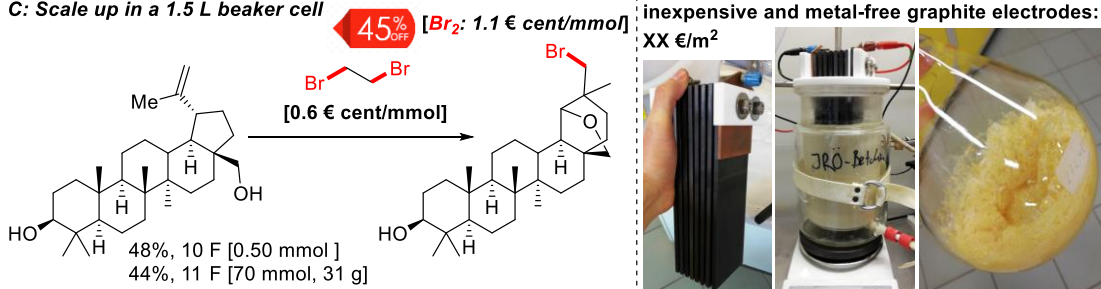
Using this protocol, a broad range of inactivated terminal alkenes (XX–XX) were readily converted to the corresponding dibromide product in good to excellent yields, in which a large variety of functional groups such as amide (XX), ester (XX), free carboxylic acid (XX), alcohol (XX), and bromide (XX) were well tolerated. Activated alkenes, such as styrene (XX-XX) and vinyl silane (XX-XX), proved to be suitable substrates as well, albeit giving slightly lower yields. This protocol was also applicable to the natural products camphene (XX) and Betulin (XX), both of which underwent desired dibromination reaction. Notably, the acid-sensitive silyl ether was well-accommodated, exhibiting an advantage over the previously reported electrochemical oxidative 1,2-dibromination of alkenes under acidic conditions²¹. While the hexa-1,5-diene (XX) underwent two-fold 1,2-dibromination to yield the tetra brominated product XX in decent yield, selective mono 1,2-dibromination was observed for several other unconjugated dienes (XX-XX). To demonstrate the easy scalability and robustness of this e-shuttle process, the dibromination of Betulin was readily scaled up to a 1.5 L beaker cell from a 10 mL reaction vial to give 33 g of product under otherwise identical reaction conditions.



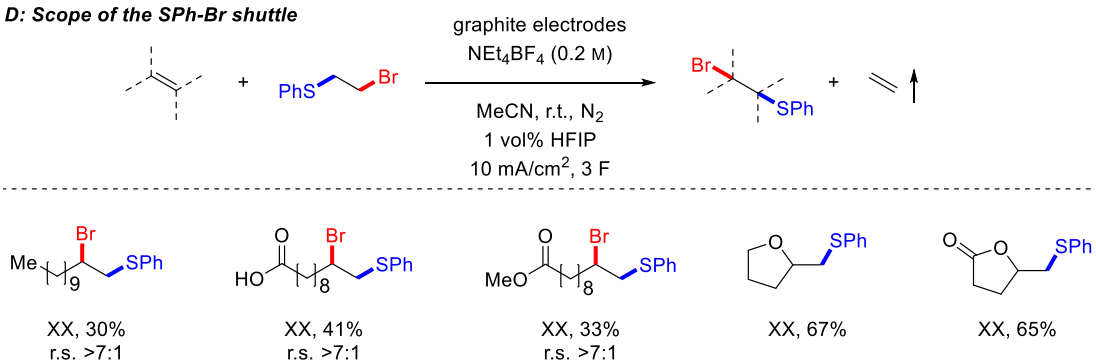
B: Scope of the Br₂-shuttle



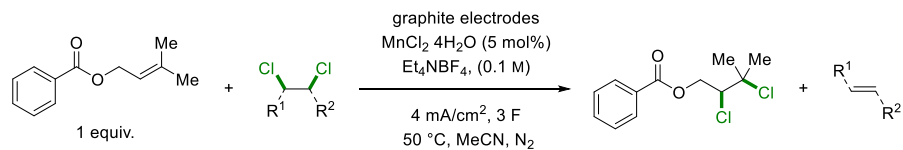
C: Scale up in a 1.5 L beaker cell



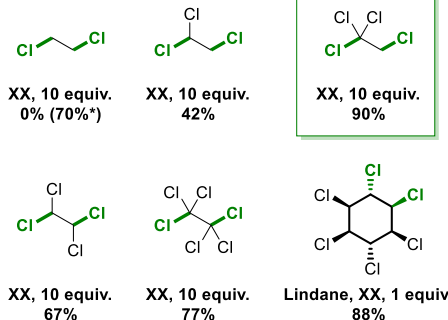
D: Scope of the SPh-Br shuttle



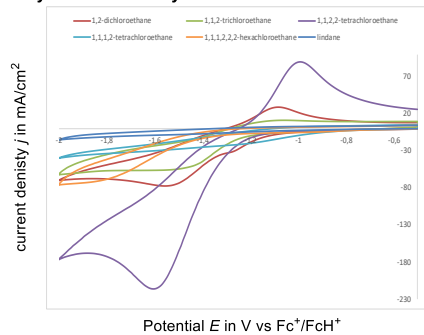
Taking advantage of the reversible elimination of a -SR group, we could next also develop a transfer bromothiolation of alkenes to access 1,2-bromothioether derivatives which are valuable synthetic intermediates usually accessed through multistep synthesis involving toxic R-SBr reagents^{26, 27}. Several terminal alkenes were successfully converted to the targeted bromothioether product with excellent regioselectivity (XX-XX), under otherwise identical conditions, taking 2-bromoethyl phenyl sulfide (10 equiv.) as the PhS-Br donor (Scheme 2). The carboxylic acid (XX) and ester (XX) functional groups were well tolerated. Interestingly, an interrupted shuttle reaction took place when pent-4-en-1-ol (XX) and pent-4-enoic acid (XX) were employed as the substrates, delivering the cyclic ether or lactam derivatives (XX-XX) via subsequent intramolecular nucleophilic attack, demonstrating the method's potential for the development of new cascade reactions.



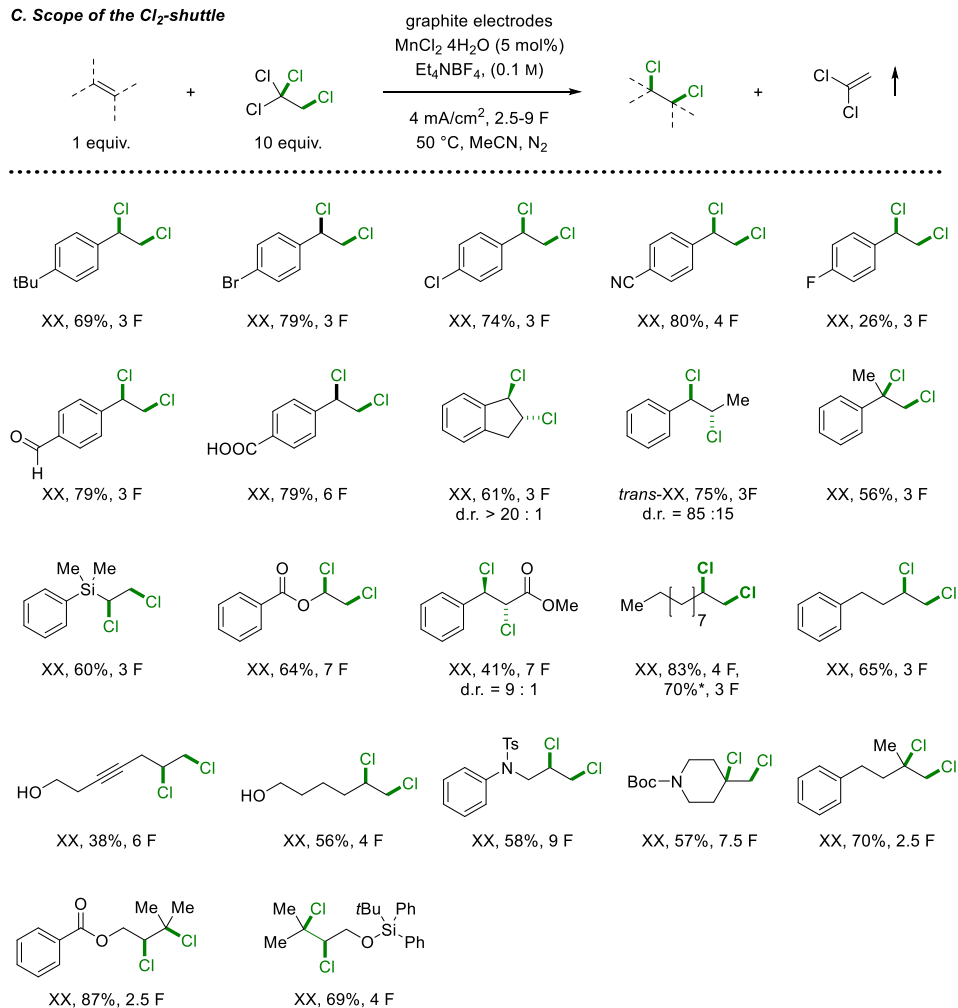
A: Reagent optimization



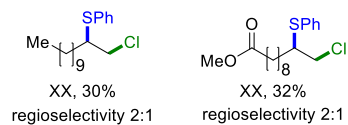
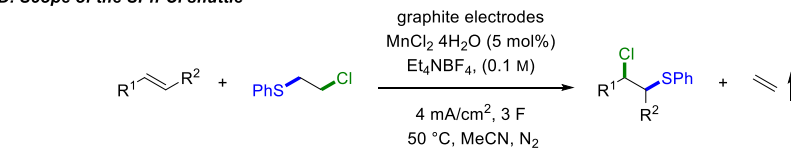
B. Cyclic voltammetry



C. Scope of the Cl₂-shuttle

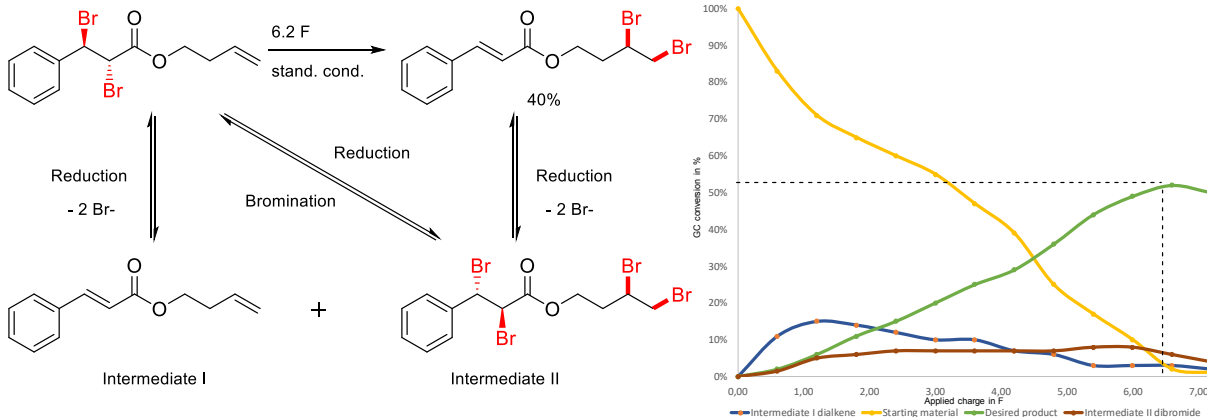


D. Scope of the SPh-Cl shuttle

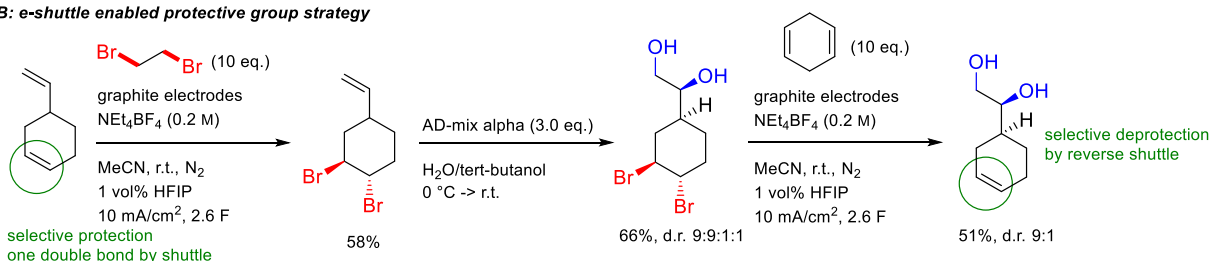


In order to further demonstrate the modularity of this conceptually new approach to shuttle catalysis, we next developed a transfer dichlorination reaction. 1,2-Dichloroethane (DCE) was selected as the donor, because it is an inexpensive bulk chemical (20 million ton/year) produced with the excess of Cl₂ gas generated during the Chlor-alkali electrolysis process²⁸. After initial fruitless attempts, the desired dichloride XX was obtained in 39% yield when 5 mol% of a Mn(II) salt (e.g. MnCl₂·4H₂O) was introduced as a mediator²⁰, and the yield was further increased to 70% when DCE (ca. 125 equiv.) was used as the solvent. While this procedure was efficient for a wide set of terminal alkenes, it failed for more challenging 1,1,2-trisubstituted alkene XX, a feature largely attributed to the undesired 1,2-dechlorinative decomposition of the product XX and alkene oligomerization of the starting material via cathodic reduction. We reasoned that these two challenges could be smoothly resolved by choosing a suitable dichloride donor, as they could not be resolved by adding an additive, such as HFIP. Among all of the polychloride donors examined, 1,1,1,2-tetrachloroethane (XX, 10 equiv.) turned out to be the best option in terms of atom economy and reaction efficiency, affording the dichloride product XX in 90% NMR yield. This can be rationalized by the low redox potential of 1,1,1,2-tetrachloroethane (Scheme 3, blue curve) and the high stability of the extruded 1,1-dichloroethene. Using this procedure, various styrene-derived alkenes were converted to the corresponding 1,2-dichlorides in good to excellent yield (XX-XX), leaving the Br, Cl, CHO, COOH and CN functional groups untouched. The indene (XX) was diastereoselectively transformed into *trans*-1,2-dichloride XX (d.r. > 19:1). The 1,2-dichloride compound XX, bearing a reactive benzylic tertiary C–Cl bond, was prepared in good yield from α -methylstyrene. Several other activated alkenes proved viable acceptors as well (XX-XX), in particular, methyl cinnamate was converted to the 1,2-dichloride XX in an excellent d.r. ratio (9:1). A series of mono- and disubstituted alkenes participated smoothly in the 1,2-dichlorination reaction, with the Boc and Ts protected amine well tolerated. To our delight, preliminary experiments show that this protocol can be readily extended to the 1,2-chlorothiolation transfer reaction using the commercially available 2-chloroethyl phenyl sulfide (10 equiv.) as the donor.

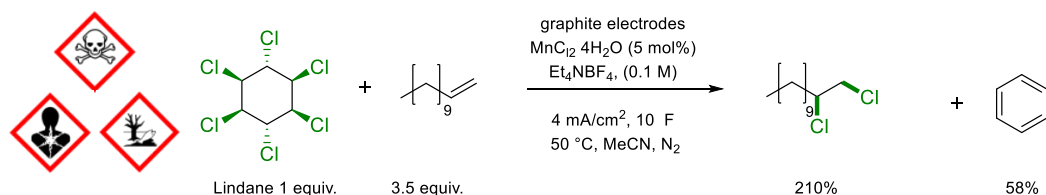
A: Formal intramolecular shuttle of Br₂



B: e-shuttle enabled protective group strategy



C: Persistent polychlorinated waste degradation



An intriguing advantage of the reaction's reversibility is the possibility to perform an intramolecular rearrangement reaction through a shuttle reaction. Indeed, taking advantage of conjugation as a driving force, we could selectively transfer a dibromide from an internal position to a terminal one (Scheme 4). The reaction's reversibility further inspired us to design a new protecting group strategy for alkenes. As shown in the figure (Scheme 4), the selective bromination of the unconjugated diene XX taking DBE as Br₂ donor leads to protected compound X, which can subsequently undergo site selective asymmetric dihydroxylation of the terminal alkene to generate the intermediate XX while the dibromide moiety remained untouched. A final retro-dibromination of XX using a sacrificial alkene (1,4-cyclohexadiene) as acceptor produces the desired dihydroxylated product XX bearing an internal alkene²⁹.

Lindane, which was once widely used as an effective insecticide in crop protection, is classified as a persistent organic pollutant due to its high toxicity and high persistency in the environment. We thus questioned whether this waste material, which can only be inefficiently degraded through normal electrochemical recycling approaches^{30,31,32}, could instead serve as an efficient Cl₂ donor in a synthetically useful transfer dichlorination. Remarkably, lindane served, through three

successive retro-dichlorination events, as an excellent donor in this reaction generating the desired dichlorinated product alongside benzene, the fully dechlorinated by-product of lindane. These results provide a conceptual blueprint for the development of ideal shuttle reactions, in which the synthetically relevant functionalization of a substrate is coupled with the recycling of a persistent environmental pollutant.

In conclusion, we have reported a scalable e-shuttle strategy to unlock previously elusive transfer difunctionalization reactions. Using an easily accessible electrochemical setup involving paired electrolysis, we have been able to take advantage of single electron transfer processes to develop four distinct, synthetically relevant transfer reactions using this unified strategy. The utility of the reaction's reversibility is demonstrated in an intramolecular rearrangement, a new protecting group strategy for alkenes and a strategy involving the concomitant degradation of a waste molecule to functionalize simple feedstocks. In a broader context, we believe that these results lay the groundwork for the development of countless new reversible reactions which take advantage of the merger between shuttle reactions and electrochemistry.

Acknowledgements:

This project received funding from the European Research Council under the European Union's Horizon 2020 research and innovation program (Shuttle Cat, Project ID: 757608).

We also thank the ETH Zürich for support. X. D. acknowledges the Marie Skłodowska-Curie Action (HaloCat, Project ID: 886102) for a postdoctoral fellowship.

J.L.R. is a recipient of a DFG fellowship through the Excellence Initiative by the Graduate School Materials Science in Mainz(GSC 266).

Author contributions: X. D. and J. R. discovered the reaction and performed all the synthetic studies. S. W. and B. M. supervised the research. All authors contributed to the writing and editing of the manuscript.

-
1. Kirk, K. L. Persistent Polyhalogenated Compounds: Biochemistry, Toxicology, Medical Applications, and Associated Environmental Issues. in *Biochemistry of the Elemental Halogens and Inorganic Halides* 191–238 (Springer, 1991).
 2. Häggblom, M. M., & Bossert, I. D. Halogenated organic compounds—a global perspective. in *Dehalogenation Microbial Processes and Environmental Applications* (eds. Häggblom, M. M.) 3–29 (Springer, 2004).
 3. Patai, S., *The Chemistry of The Carbon-Halogen Bond: Part 1*, (John Wiley & Sons, Ltd, 1973).
 4. Saikia, I., Borah, A. J., & Phukan, P. Use of bromine and bromo-organic compounds in organic synthesis. *Chem. Rev.* **116**, 6837–7042 (2016).
 5. Denmark, S. E., Kuester, W. E., & Burk, M. T. Catalytic, asymmetric halofunctionalization of alkenes—a critical perspective. *Angew. Chem. Int. Ed.* **51**, 10938–10953 (2012).
 6. Bhawal, B. N., & Morandi, B. Catalytic transfer functionalization through shuttle catalysis. *ACS Catalysis* **6**, 7528–7535 (2016).
 7. Fang, X., Yu, P., & Morandi, B. Catalytic reversible alkene-nitrile interconversion through controllable transfer hydrocyanation. *Science* **351**, 832–836 (2016).
 8. Fang, X., Cacherat, B., & Morandi, B. CO- and HCl-free synthesis of acid chlorides from unsaturated hydrocarbons via shuttle catalysis. *Nat. Chem.* **9**, 1105 (2017).

-
9. Murphy, S. K., Park, J.-W., Cruz, F. A. & Dong, V. M. Rh-catalyzed C–C bond cleavage by transfer hydroformylation. *Science* **347**, 56–60 (2015).
 10. Landis, C. R. Construction and deconstruction of aldehydes by transfer hydroformylation. *Science* **347**, 29–30 (2015).
 11. Park, Y. J., Park, J.-W. & Jun, C.-H. Metal–organic cooperative catalysis in C–H and C–C bond activation and its concurrent recovery. *Acc. Chem. Res.* **41**, 222–234 (2008).
 12. Bhawal, B. N., & Morandi, B. Catalytic Isofunctional Reactions—Expanding the Repertoire of Shuttle and Metathesis Reactions. *Angew. Chem. Int. Ed.* **58**, 10074–10103 (2019).
 13. Sakai, K., Sugimoto, K., Shigeizumi, S., & Kondo, K. A new selective dichlorination of C–C double bonds. *Tetrahedron Lett.* **35**, 737–740 (1994).
Ho, M. L., Flynn, A. B., & Ogilvie, W. W. Single-isomer iodochlorination of alkynes and chlorination of alkenes using tetrabutylammonium iodide and dichloroethane. *J. Org. Chem.* **72**, 977–983 (2007).
 14. Gribble, G. W. Naturally occurring organohalogen compounds. *Acc. Chem. Res.* **31**, 141–152 (1998).
 15. Crabtree, R. H. *The Organometallic Chemistry of the Transition Metals*, 5th Edition. John Wiley & Sons. (John Wiley & Sons, 2009).
 16. Cresswell, A. J., Eey, S. T. C., & Denmark, S. E. Catalytic, stereoselective dihalogenation of alkenes: challenges and opportunities. *Angew. Chem. Int. Ed.* **54**, 15642–15682 (2015). See page 16572
 17. Hammerich, O., & Speiser, B. *Organic Electrochemistry: Revised and Expanded*. (Taylor & Francis Group, LLC, 2015).
 18. Yan, M., Kawamata, Y., & Baran, P. S. Synthetic organic electrochemical methods since 2000: on the verge of a renaissance. *Chem. Rev.* **117**, 13230–13319 (2017).
 19. Röckl, J. L., Pollok, D., Franke, R., & Waldvogel, S. R. A Decade of Electrochemical Dehydrogenative C, C-Coupling of Aryls. *Acc. Chem. Res.* **53**, 45–61 (2019).
Wiebe, A., Gieshoff, T., Möhle, S., Rodrigo, E., Zirbes, M., & Waldvogel, S. R. Electrifying organic synthesis. *Angew. Chem. Int. Ed.* **57**, 5594–5619 (2018).
Möhle, S., Zirbes, M., Rodrigo, E., Gieshoff, T., Wiebe, A., & Waldvogel, S. R. Modern Electrochemical Aspects for the Synthesis of Value-Added Organic Products. *Angew. Chem. Int. Ed.* **57**, 6018–6041 (2018).
 20. Fu, N., Sauer, G. S., & Lin, S. Electrocatalytic radical dichlorination of alkenes with nucleophilic chlorine sources. *J. Am. Chem. Soc.* **139**, 15548–15553 (2017).
 21. Yuan, Y., Yao, A., Zheng, Y., Gao, M., Zhou, Z., Qiao, J., Hu, J., Ye, B., Zhao, J., Wen, H. & Lei, A. Electrochemical Oxidative Clean Halogenation Using HX/NaX with Hydrogen Evolution. *iScience* **12**, 293–303 (2019).
 22. Hilt, G. Basic Strategies and Types of Applications in Organic Electrochemistry. *ChemElectroChem* **7**, 395–405 (2020).
 23. Paddon, Christopher A., Mahito Atobe, Toshio Fuchigami, Ping He, Paul Watts, Stephen J. Haswell, Gareth J. Pritchard, Steven D. Bull, & Frank Marken. Towards paired and coupled electrode reactions for clean organic microreactor electrosyntheses. *J. Appl. Electrochem.* **36**, 617–634 (2006).
 24. Von Stackelberg, M. & Stracke, W. *Z. Elektrochem.* **53**, 118, (1949).
Casanova, J., & Reddy, V. P. Electrochemistry of the Carbon–Halogen Bond. in *The Chemistry of The Carbon-Halogen Bond* (eds. Patai, S.) 980–1047 (John Wiley & Sons, Ltd., 1973)
 25. D. M. Hill, *Safety Review of Bromine-Based Electrolytes for Energy Storage Applications*, Report 1 <http://energystorageicl.com/wp-content/uploads/2018/04/DNV-GL-Safety-Review-of-Bromine-Based-Electrolytes-for-Energy-Storage-Applications.pdf> (2018).
 26. Schneider, E., Darstellung & Eigenschaften von Alkylschwefelhalogeniden, *Chem. Ber.* **84**, 911–916 (1951).
 27. Drabowicz, J., Kielbasiński, P., & Mikołajczyk, M. Synthesis of sulphenyl halides and sulphenamides (eds. Patai, S.) 221–292 (John Wiley & Sons, Ltd., 1990)
 28. Hoffmann, C., Weigert, J., Esche, E., & Repke, J. U. Towards demand-side management of the chlor-alkali electrolysis: Dynamic, pressure-driven modeling and model validation of the 1, 2-dichloroethane synthesis. *Chem. Eng. Sci.* **214**, 115358 (2020).

-
29. Husstedt, U, & Schäfer, H. Selective Monoprotection of the Less Alkylated Double Bond in Dienes, *Synthesis* 964–966 (1979).
 30. Rondinini, S. & Vertova, A. Electroreduction of halogenated organic compounds. In *Electrochemistry for the Environment* (eds. Comninellis, C., & Chen, G.) 279–306 (Springer, 2010).
 31. Merz, J. P., Gamoke, B. C., Foley, M. P., Raghavachari, K., & Peters, D. G. Electrochemical reduction of (1R, 2r, 3S, 4R, 5r, 6S)-hexachlorocyclohexane (Lindane) at carbon cathodes in dimethylformamide. *J. Electroanal. Chem.* **660**, 121–126 (2011).
 32. Martin, E. T., McGuire, C. M., Mubarak, M. S., & Peters, D. G. Electroreductive remediation of halogenated environmental pollutants. *Chem. Rev.* **116**, 15198–15234 (2016).

Inhalt

1	General Methods	2
1.1	Gas Chromatography (GC/GC-MS).....	2
1.2	Liquid Chromatography	2
1.3	High Resolution Mass Spectrometry.....	2
1.4	NMR Spectroscopy.....	3
1.5	Melting Point.....	3
1.6	Cyclic voltammetry.....	3
1.7	Mechanistic experiments.....	4
1.8	Optimization	8
	Optimization of Br ₂ – shuttle conditions	8
1.9	Electrolysis setup	11
1.8.1	1.10 General procedures	13
	GP1: Electrolytic shuttle dibromination of alkenes	13
1.10.1	GP2: Electrolytic shuttle dichlorination of alkenes.....	13
1.10.2	GP3: Electrolytic shuttle bromothiolation of alkenes.....	14
1.10.3	GP4: Electrolytic shuttle chlorothiolation of alkenes	14
1.10.4	1.11 Characterization.....	15
	1.12 Spectra	63

1 General Methods

1.1 Gas Chromatography (GC/GC-MS)

Crude reaction mixtures and purified products were analyzed by gas chromatography (GC) with a GC-2010 (*Shimadzu*, Kyōto, Japan). A quartz capillary column ZB-5 (length: 30 cm, inner diameter: 0.25 mm, layer thickness of stationary phase: 0.25 μm , carrier gas: hydrogen, stationary phase: (5%-phenyl)-methylpolysiloxane (*Phenomenex*, Torrance, USA) was used. The carrier gas rate was 45.5 $\text{cm}\cdot\text{s}^{-1}$ and the injection temperature 250 °C. A flame ionization detector (FID) with an inlet temperature of 310 °C was used.

Further analysis by gas chromatography mass spectra (GC-MS) using a GC-2010 with a similar column, combined with a GC-MS-QP2010 (*Shimadzu*, Kyōto, Japan) detector with an injection temperature of 250 °C and detection inlet temperature of 310 °C was conducted.

All chromatographic data was recorded using the method “hart”, which starts at 50 °C with a heating rate of 15 °C $\cdot\text{min}^{-1}$ to 290 °C which is held for 8 min.

1.2 Liquid Chromatography

Thin layer chromatography (TLC) was performed with “DC Kieselgel 60 F₂₅₄” (*Merck KGaA*, Darmstadt, Germany) on aluminum plates and an UV lamp ($\lambda = 254 \text{ nm}$, NU-4 KL, Benda, Wiesloch, Germany). No stain was utilized as all starting materials and products absorbed in the UV light at $\lambda = 254 \text{ nm}$. An automatic silica flash column chromatography system with a control unit C-620, a fraction collector C-666 and a UV photometer C-635 (*Büchi*, Flawil, Switzerland) was used for all isolations. Silica gel 60 M (0.040 – 0.063 mm, *Macherey-Nagel GmbH & Co.*, Düren, Germany) was used as the stationary phase. Cyclohexane and ethyl acetate or dichloromethane and methanol were used as eluents. The system connected to a computer and controlled with the software *BÜCHI Sepacore Control 1.2 Standard Edition*.

1.3 High Resolution Mass Spectrometry

High resolution electrospray ionization mass spectrometry (HR-ESI) and high resolution atmospheric pressure chemical ionization (HR-APCI) was performed using an Agilent 6545 QTOF-MS (*Agilent*, Santa Clara, USA). The data given displays the mass-charge-ratio (m/z) of the corresponding compounds.

1.4 NMR Spectroscopy

Nuclear magnetic resonance spectroscopy (NMR) was measured using a multi nuclear magnetic resonance spectrometer Bruker Avance III HD 400 (400 MHz) (5 mm BBFO-SmartProbe with z gradient and ATM, *SampleXPress* 60 sample changer, Analytische Messtechnik, Karlsruhe, Germany). The chemical shifts (δ) are reported in parts per million (ppm) relative to the residue signal of the deuterated solvent (CDCl_3 or $\text{DMSO-}d_6$) used for the measurements by the solvent data chart from Cambridge Isotopes Laboratories, USA. For the ^{19}F spectra, ethyl fluoroacetate served as external standard ($\delta = -231.1\text{ppm}$).

The evaluations of ^1H and ^{13}C were executed using the software MestReNova 10.0.1-14719 (*Mestrelab Research S.L.*, Spain) with the assistance of *H,H*-COSY, *C,H*-HSQC and *C,H*-HMBC experiments. The multiplicity of the signals were abbreviated in the following manner: s (singlet), d (doublet), t (triplet), hept (heptet) pseudo-quart (pseudo-quartet), pseudo-quint (pseudo-quintet), m (multiplet), dd (doublet of doublets), ddd (doublet of doublets of doublets). The coupling constants *J* have been given in Hertz (Hz).

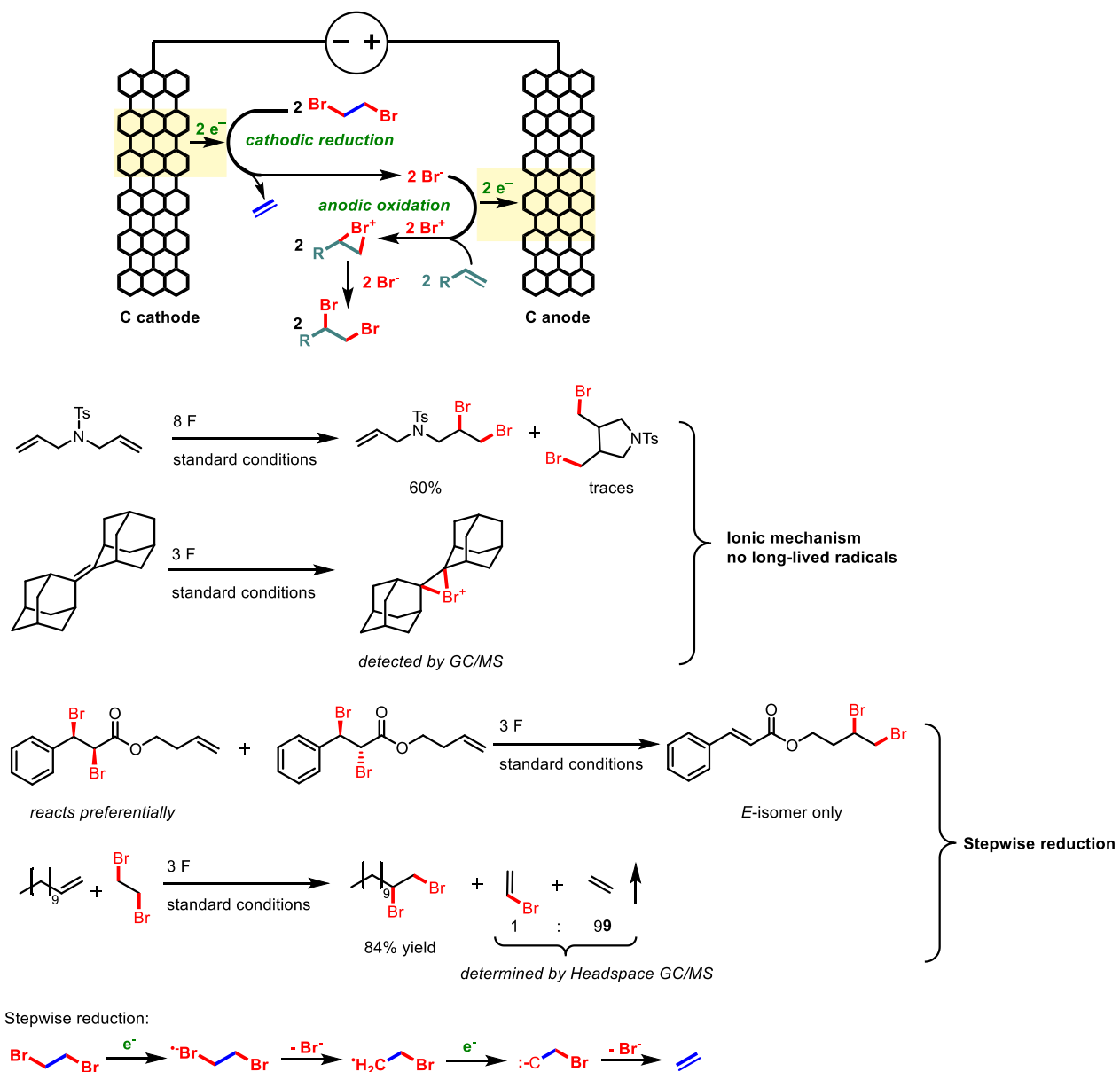
1.5 Melting Point

The melting ranges of purified products were measured using M-565 (*Büchi*, Flawil, Switzerland) with a heating rate of $2\text{ }^\circ\text{C}\cdot\text{min}^{-1}$. The given melting ranges are not further corrected.

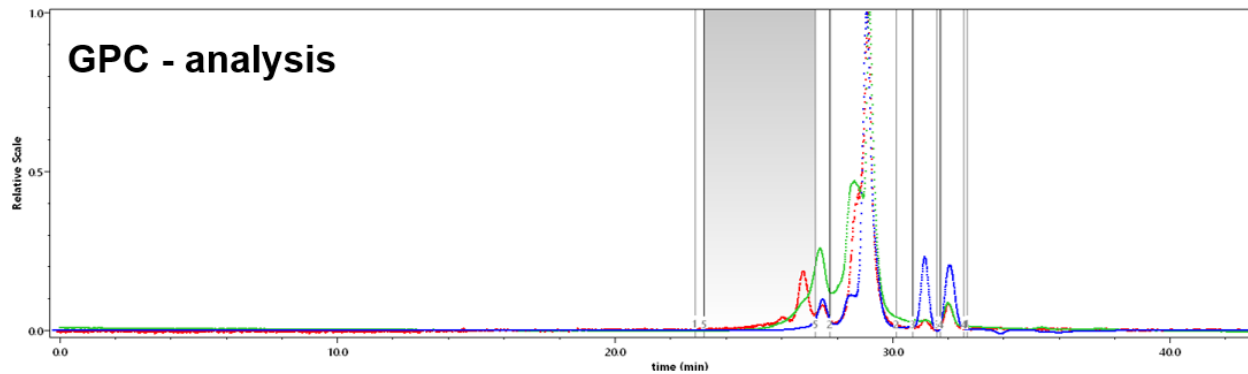
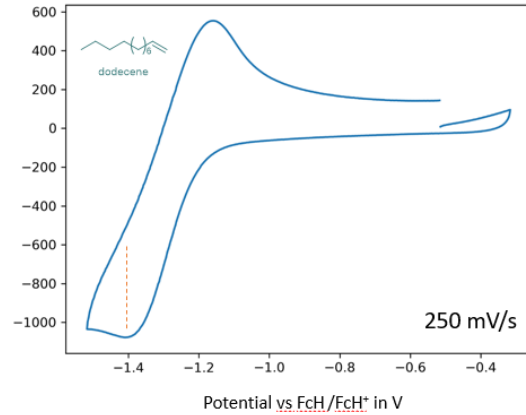
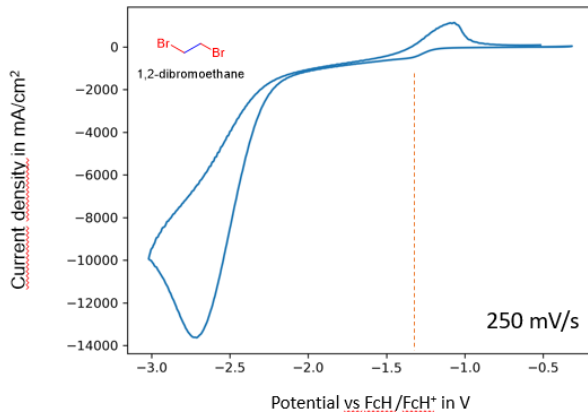
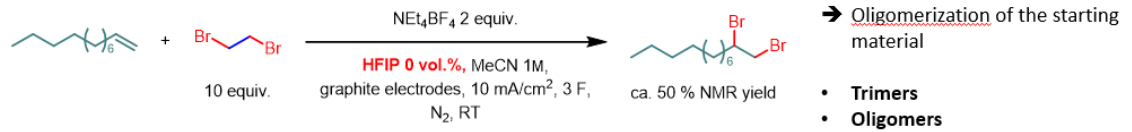
1.6 Cyclic voltammetry

Cyclic voltammetry (CV) was performed with a Metrohm 663 VA Stand equipped with a $\mu\text{Autolab}$ type III potentiostat (*Metrohm AG*, Herisau, Switzerland). Working electrode: for Br_2 – shuttle graphite electrode tip, 2 mm diameter; for Cl_2 – shuttle Pt electrode tip, 2 mm diameter; counter electrode: glassy carbon rod; reference electrode: Ag/AgCl in saturated LiCl/EtOH. Solvent: MeCN, scan rate (unless stated otherwise) $\nu = 100\text{ mV/s}$, $T = 20\text{ }^\circ\text{C}$, $c = 5\text{ mm}$, supporting electrolyte (if used): Et_4NBF_4 , $c(\text{Et}_4\text{NBF}_4) = 1\text{ M}$.

2 Mechanistic experiments



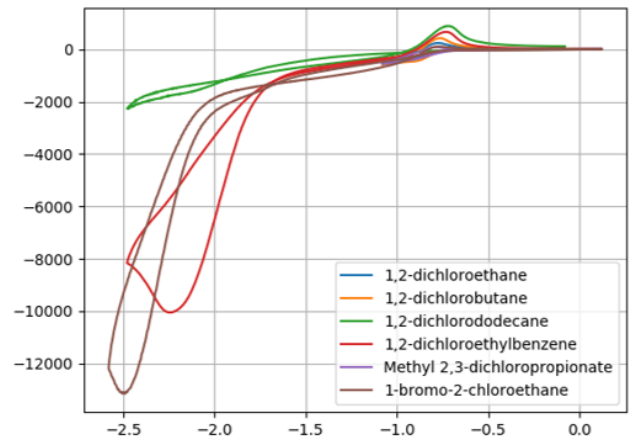
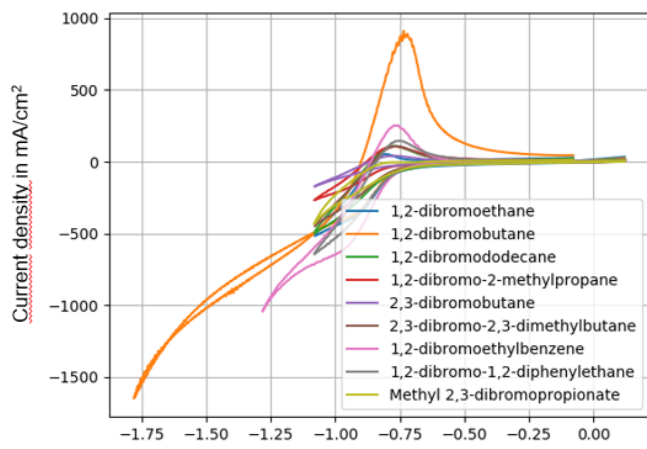
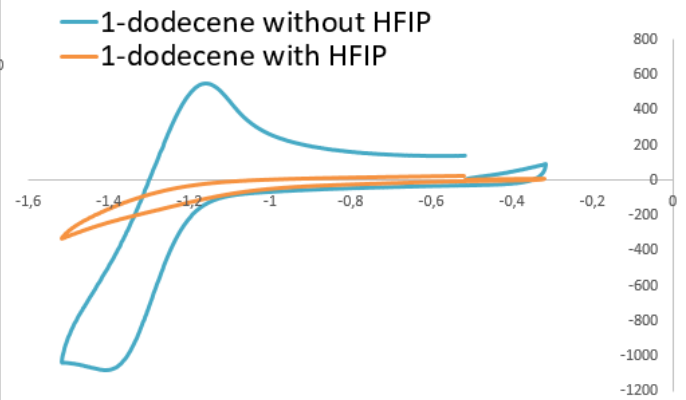
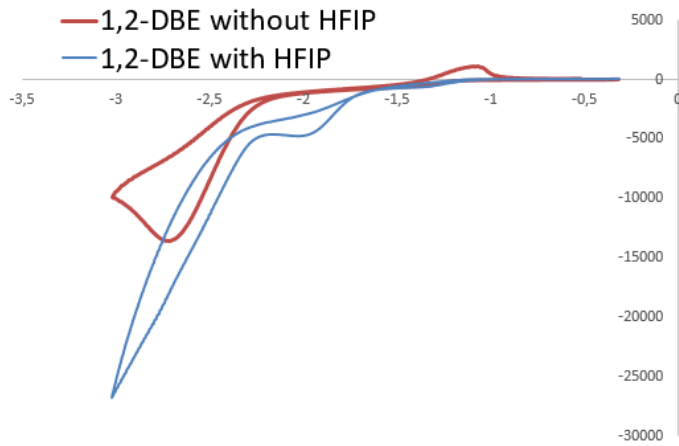
2.1 Cyclic voltammetry



Peak Results

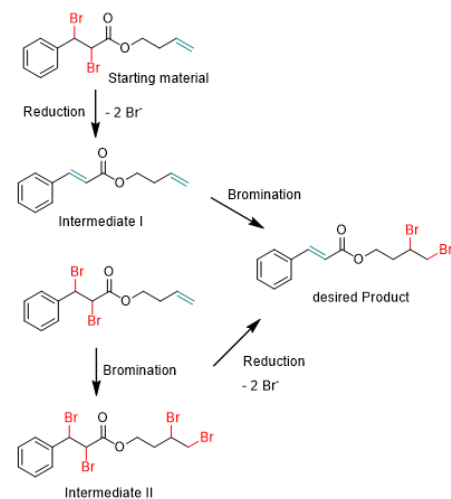
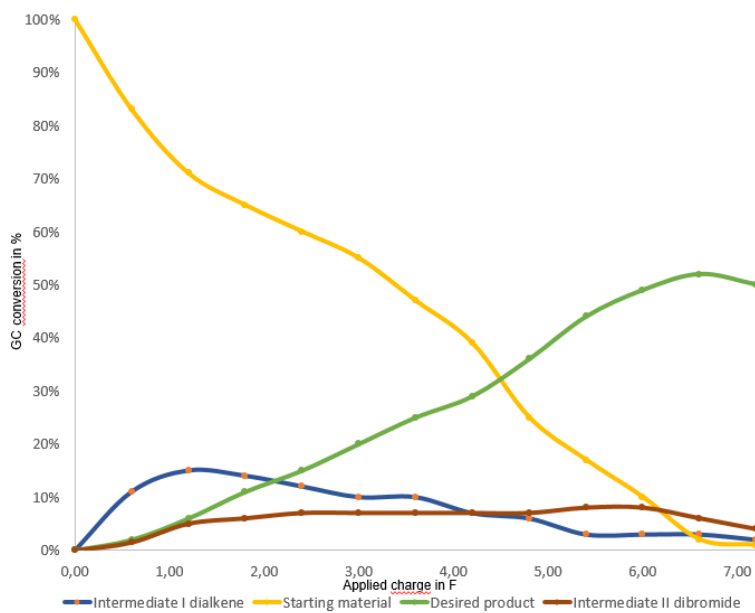
	Peak 1	Peak 2	Peak 3	Peak 4	Peak 5
Masses					
Injected Mass (µg)	365.00	365.00	365.00	365.00	365.00
Calculated Mass (µg)	1243.87	861.27	137.70	150.53	19.46
Mass Recovery (%)	340.8	236.0	37.7	41.2	5.3
Mass Fraction (%)	100.0	69.2	11.1	12.1	1.6
Molar mass moments (g/mol)					
Mn	2.287×10^3 ($\pm 11.095\%$)	4.761×10^3 ($\pm 2.919\%$)	5.636×10^3 ($\pm 10.323\%$)	1.536×10^3 ($\pm 9.215\%$)	2.478×10^3 ($\pm 3.790\%$)
Mp	4.186×10^3 ($\pm 2.453\%$)	4.186×10^3 ($\pm 2.453\%$)	4.685×10^3 ($\pm 10.250\%$)	1.590×10^3 ($\pm 7.959\%$)	7.536×10^3 ($\pm 4.237\%$)
Mv	n/a	n/a	n/a	n/a	n/a
Mw	5.074×10^3 ($\pm 4.139\%$)	5.339×10^3 ($\pm 2.622\%$)	6.768×10^3 ($\pm 20.882\%$)	1.623×10^3 ($\pm 10.204\%$)	5.442×10^3 ($\pm 6.624\%$)
Mz	2.029×10^3 ($\pm 20.800\%$)	6.645×10^3 ($\pm 5.164\%$)	9.981×10^3 ($\pm 53.896\%$)	1.746×10^3 ($\pm 25.161\%$)	8.588×10^3 ($\pm 22.291\%$)
Mz+1	1.114×10^4 ($\pm 14.631\%$)	8.932×10^3 ($\pm 5.143\%$)	2.042×10^4 ($\pm 51.770\%$)	1.938×10^4 ($\pm 42.484\%$)	1.126×10^4 ($\pm 42.914\%$)
M(avg)	3.717×10^3 ($\pm 0.155\%$)	5.685×10^3 ($\pm 0.149\%$)	5.964×10^3 ($\pm 1.947\%$)	1.479×10^3 ($\pm 0.906\%$)	3.261×10^3 ($\pm 0.191\%$)

- Oligomerization of the starting material
- Dodecene left
 - Trimers
 - Oligomers

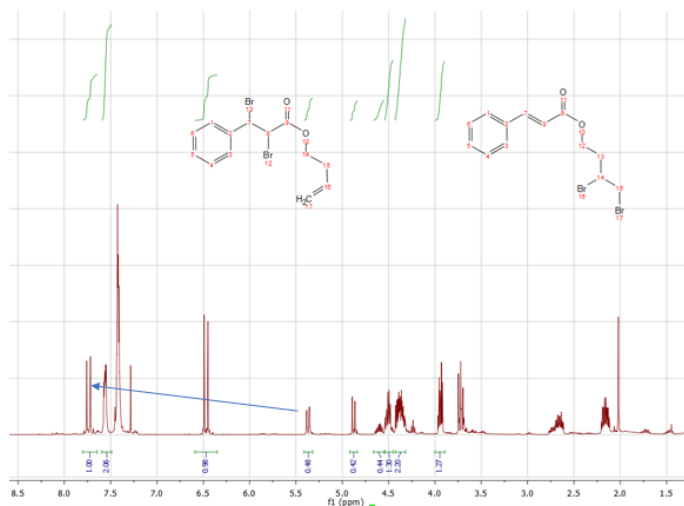
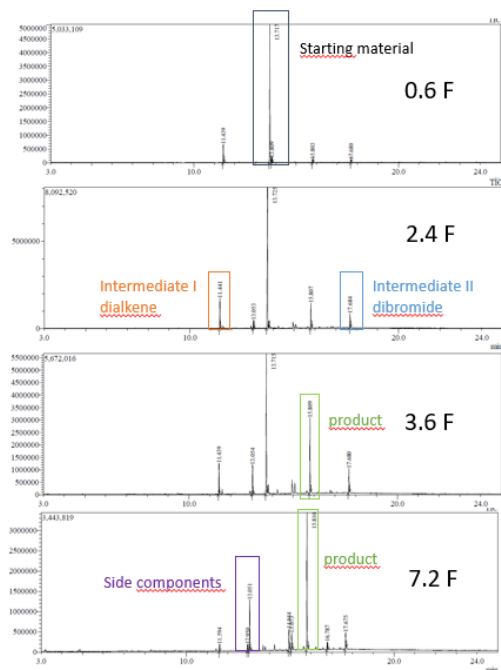


Potential vs Ag/AgCl in V

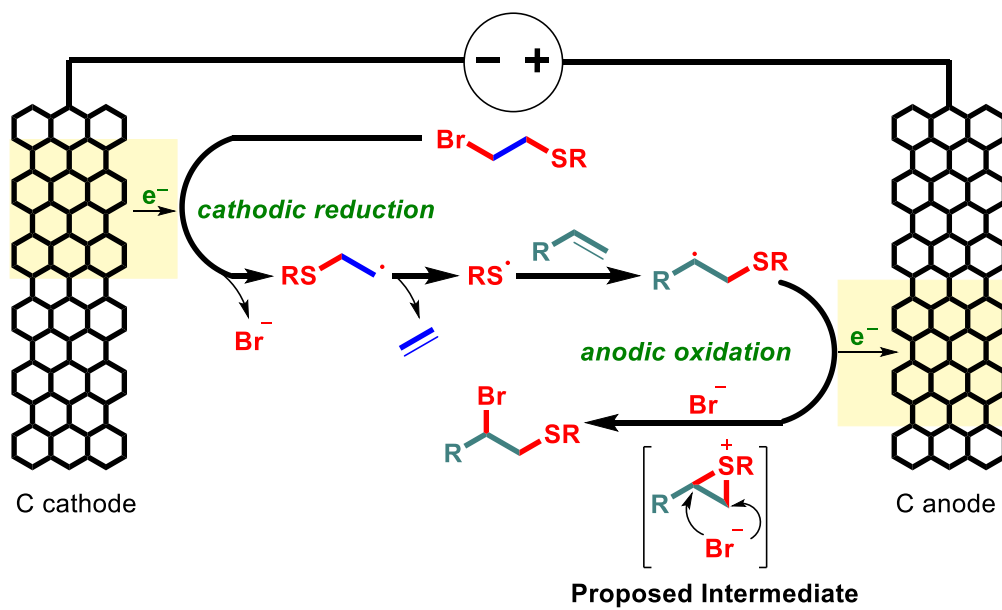
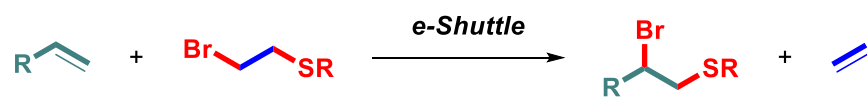
Potential vs Ag/AgCl in V



12

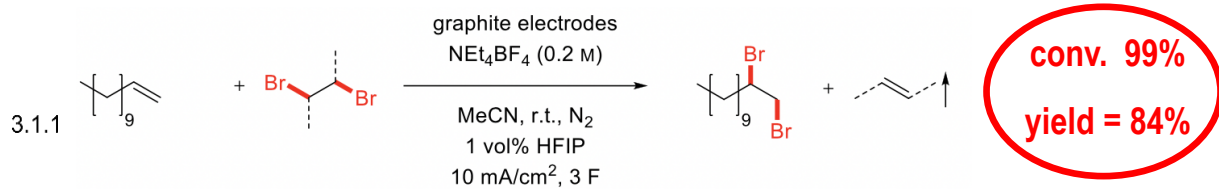


25



3 Optimization

Optimization of Br₂ – shuttle conditions

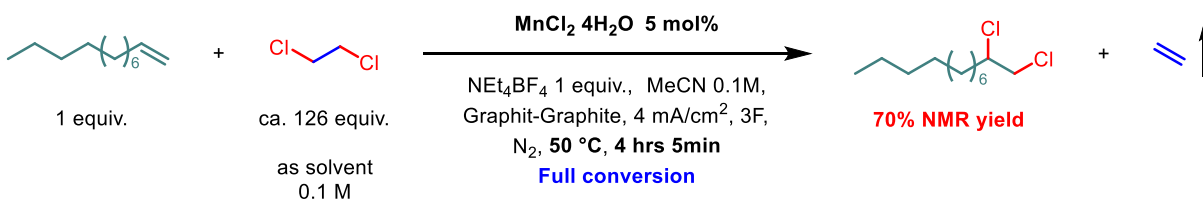
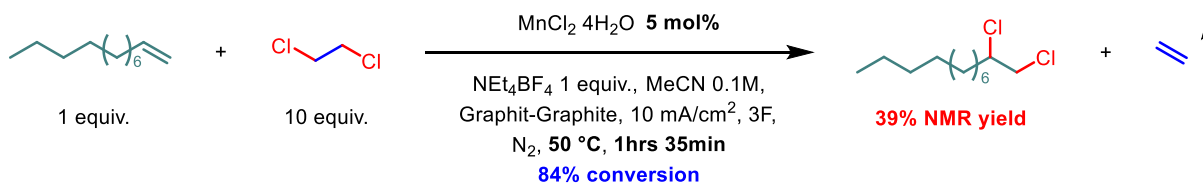


<u>anode</u>	<u>cathode</u>	<u><i>i</i> (mA/cm²)</u>	<u>donor screening (20eq.)</u>
BDD (traces)	Platinum (23%)	1.6 (25%) 8.3 (48%)	1,2-dibromoethane (50%) → 5 eq. (50%)
Glassy carbon (traces)	Graphite (50%)	3.3 (31%) 10 (50%)	1,2-dibromopropane (20%)
Graphite (50%)	Zinc (ND)	5.3 (49%) 15 (46%)	2,3-dibromobutane (6%)
	Magnesium (ND)		1,2-dibromoethylbenzene 1.eq (42%)
<u>atmosphere</u>	<u>solvent</u>	<u>additive (5 vol%)</u>	<u>supp. electrolyte (0.2 M)</u>
air (74%)	CH ₃ CN (49%)	- (49%)	-
nitrogen (84%)	1,2-dibromoethane (22%)	HFIP (82%) → 1 vol% (84%)	NBu ₄ BF ₄ (40%)
argon (84%)	MeOH (traces)	MeOH (76%)	NEt ₄ BF ₄ (50%)
	HFIP (ND)	water (messy)	
<u>applied charge (F)</u>	<u>temperature</u>	<u>additional exp.:</u>	
(conversion in %)	r.t. (50%)	Slow addition (23%)	
2.0 (63%) 2.6 (87%)	40 °C (50%)	Excell (4%)	
2.2 (75%) 2.8 (95%)	60 °C (36%)		
2.4 (80%) 3.0 (>99%)			



Optimization of Cl₂ – shuttle conditions

3.1.2



Cathode Electrodes, instead of graphite

(+)C–C(-): IKA	full conversion, 70% NMR yield
(+)C–C(-): STEINEMANN	93% conversion, 63% NMR yield
(+)C–Pt(-):	88% conversion, 55% NMR yield
(+)C–Zn(-):	89% conversion, 63% NMR yield
(+)C–Mg(-):	92% conversion, 65% NMR yield
(+)C–Ni(-): (foam)	86% GC conv, 50% NMR yield
(+)C–C(-): Glassy Carbon	67% conversion, 0% NMR yield

Cathode Electrodes, instead of graphite

(+)C–Ag(-):	87% conversion, 43% NMR yield
(+)C–Stainless(-): steel	full conversion, 74% NMR yield
(+)C–Co(-):	full conversion, 64% NMR yield
(+)C–Lead Cu(-):	81% conversion, 54% NMR yield
(+)C–Cu(-): (foam)	94% GC conv, 70% NMR yield
(+)C–Niobium(-):	Full % conversion, 70% NMR yield
(+)C–Ni(-):	Full % conversion, 69% NMR yield

Standard conditions

$j = 10 \text{ mA/cm}^2$:	81% conversion, 20% NMR yield
$j = 8 \text{ mA/cm}^2$:	XX conversion, XX% NMR yield
$j = 6 \text{ mA/cm}^2$:	XX conversion, XX% NMR yield
$j = 4 \text{ mA/cm}^2$:	full conversion, 70% NMR yield
$j = 2 \text{ mA/cm}^2$:	81% conversion, 40% NMR yield

Electrolyte (2 eq.), instead of Et₄NBF₄

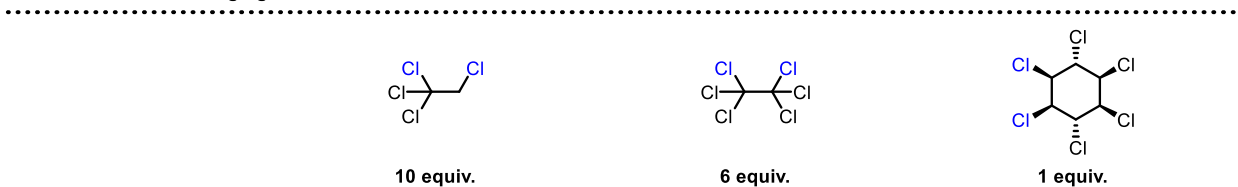
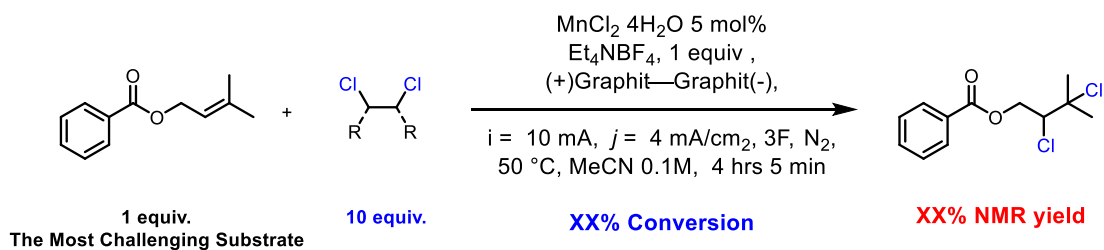
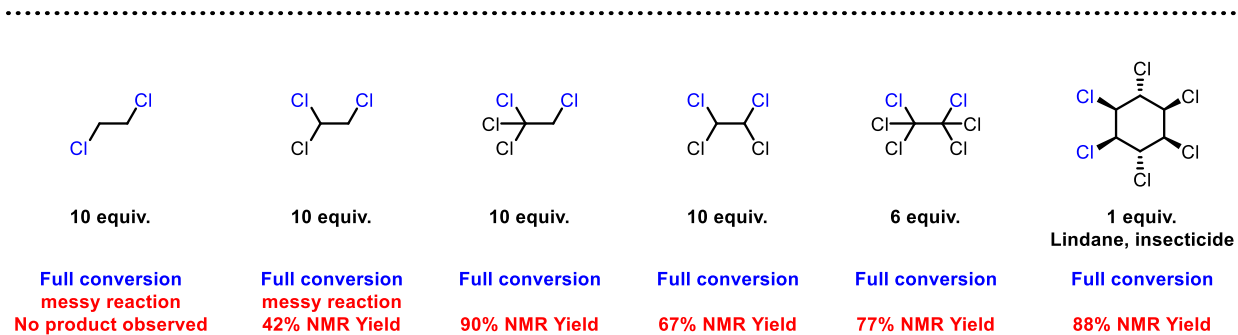
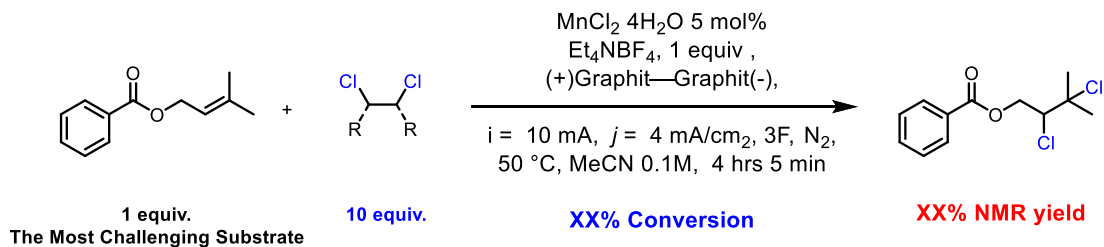
Me ₄ NBF ₄ 2 eq:	low conductivity
LiBF ₄ 2 eq:	low conductivity
LiClO ₄ 2 eq:	low conductivity
TBAI 100 mol%: Et ₄ NBF ₄ 0 eq	31% conversion, trace product
TBAI 50 mol%: Et ₄ NBF ₄ 1 eq	29% conversion, trace product
TBAI 100 mol%: Et ₄ NBF ₄ 1 eq	23% conversion, trace product

Additives,

HFIP 1 vol% :	XX% conversion, XX% NMR yield
HFIP 10 vol% :	57% conversion, 24% NMR yield
HCOOH 10 vol%:	78% conversion, 0% NMR yield
AcOH 10 vol%:	64% conversion, 0% NMR yield

Catalysts,

MnCl ₂ 4H ₂ O :	Full conversion, 70% NMR yield
Mn(OAc) ₂ 4H ₂ O :	79% conversion, 42% NMR yield
CoCl ₂ :	83% conversion, 0% NMR yield
NiCl ₂ :	70% conversion, Messy reaction, ca. 30% NMR yield



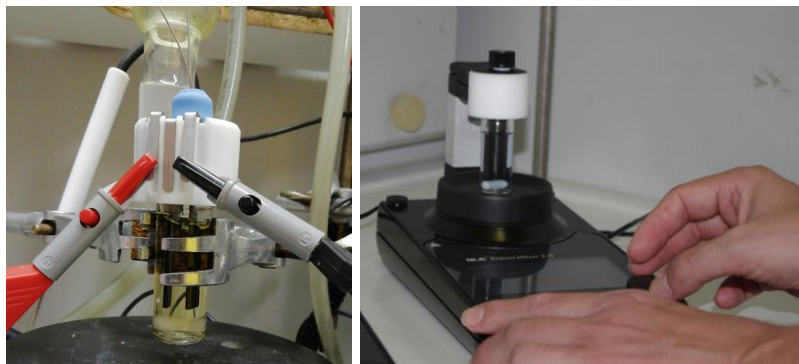
Standard Condition:	Full conversion, 90% NMR Yield	Full conversion, 77% NMR Yield	Full conversion, 88% NMR Yield
----------------------------	--	--	--

Without $\text{MnCl}_2 \cdot 4\text{H}_2\text{O}$:	Full conversion, Messy reaction < 4% NMR Yield	Full conversion, Messy reaction 7% NMR Yield	Full conversion, Messy reaction 11% NMR Yield
--	---	---	--

Without electricity:	< 5% NMR Conversion Product not observed	< 5% NMR Conversion Product not observed	12% NMR Conversion Product not observed
-----------------------------	---	---	---

4 Electrolysis setup

Electrasyn cell-setup (5 and 10 mL)



<https://www.ika.com/electrasyn/Echem-Platform.html>

Beaker-type cell (200 mL)

The beaker-type cell (200 mL) consists of a simple glass beaker and a glass adapter, closed by a PTFE plug. This cap allows precise arrangement of the electrodes. Total dimension of the electrodes are 14 cm x 3.5 cm x 0.3 cm.

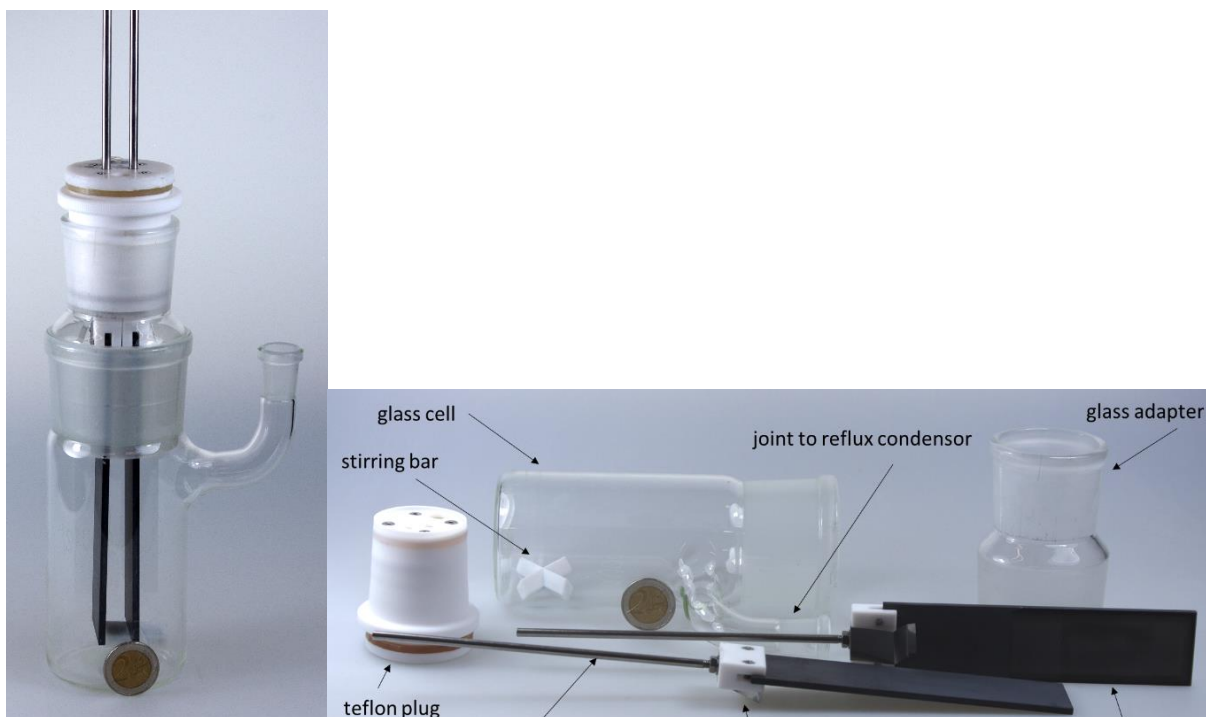


Figure X: 200 mL beaker-type cell; left: assembled; right: individual parts. For size comparison one 2 € coin (diameter 25.75 mm \approx 1.01 inches) is placed in front of the glass cell.

Beaker-type cell (1.5 L). The undivided 1.5 L vessel is equipped with a heating jacket, bottom outlet and thermometer. A bipolar stacked electrode setup of 8 isostatic graphite electrodes ($d = 5 \text{ mm}$) with a total surface area of 374 cm^2 anodic and cathodic sites was used. For power supply, a TDK Lambda Genesys™ GEN 30-50 was used providing a maximum of 1500 W at 30 V/50A.

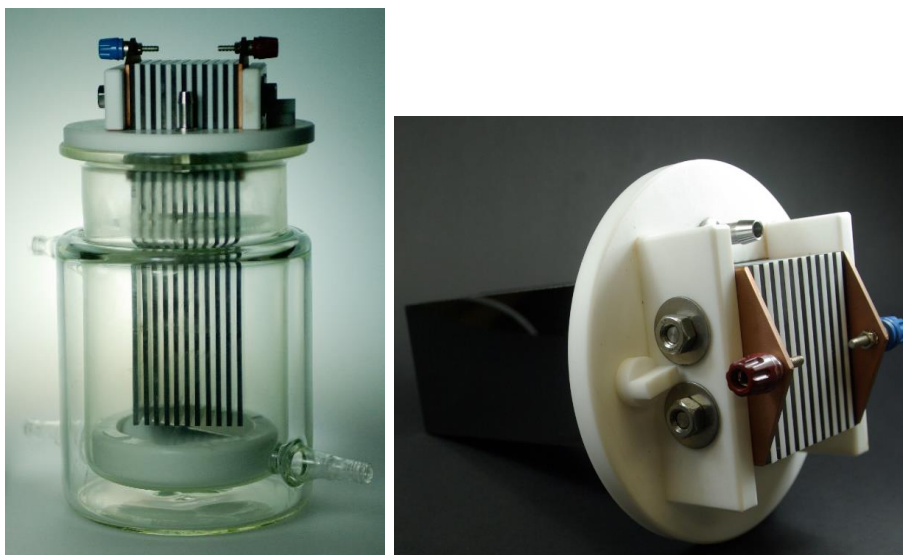


Figure X: Double-jacketed 1500 mL beaker-type cell; left: assembled; right: Electrode arrangement.

5 General procedures

GP1: Electrolytic shuttle dibromination of alkenes

Et₄NBF₄ (434 mg, 2.0 mmol, 2 equiv.) was added to an oven-dried undivided *ElectraSyn*® vial (10 mL) equipped with a Teflon-coated magnetic stir bar. Two graphite electrodes (0.8 x 0.2 x 3.25 cm, SIGRAFINE®V2100, SGL Carbon, Bonn-Bad Godesberg, Germany) were adapted to the *ElectraSyn*® vial cap. The vial was capped and connected to the Schlenk line via a canula and purged with a gentle flow of N₂ (the gentle flow was maintained during the whole electrolysis). The respective alkenes (1 mmol, 1 equiv.), 1,2-dibromoethane (939 mg, 433 μL, 2.5 mmol, 5 equiv.), HFIP (100 μL, 1 vol%) and dry MeCN (ca. 9.5 mL) were added to the reaction mixture to reach 10 mL (0.1 M). Pre-stir the reaction mixture until a clear solution was obtained. The reaction mixture was subjected to a constant current electrolysis with a current density of 10.0 mA/cm² at room temperature. The progress of the reaction was monitored by GC or TLC and the electricity was turned off until completion of the reaction (typically after 2.5 – 10 F per mole). Then, the volatile solvent was removed *in vacuo*. The residue was purified by column chromatography using silica gel and cyclohexane/ethyl acetate as eluent to afford the desired product.

5.1.2

GP2: Electrolytic shuttle dichlorination of alkenes

MnCl₂·4H₂O (5.0 mg, 25 μmol, 0.05 equiv.) and Et₄NBF₄ (109 mg, 0.5 mmol, 1 equiv.) was added to an oven-dried undivided *ElectraSyn*® vial (5 mL) equipped with a Teflon-coated magnetic stir bar. Two graphite electrodes (0.8 x 0.2 x 3.25 cm, SIGRAFINE®V2100, SGL Carbon, Bonn-Bad Godesberg, Germany) were adapted to the *ElectraSyn*® vial cap. The vial was capped and connected to the Schlenk line via a canula, which was then evacuated and backfilled with N₂ for five times. The respective alkenes (0.5 mmol, 1 equiv.), 1,1,1,2-tetrachloroethane (840 mg, 546 μL, 5 mmol, 10 equiv.) and dry MeCN (ca. 4.5 mL) was added to the reaction mixture to reach 5 mL (0.1 M). The reaction mixture was stirred until a clear solution was obtained. The reaction mixture was subjected to a constant current electrolysis with a current density of 2.0 mA/cm² at 50 °C. The progress of the reaction was monitored by GC or TLC and the electricity was turned off until completion of the reaction (typically after 2.5 – 5 F per mole). Then, the volatile solvent was removed *in vacuo*. The residue was purified by column chromatography using silica gel and n-pentane/diethyl ether or cyclohexane/ethyl acetate as eluent to afford the desired product.

GP3: Electrolytic shuttle bromothiolation of alkenes

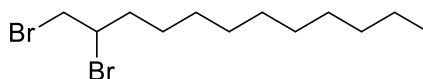
5.1.3 Et₄NBF₄ (434 mg, 2.0 mmol, 2 equiv.) was added to an oven-dried undivided *ElectraSyn*® vial (5 mL) equipped with a Teflon-coated magnetic stir bar. Two graphite electrodes (0.8 x 0.2 x 3.25 cm, SIGRAFINE®V2100, SGL Carbon, Bonn-Bad Godesberg, Germany) were adapted to the *ElectraSyn*® cap. The vial was capped and connected to the Schlenk line via a canula and purged with a gentle flow of N₂ (the gentle flow was maintained during the whole electrolysis). The respective alkenes (0.5 mmol, 1 equiv.), and (2-bromoethyl)(phenyl)sulfane (543 mg, 2.5 mmol, 5 equiv.) and dry MeCN (ca. 4.5 mL) were added to the reaction mixture to reach 5 mL (0.1 M). Pre-stir the reaction mixture until a clear solution was obtained. The reaction mixture was subjected to a constant current electrolysis with a current density of 10.0 mA/cm² at room temperature. The progress of the reaction was monitored by GC or TLC and the electricity was turned off until completion of the reaction (typically after 2.5 – 10 F per mole). Then, the volatile solvent was removed *in vacuo*. The residue was purified by reversed phase column chromatography using MeCN/water (Millipore + 0.1% formic acid) acetate as eluent to afford the desired product.

5.1.4 GP4: Electrolytic shuttle chlorothiolation of alkenes

To an oven-dried undivided *ElectraSyn*® vial (5 mL) equipped with a Teflon-coated magnetic stir bar, MnCl₂·4H₂O (5.0 mg, 25 μmol, 0.05 equiv.) and Et₄NBF₄ (109 mg, 0.5 mmol, 1 equiv.) was added. Two graphite electrodes (0.8 x 0.2 x 3.25 cm, SIGRAFINE®V2100, SGL Carbon, Bonn-Bad Godesberg, Germany) were adapted to the *ElectraSyn*® vial cap. The vial was capped and connected to the Schlenk line via a canula, which was then evacuated and backfilled with N₂ for five times. The respective alkenes (0.5 mmol, 1 equiv.), (2-chloroethyl)(phenyl)sulfane (864 mg, 738 μL, 5 mmol, 10 equiv.) and dry MeCN (ca. 4.2 mL) was added to top-up the reaction mixture to reach 5 mL (0.1 M). The reaction mixture was stirred until a clear solution was obtained. The reaction mixture was subjected to a constant current electrolysis with a current density of 2.0 mA/cm² at 50 °C. The progress of the reaction was monitored by GC or TLC and the electricity was turned off until completion of the reaction (typically after 2.5 – 5 F per mole). Then, the volatile solvent was removed *in vacuo*. The residue was purified by reversed phase column chromatography using MeCN/water (Millipore + 0.1% formic acid) acetate as eluent to afford the desired product.

6 Characterization

1,2-dibromododecane (XX)



Chemical Formula: C₁₂H₂₄Br₂

According to the **GP1** for the electrochemical Br₂ shuttle of alkenes, a mixture of dodec-1-ene (168 mg, 1 mmol, 1.0 equiv.), 1,2-dibromoethane (939 mg, 433 μ L, 5.0 mmol, 5 equiv.), HFIP (100 μ L, 1 vol%), and Et₄NBF₄ (434 mg, 2.0 mmol, 2 equiv.) in dry MeCN (0.1 M) was electrolyzed at room temperature with a current density of 10.0 mA/cm² using graphite electrodes in an undivided *ElectraSyn*[®] vial (10 mL). After 3.0 F was applied, the volatile solvent was removed *in vacuo*. The residue was purified by column chromatography (gradient: cyclohexane : ethyl acetate = from 100:0) yielding the product as a **colorless oil** (yield: 84%, 276 mg, 0.84 mmol).

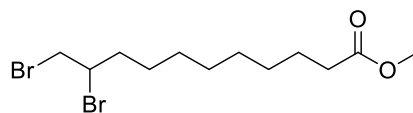
Scale-up **25x in 250 mL cell**: yield: 80%, 6.57 g, 20 mmol

¹H NMR (400 MHz, Chloroform-*d*) δ 4.24 – 4.12 (m, 1H), 3.86 (dd, *J* = 10.2, 4.4 Hz, 1H), 3.64 (t, *J* = 10.2 Hz, 1H), 2.15 (dddd, *J* = 14.6, 10.2, 5.6, 3.3 Hz, 1H), 1.80 (dtd, *J* = 14.4, 9.7, 4.6 Hz, 1H), 1.65 – 1.51 (m, 1H), 1.31 (m, 18H), 0.91 (t, *J* = 6.7 Hz, 3H).

¹³C NMR (101 MHz, Chloroform-*d*) δ 53.2, 36.4, 36.0, 31.9, 29.6, 29.5, 29.4, 29.3, 28.8, 26.7, 22.7, 14.1.

[Long, Jin](#); [Chen, Jia](#); [Li, Rong](#); [Liu, Zhuo](#); [Xiao, Xuan](#); [Lin, Jin-Hong](#); [Zheng, Xing](#); [Xiao, Ji-Chang](#)[*Synlett*, **2019**, vol. 30, # 2, p. 181 - 184]

Methyl 10,11-dibromoundecanoate (XX)



Chemical Formula: C₁₂H₂₂Br₂O₂

Molecular Weight: 358,1140

According to the **GP1** for the electrochemical Br₂ shuttle of alkenes, a mixture of Methyl 10-undecenoate (198 mg, 1 mmol, 1.0 equiv.), 1,2-dibromoethane (939 mg, 433 μL, 5.0 mmol, 5 equiv.), HFIP (100 μL, 1 vol%), and Et₄NBF₄ (434 mg, 2.0 mmol, 2 equiv.) in dry MeCN (0.1 M) was electrolyzed at room temperature with a current density of 10.0 mA/cm² using graphite electrodes in an undivided *ElectraSyn*® vial (10 mL). After 3.0 F was applied, the volatile solvent was removed *in vacuo*. The residue was purified by column chromatography (gradient: cyclohexane : ethyl acetate = from 100:0) yielding the product as a **colorless oil** (yield: 62%, 222 mg, 0.62 mmol).

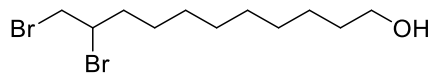
¹H NMR (400 MHz, Chloroform-*d*) δ 4.15 (tdd, *J* = 9.5, 4.4, 3.3 Hz, 1H), 3.84 (dd, *J* = 10.2, 4.4 Hz, 1H), 3.66 (s, 3H), 3.62 (t, *J* = 10.2 Hz, 1H), 2.29 (t, *J* = 7.5 Hz, 2H), 2.12 (dddd, *J* = 14.7, 10.2, 5.6, 3.3 Hz, 1H), 1.83 – 1.71 (m, 1H), 1.65 – 1.57 (m, 2H), 1.30 (m, 9H).

¹³C NMR (101 MHz, Chloroform-*d*) δ 174.4, 53.2, 51.60, 36.4, 36.1, 34.2, 29.3, 29.2, 29.2, 28.8, 26.79, 25.0.

HRMS for C₁₂H₂₂Br₂O₂ (ESI+) [M]⁺: calc.: 357.0059, found: 357.0065.

[Kabalka](#); [Yang](#); [Reddy](#); [Narayana](#)[*Synthetic Communications*, 1998, vol. 28, # 5, p. 925 - 929]

10,11-dibromoundecan-1-ol (XX)



Chemical Formula: C₁₁H₂₂Br₂O

Exact Mass: 328,0037

According to the **GP1** for the electrochemical Br₂ shuttle of alkenes, a mixture of Methyl 10-undecen-1-ol (170 mg, 1 mmol, 1.0 equiv.), 1,2-dibromoethane (939 mg, 433 μ L, 5.0 mmol, 5 equiv.), HFIP (100 μ L, 1 vol%), and Et₄NBF₄ (434 mg, 2.0 mmol, 2 equiv.) in dry MeCN (0.1 M) was electrolyzed at room temperature with a current density of 10.0 mA/cm² using graphite electrodes in an undivided *ElectraSyn*[®] vial (10 mL). After 3.0 F was applied, the volatile solvent was removed *in vacuo*. The residue was purified by column chromatography (gradient: cyclohexane : ethyl acetate = from 100:0) yielding the product as a **colorless oil** (yield: 37%, 122 mg, 0.37 mmol).

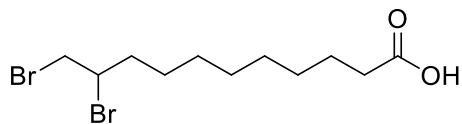
¹H NMR (400 MHz, Chloroform-*d*) δ 4.23 – 4.15 (m, 1H), 3.87 (dd, *J* = 10.2, 4.4 Hz, 1H), 3.72 – 3.58 (m, 1H), 2.16 (dddd, *J* = 14.6, 10.2, 5.6, 3.2 Hz, 1H), 1.86 – 1.73 (m, 1H), 1.59 (dq, *J* = 9.6, 6.6 Hz, 4H), 1.51 – 1.42 (m, 2H), 1.40 – 1.31 (m, 10H).

¹³C NMR (101 MHz, Chloroform-*d*) δ 63.2, 53.3, 36.5, 36.1, 32.9, 29.5, 29.4, 28.9, 26.9, 25.8.

HRMS for C₁₁H₁₄Br₂ (ESI+) [M]⁺: calc.: 328.0037, found: 328.0038.

[Camps, F.](#); [Chamorro, E.](#); [Gasol, V.](#); [Guerrero, A.](#) [*Journal of Organic Chemistry*, **1989**, vol. 54, # 18, p. 4294 - 4298]

10,11-dibromoundecanoic acid (XX)



Chemical Formula: C₁₁H₂₀Br₂O₂

Molecular Weight: 344,0870

According to the **GP1** for the electrochemical Br₂ shuttle of alkenes, a mixture of 10-undecenoic acid (184 mg, 1 mmol, 1.0 equiv.), 1,2-dibromoethane (939 mg, 433 μ L, 5.0 mmol, 5 equiv.), HFIP (100 μ L, 1 vol%), and Et₄NBF₄ (434 mg, 2.0 mmol, 2 equiv.) in dry MeCN (0.1 M) was electrolyzed at room temperature with a current density of 10.0 mA/cm² using graphite electrodes in an undivided *ElectraSyn*® vial (10 mL). After 3.0 F was applied, the volatile solvent was removed *in vacuo*. The residue was purified by column chromatography (gradient: cyclohexane : ethyl acetate = from 100:0) yielding the product as a **colorless oil** (yield: 61%, 210 mg, 0.61 mmol).

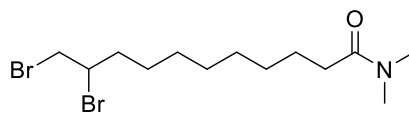
¹H NMR (400 MHz, Chloroform-*d*) δ 4.21 – 4.12 (m, 1H), 3.85 (dd, *J* = 10.2, 4.4 Hz, 1H), 3.63 (t, *J* = 10.0 Hz, 1H), 2.35 (t, *J* = 7.5 Hz, 2H), 2.13 (dddd, *J* = 14.6, 10.3, 5.6, 3.3 Hz, 1H), 1.85 – 1.71 (m, 1H), 1.70 – 1.50 (m, 2H), 1.43 – 1.25 (m, 10H).

¹³C NMR (101 MHz, Chloroform-*d*) δ 178.4, 52.3, 36.5, 36.1, 34.0, 29.3, 29.2, 29.1, 28.9, 26.8, 24.8.

HRMS for C₁₁H₁₉Br₂O₂ (ESI-) [M-H]⁻: calc.: 340.9457, found: 340.9450.

[Nishio, Yuya](#); [Yubata, Kotaro](#); [Wakai, Yutaro](#); [Notsu, Kotaro](#); [Yamamoto, Katsumi](#); [Fujiwara, Hideki](#); [Matsubara, Hiroshi](#) [*Tetrahedron*, **2019**, vol. 75, # 10, p. 1398 - 1405]

10,11-dibromo-N,N-dimethylundecanamide (XX)



Chemical Formula: C₁₃H₂₅Br₂NO

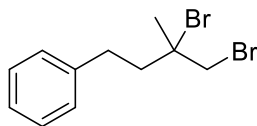
According to the **GP1** for the electrochemical Br₂ shuttle of alkenes, a mixture of N,N-dimethylundecane-10-ene amid (212 mg, 1 mmol, 1.0 equiv.), 1,2-dibromoethane (939 mg, 433 μ L, 5.0 mmol, 5 equiv.), HFIP (100 μ L, 1 vol%), and Et₄NBF₄ (434 mg, 2.0 mmol, 2 equiv.) in dry MeCN (0.1 M) was electrolyzed at room temperature with a current density of 10.0 mA/cm² using graphite electrodes in an undivided *ElectraSyn*[®] vial (10 mL). After 3.0 F was applied, the volatile solvent was removed *in vacuo*. The residue was purified by column chromatography (gradient: cyclohexane : ethyl acetate = from 100:0) yielding the product as a **colorless oil** (yield: 65%, 242 mg, 0.65 mmol).

¹H NMR (400 MHz, CDCl₃) δ 4.20 – 4.11 (m, 1H), 3.83 (dd, *J* = 10.2, 4.5 Hz, 1H), 3.62 (t, *J* = 10.2 Hz, 1H), 2.97 (s, 6H), 2.36 – 2.26 (m, 2H), 2.11 (dddd, *J* = 14.6, 10.2, 5.6, 3.3 Hz, 1H), 1.84 – 1.70 (m, 1H), 1.67 – 1.48 (m, 3H), 1.45 – 1.25 (m, 9H).

¹³C NMR (101 MHz, CDCl₃) δ 173.41, 53.16, 36.39, 36.01, 33.28, 29.43, 29.30, 29.22, 28.74, 26.72, 25.17.

HRMS for C₁₃H₂₅Br₂NO (ESI+) [M+H]⁺: calc.: 370.0376, found: 370.0382.

(3,4-dibromo-3-methylbutyl)benzene (XX)



Chemical Formula: C₁₁H₁₄Br₂
Exact Mass: 303.9462

According to the **GP1** for the electrochemical Br₂ shuttle of alkenes, a mixture of (3-methylbut-3-en-1-yl)benzene 146 mg, 1 mmol, 1.0 equiv.), 1,2-dibromoethane (939 mg, 433 μ L, 5.0 mmol, 5 equiv.), HFIP (100 μ L, 1 vol%), and Et₄NBF₄ (434 mg, 2.0 mmol, 2 equiv.) in dry MeCN (0.1 M) was electrolyzed at room temperature with a current density of 10.0 mA/cm² using graphite electrodes in an undivided *ElectraSyn*[®] vial (10 mL). After 5.0 F was applied, the volatile solvent was removed *in vacuo*. The residue was purified by column chromatography (*n*-pentane : diethyl ether = from 100:0) yielding the product as a **colorless solid** (yield: 60%, 184 mg, 0.60 mmol).

¹H NMR (400 MHz, Chloroform-*d*) δ 7.40 – 7.26 (m, 5H), 4.02 (d, *J* = 10.3 Hz, 1H), 3.93 (d, *J* = 10.2 Hz, 1H), 2.91 – 2.87 (m, 2H), 2.28 – 2.24 (m, 2H), 1.96 (s, 3H).

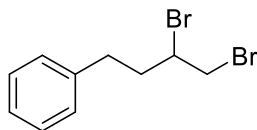
¹³C NMR (101 MHz, Chloroform-*d*) δ 141.0, 128.7, 128.6, 67.3, 44.4, 42.2, 32.3, 30.8.

HRMS for C₁₁H₁₄Br₂ (ESI+) [M]⁺: calc.: 303.9457, found: 303.9458.

The analytical data are in accordance with those reported.^[XX]

Ref: W. Chen, H.Tao, W. Huang, G. Wang, S. Li, X. Cheng, G. Li, *Chem. Eur. J.* **2016**, *22*, 9546–9550.

(3,4-dibromobutyl)benzene (XX)



Chemical Formula: C₁₀H₁₂Br₂
Exact Mass: 289.93

According to the **GP1** for the electrochemical Br₂ shuttle of alkenes, a mixture of but-3-en-1-ylbenzene (132 mg, 1 mmol, 1.0 equiv.), 1,2-dibromoethane (939 mg, 433 μ L, 5.0 mmol, 5 equiv.), HFIP (100 μ L, 1 vol%), and Et₄NBF₄ (434 mg, 2.0 mmol, 2 equiv.) in dry MeCN (0.1 M) was electrolyzed at room temperature with a current density of 10.0 mA/cm² using graphite electrodes in an undivided *ElectraSyn*[®] vial (10 mL). After 3.0 F was applied, the volatile solvent was removed *in vacuo*. The residue was purified by column chromatography (*n*-pentane : diethyl ether = from 100:0) yielding the product as a **colorless solid** (yield: 60%, 184 mg, 0.60 mmol).

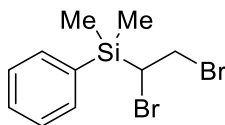
¹H NMR (400 MHz, Chloroform-*d*) δ 7.41 – 7.36 (m, 2H), 7.31 – 7.27 (m, 3H), 4.21 – 4.15 (m, 1H), 3.93 – 3.90 (m, 1H), 3.74 – 3.68 (m, 1H), 3.05 – 2.98 (m, 1H), 2.86 – 2.79 (m, 1H), 2.59 – 2.50 (m, 1H), 2.21 – 2.11 (m, 1H).

¹³C NMR (101 MHz, Chloroform-*d*) δ 140.3, 128.7, 128.6, 126.4, 52.2, 37.8, 36.3, 33.1.

HRMS for C₁₀H₁₂Br₂ (ESI+) [M]⁺: calc.: 289.9300, found: 289.9298.

[Xia, Xuanshu; Toy, Patrick H.](#)[*Beilstein Journal of Organic Chemistry*, 2014, vol. 10, p. 1397 - 1405]

(1,2-dibromoethyl)dimethyl(phenyl)silane (XX)



Chemical Formula: C₁₀H₁₄Br₂Si

Exact Mass: 319.92

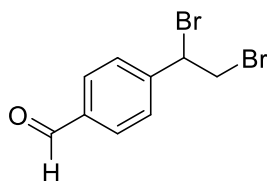
According to the **GP1** for the electrochemical Br₂ shuttle of alkenes, a mixture of dimethyl(phenyl)(vinyl)silane (162 mg, 1 mmol, 1.0 equiv.), 1,2-dibromoethane (939 mg, 433 μ L, 5.0 mmol, 5 equiv.), HFIP (100 μ L, 1 vol%), and Et₄NBF₄ (434 mg, 2.0 mmol, 2 equiv.) in dry MeCN (0.1 M) was electrolyzed at room temperature with a current density of 10.0 mA/cm² using graphite electrodes in an undivided *ElectraSyn*[®] vial (10 mL). After 4.0 F was applied, the volatile solvent was removed *in vacuo*. The residue was purified by column chromatography (*n*-pentane : diethyl ether = from 100:0) yielding the product as a **colorless solid** (yield: 48 %, 154 mg, 0.48 mmol).

¹H NMR (400 MHz, Chloroform-*d*) δ 7.60 – 7.58 (m, 2H), 7.49 – 7.40 (m, 3H), 3.94 – 3.86 (m, 1H), 3.68 – 3.61 (m, 2H), 0.56 – 0.54 (m, 6H).

¹³C NMR (101 MHz, Chloroform-*d*) δ 134.46, 134.14, 130.23, 128.27, 42.56, 36.97, -3.24, -4.65.

HRMS for C₁₀H₁₄BrSi (ESI+) [M-Br]⁺: calc.: 241.0043, found: 241.0042.

4-(1,2-dibromoethyl)benzaldehyde (XX)



Chemical Formula: C₉H₈Br₂O

Exact Mass: 289.89

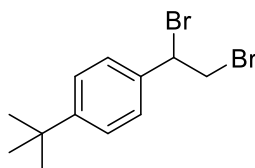
According to the **GP1** for the electrochemical Br₂ shuttle of alkenes, a mixture of 4-vinylbenzaldehyde (134 mg, 1 mmol, 1.0 equiv.), 1,2-dibromoethane (939 mg, 433 μ L, 5.0 mmol, 5 equiv.), HFIP (100 μ L, 1 vol%), and Et₄NBF₄ (434 mg, 2.0 mmol, 2 equiv.) in dry MeCN (0.1 M) was electrolyzed at room temperature with a current density of 10.0 mA/cm² using graphite electrodes in an undivided *ElectraSyn*[®] vial (10 mL). After 5.0 F was applied, the volatile solvent was removed *in vacuo*. The residue was purified by column chromatography (*n*-pentane : diethyl ether = from 100:0) yielding the product as a **colorless oil** (yield: 18 %, 52.2 mg, 0.18 mmol).

¹H NMR (400 MHz, Chloroform-*d*) δ 10.03 (s, 1H), 7.92 – 7.89 (m, 2H), 7.59 – 7.57 (m, 2H), 5.16 (dd, *J* = 11.1, 5.1 Hz, 1H), 4.11 – 3.99 (m, 2H).

¹³C NMR (101 MHz, Chloroform-*d*) δ 191.5, 145.0, 136.8, 130.3, 128.6, 49.1, 34.3.

HRMS for C₉H₈Br₂NaO (ESI+) [M+Na]⁺: calc.: 312.8834, found: 312.8833.

4-tert-butyl-1,2-dibromoethylbenzene (XX)



Exact Mass: 317,9619
Molecular Weight: 320,0680

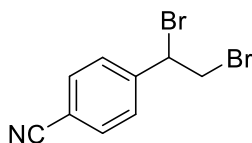
According to the **GP1** for the electrochemical Br₂ shuttle of alkenes, a mixture of 4-tert-butylstyrene (160 mg, 1 mmol, 1.0 equiv.), 1,2-dibromoethane (939 mg, 433 μ L, 5.0 mmol, 5 equiv.), HFIP (100 μ L, 1 vol%), and Et₄NBF₄ (434 mg, 2.0 mmol, 2 equiv.) in dry MeCN (0.1 M) was electrolyzed at room temperature with a current density of 10.0 mA/cm² using graphite electrodes in an undivided *ElectraSyn*[®] vial (10 mL). After 3.0 F was applied, the volatile solvent was removed *in vacuo*. The residue was purified by column chromatography (*n*-pentane : diethyl ether = from 100:0) yielding the product as a **colorless oil** (yield: 42%, 134 mg, 0.42 mmol).

¹HNMR 400 MHz, Chloroform-*d*) δ =7.40-7.31(m,4H),5.15 (dd, J1= 10.2 Hz, J2= 5.8 Hz, 1H), 4.09-4.00 (m, 1H), 1.32 (s, 9H).

¹³C NMR (100 MHz, Chloroform-*d*) δ = 152.5, 135.8, 127.5, 126.1, 51.5, 35.4, 35.0, 31.5.

HRMS for C₁₂H₁₆⁷⁹Br (APCI+) [M-Br]⁺: calc.: 239.0430, found: 239.0434.

4-(1,2-dibromoethyl)benzonitrile (XX)



Chemical Formula: C₉H₇Br₂N

Exact Mass: 286.89

According to the **GP1** for the electrochemical Br₂ shuttle of alkenes, a mixture of 4-vinylbenzonitrile (130 mg, 1 mmol, 1.0 equiv.), 1,2-dibromoethane (939 mg, 433 μ L, 5.0 mmol, 5 equiv.), HFIP (100 μ L, 1 vol%), and Et₄NBF₄ (434 mg, 2.0 mmol, 2 equiv.) in dry MeCN (0.1 M) was electrolyzed at room temperature with a current density of 10.0 mA/cm² using graphite electrodes in an undivided *ElectraSyn*[®] vial (10 mL). After 5.0 F was applied, the volatile solvent was removed *in vacuo*. The residue was purified by column chromatography (gradient: *n*-pentane : diethyl ether = from 30:1) yielding the product as a **colorless oil** (yield: 40 %, 116 mg, 0.40 mmol).

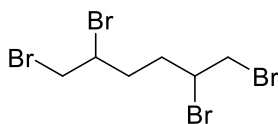
¹H NMR (400 MHz, Chloroform-*d*) δ 7.70 – 7.67 (m, 2H), 7.53 – 7.50 (m, 2H), 5.12 (dd, *J* = 11.2, 5.0 Hz, 1H), 4.07 (dd, *J* = 10.4, 5.0 Hz, 1H), 3.99 – 3.93 (m, 1H).

¹³C NMR (101 MHz, Chloroform-*d*) δ 143.7, 132.8, 128.7, 118.3, 113.1, 48.5, 34.0.

HRMS for C₉H₇Br₂NNa (ESI+) [M+Na]⁺: calc.: 309.8837, found: 309.8837.

Chinese Academy Of Sciences Lanzhou Chemical Physics Institute; Qian Bo; Li Weihe - CN110862292, 2020, A

1,2,5,6-tetrabromohexane (XX)



Chemical Formula: C₆H₁₀Br₄

Exact Mass: 397.75

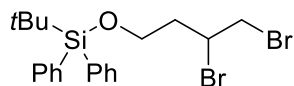
According to the **GP1** for the electrochemical Br₂ shuttle of alkenes, a mixture of hexa-1,5-diene (83 mg, 1 mmol, 1.0 equiv.), 1,2-dibromoethane (939 mg, 433 μ L, 5.0 mmol, 5 equiv.), HFIP (100 μ L, 1 vol%), and Et₄NBF₄ (434 mg, 2.0 mmol, 2 equiv.) in dry MeCN (0.1 M) was electrolyzed at room temperature with a current density of 10.0 mA/cm² using graphite electrodes in an undivided *ElectraSyn*[®] vial (10 mL). After 7 F was applied, the volatile solvent was removed *in vacuo*. The residue was purified by column chromatography (gradient: *n*-pentane : diethyl ether = from 100:0) yielding the product as a **colorless solid** (yield: 35 %, 138.9 mg, 0.35 mmol).

¹H NMR (400 MHz, Chloroform-*d*) δ 4.23 – 4.16 (m, 2H), 3.91 – 3.86 (m, 2H), 3.67 – 3.61 (m, 2H), 2.57 – 2.47 (m, 1H), 2.40 – 2.30 (m, 1H), 2.15 – 2.03 (m, 1H), 1.97 – 1.85 (m, 1H).

¹³C NMR (101 MHz, Chloroform-*d*) δ 51.6, 51.2, 35.9, 35.8, 33.8, 33.7.

HRMS for C₆H₉Br₂ (ESI+) [M–Br₂H]⁺: calc.: 238.9066, found: 238.9066.

tert-butyl(3,4-dibromobutoxy)diphenylsilane (XX)



Chemical Formula: C₂₀H₂₆Br₂OSi

Exact Mass: 468.01

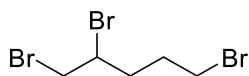
According to the **GP1** for the electrochemical Br₂ shuttle of alkenes, a mixture of (but-3-en-1-yloxy)(*tert*-butyl)diphenylsilane (311 mg, 1 mmol, 1.0 equiv.), 1,2-dibromoethane (939 mg, 433 μ L, 5.0 mmol, 5 equiv.), HFIP (100 μ L, 1 vol%), and Et₄NBF₄ (434 mg, 2.0 mmol, 2 equiv.) in dry MeCN (0.1 M) was electrolyzed at room temperature with a current density of 10.0 mA/cm² using graphite electrodes in an undivided *ElectraSyn*[®] vial (10 mL). After 6.0 F was applied, the volatile solvent was removed *in vacuo*. The residue was purified by column chromatography (gradient: *n*-pentane : diethyl ether = from 100:0) yielding the product as a **colorless oil** (yield: 75 %, 352.6 mg, 0.75 mmol).

¹H NMR (400 MHz, Chloroform-*d*) δ 7.77 – 7.72 (m, 4H), 7.51 – 7.41 (m, 6H), 4.59 – 4.52 (m, 1H), 3.96 – 3.87 (m, 3H), 3.77 – 3.72 (m, 1H), 2.55 – 2.47 (m, 1H), 1.97 – 1.89 (m, 1H).

¹³C NMR (101 MHz, Chloroform-*d*) δ 135.7, 135.7, 133.6, 133.5, 129.9, 129.9, 127.9, 61.2, 49.8, 39.1, 37.0, 27.0, 19.6.

HRMS for C₂₀H₂₆Br₂NaOSi (ESI+) [M+Na]⁺: calc.: 491.0012, found: 491.0009.

1,2,5-tribromopentane (XX)



Chemical Formula: C₅H₉Br₃

Exact Mass: 305.83

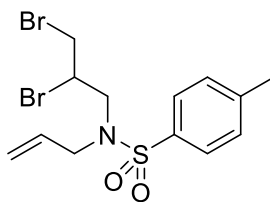
According to the **GP1** for the electrochemical Br₂ shuttle of alkenes, a mixture of 5-bromopent-1-ene (149 mg, 1 mmol, 1.0 equiv.), 1,2-dibromoethane (939 mg, 433 μ L, 5.0 mmol, 5 equiv.), HFIP (100 μ L, 1 vol%), and Et₄NBF₄ (434 mg, 2.0 mmol, 2 equiv.) in dry MeCN (0.1 M) was electrolyzed at room temperature with a current density of 10.0 mA/cm² using graphite electrodes in an undivided *ElectraSyn*[®] vial (10 mL). After 3.0 F was applied, the volatile solvent was removed *in vacuo*. The residue was purified by column chromatography (gradient: cyclohexane : ethyl acetate = from 100:0) yielding the product as a **slightly yellow oil** (yield: 64%, 306.4 mg, 0.64 mmol).

¹H NMR (400 MHz, Chloroform-*d*) δ 4.21 – 4.14 (m, 1H), 3.87 (dd, *J* = 10.3, 4.4 Hz, 1H), 3.63 (t, *J* = 10.1 Hz, 1H), 3.50 – 3.41 (m, 2H), 2.42 – 2.34 (m, 1H), 2.23 – 2.13 (m, 1H), 2.06 – 1.88 (m, 2H).

¹³C NMR (101 MHz, Chloroform-*d*) δ 51.6, 36.0, 34.8, 32.5, 30.1.

HRMS for C₅H₉Br₃ (ESI+) [M-Br]⁺: calc.: 228.9045, found 228.9046.

N-allyl-N-(2,3-dibromopropyl)-4-methylbenzenesulfonamid (XX)



Chemical Formula: C₁₃H₁₇Br₂NO₂S

Exact Mass: 408,9347

Molecular Weight: 411,1520

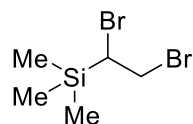
According to the **GP1** for the electrochemical Br₂ shuttle of alkenes, a mixture of N,N-diallyltosylamide (251 mg, 1 mmol, 1.0 equiv.), 1,2-dibromoethane (939 mg, 433 μ L, 5.0 mmol, 5 equiv.), HFIP (100 μ L, 1 vol%), and Et₄NBF₄ (434 mg, 2.0 mmol, 2 equiv.) in dry MeCN (0.1 M) was electrolyzed at room temperature with a current density of 10.0 mA/cm² using graphite electrodes in an undivided *ElectraSyn*[®] vial (10 mL). After 8.0 F was applied, the volatile solvent was removed *in vacuo*. The residue was purified by column chromatography (gradient: cyclohexane : ethyl acetate = from 100:0) yielding the product as a **colorless oil** (yield: 60%, 247 mg, 0.60 mmol).

¹H NMR (400 MHz, Chloroform-*d*) δ 7.76 – 7.69 (m, 2H), 7.37 – 7.31 (m, 2H), 5.56 (ddt, *J* = 16.8, 10.0, 6.6 Hz, 1H), 5.24 – 5.16 (m, 2H), 4.51 (qd, *J* = 6.9, 4.9 Hz, 1H), 3.96 (ddt, *J* = 15.1, 6.9, 1.4 Hz, 1H), 3.89 – 3.74 (m, 3H), 3.68 (dd, *J* = 15.1, 6.9 Hz, 1H), 3.34 (dd, *J* = 15.1, 7.1 Hz, 1H), 2.44 (s, 3H).

¹³C NMR (101 MHz, Chloroform-*d*) δ 144.1, 135.9, 132.4, 130.1, 127.6, 120.5, 53.4, 52.9, 52.3, 50.2, 35.1, 21.7.

HRMS for C₁₃H₁₇Br₂NO₂S (ESI+) [M+H]⁺: calc.: 409.9420, found: 409.9421.

(1,2-dibromoethyl)trimethylsilane (XX)



Chemical Formula: C₅H₁₂Br₂Si

Exact Mass: 257.91

According to the **GP1** for the electrochemical Br₂ shuttle of alkenes, a mixture of trimethyl(vinyl)silane (100 mg, 1 mmol, 1.0 equiv.), 1,2-dibromoethane (939 mg, 433 μ L, 5.0 mmol, 5 equiv.), HFIP (100 μ L, 1 vol%), and Et₄NBF₄ (434 mg, 2.0 mmol, 2 equiv.) in dry MeCN (0.1 M) was electrolyzed at room temperature with a current density of 10.0 mA/cm² using graphite electrodes in an undivided *ElectraSyn*[®] vial (10 mL). After 3.0 F was applied, the volatile solvent was removed *in vacuo*. The residue was purified by column chromatography (gradient: cyclohexane : ethyl acetate = from 100:0) yielding the product as a **colorless oil** (yield: 22 %, 56.7 mg, 0.22 mmol).

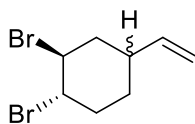
¹H NMR (400 MHz, Chloroform-*d*) δ 3.97 (dd, *J* = 11.1, 4.5 Hz, 1H), 3.73 – 3.65 (m, 1H), 3.48 (dd, *J* = 10.4, 4.5 Hz, 1H), 0.20 (s, 9H).

¹³C NMR (101 MHz, Chloroform-*d*) δ 43.05, 36.68, -2.36.

MS for C₅H₁₂Br₂Si EI *m/z* (%): 139 (37), 136 (39), 109 (4), 85 (7), 75 (4), 74 (8), 73 (100), 59 (10), 45 (13), 44 (3), 43 (10).

[Billups](#); [Saini, Rajesh K.](#); [Litosh, Vladislav A.](#); [Alemany, Lawrence B.](#); [Wilson, William K.](#); [Wiberg, Kenneth B.](#) [*Journal of Organic Chemistry*, 2002, vol. 67, # 13, p. 4436 - 4440]

E-1,2-dibromo-4-vinylcyclohexane (XX)



Chemical Formula: C₈H₁₂Br₂
Exact Mass: 265,9306

According to the **GP1** for the electrochemical Br₂ shuttle of alkenes, a mixture of 4-vinylcyclohexane (108 mg, 1 mmol, 1.0 equiv.), 1,2-dibromoethane (939 mg, 433 μL, 5.0 mmol, 5 equiv.), HFIP (100 μL, 1 vol%), and Et₄NBF₄ (434 mg, 2.0 mmol, 2 equiv.) in dry MeCN (0.1 M) was electrolyzed at room temperature with a current density of 10.0 mA/cm² using graphite electrodes in an undivided *ElectraSyn*® vial (10 mL). After 2.6 F was applied, the volatile solvent was removed *in vacuo*. The residue was purified by column chromatography (gradient: cyclohexane : ethyl acetate = from 100:0) yielding the product as a **colorless oil** (yield: 58%, 154 mg, 0.58 mmol).

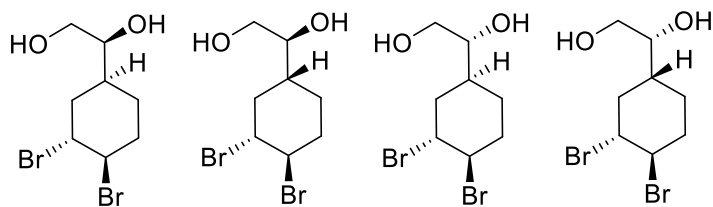
¹H NMR (400 MHz, Chloroform-*d*) δ 5.83 (ddd, *J* = 17.0, 10.4, 6.4 Hz, 1H), 5.10 (dt, *J* = 17.0, 1.4 Hz, 1H), 5.05 (dt, *J* = 10.4, 1.4 Hz, 1H), 4.75 – 4.67 (m, 2H), 2.69 – 2.46 (m, 3H), 2.02 (ddq, *J* = 14.9, 3.3, 1.7 Hz, 2H), 1.79 – 1.66 (m, 2H).

¹³C NMR (101 MHz, CDCl₃) δ 142.0, 127.0, 53.2, 52.3, 35.6, 29.6, 27.0, 21.3.

MS for C₈H₁₂Br₂ EI *m/z* (%): 189 (4), 187 (2), 119 (6), 108 (48), 107 (48), 105 (38), 91 (13), 80 (100), 79 (64), 77 (11), 54 (16), 53 (13), 41 (13), 39 (17).

Husstedt,U.; Schaefer,H.J.[*Synthesis*, 1979, p. 966 - 968]

***E*-4,5-dibromo-7,8-dihydroxyvinylcyclohexane (XX)**



Chemical Formula: $C_8H_{14}Br_2O_2$

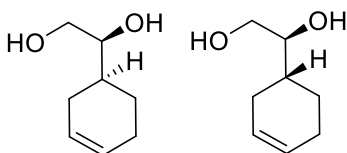
Exact Mass: 299,9361

According to the standard procedure reported by Sharpless et. al. 2 mmol of *E*-1,2-dibromo-4-vinylcyclohexane was dehydroxylated (Kolb, H. C.; Van Nieuwenhze, M. S.; Sharpless, K. B. (1994). "Catalytic Asymmetric Dihydroxylation". *Chem. Rev.* **94** (8): 2483–2547) using AD-mix alpha. The desired product was isolated in 66% yield in a d.r. of 9:9:1:1.

1H NMR (400 MHz, $CDCl_3$) δ 4.75 – 4.69 (m, 1H), 4.66 (m, 1H), 3.72 (m, 1H), 3.62 – 3.52 (m, 2H), 2.55 – 2.42 (m, 1H), 2.40 – 2.21 (m, 2H), 2.18 – 1.83 (m, 2H), 1.80 – 1.51 (m, 3H).

^{13}C NMR (101 MHz, $CDCl_3$) δ 75.4, 75.3, 64.8, 53.2, 53.2, 53.2, 53.1, 34.7, 34.6, 31.1, 30.5, 28.23, 28.2, 23.0, 22.0.

4-vinylcyclohexene-1,8-diol (XX)



Chemical Formula: C₈H₁₄O₂
Exact Mass: 142,0994

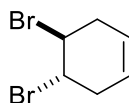
According to the **GP1** for the electrochemical Br₂ shuttle of alkenes, a mixture of **XX** (300 mg, 1 mmol, 1.0 equiv.), HFIP (100 μL, 1 vol%) Et₄NBF₄ (434 mg, 2.0 mmol, 2 equiv.) and 1,4-cyclohexadiene (801 mg, 10 mmol, 10. equiv.) as acceptor in dry MeCN (0.1 M) was electrolyzed at room temperature with a current density of 10.0 mA/cm² using graphite electrodes in an undivided *ElectraSyn*® vial (10 mL). After 3.0 F was applied, the volatile solvent was removed *in vacuo*. The residue was purified by column chromatography (gradient: cyclohexane : ethyl acetate = from 100:0) yielding the product as a **colorless oil** (yield: 51%, 72 mg, 0.51 mmol).

¹H NMR (400 MHz, CDCl₃) δ 5.75 – 5.54 (m, 2H), 4.13 – 3.38 (m, 3H), 1.92 – 1.23 (m, 7H).

¹³C NMR (101 MHz, CDCl₃) δ 127.8, 126.1, 74.5, 68.3, 36.8, 27.9, 25.0, 21.1.

MS for C₈H₁₄O₂ EI *m/z* (%): 166 (4), 124 (2), 111 (6), 106 (48), 91 (48), 78 (38), 77 (13), 43 (100).

E-4,5-dibromocyclohex-1-ene (XX)



Chemical Formula: C₆H₈Br₂

Exact Mass: 237.90

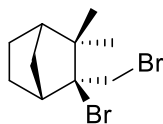
According to the **GP1** for the electrochemical Br₂ shuttle of alkenes, a mixture of cyclohexa-1,4-diene (80 mg, 1 mmol, 1.0 equiv.), 1,2-dibromoethane (939 mg, 433 μ L, 5.0 mmol, 5 equiv.), HFIP (100 μ L, 1 vol%), and Et₄NBF₄ (434 mg, 2.0 mmol, 2 equiv.) in dry MeCN (0.1 M) was electrolyzed at room temperature with a current density of 10.0 mA/cm² using graphite electrodes in an undivided *ElectraSyn*[®] vial (10 mL). After 3.0 F was applied, the volatile solvent was removed *in vacuo*. The residue was purified by column chromatography (gradient: cyclohexane : ethyl acetate = from 100:0) yielding the product as a **colorless oil** (yield: 55%, 131 mg, 0.55 mmol).

¹H NMR (400 MHz, Chloroform-*d*) δ 5.67 – 5.66 (m, 2H), 4.53 – 4.51 (m, 2H), 3.23 – 3.18 (m, 2H), 2.63 – 2.57 (m, 2H).

¹³C NMR (101 MHz, Chloroform-*d*) δ 122.3, 48.7, 31.2.

MS for C₆H₈Br₂ EI *m/z* (%): 242 (1), 240 (2), 238(1), 161 (6), 159 (6), 80 (13), 79 (100), 77 (43), 51 (12), 39 (13).

diBr2 camphene (XX)



Chemical Formula: C₁₀H₁₆Br₂

Molecular Weight: 296,0460

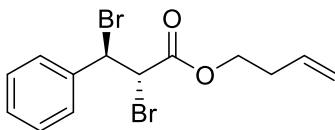
According to the **GP1** for the electrochemical Br₂ shuttle of alkenes, a mixture of 2,2-Dimethyl-3-methylenenorbornane (136 mg, 1 mmol, 1.0 equiv.), 1,2-dibromoethane (939 mg, 433 μ L, 5.0 mmol, 5 equiv.), HFIP (100 μ L, 1 vol%), and Et₄NBF₄ (434 mg, 2.0 mmol, 2 equiv.) in dry MeCN (0.1 M) was electrolyzed at room temperature with a current density of 10.0 mA/cm² using graphite electrodes in an undivided *ElectraSyn*[®] vial (10 mL). After 3.0 F was applied, the volatile solvent was removed *in vacuo*. The residue was purified by column chromatography (gradient: cyclohexane : ethyl acetate = from 100:0) yielding the product as a **colorless oil** (yield: 33%, 98.5 mg, 0.33 mmol).

¹H NMR (400 MHz, CDCl₃) δ 4.26 (dd, *J* = 8.7, 4.6 Hz, 1H), 3.77 (d, *J* = 9.9 Hz, 1H), 3.48 (d, *J* = 9.9 Hz, 1H), 2.43 (dtd, *J* = 14.4, 4.6, 3.3 Hz, 1H), 2.16 (dd, *J* = 14.4, 8.6 Hz, 1H), 2.00 – 1.88 (m, 2H), 1.84 – 1.74 (m, 1H), 1.56 (ddd, *J* = 13.4, 9.5, 4.1 Hz, 1H), 1.21 (s, 3H), 1.20 – 1.14 (m, 1H), 0.94 (s, 3H).

¹³C NMR (101 MHz, CDCl₃) δ 56.8, 53.2, 49.5, 48.5, 42.2, 37.3, 34.6, 26.5, 21.1, 20.5.

MS for C₈H₁₄O₂ EI *m/z* (%): 217 (23), (2), 215 (22), 175 (4), 173 (4), 161 (15), 159 (15), 135 (100), 121 (4), 107 (27), 93 (67), 79 (34), 77 (21), 43 (18), 41 (39).

Intra SM (XX)



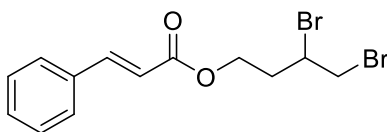
Prep.

^1H NMR (400 MHz, CDCl_3) δ 7.45 – 7.31 (m, 5H), 5.85 (ddt, J = 17.0, 10.2, 6.7 Hz, 1H), 5.34 (d, J = 11.8 Hz, 1H), 5.26 – 5.10 (m, 2H), 4.84 (d, J = 11.8 Hz, 1H), 4.36 (td, J = 6.7, 1.9 Hz, 2H), 2.51 (qt, J = 6.7, 1.4 Hz, 2H).

^{13}C NMR (75 MHz, CDCl_3) δ 168.0, 137.7, 133.5, 129.5, 129.0, 128.2, 117.9, 65.7, 50.8, 47.1, 32.8.

MS for $\text{C}_8\text{H}_{14}\text{O}_2$ EI m/z (%): 217 (23), (2), 215 (22), 175 (4), 173 (4), 161 (15), 159 (15), 135 (100), 121 (4), 107 (27), 93 (67), 79 (34), 77 (21), 43 (18), 41 (39).

Intra P (XX)



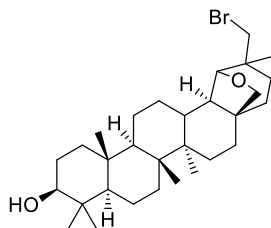
A mixture of **2,2-Dimethyl-3-methylen-norbornan** (136 mg, 1 mmol, 1.0 equiv.), HFIP (100 μ L, 1 vol%), and Et_4NBF_4 (434 mg, 2.0 mmol, 2 equiv.) in dry MeCN (0.1 M) was electrolyzed at room temperature with a current density of 10.0 mA/cm² using graphite electrodes in an undivided *ElectraSyn*[®] vial (10 mL). After 6.2 F was applied, the volatile solvent was removed *in vacuo*. The residue was purified by column chromatography (gradient: cyclohexane : ethyl acetate = from 100:0) yielding the product as a **colorless oil** (yield: 33%, 98.5 mg, 0.33 mmol).

¹H NMR (400 MHz, CDCl_3) δ 7.72 (d, J = 16.0 Hz, 1H), 7.54 (ddd, J = 5.9, 4.2, 2.7 Hz, 3H), 7.40 (dt, J = 5.9, 4.2, 1.9 Hz, 4H), 6.45 (d, J = 16.0 Hz, 1H), 4.49 (ddd, J = 10.9, 5.9, 4.8 Hz, 1H), 4.42 – 4.29 (m, 2H), 3.92 (dd, J = 10.4, 4.2 Hz, 1H), 3.70 (dd, J = 10.4, 9.7 Hz, 1H), 2.64 (dddd, J = 15.0, 8.7, 5.9, 3.1 Hz, 1H), 2.14 (ddt, J = 15.0, 9.7, 4.8 Hz, 1H).

¹³C NMR (75 MHz, CDCl_3) δ 168.0, 137.7, 133.5, 129.5, 129.0, 128.2, 117.9, 65.7, 50.8, 47.1, 32.8.

MS for $\text{C}_8\text{H}_{14}\text{O}_2$ EI m/z (%): 217 (23), (2), 215 (22), 175 (4), 173 (4), 161 (15), 159 (15), 135 (100), 121 (4), 107 (27), 93 (67), 79 (34), 77 (21), 43 (18), 41 (39).

30-Bromoallobetulin (XX)



Chemical Formula: C₃₀H₄₉BrO₂
Molecular Weight: 521,6240

According to the **GP1** for the electrochemical Br₂ shuttle of alkenes, a mixture of betulin (222 mg, 0.50 mmol, 1.0 equiv.), 1,2-dibromoethane (1880 mg, 854 μ L, 10.0 mmol, 20 equiv.), HFIP (100 μ L, 1 vol%), and Et₄NBF₄ (434 mg, 2.0 mmol, 2 equiv.) in dry MeCN (0.1 M) was electrolyzed at room temperature with a current density of 10.0 mA/cm² using graphite electrodes in an undivided *ElectraSyn*[®] vial (10 mL). After 10 F was applied, the volatile solvent was removed *in vacuo*. The residue was purified by column chromatography (gradient: cyclohexane : ethyl acetate = from 100:0 to 80:20) yielding the product as a **colorless solid** (yield: 48 %, 145 mg, 0.24 mmol).

Scale-up in 1.5 L beaker cell (x140): yield 44%, 17.8 g, 30.8 mmol.

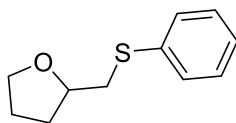
¹H NMR (400 MHz, CDCl₃) δ 3.86 – 3.74 (m, 1H), 3.54 – 3.28 (m, 2H), 3.19 (dd, *J* = 11.2, 5.0 Hz, 1H), 1.71 (dt, *J* = 13.0, 3.7 Hz, 1H), 1.65 – 1.18 (m, 20H), 1.10 (ddd, *J* = 14.3, 6.6, 3.3 Hz, 1H), 0.99 – 0.90 (m, 13H), 0.86 – 0.74 (m, 8H), 0.72 – 0.67 (m, 1H).

¹³C NMR (101 MHz, CDCl₃) δ 88.1, 83.8, 79.1, 77.5, 77.4, 77.2, 76.8, 71.7, 71.4, 55.6, 51.2, 51.2, 47.1, 46.9, 46.2, 41.7, 41.6, 40.9, 40.8, 40.7, 40.4, 39.1, 39.0, 37.4, 36.9, 36.6, 36.4, 34.3, 34.2, 34.0, 32.8, 30.4, 28.9, 28.1, 27.5, 27.0, 26.6, 26.5, 26.4, 26.1, 24.7, 21.2, 21.1, 21.0, 18.4, 16.6, 15.8, 15.5, 13.6.

HRMS for C₃₀H₅₀Br₂O₂ (ESI+) [M-Br]⁺: calc.: 520.2915, found: 520.2916.

Melting point: M_p = 217 – 220 °C.

2-thiophenylmethyl-tetrahydrofuran (XX)



Chemical Formula: C₁₁H₁₄OS
Exact Mass: 194,0765

According to the **GP3** for the electrochemical SPhBr-shuttle of alkenes, a mixture of 4-penten-1-ol (43 mg, 0.5 mmol, 1.0 equiv.), (2-bromoethyl)(phenyl)sulfane (543 mg, 2.5 mmol, 5 equiv.) and Et₄NBF₄ (217 mg, 1.0 mmol, 2 equiv.) in dry MeCN (0.1 M) was electrolyzed at room temperature with a current density of 10.0 mA/cm² using graphite electrodes in an undivided *ElectraSyn*® vial (5 mL). After 3.0 F was applied, the volatile solvent was removed *in vacuo*. The residue was purified by column chromatography (gradient: MeCN : water (0.1% HOAc) = from 70:30 to 100:0) yielding the product as a **colorless liquid** (yield: 67 %, 130 mg, 0.33 mmol).

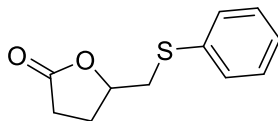
¹H NMR (400 MHz, Chloroform-*d*) δ 7.40 – 7.34 (m, 2H), 7.30 – 7.25 (m, 2H), 7.20 – 7.14 (m, 1H), 4.06 (qd, *J* = 6.9, 5.8 Hz, 1H), 3.91 (ddd, *J* = 8.3, 6.9, 6.0 Hz, 1H), 3.80 – 3.72 (m, 1H), 3.16 (dd, *J* = 13.1, 5.8 Hz, 1H), 2.97 (dd, *J* = 13.1, 6.9 Hz, 1H), 2.07 (dddd, *J* = 12.0, 8.5, 6.9, 5.3 Hz, 2H), 1.97 – 1.85 (m, 1H), 1.67 (ddt, *J* = 12.0, 8.5, 6.9 Hz, 1H).

¹³C NMR (101 MHz, Chloroform-*d*) δ 136.5, 130.4, 129.4, 129.0, 126.1, 77.8, 68.5, 39.0, 31.1, 25.9.

MS: EI *m/z* (%): 195 (2), 194 (15), 125 (2), 124 (19), 123 (7), 77 (5), 71 (100). 45 (9), 43 (35).

[Marset, Xavier](#); [Guillena, Gabriela](#); [Ramón, Diego J.](#) [*Chemistry - A European Journal*, 2017, vol. 23, # 44, p. 10522 - 10526]

5-[(phenylsulfanyl)methyl]dihydrofuran-2(3H)-2-on (XX)



Chemical Formula: C₁₁H₁₂O₂S
Exact Mass: 208,0558

According to the **GP3** for the electrochemical SPhBr-shuttle of alkenes, a mixture of 4-pentenoic acid (50 mg, 0.5 mmol, 1.0 equiv.), (2-bromoethyl)(phenyl)sulfane (543 mg, 2.5 mmol, 5 equiv.) and Et₄NBF₄ (217 mg, 1.0 mmol, 2 equiv.) in dry MeCN (0.1 M) was electrolyzed at room temperature with a current density of 10.0 mA/cm² using graphite electrodes in an undivided *ElectraSyn*® vial (5 mL). After 3.0 F was applied, the volatile solvent was removed *in vacuo*. The residue was purified by column chromatography (gradient: MeCN : water (0.1% HOAc) = from 70:30 to 100:0) yielding the product as a **colorless liquid** (yield: 65%, 68 mg, 0.32 mmol).

¹H NMR (400 MHz, Chloroform-*d*) δ 7.45 – 7.39 (m, 1H), 7.37 – 7.30 (m, 1H), 7.29 – 7.23 (m, 1H), 4.70 – 4.58 (m, 1H), 3.37 (dd, *J* = 13.9, 4.8 Hz, 1H), 3.06 (dd, *J* = 13.9, 7.7 Hz, 1H), 2.68 – 2.36 (m, 2H), 2.12 – 1.97 (m, 1H).

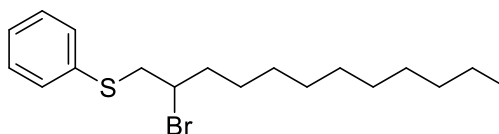
¹³C NMR (101 MHz, Chloroform-*d*) δ 175.7, 134.8, 131.1, 129.3, 127.2, 78.7, 38.7, 28.6, 27.1.

MS: EI *m/z* (%): 209 (6), 208 (46), 125 (5), 124 (21), 123 (77), 110 (18), 86 (5), 85 (100), 77 (12), 57 (15), 45 (31), 39 (10).

HRMS for C₁₁H₁₂O₂S (ESI+) [M+H]⁺: calc.: 209.0631, found: 209.0633.

[Marset, Xavier](#); [Guillena, Gabriela](#); [Ramón, Diego J.](#) [Chemistry - A European Journal, 2017, vol. 23, # 44, p. 10522 - 10526]

(2-bromododecyl)(phenyl)sulfane (XX)



Chemical Formula: C₁₈H₂₉BrS
Molecular Weight: 357,3940

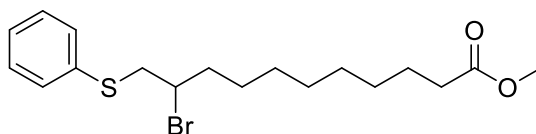
According to the **GP3** for the electrochemical SPhBr-shuttle of alkenes, a mixture of 1-dodecene (84 mg, 0.5 mmol, 1.0 equiv.), (2-bromoethyl)(phenyl)sulfane (543 mg, 2.5 mmol, 5 equiv.) and Et₄NBF₄ (217 mg, 1.0 mmol, 2 equiv.) in dry MeCN (0.1 M) was electrolyzed at room temperature with a current density of 10.0 mA/cm² using graphite electrodes in an undivided *ElectraSyn*® vial (5 mL). After 3.0 F was applied, the volatile solvent was removed *in vacuo*. The residue was purified by reversed phase column chromatography (gradient: MeCN : water (0.1% HOAc) = from 70:30 to 100:0) yielding the product as a **colorless oil** in a mixture of regioisomers (ratio 7:1) (yield: 30 %, 54 mg, 0.15 mmol).

¹H NMR (400 MHz, Chloroform-*d*) δ 7.45 – 7.39 (m, 1H), 7.37 – 7.30 (m, 1H), 7.29 – 7.23 (m, 1H), 4.70 – 4.58 (m, 1H), 3.37 (dd, *J* = 13.9, 4.8 Hz, 1H), 3.06 (dd, *J* = 13.9, 7.7 Hz, 1H), 2.68 – 2.36 (m, 2H), 2.12 – 1.97 (m, 1H).

¹³C NMR (101 MHz, Chloroform-*d*) δ 175.7, 134.8, 131.1, 129.3, 127.2, 78.7, 38.7, 28.6, 27.1.

MS: EI *m/z* (%): 356 (9), 358 (9), 277 (17), 207 (14), 188 (8), 190 (8), 123 (35), 110 (100), 97 (49), 83 (52), 69 (60), 55 (78), 41 (63).

Methyl 10-bromo-11-benzylsulfanyl-undecanoate (XX)



Chemical Formula: C₁₈H₂₇BrO₂S
Molecular Weight: 387,3760

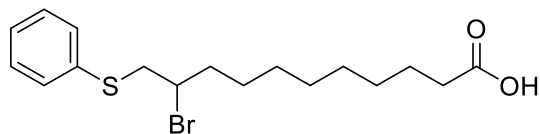
According to the **GP3** for the electrochemical SPhBr-shuttle of alkenes, a mixture of methyl 10-undecenoate (99 mg, 0.5 mmol, 1.0 equiv.), (2-bromoethyl)(phenyl)sulfane (543 mg, 2.5 mmol, 5 equiv.) and Et₄NBF₄ (217 mg, 1.0 mmol, 2 equiv.) in dry MeCN (0.1 M) was electrolyzed at room temperature with a current density of 10.0 mA/cm² using graphite electrodes in an undivided *ElectraSyn*® vial (5 mL). After X.X F was applied, the volatile solvent was removed *in vacuo*. The residue was purified by reversed phase column chromatography (gradient: MeCN : water (0.1% HOAc) = from 70:30 to 100:0) yielding the product as a **colorless oil** in a mixture of regioisomers (ratio 7:1) (yield: 33%, 64 mg, 0.16 mmol).

¹H NMR (400 MHz, CDCl₃) δ 7.39 – 7.20 (m, 5H), 4.05 (tdd, *J* = 8.9, 5.1, 3.3 Hz, 1H), 3.66 (s, 3H), 3.53 (dd, *J* = 13.8, 5.1 Hz, 1H), 3.25 (dd, *J* = 13.8, 9.3 Hz, 1H), 2.30 (t, *J* = 7.6 Hz, 1H), 2.08 (dddd, *J* = 14.5, 10.0, 5.7, 3.3 Hz, 1H), 1.77 (dddd, *J* = 14.5, 10.0, 9.3, 4.5 Hz, 1H), 1.66 – 1.57 (m, 2H), 1.55 – 1.47 (m, 1H), 1.28 (m, 10H).

¹³C NMR (101 MHz, CDCl₃) δ 173.7, 135.8, 132.4, 130.2, 129.2, 126.9, 54.4, 51.5, 42.6, 36.7, 34.1, 29.2, 29.1, 29.1, 28.8, 27.1, 24.9.

MS: EI *m/z* (%): 388 (4), 386 (3), 307 (7), 291 (14), 253 (5), 207 (36), 191 (6), 165 (16), 123 (45), 110 (98), 109 (40), 83 (29), 74 (66), 69 (39), 55 (100), 41 (62).

10-bromo-11-benzylsulfanyl-undecanoic acid (XX)



Chemical Formula: C₁₇H₂₅BrO₂S

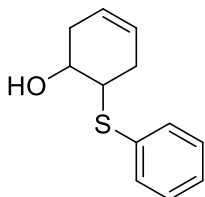
Molecular Weight: 373,3490

According to the **GP3** for the electrochemical SPhBr-shuttle of alkenes, a mixture of 10-undecanoic acid (92 mg, 0.5 mmol, 1.0 equiv.), (2-bromoethyl)(phenyl)sulfane (543 mg, 2.5 mmol, 5 equiv.) and Et₄NBF₄ (217 mg, 1.0 mmol, 2 equiv.) in dry MeCN (0.1 M) was electrolyzed at room temperature with a current density of 10.0 mA/cm² using graphite electrodes in an undivided *ElectraSyn*® vial (5 mL). After X.X F was applied, the volatile solvent was removed *in vacuo*. The residue was purified by reversed phase column chromatography (gradient: MeCN : water (0.1% HOAc) = from 70:30 to 100:0) yielding the product as a **colorless oil** and a mixture of regioisomers 7 : 1 (yield: 41%, 76.5 mg, 0.21 mmol).

¹H NMR (400 MHz, CDCl₃) δ 7.48 – 7.21 (m, 5H), 3.68 (dtt, *J* = 10.5, 7.5, 3.8 Hz, 1H), 3.17 (d, *J* = 13.1 Hz, 1H), 2.87 (dd, *J* = 13.7, 8.7 Hz, 1H), 2.36 (td, *J* = 7.5, 2.4 Hz, 2H), 1.69 – 1.60 (m, 2H), 1.54 (dt, *J* = 8.1, 5.8 Hz, 2H), 1.48 – 1.26 (m, 10H).

¹³C NMR (101 MHz, CDCl₃) δ 179.5, 135.3, 130.1, 129.1, 129.0, 126.6, 69.4, 42.2, 36.1, 34.0, 29.5, 29.3, 29.1, 29.0, 25.6, 24.6.

4-hydroxy-5-phenylsulfonylcyclohexene (XX)



Chemical Formula: C₁₂H₁₄OS
Molecular Weight: 206,3030

According to the **GP3** for the electrochemical SPhBr-shuttle of alkenes, a mixture of 1,4-cyclohexadiene (40 mg, 0.5 mmol, 1.0 equiv.), (2-bromoethyl)(phenyl)sulfane (543 mg, 2.5 mmol, 5 equiv.) and Et₄NBF₄ (217 mg, 1.0 mmol, 2 equiv.) in dry MeCN (0.1 M) was electrolyzed at room temperature with a current density of 10.0 mA/cm² using graphite electrodes in an undivided *ElectraSyn*® vial (5 mL). After 3.0 F was applied, the volatile solvent was removed *in vacuo*. The residue was purified by reversed phase column chromatography (gradient: MeCN : water (0.1% HOAc) = from 70:30 to 100:0) yielding the product as a **colorless oil** (yield: 29%, 30 mg, 0.15 mmol).

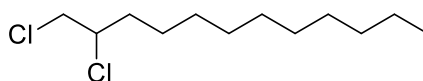
¹H NMR (400 MHz, Chloroform-*d*) δ 7.52 – 7.46 (m, 2H), 7.36 – 7.27 (m, 3H), 5.63 – 5.52 (m, 2H), 3.78 – 3.64 (m, 1H), 3.21 – 3.08 (m, 1H), 2.66 – 2.50 (m, 2H), 2.26 – 2.09 (m, 2H).

¹³C NMR (101 MHz, Chloroform-*d*) δ 133.5, 129.0, 127.8, 125.5, 124.6, 68.8, 52.1, 33.2, 32.0.

MS: EI *m/z* (%): 206 (4), 153 (1), 129 (1), 136 (11), 110 (100), 95 (11), 79 (32), 67 (17), 45 (7), 41 (18).

[Ingle, Gajendrasingh; Mormino, Michael G.; Antilla, Jon C.](#) [Organic Letters, 2014, vol. 16, # 21, p. 5548 - 5551]

1,2-dichlorododecane (XX)



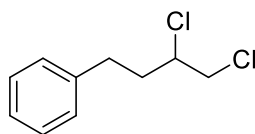
Chemical Formula: C₁₂H₂₄Cl₂

According to the **GP2** for the electrochemical Cl₂ shuttle of alkenes, a mixture of MnCl₂·4H₂O (5.0 mg, 25 μmol, 0.05 equiv.), 1-dodecene (84 mg, 0.5 mmol, 1.0 equiv.), 1,1,1,2-tetrachloroethane (840 mg, 546 μL, 5 mmol, 10 equiv.), and Et₄NBF₄ (109 mg, 0.5 mmol, 1 equiv.) in dry MeCN (0.1 M) was electrolyzed at 50 °C and a current density of 2.0 mA/cm² using graphite electrodes in an undivided *ElectraSyn*® vial (5 mL). After **3.0 F** was applied, the volatile solvent was removed *in vacuo*. The residue was purified by column chromatography (gradient: *n*-pentane : diethyl ether = from 100:0) yielding the product as a colorless oil (yield: 65 %, 66.0 mg, 0.33 mmol).

¹H NMR (400 MHz, Chloroform-*d*) δ 4.07 – 3.95 (m, 1H), 3.78 – 3.58 (m, 2H), 2.02 – 1.89 (m, 1H), 1.75 – 1.62 (m, 1H), 1.44 – 1.18 (m, 16H), 0.86 (t, J = 6.6 Hz, 3H).

¹³C NMR (101 MHz, Chloroform-*d*) δ 61.3, 48.3, 35.1, 31.9, 29.6, 29.56, 29.4, 29.3, 29.0, 25.8, 22.7, 14.1.

(3,4-dichlorobutyl)benzene (XX)



Chemical Formula: C₁₀H₁₂Cl₂

Exact Mass: 202.03

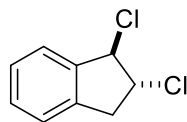
According to the **GP2** for the electrochemical Cl₂ shuttle of alkenes, a mixture of MnCl₂·4H₂O (5.0 mg, 25 μmol, 0.05 equiv.), but-3-en-1-ylbenzene (67 mg, 0.5 mmol, 1.0 equiv.), 1,1,1,2-tetrachloroethane (840 mg, 546 μL, 5 mmol, 10 equiv.), and Et₄NBF₄ (109 mg, 0.5 mmol, 1 equiv.) in dry MeCN (0.1 M) was electrolyzed at 50 °C and a current density of 2.0 mA/cm² using graphite electrodes in an undivided *ElectraSyn*® vial (5 mL). After 3.0 F was applied, the volatile solvent was removed *in vacuo*. The residue was purified by column chromatography (gradient: *n*-pentane : diethyl ether = from 100:0) yielding the product as a colorless oil (yield: 65 %, 66.0 mg, 0.33 mmol).

¹H NMR (400 MHz, Chloroform-*d*) δ 7.38 – 7.34 (m, 2H), 7.29 – 7.25 (m, 3H), 4.08 – 4.01 (m, 1H), 3.82 (dd, *J* = 11.3, 5.1 Hz, 1H), 3.71 (dd, *J* = 11.3, 7.4 Hz, 1H), 3.00 – 2.93 (m, 1H), 2.85 – 2.77 (m, 1H), 2.40 – 2.32 (m, 1H), 2.13 – 2.03 (m, 1H).

¹³C NMR (101 MHz, Chloroform-*d*) δ 140.5, 128.7, 128.6, 126.4, 60.4, 48.4, 36.8, 32.1.

HRMS for C₁₀H₁₂Cl₂ (ESI+) [M]⁺: calc.: 202.0311, found: 202.0305.

rac-1,2-dichloro-2,3-dihydro-1H-indene (XX)



Chemical Formula: C₉H₈Cl₂

Exact Mass: 186.00

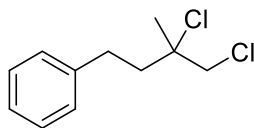
According to the **GP2** for the electrochemical Cl₂ shuttle of alkenes, a mixture of MnCl₂·4H₂O (5.0 mg, 25 μmol, 0.05 equiv.), 1H-indene (58 mg, 0.5 mmol, 1.0 equiv.), 1,1,1,2-tetrachloroethane (840 mg, 546 μL, 5 mmol, 10 equiv.), and Et₄NBF₄ (109 mg, 0.5 mmol, 1 equiv.) in dry MeCN (0.1 M) was electrolyzed at 50 °C and a current density of 2.0 mA/cm² using graphite electrodes in an undivided *ElectraSyn*[®] vial (5 mL). After 3.0 F was applied, the volatile solvent was removed *in vacuo*. The residue was purified by column chromatography (gradient: *n*-pentane : diethyl ether = from 100:0) yielding the product as a colorless oil (yield: 61.4%, 57.7 mg, 0.31 mmol).

¹H NMR (400 MHz, Chloroform-*d*) δ 7.48 – 7.45 (m, 1H), 7.38 – 7.28 (m, 3H), 5.36 (d, *J* = 3.0 Hz, 1H), 4.67 (dt, *J* = 6.3, 3.4 Hz, 1H), 3.71 (dd, *J* = 16.8, 6.0 Hz, 1H), 3.19 (dd, *J* = 16.8, 3.4 Hz, 1H).

¹³C NMR (101 MHz, Chloroform-*d*) δ 140.0, 129.8, 128.1, 125.6, 125.2, 67.8, 64.6, 40.9.

HRMS for C₉H₈Cl₂ (ESI+) [M]⁺: calc.: 185.9998, found: 185.9997.

(3,4-dichloro-3-methylbutyl)benzene (XX)



Chemical Formula: C₁₁H₁₄Br₂
Exact Mass: 303.95

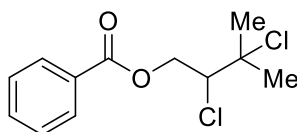
According to the **GP2** for the electrochemical Cl₂ shuttle of alkenes, a mixture of MnCl₂·4H₂O (5.0 mg, 25 μmol, 0.05 equiv.), (3-methylbut-3-en-1-yl)benzene (74 mg, 0.5 mmol, 1.0 equiv.), 1,1,1,2-tetrachloroethane (840 mg, 546 μL, 5 mmol, 10 equiv.), and Et₄NBF₄ (109 mg, 0.5 mmol, 1 equiv.) in dry MeCN (0.1 M) was electrolyzed at 50 °C and a current density of 2.0 mA/cm² using graphite electrodes in an undivided *ElectraSyn*[®] vial (5 mL). After 3.0 F was applied, the volatile solvent was removed *in vacuo*. The residue was purified by column chromatography (gradient: *n*-pentane : diethyl ether = from 100:0) yielding the product as a colorless oil (yield: 70%, 76.5 mg, 0.35 mmol).

¹H NMR (400 MHz, Chloroform-*d*) δ 7.36 – 7.32 (m, 2H), 7.29 – 7.23 (m, 3H), 3.87 – 3.76 (m, 2H), 2.87 – 2.82 (m, 2H), 2.27 – 2.12 (m, 2H), 1.74 (s, 3H).

¹³C NMR (101 MHz, Chloroform-*d*) δ 141.2, 128.7, 128.6, 126.3, 71.1, 52.5, 42.7, 30.9, 28.3.

HRMS for C₁₁H₁₄Cl₂ (ESI+) [M]⁺: calc.: 216.0467, found: 216.0470.

2,3-dichloro-3-methylbutyl benzoate (XX)



Chemical Formula:
 $C_{12}H_{14}Cl_2O_2$
Exact Mass: 260.04

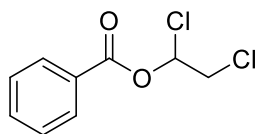
According to the **GP2** for the electrochemical Cl_2 shuttle of alkenes, a mixture of $MnCl_2 \cdot 4H_2O$ (5.0 mg, 25 μ mol, 0.05 equiv.), 3-methylbut-2-en-1-yl benzoate (96 mg, 0.5 mmol, 1.0 equiv.), 1,1,1,2-tetrachloroethane (840 mg, 546 μ L, 5 mmol, 10 equiv.), and Et_4NBF_4 (109 mg, 0.5 mmol, 1 equiv.) in dry MeCN (0.1 M) was electrolyzed at 50 °C and a current density of 2.0 mA/cm² using graphite electrodes in an undivided *ElectraSyn*[®] vial (5 mL). After 9.0 F was applied, the volatile solvent was removed *in vacuo*. After 2.5 F was applied, the volatile solvent was removed *in vacuo*. The residue was purified by column chromatography (gradient: *n*-pentane : diethyl ether = from 30:1) yielding the product as a colorless oil (yield: 87%, 113.9 mg, 0.44 mmol).

¹H NMR (400 MHz, Chloroform-*d*) δ 8.10 – 8.06 (m, 2H), 7.61 – 7.57 (m, 1H), 7.49 – 7.44 (m, 2H), 5.00 (dd, J = 11.9, 3.1 Hz, 1H), 4.57 (dd, J = 11.9, 8.4 Hz, 1H), 4.35 (dd, J = 8.4, 3.1 Hz, 1H), 1.81 (s, 3H), 1.73 (s, 3H).

¹³C NMR (101 MHz, Chloroform-*d*) δ 166.3, 133.5, 129.9, 129.8, 128.6, 69.3, 67.3, 66.2, 31.9, 28.0.

HRMS for $C_{12}H_{14}Cl_2NaO_2$ (ESI+) $[M+Na]^+$: calc.: 283.0263, found: 283.0262.

1,2-dichloroethyl benzoate (XX)



Chemical Formula: C₉H₈Cl₂O₂

Exact Mass: 217.99

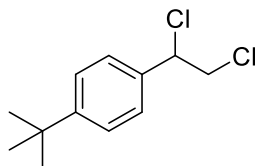
According to the **GP2** for the electrochemical Cl₂ shuttle of alkenes, a mixture of MnCl₂·4H₂O (5.0 mg, 25 μmol, 0.05 equiv.), vinyl benzoate (75 mg, 0.5 mmol, 1.0 equiv.), 1,1,1,2-tetrachloroethane (840 mg, 546 μL, 5 mmol, 10 equiv.), and Et₄NBF₄ (109 mg, 0.5 mmol, 1 equiv.) in dry MeCN (0.1 M) was electrolyzed at 50 °C and a current density of 2.0 mA/cm² using graphite electrodes in an undivided *ElectraSyn*® vial (5 mL). After 7.0 F was applied, the volatile solvent was removed *in vacuo*. The residue was purified by column chromatography (gradient: *n*-pentane : diethyl ether = from 30:1) yielding the product as a colorless oil (yield: 64%, 70.5 mg, 0.32 mmol).

¹H NMR (400 MHz, Chloroform-*d*) δ 8.12 – 8.09 (m, 2H), 7.66 – 7.61 (m, 1H), 7.51 – 7.47 (m, 2H), 6.77 (dd, *J* = 8.0, 3.6 Hz, 1H), 4.08 – 3.95 (m, 2H).

¹³C NMR (101 MHz, Chloroform-*d*) δ 164.09, 134.29, 130.30, 128.79, 128.32, 81.37, 46.10.

HRMS for C₉H₈Cl₂NaO₂ (ESI+) [M+Na]⁺: calc.: 240.9794, found: 240.9791.

1-(tert-butyl)-4-(1,2-dichloroethyl)benzene (XX)



Chemical Formula: C₁₂H₁₆Cl₂
Exact Mass: 230.06

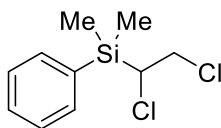
According to the **GP2** for the electrochemical Cl₂ shuttle of alkenes, a mixture of MnCl₂·4H₂O (5.0 mg, 25 μmol, 0.05 equiv.), 1-(tert-butyl)-4-vinylbenzene (81 mg, 0.5 mmol, 1.0 equiv.), 1,1,1,2-tetrachloroethane (840 mg, 546 μL, 5 mmol, 10 equiv.), and Et₄NBF₄ (109 mg, 0.5 mmol, 1 equiv.) in dry MeCN (0.1 M) was electrolyzed at 50 °C and a current density of 2.0 mA/cm² using graphite electrodes in an undivided *ElectraSyn*® vial (5 mL). After 3.0 F was applied, the volatile solvent was removed *in vacuo*. The residue was purified by column chromatography (gradient: *n*-pentane : diethyl ether = from 100:0) yielding the product as a colorless oil (yield: 69%, 80.2 mg, 0.35 mmol).

¹H NMR (400 MHz, Chloroform-*d*) δ 7.43 – 7.40 (m, 2H), 7.35 – 7.32 (m, 2H), 5.00 (t, *J* = 7.3 Hz, 1H), 4.02 – 3.91 (m, 2H), 1.33 (s, 9H).

¹³C NMR (101 MHz, Chloroform-*d*) δ 152.4, 135.1, 127.2, 125.9, 66.0, 48.6, 34.8, 31.4.

HRMS for C₁₂H₁₆Cl₂ (ESI+) [M]⁺: calc.: 230.0624, found: 230.0622.

(1,2-dichloroethyl)dimethyl(phenyl)silane (XX)



Chemical Formula: C₁₀H₁₄Cl₂Si

Exact Mass: 232.02

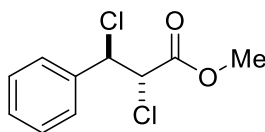
According to the **GP2** for the electrochemical Cl₂ shuttle of alkenes, a mixture of MnCl₂·4H₂O (5.0 mg, 25 μmol, 0.05 equiv.), dimethyl(phenyl)(vinyl)silane (82 mg, 0.5 mmol, 1.0 equiv.), 1,1,1,2-tetrachloroethane (840 mg, 546 μL, 5 mmol, 10 equiv.), and Et₄NBF₄ (109 mg, 0.5 mmol, 1 equiv.) in dry MeCN (0.1 M) was electrolyzed at 50 °C and a current density of 2.0 mA/cm² using graphite electrodes in an undivided *ElectraSyn*[®] vial (5 mL). After 3.0 F was applied, the volatile solvent was removed *in vacuo*. The residue was purified by column chromatography (gradient: *n*-pentane : diethyl ether = from 100:0) yielding the product as a colorless oil (yield: 60%, 70 mg, 0.30 mmol).

¹H NMR (400 MHz, Chloroform-*d*) δ 7.57 – 7.54 (m, 2H), 7.46 – 7.38 (m, 3H), 3.86 (dd, *J* = 11.1, 2.5 Hz, 1H), 3.70 – 3.60 (m, 2H), 0.50 – 0.49 (m, 6H).

¹³C NMR (101 MHz, Chloroform-*d*) δ 134.4, 134.2, 130.3, 128.3, 51.2, 48.6, -4.1, -5.3.

HRMS for C₉H₁₀ClSi (ESI+) [M-CH₄Cl]⁺: calc.: 181.0235, found: 181.0231.

rac-methyl-2,3-dichloro-3-phenylpropanoate (XX)



Chemical Formula: C₁₀H₁₀Cl₂O₂
Exact Mass: 232.01

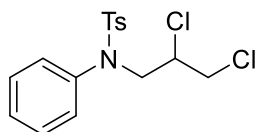
According to the **GP2** for the electrochemical Cl₂ shuttle of alkenes, a mixture of MnCl₂·4H₂O (5.0 mg, 25 μmol, 0.05 equiv.), methyl cinnamate (82 mg, 0.5 mmol, 1.0 equiv.), 1,1,1,2-tetrachloroethane (840 mg, 546 μL, 5 mmol, 10 equiv.), and Et₄NBF₄ (109 mg, 0.5 mmol, 1 equiv.) in dry MeCN (0.1 M) was electrolyzed at 50 °C and a current density of 2.0 mA/cm² using graphite electrodes in an undivided *ElectraSyn*[®] vial (5 mL). After 7.0 F was applied, the volatile solvent was removed *in vacuo*. The residue was purified by column chromatography (gradient: *n*-pentane : diethyl ether = from 30:1) yielding the product as a colorless solid (yield: 42%, 48.2 mg, 0.21 mmol, d.r. = 9 : 1).

¹H NMR (400 MHz, Chloroform-*d*) δ 7.45 – 7.36 (m, 5H), 5.19 (d, *J* = 10.7 Hz, 1H), 4.63 (d, *J* = 10.7 Hz, 1H), 3.90 (s, 3H).

¹³C NMR (101 MHz, Chloroform-*d*) δ 168.1, 136.5, 129.6, 128.9, 128.2, 61.2, 58.9, 53.5.

HRMS for C₁₀H₁₀Cl₂NaO₂ (ESI+) [M+Na]⁺: calc.: 254.9950, found: 254.9949.

***N*-(2,3-dichloropropyl)-4-methyl-*N*-phenylbenzenesulfonamide (XX)**



Chemical Formula: C₁₆H₁₇Cl₂NO₂S

Exact Mass: 357.04

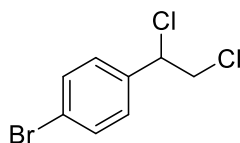
According to the **GP2** for the electrochemical Cl₂ shuttle of alkenes, a mixture of MnCl₂·4H₂O (5.0 mg, 25 μmol, 0.05 equiv.), *N*-allyl-4-methyl-*N*-phenylbenzenesulfonamide (144 mg, 0.5 mmol, 1.0 equiv.), 1,1,1,2-tetrachloroethane (840 mg, 546 μL, 5 mmol, 10 equiv.), and Et₄NBF₄ (109 mg, 0.5 mmol, 1 equiv.) in dry MeCN (0.1 M) was electrolyzed at 50 °C and a current density of 2.0 mA/cm² using graphite electrodes in an undivided *ElectraSyn*® vial (5 mL). After 9.0 F was applied, the volatile solvent was removed *in vacuo*. The residue was purified by column chromatography yielding the product as a white solid (yield: 58%, 105 mg, 0.29 mmol).

¹H NMR (400 MHz, Chloroform-*d*) δ 7.48 – 7.45 (m, 2H), 7.36 – 7.33 (m, 3H), 7.29 – 7.26 (m, 2H), 7.10 – 7.07 (m, 2H), 4.27 – 4.19 (m, 1H), 3.99 (dd, *J* = 14.2, 7.3 Hz, 1H), 3.88 – 3.87 (m, 2H), 3.82 (dd, *J* = 14.2, 6.6 Hz, 1H), 2.45 (s, 3H).

¹³C NMR (101 MHz, Chloroform-*d*) δ 144.1, 139.6, 134.4, 129.7, 129.4, 128.7, 128.5, 127.9, 58.2, 54.7, 46.4, 21.7.

HRMS for C₁₆H₁₇Cl₂NNaO₂S (ESI+) [M+Na]⁺: calc.: 380.0249, found: 380.0245.

1-bromo-4-(1,2-dichloroethyl)benzene (XX)



Chemical Formula: C₈H₇BrCl₂

Exact Mass: 251.91

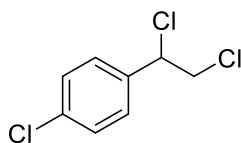
According to the **GP2** for the electrochemical Cl₂ shuttle of alkenes, a mixture of MnCl₂·4H₂O (5.0 mg, 25 μmol, 0.05 equiv.), 1-bromo-4-vinylbenzene (92 mg, 0.5 mmol, 1.0 equiv.), 1,1,1,2-tetrachloroethane (840 mg, 546 μL, 5 mmol, 10 equiv.), and Et₄NBF₄ (109 mg, 0.5 mmol, 1 equiv.) in dry MeCN (0.1 M) was electrolyzed at 50 °C and a current density of 2.0 mA/cm² using graphite electrodes in an undivided *ElectraSyn*[®] vial (5 mL). After 3.0 F was applied, the volatile solvent was removed *in vacuo*. The residue was purified by column chromatography (gradient: *n*-pentane : diethyl ether = from 100:0) yielding the product as a colorless oil (yield: 79%, 99.7 mg, 0.39 mmol).

¹H NMR (400 MHz, Chloroform-*d*) δ 7.55 – 7.51 (m, 2H), 7.31 – 7.26 (m, 2H), 4.95 (dd, *J* = 8.4, 6.1 Hz, 1H), 3.98 (dd, *J* = 11.3, 6.1 Hz, 1H), 3.88 (dd, *J* = 11.3, 8.4 Hz, 1H).

¹³C NMR (101 MHz, Chloroform-*d*) δ 137.1, 132.1, 129.3, 123.4, 60.8, 48.1.

HRMS for C₈H₇BrCl₂ (ESI+) [M]⁺: calc.: 251.9103, found: 251.9104.

1-chloro-4-(1,2-dichloroethyl)benzene (XX)



Chemical Formula: C₈H₇Cl₃

Exact Mass: 207.96

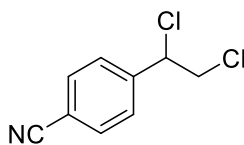
According to the **GP2** for the electrochemical Cl₂ shuttle of alkenes, a mixture of MnCl₂·4H₂O (5.0 mg, 25 μmol, 0.05 equiv.), 1-chloro-4-vinylbenzene (70 mg, 0.5 mmol, 1.0 equiv.), 1,1,1,2-tetrachloroethane (840 mg, 546 μL, 5 mmol, 10 equiv.), and Et₄NBF₄ (109 mg, 0.5 mmol, 1 equiv.) in dry MeCN (0.1 M) was electrolyzed at 50 °C and a current density of 2.0 mA/cm² using graphite electrodes in an undivided *ElectraSyn*[®] vial (5 mL). After 3.0 F was applied, the volatile solvent was removed *in vacuo*. The residue was purified by column chromatography (gradient: *n*-pentane : diethyl ether = from 100:0) yielding the product as a colorless oil (yield: 74%, 77.9 mg, 0.37 mmol).

¹H NMR (400 MHz, Chloroform-*d*) δ 7.39 – 7.34 (m, 4H), 4.97 (dd, *J* = 8.4, 6.2 Hz, 1H), 3.99 (dd, *J* = 11.3, 6.2 Hz, 1H), 3.88 (dd, *J* = 11.3, 8.4 Hz, 1H).

¹³C NMR (101 MHz, Chloroform-*d*) δ 136.64, 135.20, 129.18, 128.98, 60.81, 48.18.

HRMS for C₈H₇Cl₃ (ESI+) [M]⁺: calc.: 207.9608, found: 207.9608.

4-(1,2-dichloroethyl)benzonitrile (XX)



Chemical Formula: C₉H₇Cl₂N

Exact Mass: 198.9956

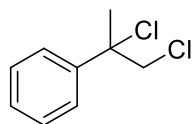
According to the **GP2** for the electrochemical Cl₂ shuttle of alkenes, a mixture of MnCl₂·4H₂O (5.0 mg, 25 μmol, 0.05 equiv.), 4-vinylbenzonitrile (70 mg, 0.5 mmol, 1.0 equiv.), 1,1,1,2-tetrachloroethane (840 mg, 546 μL, 5 mmol, 10 equiv.), and Et₄NBF₄ (109 mg, 0.5 mmol, 1 equiv.) in dry MeCN (0.1 M) was electrolyzed at 50 °C and a current density of 2.0 mA/cm² using graphite electrodes in an undivided *ElectraSyn*[®] vial (5 mL). After 4.0 F was applied, the volatile solvent was removed *in vacuo*. The residue was purified by column chromatography (gradient: *n*-pentane : diethyl ether = from 50:1) yielding the product as a colorless oil (yield: 80%, 80.2 mg, 0.40 mmol).

¹H NMR (400 MHz, Chloroform-*d*) δ 7.72 – 7.69 (m, 2H), 7.56 – 7.53 (m, 2H), 5.01 (dd, *J* = 8.7, 5.8 Hz, 1H), 4.01 (dd, *J* = 11.4, 5.8 Hz, 1H), 3.89 (dd, *J* = 11.4, 8.7 Hz, 1H).

¹³C NMR (101 MHz, Chloroform-*d*) δ 143.0, 132.7, 128.5, 118.3, 113.3, 60.1, 47.7.

HRMS for C₉H₇Cl₂NNa (ESI+) [M+Na]⁺: calc.: 221.9848, found: 221.9846.

(1,2-dichloropropan-2-yl)benzene (XX)



Chemical Formula: C₉H₁₀Cl₂

Exact Mass: 188.02

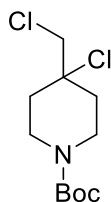
According to the **GP2** for the electrochemical Cl₂ shuttle of alkenes, a mixture of MnCl₂·4H₂O (5.0 mg, 25 μmol, 0.05 equiv.), prop-1-en-2-ylbenzene (60 mg, 0.5 mmol, 1.0 equiv.), 1,1,1,2-tetrachloroethane (840 mg, 546 μL, 5 mmol, 10 equiv.), and Et₄NBF₄ (109 mg, 0.5 mmol, 1 equiv.) in dry MeCN (0.1 M) was electrolyzed at 50 °C and a current density of 2.0 mA/cm² using graphite electrodes in an undivided *ElectraSyn*[®] vial (5 mL). After 3.0 F was applied, the volatile solvent was removed *in vacuo*. The residue was purified by column chromatography (gradient: *n*-pentane : diethyl ether = from 100:0) yielding the product as a colorless oil (yield: 56%, 53.1 mg, 0.28 mmol).

¹H NMR (400 MHz, Chloroform-*d*) δ 7.59 – 7.55 (m, 2H), 7.43 – 7.32 (m, 3H), 4.08 – 3.99 (m, 2H), 2.11 (s, 3H).

¹³C NMR (101 MHz, Chloroform-*d*) δ 141.6, 128.6, 128.5, 126.6, 70.7, 54.7, 28.4.

HRMS for C₉H₈Cl₂ (ESI+) [M-H₂]⁺: calc.: 185.9998, found: 186.0001.

***tert*-butyl 4-chloro-4-(chloromethyl)piperidine-1-carboxylate (XX)**



Chemical Formula: C₁₁H₁₉Cl₂NO₂
Exact Mass: 267.08

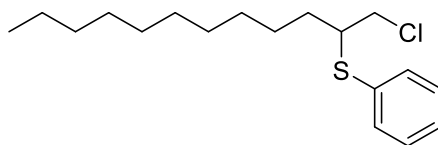
According to the **GP2** for the electrochemical Cl₂ shuttle of alkenes, a mixture of MnCl₂·4H₂O (5.0 mg, 25 μmol, 0.05 equiv.), *tert*-butyl 4-methylenepiperidine-1-carboxylate (99 mg, 0.5 mmol, 1.0 equiv.), 1,1,1,2-tetrachloroethane (840 mg, 546 μL, 5 mmol, 10 equiv.), and Et₄NBF₄ (109 mg, 0.5 mmol, 1 equiv.) in dry MeCN (0.1 M) was electrolyzed at 50 °C and a current density of 2.0 mA/cm² using graphite electrodes in an undivided *ElectraSyn*[®] vial (5 mL). After 7.5 F was applied, the volatile solvent was removed *in vacuo*. The residue was purified by column chromatography (gradient: *n*-pentane : diethyl ether = from 10:1) yielding the product as a colorless oil (yield: 57%, 76.3 mg, 0.29 mmol).

¹H NMR (400 MHz, Chloroform-*d*) δ 4.07 (m, 2H), 3.74 (s, 2H), 3.12 (m, 2H), 1.96 – 1.88 (m, 2H), 1.83 – 1.78 (m, 2H), 1.45 (s, 9H).

¹³C NMR (101 MHz, Chloroform-*d*) δ 154.7, 80.0, 71.1, 54.0, 39.6, 35.8, 28.53.

HRMS for C₁₁H₁₉Cl₂NNaO₂ (ESI+) [M+Na]⁺: calc.: 290.0685, found: 290.0686.

(1-chlorododecyl)(phenyl)sulfane (XX)



Chemical Formula: C₁₈H₂₉ClS

Exact Mass: 312,1678

Molecular Weight: 312,9400

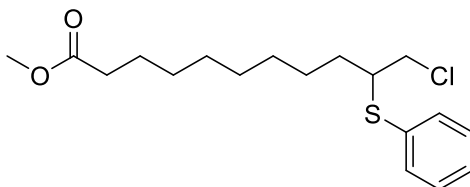
According to the **GP4** for the electrochemical SPhCl-shuttle of alkenes, a mixture of MnCl₂·4H₂O (5.0 mg, 25 μmol, 0.05 equiv.), 1-dodecene (84 mg, 0.5 mmol, 1.0 equiv.), (2-chloroethyl)(phenyl)sulfane (863 mg, 738 μL, 5 mmol, 10 equiv.), and Et₄NBF₄ (109 mg, 0.5 mmol, 1 equiv.) in dry MeCN (0.1 M) was electrolyzed at 50 °C and a current density of 2.0 mA/cm² using graphite electrodes in an undivided *ElectraSyn*® vial (5 mL). After 3.0 F was applied, the volatile solvent was removed *in vacuo*. The residue was purified by column chromatography (gradient: MeCN : water (0.1% HOAc) = from 70:30 to 100:0) yielding the product as a colorless oil and a mixture of regioisomers (ratio 2:1) (yield: 30%, 47 mg, 0.15 mmol).

¹H NMR (400 MHz, Chloroform-*d*) δ 7.48 – 7.29 (m, 5H), 3.72 (dd, *J* = 11.0, 4.0 Hz, 1H), 3.52 (dd, *J* = 11.0, 9.3 Hz, 1H), 3.28 (tt, *J* = 8.6, 4.0 Hz, 1H), 2.05 – 1.97 (m, 1H), 1.73 (ddt, *J* = 14.3, 9.3, 5.0 Hz, 1H), 1.59 – 1.49 (m, 2H), 1.36 – 1.26 (m, 12H), 0.92 (m, 4H).

¹³C NMR (101 MHz, Chloroform-*d*) δ 133.8, 132.5, 130.1, 129.2, 127.6, 126.8, 50.4, 47.5, 31.9, 31.2, 29.6, 29.5, 29.4, 29.0, 26.6, 26.1, 22.7, 15.0.

HRMS for C₁₈H₂₉ClS (ESI+) [M+HO]⁺: calc.: 329.1700, found: 329.1706.

Methyl 11-chloro-10-benzylsulfanyl-undecanoate (XX)



Chemical Formula: C₁₈H₂₇ClO₂S

Exact Mass: 342,1420

Molecular Weight: 342,9220

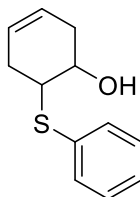
According to the **GP4** for the electrochemical SPhCl-shuttle of alkenes, a mixture of MnCl₂·4H₂O (5.0 mg, 25 μmol, 0.05 equiv.), methyl 10-undecenoate (99 mg, 0.5 mmol, 1.0 equiv.), (2-chloroethyl)(phenyl)sulfane (863 mg, 738 μL, 5 mmol, 10 equiv.), and Et₄NBF₄ (109 mg, 0.5 mmol, 1 equiv.) in dry MeCN (0.1 M) was electrolyzed at 50 °C and a current density of 2.0 mA/cm² using graphite electrodes in an undivided *ElectraSyn*[®] vial (5 mL). After 3.0 F was applied, the volatile solvent was removed *in vacuo*. The residue was purified by column chromatography (gradient: MeCN : water (0.1% HOAc) = from 70:30 to 100:0) yielding the product as a colorless oil and a mixture of regioisomers (ratio 2:1) (yield: 32%, 55 mg, 0.16 mmol).

¹H NMR (400 MHz, Chloroform-*d*) δ 7.46 – 7.27 (m, 5H), 3.71 (dd, *J* = 11.0, 4.0 Hz, 1H), 3.69 (s, 3H), 3.51 (dd, *J* = 11.0, 9.2 Hz, 1H), 3.30 – 3.23 (m, 1H), 2.33 (td, *J* = 7.5, 3.4 Hz, 3H), 2.03 – 1.95 (m, 1H), 1.68 – 1.60 (m, 1H), 1.32 (dd, *J* = 14.7, 3.1 Hz, 10H).

¹³C NMR (101 MHz, Chloroform-*d*) δ 174.9, 133.7, 132.5, 130.1, 129.2, 127.6, 126.8, 51.5, 50.3, 47.4, 34.1, 31.2, 29.2, 29.16, 29.11, 26.5, 26.0, 24.9.

HRMS for C₁₈H₂₇ClO₂S (ESI+) [M-Cl]⁺: calc.: 307.1726, found: 307.1720.

4-hydroxy-5-phenylsulfonylcyclohexene (XX)



Chemical Formula: C₁₂H₁₄OS

Exact Mass: 206,0765

Molecular Weight: 206,3030

According to the **GP4** for the electrochemical SPhCl-shuttle of alkenes, a mixture of MnCl₂·4H₂O (5.0 mg, 25 μmol, 0.05 equiv.), 1,4-cyclohexadiene (40 mg, 0.5 mmol, 1.0 equiv.), (2-chloroethyl)(phenyl)sulfane (863 mg, 738 μL, 5 mmol, 10 equiv.), and Et₄NBF₄ (109 mg, 0.5 mmol, 1 equiv.) in dry MeCN (0.1 M) was electrolyzed at 50 °C and a current density of 2.0 mA/cm² using graphite electrodes in an undivided *ElectraSyn*[®] vial (5 mL). After 3.0 F was applied, the volatile solvent was removed *in vacuo*. The residue was purified by column chromatography (gradient: MeCN : water (0.1% HOAc) = from 70:30 to 100:0) yielding the product as a colorless oil (yield: 19%, 21.5 mg, 0.10 mmol).

¹H NMR (400 MHz, Chloroform-*d*) δ 7.52 – 7.46 (m, 2H), 7.36 – 7.27 (m, 3H), 5.63 – 5.52 (m, 2H), 3.78 – 3.64 (m, 1H), 3.21 – 3.08 (m, 1H), 2.66 – 2.50 (m, 2H), 2.26 – 2.09 (m, 2H).

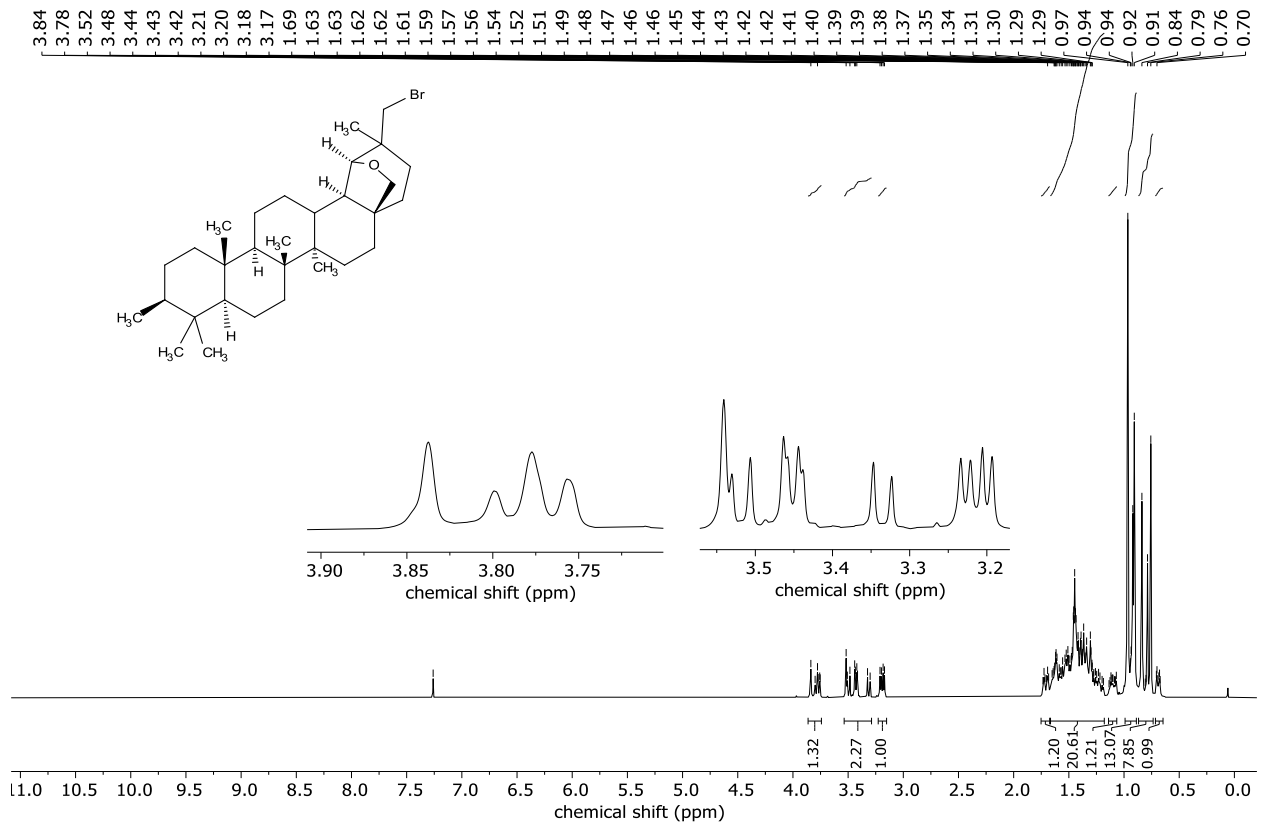
¹³C NMR (101 MHz, Chloroform-*d*) δ 133.5, 129.0, 127.8, 125.5, 124.6, 68.8, 52.1, 33.2, 32.0.

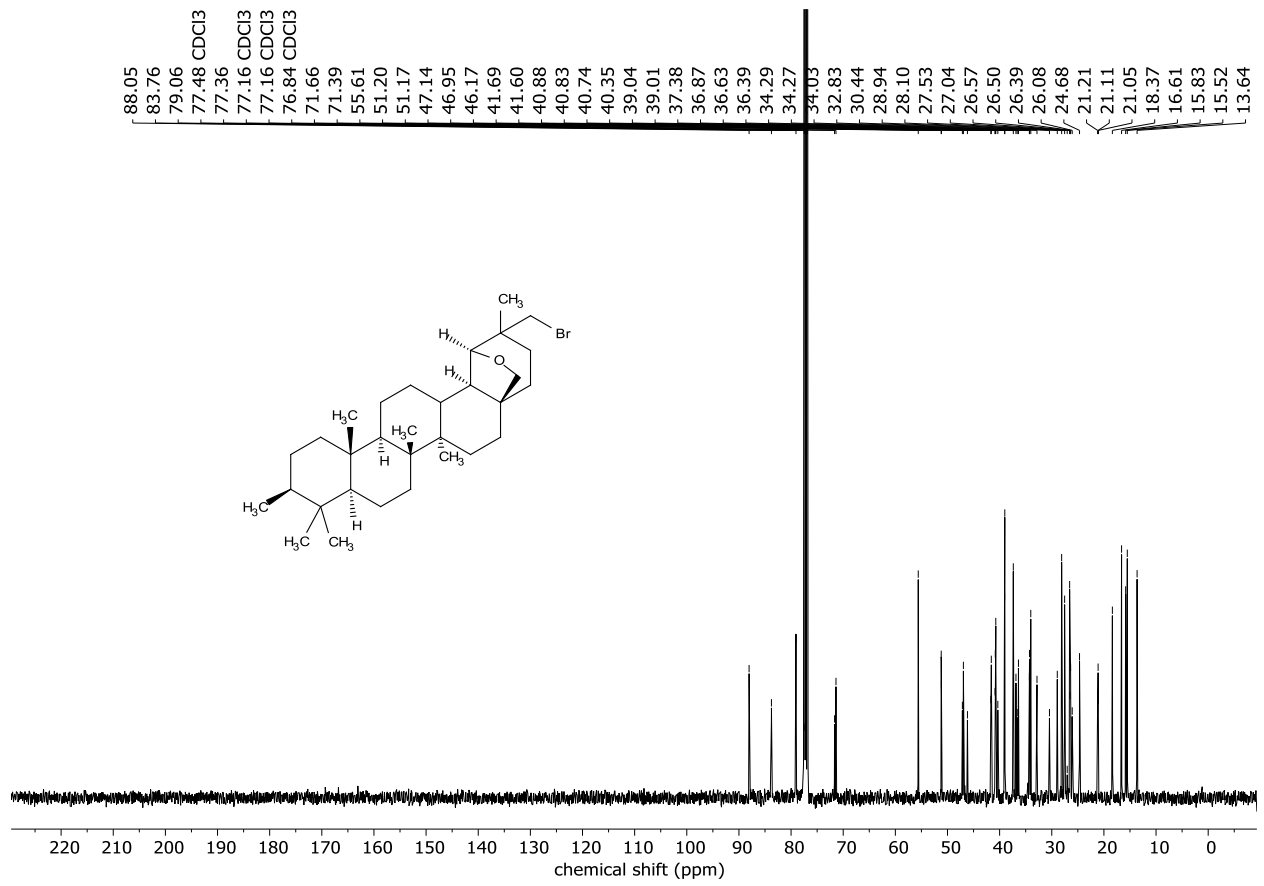
MS: EI *m/z* (%): 206 (4), 153 (1), 129 (1), 136 (11), 110 (100), 95 (11), 79 (32), 67 (17), 45 (7), 41 (18).

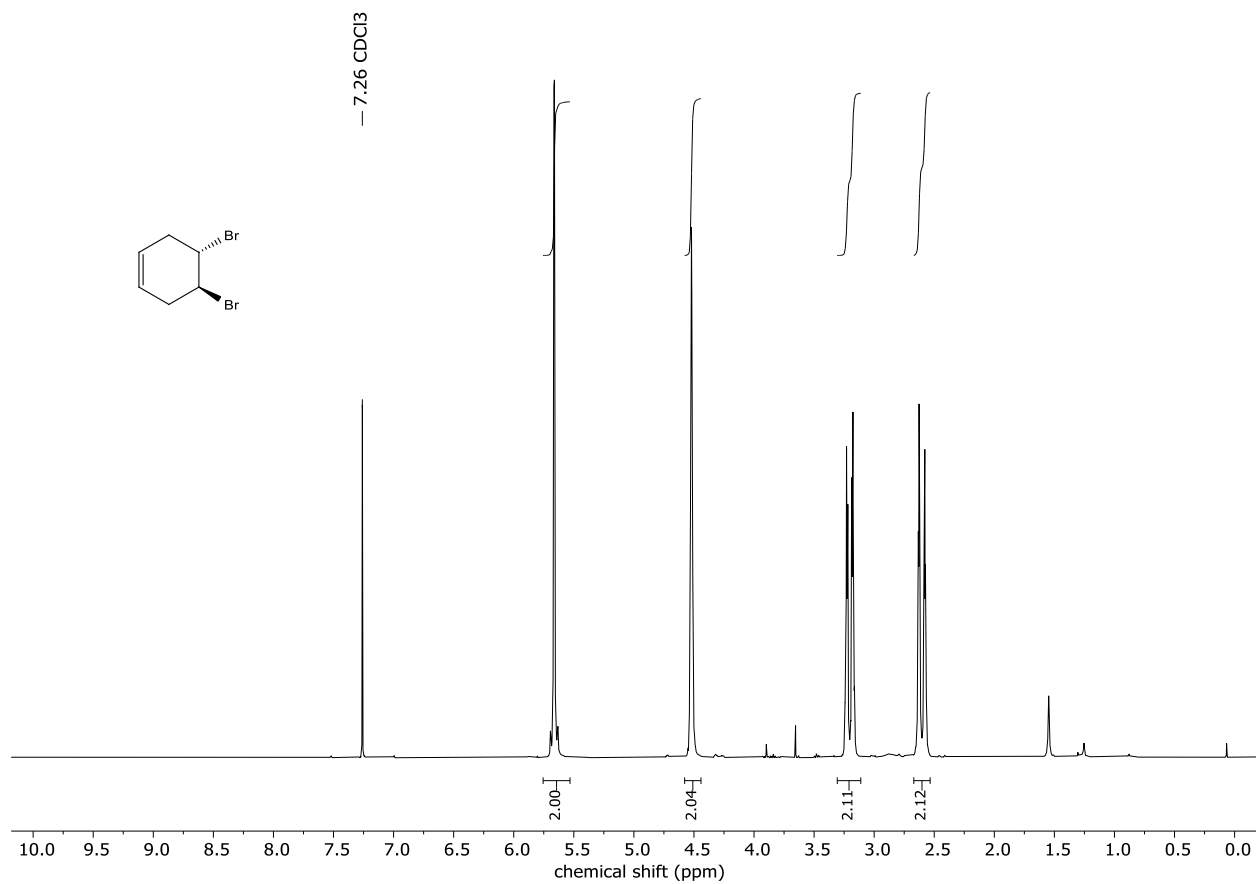
HRMS for C₁₂H₁₄OS (ESI+) [M-OH]⁺: calc.: 189.0732, found: 189.0737.

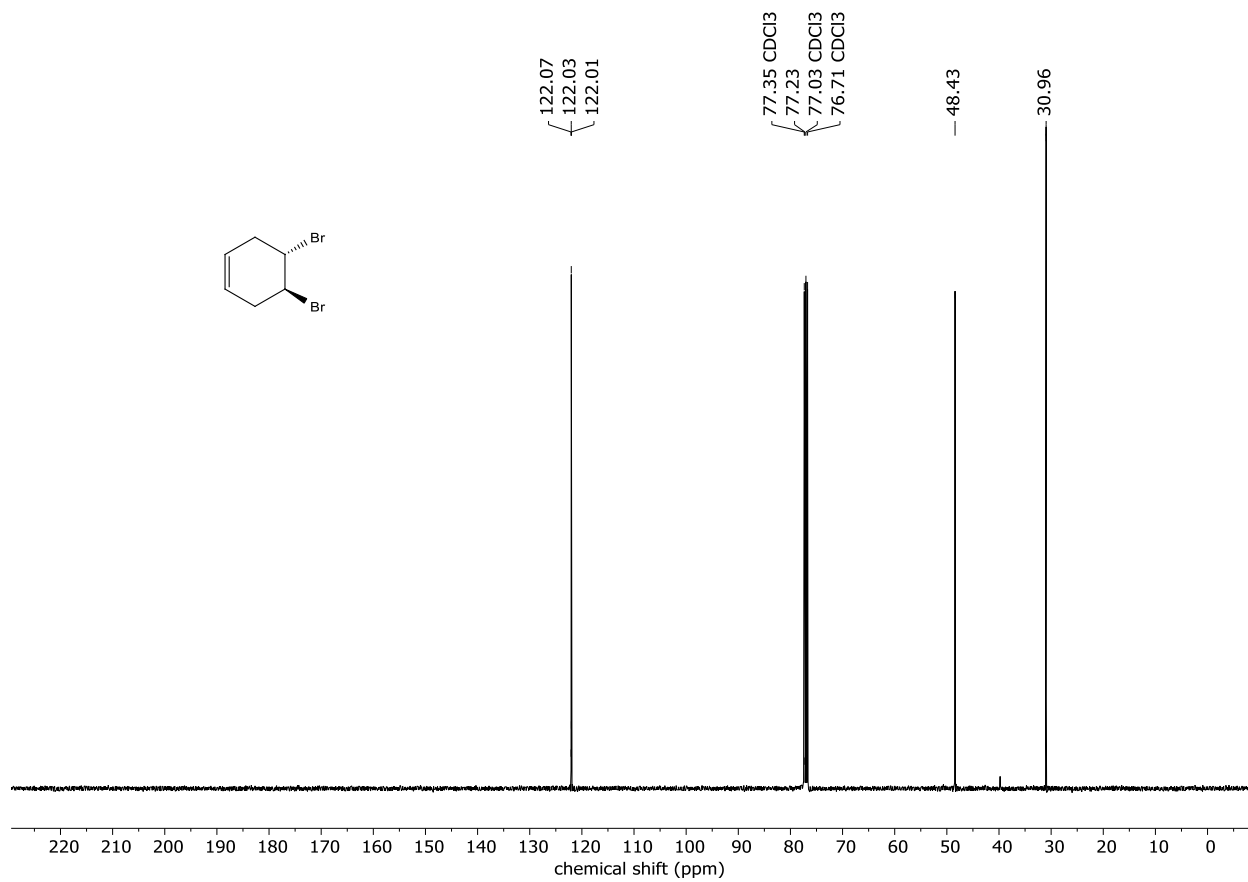
[Ingle, Gajendrasingh](#); [Mormino, Michael G.](#); [Antilla, Jon C.](#) [*Organic Letters*, **2014**, vol. 16, # 21, p. 5548 - 5551]

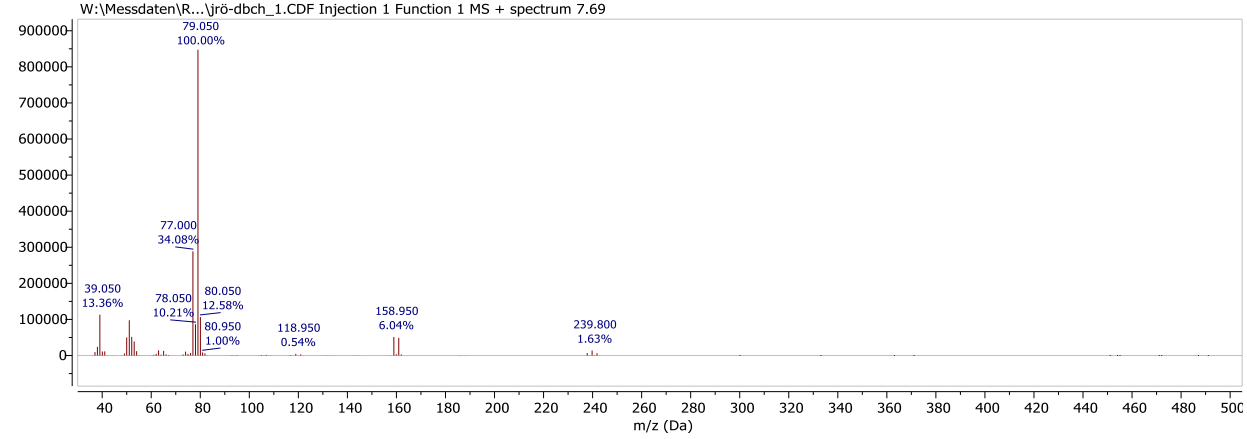
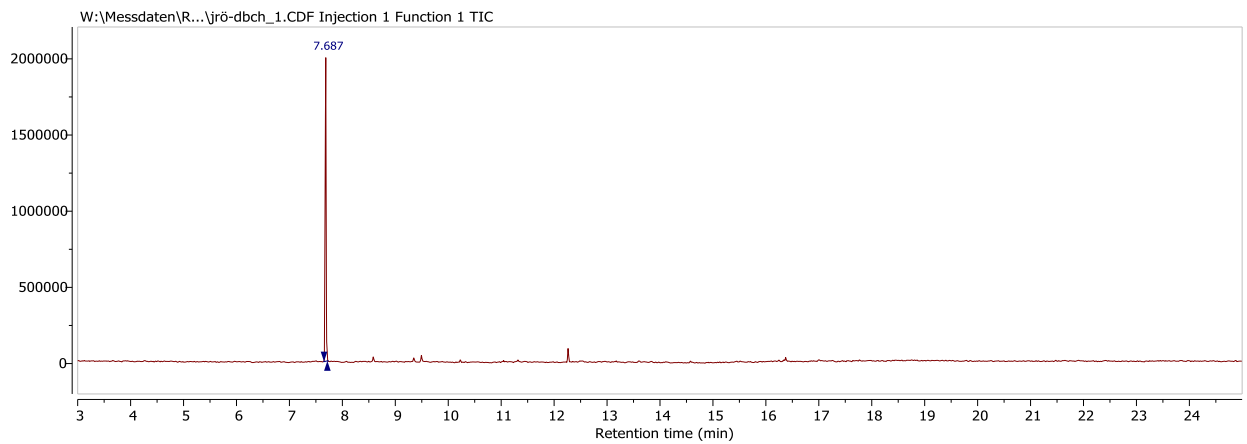
6.1 Spectra



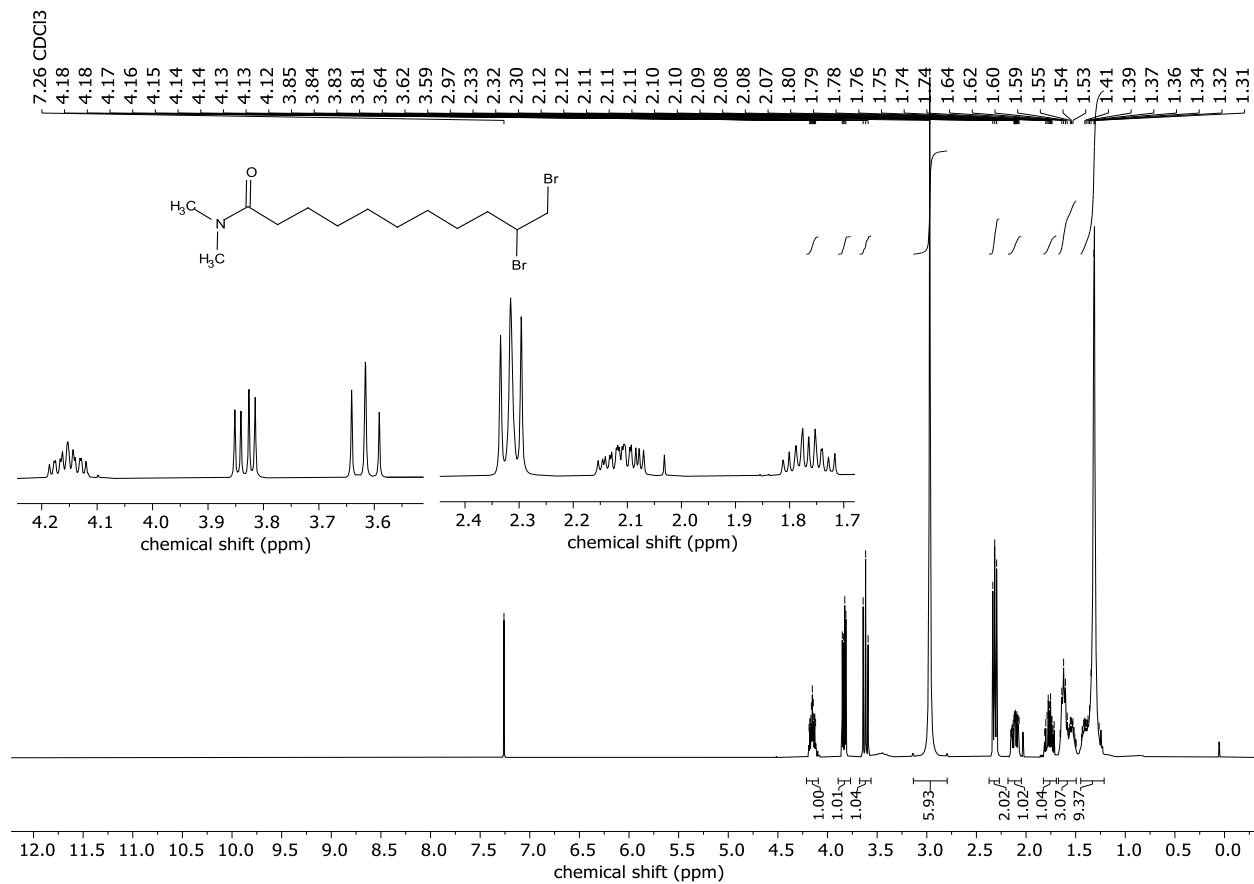


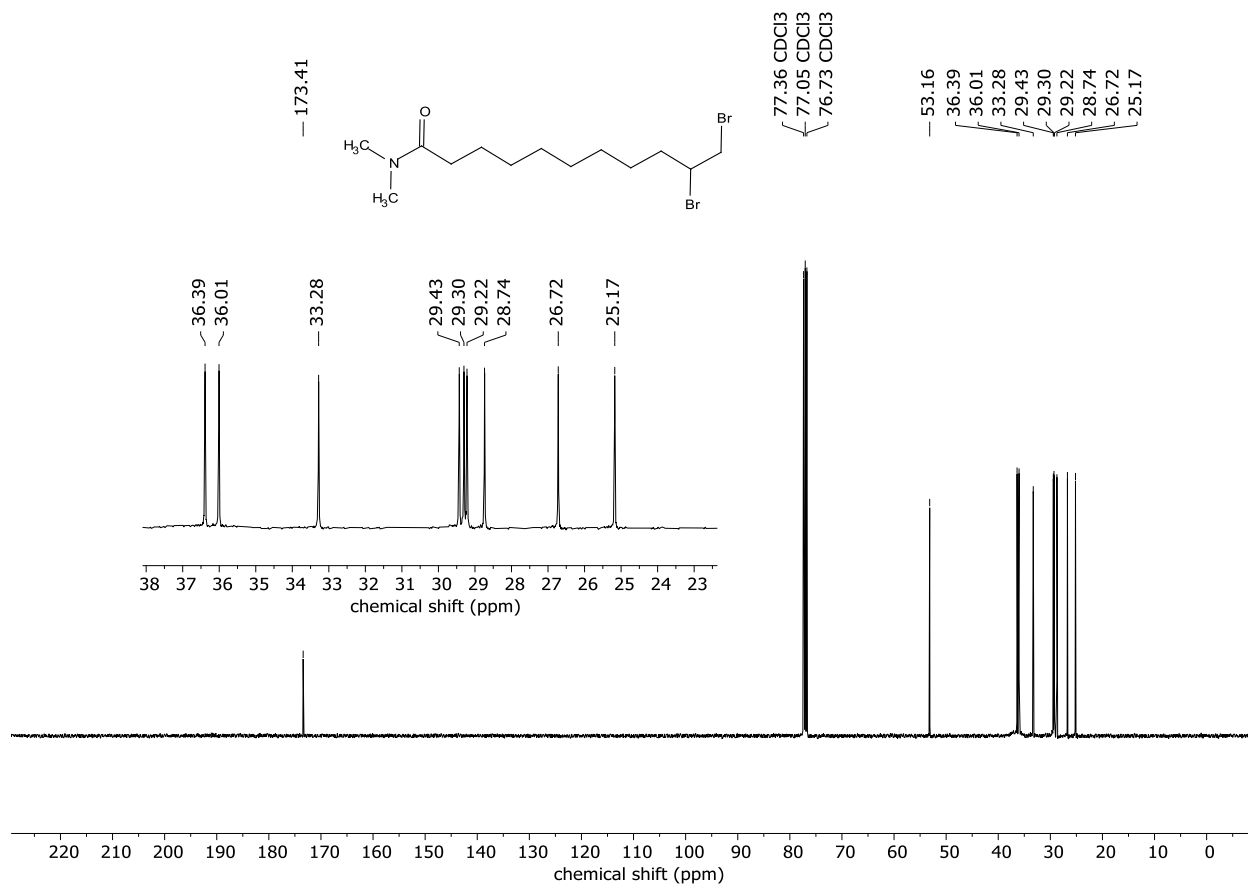


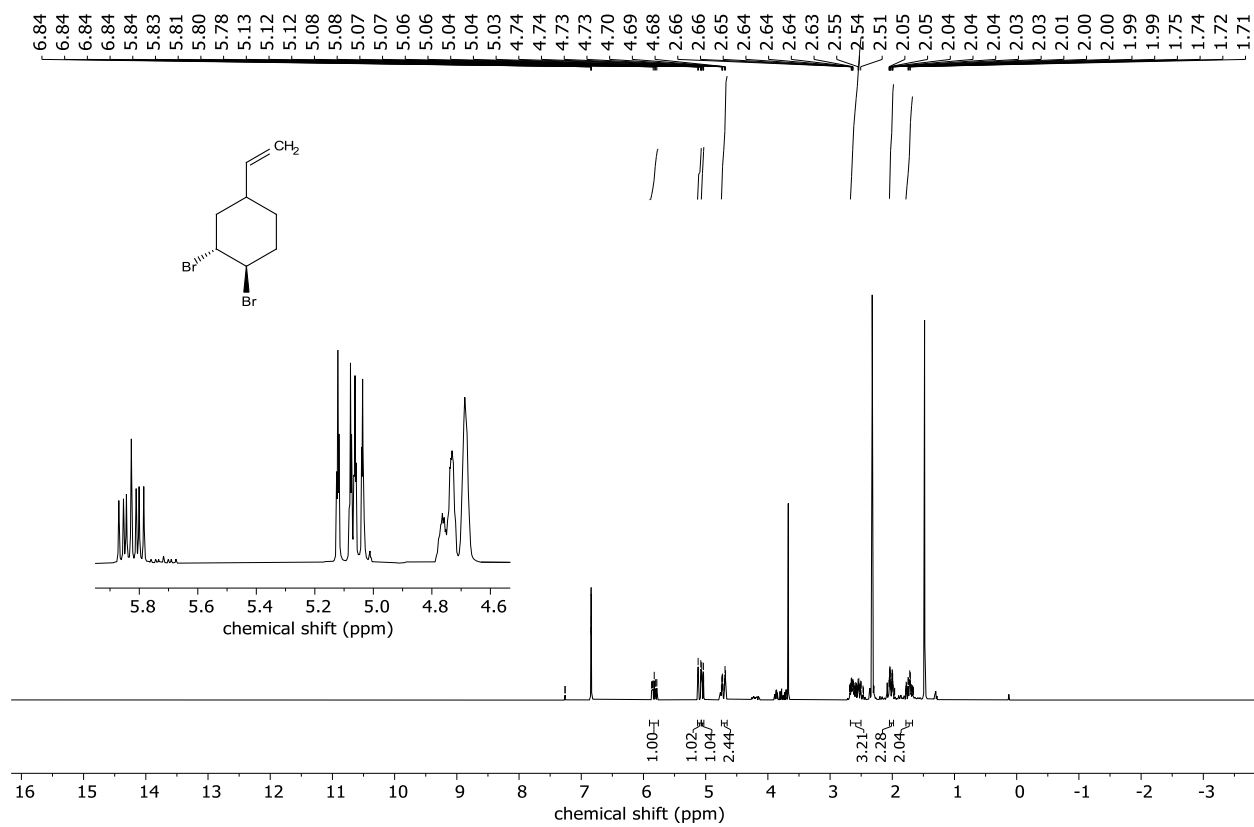


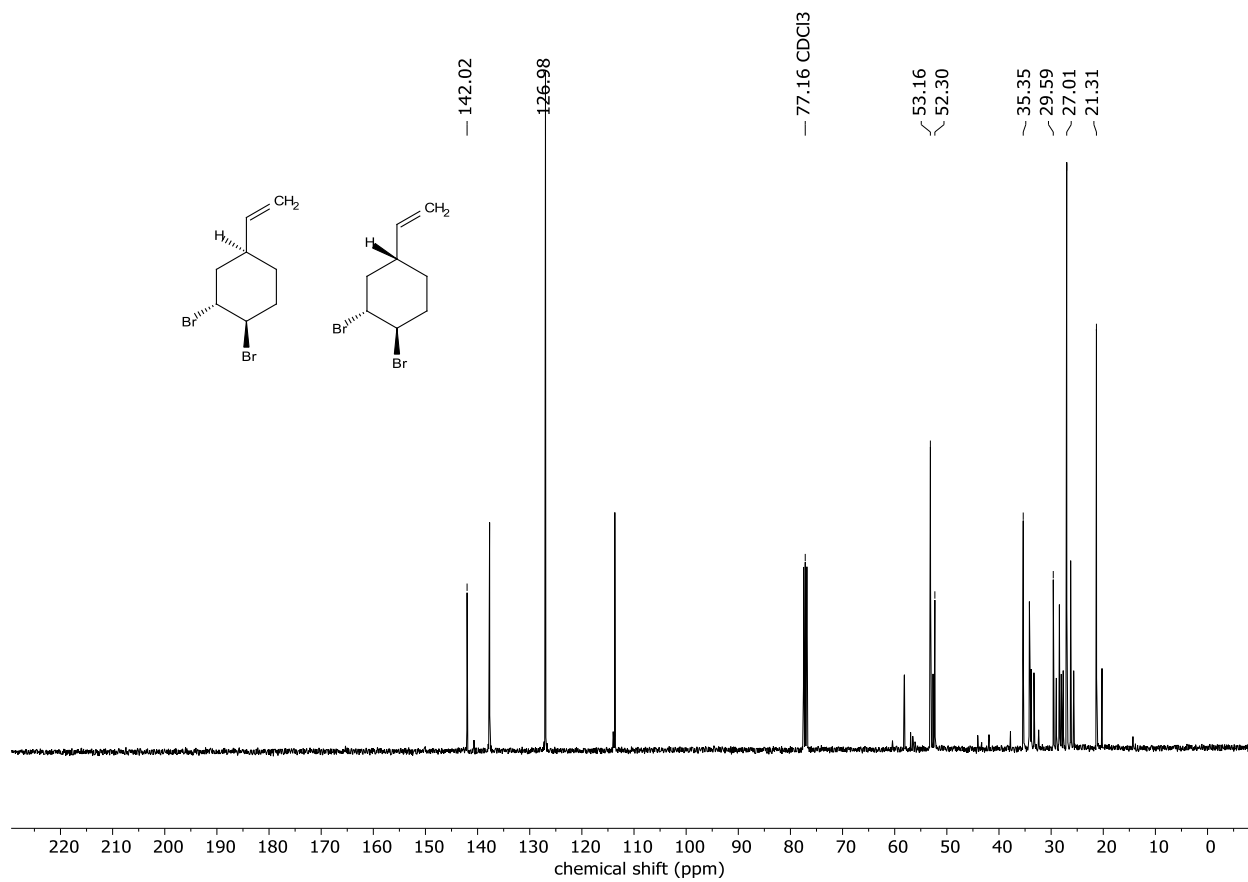


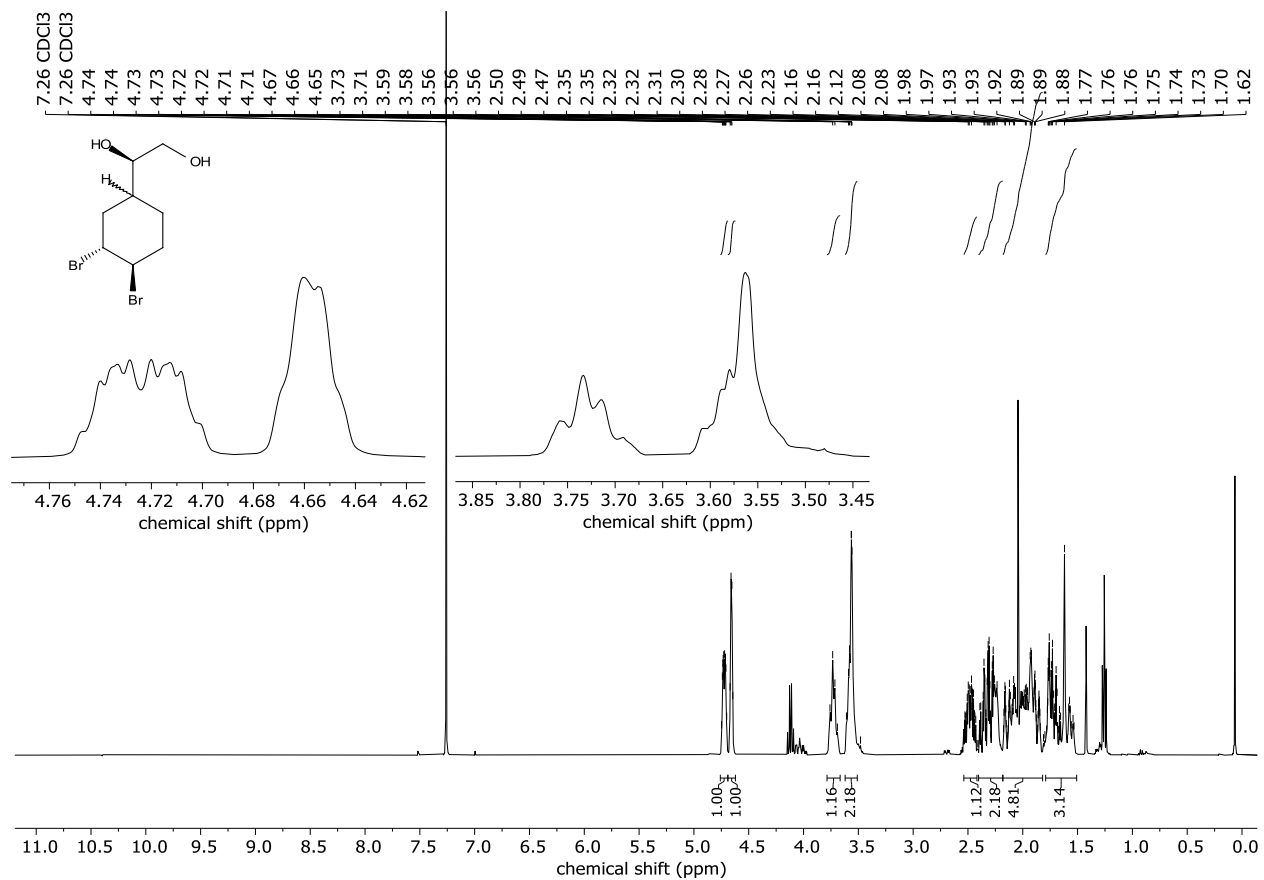
V











4 diastereomers. Mix of trans bromination and cis hydroxylation

